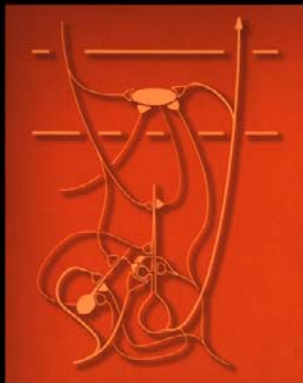


*The Synaptic
Organization
of the Brain*

FIFTH EDITION



EDITED BY

Gordon M. Shepherd

THE SYNAPTIC ORGANIZATION
OF THE BRAIN

This page intentionally left blank

THE
SYNAPTIC ORGANIZATION
OF THE BRAIN

Fifth Edition

Edited by

Gordon M. Shepherd

OXFORD
UNIVERSITY PRESS

2004

OXFORD
UNIVERSITY PRESS

Oxford New York

Auckland Bangkok Buenos Aires Cape Town Chennai
Dar es Salaam Delhi Hong Kong Istanbul Karachi Kolkata
Kuala Lumpur Madrid Melbourne Mexico City Mumbai
Nairobi São Paulo Shanghai Taipei Tokyo Toronto

Copyright © 1974, 1979, 1990, 1998, 2004
by Oxford University Press, Inc.

Published by Oxford University Press, Inc.
198 Madison Avenue, New York, New York, 10016
<http://www.oup-usa.org>

Oxford is a registered trademark of Oxford University Press

All rights reserved. No part of this publication may be reproduced,
stored in a retrieval system, or transmitted, in any form or by any means,
electronic, mechanical, photocopying, recording, or otherwise,
without the prior permission of Oxford University Press.

Library of Congress Cataloging-in-Publication Data
The synaptic organization of the brain /
edited by Gordon M. Shepherd.—5th ed.
p. cm. Includes bibliographical references and index.
ISBN 0-19-515955-1 (cloth)—ISBN 0-19-515956-X (pbk.)
1. Brain. 2. Synapses. 3. Neural circuitry.
I. Shepherd, Gordon M., 1933–
QP376.S9 2003 612.8'2—dc21 2003042914

2 4 6 8 9 7 5 3 1

Printed in the United States of America
on acid-free paper

PREFACE

The most significant event since the publication of the previous edition has been the sequencing of the mouse and human genomes, opening up new horizons for all of biology. For the brain, interpreting the functions of the genes depends on understanding how the proteins they produce function at different sites within a nerve cell, and how each nerve cell contributes to the circuits that carry out the fundamental operations of processing information in each brain region. This is the subject matter of synaptic organization.

Taking advantage of the genomic and proteomic data are new methods, including new applications of patch clamp recordings, powerful new microscopic methods based on two-photon laser confocal microscopy, gene-targeting to enable specific genes and proteins to be labeled, knocked-in or knocked-out, and fluorescent methods that provide dramatic images of cells as they interact synaptically with their neighbors under a variety of different functional states. Previously remote problems, such as the functions of dendrites and dendritic spines, are being attacked directly with the new methods. In parallel with the experimental advances have come ever more powerful computational models that are building a deeper theoretical basis for brain function.

Just as more powerful accelerators give physicists the ability to probe more deeply into the atom and the fundamental forces that determine the nature of matter and energy, so the new methods are giving neuroscientists the ability to probe more deeply into the neuron and its synaptic circuits and the fundamental properties that determine how information is processed in the brain. The results continue to constitute a quiet revolution in how we understand the neural basis of behavior, as potentially profound for brain science as the quantum theory has been for physics.

Each senior author is unique for his or her ability to bring together the molecular, anatomical, functional, and behavioral data in an authoritative integrated account. I am profoundly grateful to them for taking on the task of revising and enlarging their accounts to cover the advances made in the past six years. It is also a pleasure to welcome new co-authors and younger colleagues, not only to share the writing burdens but to show that a dedication to embracing all relevant disciplines in order to achieve an integrated understanding of brain organization has a thriving future.

As previously, this edition focuses on the brain regions best understood for their synaptic organization and functional correlates. The chapters are organized for the most part in the same format, proceeding from neural elements and synaptic connections to a basic canonical circuit for that region. This is followed by sections on synaptic physiology, neurotransmitters and neuromodulators, membrane properties, a special emphasis on dendritic properties that are crucial for action potential generation and for synaptic integration, and a final section on how the circuits mediate specific behaviors. By working within the same organizational framework for each chapter, the authors are able to highlight principles that are common to all regions, as well as the adaptations unique to each.

It can now be seen that this same organizational structure constitutes in fact the first necessary step toward building a database of the information needed to identify those

principles and adaptations. Building databases is a new goal of the funding agencies at the National Institutes of Health, and of the multiagency Human Brain Project. The study of synaptic organization may thus serve as leading model for the new field of neuroinformatics, which is dedicated to constructing databases and search tools that will enable experimentalists and theorists to construct a comprehensive multilevel, multidisciplinary database of the brain.

Among the unique aspects of this book is the combined reference list. Most scientific writing these days involves strict limits on numbers of references cited in order to save space. This means that in many cases authors are forced to cite review articles rather than the primary literature and to neglect the original literature. In current vernacular, if it isn't in pubmed, forget it. By contrast, this book continues to prize a scholarly depth behind our understanding. There has been no limit placed on referencing the studies cited. As a result, these accounts are among the most complete sources currently available for recognizing the main contributors to each field. All of the references are gathered in a common list at the back of the book, its number now grown to over 3,000. I hope its utility will justify the editorial labor in composing it!

Fiona Stevens at the Oxford University Press has been instrumental in stimulating the appearance of this new edition. Leslie Anglin has expertly overseen the production.

I would like to dedicate this new edition to Wilfrid Rall, mentor, friend and collaborator for many years, who has inspired myself and the authors of this volume and countless colleagues around the globe by pioneering the theoretical foundations of the functions of dendrites and their synaptic organization.

Finally, as always, to Grethe: tak.

Hamden, Connecticut

G.M.S.

ACKNOWLEDGMENTS

Chapter 1. Gordon M. Shepherd is grateful to the National Institutes of Health for research support from the National Institute on Deafness and Other Communicative Disorders, to the Human Brain Project/Neuroinformatics Program with support from the National Institute on Deafness and Other Communication Disorders, National Institute of Mental Health, National Institute of Neurological Disorders and Stroke, National Institute on Aging, and National Science Foundation, and to a Multiple University Research Initiative (MURI) grant from the Department of Defense. He thanks Wendolyn Hill and Gerry Domian for expert graphics, and Christof Koch for valuable contributions to an earlier version of this chapter.

Chapter 2. David A. McCormick's work has been supported by the National Institutes of Health and the Human Frontiers Science Program.

Chapter 3. Robert E. Burke's research support comes entirely from the Intramural Program of the National Institute of Neurological Disorders and Stroke (National Institutes of Health). He is grateful to his colleagues Michael O'Donovan, Jeffrey C. Smith, and William Marks for much stimulating discussion.

Chapter 4. Eric D. Young is grateful to Phyllis Taylor for help in preparing the figures. The work has been supported by the National Institute on Deafness and Other Communication Disorders (National Institutes of Health).

Chapter 5. Gordon M. Shepherd, Charles A. Greer, and Wei R. Chen are grateful to the National Institutes of Health for research support from the National Institute on Deafness and Other Communicative Disorders. Dr. Shepherd is also grateful to the Human Brain Project/Neuroinformatics Program with support from the National Institute on Deafness and Other Communication Disorders, National Institute of Mental Health, National Institute of Neurological Disorders and Stroke, National Institute on Aging, and National Science Foundation, and to a Multiple University Research Initiative (MURI) grant from the Department of Defense. Dr. Charles A. Greer is also grateful for support from the Human Frontiers Program. Dr. Wei R. Chen in addition thanks the Whitehall Foundation for research support.

Chapter 6. We thank the following members of the Sterling laboratory, past and present, for their contributions to data and ideas summarized here: Barbara McGuire, Michael Freed, Ethan Cohen, Yoshihiko Tsukamoto, Rukmini Rao-Mirotnik, David Calkins, and Andrew Hsu. We also thank the following collaborators: Robert Smith, Noga Vardi, Michael Freed, Gary Matthews, Henrique von Gersdorff, and Stanley J. Schein. The research was supported by grants from the National Eye Institute. We are grateful to Gordon Shepherd for editorial suggestions and to Sharron Fina for preparing the manuscript and illustrations.

Chapter 7. Eric Lange is grateful to the National Institute for Neurological Diseases and Stroke (NIH) and the National Science Foundation for research support.

Chapter 8. We acknowledge support for our research from U.S. Public Health Service grants from the National Institute for Eye Research.

Chapter 9. This work was supported by the National Institute of Neurological Disorders and Stroke.

Chapter 10. We thank Joshua Chover for contributing to the development of ideas. This work was supported by a National Institutes of Health grant from the National Institute on Deafness and Other Communicative Disorders and a Howard Hughes pre-doctoral fellowship.

Chapter 11. Daniel Johnston and David G. Amaral have been supported by grants from the National Institute of Neurological Disorders and Stroke and the National Institute of Mental Health during the preparation of this chapter. Dr. Johnston is also grateful to Diane Jensen for editorial assistance.

Chapter 12. The preparation of this chapter was supported by the Human Frontiers Science Program, the Koerber Foundation, and the European Union. We thank John Anderson for neuron and dendritic reconstructions, and the Physiology Department of the University of Cape Town for educating the authors.

CONTENTS

Online Resources, xi

Contributors, xiii

1. Introduction to Synaptic Circuits, 1
Gordon M. Shepherd
 2. Membrane Properties and Neurotransmitter Actions, 39
David A. McCormick
 3. Spinal Cord: Ventral Horn, 79
Robert E. Burke
 4. Cochlear Nucleus, 125
Eric D. Young and Donata Oertel
 5. Olfactory Bulb, 165
Gordon M. Shepherd, Wei R. Chen, and Charles A. Greer
 6. Retina, 217
Peter Sterling and Jonathan B. Demb
 7. Cerebellum, 271
Rodolfo R. Llinás, Kerry D. Walton, and Eric J. Lang
 8. Thalamus, 311
S. Murray Sherman and R. W. Guillery
 9. Basal Ganglia, 361
Charles J. Wilson
 10. Olfactory Cortex, 415
Kevin R. Neville and Lewis B. Haberly
 11. Hippocampus, 455
Daniel Johnston and David G. Amaral
 12. Neocortex, 499
Rodney Douglas, Henry Markram, and Kevan Martin
- References, 559
- Index, 705

This page intentionally left blank

ONLINE RESOURCES

Each of the authors has a website (URL) that provides information about the author together with supplementary materials and links to publications. These websites can be located by entering the author's name in the search engine Google.

A website is planned that will provide supplementary materials for *The Synaptic Organization of the Brain*, including illustrations in full color. Links to this website will be provided at the websites of the editor and the authors who wish to post this material.

Many sites on the web are available to support the study of the synaptic organization of the brain. Most closely related is a set of databases at the SenseLab project (senselab.med.yale.edu). These include the following:

Cell Properties Database (CellPropDB) (<http://senselab.med.yale.edu/cellpropdb>) is a database of the main membrane properties (transmitter receptors, ion channels and transmitters) expressed by each of the main cell types covered in this book.

Neuron Database (NeuronDB) (<http://senselab.med.yale.edu/neurondb>) is a database of those membrane properties as they are distributed within the dendrites, cell body and axon of each cell type.

Model Database (ModelDB) (<http://senselab.med.yale.edu/modeldb>) is a database of published computer models of each cell type and some of the circuits in which they are involved.

Each of these databases has efficient search tools for extracting arbitrary combinations of properties across the cell types, to facilitate identification of common principles of synaptic organization. The properties are documented by direct links to the original articles in PubMed.

These databases are sponsored by the *Human Brain Project* (<http://www.nimh.nih.gov/neuroinformatics/researchgrants.cfm>), a multiagency consortium whose goal is to support pilot studies in constructing databases to support research on the brain at all levels of organization, from genes to behavior.

Other resources within the Human Brain Project that are particularly relevant to synaptic organization are as follows:

Three-Dimensional Structure & Function of Synapses in the Brain (<http://synapses.mcg.edu>),

Generation and Description of Dendritic Morphology (<http://www.krasnow.gmu.edu/L-Neuron/index.html>),

Development of a 3D Cell-Centered Neuronal Database (<http://ncmir.ucsd.edu/NCDB>), and

Databases and Data Models Enabling Neuroinformatics (<http://neurodatabase.org> and <http://brainml.org>)

Reconstruction and Representations of Cerebral Cortex (<http://stp.wustl.edu>).

This page intentionally left blank

CONTRIBUTORS

DAVID G. AMARAL, PH.D.

Department of Psychiatry
University of California, Davis
Davis, California

ROBERT E. BURKE, M.D.

Laboratory of Neural Control
National Institute of Neurological Disorders
and Stroke

National Institutes of Health
Bethesda, Maryland

WEI R. CHEN, PH.D.

Department of Neurobiology
Yale University School of Medicine
New Haven, Connecticut

JONATHAN B. DEMB, PH.D.

Department of Neuroscience
University of Pennsylvania
Philadelphia, Pennsylvania

RODNEY DOUGLAS, M.D.

Institut für Neuroinformatik
ETH/UNIZ
Zurich, Switzerland

CHARLES A. GREER, PH.D.

Section of Neurosurgery
Yale University School of Medicine
New Haven, Connecticut

R. W. GUILLERY, PH.D.

Department of Anatomy
University of Wisconsin School of Medicine
Madison, Wisconsin

LEWIS B. HABERLY, PH.D.

Department of Anatomy
University of Wisconsin School of Medicine
Madison, Wisconsin

DANIEL JOHNSTON, PH.D.

Division of Neuroscience
Baylor College of Medicine
Houston, Texas

ERIC J. LANG, M.D., PH.D.

Department of Physiology & Neuroscience
New York University School of Medicine
New York, New York

RODOLFO R. LLINÁS, M.D. PH.D.

Department of Physiology & Neuroscience
New York University School of Medicine
New York, New York

HENRY MARKRAM, PH.D.

Mind and Brain Institute
EPFL
Lausanne, Switzerland

KEVAN A. C. MARTIN, D.PHIL.

Institute of Neuroinformatics
ETH/UNIZ
Zurich, Switzerland

DAVID A. MCCORMICK, PH.D.

Section of Neurobiology
Yale University School of Medicine
New Haven, Connecticut

KEVIN R. NEVILLE

Neuroscience Program
University of Wisconsin School of Medicine
Madison, Wisconsin

DONATA OERTEL, PH.D.

Department of Physiology
University of Wisconsin
Madison, Wisconsin

GORDON M. SHEPHERD, M.D., D.PHIL.

Department of Neurobiology
Yale University School of Medicine
New Haven, Connecticut

S. MURRAY SHERMAN, PH.D.

Department of Neurobiology
State University of New York
Stony Brook, New York

PETER STERLING, PH.D.

Department of Neuroscience
University of Pennsylvania
Philadelphia, Pennsylvania

KERRY D. WALTON, PH.D.

Department of Physiology
New York University School of Medicine
New York, New York

CHARLES J. WILSON, PH.D.

Department of Biology
University of Texas at San Antonio
San Antonio, Texas

ERIC D. YOUNG, PH.D.

Department of Biomedical Engineering
Johns Hopkins University School of
Medicine
Baltimore, Maryland

THE SYNAPTIC ORGANIZATION
OF THE BRAIN

This page intentionally left blank

INTRODUCTION TO SYNAPTIC CIRCUITS

GORDON M. SHEPHERD

Synapses are contacts that enable neurons to interact. Through these interactions they form the circuits that mediate the specific functional operations of different brain regions. The subject of *synaptic organization* is concerned with the principles underlying these circuits.

Synaptic organization differs from other fields of study in several ways. First, it is a *multidisciplinary* subject, requiring the integration of results from experimental work in molecular neurobiology, neuroanatomy, neurophysiology, neurochemistry, neuropharmacology, developmental neurobiology, and behavioral neuroscience. It is a *multi-level* subject, beginning (from the bottom up) with the properties of ions, transmitter molecules, and individual receptor and channel proteins and building up through individual synapses, synaptic patterns, dendritic trees, and whole neurons to the multi-neuronal circuits that are characteristic of each brain region. Finally, it is a field with a theoretical foundation, building and testing its experimentally derived results within a framework of theoretical studies in biophysics, neuronal modeling, computational neuroscience, and neural networks.

Studies of synaptic organization have been pursued vigorously for half a century, with increasing intensity. The co-authors of this book have been leaders in this effort. Each chapter lays out the synaptic organization of a specific brain region—in its full multidisciplinary, multilevel, and theoretical dimensions.

In this chapter, we introduce some of the basic principles that are common to the different regions. We show that it is possible to identify fundamental types of synaptic circuits at successive levels of organization. These types are called *basic*, or *canonical*, circuits. Like the Bohr atom in physics or gene families in molecular biology, canonical circuits are a conceptual tool for organizing the great varieties of circuits present in the nervous system. In parallel, we describe the canonical operations that the circuits perform. This provides a conceptual framework for understanding the adaptations of these operations that are unique to each of the regions considered in subsequent chapters.

It is a common lament in neuroscience that there is a lack of basic principles for understanding the vast amount of information about the brain that is accumulating. One

of the main aims of this book is to show that this lament ignores the progress that is being made in understanding synaptic organization, which is leading to a quiet revolution in our understanding of the neural basis of behavior.

THE TRIAD OF NEURONAL ELEMENTS

Figure 1.1 illustrates that the brain consists of many local regions, or centers, and of the many pathways between them. At each center, the *input fibers* make synapses onto the cell body (*soma*) and/or the branched processes (*dendrites*) emanating from the cell body of the nerve cells contained therein. Some of these neurons send out a long axon

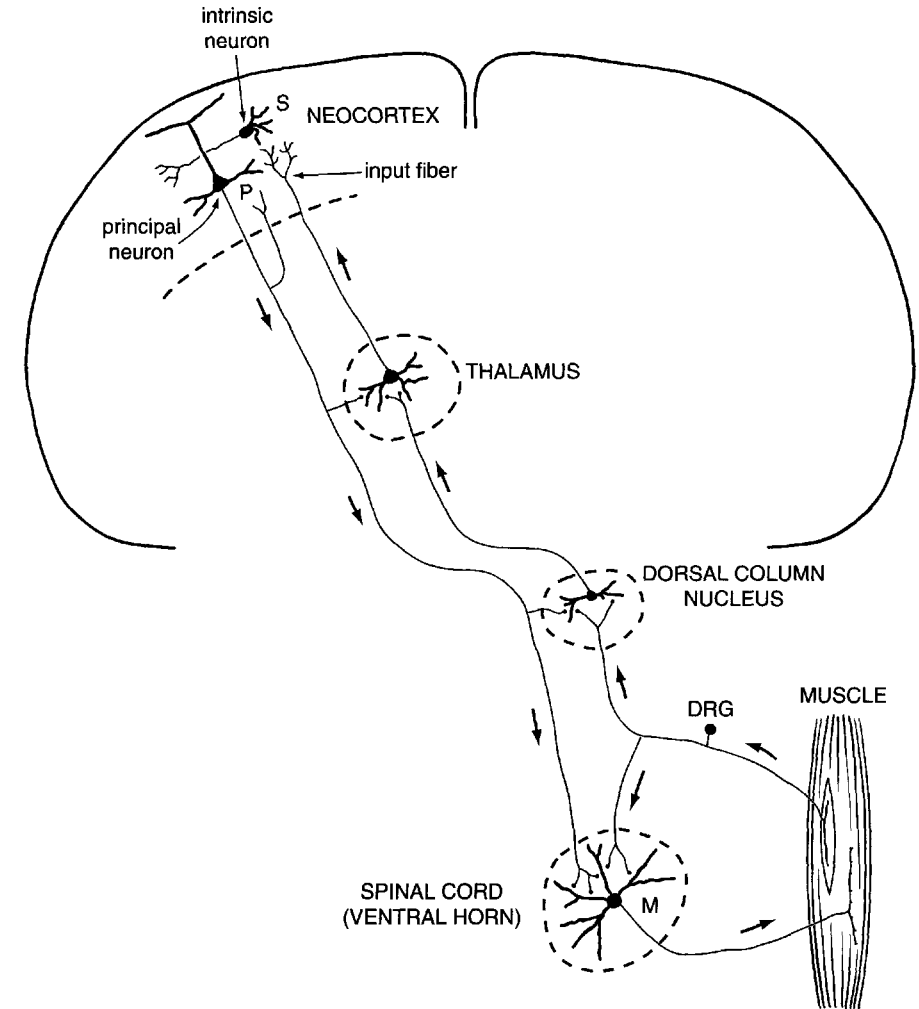


Fig. 1.1. Examples of the organization of the nervous system into local regions and interregional pathways formed by the long axons of principal neurons. Abbreviations: DRG, dorsal root ganglion cell; M, motoneuron; P, pyramidal (principal) neuron; S, stellate (intrinsic) neuron.

that, in turn, carries the signals to other centers; these are termed *principal*, *relay*, or *projection* neurons. Other cells are concerned only with local processing within the center; these are termed *intrinsic* neurons, *local* neurons, or *interneurons*. An example of this latter type is shown in the cerebral cortex in Fig. 1.1. The distinction between a principal and an intrinsic neuron cannot be rigid, because principal neurons also take part in local interactions. It is nonetheless a useful way of characterizing nerve cells, which is used throughout this book.

The principal and intrinsic neurons, together with the incoming input fibers, are the three types of neuronal constituents common to most regions of the brain. We refer to them as a *triad* of neuronal elements. The relations among the three elements vary in different regions of the brain, and these variations underlie the specific functional operations of each region.

THE SYNAPSE AS THE BASIC UNIT OF NEURAL CIRCUIT ORGANIZATION

Interactions among the triad of neuronal elements are mediated by the junctions termed *synapses*. It follows that the synapse is the elementary structural and functional unit for the construction of neural circuits. Traditionally, most concepts of neural organization have assumed that a synapse is a simple connection that can impose either excitation or inhibition on a receptive neuron. Much experimental evidence indicates that this assumption needs to be replaced by an appreciation of the complexity of this functional unit.

Figure 1.2 summarizes the current view of the synapse. Most synapses involve the apposition of the plasma membranes of two neurons to form a punctate junction, also termed an *active zone*. The junction has an orientation, thus defining the *presynaptic* process and the *postsynaptic* process. At a chemical synapse such as that depicted in Fig. 1.2, the presynaptic process liberates a *transmitter* substance that acts on the postsynaptic process. From an operational point of view, a synapse converts a presynaptic electrical signal into a chemical signal and back into a postsynaptic electrical signal. In the language of the electrical engineer, such an element is a *nonreciprocal two-port* (Koch and Poggio, 1987).

THE SYNAPSE AS A MULTIFUNCTIONAL MULTITEMPORAL UNIT

The mechanism of a synapse involves a series of steps, which are summarized in Fig. 1.2 (see Chap. 2) (for a comprehensive review, see Cowan et al., 2001). These include (1) depolarization of the presynaptic membrane; (2) influx of Ca^{2+} ions into the presynaptic terminal; (3–5) a series of steps leading to fusion of a synaptic vesicle with the plasma membrane; (6) release of a packet (quantum) of transmitter molecules; (7) diffusion of the transmitter molecules across the narrow synaptic cleft separating the presynaptic and postsynaptic processes; and (9) action of the transmitter molecules on receptor molecules in the postsynaptic membrane, (10) leading in some cases to direct gating of the conductance at an ionotropic receptor. This changes the membrane potential (11) and hence the excitability of the postsynaptic process. A depolarizing change increases the excitability; this is called an excitatory postsynaptic potential

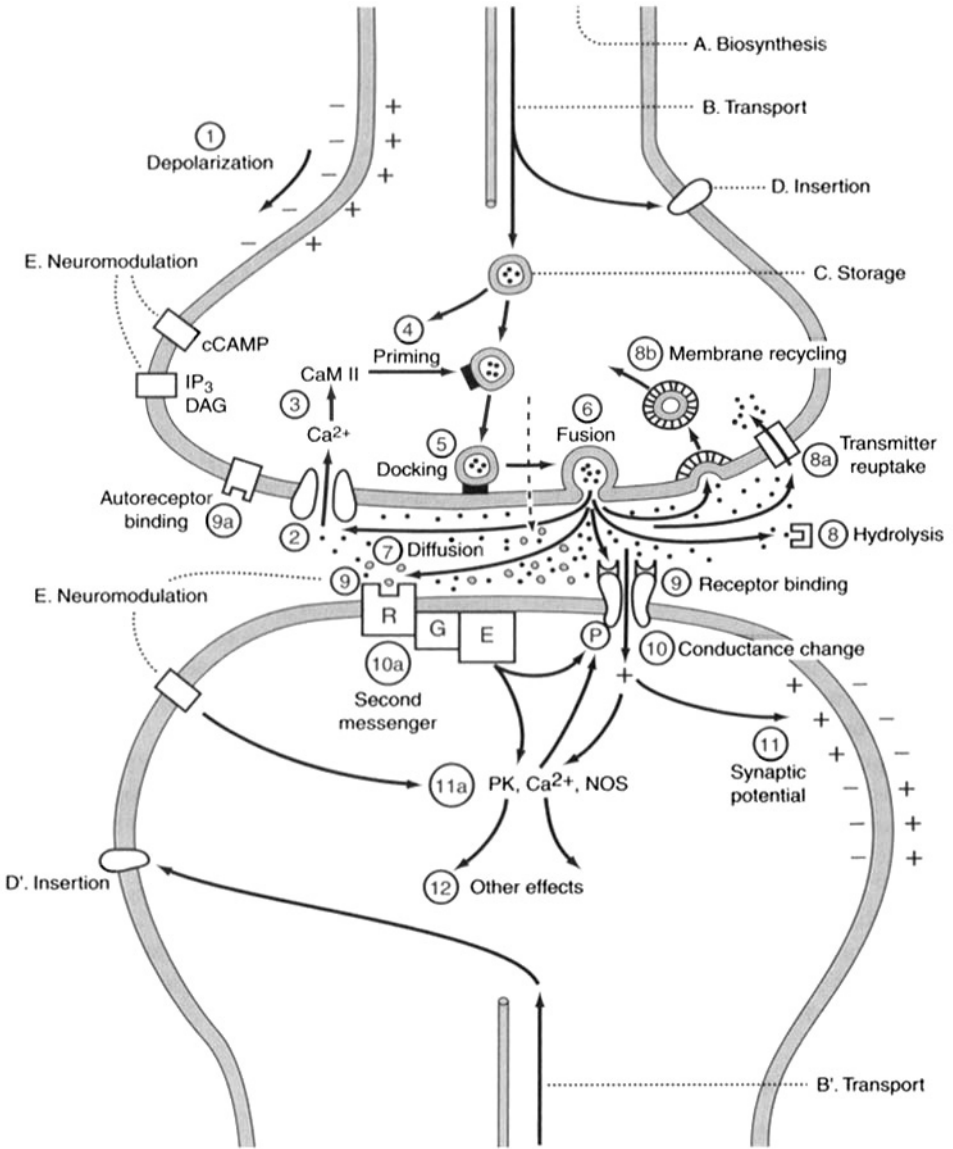


Fig. 1.2. A summary of some of the main mechanisms involved in immediate signaling at the synapse. Steps 1 through 12 are described in the text. Abbreviations: IP₃, inositol trisphosphate; AC, adenylate cyclase; CaM II, Ca/calmodulin-dependent protein kinase II; DAG, diacylglycerol; G, G protein; PK, protein kinase; R, receptor. [Modified from Shepherd, 1994b.]

(EPSP). A hyperpolarizing change decreases the excitability; this is called an inhibitory postsynaptic potential (IPSP). The mechanisms mediated by ionotropic receptors are concerned with rapid (1–20 msec) transmission of information, as in rapid sensory perception, reflexes, and voluntary movements (such as those used to type this text and you are using to read it).

The transmitter molecule may also activate a metabotropic receptor (10a) linked to a second-messenger pathway that modulates a membrane conductance or has other metabolic effects (11a and 12). The presynaptic process is itself a possible target, either of the transmitter acting on autoreceptors (8a) or of diffusible second messengers such as nitric oxide, produced by nitric oxide synthase (NOS) in the postsynaptic process, which can modulate transmitter release in an activity-dependent manner (also called *retrograde* messengers). The synapse can thus be regarded not only as a one-way relay but also as a more complicated bidirectional junction (Jessell and Kandel, 1993). Although presynaptic-to-postsynaptic activation can be fast, retrograde messengers typically act more slowly.

Activation of second messengers can have short- as well as long-lasting metabolic effects that lead to changes in synaptic efficacy. Of these, long-term potentiation (LTP) and long-term depression (LTD) are the most prominent. They are discussed in the following chapters as prime candidates for “activity-dependent” mechanisms that may underlie learning and memory. Also of interest are short-term facilitation and depression, which may occur over shorter periods of 10–100 msec (Markram and Tsodyks, 1996; Abbott et al, 1997; for a review, see Koch, 1997).

Many cellular mechanisms impinge on synaptic transmission over longer time periods. These include steps involved in axonal and dendritic transport, storage of transmitters and peptides, corelease of peptides, and direct modulation of transmitter responses (see Neuromodulation in Fig. 1.2). These effects are slow (seconds to minutes) or very slow (hours and longer); the slowest processes merge with mechanisms of development, ageing, and hormonal effects.

From these properties one can appreciate that the synapse is admirably suited to be a unit for building circuits. The multiple steps of its mechanism confer a considerable flexibility of function by means of different transmitters and modulators, different types of receptors, and different second-messenger systems linked to the different kinds of machinery in the cell: electrical, mechanical, metabolic, and genetic. This means that several mechanisms, with different time courses, can exist at the same synapse, conferring on the individual synapse the ability to coordinate rapid activity with the slower changes that maintain the behavioral stability of the organism over time. It is a multifunctional, multitemporal junctional unit.

TYPES OF SYNAPSES

In view of this tremendous potential for functional diversity, it is remarkable that synapses throughout the nervous system show such a high degree of morphological uniformity. Synapses in the brain tend to fall into two groups (see Fig. 1.3A): those with asymmetrical densification of their presynaptic and postsynaptic membranes and those with symmetrical densification. Gray (1959) termed these *type 1* and *type 2*, respectively. Depending on the histological fixatives used, type 1 is usually associated with small, round, clear synaptic vesicles, and in a number of cases has been implicated in excitatory actions. By contrast, type 2 is usually associated with small, clear, flattened or pleomorphic vesicles and is implicated in inhibitory synaptic actions.

Many examples of these types of synapses are identified throughout this book. There are well recognized exceptions to these structure–function relations—for example, inhibitory actions by synapses that do not have type 2 morphology (cf. cerebellar basket

B. Levels of Brain Organization

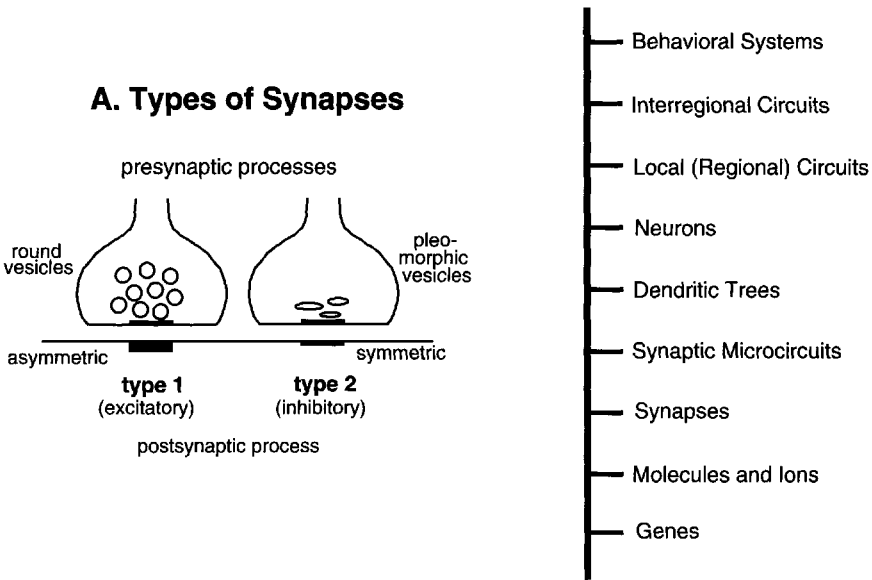


Fig. 1.3. Two key concepts for analyzing synaptic organization. **A:** Two main types of synapses. **B:** Multiple levels of organization. This book focuses on the levels from *synapses* to *local circuits* as a basis for understanding the expression of *molecules* and *ions* in an integrative context and for understanding the circuit basis of *behavioral systems*.

cells, see Chap. 7). Thus, although the type 1 and type 2 designations provide a useful working hypothesis, there is always the clear understanding that this is only a first step in classifying synaptic structure and function. For consistency in this book in the diagrams of synaptic connections in the different regions, neurons making type 1 synapses and having primarily excitatory actions are depicted by open profiles, whereas those making type 2 synapses and having primarily inhibitory actions are depicted by filled profiles.

LEVELS OF ORGANIZATION OF SYNAPTIC CIRCUITS

It might seem that one could simply connect neurons together by means of synapses and make networks that mediate behavior, but this is not the way nature does it. A general principle of biology is that any given behavior of an organism depends on a hierarchy of levels of organization, with spatial and temporal scales spanning many orders of magnitude. This is nowhere more apparent than in the construction of the brain. As applied to synaptic circuits, it means, as already indicated, that one needs to identify the main levels of organization to provide a framework for understanding the principles underlying their construction and function.

The analysis of local regions over the past two decades has led to the recognition of several important levels of circuit organization (Fig. 1.3B). The most fundamental level

is the information carried in the *genes*, which, interacting with the cellular environment, read out the basic *protein* molecular components of the cells in different regions. These molecular components are organized into *organelles* of the cell. For circuit formation, as we have seen, the most critical organelle is the *synapse*.

Synaptic organization begins at the next level, with the organization of multiple gene products into the synapse. The most local patterns of synaptic connection and interaction, involving small clusters of synapses, are termed *microcircuits* (Shepherd, 1978). The smallest microcircuits have extents measured in microns; their fastest speed of operation is measured in milliseconds. Microcircuits are grouped to form *dendritic subunits* (Rall, 1977; Shepherd, 1972b; Koch et al., 1982). The *dendritic trees* of individual neurons are a rich integrative substrate (Rall, 1977; Llinàs, 1988). The entire *neuron*, containing its several dendritic and axonal subunits, is the next level of complexity. Interactions between neurons within a region form *local circuits* (Rakic, 1976); these perform the operations characteristic of a particular region. Above this level are the interregional *pathways*, columns, laminae, and topographical maps, involving multiple regions in different parts of the brain, that form the *systems* that mediate specific types of behavior.

These many interwoven levels of organization are a feature of the brain not shared by its artificial cousin, the digital computer, in which few intermediate modular structures exist between the individual transistor, on the one hand, and a functional system, such as a random-access memory chip, on the other.

An important aim of the study of synaptic organization is to identify the types of circuits and the functional operations that they perform at each of these organizational levels. In the rest of this chapter, we consider examples at each level. Subsequent chapters show how, in each region, the nervous system rings changes on these basic themes, with variations of circuits exquisitely adapted for the specific operations and computations carried out by that region on its particular input information.

THE SYNAPSE AS AN INTEGRATIVE MICRO-UNIT

In addition to its ability to mediate different specific functions, an important property of the synapse is its small size. The area of contact has a diameter of 0.5–2.0 μm , and the presynaptic terminal (a *varicosity* or *bouton*) has a diameter that characteristically is only slightly larger. These small sizes mean that large numbers of synapses can be packed into the limited space available within the brain. For example, in the cat visual cortex (see Chap. 12), 1 mm^3 of gray matter contains approximately 50,000 neurons, each of which gives rise on average to some 6,000 synapses, making a total of 300 million (300×10^6) synapses (Beaulieu and Colonnier, 1983). It has been estimated that 84% of these are type 1 and 16% are type 2. If the cortical area of one hemisphere in the human is approximately 100,000 mm^2 , there must be on the order of 10 billion cells in the human cortex and 60 trillion (60×10^{12}) synapses. In the cerebellum (see Chap. 7), it has been estimated that the small granule cells number up to 100 billion, each making up to 100 synapses onto cerebellar nuclear and cortical cells.

Like the national debt, these numbers are so large that they lose meaning. The important point is that the number of synapses amplifies the number of neurons by several orders of magnitude, providing a rich substrate for the construction of microcircuits within the packed confines of the brain.

DEVELOPMENT OF SYNAPTIC CIRCUITS

In early development, an exuberance of synapses is generated throughout the nervous system; during this time synapses are very dynamic and appear and disappear relatively rapidly. When the animal reaches maturity, the final synaptic density may be reduced by as much as half (yet the size of the brain has expanded considerably) (Rakic et al., 1986). Studies of these kinds of mechanisms are extremely important for understanding the strategy of construction of synaptic circuits. Developmental mechanisms are a vast field of contemporary neuroscience (for a comprehensive review, see Sanes et al., 2000). Particular aspects of development are considered in this book as they relate to basic principles, but the primary focus will be the organization and functional operations of the mature nervous system.

SYNAPTIC MICROCIRCUITS

Excitation and inhibition by single synapses have little behavioral significance by themselves; it is the assembly of synapses into *patterns of connectivity* during development that produces functionally significant operations. The process can be likened to the assembly of transistors onto chips to form microcircuits in computers. By analogy, we refer to these most local synaptic patterns as neuronal *microcircuits*. Let us consider several basic (canonical) types.

ELECTRICAL COUPLING

The simplest type of microcircuit involves a connection between two or more presynaptic terminals by electrical (gap) junctions (Fig. 1.4A). Through these junctions the electrical current in one process is distributed to the other process(es) (see Chap. 2). This arrangement has several important functions in synaptic microcircuits.

Signal-to-Noise Enhancement. The distribution of current through the electrical synapse reduces the amount of current in the active process. This reduces the impact of random (noisy) activity in single processes while enhancing the impact of simultaneous (signal specific) activity in two or more processes (this mechanism is described in the retina, Chap. 6).

Synchronization. Activity in one process may tend to activate other processes at the same time, thus promoting synchronization of activity. This can occur in either pre- or postsynaptic locations (see inferior olive cells, Chap. 7).

Gating by Different Mechanisms. The conductivity of the electrical connection may be gated by different mechanisms, such as membrane depolarization or hyperpolarization, pH, metabolic products, neurotransmitters and neuropeptides (Chap. 2). This can occur in both directions, or in only one direction (rectification). Gap junctions are thus dynamic rather than static connection elements.

Exchange of Small Molecules. Gap junctions allow the free passage of small molecules, providing the means for mediating tissue homeostasis, cellular organization, cellular differentiation and other developmental processes.

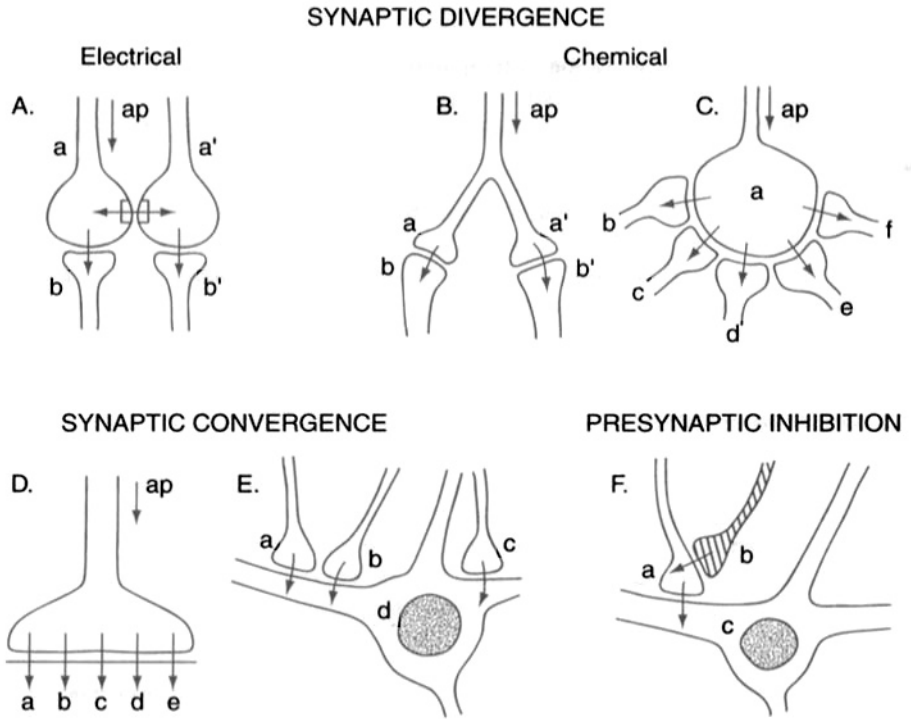


Fig. 1.4. The simplest types of synaptic microcircuits. **Synaptic divergence.** **A:** Divergence by electrical interactions through gap junctions. In this example, an action potential (ap) invades terminal (a) to activate a synapse onto (b); the current spreads through the gap junction from terminal (a) into terminal (a') to activate (b) near-synchronously. **B:** Divergence through chemical synapses. Action potential invades terminals (a) and (a'), leading to activation of (b) and (b'). **C:** Action potential invades large terminal (a), which has synapses onto (b–f). **Synaptic convergence.** **D:** Multiple synapses from a single terminal converge onto a single postsynaptic process. **E:** Synaptic convergence of several axons (a–c) onto a single postsynaptic neuron (d). **F:** **Presynaptic inhibition** by axon b onto axon a, which is presynaptic to axon c. See text.

SYNAPTIC DIVERGENCE

A fundamental and common pattern of synaptic organization is to have multiple outputs from a single source. In neural network terminology, this is called “fan-out.” A common pattern consists of multiple branches of a single axon (Fig. 1.4B). Fan-out from a single axon may be considerable, as exemplified by the several thousand synapses made by a typical cortical cell mentioned earlier. Fan-out is essential if information carried in one cell in one region is to be combined with information from cells in other regions.

Fan-out may also occur from a single terminal. As indicated in Fig. 1.4C, a presynaptic terminal (a) has excitatory synapses onto postsynaptic dendrites (b–f). An action potential (ap) invading the presynaptic terminal can thus cause simultaneous EPSPs in many postsynaptic dendrites.

The operational advantages of this arrangement are several:

Amplification. When there are multiple outputs from a single terminal, the activity in a single axon is amplified into activity in many postsynaptic neurons, conferring a high gain upon the system. This can be important in increasing the signal-to-noise ratio underlying signal detection.

Synchronization. Activation of multiple synapses from a single terminal occurs simultaneously. This retains the precise timing of the input and mediates synchronization of the postsynaptic responses. Synchronization underlies oscillatory activity, which is increasingly recognized as important for signal processing in the brain.

Retention of Sign. The synapses from a given terminal are likely to be release the same transmitter and, although not necessarily, have the same action on postsynaptic cells (e.g., excitation → excitation).

These factors may also apply to divergence from multiple terminals, although with more variation. Divergence from single terminals is found in many parts of the nervous system. A single mossy fiber terminal in the cerebellum, for example, may make synapses onto dendrites of as many as 100 or more granule cells (cf. Chap. 7). Single terminals with more modest divergence factors are made by sensory afferents in thalamic relay nuclei (see Chap. 8) and the substantia gelatinosa of the dorsal horn.

Release Probabilities and Safety Factors. Multiple outputs from a presynaptic terminal can be organized in an entirely different way, as is shown by the well-known example of the neuromuscular junction (NMJ) (see Fig. 1.4D). The NMJ also consists of a large presynaptic terminal with many release sites, but they are all made onto the same muscle fiber. It is known that of 1000 or so release sites, only 100–200 are actually activated by invasion of a single impulse into the presynaptic terminal. Thus, there is a probability of only 0.1–0.2 that a given site will release transmitter when depolarized by an impulse. The multiple release sites onto the same muscle fiber therefore raise the “safety factor” for synaptic transmission, ensuring that an action potential in the presynaptic nerve will always lead to a response in the muscle fiber. Multiple synapses by a presynaptic onto a postsynaptic process are also found between neurons; an example is discussed in the retina (see Chap. 6).

The release sites of the NMJ are equivalent to the active zones of central synapses, each with its own release probability. This implies that, in the example of Fig. 1.4C, presynaptic depolarization would cause some synapses to release transmitter (e.g., b, c) but not others (e.g., d). The divergent pattern thus has the advantages noted earlier but has the disadvantage of making each connection less reliable, dependent on probability of release and other modulatory factors (see Chap. 12).

Silent Synapses. The NMJ example illustrates that morphological studies can identify the pattern of synaptic connections, but their actual use is physiological and probabilistic (see Korn and Faber, 1987). The release probability can be up- or down-regulated by the amount and timing of presynaptic and postsynaptic activity, providing an effective mechanism for adjusting the effect that a synapse has on its postsynaptic target (Stevens and Wang, 1994; Abbott et al., 1997). Synapses that are not activated by a single action potential but depend on these multiple factors for activation are called *silent synapses*.

SYNAPTIC CONVERGENCE

The considerable divergence that characterizes the output of a single neuron is matched by the considerable convergence of many inputs onto a single neuron. In neural network terminology, this is called “fan-in.” The essence of this convergence at the microcircuit level is depicted in Fig. 1.4E, where two terminals (a, b) make synapses onto a postsynaptic dendrite (d). These simple canonical convergence patterns have a number of important properties:

Temporal Summation. Let us consider first the case in which both terminals are excitatory. Spread of an impulse into terminal (a) sets up an EPSP; slightly later, spread of an impulse into terminal (b) sets up an EPSP that summates with that of (a). This is termed *temporal summation*. Note that although the impulses in (a) and (b) may be asynchronous, their EPSPs nonetheless can summate. For relatively fast EPSPs, the prolongation that makes temporal summation possible is due mainly to the membrane capacitance, which slows the dissipation of charge across the postsynaptic membrane (cf. Johnston and Wu, 1995; Shepherd, 2003a). For slower EPSPs, the time course is controlled by biochemical processes, such as second messengers.

Quantal vs. Graded Actions. When a single synapse releases a single vesicle, the action on a postsynaptic process is *quantal* in amplitude, that is, all-or-nothing. This is likely to be the case for the postsynaptic response of a dendritic spine receiving one synapse (see later). When multiple synapses are activated by different input fibers, summation in the dendritic branches and cell body of the postsynaptic cell is *graded* in amplitude with the numbers of input fibers and their release probabilities. Thus, synaptic actions are either quantal or graded, depending on the numbers of synapses involved and the spatial extents of the summing process.

Synaptic Summation Is Fundamentally Nonlinear. Although it might appear that temporal summation involves simple linear addition of PSPs, in general this is not the case. This is because PSPs are generated by changes in membrane conductance to specific ions and not by current injection (see Chap. 2). The conductances act to shunt, or short-circuit, each other, so that the combined amplitude of a PSP is less than the sum of its parts. As first emphasized by Wilfrid Rall, this means that synaptic summation is essentially a nonlinear process (Rall, 1964, 1977; Johnston and Wu, 1995; Shepherd, 2003b).

Types of Excitatory–Inhibitory Interactions. Synaptic convergence also involves summation of excitatory and inhibitory PSPs. This process lies at the heart of the integrative mechanisms of neurons. Consider, for example, in Fig. 1.4E, that (b) is inhibitory. Activation sets up an IPSP, which opposes the EPSP set up by (a) and repolarizes the membrane toward the reversal potential for the inhibitory conductance (see Chap. 2). If the reversal potential is near the resting membrane potential, this is called *silent*, or *shunting*, inhibition. If it is more polarized, it gives rise to *hyperpolarizing inhibition*. Obviously, integration of excitatory and inhibitory synaptic responses can be highly nonlinear and complex, even without the added complication of active membrane properties (Rall, 1964; Koch et al., 1983; Koch, 1997).

Spatial Summation. It remains to note that inputs are characteristically distributed over the entire dendritic surface of a neuron [see (c) in Fig. 1.4E]. This means that, in addition to temporal summation, there is *spatial summation* of responses arising in different parts of a dendrite, as well as different parts of the whole dendritic tree. Spatial summation allows for combining many inputs into one integrated postsynaptic response. The separation of PSPs reduces the nonlinear interactions between synaptic conductances, making the summation more linear. However, it also increases the possibilities for local active mechanisms and the generation of nonlinear sequences of activation from one site to the next within the dendritic tree.

PRESYNAPTIC INHIBITION

This is a final type of simple synaptic combination involving a special type of convergence. In this arrangement (see Fig. 1.4F), a presynaptic terminal (a) is itself postsynaptic to another terminal (b). The presynaptic action may involve a conventional type of IPSP produced by (b) in the presynaptic terminal (a). Alternatively, there may be a maintained depolarization of the presynaptic terminal, reducing the amplitude of an invading impulse and with it the amount of transmitter released from the terminal. The essential operating characteristic of this microcircuit is that the effect of an input (a) on a cell (c) can be reduced or abolished (by b) without there being any direct action of (b) on the cell (c) itself. Control of the input (a) to the dendrite or cell body can thus be much more specific.

Presynaptic control may be exerted by either axon terminals or presynaptic dendrites. Note that the effect is presynaptic only with regard to the response of the postsynaptic cell. From the point of view of the presynaptic terminal, the effect is postsynaptic. There are many situations in the nervous system, involving multiple synapses between axonal and/or dendritic processes, in which sequences of pre- and postsynaptic effects can occur (see Chaps. 3, 5, 6, 8, on the spinal cord, olfactory bulb, retina, and thalamus).

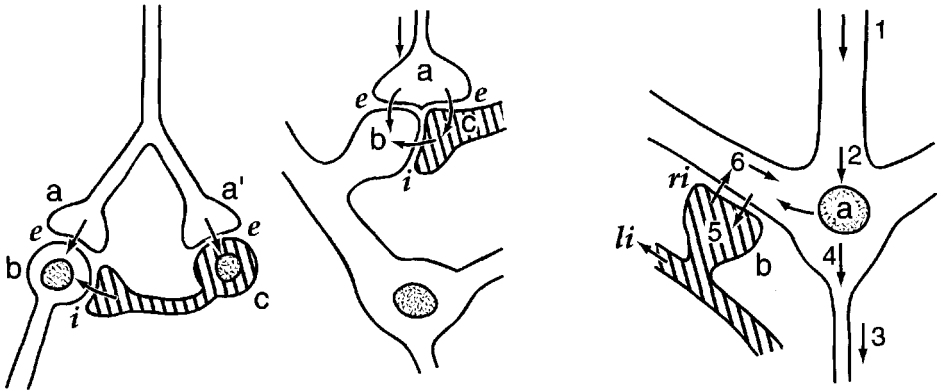
INHIBITORY OPERATIONS

The patterns of synaptic connections considered thus far mediate elementary excitatory and inhibitory operations. Let us next consider canonical arrangements that carry out operations for specific information processing functions through inhibitory interneurons.

Feedforward Inhibition. Sensory processing commonly involves an inhibitory “shaping” of excitatory events. An important mechanism for producing this is by a pattern of synaptic connections that mediates *feedforward inhibition*. The most common type involves excitatory input to both a principal neuron and an inhibitory interneuron, so that the activated interneuron “feeds forward” inhibition onto the principal neuron (Fig. 1.5A, left). A special variation of this type of arrangement (Fig. 1.5A, right) consists of an afferent terminal (a) which makes synapses onto the dendrites of both a relay neuron (b) and an interneuron (c). The dendrites of both neurons respond by generating EPSPs. However, the interneuron also has inhibitory dendrodendritic synapses onto the relay neuron; the EPSP activates these synapses, producing an inhibition of the relay neuron. The extra synapse in this pathway helps to delay the inhibitory input, so that the combined effect in (b) is an excitatory–inhibitory sequence.

A. FEEDFORWARD INHIBITION

B. RECURRENT INHIBITION



C. RECURRENT AND LATERAL INHIBITION

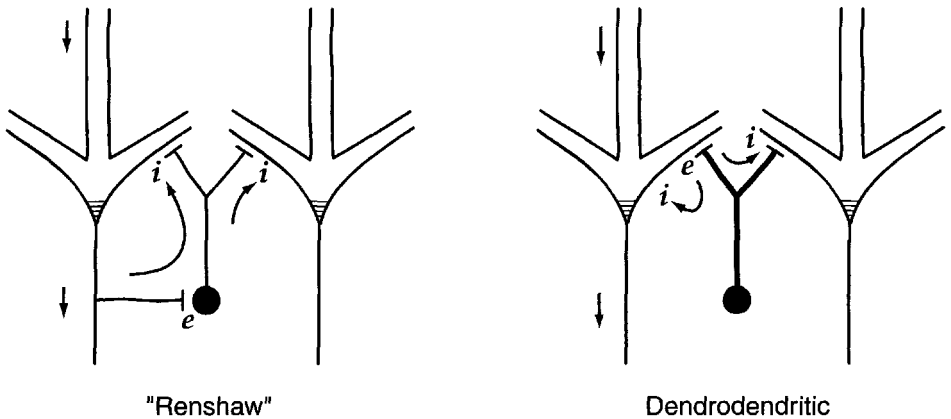


Fig. 1.5. Microcircuits that mediate different types of postsynaptic inhibition. **A:** Feedforward inhibition: on the left, through an interneuronal axon, on the right, through an interneuronal dendrite. **B:** Recurrent inhibition, in which a relay neuron (a) is both presynaptic and postsynaptic to the dendrite (d) of an inhibitory interneuron (b). This microcircuit mediates both recurrent and lateral inhibition, through the series of steps indicated by 1–6. **C:** Comparison between lateral inhibition mediated by axon collateral and interneurons and by dendrodendritic connections. See text.

This type of sequence is found in the thalamus (see Chap. 8) and many sensory pathways. By restricting the excitation of relay neurons to the onset of an excitatory input, it serves to enhance the sensitivity to changing stimulation, and thus performs a kind of *temporal differentiation* on changing sensory states (Koch, 1985). By means of spread of postsynaptic responses through dendritic trees, it may also contribute to the enhancement of spatial contrast through *lateral inhibition* (see later).

Note that the microcircuits in Fig. 1.5A are built of all three elementary patterns discussed earlier and depicted in Fig. 1.4. Thus, they combine *divergence* from terminal (a) with *convergence* of (a) and (c) onto (b) and *presynaptic* control by (a) of (c).

Recurrent Inhibition. A common type of operation in the nervous system is one in which the excitation of a neuron leads to inhibition of that neuron and/or of neighboring neurons. This is called *feedback* or *recurrent inhibition*. It can be mediated by several types of circuit, the most local of which involves reciprocal dendrodendritic synapses.

This mechanism has been worked out at the synaptic level in the olfactory bulb (see Chap. 5) and is illustrated in Fig. 1.5B. The output neurons of the olfactory bulb are mitral and tufted cells (a). They are activated by EPSPs, which spread through a primary dendrite (1) to the cell body (2) to set up an impulse that propagates into the axon (3). The impulse also backspreads into secondary dendrites (4), where it activates output synapses that are excitatory to spines of granule cell dendrites (5). The EPSP in the spine then activates a reciprocal inhibitory synapse back into the mitral cell dendrite (6); the IPSP spreads through the neuron to inhibit further impulse output.

Reciprocal synapses thus form an effective microcircuit module carrying out an elementary computation—in this case, recurrent inhibitory feedback of an activated neuron. Reciprocal synapses are found in a number of regions of the nervous system; in addition to the olfactory bulb, they include the dorsal horn of the spinal cord, retina (see Chap. 6), thalamus (see Chap. 8), and suprachiasmatic nucleus. There also is evidence for feedback from dendrites onto axon terminals in the cerebral cortex (Zilberter, 2000). Their presence in the different nuclei of the thalamus means that they play a role in the thalamocortical circuits that control cortical operations (cf. Chap. 8).

Lateral Inhibition. In addition to recurrent inhibition, the same microcircuit may mediate lateral inhibition. In Fig. 1.5B, the EPSP in the granule cell spine spreads through the dendritic branch to other spines, activating inhibitory output onto neighboring, less active, mitral cells. The more common implementation is through axon collaterals of an output neuron that feed back onto an interneuron, which inhibits other output neurons through its axonal connections. This was first described in the spinal cord, where it was named *Renshaw inhibition*, after its discoverer (see Chap. 3).

The two neural substrates for lateral inhibition are compared in Fig. 1.5C in relation to the axon hillock of the output cell. Dendrodendritic inhibition is activated by the backspreading action potential from the axon hillock. It is therefore “prehillock” in location (Fig. 1.5C, right). The pathway is local, limited to the dendritic tree of that neuron and its interconnections with local subunits of the interneuronal dendrites. By contrast, Renshaw inhibition is due to the forward-propagating action potential from the axon hillock and is therefore “trans-hillock” in nature (Fig. 1.5C, left). The pathway consists of the global output of the axon collaterals of the output neuron and the axonal branches of the activated interneurons.

Lateral inhibition is a fundamental mechanism of neural processing. We will see numerous examples of how it is implemented in virtually every region of the brain.

DENDRITIC INTEGRATION AND DENDRITIC SUBUNITS

We now move to the next higher level of organization, of dendritic trees. Understanding of the functional properties of dendritic trees began with the pioneering studies of Wilfrid Rall (Rall, 1957; 1959a,b; Segev et al., 1995). Neuronal dendrites are characteristically highly branched, which obviously increases the surface area for receiving synaptic inputs. Despite this wide distribution of synapses on the dendrites, it is common practice in neuroanatomical textbooks, and it is the common assumption underlying the vast majority of neural network simulations, to consider nerve cells to be single-node, linear integration devices, in which the effects of dendritic morphology and synaptic patterns on the functions of individual cells are totally neglected.

In fact, the patterns of dendritic branching impose critical geometrical constraints on the integration of activity in different branches. The rules for integration were developed in a comprehensive theoretical framework by Wilfrid Rall (summarized in Segev et al., 1995) which applies to the analysis of dendritic properties in all the chapters of this book. The geometry of the branches and the sites of specific inputs combine with the electrotonic properties to ensure that parts of a dendritic tree can function semi-independently of one another. If one adds the fact that voltage-gated channels can confer excitable properties onto local dendritic regions, it is clear that the dendrites, far from being functionally trivial appendages of a cell body, are the substrate for generating a rich repertoire of computation that contributes critically to the overall input-output functions of the neuron. It is thus evident that single-node network models ignore several levels of dendritic organization responsible for much of the computational complexity of the real nervous system.

Four factors—dendritic branching architecture, synaptic placement, and passive and active membrane properties—must be taken into account in assessing the nature of the integrative activity of dendrites. Characterization of the electrotonic spread of potentials is difficult because of the complex branching patterns of many dendrites. An introduction to one-dimensional passive cable theory is provided in several accounts (Rall, 1977; Johnston and Wu, 1995; Segev, 1995; Shepherd, 2003a). The ways that active conductances can contribute to dendritic activity are considered in Chap. 2.

The functional role of dendritic activity in information processing within synaptic circuits is a common theme running through the accounts of most of the cells in the brain regions considered in this book. Here we provide a brief introduction to the nature of dendritic integration and the ways that functional compartments are created at several levels of dendritic organization. Although dendritic branching patterns seem infinitely variable, canonical operations can be seen to apply across most of these patterns.

DENDRITIC COMPUTATION

In assessing the nature of dendritic integration, it is increasingly fashionable to use computational metaphors. Although this obscures many functional roles of dendrites that are not strictly “computational” (e.g., mechanisms involved in development, maturation, activity-dependent changes, etc.), it has the advantage of providing a specific framework within which the capacity of dendrites to carry out well-characterized types of operations can be assessed.

The importance of the sites and types of synaptic inputs on a dendritic branch can be illustrated by using the paradigm of logic operations. In the diagram of Fig. 1.6A, alternating excitatory and inhibitory synapses are arranged along a dendritic branch. Given the nonlinear interactions between these synapses, as discussed earlier, an inhibitory synapse (i_1 , i_2 , i_3) with a synaptic reversal potential close to the resting potential of the cell (“shunting” or “silent” synapse, see Chap. 2) can effectively oppose

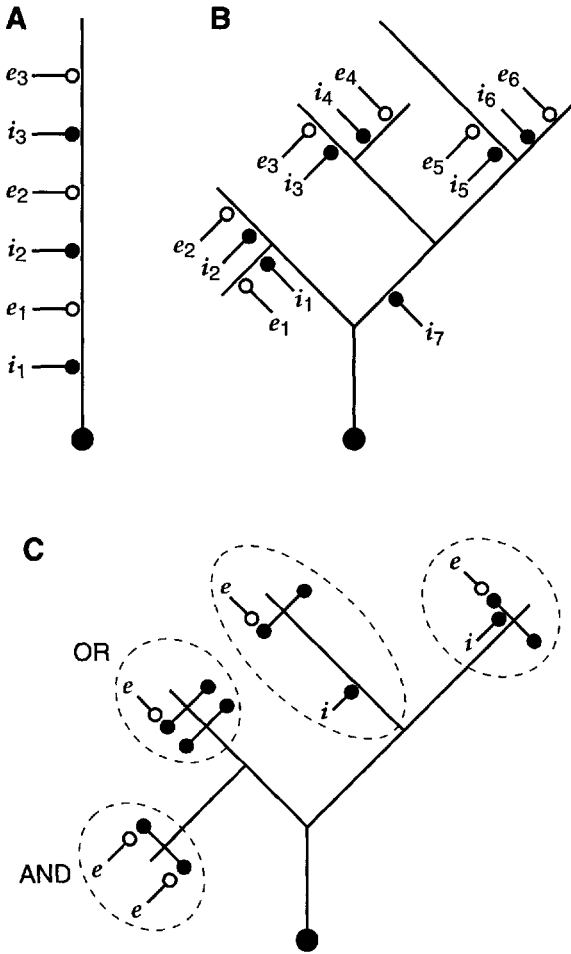


Fig. 1.6. Arrangements of synapses that could subserve logic operations. **A:** A single dendrite receives excitatory (e_1 – e_3) and inhibitory (i_1 – i_3) synapses. An inhibitory input can effectively veto only more distal excitatory responses; this approximates an AND-NOT logic operation, e.g., [e_2 AND NOT i_1 or i_2]. **B:** Branching dendritic tree with arrangements of excitatory and inhibitory synapses. As in **A**, inhibitory inputs effectively veto only the excitatory response more distal to it, e.g., [e_5 AND NOT i_5] AND NOT i_7 . **C:** Branching dendritic tree with excitatory synapses on spines and inhibitory synapses either on spine necks or on dendritic branches. Different types of logic operations arising out of these arrangements are indicated. In all cases (**A**–**C**), inhibition is of the shunting type. See text. [**A**, **B** adapted from Koch, 1983; **C** based on Shepherd and Brayton, 1987.]

(“veto”) the ability of a membrane potential change generated by any more distal excitatory synapse to spread to the soma and generate impulses there. By contrast, an inhibitory synapse has little effect in vetoing the voltage change initiated by more proximal excitatory synapses. This operation is an analog form of a digital AND-NOT gate (*e and not more proximal i*) and has been postulated to be a mechanism underlying various computations, such as direction selectivity in retinal ganglion cells.

This type of synaptic arrangement can also be found in more localized parts of dendritic trees. Figure 1.6B depicts a case in which a dendrite has numerous distal branches, each with an excitatory and an inhibitory synapse. The same “on-path” rule still applies: an inhibitory synapse effectively vetoes a more distal excitatory synapse on the same branch but has little effect in opposing excitatory responses originating anywhere else in the dendritic tree, which are effectively sited more proximally to the soma. Thus, the combination of dendritic morphology in conjunction with synaptic placement enables the cell to “synthesize” analog versions of logical, boolean operations.

In summary, local dendrites can be considered canonical structures that apply across most types of dendritic branching. In addition, logic operations can be considered canonical operations, in terms of basic properties of coincidence detection and excitatory-inhibitory interactions, that also apply across most types.

DENDRITIC SPINE UNITS

The smallest compartment, structurally and functionally, within a dendritic tree is the dendritic spine, a small (1–2 μm), thornlike protuberance. It is already evident from Fig. 1.5 that spines are an important component in many kinds of microcircuits. An electron micrograph of a spine in the cerebral cortex is shown in Fig. 1.7. Spines are extremely numerous on many kinds of dendrites; in fact, they account for the majority of postsynaptic sites in the vertebrate brain. They are especially prominent in the cerebellar cortex (see Chap. 7), basal ganglia (see Chap. 9), and cerebral cortex (see Chaps. 10–12). Within the cerebral cortex, about 79% of all excitatory synapses are made onto spines and the rest are made directly onto dendritic branches, whereas 31% of all inhibitory synapses are made onto spines. A spine with an inhibitory synapse always carries an excitatory synapse as well (Beaulieu and Colonnier, 1983). Given the dominance of excitatory synapses, about 15% of all dendritic spines carry both excitatory and inhibitory synaptic profiles.

On dendrites of cortical pyramidal cells, spine densities may reach several spines per micrometer of dendritic length. Because spines are characteristically located on dendrites at some distance from the cell body, experimental evidence regarding their physiological properties is still difficult to obtain. However, their obvious importance has stimulated considerable interest (Shepherd, 1996; Harris, 1999; Yuste and Majewska, 2001; Nimchinsky et al., 2002; Segal, 2002). It is now possible to obtain direct structural, molecular, and functional data on spine properties. Subsequent chapters will give abundant testimony to this new work.

Specific Information Processing. To illustrate the potential importance of spines for information processing in synaptic circuits, the paradigm of logic operations is useful. The diagram in Fig. 1.6C represents a dendritic tree with its distal branches covered by spines. Assume that there are patches of active membrane in the distal dendrites and

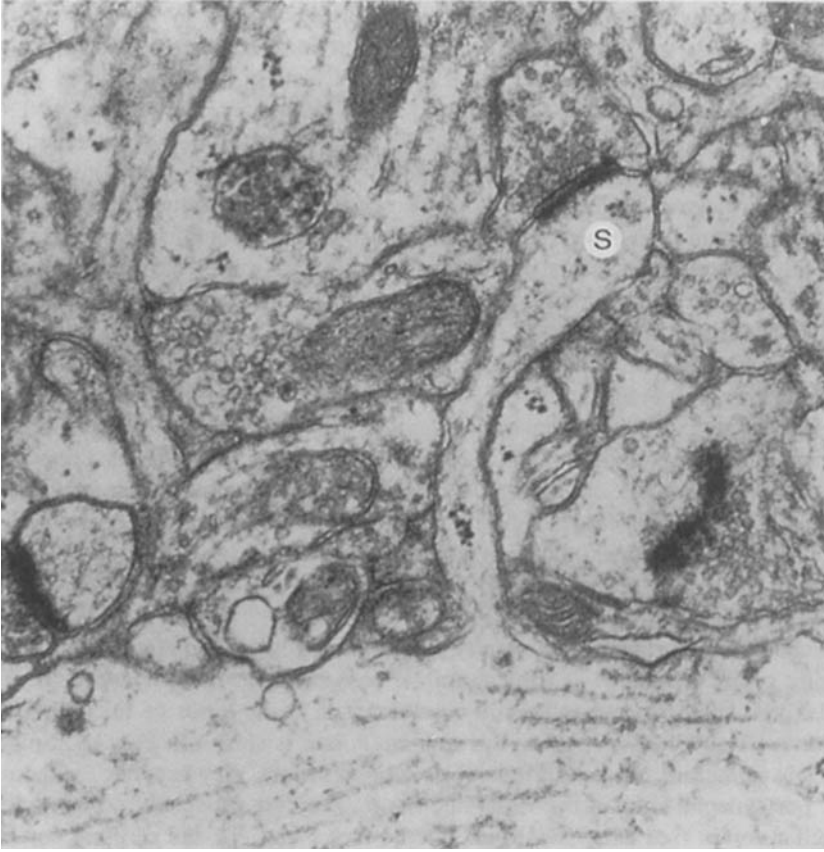


Fig. 1.7. The fine structure of a dendritic spine. This electron micrograph shows (bottom) a longitudinally cut dendrite from which arises a spine (s). The spine is approximately $1.5 \mu\text{m}$ in length and $0.1 \mu\text{m}$ at its narrowest width. At its head it receives a synapse, which has the round vesicles and asymmetrical density characteristic of Gray's type 1. In the neck and head are small clumps of ribosomes; in the dendrite are longitudinally cut microtubules. [From Feldman, 1984.]

that these give rise to a regenerative membrane event if there is sufficient depolarization by an excitatory synaptic response (Miller et al., 1985; Perkel and Perkel, 1985; Shepherd et al., 1985). One possible arrangement is that the impulse would fire if any one of several spines in a cluster should receive an excitatory input; this would be equivalent to an OR gate in the logic paradigm. Alternatively, two simultaneous inputs might be required; this would constitute an AND gate. Finally, one might have AND-NOT gates. Depending on the placement of the inhibition, the gate might be localized to an individual spine, or it might involve a dendritic branch containing a cluster of spines. These possibilities can all be traced in the diagram of Fig. 1.6C. Experimental studies suggest that these simple combinations of excitatory and inhibitory interactions do occur in natural activity, and computer simulations have shown that the logic operations arise readily out of these arrangements (Shepherd and Brayton, 1987; Shepherd et al., 1989).

These studies indicate that interactions in the smallest compartments of the nervous system—terminal dendritic branches and dendritic spines—may be capable of powerful and precise types of information processing. A further interest is that, through sequential activation of active sites along branches within the dendritic tree, synaptic responses initiated in the most distal parts of the tree nonetheless can exert precise control over the generation of impulses in the cell body and initial axonal segment.

In summary, the spine may be considered as a canonical unit for synaptic reception and in some cases synaptic output as well. It does not have a single function, however; rather, it appears to be a unit with multiple canonical functions (Shepherd, 1996). Some of those functions are summarized in Table 1.1. They are described in detail in subsequent chapters.

Associative Learning. In recent years considerable attention has been focused on the possibility that LTP of cortical neurons may underly learning and memory (reviewed in Nicoll and Malenka, 1995). This involves a long-term (hours to weeks) increase in synaptic efficiency in response to a presynaptic input volley. There is growing evidence of anatomical, biochemical, and physiological changes in dendritic spines of these cells during LTP. It has been shown, for example, that sufficient depolarization of a spine increases calcium ion (Ca^{2+}) conductance; the calcium ions are then available to bring about biochemical and structural changes in the spine that could function in the storage of information (see Fig. 1.2; these mechanisms are discussed in detail in Chap. 11). To the extent that these changes involve activation thresholds and nonlinear properties, they can be incorporated into the logic paradigm of spine interactions illustrated in Fig. 1.6C.

DENDRITIC BRANCH SUBUNITS

Functional compartments can be created in dendritic trees in various ways. The interactions between excitatory and inhibitory synaptic responses described earlier define relatively small functional subunits. By contrast, larger functional compartments are built into the branching structure of dendrites during development.

The mitral cell of the olfactory bulb provides a clear example of this level of organization. As shown in Fig. 1.8A (left), each mitral cell has a primary dendrite, divided into two subunits: a terminal tuft (T) and a primary dendritic shaft (1°). The function of the terminal tuft is to receive the sensory input through the olfactory nerves and process the responses through dendrodendritic interactions (see inset). The function of the primary dendritic shaft is to pass on this integrated response to the cell body. The third dendritic subunit in this cell consists of the secondary (2°) dendrites, which take part in dendrodendritic interactions with the granule cells and thereby control the output from the cell body (these have been described above; see Fig. 1.5B). Thus, the mitral cell dendritic tree is fractionated into three large subunits, each with a distinct function that is carried out semi-independently of the others (see Chap. 5 for further details).

Another example of dendritic compartmentalization is provided by the starburst amacrine cell of the retina. This cell (see Fig. 1.8B) has a widely radiating dendritic tree. Like olfactory granule cells, amacrine cells lack axons; the distal dendritic branches are the sites of synaptic output, whereas synaptic inputs are present both

Table 1.1. Functions That Have Been Ascribed to Spines

Site of synaptic connection
Receives synaptic input
Site of excitatory synaptic input
Site of inhibitory synaptic input (axon initial segment)
The spine only connects
Developmental synaptic target
Increases dendritic surface area
Makes synaptic connections tighter
Critical for development of synaptic connections
Matching of pre- and postsynaptic elements
Local dendritic input-output unit
Mediates prolonged synaptic output
Serves as dendrodendritic input-output unit
Passive synaptic potential modification
Spine: dendrite impedance matching
Synaptic potential attenuation
Constant current device
Large amplitude, rapid local responses (EPSP amplification)
Unit for synaptic plasticity
Spine stem modulates synaptic spread into dendrite
Spine stem involved in memory (EPSP amplitude modulation)
Site of LTP/LTD
Rapid mechanical changes: do spines twitch?
Active synaptic boosting unit
Site of local impulse amplification
Site of pseudosaltatory conduction
Information processing unit
Thresholding operational unit
Active logic gate: specific information processing in distal dendrites
Temporal processing unit
Acts as coincidence detector
Biochemical compartment
Absorbs nutrients
Provides for biochemical isolation related to single synapse
Site of local protein synthesis (polyribosomes)
Site of local Ca ²⁺ increase
Neuroprotection: isolates the dendrite from toxic Ca ²⁺ levels
Membrane surface shape properties
Target for electrophoretic membrane migration
Increases dendritic membrane capacitance
Shortest wire in the nervous system
Increases intersynaptic distance

For references, see text. EPSP, excitatory postsynaptic potential; LTP, long-term potentiation; LTD, long-term depression.

Source: Shepherd, 1996, with permission.

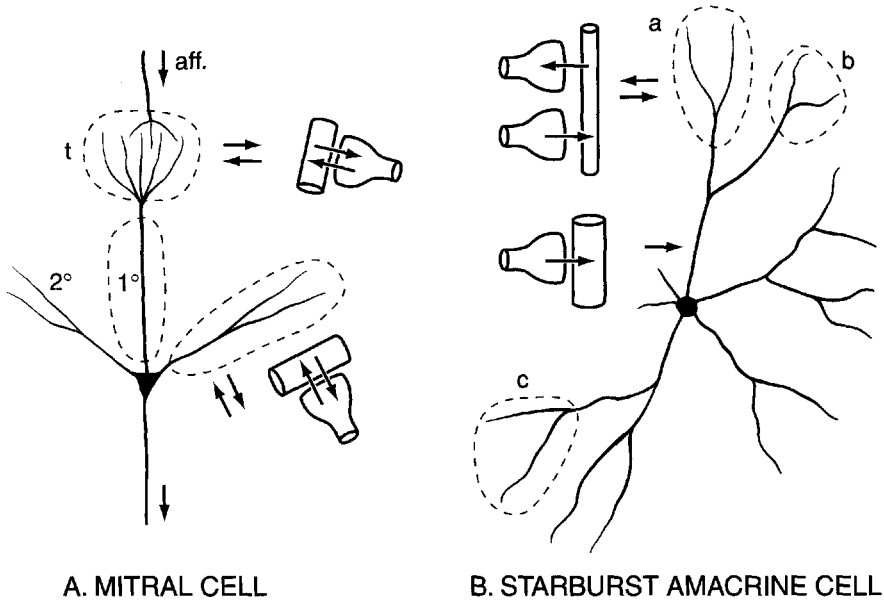


Fig. 1.8. Organization of subunits within dendritic trees. **A:** Mitral cell of the olfactory bulb, showing division of the dendritic tree into three main subunits. Abbreviations: aff., afferent; t, dendritic tuft; 1°, 2°, primary and secondary dendrites. Synaptic microcircuits are indicated in insets. **B:** Starburst amacrine cell in the retina, showing division of dendritic tree into functional subunits, as exemplified by *a-c*. Microcircuits are indicated in the insets. [**A** after Shepherd, 1979; **B** based in part on Koch, 1982.]

distally and proximally (see insets). Thus, each dendrite appears to function as a relatively independent input-output unit (Koch et al., 1982; Miller and Bloomfield, 1983). These dendritic subunits appear to be part of the circuits for computing the direction of a moving stimulus in the vertebrate retina (see later, and see Chap. 6 for further details).

This information can be combined with other information to begin to give an integrated understanding of this particular type of microcircuit. The starburst cells synthesize and release acetylcholine (ACh), providing excitatory input to direction-selective ganglion cells. Pharmacological evidence suggests that the most common inhibitory neurotransmitter, gamma-aminobutyric acid (GABA), provides the inhibitory input in the cell's null direction. Thus, an excitatory bipolar cell input to the amacrine cell could, in conjunction with GABAergic input from inhibitory bipolar or inhibitory cells, function as an AND-NOT gate, in analogy with the corresponding arrangement illustrated in Fig. 1.6B. Paradoxically, starburst amacrine cells also appear to synthesize, store, and release GABA (see Chap. 6). Until recently, such a colocalization of two fast-acting neurotransmitters was thought not to exist. Its presence obviously increases the opportunities for more complex synaptic interactions at the local level. We discuss retinal circuits for movement detection further later.

A BIOPHYSICS OF COMPUTATION

We have seen that a neuron generally contains several levels of organization within it, starting with the synapse as the basic functional unit. The different patterns of synapses, coupled with passive and active membrane properties and the geometry of the dendrites, provide a rich substrate for carrying out neuronal computations. The time scale of these computations varies greatly, from the fraction of a millisecond required for inhibition to suppress EPSPs in dendritic spines to many hundreds of milliseconds or seconds in the case of the slowly acting effects of neuropeptides on the electrical properties of neurons.

A description of the way that different types of membrane conductances, each with a characteristic distribution in the cell body and dendrite, combine to control the flow of information through the neuron is given in Chap. 2. Table 1.2 provides a brief compendium of some elementary synaptic circuits and biophysical mechanisms relevant for carrying out specific computations in the nervous system. In addition to their interest for neuroscience, these operations are of considerable potential relevance in computer science, where work on the “physics of computation” attempts to characterize the physical mechanisms that can be exploited to perform elementary information processing operations in artificial neural systems (Mead and Conway, 1980). These mechanisms constrain in turn the types of operations that can be exploited for computing. It has been suggested that a “biophysics of computation” is needed for understanding the roles of membranes, synapses, neurons, and synaptic circuits in information processing in biological systems, to bridge the gap between computational theories and neurobiological data (Koch, 1999; Shepherd, 1990). This knowledge will also enable us to understand the fundamental limitations in terms of noise, accuracy, and irreversibility on neuronal information processing.

The vast majority of neural network simulations—in particular, connectionist models—consider individual nerve cells to be single-node, linear integration devices. They thus neglect the effect of dendritic, synaptic, and intrinsic membrane properties on the function of individual cells. An important goal of the study of synaptic organization is therefore to identify the specific operations, such as those summarized in Table 1.2, that arise from these properties and incorporate them into more realistic network simulations of specific brain regions.

THE NEURON AS AN INTEGRATIVE UNIT

How are these different levels of dendritic functional units coordinated with the soma and initial segment of the axon to enable neurons to function as complex integrative units? The answer to this question requires an understanding of how synaptic activity in the dendrites is related to action potential generation in the axon hillock and initial axonal segment. These points are amplified in Chap. 2 and in subsequent chapters for specific neuronal types.

ACTION POTENTIAL INITIATION

The modern view of how a neuron generates an action potential arose in the 1950s, when the first intracellular recordings from spinal motoneurons showed that EPSPs in

Table 1.2. Some Neuronal Operations and Their Underlying Biophysical Mechanisms

Biophysical Mechanism	Neuronal Operation	Example of Computation	Time Scale
Action potential initiation	Threshold, one-bit analog-to-digital converter		0.5–5 msec
Action potentials in dendritic spines	Binary OR, AND, AND-NOT gate	^a	0.1–5 msec
Nonlinear interaction between excitatory and inhibitory synapses	Analog AND-NOT veto operation	Retinal directional selectivity ^b	2–20 msec
Spine–triadic synaptic circuit	Temporal differentiation high-pass filter	Contrast gain control in the LGN ^c	1–5 msec
Reciprocal synapses	Negative feedback	Lateral inhibition in olfactory bulb ^d	1–5 msec
Low-threshold calcium current (I_T)	Triggers oscillations	Gating of sensory information in thalamic cells ^e	5–15 Hz
NMDA receptor	AND-NOT gate	Associative LTP ^f	0.1–0.5 sec
Transient potassium current (I_A)	Temporal delay	Escape reflex circuit in Tritonia ^g	10–400 msec
Regulation of potassium currents (I_M , I_{AHP}) via neurotransmitter	Gain control	Spike frequency accommodation in sympathetic ganglion ^h and hippocampal pyramidal cells ^f	0.1–2 sec
Long-distance action of neurotransmitters	Routing and addressing of information	^j	1–100 sec

Note: The time scales are only approximate. LGN, lateral geniculate nucleus; LTP, long-term potentiation; NMDA, *N*-methyl-D-aspartate.

Sources: Includes the chapter in which the mechanism is discussed and the original reference.

^aChap. 1; see also Shepherd and Brayton, 1987.

^bChap. 1; see also Koch et al., 1982, 1983.

^cChap. 8; see also Koch, 1985.

^dChap. 5; see also Rall and Shepherd, 1968.

^eChaps. 2 and 8; see also Jahnsen and Llinás, 1984a,b.

^fChap. 2; Jahr and Stevens, 1986.

^gSee Getting, 1983.

^hChap. 3; see also Adams et al., 1986.

ⁱChap. 11; see also Madison and Nicoll, 1982.

^jSee Koch and Poggio, 1987.

the dendrites spread through the soma to initiate the action potential in the axon hillock-initial segment. These early studies are reviewed elsewhere (Shepherd, 2003b). The problem has been re-investigated thoroughly since the introduction of the multiple patch recording method by Stuart and Sakmann in 1993. The classical concept holds for low-to-medium levels of synaptic input, but there can be a shift to dendritic sites of action

potential initiation with medium to high levels of input. We discuss two examples in relation to Fig. 1.9.

Cortical Pyramidal Neurons. In pyramidal cells of the hippocampus and neocortex, the action potential in response to synaptic excitation in the dendrites arises in the initial axonal segment and propagates both down the axon and back into the soma-

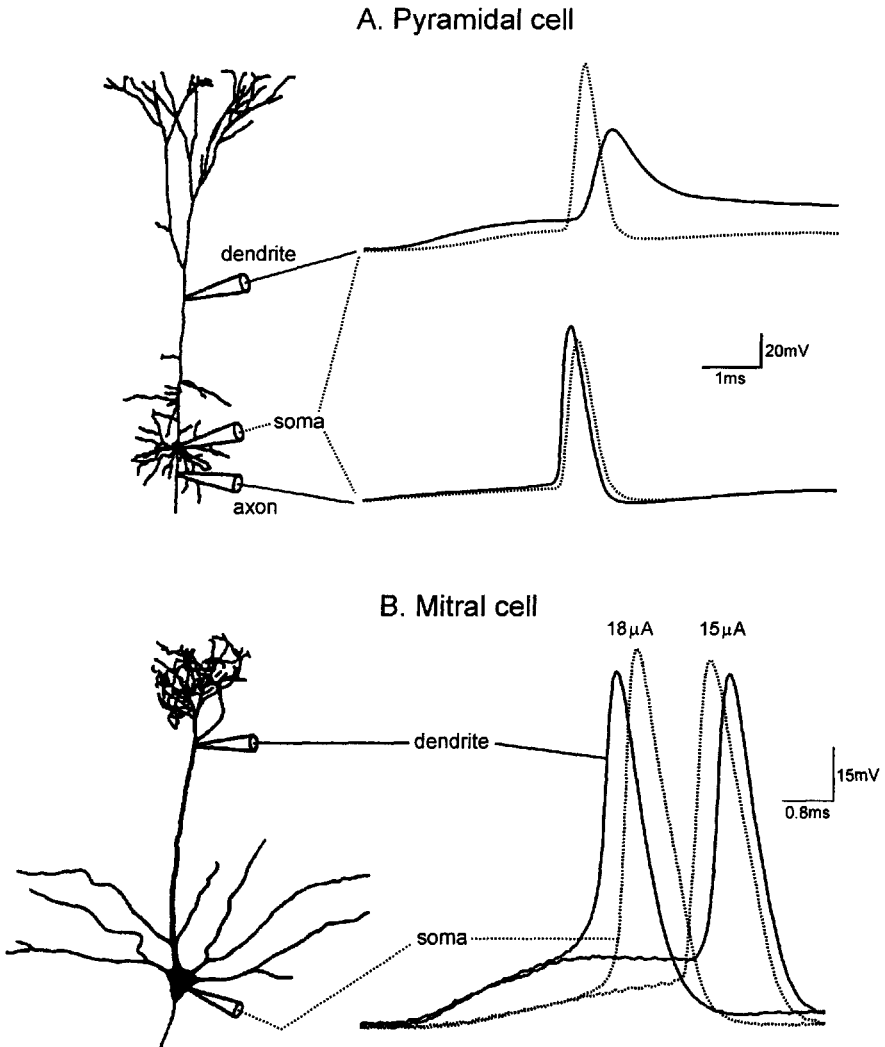


Fig. 1.9. Sites within the neuron for action potential initiation. **A:** Pyramidal cell in the rat cerebral cortex. [From Stuart et al., 1997.] **B:** Mitral cell in the rat olfactory bulb. [From Chen et al., 1997.] See text.

dendrites (Fig. 1.9A). Action potential initiation and forward propagation in the axon of course are supported by high densities of sodium (Na) channels in the initial segment and nodes of Ranvier, respectively. By contrast, the soma-dendrites have a low density of Na channels, which are not sufficient to generate action potentials directly in response to the relatively low amplitudes of dendritic EPSPs but can be activated by the large-amplitude depolarizations of backpropagating action potentials. In general, EPSPs in the distal dendrites by themselves give rise to slow low-amplitude regenerative “spikes” that forward propagate only under special conditions; this is explained further in Chaps. 11 and 12.

The back propagating action potentials are believed to have several possible roles in the integrative activity of cortical pyramidal neurons (reviewed in Stuart et al., 1999; Spruston et al., 2000). (1) They may function as “hot spots” to boost EPSPs in spreading from distal dendrites to the soma and axon hillock. (2) They may serve as sites of local integration and thresholding operations at dendritic branch points. (3) Their activity may contribute to synaptic plasticity and memory mechanisms. (4) Finally, they appear to boost the backspreading impulse so that it may send a more global retrograde signal to the entire dendritic tree that an impulse output has occurred. These and other possibilities are discussed in the appropriate chapters of this book; see especially Chap. 8 (cerebellum), Chap. 11 (hippocampus), and Chap. 12 (neocortex).

Mitral Cells. As described earlier, the sensory-evoked EPSP in the distal dendritic tuft spreads through the primary dendrite and soma to the axon hillock to initiate the action potential, which both propagates into the axon and spreads back into the soma and dendrites. Double-patch recordings have confirmed this classic model with weak synaptic excitation (Fig. 1.9B, 17 μA). However, with stronger excitation, the site of initiation shifts to the distal dendritic region, and a full action potential propagates through the primary dendrite to the soma and out the axon (Fig. 1.9B, 33 μA). An action potential in the soma has been shown experimentally under direct observation to propagate actively through the secondary dendrites. These experiments, together with computer simulations, are discussed further in Chap. 5.

As discussed earlier in this chapter, the backpropagating action potential in the secondary dendrites of mitral cells is believed to mediate several specific functions: recurrent inhibition of the activated mitral cell, lateral inhibition of neighboring mitral cells; and oscillatory firing of the mitral cell population. The functions associated with the backpropagating action potential in the primary dendrite, analogous to the apical dendrite of cortical pyramidal neurons, are less well understood. These questions are discussed further in Chap. 5.

The Concept of the Canonical Neuron. From these experiments on cortical pyramidal neurons and mitral cells, it is clear that the central neurons are much more complex integrative units than is usually realized. A key question that follows is: How much of this complexity is necessary to build realistic neuronal and network models in order to simulate brain functions?

The pyramidal neuron of the cerebral cortex is a prime example of this problem. Clearly, an understanding of the functional organization of this type of neuron is critical for an understanding of cognitive functions. Pyramidal neurons are the principal

neurons in all three basic types of cortex: olfactory (see Chap. 10), hippocampal (see Chap. 11), and neocortex (see Chap. 12). Although they vary in size and shape, one can identify a “canonical” pyramidal neuron in the same way that one identifies a gene family by certain shared characteristics. What we particularly need to know is: *What is the minimum architecture necessary to capture the integrative structure of the pyramidal neuron?*

An approach to this answer is illustrated by the reduced representation in Fig. 1.10, left. It consists of (1) division of the dendritic tree into apical and basal parts, (2) dendritic spines on both apical and basal dendrites, and (3) different excitatory and inhibitory synaptic inputs to different levels of the apical and basal dendritic trees. A final feature (4) (not shown) is a long axon that gives off axon collaterals that makes synapses on targets within the neighborhood of the cell and at different distances from the cell.

This canonical cell can be converted into a *canonical model* by representing it as a series of compartments, as shown in Fig. 1.10, right. Each compartment can be seen to form a local subunit that can play a critical role in information processing within the neuron by virtue of its unique combination of synaptic inputs, passive properties, active properties, and relation to other subunits. Thus, the spines (A1, A2) represent principal sites of excitatory inputs; their interactions may generate *specific local information processing* and *local activity-dependent changes*, as discussed earlier. The activity spreading in dendritic branches (B, C) is summed at a branch point (D), which acts as a *local decision point* for passing activity toward the soma. Whether this ac-

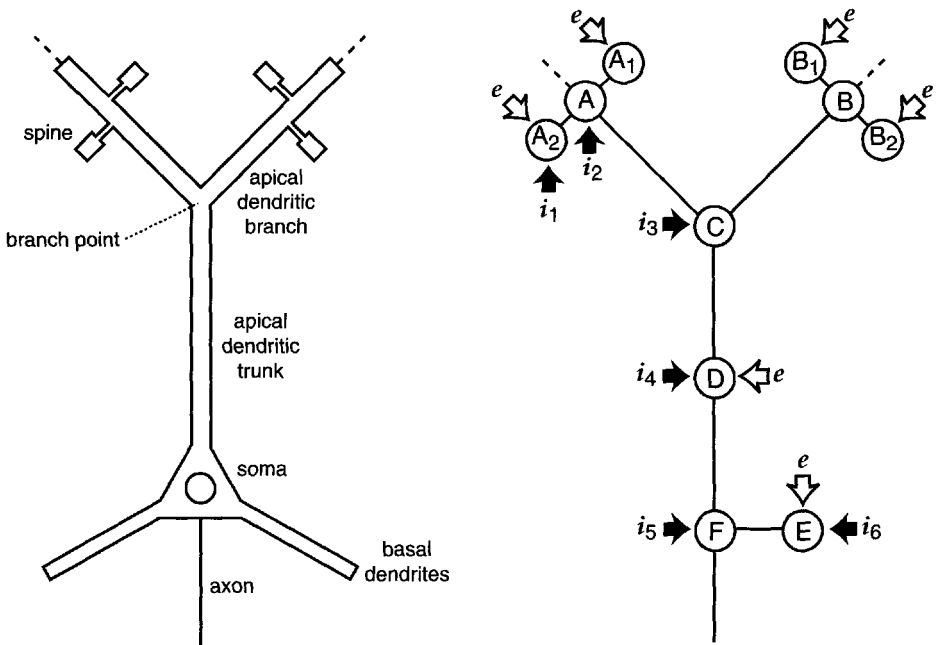


Fig. 1.10. **Left:** Canonical representation of a cortical pyramidal neuron. **Right:** Further abstraction of a cortical pyramidal neuron as a branching system of integrative units. See text. [Modified from Shepherd, 1994.]

tivity spreads effectively to the soma depends on *modulatory gating* by both excitatory and inhibitory inputs along the apical shaft (D). There is a further stage of summation between the activities spreading to the soma from the apical (D) and basal (E) dendrites. Finally, there are direct inputs to the soma, many of them inhibitory, which provide for *global integration and modulation* of the neuronal output, in contrast to the local activities taking place within each dendritic branch and field. When the impulse is initiated in the axon hillock, in addition to propagating along the axon, it back-propagates into the dendrites, thus sending a global signal that an output has occurred to the local subunits, modulating the excitability of the dendrites in relation to further synaptic inputs and perhaps triggering dendritic outputs onto those input terminals.

In summary, a logical parsing of the canonical structure indicates a sequence of functional operations, proceeding from the local to the global, which is likely to underlie the roles of pyramidal neurons in cortical functions. The diagram indicates the minimal structure necessary to capture the essential functional organization of the pyramidal neuron. Just as the classical Bohr atom gave a working representation of the essentials of atomic structure, so does the canonical neuron give a working representation of the essentials of neuronal structure. The canonical neuron becomes the basis for construction of canonical circuits (see later).

LOCAL CIRCUITS

No matter how complicated a single neuron may be, it cannot play a role in the processing of information without interacting with other neurons. The circuits that mediate interactions between neurons within a region are called *local*, or *intrinsic*, circuits. They include all of the levels of organization we have considered previously, plus the longer-distance connections made by axons and axon collaterals within a given brain region. In turning our attention to these more extensive circuits, we continue to distinguish between simple excitatory and inhibitory synaptic actions. Although the types of neurons and their circuits appear to be distinctive for each region, we will see that the operations they carry out can be grouped into several basic types.

EXCITATORY OPERATIONS

Excitatory local circuits can be grouped into two main types: feedforward excitation in input pathways and feedback excitation between output cells. We will discuss these operations with particular reference to the organization of the cerebral cortex.

In many regions of the nervous system, the input fibers (arising from output cells in other regions) are excitatory. Thus, nearly all of the long-range projections to, from, and within the cerebral cortex are excitatory, as are the projections to and from the specific thalamic nuclei. The rules of connectivity for the targets of these excitatory inputs vary, however, in different regions.

We begin by noting that in many regions there are inputs that connect directly to the output neurons of that region. The target may be the distal or proximal dendrites of a cortical pyramidal neurons (Fig. 1.10). Other cells in which synaptic excitation of distal dendrites is important are mitral cells (see Chap. 5) and cerebellar Purkinje cells (see Chap. 7). The incoming fibers converge and diverge according to the canonical arrangements described in Fig. 1.4.

Feedforward Excitation. A common pattern of excitatory input is that input fibers connect to excitatory interneurons, which provide circuits for feedforward excitation. In the cerebellar cortex, for example, mossy fibers make excitatory synapses onto granule cells, which then make excitatory connections onto the Purkinje cell dendrites. The advantage of this arrangement is that it gives the opportunity for additional patterns of convergence and divergence (Fig. 1.11A). These complex patterns through granule cells are in parallel with the direct access of excitatory climbing fiber inputs to the Purkinje cells (see Chap. 7).

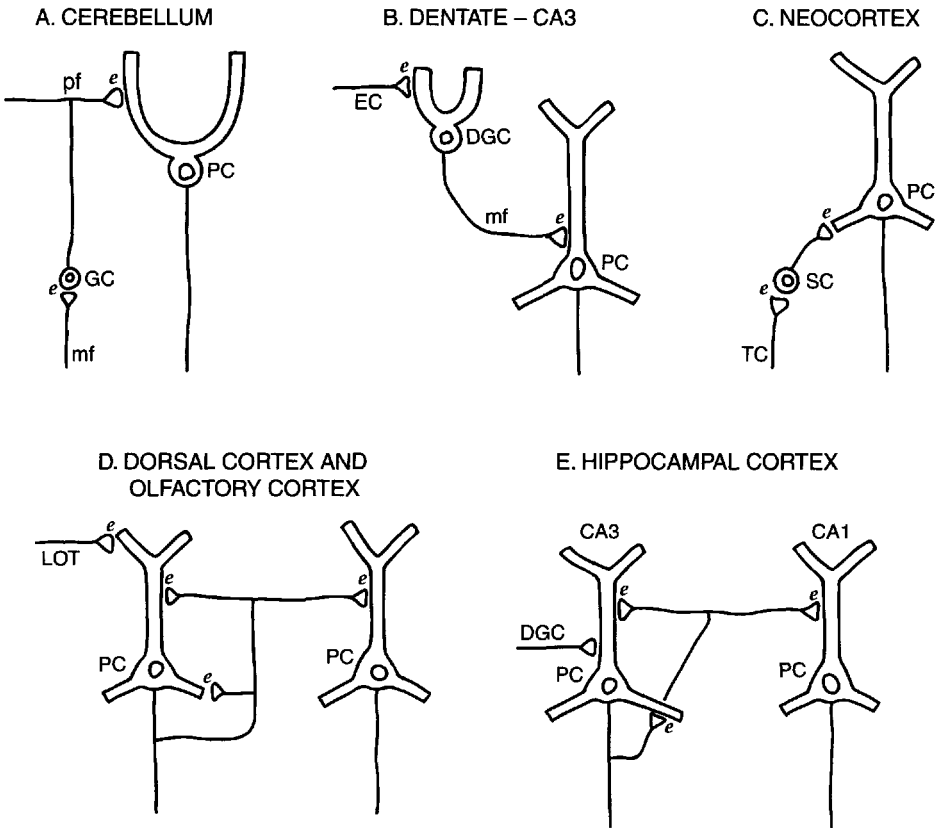


Fig. 1.11. Excitatory local circuits in different brain regions. **A–C:** Excitatory feedforward circuits. **A:** Cerebellum. Mossy fibers (mf) have excitatory (e) connections onto granule cells (GC) whose parallel fibers (pf) excite Purkinje cells (PC). **B:** Dentate-CA3 region of hippocampus. Perforant pathway axons from entorhinal cortex (EC) excite dentate granule cells (DGC) whose mossy fibers (mf) excite pyramidal cells (PC). **C:** Neocortex. Thalamocortical cells (TC) excite stellate cells (SC) whose axons excite pyramidal cells (PC). **D–E:** Mixed excitatory feedforward and feedback connections. **D:** Dorsal cortex of reptiles and olfactory cortex of mammals. Lateral olfactory tract (LOT) axons excite pyramidal cells (PC) whose axon collaterals feedback excitation onto the same and neighboring pyramidal cells. **E:** Hippocampal complex. Mossy fibers (see **B**) from dentate granule cells (DGC) excite CA3 pyramidal cells (PC) whose axon collaterals feedback excitation onto the same PCs and feedforward excitation on CA1 PCs. See text and relevant chapters.

In the hippocampus, there is a feedforward excitatory pathway from the dentate granule cells through relatively short mossy fibers to the CA3 hippocampal pyramidal cells (Fig. 1.11B; see Chap. 11).

In the cerebral cortex, excitatory interneurons in input pathways are exemplified by the spiny stellate cells of laminar IV, found in sensory areas and association areas of granular cortex. As shown in Fig. 1.11C, this provides for an intracortical feedforward excitatory relay from the afferents onto the output neurons. As in the cerebellum, this can be regarded as a staging step in the processing of afferent information and presenting it to the cortex, by convergence–divergence patterns of connections (cf. Fig. 1.4). In addition to such serial excitatory sequences, there are parallel input pathways, including direct afferent inputs to the pyramidal neurons, which contribute to the abstraction of receptive field properties. Inhibitory interactions also contribute very importantly to these properties (see later).

In summary, feedforward excitation is built into local circuits by expansion of canonical arrangements of convergent, divergent, and multiple synaptic connections. The resulting control of different inputs in exciting their target neurons gives a range of safety factors for inputs in activating their targets. This varies from high safety factors through multiple synapses onto the same target (climbing fibers onto cerebellar Purkinje cells; see Chap. 7) to low safety factors through massive divergence–convergence (cerebellar parallel fibers (see Chap. 7), Ia inputs to motoneurons (see Chap. 3), striatal inputs (see Chap. 9), etc.).

Feedback Excitation. Within a region, there are mechanisms that provide for re-excitation of activated neurons. The simplest type of re-excitation is implemented by the action of a released excitatory neurotransmitter onto the releasing process. This action on autoreceptors (Fig. 1.2, 9a) is found in many synaptic circuits. It has the advantage of being very localized in its action.

An important type is excitatory feedback through synaptic connections from an output neuron onto itself and/or neighboring output neurons. This has the advantage of extending the possibilities for more complex information processing. Also called *recurrent excitation*, or simply *re-excitation*, it is rarely fed back through an excitatory interneuron. An obvious reason is that this would create a loop for amplifying positive feedback that would lead to powerful and widespread excessive excitation and seizure activity. Thus feedback excitation is usually mediated only by direct connections of the dendrites and/or recurrent collaterals onto other principal neurons.

Clear examples of re-excitation through axon collaterals are found in the vertebrate cerebral cortex. The simplest case is olfactory cortex, where the pyramidal neurons give off recurrent collaterals that feed back excitation onto the dendrites of nearby pyramidal neurons (Fig. 1.11D; see Chap. 10). Similar evidence for direct feedback excitation has been obtained in reptilian dorsal general cortex (Fig. 1.11D), which is regarded as a model for the evolutionary precursor of mammalian neocortex (Kriegstein and Connors, 1986), indicating that this has been a fundamental property in the evolution of the cerebral cortex. Another example is the Schaffer collateral system of the hippocampus, in which recurrent collaterals from pyramidal neurons of CA3 make excitatory connections onto the dendrites of pyramidal neurons in CA3 and CA1 (see Fig. 1.11E; see Chap. 11). In the neocortex itself, pyramidal neurons have well-

developed recurrent axon collateral systems, and there has long been evidence for excitatory actions attributable to them. In addition to this intraregional excitatory feedback, there is a massive interregional feedback system originating among the pyramidal cells in the lower layers of cortex which projects back to those specific thalamic nuclei that provide the input to the cortex (see later and Chap. 12). Reciprocal excitatory connections between cortical areas are described in Chap. 12.

The significance of the local feedback connections is that activated pyramidal neurons can respond to an initial excitatory input with subsequent waves of re-excitation. Through this means, a subset of activated pyramidal neurons imposes a subsequent pattern of activation onto an overlapping subset of pyramidal neurons in the same region. It is believed that this is a powerful mechanism for achieving combinatorial patterns of activation reflecting both the pattern of the input signal and the experience-dependent patterns stored within the distributed connections of the local circuits of the region in question (see Haberly, 1985; Granger et al., 1988; Wilson and Bower, 1988; Douglas et al., 1995).

In summary, feedback excitatory connections constitute a canonical circuit element that is fundamental to combinatorial information processing within and between cortical regions.

INHIBITORY OPERATIONS

As is already clear, inhibitory circuits play large roles in determining the types of operations generated within a region. This was supported by early studies showing that if synaptically mediated inhibition is blocked pharmacologically, cells lose most of their distinguishing features; an example is the loss of orientation and directional sensitivity of visual cortical neurons (see Chap. 12).

A wide range of types of inhibitory actions in local neural circuits is suggested by a veritable explosion of different types of inhibitory neurons shown by recent experimental studies. For example, over two dozen types of inhibitory interneurons have been identified in the hippocampus on the basis of dendritic morphology and axonal connection patterns (see Chap. 11). Similarly, the retina is well known for the dozens of different types of amacrine cells, most of which are presumably inhibitory in their actions (see Chap. 6).

How do we see order in this diversity? The answer lies in the canonical approach, with a focus not so much on types of neurons but rather on types of local circuits. The basis for this is the expectation that there is a limited family of different types of inhibitory operations implemented by the circuit connections of different types of neurons in different brain regions.

We examine here four examples of inhibitory local circuits that perform distinct canonical functions. Our aim, first, is to show how inhibitory circuits can give rise to specific functions. A second aim is to consider these circuits within a comparative framework. This will allow us to see that each circuit employs an inhibitory neuron in a slightly different way. This enables different operations to be generated by relatively fine tuning of the connections of a generic inhibitory interneuron, in a manner analogous to the way that G protein-coupled receptors, all with the same basic seven-transmembrane domain architecture, are fine tuned by specific residue substitutions to respond to different neurotransmitter ligands.

Rhythmic Generation. Rhythmic activity is fundamental to the activity of the nervous system. It can be generated by two main mechanisms: intrinsic membrane properties and synaptic circuits.

Intrinsic membrane properties were first found in pacemaker neurons in central pattern generator circuits controlling breathing, walking, and other highly stereotyped behaviors in invertebrates. Since the early 1980s, research carried out on brain slices has shown that many types of neurons in the vertebrate central nervous system possess complex and highly nonlinear ionic conductances that endow these cells with the ability to respond to inputs with oscillations at various frequencies (Llinas, 1988). Thus, intrinsic oscillatory neurons may be far more common in the central nervous system than previously thought, enhancing the computational power of the system. An introduction to these ionic conductances is provided in Chap. 2, and examples are described throughout this book for virtually every brain region.

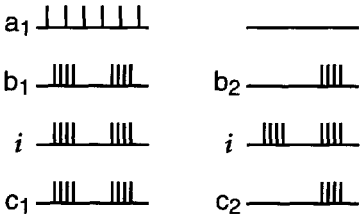
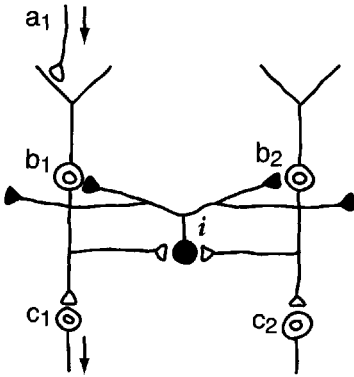
Rhythmic activity can also be a property of *local circuit interactions*. A common model, shown in Fig. 1.12A, consists of output neurons (b) connected through axon collaterals to inhibitory neurons (i), which in turn connect back into the output neurons. When an input (a) activates the output neurons, they begin to generate impulses, which leads to activation of the interneurons. This activation leads to feedback inhibition of the output neurons, which now can no longer respond to the input and thus also deprives the interneurons of their source of activation; they are, in a sense, presynaptically inhibited by themselves. Both populations, therefore, are silent until the IPSPs in the output neurons wear off and the cycle is ready to be repeated. The degree of synchronization of a region will obviously depend on the extensiveness of the connections. The circuit could thus be laid down during development by a simple rule for the interneurons to make extensive random connections on the output cell populations.

Rhythmic activity can also be generated by dendrodendritic microcircuits, as discussed above (see Fig. 1.5B and Chap. 5). Although the neural elements are different, the principles underlying the interactions are similar. This illustrates an important concept, that *similar functions can be mediated by different neural substrates*. Conversely, *similar substrates can mediate different functions*, by specific adaptations of general mechanisms.

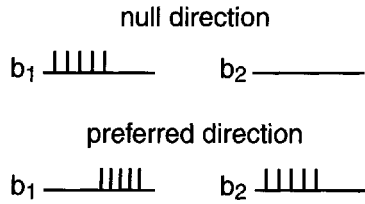
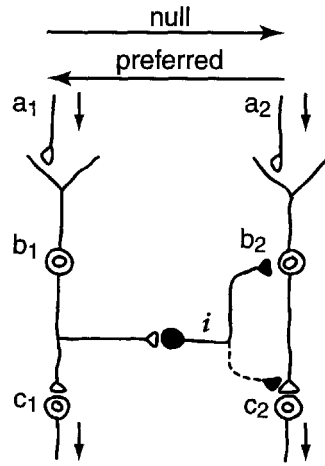
In summary, three canonical mechanisms (membrane channels, circuits involving axon collaterals, and circuits involving dendritic interactions) can generate the same canonical operation: oscillatory activity. Conversely, each of these canonical mechanisms can potentially be refined to generate different oscillatory frequencies. This illustrates a recurrent theme in synaptic organization—that the same substrate can generate different functions and that different substrates can generate the same function. These are neural examples of general phenomena in biological organization. They reflect the ability of organisms to respond to adaptive pressures in multiple ways that ensure the survival of the organism.

Directional Selectivity. A second type of local circuit in which an inhibitory interneuron plays an essential role is in direction selectivity. The best known model is the retina, where ganglion cells in most vertebrate species show selective activation by stimuli moving in one direction. The proposed model is shown schematically in Fig. 1.12B. The essential element is an inhibitory interneuron whose connections are made in one

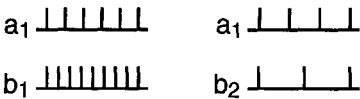
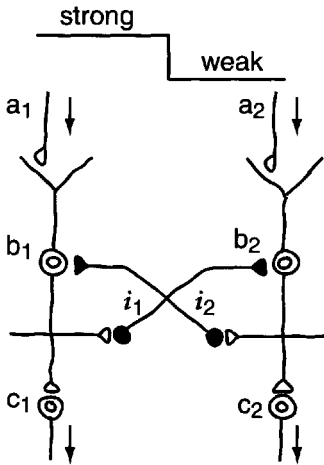
A. RHYTHM GENERATION



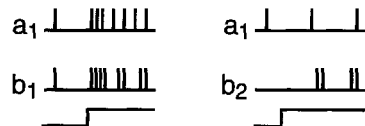
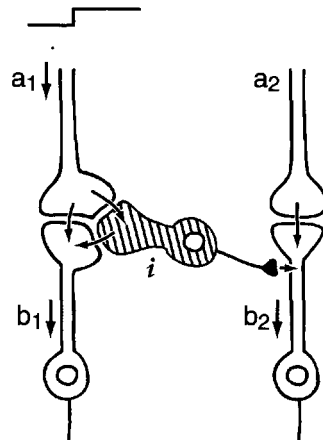
B. DIRECTION SELECTIVITY



C. SPATIAL CONTRAST



D. TEMPORAL CONTRAST



direction, *opposite* to the preferred direction. This means that stimuli moving in that direction (called the “null” direction) activate the inhibitory connections in that direction, so that cells farther along cannot respond. In the opposite, preferred, direction, by contrast, the cells are free to respond.

Several types of circuit connections might mediate this selectivity. In the retina, the most likely involves connections onto the dendrites and somata of ganglion cells (dashed line in Fig. 1.12B). The starburst amacrine cell has been proposed to play this role. The organization of this cell was discussed earlier (see Fig. 1.8B). These cells synthesize, store, and release the two most common fast-acting excitatory (ACh) and inhibitory (GABA) neurotransmitters, suggesting that one and the same cell could potentially act as both an excitatory and an inhibitory circuit element.

Directionally selective cells are also found in visual cortex, where this property is mediated by a combination of excitatory inputs and inhibitory interneurons (Ferster and Koch, 1987), whose connections are mainly onto cell bodies and proximal dendrites (solid line in Fig. 1.12E). This site is less selective but might be easier to target during development. Blocking the action of the inhibitory cells by an appropriate chemical substance leads to the almost total loss of direction selectivity (Sillito et al., 1980).

In summary, we again see that the same canonical function—directional selectivity—can be implemented by circuits with the same operational characteristics but different neuronal substrates.

Spatial Contrast. These concepts are further exemplified by the role of inhibitory circuits in mediating enhancement of spatial contrast, a common property of receptive field organization in many sensory systems. This property is illustrated in Fig. 1.12C, where there is strong stimulation of input (a_1) and all elements to the left in the diagram (not shown) and weaker stimulation of input (a_2) and elements lying to the right. The responses of b_1 and b_2 would start out being proportional; however, the stronger inhibition by b_1 and i_1 suppresses b_2 more than the suppression of b_1 by b_2 and i_2 , thereby enhancing the difference in firing rates of b_1 and b_2 . This effect falls off the farther away the elements are from the border, thereby enhancing the contrast between strong and weak stimulation at the border.

This is the basis for the classic description of Mach bands in the visual system, as first demonstrated in the *Limulus* eye (see Ratliff, 1965). It has turned out that the circuit for mediating this effect in *Limulus* appears to involve dendrodendritic connections without intervention of an inhibitory interneuron (Fahrenbach, 1985). In mammalian sensory systems, however, it characteristically involves inhibitory interneurons. An example is indicated in Fig. 1.12C, in which spatial contrast is mediated by a canon-

←
 Fig. 1.12. Intrinsic inhibitory circuits are organized to mediate different types of functional operations within a given region. **A:** Rhythm generation (a_1 , input; b_1 , b_2 , relay neurons; c_1 , c_2 , targets of relay neurons; i , inhibitory interneuron). Impulse firing patterns are shown below. **B:** Direction selectivity. Arrows indicate movement of a stimulus in the null and the preferred direction. **C:** Spatial contrast. Stimulation consists of strong and weak areas of stimulation, with a sharp edge between them. **D:** Temporal contrast. Feedforward inhibition synchronizes driving input from a_1 to b_1 , and entrains neighboring pathway a_2 to b_2 . See text.

ical circuit involving axon collaterals and inhibitory interneurons. It can also be mediated by the canonical dendrodendritic pathway through an interneuron, as described in Fig. 1.5.

In summary, the spatial organization of receptive fields can be implemented by several types of canonical circuits; the resulting receptive fields can subserve processing of information in different modalities.

Temporal Contrast. Just as there is enhancement of spatial contrast between the activities of populations of cells, so is there enhancement of temporal contrast between successive activity states. This can also be mediated by intrinsic membrane properties or circuit properties. Membrane mechanisms are described in Chap. 2. Circuit mechanisms commonly involve the sequential action of synaptic excitation followed by inhibition. An example is illustrated in Fig. 1.12D as it might apply to the thalamic triad, in which excitation of an output neuron is followed by feedforward inhibition. As shown, this converts a step increase in activity in the input to a brief spike burst in the output. As for spatial contrast enhancement, the nervous system cares more about changes in stimulus conditions than in the steady state conditions. In summary, local inhibitory circuits are critical elements in extraction of changes in activity in both the spatial and temporal domains.

REGIONAL CANONICAL CIRCUITS

How can one represent the different canonical excitatory and inhibitory local circuits, each with its underlying levels of canonical functional units, in a way that is not merely a catalog but gives insight into the functions of each region? A useful way to do this is by means of a *basic (canonical) regional circuit*, defined as a representation of the main patterns of synaptic connections and interactions most characteristic of a given region. Such a representation is useful in several ways: for identifying the principles of circuit organization of a region, for better understanding of relations between synaptic actions and dendritic properties, and for identifying the minimum of essential properties that must be included if a network simulation is to have validity as an accurate representation of that region.

RETINA AND OLFACTORY BULB

An advantage of thinking in this way about synaptic organization in terms of regional canonical circuits is that it provides a logical basis for comparing the functional organization of different brain regions. The olfactory bulb and retina provide useful examples. The similarities of their neural organization were already recognized by Cajal (1911). Their basic circuits were formulated independently by subsequent studies at the cellular level (Dowling, 1968; Shepherd, 1963, 1974) and are illustrated in Fig. 1.13. On the left is shown a basic circuit of the retina; on the right, the olfactory bulb. Despite the fact that these regions process entirely different sensory modalities, the basic circuits are similar in outline and in several details. In each case, there are parallel vertical pathways for straight-through transmission of information. In addition, there are horizontal connections, arranged in two main levels, for processing of information by lateral interactions. Within this framework are further similarities, such as recipro-

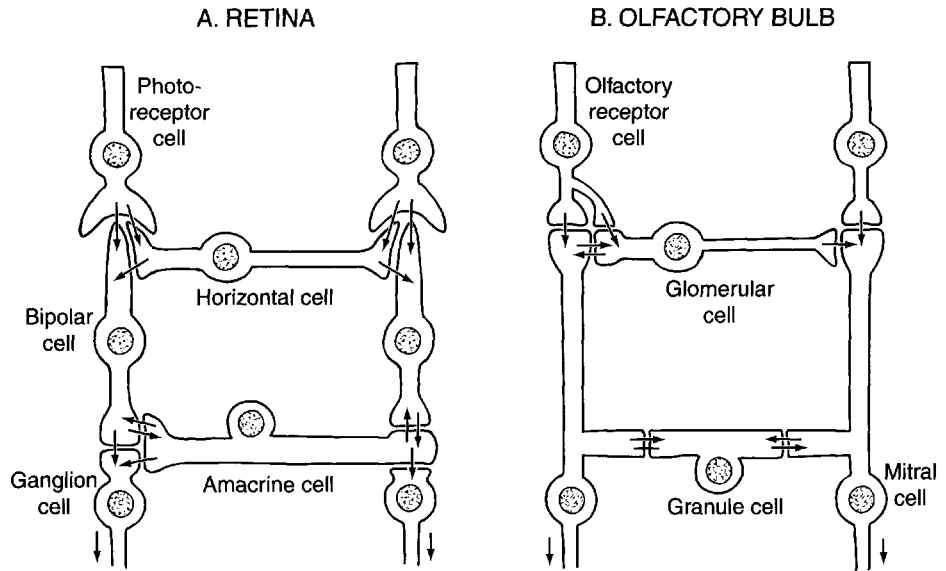


Fig. 1.13. Comparison between basic (canonical) circuits for the retina (A) and olfactory bulb (B). [From Shepherd, 1988.]

cal synapses and interneurons that lack axons. All of these features are described in detail in Chaps. 5 and 6.

The purpose of such a comparison is not, of course, to suggest that the two regions are identical; rather, it is to be able to identify more clearly the principles that are common across regions, so that one can better analyze and understand the adaptations that make each region unique. Among the common principles are the notions that in each region there are three stages of information processing: an initial stage of *input processing*, a second stage of *intrinsic operations* within the synaptic circuits of the region, and a final stage of *output control*. These three levels can be seen most clearly in the basic circuits of tightly organized and highly laminar regions like the olfactory bulb and retina (see Fig. 1.12) but also are evident as we shall see in more spread-out regions like the cerebral cortex.

The regional canonical circuit thus provides a useful starting point for categorizing the organization of a region. In addition, it provides a rational framework for comparing the organization of disparate regions, a crucial step toward developing comprehensive theories of brain organization.

An objection to the idea of a regional basic circuit is that it does not adequately represent the rich diversity of neural elements and synaptic connections that can be found in most brain regions. However, the problem with this diversity is that it can obscure the crucial issue, of determining which properties are essential for which operations. This issue is critical, not only for experimentalists attempting to analyze these operations but also for theorists who seek to incorporate these essential properties into network simulations. The basic regional circuit can be expanded with subcircuits for specific functions as needed.

CEREBRAL CORTEX

The cerebral cortex presents perhaps the greatest challenge in elucidating principles of organization. How far can the canonical approach give insight into these principles?

Comparisons between the local circuits in the different types of cortex, as discussed earlier, give a different perspective on cortical organization from that derived from traditional views based on cortical cytoarchitectonics. From this new perspective, what is striking is the local circuit elements that are common to the different types.

We illustrate this comparative approach by considering three examples of basic circuits that have been proposed to account for experimental findings in cortical studies. First is dorsal turtle cortex. This relatively simple cortex in the reptilian forebrain is regarded as the evolutionary precursor of mammalian neocortex. A combined morphological and electrophysiological study (Kriegstein and Connors, 1986) led to the basic circuit shown in Fig. 1.14A. In this circuit, the afferent input (1, a, b) excites both pyramidal cells (P) and inhibitory interneurons (I). The I neuron feeds forward inhibition (2) to the P cells. The P cells feed back excitation (3) onto themselves and onto the I cells (4), which also receive other inhibitory modulation (5). The P cells send the output through their axons (6). The incorporation of many of the basic elements of excitatory and inhibitory local circuits that we have discussed earlier is obvious in the diagram.

An elaboration on this basic pattern to a sensory area of mammalian cortex is shown in Fig. 1.14B. This reflects the fact that mammalian cortex is characterized by six layers, involving superficial and deep populations of pyramidal cells (P 1, P 2) and stellate cells (S) in layer 4. In this cortex, afferent inputs (AFFd) excite pyramidal (P) cells (1,2) as well as inhibitory cells (i 1) (1). In addition, there is feedforward excitation (AFF3) through stellate cells (S), as described earlier (Fig. 1.11). The excited P cells have recurrent axon collaterals (rac) that recurrently and laterally excite the P cells (rac 1) as well as inhibitory cells (i 2) that provide for feedback and lateral inhibition. The balance of excitation and inhibition controls the output of the P cells (EFF 1,2). Note how the properties of the canonical pyramidal neuron depicted in Fig. 1.9 are incorporated into the basic circuit that contains it.

Close comparison of this circuit with dorsal cortex gives clues to the critical circuits added in the evolution from reptiles to mammals; these obviously include the extra layer of deep pyramidal cells (P 2), and the feedforward excitation through stellate cells (S). Other circuits can be added to the basic circuits to focus on more specific differences.

A third example is the canonical cortical circuit suggested by the studies of Douglas et al. (1989) (Fig. 1.14C). In their model the superficial population of excitatory pyramidal cells is represented by P2 and 3 (stellate cells in layer 4 (4) are also included) and deep cells in layers P5 and 6, and inhibitory cells by GABA cells. The excitatory and inhibitory interactions shown by their study are indicated by the diagram. The authors suggest that this set of connections and interactions may reflect a basic "canonical" circuit that can apply to all neocortex. The evidence for this is fully discussed in Chap. 12.

In order to compare this canonical circuit with the basic circuits of A and B, it is rearranged in the diagram to the right in (C) to conform more closely to the conventions used in the other diagrams. It can be seen that this brings out more clearly the basic similarities between the three basic circuits: the excitatory inputs to the P cells and inhibitory interneurons; the feedback and lateral excitatory actions of the P cell recur-

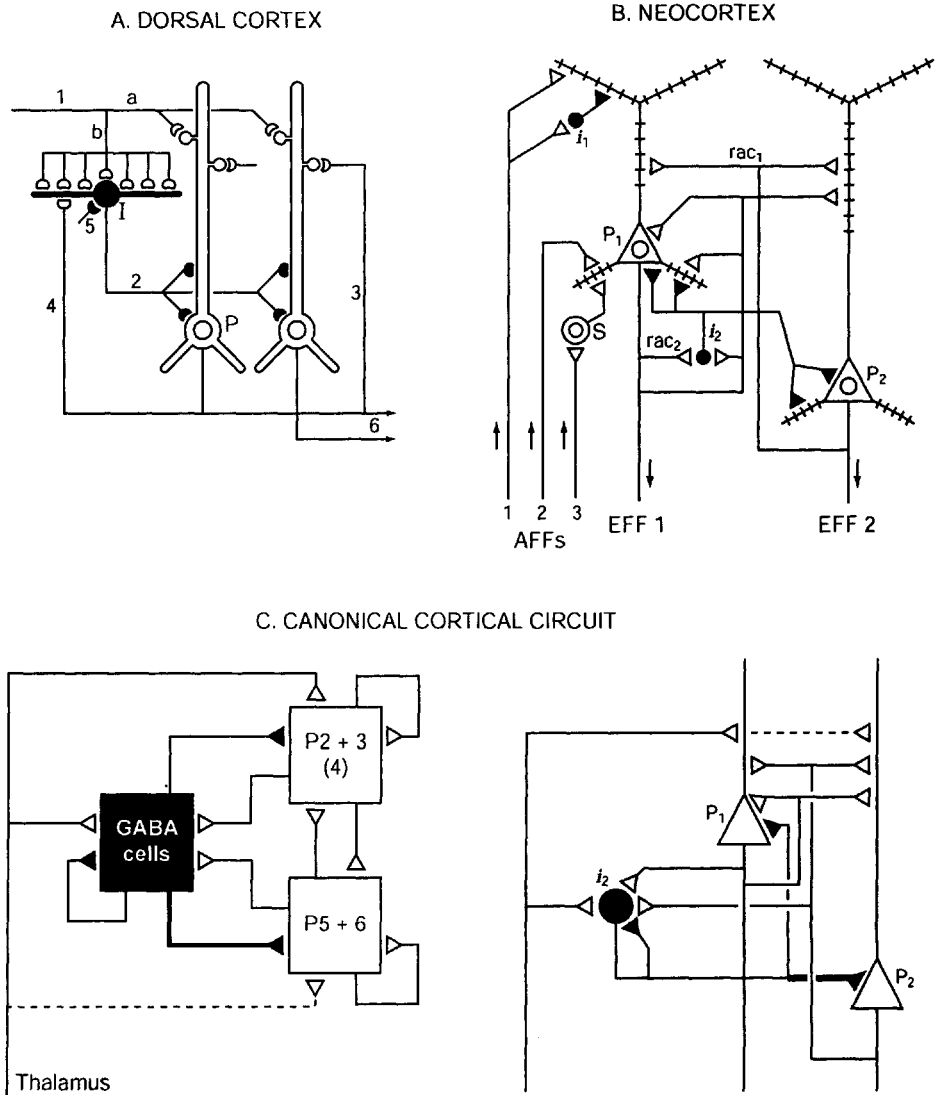


Fig. 1.14. Basic circuits to show principles of organization of local circuits in cerebral cortex. **A:** Reptilian three-layered dorsal cortex [Modified from Kriegstein and Connors, 1986]. **B:** Mammalian neocortex (sensory areas) [Modified from Shepherd, 1988.] **C:** Canonical cortical circuit [Left, modified from Douglas et al. (1989); right, re-drawn for comparison with **B.**] For labels and explanation, see text.

rent axon collaterals, and their excitation of the interneurons to provide feedback and lateral inhibition.

Building on the concept of the canonical neuron, we can thus designate a basic “cortical canonical circuit,” which may be defined as the minimum architecture necessary for capturing the most essential cortical input-output operations.

The sets of local circuits depicted in Fig. 1.14 can be considered a superfamily unique to the vertebrate cerebral cortex, which is adapted and elaborated in the different types of cortex and the different cortical regions in order to carry out the set of operations characteristic of each (Shepherd, 1974; 1988). There is current debate about whether there is one basic cortical circuit or a diversity of circuits (Nelson, 2002). A full exposition of these basic circuits and their roles in different cortical functions is given in Chaps. 10–12.

In conclusion, the canonical circuit approach provides a useful first step for characterizing the essential organization of a brain region. As discussed above, for closer examination of a given region, one begins with the canonical circuit and introduces the particular adaptations and elaborations that underlie its unique properties. The canonical circuit is thus a flexible tool, not rigidly defined; the purpose is to represent the minimum of elements and connections that will capture the essence of the functional operations of a region. It provides the experimentalist and theorist a conceptual framework for integrating their analyses to give a more accurate representation and simulation of the functional operations of each region. Finally, it provides the reader of this book with a key to understanding and comparing the principles of synaptic organization across different brain regions.

MEMBRANE PROPERTIES AND NEUROTRANSMITTER ACTIONS

DAVID A. McCORMICK

Information processing depends not only on the anatomical substrates of synaptic circuits but also on the electrophysiological properties of neurons and neuronal elements and on how these properties are altered and tuned by the plethora of neuroactive substances impinging upon them. Even if two neurons in different regions of the nervous system possess identical morphological features, they may respond to the same synaptic input in very different manners due to each cell's intrinsic properties. Understanding synaptic organization and function in different regions of the nervous system therefore requires an understanding of the electrophysiological and pharmacological properties of each of the constituent neuronal elements.

The electrophysiological behavior of a neuron is determined by the presence and distribution of different ionic currents in that cell and by the ability of various neurotransmitters either to increase or decrease the amplitude, or to modify the properties, of these currents. The present chapter gives a general overview of neuronal currents known to exist in brain cells, how they may be modulated by neurotransmitters, and how the interplay between the two can result in complicated patterns of activity in synaptic circuits. For a more detailed introduction to the biophysical mechanisms of ionic currents in neurons, the reader is referred to Huguenard and McCormick (1994), Johnston and Wu (1995), and Hille (2001).

MEMBRANES AND IONIC CURRENTS

Neurons, like cells elsewhere in the body, are bounded by a lipid bilayer membrane that contains a large number of protein macromolecules. The lipid bilayer allows the composition of the medium on each side to be very different. Of particular importance for electrical signaling is the fact that certain key ions have different concentrations on the inside and outside of the neuron (Fig. 2.1). On the outside, Na^+ , Ca^{2+} , and Cl^- exist in much higher concentrations; by contrast, K^+ ions and membrane impermeant anions (denoted as A^-) are concentrated on the inside.

Protein macromolecules in the membrane subserve a variety of functions. Those that underlie electrical signaling are large molecules that form ionic channels (see

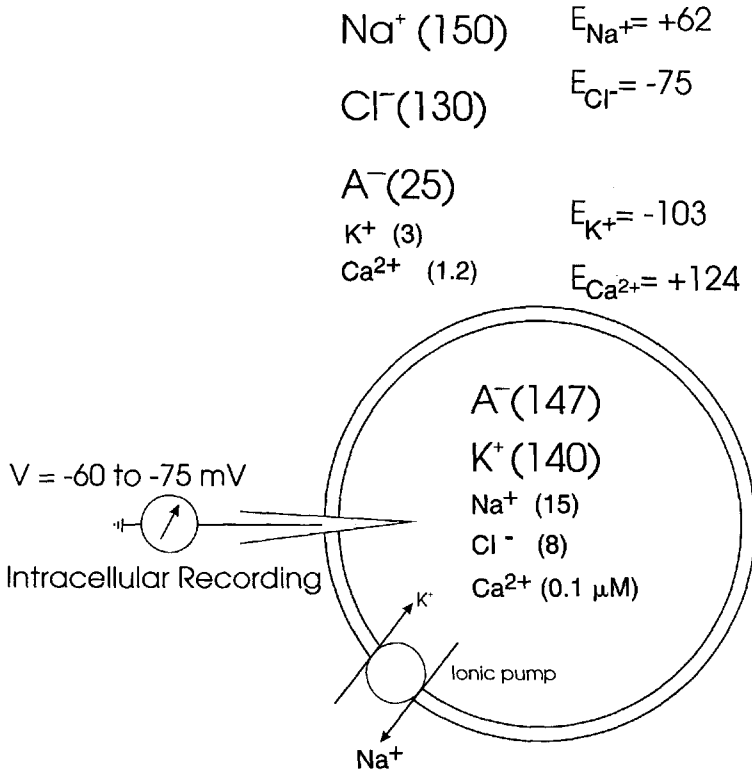


Fig. 2.1. Distribution of ions across neuronal membranes and their equilibrium potentials. At rest the cell membrane is permeable to K^+ , Na^+ , and Cl^- and exhibits a voltage difference (inside versus outside) of approximately -60 to -75 mV, as seen with an intracellular recording electrode.

Ionic Channels). Membrane channels possess a number of important features, including the presence of a water-filled pore through which ions flow; selectivity for one or more types of ions (e.g., K^+ , Na^+ , Cl^- , Ca^{2+}); sensitivity to (i.e., opened or closed by) the electrical potential across the membrane or to a neurotransmitter substance, or to both; and the ability to be modified by a variety of intracellular biochemical signals.

Because ions are unequally distributed across the membrane, they tend to diffuse down their concentration gradient through ionic channels. This tendency arises from the fact that the intrinsic movements of ions in a solution tend to disperse them from regions of higher to lower concentration. However, because ions are electrically charged molecules, their movements are dictated not only by concentration gradients but also by the voltage difference across the membrane. For example, if the membrane of a neuron were made permeable to K^+ ions by opening K^+ channels, the higher concentration of these ions on the inside versus the outside of the cell would make it more probable that K^+ ions would leave, rather than enter, the cell. As K^+ ions exit the cell they carry positive charge with them, thereby leaving behind a net negative charge (made up in part of impermeant anions; see Fig. 2.1). However, this negative charge

(expressed as a *voltage difference*) on the inside versus the outside of the cell will attract the K^+ ions and slow down the rate at which they leave. At some point, the tendency for K^+ to flow out of the cell will be offset exactly by the attraction of the negative charge left inside the cell. The voltage difference at which this occurs is known as the *equilibrium potential* (denoted as E) and is different for each ionic species (Fig. 2.2; see Fig. 2.1). It is shown later in this and other chapters that the equilibrium potential is important for determining the effect of activation (synaptic or intrinsic) of an ionic current.

The flow of ions across the membrane obeys physical laws in a consistent and reproducible manner. Considering the basic forces involved in determining the passive distribution of ions (e.g., thermodynamic and electrical), it becomes clear that four of the important factors influencing the equilibrium potential are as follows: (1) the concentration of the ion inside and outside the cell, (2) the temperature of the solution, (3) the valence of the ion, and (4) the amount of work associated with separating a given quantity of charge. The German physical chemist Walter Nernst derived an equa-

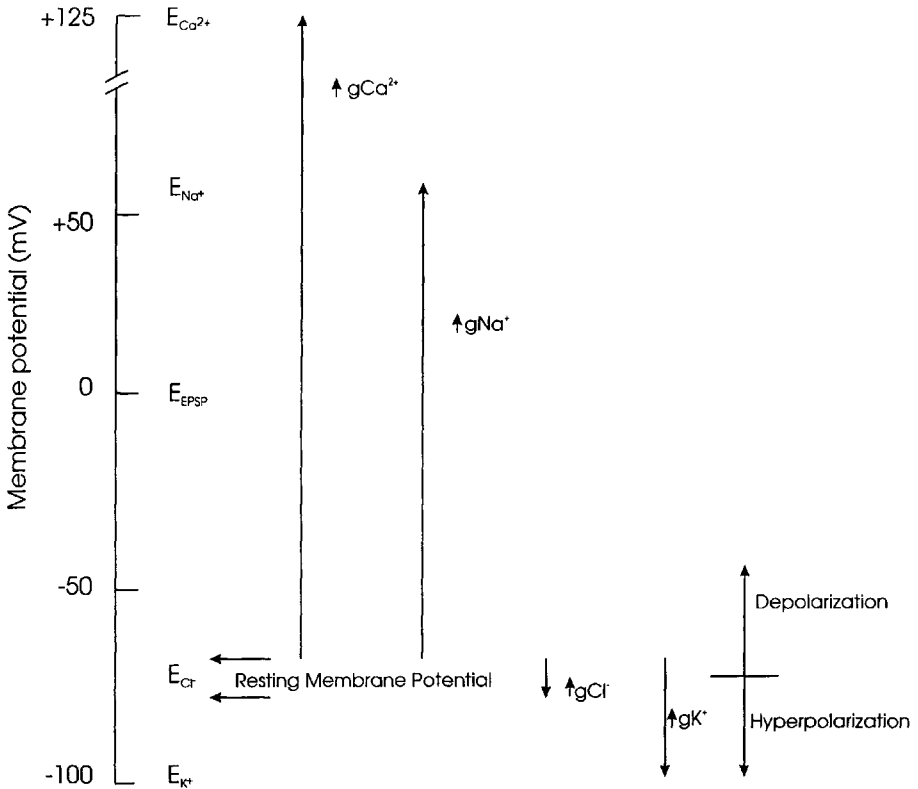


Fig. 2.2. Effect of increasing membrane conductance (denoted as g) to Ca^{2+} , Na^+ , Cl^- , or K^+ . Increases in gCa^{2+} or gNa^+ bring the membrane potential toward more positive values (depolarization), whereas increases in gCl^- or gK^+ bring it toward more negative values (hyperpolarization).

tion in 1888 that related such factors, allowing for the calculation of the equilibrium potential (Nernst, 1888).

$$E_{\text{ion}} = RT/zF \cdot \ln [\text{Ion}]_o/[\text{Ion}]_i \quad (2.1)$$

where E_{ion} is the membrane potential at which the ionic species under consideration (e.g., K^+ , Na^+ , Cl^-) is at equilibrium, R is the gas constant (8.315 Joules/Kelvin · mole), T is the temperature in degrees Kelvin ($T_{\text{Kelvin}} = 273.16 + T_{\text{Celsius}}$), F is Faraday's constant (96,485 Coulombs/mole), Z is the valence of the ion (typically ± 1 or 2), and $[\text{Ion}]_o$ and $[\text{Ion}]_i$ are the concentrations of the ion in question on the outside and inside of the cell, respectively. Substituting the appropriate numbers as well as converting from natural log (\ln) to log-base-10 (\log_{10}) results in the following equation at room temperature (20° C) for a monovalent, positively charged ion (cation):

$$E_{\text{ion}} = 58.2 \log_{10} [\text{Ion}]_o/[\text{Ion}]_i \quad (2.2)$$

and at a body temperature of 37° C, the Nernst equation is

$$E_{\text{ion}} = 61.5 \log_{10} [\text{Ion}]_o/[\text{Ion}]_i \quad (2.3)$$

As an illustrative example, consider the passive distribution of K^+ ions in the squid giant axon as studied by Alan Hodgkin and Andrew Huxley (1952a–d). The squid giant axon is very large, approximately 1 mm in diameter, as its name implies, and is used by the squid for the generation of escape reflexes (because large axons conduct quickly). The large size and robust nature of the squid giant axon allowed Hodgkin and Huxley in the 1940s and 1950s to perform many different experiments, such as intracellular recording, that could not be performed at that time on mammalian neurons.

The inside of the squid giant axon has a concentration of K^+ of about 400 mM, while the outside of the axon is exposed to about 20 mM K^+ . K^+ ions, being in much higher abundance on the inside versus the outside of this axon, will tend to flow down their concentration gradient, taking positive charge with them as they do. The membrane potential at which the tendency for K^+ to flow down its concentration gradient will be exactly offset by the attraction for K^+ to enter the cell due to the negative charge on the inside of the cell at a room temperature of 20° C is as follows:

$$E_{\text{K}} = 58.2 \log_{10}(20/400) = -76 \text{ mV} \quad (2.4)$$

Therefore, at a membrane potential of -76 mV, there will be no net tendency for K^+ ions to flow either into or out of the axon.

The concentrations of K^+ experienced by mammalian neurons and glial cells are considerably different from that of the squid giant axon. In the mammalian brain the extracellular concentration of K^+ is approximately 3 mM, whereas the intracellular concentration is approximately 140 mM (see Fig. 2.1). Therefore, at a body temperature of 37° C, the equilibrium potential for K^+ in mammalian neurons is as follows:

$$E_{\text{K}} = 61.5 \log_{10}(3.1/140) = -103 \text{ mV} \quad (2.5)$$

At membrane potentials positive to -103 mV in mammalian cells, K^+ ions will tend to flow out of the cell, down their concentration gradient (see Fig. 2.2). Therefore, at these membrane potentials, increasing the ability of K^+ ions to flow across the membrane, in other words increasing the *conductance* of the membrane to K^+ (abbreviated as gK), will result in the membrane potential becoming more negative, or *hyperpolarizing*, owing to the exiting of positively charged ions from the inside of the cell.

The ease with which an ion diffuses across the membrane is expressed as the ion's *permeability*. Increasing the permeability of the membrane to a particular ionic species (e.g., by increasing the probability that membrane channels conducting that ion will be open) increases the electrical conductance and will bring the membrane potential of the cell closer to the equilibrium potential of that ion. This is true whether the membrane potential becomes more negative (i.e., hyperpolarized) or more positive (i.e., depolarized) toward the equilibrium potential. Of course, if the membrane potential is already at the equilibrium potential, then its value will not change in response to a further increase in conductance. In this circumstance, the most significant change will be that the ability of other currents to move the membrane potential away from its present potential will be diminished. If the membrane were only slightly permeable to Cl^- ions, then increases in membrane conductance to other ionic species could easily move the membrane potential away from E_{Cl} . However, if the permeability to Cl^- was greatly increased, the membrane potential would be effectively "clamped" close to E_{Cl} . In this circumstance, movements of other ions into or out of the cell would now be largely offset by compensating movements of Cl^- ions, thereby keeping the membrane potential close to E_{Cl} .

Consider the following example. Assume that the membrane is highly permeable to Cl^- and that the membrane potential is at E_{Cl} . If the membrane is now also made permeable to sodium, Na^+ ions will enter the cell. However, as the positive ions enter the cell and move the membrane potential away from E_{Cl} , Cl^- ions will also move into the cell, bringing the cell back toward E_{Cl} and negating some of the depolarizing influence of the increased permeability to Na^+ . If the permeability to Cl^- is much higher than that to Na^+ , then the membrane potential will stay close to E_{Cl} . As we shall see, this type of "shunting" of the membrane potential near E_{Cl} is important in the actions of some types of inhibitory neurotransmitters.

RESTING MEMBRANE POTENTIAL

When there is no synaptic input, or when the neuron is "at rest," the cellular membrane is dominated by its permeability to K^+ . This permeability to K^+ ions draws the membrane potential of the cell toward approximately -103 mV (see Figs. 2.1 and 2.2). If the membrane were permeable only to K^+ , then the membrane potential would be equal to E_K . However, even at rest, neuronal membranes are also permeable to other ions, Na^+ and Cl^- in particular, so the membrane potential is pulled toward E_{Na} ($+62$ mV) and E_{Cl} (-75 mV). The point at which the movements of these various ions come into equilibrium such that there is no *net* current (denoted as I) flow across the membrane corresponds to the resting membrane potential and is typically between -60 to -80 mV (see Fig. 2.2).

The weighted mixture of all of the ionic currents flowing across the membrane determines the resting membrane potential, as well as the membrane potential during nearly all types of activity. This principle allows the calculation of the membrane potential at any given point in time using the *Goldman-Hodgkin-Katz* (GHK) equation based upon the concentration gradient and membrane permeability of each ion (Goldman, 1943; Hodgkin and Katz, 1949).

$$V_m = \frac{RT}{F} \cdot \ln \left[\frac{P_K[K^+]_o + P_{Na}[Na^+]_o + P_{Cl}[Cl^-]_i}{P_K[K^+]_i + P_{Na}[Na^+]_i + P_{Cl}[Cl^-]_o} \right] \quad (2.6)$$

A consequence of this relationship of ionic currents and membrane potential is that, in general, the membrane potential of the cell will be closest to the equilibrium potential of the ion to which the membrane is most permeable (e.g., P_K , P_{Cl} , or P_{Na}). In this equation, each of the three different ions, K^+ , Na^+ , and Cl^- , influences the membrane potential. The relative contribution of each is determined by the concentration differences across the membrane and the relative permeability (P_K , P_{Na} , and P_{Cl}) of the membrane to each different type of ion. If the membrane were permeable to only one ion, for example, K^+ , then the GHK equation reduces to the Nernst equation. Experiments on the squid giant axon at resting membrane potential reveal permeability ratios of the following:

$$P_K:P_{Na}:P_{Cl} = 1:0.04:0.45 \quad (2.7)$$

In other words, the membrane of the squid giant axon at rest is most permeable to K^+ ions, followed by Cl^- , followed by a small permeability to Na^+ . (Chloride appears to contribute considerably less to the determination of the resting potential of mammalian neurons.) These results indicate that the resting membrane potential is determined by the resting permeability of the membrane to K^+ , Na^+ , and Cl^- and that this resting membrane potential may be, at least in theory, anywhere between E_K (e.g., -76 mV) and E_{Na} ($+55$ mV). Substituting the values for the concentrations of Na^+ , K^+ , and Cl^- as well as their relative permeabilities into the GHK equation at a temperature of 20° C reveals the following:

$$V_m = 58.2 \log_{10} \left[\frac{1 \cdot 20 + 0.04 \cdot 440 + 0.45 \cdot 40}{1 \cdot 400 + 0.04 \cdot 50 + 0.45 \cdot 560} \right] = -62 \text{ mV} \quad (2.8)$$

This suggests that the squid giant axon should have a resting membrane potential of -62 mV. In fact, the resting membrane potential may be a few millivolts hyperpolarized to this value through the operation of the electrogenic Na^+ - K^+ pump (see later).

In the mammalian nervous system, the exact value of the resting membrane potential varies between different types of neurons and is very important in determining the manner in which a particular neuron behaves both spontaneously as well as in response to extrinsic inputs. For example, cortical pyramidal cells (see Chap. 12) have a resting membrane potential in the absence of synaptic input of approximately -75 mV, thalamic relay neurons (see Chap. 8) are at approximately -65 to -55 mV at rest in the waking animal, and retinal photoreceptor cells have a resting membrane potential of

approximately -40 mV (see Chap. 6). Some types of neurons do not have a true “resting” membrane potential in that they are spontaneously active even during the lack of all synaptic input (see later).

ACTION POTENTIAL

Rapid signaling in nerve cells is accomplished by brief changes in the membrane potential. Traditionally, the most characteristic type of signal has been considered to be the *action potential*, or *nerve impulse* (also referred to as a “spike”). Local action potentials in patches of dendritic membrane can also serve as boosters for the spread of synaptic potentials to the soma (as discussed in Chap. 1).

As with the resting membrane potential, the basic changes in membrane ionic permeability that underlie the action potential were first well characterized by Hodgkin and Huxley (1952a–d) using the squid giant axon preparation. The large size of the squid giant axon allowed Hodgkin and Huxley to thread a wire into the axon, giving them the ability to control accurately the membrane potential through a procedure known as *voltage clamp*. Currents typically display both a voltage dependence and characteristic kinetics of turning on and off. In the voltage-clamp procedure, the amount of current injected into the cell is adjusted so that the voltage across the membrane is kept constant (i.e., the voltage is “clamped”). This technique allows one to observe directly the transmembrane currents responsible for the electrical behavior of the cell and, importantly, to separate the voltage and time (*kinetics*) dependence of the underlying currents. The isolation of the squid giant axon *in vitro* meant that Hodgkin and Huxley could also control the ionic composition of the medium on both the outside and the inside of the axon. These experiments revealed that the rapid upswing of the action potential is mediated by a regenerative increase in a transient Na^+ current, denoted as $I_{\text{Na,t}}$ (Fig. 2.3). Because $I_{\text{Na,t}}$ is rapidly activated by depolarization and is itself a depolarizing influence, it forms a positive feedback loop in the unclamped axon, as shown diagrammatically in Fig. 2.3A. Depolarization of the membrane causes a rapid increase in the number of Na^+ channels that are open, thereby allowing more Na^+ ions to enter the cell, resulting in even more depolarization of that portion of membrane, increased entry of Na^+ , and so on.

Membrane currents that change their amplitude in response to changes in the voltage across the membrane in a “nonlinear” manner, such as $I_{\text{Na,t}}$, are referred to as *voltage sensitive*, whereas the ionic channels that underlie these currents are said to be *voltage gated*. The depolarization caused by entry of Na^+ ions into the cell spreads to neighboring membrane via *electrotonic* current flow. The depolarization of one patch of membrane will also depolarize neighboring patches of membrane. The subsequent activation of the same regenerative mechanisms at these sites underlies the propagation of the action potential along the axon.

Repolarization of the action potential is very important not only because of the obvious need to be able to generate more than one action potential during the life of the cell but also in determining the way the cell responds to repetitive inputs. Two processes are essential for the repolarization of the action potential in most neurons: the rapid inactivation of $I_{\text{Na,t}}$ and the activation of K^+ currents. The rate of *inactivation* (termed *inactivation kinetics*) of $I_{\text{Na,t}}$ is only slightly slower than the rate of activation.

THE ACTION POTENTIAL

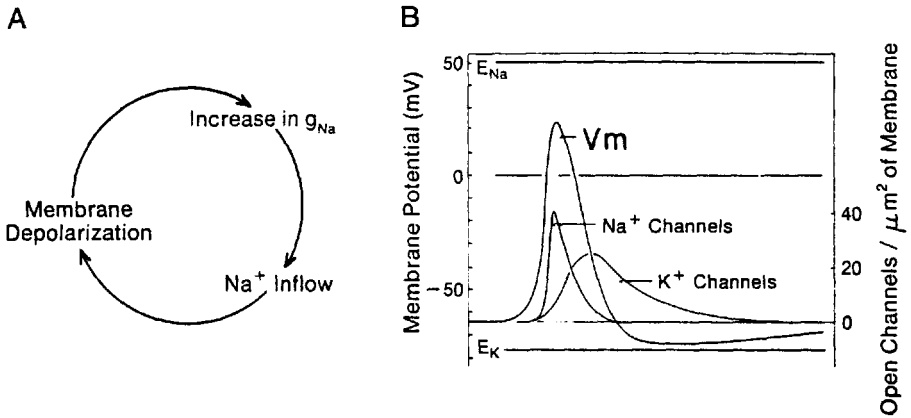


Fig. 2.3. **A:** Regenerative relation between membrane depolarization, increase in membrane conductance to Na^+ (g_{Na}), and Na^+ current that underlies the action potential. **B:** Reconstruction of changes in ionic conductance underlying the action potential in squid giant axon; scale for the membrane potential (V_m) is shown on the left. The equilibrium potentials for Na^+ (E_{Na}) and K^+ (E_K) are also indicated on the left. Changes in Na^+ and K^+ ionic conductances are scaled on the *right* in terms of calculated open channels per square micrometer of membrane. [Adapted from Hodgkin and Huxley, 1952; and Hille, 1984.]

Even during the rising phase of the action potential, the available Na^+ current becomes less and less due to inactivation. Simultaneously, but with a slower time course, a K^+ current, known as I_K , is activated by the membrane depolarization associated with the action potential, allowing K^+ to leave the cell. These two currents, flowing through their respective ionic channels, are indicated in Fig. 2.3B. At some point, the hyperpolarizing influence of K^+ leaving overcomes the depolarizing influence of Na^+ entering, thereby terminating the action potential and repolarizing the membrane.

The triggering of an action potential occurs when the membrane potential of the neuron is depolarized sufficiently to reach action potential *threshold*. In many cells, this potential is approximately -50 to -55 mV. Action potential threshold is the membrane potential at which the regenerative activation of depolarizing currents (e.g., $I_{Na,t}$) is strong enough to overcome the inactivation of these currents as well as the activation of others that hyperpolarize the neuron back toward rest. At threshold, the generation of an action potential is an "all-or-nothing" event. If threshold is surpassed, an action potential is generated and the information is transferred down the axon to cause the release of neurotransmitter at synapses. If firing threshold is not reached by a depolarizing event, an action potential is not produced and the event is not relayed to other cells. However, as we shall see, the depolarization can still serve to modify the probability that other postsynaptic potentials in the neuron may cause the cell to discharge.

Since 1952, it has become apparent that $I_{Na,t}$ is the dominant current in the generation of action potentials in axons, axon hillocks, and cell bodies. However, in somatic

and dendritic regions, voltage-gated Ca^{2+} currents are also involved, as documented later here and in ensuing chapters (e.g., see Fig. 2.5B, C, and E). In mammalian somata and dendrites, in contrast to squid giant axon, repolarization of action potentials is accomplished not only by I_K but also by a complicated array of different K^+ currents (see sections on I_K , I_C , and I_A later).

IONIC CHANNELS

The generation of ionic currents useful for the propagation of action potentials requires the movement of significant numbers of ions across the membrane in a relatively short period of time. The rapid rate of ionic flow occurring during the generation of an action potential is far too high to be achieved via an active transport mechanism. Rather it results from the opening of ion channels. Although the existence of ionic channels in the membrane has been postulated for decades, their properties and structure have only recently become known in detail. The development by Erwin Neher and Bert Sakmann of the patch-clamp technique, in which a small patch of membrane containing a single or small number of ionic channels is drawn up into a blunt microelectrode, allowed for the minuscule (10^{-9} Amps or picoamps) current flowing through single channels to be recorded in intact biological membranes for the first time (Neher and Sakmann, 1976, 1992; Hamill et al., 1981; Sakmann, 1992). In addition, the rapid advances made in molecular biology regarding the isolation, cloning, and sequencing of the proteins making up ionic channels have revealed much about their primary structure. Especially exciting is the recent crystallization of K^+ and Cl^- channels in some of their different conformations, allowing their tertiary structure to be detailed with X-ray diffraction (Jiang et al., 2002a,b). The powerful combination of electrophysiological and molecular techniques have yielded valuable insights into the structure-function relationships of ionic channels (see Catterall, 1995, 2000a,b; Yellen, 2002).

Voltage-sensitive ionic channels appear to have several shared features. First, they are large proteins that span the 6–8 nm of the plasma membrane and are typically made up of subunits. Second, through protein folding, they form a cylinder surrounding a central water-filled pore that permits the passage of only certain classes of ions between the inside and outside of the cell. The selection of which ions are allowed to pass through each different type of ionic channel is based upon the size, charge, and degree of hydration of the different ions involved (see Hille, 2001). Finally, voltage-gated ion channels possess one or more *gates*, or voltage-sensing regions, within the ionic pore, and the flow of ions through the channels is regulated by these gates.

IONIC PUMPS

The quantity of ions that enter and exit the cell during electrical activity is actually very small in comparison with the number of ions present. For example, the generation of a single action potential in a hypothetical spherical cell 25 μm in diameter should result in an increase of intracellular concentration of Na^+ of only approximately 6 μM (from approximately 15 mM to 15.006 mM)! This means that the action potential is an electrical event that is generated by a change in the distribution of charge

across the membrane and not by a marked change in intracellular or extracellular concentration of Na^+ or K^+ .

However, even these small exchanges of ions across the membrane, coupled with a constant "leak" at rest, can eventually destroy the correct ionic distribution and thereby render a neuron nonfunctional. To compensate for this "rundown," neuronal membranes possess specialized protein macromolecules known as *ionic pumps*. Ionic pumps maintain the correct distribution of all of the ions involved in electrical activity by actively transporting these ions "upstream" against their concentration gradient. The energy required to perform this task is sometimes obtained through the hydrolysis of ATP (adenosine triphosphate). The ionic pump that has been best characterized is the "electrogenic sodium-potassium" pump (see Thomas, 1972; Skou, 1988). This ionic pump carries approximately three Na^+ ions out for every two K^+ ions it brings in, thereby generating an electric current (see Fig. 2.1). The exact amplitude of this current depends upon the rate at which the pump is active, which is in turn related to the intracellular concentration of Na^+ and the extracellular concentration of K^+ .

Besides the electrogenic Na^+ - K^+ pump, neurons and glia also contain many other types of ionic pumps in their membranes (e.g., Läuger, 1991; Andersen and Bittar, 1998). Many of these pumps are operated by the Na^+ gradient across the cell, whereas others operate through a mechanism similar to the Na^+ - K^+ pump (i.e., the hydrolysis of ATP). For example, the Ca^{2+} concentration inside neurons is kept to very low levels (typically 50–100 nM) through the operation of both types of ionic pumps as well as special intracellular Ca^{2+} -buffering mechanisms. Ca^{2+} is extruded from neurons through both Ca^{2+} - Mg^{2+} -ATPase as well as an Na^+ - Ca^{2+} exchanger. The Na^+ - Ca^{2+} exchanger is driven by the Na^+ gradient across the membrane and extrudes one Ca^{2+} ion for each Na^+ ion allowed to enter the cell.

The Cl^- concentration in neurons is actively maintained at a low level through the operation of a chloride-bicarbonate exchanger, which brings in one ion of Na^+ and one ion of HCO_3^- for each ion of Cl^- extruded (e.g., Reithmeier, 1994; Thompson et al., 1988). Finally, intracellular pH can have marked effects on neuronal excitability, and therefore pH is also tightly regulated, in part through the efforts of a Na^+ - H^+ exchanger that, again, extrudes one proton for each Na^+ that is allowed to enter the cell.

Ionic pumps are essential and important constituents of neurons and neuronal membranes. Their time scale of action is seconds to minutes, and they are therefore thought of as being more involved in long-term rather than short-term neuronal processing.

TYPES OF IONIC CURRENTS

Neurons in the nervous system do not simply lie at rest and occasionally generate an action potential. Rather, neuronal membranes are in a constant state of flux due to the presence of a remarkable variety of different ionic currents (Table 2.1). These currents are distinguished not only by the ions that they conduct (e.g., K^+ , Na^+ , Ca^{2+} , Cl^-) but also by their time course, sensitivity to membrane potential, and sensitivity to neurotransmitters and other chemical agents (for reviews, see Huguenard and McCormick, 1994; Johnston and Wu, 1995; Stea et al., 1995; Hille, 2001; Yellen, 2002). As the various ionic currents were discovered, they were divided into two general categories: those that are sensitive to changes in membrane potential and those that are altered by

Table 2.1. Neuronal Ionic Currents

Current	Description	Function
Na⁺		
$I_{Na,t}$	Transient; rapidly activating and inactivating	Action potentials
$I_{Na,p}$	Persistent; noninactivating	Enhances depolarization; contributes to steady state firing
Ca²⁺		
I_T , low threshold	“Transient”; rapidly inactivating; threshold negative to -65 mV	Underlies rhythmic burst firing
I_L , high threshold	“Long-lasting”; slowly inactivating; threshold around -20 mV	Underlies Ca ²⁺ spikes that are prominent in dendrites; involved in synaptic transmission
I_N	“Neither”; rapidly inactivating; threshold around -20 mV	Underlies Ca ²⁺ spikes that are prominent in dendrites; involved in synaptic transmission
I_P	“Purkinje”; threshold around -50 mV	
K⁺		
I_K	Activated by strong depolarization	Repolarization of action potential
I_C	Activated by increases in $[Ca^{2+}]_i$	Action potential repolarization and interspike interval
I_{AHP}	Slow afterhyperpolarization; sensitive to increases in $[Ca^{2+}]_i$	Slow adaptation of action potential discharge; the block of this current by neuromodulators enhances neuronal excitability
I_A	Transient; inactivating	Delayed onset of firing; lengthens interspike interval; action potential repolarization
I_M	“Muscarine” sensitive; activated by depolarization; noninactivating	Contributes to spike frequency adaptation; the block of this current by neuromodulators enhances neuronal excitability
I_h	Depolarizing (mixed cation) current that is activated by hyperpolarization	Contributes to rhythmic burst firing and other rhythmic activities
$I_{K,leak}$	Contributes to neuronal resting membrane potential	The block of this current by neuromodulators can result in a sustained change in membrane potential

neurotransmitters and internal messengers. However, with the discovery of a number of voltage-sensitive ionic channels that are also gated by neurotransmitters, and vice versa, it became apparent that there is substantial overlap between these two groups. The currents that possess both voltage and neurotransmitter sensitivity have received attention because of their ability to modulate the electrical behavior of neurons in unusual and interesting ways (see Chemical Synapses later).

Most currents that are sensitive to membrane potential are turned on (*activated*) by depolarization. The rate at which they activate and the membrane potential at which they start to become active (*threshold*) are important characteristics. Many voltage-dependent currents do not remain on once they are activated, even during a constant shift in membrane potential. The process by which they turn off despite a stable level of membrane potential in their activation range is known as *inactivation*. Inactivation is a state of the current and ionic channels that is distinct from simple channel closure. Once a current becomes inactive, this inactivation must be removed before it can again be activated. *Removal of inactivation* is generally achieved by repolarization of the membrane potential. Like the process of activation, inactivation and removal of inactivation are time and membrane potential dependent. Together, all of these characteristics define the temporal and voltage domain over which the current influences the electrical activity of the neuron.

The names given to each ionic current often reflect a distinguishing property of the current. If the current is activated by relatively small deviations in the membrane potential (denoted as V_m) from rest, then it may be known as *low threshold* (e.g., low-threshold Ca^{2+} current), whereas if the current is activated only at levels that are substantially positive (depolarized) from rest, the current may be known as *high threshold* (e.g., high-threshold Ca^{2+} current). In addition, if activation of the current through a constant and steady change in membrane potential (i.e., under voltage-clamp conditions in which the membrane potential is held constant) leads to only a transient response, then it is known as *transient* or *rapidly inactivating* (examples are the A-current and the T-current). Likewise, a current that persists during constant activation (i.e., that is noninactivating) is known as *sustained*, *persistent*, or *long lasting* (e.g., persistent Na^+ current and the L, or long-lasting, Ca^{2+} current).

The ionic currents that determine the neuronal firing behavior of neurons in different regions of the nervous system have been intensively investigated. To date, at least a dozen distinct types of neuronal current, many of which are common to neurons at all levels of the neuraxis, have been identified (see Table 2.1). We briefly summarize these currents and the unique contribution that each makes to the firing behavior of neurons (Fig. 2.4).

SODIUM (Na^+) CURRENTS

Two Na^+ currents— $I_{\text{Na,t}}$ (transient) and $I_{\text{Na,p}}$ (persistent)—are widely distributed in neurons from different regions of the nervous system. These two currents are distinguished from one another by their rate of inactivation, their threshold for activation, and their amplitude.

$I_{\text{Na,t}}$, Transient Sodium. As we have noted, the transient Na^+ ($I_{\text{Na,t}}$) current rapidly inactivates within a few milliseconds during steady depolarization. All central neurons studied to date possess a large $I_{\text{Na,t}}$, whereas $I_{\text{Na,p}}$ is considerably smaller in amplitude. The rapid activation and inactivation properties of $I_{\text{Na,t}}$ make this current ideal for its role in the generation of action potentials (see Fig. 2.4A).

$I_{\text{Na,p}}$, Persistent Sodium. In contrast to $I_{\text{Na,t}}$, the persistent Na^+ ($I_{\text{Na,p}}$) current shows little, if any, inactivation. This current is also rapidly activated by membrane depolariza-

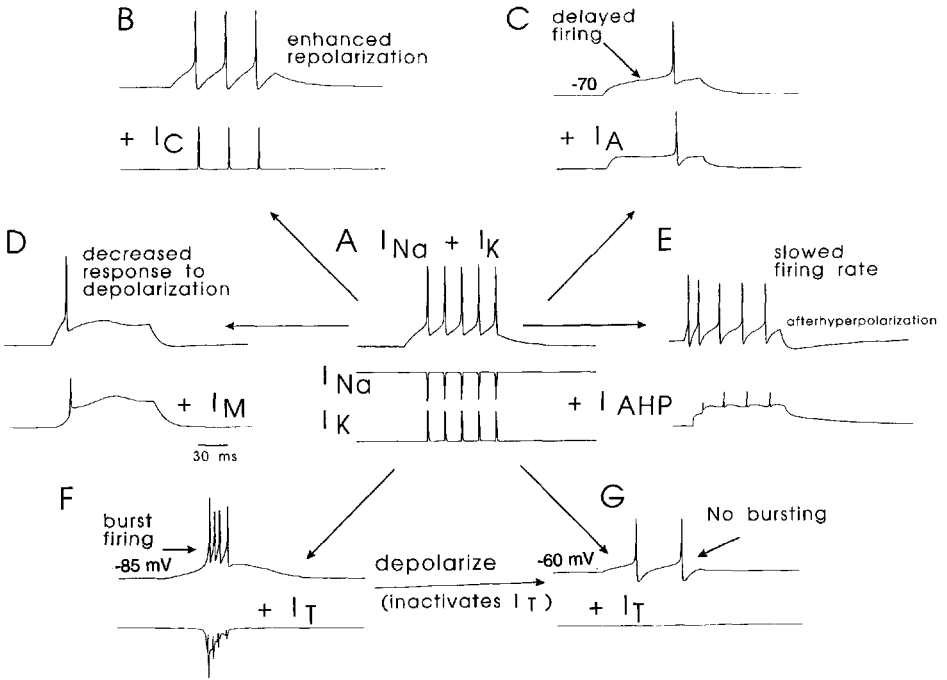


Fig. 2.4. A summary of different types of voltage-gated currents and the impulse firing patterns they produce in a neuron in response to steady injection of depolarizing current. At the center (A) is shown the repetitive impulse response of the classic Hodgkin-Huxley model (voltage recording above, current recordings below). Radiating out from this are changes in this pattern associated with the different types of ionic channels. **B:** Addition of the Ca^{2+} -activated K^+ current I_C (and the high threshold Ca^{2+} current I_L) facilitates the repolarization of each action potential. **C:** Addition of the depolarization-activated, but transient, K^+ current I_A results in a delay to onset of action potential generation. **D:** Addition of the depolarization-activated, but persistent, K^+ current I_M results in a marked decrease in neuronal excitability. **E:** Addition of the slow Ca^{2+} -activated K^+ current I_{AHP} results in spike frequency adaptation and the generation of a slow hyperpolarization after the action potential train (afterhyperpolarization). **F:** Addition of the low threshold and transient Ca^{2+} current I_T results in the generation of a burst of action potentials at -85 mV. **G:** Depolarization of the cell in **F** to -60 mV results in inactivation of I_T and now the cell generates a train of two action potentials. [Modified from Shepherd, 1994.] These traces are the result of computer simulations (Huguenard and McCormick, 1994).

tion, but its noninactivating nature allows it to serve a very different role in neuronal function (see Llinás, 1988; Ogata and Ohishi, 2002). A large percentage of neuronal computations occur in a narrow range of membrane potential between approximately -75 and -50 mV. This range is between resting membrane potential and a level of depolarization at which the neuron is firing repeatedly at a high rate. The nature of $I_{\text{Na,p}}$ is such that it is activated by depolarizations, such as synaptic potentials, that bring the membrane potential from rest to near action potential firing threshold. The added depolarizing influence of the influx of Na^+ ions resulting from the activation of $I_{\text{Na,p}}$ serves to markedly enhance the response of the neuron to excitatory inputs and may result in the generation of “plateau potentials” (Fig. 2.5C). Plateau potentials are pro-

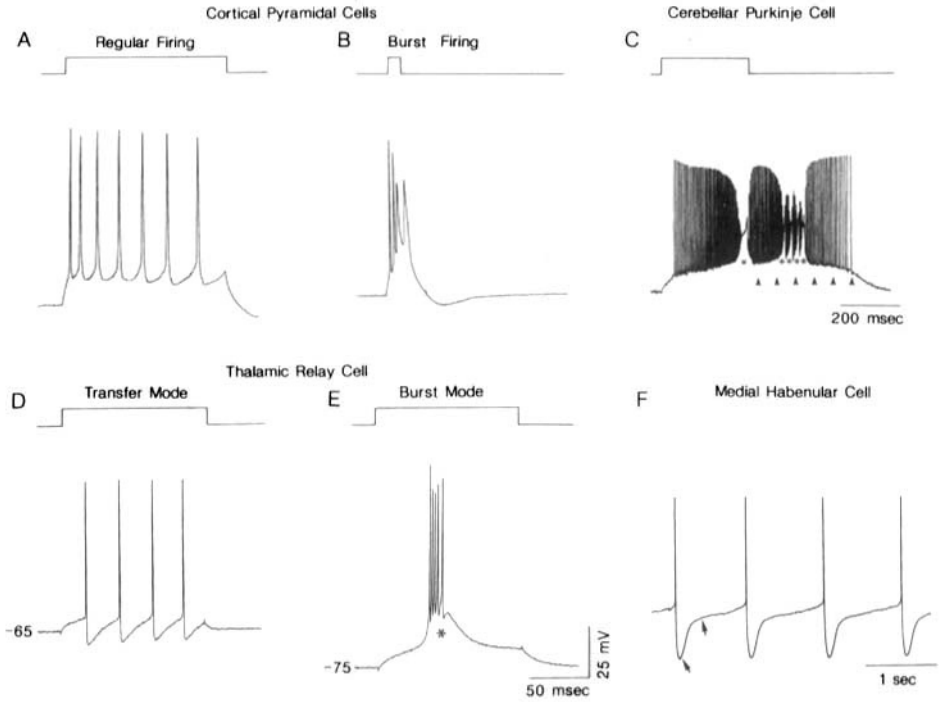


Fig. 2.5. Electrophysiological behavior of neurons in different regions of the mammalian brain. **A:** Example of a “regular” firing cortical pyramidal neuron. Intracellular injection of a depolarizing current pulse (top trace) results in the generation of a train of action potentials that occur at progressively slower frequencies (spike frequency adaptation). **B:** By contrast, intracellular injection of depolarizing current pulses in a “burst” generating cortical pyramidal neuron results in the clustering of action potentials together on top of a slow potential. **C:** Electrical activity of a cerebellar Purkinje cell in response to intracellular injection of a depolarizing current pulse. The cell generates initially a high-frequency discharge of fast Na^+ -dependent action potentials (generated in the soma). This discharge is modulated by the occurrence of dendritic Ca^{2+} spikes (asterisks). The discharge outlasts the duration of the intracellular depolarizing pulse (top trace) due to the presence of a plateau potential mediated by $I_{\text{Na,p}}$ and calcium currents (arrowheads). **D:** Depolarization of thalamic relay neuron results in the generation of a train of four action potentials if the membrane potential is positive to approximately -65 mV, but a burst of action potentials if the cell is at or negative to -75 mV (**E**). The low-threshold Ca^{2+} spike underlying this burst discharge is indicated by an asterisk. **F:** Example of a neuron in the medial habenula that generates intrinsic “pacemaker” discharge. Intracellular recording reveals the presence of large hyperpolarizations after each action potential that are complicated in time course and help determine the rate at which the neuron fires (arrows). Videos of electrical activity in different types of neurons can be obtained at www.mccormicklab.org.

longed depolarizations that persist despite the removal of all other depolarizing influences in the cell (e.g., a synaptic potential or the intracellular injection of current).

The amplitude and cellular distribution of $I_{\text{Na,p}}$ can therefore have an important role in determining the responsiveness of neurons. The persistent nature of $I_{\text{Na,p}}$ allows this current to participate in the determination of the baseline firing rate of neurons. $I_{\text{Na,p}}$

appears especially important to the ability of some neurons to maintain intrinsic *pace-maker* activity (e.g., the generation of action potentials in a repeated temporal pattern in the absence of synaptic input). In these cells, the steady influx of Na^+ ions into the neuron depolarizes the cell to above firing threshold, thereby triggering baseline activity. The membrane potential of these cells is in a state of constant change, cycling through the generation of an action potential to the repolarization of the cell (see K Currents) to the generation of an action potential again. Examples of such neurons in the central nervous system (CNS) are those of the locus coeruleus, dorsal raphe, medial habenula nuclei, and cerebellar Purkinje cells (see Fig. 2.5F) (see McCormick and Prince, 1987; Raman and Bean, 1999; Alvarez et al., 2002; Liu et al., 2002).

CALCIUM (Ca^{2+}) CURRENTS

Ca^{2+} ions lead with a dual role in neurons, as modulators of neuronal firing pattern and as intermediaries in a number of nonelectrical cellular activities, including neurotransmitter release, enzyme activation, metabolism, and even gene expression. This diverse involvement of Ca^{2+} ions, as well as the ubiquitous nature of Ca^{2+} currents, has led to intense investigation of these Ca^{2+} currents.

Ionic channels that conduct Ca^{2+} are present in all neurons. These channels are special in that they serve two important functions. First, Ca^{2+} channels are present throughout the different parts of the neuron (dendrites, soma, synaptic terminals) and contribute greatly to the electrophysiological properties of these processes (Llinás, 1988; Hausser et al., 2000; Migliore and Shepherd, 2002). Second, Ca^{2+} channels are unique in that Ca^{2+} is an important second messenger in neurons and the entry of Ca^{2+} into a cell can affect numerous physiological functions, including neurotransmitter release, synaptic plasticity, neurite outgrowth during development, and even gene expression.

Ca^{2+} currents have been separated into at least four separate categories based upon their voltage sensitivity and kinetics of activation and inactivation as well as their block by various pharmacological agents. Differences in the kinetics and pharmacology of three different categories of Ca^{2+} currents led Richard Tsien and colleagues (Nowycky et al., 1985) to name them I_T (“transient”), I_L (“long-lasting”), and I_N (“neither”) (see also Carbonne and Lux, 1984). More recent experiments by Rodolfo Llinás and colleagues (reviewed in Llinás et al., 1992) demonstrated that Purkinje cells of the cerebellum, as well as many different cell types of the CNS, also possess another Ca^{2+} current termed I_p . Molecular biology has revealed a wide variety of genes involved in the production of Ca^{2+} channels, and it is certain that more Ca^{2+} currents have yet to be characterized (e.g., see Catterall, 2000a; Ertel et al., 2000).

High-Threshold Ca^{2+} Currents. Most Ca^{2+} channels are activated at membrane potentials positive to approximately -40 mV and are termed *high-voltage activated* (HVA). These Ca^{2+} channels include at least those underlying the currents I_L , I_N , and I_p . These three different ionic currents can be separated from each other through examination of their voltage dependence and kinetics of activation and inactivation and through their sensitivity to various Ca^{2+} channel blockers and neural toxins. The Ca^{2+} channel antagonists known as dihydropyridines, which clinically are useful for their effects on the heart and vascular smooth muscle (e.g., for the treatment of arrhythmias, angina, migraine headaches), selectively block the L-type Ca^{2+} channels (reviewed in

Stea et al., 1995; Catterall, 2000a). L-type Ca^{2+} currents exhibit a high threshold for activation (around -10 mV) and give rise to rather persistent, or long-lasting, ionic currents. In contrast to I_L , I_N is not blocked by dihydropyridines but rather is selectively blocked by a toxin found in Pacific cone shells (ω -conotoxin-GVIA). N-type Ca^{2+} channels have a threshold for activation of around -20 mV, inactivate with maintained depolarization, and are modulated by a variety of neurotransmitters. In at least some cell types, I_N is involved in the Ca^{2+} -dependent release of neurotransmitters at presynaptic terminals (e.g., Wheeler et al., 1994).

P-type Ca^{2+} channels are distinct from N and L types in that they are not blocked by either dihydropyridines or ω -conotoxin-GVIA, but they are blocked by a toxin (termed ω -agatoxin-IVA) that is present in the venom of the Funnel web spider (Linás et al., 1992; Catterall, 2000a). P-type calcium channels activate at relatively high thresholds and do not inactivate. This type of calcium channel appears to be prevalent in Purkinje cells of the cerebellum, as well as other cell types, and participates in the generation of dendritic Ca^{2+} spikes, which can strongly modulate the firing pattern of the neuron in which they occur (e.g., Fig. 2.5C).

Collectively, the high-threshold-activated Ca^{2+} channels also contribute to the generation of action potentials in mammalian neurons. The activation of these Ca^{2+} currents adds a bit to the depolarizing portion of the action potential, but, more importantly, they allow Ca^{2+} to enter the cell, and this has the secondary consequence of activation of various Ca^{2+} -activated K^+ currents (see Sah and Faber, 2002). The activation of these K^+ currents then modifies the pattern of action potentials generated in the cell, as mentioned earlier (see Fig. 2.4B, E).

Molecular biological studies have demonstrated that high-threshold Ca^{2+} channels are similar to the Na^+ channel in that they contain a central α_1 subunit that forms the aqueous pore and several regulatory or auxiliary subunits. As in the Na^+ channel, the primary structure of the α_1 subunits of Ca^{2+} channels consists of four homologous domains (I–IV), each of which contains six regions (S1–S6) that may generate transmembrane α -helices. The genes for at least 10 different Ca^{2+} channel α subunits have been cloned (α_{1A-I} and α_{1s}). These different α subunits are grouped into three different subfamilies and have been renamed with the current convention of $\text{Ca}_v1.x$ to $\text{Ca}_v3.x$ (Ertel et al., 2000). The Ca_v1 subfamily corresponds to I_L , whereas the Ca_v3 family corresponds to I_T . I_P , I_N , and I_R are within the Ca_v2 subfamily (Ertel et al., 2000).

Low-Threshold Ca^{2+} Currents. Low-threshold Ca^{2+} currents, also known as the transient Ca^{2+} current I_T , are also present in many different cell types in the nervous system and are often involved in the generation of rhythmic bursts of action potentials (Figs. 2.4F and 2.5E). The low-threshold Ca^{2+} current is characterized by a threshold for activation of around -65 mV, which is below the threshold for generation of typical Na^+ - K^+ -dependent action potentials (-55 mV). Another important feature of this current is that it inactivates with maintained depolarization. Owing to these properties, this Ca^{2+} current can perform a markedly different function in neurons from that of the high-threshold Ca^{2+} currents. Through activation and inactivation of the low-threshold Ca^{2+} current, neurons can generate slow (around 50–100 msec) Ca^{2+} spikes, which can result, owing to their prolonged duration, in the generation of a high-frequency “burst” of short-duration Na^+ - K^+ action potentials (Figs. 2.4F and 2.5E).

In the mammalian brain, this pattern is especially well exemplified by the activity of thalamic relay neurons, which in the visual system receive direct input from the retina and transmit this information to the visual cortex. During periods of slow-wave sleep, the membrane potential of these relay neurons is relatively hyperpolarized, resulting in the removal of inactivation (de-inactivation) of the low-threshold Ca^{2+} current. This allows these cells to spontaneously generate low-threshold Ca^{2+} “spikes” and bursts of two to five action potentials (Fig. 2.5E). The large number of thalamic relay cells bursting during sleep in part gives rise to the spontaneous synchronized activity that early investigators were so surprised to find upon recording from the brains of sleeping animals (reviewed in McCormick and Bal, 1997). It has even proved possible to maintain one of the sleep-related brain rhythms (spindle waves) intact in slices of thalamic tissue maintained *in vitro*, owing to the activation of low-threshold Ca^{2+} spikes and burst of action potentials in networks of interacting thalamic cells (see McCormick and Bal, 1997).

The transition to waking or the period of sleep when dreams are prevalent (rapid-eye-movement sleep) is associated with a maintained depolarization of thalamic relay cells to membrane potentials of around -60 to -55 mV. This maintained depolarization results in the inactivation of the low-threshold Ca^{2+} current and therefore an abolition of burst discharges in these neurons (e.g., Figs. 2.4G and 2.5D). In this way, the properties of a single ionic current (I_T) help to explain in part the remarkable changes in brain activity occurring in the transition from sleep to waking.

POTASSIUM (K^+) CURRENTS

Neuronal K^+ currents form a large and diversified group. They are intimately involved in determining the pattern of activity generated by neurons. Because they are hyperpolarizing, they are responsible not only for the repolarization of the action potential but also for the determination of the *probability* of generation of an action potential at any given point in time. As with other neuronal currents, K^+ currents are distinguished by their voltage and time dependency, as well as by pharmacological techniques (reviewed in Storm, 1990; Johnston and Wu, 1995; Yellen, 2002).

Molecular biological studies of voltage-sensitive K^+ channels, first done in *Drosophila* and later in mammals, have revealed a large number of genes that generate K^+ channels. They consist of four distinct families (K_v1-4) (Chandy and Gutman, 1995; Yellen, 2002). These genes generate a wide variety of different K^+ channels not only due to the large number of genes involved but also due to alternative RNA splicing, gene duplication, and other posttranslational mechanisms. Functional expression of different K^+ channels reveals remarkable variation in the rate of inactivation, such that some are rapidly inactivating (A current-like), whereas others inactivate more slowly. Finally, some K^+ channels do not inactivate, such as those underlying I_K . One of the largest subfamilies of K^+ channels are those that give rise to the resting membrane potential, so-called leak channels. Interestingly, these channels appear to be opened by gaseous anesthetics, indicating that hyperpolarization of central neurons is a major component of general anesthesia. It is now clear that each type of neuron in the nervous system contains a unique set of functional voltage-sensitive K^+ channels that are selected, modified, and placed in particular spatial locations in the cell in a manner to facilitate the unique role of that cell in neuronal processing.

I_K, Delayed Rectifier. As we have seen, the early studies in the squid giant axon not only defined the role of the transient Na⁺ current in the generation of the action potential but also identified an important outward K⁺ current known as the delayed rectifier, or *I_K*. The activation kinetics of *I_K* are slower than those of the transient Na⁺ current and therefore *I_K* appears somewhat “delayed” (see Fig. 2.3B). This K⁺ current is voltage sensitive, being activated at membrane potentials positive to approximately -40 mV, and only slowly inactivates. *I_K* is found in neurons throughout the nervous system and typically contributes to the repolarization of action potentials and the hyperpolarization that follows them (see Figs. 2.3B and 2.4A).

Ca²⁺-Activated K⁺ Currents. An additional class of K⁺ currents that are important for determining the firing behavior of neurons are those that are Ca²⁺ sensitive (denoted *I_{K,Ca}*). This family of K⁺ currents is activated by increases in the intracellular concentration of unbound Ca²⁺ ([Ca²⁺]_i). Two *I_{K,Ca}* currents have been widely identified in neurons: *I_C* and *I_{AHP}* (see Storm, 1990; Sah and Faber, 2002). *I_C* is not only sensitive to increases in [Ca²⁺]_i in the micromolar range but is also strongly voltage dependent, becoming larger with depolarization. *I_C* helps control the frequency of action potential generation during a steady depolarization by causing a marked hyperpolarization after the occurrence of each spike (see Fig. 2.4B). *I_C* may even be important in some neurons in repolarization of the action potential. The voltage dependence of *I_C* results in its rapid inactivation once the membrane potential is repolarized. This inactivation constrains the influence of *I_C* in the temporal domain to tens of milliseconds or less.

I_{AHP}, in contrast to *I_C*, is much slower in time course and not very voltage dependent. Its influence on the membrane potential of the cell is best seen after the generation of a number of action potentials as a prolonged *afterhyperpolarization*, for which it is named. This K⁺ current contributes significantly to the tendency of the firing frequency of some types of neurons (e.g., cortical and hippocampal pyramidal neurons) to decrease during maintained depolarizations, a process known as *spike frequency adaptation* (see Fig. 2.4E and later).

The generation of action potentials, by increasing [Ca²⁺]_i through L- or N-type Ca²⁺ channels, triggers *I_C* and *I_{AHP}*. The hyperpolarizations of the membrane potential resulting from K⁺ leaving the cell during these currents regulates the rate at which the neuron fires. Due to its short time course, *I_C* contributes substantially to short interspike intervals. In contrast, because of its slow activation and prolonged time course, *I_{AHP}* contributes more to the overall pattern of spike activity. The relatively non-voltage-dependent nature of *I_{AHP}* means that the influence of this current on the membrane potential is more closely related to changes in [Ca²⁺]_i than is *I_C*. Importantly, the amount of *I_{AHP}* appears to be under the control of a number of putative neurotransmitters (see Decrease of *I_{AHP}*).

Transient K⁺ Currents. The first of a family of K⁺ currents that are activated by membrane depolarization and then undergo relatively rapid inactivation was discovered in molluscan neurons (Connor and Stevens, 1971; Neher, 1971) and termed *I_A*. The A-current is a transient K⁺ current: after its activation by depolarization of the membrane potential positive to approximately -60 mV, it rapidly inactivates. Like other transient and voltage-activated currents (e.g., *I_{Na,t}* and *I_T*), this inactivation is removed by repo-

larization of the membrane potential. I_A is involved in the response of neurons to a sudden depolarization from hyperpolarized membrane potentials and serves to delay the onset of the generation of the first action potential (see Fig. 2.4C). I_A can also slow a neuron's firing frequency during a maintained depolarization and help to repolarize the action potential. For example, in a spontaneously active neuron, the hyperpolarization that occurs after the generation of an action potential will remove some of the inactivation of I_A . As the membrane potential depolarizes back toward the firing threshold, I_A will be activated and slow down the rate of depolarization. Once the firing threshold is reached and an action potential is generated, the rapid depolarization may activate more of I_A , which then helps to repolarize the cell. In this manner, I_A can be an important current in the determination of firing behavior of neurons.

Muscarine-Sensitive K^+ Currents. Another type of K^+ current was discovered in sympathetic ganglion neurons of bullfrogs by David Brown and Paul Adams (1980). This K^+ current is activated by depolarization of the membrane potential positive to approximately -65 mV, does not inactivate with time, and is blocked by stimulation of muscarinic cholinergic receptors (hence its name, I_M). I_M is found in neurons throughout the nervous system, including pyramidal cells of the cerebral cortex and hippocampus (reviewed in Marrion, 1997; Jentsch, 2000). Depolarizations that are large enough to result in the generation of action potentials also cause the activation of I_M . However, because of its relatively slow kinetics and modest amplitude, I_M probably does not affect substantially the waveform of a single action potential but rather contributes to the slow adaptation of spike frequency seen during a maintained depolarization (see Fig. 2.4D).

Currents Activated by Hyperpolarization. Hyperpolarization of neurons in many regions of the nervous system results in the activation of a current that brings the membrane potential toward more positive values (e.g., back toward rest). This current, or family of currents, is generally referred to as I_h ("hyperpolarization activated), although it has also been given such lively names as I_Q ("queer") and I_f ("funny") (see Pape, 1996). The currents in this family are carried by both Na^+ and K^+ ions and are relatively slow in time course, although this varies widely between different cell types. H-channels are found in the dendrites of cortical pyramidal cells and appear to control the communication of synaptic inputs to the soma (Magee, 1998; Lorincz et al., 2002).

The cloning of H-channels reveals that they are related to both K^+ channels and cyclic nucleotide-gated channels. The modulation of the voltage dependence of I_h through the direct binding of cyclic AMP to h-channels can control diverse neuronal functions, including neuronal excitability and rhythmogenesis. For example, the activation of I_h has been demonstrated to be important in the generation of rhythmic oscillations in at least thalamic relay neurons and some types of cardiac cells (DiFrancesco, 1985; McCormick and Pape, 1990). The activation of the h-current results in the slow depolarization of the cell and, in so doing, generates a "pacemaker" potential that can activate repetitive Na^+ and/or Ca^{2+} spikes. Changes in the intracellular levels of cyclic AMP modulate the voltage dependence of activation of the h-current and, through this mechanism, can modulate the rate of repolarization of the membrane potential, resulting, for example, in a change in heart rate.

SUMMARY OF INTRINSIC MEMBRANE PROPERTIES

Neurons possess a virtual cornucopia of different ionic currents. The magnitude, cellular distribution, and sensitivity to pharmacological manipulation of each of these ionic currents are different for every major neuronal region in the central and peripheral nervous systems. These differences result in widely varying electrophysiological properties and patterns of neuronal activity generated by cells in different parts of the brain. Each class of neuron is exquisitely “tuned” to do its particular task in the nervous system through its own special mixture of the basic ionic currents available and through the precise modulation of these currents by neuroactive substances. An analogy to this situation would be “nature versus nurture” in determining human behavior. The cells are endowed with a particular mixture of ionic currents through genetic programming (nature) that can then be modified on either a short- or long-term basis through development or actions of a number of substances impinging upon the cell (nurture).

Examples of the different electrophysiological “behaviors” of neurons due to different combinations of ionic currents are illustrated in Fig. 2.5. Cortical pyramidal neurons respond to a depolarizing current pulse with a train (Fig. 2.5A) or a burst (Fig. 2.5B) of action potentials (see Gray and McCormick, 1996). The spike frequency adaptation of cortical pyramidal neurons (Fig. 2.5A) is due to the presence of I_{AHP} and I_{M} . In contrast to neocortical pyramidal neurons, the major output cell of the cerebellar cortex, the Purkinje cell, responds to a depolarizing current pulse with a high-frequency discharge of short-duration action potentials (Fig. 2.5C). This high-frequency discharge is modulated by dendritic calcium spikes (Fig. 2.5C, asterisks) as well as by prolonged Na^+ ($I_{\text{Na,p}}$) and Ca^{2+} currents (I_{p} ; Fig. 2.5C, arrowheads).

Thalamic relay neurons are unusual in that they possess two distinct modes of action potential generation: single-spike activity when depolarized above -65 mV (Fig. 2.5D) and burst firing when depolarized at or negative to -75 mV (Fig. 2.5E). Thalamic neurons respond with a burst of action potentials at -75 mV due to the presence of a large I_{T} , which is completely inactivated at membrane potentials positive to -65 mV.

Some neurons display spontaneous activity in a regular and stereotyped manner, even in the lack of all synaptic input, such as the medial habenular neuron illustrated in Fig. 2.5F. These cells appear to possess prolonged and complicated spike after hyperpolarizations (arrows), which help to determine the rate at which the action potentials are generated.

Although the electrophysiological behavior of neurons can be markedly changed by the neurotransmitter “environment,” they also remain distinct in that it is generally not possible to cause one class of neuron (e.g., cortical pyramidal neuron) to behave electrophysiologically *identical* to another (e.g., cerebellar Purkinje cell). However, substantial and interesting transformations take place in response to neuron-to-neuron communication.

TYPES OF NEURONAL COMMUNICATION

Communication from one neuron to another in the nervous system occurs through at least three different mechanisms: (1) gap junctions, (2) ephaptic interactions, and (3) the release of neuroactive substances.

GAP JUNCTIONS

Gap junctions are actual physical connections between neighboring neurons made by large macromolecules that extend through the membranes of both cells and contain water-filled pores (Fig. 2.6). Gap junctions allow for the direct exchange of ions and other small molecules between cells. Ionic current through these channels directly couples the electrical activity of one cell to that of the other. Although in some cases gap junctions can be viewed as simple linearly conducting connections, in many other cases they are known to *rectify* (i.e., pass current in one direction much better than in the other). Gap junctions are known to be a prominent feature of neuron-to-neuron connections in many submammalian species. In mammals, gap junctions are prevalent in the retina, olfactory granule cells (see Chap. 5), and some brainstem nuclei (vestibular nucleus and the mesencephalic nucleus of the fifth cranial nerve). Interestingly, gap junctions have been found to couple together GABAergic interneurons within the cortex and thalamus in young animals (Beierlein et al., 2000; Landisman et al., 2002), suggesting that these cells may synchronize their activities through this electrical coupling. The ability of neurotransmitters to alter the conducting properties of gap junctions in some regions (e.g., retina) gives additional complexity to this system of communication.

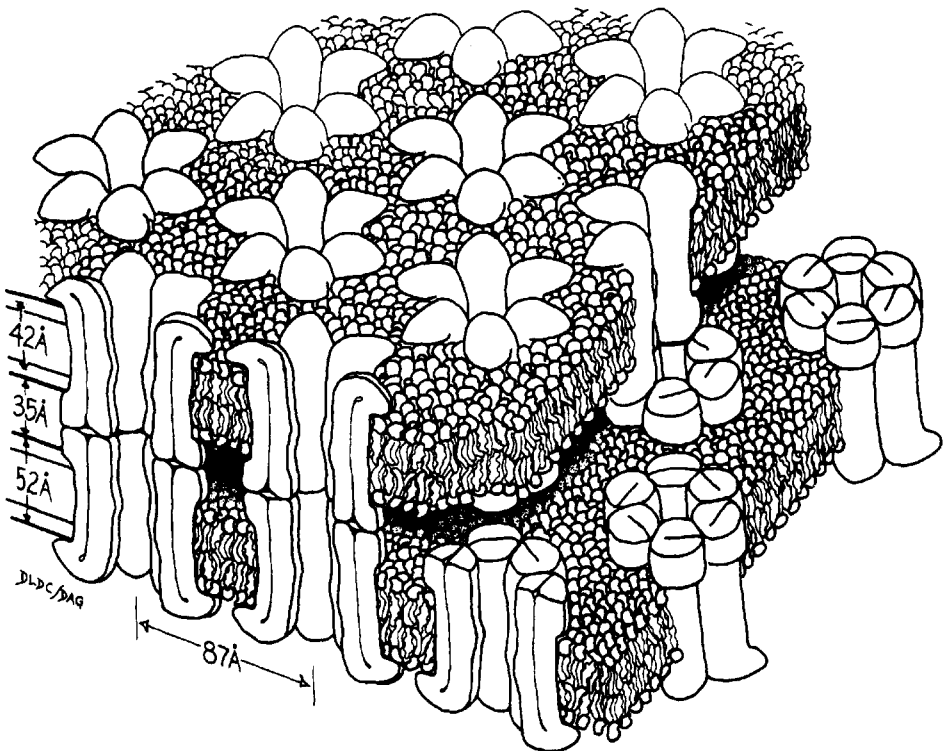


Fig. 2.6. Diagram of direct electrical connection between cells (gap junction). Channels provide cell-to-cell exchange of low-molecular-weight substances and electric ionic current (in the form of ions). [From Makowski et al., 1977.]

EPHAPTIC INTERACTIONS

Ephaptic interactions refer to interactions between neurons based largely upon their close physical proximity (Fig. 2.7). The flow of ions into and out of one neuron will set up local electrical currents that can partially pass through neighboring neurons. The degree to which a neuron can be influenced by the activity of its neighbor is determined in part by the proximity of the cells and their processes (i.e., dendrites, cell bodies, and axons). In regions that possess closely spaced neuronal elements, such as the close packing of cell bodies in hippocampus and cerebellum or the bundling of dendrites in the cerebral cortex, there is the possibility of significant ephaptic interaction. Ephaptic interactions, like gap junctions, serve to synchronize local neuronal activity

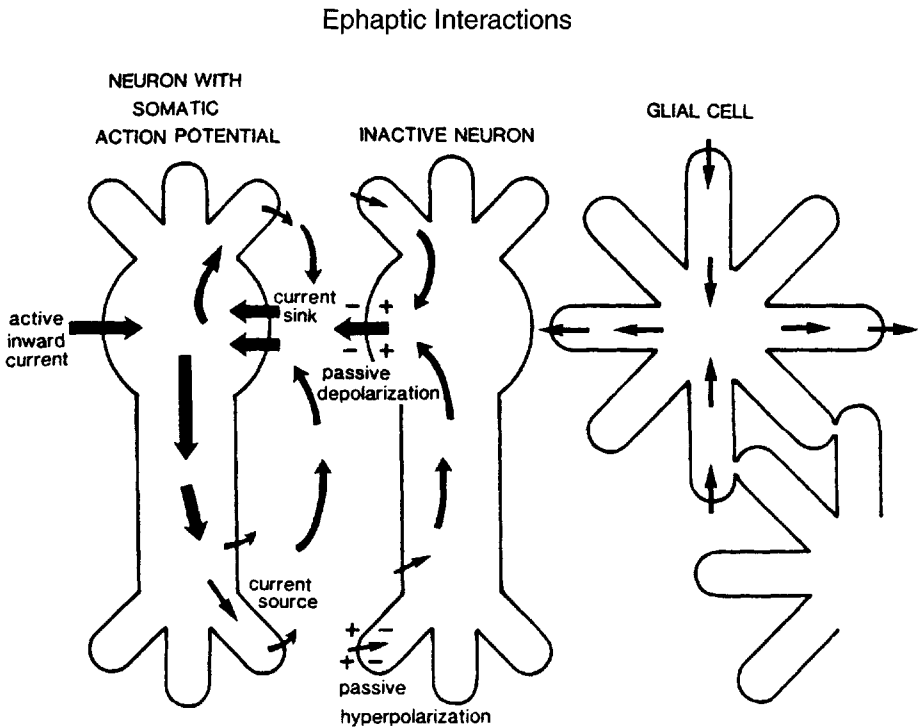


Fig. 2.7. Schematic diagram of current flow proposed to underlie excitatory electrical field effects between pyramidal neurons in the hippocampus (an example of ephaptic interactions). Arrows denote current flow of positive charges. The driving force of the ephaptic electrical field effect is the flow of positive current into somata produced by the synchronous firing of a population of hippocampal pyramidal cells (left). Positive current then flows passively out dendrites of active cells and returns through extracellular space. The relative decrease in positive charge in the extracellular space at the cell body layer causes the voltage on the inside of inactive cells (center) to appear relatively more positive (i.e., depolarized) than previously. Likewise, the addition of positive current to the extracellular space at the levels of the dendrites by the neuronal activity causes the intracellular potentials of inactive dendrites to appear more negative (hyperpolarized) than previously. Depolarization of the neuronal somata increases the probability that neighboring cells will generate action potentials in synchrony. Passive glial cell also develops transmembrane current flow within electrical field (right). From Taylor and Dudek, 1984.

and may influence the general firing pattern of functionally related neurons (e.g., Jefferys, 1995).

CHEMICAL SYNAPSES

The release of neuroactive substances at the specialized connections called *synapses* is by far the most common method by which neurons influence other neurons. Some neuroactive substances can also diffuse over rather long distances to activate extra-synaptic sites, although it is not yet clear how common this type of transmission is.

As discussed in Chap. 1, neurotransmitters are released by neurons through exocytosis of packets (*vesicles*) of the substance from synaptic specializations into the space (*synaptic cleft*) between the cells. Examples of two of the most prevalent types of synapses are shown in Fig. 2.8. The release of transmitter is triggered by the entry of

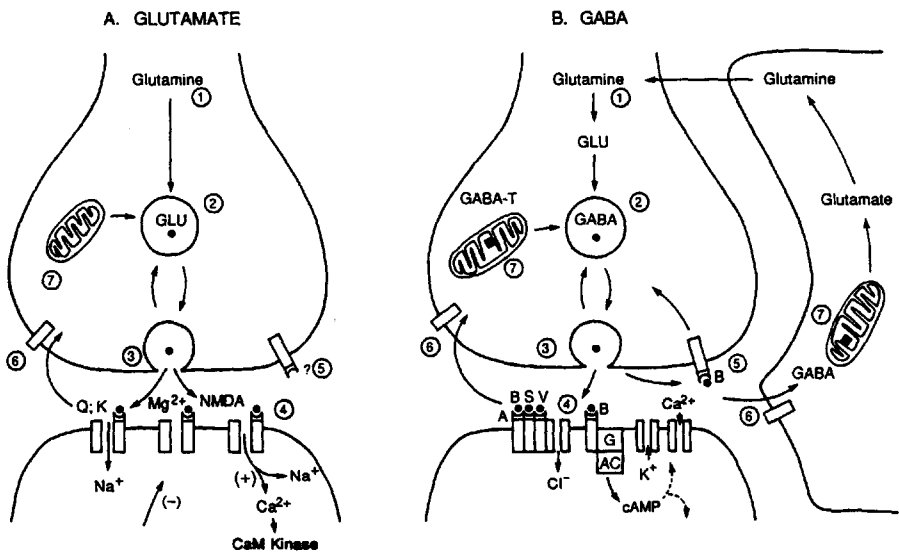


Fig. 2.8. Molecular mechanisms of ionotropic amino acid synapses. **A:** Glutaminergic synapses: (1) synthesis of glutamate (GLU) from glutamine, (2) transport and storage, (3) release of GLU by exocytosis, and (4) binding of GLU to AMPA, kainate (K), and NMDA receptors. The Q (quisqualate or AMPA) and K (kainate) receptors typically gate Na^+ and K^+ flux; the NMDA receptor also typically allows Ca^{2+} entry when the membrane potential is depolarized (+). When the membrane potential is hyperpolarized (-), Mg^{2+} blocks the channel. The release of GLU may be regulated by presynaptic receptors (?5). Once GLU is released, it is removed from the synaptic cleft by re-uptake (6) and processed intracellularly (7). [From Shepherd, 1994; based on Cooper et al., 1987; Cull-Candy and Usowicz, 1987; Jahr and Stevens, 1987.] **B:** GABAergic synapse. (1) synthesis of GABA from glutamine; (2) transport and storage of GABA; (3) release of GABA via exocytosis; (4) binding to a GABA_A receptor that can be blocked by bicuculline (B), picrotoxin, or strychnine (S) and can also be modified by benzodiazepines, such as valium (V); GABA_B receptors, by contrast, are linked via a G-protein to the opening of K^+ , or the reduction in Ca^{2+} , channels; (5) release of GABA is under the control of presynaptic GABA_B receptors; GABA is removed from the synaptic cleft by uptake into terminals or glia (6); and (7) processing of GABA back to glutamine. [From Shepherd, 1994; Nicoll, 1982; Aghajanian and Rasmussen, 1987; modified from Cooper et al., 1987.]

Ca^{2+} into the presynaptic terminal. This Ca^{2+} entry results from the depolarization associated with the arrival of the action potential. Once the neurotransmitter is released, it rapidly traverses the short distance between the neurons and binds to specific proteins (*receptor molecules*) on the postsynaptic cell. The activation of the receptors by the neurotransmitter may then cause a myriad of postsynaptic responses, many of which are expressed as an altering of the probability that a particular type of ionic channel will be open.

The actual receptor binding site may be part of, or separate from, the macromolecule making up the ionic channel. Examples of ionic channels to which the neurotransmitter directly binds include the glutamate and γ -aminobutyric acid (GABA)-activated channels (see Fig. 2.8) and the nicotinic cholinergic receptor. The latter is activated by acetylcholine (ACh) at the neuromuscular junction, in sympathetic ganglion neurons, and in many other regions of the nervous system. The binding of ACh to the nicotinic postsynaptic receptor induces a conformational change in the ionic channel, thereby opening the “gate” and allowing ions (in this case, Na^+ , Ca^{2+} , and K^+) to flow through the pore (reviewed in Hille, 2001).

An example of a receptor site that appears to be separate from the channel molecule is the muscarinic receptor in the heart, which when activated by ACh results in an increase in membrane K^+ conductance, a response that also occurs in some parts of the brain. This response to ACh is associated with the receptor-mediated activation of an intracellular second messenger known as a G-protein. G-proteins are a class of molecule that require the binding of guanyl nucleotides to be active. The active component (catalytic subunit) of the G-protein is then thought to act as an intermediary between the receptor molecule and the ionic channel (reviewed by Neer, 1995; Neves et al., 2002).

Once a neurotransmitter is released, the length of time that it is present in the synaptic cleft is controlled by either hydrolysis of the transmitter, re-uptake into the presynaptic terminal, uptake into neighboring cells, or diffusion out of the cleft.

Neurotransmission versus Neuromodulation. Neuroactive substances in the nervous system have often been classified as either “neurotransmitters” or “neuromodulators” according to the duration and the functional implications of their actions. Substances released by neurons that have typical neurotransmitter roles cause postsynaptic responses that are both quick in onset (e.g., <1 msec) and relatively short in duration (e.g., less than tens of milliseconds). The summation of phasic excitatory and inhibitory postsynaptic potentials (EPSPs and IPSPs, respectively) and the way in which they interact with the intrinsic electrophysiological and morphological properties of the neuron form to a large extent the manner in which neuronal computations occur.

In contrast, modulatory actions of neuroactive substances are characterized by their prolonged duration and the ability to *modulate* the response of the neuron to other, perhaps more phasic, inputs. Although the distinction between these two types of neurotransmitter actions is not always easy, it is nonetheless useful. Receptors acted on directly by a neurotransmitter are called *ionotropic*, whereas those acted on indirectly by second messengers are sometimes referred to as *metabotropic*.

It is probably safe to say that most neurons in the brain are under the influence of as many as a dozen or more neuroactive substances (Table 2.2). The wide range of cel-

This page intentionally left blank

receptor molecules. In this manner, a neuroactive substance released onto a pyramidal neuron in the cerebral cortex may have a very different effect from the release of the same neurotransmitter onto a relay neuron in the thalamus (see later). Indeed, the same neurotransmitter may have very different, or even opposite, postsynaptic effects on neighboring neurons in the same neuronal region, depending upon the particular function of the neuron in the local circuit.

Many of the ionic currents in neurons are under the control of neuroactive substances. It has become apparent that different neurotransmitters, each acting through its own distinct class of receptor molecules, can modify the same ionic current. For this reason, I review here the more common postsynaptic actions of neurotransmitters in terms of the physiological action rather than the type of neurotransmitter.

FAST POSTSYNAPTIC POTENTIALS

The classic postsynaptic potential (PSP) occurs through a temporally (e.g., milliseconds) and spatially (i.e., local) limited increase in membrane ionic conductance. The relatively brief time course of these PSPs allows neurons to perform a large number of computations within short time periods, limiting the interactions between events that are widely separated in time. Synaptic potentials, especially those brief in duration, are usually classified by whether they increase (excitatory) or decrease (inhibitory) the probability of action potential discharge. However, it is always better to know the actual biophysical and biochemical actions of the neuroactive substance than to refer to them as being just “excitatory” or “inhibitory,” especially when considering the *modulatory* actions of many putative neuroactive substances (see later).

Fast EPSPs. Two main types of brief-duration EPSPs have been identified in the nervous system: those due to the activation of nicotinic receptors by ACh and those caused by the release of excitatory amino acids.

Nicotinic cholinergic responses: Fast nicotinic EPSPs mediated by ACh have so far been shown to occur in the spinal cord, peripheral nervous system, and skeletal muscle. Nicotinic receptors are also located throughout the CNS (e.g., Albuquerque et al., 1995).

The activation of the nicotinic receptor–ionic channel complex by ACh results in a conformational change in the shape of critical portions of this macromolecule, thereby allowing ions to flow through. The nicotinic ionic channel is a “nonselective” cation channel, meaning that positively charged ions (e.g., Na^+ , Ca^{2+} , and K^+) pass through the channel with about equal proficiency. Because of the mixed nature of the ions flowing through the nicotinic channel, the equilibrium (reversal) potential of the nicotinic response, approximately -5 mV, lies between the equilibrium potentials of the various cations (see Fig. 2.2).

The nicotinic receptor-channel is a pentameric structure composed of, in order of mobility on SDS polyacrylamide gels, two α , one β , one γ (expressed in development; replaced by ϵ in adults), and one δ subunit surrounding a water-filled pore. Amino acid sequencing of α subunits, which contain the binding site for receptor activation, revealed the presence of at least eight distinct subtypes, termed $\alpha 1$ – $\alpha 8$. These eight different α subunits ($\alpha 1$, muscle; $\alpha 2$ – $\alpha 8$, neural) differ not only in their primary structure but also in their pharmacological properties and their distribution in the CNS.

The actions of ACh through nicotinic receptors in the nervous system is of particular interest because nicotine, in the form of tobacco products, is still one of the most widely used drugs of addiction. It has been proposed that the activation of dopaminergic neurons in the basal forebrain (ventral tegmental area) may be important in the pleasurable, and addictive, aspects of nicotine use (e.g., Balfour et al., 2000).

Excitatory Amino Acid Responses: A substantial portion of the fast EPSPs in the brain, particularly those in the cerebral cortex and hippocampus, are due to the release of an excitatory amino acid such as glutamate or aspartate. Postsynaptic ionotropic receptors for glutamate have been categorized according to their affinity for three different exogenous agonists: AMPA, kainate, and *N*-methyl-D-aspartate (NMDA). Molecular biological studies of glutamate receptors have revealed that each of these three subgroups is encoded for by a number of different genes, including GluR1–4 for AMPA receptors; GluR5–7, KA1, and KA2 for kainate receptors; and NR1 and NR2A–D for NMDA receptors (for a review, see Madden, 2002). Hetero-oligomers formed by the different subunits generated by these genes are of a wide variety and exhibit varying electrophysiological and pharmacological properties, depending upon the combinations of subunits expressed.

Activation of excitatory amino acid receptors underlies fast glutamatergic EPSPs. The PSPs mediated by AMPA and kainate receptors, like those associated with nicotinic channels, are typically caused by an increase in a mixed cation conductance (mainly Na^+ and K^+ , but sometimes Ca^{2+} as well) such that the reversal potential is approximately 0 mV (see Hollmann and Heinemann, 1994). These synaptic potentials have a very short delay from the arrival of the action potentials at the presynaptic terminal to the appearance of the PSP and a rapid rate of rise. The falling phase is much slower, being determined in large part by the membrane properties of the neuron (see Fig. 2.9B).

In contrast to the fast PSPs mediated by AMPA-kainate receptors, the action of glutamate through NMDA receptors is more complicated (reviewed by Ascher and Nowak, 1987). Stimulation of NMDA receptors results in the activation of a voltage-dependent current that is carried not only by Na^+ and K^+ but also, importantly, by Ca^{2+} . The voltage-dependent nature of this NMDA receptor-mediated current is due to the differential block of the ionic channel by magnesium ions (Mg^{2+}) at different membrane potentials (Mayer et al., 1984). At resting membrane potential (e.g., -75 mV), the driving force on Mg^{2+} , which is concentrated on the outside of the cell, to enter the neuron is quite high. Because of this, Mg^{2+} ions compete with Ca^{2+} and Na^+ ions for access to the pore of the channel. Because Mg^{2+} ions cannot flow through the pore, the channel is effectively blocked whenever one of the ions enters, thereby reducing the amount of time that the channel is open and conducting (see Fig. 2.9C).

When the cell is depolarized, the tendency for Mg^{2+} to fill the pore is substantially reduced, thereby lessening the block and allowing a larger $\text{Na}^+/\text{Ca}^{2+}/\text{K}^+$ current to flow. Because of this voltage dependence, activation of a glutaminergic synapse onto a neuron at resting membrane potentials may result in a fast EPSP mediated through the activation of kainate and AMPA (also known as quisqualate) receptors with little contribution of NMDA receptor-mediated current, even though glutamate may be binding to these receptors (Fig. 2.9C). However, repetitive activation of the same synapse may cause a large depolarization of the cell through temporal summation of the

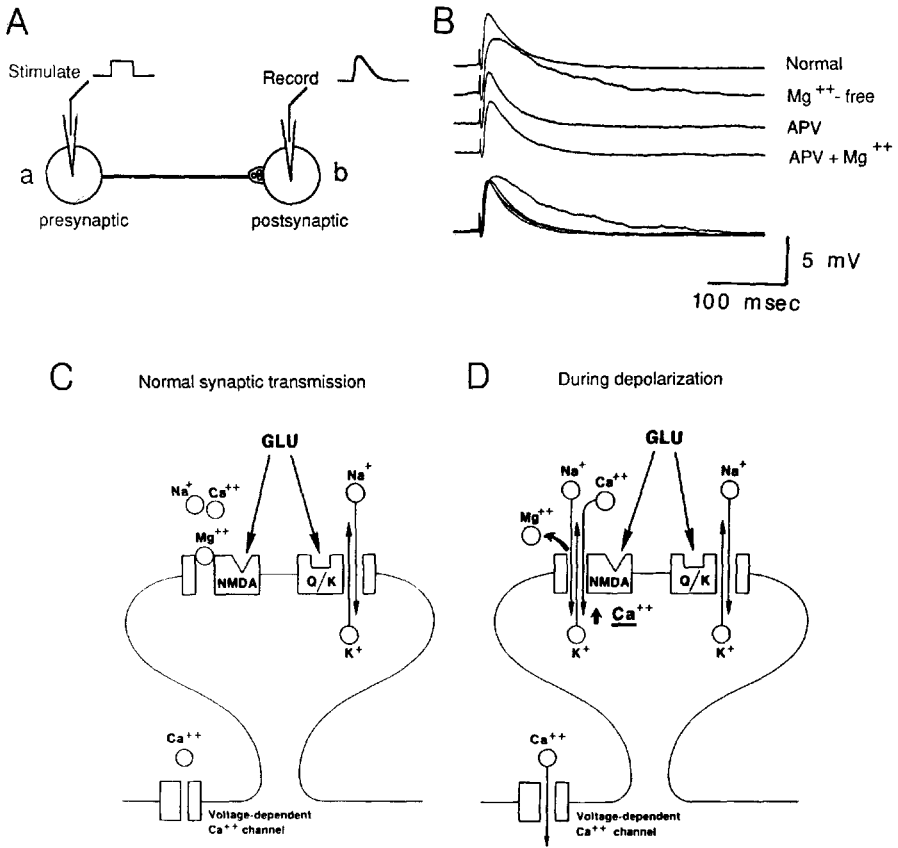


Fig. 2.9. Synaptic potentials mediated by the release of glutamate. **A:** Schematic diagram of experimental protocol in which the actions and pharmacology of monosynaptic connections between cultured cortical pyramidal cells is investigated. Intracellular recordings are used to stimulate a generator cell (a) that is monosynaptically connected to a follower cell (b). **B:** Activation of an action potential in the generator cell (a) causes a monosynaptic EPSP in the follower cell (b) through the stimulation of AMPA and kainate receptors (top trace; normal). Removal of Mg^{2+} from the medium bathing the cultures enhances the late components of this EPSP (second trace; Mg^{2+} -free). Addition of the NMDA receptor antagonist APV abolishes this late component, indicating that it was due to the activation of NMDA receptors (third trace; APV). Returning Mg^{2+} to the bathing medium now has no additional effect on the EPSP (fourth trace, Mg^{2+}). At the bottom of **B**, the traces are superimposed for comparison. These data illustrate that the release of glutamate can activate AMPA/kainate and NMDA receptors and that NMDA, but not AMPA/kainate, ionic channels can be blocked by Mg^{2+} ions. **C:** Schematic summary diagram illustrating that glutamate release from the presynaptic terminal at a low frequency ("normal synaptic transmission") acts on both the NMDA and AMPA/kainate type of receptors. Na^+ and K^+ flow through the AMPA/kainate channel, but not through the NMDA receptor channel due to Mg^{2+} block. **D:** Depolarization of the membrane potential, or activation of the glutamatergic inputs at a high frequency, relieves the Mg^{2+} block of the NMDA channel, thereby allowing Na^+ , K^+ , and, importantly, Ca^{2+} to flow through the channel. Depolarization due to the synaptic potential now also activates other voltage-dependent channels, such as those that conduct Ca^{2+} . [**B** from Huettner and Baughman, 1989; **C** and **D** from Nicoll et al., 1988.]

unitary PSPs. The more that these PSPs depolarize the cell, the more the degree of magnesium block will be removed, and thus the greater will be the activation of the NMDA current (Fig. 2.9D). Because NMDA channels conduct Ca^{2+} as well as Na^{+} and K^{+} , Ca^{2+} will flow into the postsynaptic cell and, by activating further biochemical mechanisms, can result in a *potentiation* of the strength of the unitary excitatory PSP. This enhancement of the PSP can last for prolonged periods (hours, days, and maybe longer) and therefore is known as LTP (see Bliss and Collingridge, 1993; Malinow and Malenka, 2002 for review). LTP is one of the leading models of the mechanisms by which synapses change their efficacy to participate in the encoding of memories in the nervous system (see Chaps. 10–12).

In addition to the activation of fast EPSPs, glutamate may also activate slow (seconds to minutes) EPSPs through the activation of glutamate “metabotropic” receptors (see later).

Fast IPSPs. Postsynaptic potentials that are quick in onset and inhibit the postsynaptic activity of the neuron are known to be mediated by two different neurotransmitters in the CNS: GABA and glycine.

GABA-Mediated IPSPs. GABA is the major inhibitory neurotransmitter of the nervous system. GABA-releasing cells are present throughout all levels of the neuraxis. In the cerebral cortex and thalamus, they account for approximately 20%–30% of all neurons. Neurons that use GABA as a neurotransmitter form a diverse group, with several different morphologies specific for their own role in neuronal processing. They are instrumental in defining and confining the response properties not only of single neurons but also of large neuronal circuits. They figure prominently as interneurons in the types of inhibitory circuits illustrated previously in Chap. 1. It would be fair to say that without GABAergic neurons the nervous system would not function in any logical manner.

There are three major types of GABA receptor, which are referred to as GABA_A , GABA_B , and GABA_C (Bowery et al., 2002; Jentsch et al., 2002). Here we consider only the GABA_A receptor (GABA_B - and GABA_C -mediated responses are discussed later). Many fast IPSPs in the brain are believed to result from the release of GABA acting upon the GABA_A subclass of receptor (see early IPSP, Fig. 2.10). Binding of GABA to this class of receptor opens ion channels that are selective for Cl^{-} ions, and therefore the reversal potential of GABA_A -mediated responses is at the equilibrium potential for Cl^{-} (i.e., ≈ -75 mV). Like the fast EPSPs in the nervous system, fast GABA_A -mediated IPSPs possess a rapid rising phase and a slower decay. These IPSPs are only tens of milliseconds in duration and are involved in rapid computations by neuronal networks (see Chap. 1).

GABA_C receptors also conduct Cl^{-} ions and are most pronounced in the retina, although it is likely that they will be found in other parts of the CNS (see Bormann and Feigenspan, 1995).

Glycine-Mediated IPSPs. Glycinergic interneurons were first identified in the spinal cord and the brainstem. Glycine inhibits neuronal activity by increasing a Cl^{-} conductance similar to that activated by GABA (see Jentsch et al., 2002). Recent evidence suggests that glycine also serves as a classic neurotransmitter function in the forebrain

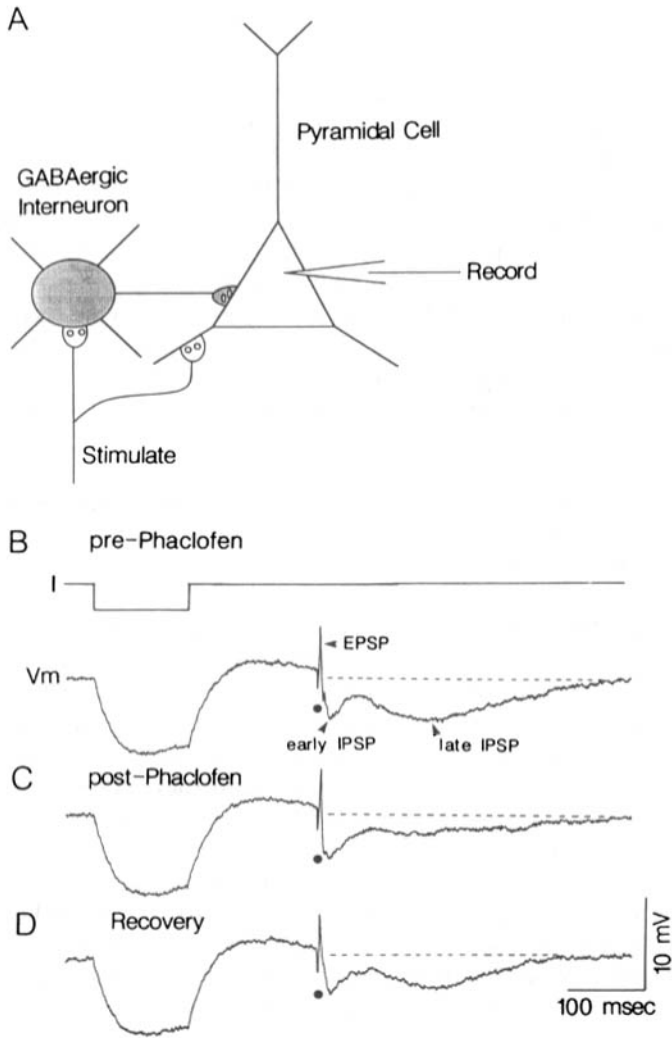


Fig 2.10. Synaptic potentials generated in cortical pyramidal cells. **A:** Schematic diagram of stimulation and recording situation. Stimulation of afferent fibers activates both pyramidal cells and GABAergic interneurons, which subsequently inhibit pyramidal cells. **B:** Intracellular recording from a human cortical pyramidal cell during stimulation of ascending axons. Injection of a hyperpolarizing current pulse (I) is used to investigate the apparent input resistance of the neuron. Electrical stimulation (dot) results in the generation of a fast EPSP followed by an early (fast) and late (slow) IPSP. Activation of the axons excites local GABAergic interneurons that subsequently release GABA onto the recorded pyramidal cell. GABA then activates both GABA_A and GABA_B receptors. Activation of GABA_A receptors causes an increase in Cl⁻ conductance and underlies the early IPSP, whereas activation of GABA_B receptors causes an increase in K⁺ conductance and is responsible for the generation of the late IPSP. **C:** Local application of the GABA_B-specific antagonist phaclofen substantially reduces the late IPSP, confirming that this PSP is due to the activation of GABA_B receptors. The effect of phaclofen is reversible (**D**).

(Betz, 1991; Trombley and Shepherd, 1994). Very low doses of glycine can greatly potentiate the actions of glutamate at NMDA receptors (Johnson and Ascher, 1987). This potentiating action occurs at sufficiently low doses that even the concentrations of glycine occurring in the extracellular fluid are large enough to have a significant effect.

SLOW SYNAPTIC POTENTIALS

Like fast PSPs, slow PSPs are found at all levels of the nervous system. They have a large variety of sizes, shapes, and effects on the functional properties of neurons and neuronal circuits. Because of their delayed onset and prolonged duration, these PSPs are probably more involved in the regulation of the *excitability* of single neurons and neuronal circuits as opposed to underlying the relatively high frequency transfer of information.

Increase in K^+ Conductance. Applications onto neurons of a large variety of putative neurotransmitters, including ACh, adenosine, norepinephrine, serotonin, GABA, dopamine, and various peptides, have been found to cause an increase in membrane K^+ conductance (gK; Fig. 2.10 and Table 2.2) (reviewed in Nicoll et al., 1990; McCormick, 1992). This occurs through a specific subtype of neuronal receptor for each neuroactive substance. Although all of these substances have the ability to increase K^+ conductance in some region of the nervous system, the nonhomogeneous distribution of receptors that mediate this response means that some neurons exhibit it and others do not. For example, the application of ACh to GABAergic interneurons in the feline thalamus results in an *increase* in gK, whereas in neighboring thalamocortical relay cells, this neurotransmitter causes a *decrease* in gK (see McCormick, 1992; Pape and McCormick, 1995; see Chap. 8). Furthermore, in many regions of the nervous system there is convergence of different neuroactive substances, with each one generating an increase in gK in the same postsynaptic neuron. For example, hippocampal pyramidal cells respond to serotonin, GABA (through GABA_B receptors), and adenosine with an increase in the same K^+ conductance (Nicoll et al., 1990; see Chap. 11). In this manner, a variety of neuroactive substances can activate or inactivate the same ionic currents in a given neuron and perhaps even converge onto the same ionic channel.

Functionally, an increase in membrane K^+ conductance is considered inhibitory in that it usually decreases the probability of action potential discharge, and this can have important functional consequences. For example, GABA can increase both gCl (through GABA_A or GABA_C receptors) and gK (through GABA_B receptors); the result is a fast GABA_A-mediated increase in gCl followed by a slow GABA_B-mediated increase in gK in the postsynaptic neuron (see late IPSP, Fig. 2.10) (e.g., Dutar and Nicoll, 1988; Kim et al., 1997). In addition, there are many differences between the fast and slow GABA-mediated IPSPs other than just their time course. The conductance increase associated with the late IPSP is much smaller than that associated with the fast IPSP even though the amplitude of the voltage deviation associated with each may be similar. Indeed, if the membrane potential is negative to E_{Cl} , the fast IPSP will be *depolarizing* (although it is still inhibitory), whereas the late IPSP will still be hyperpolarizing. In addition, the GABA-activated late IPSP is mediated through a second-messenger system (G-proteins), whereas the fast IPSP is the result of GABA binding to a receptor located directly on the ion channel.

These physiological differences make fast IPSPs more of a *shunting* inhibition (i.e., the membrane potential of the cell is held close to E_{Cl} and the input resistance of the cell is “shunted”), and the late IPSP operates more through the *hyperpolarization* of the neuron. Fast IPSPs are useful for local (e.g., particular subparts of the cell) “yes-no” decisions, whereas the late IPSP is useful for the *modulation* of the overall excitability of the neuron. The restricted time and space domains of the fast IPSPs allow them to participate in relatively high-frequency neuronal processing, and the slow IPSP is important for setting a particular level of excitability in the neuron for more prolonged periods of time.

The postsynaptic morphological locations of IPSPs are also very important in determining their consequences for processing within synaptic circuits. Many types of GABAergic neurons form synaptic contacts at specific locations of the postsynaptic neuron. For example, *chandelier cells* of the cerebral cortex give rise to chains of synaptic terminals on the axon hillocks of cortical pyramidal cells (see Chap. 12), whereas *basket cells* give rise to a “basket” or “pericellular nest” of terminals around the cell bodies of pyramidal neurons. In this way, both of these inputs have powerful effects on the output of the entire neuron. It may even be possible for the chandelier cell to prevent the propagation of an action potential down the axon after its generation in the cell body and/or dendrite or to determine the precise timing of action potential generation.

The opposite extreme of the above two examples of a rather global inhibition by GABA of the output of the neuron is found in the very localized synaptic processing in dendritic microcircuits (see Chap. 1). At this level of organization, individual GABAergic terminals may have effects that are relatively independent of one another, as well as independent of the output activity of the neuron itself. In these situations, the GABAergic process may affect only a particular portion of the postsynaptic dendritic tree or, perhaps, only particular synaptic terminals. Numerous examples of GABAergic contributions to processing in synaptic glomeruli, dendritic trees, and other types of microcircuits are discussed in subsequent chapters.

Decrease in K^+ Currents. Neuroactive substances can not only increase, but also decrease, neuronal K^+ currents. To date, there are four different K^+ currents that can be decreased in amplitude in response to various neurotransmitters: I_{AHP} , I_M , I_A , and a resting “leak” K^+ current that I shall denote as $I_{K,leak}$.

Decrease in I_{AHP} : I_{AHP} has been shown to be decreased by a number of putative neurotransmitters (norepinephrine, ACh, serotonin, histamine, glutamate, etc.) (reviewed in Nicoll et al., 1990; McCormick, 1992). In the case of norepinephrine, the decrease in I_{AHP} is achieved through an increase in the intracellular activity of a second messenger, cyclic adenosine monophosphate (cAMP) (Madison and Nicoll, 1986b; Pedarzani and Storm, 1993).

As stated previously, I_{AHP} contributes substantially to spike frequency adaptation. Therefore, block of this current greatly reduces the tendency for cells to slow down their firing rate during maintained depolarization (Fig. 2.11). This is an important effect because it allows a neurotransmitter to increase the response of a cell to barrages of EPSPs with little or no change in the resting membrane potential, or the response to IPSPs. Indeed, if the putative neurotransmitter simultaneously increases membrane conductance to K^+ or Cl^- as well as blocking I_{AHP} , the result may actually be an in-

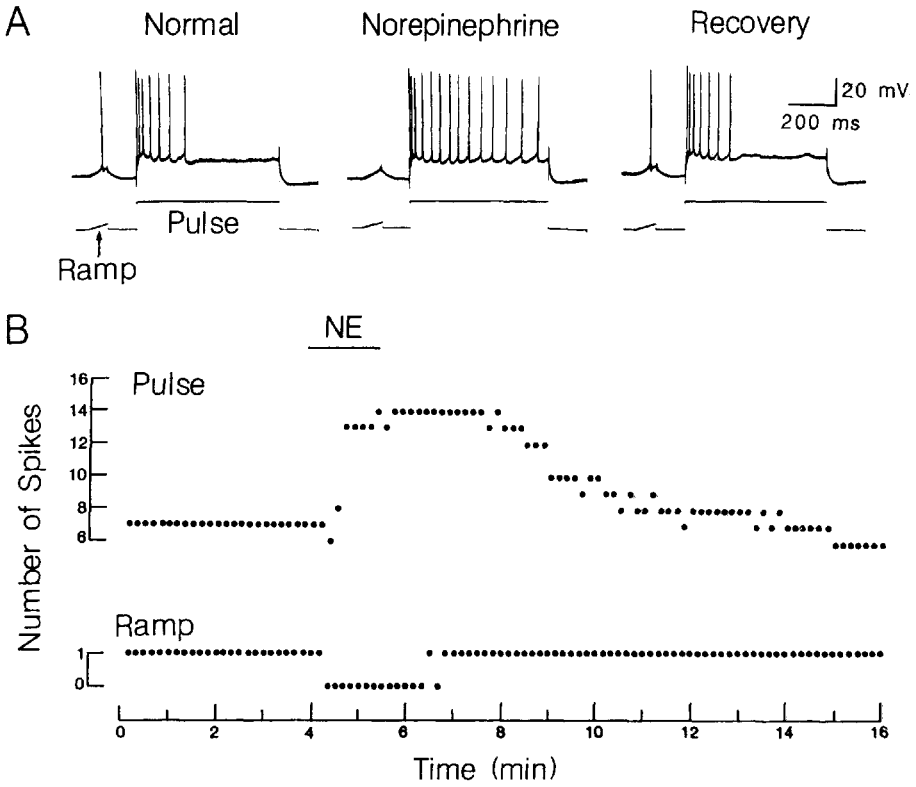


Fig. 2.11. Effect of norepinephrine on the excitability of cortical pyramidal neurons. The response of this hippocampal pyramidal neuron to two different types of input was examined: a small depolarizing ramp (to mimic weak EPSPs) and a prolonged depolarization (to mimic a train of strong EPSPs). **A**: In normal condition, the small ramp input causes the generation of a single action potential (asterisk), whereas the prolonged depolarization results in a train of action potentials that show strong spike frequency adaptation ([A, left]). Addition of norepinephrine to the bathing medium results in a small hyperpolarization of the membrane potential (not shown). During the hyperpolarization, the small depolarizing input no longer generates an action potential, whereas the response to the prolonged input is actually potentiated due to the block of spike frequency adaptation (A, norepinephrine). The reduction in spike frequency adaptation is a secondary effect due to the block of I_{AHP} (not shown). This effect of norepinephrine is fully reversible (A, recovery). **B**: Graphic representation of the data in A. The generation of an action potential by the small ramp input is blocked, whereas the response to the prolonged input is greatly enhanced. In this manner, norepinephrine can increase the “signal-to-noise” ratio of the cell. [From Madison and Nicoll, 1986a.]

crease in “signal-to-noise” ratio. The baseline spontaneous firing of the cell will be reduced by the increase in K^+ and/or Cl^- currents, whereas the cell’s response to barrages of large EPSPs may actually be enhanced by the decrease in I_{AHP} (see Fig. 2.11).

Decrease in I_M : As stated earlier, I_M is a K^+ current that is slowly (tens of milliseconds) activated by depolarization of the membrane potential above approximately -65 mV (Brown and Adams, 1980; Marrion, 1997). This current has been shown to be potently reduced by stimulation of muscarinic receptors by ACh. Like I_{AHP} , I_M con-

tributes to spike frequency adaptation; blocking it subsequently increases the response of a neuron to barrages of EPSPs. Because I_M is active only at depolarized potentials, its blockade may have little effect on the cell's resting membrane potential or response to IPSPs. The M-current may be reduced following the activation of a variety of receptors, including some types of peptide receptors (see Marrion, 1997).

Decrease in I_A : Many of the different K^+ currents in neurons are differentiated by different rates of activation and inactivation. One of these, the A-current, and probably others, can be modulated by the application of neurotransmitters (Aghajanian, 1985). Because I_A contributes to an increase in the interval between action potentials during certain types of neuronal activity, the block of I_A will enhance the response of the neuron by increasing the frequency of action potential discharge.

Decrease in Ca^{2+} Currents: Numerous putative neurotransmitters, including ACh, norepinephrine, serotonin, and GABA, can reduce the flow of Ca^{2+} across the membrane (see Tsien et al., 1988; Stea et al., 1995). The functional consequences of neurotransmitter suppression of Ca^{2+} currents has not been well studied in the CNS. One possible effect is related to the actions of neurotransmitters at presynaptic terminals. The amount of transmitter that is released after the invasion of the terminal by an action potential is under the control of neuroactive agents binding to receptors located on these terminals. In most (perhaps all) systems, the binding of the transmitter that is released by the terminal *reduces* the quantity released by subsequent action potentials. This *autoinhibition* then forms a negative feedback loop that is useful for regulating the concentration of transmitter in the area of the synaptic cleft. The ionic mechanisms of this negative feedback are not known. However, because neurotransmitter release is highly dependent upon Ca^{2+} entry, transmitter-mediated decreases in Ca^{2+} currents may be involved.

Possible Gating Actions of Neurotransmitters. As discussed previously, many different types of neurons in the nervous system possess two intrinsic and physiologically distinct firing modes: single spike and burst activity (e.g., Llinás and Yarom, 1981a,b; Jahnsen and Llinás, 1984a,b; Llinás, 1988). The cell's membrane potential determines in part which of these two firing patterns the neuron will exhibit. Burst firing occurs in response to excitatory inputs whenever the membrane potential is negative to approximately -65 mV, whereas single-spike activity occurs at membrane potentials positive to approximately -55 mV (see Fig. 2.5D and E). Therefore, a neuroactive substance that activates a K^+ conductance can actually increase the probability of a neuron firing by hyperpolarizing the cell into the burst firing mode of action potential generation (e.g., from -60 to -70 mV). In this situation, the increase in membrane conductance is acting more as a "switching" or modulatory mechanism than as a strict "yes-no" inhibition (McCormick, 1992). Likewise, decreasing resting conductance to K^+ is an effective mechanism by which a neuron can be tonically depolarized out of the burst firing mode and brought closer to threshold for generation of the more unmodulated single-spike discharge (Fig. 2.12). Such changes in membrane potential have been found to occur during shifts in arousal (Hirsch et al., 1983) and may underlie the well known shift in the characteristics of the electroencephalogram (EEG) from synchronized slow waves to desynchronized, higher frequencies during increases in arousal (e.g., Moruzzi and Magoun, 1949; Steriade et al., 1993).

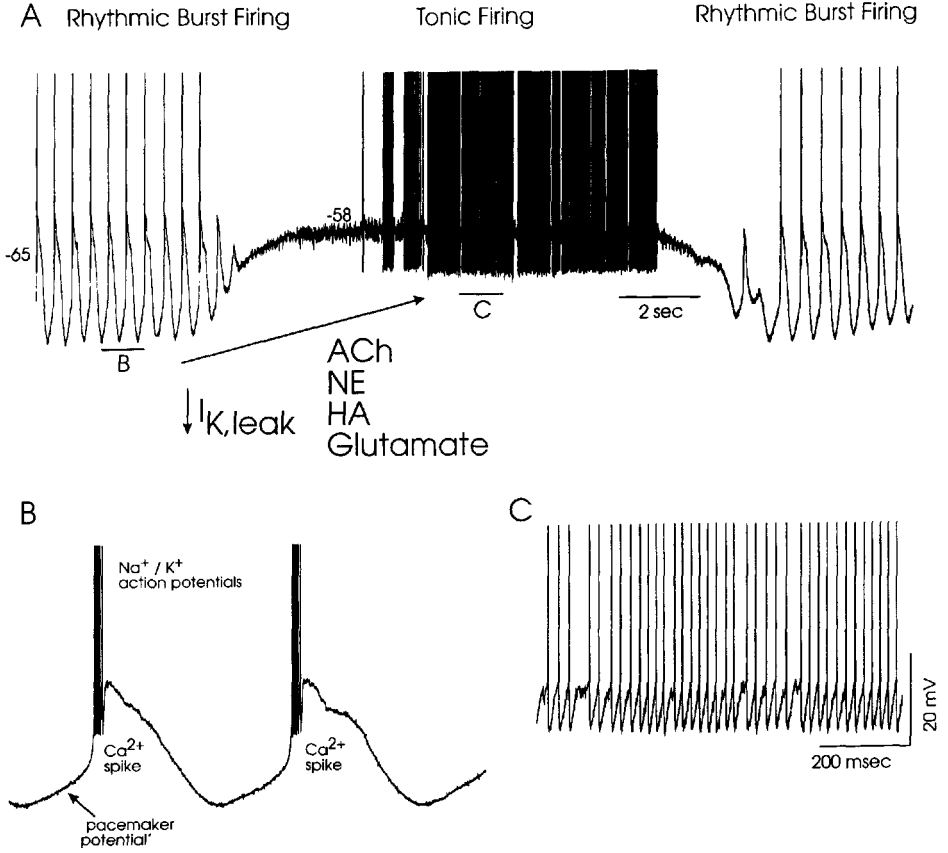


Fig. 2.12. Neurotransmitters control the firing mode in thalamic relay neurons. **A**: Thalamic relay neurons can spontaneously generate rhythmic bursts of action potentials (Rhythmic Burst Firing) through the generation of repetitive low-threshold Ca^{2+} spikes (see **B**). Application of a variety of neurotransmitters, including acetylcholine (ACh), norepinephrine (NE), histamine (HA), and glutamate, can reduce a “leak” K^+ current, $I_{K,leak}$, and therefore depolarize the thalamic cell. This depolarization inactivates the low threshold Ca^{2+} current and therefore blocks rhythmic burst firing. Now the cell generates tonic trains of action potentials. Once the block of $I_{K,leak}$ wears off, the cell returns to rhythmic burst firing. **B**: Expansion of the rhythmic burst firing in **A** illustrating the rhythmic Ca^{2+} spikes interspersed by a “pacemaker potential.” **C**: Expansion of part of the tonic firing in **A**. [Modified from McCormick and Pape, 1990.]

Retrograde Signaling: Synaptic Transmission in Reverse. The overwhelming majority of synaptic communication in the brain occurs through the traditional mechanism: vesicular release from the presynaptic terminal followed by diffusion of the neurotransmitter to receptors on the postsynaptic neuron. However, it is becoming increasingly apparent that signaling can also occur in reverse. In some cases, the postsynaptic neuron can release neuroactive agents that diffuse locally, bind to receptors on presynaptic terminals, and influence the subsequent release of neurotransmitter. Perhaps the best example of this retrograde signaling is in the cannabinoid pathway. *Cannabis sativa* derivatives such as marijuana and hashish have been used medicinally and recreation-

ally for thousands of years. The active ingredient in these, Δ^9 -tetrahydrocannabinol (Δ^9 -THC), binds to a cannabinoid receptor (CB1) typically found on a subset of presynaptic terminals within wide regions of the nervous system and reduces the probability of release of synaptic transmitter. The brain contains its own endogenous cannabinoids. Depolarization of postsynaptic cells can result in an influx of Ca^{2+} and the subsequent synthesis and release of an endogenous cannabinoid (e.g., anadamide). This agent then diffuses locally, resulting in a long-lasting inhibition of presynaptic terminals (reviewed in Wilson and Nicoll, 2002). Through this mechanism, the postsynaptic neuron does not have to only listen to its presynaptic partners; it can also talk to them.

INTRINSIC AND SYNAPTIC CURRENTS: PUTTING IT ALL TOGETHER

With our new armament of knowledge of the intrinsic properties of neurons and how they may be affected by neurotransmitters, we can proceed (with due caution) to propose a scenario of how synaptic computations may be implemented and modulated in a representative neuron. We take as our example one of the most abundant and important neuronal cell types in the human brain: the cerebral cortical pyramidal cell (Chaps. 1 and 10–12).

Like neurons in most other parts of the brain, cortical pyramidal cells receive excitatory, inhibitory, and modulatory inputs from a variety of sources. Putative glutamergic synapses, which have typical fast excitatory actions, are found on the spines of apical and basilar dendrites (Fig. 2.13). Notable sources of excitatory inputs are other pyramidal cells (located in neighboring or distant cortical regions), spiny stellate neurons of layer IV, and inputs from the thalamus (see Chap. 12). In contrast to excitatory inputs, GABAergic inhibitory synapses are found on the soma, proximal and distal dendrites, and initial segment of the axon; they arise largely from intrinsic cortical interneurons, which are morphologically and functionally heterogeneous. Putative neuromodulatory substances arrive from a variety of subcortical (cholinergic, noradrenergic, and serotonergic) and intracortical (cholinergic and peptidergic) neurons. Their synaptic contacts on pyramidal neurons are found largely on dendrites. Some types of GABAergic neurons also contain, and may release, one or more peptides. The ionic actions of these peptides and how they interact with the actions of GABA are not yet known.

Let us imagine that our cortical pyramidal cell is in the visual cortex and that, although the animal is awake and attentive, the cell is not yet receiving any specific visual input. The resting potential of our hypothetical cell will probably be somewhere around -65 mV, depending upon the state of input from the slowly acting neurotransmitters, especially those (e.g., ACh) that can alter the level of resting K^+ conductance. This resting potential is about 10 mV below (more hyperpolarized than) the threshold of around -55 mV for the generation of action potentials by a cortical pyramidal neuron.

Now let us stimulate the visual receptive field of our cell with an adequately adjusted light stimulus to the retina (e.g., a moving bar of light). This input will first cause excitation of the thalamic neurons (see Chap. 8). Because the animal is awake and at-

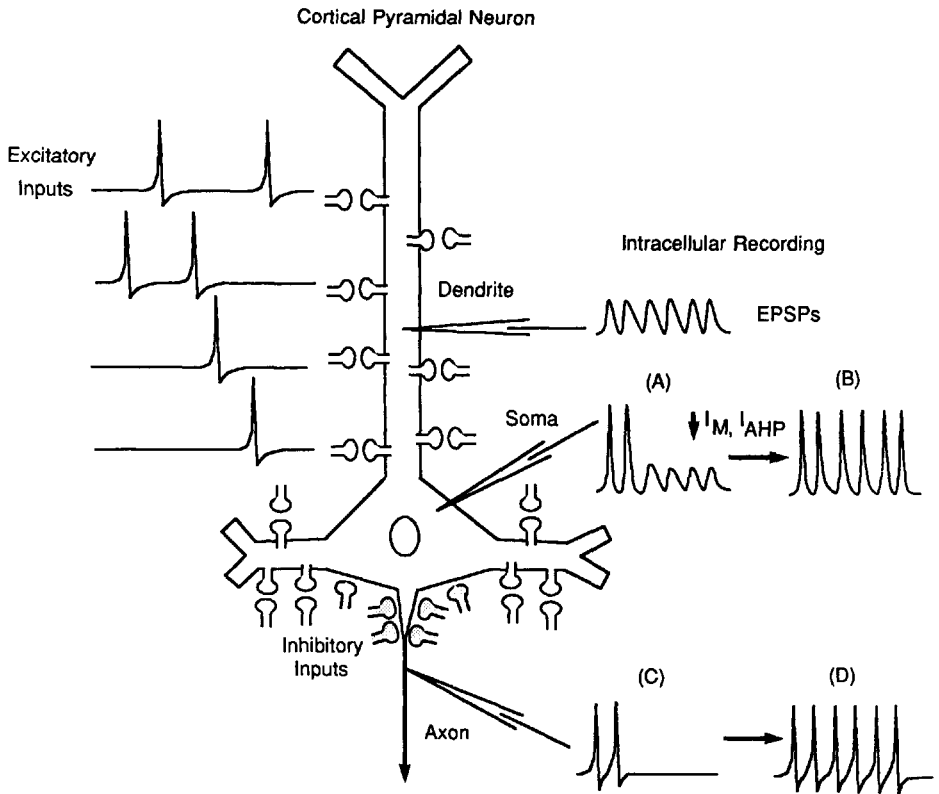


Fig. 2.13. Effect of activation of excitatory inputs to a cortical pyramidal cell. A train of action potentials arriving at different synaptic endings on the apical dendrite of the pyramidal cell results in the generation of a train of EPSPs. The first two EPSPs generate action potentials in the somatic region, and the last four fail due to activation of I_M and I_{AHP} (A). This is further reflected in the axonal output of the neuron (C). Block of these two currents reduced spike frequency adaptation and allows all six EPSPs to generate action potentials (B and D). See text for details.

tentive, the thalamic neurons respond to the input in a one-spike-out-per-spike-in fashion (e.g., Fig. 2.5D) and in turn give rise to a train of action potentials that reach some of the presynaptic terminals onto our cell. Each action potential causes an increase in $[Ca^{2+}]_i$ in the presynaptic terminal that in turn causes the release of excitatory transmitter from a variable number of synaptic vesicles in a probabilistic manner (see Chaps. 1 and 3). The transmitter travels across the synaptic cleft and binds to specific receptor molecules on the postsynaptic spine, increasing the probability that certain ionic channels (assume they conduct Na^+ and K^+ ions) will be in the open and conducting state. In this manner, each presynaptic spike will cause an EPSP in the postsynaptic dendrite (see Fig. 2.13). The exact amplitude-time course of each EPSP depends upon a large number of factors, including the amount of transmitter released, the density of postsynaptic receptor molecules, the sensitivity of the postsynaptic element to the transmitter, the size and shape of the postsynaptic element, and, finally, the amplitude and

distribution of active currents that the postsynaptic element possesses. Indeed, the “efficacy” of each synaptic connection is not a static number, because it is probably modified during the acquisition of new information, as well as new strategies to analyze that information, perhaps through a process similar to LTP (see Fast EPSPs).

In order for the barrage of EPSPs generated by the train of inputs from the thalamus to cause our cell to fire, it must cause the output decision point of the cell (the cell body and axon hillock in this case) to rise above firing threshold (e.g., -55 mV). To do this, the EPSPs must spread from their points of generation in the dendrites, through the cell body, to the axon hillock. What happens to these EPSPs as they make this trip is determined by the intrinsic properties of our cell and the state of other neuroactive substances impinging upon it. The dendritic EPSPs will probably be large enough to activate $I_{Na,p}$, or a Ca^{2+} current and thereby receive an extra “boost” from these depolarizing currents. This enhancement is needed to help overcome the fact that cell membranes are not perfect insulators, and some of the current will leak out, thereby reducing the size of the EPSP as it travels toward the cell body. If the train of EPSPs comes at a sufficiently high frequency, they will exhibit temporal summation, whereas EPSPs that arise from more than one point in the cell will also exhibit spatial summation. If the summated EPSP is large enough, it may be capable of causing the generation of a dendritic Na^+/Ca^{2+} -mediated action potential that will, of course, greatly enhance and transform the response of the cell to the synaptic input (see Fig. 2.5C). However, for simplicity, assume that the threshold for the generation of a dendritic Na^+/Ca^{2+} spike is not reached.

Now consider the situation in which many of the EPSPs in the train are large enough to cause the generation of an action potential in the cell body and axon hillock. In this circumstance, the initial EPSPs in the train will be more likely to cause the generation of spikes than the latter ones due to the progressive activation of I_{AHP} and I_M , both of which contribute to spike frequency adaptation (see Fig. 2.13A and C). Thus, although the cell may fire to the initial few EPSPs, the later ones will not reach firing threshold and the cell’s firing will cease. This is where our modulatory transmitters come into play. If we were to arouse our animal such that there were an increase in the release of, for example, norepinephrine and ACh, then I_{AHP} and I_M (and perhaps $I_{K,l}$) would be reduced. Reduction in these K^+ currents would enhance the response of the neuron by reducing spike frequency adaptation as well as by moving the cell’s membrane potential closer to firing threshold (see Fig. 2.13B and D).

As the visual stimulus moves out of the cell’s excitatory receptive field and into those of neighboring cortical neurons, our pyramidal cell may now be actively inhibited through the connections of intrinsic GABAergic neurons. These barrages of IPSPs will meet with many of the constraints as did the previous EPSPs, although they may occur in a more “linear” portion of the membrane potential (i.e., between -65 and -75 mV). The fast GABAergic IPSPs will be important in terminating the residual excitation from the previous barrage of EPSPs by causing an increase in Cl^- conductance. The influential position of the IPSPs on or near the soma and initial portion of the axon (axon hillock) makes them particularly effective.

Now consider the situation when the animal or person falls to sleep. As drowsiness sets in, the rate of release of the ascending modulatory neurotransmitters, such as ACh, norepinephrine, and histamine, will decrease. The decreased release of these modula-

tory transmitters will result in a hyperpolarization of many cell types owing to increases in various K^+ conductances. For example, thalamocortical neurons in the thalamus (see Chap. 8) may hyperpolarize by up to 20 mV, owing to the increase in a resting K^+ conductance that is normally reduced by the release of these agents. This hyperpolarization of neurons in the CNS and the increase in amplitude of various K^+ currents result in a decreased excitability of these cells. In addition, the hyperpolarization results in the removal of inactivation of some ionic currents, most notably the low-threshold Ca^{2+} current I_T . The removal of inactivation of I_T allows for the generation of low-threshold Ca^{2+} spikes, and the activation of these in thalamocortical networks results in the generation of the spontaneous rhythms of sleep (Steriade et al., 1993).

The presentation of a visual (or other sensory) stimulus to our drowsy or sleeping friend will now result in a reduced response in the visual cortex: his or her brain will be less responsive and less able to respond quickly. This reduction in responsiveness becomes more and more pronounced as the person falls deeper and deeper in sleep.

Many of the properties outlined for our hypothetical cortical pyramidal and thalamic neurons can be generalized to neurons in all regions of the nervous system. However, each type of neuron is an individual and generalizations must be used with caution so as not to neglect the important features of each neuronal type that allow it to perform its unique brand of cellular processing and thereby make its specific contributions to the synaptic circuits of which it is a part.

This page intentionally left blank

SPINAL CORD: VENTRAL HORN

ROBERT E. BURKE

The spinal cord is a remarkably complex system of neurons that subserves sensory, motor, and autonomic functions. The modern era of research on synaptic organization within the mammalian central nervous system (CNS) began with the pioneering work of the English physiologist Sir Charles Sherrington on spinal cord reflexes (see Creed et al., 1932). These stereotyped motor responses to specific sensory stimuli in intact animals are much the same in reduced preparations that can be studied in the laboratory. Sensory inputs to and motor outputs from the spinal cord are physically accessible and functionally meaningful; therefore, it is possible to attach behavioral significance to the organization of the synaptic linkages between them—an elusive goal in most other parts of the CNS. More recently, the analysis of spinal circuits has expanded to include the mechanisms that generate and control rhythmic movements like locomotion and scratching that can also be produced in reduced preparations. This chapter focuses on the organization of neuronal elements and synaptic interconnections in the ventral horn that are relevant to the control of movement.

Why limit the focus to the ventral horn? Certainly the dorsal horn contains circuitry at least as complex as that in more ventral regions (Brown, 1981; Willis and Coggeshall, 1991). However, dorsal horn circuitry is largely devoted to processing sensory information from primary afferents that is destined for supraspinal centers. This function is less amenable to a full input-to-output circuit analysis than the reflex circuitry located in more ventral regions.

NEURONAL ELEMENTS

There are three major categories of neuronal elements in the spinal cord: (1) axons that originate either from sensory afferent neurons in the dorsal root ganglia or descending fiber systems that carry motor command signals into the cord from the supraspinal brain; (2) spinal neurons with axons that leave the cord to innervate skeletal muscle fibers (motoneurons) or autonomic ganglia (preganglionic neurons); and (3) spinal interneurons with axons that terminate exclusively within the CNS, either within the spinal cord itself (interneurons) or that leave the spinal cord to project to supraspinal targets (tract cells). Some of the latter also have local collateral branches, so these last categories are not mutually exclusive.

The diagram in Fig. 3.1A illustrates some aspects of the structure of the spinal cord as viewed in cross section. In contrast to cerebral hemispheres and cerebellum, where large bundles of axons (white matter) are located inside cortical regions dominated by neuron cell bodies, the spinal cord is organized in an inside-out pattern. The outermost part of the spinal cord is white matter, composed of axons from spinal and supraspinal neurons running up and down the long axis. The inner gray matter core contains the cell bodies of spinal neurons and most of the synaptic neuropil in which they interact. The dorsal and ventral horns of the gray matter can be subdivided into layers, numbered I through X, on the basis of neuron sizes and densities (“cytoarchitectonic” divisions; Rexed, 1952; left half of Fig. 3.1A). Identifiable classes of spinal interneurons (e.g., “Ia/Ib INs,” “Ia INs,” “Renshaw INs”) and motoneurons (or motor neurons, if you prefer) occupy predictable parts of the ventral horn gray matter, although there are few precisely delimited “nuclei” that match those found in the supraspinal brain. The intermixing of different categories of interneurons within the spinal gray matter has made it technically difficult to work out the synaptic organization of specific functional circuits.

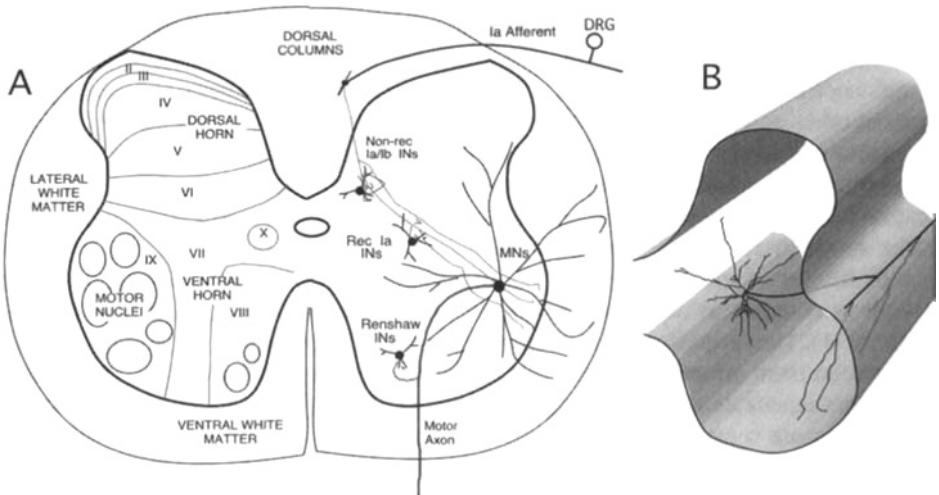


Fig. 3.1. Spinal cord anatomy. **A:** Cross-sectional diagram of the spinal cord showing the main white matter regions on the outside and the gray matter within. The thin lines in the left half of the gray matter denote the cytoarchitectonic laminations (Rexed, 1952). The right half shows the trajectory of a group Ia afferent with one collateral branch that enters the gray matter to deliver synaptic contacts to two groups of interneurons (Non-rec. Ia/Ib Ins and Rec. Ia Ins) along its course into the ventrolateral gray matter, where it makes contact with motoneurons (MN). Note the wide extent of the motoneuron dendrites and the approximate locations of three groups of interneurons discussed in the text. **B:** Diagram of a reciprocal group Ia inhibitory interneuron to show the projection of its main axon into the lateral white matter, where it divides into rostral and caudal branches that in turn drop collaterals back into the gray matter to make inhibitory synapses on motoneurons.

PRIMARY AFFERENTS

Primary afferents fall into a wide variety of categories based on anatomical and functional differences, including the tissue innervated (muscle, skin, joints and other deep tissues, or the viscera) and the characteristics of their peripheral structure, which govern the response to natural stimuli. The axonal size (diameter) and the presence or absence of myelin control the speed with which its information can be conducted to the spinal cord. As might be expected, there are systematic interrelations between these characteristics and the type of peripheral receptor (for reviews, see Brown, 1981; Darian-Smith, 1984; Fyffe, 1984). There also is evidence that different classes of afferent neurons exhibit distinctive intrinsic membrane properties (Koerber et al., 1988).

Primary afferents entering the spinal cord are often grouped into two functional classes, called *exteroceptive* and *proprioceptive*. Exteroceptors are viewed as primarily responsive to events in the environment as sensed by the skin (touch, temperature, pain, etc.). Proprioceptors, on the other hand, are viewed as activated mainly by the animal's own movements, as signaled by sensory structures in muscles, joints, and deep tissues of the trunk and limb. This dichotomy is useful and well entrenched, but it is important to remember that movements can, and do, activate many kinds of skin afferents as well as those from muscle and deep tissues. Still other systems group sensory afferents according to the type of reflex response they produce when activated. An example of this is the *flexor reflex afferents* (FRAs), an assortment of skin, joint, and muscle afferents with relatively high electrical thresholds that under some conditions tend to activate flexor muscles and inhibit extensors (i.e., the "flexor reflex"; reviewed in Baldissera et al., 1981). The name "FRA" is somewhat misleading, however, because these afferents are likely to be an important source of proprioceptive information that influence all types of movements (Lundberg et al., 1987).

MOTONEURONS

Motoneurons are the only CNS neurons that make synaptic contacts on non-neuronal tissue (i.e., skeletal muscle fibers). They are also one of the relatively few classes of neurons within the CNS that have a precisely defined functional role. Motoneuron cell bodies and their dendritic extensions lie within the ventrolateral gray matter of the spinal cord (see Fig. 3.1A) and in certain cranial nerve nuclei in the brainstem. The somata of motoneurons that innervate a given muscle in the limbs or trunk lie clustered together in elongated, cigar-shaped collections along the rostrocaudal axis of the ventrolateral horn ("motor nuclei"; Burke et al., 1977). The relative positions of the motor nuclei that innervate functionally related muscles exhibit fundamental similarities throughout the vertebrate series, from amphibia to humans (Romanes, 1951; Sharrard, 1955; Landmesser, 1978; Fetcho, 1987). The number of motoneurons that project to a given muscle varies from dozens to hundreds, depending on muscle size and function.

Motoneurons are the largest neurons in the CNS. Their dendrites can extend more than 1.5 mm from the cell body (Fig. 3.2; see also Cullheim et al., 1987), well outside of the motor nucleus. Within the gray matter they intertwine in an intricate feltwork where they receive synaptic contacts over their entire length (Brännström, 1993), including the distal parts that project into the white matter (Rose and Richmond, 1981). The myelinated axons of motoneurons are correspondingly large in both diameter and

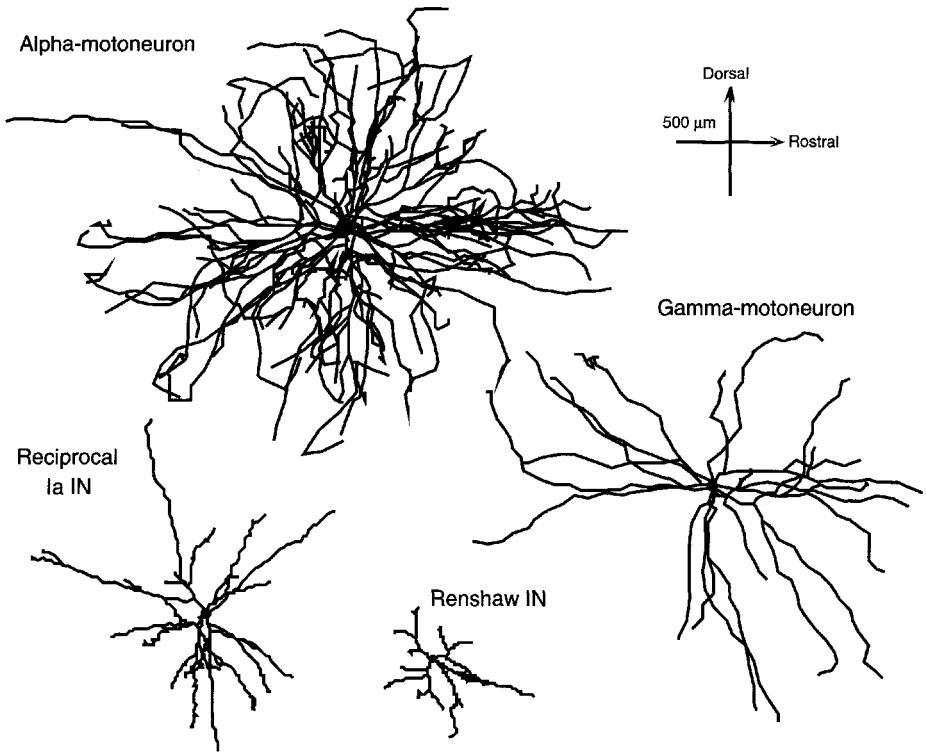


Fig. 3.2. Reconstructions of intracellularly labeled alpha- and gamma-motoneurons and two interneurons, all at the same scale (500- μm scale bars at upper right). The dendritic trees of the motoneurons have similar extents, but that of the gamma-motoneuron was considerably less dense. In contrast, the dendritic trees of the interneurons are much smaller. Note that the dendrites are not drawn to scale. If they were, most would be invisible. [The motoneurons were reconstructed in the author's laboratory (see Cullheim et al., 1987; Moschovakis et al., 1991a), and the interneuron reconstructions were kindly provided by Diane Dewey and R. E. W. Fyffe.]

length. Their large diameter and heavy myelin sheaths ensure that they conduct action potentials rapidly and reliably (conduction velocities of 20 to >100 m/s in cats). The length of motoneuron axons obviously depends on body size and the distance to their target muscle. In humans, for example, motor axons that supply the intrinsic muscles in the foot can be over 1 meter in length, and this can be multiplied many times in large mammals such as elephants and whales. The large size of motoneurons is at least in part due to the large cellular volume needed to maintain the huge amount of axonal material, which can be over an order of magnitude larger than the motoneuron itself.

There are two distinct types of motoneurons in mammals: alpha and gamma. These names were applied on the basis of the fact that alpha-motoneuron axons have faster conduction velocities (generally >60 m/s, in the "alpha peak" of the compound action potential recorded from muscle nerves) than the gamma-motoneurons (conduction velocities <40 m/s, in the "gamma peak"; Matthews, 1972, 1981). The axon of an alpha-motoneuron splits into dozens to thousands of terminal branches in and near its target

muscle. Each terminal branch innervates one large “extrafusal” striated muscle fiber via a specialized synapse called the *neuromuscular junction*. The extrafusal muscle fibers make up the major bulk of muscles and produce output force. Normally, extrafusal fibers receive innervation from only one motoneuron but that motoneuron can innervate dozens to hundreds of muscle fibers. The combination of a motoneuron and the multiple extrafusal muscle fibers that it controls (called its *muscle unit*) make up a *motor unit* (see Burke, 1981).

In contrast, gamma-motoneurons exclusively innervate one or more of the three kinds of small, highly specialized “intrafusal” muscle fibers that exist only within the muscle spindle stretch receptors. Their action is to modulate the sensitivity of the two types of muscle spindle afferents, group Ia and group II, that emerge from the muscle. There are two functional classes of gamma-motoneurons, called *static* and *dynamic*, that have different effects on stretch receptor sensitivity. The static gamma-motoneurons enhance the sensitivity to muscle length *per se*, whereas the dynamic cells promote sensitivity to the velocity of length change. The details of the operation of this remarkable sensory system can be found elsewhere (Hasan and Stuart, 1984; Matthews, 1981).

The somata of alpha-motoneurons are larger and their dendritic trees are more numerous and highly branched than those of gamma-cells (Ulfhake and Cullheim, 1981; Ulfhake and Kellerth, 1981; Moschovakis et al., 1991a). The extent of this difference is apparent in the drawings in Fig. 3.2. Although the two neuron types are quite thoroughly intermixed within motor nuclei (Burke et al., 1977), they do not receive identical synaptic inputs. The most striking difference is that gamma-motoneurons receive no monosynaptic excitation from large-diameter group Ia muscle spindle afferents (see later), whereas virtually all alpha-motoneurons do. The lack of direct excitation of gamma-motoneurons by group Ia spindle afferents presumably prevents a positive feedback loop that might produce instability in the spindle servo-control system. On the other hand, group II spindle afferents do make monosynaptic excitatory projections to some static gamma-motoneurons (Gladden et al., 1998), but the functional significance of this remains unclear.

This simple alpha-gamma dichotomy became more complicated with the discovery that some motoneurons in cats innervate *both* extrafusal and intrafusal muscle fibers (Bessou et al., 1965; Emonet-Denand et al., 1975). Such “beta-motoneurons” are fairly common in certain limb muscles in cats (Jami et al., 1982), and they can also be found in primates (Murthy et al., 1982). In contrast to their gamma-motoneuron cousins, it is probable that most, if not all, beta-motoneurons receive monosynaptic excitation from group Ia afferents (Burke and Tsairis, 1977). This would appear to form a positive feedback system with still uncertain functional consequences (Grill and Rymer, 1987).

Motor Units. One of the many key concepts that we owe to Sherrington (Liddell and Sherrington, 1925) is that of the motor unit—the combination of a motoneuron (alpha or beta) and the group of muscle fibers that it innervates (for convenience, called the *muscle unit*). Motoneurons are anatomically and functionally inseparable from the muscle units that they innervate. They are the irreducible, “quantal” elements that produce all body movements. Most limb and trunk muscles in mammals contain two fundamental motor unit types—fast twitch (type F) and slow twitch (type S)—based primarily on the morphology, biochemistry, and mechanical properties of the innervated

muscle fibers (Burke et al., 1973a; Burke, 1981, 1999a). The type F population can be further divided into two major subtypes: one relatively fatigable (type FF) and the other much more resistant to fatigue (type FR). In general, all of the muscle fibers in a given muscle unit share the same morphology, chemistry, and (by inference) mechanical characteristics (Nemeth, 1990).

Most type F motor units produce considerably more force than type S units, although there is a continuous gradation in maximum force outputs within the population in any muscle (Fig. 3.3A). There is a long list of intrinsic motoneuron properties, as well as the organization of synaptic inputs to them, that are systematically related to motor unit type (reviewed in Burke, 1981; Binder et al., 1996; Powers and Binder, 2001). Some of these are shown schematically in Fig. 3.4. Those properties that have larger values in S motor units than in F units are denoted in gray, whereas the reverse is indicated by hatching. These differences represent functional specializations that enable the different types of motor units to play particular roles during reflex and voluntary movements. Material in this figure is discussed and referenced later.

INTERNEURONS

It is useful to define three subgroups of spinal cord interneurons, based on their axonal targets. *Segmental*, or *local*, interneurons project to spinal cord regions relatively close to the parent cell body, i.e., within the same spinal segment or in nearby segments. Segmental interneurons participate in reflexes to coordinate the action of motoneuron groups within a given limb. Interneurons with axons that end at greater distances but still within the spinal cord itself are referred to as *propriospinal* cells. Propriospinal neurons link activities over multiple spinal segments, which are required to coordinate

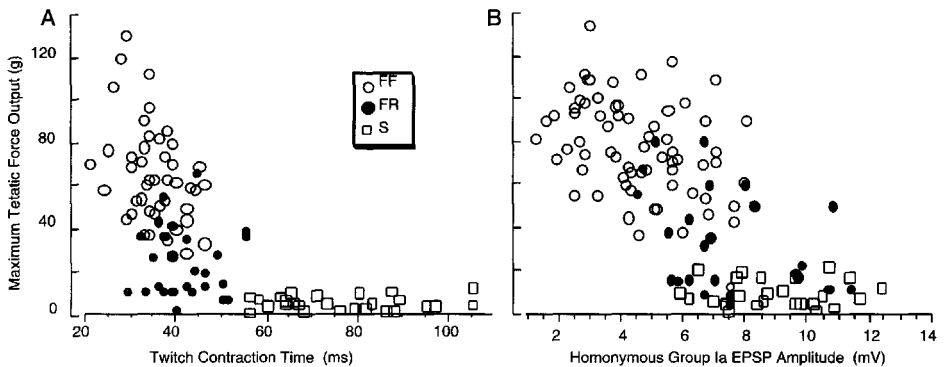


Fig. 3.3. Interrelations of some properties of type-identified motor units in cat medial gastrocnemius (MG) motor units [data from Burke et al., 1976]. **A:** Correlation of maximum tetanic force (ordinate) with twitch contraction time (abscissa) shows that fast twitch muscle units (types FF and FR) produce a wide range of force, generally largest in type FF, whereas slow twitch (type S) units produce uniformly small force outputs. **B:** Correlation of maximum tetanic force (ordinate) with peak amplitude of monosynaptic group Ia EPSPs (abscissa) in the same set of MG motor units. The large force type FF units exhibit generally smaller EPSPs than type FR units, which are in turn generally smaller than those in type S units. However, the relation is continuous and there is a great deal of overlap between the unit groups.

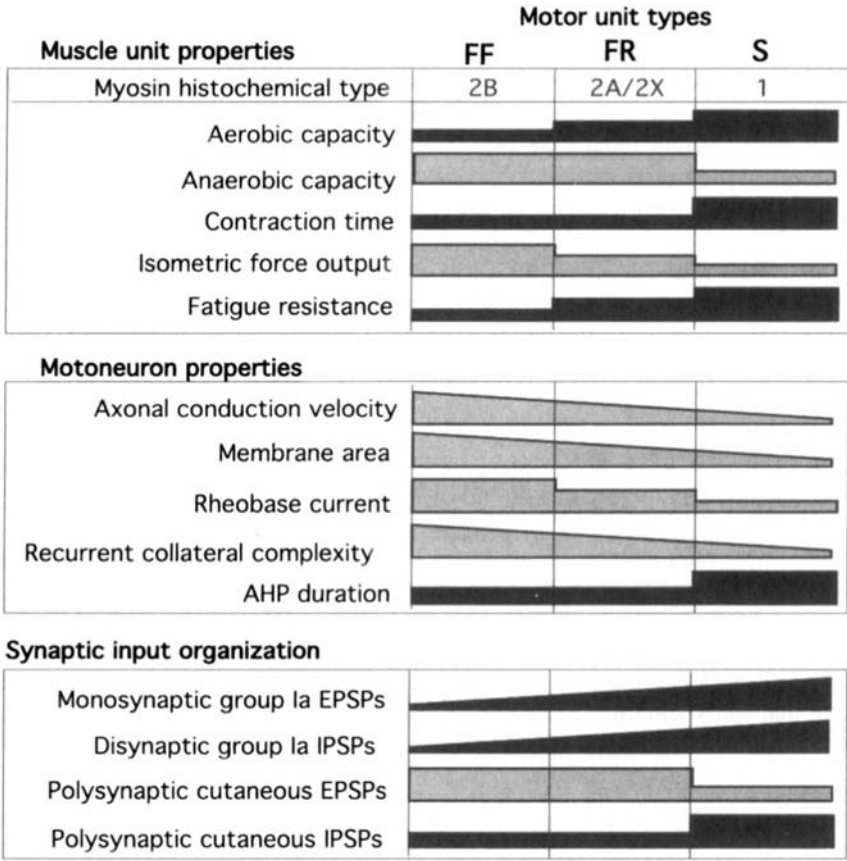


Fig. 3.4. Coordinated properties of the three main types of motor units. Properties that increase in the sequence FF < FR < S are shown in black while reverse orderings are shown in gray. This summary represents approximations that are not drawn to scale. The histochemical typing of muscle fibers is based on the chemical characteristics of the myosin proteins in them (see Burke, 1981; 1999a). References for the data in this figures are given in the text.

muscle activities within and between limbs, as well as in widely distributed trunk muscles, during postural control and locomotor movements. Spinal interneurons that send their axons primarily to supraspinal destinations can be referred to as *tract cells*. One example of the latter is the large neurons in Clarke’s column in the upper lumbar spinal segments, one of the few clearly defined nuclear groupings in the spinal cord. These neurons project to the cerebellum in the dorsal spinocerebellar tract (DSCT), ending as mossy fibers in the cerebellar cortex (Bloedel and Courville, 1981). The most obvious role for tract neurons is to deliver information to supraspinal regions of the brain that are specifically associated with movement control or sensory perception.

Of course, as with most biological systems, these neat categories are oversimplifications because they are not mutually exclusive (Jankowska, 1992). For example, some

tract cells also have axon collaterals that end locally within the spinal cord (Brown et al., 1977). Such neurons may therefore also function as local interneurons. As information about the structure and function of spinal interneurons improves, it seems quite likely that many of these neurons will be shown to have multiple sites of action, and therefore multiple functional roles (see later).

Most spinal cord interneurons are considerably smaller than motoneurons in both soma size and dendritic extent (see Fig. 3.2). The laminar organization and neuron shapes and sizes have led to detailed analyses of the organization of sensory systems in the dorsal horn of the spinal cord (reviews in Brown, 1981; Darian-Smith, 1984; Willis and Coggeshall, 1991). Although there are at present relatively few such morphological clues to guide a functional taxonomy of interneurons in the ventral horn, a combination of anatomical and electrophysiological studies has identified the locations of particular functional groups of ventral horn interneurons. These include Renshaw cells that produce recurrent inhibition of motoneurons, interneurons that mediate disynaptic reciprocal group Ia afferent inhibition of antagonist motoneurons, and interneurons that mediate nonreciprocal muscle and cutaneous afferents reflex effects (see Fig. 3.1A). These are discussed in more detail later.

Ventral horn interneurons of all types appear to have one important feature in common—this is that their axons leave the gray matter relatively close to the cell body to run rostrally and caudally in the white matter. They make most of their synaptic contacts on motoneurons and other interneurons by dropping collaterals at various distances back into the gray matter (see Fig. 3.1B). This axonal organization makes sense in that spinal circuitry is distributed longitudinally along the cord, rather than in discrete nuclei as in the supraspinal brain.

SYNAPTIC ACTION IN THE SPINAL CORD

There are three basic types of synaptic boutons found in electron microscopic studies of the ventral horn (see Conradi et al., 1979; Brännström, 1993) (Fig. 3.5): (1) type S synaptic boutons that range from 0.5 to 8 μm in average diameter and contain spherical synaptic vesicles, (2) type F boutons that range from 0.5 to 7 μm in diameter but contain vesicles that appear irregular (pleomorphic) or flattened with many types of fixation, and (3) type P boutons that are small (0.5–1.5 μm in diameter) and contain flat or pleomorphic vesicles. The S and F boutons contact the somata and dendrites of neurons with synaptic specializations, or “active zones,” at which the vesicles congregate. The P (for *presynaptic*) boutons end on type S boutons with synaptic specializations that indicate functional synaptic connections onto the larger S that they contact. Such “axo-axonic contacts” are believed to modulate the release of transmitter from the recipient boutons, producing *presynaptic inhibition* (discussed later). A subtype of large type S bouton, called the C type, that exhibits a postsynaptic “cistern” instead of a postsynaptic density, has also been recognized (Conradi et al., 1979). Type C synapses on motoneurons are known to be cholinergic but probably do not originate from motoneurons (Hellstrom et al., 1999).

Vesicle shape correlates with excitatory or inhibitory action on the postsynaptic target; type S boutons are excitatory, whereas the F boutons with flat/pleomorphic vesicles are generally inhibitory. Synaptic boutons with pleomorphic vesicles on and near

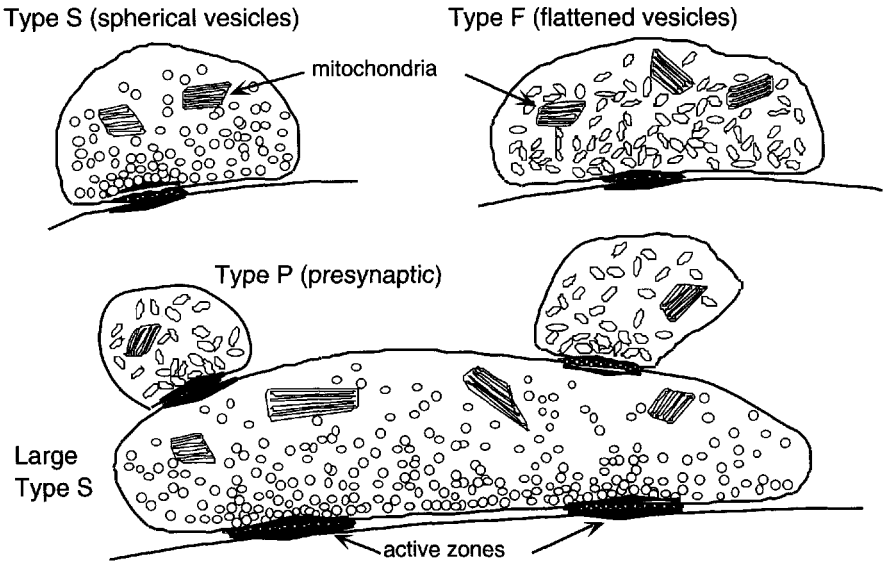


Fig. 3.5. Synaptic types in the cat ventral horn. Drawings of the ultrastructural appearance of the major types of synapses found in the ventral horn. [Adapted from Fig. 2 in Conradi et al. (1979), with permission.]

the somata of large ventral horn neurons (presumably motoneurons) are immunopositive for the inhibitory transmitter glycine (Destombes et al., 1992; Shupliakov et al., 1993). Synaptic boutons that are immunopositive for the other major inhibitory neurotransmitter, γ -aminobutyric acid (GABA), are also found on motoneuron somata (Destombes et al., 1996). In fact, a substantial proportion of boutons immunopositive for GABA are also reactive for glycine, suggesting that some inhibitory synapses may liberate both neurotransmitters (Örnung et al., 1994). Synaptic boutons with other neurotransmitters, such as serotonin, are also present on motoneurons (Alvarez et al., 1998). The soma and dendritic trees of motoneurons are covered by S and F boutons, although the density of coverage decreases with distance from the soma (Brännström, 1993). Cat alpha-motoneurons receive, on average, about 50,000 synapses from all sources.

Motoneurons in amphibians can communicate with one another directly via “ephaptic” interactions mediated by gap junction connections in their dendrites (Sonnhof et al., 1977). Direct dendrodendritic synaptic arrangements that are found in some specialized CNS regions (see Chap. 5) are not present in the spinal ventral horn, although weak electrical interactions have been found between some mammalian motoneurons (Nelson, 1966; Gogan et al., 1977). There are sites of apparent close apposition, without membrane specializations, between cat motoneuron dendrites, especially in regions where dendrites are “bundled” closely together (Matthews et al., 1971). Electrical coupling between motoneurons has been demonstrated to produce sharply timed synchronous discharge of motoneurons in electric fish (Bennett, 1977), and this might be of use in frogs. However, there is little evidence, nor much functional reason, for this type of tight coupling among mammalian spinal motoneurons. Oddly enough, however, motoneurons apparently also interact directly via monosynaptic connections from re-

current collaterals that arise from the motoneuron axons before they leave the spinal cord (Cullheim et al., 1977). These contacts are rare and their function remains unknown.

POSTSYNAPTIC EXCITATION: GROUP Ia AFFERENTS

The group Ia, or primary, muscle spindle afferents are of special significance to a discussion of synaptic action in the spinal cord. Group Ia afferents make direct, or monosynaptic, excitatory synaptic connections with alpha-motoneurons, giving rise to excitatory postsynaptic potentials (EPSPs) that were the first synaptic potentials in the CNS to be recorded with intracellular electrodes (Brock et al., 1952). Many of our fundamental ideas about synaptic mechanisms within the CNS are based on a half century of work on this monosynaptic system.

Anatomy. Group Ia afferents arise from specialized “annulospiral” end organs in muscle spindles that are activated by muscle stretch, producing the familiar stretch reflex. In mammals, group Ia afferents are among the largest diameter and fastest conducting primary afferents that enter the spinal cord. The Ia afferents from a given muscle enter the cord in the spinal segments that contain the motoneurons that innervate that muscle (called *homonymous* motoneurons), as well as motoneurons that innervate synergistic muscles (called *heteronymous* motoneurons) (Eccles et al., 1957).

The intraspinal anatomy of group Ia afferents is representative of synaptic systems in many other parts of the CNS. As shown in Fig. 3.6A, after entry into the cord, each Ia afferent divides into a thick ascending (rostral) and a thinner and shorter descending (caudal) branch. The ascending branch travels in the ipsilateral dorsal column up to the cuneate nuclei in the lower brain stem. These dorsal column axons give off local collateral branches that drop into the gray matter at roughly 0.5- to 2-mm intervals in and near the segment the site of entry (Ishizuka et al., 1979). Each local Ia collateral then descends into the gray matter where it gives rise to preterminal arborizations and associated synaptic boutons in three defineable locations (see Fig. 3.1A): (1) the intermediate nucleus (the medial part of Rexed laminae V and VI, where they contact a variety of spinal interneurons (Czarkowska et al., 1981); (2) in lamina VII, just dorsomedial to lamina IX, where they make contacts with a more specific group of inhibitory interneurons (Jankowska and Lindström, 1972; see later); and (3) in lamina IX, where they intersect with and form contacts on the somata and dendrites of alpha-motoneurons (Fig. 3.6B) (Brown and Fyffe, 1981; Redman and Walmsley, 1983b; Burke and Glenn, 1996). The rostral branch in the dorsal column also drops collateral branches into a specialized nucleus called Clarke’s column, located in the upper lumbar and lower thoracic segments of the spinal cord, where they make powerful excitatory connections with neurons that give rise to the dorsal spinocerebellar tract (Walmsley, 1991).

The monosynaptic group Ia contacts on alpha-motoneurons arise from elaborate arborizations of the local collaterals in lamina IX, either as *en passant* boutons (simple swellings along the course of a collateral where the myelin sheath disappears) or as terminal boutons, where a fine collateral branch ends in a synaptic swelling (see Fig. 3.6B). There are about 70 group Ia afferents in the cat medial gastrocnemius muscle nerve (Boyd and Davey, 1968); one can envision the interstices between collaterals from any given afferent as filled in by the collaterals of others (see Fig. 3.6A) (Ishizuka

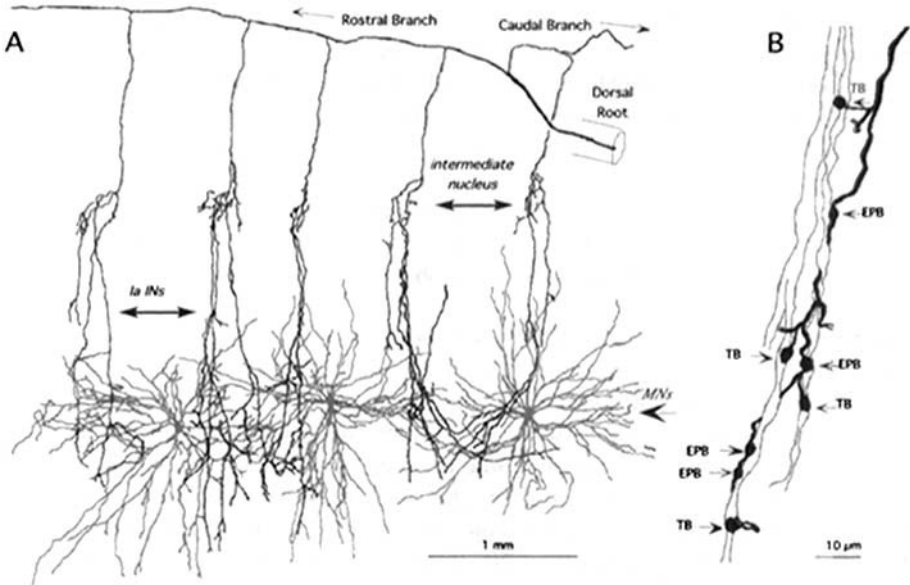


Fig. 3.6. Anatomy of group Ia afferents. **A:** Drawing of a cat triceps surae group Ia afferent (black lines) and three alpha-motoneurons (gray lines), all filled by intracellular injection of horseradish peroxidase tracer, reconstructed from a series of parasagittal section (see Burke and Glenn, 1996). Note the close spacing of Ia collaterals that begin to branch in the intermediate nucleus (see Fig. 3.1A) and then deliver additional synaptic terminals to reciprocal Ia inhibitory interneurons and the dendrites of motoneurons. **B:** High-magnification drawing of *en passant* (EPB) and terminal (TB) boutons along one afferent collateral branch (thick lines) on two fine motoneuron dendrite branches (thin lines) of one of the motoneurons shown in A. A majority of the bouton swellings occur along the afferent collateral (EPBs) rather than terminal branches (TBs). This was also true of the entire sample of more than 200 bouton contacts on identified motoneurons (Burke and Glenn, 1996).

et al., 1979; Burke and Glenn, 1996). The terminal fields of Ia synapses from a given muscle in the ventral horn can be viewed as longitudinal clouds of synaptic boutons in these three gray matter loci.

Motoneurons in a given motor nucleus receive functional Ia contacts from nearly all of the group Ia afferents originating in the innervated muscle (the “homonymous” connection; Mendell and Henneman, 1971; Fleshman et al., 1981a). The projection frequency is somewhat smaller but still considerable among motoneurons that innervate muscles that act synergistically (“heteronymous” connections). Presumably, such Ia connections facilitate the coordinated action of different muscles during movement (Eccles and Lundberg, 1958). Muscles that are linked by Ia interconnections are sometimes referred to as a *myotatic unit* (Lloyd, 1960) because they participate together in stretch (or “myotatic”) reflexes. Muscles in a myotatic unit often act together in a variety of movements, but there are some interesting exceptions to this rule (Fleshman et al., 1984; see later).

Intracellular injection of the tracer horseradish peroxidase (HRP) into Ia afferents and their postsynaptic motoneuron targets has shown that individual afferents can con-

tribute as many as 35 boutons to a given motoneuron (average about 10) and these boutons often exhibit wide spatial dispersion in the dendritic tree (Burke and Glenn, 1996). Two and sometime three neighboring collaterals from the same afferent can make contact in different parts of the dendritic tree of a single motoneuron. This anatomical evidence has confirmed earlier inferences about wide spatial dispersion of Ia synapses that were based on electrophysiological information (Burke, 1967; Rall et al., 1967; Jack et al., 1971). Between 500 and 1000 group Ia boutons terminate on an average lumbosacral cat motoneuron (Burke and Glenn, 1996), which is 1–2 percent of the roughly 50,000 total synaptic boutons that probably end on these cells.

Physiology. Using relatively simple but ingenious methods, David Lloyd (Lloyd, 1960) demonstrated that the stretch reflex is generated by electrical stimulation of the fastest-conducting (i.e., group Ia) afferents from muscle spindles with a central latency so short (<1.0 ms) that the connection between Ia afferents and motoneurons had to be direct (monosynaptic). Central latency is the time between the arrival of synchronized afferent action potentials at the spinal cord and the onset of synaptic potentials in their target neurons. Group Ia EPSPs in alpha-motoneurons (Fig. 3.7D) were the first synaptic potentials to be recorded within the CNS (Coombs et al., 1955a; Eccles, 1964). Extracellular recordings in the ventral horn also revealed small “terminal potentials” (see Fig. 3.9B, arrow) that signal the arrival of the Ia volley at the motoneurons, allowing estimation of the synaptic delay of 0.2–0.4 ms before the onset of the intracellular EPSP (Munson and Sypert, 1979a, b).

The anatomy of Ia afferents defines a functional hierarchy (see Fig. 3.7A) for group Ia synaptic action on motoneurons: (1) *single bouton* EPSPs produced by an individual Ia synapse (Fig. 3.7B), (2) *single-fiber* EPSPs produced by all of the boutons belonging to an individual Ia afferent (Fig. 3.7C), and (3) *composite* EPSPs produced by synchronous action in many Ia afferents (Fig. 3.7D). This hierarchy is the same throughout the CNS. Single-fiber Ia EPSPs were first recorded by Kuno (1964) more than a decade after the first intracellular experiments. Subsequently, others (Burke, 1967; Jack et al., 1971; Mendell and Henneman, 1971) showed that single-fiber Ia EPSPs in motoneurons varied in shape exactly as predicted by Wilfrid Rall (1964) for synapses that are widely dispersed throughout the dendritic tree (Fig. 3.8). The resulting conclusion that Ia synapses are widely distributed along motoneuron dendrites was later confirmed directly by anatomical studies discussed earlier. Single-bouton Ia EPSPs have only rarely been observed in isolation (see Fig. 3.6B) because in most motoneurons they are much smaller than the background synaptic “noise” from other sources.

The Influence of Dendrites on Synaptic Action. In most CNS neurons, the major fraction of the cell membrane that receives synapses is in the dendrites. The dendrites dominate the electrical properties of the neuron and influence the synaptic currents that are delivered to the membrane region, called the *initial segment of the axon*, where action potentials are generated (Eccles, 1957; Stuart et al., 1997). Most of our current understanding of dendritic function is based on pioneering work of Wilfrid Rall on the flow of subthreshold electrotonic currents that spread through the cell interior (Rall, 1959, 1960; see also Segev et al., 1995). Much of the early experimental work on dendritic electrotonus was done in spinal motoneurons (Ianssek and Redman, 1973; Barrett and

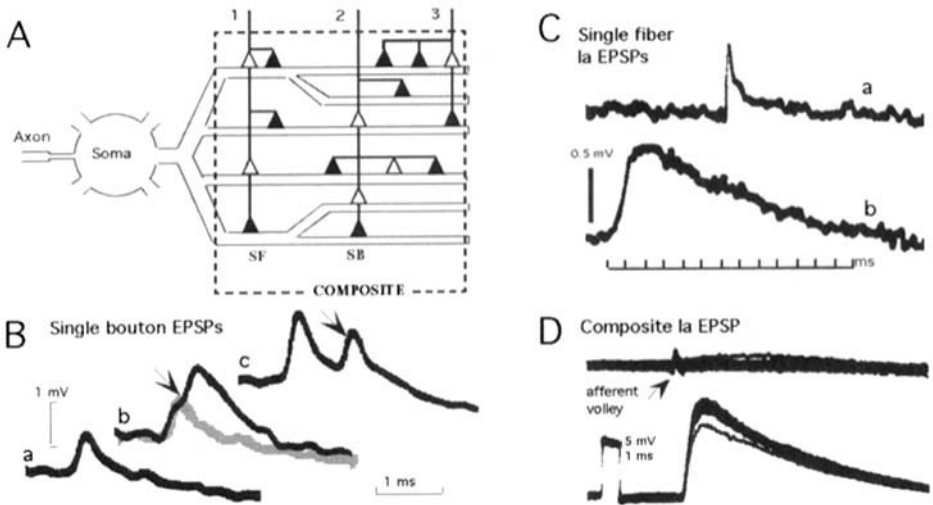


Figure 3.7. Synaptic hierarchy in a primary afferent system. **A:** Cartoon showing spatial dispersion of *en passant* (open triangles) and terminal boutons (filled triangles) belonging to three afferent fibers ending on the same dendrite. When simultaneously activated, the complete set (dashed line) generates a “composite” EPSP (as in **D**). Activating an individual afferent fiber produces a “single-fiber” EPSP (**C**), in which the amplitude and shape depend on the number of synapses associated with that fiber and their spatial dispersion with respect to the soma where they are recorded. Individual synaptic boutons produce “single-bouton” EPSPs (as in **B**), which are only rarely detectable in spinal cord neurons. **B:** Unusually large single-bouton EPSPs recorded in a cat motoneuron during repetitive firing in a group Ia afferent. All-or-none components were identified because of occasional latency jitter (traces b and c). These had the same shape and amplitude as apparently single all-or-none events (trace a). **C:** Single-fiber EPSPs produced by two individual group Ia afferents in the same motoneuron during controlled muscle stretch. Both were relatively large in amplitude but had very different shapes. The shape difference could be accounted for by different spatial locations in the dendritic tree; EPSP (a) must have been generated at or very near the cell soma, whereas EPSP (b) involved many synapses located at relatively distant points in the dendrites. **D:** Composite EPSP produced by electrical stimulation of the entire muscle nerve (lower trace) in the same motoneuron as in **C**. The upper trace is the potential recorded on the cord surface showing the arrival of a synchronized volley in all of the Ia afferents in the nerve (sharp deflection just before the EPSP onset). The overall shape of the composite EPSP was intermediate between the two single fiber components shown in **C**. The record shows superimposed multiple sweeps in which there was some fluctuation in EPSP amplitudes. [Records in **B–D** from Burke, 1967, with permission.]

Crill, 1974). One might expect that, after decades of work, the electrophysiological properties of motoneuron dendrites would be well understood. In some respects they are, but work on this problem also illustrates how difficult it is to extract fundamental information about dendritic membrane properties from real neurons *in situ* within the CNS.

The specific resistivity and capacitance of the neuron membrane (denoted R_m and C_m , respectively) and the resistivity of its cytoplasm (R_i) are values critical to any discussion of the electrotonic properties of neural dendrites (Rall, 1977). These parameters can only be estimated indirectly from the anatomy of the whole neuron (e.g.,

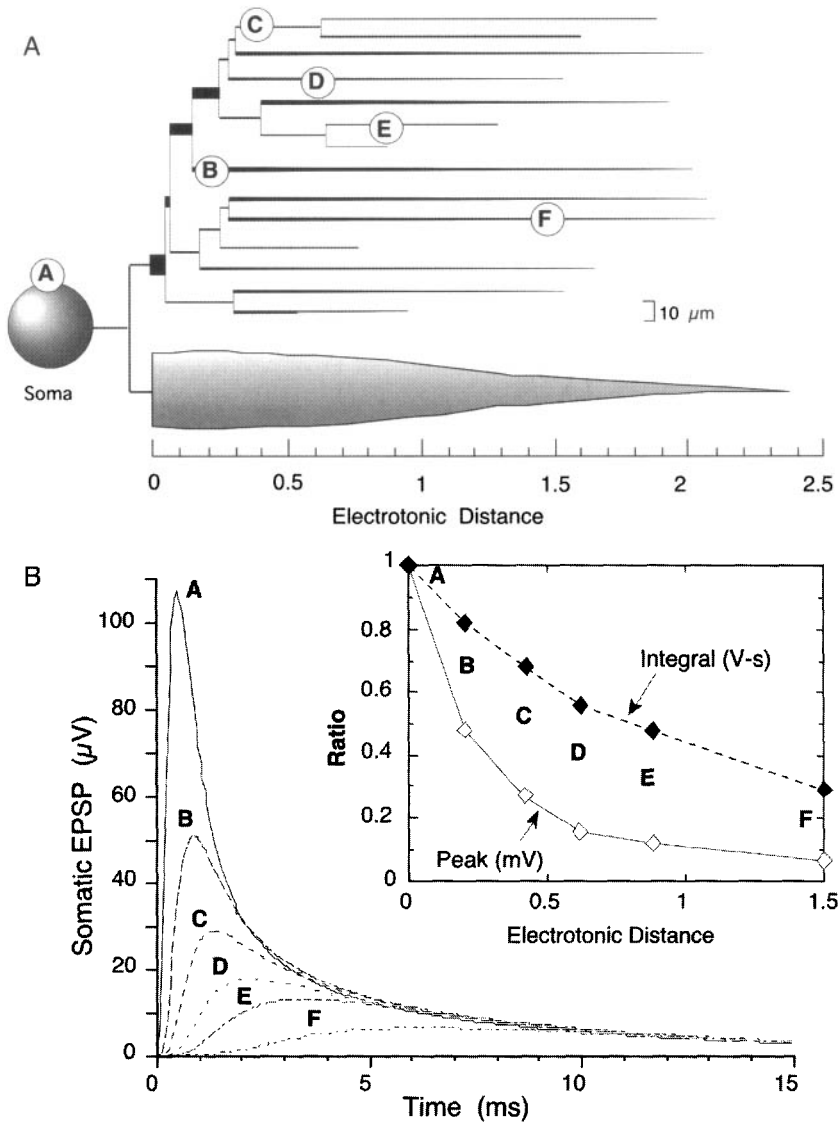


Fig. 3.8. Effect of dendritic location on somatic EPSPs. **A:** An electrotonic model of a type FR cat alpha-motoneuron (cell 43/5 in Fleshman et al., 1988) that includes the soma, 1 fully branched dendrite, and a tapered equivalent cable representing the other 10 dendrites (Clements and Redman, 1989; Burke, 2000). All parts of the dendritic tree are aligned according to their electrotonic distances from the soma, calculated from the cell morphology and estimates of specific electrical properties ($R_{m,soma} = 225 \Omega \text{ cm}^2$, $R_{m,dend} = 11,000 \Omega \text{ cm}^2$, $R_i = 70 \Omega \text{ cm}$, $C_m = 1 \mu\text{F}/\text{cm}^2$). The circles (A–F) indicate positions of simulated group Ia synapses, each of which produced a peak synaptic conductance of 5 nS at 0.2 ms (Finkel and Redman, 1983). The spatial distribution is based on the observed distribution of group Ia boutons in cat motoneurons (Burke and Glenn, 1996). **B:** The main graph shows somatic EPSPs generated by the individual synapses in the model cell. Note the progressive decrease in amplitude and slowing of time courses produced by increasing electrotonic distance, as well as the fact that all EPSPs eventually decay with the same time course. The inset graph shows peak EPSP amplitudes (open diamonds) and the integral over the first 20 ms (filled diamonds) that represents the current delivered to the soma. Note that the current falls off less rapidly than peak amplitude with electrotonic distance.

Fig. 3.2) as well as the steady-state input resistance of the cell (R_N) and its dynamic response to short and/or long pulses of current. The generally accepted value for C_m is $1.0 \mu\text{F}/\text{cm}^2$ in most biological membranes (Cole, 1968), although estimates range from $0.66 \mu\text{F}/\text{cm}^2$ in hippocampal pyramidal neurons (Major et al., 1994) to over $2 \mu\text{F}/\text{cm}^2$ in neonatal rat motoneurons *in vitro* (Thurbon et al., 1998). Estimates for R_i are about $70\text{--}90 \Omega\text{-cm}$ in cat motoneurons (Barrett and Crill, 1974; Burke et al., 1994; Thurbon et al., 1998), although values as high as $390 \Omega\text{-cm}$ have been calculated for hippocampal neurons (Major et al., 1994). Relatively small changes in either of these parameters, as well as the assumption of spatial uniformity, greatly affect estimates of R_m (e.g., Burke et al., 1994).

All reports of specific electrical properties depend on assumptions that are oversimplifications (Rall et al., 1992). For example, neuron membranes have nonlinear voltage-gated conductances that can distort experimental records. It is also likely that R_m is not uniform everywhere in the cell. Studies in spinal motoneurons using conventional intracellular electrodes suggest that the effective R_m in and near the soma is orders of magnitude lower than that in the dendrites (Ianseck and Redman, 1973; Fleshman et al., 1988b; Clements and Redman, 1989). Estimates of R_m in the presence of such “leaky” somatic membrane range from 10 to $20 \text{K}\Omega\text{-cm}^2$ in cat alpha-motoneurons and over $30,000 \Omega\text{-cm}^2$ in gamma-motoneurons (Burke et al., 1994). There also is evidence suggesting that dendritic R_m in small (i.e., type S) motoneurons is higher than that in fast twitch (FR and FF) motoneuron types (Fleshman et al., 1981b; Gustafsson and Pinter, 1984). In contrast, Thurbon and coworkers (1998) found it unnecessary to postulate a somatic leak in 4/10 neonatal rat motoneurons studied with whole-cell patch electrodes in spinal cord slices. Although a relative “somatic shunt” could result from local injury caused by conventional microelectrode (Spruston and Johnston, 1992; Staley et al., 1992), it is possible that the soma may have lower effective R_m even in uninjured neurons. For example, a K^+ -channel with “leak” conductance properties (i.e., voltage independent) is highly concentrated on the soma and proximal dendrites of spinal motoneurons (Talley et al., 2001).

The dendrites of many CNS neurons exhibit a wide variety of voltage-gated active channels (Magee, 1999), and motoneurons are no exception. For example, action potentials that arise in the initial axon segment propagate antidromically to involve the motoneuron soma and proximal dendritic membrane (Eccles, 1957), indicating the presence of fast voltage-dependent conductance channels in proximal regions (Traub and Llinas, 1977). These active dendritic channels can, at least in principle, contribute to net membrane conductivity at rest as well as during voltage perturbations. Other voltage-sensitive dendritic conductances are discussed later.

Despite these uncertainties, passive membrane models provide a critical baseline for interpreting the effects produced by relaxing the starting assumptions and adding active membrane properties (Rall et al., 1992; Spruston et al., 1994; Segev and London, 1999). The weight of evidence suggests that the dendritic R_m in motoneurons (and probably most other CNS neurons) is sufficiently high that they are relatively short in electrotonic terms, despite their anatomical extent (see Fig. 3.2). Thus, even distal synapses can have appreciable effects at the soma. This is illustrated in a neuron model shown in Fig. 3.8, which is based on data from a cat alpha-motoneuron (Fleshman et al., 1988b). Given a rather long list of starting assumptions (Rall et al., 1992), such equiv-

alent cables provide an approximate simulation of the electrotonic load of dendrites that do not receive simulated synaptic inputs.

The circles with letters in Fig. 3.8A denote the positions of six simulated synapses on the soma (A) and at various electrotonic distances from it (B through F). Figure 3.8B shows that the simulated synaptic conductance transient produced a rapidly rising and falling somatic EPSP of about $100 \mu\text{V}$ when applied across the soma membrane (A), whereas somatic EPSPs were progressively slower and smaller when the same conductance transient was applied at increasing electrotonic distances (B \rightarrow F). The inset graph in Fig. 3.8B shows that decline of peak amplitude with increasing electrotonic distance (open diamonds) was much faster than that of the integral of voltage over a relatively long time (20 ms in this case; filled diamonds), which represents the electrical charge delivered by the synapses to the soma (Edwards et al., 1976). By this measure of synaptic efficacy, boutons at almost one length constant (λ) from the soma are about half as effective as a bouton directly on the soma.

In contrast to somatic EPSPs, the peak amplitude of *local* EPSPs recorded at the site of generation *increase* markedly with progressively distant sites of generation (from B to F; see Williams and Stuart, 2002, for a remarkable experimental example with multiple intradendritic recordings). This occurs because the local input resistance is high and capacitance is low at these sites in branched dendritic trees (Rinzel and Rall, 1974). The local EPSPs in the dendrites are sufficiently large that they reduce the synaptic current that can be injected by a given conductance change because of reduced synaptic driving potential (see Chap. 2).

Mechanisms of Group Ia Excitatory Transmission. Synaptic transmission between muscle afferents and motoneurons in frogs has both electrical (ephaptic) and chemical components (Shapovalov and Shiraev, 1980; see Chap. 2). In mammals, however, group Ia EPSPs behave as expected for a purely chemically mediated event. "As expected" means that composite group Ia EPSPs exhibit an equilibrium potential ($E_{\text{eq,syn}}$; see Chap. 2) near 0 mV and reverse to hyperpolarizing polarity at more positive membrane potentials (Engberg and Marshall, 1979). This suggests that Na^+ ($E_{\text{eq,Na}}$ about +40 mV), K^+ ($E_{\text{eq,K}}$ about -90 mV), and possibly Ca^{2+} ($E_{\text{eq,Ca}}$ about +145 mV), pass through the activated channels (see Chap. 2). The reversal potential of Ia EPSPs is difficult to measure accurately (Smith et al., 1967), not only because most Ia boutons are electrotonically isolated from the soma but also because injection of strong depolarizing currents into cat motoneurons can activate membrane conductances that limit their effectiveness. Similar problems have been encountered in other parts of the CNS (e.g., the spiny neuron of the neostriatum; see Chap. 9).

Neurotransmitter Receptors. The neurotransmitter released by group Ia synapses is the excitatory amino acid (EAA) glutamate. Of the three types of postsynaptic glutamate receptor types (GluRs; see Chap. 2), the fast AMPA GluR is predominant in adult cats. Walmsley and Bolton (1994) demonstrated that local perfusion with AMPA GluR antagonists (CNQX and NBQX) near the soma of intracellularly recorded alpha-motoneurons blocked composite- and single-fiber Ia EPSPs. Short-duration single-fiber EPSPs generated at boutons relatively close to the soma were completely blocked, whereas blockade was incomplete for more distant EPSPs with slower time courses.

These authors found no evidence for a slow NMDA GluR component in adult cats. However, there is other evidence that NMDA receptors may be more important in other synaptic systems (Rekling et al., 2000).

On the other hand, group Ia synapses in immature rat spinal cords studied *in vitro* do exhibit variable levels of NMDA GluR action. Ziskind-Conhaim (1990) found that NMDA receptors are predominant in the response of embryonic motoneurons, but their contribution to Ia EPSPs in neonatal rodents, as judged by sensitivity to the NMDA blocker 2-amino-5-phosphovalerate (APV), is much smaller (Pinco and Lev-Tov, 1993; Li and Burke, 2001) or undetectable (Jahr and Yoshioka, 1986). Thus, like many CNS synapses (Cline, 1999), there appears to be a developmental switch between ionotropic NMDA and AMPA GluRs during early development of the spinal cord.

Quantization of Synaptic Action. Synaptic potentials at the neuromuscular junction exhibit all-or-none components that represent liberation of equal-sized packets (quanta) of the transmitter acetylcholine (Katz, 1966). Under certain conditions, transmission can fail to occur. Single-fiber group Ia EPSPs (sfEPSPs) also sometimes fail to occur during repetitive activation, leading to the conclusion that synaptic action at this CNS synapse is also quantized (Kuno, 1964; Jack et al., 1981a; Redman and Walmsley, 1983a; Redman, 1990). Given that most group Ia afferents contribute more than one synaptic bouton to each motoneuron, there are two possible explanations for such transmission failures. Action potentials might sometimes fail to invade some distal branches within the complex Ia collateral arborizations (*branch point failure*; Lüscher and Clamann, 1992). Alternatively, fully activated synaptic boutons might sometimes fail to liberate transmitter (*release failure*). These alternatives are not mutually exclusive. The weight of available evidence favors release failure from fully active boutons (Lev-Tov et al., 1983b; Redman and Walmsley, 1983a; Burke, 1998), but it is very difficult to rule out any contribution from branch point failure. In either case, it seems safe to say that the all-or-none EPSP components that make up an Ia sfEPSP probably represent events that are generated at the individual boutons belonging to that afferent.

A variety of statistical approaches (reviewed in Faber et al., 1998) have been used to infer the quantal size of group Ia sfEPSPs. In the rare cases studied both physiologically and morphologically, the maximum numbers of quantal components in Ia sfEPSPs pretty well match the numbers of HRP-labeled boutons from the same Ia afferents observed anatomically (Redman and Walmsley, 1983a). Given that boutons from a single Ia afferent are scattered at different distances from the motoneuron soma, one would expect them to generate different size somatic EPSPs (see Fig. 3.8B). Surprisingly, however, statistical deconvolution studies suggest that, on average, quantum intervals from Ia sfEPSPs are about the same size irrespective of EPSP shape (Jack et al., 1981a; Redman and Walmsley, 1983a). Although this might result from a statistical artifact (Walmsley, 1995), the idea of some nonlinear amplification at distal synapses in motoneurons is consistent with recent data from other neuron types (Spruston et al., 1999; Lee and Heckman, 2000). In addition, the size of identified Ia boutons, as well as the size and number of their active zones (all morphological indices of synaptic efficacy), are larger on thin, presumably distal, motoneuron dendrites than on thick ones (Pierce and Mendell, 1993; see also Oleskevich et al., 1999). The issue of dendritic amplification is discussed further later.

Modulation of Transmitter Release at Ia Synapses. Composite Ia EPSPs fluctuate in amplitude from trial to trial (e.g., Fig. 3.7D). There are multiple sources for such fluctuations (Gossard et al., 1994), one of which is the probability of transmitter release at individual synaptic boutons (see earlier). Release probabilities may differ from one bouton to another (Walmsley and Edwards, 1988), and they also vary with time (Henneman et al., 1984) and prior history of activation (Zucker and Regehr, 2002). For example, Ia EPSP amplitudes are depressed during repetitive activation at moderate to high frequencies (>50 Hz; Curtis and Eccles, 1960) due to an apparent depletion of the amount of transmitter immediately available for release by the active synapses (*tetanic depression*; see Zucker and Regehr, 2002). This depression often persists for several seconds immediately after the end of a tetanus (*post-tetanic depression* [PTD]). However, the relatively brief PTD is followed by a prolonged period during which Ia EPSPs are usually considerably larger than pretetanic control responses, called *post-tetanic potentiation* (PTP) (Curtis and Eccles, 1960). After long, high-frequency tetanization, PTP rises to maximum over several tens of seconds and then decays to control amplitudes over a period of tens of minutes (Lev-Tov et al., 1983b). These forms of short-term synaptic potentiation and depression are quite different from the sustained *long-term potentiation* (LTP) and *long-term depression* (LTD) that are found in other areas of the brain (see Chaps. 2 and 11). Neither LTP nor LTD seems to occur in motoneurons.

The co-existence of simultaneous PTD and PTP can be revealed by the administration of the drug *l*-baclofen (Lev-Tov et al., 1983b), which activates presynaptic GABA-B receptors. Baclofen reduces Ca^{2+} entry into synaptic terminals (Dunlap and Fischbach, 1981; Dolphin and Scott, 1986), which in turn reduces transmitter output and consequently eliminates the PTD produced by transmitter depletion. The net effect is to reveal uncontaminated PTP, in which EPSPs immediately after the end of the conditioning tetanus can be up to six times larger than the pretetanic EPSPs (Lev-Tov et al., 1983b). The drug 4-aminopyridine, which prolongs the afferent action potential and allows greater influx of Ca^{2+} , also produces marked enhancement of Ia EPSP amplitudes (Jankowska et al., 1977) and increases the average probability of single-fiber quantal Ia EPSPs without changing their size (Jack et al., 1981b). In all of these respects, the behavior of group Ia EPSPs within the CNS closely resembles that of cholinergic end plate potentials at the neuromuscular junction (Barrett and Magleby, 1976). Despite the great anatomical differences between the consolidated neuromuscular junction and the distributed, individual synaptic boutons belonging to a single Ia afferent, these results strongly suggest that the basic mechanism of transmitter release is the same at both synapses.

PRESYNAPTIC INHIBITION

If the probabilities of release at all 500 or so Ia boutons ending on an average motoneuron varied independently, then the amplitude of the resulting composite Ia EPSPs would change very little from moment to moment because random fluctuations at individual boutons would cancel each other. However, composite Ia EPSPs, as well as the monosynaptic reflexes produced by them, exhibit large, correlated fluctuations from trial to trial (Gossard et al., 1994). In addition, when composite Ia EPSPs are recorded simultaneously in two motoneurons in the same motor nucleus, their amplitude fluctuate

tuations are correlated (Rudomin et al., 1975). These observations indicate the existence of a mechanism that can synchronize the fluctuations in transmitter release among large numbers of presynaptic group Ia boutons, whether ending on the same or different motoneurons.

In the mid-1950s, Frank and Fuortes (1957) discovered that conditioning stimulation of group I afferents in certain flexor muscle nerves reduced the amplitude of subsequent homonymous group Ia EPSPs in extensor motoneurons without producing other detectable changes in the postsynaptic cell. Frank (1959) later suggested that such “remote inhibition” of somatic EPSPs might result from interactions between Ia boutons and nearby inhibitory synapses located on the same distal, electrotonically remote dendrites, such that the responsible inhibitory conductances would themselves not be “seen” at the soma. This was a revolutionary notion at the time, because synapses on distant dendrites were generally regarded as irrelevant. Moreover, Frank suggested that transmission at Ia boutons might be reduced by some mechanism that presynaptically reduces transmitter release. This is now called *presynaptic inhibition*, whereas negative postsynaptic interactions on distal dendrites are still referred to as *remote inhibition*. These alternatives are not mutually exclusive and there is evidence that both mechanisms exist (Burke and Rudomin, 1977; Rudomin and Schmidt, 1999).

Conditioning stimuli that produce presynaptic inhibition usually also generate depolarizing potentials, called *primary afferent depolarization* (PAD), in the intraspinal arborizations of the target primary afferents (Rudomin and Schmidt, 1999). There is now abundant evidence that PAD is produced by GABA liberated by the type P “axo-axonic” synapses (see Fig. 3.5) that synapse directly on group Ia and other primary afferent synapses (Pierce and Mendell, 1993; Destombes et al., 1996). GABA-A receptor blockers such as picrotoxin block PAD (Eccles et al., 1963). The depolarizing action of GABA on primary afferent terminals may seem somewhat odd because this transmitter usually produces hyperpolarization by increasing Cl^- conductances in motoneurons and many other types of neurons (reviewed in Rekling et al., 2000). However, the Cl^- equilibrium potential in primary afferent terminals is more positive than the resting membrane potential (Alvarez-Leefmans et al., 1998), so that an increased Cl^- conductance generates depolarizing potentials in afferent terminals.

There is some debate about whether PAD *causes* presynaptic inhibition and, if so, via what mechanism (reviewed in Rudomin and Schmidt, 1999). Current evidence suggests that, in most instances, PAD generated by axo-axonic boutons indeed reduces glutamate release by reducing the entry of Ca^{2+} into afferent boutons by reducing the amplitude and duration of the afferent action potential (Stuart and Redman, 1992; Graham and Redman, 1994). There is little evidence for actual blockade of action potential invasion in afferent arborizations (Graham and Redman, 1994; Rudomin and Schmidt, 1999). Local increases in extracellular K^+ from neuronal activity can also produce PAD, but this is not associated with presynaptic inhibition. The close quantitative association between the magnitude and time course of PAD and presynaptic inhibition of group Ia EPSPs (e.g., Lev-Tov et al., 1983a) has led many investigators to conclude that the relation represents cause and effect.

This simple conclusion is complicated by the fact that afferent boutons also have GABA-B receptors (Bowery et al., 1987), which are co-activated by axo-axonic GABA release and also reduce Ca^{2+} entry (Dolphin and Scott, 1986) by a G-protein-coupled

metabotropic action (see Chap. 2). Baclofen produces marked depression of postsynaptic PSPs (Shapovalov and Shiraev, 1982; Lev-Tov et al., 1988), without inducing ionotropic changes in postsynaptic membrane potential (Curtis et al., 1981). Although this evidence might suggest that presynaptic inhibition and PAD may not in fact be causally linked, Stuart and Redman (1992) used the GABA-B blocker, saclofen, to conclude that GABA-B activation, although clearly present during presynaptic inhibition, plays a subsidiary role in its production. It is likely, therefore, that PAD and GABA-B receptor activation act cooperatively to modulate Ca^{2+} entry into afferent terminals, with additive effects on net transmitter output (see also Peng and Frank, 1989). Presynaptic inhibition cannot completely block afferent information, but it can certainly modify its strength and target effects.

Presynaptic inhibition is widespread among large-diameter afferents, both muscle and cutaneous, but there is no convincing evidence that it occurs in supraspinal descending pathways, nor in the connections made by spinal interneurons. The functional organization of presynaptic control of afferent transmission is highly complex and beyond the scope of this chapter (see Rudomin and Schmidt, 1999). However, it should be noted that PAD can be localized within individual collaterals of a given afferent; giving the CNS a remarkable degree of specific control (Eguibar et al., 1997). In the functioning spinal cord, there appears to be a constant background of presynaptic inhibition that can modulate afferent information to sharpen as well as defocus sensory input within the segmental circuitry. This includes the flow of information to tract interneurons that forward afferent information to the brain.

OTHER EXCITATORY SYSTEMS

The group Ia afferent system is obviously only one of many synaptic systems that control activity within the spinal cord ventral horn. Many segmental interneurons make excitatory synapses on one another as well as on motoneurons, but these synaptic systems are not well characterized because they are difficult to study in isolation. Some functionally defined systems that descend from the brain have been studied with experimental methods analogous to those applied to the group Ia system. Perhaps the best known are the corticospinal and rubrospinal tracts, which contain fibers that make direct, monosynaptic excitatory contact with certain species of alpha-motoneurons in primates (see reviews by Phillips, 1969, and Porter, 1987). The collaterals of corticospinal axons in monkeys and cats are more sparsely distributed along the cord than those of Ia afferents (Shinoda et al., 1986b), and their terminal arborizations also differ in shape and density (Lawrence et al., 1985).

Corticospinal EPSPs recorded in primate motoneurons share some characteristics with group Ia EPSPs (Clough et al., 1968) but differ in that they exhibit considerable facilitation during double-pulse or short-train repetitive activation (Muir and Porter, 1973). Other descending systems, such as the vestibulospinal tract, exhibit much less such facilitation (Burke and Rudomin, 1977). The morphology of vestibulospinal fibers is also more like that of group Ia afferents (Shinoda et al., 1986a). The evidence at hand suggests that the transmitter and/or receptor kinetics may be different for these various species of spinal afferent systems. The transmitter(s) liberated by descending systems remain unknown, although glutamate is the most likely excitatory transmitter. It should be noted that electrical stimulation of descending tracts is much less easily

controlled than that of afferents in peripheral nerves and there is much less assurance that one is activating fibers with similar physiological roles.

POSTSYNAPTIC INHIBITION: THE DISYNAPTIC Ia RECIPROCAL SYSTEM

Inhibitory synaptic mechanisms are extremely important in controlling neural activity throughout the CNS. In the spinal cord, all of the various types of primary afferents, as well as the majority of long axonal systems that descend into the spinal cord from the brain, make excitatory synapses with their target neurons. Thus, inhibition in the ventral horn is largely produced by segmental interneurons, making information about specific inhibitory systems less detailed than is the case with group Ia excitation discussed earlier.

The first inhibitory postsynaptic potentials (IPSPs) recorded in the mammalian CNS were found by Eccles and colleagues in alpha-motoneurons after stimulation of group Ia afferents from antagonist group Ia afferents (Brock et al., 1952). The central latency of these “reciprocal Ia IPSPs” is sufficiently long (1.2–1.8 ms) to indicate the presence of one level of interposed interneurons (Eccles et al., 1956) (Fig. 3.9). Reciprocal Ia inhibition is referred to as *disynaptic* because there are two synaptic layers (and one layer of interneurons) interposed between the afferents and the target neurons. The identification and elucidation of the synaptic organization of the inhibitory interneurons in this pathway came much later (see later).

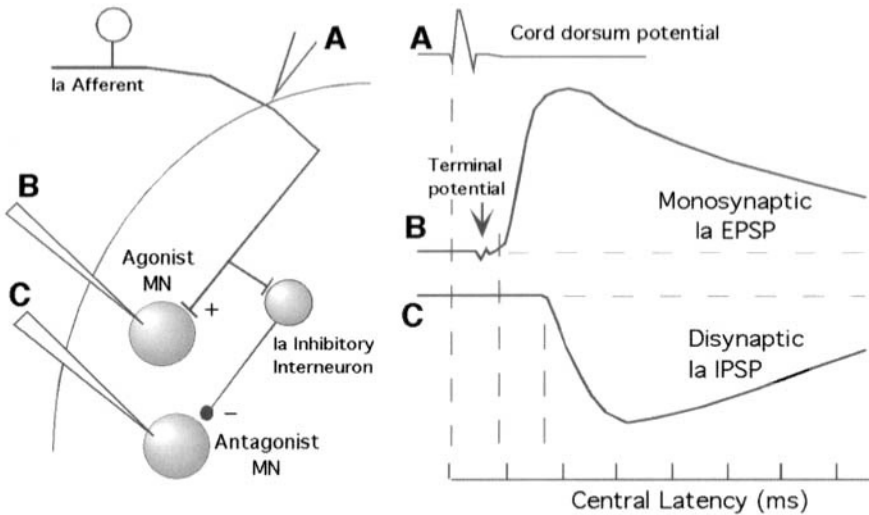


Fig. 3.9. Latencies of monosynaptic and disynaptic PSPs. The cartoon at the left illustrates the point of recording for afferent volleys entering at the dorsal root (A) and the intraspinal circuits for monosynaptic EPSPs and disynaptic IPSPs generated in homonymous (B) and antagonist (C) motoneurons. The drawing on the right illustrates the time differences (central latency) between the entering volley and the onsets of the monosynaptic EPSP (about 0.8 ms) and the disynaptic IPSP (about 1.7 ms), produced by the time needed to fire the intervening interneurons that generate the IPSP. Note that the arrival of the group Ia volley in the ventral horn, signaled by the “terminal potential” just before EPSP onset (arrow), is about 0.3 ms before the EPSP begins.

At normal motoneuron resting potentials (about -70 mV), group Ia disynaptic IPSPs are hyperpolarizing, indicating that the equilibrium potential for the process is more negative than the resting potential. The IPSPs can be reversed into depolarizing synaptic potentials by injecting hyperpolarizing current to move the transmembrane potential to values more negative than the inhibitory E_{eq} (usually about -75 mV to -80 mV; Coombs et al., 1955b). Intracellular injection of Cl^- ions reverses Ia IPSPs at normal resting potentials by moving the inhibitory E_{eq} to more positive values. Therefore, it is generally accepted that Cl^- is the major ionic species involved in this inhibition (see Chap. 2). Motoneuron responses to direct application of the amino acid, glycine, behave in exactly the same manner as Ia IPSPs (reviewed in Young and Macdonald, 1983). Group Ia IPSPs are blocked by the convulsant drug strychnine, which also blocks postsynaptic glycine receptors. Because group Ia IPSPs are readily influenced by the injection of electrical current or small amounts of Cl^- ions into the motoneuron soma, it seems likely that many of the synapses of Ia inhibitory interneurons are located on and near the cell soma (Burke et al., 1971).

REFLEXES AND BEYOND: THE SYNAPTIC ORGANIZATION OF SPINAL CIRCUITS

Unraveling the specific patterns of interconnections between CNS neurons is a major goal of neuroscience. As mentioned earlier, one of the great advantages of the spinal cord for neural circuit analysis is the fact that both primary afferents and motoneurons, the two linchpins of functional identification in the motor system, are locally present, separately accessible, and readily identifiable. A set of interneurons known to receive direct (monosynaptic) input from a particular afferent system and to project, directly or indirectly, to motoneurons can be defined in terms of spinal cord circuitry and probable function. Such aggregates are *reflex pathways*.

REFLEX PATHWAYS

The history of neuroscience began with studies of reflexes, which are predictable patterns in activity in muscles or autonomic effector organs that are produced by particular inputs. The simplest example, as already noted, is the monosynaptic stretch reflex. An even more classic example is the withdrawal of a limb away from a painful stimulus (the *flexion reflex*), which can be accompanied by generalized autonomic effects such as the constriction of arterioles and pupillary dilation. Indeed, some reflexes can involve precisely coordinated action of many muscles, such as the rhythmic scratching movements in a dog's hindleg in response to tickling its ear (the "scratch reflex") or the shifts in activity in many limb and trunk muscles that accompany limb withdrawal away from a painful stimulus. These and other reflexes have been used to elucidate the neuronal circuits and synaptic interactions that produce them. One cannot overstate the importance of reflexes in the development of ideas about CNS function that we now take for granted (e.g., see Brazier, 1960).

Until relatively recently, *automatic* reflex responses have usually been regarded as qualitatively different from *voluntary* motor acts, which implies that the two are produced by separate bits of neural machinery even though both kinds of action require the same motoneurons. However, over the past three decades research on synaptic or-

ganization in the spinal cord has revealed that both reflex and voluntary actions also utilize many of the same spinal *interneurons*. The ventral horn of the spinal cord is a region in which incoming sensory information is integrated with “motor command” signals descending from supraspinal brain regions, forming an efficient feed-forward control system. The following section stresses two points: (1) the spinal pathways of nominally different “reflexes” in fact interact extensively, often by sharing common interneurons; and (2) control of movement by the supraspinal brain is mediated mainly through interneurons in “reflex” pathways (Lundberg, 1975). This is likely to be true even in primates, including humans, despite the existence of direct (monosynaptic) corticospinal control of some motoneurons.

SYNAPTIC ORGANIZATION IN THE STRETCH REFLEX

Contraction of a muscle after sudden stretch depends on the monosynaptic excitation of motoneurons by group Ia afferents. The monosynaptic projections of group Ia afferents are directed not only to motoneurons of the muscle from which those Ia afferents arise, called the homonymous muscle, but also to those of its functional synergists (heteronymous muscles). These synergists can act at the same joint, as with the potent heteronymous Ia connections between the three ankle extensor muscles that comprise the triceps surae group (soleus plus medial and lateral gastrocnemius), or at different joints, such as gluteus (hip extensor) and soleus (Eccles et al., 1957). In general, the heteronymous composite EPSPs are smaller than the homonymous ones because a smaller proportion of heteronymous Ia afferents reach synergist motoneurons than their homonymous targets (Fleshman et al., 1981a). It is now known that the smaller-diameter, slower-conducting group II muscle spindle afferents also produce monosynaptic excitation in many motoneurons, albeit considerably weaker than that produced by Ia afferents (Sybert and Munson, 1984). The only primary afferent systems that make direct connections onto motoneurons are thus the groups Ia and II muscle spindle afferents.

The monosynaptic stretch reflex is obviously designed for speed, but it is important to recognize that it is also reliable, in the sense that a monosynaptic connection cannot be completely interrupted, despite modulation by presynaptic inhibition (see earlier). One clear role of stretch reflexes is to increase motor unit activity to resist externally imposed stretch, which increases muscle stiffness and tends to restore the muscle to its original length (Houk and Rymer, 1981; Prochazka, 1996). The apparent simplicity of the monosynaptic pathway is deceptive, however, because the sensitivity of stretch receptor afferents can be controlled by the CNS through the gamma- and beta-motoneurons. In addition, both Ia and group II spindle afferents exert significant effects on motoneurons indirectly through interneuron pathways (Lundberg et al., 1987; Jankowska, 1992), which are themselves targets of CNS control (see later). This functional roles of this remarkable system continue to be a matter of intense research interest.

MULTISYNAPTIC REFLEXES: INTERNEURONS

The fact that a monosynaptic reflex arc cannot be completely disabled is a weakness as well as a strength. Significant advantages accrue when at least one layer of interneurons is interposed between an afferent system and the target motoneurons, as in the disynaptic group Ia inhibitory circuit discussed earlier. The sign of the effect at moto-

neurons can be changed from excitation to inhibition. In addition, transmission in a multisynaptic reflex pathway can vary from zero to considerable amplification, by virtue of other excitatory and inhibitory effects that converge onto the interposed interneurons, thus regulating their excitability. Thus, multisynaptic circuits can function as logical elements (in effect, digital gates of any configuration) and as signal amplifiers, depending on circuit organization. The convergence of multiple input systems onto specific groups of interneurons in spinal reflex pathways is so common that few if any of them are "private" to a particular category of input or output (Lundberg, 1969, 1975; Baldissera et al., 1981). It seems quite likely that the spinal interneurons that are interposed in the long-recognized spinal reflex pathways can under other conditions subserve quite different functions and obey other masters.

Disynaptic Recurrent Inhibition: Renshaw Cells. The first spinal interneurons to be functionally identified were the "Renshaw cells," so-called by Sir John Eccles and coworkers (1954) in honor of Birdsey Renshaw, who first described *recurrent inhibition* of motoneurons following antidromic activation of motor axons. Renshaw cells are monosynaptically excited by cholinergic synapses from collaterals that arise along the course of motoneuron axons before they exit from the cord. In turn, Renshaw cells project back to the same and related motoneurons where they produce inhibitory synaptic potentials (for reviews, see Burke and Rudomin, 1977; Baldissera et al., 1981). The central latency of onset for recurrent IPSPs (about 1.5 ms) in motoneurons indicates interposition of a single layer of intermediate interneurons (i.e., a "disynaptic" connection).

The key to functional identification of Renshaw interneurons was that the input and output sources were the same (i.e., motoneurons). Individual Renshaw cells were identifiable during microelectrode recording (Eccles et al., 1954) because the EPSPs produced by motor axon collaterals are powerful and of relatively long duration (Walmsley and Tracey, 1981). As a result, Renshaw cells have distinctive, very high frequency (up to 1000 Hz) repetitive action potentials when activated by stimulating a ventral root (Fig. 3.10A), making their identification possible without the considerable difficulty of proving that an individual cell indeed projects monosynaptically to motoneurons (Van Keulen, 1981).

Individual Renshaw cells have been studied morphologically, and their projections confirmed directly (Lagerbäck and Kellerth, 1985; Fyffe, 1991). Although Renshaw cells are located deep in Rexed's lamina VII, ventromedially adjacent to the motor nuclei (see Fig. 3.1), only a few of their axonal collaterals take the shortest route (i.e., within the gray matter) to the adjacent motor nuclei. Like other spinal interneurons (see Fig. 3.1B), their main axons enter the ventral and lateral white matter and then drop finer collaterals back into the ventral horn as they run along the spinal cord. Surprisingly, the cholinergic synapses that produce the intense discharge in Renshaw cells are located mainly on the proximal dendrites (Alvarez et al., 1999), whereas their somata are dominated by inhibitory glycinergic synapses (Alvarez et al., 1997).

The recurrent IPSPs produced in motoneurons after ventral root stimulation are longer and less sharply peaked (see Fig. 3.10A) than group Ia IPSPs discussed earlier (see Fig. 3.9) because they are produced by high-frequency bursts from the Renshaw cells. Consequently, recurrent IPSPs can exhibit more or less synchronous wavelets,

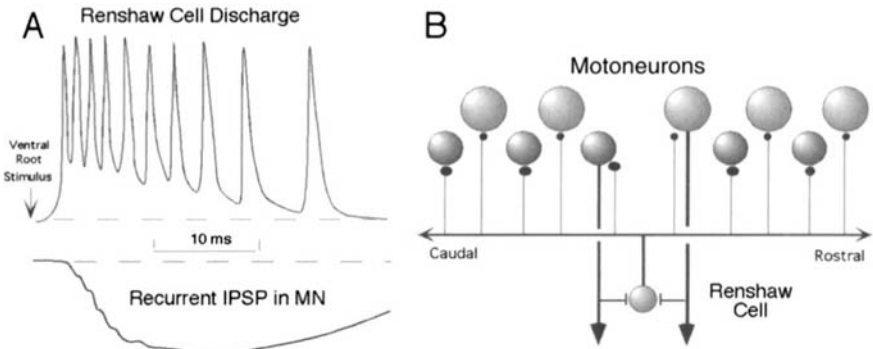


Fig. 3.10. Recurrent inhibition through Renshaw interneurons. **A:** Diagram of the intracellular potential in a Renshaw interneuron, in which a powerful EPSP produced by motoneuron recurrent collaterals generates fast repetitive firing (upper trace) that in turns results in a prolonged IPSP in motoneurons (lower trace). **B:** Circuit diagram of the recurrent inhibitory pathway. Relatively localized motor axon collaterals project to nearby Renshaw cells that have axons that project more widely to motoneurons along the axis of the spinal cord. The relative efficacy of Renshaw cell projections to small and large motoneurons is denoted by the sizes of the recurrent synapses.

each generated by the relatively synchronized spikes in the multiple Renshaw cells that converge onto the motoneuron. The reversal potential for recurrent IPSPs is similar to that of disynaptic Ia IPSPs, indicating that increased Cl^- conductance is responsible. However, it has been reported that recurrent IPSPs are only partially blocked by the glycine antagonist strychnine (Cullheim and Kellerth, 1981; Schneider and Fyffe, 1992). The strychnine-resistant remnant is instead blocked by the GABA-A receptor blocker picrotoxin. There may be two populations of Renshaw interneurons, one that secretes glycine and the other that secretes GABA (Fyffe, 1990), although it is also possible that individual Renshaw interneurons may co-release both inhibitory transmitters (Örnung et al., 1994).

Interestingly, recurrent IPSPs are less readily reversed by small injections of Cl^- into the motoneuron soma than are Ia IPSPs in the same motoneuron, even though both are about equally affected by current injected at the soma (Burke et al., 1971). This suggests that Renshaw cell synapses end mainly on proximal motoneuron dendrites, where they are relatively isolated from small alterations of intrasomatic Cl^- concentration but less so from voltage perturbations. This conclusion has been confirmed by direct anatomical reconstructions (Fyffe, 1991). If Renshaw cell synapses are located on some proximal motoneuron dendrites and not others, it is possible that they might strategically reduce the effects of synapses located more distally on just those dendrites.

The basic circuit diagram of the Renshaw system (see Fig. 3.10B) is relatively simple, but one must appreciate that many neurons are symbolized by the single element labeled "Renshaw cell." It is also clear that a given Renshaw cell receives input from many motoneurons (*input convergence*) and almost certainly projects to many individual motoneurons (*output divergence*). Recurrent inhibition obviously provides negative feedback from active motoneurons to the same and other motoneurons, but there

are a few interesting complexities in their organization that lend spice to this apparently simple circuit.

The collaterals of motoneuron axons spread rostrocaudally for only about 1 mm away from their point of origin, limiting recurrent input to nearby Renshaw cells (Cullheim and Kellerth, 1978a). Because most motor nuclei in the cat spinal cord are 7–10 mm in length, this means that only a fraction of the motoneurons belonging to a given nucleus can contribute input to any local group of Renshaw cells. In addition, recurrent collaterals from the motoneurons that innervate fast contracting muscle units (most notably, those of type FF motor units) are more luxuriant than those of cells innervating slow twitch muscle units (type S; Cullheim and Kellerth, 1978a). It is interesting that motoneurons that innervate small, distal muscles do not have recurrent axon collaterals at all, irrespective of motor unit type (Cullheim and Kellerth, 1978b; McCurdy and Hamm, 1992). Motor axon collaterals are not the only source of synaptic input to Renshaw cells. Groups of Renshaw cells inhibit one another, producing “recurrent excitation” (see Fig. 3.12) (Ryall, 1981), and they receive both excitatory and inhibitory input from a variety of primary afferents and supraspinal regions (Burke and Rudomin, 1977; Baldissera et al., 1981). Thus, it is clear that Renshaw cells do not constitute a “private pathway” exclusive to motor axon collaterals.

On the output side, Renshaw cell axons can project over 12 mm rostrocaudally, thus extending their influence to large fractions of the motor nuclei (Jankowska and Smith, 1973) (see Fig. 3.10B). In contrast to the apparent strength of type-related motoneuron input to Renshaw cells noted earlier, recurrent IPSPs are largest among type S motoneurons and smallest in type FF (Friedman et al., 1981). Despite some contrary evidence (Lindsay and Binder, 1991), the weight of available observations suggests that, in general, motoneurons that excite Renshaw cells most strongly receive the weakest recurrent inhibition, and vice versa. The spatial relations between motor nuclei that activate Renshaw cells versus those that receive recurrent inhibition can be quite complex. As a general rule, recurrent inhibition is not found between motor nuclei of muscles that are strict functional antagonists at a particular joint (Baldissera et al., 1981). Particular motor nuclei can be joined as input-output partners in recurrent inhibition even though separated by considerable distances, whereas near neighbors may not be. Recent work has provided evidence for quite specific input-output patterns among cat hindlimb motor nuclei that include both recurrent inhibition and facilitation (Turkin et al., 1998). However, motoneurons and other Renshaw cells are not the only targets for Renshaw cell output; they powerfully inhibit interneurons in the reciprocal disinaptic pathway between group Ia afferents and motoneurons but not cells in most other oligosynaptic reflex pathways (Hultborn et al., 1971a,b; see later).

A modeling study suggests that one role for recurrent inhibition is to promote desynchronized firing among motoneurons (Maltenfort et al., 1998), which could provide more accurate control of muscle force. Beyond that, however, the complexity of synaptic organization among Renshaw interneurons, particularly the fact that they inhibit reciprocal group Ia interneurons (see later), suggests that they subserve functions that go well beyond negative feedback. What appears at first glance to be a rather simple neuronal organization has, on closer inspection, remarkable complexity, with functional implications that remain to be clarified.

Disynaptic Group Ia Reciprocal Inhibition. Identification of individual interneurons in the reciprocal Ia inhibitory pathway was not as simple as in the case of Renshaw cells. Many spinal interneurons receive monosynaptic group Ia excitation (Eccles et al., 1960), and for a long time it was not clear which of the candidates directly inhibit antagonist motoneurons. The key to this problem was found by Hultborn and coworkers (1971a,b) who discovered that of all the group Ia inhibitory reflex pathways tested, only disynaptic reciprocal Ia inhibition is subject to recurrent inhibition by Renshaw cells. Thus, an individual interneuron that is monosynaptically excited by group Ia afferents and disynaptically inhibited after ventral root stimulation can be inferred to belong to the reciprocal Ia inhibitory reflex pathway.

Subsequent elegant work by Jankowska and Roberts (1972), using the technique of spike-triggered averaging (using the action potentials of a single interneuron to trigger a computer to average intracellular potentials from the target motoneuron), showed directly that such interneurons indeed directly inhibit the appropriate motoneurons. The morphology of Ia inhibitory interneurons has been examined using intracellular injection of tracer substances (Jankowska and Lindström, 1972). Like Renshaw cells, Ia inhibitory interneurons have axons that travel in the white matter, dropping collaterals back into the gray matter to make synaptic contacts with both alpha- and gamma-motoneurons (see Fig. 3.1B).

The disynaptic reciprocal Ia inhibitory pathway provides a striking example of the complexity of CNS control of interneurons. Synaptic organization in this pathway was worked out largely using the technique of “spatial facilitation” that allows inferences about the convergence of multiple synaptic input systems onto interneurons that project directly to motoneurons (Lundberg, 1975). With intracellular recording from a motoneuron, stimulation of one input system (a “conditioning” input, usually a primary afferent system) can nonlinearly enhance or diminish the amplitude of “test” synaptic potentials produced by another input source when the two inputs converge on common interneurons (Fig. 3.11). When postsynaptic changes in the motoneuron and presynaptic inhibition can be excluded, this method can give information about the CNS circuits that may control those interneurons during various behaviors.

Using spatial facilitation, Hultborn, Jankowska, and their colleagues (for reviews, see Baldissera et al., 1981) have shown that the reciprocal Ia inhibitory interneurons receive excitatory inputs from a wide variety of input systems in addition to Ia afferents (Fig. 3.12, left panel), including other primary afferents and descending systems from supraspinal centers. In addition to inhibition by Renshaw cells, groups of Ia inhibitory interneurons also directly inhibit other groups of reciprocal Ia inhibitory interneurons. Finally, Ia reciprocal interneurons can be driven in phase-related bursts during rhythmic motoneuron activity, called *fictive locomotion*, that mimics the patterns seen in actual locomotion (Feldman and Orlovsky, 1975; see later) without any drive at all from Ia afferents.

Although seemingly bewildering in complexity, the synaptic organization of reciprocal Ia inhibitory interneurons displays patterns that suggest important functional correlates (Baldissera et al., 1981; Jankowska, 1992). For example, descending systems like the vestibulospinal tract directly excite certain extensor motoneurons as well as Ia inhibitory interneurons that receive Ia input from the same muscle and then inhibit its

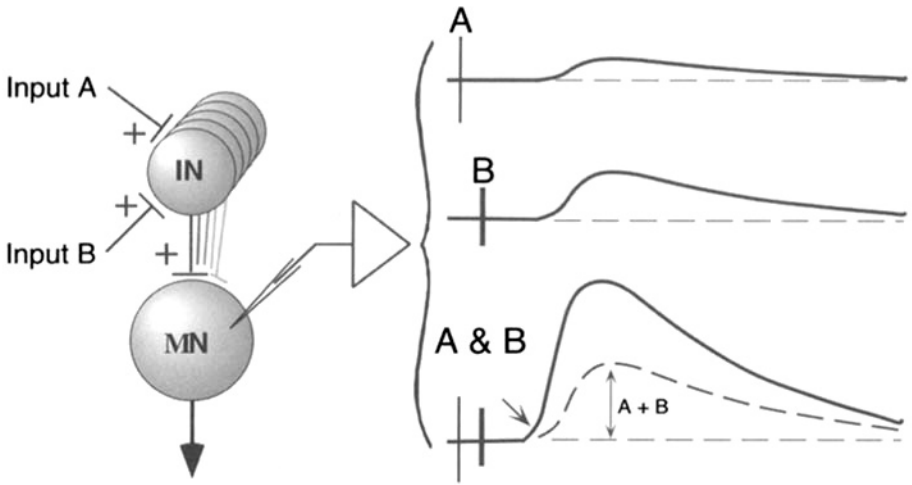


Fig. 3.11. Spatial facilitation of transmission through a disynaptic pathway to motoneurons. [Adapted from Lundberg, 1975.] The cartoon at the left shows a motoneuron (MN) receiving projections from a set of last-order interneurons that in turn receive synaptic excitation from two sources (inputs A and B). When activated by either input alone, the interneurons produce small disynaptic EPSPs in the motoneuron (right diagram). Activating the two inputs together with the proper timing produces an EPSP that is much larger than the algebraic sum of A and B alone. In addition to being larger, the facilitated EPSP can also sometimes exhibit reduced central latency because some of the interposed interneurons fire earlier than they do with either input alone (A and B, arrow). This is due to the fact that the EPSPs in some interneuron reach threshold for firing earlier when the cells are depolarized by both inputs.

flexor antagonists. These same “extensor” Ia inhibitory interneurons also inhibit the Ia inhibitory interneurons that receive *flexor* Ia input and inhibit the extensor motoneurons (see Fig. 3.12). Working through this organization, it becomes apparent that activation of an extensor muscle by, for example, descending vestibulospinal “commands,” would simultaneously increase inhibition of the antagonist flexor nucleus and reduce any ongoing extensor inhibition due to “flexor” Ia interneurons activated by passive stretch of the antagonist flexor muscle. This antagonist suppression presumably can be kept within bounds, at least to some extent, by superimposed recurrent inhibition. Activation of the agonist (extensor) motor nucleus would, through recurrent inhibition, suppress “its” Ia interneurons and remove the antagonist suppression. This is, of course, only one possible scenario. Given the variety of inputs present, reciprocal Ia inhibitory interneurons can presumably participate in a wide variety of actions in addition to their “simple” reflex function. The fact that they can be driven rhythmically during fictive locomotion provides a striking example of this (see later).

Other Disynaptic Reflex Systems: State Dependence. The spatial facilitation approach is most informative when applied to disynaptic reflex pathways. The synaptic organization of most spinal reflex systems is unknown because they involve multiple layers of interneurons between the incoming afferents and motoneurons. However, there are muscle and cutaneous afferents that do produce disynaptic PSPs in specific groups of

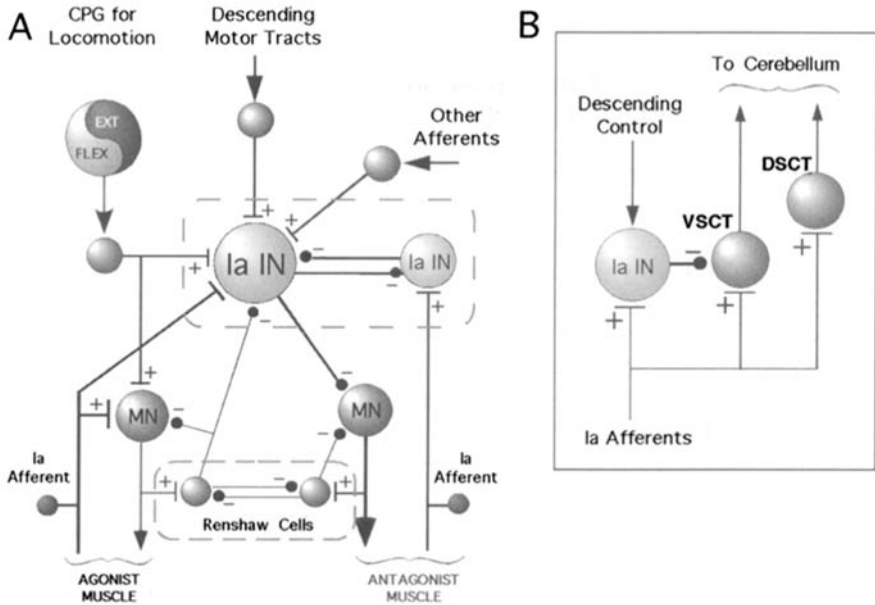


Fig. 3.12. Synaptic organization of group Ia inhibition. **A:** The schematic diagram shows the main features of synaptic organization in interneurons in the disynaptic reciprocal inhibitory pathway from group Ia afferents to antagonist motoneurons (thicker lines). Because of its importance in the identification of these interneurons, the organization of Renshaw interneurons is also shown. Note the reciprocal inhibitory connections between groups of Ia inhibitory and Renshaw interneurons (within dashed boxes). (See the text for other details.) [Diagram adapted from Baldissera et al., 1981, with permission.] **B:** The schematic diagram within the box on the right illustrates one aspect of contrasting synaptic organization in dorsal (DSCT) and ventral (VSCT) spinocerebellar tract neurons. [Adapted from Fig. 1 in Lundberg, 1971, with permission.] Note that VSCT neurons receives monosynaptic excitation and disynaptic inhibition from the same set of group Ia afferents. With this basic arrangement, the signal in the VSCT pathway depends on the balance between monosynaptic Ia excitation and disynaptic inhibition, whereas that in the DSCT reflects only Ia excitation. In principle, comparison of the two signals in the cerebellum carries information about transmission through the Ia inhibitory interneurons. See text for full discussion.

motoneurons. Most of these disynaptic effects were not detected in conventional, deeply anesthetized preparations because they are “open” only under certain conditions, or *CNS states*, such as during fictive locomotion (Burke, 1999a; see later). For example, group I afferents (including group Ia muscle spindle afferents) produce disynaptic EPSPs that are superimposed on monosynaptic EPSPs in many extensor or flexor motoneurons only during the phase of fictive locomotion when the recipient motoneurons are active (Schomburg and Behrends, 1978; Angel et al., 1996; Degtyarenko et al., 1998). These disynaptic EPSPs can be quite large, amplifying the effects of group Ia input that supports firing in the already active motoneurons. These effects appear to be due to convergence of drive from circuits that produce locomotion (see later) onto the same interneurons that receive group I input, rather than modulation of presynaptic control of group I synaptic action (Gossard, 1996). The central pathways from group

II spindle afferents are also subject to such state-dependent control (Lundberg et al., 1987; Jankowska, 1992).

The Golgi tendon organ afferents (group Ib) that sense muscle tension also generate disynaptic excitatory and inhibitory reflex effects (Baldissera et al., 1981; Jankowska, 1992). There are also disynaptic excitatory pathways from skin afferents to some motoneurons (Illert et al., 1976; Fleshman et al., 1984, 1988a), and some of them become evident only during particular phases of fictive locomotion (see later). However, most cutaneous and some muscle afferent reflexes operate through at least two levels of interneurons (referred to simply as *multisynaptic*). It is difficult to make inferences about the synaptic organization in multisynaptic reflex pathways using the spatial facilitation approach because the neurons that receive direct afferent input are *not* the same as those that project to the output motoneurons. Nevertheless, many of these more complex pathways appear to exhibit the same kind of convergent control that is characteristic of disynaptic systems (Baldissera et al., 1981).

THE SYNAPTIC ORGANIZATION OF ASCENDING TRACTS

The basic function of some ascending tract neurons is clearly to relay sensory information from primary afferents to regions of the brain that produce conscious sensation and/or guide the formation of appropriate actions. There is a great deal of information about such systems that, being located in the dorsal horn, are beyond the scope of this chapter (see Willis and Coggeshall, 1991). However, some ascending systems appear to reflect a more “integrative” function at the spinal cord level that complements the organizations found in the reflex interneuron pathways discussed earlier.

The contrast between “relay” and “integrative” functions is apparent when comparing the synaptic organization of two major spinocerebellar systems that project from the lumbosacral enlargements of carnivores and primates to the cerebellar cortex and certain brain stem nuclei. The dorsal spinocerebellar tract (DSCT) originates from cells in Clarke’s column, one of the few anatomically distinct groups of spinal cord neurons, located in the upper lumbar segments of the cord. Individual DSCT neurons receive powerful input from particular afferent species, either from muscle (e.g., group Ia afferents from one muscle or a functionally related group of muscles) or from cutaneous and some high-threshold muscle afferents (for a review, see Bloedel and Courville, 1981). The firing of a given DSCT cell is tightly coupled to, and relays with reasonable accuracy, the input from the afferents that project to it (Kröller and Grüsser, 1983). As always in nature, the “relay” analogy is not perfect because there is evidence that DSCT neurons also receive input from segmental and local interneurons (Hongo et al., 1983), leading to a degree of integration within Clarke’s column (reviewed in Bosco and Poppele, 2001). Nevertheless, DSCT neurons provide the cerebellar cortex with a relatively “unprocessed” version of information from particular kinds of primary afferents, which is markedly different from its counterpart, the ventral spinocerebellar tract (VSCT).

Individual neurons of the VSCT receive a complex mixture of cutaneous and muscle afferent inputs, some directly from primary afferents and some indirectly via segmental interneurons, including those in the reciprocal group Ia inhibitory pathway

(Lundberg and Weight, 1971). In general, no single afferent system dominates the synaptic inputs to VSCT. What use can the cerebellum make of such diverse mixtures? Lundberg (1971) suggested an intriguing hypothesis, based in part on the observation that some VSCT cells receive monosynaptic excitation from group Ia afferents from a particular muscle nerve and, at the same time, disynaptic inhibition apparently produced by the same Ia afferents (see Fig. 3.12, right panel) (Lundberg and Weight, 1971). When the two co-exist, the probability of discharge from VSCT cells might cancel if they were of equal efficacy or modulated up or down depending on which input was stronger. This arrangement would enable VSCT neurons to function as comparators, signaling the level of transmission through the disynaptic Ia inhibitory pathway. Given the complexity of peripheral, local, and descending input to the reciprocal Ia inhibitory interneurons, it would seem important to forward information about the “state of affairs” at the segmental level to the supraspinal brain (Lundberg, 1971). Although much work is required to validate this hypothesis, it is in principle testable.

Synthesis. The synaptic organization found in spinal interneuronal pathways implies great functional flexibility in the spinal cord. This phylogenetically old part of the CNS evidently retains mechanisms capable of sophisticated local integration of sensory information with descending motor commands. The convergence of control on reflex pathway interneurons enables descending motor commands to take advantage of the fact that these cells have immediate access to the sensory information that signals, for example, current limb position, muscle lengths and tensions, and the presence of external obstacles. By operating through interneurons of segmental reflex pathways, descending motor commands can be effectively filtered according to the existing “state of affairs” in the limb and trunk before they reach the motoneurons, which is updated continuously as conditions change. This feed-forward organization can operate in an efficient, predictive way, in contrast to feed-back mechanisms that depend on sensory signals about the *results* of a movement, which are inherently slower and less efficient in controlling movements of even modest speed (Rack, 1981). There is evidence that this type of organization is present in humans, where it appears to operate during voluntary movements (Pierrot-Deseillegnny, 1996).

THE SPINAL CORD IN ACTION

Aspects of the synaptic organization of the ventral horn have been discussed earlier at the level of individual synapses, neuron groups, and small neuronal circuits. This section deals with the influence of synaptic organization on two important aspects of dynamic spinal cord function: (1) the recruitment of motor units during a variety of movements, and (2) the operation of some interneuronal circuits during the generation of rhythmic motoneuron firing that resembles the patterns found in locomotion (fictive locomotion).

MOTOR UNIT RECRUITMENT

Control of muscle action during movement is obviously a major function of the spinal cord. Muscles are essentially conglomerates of motor units, and regulation of muscle force is a matter of activating and de-activating these quantum elements (*recruitment*

and *derecruitment*, respectively). The force produced by individual motor units is controlled by regulating motoneuron firing frequency (often referred to as *rate coding*). Because of the wide but systematic interrelations among motor unit properties (see Fig. 3.3) (see also Burke, 1981; Henneman and Mendell, 1981; Binder et al., 1996), understanding the recruitment process requires information about the *identities* as well as the numbers of active motor units. In addition to its importance in motor control, the process of motor unit recruitment has a wider significance for understanding the regulation of activity in functionally related groups of neurons throughout the CNS.

The fact that small motor units are recruited before large ones during stretch reflexes was first described by Denny-Brown (1929). Later, an influential series of papers from the laboratory of Elwood Henneman re-affirmed this observation and showed that derecruitment usually proceeds in the reverse order (Henneman and Olson). Henneman coined the term *size principle* not only to describe the small-to-large recruitment sequence but also to encapsulate the idea that the phenomenon somehow depends on the anatomical size of the motoneurons (Henneman et al., 1965). This idea generated wide interest in the basic mechanisms that underlie recruitment sequences (for reviews, see Burke, 1981; Binder et al., 1996; Powers and Binder, 2001). The results can be summarized by saying that recruitment in a wide variety of reflex and voluntary activities is usually, but not always, in a size-ordered sequence and that such sequences are determined by the interaction between intrinsic motoneuron properties and the organization of synaptic input to them. All of these factors are related to motoneuron size, but *size per se* is not a causal factor.

Intrinsic Motoneuron Properties Related to Recruitment. Intrinsic membrane properties that control cell excitability vary among the motoneurons in a given motor nucleus in relation to the properties of their muscle units (i.e., motor unit type). Whole neuron input resistance, R_N , is proportional to the effective membrane resistivity, R_m (see earlier), divided by the membrane area of the cell, A_N . In cat motoneurons, R_N varies over a 10-fold range, but A_N varies only about 3-fold (Fleshman et al., 1981b; Burke et al., 1982; Gustafsson and Pinter, 1984). Both factors exhibit the same gradation with motor unit type, suggesting that effective membrane resistivity of cat motoneurons increases in the same sequence. The same effective synaptic current delivered to the soma would thus generate the largest PSPs in type S motoneurons (Binder et al., 1996), as observed with some synaptic inputs (see Fig. 3.4).

Motoneurons exhibit a variety of nonlinear, time- and voltage-dependent properties that have important functional consequences on their relative excitability (reviewed in Binder et al., 1996; Powers and Binder, 2001). The rheobase current (the depolarizing current necessary to bring a neuron to its firing threshold) is a good measure of intrinsic excitability. Rheobase current in motoneurons increases systematically in the sequence $S < FR < FF$ after adjustment for differences in R_N (Fleshman et al., 1981b; Zengel et al., 1985). Another property called *accommodation* increases the firing threshold of some type F motoneurons during sustained depolarization, leading to eventual cessation of firing (Burke and Nelson, 1971).

Although motoneurons have long been known to possess nonlinear voltage-dependent conductances (Schwindt and Crill, 1977; see Crill, 1996), most of the early work on motoneuron properties was done in anesthetized or spinalized ani-

mals in which membrane nonlinearities are not prominent. It has become quite clear that voltage-dependent nonlinearities can dominate motoneuron behavior under other conditions. Motoneurons exhibit what has been called *bistable* membrane responses, or sustained depolarizing *plateau potentials*, in decerebrate cats (Crone et al., 1988), in which there is a strong monoaminergic descending drive from reticulospinal systems, or when exposed to the neurotransmitter serotonin (5-hydroxytryptamine [5-HT]; Hounsgaard et al., 1988) or drugs like L-DOPA that cause the release of noradrenaline (Conway et al., 1988). The ventral horn is liberally supplied by 5-HT synapses from bulbospinal descending axons (Alvarez et al., 1998; Rekling et al., 2000), which potentially provide the brain with a route for controlling plateau potential modulation during various motor acts (Delgado-Lezama and Hounsgaard, 1999).

In the presence of exogenous or endogenous 5-HT, transient depolarizations produced by current injection or synaptic action can activate a persistent inward (depolarizing) current (IPIC). This effect is an example of *neuromodulation* as described in Chap. 2. Although motoneurons exhibit an IPIC that is carried by Na^+ (Crill, 1996), the pharmacology of plateau potentials suggests that they are due largely to increased Ca^{2+} conductances through L-type channels in the dendrites (Svirskis and Hounsgaard, 1997; Carlin et al., 2000). This conductance can generate step-like increases in motoneuron firing that can outlast the activating event (Fig. 3.13). Plateau potentials either de-activate spontaneously or can be terminated by a short hyperpolarization from injected current or inhibitory synaptic input. Evidence suggests that the prevalence and voltage threshold for plateau potentials favor their operation in motoneurons with relatively slow axonal conduction velocities and low rheobase currents, suggesting that they are particularly prominent in type S motoneurons (Lee and Heckman, 1998).

Unlike many types of CNS neurons (see Chap. 2), motoneurons have a relatively limited range of firing frequency, largely because of their long-duration post-spike afterhyperpolarizing potentials (AHPs) (Kernell, 1965; reviewed in Kernell, 1992; Powers and Binder, 2001), which depend largely on Ca^{2+} -activated K^+ conductances (Barrett and Barrett, 1976). Motoneurons can fire at short intervals (10–20 ms; called *doublets*) when they begin firing, but the AHP conductance increases during repetitive firing (Baldissera and Gustafsson, 1971), resulting in longer inter-spike intervals (*adaptation*) as firing continues. Doublets can enhance subsequent force output, particularly in type S muscle units, despite lower sustained frequencies (the “catch” property; Burke et al., 1970b).

All of these features are closely related to the mechanical properties of the innervated muscle units and the ways in which they are used during movement. Muscle units of all types produce their full effective range of force output modulation over a relatively limited range of sustained frequencies (10–40 Hz in most limb muscles). In a given motor unit, this “optimum” range is related to the twitch contraction time, so the range is lower in type S than in type F units (Burke et al., 1976a). When activated, plateau potentials can produce sustained firing rates near the upper limits, ensuring near-maximum force production that is relatively independent of excitatory synaptic drive. The prevalence of plateau potentials in type S motoneurons would be particularly useful in postural control that demands sustained generation of relatively small forces (Walmsley et al., 1978).

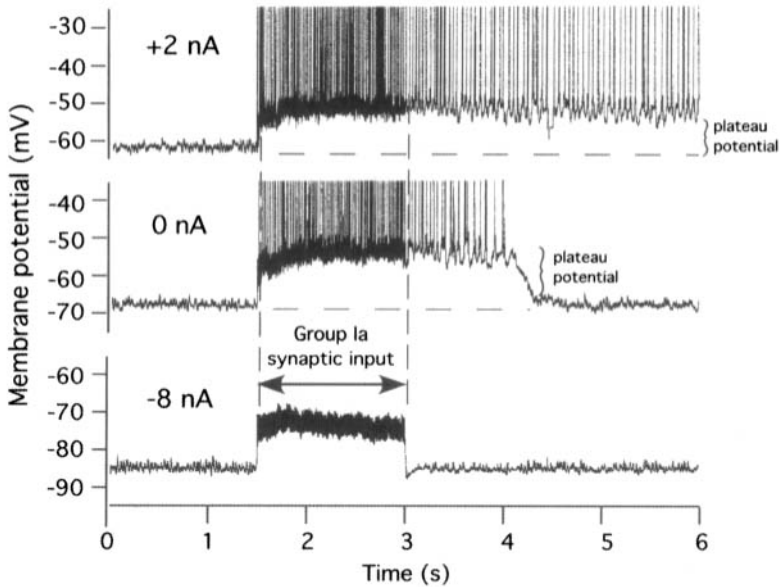


Fig. 3.13. Plateau potentials in a cat alpha-motoneuron. Three intracellular records from the same triceps surae motoneuron at different membrane potentials (ordinates; note different scales) produced by the injection of depolarizing (top trace) or hyperpolarizing (bottom trace) currents or at the resting potential without current (middle trace). For each trace, a barrage of group Ia synaptic input was generated by high-frequency vibration of the triceps surae tendon between the double-headed arrow (vertical dashed lines). The resulting synaptic depolarization was limited to the duration of vibration and produced no action potentials when the cell was hyperpolarized (bottom trace). However, at the resting potential (middle trace), the same input generated spiking not only during the input but also during a period of sustained depolarization (plateau potential) that outlasted the stimulus before its spontaneous termination. During depolarization (top trace), the plateau potential and resulting spikes persisted until the end of the record. Decerebrate cat preparation treated with a noradrenergic agonist, methoxamine, to enhance activation of plateau potentials. [Adapted from Fig. 1A in Lee and Heckman, 1998, with permission.]

Synaptic Organization Underlying Recruitment. Although intrinsic motoneuron properties are undoubtedly important in recruitment control, the organization of synaptic input is also critical. If recruitment were governed only by motoneuron properties, it would be essentially invariant, but this is clearly not the case. For example, the excitability of individual motoneurons within a motor nucleus fluctuates with relative independence from the whole population during repeated stimulation of group Ia afferents (Rall and Hunt, 1956). During such experiments, the degree of independence between population and individual motoneuron responses can be increased by conditioning the same system with other synaptic inputs (Gossard et al., 1994). Such observations are best explained by variations in synaptic organization between motoneurons, even within the same motoneuron pool. Some synaptic systems are organized to re-enforce the spectrum of intrinsic motoneuron properties, whereas others exhibit quite different gradations of efficacy.

Monosynaptic group Ia EPSPs provide an example of synaptic organization that works in concert with the spectrum of intrinsic motoneuron properties to produce size-ordered recruitment. The peak amplitudes of composite EPSPs produced by group Ia afferents increase in the sequence $FF < FR < S$ (see Fig. 3.3B) (Burke et al., 1976b; Fleshman et al., 1981a). There is a clear correlation between Ia EPSP amplitude and the functional thresholds of slow and fast twitch motor units in the stretch reflex (Burke, 1968), as predicted by the size principle (Henneman and Olson, 1965). Moreover, assessment of the effective synaptic current delivered to the spike generation zone from group Ia synapses reveals the same ordering (Heckman and Binder, 1988). Because motor units are generally recruited from small to large force units under many conditions, we can infer that many other synaptic systems probably exhibit the same gradation of synaptic efficacy as found for group Ia afferents. For example, amplitudes of disynaptic group Ia IPSPs in motoneurons are strongly correlated with those of Ia EPSPs in the same cells (Burke et al., 1976b). On the other hand, the relative efficacy of monosynaptic vestibulospinal EPSPs is more or less equal in all motor unit types in cat medial gastrocnemius motor units (Burke et al., 1976b; see also Powers and Binder, 2001).

Factors That Control Synaptic Efficacy. One obvious measure of synaptic strength, or *efficacy*, is the peak amplitude of monosynaptic potentials measured by an intracellular electrode in the cell soma (see Figs. 3.3B and 3.7D) (for additional perspectives, see Kirkwood et al., 1999). The magnitude of steady-state “effective” synaptic currents at the soma can also be estimated, making it possible to estimate synaptic efficacy in polysynaptic as well as monosynaptic inputs (Powers and Binder, 2001). Such currents multiplied by the neuron’s input resistance give the somatic voltage change produced by the input, after factoring in the equilibrium potential for the synapses in question. Because the spike generator in most CNS neurons is in the axon initial segment (see earlier), the somatic currents/potentials translate quite well into the output firing rate (Binder et al., 1993).

There are three levels of synaptic organization at which interactions between presynaptic and postsynaptic factors can affect the synaptic efficacy. At the level of *single synaptic boutons*, one must consider the amount of transmitter released presynaptically and the sensitivity and density of postsynaptic receptors for it. The interaction between these presynaptic and postsynaptic factors results in the transmembrane conductance change that generates a single-bouton EPSP. There is evidence that variations at this level are systematically related to motoneuron type (Honig et al., 1983; Mendell et al., 1990), possibly due to some retrograde message from motoneurons to synapses.

The next level of analysis is the *synaptic system*, e.g., all of the Ia synapses that impinge on a given motoneuron. Effective synaptic strength can vary from cell to cell as a function of the total number of Ia synapses that release transmitter during any given presynaptic action potential (see earlier). However, synaptic number alone has little meaning without considering the total amount of postsynaptic membrane over which they are distributed. The ratio between synaptic number and membrane area is the *synaptic density*. When all other things are equal, increasing synaptic density should result in increasing synaptic efficacy.

The last level of analysis concerns *electrotonic interactions* that depend on the spatial distribution of the active boutons and the electrotonic characteristics of the cell

(soma and dendrites) on which they are distributed (see Fig. 3.8). For example, if most of the Ia synapses to one motoneuron were electrotonically closer to the soma than in another, an equal density would still result in larger and faster EPSPs in the former than in the latter. Equivalent spatial distributions of the same number of synapses to cells with very different electrotonic architectures could in principle give the same result. The electrotonic factor is of somewhat less consequence if EPSPs are measured by the electrical charge injected into the soma (see Fig. 3.8) (Ianssek and Redman, 1973; Heckman and Binder, 1988). It should be noted also that synaptic inputs operate normally during repetitive action, so that the voltage changes at the spike generation site in the axon initial segment depend on timing and frequency of input. This factor can interact with spatial location because of its effect on PSP shape as well as amplitude (see Fig. 3.8).

All of these mechanisms operate whether the postsynaptic membrane is passive or active. Two kinds of nonlinear mechanisms must be added to this mix. In the first, repetitive activation of group Ia afferents produces less than expected EPSP summation in low-rheobase, high-resistance motoneurons with large EPSP amplitudes than in the high-rheobase, low-resistance cells that have smaller Ia EPSPs, thus tending to "equalize" differences between low- and high-threshold motoneurons during repetitive activation such as occurs in actual movements (Mendell et al., 1990). An opposite effect results from nonlinear amplification of Ia EPSPs due to activation of dendritic conductances that underlie plateau potentials. Evidence that the persistent inward current (IPIC) that produces plateau potentials and bistable motoneuron firing (see earlier) can be activated by the large local EPSPs generated in the dendrites (Lee and Heckman, 2000). The operation of this mechanism can be controlled by reticulospinal descending systems. Because this effect is larger and more easily activated in low-threshold, type S motoneurons, this mechanism provides an additional level of CNS control that favors size-ordered recruitment that can be modulated by descending motor commands (Lee and Heckman, 2000).

Alternative Recruitment Patterns. If all synaptic input systems to motoneuron were qualitatively the same, understanding recruitment order would simply be a matter of the quantitative interactions described above. However, there is evidence that normally high-threshold motor units can be selectively recruited under special conditions. This suggests the synaptic systems responsible may project primarily, if not exclusively, to these units. For example, stimulation of distal skin regions can sometimes markedly re-order the relative excitability of cat ankle extensor (triceps surae) motor units during activation by group Ia afferents in animals (Kanda et al., 1977; Gossard et al., 1994; but cf. Cope and Pinter, 1995). Low-threshold afferents from distal skin regions in the cat hindlimb produce polysynaptic excitation that is ordered quite differently from Ia input. These polysynaptic EPSPs are small or even undetectable in many type S motoneurons but are present and sometimes quite powerful in motoneurons of FR and FF units (Fig. 3.4; see Burke et al., 1970a, 1973b). The responsible multisynaptic pathway in the cat receives convergent supraspinal excitation (Pinter et al., 1982).

A similar phenomenon has been observed in human subjects during voluntary abduction of the forefinger (Datta and Stephens, 1981; Garnett and Stephens, 1981). The recruitment thresholds of motor units in the first dorsal interosseous muscle during vol-

untary ramp contractions of the index finger exhibit marked reversals during and for some time after repetitive electrical stimulation of the distal skin of the same finger. A quite different example of differential recruitment in humans occurs during controlled voluntary lengthening of triceps surae muscles against a steady load (Nardone et al., 1989). In this rather unusual situation, motor units with large electromyographic (EMG) signals were preferentially recruited while units with smaller EMG signatures fell silent. This was the reverse of the normal recruitment pattern, when these muscles were voluntarily shortened against the same load. In fact, many of the large signal units were not recruited during ankle extension, except in very rapid (ballistic) contractions.

These observations suggest that there are at least two qualitatively different patterns of synaptic organization to motor units in mixed muscles. These are illustrated schematically in the left panel of Fig. 3.14, in which the width of the lines denotes relative input efficacy. The existence of just two different orderings of synaptic efficacy provides the CNS with at least three options: (1) a "size-ordered" recruitment sequence when input A is dominant, (2) essentially synchronous activation of all pool motor units when both A and B are active, and (3) selective recruitment of otherwise high-threshold motor units when input B is dominant. It may well be that selective recruitment of large force, fast twitch motor units is useful only in situations that demand both large forces and rapid relaxation, such as occurs during the very rapid alternation when a cat shakes a wet hindpaw (the "paw shake reflex"; Smith et al., 1980). However, the option of combining A and B input organizations would reduce the firing threshold range inherent with input A alone (threshold compression; right panel in Fig. 3.14; see Garnett and Stephens, 1981) and facilitate the more or less synchronous activation of the en-

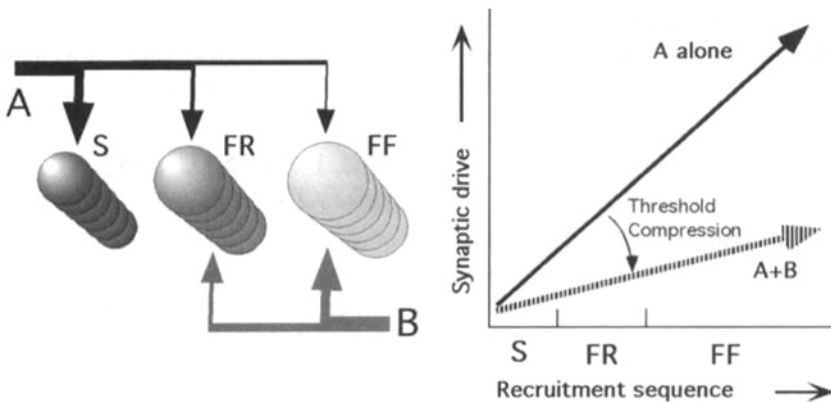


Fig. 3.14. Synaptic organization and motoneuron recruitment. The cartoon on the left depicts the type S, FR, and FF subsets of motor units in a given motor pool. The strength of excitatory synaptic input A is largest in S motoneurons, smaller in FR, and smallest in FF, as observed for monosynaptic Ia EPSPs (see Fig. 3.3B). The FF and FR units in same pool also receive excitation from a second source, B, that does not project to type S motoneurons (Burke et al., 1970). (See text.) Increasing drive through input A should recruit motor units in an S \rightarrow FR \rightarrow FF sequence, as in the graph on the right. Combining drive from both A and B should result in greater synchrony in recruitment because it would narrow the difference between low- and high-threshold units established by synaptic inputs organized like input A.

tire motor unit population that is in fact observed during ballistic contractions (Desmedt and Godaux, 1977).

It should be noted that the importance, if not the existence, of selective motor unit recruitment is controversial (e.g., Calancie and Bawa, 1990; Cope and Pinter, 1995; Cope and Sokoloff, 1999; Burke, 2002). The spectrum of motoneuron intrinsic properties and the organization of many types of synaptic input discussed earlier strongly favor size-ordered recruitment. Perhaps because of this, instances of clear selective recruitment are infrequent and require special conditions. Nevertheless, there seems to be sufficient evidence that motor unit recruitment sequences are not immutable, which emphasizes the importance of synaptic organization in recruitment control.

Functional Consequences. In size-ordered recruitment sequences, the lowest-threshold motor units produce small forces that are resistant to fatigue (i.e., type S), which is advantageous for motor units that are used often and for prolonged periods of time (high “duty-cycle” units). The small force outputs of individual type S motor units permits precise incremental control of total muscle force by recruitment and rate coding. Both features are important for the maintenance of posture, which requires relatively small total force outputs (Walmsley et al., 1978). As force demand increases, size-ordered recruitment activates larger force type FR motor units that are still relatively fatigue resistant. These medium duty-cycle units are called into play for movements like walking and running that require more total force and faster contraction and relaxation. Type FF motor units ordinarily have the highest functional thresholds and are used relatively infrequently (low “duty-cycle” units) in short bursts of activity that require large force outputs (galloping and jumping in cats; Walmsley et al., 1978) but little resistance to fatigue. Thus, size-ordered recruitment is precisely tailored for a wide range of movements. On the other hand, some actions like ballistic or rapidly alternating movements, and perhaps controlled active lengthening, appear to require more selective activation of ordinarily high-threshold motor units, with or without the smaller, low-threshold units.

DYNAMIC CONTROL OF SPINAL INTERNEURONS: FICTIVE LOCOMOTION

A long-term goal of systems neuroscience is to explain behavior in terms of the responsible neural circuits. Although information about the synaptic organization of reflex pathways is a step in this direction, reflexes are not really behaviors. We need experimental models in which the CNS emits outputs that clearly resemble those that occur in intact, behaving animals but that can be studied using the invasive methods developed for studying reflexes.

At the spinal cord level, one such model system is *fictive locomotion*. Under certain conditions, motor nuclei produce coordinated patterns of cyclic firing that closely resemble the patterns observed in intact animals (Fig. 3.15) (see Grillner, 1981; Rossignol and Dubuc, 1994; Rossignol, 1996). Such patterns can be elicited by electrical stimulation of sites in the hind brain (e.g., the mesencephalic locomotor region [MLR]) (Shik et al., 1966) or by drugs administered after spinal cord interruption in paralyzed animals in which the supratentorial brain is removed (decerebrated; see Schmidt and Jordan, 2000). Such immobilized preparations are suitable for extracellular and intra-

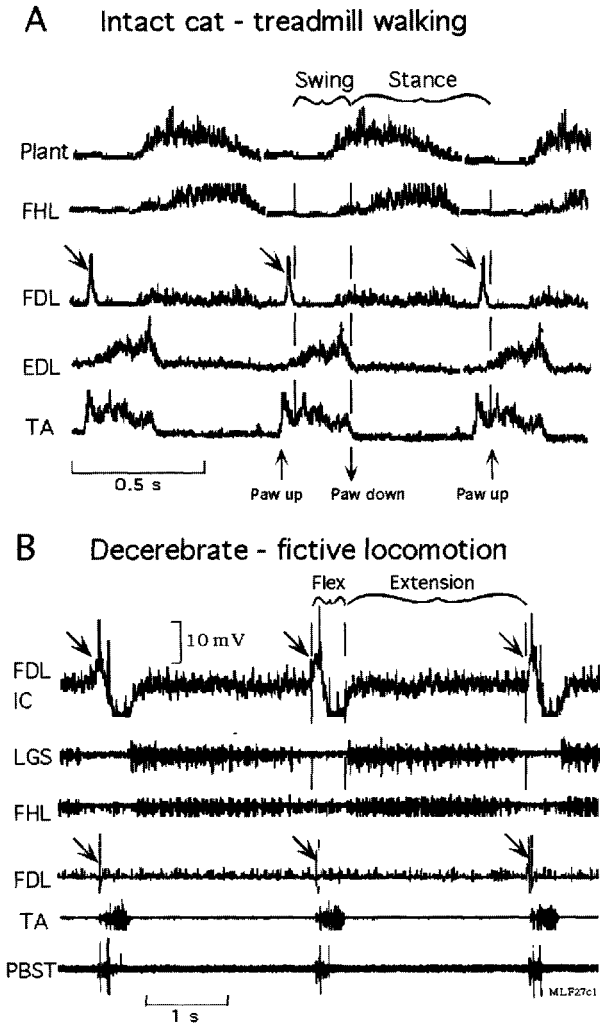


Fig. 3.15. Motoneuron activity patterns are similar in normal and fictive locomotion. **A:** Rectified and integrated electromyographic (EMG) signals produced from five hindlimb muscles during three step cycles in a normal cat walking on a treadmill. Note the alternation between extensor muscles plantaris (Plant) and flexor hallucis longus (FHL), and flexor muscles extensor digitorum longus (EDL) and tibialis anterior (TA). The middle trace is from the flexor digitorum longus (FDL), which is the mechanical synergist of FHL but exhibits a different activity pattern, with little activity during the extension phase but a large, brief burst at the onset of the flexion phase (arrows). [Adapted from Fig. 9 in Carlson-Kuhta et al., 1998, with permission.] **B:** The bottom five traces show a closely similar activity pattern recorded directly from five muscle nerves (electroneurograms, ENGs, no rectification) during spontaneous fictive locomotion in an immobile decerebrate cat treated with a neuromuscular blocking agent to prevent muscle movement. [Records from the author's laboratory; see Degtyarenko et al., 1998.] As in the normal case, there was alternation between extensor muscles (*lateral gastrocnemius-soleus*, LGS, and FHL), and flexors (TA and posterior biceps plus semitendinosus, PBST). The brief bursts in FDL at the onset of the flexion phases (arrows) are exactly as in the intact animal. The top trace is a simultaneous intracellular record from an FDL motoneuron, showing sharp depolarizations in the first third of flexion (arrows) that drive the early flexion bursts, and subsequent strong hyperpolarization (inhibition) through the subsequent two-thirds, which prevent FDL firing during this period.

cellular recording from individual neurons, which permits analysis of synaptic organization in the ventral horn circuits that are involved. In this case, rhythmic motoneuron activity is recorded in muscle nerves (electroneurograms [ENGs]) (Fig. 3.15, B) rather than from muscles (EMGs; Fig. 3.15, A).

The basic pattern of coordinated motoneuron activations in locomotion is produced by a system of spinal interneurons organized into what is called the *central pattern generator* (CPG) for locomotion (Grillner, 1981; Stein and Smith, 1997; Selverston et al., 1998). Such a CPG can generate rhythmic motoneuron activity without any afferent activity or other source of rhythmic external drive. Coordinated patterns of motoneuron activity are the hallmark of CPG operation, but interneurons also receive rhythmic drive from the locomotor CPG. For example, the locomotor CPG regulates the excitability of group Ia reciprocal inhibitory interneurons (see Fig. 3.12; Feldman and Orlovsky, 1975; Pratt and Jordan, 1987; Degtyarenko et al., 1998). Moreover, the locomotor CPG can drive reciprocal Ia inhibitory interneurons to rhythmic discharge in the absence of any phasic contribution from Ia afferents at all (Feldman and Orlovsky, 1975), essentially co-opting them to generate “locomotor” inhibition rather than “stretch reflex” inhibition. In this situation, these “reflex” interneurons might better be called “CPG inhibitory interneurons.” It seems inevitable that the more we learn about synaptic organization among spinal interneurons, the more difficult it will be to assign them to the precise categories that we usually use to organize and communicate information.

Spatial Facilitation of Cutaneous Reflexes During Fictive Locomotion. Modulation of transmission through the reciprocal group Ia pathway during fictive locomotion is an example of the convergence of multiple sources of CNS control onto common interneurons (i.e., spatial facilitation; see Fig. 3.11). Repeated electrical stimulation of an afferent nerve can be used to probe the convergence of drive from the locomotor CPG onto other disynaptic reflex interneurons during cycling from flexion to extension. The observed “state-dependent” changes in transmission through segmental interneurons provides information about their synaptic organization (Burke, 1999b) and in turn permits inferences about the structure of the CPG itself (Burke et al., 2001). This can be illustrated using synaptic inputs to the motor nuclei of two small muscles in the cat hindlimb, flexor digitorum longus (FDL), and extensor digitorum longus (EDL).

The FDL muscle plantar flexes the hindpaw toes, whereas the EDL extends them. Coactivation of the two muscles protrudes the claws. Motoneurons that innervate both of these muscles receive disynaptic and trisynaptic PSPs from two sets of fast-conducting cutaneous afferents, one via the superficial peroneal (SP) nerve that innervates skin on the dorsal surface of the hindpaw and the other via the medial plantar (MPL) nerve that innervates the ventral (plantar) skin (Moschovakis et al., 1991b; Degtyarenko et al., 1998). The unusual prevalence of disynaptic cutaneous PSPs in these two sets of motoneurons suggests that these are functionally specialized pathways, because cutaneous afferents produce only trisynaptic PSPs in many other hindlimb motoneurons (see earlier). The behavioral relevance of these functional specializations becomes apparent when the pathways are examined during fictive locomotion.

Figure 3.16A illustrates an example of fictive locomotion in which SP and MPL PSPs were generated at regular intervals (100 ms), superimposed on rhythmic bursting in extensor and flexor muscle nerves. With sufficiently long periods of rhythmic

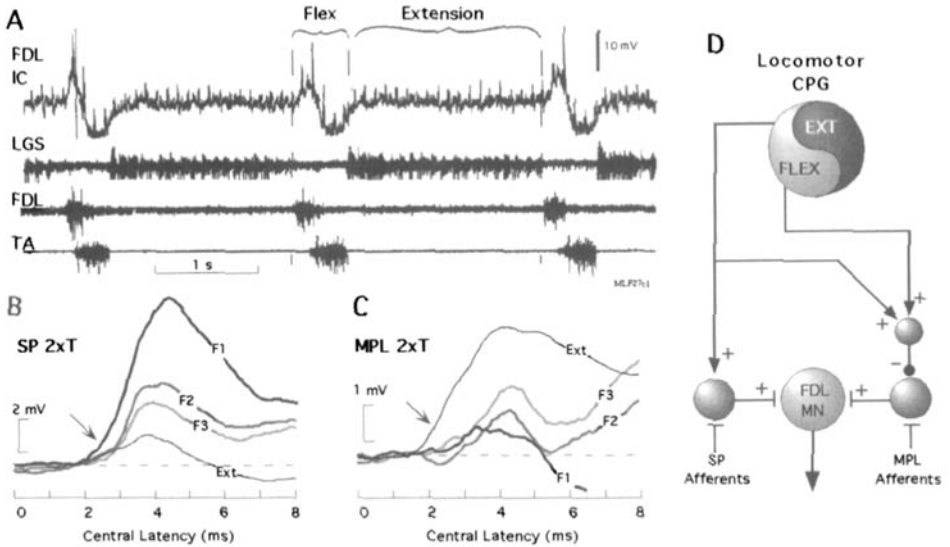


Fig. 3.16. Modulation of cutaneous reflex pathways during fictive locomotion. **A:** A sample of intracellular and ENG records from another bout of fictive locomotion involving the same FDL motoneuron shown in Fig. 3.15B. During a long sequence of step cycles, two cutaneous nerves, superficial peroneal (SP) and medial plantar (MPL), were alternately stimulated electrically at 10 Hz to sample changes at all phases of the stepping cycles (see Moschovakis et al., 1991b). A computer program was used to average together responses produced in specific phases, shown in **B** and **C**. **B:** Averaged PSPs produced by the SP nerve during early (F1), middle (F2), and late (F3) flexion, as well as throughout extension (Ext). Note the large enhancement of SP EPSPs in F1, with the appearance of a disynaptic component (arrow; central latency, 1.9 ms) that was not present in any other phase. **C:** As in **B** but showing PSPs produced by MPL stimulation during the same step cycle phases. In marked contrast to the SP pattern, disynaptic MPL EPSPs were completely suppressed throughout flexion, and later components were much reduced in amplitude. The suppression during F1 is not explained by postsynaptic inhibition, which only begins later (**A**). **D:** A simple circuit diagram that is consonant with the observations in **A** through **C**. Input from the SP and MPL nerve project to FDL motoneurons via independent sets of last-order excitatory interneurons. The disynaptic SP pathway cells receive excitation from the CPG for locomotion mainly during the early part of the flexion phase. In contrast, the MPL pathway cells are actively inhibited through the entire flexion phase, via inhibitory interneurons that must exist if the CPG output is assumed to be purely excitatory (arrows denote unknown circuitry).

stepping, cutaneous PSPs were generated during all phases of the step cycle and were then averaged together, using a computer program (Degtyarenko et al., 1996b). The intracellular record in Fig. 3.16A (FDL IC) shows that the FDL motoneuron was depolarized during the first third (F1) of the flexion phase of locomotion, producing the short burst of firing in the FDL nerve, but is powerfully inhibited during the subsequent two-thirds of flexion (F2 and F3). These synaptic effects are often called *locomotor drive potentials* (LDPs) (Jordan, 1983). During the F1 period, SP EPSPs were markedly enhanced, and an otherwise inconspicuous disynaptic EPSP appeared (central latency <2 ms; Fig. 3.16B, arrow). The enhancement decreased during the later flexion phases (F2 and F3) and the EPSP returned to its control amplitude during the

extension phase (Ext). In marked contrast, the MPL EPSP was *suppressed* during the entire flexion phase (Fig. 3.16C). This differential modulation clearly shows that the SP and MPL EPSPs, although both disynaptic, are produced in FDL motoneurons by different sets of last-order interneurons (Fig. 3.16D) (Moschovakis et al., 1991b).

The available observations about modulation of cutaneous input to FDL and EDL motoneurons in the cat lead to the circuit diagrams in Fig. 3.17. The data suggest that the locomotor CPG has two functional components: (1) a circuit that generates the basic flexion-extension rhythm (clock network) and (2) circuits driven by that rhythm that distribute CPG output to target interneurons (called "last-order" interneurons) that in turn project directly to specific motoneurons. This pattern-forming network appears to be needed to generate the precise temporal patterns found in different motor nuclei during the flexion and extension phases (e.g., Figs 3.15; see also Burke et al., 2001). In the case of circuits to the FDL motor nucleus (Fig. 3.17A), the pattern forming network is complicated by the fact that FDL motoneurons can sometimes fire during the extension phase of stepping in normal cats (O'Donovan et al., 1982) or in fictive locomotion (Fleshman et al., 1984). When firing in extension, the FDL assists the anti-gravity action of its mechanical synergist FHL, which is invariably active only during the stance (extension) phase of locomotion (see Fig. 3.15). These alternative actions of FDL are denoted by the switch symbol included in the network.

There are four sets of last-order interneurons in the FDL diagram, one each for the two afferent inputs, one that excites FDL cells during F1, and one that inhibits them during the remainder of flexion (here called F2). The latter two sets can account for the succession of EPSP and IPSP LDPS evident in the intracellular record in Fig. 3.16A. Finally, there must be a set of inhibitory interneurons that project onto the last-order cells in the MPL pathway, to account for the suppression of disynaptic MPL EPSPs throughout the flexion phase (note arrow in Fig. 3.16C). This diagram attributes the observed effects of SP and MPL afferents in FDL motoneurons to convergence of afferent input and CPG drive onto common interneurons. It is impossible to rule out some contribution of modulated presynaptic inhibition in the afferent terminals because of evidence that PAD exhibits phase-related changes during fictive locomotion (reviewed in Rossignol, 1996; Rudomin and Schmidt, 1999). However, the details of pattern and timing of the modulation favor the view that most, if not all, of the observations are due to the convergence mechanism. Amplification of PSPs by active membrane properties in the postsynaptic motoneurons (see earlier) would not explain EPSP suppression (Fig. 3.17C) or the precise timing of appearance and disappearance of disynaptic components in EPSPs (Fig. 3.16B and C).

Locomotor control of cutaneous inputs to EDL motoneurons has two remarkable features. First, electrical stimulation the SP nerve produces disynaptic IPSPs in EDL motoneurons that exhibit the same pattern of modulation during locomotion as found in the SP EPSPs in FDL motoneurons (Degtyarenko et al., 1996a). Enhancement of the SP IPSP is maximal during the first third of flexion and then declines rapidly. The disynaptic IPSPs disappear entirely during the extension phase and they are rarely evident outside of fictive locomotion. The second feature of interest is that EDL motoneurons, like FDL cells, receive disynaptic and trisynaptic EPSPs from the MPL nerve, and these are also powerfully suppressed during the entire flexion phase (Degtyarenko et al., 1996a). This observation suggests, but cannot prove, that the same last-order

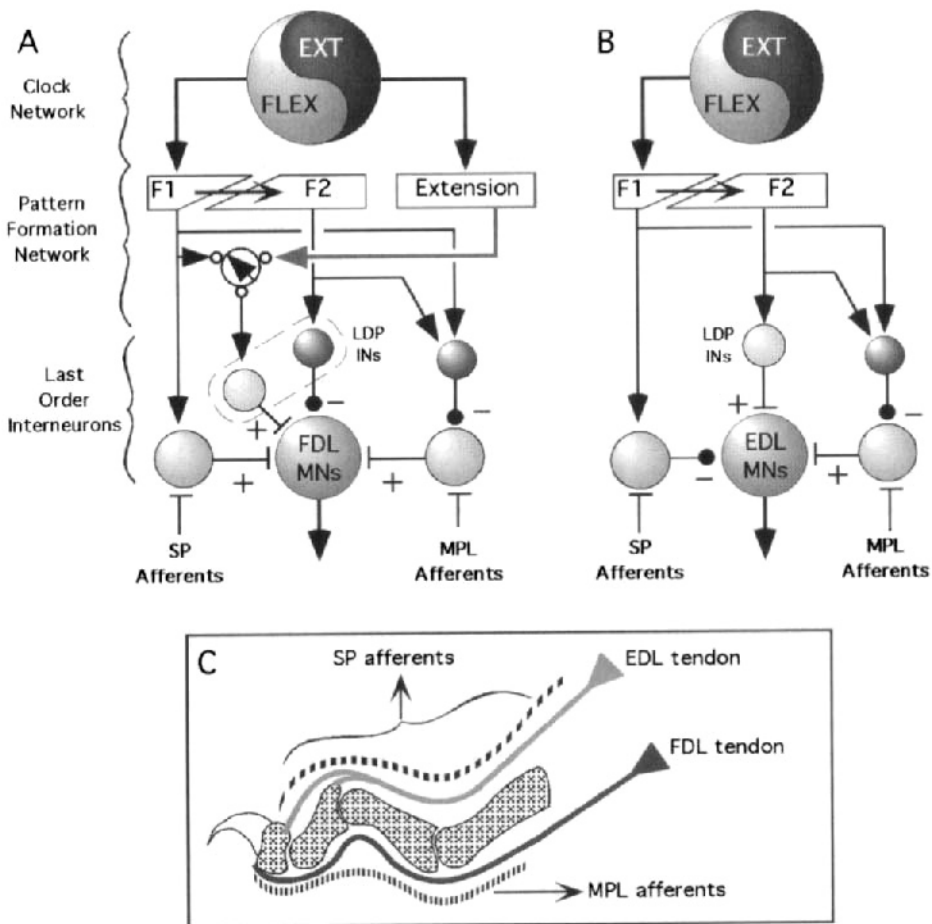


Fig. 3.17. A more complete diagram of CPG control of cutaneous input to FDL and EDL motoneurons. It embodies two messages: (1) the locomotor CPG is a complex set of circuits, one of which functions to generate the basic rhythm, and (2) a set of circuits that shapes the temporal and spatial aspects of the rhythmic drive to deliver it to both motoneurons and interneurons at appropriate time points in the step cycle (see Burke et al., 2001). **A**: This diagram is an elaboration of the one in Fig. 3.16D. The CPG icon is expanded into a circuit that generates the locomotor rhythm (clock network), which drives another network (pattern formation network) that provides timing delays and distribution of locomotor drive to appropriate interneurons and motoneurons. FDL motoneurons can be active either during flexion or extension but usually not both. Therefore, the pattern network must contain a subnetwork that allows this phase switch, which is accomplished without changing the drive to SP interneurons (Burke et al., 2001). Therefore, there must be excitatory last-order interneurons that produce the relevant locomotor drive potentials (LDP INs). There must also be inhibitory LDP interneurons that produce the IPSPs found in FDL cells irrespective of whether they fire in early flexion or in extension. The circuit that controls MPL transmission is as in Fig. 3.16. **B**: An analogous diagram to summarize observations on disynaptic cutaneous PSPs in EDL motoneurons (Degtyarenko et al., 1996). There are two differences from the FDL circuit: (1) the disynaptic SP pathway that is enhanced during early flexion is inhibitory rather than excitatory, and (2) the LDP interneurons driven later during flexion are excitatory. The MPL pathway control is exactly as that found in FDL motoneurons, which suggests (but does not prove) that a single set of last-order interneurons projects to both sets of motoneurons. **C**: Diagram of the insertions of the EDL and FDL tendons on the distal phalanges of the cat hind toes, showing complex, multijoint antagonistic action of the two muscles when activated individually. When co-active, the FDL rotates the distal phalanx to protrude the claws. Note that the SP and MPL innervations are closely adjacent.

interneurons are involved in transmitting MPL information to both motor nuclei (Burke, 1999b), even though the two muscles are functional antagonists. Thus the cutaneous PSPs and their control during fictive locomotion are virtually identical in FDL and EDL motoneurons, except for the inversion of sign in the SP PSPs. The circuit diagram based on these observations (Fig. 3.17B) is the same as that in panel A, with three exceptions: (1) there is no switch because EDL fire only during the flexion phase of fictive locomotion, (2) the disynaptic interneurons in the SP pathway are inhibitory instead of excitatory, and (3) excitatory LDP interneurons drive EDL motoneurons to fire during F2 while analogous LDP cells simultaneously inhibit FDL motoneurons.

Functional Considerations. It seems remarkable that information from two adjacent skin regions at the tip of the hindpaw should project to FDL and EDL motoneurons through separate sets of segmental interneurons. The reason for this precision in synaptic organization lies in the functional roles of the two muscles. When the skin on the dorsal surface of a cat's hindpaw, innervated by the SP nerve, encounters an obstacle during the early swing (flexion) phase of locomotion, the entire hindlimb undergoes an immediate exaggerated flexion called the "stumbling corrective reaction" that lifts the leg over the obstacle (Forssberg, 1979). The CPG enhancement of transmission through the SP interneurons at exactly this time prepares FDL (and presumably many other) motoneurons to generate this reaction. At the same moment, such an unexpected input powerfully inhibits the antagonist EDL motoneurons, preventing co-contraction of FDL and EDL that would produce unwanted claw protrusion that could disturb the movement. Speed is essential in order to preserve balance.

What about the MPL pathway? Information from the ventral (plantar) surface of foot is presumably important to the proper functioning of both FDL and EDL motoneurons during the stance (extension) phase of locomotion, because cats walk and run essentially on their toes. Therefore this pathway is gated on by the CPG during this phase of the step cycle. But why is it gated off during the swing (flexion) phase? We can only speculate that information from the plantar skin, activated during the normal curling and uncurling of the toes during swing, might interfere with the coordinated action of the muscles that produce these movements.

Finally, it should be noted that gating and modulation of reflex gain such as described above in the cat during fictive locomotion are also found in humans during normal walking (Duyssens et al., 1990).

SUMMARY

This chapter has attempted to present an overview of the neuron types present in the ventral spinal cord, some features of their cellular and synaptic physiology, and some of their known circuit interactions. What we now call neuroscience began with systematic study of the spinal cord, but it still has much to teach us. The precise synaptic organization evident in the example discussed in the last section is certainly not unique. The specializations found among last-order interneurons to just a handful of hindlimb motor nuclei suggest that there must be an enormous number of other such circuits waiting to be uncovered.

The spinal cord is phylogenetically the oldest part of the CNS. In that sense it is not surprising that millions of years of evolution have tailored its circuitry for the wide range of motor behaviors exhibited by mammals. It remains one of the few parts of the CNS in which inputs and outputs are both accessible and can be interpreted in functional terms. These linchpins can serve, given sufficient energy and time, to permit definition of neuronal properties and synaptic circuits that can be directly linked to motor behavior that are ultimately dependent on the interneurons and motoneurons of the ventral horn.

This page intentionally left blank

COCHLEAR NUCLEUS

ERIC D. YOUNG AND DONATA OERTEL

The cochlear nucleus contains the circuits through which information about sound is coupled to the brain. In the cochlear nucleus, fibers of the auditory nerve contact neurons that form multiple, parallel representations of the acoustic environment. These circuits vary from simple synapses that preserve the timing of auditory events to complex neuropils that are sensitive to features that identify sounds. The parallel pathways each perform a different analysis of the auditory signal. Thus calculations such as the localization of a sound source in space or the identification of a sound are separated in the cochlear nucleus and performed in parallel as signals ascend through the brainstem auditory nuclei.

A tonotopic map of sound is generated in the cochlea, shown schematically in Fig. 4.1. Sound causes a traveling-wave of displacement on the basilar membrane. The location of the largest displacement depends on the frequency of the sound, with low frequency sounds causing displacement at the apex and high frequencies at the base of the cochlea. The resulting map of stimulus frequency as a function of place along the basilar membrane is shown in Fig. 4.1 for the cat cochlea (for descriptions of cochlear anatomy and physiology, see Pickles, 1988; Patuzzi, 1996). Transduction of basilar membrane motion occurs in hair cells (Kros, 1996). Fluctuations of hair-cell membrane potential reflect motion of the basilar membrane. Depolarization in hair cells excites dendrites of auditory-nerve fibers (ANFs), synaptically evoking action potentials whose rate reflects the degree of excitation. Thus any given ANF responds to sound in proportion to the degree of basilar membrane motion at the point on the membrane innervated by the fiber. Each ANF responds to a limited range of frequencies. The frequency to which a fiber is most sensitive is its *best frequency* (BF). The best frequencies of ANFs vary systematically, forming a *tonotopic map*. Perceptually, position along the tonotopic map, or frequency of sound, corresponds to the sense of highness or lowness of the sound, which is like its position along a musical scale (Moore, 1997). In contrast with the visual and somatosensory systems, the tonotopic organization of the auditory system does not reflect location in space. The auditory system's frequency map is more like the olfactory system's map of odor molecular structure (Chap. 5).

There are two groups of hair cells and ANFs (Spoendlin, 1973; Kiang et al., 1982; Ryugo, 1992). Inner hair cells and type I ANFs form the major afferent pathway to the cochlear nucleus; each type I fiber innervates one inner hair cell. Type I fibers are

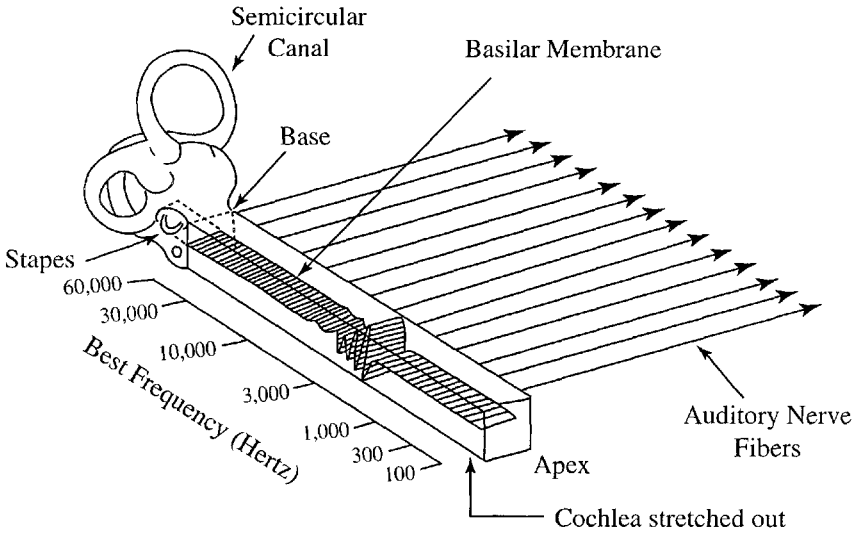


Fig. 4.1. Schematic representation of the cochlea illustrating the transduction of sound according to frequency on the basilar membrane. The cochlea is shown unrolled but is actually coiled like a snail. Sound energy enters the cochlea at the stapes and causes a traveling wave of displacement of the basilar membrane; the traveling wave peaks at a particular place, which depends on the frequency of the sound. Shown is a traveling wave for a ≈ 3000 -Hz sound. The mapping of sound frequency into place, or distance along the basilar membrane, is shown by the scale for the cat cochlea (Liberman, 1982). Type I auditory nerve fibers (ANFs) are indicated schematically by the parallel lines. Each fiber innervates one inner hair cell and thereby samples the basilar membrane displacement at that hair cell's location. The array of ANFs carries a tonotopic representation of sound, in which each fiber conveys information primarily about sound frequencies near the best frequency of the point on the basilar membrane innervated by the fiber.

myelinated, constitute 90%–95% of the fibers in the auditory nerve, and are the primary afferent input to most of the cell types in the cochlear nucleus. Outer hair cells are innervated by type II fibers, which are unmyelinated and project to nonprincipal cell regions of the cochlear nucleus (Brown et al., 1988a; Brown and Ledwith, 1990). To date, responses to sound have not been recorded from type II fibers, and it is not clear what role they play. Outer hair cells appear to participate in the mechanical response of the basilar membrane; loss of outer hair cells leads to a loss of sensitivity to soft sounds and a decrease in the sharpness of tuning (i.e., the frequency selectivity) of the basilar membrane (Patzuzzi, 1996). In the rest of the chapter, the term *auditory nerve fiber*, or ANF, will refer to type I fibers only, unless otherwise stated.

NEURONAL ELEMENTS AND THEIR SYNAPTIC CONNECTIONS

OVERVIEW

The modern definitions of the cell types in the cochlear nucleus were developed by Kirsten Osen on the basis of cytoarchitecture (Osen, 1969) and modified by Morest

and colleagues (Brawer et al., 1974; Cant and Morest, 1984) on the basis of Golgi material. In some cases the correspondence between cell types was initially unclear so that multiple terms have come to be used to describe the same group of cells. Figure 4.2 shows the distribution of cell types in the cochlear nucleus of the cat in a sagittal view of the nucleus. Incoming ANFs bifurcate in the central region of the ventral cochlear nucleus (VCN) and send an *ascending branch (a.b.)* rostrally to the anterior division of the VCN (AVCN) and a *descending branch (d.b.)* caudally to the posterior division of the VCN (PVCN); the descending branch curves back rostrally to innervate the dorsal cochlear nucleus (DCN). The innervation of the cochlear nucleus by ANFs is orderly and reflects the tonotopic organization of the cochlea: low BF fibers bifurcate proximally and innervate the most ventral and lateral portions of the nucleus, whereas high BF fibers innervate more dorsal and medial portions of the nucleus (Osen, 1970a; Bourk et al., 1981).

The symbols in Fig. 4.2 show the distribution of eight cell types that can be defined on the basis of cytoarchitecture. These are principal cells except for the granule cells and some of the small cells. Note that the principal cells are arranged in such a way that each type receives input from ANFs over the whole tonotopic range. In this sense, each principal cell type carries a separate but complete representation of the sound coming to the ear on that side of the head.

In projecting to different targets in the brain stem, the principal cell types form separate, parallel pathways. Figure 4.3 shows the projection patterns of six of the cell types

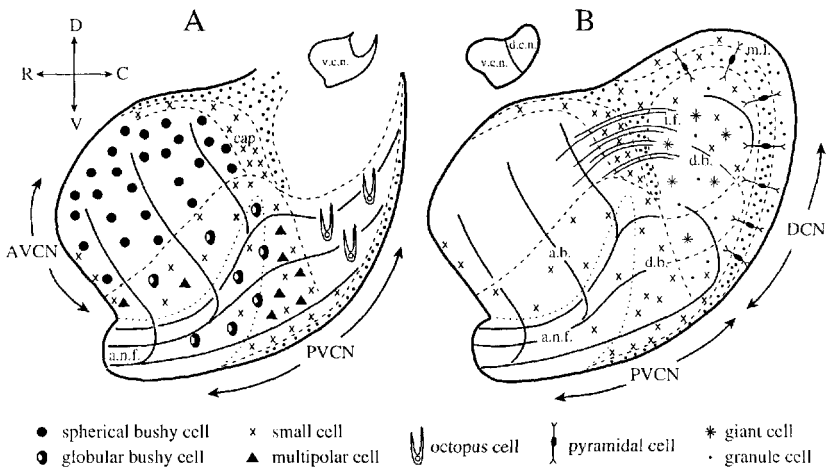


Fig. 4.2. Distribution of cell types shown schematically in sagittal views of the cat cochlear nucleus. **A:** Ventral cochlear nucleus (VCN) by itself. **B:** VCN partly covered by the dorsal cochlear nucleus (DCN). Lines marked *a.n.f.* show auditory nerve fibers with their ascending branches *a.b.* projecting to the anteroventral cochlear nucleus (AVCN) and descending branches *d.b.* projecting to the posteroventral cochlear nucleus (PVCN) and DCN. Fibers are shown at three points on the tonotopic scale, with the lowest-frequency fiber in the most ventral position at the point where the fibers enter the nucleus. Cell types are indicated by symbols. Lines marked *i.f.* in **B** are axons interconnecting the VCN and DCN. *m.l.* is the superficial or molecular layer of the DCN; *cap* is the small-cell cap. [Modified from Osen, 1970a, with permission.]

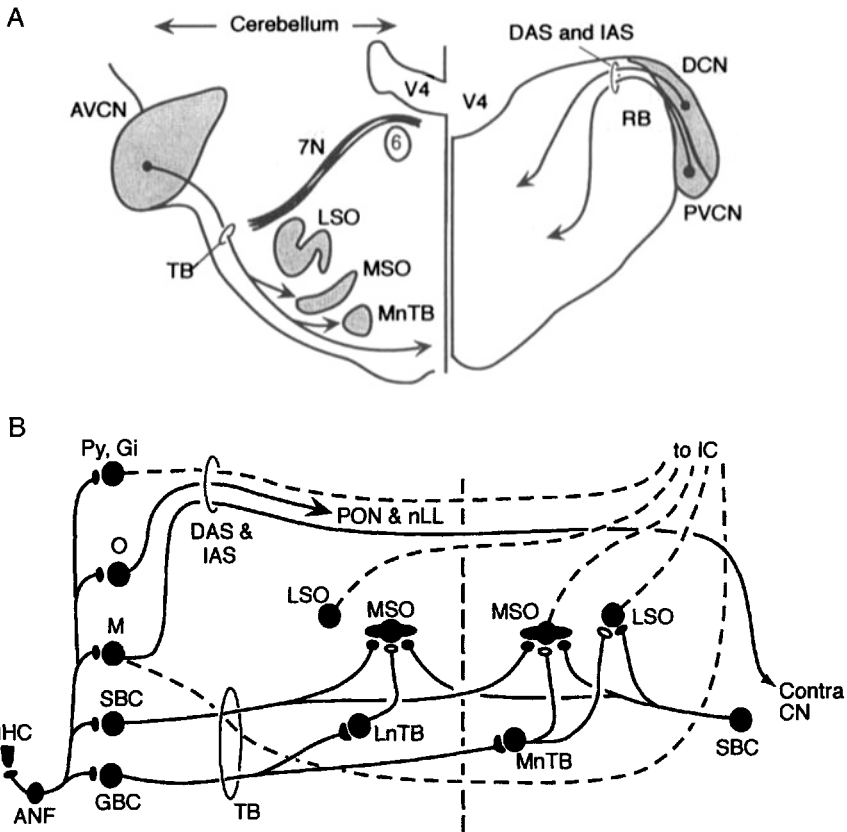


Fig. 4.3. Ascending pathways from the cochlear nucleus through the brainstem. **A:** The cat brainstem is shown in frontal-plane cross sections: the left half section is at the level of the anteroventral cochlear nucleus (AVCN) and superior olive; the right half section is slightly caudal, at the level of the dorsal (DCN) and posteroventral (PVCN) cochlear nuclei. The auditory nerve enters the nucleus between these two planes of section. Output fibers from the cochlear nucleus pass through the trapezoid body *TB* and dorsal and intermediate acoustic striae *DAS* and *IAS* (shown as arrows). Other abbreviations: *V4*, fourth ventricle; *6*, abducens nerve nucleus; *7N*, seventh (facial) nerve. **B:** Some of the cochlear nuclear principal cell types with their projections to the nuclei of the superior olivary complex and the inferior colliculus (*IC*). The auditory pathway begins with the transducer cell, the inner hair cell (*IHC*). Auditory nerve fibers (*ANF*) carry action potentials from the inner ear to the cochlear nucleus. From the VCN, bushy cells (*SBC* and *GBC*) innervate the medial (*MSO*) and lateral (*LSO*) superior olivary nuclei. The innervation is bilateral, with symmetrical connections on the two sides, only some of which are shown (the midline of the brainstem is shown by the dashed vertical line). The *GBCs* form large calyceal synapses on principal cells of the medial nucleus of the trapezoid body (*MnTB*) that in turn provide glycinergic inhibition to *MSO* and *LSO* principal cells. Neurons of the lateral nucleus of the trapezoid body (*LnTB*) are also inhibitory and project to the *MSO* as well as projecting back to the cochlear nucleus (not shown). T-multipolar cells (*M*, dashed line) in the VCN project through the *TB*, and pyramidal (*Py*) and giant (*Gi*) cells from the DCN project through the *DAS* to the contralateral *IC*; D-multipolar cells (*M*-solid line) project to the contralateral cochlear nucleus. Octopus cells (*O*) project from the VCN via the *IAS* to the contralateral superior paraolivary nucleus (*PON*) and to the ventral nucleus of the lateral lemniscus (*nLL*; neither is shown).

from Fig. 4.2. Figure 4.3A is a drawing of coronal sections of the cat brainstem at two levels, through the AVCN (left side) and PVCN/DCN (right side). This figure shows the two major fiber bundles that leave the cochlear nucleus in relation to other structures in the brainstem. Figure 4.3B shows some of the auditory neuronal circuits of the brainstem. At the output of the cochlear nucleus, spherical and globular bushy cells (*SBC* and *GBC*, solid lines) project to the medial (*MSO*) and lateral (*LSO*) superior olivary nuclei and the medial and lateral nuclei of the trapezoid body (*MnTB* and *LnTB*). The *MSO* and *LSO* compare input from the two ears and perform the initial computations necessary for sound localization in the horizontal plane (Yin, 2002). Excitatory inputs to the superior olive come from the *SBC* and inhibitory inputs come from the *GBC*; the latter are relayed through inhibitory interneurons in the *LnTB* and *MnTB* (Cant and Hyson, 1992). The characteristics of bushy cells described later will be interpreted in terms of the needs of these circuits for localizing sounds.

Multipolar (*M*), giant (*Gi*), and pyramidal (*Py*) cells project directly to the inferior colliculus (*IC*; Adams, 1979; Brunso-Bechtold et al., 1981). One population of multipolar cells, the *T-multipolars*, project through the trapezoid body (*TB*) to the *IC*, whereas another population, the *D-multipolars*, is inhibitory and projects to the contralateral cochlear nucleus (Cant and Gaston, 1982; Wenthold, 1987; Schofield and Cant, 1996). The octopus cells (*O*) project to the superior paraolivary nucleus (Schofield, 1995) and to the ventral nucleus of the lateral lemniscus (*VnLL*; Adams, 1997). These nuclei are not shown in Fig. 4.3 but are located dorsal to the *LSO*, between the superior olive and *IC*; the *nLL* receive collateral projections from most of the cells shown. All parallel ascending auditory pathways through the brain stem converge in the *IC*. It receives direct projections from the cochlear nucleus and superior olive and also projections from periolivary nuclei (*PON*) and from the *nLL*. The axons of most of these projections end in partially segregated bands within the colliculus (Oliver and Huerta, 1992).

Two nonprincipal cell regions of the cochlear nucleus are shown in Fig. 4.2: the granule cell areas (dotted) and the small cell cap (*cap*). The granule cells resemble and are developmentally related to those in the cerebellum (Mugnaini et al., 1980b; Berrebi et al., 1990; Fünfschilling and Reichardt, 2002); their axons project to the molecular layer of the *DCN* (*m.l.* in Fig. 4.2), where they form *parallel fibers*. The small cell cap is a collection of small multipolar cells that lies between the principal cell regions of the *VCN* and the granule cells (Osen, 1969; Cant, 1993). This region receives collaterals of ANFs (Brown and Ledwith, 1990; Liberman, 1991) and collaterals of efferent neurons that project from the superior olive to the cochlea (Benson and Brown, 1990; Benson et al., 1996). These olivocochlear efferent neurons receive input from small-cell-cap axons (Ye et al., 2000) as well as from *T-multipolar* cells (Thompson and Thompson, 1991; Smith et al., 1993). It has been suggested that the olivocochlear efferent feedback circuit regulates the sensitivity of the cochlea (Guinan, 1996) and of the *T-multipolars* (Fujino and Oertel, 2001).

Each cochlear nucleus cell type has a unique pattern of response to sound, consistent with the idea that each type is involved in a different aspect of the analysis of the information in the auditory nerve. The diversity of these patterns can be accounted for by three features that vary among the principal cell types: (1) the pattern of the innervation of the cell by ANFs, (2) the electrical properties of the cells that shape synaptic inputs, and (3) the interneuronal circuitry associated with the cell. In the following

sections, these aspects of the principal cell types are described and related to the cells' responses to sound.

CELL TYPES IN THE VENTRAL COCHLEAR NUCLEUS

Figure 4.4 shows examples of four neuron types found in the VCN and one from the DCN. These are taken from studies in which cells were filled with horseradish peroxidase after intracellular recording was performed to correlate their physiological and anatomical properties.

Bushy cells have short ($<200\ \mu\text{m}$), bushy dendritic trees. Their synaptic input is located mainly on the soma, with few synapses on their dendrites (Ostapoff and Morest, 1991). Two subtypes of bushy cells are recognized. As discussed earlier, SBCs and GBCs differ in their locations (see Fig. 4.2) and their projections (see Fig. 4.3). They also differ in the number of converging ANF inputs. Figures 4.4A and 4.4B show examples of their cellular morphology; SBCs have one or a few short dendrites that terminate in a dense bush-like structure near the soma (Fig. 4.4A; Brawer et al., 1974; Cant and Morest, 1979a), and GBCs have more ovoid somata and larger, more diffuse dendritic trees (Fig. 4.4B; Tolbert and Morest, 1982a; Smith and Rhode, 1987). Bushy cells are innervated at the cell body by ANFs through large synaptic terminals, described later.

Multipolar cells have multiple, long dendrites that extend away from the soma in several directions (Fig. 4.4C; Brawer et al., 1974; Cant and Morest, 1979a). Two major classes of multipolar cells have been described (Cant, 1981, 1982; Smith and Rhode, 1989; Doucet and Ryugo, 1997; Fujino and Oertel, 2001). The cells of one group, T-multipolars (planar), have a stellate morphology with dendrites aligned with ANFs, suggesting that these cells receive input from a restricted range of best frequencies. Their axons project through the trapezoid body (hence the "T") to the contralateral IC (dashed line from cell *M* in Fig. 4.3B). Cells of the second group, D-multipolars (radiate), have dendritic fields that are not aligned with ANFs. Their axons leave the nucleus through the intermediate acoustic stria and project to the contralateral cochlear nucleus (solid line from cell *M* in Fig. 4.3B). The axons of both multipolar types have collaterals that terminate locally near the cell body and in the DCN to form intrinsic circuits (Smith and Rhode, 1989; Oertel et al., 1990). T-multipolar cells are excitatory, and D-multipolar cells are inhibitory and glycinergic (Wenthold, 1987; Ferragamo et al., 1998a; Doucet et al., 1999). Small cells in the cap are also sometimes referred to as "multipolar cells," and multipolar cells are sometimes referred to as "stellate."

Octopus cells (see Fig. 4.4D) occupy a teardrop-shaped area in the posterior and dorsal PVCN (Fig. 4.2) where the ANFs converge to form a tonotopically organized bundle that courses toward the deep layer of the DCN (Osen, 1969; Kane, 1973; Oertel et al., 1990). Octopus cell dendrites are oriented, inspiring their name (the cell illustrated in Fig. 4.4D has a single dendrite extending opposite to the remaining dendrites, which is not typical). The orientation is perpendicular to the ANFs so that they receive input from fibers with a relatively wide range of BFs. The cell bodies encounter fibers with the lowest best frequencies, and the large dendrites extend toward fibers that encode higher frequencies.

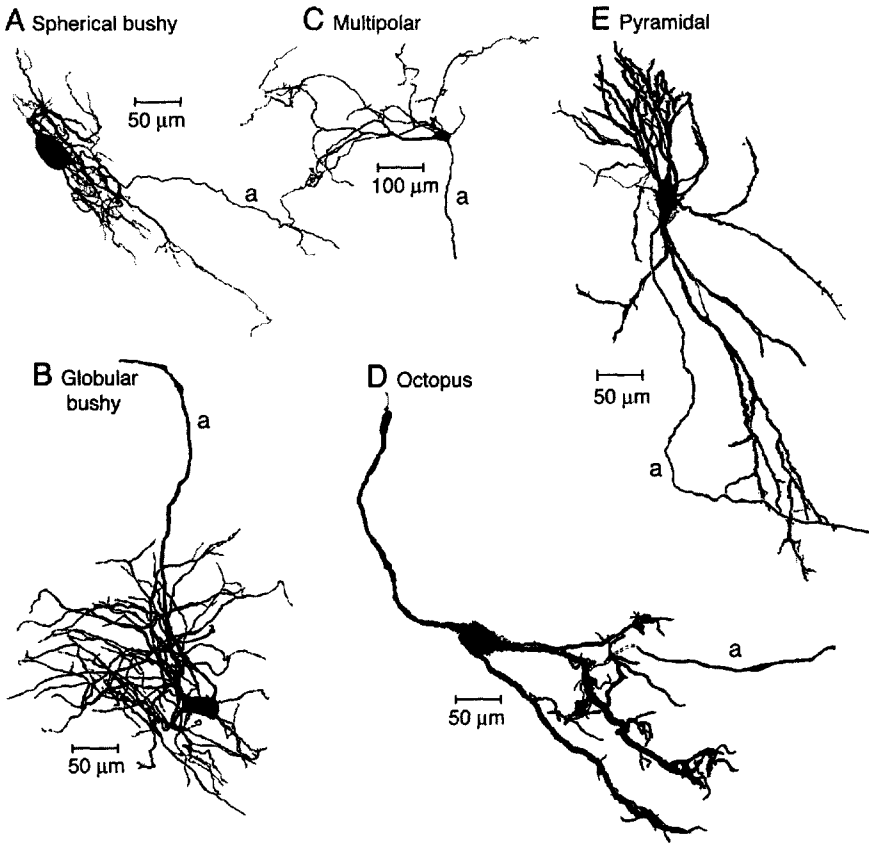


Fig. 4.4. Camera lucida drawings of labeled cochlear nucleus principal cells illustrating characteristic features of each type in the cat. **A:** Spherical bushy cell. [Provided by W. S. Rhode.] **B:** Globular bushy cell. [From Smith and Rhode, 1987.] **C:** Multipolar cell. [From Rhode et al., 1983a.] **D:** Octopus cell. [From Rhode et al., 1983a.] **E:** Pyramidal cell, also called a fusiform cell. [From Rhode et al., 1983b.] All cells are from the cat, drawn to the same scale. Cell types in other mammals have similar configurations (for the mouse, Wu and Oertel, 1984; Oertel and Wu, 1989; Oertel et al., 1990; and the gerbil, Feng et al., 1994; Ostapoff et al., 1994). Axons are indicated by *a*. [Taken from the sources listed with permission of Wiley-Liss.]

CELL TYPES IN THE DORSAL COCHLEAR NUCLEUS

In contrast to the VCN, the DCN is layered and contains a substantial interneuronal neuropil that is important in generating its responses to sound. Figure 4.5 is a drawing of a Golgi preparation showing the neural elements of the DCN (Osen et al., 1990). The first and outermost layer, called the *superficial* or *molecular* layer, contains the axons of granule cells (*gr*), along with other populations of small interneurons. The second layer, called the *pyramidal cell* layer, is defined by the cell bodies of the pyramidal cells (*Py*), the most numerous of the DCN's principal cell types, and cartwheel (*Ca*) and granule cells. The innermost, deep layer is sometimes subdivided into layers

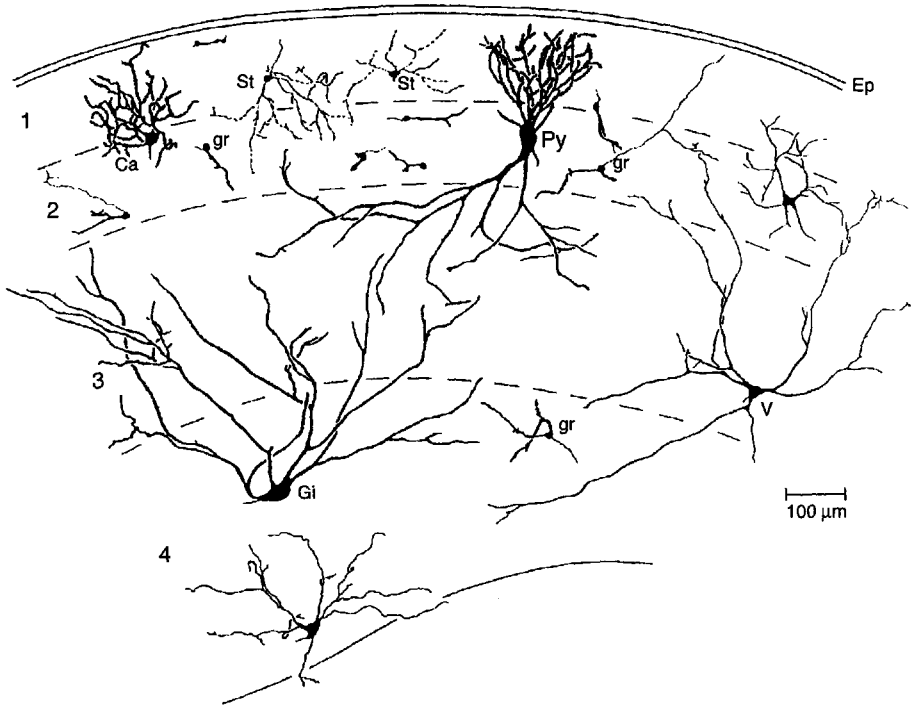


Fig. 4.5. Cell types of the DCN shown with respect to the layers of the nucleus in a plane approximately parallel to an isofrequency sheet; granule cell axons run approximately perpendicular to the page in layer 1, and ANFs run parallel to the page mainly in layer 3. The surface of the DCN (top) is covered by the ependymal layer (*Ep*), which forms the floor of the fourth ventricle. The layers are often named rather than numbered (at left): layer 1 is the superficial or molecular layer, layer 2 is the pyramidal (or fusiform) cell layer, layers 3 and 4 form the deep layer. Abbreviations: *Ca*, cartwheel cell; *Gi*, giant cell; *gr*, granule cell; *Py*, pyramidal or fusiform cell; *St*, stellate cell; *V*, vertical cell, also called a tuberculoventral or corn cell. Some unidentified cell types are shown unlabeled. [From Osen et al., 1990, with permission.]

3 and 4. It contains the axons of ANFs as well as giant cells (*Gi*), the second principal cell type, and vertical cells (*V*).

The two major afferent systems of the DCN, the ANFs and the parallel fibers (granule cell axons), are orthogonal to one another and innervate separate layers. The principal cells integrate inputs from both systems of afferents (Manis, 1989; Zhang and Oertel, 1994; Kanold and Young, 2001). Auditory nerve fibers innervate only the deep layer (layer 3) and do so tonotopically. Fibers with low BFs innervate the most ventral and lateral part of the DCN, whereas those with high BFs innervate the most dorsal and medial part (see Fig. 4.2B). Strips of cells receiving input from fibers with similar BFs form *isofrequency sheets* (Osen, 1970a; Wickesberg and Oertel, 1988; Spirou et al., 1993). In the deep layer the dendrites and terminal arbors of many DCN neurons are confined to the isofrequency sheets, so that the deep layer is organized into a succession of modules, each dealing with a narrow range of frequencies. The drawing in Fig. 4.5 is made in a plane roughly parallel to the path of ANFs through the

DCN. Parallel fibers innervate only the molecular layer running orthogonally to ANFs, thus crossing the isofrequency sheets.

Pyramidal (fusiform) neurons (Py) are bipolar (see Figs. 4.4E and 4.5), with a spiny apical dendritic tree in the molecular layer and a smooth basal dendritic tree in the deep layer (Kane, 1974; Rhode et al., 1983b; Smith and Rhode, 1985). The cell bodies of pyramidal cells form a band in the pyramidal cell layer. The basal dendrites have few branches and are flattened in the plane of the isofrequency sheets, where they receive input from the auditory nerve (Blackstad et al., 1984; Zhang and Oertel, 1994). The apical dendrites branch profusely and span the molecular layer. They are densely covered with spines that are contacted by parallel fibers.

Giant cells (Gi) are large multipolar cells located in the deep layers of the DCN. They are the DCN's second principal cell type (Kane et al., 1981; Zhang and Oertel, 1993b). Giant cells have large, sparsely branching, dendritic trees that cross isofrequency sheets. Most of the dendrites are confined to the deep layers and are smooth, but where the tips of dendrites reach into the molecular layer, they are covered with spines. Giant-cell axons join those of the pyramidal cells to form the DAS and project to the contralateral IC (see Fig. 4.3; Adams, 1979; Ryugo and Willard, 1985).

Vertical (tuberculoventral) cells (V) are inhibitory interneurons found in the deep layer (Lorente de Nó, 1981; Zhang and Oertel, 1993c; Rhode, 1999). Their cell bodies and dendrites are intermingled among the basal dendritic trees of pyramidal cells. Their smooth dendritic trees are flattened in the plane of the isofrequency sheet so that when they are examined in tissue cut coronally, they appear to be oriented vertically, perpendicular to the plane of the layers (Osen, 1983). Vertical cell axons ramify parallel to their own isofrequency sheet within the DCN; many, perhaps most, of them also project to the VCN, where axons terminate tonotopically on cells with BFs corresponding to the vertical cells (Wickesberg and Oertel, 1988). Cells that project from the DCN, or *tuberculum acousticum*, to the VCN are called *tuberculoventral* cells. Vertical cells stain prominently for glycine (Wenthold et al., 1987; Saint Marie et al., 1991; Wickesberg et al., 1994). They are a prominent source of glycinergic inhibition in both DCN and VCN (Voigt and Young, 1990; Wickesberg and Oertel, 1990).

Cartwheel (Ca) cells are inhibitory interneurons whose numerous cell bodies lie in the pyramidal cell layer of the DCN (Wouterlood and Mugnaini, 1984). Their dendrites span the molecular layer and are densely covered with spines that are contacted by parallel fibers. Although these cells stain for glycine as well as for GABA and GAD (Osen et al., 1990; Kolston et al., 1992), they contact pyramidal, giant, and other cartwheel cells through glycinergic synapses (Golding and Oertel, 1997; Davis and Young, 2000). Cartwheel and cerebellar Purkinje cells share many features. Like Purkinje cells, cartwheel cells fire complex action potentials (Zhang and Oertel, 1993a; Manis et al., 1994). Both contain PEP19 (Berrebi and Mugnaini, 1991), cerebellin (Mugnaini and Morgan, 1987), and GAD (Mugnaini, 1985). Both cartwheel and Purkinje cells have mGluR1 α located in spines (Petralia et al., 1996; Wright et al., 1996). The dendrites of both contain IP3 receptors (Rodrigo et al., 1993; Ryugo et al., 1995). Genetic mutations affect Purkinje cells and cartwheel cells similarly (Berrebi et al., 1990).

Granule cells are microneurons whose axons, the parallel fibers, provide a major excitatory input to DCN through the molecular layer (Mugnaini et al., 1980a,b). They have short dendrites whose claw-like endings receive input from large mossy terminals

in *glomeruli*. Granule cells are found in domains around the VCN (see Fig. 4.2) and in the pyramidal cell layer of the DCN (see Fig. 4.5). In the molecular layer, the granule cell axons run perpendicularly to the isofrequency sheets from ventrolateral to dorsomedial. As in the cerebellum, the granule cells in the cochlear nuclei are associated with inhibitory interneurons.

Golgi cells provide both feedforward and feedback inhibition to granule cells (Mugnaini et al., 1980a; Ferragamo et al., 1998b). Golgi axons ramify locally and extensively within the granule cell domains. They contain both GABA and glycine (Mugnaini, 1985; Kolston et al., 1992) but are assumed, by analogy with cerebellar Golgi cells, to be GABAergic.

Stellate (St) cells are confined to the molecular layer. They have smooth dendrites and their axons arborize extensively in the plane of the molecular layer (Wouterlood et al., 1984; Zhang and Oertel, 1993a). Their cell bodies are labeled by GABAergic markers (Osen et al., 1990; Kolston et al., 1992).

Unipolar brush cells and *chestnut cells* are excitatory interneurons, slightly larger than granule cells, that reside in the two most superficial layers (Florin et al., 1994; Weedman et al., 1996). Not only do unipolar brush cells receive input through large, mossy terminals, but also their axons terminate in mossy endings, presumably supplying input to granule cells. The unipolar brush cells have been shown in the cerebellum to convert a single action potential from mossy fiber inputs into a prolonged train of action potentials (Rossi et al., 1995). Chestnut cells have a single stubby dendrite that receives multiple inputs (Weedman et al., 1996).

SYNAPTIC CONNECTIONS

ANFs and mossy terminals to granule cells (and their parallel fiber axons) comprise the two major systems of extrinsic excitatory inputs to the cochlear nucleus. ANFs bring acoustic information from the cochlea. Through mossy terminals on granule cells, perhaps through unipolar brush cells, parallel fibers bring multimodal input from widespread regions of the brain, including somatosensory (Itoh et al., 1987), vestibular (Burian and Gstoettner, 1988), auditory (Brown et al., 1988a; Caicedo and Herbert, 1993; Feliciano et al., 1995; Weedman and Ryugo, 1996), and pontine motor systems (Ohlrogge et al., 2001).

In addition neurons receive excitatory and inhibitory input from local arborizations of cochlear nuclear neurons and excitatory and inhibitory efferent inputs from other brain stem nuclei (Cant, 1992). Through local collateral terminals, pyramidal and T-multipolar cells provide glutamatergic excitation (Smith and Rhode, 1985, 1989; Ferragamo et al., 1998a). D-multipolar, vertical, and cartwheel cells are inhibitory and glycinergic (Wickesberg and Oertel, 1990; Golding and Oertel, 1997; Ferragamo et al., 1998a), and stellate and Golgi cells are probably inhibitory and GABAergic (Osen et al., 1990; Kolston et al., 1992). Collaterals of olivocochlear neurons in the ventral nucleus of the trapezoid body provide cholinergic excitation to some neurons (Brown et al., 1988b; Horvath et al., 2000; Fujino and Oertel, 2001; Mulders et al., 2002). Many of the efferent inputs from the periolivary regions are inhibitory (Potashner et al., 1993; Ostapoff et al., 1997).

ANFs make synapses on all of the cell types in the cochlear nucleus, except the cells of the molecular layer of the DCN and those in the granule cell regions. Their terminals range in size from small boutons to large endbulbs (Rouiller et al., 1986). Figure 4.6 shows a reconstruction of an ANF that illustrates the variety of synaptic contacts

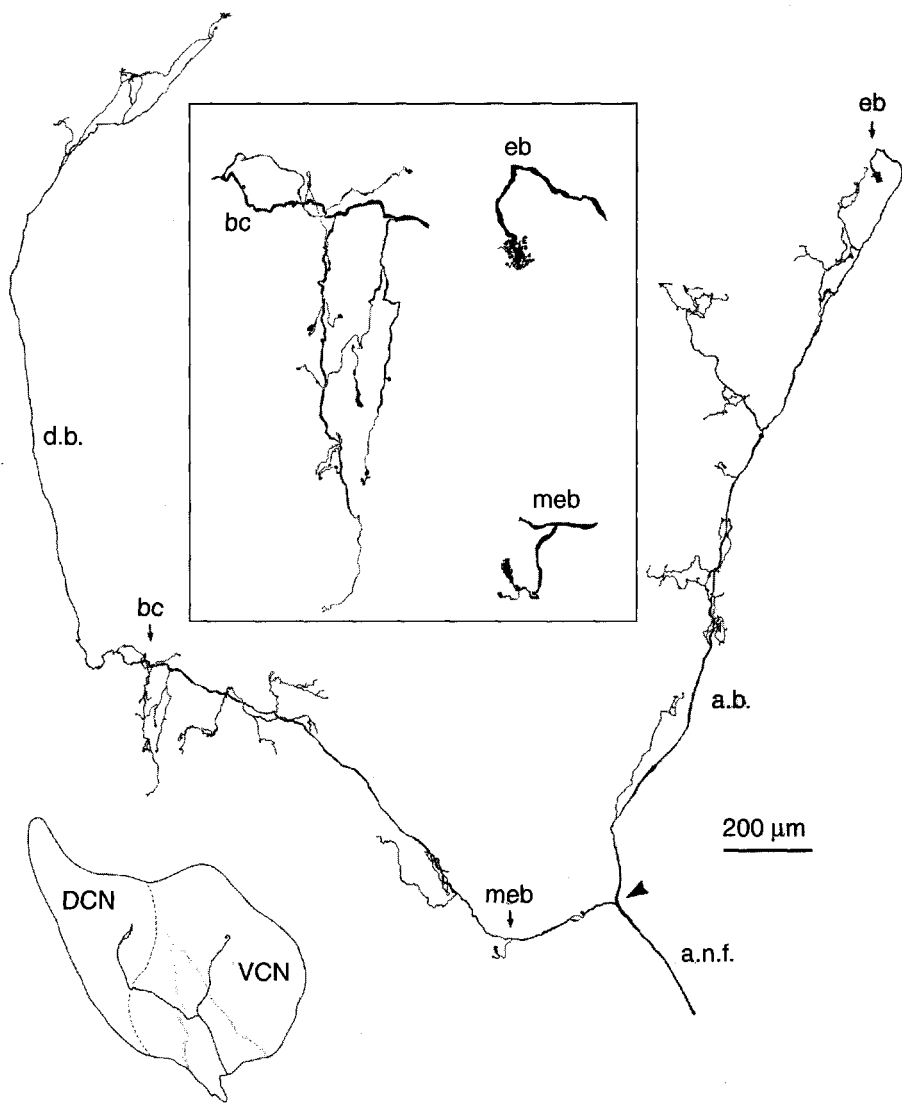


Fig. 4.6. Camera lucida drawing in the parasagittal plane of the complete branching pattern of an ANF in the cochlear nucleus of a cat. The inset at bottom left shows the position of the fiber relative to the nucleus. *a.n.f.* is the main branch of the fiber from the auditory nerve; *a.b.* and *d.b.* are the ascending and descending branches. Three types of synaptic termination are shown expanded three times in the box at top center; these are labeled in the same way as in the main diagram. *bc*, collaterals ending in boutons in the central region of the PVCN; these often end in the neuropil away from cell bodies. Similar bouton collaterals can be seen in DCN and in the AVCN. *m.e.b.*, modified endbulb terminal associated with the soma of a GBC; *eb*, endbulb of Held, a calyceal terminal that contacts the soma of an SBC, at the rostral end of the fiber. [From Fekete et al., 1984, with permission.]

made by each fiber (Fekete et al., 1984). The largest endings are the endbulbs of Held (*eb* and *meb*) that terminate on bushy cells. Smaller bouton terminals are found on collaterals (*bc*) throughout the nucleus. At the ultrastructural level all are characterized by asymmetric, often concave, synaptic contacts with large spherical vesicles; these will be referred to as *ANF type* (Fig. 4.7A; Lenn and Reese, 1966; Cant, 1992).

SYNAPSES IN VENTRAL COCHLEAR NUCLEUS

Neurons in the ventral cochlear nucleus characteristically respond to sound by firing well-timed action potentials. Both the characteristics of the synaptic current and the

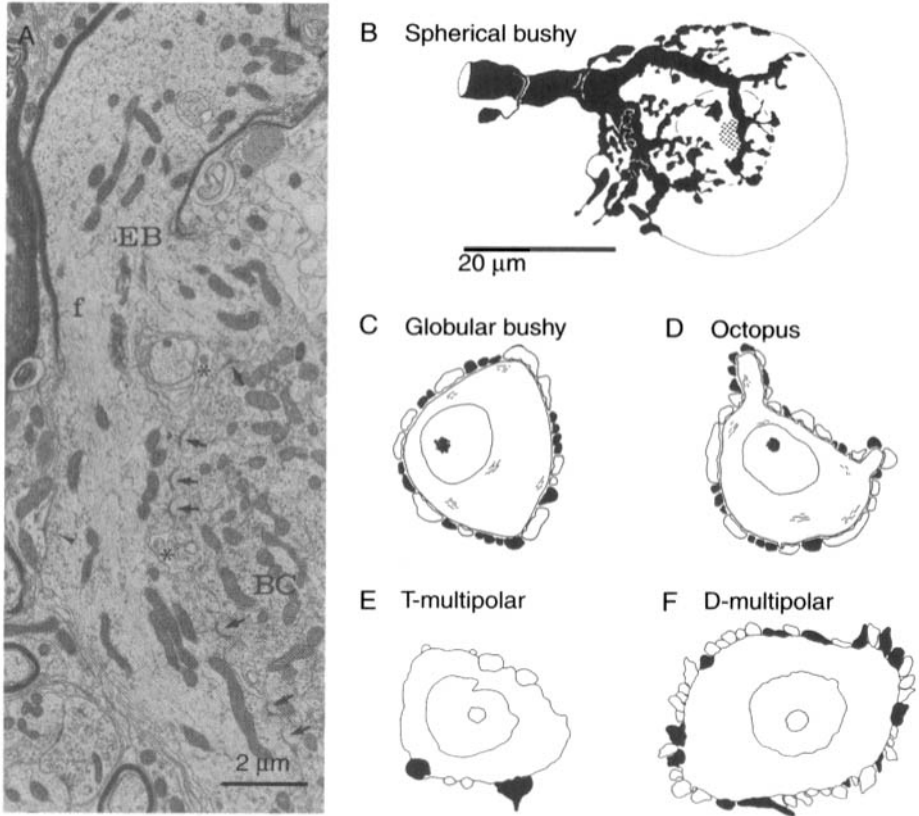


Fig. 4.7. Illustrations of synapses on the somata of five VCN cell types in cats. **A:** Cross section of an endbulb terminal (*EB*) on the soma of an SBC (*BC*). [From Cant and Morest, 1979b.] Arrowheads show synaptic release sites; note the characteristic curvature of the synaptic contact. The arrowhead on the left side of the endbulb shows a synaptic contact on the dendrite of another bushy cell. **B:** Drawing of an endbulb on an SBC soma (Sento and Ryugo, 1989). **C–F:** Drawings of somata showing the distribution of excitatory-type (unfilled, mainly ANF type) and inhibitory-type (filled) terminals. Octopus, T- and D-multipolar cells receive not only somatic but also substantial dendritic inputs. The scale bar in **B** applies to **C–F** as well. **C:** Globular bushy cell. **D:** Octopus cell. **E** and **F:** T- and D-multipolar cells, respectively. [Bushy and octopus cells from Cant, 1992; multipolar cells from Smith and Rhode, 1989.] [Taken from the sources listed with permission; **B**, **E**, and **F** reprinted with permission from Wiley-Liss.]

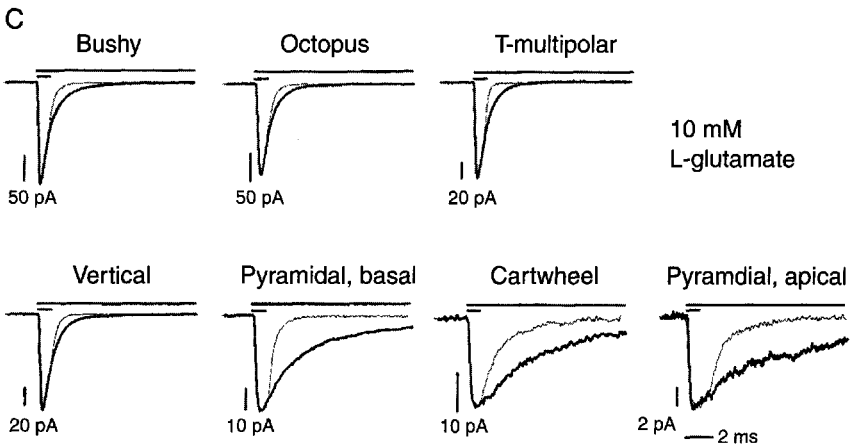
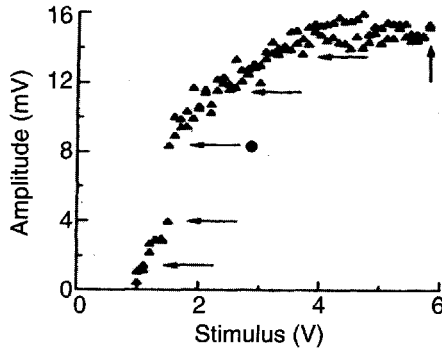
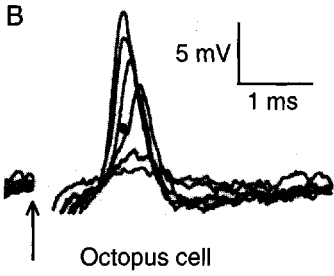
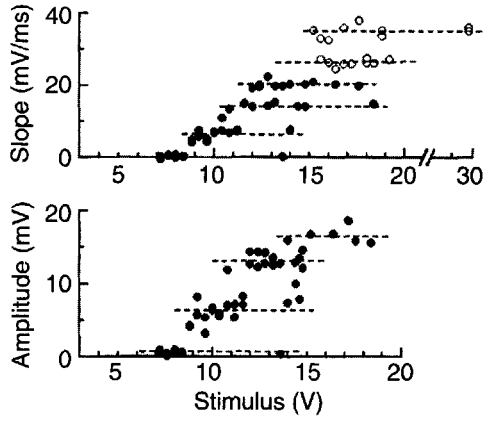
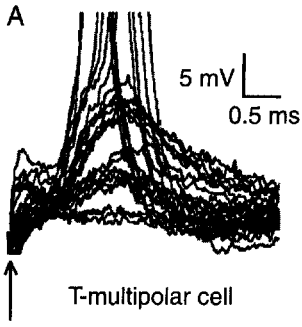
electrical characteristics of the cells on which those currents act shape the timing of the response. The sharp timing of action potentials is manifested in the small temporal jitter in the responses to the onset of a tone. The standard deviations in the time of occurrence of the first spike of a response in bushy, D-multipolar, and octopus cells range between 100 and 600 μsec ; in T-multipolar cells, they are about 1 msec (Rhode and Smith, 1986). Here we describe the specializations of the synapses in cochlear nucleus that allow this precision.

In the AVCN individual ANFs wrap the cell bodies of bushy cells with calyceal endings (*eb* in Fig. 4.6) or with clusters of boutons and fingerlike endings (*meb* in Fig. 4.6). The SBCs in the AVCN receive input through *endbulbs of Held* from about three ANFs per cell (see Fig. 4.7B; Brawer and Morest, 1975; Ryugo and Fekete, 1982; Ryugo and Sento, 1991). The GBCs are contacted by smaller modified endbulbs from between 4 and 40 fibers (Tolbert and Morest, 1982b; Smith and Rhode, 1987; Ostapoff and Morest, 1991; Nicol and Walmsley, 2002), mainly on the soma and proximal dendrites (Fig. 4.7C). Endbulbs (*EB*) contain 100 or more synaptic release sites (Fig. 4.7A, arrowheads; Lenn and Reese, 1966; Cant and Morest, 1979b; Nicol and Walmsley, 2002). Both SBCs and GBCs also receive terminals other than those from ANFs; in GBCs, where this question has been examined directly (Ostapoff and Morest, 1991), ANF endings predominate on the soma and initial segment of the axon (27/52 somatic endings per cell), whereas inhibitory-type endings predominate on the dendrites (27/38 dendritic endings per cell). Small numbers of excitatory-type endings that are not from ANFs are also seen scattered everywhere on the cell (≈ 4 per cell).

Multipolar cells receive bouton endings from collaterals of ANFs (*bc* in Fig. 4.6). In cats differences in the somatic innervation of T- and D-multipolar cells define a clear distinction between two types of multipolar cells (Cant, 1981; Smith and Rhode, 1989). The cell bodies of D-multipolars are densely covered with terminals, about half of which arise from ANFs (Fig. 4.7F). The cell bodies of T-multipolars, in contrast, receive few terminals on the soma and only one-tenth of those arise from ANFs (Fig. 4.7E). In multipolar cells many ANFs terminate on proximal dendrites. The remaining synapses are a mixture of the inhibitory types. The difference in somatic innervation is less clear in rats (Alibardi, 1998).

The number of terminals made by ANFs on multipolar cells has not been counted anatomically, but the electrophysiological evidence indicates that only about five ANFs contact a T-multipolar cell in mice (Ferragamo et al., 1998a). At left in Fig. 4.8A are shown the EPSPs evoked in a T-multipolar cell by electrical stimulation of the auditory nerve. As the stimulus strength increased in small increments, EPSPs increased in size by jumps until action potentials were produced. The scatter plots at the right show that the EPSP amplitudes evoked by a range of stimulus strengths clustered into about four groups, for subthreshold potentials (filled symbols in the bottom plot). When the slope of the rise of the EPSP was considered, two additional groups could be recognized in suprathreshold responses (open circles in the top plot). The five jumps in the rate of rise reflect the recruitment of five ANF inputs as the stimulus strength was increased.

Octopus cells are contacted by short collaterals of large numbers of ANFs through uniformly small terminal boutons; the innervation of the soma is dense (see Fig. 4.7D), but terminals are also found on the dendrites (Kane, 1973). Octopus cell dendrites extend across the auditory nerve array, receiving inputs from roughly one-third of the



tonotopic range. *In vivo* the convergence of many fibers is manifested as broad tuning, i.e. by responsiveness to a wide range of stimulus frequencies (Godfrey et al., 1975a; Rhode and Smith, 1986). *In vitro* the convergence of many ANFs is manifested by synaptic responses to shocks of the auditory nerve that grow in tiny increments as a function of the strength of shock, so that contributions of individual fibers to the EPSPs cannot be seen (Fig. 4.8B). Assuming that an ANF innervates only one octopus cell in mice, each octopus cell receives about 60 ANF inputs (Willott and Bross, 1990; Golding et al., 1995). EPSPs in octopus cells are very brief, between 1 and 2 msec in duration (Fig. 4.8B; Golding et al., 1995).

Most evidence suggests that the auditory-nerve neurotransmitter is glutamate: glutamate levels and levels of its precursor, glutamine, are high in the terminals of ANFs (Hackney et al., 1996), its release is Ca^{2+} dependent (Wentholt, 1979), its extrinsic application mimics the action of the neurotransmitter (Raman et al., 1994; Gardner et al., 2001), and the receptors clearly belong to the family of glutamate receptors (GluRs; Petralia et al., 1996; Wang et al., 1998).

The postsynaptic GluRs at ANF synapses in the VCN are mainly of the AMPA subtype. In young animals NMDA receptors contribute significantly to responses evoked by stimulation of the auditory nerve, but their contribution decreases with development and becomes insignificant in mature animals (Wickesberg and Oertel, 1989; Bellingham et al., 1998). Auditory AMPA receptors have rapid kinetics and high unitary conductances. It was first shown in targets of avian ANFs that the GluRs of the AMPA subtype have exceptionally rapid kinetics (Raman et al., 1994). The finding has been confirmed in mammals. Spontaneous release of neurotransmitter activates miniature synaptic currents whose time constants of decay are shorter than 1 msec (Gardner et al., 1999).

←

Fig. 4.8. Synaptic physiology of VCN neurons in slice preparations from mice. **A:** EPSPs evoked in a T-multipolar cell by electrical stimulation of the auditory nerve with shocks whose strength was varied in small increments (Ferragamo et al., 1998a). The stimuli were applied at the arrow. Suprathreshold traces are cut off. Note that the subthreshold traces cluster at certain amplitudes. At the right, the rising slope (top) and amplitude (bottom) of EPSPs are plotted against the stimulus strength. The dashed lines show mean amplitudes and slopes of the EPSPs after clustering (using k-means). Solid symbols show subthreshold cases, and unfilled symbols (slope only) show suprathreshold cases. Presumably the clusters correspond to recruitment of ANFs by the stimulus; this experiment shows that the T-multipolar cell was contacted by at least five ANFs. **B:** Similar analysis for an octopus cell (Golding et al., 1995); only amplitude data are shown in the plot. Amplitudes show a jump at the filled circle, where the EPSPs become suprathreshold. Horizontal arrows in the plot at right identify the synaptic responses illustrated at left. No subthreshold clusters are seen in octopus cells, presumably because they receive a large number of inputs, each of which contributes only a very small EPSP. **C:** Synaptic receptor currents produced by AMPA receptors in membrane patches from six cell types (Gardner et al., 2001). Inward currents were evoked by 1-ms or 10-ms pulses (indicated by the short and long horizontal lines, respectively) of 10 mM L-glutamate applied rapidly by moving the interface of control and test solutions across the patches. The responses to the 10-ms applications (heavy traces) illustrate desensitization of the receptors; light traces, the responses to 1-ms applications, show deactivation kinetics. Currents in cells of the VCN and in dendrites in the deep layer of the DCN that are contacted by ANFs have more rapid kinetics than receptors in the molecular layer of the DCN that are contacted by parallel fibers. [Reproduced from the sources listed with permission.]

GluRs are tetramers formed from any combination of the GluR family of subunits. In addition, alternative splicing gives these subunits “flip” or “flop” configurations. In VCN, most receptors associated with ANF terminals contain GluR3 and GluR4 subunits in the flop configuration (Petrálie et al., 2000; Schmid et al., 2001). The presence of flop suggests that the gating kinetics of these receptors are fast (Mosbacher et al., 1994) and the absence of GluR2 should give them high single-channel conductances and make them permeable to Ca^{2+} (Swanson et al., 1997). Figure 4.8C shows currents evoked by rapid application of glutamate recorded from three typical VCN cells (Gardner et al., 2001). The kinetics are fast for activation, deactivation, and desensitization; in fact, they match the most rapid that have been measured anywhere. Conductances of single GluRs on VCN cells average 28 pS. On average 40–50 receptors are activated in a miniature synaptic event.

The large conductance and rapid kinetics of receptors in the VCN can be understood in terms of the properties of the postsynaptic cells. Bushy and octopus cells have low input resistances that give them short time constants and allow them to encode brief events with temporal precision but also require large synaptic currents to bring them to threshold (Oertel, 1983; Manis and Marx, 1991; Golding et al., 1995). In the avian homolog of SBCs, activation of an action potential in one ANF opens $\approx 10,000$ AMPA receptors and produces a conductance increase of over 200 nS through the release of ≈ 100 quanta (Zhang and Trussell, 1994). In rodent GBCs, each ANF activates an average conductance between 34 and 45 nS, evoking a synaptic current of over 10 nA (Isaacson and Walmsley, 1995; Bellingham et al., 1998).

Synapses in many parts of the brain show short-term and long-term changes in strength, including facilitation, depression, long-term potentiation (LTP), and long-term depression (LTD). Synaptic transmission by mature ANFs is remarkable in showing little plasticity, a feature that is useful for transmitting ongoing acoustic information faithfully and with minimal distortion by preceding sounds. In responding to sounds, mammalian ANFs fire up to 300 action potentials/sec *in vivo* (Sachs and Abbas, 1974). *In vitro* studies show that synaptic depression is prominent in very young animals and decreases as animals mature (Wu and Oertel, 1987; Brenowitz and Trussell, 2001). In relatively mature animals synaptic depression is detectable only at the highest natural firing rates (Wu and Oertel, 1987; Golding et al., 1995; Oertel, 1997). The depression seen in these records is likely to be greater than under physiological conditions, because these *in vitro* recordings were made at lower than physiological temperatures and synaptic depression decreases as temperature increases and because other mechanisms further decrease depression (Brenowitz et al., 1998).

SYNAPSES IN DORSAL COCHLEAR NUCLEUS

Pyramidal cells, the principal cells of the DCN, integrate input from two different circuits, one in the molecular layer and the other in the deep layer, through separate apical and basal dendrites. In the molecular layer the parallel fibers excite pyramidal cells through spines on apical dendrites (Smith and Rhode, 1985). The shafts of apical dendrites and the cell bodies of pyramidal cells are densely packed with inhibitory-type terminals (Juiz et al., 1996). Many of these inhibitory terminals arise from glycinergic cartwheel cells. Cartwheel cells are themselves excited by parallel fibers on dendritic spines in the molecular layer and are also interconnected among themselves (Wouter-

lood and Mugnaini, 1984; Golding and Oertel, 1997). In the deep layer, terminals from ANFs end on the mostly smooth basal dendrites, where they account for $\approx 10\%$ of the terminals on the proximal dendrites and $\approx 38\%$ on distal dendrites; the remaining terminals on the basal dendrites are inhibitory type. Indirectly ANFs drive glycinergic inhibition on basal dendrites through vertical cells (Voigt and Young, 1990; Zhang and Oertel, 1993c, 1994).

The AMPA receptors that mediate excitation to DCN neurons differ in the various neurons and, in the case of pyramidal cells, differ in the apical and basal dendrites. GluR2 and GluR3 subunits are found in both pyramidal and cartwheel cells (Petralia et al., 2000). The basal dendrites of pyramidal cells also contain GluR4 subunits but the apical dendrites do not (Rubio and Wenthold, 1997). Cartwheel cell dendrites do not contain GluR4 subunits but do contain GluR1 subunits (Petralia et al., 1996). The dendrites receiving terminals from ANFs, both vertical cells and basal pyramidal dendrites, show faster receptor currents than those receiving terminals from granule-cell axons, the cartwheel and apical pyramidal dendrites (Fig. 4.8C; Gardner et al., 2001). This difference may reflect the presence of GluR4 subunits, as in the VCN. In the case of vertical cells, the receptor kinetics are almost as fast as in VCN neurons, but the underlying receptor subunits have not been studied. A similar pattern is seen in miniature synaptic currents (Gardner et al., 1999).

There are dramatic differences in the way excitatory, glutamatergic synapses in the deep layer and those in the molecular layer of the DCN are modulated by activity (Fujino and Oertel, 2002). Synapses between parallel fibers and their pyramidal and cartwheel cell targets in the molecular layer show LTP and LTD. Examples are shown in Fig. 4.9. When parallel fibers are induced to fire rapidly (100 Hz) and their synaptic inputs are associated with a depolarization of the target neurons, synaptic currents increase in amplitude (Fig. 4.9A, B); when parallel fibers are induced to fire slowly (0.1 Hz) and their activity is paired with postsynaptic depolarization, synaptic currents decrease in amplitude (Fig. 4.9C, D). The strength of synapses between parallel fibers and their targets is thus continually modulated upward and downward by synaptic traffic. Those between ANFs or T-multipolar neurons and dendrites in the deep layer do not show LTP or LTD (Fig. 4.9E, F).

Plasticity in the molecular layer of the DCN has much in common with long-term plasticity in the hippocampus and cerebellum (see Chaps. 7 and 11). Synapses on spines, but not those on the shafts of dendrites, show LTP and LTD, supporting the idea the spines serve as biochemical compartments. Furthermore, long-term changes in synaptic strength are governed by changes in the intracellular Ca^{2+} concentration, because plasticity is not observed when recordings are made with patch-pipettes that contain high concentrations of Ca^{2+} buffers (9 mM EGTA). Both LTP and LTD require a rise of intracellular Ca^{2+} . There are several potential sources of Ca^{2+} in fusiform and cartwheel cells. Some Ca^{2+} enters neurons from the extracellular space through the NMDA subtype of GluRs (Manis and Molitor, 1996). Blocking these receptors with DL-2-amino-5-phosphonovaleric acid (APV) reduces LTP in pyramidal and cartwheel cells, and it consistently blocks LTD in cartwheel cells (Fujino and Oertel, 2003). Antagonists of metabotropic GluRs also reduce LTP and LTD in pyramidal and cartwheel cells. Voltage-sensitive Ca^{2+} channels are prominent in cartwheel (Zhang and Oertel, 1993a; Manis et al., 1994; Golding and Oertel, 1997) and pyramidal (Hirsch and

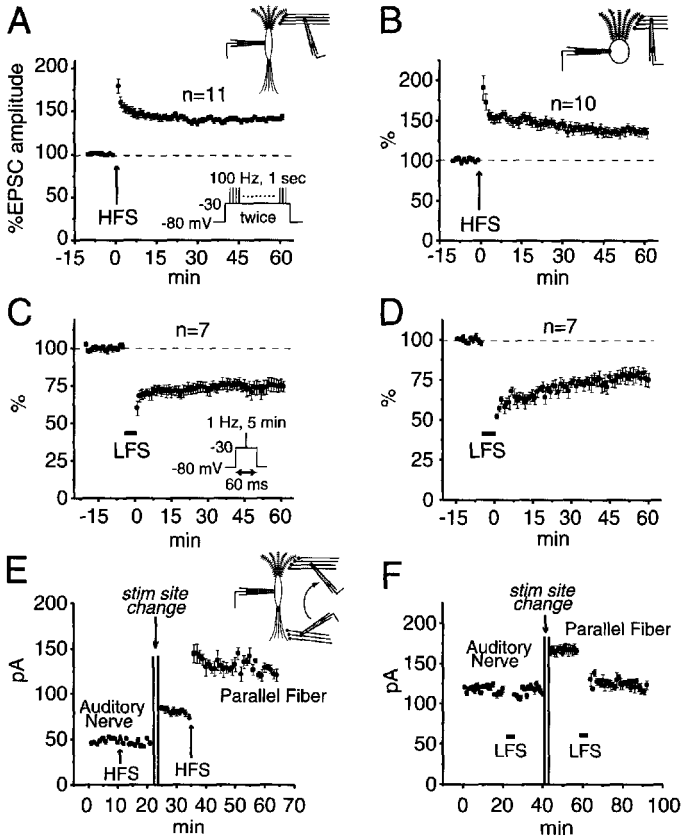


Fig. 4.9. Long-term potentiation (LTP) and depression (LTD) in parallel fiber synapses in the DCN (Fujino and Oertel, 2003). Excitatory synaptic currents (EPSCs) were recorded from the soma of pyramidal cells (left column) or cartwheel cells (right column). Shocks were applied at 0.1 Hz to parallel fibers or ANFs to monitor the strength of synapses. **A** and **B**: EPSC amplitude, averaged over 10 or 11 cells for parallel fiber stimulation. At the point marked *HFS*, a 100-Hz, 1-s-long pulse train was applied twice while the cell was depolarized to -30 mV. The amplitude of the EPSC increased by $\approx 50\%$ and remained elevated for at least 1 h (LTP). **C** and **D**: When parallel fibers were stimulated at 1 Hz for 5 min, also while depolarizing the cell (LFS), the amplitudes of EPSCs decreased and remained small for at least 1 h (LTD). **E** and **F**: Pyramidal cells tested for LTP (**E**) or LTD (**F**) with both auditory nerve and parallel fiber stimulation. LTP and LTD were observed only at the parallel fiber synapse. [Adapted from the source listed, with permission.]

Oertel, 1988; Molitor and Manis, 1999) cells and probably also contribute to the rise in intracellular Ca^{2+} levels. In addition to the entry of Ca^{2+} from the extracellular space, plasticity requires Ca^{2+} -induced Ca^{2+} release through ryanodine receptors from intracellular stores (Fujino and Oertel, 2003).

Granule cells receive inputs at specialized *glomerular synapses* in which a large synaptic terminal (mossy fiber) is partially surrounded by claw-like granule cell dendrites, which also receive inhibitory synapses from other cells, probably including Golgi cells (Mugnaini et al., 1980a).

As was discussed for the VCN, neurons in the DCN are influenced by inhibition both from intrinsic inhibitory neurons and from descending inputs from periolivary regions. Stellate neurons in the molecular layer of the DCN label for GABA, cartwheel and Golgi cells double-label for GABA and glycine, and vertical and D-multipolar cells label for glycine (Osen et al., 1990; Saint-Marie et al., 1991; Kolston et al., 1992; Doucet et al., 1999). One question raised by these findings is whether neurons that are labeled for both GABA and glycine release both neurotransmitters. Cartwheel cells have been shown to produce purely glycinergic synaptic potentials in their targets (Goldring and Oertel, 1996, 1997). Whether this results from only glycine being released or from only glycine receptors being present postsynaptically is not known. Both GABA and glycine receptors that are typical of such receptors elsewhere in the brain are present in DCN (Wu and Oertel, 1986; Harty and Manis, 1996). *In vivo* antagonists of both glycine and GABA affect responses to sound, although the effects of glycine antagonists are usually stronger (Caspary et al., 1987; Evans and Zhao, 1993; Caspary et al., 1994; Davis and Young, 2000). A second question concerns why there should be two types of inhibition. Glycinergic, strychnine-sensitive IPSPs are prominent in circuits that can be activated in slices; GABA_Aergic inhibition is subtle (Ferragamo et al., 1998a; Lim et al., 2000). It is possible that GABA mediates mainly presynaptic inhibition through GABA_B receptors and that, when GABA and glycine are released together, the glycine serves as the signaling molecule to the postsynaptic cell and the GABA serves to regulate the synapse presynaptically (Lim et al., 2000).

NUMBERS OF CELL TYPES AND CONVERGENCE

In cat, there are ≈ 3000 IHCs and $\approx 50,000$ type I ANFs (Ryugo, 1992). The total population of cells in the cochlear nucleus is similar in number to the ANFs. Most numerous are the bushy cells, with 36,600 SBCs and 6300 GBCs (Osen, 1970b). These numbers are consistent with the innervation ratios described above for SBCs (1–3 ANFs per cell) and GBCs (≈ 35 ANF-type terminals per cell), given that each ANF contacts, on average, 1 SBC soma and 3–6 GBC somas (Liberman, 1991). There are ≈ 9400 multipolar cells (Osen, 1970b), most of which are T-multipolars; the ratio of T- to D-multipolars is $\approx 15:1$ (Doucet and Ryugo, 1997). Anatomical convergence ratios onto multipolar cells have not been estimated, but it was argued earlier based on physiological data to be ≈ 5 ANFs/T-multipolar (Fig. 4.8A). There are ≈ 1500 octopus cells (Osen, 1970b), and each ANF contacts ≈ 2 somas in the octopus cell area (Liberman, 1993), yielding a convergence ratio of ≈ 67 ANFs/octopus cell, similar to the minimal value estimated earlier for mouse. In DCN, there are ≈ 4400 pyramidal cells and ≈ 1300 giant cells (Osen, 1970b; Adams, 1976). The most numerous DCN cell types are the granule cells (60,000) and cartwheel cells (18,000), with fewer stellates (4000) and Golgi cells (2300) (Wouterlood and Mugnaini, 1984). The degree of convergence onto and among DCN cell types cannot be estimated from existing data.

BASIC CIRCUIT

The intrinsic organization of neuronal elements and synaptic connections in the cochlear nucleus is summarized in Fig. 4.10. All of the principal cells of the ventral and dorsal

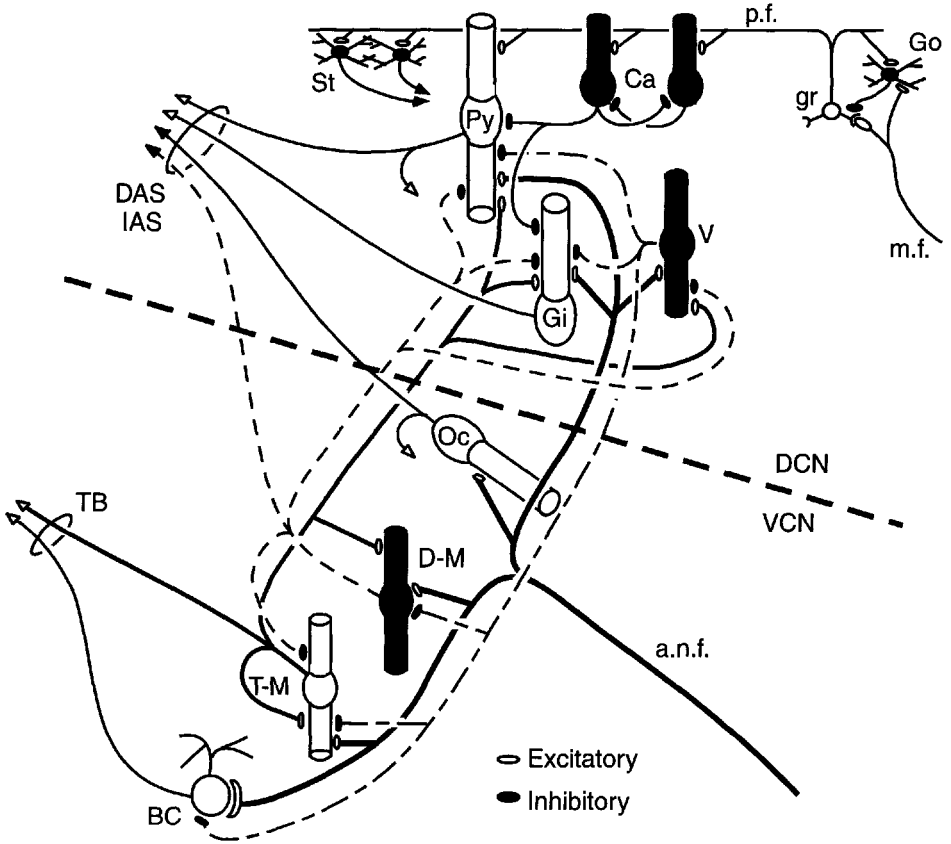


Fig. 4.10. Schematic drawing of the neuronal circuits in the cochlear nucleus. Excitatory neurons and terminals are shown unfilled; inhibitory elements are shown filled. Inputs to the cochlear nucleus come from auditory nerve fibers (*a.n.f.*) and mossy fibers (*m.f.*); additional inputs from the central auditory system are not shown. The axons of the principal cells exit the cochlear nucleus through the trapezoid body (*TB*), and the dorsal (*DAS*) and intermediate acoustic striae (*IAS*). Abbreviations: *BC*, spherical and globular bushy cells; *T-M* and *D-M*, T- and D-multipolar; *Oc*, octopus cells; *Gi*, giant cells; *Py*, pyramidal cells. Vertical cells (*V*) project to all principal cell types except the octopus cells. Both T- and D-multipolar cells form intrinsic connections through collaterals in the VCN and DCN. The axons of multipolar and vertical cells that travel between DCN and VCN make up the prominent bundle of fibers labeled *i.f.* in Fig. 4.2B. Pyramidal cells in cats (but not in mice) and octopus cells have collaterals that terminate near their cell bodies. The axons of granule cells are termed *parallel fibers* (*p.f.*); they terminate on pyramidal, cartwheel (*Ca*), and stellate (*St*) cells in the molecular layer.

cochlear nucleus are innervated by ANFs (*a.n.f.*). Innervation by ANFs both in the VCN and in the deep layer of the DCN is tonotopically organized, with low-frequency encoding fibers innervating bands ventrally and high-frequency encoding fibers innervating bands dorsally. The principal cells of the DCN integrate two sets of circuits—one associated with the ANF inputs (*a.n.f.*) in the deep layer and a second associated with the granule cells (*gr*) and parallel fibers (*p.f.*).

The vertical cells are inhibitory interneurons that project to their isofrequency sheets in both DCN and VCN (Wickesberg and Oertel, 1988; Zhang and Oertel, 1993c; Rhode, 1999); they inhibit all of the principal cells in the cochlear nucleus, except the octopus cells (Voigt and Young, 1990; Wickesberg and Oertel, 1990, 1991). Vertical cells are narrowly tuned, and they respond most strongly to tones at a frequency near their BF (Spirou et al., 1999). Consistent with the tonotopic projection of vertical cell axons, cells in both DCN and VCN have a glycinergic inhibitory input whose BF is very close to the cell's own BF (Wickesberg and Oertel, 1988; Caspary et al., 1994; Davis and Young, 2000).

Both T- and D-multipolar cells in the VCN serve the role of interneurons through their axon collaterals. These terminate locally within VCN as well as projecting to the deep DCN (Smith and Rhode, 1989; Oertel et al., 1990). T-Multipolars are excitatory and D-multipolars are inhibitory. T-multipolars are the likely source of polysynaptic EPSPs in vertical and principal cells in DCN and in T-multipolars in VCN (Ferragamo et al., 1998a). D-multipolars seem likely to be the source of IPSPs in the same cells. The properties of D-multipolar cell responses to sound are complementary to those of vertical cells, in that D-multipolars are broadly tuned and respond best to stimuli like noise but only weakly to tones (Palmer et al., 1996; Paolini and Clark, 1999). In this sense, the vertical D-multipolar cells provide complementary inhibitory inputs to cells throughout the cochlear nucleus. The role of their interaction in the DCN is discussed later. Notice that these two inhibitory circuits are mutually inhibitory (Fig. 4.10).

Pyramidal cells in cats (but not in mice) and octopus cells give axon collaterals that terminate locally (shown as recurving arrows in Fig. 4.10); both are excitatory (Smith and Rhode, 1985; Golding et al., 1995). The pyramidal cell axons project to other pyramidal cells, and the octopus cell axons terminate in the octopus cell area and in granule cell areas.

Granule-cell axons (*p.f.* in Fig. 4.10) terminate on spines of the apical dendrites of pyramidal cells, on spines of cartwheel cells, and on the stellate cells of the superficial DCN. The axons of cartwheel cells end in the pyramidal and deep layers of the DCN, where they produce IPSPs in pyramidal and giant cells (Zhang and Oertel, 1993b, 1994; Golding and Oertel, 1997). In addition, cartwheel cells interact with one another in a network (Wouterlood and Mugnaini, 1984; Berrebi and Mugnaini, 1991; Golding and Oertel, 1996). The reversal potential of the cartwheel-to-cartwheel cell synapses lies a few millivolts above the resting potential and the threshold for firing so that its effect is depolarizing for the cell at rest but hyperpolarizing when the cell has been depolarized by other inputs. Thus, the effects of the cartwheel cell network are likely to be context dependent—excitatory when the cells are at rest but stabilizing when the cells are excited. The cartwheel cells are the most numerous neuron in the DCN, except for the granule cells; by virtue of their numbers, their network of interconnections, and their profuse terminal distribution, cartwheel cells represent a substantial computational resource for the DCN.

Not shown in Fig. 4.10 are some circuits in the granule cell regions, including the unipolar brush and chestnut cells and some of the connections of the Golgi cells. The latter form inhibitory feedforward and feedback connections with granule cells, as in the cerebellum (Mugnaini et al., 1980a) and probably also inhibit T-multipolar cells in VCN (Ferragamo et al., 1998b).

MEMBRANE PROPERTIES AND INTEGRATION OF INPUTS

Previous sections have described the morphology, connections, and synaptic physiology of the circuits of the cochlear nucleus. In the remainder of this chapter, the properties of these circuits are related to the cells' responses to sound. Figure 4.11 shows that the electrophysiological properties of neurons influence their responses to sound and thus determines the computational role of cells. Responses to short bursts of sound recorded *in vivo* using extracellular electrodes are shown in the left column; responses *in vitro* to intracellular injections of hyperpolarizing and depolarizing currents are shown in the right column. The sounds in this case were tones at the BF of the neuron at a loudness significantly above threshold, where the neurons' responses are stable and assume their typical form (Pfeiffer, 1966; Bourk, 1976). For comparison, the responses of ANFs to this stimulus resemble those shown in Fig. 4.11C1: following stimulus onset there is a rapid increase in discharge rate to a maximum, followed by a slower decline to a fairly steady discharge, the so-called *primarylike response*. An important aspect of auditory-nerve responses that is not shown is their *irregularity*, meaning a lack of repetitive firing behavior; the spikes of an ANF occur randomly in time, so the intervals between spikes are highly variable and the pattern of action potentials is different for each stimulus repetition.

CHOPPER RESPONSES FROM T-MULTIPOLAR CELLS

Figures 4.11A and 4.11B show responses characteristic of T-multipolar cells (Rhode et al., 1983a; Wu and Oertel, 1984; Smith and Rhode, 1989; Feng et al., 1994). T-multipolar cells receive irregular, phasic input from ANFs, yet respond to tones by firing tonically at regular intervals, a pattern called *chopping*. The contrast between the regularity in firing of T-multipolar cells and the irregularity of their ANF inputs indicates that the temporal firing pattern is not imposed by the inputs but arises from the intrinsic properties of the cells themselves. Depolarization with steady current pulses causes T-multipolar cells to fire regularly with the same sort of chopping pattern (Fig. 4.11B; Oertel et al., 1988; Manis and Marx, 1991). The reproducibility of firing gives PST histograms of responses to sound a series of characteristic modes that is independent of the fine structure of the sound (Fig. 4.11A). The intervals between nodes are of equal duration and correspond to the intervals between spikes, with one spike per node. The peaks are large at the onset of the response because the latency to the first spike is quite reproducible in chopper neurons; the peaks fade away over the first 20 msec of the response as small variations in interspike interval accumulate and spike times in successive stimulus repetitions diverge (Young et al., 1988). As is shown later, the regular firing is expected from properties of neuronal spike initiation.

PRIMARYLIKE RESPONSES FROM BUSHY CELLS

Figure 4.11C shows typical responses to tones of bushy cells (Rhode et al., 1983a; Rouiller and Ryugo, 1984; Wu and Oertel, 1984; Smith and Rhode, 1987). Large EPSPs from between one and three endbulbs (Fig. 4.7A,B) cause SBCs to fire whenever the ANFs do (except when the cell is refractory). This one-spike-in, one-spike-out mode of processing means that the responses to sound of SBCs resemble those of ANFs, so they are called *primarylike* (Fig. 4.11C1). Evidence that primarylike responses re-

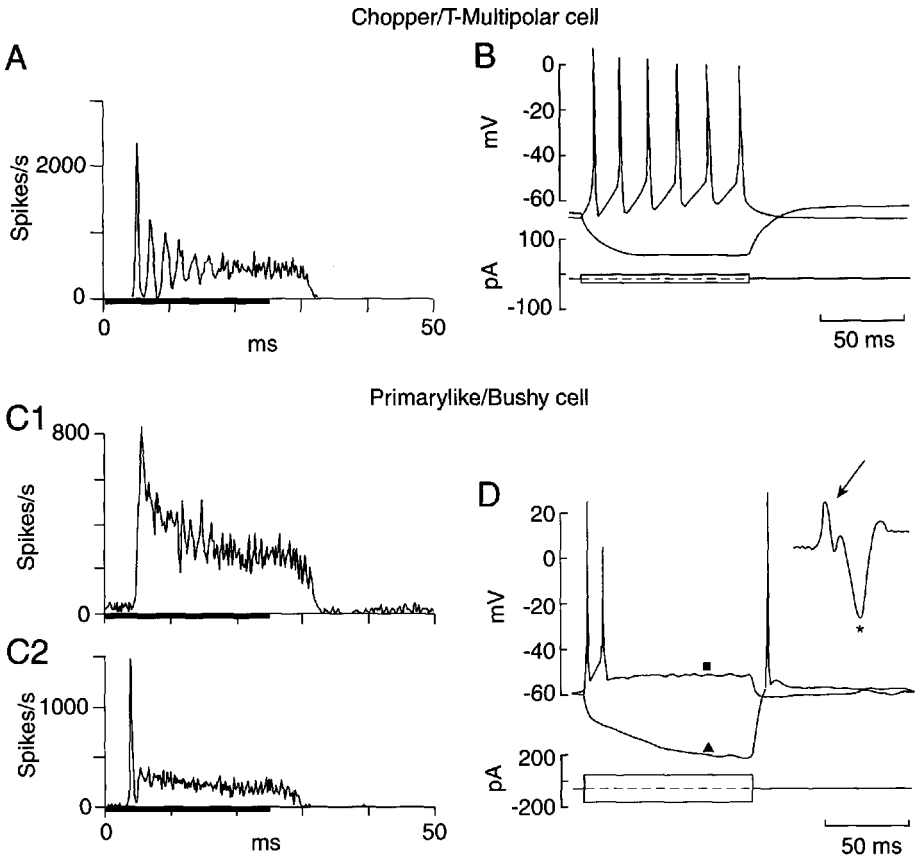


Fig. 4.11. Responses of T-multipolar and bushy cells to tones and to the intracellular injection of current. **A**, **C1**, and **C2** show poststimulus time histograms (PSTHs) of responses to BF tone bursts from extracellular recordings. The PSTH plots average discharge rate as a function of time over several stimulus repetitions. The stimulus is on during the first 25 ms, as shown by the heavy lines on the abscissae. The delay between stimulus onset and the beginning of the response (and at the offset) reflects acoustic delay in the stimulus system, the activation and propagation of the traveling wave on the basilar membrane of the cochlea, synaptic delays in the cochlea and in the cochlear nucleus, and the integration time in the neurons. **B** and **D**: Superimposed responses to intracellular injection of depolarizing and hyperpolarizing currents. Each panel shows the membrane potential of a neuron (top) and the current injected (bottom). Positive (depolarizing) currents produce action potentials, whereas negative (hyperpolarizing) currents produce passive charging of the cell membrane. Response types and the cells from which they are typically recorded are as follows. **A** and **B**: Chopper responses from T-multipolar cells. [From Blackburn and Sachs, 1989; Manis and Marx, 1991.] **C**: Primarylike (C1) response from an SBC and primarylike-with-notch (C2) response from a GBC (Blackburn and Sachs, 1989). **D**: Bushy cell responses to current pulses (Manis and Marx, 1991). The inset in **D** shows a complex action potential with a prepotential (arrow), probably from an SBC. [Redrawn from the sources indicated with permission.]

flect a one-spike-in, one-spike-out mode of processing is provided by their action potential shapes, an example of which is shown in the inset of Fig. 4.11D. The action potential (asterisk) is preceded by a *prepotential* (arrow), which is the action potential of the presynaptic cell (Guinan and Li, 1990); prepotentials are seen in the AVCN and in the MnTB, which also contains bushy-like cells with calyceal endings. In both places,

prepotentials are almost always followed by the postsynaptic component of the spike, demonstrating that this is a very secure synapse (Goldberg and Brownell, 1973; Bourk, 1976; Kopp-Scheinpflug et al., 2002). As expected, primarylike neurons fire as irregularly as ANFs (Rothman et al., 1993).

GBCs give a similar response, called *primarylike-with-notch*, or pri-N (Fig. 4.11C2). Pri-N responses differ from primarylike (and ANF) responses in their behavior at the beginning of the response, where a precisely timed peak followed by a brief notch is observed. The convergence of multiple large inputs from ≈ 35 ANFs (Ostapoff and Morest, 1991) makes the timing of firing and the encoding of the fine structure of auditory stimuli precise (Joris et al., 1994a, 1994b). For example, consider the large peak at the onset of the stimulus in Fig. 4.11C2; this peak contains a spike in every repetition of the stimulus. If the GBC fires in response to the first input spike it receives from any one of its inputs, then the more inputs that converge on the cell, the less time it will take for the first input spike to occur and the sharper will be the onset peak in the PSTH (Rothman et al., 1993). The small notch following the peak results from refractoriness.

The electrical characteristics of bushy cells are shown in Fig. 4.11D (Wu and Oertel, 1984; Manis and Marx, 1991). When depolarized, these cells fire one to three spikes at stimulus onset and then their membrane potential settles to a steady, slightly depolarized value (filled square). This behavior is produced by a *low-threshold potassium conductance* that is in part activated at rest and is strongly activated by depolarization, producing a membrane *rectification* (Manis and Marx, 1991; Reyes et al., 1994). The rectification (low input resistance in the physiological voltage range) has two important consequences: (1) large synaptic currents, provided by the calyceal endings of ANFs, are required to overcome the input resistance when the cell is depolarized; and (2) the membrane time constant of the cell is fast (2–4 msec at rest). The fast time constant can be seen from the rapid initial drop of the response to hyperpolarizing current and from the fall in voltage at the end of the depolarizing current pulse in Fig. 4.11D (compare with Fig. 4.11B). The short time constant of bushy cells blocks temporal integration of synaptic inputs (Oertel, 1983; Smith and Rhode, 1987; Paolini et al., 1997). Figure 4.12 shows postsynaptic potentials produced in a multipolar cell

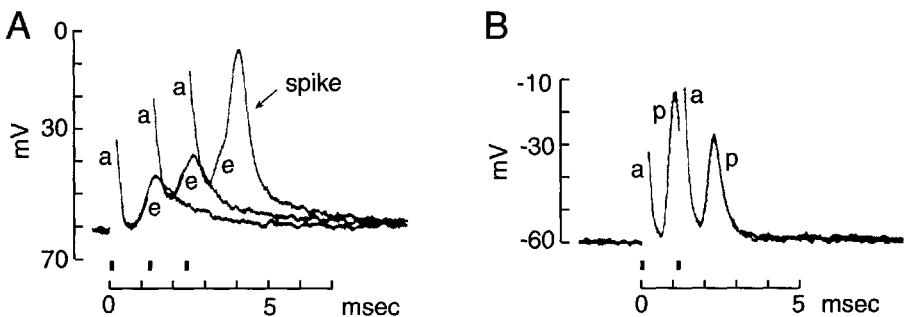


Fig. 4.12. Postsynaptic potentials in a multipolar (A) and a bushy (B) cell produced by repetitive electrical stimulation of the auditory nerve (heavy vertical bars on the time axis). **A:** Responses to one, two, and three stimuli are shown. *a*, stimulus artifact; *e*, EPSPs. Temporal summation leads to a spike after three stimuli. **B:** Large postsynaptic potentials (*p*) show rapid recovery time constants and no temporal summation. [Redrawn from Oertel, 1983, with permission.]

(A) and a bushy cell (B) by trains of electrical stimuli delivered to the auditory nerve. Temporal summation of successive EPSPs (*e*) is clear in the multipolar cell but is minimal in the bushy cell, where each EPSP leads to a spike (*p*). Recall from Fig. 4.8C that bushy and multipolar cells have AMPA receptors with similar rapid kinetics. The differences between EPSPs arise because the decay of the EPSP, and therefore the degree of temporal integration, is determined by the membrane time constant of the cell. For bushy cells this is short (2–4 msec), whereas for multipolar cells it is longer (5–10 msec; Oertel, 1983; White et al., 1994). Rapid temporal processing permits bushy cells to preserve information about the stimulus waveform information that is necessary for sound localization (Yin, 2002).

ONSET RESPONSES FROM OCTOPUS CELLS

Octopus cells respond to the synchronous firing of groups of ANFs that occurs at stimulus transients, such as the sudden increase in loudness at the onset of a syllable. The tones that are usually used to characterize neurons activate relatively few ANFs and bring octopus cells to threshold only at the beginning of the tone, which has led to the term *onset units* (Fig. 4.13A; Godfrey et al., 1975a; Rhode et al., 1983a). When presented with a train of broadband transients, such as a train of clicks, octopus cells fire to each click up to very high rates (>500 spikes/sec). Octopus cells also respond vigorously to low frequency tones, tones that evoke synchronous firing of ANFs to each cycle of the tone (Rhode and Smith, 1986). This behavior reflects the unusual biophysical properties of octopus cells that allow EPSPs to be brief and the responses well timed.

Octopus cells are like bushy cells in that the resting input resistance of octopus cells is low, $\approx 6 \text{ M}\Omega$ (Bal and Oertel, 2000). As was shown for bushy cells in Fig. 4.12, the low input resistance prevents temporal summation of nonsynchronous inputs. Instead of receiving large inputs from few fibers, however, octopus cells receive small inputs from many ANFs. Thus simultaneous firing of many inputs is necessary to drive an octopus cell to fire.

Octopus cells show a strong membrane rectification, like bushy cells (Fig. 4.13B). In the case of octopus cells, the low input resistance results from the activation of two opposing voltage-sensitive conductances: a hyperpolarization-activated, mixed cation conductance (g_h) that pulls the membrane potential toward -40 mV and a depolarization-activated K^+ conductance (g_{KL}) that pulls the membrane toward -80 mV (Golding et al., 1995; Bal and Oertel, 2000, 2001). Both are large conductances. The maximal g_h is 150 nS ; the maximal g_{KL} is over 500 nS . The voltage sensitivity of these conductances overlaps at rest so that both conductances are partially activated, each with a resting current over 1 nA . The voltage sensitivity of these conductances is high near the resting potential, so that each conductance is activated steeply by small changes in the membrane potential. These voltage-sensitive conductances shape EPSPs and affect the firing of octopus cells in three important ways. (1) The low input resistance of octopus cells makes EPSPs small ($<1 \text{ mV}$) and brief ($\approx 1 \text{ msec}$), thus making the cell sensitive only to synchronous inputs. (2) When octopus cells are depolarized synaptically, g_{KL} is activated rapidly and cuts short EPSPs, so that the timing of the peaks of synaptic depolarizations is nearly invariant over a large amplitude range. (3) g_{KL} causes octopus cells to be sensitive to the rate at which they are depolarized (Ferragamo and Oertel, 2002). Slow depolarizations activate g_{KL} and prevent the generation of action potentials. This

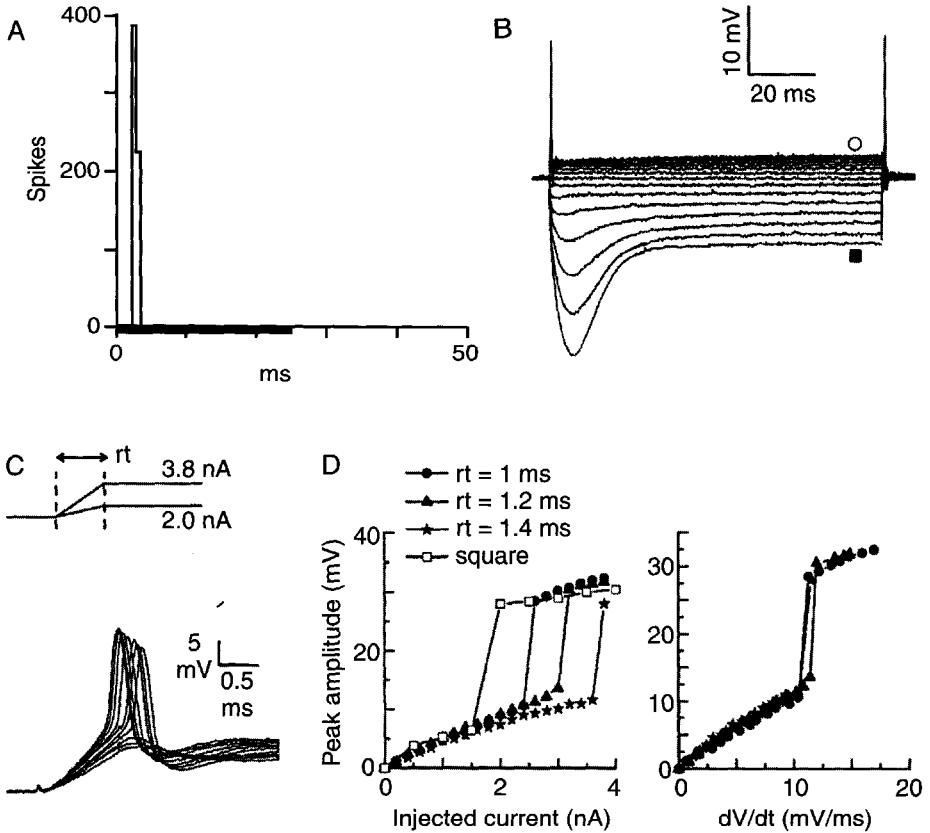


Fig. 4.13. Responses of octopus cells to tones and current pulses. **A:** PSTH of responses to a tone at BF, showing a single-spike *onset* response to the turning-on of the tone (Kiang et al., 1973). **B:** Whole-cell patch-clamp recording of responses to pulses of current from -2.8 to 2.8 nA in 0.4 nA steps (Golding et al., 1999). Note that the responses to depolarizing current (unfilled circle) are smaller than the responses to hyperpolarizing current of equal amplitude (filled square). This *rectification* is similar to that seen in bushy cells, except that the response to hyperpolarization reflects both deactivation of the low-threshold potassium conductance (g_{KL}) and activation of a mixed-cation hyperpolarizing current (g_h). **C:** Intracellular responses, in a whole-cell patch-clamp recording, of an octopus cell to ramps of current from zero to final levels varying between 2 and 3.8 nA (sketched at top). The rise time rt of ramps was 1 ms in this case. Threshold was reached between the third and fourth ramp. **D:** Peak amplitude of response to current ramps of varying rt (see legend) are plotted against the maximum current in the ramp (at left) and against the rate at which the voltage rises from rest to the foot of the action potential (at right); (Ferragamo and Oertel, 2002). The vertical jump in these curves shows the threshold for action potential initiation. Note the thresholds are independent of the final level of currents but are a consistent function of the rate of rise of voltage. [Taken from the sources listed with permission.]

mechanism makes octopus cells sensitive to the rate of rise, or the time derivative, of their inputs. Figure 4.13C shows intracellular potentials produced by depolarizing ramps with a rise time, rt , of 1 msec. As the ramp increased in amplitude, action potentials were eventually produced. The threshold for generation of action potentials depended on the rate of rise of the depolarization, not its amplitude; Fig. 4.13D shows that

input/output functions for the cell superimpose when the input is plotted as dV/dt (right) but not when it is plotted as the amplitude of the ramp (left). Because the rate of rise of synaptic responses depends on the synchronicity of the activation of ANF inputs, the intrinsic electrical properties of octopus cells enable them to respond to synchronized activation and to fail to respond if the activation is too asynchronous.

D-multipolar neurons also respond to the onset of sounds but have not been characterized as well as octopus cells. Like octopus cells, D-multipolars receive innervation by many ANFs on their somata and on dendrites that spread across the tonotopic axis (Smith and Rhode, 1989; Oertel et al., 1990; Doucet and Ryugo, 1997), and both are broadly tuned (Jiang et al., 1996). D-multipolars also respond with a precisely timed onset spike to tones (as in Fig. 4.13A) but differ from octopus cells in that they give some steady discharge after the onset spike (Smith and Rhode, 1989; Rhode and Greenberg, 1994a; Paolini and Clark, 1999). Unlike octopus cells, the firing pattern in response to tones is shaped by inhibition along with the intrinsic electrical properties (Paolini and Clark, 1999).

PYRAMIDAL AND CARTWHEEL CELLS

Pyramidal neurons in the DCN show *pauser* and *buildup* responses to sound (Fig. 4.14A; Godfrey et al., 1975b; Rhode et al., 1983b). The examples shown in Fig. 4.14A are typical of anesthetized animals, where the inhibitory circuits of the DCN are weakened. The response shows a poorly timed, long latency onset spike followed by a prominent pause (Fig. 4.14A1) or a slow buildup in response with a long latency (Fig. 4.14A2). The membrane properties of pyramidal cells include the typical complement of potassium, calcium, and sodium channels (Hirsch and Oertel, 1988; Manis, 1990; Kanold and Manis, 1999; Molitor and Manis, 1999). The pauser and buildup characteristics seem to derive from a transient potassium conductance. Figure 4.11B shows intracellular responses to depolarizing currents in cells that were held hyperpolarized between depolarizing current pulses; the dotted lines in the current waveforms show the holding current necessary to place the cell at its resting potential. Depolarization following hyperpolarization produced a pauser response (Fig. 4.14B1) or a buildup response (Fig. 4.14B2), depending on the strength of the depolarizing current. If the cell was not hyperpolarized between depolarizations, the pause did not occur and the cell gave a simple tonic response, similar to Fig. 4.11B. The pause is produced by activation of a transient potassium conductance that is normally inactivated at rest. If the cell is hyperpolarized, inactivation is removed, so that the transient conductance can be activated by a subsequent depolarization (Manis, 1990; Kanold and Manis, 1999, 2001). *In vivo* a hyperpolarization that is sufficient to remove the inactivation is observed as an aftereffect of a strong response to an acoustic stimulus (Rhode et al., 1983b) or from inhibitory synaptic inputs. Properties of the transient potassium current are reviewed in Chap. 2.

Figure 4.14C shows responses to sound of cartwheel cells. Cartwheel cells are the only cells in the cochlear nucleus with complex action potentials, which reflect a combined calcium and sodium spike (Fig. 4.14D; Zhang and Oertel, 1993a; Manis et al., 1994; Golding and Oertel, 1997). Many cartwheel cells respond weakly to sound (Fig. 4.14C1), whereas others give robust responses more like those of other cochlear nucleus cells (Fig. 4.14C2; Parham and Kim, 1995; Davis and Young, 1997). No partic-

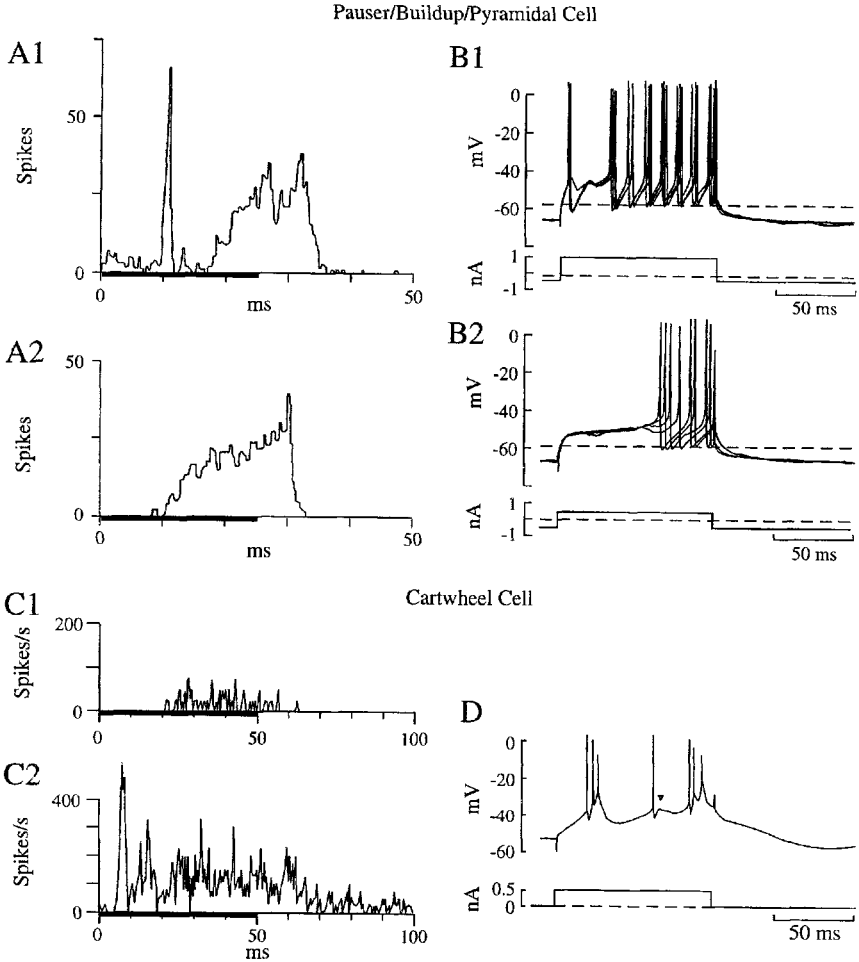


Fig. 4.14. PSTHs of responses to tones at BF (left column) and responses to intracellular current (right column) for two DCN cell types. Response types and the cells from which they are typically recorded are as follows. **A:** Pauser (A1) and build-up (A2) responses from pyramidal cells (Godfrey et al., 1975b). The ordinates of these PSTHs are scaled as spike counts and not as discharge rate. **B:** Responses to current of a pyramidal cell; hyperpolarizing current was used to hold the cell below its resting potential (dashed line is the holding current for the resting potential) to de-inactivate transient K^+ channels (Manis, 1990). **C:** Examples of weak (C1) and strong (C2) acoustic responses of cartwheel cells (Parham and Kim, 1995). **D:** Mixed complex and simple (triangle) spikes from a cartwheel cell (Manis et al., 1994). [Redrawn from the sources indicated with permission.]

ular pattern of response is consistently observed in PSTHs of cartwheel cell responses. The excitatory inputs to cartwheel cells are through granule cells as discussed earlier (Fig. 4.10). Responses to sound of DCN neurons do not change significantly in animals with a congenital absence of cartwheel cells (Parham et al., 2000), suggesting that these cells generally convey mainly nonauditory information to the principal cells of the DCN.

MODELS OF SOMATIC AND DENDRITIC PROPERTIES

As data on the membrane properties of cochlear nucleus neurons have accumulated, it has become possible to use models to explore the different behaviors described in the previous section. These models are based on the gating of ion channels. Such models make explicit the qualitative hypotheses discussed earlier and provide rigorous quantitative tests of them. For example, the slope sensitivity of octopus cells can be accounted for by gating of the low-threshold potassium conductance (Cai et al., 2000), and the pausing behavior of DCN pyramidal neurons can be accounted for by transient potassium channels (Kim et al., 1994; Hewitt and Meddis, 1995; Kanold and Manis, 2001). In the following, two early models of T-multipolar and bushy cells are described to show how patterns of activation can be affected by the channels present in a membrane.

CHOPPER NEURONS

The transformation in firing pattern that is observed between ANFs and chopper neurons is primarily a change from the irregular discharge of ANFs to regular firing in choppers. Computational models show that the transformation is a property of the action potential generation mechanism itself (Arle and Kim, 1991; Banks and Sachs, 1991; Hewitt and Meddis, 1993).

Figure 4.15A shows the structure of a simple neuronal model consisting of a soma and an axon containing voltage-gated sodium and potassium channels, with characteristics like those in the squid axon, connected to a dendritic tree model (Banks and Sachs, 1991). Auditory-nerve inputs are applied to the model through the excitatory conductances g_E . The model ANF spike trains are irregular and accurately duplicate the statistical features of real auditory-nerve spike trains. Figure 4.15B shows the excitatory synaptic conductance of the model (below) and the resulting spike train (above). In this model, there is little correspondence between the time of arrival of auditory-nerve spikes, as judged by the EPSPs, and the postsynaptic spikes. There is, of course, an EPSP preceding each output spike, but the basic pattern of the output is determined by the tendency of the neuron to fire regularly, and not by the time of occurrence of input spikes. Figure 4.15C is a PSTH of the model's output, showing the chopper pattern. Note the correspondence of spike times in Fig. 4.15B and peaks in the PSTH in Fig. 4.15C. Regular firing, or chopping, is thus a property of the voltage-sensitive conductances summarized in the Hodgkin-Huxley membrane model. Real multipolar cells have additional conductances that modulate the cells' behavior, but the basic result shown here does not change (Rothman, 1999).

PRIMARYLIKE NEURONS

Figure 4.15D shows a membrane model for a bushy cell (Rothman et al., 1993). Because the synaptic input to bushy cells is on the soma, the model consists of only one somatic compartment, containing the same conductances as in the multipolar cell model plus a low-threshold voltage-dependent potassium conductance, g_M . This conductance is activated at and just above the resting potential and gives the model electrophysiological characteristics similar to those of real bushy cells (see Fig. 4.11D). As the number and strength of independent auditory-nerve inputs are varied, the model accurately duplicates bushy cell PSTHs, producing primarylike responses (Fig. 4.11C1) if supplied

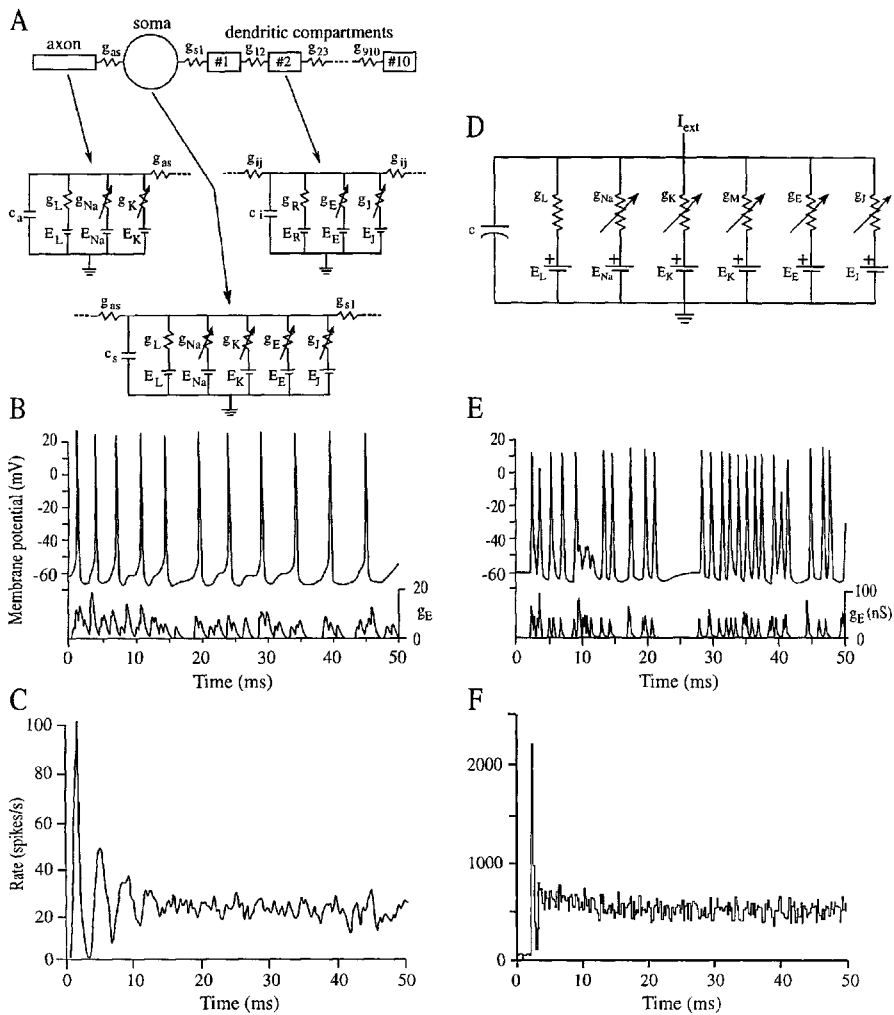


Fig. 4.15. Computational models used to study the input/output transformations in multipolar and bushy neurons. **A**: The multipolar neuron is broken into 12 compartments (Banks and Sachs, 1991). The axon and soma are each one compartment, containing a capacitance c_i , a leak conductance g_L , and voltage-dependent sodium g_{Na} and potassium g_K channels. The dendritic tree is collapsed into a single equivalent cylinder of 10 compartments, each containing a capacitance c_i , a resting conductance g_R , and excitatory g_E and inhibitory g_I synaptic conductances. The soma also contains excitatory and inhibitory synaptic conductances. **B**: Somatic membrane potential (above) and synaptic conductance (below) for the multipolar-cell model with eight independent subthreshold excitatory inputs to the second dendritic compartment. **C**: PSTH of the model responses for the same input as in **B**. **D**: The bushy cell is modeled as a single somatic compartment containing capacitance c , leak conductance g_L , voltage-gated sodium g_{Na} and potassium g_K, g_M channels, and inhibitory g_I and excitatory g_E synaptic channels (Rothman et al., 1993). **E** and **F**: Membrane potential, synaptic conductances, and PSTHs for the bushy-cell model with five independent suprathreshold excitatory inputs. In both models, ANF-like spike trains drive the excitatory conductances; each spike arrival produces a transient alpha-wave conductance change $A(t/t_p) \exp[-(t_p - t)/t_p]$, where $t_p = 0.1$ (bushy) or 0.25 (multipolar) ms. [Redrawn from the sources listed with permission.]

with only one or two large (suprathreshold) auditory-nerve inputs and pri-N responses (Fig. 4.11C2) if supplied with more inputs (e.g., Fig. 4.15F, with five suprathreshold inputs). The model's spike trains are as irregular as those of ANFs and real bushy cells, if supplied with suprathreshold inputs. The difference in input/output behavior between multipolar and bushy cells can be appreciated by comparing Figs. 4.15B and 4.15E. In contrast with the multipolar model, the bushy model shows a good temporal register of EPSPs and postsynaptic spikes. This correspondence results mainly from the lack of temporal summation of inputs (Fig. 4.12) caused by the low-threshold potassium conductance.

The model in Fig. 4.15D accounts for the properties of SBCs and for some properties of GBCs. However, there are problems in trying to account for all the properties of GBCs. One issue is that GBCs receive a large number of ANF inputs, up to 50 (Liberman, 1991; Ostapoff and Morest, 1991). Not only do these inputs vary in strength, but their firing may be strongly correlated because they presumably receive input from the same or from neighboring hair cells. Most of these inputs probably come from ANFs with significant spontaneous discharge. Because the inputs have to be suprathreshold to produce an irregular output, the result of applying a large number of spontaneously active inputs to the bushy cell model is to give the model substantial spontaneous activity. However, pri-N neurons frequently have low or no spontaneous activity (Blackburn and Sachs, 1989; Spirou et al., 1990). In addition, there are problems accounting for all aspects of the phase-locking behavior of pri-N neurons (phase locking is explained later in Fig. 4.16). The details of this issue are beyond the scope of this chapter and are discussed elsewhere (Joris et al., 1994b; Rothman and Young, 1996). Inhibitory inputs to GBCs, which are not present in the model, could account for some of the differences.

CIRCUIT FUNCTIONS

We have seen that each neuron type of the cochlear nucleus has specific structural and functional properties that, together with its distinctive synaptic connections, enable it to respond in a specific way to auditory stimuli. We are now in a position to assess how the multiple features of the auditory stimulus are encoded by the parallel processing lines of the cochlear nucleus. It is the simultaneous extraction of these multiple features that permits the auditory system to be able to localize sound sources, whether the source is prey or predator or a person to whom one speaks, to interpret the meaning of sounds and, in humans, to understand language and appreciate song and instrumental music.

PHASE-LOCKING IN BUSHY CELLS AND SOUND LOCALIZATION IN THE HORIZONTAL PLANE

The computation of the location of a sound source in the horizontal plane begins in the superior olivary nuclei (see Fig. 4.3B), where neurons compare the time of arrival (MSO; Goldberg and Brown, 1969) and the relative loudness (LSO; Boudreau and Tsuchitani, 1970) of the stimuli in the two ears. Such comparisons are useful because a sound originating on, say, the left will reach the left ear before it reaches the right ear and will be louder in the left ear (Yin, 2002). The inputs to the MSO and LSO are from the bushy cells of the VCN. In the following paragraphs, the anatomical and mem-

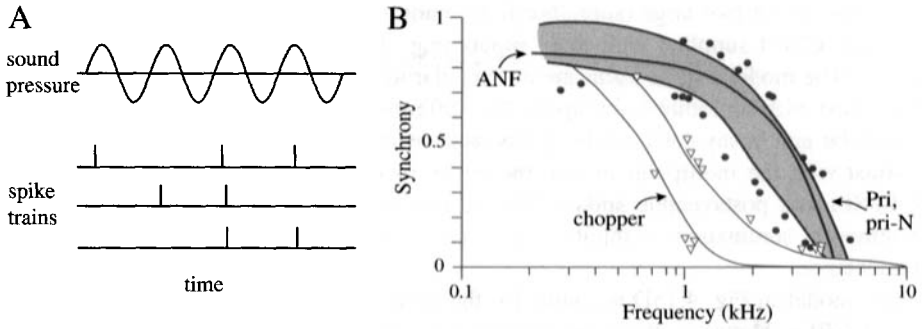


Fig. 4.16. Phase-locking in ANFs and VCN units. **A:** Top line shows the waveform of a tone as the sound pressure at the eardrum. The next three lines show how three hypothetical neurons might respond to the tone. *Phase-locking* is the tendency of spikes to occur at a particular point during the stimulus cycle, in this case near the positive peak. Note that each neuron does not necessarily produce a spike in every stimulus cycle. **B:** Plot of the strength of phase-locking versus tone frequency for ANFs (line; Johnson, 1980), primarylike and pri-N neurons (shaded region), and choppers (unfilled region; Blackburn and Sachs, 1989). Data points show the outliers from the cochlear nucleus populations. Phase locking is measured as synchrony which varies from 0 (random spike patterns with no phase locking) to 1 (perfect locking, spikes all occur at the same point in the cycle). [Redrawn from Blackburn and Sachs, 1989 with permission.]

brane specializations of bushy cells are interpreted as necessary to support interaural time difference analysis in the MSO.

Interaural time differences are best encoded by phase locking to low frequency sounds because interaural time is encoded with every cycle of a sound. The means by which temporal information about the stimulus is encoded is shown in Figure 4.16A. This figure shows the spike trains of three neurons responding to a low-frequency tone; the responses are *phase locked* to the stimulus, in that spikes occur near a particular preferred portion of the stimulus waveform. Figure 4.16B shows that phase locking occurs in cat ANFs (line) for frequencies up to ≈ 5 kHz (Johnson, 1980). The shaded region shows that the phase-locking ability of primarylike and pri-N neurons (bushy cells) is similar to that of ANFs (Blackburn and Sachs, 1989; Joris et al., 1994a). Bushy cells actually display enhanced phase locking at low frequencies, below 1 kHz, where they may be entrained precisely to the stimulus waveform (Joris et al., 1994a,b). By contrast, the phase locking of chopper neurons (T-multipolars) is much weaker, essentially disappearing by 2 kHz.

The differences between primarylike and chopper neurons derive from their membrane properties. Because of membrane capacitance, the postsynaptic processing of all neurons tends to be low pass; i.e., fast fluctuations in the synaptic inputs are filtered out. In T-multipolars, where the inputs are on the dendritic tree, there is an additional component of low-pass filtering due to the dendrites (White et al., 1994). As a result, frequencies in the input above a few hundred Hertz are severely attenuated. By contrast, in bushy cells postsynaptic filtering is minimized by placing the synapses on the soma, by making the postsynaptic currents large so as to quickly charge the membrane capacitance, and by minimizing temporal integration of inputs, as described in Fig. 4.12. The tendency of bushy cells to follow the temporal patterns of their inputs, as

opposed to T-multipolar cells is also apparent in the model results in Figs. 4.15B and 4.15E.

A particularly strong cue for sound localization is the interaural delay in the *waveform* of the stimulus. In fact, perceptual experiments show that the strongest cue for localization of sound in azimuth is the interaural delay at frequencies below 1 kHz (Wightman and Kistler, 1992). If the waveform of a stimulus like the tone in Fig. 4.16A is delayed in one ear, the ANF spikes that are phase locked to the tone will be delayed by the same amount. In other words, an interaural time delay produces a change in the relative phase-locking point in the two ears. Thus MSO neurons can compare the time of arrival of the stimulus waveforms in the two ears by comparing the time of arrival of phase-locked spike trains from the two cochlear nuclei. MSO neurons accomplish this comparison by functioning as coincidence detectors (Goldberg and Brown, 1969), meaning that they respond when they receive coincident spikes from their bushy cell inputs on the two sides. Coincidence detection is possible in MSO cells only because they share the short membrane time constant and the low threshold potassium channel described earlier for bushy cells (Smith, 1995). Inhibitory inputs from the MnTB and LnTB serve to sharpen the coincidence detection (Brand et al., 2002). Thus the membrane specializations of both bushy and MSO cells allow precision in the timing of firing that is necessary for binaural comparison of interaural time difference.

STIMULUS SPECTRUM REPRESENTATION IN CHOPPER NEURONS

In addition to localizing a sound, it is important to identify it and to extract its meaning. The auditory system identifies sounds based on their frequency content and their temporal fluctuations. An illustration of the importance of frequency content, or *spectrum*, is provided by the vowels of human speech. Figure 4.17A shows the frequency content of the vowel EH, as in “met.” There are prominent peaks of energy at 512, 1792, and 2432 Hz (arrows); these peaks are called *formants* and correspond to the resonant frequencies of the vocal tract. Each vowel is characterized by a different combination of formant frequencies (Peterson and Barney, 1952), and our perceptual recognition of different speech sounds is closely tied to the frequencies of their first three formants (Remez et al., 1981).

Because of the importance of the frequency content of sounds for their perception, it is natural to consider the neural representation of sounds in terms of a plot of neural response versus BF (Pfeiffer and Kim, 1975; Sachs and Young, 1979). That is, we consider the representation of a sound in terms of the tonotopic map established in the cochlea (see Fig. 4.1), where each ANF represents the energy in the stimulus at frequencies near its BF. Figures 4.17B–E compare the tonotopic representation of the frequency spectrum of the EH for two subpopulations of ANFs and for chopper neurons (Blackburn and Sachs, 1990); the chopper neurons appear to derive a stable representation of the stimulus spectrum at all sound levels from the more variable ANF representation.

The plots in Figs 4.17B–E show discharge rate versus BF; these plots were constructed by recording the responses of several hundred neurons to the vowel, plotting each neuron’s discharge rate at an abscissa position equal to its BF, and then averaging the data using a moving window filter (Blackburn and Sachs, 1990). The lines show the average values. Response profiles are shown for three populations of neurons:

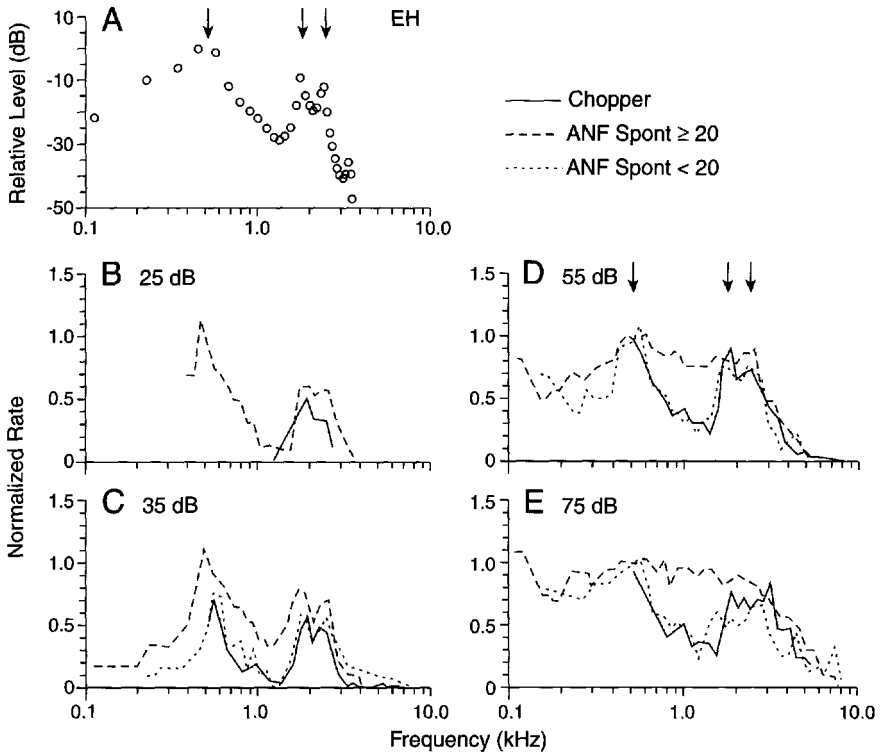


Fig. 4.17. Frequency content of a vowel-like sound and its neural representation in populations of ANFs and chopper units (Blackburn and Sachs, 1990). **A**: Distribution of energy across frequency for a synthetic version of the vowel EH, as in “met”; the points show the amplitudes of a series of tones of different frequencies that are added together to make the vowel. The energy peaks (arrows) are the formants. **B–E**: Responses of populations of ANFs and chopper units to the vowel at four sound levels, ranging from very soft (25 dB, **B**) to conversational levels (75 dB, **E**). Response is plotted as normalized rate that varies from 0 (spontaneous rate) to 1 (maximal or saturated rate). The abscissa shows the BFs of the neurons. The lines represent averages of the responses of neurons of similar BFs, computed from populations of several hundred neurons. The three line types correspond to three neural populations, as given in the legend. ANFs are separated into two groups that differ in their spontaneous firing rates. Lines are plotted only over the frequency range where significant numbers of neurons of each type were studied. For technical reasons, few chopper neurons with low BFs were studied, so those data are missing. The chopper data are from a subgroup of the chopper population, called chop-T, but are typical of all choppers. [Redrawn from Blackburn and Sachs, 1990, with permission.]

(1) ANFs with spontaneous rates of less than 20/sec (dotted), (2) fibers with spontaneous rates above 20/sec (dashed), and (3) cochlear-nucleus choppers (solid). The two populations of ANFs are separated because they have different dynamic ranges. High spontaneous rate fibers have low thresholds but have limited dynamic ranges, so these fibers provide rate information mainly at low sound levels. At the lowest sound level (25 dB; Fig. 4.17B), the dashed-line rate profile provides a good representation of the vowel in that there are peaks of discharge rate among fibers with BFs equal to the formant frequencies. As the sound level increases, this representation is lost as high spon-

taneous rate fibers of all BFs approach their maximal discharge rates (Fig. 4.17D,E), meaning normalized rates near 1. Note that 75 dB is conversational sound level; i.e., we comfortably communicate using speech at ≈ 75 dB.

Low spontaneous rate fibers, by contrast, have higher thresholds and wider dynamic ranges. At the lowest level (25 dB; Fig. 4.17B) there is no response from the low spontaneous rate fibers, because the stimulus is below threshold. As stimulus level increases, a good rate representation is provided (dotted line), which is maintained to the highest level shown; there are clearly defined peaks of response near the first and the second/third formant peaks (arrows) with a minimum of response in between.

The solid lines in Fig. 4.17 show responses of chopper neurons to the same stimulus. Note that the choppers maintain a representation that is at least as good as that of the better ANF group; there is a clear peak at BFs equal to the formants at all sound levels (Blackburn and Sachs, 1990; May et al., 1998). This behavior could be explained at high levels if T-multipolar cells receive inputs predominantly from low spontaneous rate ANFs. However choppers also respond at low sound levels (Fig. 4.17B) and therefore must receive inputs from high spontaneous rate fibers (Bourk, 1976; Sachs et al., 1993). This raises the question of how choppers avoid saturation of their discharge rates by their high spontaneous rate inputs. It is likely that inhibitory inputs play a role (Blackburn and Sachs, 1992; Caspary et al., 1994; Rhode and Greenberg, 1994b; Palmer et al., 1996). Known sources of inhibition on T-multipolars include D-multipolar and vertical cells in the cochlear nucleus (see Fig. 4.10; Wickesberg and Oertel, 1990; Ferragamo et al., 1998a) as well as neurons in the superior olive (Ostapoff et al., 1997). These inhibitory inputs have diverse responses to sound. Particularly interesting with respect to responses to speech are the D-multipolars, which respond strongly to broadband stimuli like speech (Winter and Palmer, 1995). From Fig. 4.10, it is clear that the D- and T-multipolars form a network in which T-multipolars receive both excitatory and inhibitory recurrent inputs, as well as ANF inputs. Such networks can perform several types of computations, including a winner-take-all computation in which the strongest input dominates, reducing other inputs to zero (Shamma, 1998; Wilson, 1999). In the case of the T-multipolars, the response peak among low spontaneous rate ANFs with BFs near a formant peak could suppress the saturated inputs from high spontaneous rate units, giving the robust chopper representation. Another possibility is that T-multipolars arrange the low and high spontaneous rate inputs on their dendritic trees in such a way that they can switch from one input to the other (Lai et al., 1994). This sort of switching is based on theoretical calculations showing that inhibitory inputs can cancel excitatory inputs located more distally on a dendritic tree (Koch et al., 1983). Thus high spontaneous rate inputs located distally on the tree could be cancelled by inhibitory inputs (from D-multipolars) at high levels to allow the neuron to respond to low spontaneous rate inputs located proximally. The dynamic range of T-multipolars might also be extended by cholinergic modulation. Cholinergic inputs from olivocochlear efferent neurons reduce the sensitivity of the cochlea in the presence of loud sounds, reducing saturation (Guinan, 1996). They also excite T-multipolar cells but do not affect D-multipolar cells (Fujino and Oertel, 2001). The cholinergic efferents would thus be expected differentially to boost excitation of those chopper neurons that encode the formants, boosting the encoding of spectral peaks more than other excitation, and to increase the balance of excitation over inhibition.

In addition to the frequency information discussed in Fig. 4.17, natural auditory stimuli also contain information in their temporal structure. An example of temporal structure is the fluctuation in sound amplitude corresponding to the sequence of syllables in an utterance. In experiments in which the information encoded in the frequency content of the sound (like Fig. 4.17A) is removed, leaving only the temporal structure, listeners can make many basic speech discriminations (Van Tasell et al., 1987). Indeed the cochlear implant, an auditory prosthesis for the deaf in which the ANFs are directly stimulated electrically, conveys much of its information via the temporal structure of the stimulation (Shannon et al., 1995). Cochlear nucleus neurons are sensitive to temporal fluctuations like those in speech and generally sharpen the representation of temporal information, i.e. give enhanced responses, compared with ANFs, to increases or decreases in stimulus amplitude (Wang and Sachs, 1994; Delgutte et al., 1998; Frisina, 2001). Onset neurons show the largest enhancement, followed by choppers and then primarylike neurons.

The representation of temporal and spectral information encoded in onset and chopper neurons allows the identity of sounds to be determined—one speech sound versus another, for example. This information complements the information about sound source location provided by the bushy cell–superior olive pathway. Thus we begin to see how aspects of the acoustic environment are separated out at the brainstem level and selectively processed and represented. It is important to point out, however, that the separation is not complete. Information about the stimulus frequency spectrum is also encoded in the bushy cell pathway, and information about sound localization is encoded in the chopper pathway.

FEATURE DETECTION IN DORSAL COCHLEAR NUCLEUS

As discussed earlier, principal cells of the DCN integrate two systems of inputs (see Fig. 4.10): ANFs and related inhibitory inputs and parallel fibers and their associated inhibitory circuits. The former carry mainly auditory information, but the latter carry a mixture of auditory and nonauditory information. In contrast to the VCN, where effects of inhibition are relatively weak, DCN neurons in unanesthetized animals receive strong inhibition from both sets of inputs. In the DCN, spectrally complex sounds evoke a summation of excitation and inhibition that enables neurons to detect spectral features, which are often the information-bearing elements of sounds (Nelken and Young, 1996; Parsons et al., 2001).

Figure 4.18B shows a tone response map typical of what are almost certainly pyramidal cells (so-called type IV units) in unanesthetized animals (Evans and Nelson, 1973; Young and Brownell, 1976). The map shows discharge rate as a function of frequency and sound level. Two inhibitory areas (gray) are consistently observed in such maps—one located at and below BF (≈ 13 – 20 kHz in this case) and a second above BF (>22 kHz here; Spirou and Young, 1991). Excitatory areas are seen at low sound levels at BF (≈ 18 kHz) and usually, but not always, between the two inhibitory areas (≈ 21 kHz here) and at low frequencies (<10 kHz). In gerbil DCN, response maps are similar but inhibition is weaker (Davis et al., 1996b; Davis and Voigt, 1997).

Figure 4.18D schematically shows how the excitatory and inhibitory areas in type IV response maps could arise from what is known about the connections and the responses to sounds of interneurons (Spirou and Young, 1991; Davis and Young, 2000).

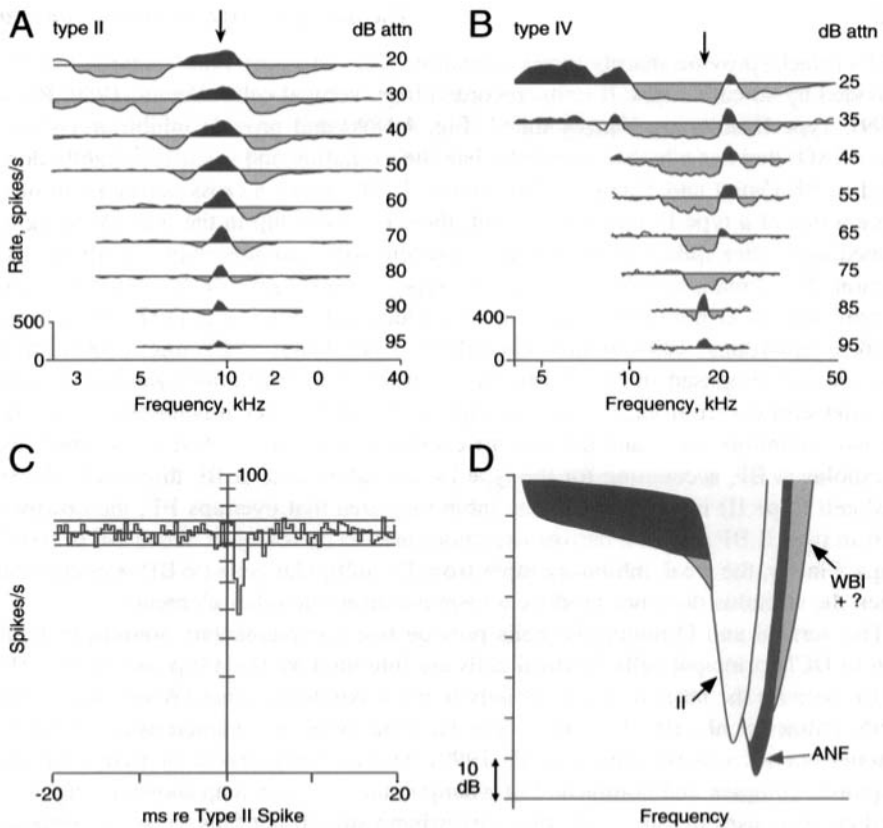


Fig. 4.18. Response maps of type II (probably vertical) and type IV (probably pyramidal) neurons in DCN. **A:** Type II response map showing excitatory and inhibitory areas as a function of frequency and sound level of a tone stimulus. Each trace shows discharge rate of the neuron versus tone frequency at a fixed sound level, given at right. Sound levels become louder from bottom to top. Because the type II neuron had no spontaneous activity, a BF tone slightly above threshold was presented along with the test tones to generate the background activity necessary to reveal inhibition. The straight horizontal lines are the background rate, i.e., the rate in response to the background tone alone. The rate scale is given at the bottom left. Excitatory responses are increases in rate above background, black area; inhibitory regions are decreases in rate below background, shaded area. The arrow at top points to BF. Type II responses are recorded from vertical cell interneurons (Young, 1980; Rhode, 1999). **B:** Response map for a type IV neuron. No background tone was presented; the horizontal lines are the neuron's spontaneous discharge rate. BF tones are excitatory at low sound levels but inhibitory at higher levels; the arrow at the top points to BF. Type IV responses are recorded from DCN principal cells, both pyramidal and giant cells (Young, 1980). **C:** Cross-correlogram of the spike trains of a type II and a type IV neuron (Young and Voigt, 1981). The plot shows the average discharge rate of the type IV neuron relative to spikes in the type II neuron. Note the *inhibitory trough* just to the right of the origin; this dip in the type IV rate following type II spikes suggests that these neurons are connected by a monosynaptic inhibitory synapse. The horizontal lines show the range of type IV rates (± 2 S.D.) if the neurons were not connected. **D:** Schematic to explain the shape of the response map of type IV neurons in terms of excitatory ANF (black), inhibitory type II (white), and WBI plus unknown other (gray) response maps. Response maps are superimposed in order of the strength of synapses, weakest in the back, strongest in front. Estimates of synaptic strength are based on cross-correlation analysis (Voigt and Young, 1990), analysis of responses to sound (Nelken and Young, 1994), and the effects of inhibitory antagonists (Davis and Young, 2000). Two type II maps are placed side by side, because the bandwidth of the type IV inhibitory area is wider than the excitatory area of type II units. [Reproduced with permission from Young and Voigt, 1981; Young and Davis, 2002.]

ANFs (black) provide sharply tuned excitation. The inhibitory input centered on BF is provided by so-called type II units, recorded from vertical cells (Young, 1980; Rhode, 1999). Type II units are sharply tuned (Fig. 4.18A) and provide inhibition (white in Fig. 4.18D) that has a higher threshold than the excitation and is shifted slightly downward in BF (Voigt and Young, 1990). Figure 4.18C shows a cross-correlogram of the spike trains of a type II and type IV unit; there is a brief dip in the type IV firing rate immediately after spikes in the type II, consistent with a monosynaptic inhibitory connection. The remaining inhibitory input to type IV units (gray, *WBI+?* in Fig. 4.18D) is provided by D-multipolar cells and an additional, unknown, GABAergic source (Nelken and Young, 1994; Winter and Palmer, 1995; Davis and Young, 2000). The inputs are superimposed in Fig. 4.18D in the order of their relative synaptic strengths, with the strongest in front. Comparing Figs. 4.18B and 4.18D, it is possible to see how the two inhibitory areas and the various excitatory areas arise. ANFs have the lowest thresholds at BF, accounting for the type IV excitatory area at BF threshold. The vertical cell (type II) input produces the inhibitory area that overlaps BF; the downward shift in type II BF allows a narrow excitatory area to be seen just above BF in type IV maps. Finally, the weak inhibitory input from D-multipolar cells (*WBI*) is evident only when the stimulus does not produce a response from the other elements.

The vertical and D-multipolar cells provide two complementary sources of inhibition to DCN principal cells. Vertical cells are inhibited by D-multipolar neurons (Fig. 4.10); because the latter respond strongly to noise but not to tones (Winter and Palmer, 1995; Palmer et al., 1996), vertical cells have the opposite characteristic, responding to tones but not to noise (Spirou et al., 1999). This circuitry makes the pyramidal cell's responses complex and nonlinear. For example, the response map shown in Fig. 4.18B predicts responses to tones and other narrowband stimuli but fails to predict responses to broadband stimuli like noise (Spirou and Young, 1991; Yu and Young, 2000). For broadband stimuli, the type II inhibitor is itself inhibited, by the D-multipolar, so the large central inhibitory area disappears.

Natural stimuli are mixtures of narrowband and broadband features. Pyramidal cells are inhibited (from their spontaneous rate, averaging $\approx 40/\text{sec}$) by either narrowband peaks in the stimulus' frequency content (as at a formant peak in speech) or notches in the frequency content of a broadband noise (Nelken and Young, 1994). The latter is a stimulus feature produced by the external ear that is used by humans and cats to localize sound sources (Musicant et al., 1990; Middlebrooks, 1992; Huang and May, 1996). Cats appear to process the narrowband notch cue in the DCN, because lesions there specifically degrade performance in vertical sound localization, which depends on the notch cue (May, 2000). Thus, DCN principal cells seem to signal "interesting" features in the stimulus spectrum by being inhibited where such features lie near BF.

The second set of inputs to DCN principal cells, from granule cells and their associated inhibitory interneurons, conveys multimodal sensory information. Auditory responses are weak in cartwheel cells (Parham and Kim, 1995; Davis and Young, 1997), which probably reflects a generally weak acoustic response in the granule cell system. However granule cells strongly excite and, through cartwheel cells, inhibit pyramidal cells when the superficial DCN circuitry is activated from the somatosensory spinal nuclei (Davis et al., 1996a; Kanold and Young, 2001). The somatosensory input comes predominantly from the muscles connected to the pinna in cat. This fact raises a num-

ber of interesting possibilities because of the importance of pinna movements for hearing (or analogously head movements in animals that do not have mobile pinnae). One possibility is that the DCN is involved in coordinating motor and sensory information in sound localization (May, 2000; Young and Davis, 2001).

The similarity of the granule cell circuitry in DCN to that in the cerebellum (Mugnaini and Morgan, 1987) and similar structures in electric fish (Montgomery et al., 1995; Bell, 2002) suggests that the DCN might be performing a role similar to one kind of cerebellar learning (Medina et al., 2000). A wide range of information about movements of the pinna, turning of the head, and movement of the body, which can make noise or cause changes in the environmental sounds reaching the ear, is represented in the parallel fiber array. Synaptic plasticity in the apical dendrites of the cartwheel and pyramidal cells (see Fig. 4.9) could then be used to learn associations between sound and the information present on the parallel fibers. In electric fish, a system like this is used to subtract off self-generated electric fields (Bell et al., 1997). In the auditory system, such information could be important in interpreting self-generated acoustic changes and the DCN could be used to discover when such changes are expected.

This page intentionally left blank

OLFACTORY BULB

GORDON M. SHEPHERD,
WEI R. CHEN, AND CHARLES A. GREER

The olfactory bulb is an outgrowth of the forebrain, specialized for processing the molecular signals that give rise to the sense of smell. It receives sensory input from the olfactory sensory neurons (Fig. 5.1), and sends its output directly to the olfactory cortex (see Chap. 10). This basic relationship has endured throughout the evolution of nearly all vertebrates.

As a region for experimental analysis, the olfactory bulb is attractive for several reasons. In its position in front of the brain, it is easily accessible. The sensory nerves to the bulb are separated from its output fibers to the brain; this enables input and output to be manipulated separately, whether by electrical stimulation or tracer injection, similar to the situation in the spinal cord (see Chap. 3). Within, the bulb is a distinctly laminated structure, containing sharply differentiated cell types, particularly in terrestrial animals. All of these features facilitate the application of different experimental techniques and the interpretation of results. In addition, there is continual turnover of the sensory neurons and the bulbar interneurons, making the bulb unique among central brain structures and of special interest with regard to neurogenesis and neural transplants in the brain.

During the 1900s, these advantages were put to good use. Work on the olfactory bulb by Ramon y Cajal and the classic histologists in the nineteenth century contributed to the evidence that led to acceptance of the neuron doctrine (reviewed in Shepherd, 1991; Jones, 1994). Modern studies have contributed to the new principles of synaptic organization, as outlined in Chap. 1.

Traditionally, a disadvantage of working on the olfactory bulb has been the limited understanding of the neural basis of the sense of smell. However, advances have led to an emerging consensus on the outlines of the mechanisms whereby information carried in odor molecules is first transduced by the sensory neurons and then processed by olfactory bulb circuits. A full discussion of olfactory transduction lies outside the bounds of this chapter (see Ache, 1994; Breer, 1994; Hildebrand and Shepherd, 1997, for reviews). Studies of the olfactory bulb itself have also become too extensive to review completely here (see Ennis and Shipley, 1997; Nagao et al., 2002). Our focus therefore is on the principles of synaptic organization underlying a critical function of the olfactory system: the ability to discriminate between different odor molecules.

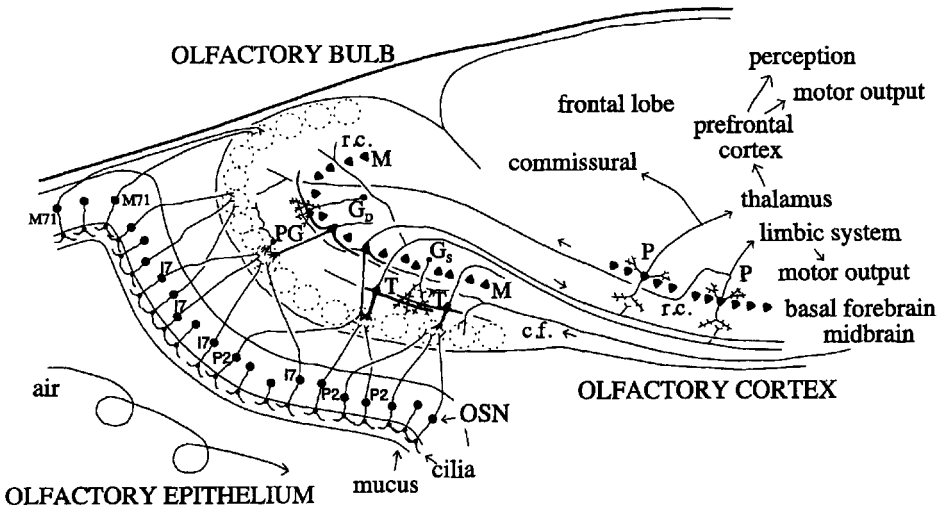


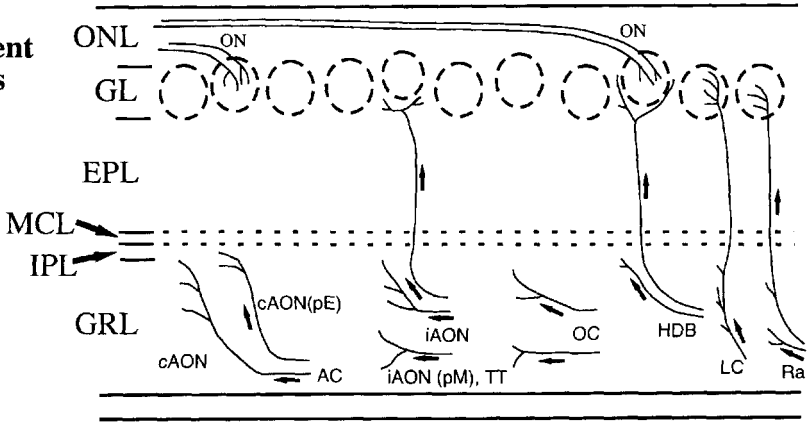
Fig. 5.1. Overview of the olfactory pathway. The olfactory bulb receives input from the olfactory sensory neurons in the olfactory epithelium and projects to the olfactory cortex. The diagram indicates some essential aspects of the projection patterns between the regions, as well as the main neural elements within the olfactory bulb. Note that the olfactory epithelium is arranged in overlapping populations of olfactory sensory neurons (e.g., M71, I7, P2) which project to individual glomeruli. Some of the central olfactory connections to limbic brain structures are also indicated. Abbreviations: c.f., centrifugal fiber; G_D, deep granule cell; G_S, superficial granule cell; M, mitral cell; OSN, olfactory sensory neuron; P, pyramidal cell; PG, periglomerular cell; r.c., recurrent axon collateral; T, tufted cell.

NEURONAL ELEMENTS

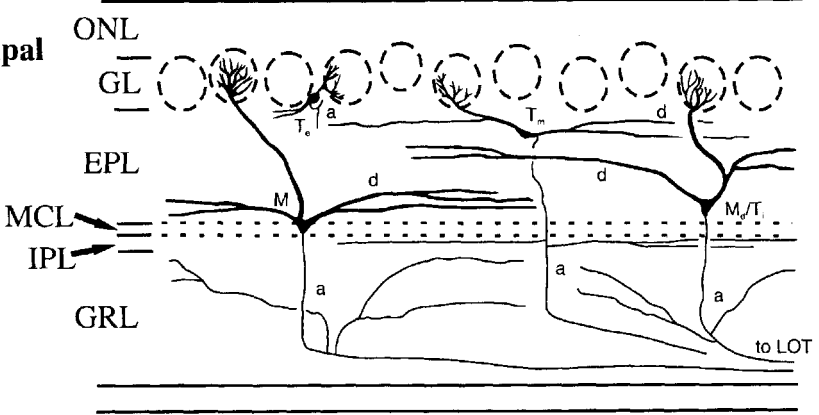
As in other brain regions, the neuronal elements fall into three categories: input, output, and intrinsic. We describe these elements and relate them to their histological layers (Fig. 5.2). Classic descriptions of olfactory bulb neurons were based on Golgi-impregnations (cf. Cajal, 1911); these have been confirmed and extended by contemporary methods, including intracellular staining and genetic engineering (see later).

Fig. 5.2. Neural elements of the mammalian olfactory bulb, grouped according to subdivision into (A) afferent fibers, (B) principal cells, and (C) local interneurons. Diagrams based on various studies using the Golgi method and HRP (see text). Abbreviations for layers: EPL, external plexiform layer; GL, glomerular layer; GRL, granule cell layer; IPL, internal plexiform layer; MCL, mitral cell body layer; ONL, olfactory nerve layer. **A:** ON indicates afferent olfactory nerve fibers. Centrifugal afferents are from the contralateral anterior olfactory nucleus (cAON), ipsilateral anterior olfactory nucleus (iAON), tenia tecta (TT), olfactory cortex (OC), horizontal limb of the diagonal band (HDB), locus coeruleus (LC), and raphe nucleus (Ra). pE, pars externa of the AON; pM, pars medialis of the AON. **B:** The dendrites and axon collaterals of the mitral cell (M), an internal tufted cell (Ti, or displaced mitral cell, Md), a middle tufted cell (Tm), and an external tufted cell (Te), a, axon, d, dendrite; LOT, lateral olfactory tract. **C:** Three types of granule cells (GI, GII, GIII); PG, periglomerular cell; SA(B) Blanes' cell; SA(C), Clandins' cell; SA(G), Golgi cell; SA(H), Hensen's cell; SA(S) Schwann cell; SA(V), van Gehuchten cell. [Modified from Mori, 1987, with permission.]

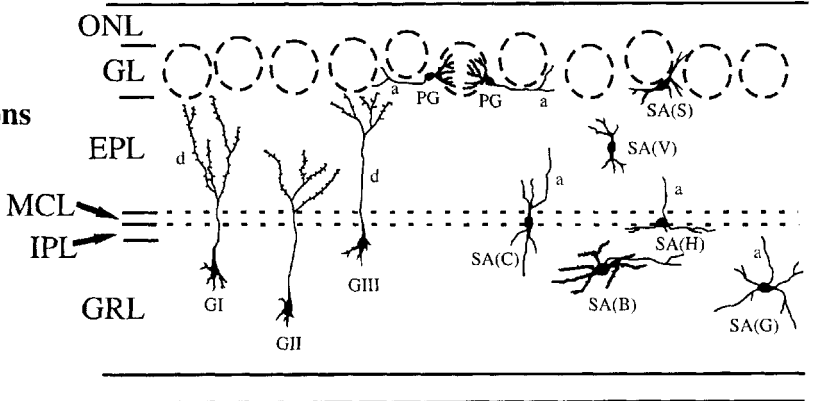
**A.
Afferent
Fibers**



**B.
Principal
Cells**



**C.
Local
Inter-
neurons**



INPUTS

Afferents. The sensory input consists of a complex array of axons from the olfactory sensory neurons that line the neuroepithelium of the nasal cavity. A detailed consideration of the sensory neurons is not possible here (Mombaerts, 2000), but several facts are relevant.

Within the epithelium, olfactory sensory neurons appear generally morphologically homogeneous, with several exceptions (Jourdan, 1975; Moran et al., 1982). The somata of the sensory neurons in the rat average 10 μm in diameter and are distributed in the middle of the epithelium, between the deeper generative basal cells at the basal lamina and the more superficial nuclei of supportive sustentacular cells. A thin apical dendrite extending from the cell body ends in a spherical enlargement, the dendritic knob, at the surface of the epithelium. Thin tapering cilia, up to 200 μm in length in different species, extend from the knob. The sensory neuron axons, averaging 0.2 μm in diameter (range of 0.1–0.4 μm), arise from the basal pole, penetrate the basal lamina, and fasciculate to form bundles that are surrounded by ensheathing mesaxons of a highly specialized glial cell, the olfactory ensheathing cell.

In contrast to the morphological uniformity of the sensory neurons, their molecular phenotype is highly diverse. In rodents, a large multigene family encodes more than 1,000 different olfactory receptors (Buck and Axel, 1991; Zhang and Firestein, 2002). The mechanism, *allelic exclusion*, by which only the maternal or paternal allele expresses a given receptor in a single neuron, is not understood, although it has been useful for studying the role of the odor receptor in axon guidance (see later). Subsets of neurons expressing the same olfactory receptor are distributed in an apparently random pattern mainly within one of several zones across the epithelium, although the precise nature of the distribution remains under study (see Mombaerts, 1999). Because of the large number of different receptors together with other biochemical differences (cell surface antigens, second messenger pathways) the molecular phenotype of the sensory neurons is arguably the most diverse in the nervous system (see later).

The tight packing of axons as they exit the epithelium, pass through the cribriform plate, and form the outermost layer of the olfactory bulb, the olfactory nerve layer, provides an opportunity for ephaptic interactions between axons. Extracellular K^+ extruded during impulse activity or gap junctions between apposed axons may play roles in modulating activity in neighboring axons (Zhang and Restrepo, 2002). Evidence suggesting neurotransmitter-mediated interactions in the nerve layer has also been presented (Ennis et al., 2001).

The Olfactory Glomerulus. The olfactory sensory axons are initially organized in bundles (fascicles) that reflect their point of origin in the epithelium. However, upon reaching the olfactory bulb they defasciculate and begin to reorganize as they target different regions of the bulb (Au et al., 2002; Treloar et al., 2002). The axons terminate in *glomeruli*, spherical regions of neuropil that form the second layer of the bulb. The olfactory glomeruli are among the clearest examples in the brain of the principle of grouping neural elements and synapses into anatomically defined modules. They are analogous to the multineuronal “barrels” and “columns” in cerebral cortex (see Chap. 12), representing a higher level of organization than the synaptic glomeruli of the cerebellum (see Chap. 7) and thalamus (see Chap. 8).

An important advance has been the demonstration that a glomerulus is molecularly homogeneous; all of the sensory axons terminating in a glomerulus express the same olfactory receptor (Mombaerts et al., 1996; Treloar et al., 2002). Homogeneous fasciculation of axons, however, does not appear to be a prerequisite for correct glomerular targeting because single axons routinely approach and target the correct glomerulus. Although several studies have shown that the olfactory receptor itself is necessary for correct glomerular targeting, it seems likely that additional types of molecules will also be implicated as well as functional activity (Mori and Yoshihara, 1995; Mombaerts et al., 1996; Schwarting et al., 2000; St. John et al., 2000). Of the olfactory receptors that have been mapped to the rodent olfactory bulb thus far (<20 of the 1,000), most have two target glomeruli, in the medial and lateral walls of the bulb.

Glomeruli come in different sizes. In fish and amphibians, the glomeruli are small (20–40 μm in diameter) and not distinctly demarcated; in mammals, they are spherical with sharp borders, ranging from 30- to 50- μm diameter in small mammals (e.g., mice) to 100–200 μm in rabbits or cats (cf. Allison, 1953). Microglomeruli have been described (Lipscomb et al., 2002).

The olfactory sensory neuron axons do not branch on their way to the glomeruli, but once inside, they branch on average seven times and make up to 18 *en passant* and terminal bouton appositions (see later) (Halasz and Greer, 1993; Klenoff and Greer, 1998). During embryonic development most axons remain restricted to the nerve layer and do not form glomeruli (Treloar et al., 1999), although a subset do transiently penetrate the deepest layers of the olfactory bulb primordium (Monti-Graziadei et al., 1980; Gong and Shipley, 1995).

A notable feature of the sensory neurons is that they are continuously replaced throughout life from basal cells in the epithelium (Graziadei and Monti-Graziadei, 1979; see Schwob, 2002, for review). Nevertheless, the molecular specificity of the glomeruli and their sensory input appears to be maintained despite the constant turnover and remodeling of the sensory terminals. This degree of plasticity is unique in the brain, although evidence suggests that ongoing neurogenesis among interneurons in the olfactory bulb (see later) as well as dentate granule cells (see Chap. 11) may also reflect a dramatic capacity for rewiring of the brain.

Central Inputs. There are several types of inputs to the olfactory bulb from the brain, each of which has a distinctive laminar pattern of termination (reviewed in Macrides and Davis, 1983; Mori, 1987; Scott and Harrison, 1987; Nickell and Shipley, 1993). One type consists of axon collaterals from pyramidal neurons in the *olfactory cortex* (see Chap. 10); these end mostly in the granule cell layer (see OC in Fig. 5.2A). Extensive connections are made by fibers from different parts of the *anterior olfactory nucleus* (AON); their different laminar projections possibly relate to different populations of granule cells (see later). The nucleus of the *horizontal limb of the diagonal band* (HDB), one of the basal forebrain cholinergic centers, sends fibers to both the granule cell layer and the periglomerular parts of the glomerular layer. From the brainstem, the *locus coeruleus* (LC) and the *raphe nucleus* (Ra) send fibers diffusely to the granule cell layer and specifically to the interiors of the glomeruli (see Fig. 5.2A).

These central inputs are also referred to as *centrifugal* inputs, to indicate their outward orientation from the brain. It is obvious that the olfactory bulb is under extensive

and highly differentiated control by the brain. This is true of many other sensory regions in the brain. The retina (see Chap. 6), by contrast, receives few centrifugal fibers.

PRINCIPAL NEURONS

The output from the olfactory bulb is carried by the axons of mitral and tufted cells (see Fig. 5.2B). The morphology of these cells has been the subject of several studies (Mori et al., 1981a, 1983; Macrides and Schneider, 1982; Kishi et al., 1984; Orona et al., 1984).

Mitral Cells. In fish and amphibia, the principal neurons are relatively undifferentiated. In reptiles, birds, and mammals, however, distinctive mitral cell bodies lie in a thin sheet 200–400 μm deep to the glomerular layer (see Fig. 5.2B). The cell bodies are 15–30 μm in diameter, a medium size for a principal neuron in the brain.

In mammals, each mitral cell tends to give rise to a single *primary* (apical) dendrite, which traverses the external plexiform layer (EPL) and terminates within a glomerulus in a tuft of branches. The tuft has a diameter of 30–150 μm , extending throughout most of its glomerulus. The diameter of the dendrite ranges from 2 to 10 μm (depending on the size of the cell body from which it arises). The length is 200–800 μm , depending on how much it angles across the EPL. Each mitral cell also gives rise to several laterally directed *secondary* (basal) dendrites, which branch sparingly and terminate in the EPL. They are 1–6 μm in diameter, and in mammals extend at least 500 μm to over 1,000 μm . In turtles, horseradish peroxidase (HRP)-injected mitral cells commonly display two thin (1–2 μm) primary dendrites up to 700 μm in length and several thin secondary dendrites that extend over 1 mm and may reach up to halfway around the circumference of the EPL (Mori et al., 1981a).

Subtypes of mitral cells have been identified on the basis of the branching pattern of their secondary dendrites (Macrides and Schneider, 1982; Mori et al., 1983; Orona et al., 1984). As shown in the HRP-stained cells in Fig. 5.2B, type I mitral cells send their secondary dendrites into the deepest region of the EPL, whereas type II (displaced) mitral cells send their secondary dendrites into the middle region of the EPL. These two types form synaptic microcircuits with corresponding subtypes of granule cell interneurons (see later). The field of the secondary dendrites may be “disklike” (Mori, 1987) or oriented in the anteroposterior axis (Shepherd, 1972a).

The primary and secondary dendrites of mitral cells have generally smooth surfaces. They thus are *aspiny* neurons, like motoneurons, but unlike *spiny* principal neurons such as cortical pyramidal cells. The bushy terminal tuft of the primary dendrite, which segregates primary sensory afferents and their associated microcircuits within the glomeruli from the rest of the bulb, is virtually unique among principal neurons and exemplifies the attractiveness of the olfactory bulb as an experimental model.

The mitral cell axons proceed to the depths of the bulb and then pass caudally to gather at the posterolateral surface to form the lateral olfactory tract (LOT). Within the bulb the axons give off *recurrent collaterals*. According to the classic studies (Cajal, 1911), some collaterals recur to terminate in the EPL and some remain in the deep granule cell layer. However, studies of cells visualized by intracellular (Kishi et al., 1984) or extracellular (Orona et al., 1984) injections of HRP show that the collaterals remain within the granule cell layer (GCL) and internal plexiform

layer (IPL) (Kishi et al., 1984; Orona et al., 1984). Age or species differences may account for some of this discrepancy. The collaterals distribute diffusely within the deeper layers.

The output axons in the LOT give off numerous collateral branches that terminate in layer Ia of the olfactory cortex (see Chap. 10). The distances over which they extend are relatively short, up to 10–15 mm. This is similar to the projection distances of some other principal neurons, such as cerebellar Purkinje cells (see Chap. 7) or dentate granule cells (GCs) (see Chap. 11), but contrasts with the extremely long axons of motoneurons (see Chap. 3) and neocortical pyramidal cells (see Chap. 12). Studies using mice engineered to express transsynaptically transported markers suggest that the collateral branches maintain the molecular specificity of the glomeruli (Zou et al., 2001). This suggests that the targeting of axons from the LOT is influenced by the glomerulus in which the mitral cell apical dendrite terminates.

Tufted Cells. Output cells similar to mitral cells but located more superficially in the EPL are called *tufted cells* (see Fig. 5.2B). The subgroups and their nomenclature have become rather complex, but for the present purposes we can identify three main groups according to their laminar position.

The main population, *middle tufted cells* (T_m), lies near the middle of the EPL. These have a cell body diameter of 15–20 μm , several thin basal dendrites (300–600 μm), and a primary dendrite (200–300 μm) ending in a relatively confined tuft of branches in a glomerulus. The axon gives off collaterals that are mostly confined within the IPL and then joins the LOT. Its projection sites in olfactory cortex differ from those of mitral cells (see Chap. 10).

There are also several varieties of *external tufted cells* (T_e), whose dendrites have distinctive branching patterns (see contrasting examples in Fig. 5.2B). All of these give off collaterals in the IPL or adjacent GRL, where they constitute a topographically ordered intrabulbar association system (Schoenfeld et al., 1985) that appears to link glomeruli receiving input from sensory neurons that express the same odor receptor but are located in medial and lateral walls of the olfactory bulb (Belluscio et al., 2002). Some external tufted cells send an axon into the LOT, whereas others do not and thus should be classified as intrinsic neurons (see later).

Finally, some *internal tufted cells* (T_i) overlap in distribution and morphology with outwardly displaced type II mitral cells.

Traditionally, tufted cells were considered to be smaller versions of mitral cells (Allison, 1953). However, Cajal (1911) noted that their axon collateral patterns are different, and it was suggested that this could provide for distinctive types of modulation of GCs (Shepherd, 1972a). Subsequent work has established that mitral and tufted cells have different molecular phenotypes: in the mutant mouse PCD (Purkinje Cell Degeneration), mitral cells degenerate postnatally with no loss of tufted cells (Greer and Shepherd, 1982; Greer, 1987; Bartolomei and Greer, 1998). Moreover, the careful studies of Macrides et al. (1985), Orona et al. (1984), and Mori (1987) have documented the detailed morphology of the different subtypes of mitral and tufted cells. Transmitter differences are noted later. It thus appears that, as in many other regions of the brain, the principal neurons are differentiated into multiple subgroups, on the basis of molecular phenotype, position, dendritic morphology, intrabulbar axonal connections,

extrabulbar projection sites, and neurotransmitters and modulators, thus providing multiple parallel paths for processing the input information.

INTRINSIC NEURONS

The intrinsic neurons are organized in three layers: glomerular, external plexiform, and granule cell. There are two main types of intrinsic neuron in the olfactory bulb: glomerular layer (GL) cells and granule cells (GCs) (see Fig. 5.2C).

Glomerular Layer Cells. Several types of intrinsic neuron are found within or near the glomerular layer.

The main type is the *periglomerular* (PG) cell, whose cell bodies surround the glomeruli. The cell body is only 6–8 μm in diameter, among the smallest of neurons in the brain. As shown by Cajal (1911) and confirmed by modern studies (see Pinching and Powell, 1971a,b; Schneider and Macrides, 1978), each PG cell has a short bushy dendrite that arborizes to an extent of 50–100 μm within a glomerulus; bitufted PG cells, connecting to two glomeruli, are infrequently seen. The dendritic branches intermingle with the terminals of olfactory axons and the dendritic branches of mitral and tufted cells. The PG axon distributes laterally within extraglomerular regions, extending as far as five glomeruli away (Pinching and Powell, 1971a,b). Some PG cells appear to lack axons.

PG cells appear morphologically homogeneous, but biochemical subpopulations containing different neurotransmitters have been identified (see later). Moreover, subpopulations of PG cells have been characterized for their expression of calcium binding proteins (e.g., Toida et al., 2000) that correlates with differences in their synaptic organization (Kosaka et al., 2001). This suggests that the functional roles of PG cells in glomeruli may be quite diverse. The molecular and functional diversity is discussed later.

PG cells are generated predominantly in the postnatal period (Bayer, 1983) and continue to be generated in the adult. Neurogenesis begins in a specialized germinative zone of the anterior horn of the lateral ventricle, and neuroblasts migrate in a specialized tube, the rostral migratory stream (Doetsch et al., 1997). Of interest, the neuroblasts appear to migrate in a chain-like fashion to the ependymal core of the olfactory bulb without supporting radial glia. Radial migration in the olfactory bulb to their final destinations in the glomerular layer has not been fully elucidated but also appears to occur in the adult without radial glia (Chiu and Greer, 1996; Treloar et al. 1999). In the adult, the newly generated PG cells correctly target the glomerular layer, differentiate, and become incorporated into synaptic circuits (e.g., Baker et al., 2001; Rochefort et al., 2002; for review, see Coskum and Luskin, 2002). The functional significance of ongoing genesis of PG cells is not known but may reflect a basic mechanism for rewiring that accommodates learning (e.g., Rochefort et al., 2002).

There are several other types of cell within the glomerular layer that are slightly larger than the classical PG cell. These have been designated short-axon (SA) cells or juxtglomerular (JG) cells. The larger SA cells have axons that reach to glomeruli further away than the smaller classical short-axon PG cells. They are also believed to be glutamatergic, in contrast to PG cells many of which are believed to be GABAergic (see later). JG cells have dendrites that branch in the interglomerular spaces. Another type of GL cell is the external tufted cell, as described earlier.

External Plexiform Layer. The EPL is primarily constituted of the primary and secondary dendrites of mitral and tufted cells, and the cell bodies of tufted cells and displaced mitral cells (see earlier). Traditionally, scattered local interneurons first identified by van Gehuchten are seen (see Fig. 5.2C). A type of intrinsic neuron has been identified that expresses parvalbumin (Toida et al., 2000) and forms dendrodendritic synapses with mitral/tufted cells (see later).

Granule Cell Layer. The granule cell layer is dominated by the GCs and a sparse population of short-axon cells (see Fig. 5.2C).

Within and deep to the mitral cell bodies is a thick layer containing the cell bodies of GCs (GRL in Fig. 5.2). These cell bodies are very small (6–8 μm in diameter); they appeared as grains (hence the term “granule”) to the early microscopists, who applied this term to many types of small cells in the brain. The cell bodies are grouped in horizontal clusters called *islets*.

Each GC gives rise to a superficial process that extends radially toward the surface and ramifies and terminates in the EPL, the branching field extending laterally some 50–200 μm . There are also deep processes that branch sparingly in the granule cell layer. It was noted early that GCs located at different depths would have different functional roles to play in intrabulbar circuits (Shepherd, 1972a). This notion has been greatly amplified by recent studies.

Both intracellular and extracellular HRP injections and Golgi impregnations have shown that there are three main cell types in rodents (see Fig. 5.2C). *Superficial* GCs (type G_{III} of Mori et al., 1983; Orona et al., 1983; Greer, 1987) have peripheral dendrites that ramify mainly in the superficial EPL, among the dendrites of tufted cells. *Deep* GCs (G_{II}) send their dendrites mainly to the deep EPL, among the dendrites of mitral cells. *Intermediate* GCs (G_I) have dendrites that ramify at all levels of the EPL. It thus appears that mitral and tufted cells have both segregated and overlapping microcircuits through GCs (see later, and Macrides et al., 1985). Other subtypes of GCs have been reported on the basis of light and dark staining of the cell bodies by toluidine blue (Struble and Walters, 1982) and localization of neuropeptides (see later).

Like PG cells, GCs are generated predominantly during the postnatal period and continue throughout life. They travel to the olfactory bulb via the rostral migratory stream, where they differentiate and are incorporated into synaptic circuits. As suggested for the PG cells, this continuing neuronal and synaptic remodeling of local circuits indicates that odor processing in the olfactory bulb is likely to be a dynamic process that can adapt to shifting odor environments.

The GC dendrites are notable for bearing numerous spines (also called *gemmules*). In general, the spines are larger but less numerous than spines of dendrites of pyramidal cells in the cerebral cortex. In a developmental study, Greer (1984) found that the density of spines increased from 1 per 10 μm of dendritic branch length at birth to a peak of 2 or 3 at 12 days, settling to an adult value of approximately 2. This is much lower than the spine densities of striatal cells (see Chap. 9) and of pyramidal neurons in the hippocampus (see Chap. 11) and neocortex (see Chap. 12).

The most notable feature of the GC is that it lacks an axon. This was evident in the first studies by Golgi (1885) and has been repeatedly confirmed by the use of Golgi methods, HRP, and EM. The resemblance to amacrine cells in the retina was early rec-

ognized. EM studies have clearly shown that the GC processes are dendrites on the basis of their fine structural features and their close resemblance to cortical dendrites (Price and Powell, 1970a,b). The lack of an axon meant that these cells always stood out as exceptions to the classic "law of dynamic polarization" (Cajal, 1911). This problem was solved by the discovery of the output functions of the dendritic spines of these cells (see Chap. 1 and later).

Deep Short-Axon Cell. It remains to note that a third type of intrinsic neuron, the *short-axon cell*, is represented sparingly in the glomerular layer and more frequently in the granule cell layer. The latter consists of several subtypes (Pinching and Powell, 1971a,b; Schneider and Macrides, 1978), with dendritic trees of varying extent and axons that ramify in the EPL or granule cell layer (see Fig. 5.2C).

CELL POPULATIONS

Olfactory sensory neurons on one side of the nose number approximately 50×10^6 in the rabbit, giving rise to as many axons entering each olfactory bulb. This is a relatively large array of sensory input channels, exceeded only by the photoreceptors in the retina (see Chap. 6). This array converges onto approximately 2,000 glomeruli, to which are connected approximately 50,000 mitral cells and 100,000 tufted cells (see Allison, 1953). The convergence ratios are very high: onto glomeruli, 25,000:1; onto mitral cells, 1,000:1; and onto tufted cells, 500:1. These convergence ratios are now interpreted in terms of the rule that each subset of olfactory sensory neurons expressing 1 of 1,000 receptors projects to two glomeruli (see earlier).

The data are incomplete, and there are inconsistencies (see Royet, 1998), but it appears that most species have fewer numbers of sensory neurons and therefore less axonal convergence. For example, estimates of the number of sensory neurons in rodents is approximately 20×10^6 (J. Schwob, personal communication), and the number of glomeruli is approximately 1,800 (Royet et al., 1988), yielding a convergence ratio of approximately 11,000 sensory axons per glomerulus. Although more complete data are necessary, it is still evident that the convergence of receptor cell axons onto glomeruli and projection neurons is very high.

The ratios of intrinsic neurons to principal neurons are also high. Some order-of-magnitude estimates for these ratios are PG to mitral, 20:1; granule to mitral, 50–100:1; and short axon to mitral, 1:1 (Shepherd, 1972a). Better data are needed for different species. However, even these rough estimates suggest an extensive array of intrinsic circuits for information processing in the bulb.

SYNAPTIC CONNECTIONS

The distinct laminae and cell types of the olfactory bulb have greatly simplified the EM analysis of synaptic connections. In many cases, identification of processes has been further confirmed by serial reconstructions. Because of these advantages, the olfactory bulb was among the first brain regions in which identification of the main patterns of synaptic connection was made on a secure basis. These patterns are found in the three main layers of synaptic neuropil in the bulb, which we describe in sequence.

GLOMERULAR LAYER

Intraglomerular Connections. As discussed earlier, all sensory neuron axons terminating in a glomerulus express the same olfactory receptor. This means that the identity of a single glomerulus can be defined based on a molecular subset of the sensory neuron population.

Early anatomical studies suggested that within the glomerulus, subsets of axons do not ramify randomly but rather occupy distinct intraglomerular compartments (Land et al., 1970; Land and Shepherd, 1974). This has been extended by studies using molecular markers (Treloar et al., 1996); LacZ reporters, driven by olfactory marker protein, labeled subsets of sensory neuron axons that only partially innervated glomeruli, suggesting the input may be heterogeneous. Studies with markers of cell surface carbohydrates have suggested similar conclusions (Lipscomb et al., 2002), as have ultrastructural studies of glomerular synaptic organization (Kasowski et al., 1999).

Within the glomeruli, the olfactory sensory terminals make axodendritic synapses onto the dendritic tufts of both the relay neurons (mitral and tufted cells) and the intrinsic neurons (PG cells) (Pinching and Powell, 1971a,b; Kasowski et al., 1999). As shown in Fig. 5.3A, the axon terminals are relatively large, especially compared with the thin axons from which they arise. The terminals are filled with small, round vesicles. The contacts are Gray type 1 chemical synapses.

The dendrites within the glomerulus not only receive the sensory input but are themselves presynaptic in position (Fig. 5.3B). The most common pattern is dendrodendritic contacts from mitral/tufted cells to PG cells; these are Gray type 1 synapses. The presynaptic dendrites contain only a few synaptic vesicles at the synaptic sites, in contrast

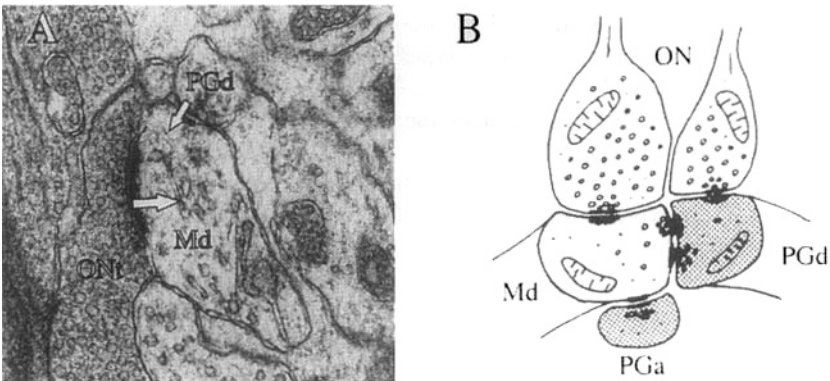


Fig. 5.3. Synaptic connections in the mammalian olfactory bulb glomerulus. In (A) an axodendritic synapse from an olfactory sensory neuron axon terminal (ONt) onto a presumed mitral/tufted cell dendrite (Md) is shown. The polarity of the synapse is indicated with the large arrow. Also shown is a periglomerular cell dendrite (PGd) making a symmetrical synapse onto the mitral/tufted cell dendrite. The small arrow indicates the polarity. In (B) the typical synaptic connections of the glomerulus are summarized. These include the axodendritic and dendrodendritic connections in the olfactory glomerulus. ON, olfactory nerve; Md, mitral dendrite; PGd, periglomerular cell dendrite; Pga, periglomerular cell axon. Note the serial and reciprocal synaptic sequences. [After Reese and Brightman, 1970; Pinching and Powell, 1971a,b; White, 1972; Toida et al., 2000.]

to the sensory axon terminals (see earlier). Another common pattern is dendrodendritic contacts in the opposite direction, from PG cells to mitral/tufted cells; these are Gray type 2 synapses. As indicated in Fig. 5.3, the two types of synapse may be arranged in reciprocal, side-by-side pairs (approximately 25% of the total), or in more widely spaced serial sequences. The presynaptic PG cell dendrite may in turn receive a type 2 synapse from another, presumably also PG, dendrite. No dendrite has been observed to be presynaptic to an axon terminal (in contrast to dorsal horn [Gobel et al., 1980] and retina [Dowling and Boycott, 1966]); however, there is evidence for presynaptic actions (see later).

The intraglomerular organization of primary sensory and local circuit synapses is complex (Kasowski et al., 1999; Toida et al., 2000). Dendritic bundles within the glomerulus are often surrounded by a glia sheath that segregates them from large fields of sensory axon terminals. The dendrodendritic synapses tend to occur predominantly within the dendritic bundles, whereas the axodendritic synapses from the sensory terminals are onto dendrites that are more isolated or alone. In contrast to elsewhere in the nervous system, individual synapses are not wrapped with a glia sheath. As discussed further later, this organization may aid in synchronizing postsynaptic activity in the glomerulus by allowing the diffusion of neurotransmitter to adjacent sites (Carlson et al., 2000; Schoppa and Westbrook, 2001).

Interglomerular Connections. In addition to the GL cell bodies, there is an extraglomerular neuropil between the glomeruli. Several types of synaptic connections have been identified here (Pinching and Powell, 1971a,b). First, the axons of PG cells make type 2 synapses onto the somata and dendrites of other PG cells and onto the primary dendrites of mitral and tufted cells as they emerge from the glomeruli. Second, there are type 1 synapses from tufted cell axon collaterals onto tufted cell dendrites. Third, there are synaptic terminals of various types of centrifugal fibers.

Development and Plasticity. How does the glomerular array of molecularly defined sensory projections develop? This remains an area of intense study, but several facts are emerging. First, the olfactory receptors themselves appear to play an important role in the targeting of axons to the glomeruli. The substitution of one olfactory receptor for another will redirect the sensory axons to a new site, whereas removal of the olfactory receptor appears to render the axons unable to target a glomerulus (e.g., Mommaerts et al., 1996; Wang et al., 1998). Other factors, such as the expression of cell surface molecules and an array of extracellular matrix molecules, are also likely to be involved (for a review, see Key and St. John, 2002) in directing the sensory axons to the correct region of the bulb.

When sensory axons first approach the olfactory bulb, they do not penetrate to form glomeruli but instead have a waiting period of several days (Bailey et al., 1999; Treloar et al., 1999). It may be that during this period the axons are sorting into broadly defined domains of the olfactory bulb, with the final coalescence into specific glomeruli occurring during the perinatal and postnatal period (Royal and Key, 1999; Kim and Greer, 2000; Potter et al., 2001). Following perinatal odor deprivation (for a review, see Brunjes, 1994) or interruption of the sensory transduction cascade in cyclic nucleotide-gated (CNG) channel knockouts (Lin et al., 2000; Zheng et al., 2000), glomeruli appear

somewhat smaller but are otherwise unremarkable. The specificity of axon targeting to the glomeruli is perturbed in the absence of functional activity, for at least some olfactory receptors, but much work remains to be done to understand fully the mechanisms involved.

The first synapses in the nascent glomeruli in the mouse appear around embryonic day (E) 14 (Hinds and Hinds, 1976). These are axodendritic and are believed to represent the first arrival of sensory afferents. Thereafter, the number of synapses, both axodendritic and dendrodendritic, increases rapidly until the numbers asymptote around 15 days postnatally. Although deafferentiation can cause a decrease in the number of dendrodendritic synapses in the EPL (see later), it is not known if the absence of sensory input has an effect on the intrinsic synaptic organization of the glomerulus.

EXTERNAL PLEXIFORM LAYER

In the EPL, the dominant type of synaptic connection is a pair of reciprocal contacts (Hirata, 1964; Andres, 1965; Rall et al., 1966). Serial reconstructions (Rall et al., 1966) established that these contacts occur, as indicated in Fig. 5.4, between the secondary dendrite (Md) of a mitral/tufted cell and the spine (gemmule) of a GC dendrite (Grs). The dendritic spines of GCs impregnated with gold are shown in high-voltage EMs in Fig. 5.4A,B. The synapses between GC dendritic spines and mitral/tufted cell secondary dendrites were the first dendrodendritic synapses identified in the nervous system. An EM of a typical reciprocal synapse is shown in Fig. 5.4C. In the reciprocal pair, the mitral-to-granule synapse is type 1, whereas the granule-to-mitral synapse is type 2 (Price and Powell, 1970a). More than 80% of all synapses in the EPL are involved in such reciprocal pairs. Remaining synapses may be accounted for in part by short-axon cells making synapses in the EPL (Toida et al., 2000).

It is notable that nearly all of the synapses onto mitral cells in the EPL are members of the reciprocal synapses onto secondary dendrites. There are few or no synapses onto the primary dendrites. The primary dendrites are thus specialized for transmission from the glomerulus to the cell body, whereas the secondary dendrites are specialized for synaptic interactions, both output and input. The significance of this compartmentalization is discussed further later.

EMs show the EPL to be a neuropil composed almost entirely of mitral/tufted and GC dendrites and their synaptic interconnections (see Reese and Shepherd, 1972). If we consider that there are up to 100 GCs for each mitral cell and that each GC has 50–100 spines in the EPL (Greer, 1987; Mori, 1987), it is obvious that these dendrodendritic microcircuits provide for extremely powerful and specific interactions with the mitral cells. Because as we have seen that the secondary dendritic fields of most mitral and tufted cells occupy separate levels in the EPL, their microcircuits through granule dendrites are correspondingly separated.

In single EM sections, the granule-to-mitral/tufted synapse sometimes appears indistinct or missing. Ramon-Moliner (1977) suggested that the inhibitory action of GCs might therefore be mediated by a nonsynaptic mechanism. However, Lieberman and his colleagues carefully reinvestigated the question (Jackowski et al., 1978) using several EM techniques and confirmed that the granule-to-mitral synapses are approximately equal partners in the reciprocal pairs, as originally described. This of course

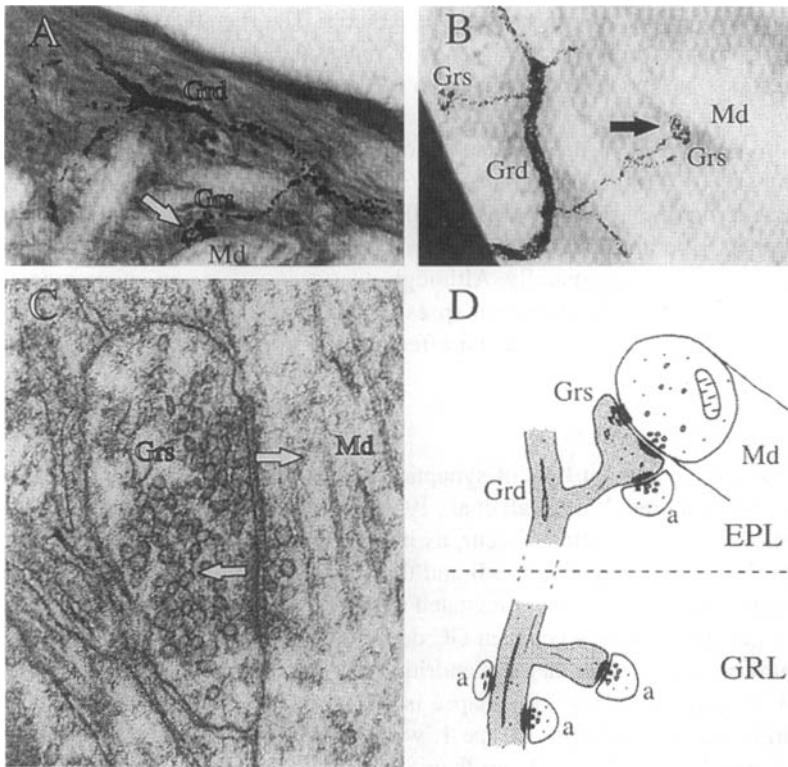


Fig. 5.4. Synaptic connections in the external plexiform layer of a mammalian olfactory bulb. High voltage electron micrographs illustrate the structure of gold-labeled granule cell dendrites (Grd) and granule cell dendritic spines (Grs) in (A) and (B). The arrows indicate two spine heads that are closely apposed to mitral/tufted dendrites (Md). The latter are not readily seen because they are not labeled. Note that the necks of the granule cell dendritic spines can be very long ($> 5\mu\text{m}$) and that they can branch yielding multiple spine heads that are connected to the parent dendrite via a common neck. In (C) a dendrodendritic synaptic connection between a mitral secondary dendrite (Md) and a granule cell dendritic spine (Grs) in the external plexiform layer is shown. Note that $\text{Md} \rightarrow \text{Grs}$ synapse has round presynaptic vesicles and a thick postsynaptic density, indicative of a Gray type 1, whereas the $\text{Grs} \rightarrow \text{Md}$ synapse has flattened presynaptic vesicles and more symmetrical membrane densities, indicative of Gray type 2. In (D) the synaptic organization of the external plexiform (EPL) and granule cell (GRL) layers is summarized. Granule cell spines establish reciprocal dendrodendritic synapses with mitral/tufted cell secondary dendrites in the external plexiform layer. In addition, the axons of centrifugal axons make Gray type 1 synapses on granule cells. In the granule cell layer, the axons of both recurrent collaterals from mitral/tufted cells, short axon cells and centrifugal axons make both Gray type 1 and type 2 synapses on the basal granule cell processes (see text). [After Andres, 1965; Hirata, 1965; Rall et al., 1966; Reese and Brightman, 1970; Price and Powell, 1970a; Kasowski et al., 1999.]

does not rule out the possibility of additional nonsynaptic interactions between the cells (see Transmitters).

In addition to synapses made by dendrites, the EPL contains axon terminals from several sources: intrinsic short-axon cells and centrifugal fibers (as noted earlier, recurrent mitral collaterals, thought by Cajal to terminate in the EPL, are now believed

to be restricted to the IPL). These axon terminals make type 1 synapses predominantly on the presynaptic granule spines (Price and Powell, 1970a); no contacts have been seen on mitral cell dendrites.

Development and Plasticity. How is the dendrodendritic microcircuit assembled during development? The mechanism in fact appears to be relatively simple. According to Hinds (1970), the mitral/tufted-to-granule synapse appears first, at about E17 in the mouse, followed 1 day later by the granule-to-mitral/tufted synapse. Whether each neuron has its own genetic timetable of synapse expression, or the earlier mitral synapse induces the granule synapse, requires further study. The later expression of granule synapses is consistent with the general rule that intrinsic neurons develop later than do projection neurons (Jacobson, 1978). In the retina, more complex microcircuits also appear to be assembled according to a similar genetic algorithm consisting of sequential expression of individual synaptic types (Nishimura and Rakic, 1987).

Studies have revealed a great deal of plasticity in these microcircuits. In the mutant mouse strain PCD (Purkinje cell degeneration), the specific degeneration of mitral, but not tufted, cells occurs at about 3 months of age (Greer and Shepherd, 1982). The number of reciprocal synapses between granule cell spines and tufted cell dendrites increases in compensation, suggesting that many denervated granule-to-mitral spines survive and establish new efferent and afferent synapses with tufted cell dendrites (Greer and Halasz, 1987). By contrast, olfactory deprivation causes a reduction in incidence of dendrodendritic synapses, more severe in the granule-to-mitral contacts (Benson et al., 1984). It has been suggested that “the reciprocal pair of synapses exists in a dynamic equilibrium in which each sustains the other through trophic or feedback mechanisms” (Shepherd and Greer, 1988).

Odor deprivation has been effectively used to demonstrate the role of afferent input during bulb development (Brunjes, 1994). Unilateral deprivation leads to down-regulation of global metabolic indices such as 2-deoxyglucose (2DG), as well as a loss of dopamine in subsets of periglomerular cells (Baker et al., 1984). Deprivation also causes changes in the membrane properties of mitral and tufted cells through a down-regulation of Na⁺ channel subunits (Sashihara et al., 1996). By contrast, pairing of specific odors with arousal during early development may lead to structural changes within the bulb, including the appearance of supernumerary glomeruli (Woo et al., 1987). Odor deprivation also causes a reduction in the incidence of dendrodendritic synapses, most severe in the granule-to-mitral contacts (Benson et al., 1984). This is consistent with the suggestion of Hinds (1970) that the mitral-to-granule contacts form first, followed by the granule-to-mitral contacts.

GRANULE CELL LAYER

In the granule cell layer, axon terminals are found on the shafts and spines of the GC dendrites (see Fig. 5.4D). The studies of Price and Powell (1970b) showed that these axon terminals derive from both intrinsic and extrinsic (central) inputs. The *intrinsic* sources include the axon collaterals of mitral and tufted cells and the axons of the deep short-axon cells. There is evidence that the synapses of these terminals are types 1 and 2, respectively. The *extrinsic* sources make connections at different levels of the granule dendritic tree (see Fig. 5.2A). Anterior commissure axons distribute mainly to the

deep processes. The anterior olfactory nucleus distributes over the middle part of the dendrites, including the spines in the EPL. The horizontal limb of the diagonal band distributes mainly to the spines in the EPL; some terminals are also found at the borders of the glomeruli. The synapses made by these inputs from the brain appear to be type 1.

Note that all of the synaptic connections in which the GC takes part are oriented toward the GC, with the sole exception of the dendrodendritic synapses from the granule spines onto the mitral dendrites in the EPL. The latter are, therefore, the only output avenue from the GCs.

Gap junctions are also found between adjacent perikarya in the GCL (Reyher et al., 1991; Paternostro et al., 1995). Freeze fracture replicas show particle aggregates in the perikaryon membrane, whereas immunocytochemical analyses revealed punctate staining for gap-junction proteins. Lucifer yellow injections into single GCs result in the staining of small subsets of adjacent cells. These findings suggest that GCs may be organized into syncytial subsets (Paternostro et al., 1995).

GLIA

As noted earlier, olfactory receptor axons are organized into bundles of 100–200 axons surrounded by the ensheathing glial cell of the olfactory nerve (Valverde and Lopez-Mascaraque, 1991; Doucette, 1993; Ramon-Cueto and Valverde, 1995; Au et al., 2002). These specialized glia have several properties that distinguish them from peripheral nervous system Schwann cells as well as oligodendrocytes, including a low expression of GFAP, p75, neuropeptide Y, and laminin, among others. Recent years have seen a great deal of interest in the ensheathing cells for their role in supporting the continued growth of sensory axons in the olfactory system. In addition, when transplanted into other regions of the nervous system, such as the spinal cord, the ensheathing cells have the potential to increase successful regeneration of axons following lesions (for a review, see Raisman, 2001). This is to be distinguished from their role in the olfactory pathway, where they support the extension of axons from newly differentiated sensory neurons.

Ensheathing cells express laminin throughout life as well as the low-affinity nerve growth factor receptor, both of which may be associated with the continued turnover of the olfactory receptor cell axons (Leisi, 1985; Turner and Perez-Polo, 1993; Kafitz and Greer, 1996).

At the juncture of the olfactory nerve layer and the glomerulus, the glial phenotype changes abruptly (Gonzalez et al., 1993; Au et al., 2002). Conventional central nervous system astrocytes surround the glomerulus and extend processes into the glomerular neuropil, where they isolate bundles as dendrites (see earlier) (Kasowski et al., 1999). This is similar to, although not nearly as distinct as, the synaptic glomeruli of the cerebellum and thalamus (Pinching and Powell, 1971a,b). Glial folds are also sometimes seen around the reciprocal dendrodendritic synapses in the EPL. This appears generally consistent with the role of glia in isolating synaptic complexes elsewhere in the central nervous system.

Within the EPL, in most vertebrate species, several loose folds of glial membrane surround the primary dendrites of mitral and tufted cells near the glomerular boundary. In mice and primates, typical myelin has been found at this site, which may not

only surround the primary dendrite but even extend to the cell body in the case of tufted cells (Pinching, 1971; Burd, 1980). This shows that a dendrite may be myelinated and that myelin is not exclusively associated with axons. The function of the myelin around dendrites may be associated with voltage-gated properties in the primary dendrite (Mori et al, 1983; see later).

BASIC CIRCUIT

The synaptic organization of the olfactory bulb is summarized in the basic circuit diagram of Fig. 5.5. The output cells (mitral and tufted cells) receive the sensory input in their glomerular tufts and give rise to the bulbar output from their cell bodies. The two main functions of *input processing* and *output control*, which characterize all local regions of the brain (see Chap. 1), are therefore separated into two distinct levels in relation to the output cells. We summarize the organization at these two levels.

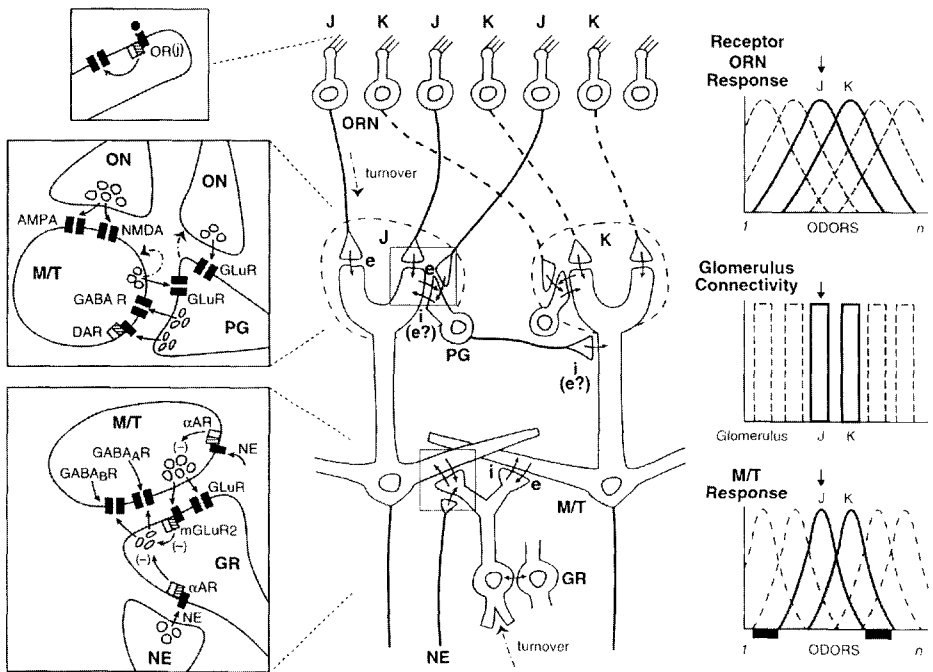


Fig. 5.5. Basic circuit of the mammalian olfactory bulb, integrating molecular, cellular, and functional organization. Abbreviations: left (molecular components): OR, olfactory receptor; ON, olfactory nerve; AMPA, 2-amino-5-phosphonovaleric acid; NMDA, N-methyl-D-aspartate; M/T, mitral/tufted cell; PG, periglomerular cell; GluR, ionotropic glutamate receptor; GABA R, GABA receptor; DAR, dopamine receptor; NE, norepinephrine; αAR, alpha adrenoreceptor; mGluR2, metabotropic glutamate receptor; GR, granule cell. Middle (synaptic circuit): ORN, olfactory receptor neuron; J, K, ORN subsets; e, excitatory; i, inhibitory. Right (structure/function relations): above, overlapping response spectra of ORNs to a range of odors (1–n); middle, connectivity of subsets to individual glomeruli; bottom, response spectra of M/T cells show less overlap due to lateral inhibition (black bars below abscissa).

INPUT PROCESSING

Intraglomerular Microcircuits. Within the glomeruli, the basic elements of the synaptic triad (see Chap. 1) come together: input (olfactory axon terminals), output (mitral/tufted cell dendrites), and intrinsic (PG cell dendrites). The same type of arrangement is found in the retina, cerebellum, and thalamus (see Fig. 1.5). In the latter regions, the synapses onto the principal and intrinsic elements arise from a single large input terminal, whereas in the olfactory glomeruli, the synapses are made by separate terminals (see Chaps. 1 and 6–8). The arrangement of separate terminals appears to permit considerable combinatorial complexity in processing odor information.

There is increasing evidence that a glomerulus operates as a functional unit, coordinating input from sensory neurons expressing the same odor receptor. There is also mounting evidence that the glomerular population forms activity maps representing the odor stimuli (see later). Monoclonal antibody staining for several cell surface glycoproteins shows sharply defined glomerular borders (reviewed in Schwob, 1992; Mori and Yoshihara, 1995). As noted earlier, olfactory receptor cell axons containing the mRNA for an olfactory receptor converge and terminate in (with few exceptions) two specific glomeruli on the medial and lateral aspects of the olfactory bulb (Ressler et al., 1994; Vassar et al., 1994; Mombaerts et al., 1996).

If glomeruli have this functional specificity, then the group of mitral, tufted, and PG cells with dendrites connected to a particular glomerulus all share this specificity. There is growing evidence to support this suggestion (Wilson and Leon, 1987; Buonviso and Chaput, 1990; Mori et al., 1992; Mori and Yoshihara, 1995; Belluscio et al., 2002). Mitral cells near each other and innervating the same glomerulus tend to have more similar responses to odor stimuli than do mitral cells that are distant from each other. Radial arrays of active glomeruli and deeper cells have in fact been visualized, using both 2DG (Stewart et al., 1979) and voltage-sensitive dyes (Kauer and Cinelli, 1993). This horizontal constraint on the organization of functionally related neurons in the bulb may be analogous to the functional columns of the cerebral cortex (Shepherd, 1972; see later).

After the initial input to the principal and intrinsic elements, further processing takes place within the glomerulus through dendrodendritic microcircuits. There is evidence that these are organized in relation to specific types of glomerular layer cells (Toida et al., 2000).

Interglomerular Microcircuits. Activity in one glomerulus can affect other glomeruli through interglomerular connections. The main route is PG cell axons, which, through their terminals, can affect the transmission of information out of neighboring glomeruli (see Fig. 5.4). There is evidence that these interglomerular actions may be excitatory (Shepherd, 1963; Freeman, 1974) or inhibitory (Getchell and Shepherd, 1975a,b). If glomeruli function as units, then one function of the interglomerular microcircuits could be to enhance the contrast between glomeruli of different specificities, in analogy with intercolumnar interactions in neocortex (see Chap. 12). Conversely, the connections might function to recruit neighboring glomeruli as the concentration of an odor increases. Studies are needed to distinguish clearly between these alternatives.

OUTPUT CONTROL

The connection between the levels of input processing in the glomeruli and output control from the mitral and tufted cell bodies is made by the primary dendrites of the mitral and tufted cells. Thus, in species in which there are single primary dendrites, a *glomerulus* defines a a translaminar “glomerular unit” formed of all of the mitral and tufted (and PG) cells connected to it. This anatomical unit has also been shown to be a functional unit in the processing of odor stimuli. This was first seen in 2DG studies as translaminar densities (cf. Stewart et al., 1979); it has also been seen in in situ hybridization for early-immediate genes (Guthrie et al., 1993; Sallaz and Jourdan, 1993) and in salamanders using voltage-sensitive dyes (VSDs) (cf. Kauer and Cinelli, 1993; Cinelli and Kauer, 1994). One may refer to these as “olfactory columns,” in analogy with ocular dominance columns and orientation columns in the visual cortex (see Chap. 12). These columns thus define the units that are the basis for generating the output from the olfactory bulb.

At the level of output control, the main type of microcircuit is the reciprocal dendrodendritic synapse between mitral/tufted cells and GCs. At this level, the mitral/tufted primary dendrite functions as the afferent element of the synaptic triad, conveying the input directly to the soma and secondary dendrites, which function as the principal neuron component. The triad is completed by the intrinsic element, the GC spine.

As we shall soon see, the mitral-to-granule synapse is excitatory and the granule-to-mitral synapse is inhibitory. Because the granule-to-mitral/tufted synapse is the sole output of the GC, the inhibition it delivers is very powerful and is the main means for mediating control of output from the olfactory bulb. Although the reciprocal synaptic microcircuit seems to be a simple and inflexible arrangement, in fact it can generate several types of functions. The most obvious are self- and lateral inhibition of the mitral/tufted cells, but it is also involved in temporal patterning and memory storage as well, as is discussed later.

The spatial constraints on these circuits controlling output obviously contrast with those involved in processing the input. As we have seen, input processing is organized according to glomerular modules, each presumably limited to processing a specific subset of sensory inputs. By contrast, output control is mediated through the long mitral/tufted secondary dendrites, whose fields are extensive and overlapping. A given output neuron is modulated according to a graded summation of effects from a wide range of other output cells. The activity of a given mitral cell therefore reflects the context of information being processed in neighboring parallel channels. This *contextual modulation* is important in determining not only the patterns of excitation and inhibition in space but also sequences of excitation and inhibition in time.

PARALLEL PATHWAYS

Parallel processing is an important feature of neural circuits. The olfactory bulb contains several types of parallel pathways for processing olfactory information.

Main Olfactory Pathway. The most obvious parallel paths consist of the 2,000 or more glomerular units. Although traditionally it has been believed that in the vertebrate all of these ordinary glomeruli and their columns are similar, anatomically identifiable glomeruli have begun to be recognized.

Modified Glomerular Complex. The first and most clearly identifiable is a “modified glomerular complex” (MGC) that forms a separate “labeled line” within the main olfactory bulb (Teicher et al., 1979; Greer et al., 1982). It is believed to mediate information concerning odor cues related to suckling in young animals (Pedersen et al., 1987). The possible analogy between this MGC and the macroglomerular complex involved in pheromone signaling in insects is intriguing (reviewed in Hildebrand and Shepherd, 1997).

Necklace Glomeruli. Related to the MGC in vertebrates are “necklace glomeruli” at the border of the main olfactory bulb facing the accessory olfactory bulb (AOB) (Zheng and Jourdan, 1988). In addition to the anatomical specificity of the necklace glomeruli, they are also the recipients of afferent input from a subpopulation of olfactory sensory neurons that express a guanylyl cyclase and a cyclic GMP–stimulated phosphodiesterase and are not dependent on the CNG channel to process odor information (Juliffs et al., 1997). Thus, in the CNG channel knockout mice, functional activity in the necklace glomeruli appears to be normal (Baker et al., 1999).

Mitral and Tufted Cells. In addition to these parallel pathways related to the glomeruli, there are also parallel pathways provided by the mitral and tufted cell populations (see Fig. 5.5). It is not known whether, at the level of input processing within the glomeruli, the dendritic tufts of the two types receive input from different receptor cell axons or if they interact with common (as shown in the diagram) or different PG cell dendrites. At the level of output control in the EPL, each type interacts with different subpopulations of granule cells: superficial GCs (G_S) control superficial and middle tufted cells (T_M), and deep GCs (G_D) control mitral cells (M_1). GCs forming a third subpopulation appear to interact with both tufted and mitral cells. These cell types can be identified in the drawings in Fig. 5.2.

When differing projection sites of mitral and tufted cells in olfactory cortical areas were first recognized, it was suggested by Skeen and Hall (1977) that there might be an analogy in this regard with the different classes of retinal ganglion cells. The differing morphologies of the dendritic trees of these cells further support that analogy (Macrides and Schneider, 1982). As noted by Orona et al. (1984), in the retina, the particular sublamina of dendritic ramification of a ganglion cell has been found to be the main morphological feature correlated with the physiological type of its response (see Chap. 6). The fact that both mitral and tufted cells are further divided into subclasses on the basis of dendritic morphology indicates that multiple parallel pathways exist. This may be important in the mediation of different types of information about molecular stimuli. As already noted, mitral cells have distributed but precise projections within the olfactory cortex (Zou et al., 2001) (see Chap. 10).

A point of interest is that tufted cells are more readily excited by orthodromic stimulation than mitral cells. This may be a reflection of the size principle (Henneman, 1957)—that small cells tend to be more excitable due to their higher input impedance (see Chap. 3). Other differences such as in primary afferent input, local circuit connectivity, or intrinsic properties, could also be involved.

Accessory Olfactory Bulb. Odor information is processed via the AOB in parallel with the main olfactory system; the AOB appears to be receptive to both volatile and non-

volatile ligands. The sensory neurons are found in a tube-like structure, the vomeronasal organ (VNO), located at the base of the nasal septum. Similar to the sensory neurons in the main epithelium, the vomeronasal receptor cells express mRNAs for GPCRs (Dulac and Axel, 1995). There are two main classes: V1R and V2R (the latter have large N-terminal domains resembling metabotropic glutamate receptors). Cells expressing V1Rs are localized in the apical part of the VNO epithelium, whereas those expressing V2Rs are localized in the basal part (cf. Buck, 2000).

The axons of the vomeronasal cells run in several distinct fascicles along the medial surface of the main olfactory bulb toward its dorsal-caudal aspect where the AOB is located. The V1R cell type projects to the anterior part of the AOB, whereas the V2R type projects to the posterior area (see Mori et al., 1999). The cytoarchitecture and synaptic organization of the AOB are similar to those of the main olfactory bulb, although the laminar organization is less distinct. The receptor cell axons terminate in glomerular regions on the dendrites of the primary projection neuron, the mitral cells. Glomeruli receive inputs from more than one subset; however, mitral cells also connect to more than one glomerulus (Del Punta et al., 2002). Periglomerular cells are few in number and are also likely to receive direct afferent input. Intraglomerular circuits appear similar to those described for the main bulb. Modulation of mitral cell output occurs in the EPL where reciprocal dendrodendritic synapses are formed with GCs. Despite these similarities, there are also differences. The glomeruli are small and fewer in number. Although the projection neurons are called *mitral cells*, they are generally smaller and more polymorphic than their counterparts in the main bulb. There are also differences in some neurotransmitters (see later).

The output of the AOB is exclusively to the medial anterior, medial posterior, and posterior cortical nuclei of the amygdala and to the bed nucleus of the stria terminalis. From these regions, multiple paths carry AOB information to the hypothalamus. The accessory pathway is believed to be involved in processing contact signals involved in mating in many mammals, as well as hormonally regulated odor-stimulated behaviors (see Keverne, 1995, for a review). In fact, the AOB provides one of the clearest examples of a correlation between a synaptic circuit and a specific learned behavior in the nervous system (see later).

CENTRIFUGAL MODULATION

In addition to processing sensory information, the bulbar microcircuits are also involved in gating and modulating that information by centrifugal fibers from the brain. A key site for this control is the dendritic spine of the GC. As can be seen in Fig. 5.5, a synaptic triad is formed by the centrifugal fiber terminal, granule spine, and mitral/tufted dendrite. Through this triad, the centrifugal fiber can exert direct and exquisite control over the function of the reciprocal microcircuit.

As discussed in an earlier section, there are four main types of centrifugal control. Their synaptic actions within the basic circuit are discussed later (see Neurotransmitters).

From these considerations, it will be seen that mitral/tufted and intrinsic cell synapses are concerned both with olfactory processing and with integration of information passing forward from the brain. Some of the information from the brain is in the form of feedback through long loops from the olfactory projection areas. Some of it is in the form of nonolfactory signals from hypothalamic and limbic structures. The granule-to-mitral synapse is a specific site at which there is an overlap of these functions. One

may characterize it in this regard as a *multifunctional*, or *multiplex*, synapse. It is, in this regard, a good example of the spine as a multifunctional microintegrative unit (see Chap. 1).

SYNAPTIC ACTIONS

Synaptic circuits in the olfactory bulb have been analyzed using many different types of preparations. In the 1960s and 1970s, selective stimulation of input and output pathways in anesthetized preparations, particularly rabbit, rat, and salamander, enabled the identification of the basic types of synaptic actions and synaptic circuits. Around 1980, the isolated turtle olfactory bulb facilitated pharmacological analysis of olfactory bulb circuits. In the 1990s, tissue slices of the rat and mouse olfactory bulb became standard preparations for detailed studies of membrane properties and neurotransmitters. These different approaches have benefited from the close application of dendritic modeling to the interpretation of experimental results.

DENDRODENDRITIC SYNAPTIC ACTIONS

The best understood synapses in the olfactory bulb, and among the best understood in the brain, are the reciprocal synapses between the secondary dendrites of mitral cells and the apical dendritic spines of GCs.

A key finding, in single-cell recordings in the anesthetized rabbit, was that antidromic invasion of a mitral cell is followed by long-lasting inhibition (Yamamoto et al., 1962; Phillips et al., 1963). Recordings from presumed GCs suggested that the inhibition could be mediated by a pathway involving mitral cell excitation of GCs, with subsequent feedback and lateral inhibition of the mitral cells by the GC dendrites operating in an output mode (Shepherd, 1963). This raised the question of the source of activation of the GCs and the nature of their synaptic output.

This question was analyzed by computational models of the mitral and GC dendrites (Rall et al., 1966; Rall and Shepherd, 1968), among the first such models using the methods introduced by Rall (1964). The models generated the intracellular potentials and the associated extracellular potentials recorded experimentally. The fundamental insights were that an action potential at the cell body spreads backward into the mitral secondary dendrites and that it is appropriately timed and placed to make these dendrites the presynaptic elements for synaptic excitation of the GC spines. The EPSP in the GCs in turn is appropriately timed and placed to mediate the long-lasting inhibition of the mitral cells.

These combined physiological and theoretical studies thus predicted novel dendrodendritic reciprocal synaptic interactions. The last step was to test this prediction by EM analysis. Using serial reconstructions, Thomas Reese and Milton Brightman showed that the mitral secondary dendrites and the GC spines are interconnected by side-by-side synapses oriented in opposite directions appropriate for mediating the predicted interactions (Rall et al., 1966; see Fig. 5.3).

The functioning of the reciprocal synapses as a microcircuit module is mentioned in Chap. 1 (see Fig. 1.5B) and is illustrated in greater detail in Fig. 5.6A. During the initial time period (A, I-II), depolarization (D) of the mitral cell dendrite by the invading action potential activates the excitatory (⊕) synapse onto the GC spine (shaded).

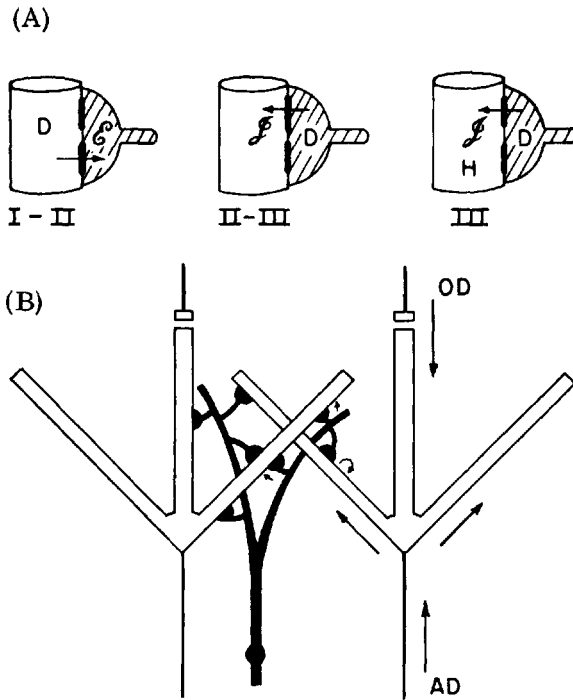


Fig. 5.6. **A:** Postulated mechanisms of action of the dendrodendritic synaptic pathway between mitral (open) and granule (shaded) cells, during successive time periods I, II, and III following an antidromic volley. D, depolarization; H, hyperpolarization; E, excitation; I, inhibition. **B:** Diagram of the pathways for self- and lateral-inhibition through dendrodendritic connections. OD, orthodromic (normal) activation; AD, antidromic activation. [From Rall and Shepherd, 1968.]

In period II–III, the EPSP in the spine activates the inhibitory (I) synapse back onto the mitral cell dendrite. In period III, this causes a hyperpolarizing (H) IPSP in the mitral cell dendrite. In addition to feedback inhibition of an activated mitral cell, the dendrodendritic synapses also initiate lateral inhibition by electrotonic spread of the EPSP in the GC to spines connected to neighboring mitral cells (Fig. 5.6B).

Both orthodromic and antidromic activation of mitral cells can involve action potential generation in the initial axonal segment, as in classic concepts of the functional organization of the neuron (Eccles, 1957; Fuortes et al., 1957; see Chaps. 1 and 3). Both routes lead to extensive action potential invasion of the secondary dendrites, whether via active or passive spread (see Fig. 5.6B). The dendrodendritic interaction model predicts a sequence of specific functions—feedback and lateral inhibition—for the backspreading action potential. These functions in turn underlie several specific operations in the processing of sensory input, including generation of oscillatory behavior, tuning of odor response spectra, and memory storage, as discussed later.

Oscillatory Activity. In addition to providing for recurrent and lateral inhibition, the dendrodendritic interaction model provides a possible basis for the generation of rhythmic activity in neuronal populations of the olfactory bulb (Rall and Shepherd, 1968;

Freeman, 1975). As illustrated in Fig. 5.7, the sequence begins with a long-lasting EPSP in the mitral cell dendritic tuft (MT in Fig. 5.7) in the glomeruli, due to olfactory nerve input or the intrinsic activity of the glomerular layer. The initial mitral cell action potential generated by the EPSP (MC in Fig. 5.6) synchronously activates all of the granule (Gr) cells with which it has connections. These GCs deliver synchronous feedback inhibition of the activated mitral cell and lateral inhibition of neighboring mitral cells as already described (Fig. 5.7), shutting off further activation from the EPSP in the glomerular tuft. As the mitral cell IPSP subsides, a point is reached at which the EPSP can again generate an action potential, and the cycle repeats itself. Through the extensive interconnections between mitral cells and GCs, a prolonged input in the glomeruli is converted into a rhythmic output in the mitral cell population, locked to a rhythmic activation of the granule cell population.

Hypotheses have been proposed for the role of these oscillations in processing sensory input (cf. Freeman, 1983; Laurent et al., 2001). Studies of membrane mechanisms underlying oscillatory activity are considered further later (see Dendritic Properties).

Field Potentials. Activity in the mitral cell and GC populations generates electric current, which spreads through their dendritic trees according to electrotonic properties (Johnston and Wu, 1995; Segev, 1995; Shepherd, 2003b). The currents of the individual neurons summate in the extracellular spaces to give rise to extracellular field potentials, which can be recorded as evoked field potentials. These were an important constraint in the study leading to the identification of the dendrodendritic synaptic interactions (Rall and Shepherd, 1968). They are also recorded as local field potentials (LFPs) by a microelectrode or electroencephalographic (EEG) waves by larger electrodes placed on the bulbar surface. Rhythmic EEG waves are a prominent character-

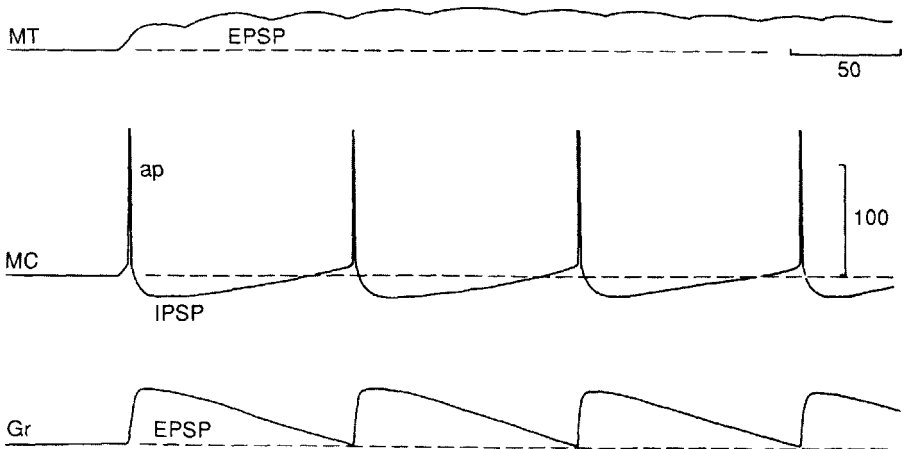


Fig. 5.7. Postulated mechanism whereby the dendrodendritic pathway may provide for rhythmic activity in the olfactory bulb. Postulated intracellular potentials are shown for the mitral cell dendritic tuft in the glomerulus (MT), mitral cell body (MC), and granule cell (Gr). See text. [From Shepherd, 1979.]

istic of the olfactory bulb in the resting state as well as during olfactory-induced activity, as first shown by Adrian (1950). We discuss them further later.

Physiological Tests of Dendrodendritic Interactions. Direct experimental testing of the model for dendrodendritic synaptic interactions began with the isolated turtle olfactory bulb, in which intrinsic circuits are well preserved (Mori et al., 1981). Jahr and Nicoll (1982) carried out an elegant experiment to test the presynaptic role of mitral cell dendrites. As shown in Fig. 5.8A, in a normal mitral cell, injected depolarizing current elicited a fast spike (left, above), which was followed by a slow IPSP (left, below). When tetrodotoxin (TTX) was added to the bath to block Na^+ conductance (Fig. 5.8B), the cell responded with a smaller, slower spike (above), presumably due to Ca^{2+} ions.

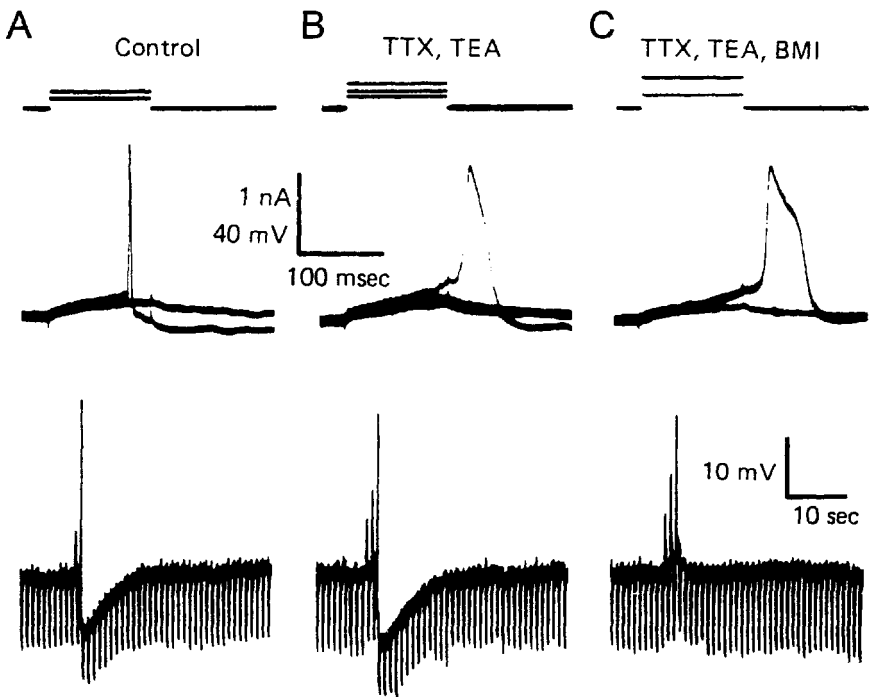


Fig. 5.8. An electrophysiological test of the reciprocal dendrodendritic microcircuit between mitral and granule cells. These tracings are intracellular recordings from a mitral cell in the *in vitro* turtle olfactory bulb. The top trace is a monitor of the depolarizing pulses injected into the cell. The middle trace is the intracellular recording of the response of the cell on a fast sweep. The bottom trace is a slow trace, showing the intracellular impulse response and the hyperpolarizing pulses used to monitor input resistance. **A:** Control responses, showing rapid spike (middle) followed by inhibition (bottom). **B:** In TTX (to block Na^+ conductances) and TEA (to block K^+ conductances, which would shunt Ca^{2+} currents), the spike is broader, but is still followed by inhibition. **C:** Addition of bicuculline (BMI), a GABA_A blocker, removes the inhibition, presumably by blocking granule-to-mitral inhibition. See text. [Modified from Jahr and Nicoll, 1982.]

This spike was still followed by the slow IPSP (below). When bicuculline (a GABA_A receptor blocker) was added to the bath, the mitral cell still responded with an impulse, but the IPSP was eliminated (Fig. 5.8C). Because the only active mitral cell was the one injected, this experiment showed several critical features: that the mitral cell somadendritic region is presynaptic to the GC, that the circuit is recurrent onto the injected cell, and that the inhibitory transmitter is GABA.

There has been a detailed analysis of dendrodendritic mechanisms. This has shown that glutamate (GLU) is the transmitter from mitral cell dendrites onto GCs in the salamander and the rodent olfactory bulb slice. GLU released by the M/T cell dendrites acts on both NMDA and non-NMDA receptors (Trombley and Shepherd, 1992; Wellis and Kauer, 1994; Chen and Shepherd, 1998; Isaacson and Strowbridge, 1998; Schoppa et al., 1998) (Fig. 5.9A).

What is the role of the AMPA and NMDA components? The traditional view of central synapses is that rapid AMPA EPSPs drive individual action potentials, acting in what is termed the “transmission mode,” whereas slower NMDA EPSPs, requiring coincident depolarization to relieve the Mg²⁺ block, are believed to be modulatory. By contrast, at the mitral-to-granule synapse, information transfer is carried mainly by the NMDA receptor. The released GLU gives rise to an EPSP in the GC spine, and the spine releases GABA to produce an IPSP in the M/T cell dendrites through GABA_A receptors. Spread of the depolarization through the dendritic tree mediates lateral inhibition, as demonstrated in paired cell recordings (see Fig. 5.9B).

Recurrent Excitation. Recurrent and lateral excitatory effects between mitral cells are emerging as possible mechanisms in olfactory bulb studies. The evidence began with excitatory interactions between mitral cells (Nicoll, 1971). At the level of the secondary dendrites, immunohistochemical staining has been shown for NMDA (Petralia et al., 1994) and AMPA (Montague and Greer, 1999) receptor subunits. Metabotropic GLU receptors along secondary dendrites have also been demonstrated (van den Pol, 1995).

Physiological evidence for the action of GLU released from secondary dendrites back onto the same dendrites was obtained by Nicoll and Jahr (1982) in the turtle. Several groups have reported more detailed evidence in the rodent olfactory bulb slice (Chen and Shepherd, 1997; Aroniadou-Anderjaska et al., 1999; Isaacson, 1999; Friedman and Strowbridge, 2000; Salin et al., 2001).

The recurrent action has been called a “spillover effect” of excess GLU released from the secondary dendrites and acting on extrasynaptic receptors on those dendrites. This kind of “action at a distance” (also called “volume conduction”) was first demonstrated for monoamine synapses. This kind of action has been postulated for GLU synapses, where a differential action on high-affinity NMDA and lower-affinity non-NMDA extrasynaptic receptors could occur. The NMDA receptors may be associated with “silent synapses,” which become active only when coupled with postsynaptic depolarization to relieve their Mg²⁺ block (Kullman and Asztely, 1998). The NMDA-mediated responses in the secondary dendrites are modulated by GLU re-uptake inhibitors (Isaacson, 1999), further consistent with diffusion of GLU beyond the synaptic region. The mitral-to-granule synapse thus serves as an excellent test site for neurotransmitter spillover mechanisms and silent synapses.

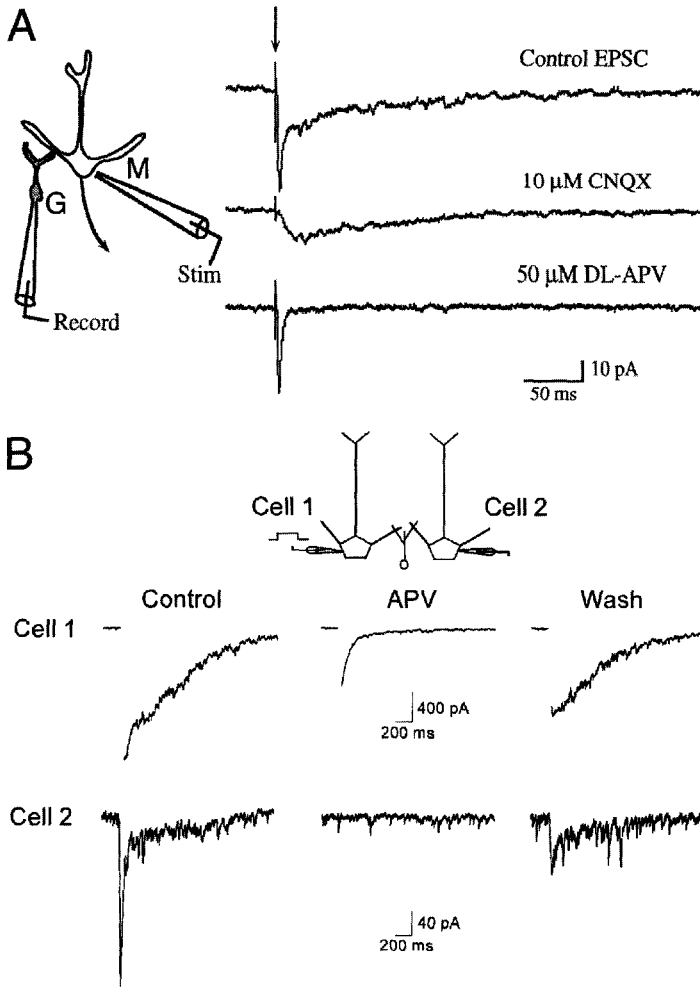


Fig. 5.9. Tests of dendrodendritic interactions in the rat olfactory bulb slice. **A:** Mitral-to-granule excitation: current pulse in mitral (M) cell, recording from granule (G) cell, showing that EPSCs are mediated by both AMPA and NMDA receptors. CNQX blocks AMPA glutamate receptors, revealing the relatively slow NMDA glutamate receptor response, whereas APV blocks NMDA receptors, revealing the relatively rapid AMPA glutamate receptor response. [From Schoppa et al., 1998.] **B:** Feedback and lateral inhibition, as recorded by dual patch electrodes in neighboring mitral cells. Depolarizing pulse in cell 1 causes feedback inhibition (reversed Cl^- IPSC) in cell 1, and lateral inhibition in cell 2; both are sensitive to APV. The lateral (secondary) dendrites are much longer than here depicted schematically (extending as far as 1,000 μm , as discussed earlier), so that lateral inhibition spreads widely, aided by action potential invasion of the secondary dendrites (see later). See text. [From Isaacson and Strowbridge, 1998.] Abbreviations: CNQX, 6-cyano-7-nitroquinoxaline-2,3-dione; AMPA, α -amino-3-hydroxy-5-methyl-4-isoxazole propionic acid; NMDA, N-methyl-D-aspartate; APV, D-2-amino-5-phosphonovalerate.

Spillover of GLU also appears to occur in the glomerulus, where it contributes to synchronization of mitral cell responses (see Dendritic Properties).

Presynaptic Mechanisms. In their presynaptic role, the mitral cell soma and dendrites can be considered analogous to the large terminal arborization at the NMJ (neuromuscular junction). The NMJ has multiple active zones that are activated by an impulse to release ACh into the postsynaptic muscle endplate membrane (cf. Chap. 1). Similarly, the mitral soma-dendrites have multiple synapses (see earlier), which are activated by an impulse to release their neurotransmitter onto postsynaptic GC spines. The mitral cell is therefore an attractive model for analysis of presynaptic release mechanisms at central synapses.

Studies have tested these mechanisms. A key step for vesicle release at most synapses is the influx of Ca^{2+} through voltage-gated Ca^{2+} channels (VGCCs). These channels appear to be present at both the mitral cell dendritic and GC dendritic spine membranes (Isaacson and Strowbridge, 1998; Schoppa and Westbrook, 1999; Chen et al., 2000). The close proximity of the reciprocal synapses to each other suggested the hypothesis that Ca^{2+} entering through NMDA receptors could also trigger vesicle release from the GABAergic synapses. This was tested in slices in which GLU could be flash-released from the mitral cell dendrite filled with caged Ca^{2+} compounds in the presence of Ca^{2+} channel blockers and 0 Mg^{2+} to facilitate NMDA receptors. The results (Chen et al., 2000; Halabiski et al., 2000; but see Schoppa and Westbrook, 1999; Isaacson, 2001) showed that the flash-released GLU still led to recurrent inhibition, presumably through NMDA Ca^{2+} influx into the spine. In summary, Ca^{2+} for vesicle release can come from Ca^{2+} influx through NMDA receptors as well as VGCCs.

GLOMERULAR SYNAPTIC ACTIONS

The other main type of synaptic connection in the olfactory bulb is between the olfactory nerve terminals and the dendritic tufts of bulbar neurons in the glomeruli. This is the first synapse in the olfactory pathway and thus is critical to the synaptic organization underlying olfactory processing.

Mitral Cells. As the largest cells in the olfactory bulb, the mitral cells have been the primary focus of analysis of glomerular synaptic activation. Early studies in the turtle showed that a volley elicited by a single shock to an olfactory nerve bundle sets up an EPSP in a recorded mitral cell, which is characteristically followed within a few milliseconds by the abrupt onset of a hyperpolarizing IPSP that may be long-lasting (several seconds or more) (Fig. 5.10A, E1, E2, I1, I2). According to the classic model of the functional organization of the neuron (see Chap. 1), the EPSP in the distal dendritic tuft spreads to elicit the action potential in the initial axonal segment. The inhibition is presumed to be due to subsequent interactions with the interneurons (PG cells and/or GCs). A sequence of excitation followed by inhibition is characteristic of the response to an input volley in neurons in many regions of the nervous system, reflecting monosynaptic excitation followed by polysynaptic inhibition (see Chap. 1 as well as other chapters).

As with other GLUergic EPSPs in central neurons, the mitral cell EPSP has a rapid and a slow component correlated with AMPA and NMDA receptors, respectively, shown

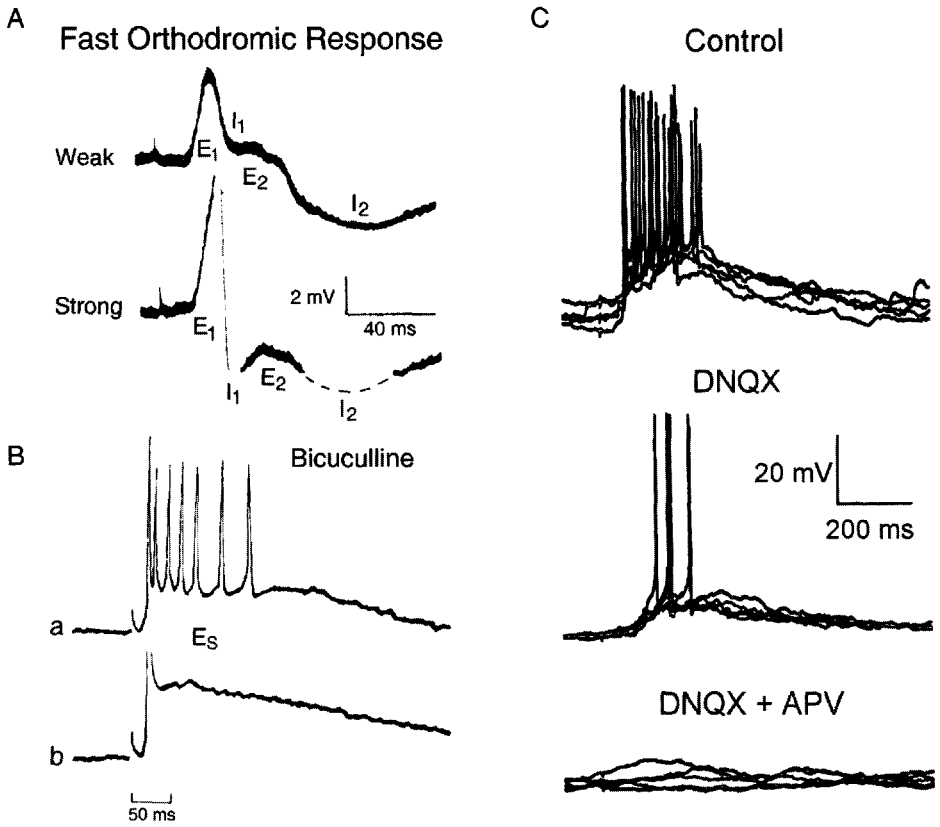


Fig. 5.10. Synaptic activation of mitral cells by olfactory nerve volleys. **A:** Intracellular recordings from the *in vitro* turtle olfactory bulb show fast orthodromic response, just below (a) and above (b) threshold for action potential generation. The synaptic potentials consist of excitatory (E1, E2) and inhibitory (I1, I2) components. See text. [From Mori et al., 1981b.] **B:** Prolonged slow ON-evoked EPSP (Es) revealed by blockade of inhibition by bicuculline. [From Nowycky et al., 1981b.] **C:** NMDA and non-NMDA components of the GLU response to an ON volley in the turtle mitral cell. See text. [From Berkowicz et al., 1994.]

in the turtle (Fig. 5.10C) and in the rat tissue slice (Ennis et al, 1996) and many subsequent studies. Blockade of the inhibition by bicuculline shows that the EPSP is long-lasting (Fig. 5.10B).

The EPSP is augmented by several mechanisms. The mitral cell is itself glutamatergic; its dendrites release GLU, which acts on autoreceptors to re-excite the cells, as first shown *in vitro* by Jahr and Nicoll (1982). As with the secondary dendrites, GLU receptors are present on the apical dendritic tuft. The EPSP amplitude is also enhanced by excitatory interactions between the glomerular tufts (Carlson et al., 2000; Schoppa and Westbrook, 2002; Urban and Sakmann, 2002). This enhanced EPSP has been called a long-lasting depolarization (LLD). It is dependent on the AMPA, but not the NMDA, component of the EPSP. The depolarization of the EPSP is further amplified by voltage-gated channels in the tuft membrane (see later). There is evidence for self-inhibition of PG cells through GABA_A receptors, which can contribute to intensifica-

tion of mitral/tufted cell excitation (Smith and Jahr, 2002). These mechanisms give the mitral cell response an all-or-nothing property (first observed by Levetau and MacLeod *in vivo*, 1965), which may be important for signal-to-noise enhancement.

Tufted Cells. As discussed earlier, these are divided into several types, with genetic and biochemical properties different from those of mitral cells.

Early experiments revealed that tufted cells have lower thresholds than mitral cells for activation by ON volleys (Scott, 1981; Schneider and Scott, 1983; Orna et al., 1984). As noted earlier, this appears to be an expression of the size principle, first laid down in the spinal cord, where motoneurons are recruited starting with the smallest and ending with the largest (see Chap. 3). It is believed that this reflects the fact that small motoneurons are activated by low to moderate levels of afferent activity, with the largest motoneurons activated only for extremes of motor output. By analogy this would imply that tufted cells transmit most of the activity through the olfactory bulb, with mitral cells activated only by the strongest inputs. This hypothesis awaits testing. Others have suggested that the mitral and tufted cell populations are similar to the different classes of ganglion cell in the retina in providing for parallel processing channels with different properties (see earlier).

As in mitral cells, tufted cells respond to a single ON volley with an EPSP–IPSP sequence. Christie et al. (2001) report that in identified tufted cells in the rat olfactory bulb slice, dendrodendritic recurrent inhibitory currents in response to an injected voltage pulse are dependent on NMDA, but not on non-NMDA, receptors, similar to the results of Schoppa et al. (1998) in mitral cells (see earlier). Because of the difference in cell size, the extent of lateral inhibition in tufted cells is less than that in mitral cells.

Glomerular Layer Cells. As we have seen, the glomerular layer contains several types of cell. Early *in vivo* studies indicated that an ON volley can elicit either limited spike responses (one or two spikes) or an intense burst in single cells in the glomerular layer, in rabbit (Shepherd, 1963; Getchell and Shepherd, 1975a,b; Fig. 5.11A), in cat (Freeman, 1974), and in rat (Schneider and Scott, 1987; Wellis and Scott, 1990). The spikes in some of the burst responses showed fast prepotentials, suggesting patches of excitable membrane in the dendrites (Shepherd, 1963). The decrementing spike amplitudes during the burst were indicative of a large underlying depolarization.

Recent studies in the rodent olfactory bulb slice have confirmed and extended these findings and have showed that different types of glomerular layer cells have different spiking patterns, giving insight into the mechanisms. If we focus on the burst response, it has been shown to have three components: the initial EPSP, a slow LTS, and rapid action potentials. The action potentials are Na^+ dependent (blocked by QX314 in the pipette), whereas the LTS has the properties of a low-voltage activated (LVA) Ca^{2+} current (blocked by Ni^{2+} and MPS [α -methyl- α -phenylsuccinimide]) (McQuiston and Katz, 2001). The LTS and spikes can be evoked by both injected depolarizing current and synaptically by a single ON volley (see Fig. 5.11B).

The burst responses have been of particular interest because of their similarity to the LVA bursts of thalamic neurons (see Chap. 8). It has been noted (McQuiston and Katz, 2001) that, as in the thalamus, the bursts give these cells the ability to oscillate spontaneously. This connects with previous work (Freeman, 1974a,b; Wellis and Scott, 1990)

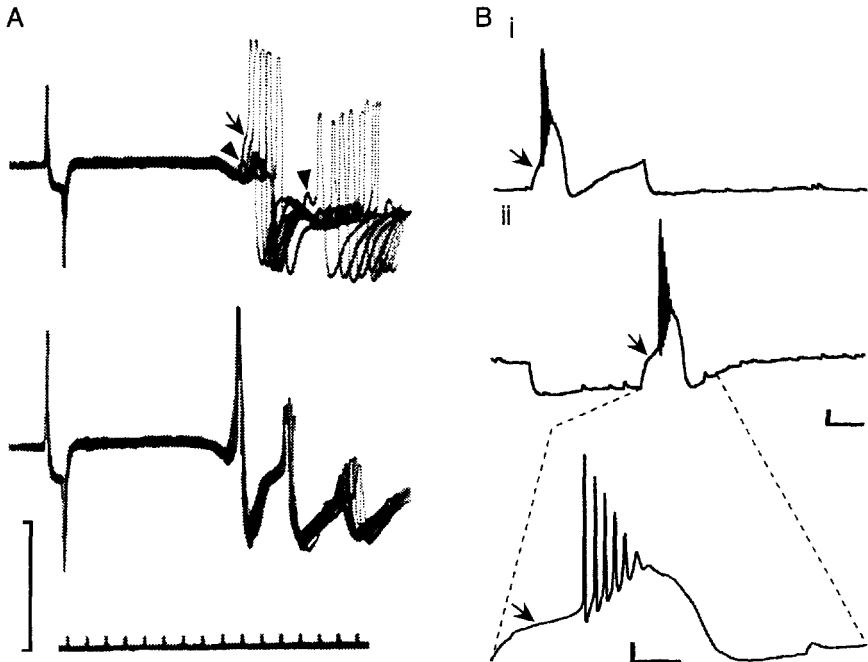


Fig. 5.11. Excitability properties of glomerular layer cells. **A**: Examples of a bursting spike response to a single ON volley in the in vivo rabbit. Note A-B inflection (arrow) and fast prepotentials (arrowhead) in top recording trace. [Modified from Shepherd, 1963.] **B**: Patch recordings of burst responses in mouse olfactory bulb slice, showing Na spikes arising from LTS (arrows). see text. [From McQuiston and Katz, 2002.]

indicating that PG cells are extensively interconnected, a necessary condition for spread of synchronization. This network may be the basis for the rhythmical reciprocal activation and depression of PG cell populations during sniffing (Onoda and Mori, 1980), which is believed to contribute to the control of the oscillatory responses of mitral cells during sniffing and odor processing. The LVA responses would appear to be well suited to contribute to this oscillatory control (McQuiston and Katz, 2001).

Which cells are responsible for the different response types? Staining of recorded cells shows that most cells producing bursts are either external tufted cells or PG cells. Of the nonbursters, most were short-axon cells. However, there was overlap of physiological type among most of the morphological types. A similar lack of strict structure-function correlation has been found in other interneuron populations, for example, in the hippocampus (see Chap. 11).

The basis for these differences in firing patterns obviously depends in the first instance on the expression of genes for different channel types and their subunits (see Chap. 2). Na^+ currents have been demonstrated in PG cells of the frog olfactory bulb (Bardoni et al, 1995), whereas considerable heterogeneity has been found in K^+ channel distributions. There is evidence from a number of studies in other cell types that dendritic K^+ channel properties and distributions mediate exquisite control over spike

firing patterns (e.g., hippocampal pyramidal neurons, see Chap. 11). These studies serve as a caution that there is no simple relation among genotype, morphological type, and functional phenotype in neurons.

Different subpopulations of glomerular layer cells are believed to have excitatory or inhibitory actions on neighboring glomeruli (Shepherd, 1963; Freeman, 1974; Getchell and Shepherd, 1975b). Recent studies suggest that GABA-containing PG cells are inhibitory to nearby glomeruli, whereas SA cells are excitatory to more distant glomeruli (A. Puche, personal communication). Depending on the cell and dendritic targets, these actions may ultimately be excitatory or inhibitory on transmission from the glomeruli through the mitral/tufted cell dendrites to output to the olfactory cortex. Glomerular layer cells thus appear to play complex roles in glomerular layer processing. The different subpopulations of glomerular layer cells, on the basis of biochemical markers, adds to this complexity (see next section).

NEUROTRANSMITTERS AND NEUROMODULATORS

One might suppose that the olfactory bulb, with its relatively stereotyped architecture, would have a simple set of neurotransmitters to mediate its synaptic interactions. In fact, the opposite is true: the olfactory bulb is enormously rich in neuroactive substances, rivaling any other brain region in this respect. Why this should be so is likely related to the fact that the olfactory bulb mediates information about crucial behaviors such as feeding, social organization, and reproduction, which are dependent on a number of behavioral state variables controlled through multiple neuroactive substances.

A summary of the putative neurotransmitter and neuromodulator substances of the main type of neurons is shown in Fig. 5.12. Glutamate and GABA have been discussed; here, we focus on the neuromodulators as they relate to the main types of synaptic connections within the basic circuit (reviewed in Halasz and Shepherd, 1983; Nickell and Shipley, 1994; Trombley and Shepherd, 1994; Shipley and Ennis, 1996).

OLFACTORY SENSORY NEURONS

The sensory neurons contain a special peptide (olfactory marker protein [OMP]) and have a high concentration of the dipeptide carnosine (reviewed in Margolis, 1988). As indicated in the previous section, many studies have indicated that glutamate is a transmitter at the olfactory nerve synapse onto the mitral, tufted, and PG cell dendrites in the glomeruli, with both AMPA and NMDA components. Glutamate is co-localized with carnosine in axon terminals in the glomeruli (Margolis et al., 1994). Several glutamate receptor ionic and metabotropic subtypes are found in the glomerular layer (see Giustetto et al., 1997), but it is not yet determined whether they are related to post-synaptic targets of the olfactory nerves or of the presynaptic dendrites in the glomeruli (see Shipley and Ennis, 1996, for a review).

GLOMERULAR LAYER CELLS

Dopaminergic Cells. Histofluorescence and EM autoradiography showed that some PG cells are positive for the DA-synthesizing enzyme tyrosine hydroxylase (TH) (Halasz et al., 1977). The dopamine is transneuronally regulated; degeneration and regeneration of olfactory nerves following olfactory nerve transection are paralleled by a decrease and

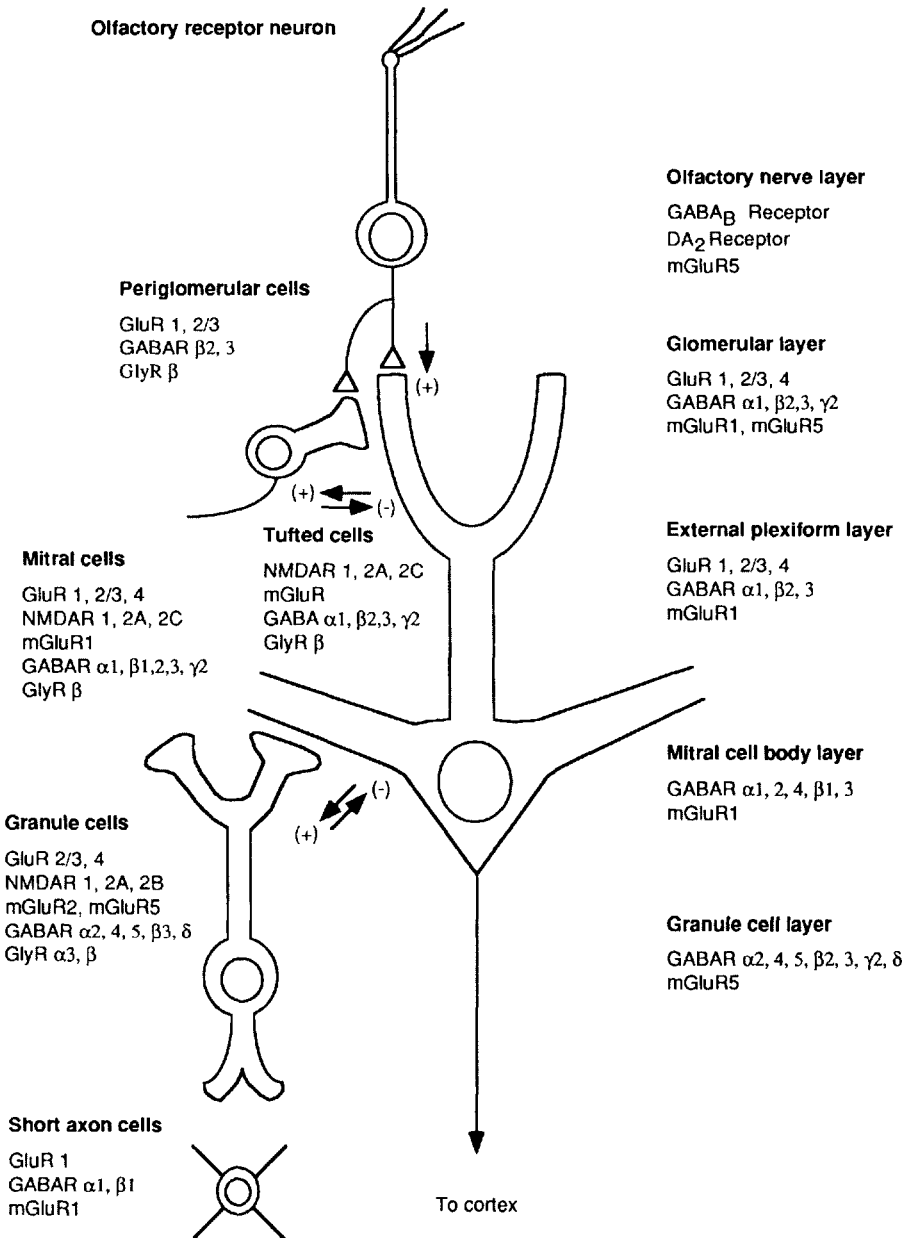


Fig. 5.12. Schematic diagram summarizing the cellular and laminar distribution of receptor subunits for amino acid transmitters in the olfactory bulb. Glutamate AMPA receptor subunits: GluR1, 2/3, 4. Glutamate NMDA receptor subunits: NMDA R1, 2A, 2B, 2C. Metabotropic glutamate receptors: mGluR1, 2, 5. GABA_A receptor subunits: α1, 2, 3, 4, 5; β1, 2, 3; γ2. Glycine receptor subunits: α3,β. [From Trombley and Shepherd, 1997.]

increase in DA and dihydroxyphenylacetic acid (DOPAC) levels in the olfactory bulb (Baker et al., 1983; Baker, 1988). Dopamine has been shown to inhibit synaptic transmission from the olfactory nerves by acting presynaptically on D2 receptors (Hsia et al., 1998; Berkowicz and Trombley, 2000; Ennis et al., 2001) and postsynaptically on GABA_A receptors (Brunig et al., 1999).

A summary of the relations between TH-positive cells and other glomerular layer cells based on immuno-EM is shown in Fig. 5.13. There are at least four distinct populations of glomerular layer cells that interact within the glomerulus via dendrodendritic synapses. One of these has calbindin immunoreactive dendrites that do not receive any direct olfactory nerve input, although they do establish a reciprocal synaptic arrangement with mitral/tufted cell dendrites. In contrast, GABA immunoreactive dendrites receive direct olfactory nerve synapses, and in turn make symmetrical (type 2, presumably inhibitory) synapses onto mitral/tufted cell dendrites. TH immunoreactive dendrites receive asymmetrical synapses from both the olfactory nerve and mitral/tufted cell dendrites and in turn, make symmetrical synapses onto mitral/tufted cell dendrites. The degree to which the olfactory nerve input onto each of the types of cells, including the mitral/tufted cells, is homogeneous is not known. If the MRR or threshold differed only slightly for olfactory receptor cell axons that terminate on GABA immunoreactive cells versus mitral/tufted cells within a glomerulus, a complex sequence of information processing could occur that would include not only the feedback inhibition associated with dendrodendritic synapses, but a proactive feedforward inhibition as well. Improving our understanding of the dendritic targets of single olfactory receptor cell axons and continuing efforts to unravel the Gordian Knot of the glomerulus will help to address this question.

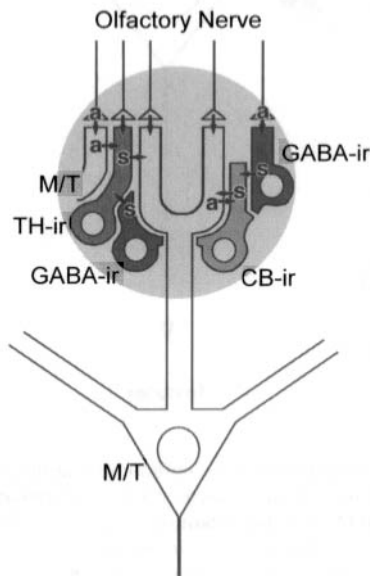


Fig. 5.13. Summary of synaptic relations between glomerular layer cells as demonstrated by immuno-labelling with electron microscopy (ir). Abbreviations: a, asymmetrical synapses; CB, calbindin; M/T, mitral/tufted cell; s, symmetrical synapses; TH-ir, tyrosine hydroxylase immunoreactive. See text. [Courtesy of K. Toida.]

GABAergic Cells. Some PG cells (approximately 20% in rat) and their dendrites contain glutamic acid decarboxylase (GAD), the GABA-synthesizing enzyme, as well as taking up GABA (Ribak et al., 1977). In rabbit olfactory bulb slice preparations, GABA-activated whole cell currents and single channel currents recorded from PG cells show GABA_A receptor properties (e.g., block by bicuculline: Bufler et al., 1992). GABA also acts on GABA_A receptors to elicit inhibitory currents in cultured rat olfactory bulb cells (Trombley and Shepherd, 1994). Evidence for inhibitory actions of glycine on PG and other bulbar neurons has also been obtained (see later).

DA and GABA may be co-localized in the same PG cell in some species and restricted to separate PG cell subpopulations in others (Mugnaini et al., 1984; Baker, 1988; see Fig. 5.12). This demonstrates two general principles: (1) a single morphological cell type may be fractionated into more than one neurotransmitter subtype, and (2) the mix of neurotransmitters in a single morphological cell type is phylogenetically flexible. Dopaminergic and GABAergic subpopulations of intrinsic neurons are also seen in other parts of the nervous system (cf. retina, see Chap. 6). As pointed out by Oertel et al. (1982), such dual subtypes may reflect an important principle of synaptic circuits.

PG cells have been postulated to have either excitatory or inhibitory synaptic actions at their dendrites and axons (see earlier). It is tempting to presume that both DA and GABA (as well as glycine) have inhibitory actions. However, the issue may not be that simple. For example, there is still controversy about whether DA has excitatory or inhibitory actions in the basal ganglia (see Chap. 9). Excitatory actions of GABA mediated by GABA_A receptors are well known during early development and at distal dendritic sites (cf. Chap. 1, 2). In the olfactory glomerulus, there is electrophysiological evidence that GABA may have excitatory actions (Rhoades and Freeman, 1990), as well as electron spectroscopic evidence for accumulations of Cl⁻ in intraglomerular dendrites, which could reflect reversed chloride gradients underlying excitatory GABAergic actions (Siklos et al., 1995).

MITRAL CELLS

Glutamate as the transmitter from the presynaptic mitral cell soma-dendrites was first indicated by the finding of NMDA receptors in the EPL of the olfactory bulb (Colman et al., 1987). The functional evidence for glutamate, acting at both AMPA and NMDA receptors on mitral/tufted and PG cell dendrites, to mediate activation of the granule cells, has been fully explained earlier. As also indicated, the released GLU acts on auto-receptors on the mitral cell dendrites (see Fig. 5.12). Glutamate also appears to be the transmitter of the mitral axon terminals in the olfactory cortex (see Chap. 10). Because the mitral cell has synaptic output from both its dendrites and axon, it provides a model for testing whether the same transmitter is released from all synapses of a neuron, a generalization known as *Dale's law* (Dale, 1935).

TUFTED CELLS

It is generally believed that tufted cells share the same neurotransmitters at their dendritic and axonal output synapses with mitral cells. However, some tufted cells appear to be dopaminergic, which makes them more similar to PG cells (Halasz et al., 1977). This may be correlated with other differences between mitral and tufted cells, as noted earlier.

GRANULE CELLS

GABA. Numerous studies point to GABA as the neurotransmitter released by the dendrodendritic synapses of the granule spine onto the mitral/tufted cell dendrites. GCs take up GABA (Halasz et al., 1978). The GABA-synthesizing enzyme GAD has been localized to the granule cells and their dendritic spines by EM immunohistochemistry (Ribak et al., 1977).

In the *in vitro* preparation of the turtle olfactory bulb, the early hyperpolarizing components of the IPSP in a mitral cell have several GABAergic properties: they are blocked by bicuculline and low Cl^- in the bathing medium, reversed by Cl^- filled electrodes, associated with an increased conductance, and have clear reversal potentials (Mori et al., 1981b; Nowycky et al., 1981a,b; Jahr and Nicoll, 1982). These reflect properties of GABA_A receptors. Similar evidence has been obtained in the salamander (Wellis and Kauer, 1993). The later, slow, inhibitory potential (I_S) does not have a reversal potential, suggesting that it may be mediated by a different synaptic receptor (possibly GABA_B receptors) or at a more distant locus on the mitral cell dendrites (Mori et al., 1981c).

The AMPA receptors on olfactory bulb GCs have a low permeability to Ca^{2+} (Jarde-mark et al., 1997).

Glycine. Glycine was found to evoke chloride-mediated membrane currents in rabbit olfactory bulb slices (Bufler et al., 1992) and to have powerful inhibitory effects on both mitral/tufted cells and GCs in culture (Trombley and Shepherd, 1994). Immunoreactivity for monoclonal antibodies against glycine and glycine receptors is found in the EPL and around mitral cell bodies (van den Pol and Gorcs, 1988). *In situ* hybridization experiments have shown that the alpha 3 glycine receptor subunit, the ligand-binding subunit of the strychnine-sensitive glycine receptor, is present in the olfactory bulb (Malioso et al., 1991). Studies in the olfactory bulb thus provide some of the best indications that glycine is a neurotransmitter in the brain as well as in the spinal cord (cf. Kuhse et al., 1991).

PEPTIDES

The olfactory bulb offers a smorgasbord of delectable peptides. Besides carnosine, it is especially rich in taurine, thyroid hormone-releasing hormone (TRH), insulin, and cholecystokinin (CCK).

Absolute levels are not the only measure of the significance of a neuroactive substance; location at a critical site in a synaptic circuit is even more significant. Examples of this are substance P, present in tufted cells, and enkephalins, present in both PG cells and GCs. Nicoll et al. (1980) studied the effect of a stable enkephalin analogue D-Ala-Mets-enkephalin (DALA) in the *in vitro* turtle olfactory bulb. DALA in the bathing medium reduced the IPSPs induced in mitral cells, especially the recurrent inhibition elicited by intracellular activation of a mitral cell. They suggested that the primary action of enkephalins is to suppress inhibitory interneurons, thereby producing indirectly an increase in excitability of the principal neurons. This would be an example of disinhibition within a synaptic circuit (see Chap. 1) and illustrates again how an understanding of synaptic organization is essential for interpreting pharmacological actions.

Peptides are co-localized with neurotransmitters at most synapses in the olfactory bulb, but the significance is not yet understood. There is evidence that some enkephalin is contained in granule cells, suggesting that it may be co-released with GABA and have a direct action on mitral cells (Bogan et al., 1982; Davis et al., 1982). One possibility is that it produces the slow inhibitory potential (see earlier). There are, however, many types of interactions between transmitters and peptides, as discussed in Chap. 2.

GASEOUS MESSENGERS

Histochemical staining for nitric oxide synthase (NOS) and NADPH diaphorase has shown that the highest densities of NOS occur in the cerebellum and olfactory bulb, a finding supported by in situ mRNA hybridization for NOS (Bredt et al., 1991). The stained elements include mainly fibers within the glomeruli, subpopulations of PG cells, and fibers around the GCs. Neighboring glomeruli characteristically show distinct levels of staining (Zhao et al., 1994). Mitral, tufted, and granule cells are not stained.

An interesting point regarding the NO released from subsets of fibers and from PG cell dendrites within a glomerulus is that their action would likely be confined to that glomerulus because of the short-acting nature of NO (Breer and Shepherd, 1993). NO thus appears well adapted to contribute to the functioning of the glomerulus as a unit. Neighboring glomeruli could function relatively independently because of the confinement of NO in the glomerulus within which it is released.

It has been hypothesized (Breer and Shepherd, 1993) that the NO released from PG cell dendrites may act on neighboring dendrites, a novel form of local diffuse dendrodendritic interaction to supplement the specific synaptic interactions between PG dendrites and the dendrites of mitral/tufted cells (see earlier). A likely target of NO is soluble guanylate cyclase (sGC). In situ hybridization studies indicate localization of sGC mRNA in mitral/tufted cells as well as mRNA for subunits of the cyclic nucleotide-gated (CNG) channel (Kingston et al., 1996). It can therefore be hypothesized that activation of subsets of PG cells may lead to modulation of CNG channels in mitral/tufted cells, which could alter the excitability of those cells and the processing of odor output from the glomeruli.

CENTRIFUGAL FIBERS

As noted previously, there are three main types of centrifugal fiber, each associated with a specific classic neurotransmitter.

Noradrenaline (NA)-containing fibers arrive from the LC and distribute mostly within the granule cell layer and IPL, as well as the glomerular layer (see Fig. 5.2 above). The actions of NA on mitral cells are complex. One action suggested by the ionophoretic studies of Jahr and Nicoll (1982) is that NA acts on GCs to reduce their release of GABA. In primary cultures of bulb cells, NA acts on an alpha 2 receptor to suppress inhibition of mitral cells (Trombley and Shepherd, 1993). The mechanism appears to involve reduction of a Ca^{2+} conductance in the presynaptic terminal (Trombley, 1993). Recent studies support this mechanism (Czesnik et al., 2001). In addition, evidence has been obtained for a direct excitatory action of NA on mitral cells (Hayar et al., 2001).

Serotonin-containing fibers arrive from the dorsal raphe. They distribute preferentially to different laminae in different species (Takeuchi et al., 1982). Of special inter-

est are the fibers that terminate within the glomeruli, thus permitting a brainstem system direct access to the initial level of input processing of olfactory signals. These could be significant in mediating behavioral-state variables set by brainstem systems involved in hunger, satiety, arousal, and sleep. Judging from ionophoresis experiments, the action of serotonin on mitral cells is inhibitory (Bloom et al., 1971).

Cholinergic fibers arrive from the basal forebrain and distribute relatively evenly through the laminae. According to Rotter et al. (1979), the external plexiform layer "has the highest concentration of muscarinic receptors in the brain . . . and high levels occur in the glomerular layer, mitral cell layer, and the granule cell layer" as well. Because these fibers terminate mainly on GC spines, they are well placed to modulate the dendrodendritic inhibition of mitral cells at the level of output control. Ionophoresis of ACh in vivo has mostly depressant effects on mitral cell firing (Bloom et al., 1971), but ACh action has not yet been studied in vitro or interpreted in relation to the specific details of synaptic organization. A recent study has revealed multiple and opposing actions of ACh in modulating bulbar neurons (Castillo et al., 1999).

DENDRITIC PROPERTIES

Each of the three main cell types of the bulb provides a model for illustrating important principles of dendritic signal processing.

MITRAL CELL

The mitral cell dendritic tree is not one homogeneous unit; rather, it is divided into several compartments, each with its own distinct function. The *glomerular dendritic tuft* is concerned primarily with reception of the olfactory input and initial synaptic processing; it is analogous in this respect to the entire dendritic tree of many other neuronal types, such as a thalamic relay neuron. The *primary dendritic shaft* has a distinct function: the transfer of information from the glomerular tuft to the cell body; in this radial transfer function, it is analogous to a retinal bipolar cell. The *secondary dendritic branches*, finally, are mainly concerned with controlling bulbar output through interactions with the GCs. These divisions are so distinct that one can regard the mitral cell as not one but three cells, with transfer between them taking place through intraneuronal continuity rather than interneuronal synapses. This means that we must assess dendritic properties in relation to the different functions of each of these entities. We consider their electrotonic and active properties.

Glomerular Tuft. We have seen that the glomerular tuft forms a small dendritic tree within an olfactory glomerulus. The trunks of the tuft have relatively small diameters of 1–3 μm . As a first approximation, assume that each dendritic trunk divides in such a way as to conform to the $3/2$ power constraint on the diameter (see Rall, 1977; Johnston and Wu, 1995; Segev, 1995; Shepherd, 2003a). Each trunk will thus give rise to a small equivalent cylinder; taken together, they will form an equivalent cylinder for the entire tuft. Assuming a range of values for electrical parameters that is typical of neurons, we can obtain an estimate of a characteristic length of 150–600 μm for the case of 1- μm -diameter trunks and 300–1000 μm for 3- μm -diameter trunks.

These estimates are considerably higher than the actual extents of the tufts, which range up to 150–200 μm . The electrotonic length ($L = x/\lambda$) of an equivalent cylinder for the tuft might, therefore, be estimated at less than 1, and possibly less than 0.5. Thus, the smaller branches of the tuft are counterbalanced by their shorter lengths, an expression of the *scaling principle* (see Shepherd, 2003a). Because of the short electrotonic length of the tuft, current flow through the tuft must be relatively effective by passive means alone, and synaptic responses to sensory inputs can spread effectively to the primary dendrite. Evidence for this effective spread is seen in dual patch recordings from the distal dendrites and computational simulations (Midtgaard et al., 2002), which are discussed further later.

Primary Dendrite. This is usually a single unbranched process and therefore easy to model. In the mammal, a diameter of 6 μm , R_m of 50,000 ohm cm^2 , and R_i of 200 ohm cm gives an estimate of the characteristic length of a typical primary dendrite in the range of 2000 μm . Because a primary dendrite in the rat has a length of about 400 μm , the electrotonic length is much less than 0.5. Electrotonic spread should, therefore, be relatively effective through such a process (Rall and Shepherd, 1968).

These calculations are relevant to understanding action potential initiation in this neuron. Experiments show how, as the amount of distal depolarization increases, the site shifts from the initial segment to the distal dendrite (Fig. 1.9). Simulations provide insight into how this shift is dependent on an interplay between the gradients of electrotonic depolarization and the density of Na^+ channels. First, a realistic compartmental model of the mitral cell was constructed that could simulate the action potentials recorded experimentally at the soma and distal dendrite (Fig. 5.14A) as they shifted from initiation first in the soma (s) for the case of weak distal currents (A, left) to the dendrite (d) for strong currents (A, right) (see the experimental recordings in Fig. 1.9). Plotting of gradients of membrane potential in Fig. 5.14B along the axon-soma-dendritic axis in response to the weak distal stimulation shows that the much higher excitability of the initial axon segment causes it to respond first. With stronger distal stimulation (Fig. 5.14C) the stronger depolarization combined with the moderate local excitability of the dendrite causes action potential initiation to shift to the dendrite. The gradients of depolarization thus reflect the combined electrotonic and active properties of the axon-soma-dendritic axis.

Secondary Dendrites. The steps for modeling the passive properties of the secondary dendrites follow those already outlined. Individual secondary dendrites are typically 1–3 μm in diameter and 500–1000 μm in length. Their electrotonic lengths, as well as the values for the equivalent cylinder for the entire tree, have been estimated to lie in the range of 0.5–1.0. Thus, electrotonic coupling is relatively close along the secondary dendrites, meaning that passive potentials spread effectively through them. What about action potentials?

Evidence regarding the extent of active invasion has been obtained by patch recordings and Ca^{2+} imaging from microscopically observed secondary dendrites in rodent olfactory bulb slices. In these experiments, a secondary dendrite has been shown to be capable of supporting full action potential propagation throughout its extent (Fig. 5.15). It has further been shown that propagation is controlled by GC inhibition (Margrie et

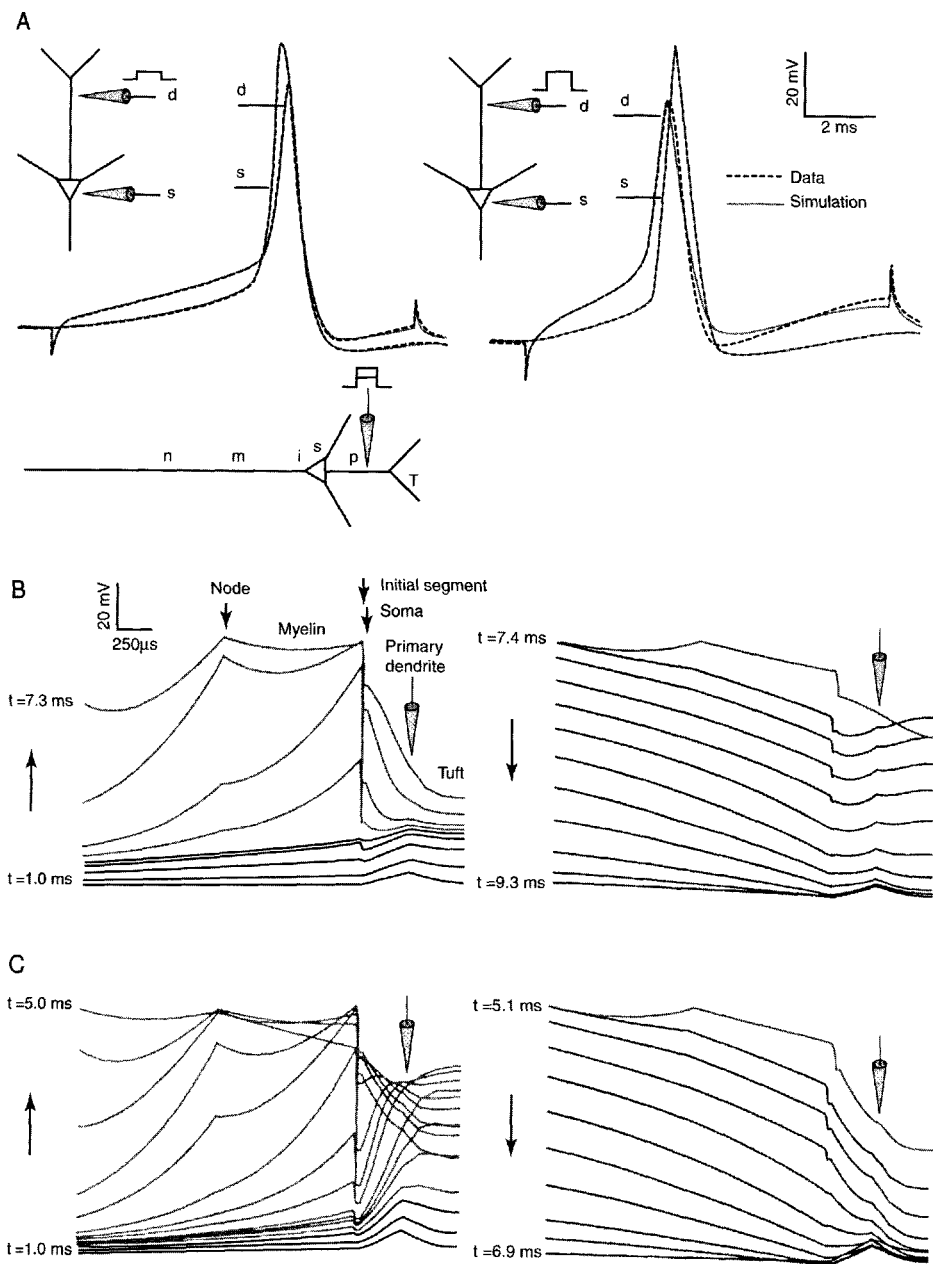


Fig. 5.14. Simulations of shifts of action potential initiation in a mitral cell. **A**: Experimental and simulation traces superimposed for weak (left) and strong (right) distal current stimulation. **B**: Radial voltage gradients for weak distal stimulation. **C**: Radial voltage gradients for strong distal stimulation. Abbreviations: n, nerve axon; m, myelinated segment; i, initial segment; s, soma; p, primary dendrite; t, terminal dendritic tuft. See text. [From Shen et al., 1999.]

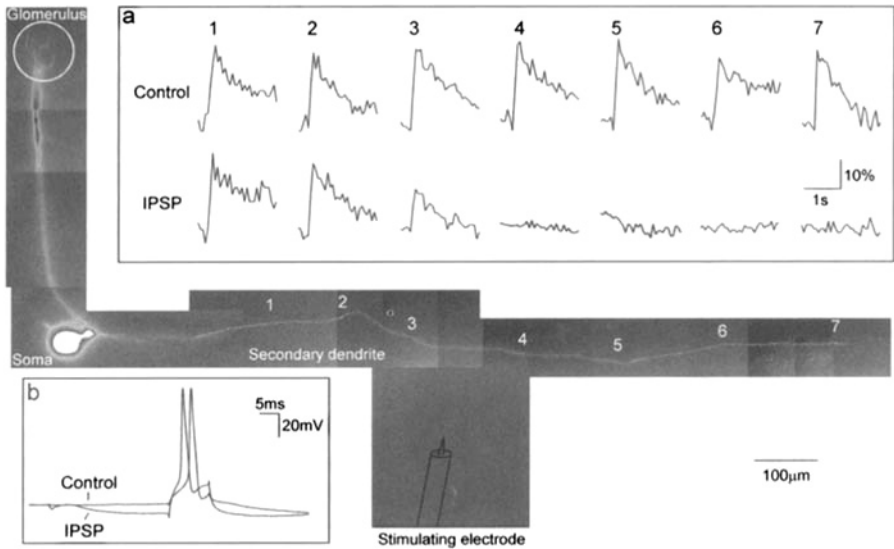


Fig. 5.15. Action potential invasion of a secondary dendrite of a mitral cell. **a**: Control: invasion of an action potential from the soma to the end of the secondary dendrite (site 7), as shown by Oregon green BAPTA-1 fluorescence, a Ca^{2+} -sensitive dye. IPSP: local IPSP at site 3 blocks action potential invasion. Fluorescence image retouched from color original. **b**: Patch recording from soma showing action potential response and IPSP. See text. [From Xiong and Chen, 2002.]

al., 2001; Lowe, 2002; Xiong and Chen, 2002) and intrinsic K^+ conductances (Christie and Westbrook, 2002). These results suggest that the long lengths of secondary dendrites provide a wide anatomical substrate for mitral cells in one glomerular module to interact with mitral cells in many other modules and that their actual functional domains are subject to constant regulation depending on the interactions between neighboring glomerular modules.

As we have seen, regenerative calcium conductances are important properties of dendritic membranes. In many neurons, they play key roles in promoting intradendritic transmission and synaptic integration (see Chap. 2, and most other chapters). The experiment shown in Fig. 5.11B demonstrates that, in addition, they may control Ca^{2+} entry and synaptic transmitter release in presynaptic cell bodies and dendrites. In fact, a number of types of Ca^{2+} currents have been identified in acutely isolated mitral cells of the rat, including I_T , I_L , and I_N (Wang et al., 1996).

GRANULE CELL

Because the GC lacks an axon, its dendritic properties are obviously crucial to understanding its input-output functions.

The branching tree within the EPL can be represented by an equivalent cylinder; assuming branch diameters of $0.2\text{--}0.8\ \mu\text{m}$, an electrotonic length of about 0.4 can be estimated (Rall and Shepherd, 1968). The shaft diameter of the granule cell is of the order of $1\ \mu\text{m}$; for an average shaft length of $600\ \mu\text{m}$, an electrotonic length of 1.7 can be estimated for the model of the combined tree and shaft.

Such a model was used to simulate synaptic depolarization of the granule spines in the EPL. It indicated that synaptic depolarization gives rise to the extracellular potentials generated just after an antidromic impulse invades the mitral cell dendrites (Phillips et al., 1963). When the mitral cell model and the GC model were joined in sequence, it could be postulated that the EPSP in the granule dendritic spines is due to a dendrodendritic input from the mitral secondary dendrites. As described in a previous section, the localization and timing indicated that the spine EPSP activates inhibitory synapses onto the same secondary dendrites, to produce the long-lasting IPSP recorded in the physiological experiments (Phillips et al., 1963).

Dendritic Spines. The properties of the GC dendritic spines were postulated to be critical in controlling the relative effectiveness of recurrent inhibition from a single spine as well as lateral inhibition mediated by spread of activity to neighboring spines (see Fig. 5.6, above). This question was first addressed directly by making precise measurements of dendrites and spines in reconstructions from serial electron micrographs (Woolf et al., 1991) and in material observed in the high-voltage EM (Greer, 1988). Computational models of these measured structures were constructed to explore the spread of activity.

An example of two common arrangements of spines is shown in Fig. 5.16. In the top panel, spines (A–D) are arranged in a linear fashion along the dendritic branch (E). Excitatory input (from a mitral/tufted cell dendrite) to spine C produces a large EPSP in C, which undergoes electrotonic decrement in spreading into the branch E. However, there is very little decrement in spreading in the other direction, from the branch into the other spines (A, B, D), because of the impedance mismatch between dendrite and spines. A different arrangement is shown in the bottom panel, where several spines (B–D) arise from a common stem, a so-called complex spine. Spread of activity from C to the neighboring spines now occurs in distinct steps. We have discussed these considerations in terms of spread of electrical potential, but they also apply to the diffusion of Ca^{2+} and other ions and metabolites between spine head and dendritic branch (Woolf and Greer, 1994).

These results support the conclusion that electrotonic spread from spine to spine is considerable over the short distances involved. It appears therefore that lateral inhibition can be mediated by passive spread alone through the dendritic tree in the EPL. The inhibition is spatially graded according to the electrotonic decrement of the potentials in the tree. Depending on the spatial arrangements, individual spines may act as functional subunits in the manner discussed in Chap. 1. A computational study has shown how groups of spines may function together as a complex input-output population (Woolf et al., 1991), dependent on the underlying membrane electrotonic properties, in much the same way that such units arise in the dendrites of amacrine cells (Koch et al., 1982).

These considerations do not rule out the possibility of active properties of the granule dendritic membrane in addition to electrotonic properties. The original model of the GC did not rule out active spine properties but rather indicated that active properties must be limited and not lead to propagation from the branches in the EPL into the main dendritic shaft (Rall and Shepherd, 1968). Subsequently, Jahr and Nicoll (1982) found that recurrent inhibition persists despite the presence of TTX (see Fig. 5.8, above),

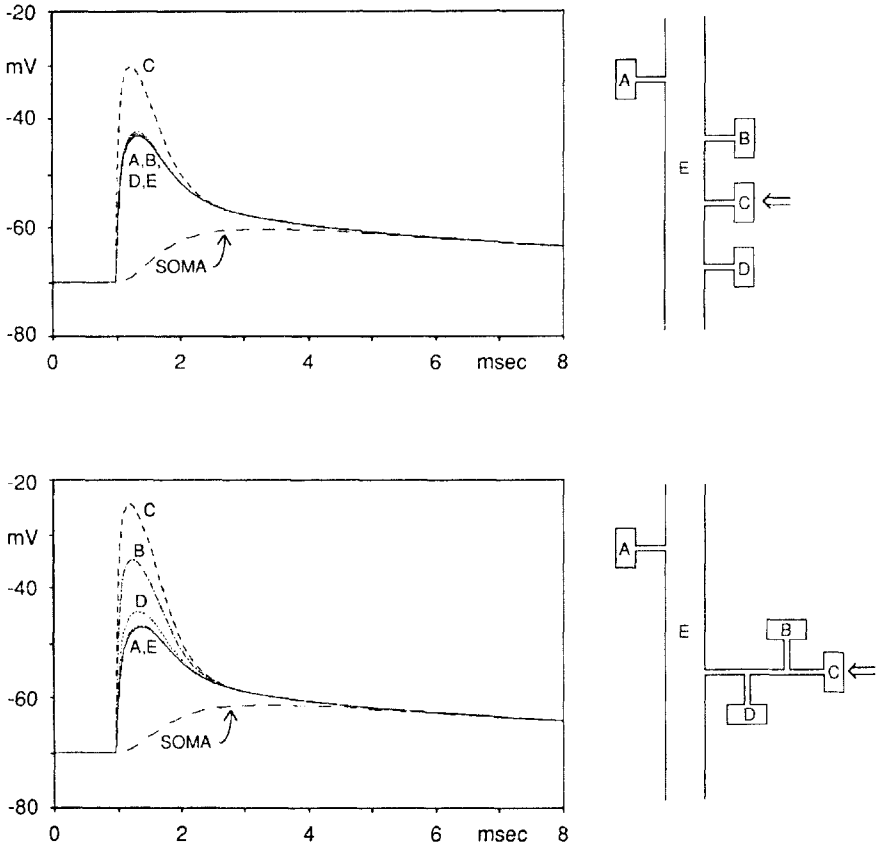


Fig. 5.16. Electrotonic models of granule cell dendrites and spines, based on reconstructions of serial electron micrographs. An excitatory synaptic conductance change was simulated in spine C, and the synaptic potentials were measured in each spine (A–D) and in the dendritic branch. Upper panels: linear arrangement of spines. Lower panels: a single and a complex spine. For these simulations, $R_m = 4000 \text{ ohm cm}^2$. [From Greer, 1988; T. B. Woolf, C. A. Greer, and G. M. Shepherd, unpublished observations.]

implying that voltage-gated sodium channels do not contribute to the potentials in granule dendritic spines. Further evidence is needed on how granule cell active properties may contribute to lateral inhibition.

PERIGLOMERULAR CELL

Taking into account both the smaller diameters and the shorter lengths of the branches, it is reasonable to conclude that an equivalent cylinder for a PG cell tuft would be similar to that for the mitral tuft, that is, with a characteristic length of less than 1 and perhaps of less than 0.5. This is, again, an expression of the scaling principle for dendritic trees of different size. The intense depolarization underlying a burst response (see earlier) indicates a close electrotonic coupling between the EPSP elicited by the ON volley, the site of generation of the LTS-dependent depolarization, and the Na^+ action potentials riding the slow depolarization.

PG cell functions appear to be exquisitely dependent on levels of input activity. Electrophysiological studies have suggested that at threshold there is mainly straight-through excitation of mitral cells by receptor axons; long-lasting facilitation is sometimes detectable (Getchell and Shepherd, 1975a,b). As input activity increases, the activation of PG cells, both by direct olfactory axon input and by indirect dendrodendritic synapses, begins to bring about inhibitory feedback from the PG cell dendrites. Small EPSPs probably mediate only local input-output paths through the dendrites; moderate EPSPs will lead to more extensive inhibitory actions within a glomerulus; and large EPSPs, by spreading to the axon hillock, set up impulses that mediate inhibition of dendrites belonging to neighboring glomeruli.

Studies of responses to natural stimulation with odors have demonstrated even more complex interactions, including the presence of an initial brief hyperpolarization at weak levels of stimulation (see next section). It thus appears that several levels of interaction can be identified within the glomerular layer, governed by the amplitudes of EPSPs and their electrotonic spread within the PG cell dendrites. Functionally, these interactions enhance transmission at detection thresholds and provide the lateral inhibition necessary for discrimination between odors at higher odor concentrations. The PG cell dendritic tree thus provides for *multiple state-dependent input-output functions*. Similar properties have been postulated for thalamic cells and may apply to other types of cells.

SYNCHRONIZATION DEPENDS ON DENDRITIC PROPERTIES

It has been known since the early work of Adrian (1950) that sensory stimulation leads to oscillatory activity in the olfactory bulb. We discuss three possible contributions to these mechanisms, before taking up the spatial organization of the olfactory bulb in the next section.

Synchronization by GCs. As noted previously, the dendrodendritic interactions have inherent in them a mechanism for temporal gating of mitral cell output. Recent work has added greatly to our understanding of how this may work.

We have seen that GLU released by the mitral cell activates both AMPA and NMDA receptors on the GC spines. It is believed that the long time course of the NMDA receptor-mediated response determines the time course of the GABA output to the mitral cells and thereby the duration of temporal gating of mitral cell output. This duration is under dynamic control by active properties of the granule dendritic membrane, particularly the I_A current (Schoppa and Westbrook, 1999; Segev, 1999). In normal conditions, the AMPA component of the GLU response is sufficient to relieve the Mg^{2+} block but is shunted out by the rapid I_A conductance increase. This leaves the slow NMDA depolarization, which inactivates the I_A channels and persists to control the release of GABA over a long time course to generate the long-lasting IPSP in the mitral cell secondary dendrites. Thus, the duration of the IPSP, and hence the frequency of oscillatory output of the mitral cells, is controlled by the differential interaction of the dendritic I_A conductance with the AMPA and NMDA components of the GC dendritic spine responses.

Synchronization by the Glomerular Tuft. We have seen that an olfactory nerve volley elicits long-lasting depolarizations in mitral cell dendritic tufts through GLU ac-

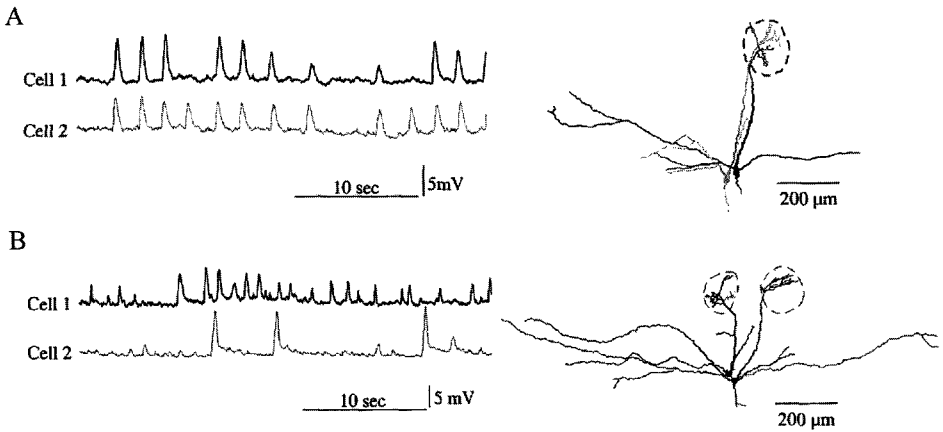


Fig. 5.17. Membrane properties underlying oscillatory activity in olfactory bulb neurons. Oscillatory activity in the glomerular dendritic tufts of mitral cells synchronizes two mitral cells connected to the (A) same but not to different (B) glomeruli. See text. [From Carlson et al., 2000.]

tivation of NMDA receptors and that this slow EPSP is augmented by several mechanisms, including GLU autoreceptors. Studies (Carlson et al., 2000; Schoppa and Westbrook, 2001; Puopulo and Belluzi, 2001) show that stronger volleys elicit a depolarization that oscillates at approximately 2 Hz (see Fig. 5.17). Similar oscillations are elicited by adding NMDA to the bath. Paired recordings showed that mitral cells have synchronous oscillations only if they are connected to the same glomerulus (Fig. 5.17A,B). A persistent depolarizing current dependent on NMDA and metabotropic GLU receptors underlies the oscillating potentials. The depolarization phases appeared to be due to an action potential-evoked GLU release from a network of mitral cells, whereas the repolarizing phases appeared to be due to local inhibitory circuits and K^+ channels. Evidence was obtained that the oscillations are driven by GLU released from the mitral primary dendrites (and dendritic tuft), presumably due to GLU spillover. The oscillations could be entrained by ON volleys at frequencies up to 8 Hz, indicating that they may operate over physiological ranges. Glial wrapping is absent around individual olfactory nerve terminal to mitral dendrite synapses, which could contribute to synchronization (Kasowski et al., 1999). Faster oscillations are mediated by gap junctions between mitral cell dendritic tufts (Schoppa and Westbrook, 2002).

Synchronization by Mitral/Tufted Cell Membrane Properties. The ionic channels of mitral/tufted cells are a third source of synchronizing mechanisms. Recordings from mitral cell bodies indicate intrinsic membrane oscillations dependent on persistent Na^+ currents and a K^+ current (Chen and Shepherd, 1997; Desmaisons et al., 2000; Davison et al., 2001; Heyward et al., 2001). Further experiments are needed to determine the distribution of these currents in the dendrites, and their contribution to the oscillatory patterns of mitral/tufted cells in response to sensory inputs.

FUNCTIONAL CIRCUITS

How do the interactions between mitral/tufted cells and their two sets of intrinsic neurons—glomerular layer and granule cells—provide the neural basis for the ability to discriminate between odor stimuli? We summarize briefly three key mechanisms: how the olfactory glomeruli are organized to generate odor maps; how the deeper microcircuits may be involved in contrast enhancement; and how the microcircuits may provide for odor memory.

GLOMERULAR MODULES FORM AN ODOR IMAGE

To analyze synaptic circuits during normal function, one must know where one is in the neural map representing the sensory space. Odor stimuli do not carry information about external space as do visual or somatosensory stimuli. The olfactory pathway can therefore use its “neural space” to represent the intrinsic properties of the odor molecules.

These properties are mapped into spatial patterns of glomerular activation, as first shown by the 2 DG method (Sharp et al., 1975) and voltage-sensitive dyes (Kauer and Cinelli, 1987) and by a number of subsequent methods (Table 5.1). Two current examples are shown in Fig. 5.18. The intrinsic optical signal images (A) show differential activation of glomeruli on the dorsal surface of the olfactory bulb by aldehydes from C4 to C7. The fMRI images (B) show differential activation patterns of the entire glomerular sheet for the same compounds.

The general principles of the formation of these maps include the following. The patterns tend to be bilaterally symmetrical. They differ with different odors. The patterns for a given odor are consistent across animals. The patterns increase in extent with increasing odor concentration. The weakest odor concentrations elicit activity in one or a few glomeruli, reflecting input from the olfactory cells with the highest affinity receptors for that odor; stronger stimuli elicit activity more widely within a domain, reflecting input from cells with lower affinity receptors.

The connectivity underlying these maps has been revealed by the finding of olfactory receptor mRNA in the olfactory axons and terminals within the glomeruli (see earlier), showing that receptor-specific glomeruli are bilaterally symmetrical and reproducible from animal to animal (Ressler et al., 1994; Vasssar et al., 1994). In gene-targeted animals, these studies have revealed striking evidence for olfactory receptor-determined maps that could underlie the functional maps (Mombaerts et al., 1996).

Table 5.1. Methods for Demonstrating Odor Maps in the Olfactory Bulb

2-Deoxyglucose (Sharp et al., 1975)
Voltage-sensitive dyes (Kauer and Cinelli, 1993; Cinelli and Kauer, 1994)
Electrophysiological recordings of single units (Mori et al., 1992)
Electrophysiological recordings of local field potentials (Mori et al., 1992)
<i>c-fos</i> mRNA (Sallasz and Jourdan, 1992; Guthrie et al., 1993; Guthrie and Gall, 1995)
Ca ²⁺ -sensitive dyes (Friedrich and Korsching, 1996)
Intrinsic optical signal imaging (Rubin and Katz, 1999; Yoshida et al., 1999)
High-resolution fMRI (Yang et al., 1998)

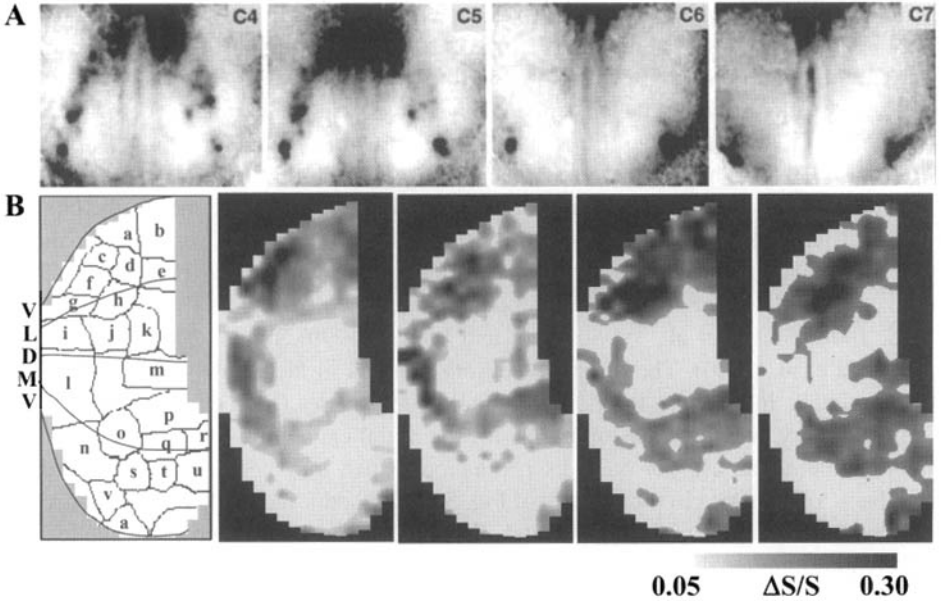


Fig. 5.18. Activity patterns elicited in the olfactory bulb by odor stimulation. **A:** Intrinsic optical signal imaging of glomerular responses in the dorsal bulbar surface to aliphatic aldehydes from C4 to C7. [From Belluscio and Katz, 2001.] **B:** High-resolution fMRI of responses in the glomerular layer throughout the olfactory bulb to the same compounds. (From Xu et al., 2003.)

Taken together, these studies suggest that odors are represented as “odor images” (“odotopic maps,” “epitopic maps”) in the glomerular sheet. Within these maps, individual activated glomeruli can be identified (Teicher et al., 1979; Lancet et al., 1981; Belluscio and Katz, 1999; Meister and Bonhoeffer, 2001), consistent with a variety of anatomical and molecular evidence that the glomerulus is the basic functional unit in the processing of odor stimuli (reviewed in Shepherd, 1994; Hildebrand and Shepherd, 1996).

For the analysis of synaptic circuits, these findings mean, first, that it is essential to know where one is recording in the glomerular sheet when stimulating with a given odor. Second, they mean that the role of microcircuits is in relation to the glomerular functional units as they process the input from a given odor relative to others.

THE CONCEPT OF MOLECULAR RECEPTIVE RANGE

Following these guidelines, Mori and his colleagues have carried out electrophysiological recordings to analyze the responses of mitral cells in the rabbit to stimulation with homologous series of odor compounds (Mori et al., 1992; summarized in Mori and Yoshihara, 1995). Their recordings were made from functionally identified regions of the glomerular sheet, in order to explore systematically the responses to a wide range of chemically related odor compounds. The spectrum of odor molecules that can activate a given cell was called its “molecular receptive range (MRR),” in analogy with the “spatial receptive field” of a cell in the visual pathway. A key finding was that the

mitral cells all show relatively narrow MRRs, with responses to only two or three neighbors in a given series of compounds from C2 to C12. Compounds of the same or similar carbon lengths were often activated in different series.

These results provided the first direct physiological evidence that “conformational features” of odor molecules are mapped spatially in the olfactory bulb (Mori and Yoshihara, 1995). The fact that these recordings were from mitral cells implies that the olfactory sensory neurons providing direct input to the mitral cells encode the conformational features (also called odotopes, determinants, or epitopes) of the odor molecules. Evidence for these conformational features has come from experimental (Zhao et al., 1998; Malnic et al., 1999) and modeling studies of receptors (Singer and Shepherd, 1994; Singer et al., 1995; Pilpel and Lancet, 1999; Singer, 2000) and ligands (Araneda et al., 2000). The olfactory sensory neurons in fact show similar properties to mitral cells in response to odors in a homologous series (Sato et al., 1994).

In summary, we now have an outline for the initial encoding of odor information in the mammal as a basis for odor discrimination, which may be summarized by referring back to the basic circuit diagram of Fig. 5.5. First, odor molecule functional groups interact with receptor molecule subsites. Second, second messenger pathways lead to differential impulse discharges. Third, the axons of a given subset converge on a few target glomeruli in the olfactory bulb. Fourth, an olfactory glomerulus is thus a functional unit reflecting the MRR of the subset(s) projecting to it. Finally, the map of olfactory glomeruli encodes odor space; given odor stimuli thus elicit “odor images” within the neural space of the glomeruli sheet. It is these “images” that are the basis for further processing by the synaptic circuits of the olfactory bulb.

FUNCTIONAL MECHANISMS IN ODOR DISCRIMINATION

In analyzing synaptic mechanisms underlying odor processing, it is critical to have precise control over the stimulus so that very brief step-pulses of odor can be used as stimuli, in the same manner as brief flashes of light or sound tones. Mitral cell responses to such stimuli show three main response patterns (Kauer, 1974; Kauer and Shepherd, 1977). First, the neuron may be suppressed at all odor concentrations, the S (suppression) type. Second, a slow spike discharge at low odor concentrations may change to an early brief spike burst followed by suppression at higher concentrations, the E (excitatory) type. Finally, there may be no detectable response to a given odor, the N (no response) type. These types have many minor variations; they are seen in their simplest form in fish and salamander, and in more complex forms in mammals (cf. Wellis and Scott, 1987).

Intracellular recordings (Hamilton and Kauer, 1985; Wellis and Scott, 1987) have revealed the synaptic potentials underlying these response types. In the experiment illustrated in Fig. 5.19B, an orthodromic volley produced an EPSP and a sequence of impulse activation followed by hyperpolarizing potentials, as in turtles (cf. Fig. 5.10 above). Sensory stimulation (Fig. 5.19A) with a brief pulse of cineole produced an E-type response in this neuron; note the similarity between this and the response to the artificial synchronous volley in B. This suggests that activation of the synaptic circuits is similar—that is, that the natural stimulus pulse caused a near-synchronous EPSP in the glomerular tuft, leading to the impulse burst, followed by activation of dendrodendritic synaptic inhibition. The large amplitude of the hyperpolarizing potentials suggests that IPSPs are generated at or near the site of recording in the mitral cell soma,

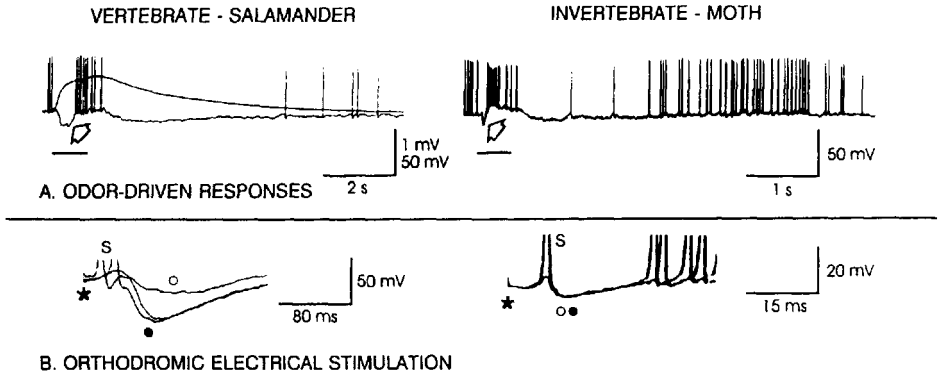
POSTSYNAPTIC RESPONSES OF OUTPUT NEURONS
IN THE OLFACTORY BULB AND THE ANTENNAL LOBE

Fig. 5.19. Intracellular responses of vertebrate mitral cells and invertebrate antennal lobe output cells, showing close similarity of response properties across phyla. **A:** Odor stimulation (horizontal bar) produces a sequence of potentials in the salamander mitral cell consisting of a brief hyperpolarization (open arrowhead) followed by an EPSP giving rise to a burst of action potentials, followed by a long-lasting IPSP. A similar sequence is produced in the moth output neuron. **B:** An electrical shock (*) to the olfactory nerves in the salamander produces, below impulse threshold, an EPSP-IPSP sequence (o); above threshold the larger EPSP elicits spikes (s), followed by a larger IPSP (•). There is a similar EPSP-IPSP sequence in the moth output neuron. [Salamander recordings adapted from Hamilton and Kauer, 1988, 1989; moth recordings adapted from Christensen and Hildebrand, 1987, and Christensen et al., 1993; in Christensen et al., 1996.]

where GC inhibition predominates (as in the antidromically activated case). It thus appears that strong synchronous artificial and natural stimulation activate the basic circuit in a similar fashion.

An intriguing and as yet unexplained property of the responses of vertebrate mitral cells to odor pulses is the presence of an initial brief hyperpolarization of the membrane, followed by the EPSP and, when of sufficient amplitude, the generation of action potentials, followed finally by the long-lasting hyperpolarization (see open arrowhead in Fig. 5.19A). The initial hyperpolarization is not seen in responses to shock stimuli. Its large amplitude points to granule cell inhibition, but, as can be appreciated by referring to the basic circuit of Fig. 5.5, the mitral cells are the route for activation of GCs; how then can granule cell inhibition of mitral cells precede mitral cell activation? One possibility is that the granule cells may be activated initially by tufted cells, which have lower thresholds for activation than the larger mitral cells (Schneider and Scott, 1983), an expression of the size principle (see Chap. 3). Another possibility is that the hyperpolarization is due to a large IPSP in the glomerular tuft mediated by dendrodendritic connections through PG cells. This would require sensory input to PG cell dendrites.

Analysis of odor responses in principal neurons of the antennal lobe of the insect has yielded excitatory-inhibitory sequences very similar to those described earlier in vertebrates (cf. Christensen et al., 1996). The similarity extends even to the brief hyperpolarization that precedes the initial EPSP and impulse burst. This suggests that de-

spite differences in the morphological types of neurons, the synaptic circuits provide for common principles of odor processing across phyla (reviewed in Hildebrand, 1995, 1996; Hildebrand and Shepherd, 1997).

LATERAL INHIBITION MEDIATES ODOR CONTRAST ENHANCEMENT

With the evidence that the fundamental units of odor information are sets of odor determinants processed by individual glomeruli, Mori and his collaborators tested for the role of the dendrodendritic microcircuits in processing that information (Yokoi et al., 1995). As noted above, the response of a mitral cell to a homologous series is limited to two or three neighboring members of a homologous series. A characteristic finding was that the members immediately flanking these compounds in a series elicited inhibition of the mitral cell (Fig. 5.20). This appears to be directly analogous to the contrast enhancement that characterizes the receptive field properties of cells in other systems, except that here it involves not spatial contrast to enhance edge detection between light and dark fields but rather molecular determinant contrast to enhance detection between differing odotopes (functional groups) in related compounds. Appli-

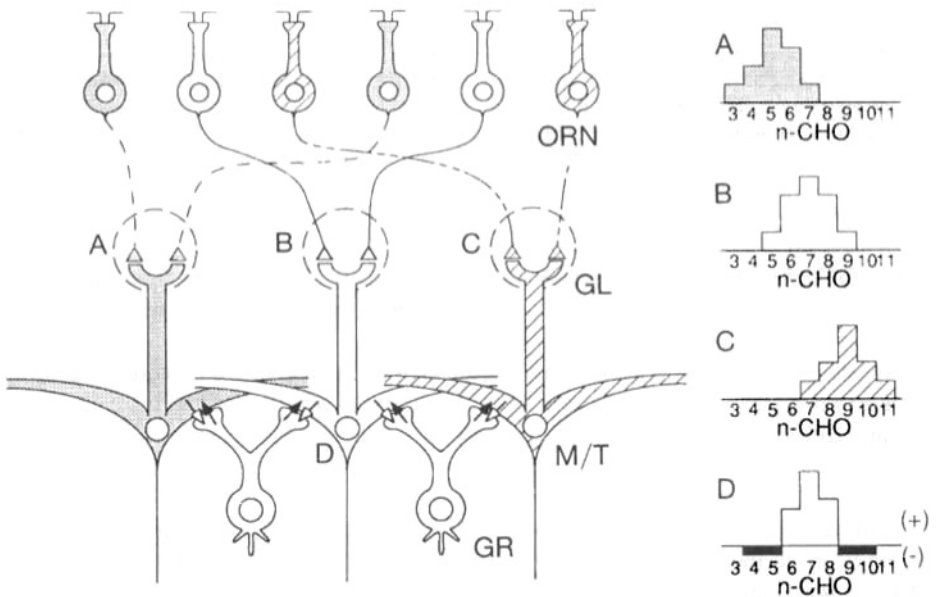


Fig. 5.20. Summary of the physiological evidence for contrast enhancement between responses of mitral cells connected to neighboring glomeruli. Diagram illustrates response spectra of ORN subsets that project to three neighboring glomeruli, and the role of dendrodendritic lateral inhibition in sharpening the contrast. Abbreviations: ORN, olfactory receptor neuron; GL, glomeruli; M/T, mitral/tufted cell; GR, granule cell; open arrowhead, excitatory mitral-to-granule synapse; closed arrowhead, inhibitory granule-to-mitral synapse; A–C, different glomeruli receiving inputs from different ORN subsets, with different response spectra (A–C at right) to a series (3–11) of aliphatic aldehydes (n-CHO); D, mitral cell receiving input from glomerulus B has narrower response range because of lateral inhibition of neighbors, shown by horizontal black bars below abscissa in D on right. [From Yokoi et al., 1995.]

cation of bicuculline abolished the inhibition, indicating that it is mediated by GABA_A receptors; further evidence suggested that this GABAergic inhibition is mediated by the interactions of GCs with the mitral/tufted cells.

These experiments thus provide the most direct evidence to date that a critical role of the dendrodendritic lateral inhibition of mitral cells by granule cells is to enhance contrast between the activity of mitral cells transmitting information about different odor stimuli. In view of the evidence for the action of the glomerulus as a functional unit, it is reasonable to hypothesize that the contrast enhancement occurs between mitral cells relating information from different glomeruli (see Figs. 5.5 and 5.16). These mechanisms are likely to play a critical role in the ability to carry out odor discrimination, whether between single odor compounds or between complex odors.

The combinations of excitatory and inhibitory MRRs have further suggested that “odor opponent” interactions exist between mitral cells belonging to different glomerular units, in analogy with color opponent interactions in the retina (Shepherd, 1992; Mori et al., 1992; Mori and Shepherd, 1994; Mori and Yoshihara, 1995). This is a useful hypothesis to be tested.

MODULATION OF RECURRENT INHIBITION MEDIATES ODOR MEMORY

The dendrodendritic synaptic microcircuit has emerged as an attractive model for examining the factors underlying plasticity at single synapses. Olfactory learning can be demonstrated early in development; rat pups, for example, use odors present *in utero* to identify the location and behavioral meaning of their mother’s nipple after birth. Olfactory learning is not restricted to early development and can be demonstrated at all ages. Adult female mice, for example, learn the odor of an impregnating male. However, if she later is exposed to the odor of a strange male, the pregnancy is blocked because the fertilized egg is rejected. This blockade, known as the *Bruce effect* (Bruce, 1959), is believed to enhance outbreeding by the female mice.

Many of the morphological, metabolic, and physiological changes that result from olfactory learning occur in the olfactory bulb. Early studies demonstrated the involvement of glutamate receptors and GABAergic transmission in olfactory learning. Several types of olfactory learning are also dependent on the presence of NA, and noradrenergic modulation of dendrodendritic inhibition has been proposed as its site of action.

Studies suggest that changes in the efficacy of dendrodendritic reciprocal excitatory—inhibitory synapses between mitral cells and GCs in the accessory olfactory bulb mediate the olfactory learning represented by the Bruce effect. The mGluR₂ subtype of the metabotropic glutamate receptor family, found predominantly on GC dendrites, may play a critical role in this learning. The evidence for this role may be summarized as follows (see Fig. 5.21). Release of glutamate from a mitral cell activates the mGluR₂ receptor on the GCs it contacts and reduces reciprocal inhibitory transmission from those GCs, thereby enhancing the mitral cell’s output to the cortex. Infusions of a specific mGluR₂ agonist, DCG-IV, into the accessory olfactory bulb of a female mouse, coupled with exposure to the odor of a male mouse, induces the formation of a memory of that pheromone that ordinarily would occur only during mating to this male. If the female now mates with a second male, she forms a memory for the second male’s odor in the usual manner. However, the memory for the first odor, formed by mGluR₂ activation but without mating, prevents the pregnancy block that ordinarily would oc-

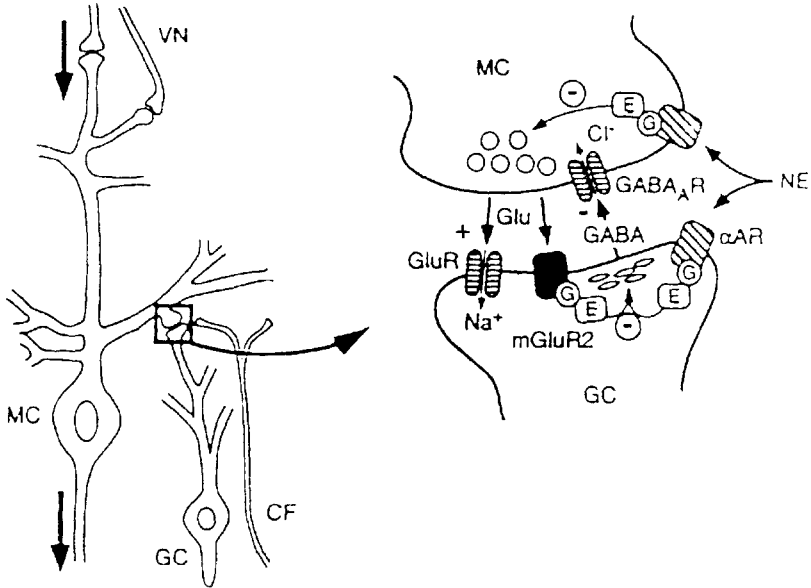


Fig. 5.21. Synaptic mechanism proposed to underly memory storage in the mouse accessory olfactory bulb. Left, schematic diagram of basic circuit, showing axons from vomeronasal (VN) organ making synapses on mitral cell. Right, diagram of synaptic receptors and second messenger actions at the dendrodendritic reciprocal synapses between mitral cell (MC) dendrite and granule cell (GC) dendritic spine. Activated mitral cell releases glutamate, acting on GluR to generate EPSP but also activating mGluR which produces long-term depression of GABAergic inhibition of the activated mitral cell. See text. Abbreviations: CF, centrifugal (noradrenergic) fibers; G, G protein; E, intracellular effector; for other abbreviations, see Fig. 5.4. [From Kaba et al., 1995.]

cur on re-exposure to the first male after the female has mated with the second male. Thus, a reduction of reciprocal inhibition from GCs to mitral cells, through mGluR₂ activation, mimicks the memory formation that occurs during mating.

It has been suggested (Llano and Marty, 1995) that these data constitute the best evidence in a mammalian system of a link between a specific learned behavior and changes in the efficacy of an identified synapse.

RETINA

PETER STERLING AND JONATHAN B. DEMB

The *retina* is a thin sheet of neural tissue lining the posterior hemisphere of the eye ball. It is actually part of the brain itself ($\approx 0.5\%$), evaginating from the lateral wall of the neural tube during embryonic development. The *optic stalk* grows out from the brain toward the ectoderm, inducing it to form an optical system (cornea, pupil, lens), which projects a physical image of the world onto the retina. The retina's task is to convert this optical image into a "neural image" for transmission down the optic nerve to a multitude of centers for further analysis. The task is complex—which is reflected in the synaptic organization.

The transformation from optical to neural image involves three stages: (1) transduction of the image by *photoreceptors*; (2) transmission of these signals by excitatory chemical synapses to *bipolar neurons*; and (3) further transmission by excitatory chemical synapses to *ganglion cells*. Ganglion cell axons collect in the optic nerve and project forward to the brain. At each synaptic stage there are specialized laterally connecting neurons called *horizontal* and *amacrine* cells. These modify (largely by inhibitory chemical synapses) forward transmission across the synaptic layers. These elements are shown schematically in Fig. 6.1.

A closer look at this apparently simple design (three interconnected layers and five broad classes of neuron) reveals additional complexity (Figs. 6.2 and 6.3). Each neuron class is represented by several or many specific *types*. Each cell type is distinguished from others in its class by its characteristic morphology, connections, neurochemistry, and function (Rodieck and Brening, 1983; Sterling, 1983). This diversity, amounting to some 80 cellular types (Kolb et al., 1981; Sterling, 1983; Vaney, 1990; Masland, 2001), was puzzling at first, but a broad explanation has gradually emerged: it is impossible to encode all the information in an optical image using a single neural image. Therefore, the retina uses different cell types to create parallel circuits for simultaneous transmission of *multiple neural images* to the brain. The retina also creates separate circuits for different light levels—daylight, twilight, and starlight—but these share certain circuit components and use the same final pathways to the brain (Smith et al., 1986).

This chapter describes key cell types and their interconnection in parallel circuits. It also discusses how the functional architecture of a circuit depends on the functional architecture of its synapses. Finally, it suggests how the flow of visual information

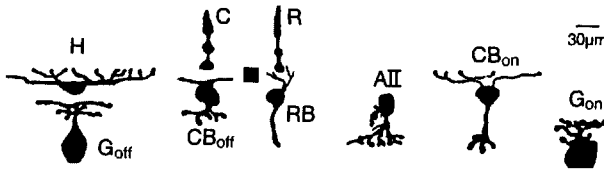


Fig. 6.1. Neuronal elements of the mammalian retina (same scale as diagrams for other regions). Symbols are defined in legend for Fig. 6.2.

shifts between circuits that are specialized for different light levels and how the circuits are switched. The chapter focuses on mammalian retina because that is where the combined knowledge of circuitry and cell physiology is best known. Early efforts centered on cat, so specific measurements, counts, etc. cited here refer to cat central retina. However, efforts have broadened to include rabbit, guinea pig, rat, mouse, monkey, and human. These demonstrate strongly conserved patterns in the circuitry, as well as special adaptations, and some of both are mentioned.

NEURONAL ELEMENTS

INPUT ELEMENTS: RECEPTORS

Photoreceptors are elongated (Fig. 6.4). The distal tip points toward the back of the eye, away from the light, and is embedded in folds of melanotic epithelium. The outer

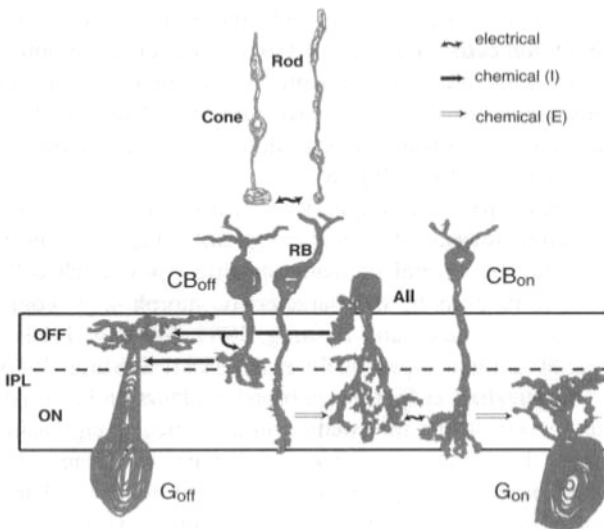


Fig. 6.2. Neuronal elements, scale enlarged in the vertical axis, to show more clearly the cell morphology and layers. Inputs: rod and cone photoreceptors. Principal neurons: ON and OFF ganglion cells (G_{on} , G_{off}). Intrinsic neurons: rod bipolar (RB) and cone bipolar (CB) neurons; horizontal (H), and amacrine neurons (A). IPL, inner plexiform layer. AII designates a specific type of amacrine cell that serves the starlight circuit (see text).

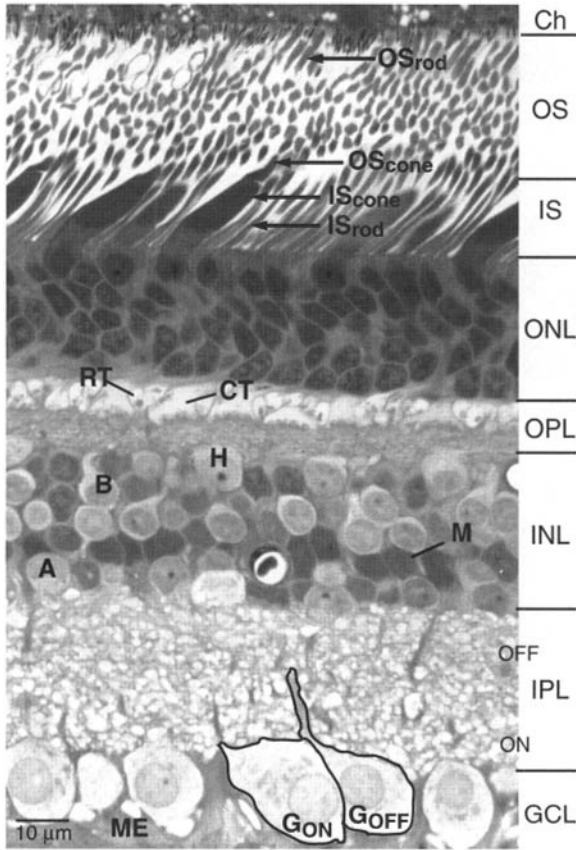


Fig. 6.3. Radial section through monkey retina about 5 mm (≈ 25 degrees) from the fovea. Here, cone and rod inner segments are easily distinguished from each other, as are their terminals in the outer plexiform layer. Pigmented cells of the choroid layer (Ch) attach the active form of vitamin A (aldehyde) to opsin and return it to the outer segment. Pigment cells also phagocytose membrane discs, shed daily from the outer segment tips. Abbreviations: OS, outer segments; IS, inner segments; ONL, outer nuclear layer; CT, cone terminal; RT, rod terminal; OPL, outer plexiform layer; INL, inner nuclear layer; IPL, inner plexiform layer; GCL, ganglion cell layer; B, bipolar cell; M, Müller cell; H, horizontal cell; A, amacrine cells; ME, Müller end feet; G_{ON}, ON ganglion cell; G_{OFF}, OFF ganglion cell. [Light micrograph from N. Vardi.]

segment contains about 900 membranous discs, stacked perpendicular to the cell's long axis (Fig. 6.4B). The disc surface is densely packed with molecules of the photopigment rhodopsin, at nearly 60,000 per disc (reviewed in Pugh and Lamb, 1993). The inner segment is filled with mitochondria. These fuel the ion pumps essential for transduction and raise the refractive index, thereby creating a wave-guide that traps photons and funnels them to the outer segment (Enoch, 1981).

The region of the photoreceptor, between the inner segment and the soma, contains the usual machinery for protein synthesis and packaging. Because the soma is stouter than the inner segment (which packs densely with its neighbors), the somas pile up

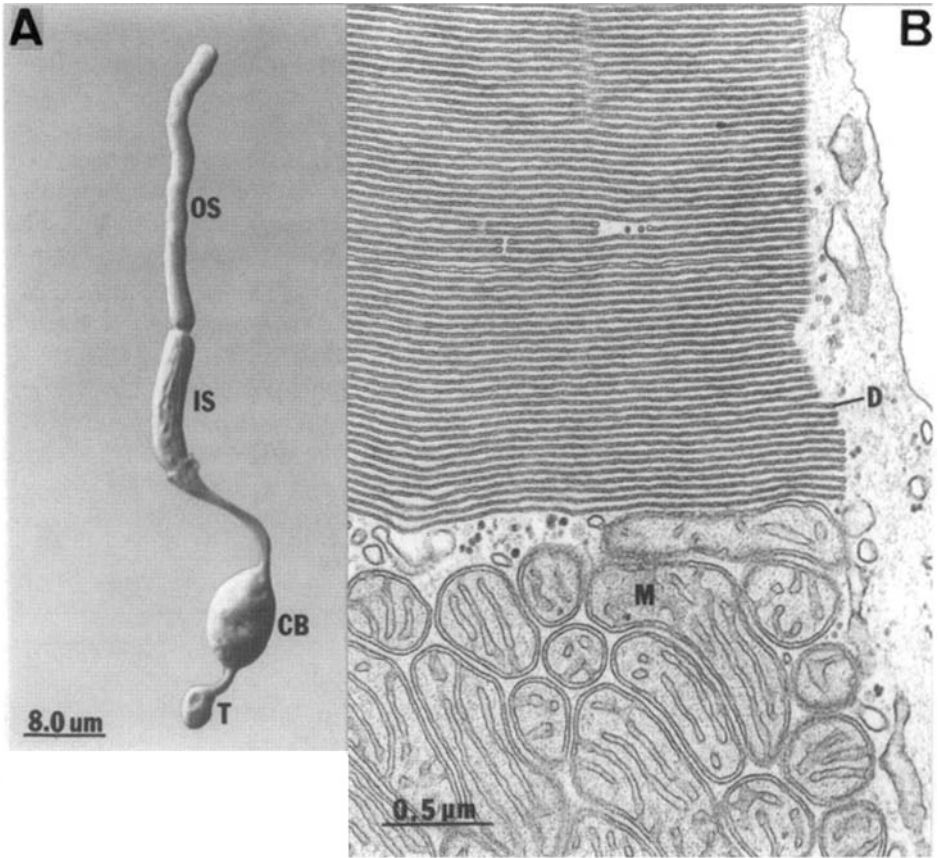


Fig. 6.4. **A:** Isolated rod photoreceptor (rabbit) showing the cell's distinct regions. Light micrograph. **B:** Radial section through rod outer/inner segment junction (salamander) showing regularly spaced membranous discs (D) and densely packed mitochondria (M). Abbreviations: CB, cell body; T, terminal. [Electron micrographs from Townes-Anderson et al., 1985, 1988, with permission.]

in tiers (outer nuclear layer; see Fig. 6.3). The photoreceptor axon is generally short, $50\ \mu\text{m}$ or less, except those in the fovea, where extremely dense packing of cones leaves no room for connections to the second- and third-order neurons. A foveal cone axon can be as long as $500\ \mu\text{m}$ (Polyak, 1941; Schein, 1988; Hsu et al., 1998). The photoreceptor axon ends, without branching, in a single, highly specialized synapse that contains one or more synaptic “ribbons” (see Figs. 6.4 and 6.13).

Intensity Range. Light intensity in the natural environment varies over a range of about 10^{10} , and we can see over this entire range. Two types of receptor divide the range: rods for night and cones for day. In mammals both have a narrow outer segment: 1- to $2\text{-}\mu\text{m}$ diameter for the rod and 3- to $5\text{-}\mu\text{m}$ diameter for the cone. This ensures a small cytoplasmic volume, which is essential to a rapid response time, and this is suited to the rapid image motion generated by rapid movements of the organism. By comparison, the

rod of sluggish amphibians has a 5-fold greater diameter (25-fold greater volume) and partly as a consequence is 10-fold slower (Pugh and Lamb, 1993). So, if our photo-receptors were large, sports such as baseball or tennis would be out of the question.

A narrow outer segment limits the number of photons that a receptor can collect within an “integration time.” A rod integrates photon signals over about 300 ms (Yau, 1994), yet starlight presents it with only 1 photon per 10 minutes! So even when the light is 2000 times brighter, there is still only 1 photon per rod per integration time. Thus, from dusk to dimmest starlight the rod detects single photons and needs to transmit only a *binary signal*: 0 or 1 photon. The task of transmitting this irreducibly simple message shapes the circuit design at all stages proximal to the outer segment. For example, the rod axon is extremely thin (0.25 μm diameter), and the synaptic terminal is small, with a single ribbon synapse (see Figs. 6.4 and 6.13).

A cone integrates photon signals over about 50 ms. During this interval, twilight (with color just barely discernible) delivers about 10^2 photons per cone, and bright sun delivers about 10^5 photons per cone (Schnapf et al., 1990). Thus, a cone integrates many photons to give a *graded signal* with good temporal resolution. The cone, having much more information to transmit than a rod, employs a thicker axon (1.6 μm diameter) and a larger terminal with many ribbon synapses (see Fig. 6.13). At dusk, as light intensity drops below cone threshold (marked by loss of color perception), the rod is collecting up to 10^2 photons per integration time. Thus, over a modest range (2 log units of intensity), the rod produces a graded signal that fills in for the failing cone. This graded rod signal for twilight is routed differently from the binary signal for starlight (see Circuits, later).

Spectral Sensitivity. Mammals have a single type of rod (peak sensitivity at ≈ 500 nm). This makes sense because at night photons are too sparse to be worth segregating by wavelength. But in daylight, there are plenty of photons, so most mammals gain extra information by using two cone types with different spectral sensitivity (Barlow, 1982). Most cones (at least 90%) are tuned to middle wavelengths (peak at ≈ 550 nm), termed “M” or *green* (reviewed in Jacobs, 1993). A few are tuned to short wavelengths (peak at ≈ 450 nm), termed “S” or *blue*. Because S cones can be distinguished by morphology and by antibody labeling, we know that they form a sparse but regular mosaic (de Monasterio et al., 1981; Szél et al., 1988; Ahnelt et al. 1990; Curcio et al., 1991). These anatomical methods confirm psychophysical maps of punctate sensitivity to S cone stimuli (Williams et al., 1981). S cones connect via a selective circuit to a special type of ganglion cell (see Circuits, later).

Old World primates (including humans) are special in being “trichromatic,” meaning that there is an additional cone type tuned to long wavelengths (peak at ≈ 570 nm), termed “L” or *red*. The M and L cone pigments are nearly identical except for a few critical amino acids in the transmembrane region, so antibodies have not yet distinguished them (Neitz et al., 1991). Spectral sensitivity mapped for cone populations in situ shows M and L cones in monkey and human to distribute randomly in clusters. M and L cones in humans distribute differently across an individual retina and differ greatly between individuals—with surprisingly little effect on color vision (Roorda and Williams, 1999; Brainard et al., 2000; Neitz et al., 2002). How these cones connect to ganglion cells is naturally of great interest and is presently

controversial (Dacey, 1996; Calkins and Sterling, 1999; Martin et al., 2001; Reid and Shapley, 2002).

Some animals using three cone pigments, such as fish, turtles, and birds, may express up to seven types of cone! This trick is accomplished by fitting the inner segment with an oil droplet of specific color/absorbance (red, yellow/ultraviolet [UV]). These serve as filters to limit the spectral composition of the light entering the outer segment (e.g., Ohtsuka, 1985). Also, evolution tunes cone pigments to match the environment's spectral content. For example, Lake Baikal is very clear and deep, but longer wavelengths fail to penetrate at greater depths. Consequently, fish species at greater depths shift their cone pigments down the spectrum (Bowmaker et al., 1994). Equally wonderful in its vision capability is the kestrel (a falcon), which has a cone type tuned to UV (≈ 350 nm). Soaring high with this receptor, it can identify the urine trails of its prey (meadow vole), which in sunlight fluoresce UV (Viitala et al., 1995).

INTRINSIC ELEMENTS FOR FORWARD TRANSMISSION: BIPOLAR AND AII CELLS

Bipolar Cells. Bipolar somas occupy the middle region of the inner nuclear layer (see Fig. 6.3). Their dendrites ascend to collect synapses from photoreceptors. One bipolar type collects only from rods, and most other types collect only from cones. However, one bipolar type in rodent retina receives chemical synaptic input directly from both rods and cones (Soucy et al., 1998; Hack et al., 1999; Tsukamoto et al., 2001). Bipolar axons descend to the inner plexiform layer where they provide ribbon synapses, each directed at a pair of postsynaptic processes, termed a *dyad* (see later; Dowling and Boycott, 1966).

The rod bipolar soma ($7 \mu\text{m}$ diameter) is located high in the outer nuclear layer (Fig. 6.5). The narrow, candelabra-like, dendritic arbor penetrates the stratum of cone terminals to reach the overlying rod terminals where it collects signals from 20 rods in cat, 15–45 in human, and up to 80 rods or more in rabbit (Boycott and Dowling, 1969; Dacheux and Raviola, 1986; Young and Vaney, 1991). The rod bipolar axon descends without branching to the deepest stratum of the inner plexiform layer where it contacts not ganglion cells, but a third-order, intrinsic neuron, termed the *AII* amacrine cell (see Fig. 6.2; Kolb and Famiglietti, 1974; McGuire et al., 1984; Freed et al., 1987; Strettoi et al., 1990; Wässle et al., 1991). The cat rod bipolar terminal employs 30 ribbon synapses, with little variation within or between animals (McGuire et al., 1984; Rao and Sterling, 1991).

The cone bipolar somas are also small ($\approx 8 \mu\text{m}$), and the dendritic fields are narrow ($\approx 15 \mu\text{m}$; Fig. 6.6). The dendritic arbor typically collects signals from 5–10 overlying cone terminals without skipping any (Cohen and Sterling, 1990a,b; Boycott and Wässle, 1991; Calkins and Sterling, 1996). An exception is the S cone bipolar cell, which *does* skip overlying M and L cones to contact S cones exclusively (Mariani, 1984; Kouyama and Marshak, 1992). The S cone bipolar cell has been defined clearly in monkey and probably corresponds to the wide-field cone bipolar in cat and other mammals that also skips certain cones (e.g., type b_5 , Fig. 6.6). Cone bipolar axons descend to the inner plexiform layer, where each type selects a particular stratum and contacts both amacrine and ganglion cells (Fig. 6.6). Cone bipolar terminals employ 30–130 ribbon synapses, depending on cell type (Cohen and Sterling, 1990b; Calkins et al., 1994; Tsukamoto et al., 2001).

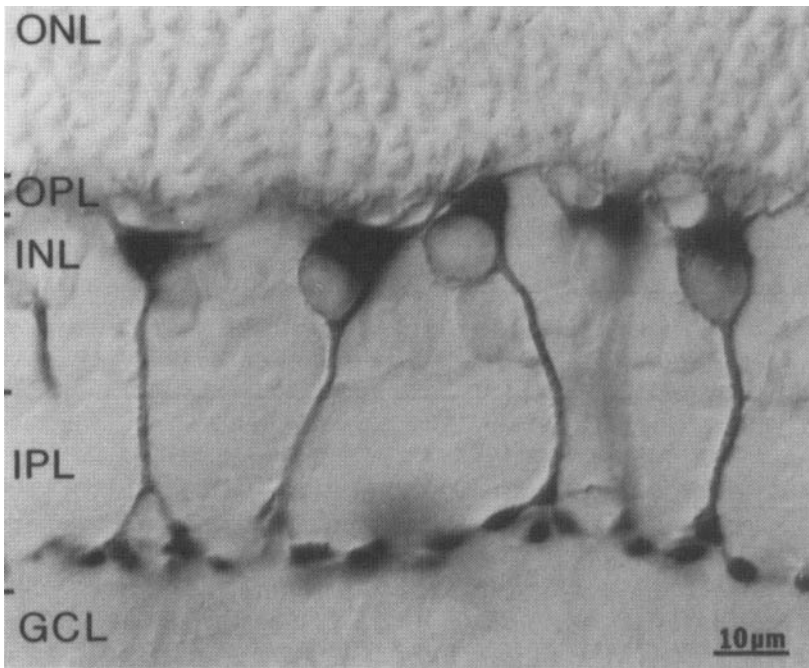
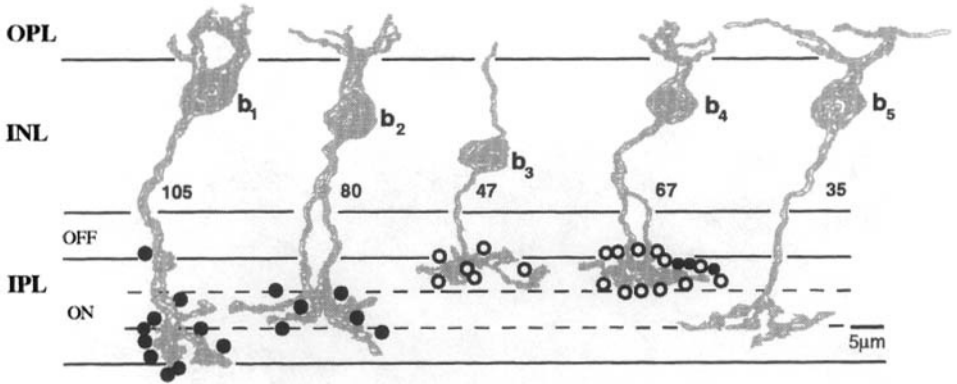


Fig. 6.5. Rod bipolar array (rabbit) immunostained for protein kinase C. Dendrites of adjacent cells overlap modestly in OPL, but axon terminals simply “tile” the deepest level of the IPL without overlap. [Light micrograph from Young and Vaney, 1991, with permission.]

ON vs. OFF Bipolar Types. It was discovered early that some bipolar cells are excited (i.e., depolarized) by light onset, whereas others are excited by light offset (Werblin and Dowling, 1969; Kaneko, 1970). How the cone synapse manages to drive these cells in opposite directions is explained later (see Fig. 6.15). Here we note that the two categories of axon terminate at different levels: OFF axons arborize in the upper half of the inner plexiform layer, and ON axons arborize in the lower half (see Fig. 6.2). Within these OFF and ON regions, multiple types segregate in different strata (see Fig. 6.6; Kolb et al., 1981; Cohen and Sterling, 1990b; Boycott and Wässle, 1991; Euler et al., 1996). It was unexpected that ON and OFF bipolar cells would comprise so many types (≈ 4 or 5 types for each category). Because all types (except for the S cone bipolar cell) collect from the same cones, their spatial and spectral inputs are identical. Therefore, one surmises that they carry different *temporal* components of the cone signal. Indeed, two types of ON bipolar cell do differ temporally, some depolarizing sustainedly to steady illumination, and others depolarizing transiently (Saito et al., 1985; Dacey et al., 2000; Euler and Masland, 2000).

AII Cell. The AII soma in the amacrine cell layer sends a thick stalk to the ON level of the inner plexiform layer where it arborizes richly to collect chemical synapses from rod bipolar terminals (see Fig. 6.2; Kolb and Famiglietti, 1974; Vaney, 1985; Sterling et al., 1988; Strettoi et al., 1990; Mills and Massey, 1999). This arbor also forms nu-

A



B

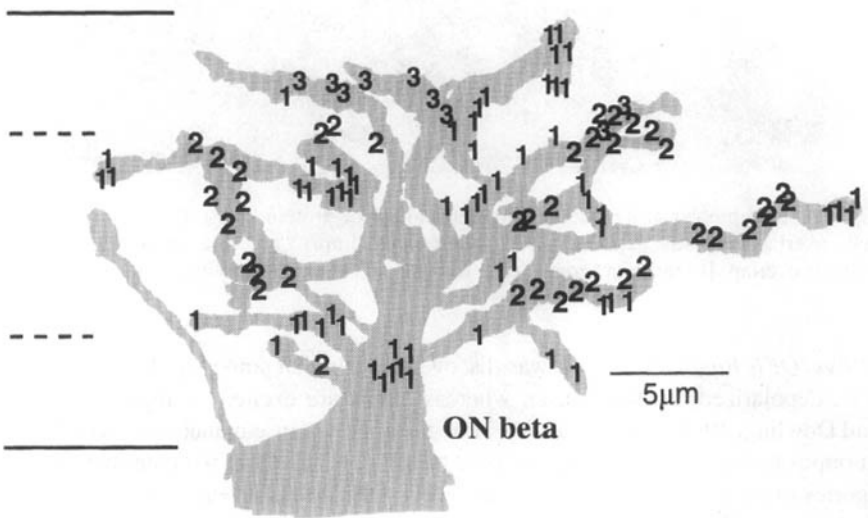


Fig. 6.6. **A:** Multiple types of ON cone bipolar cell with axons in the ON region of the IPL. Each type expresses a different number of ribbon outputs (noted at the right of each axon) and a different pattern of gap junctions (filled circles, CB–AII; open circles, CB–CB). Types b_1 – b_4 collect from all the overlying cones without skipping any; type b_5 ignores the immediately overlying cones and reaches widely to collect from outlying cones. [Reconstructions from Cohen and Sterling, 1990a,b.] **B:** ON beta ganglion cell arborizes among all types of ON cone bipolar axon, but collects ribbon synapses from only three types (b_1 , b_2 , b_3) in the proportion 80:40:20. [From Cohen and Sterling, 1992, with permission.]

merous, large gap junctions with the axon terminals of ON cone bipolar cells. When these gap junctions are in a conducting state, rod bipolar excitation spreads from AII into the cone bipolar terminals, evoking their transmitter release onto ganglion cells (see Fig. 6.21). The AII also forms “lobular appendages” at the OFF level of the inner plexiform layer. These structures, which are jammed with mitochondria and synaptic

vesicles, provide inhibitory chemical synapses to OFF bipolar terminals and OFF ganglion cell dendrites (McGuire et al., 1984; Kolb and Nelson, 1993). This wiring explains how a single type of rod bipolar cell can simultaneously excite the ON and inhibit the OFF ganglion cells (Mastrorarde, 1983; Sterling, 1983).

OUTPUT ELEMENTS: GANGLION CELLS

Ganglion cell bodies form the innermost cellular layer of the retina (see Figs. 6.2 and 6.3). Their dendrites penetrate the inner plexiform layer to collect excitatory synapses from bipolar axons and both excitatory and inhibitory synapses from amacrine cells. Ganglion cell axons enter the optic nerve and extend to the brain. The domestic cat optic nerve contains about 160,000 axons (260,000 for its wild progenitor; Williams et al., 1993b); the human nerve contains about 1.2 million axons, and the macaque optic nerve contains about 1.8 million axons (Potts et al., 1972). Because the number of fibers in the optic nerve can vary 10-fold, it does not seem to be a physical “bottleneck” for information outflow as was commonly thought. Thus, the reason that many cones converge onto a single ganglion cell is not to reduce the number of transmission channels in the nerve but rather for deeper reasons to which we shall return.

Ganglion cell somas look pretty much alike (see Fig. 6.3), but Golgi impregnations revealed the dendritic arbors to be remarkably diverse—on the order of 20 types (e.g., Polyak, 1941; Boycott and Dowling, 1969; Cajal, 1972; Boycott and Wässle, 1974; Kolb et al., 1981). Now that one can record data from a ganglion cell *in vitro* and render its dendritic arbor visible by injecting dye, we realize that each morphological type has a distinctive physiology. For example, the ganglion cell with a planar, “loopy” dendritic arbor responds selectively to stimuli moving in a particular direction (see Fig. 6.11C; Amthor et al., 1989a). This specific structure–function correspondence was first shown in rabbit but also holds for cat, and probably also for primate (Berson et al., 1998, 1999; Isayama et al., 2000). Thus, a ganglion cell type carrying a particular sort of information can (like a gene) be conserved across species.

Each type of ganglion cell distributes to a particular brain region, which uses the special information carried by that cell. Thus, the nucleus of the optic tract, which controls optokinetic eye movements, collects from the directionally selective ganglion cell (Pu and Amthor, 1990). And the suprachiasmatic nucleus, which uses light to reset circadian rhythms, collects from another type that branches over extremely wide areas. This ganglion cell type is unusual because it expresses its own visual pigment, melanopsin, and thus monitors light levels independently of the rods and cones (Berson et al., 2002; Hattar et al., 2002). Still other types of motion-selective ganglion cell project to the superior colliculus—which uses the information to orient the head and eyes (Rodieck and Watanabe, 1993; Berson et al., 1998, 1999; Isayama et al., 2000). Such subcortical “house-keeping” centers use about 40% of the cat’s ganglion cells. But these cells have small somas ($\approx 10 \mu\text{m}$) and fine axons ($0.3 \mu\text{m}$ diameter), so they occupy less than 5% of the optic nerve cross section. Similar *numbers* of house-keeping ganglion cells are required in primates, but their *proportion* of all ganglion cells is much smaller—due to the high density of midget cells (see later; Rodieck et al., 1993).

The key region for mammalian visual processing is the striate cortex, which receives its main thalamic input from the dorsal lateral geniculate nucleus. Thus, it is to this nucleus that most ganglion cells project (60% in cat; 90% in monkey). Two major

classes of ganglion cell in cat are geniculate-bound: “beta” and “alpha” cells (Fig. 6.7) (Boycott and Wässle, 1974; Wässle et al., 1981a,c; Stein et al., 1996). The beta cell has a narrow, bushy dendritic tree and a sustained (tonic) discharge of action potentials to a maintained stimulus (Figs. 6.2 and 6.7). The alpha cell has a wider, sparser dendritic tree and a transient (phasic) discharge (Cleland and Levick, 1974; Stone and Fukuda, 1974; Saito, 1983). The beta and alpha cells are each of two types, one with dendrites in the ON strata of the inner plexiform layer and the other with dendrites in the OFF strata (Fig. 6.7) (Famiglietti and Kolb, 1976). The former are excited by light onset; the latter are excited by light offset (Fig. 6.7) (Nelson et al., 1978). Thus, they are termed ON beta, OFF beta, ON alpha, and OFF alpha.

The primate retina expresses a similar division into ON and OFF versions of narrow-field, tonic cells and wider-field, phasic cells (e.g., de Monasterio, 1978). The narrow-field types are termed *midget cells* because in central retina the dendritic arbor collects from a midget bipolar cell with input from a single cone (Polyak, 1941; Kolb and Dekorver, 1991; Calkins et al., 1994), but more peripherally the arbor broadens to collect from many midget bipolar axons (Watanabe and Rodieck, 1989; Dacey, 1993; Goodchild et al., 1996b). Midget cells are also termed “P” cells because they project to the lateral geniculate’s parvocellular layers. The wider-field cells are morphologically diverse (Polyak, 1941; Boycott and Dowling, 1969). Some are termed *parasol* because of their broad, flat dendritic arbors. These are also termed “M” cells because they project to the geniculate magnocellular layers (Perry et al., 1984; Watanabe and Rodieck, 1989). However, other types of wide-field ganglion cell probably also project to the magnocellular layers, so the term *M cell* probably includes diverse types (e.g., Kaplan and Shapley, 1982; Shapley and Perry, 1986).

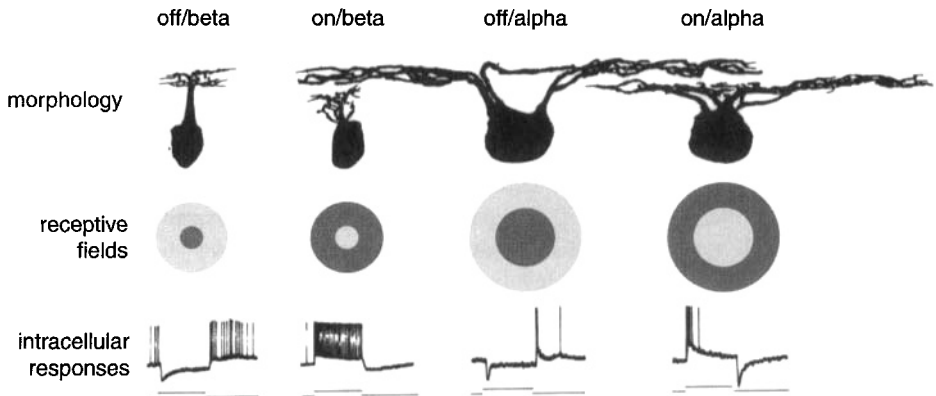


Fig. 6.7. Form and function of cat ganglion cells. Beta cells have a narrow dendritic field, and alpha cells, a broad one (top row, vertical views). Cells are maximally excited by stimuli covering the whole dendritic field, corresponding to the *receptive field* “center” and maximally suppressed by stimuli filling the outer annulus, termed the *receptive field* “surround” (middle row, tangential views). ON cells, excited by *increased* intensity on the center, arborize deep in the inner plexiform layer; OFF cells, excited by *decreased* intensity on the center, arborize superficially. Beta cells give a transient plus sustained response; alpha cells give mainly a transient response. [Intracellular recordings from Saito, 1983.]

Over a decade of intense description, physiologists divided ganglion cells into different functional categories: Y (brisk-transient), X (brisk-sustained), and W (other, including edge-detector, directionally sensitive, etc.). Simultaneously, morphologists categorized ganglion cells by dendritic branching patterns: alpha (planar-radiate), beta (3-D-bushy), and gamma (other, including planar-sparse, planar-loopy, etc.). It was quickly appreciated that functional categories might map onto the morphological ones, but to prove this directly by recording followed by tracer injection required almost another decade (e.g., Saito, 1983). This correspondence of structure to function in ganglion cells is now firmly established as a principle of retinal organization, and consequently a type can be named for its function (e.g., directionally sensitive; see Fig. 6.11C) or its morphology without any confusion (see Fig. 6.7). However, when a category is named for its central projection, such as M or P, one must remember that several types can project to the same locus. Thus, one expects multiple types of M and P cell (Amthor et al., 1989a,b; Dacey and Lee, 1994).

INTRINSIC ELEMENTS FOR LATERAL TRANSMISSION: HORIZONTAL AND AMACRINE CELLS

Horizontal Cells. Horizontal cell somas form the upper tier of the inner nuclear layer (see Fig. 6.3), and the processes connect exclusively within the outer plexiform layer. Collecting widely from receptors, their main task is to average the signals and feed negatively back onto receptor terminals and forward onto bipolar dendrites. Horizontal cells couple to each other electrically. The strength of this coupling changes with adaptive state and is modulated by dopamine secreted by certain cells in the amacrine layer (reviewed in Weiler et al., 2000).

Two types of horizontal cell in diurnal mammals connect with cones (Fig. 6.8). One has thick dendrites, a wide field and couples strongly to its neighbors; the other has thin dendrites, a narrow field and couples weakly (Mills and Massey, 1994; Peichl and Gonzalez-Soriano, 1994; Vaney, 1994a; Sandmann et al., 1996). Generally, each type connects to all the cone terminals in its dendritic field. However, in primate the large-field cell avoids S cones, and the narrow-field cell connects especially strongly to them (Dacey, et al., 1996; Goodchild et al., 1996a; see also Sandmann et al., 1996). Within this general framework are some quite spectacular morphological variations whose functions remain mysterious (see, e.g., Müller and Peichl, 1993).

One of the two types of horizontal cell connects with rods. It does so by emitting a fine axon that in cat meanders for several millimeters and then breaks into an elaborate arbor that contacts several thousand rods (see Fig. 6.8). This axon also couples to its neighbors and thus pools signals from tens of thousands of rods (Vaney, 1993). This is not the usual sort of axon because it lacks action potentials; further, cone input to the dendrites does not reach the rod axon arbor, so it must be electrically isolated from the soma (Nelson, 1977). On the other hand, the horizontal cell soma *does* receive strong rod signals (e.g., Steinberg, 1969; Nelson, 1977; Lankeet et al., 1996), which must therefore come via rod-to-cone gap junctions (Raviola and Gilula, 1973; Kolb, 1977; Smith et al., 1986). Thus, the soma serves metabolically two processes with utterly different connections. It does not seem to matter which type of horizontal cell produces the axon, because in cat and rabbit it is the wide-field cell and in primate it is the narrow-field cell (reviewed in Sandmann et al., 1996).

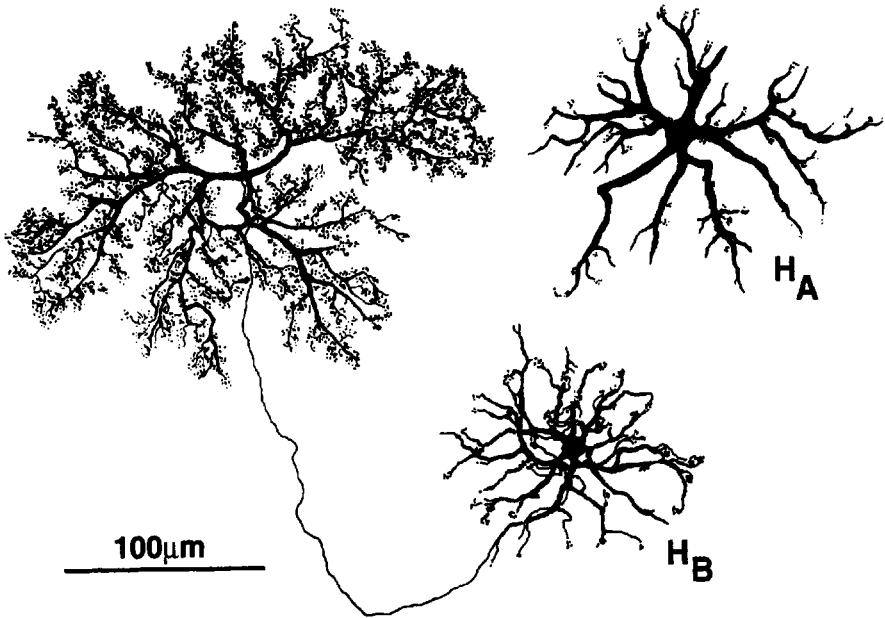


Fig. 6.8. Two types of horizontal cell from cat retina as seen in tangential view following Golgi impregnation. Dendrites of types A and B both connect with cones; axon arbor of type B connects with about 3000 rods. [From Kolb, 1974, with permission.]

Amacrine Cells. Amacrine somas form the lower tier of the inner nuclear layer and are also numerous in the ganglion cell layer, where they are called *displaced*. Amacrine cells connect exclusively within the inner plexiform layer (plus some synapses in the ganglion cell fiber layer) and are diverse in the extreme; there are about 40 types (Kolb et al., 1981; MacNeil and Masland, 1998; Vaney, 1990). Given such diversity, attempts to generalize are likely to be inadequate, but consider the following:

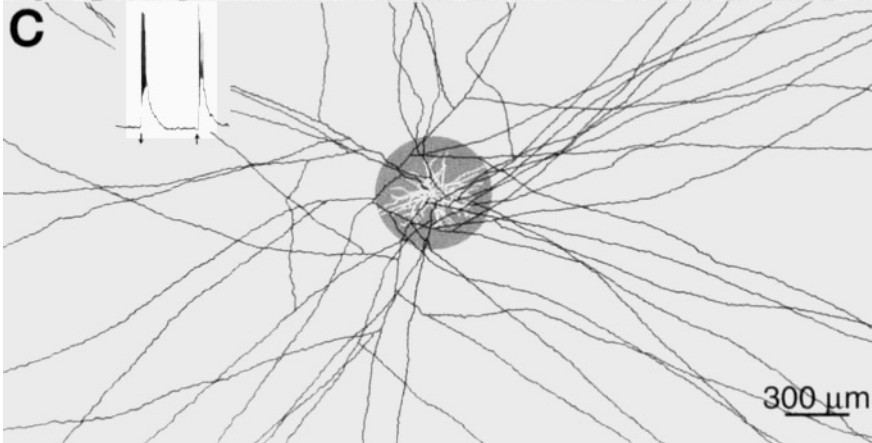
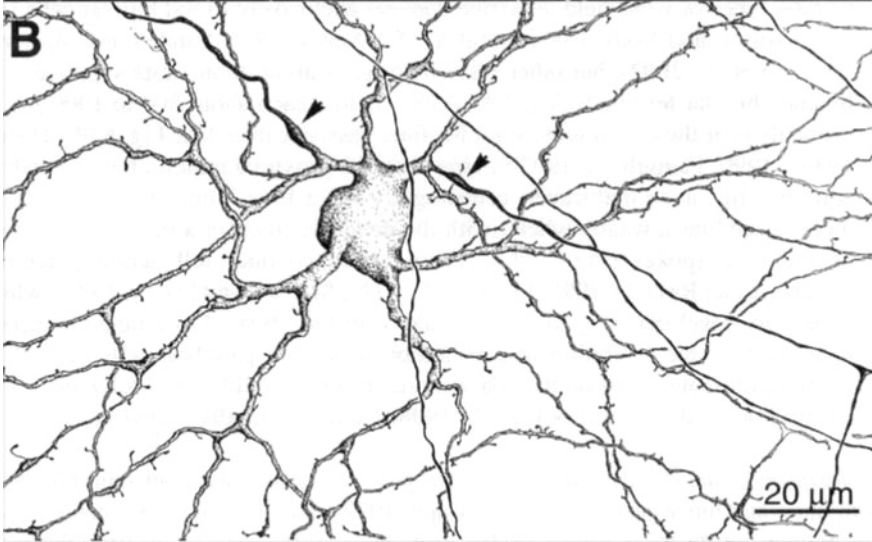
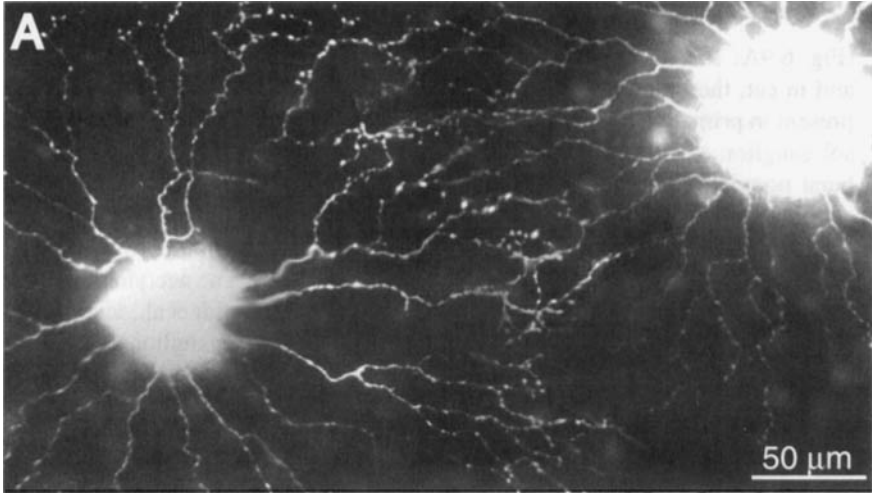
1. The AII amacrine, being narrow-field, distributes densely and thus constitutes about 20% of the amacrine layer cells (see Fig. 6.2). As noted, the AII collects purely from rod bipolars and serves a feedforward link in the rod's starlight pathway.
2. Certain narrow-field amacrine cells collect purely from cone bipolar terminals. These amacrine cells feed back reciprocally onto the bipolar terminal and forward onto the ganglion cell (see Fig. 6.14). These types, which exist as both ON and OFF forms, must distribute densely to tile the plane (Polyak, 1941; Kolb et al., 1981). This pattern of connection may reflect lateral inhibition across a small spatial scale covering tens of microns rather than hundreds as for the horizontal cells.
3. Certain medium-field amacrine cells collect from cone bipolars and arborize intimately with dendrites of certain ganglion cell types. For example, the starburst amacrine cell associates with other members of its own type to form a loopy pattern that in rabbit associates with dendrites of the direction-selective ganglion cell

(Fig. 6.9A; Tauchi and Masland, 1984; Vaney et al., 1989a; Famiglietti, 1992a), and in cat, the alpha ganglion cell (Vardi et al., 1989). The starburst cell is also present in primate, where it probably associates with the co-planar arbors of parasol ganglion cells (Rodieck, 1989; Jacoby et al., 1996). There are separate starburst populations for the ON and OFF levels of the inner plexiform layer. The starburst cell responds phasically to glutamatergic bipolar input (kainate receptors; Linn et al., 1991) and releases a pulse of acetylcholine onto the ganglion cells (Masland et al., 1984; Massey and Redburn, 1985). The acetylcholine, binding to nicotinic receptors, excites ganglion cells (e.g., Schmidt et al., 1987; Kaneda et al., 1995). Thus, the starburst circuit probably boosts ganglion cell transient responses, enhancing sensitivity to motion. Several studies suggest that the starburst cell fires action potentials (Bloomfield, 1992; Jensen, 1995; Cohen, 2001), but other studies report purely passive responses (Taylor and Wässle, 1995; Zhou and Fain, 1995; Peters and Masland, 1996).

4. Certain types of wide-field amacrine connect exclusively to rod bipolar cells (cat A17; Nelson and Kolb, 1985; rabbit S1, S2, Vaney, 1986; Sandell and Masland, 1986; Li et al., 2002), but other wide-field types arborize in strata supplied only by cone bipolar terminals. The “dendritic” fields reach about 500 to 1000 μm —probably near the electrotonic limit for fine, passive cables (see Fig. 6.9C; Dacey, 1989a, 1990; Famiglietti, 1992b). However, the proximal region of each dendrite sprouts a fine axon that travels centrifugally for at least 3 mm (Fig. 6.9B). Such a cell resembles a wagon wheel, with the dendritic field for a hub and the axons as radiating spokes (Fig. 6.9C). These axons conduct full action potentials (Dacheux and Raviola, 1995; Freed et al., 1996; Stafford and Dacey, 1997), which appear to travel centrifugally (Cook and Werblin, 1994). Long-range amacrine cells mediate the inhibition and excitation of certain ganglion cells evoked by stimuli millimeters beyond the conventional receptive field (e.g., McIlwain, 1966; Derrington et al., 1979; Cook et al., 1998; Demb et al., 1999; Taylor, 1999).

Interplexiform Cells. These cells have somas in the amacrine layer but send processes to both outer and inner plexiform layers (Cajal, 1972). The interplexiform cell receives synapses only on its inner processes but provides synaptic outputs in both the inner and outer plexiform layers. In cat, it forms chemical synapses upon both rod bipolar and cone bipolar dendrites (Kolb and West, 1977; Nakamura et al., 1980; McGuire et al., 1984; Cohen and Sterling, 1990b), and in fish it contacts horizontal cells (Downing, 1986). Some authors refer to the interplexiform as a “sixth cell class,” but it seems equally reasonable to consider it as one more extraordinary type of amacrine cell.

The interplexiform cell in New World monkey and fish contains dopamine (Downing, 1986). In cat, the dopaminergic amacrine cell also sends sporadic processes to the outer plexiform layer (Oyster et al., 1985). Because dopamine regulates horizontal cell coupling (Piccolino et al., 1984; Teranishi et al., 1984; Hampson et al., 1992; reviewed in Weiler et al., 2000), which shapes the inhibitory surround of cones and bipolar cells (see Fig. 6.17), the dopamine cell may adjust the surround’s depth and extent to ambient image statistics. Cat and rabbit interplexiform cells use γ -aminobutyric acid (GABA) and contact bipolar dendrites, so they probably have a different function.



Centrifugal Fibers. Specific brain regions in certain vertebrates, including fish, amphibians, reptiles, and birds, produce efferent axons that travel in the optic nerve to terminate in the inner retina. In birds, the isthmo-optic nucleus, a substantial structure with a definite retinotopic organization, projects about 10,000 fibers centrifugally to the inner retina to terminate on a special type of amacrine cell (Dowling and Cowan, 1966; Uchiyama and Ito, 1993). In fish, the olfactory bulb sends fibers containing a peptide luteinizing hormone–releasing hormone (LHRH) to contact interplexiform cells (Zucker and Dowling, 1987). Thus, the idea is not entirely far fetched that an odor, a memory, or a feeling could modify the construction of a visual image in the retina—that beauty could be literally in the eye of the beholder. However, little is known regarding the function of these centrifugal pathways (Uchiyama and Barlow, 1994).

Glial Cells. The retina contains a single, highly stereotyped glial cell, termed the *Müller cell*. Its cell body, recognized by its dark cytoplasm and polygonal shape, lies in the deeper tiers of the inner nuclear layer (INL) (see Fig. 6.3). Processes extend from this cell outward to reach the choroid layer and inward to ensheath the ganglion cells and terminate as “endfeet” at the vitreal surface (Fig. 6.3). Thus, each Müller cell spans the full thickness of the neural retina. One important consequence is that the cell accumulates potassium from the extracellular space (where it is released through neuronal activity) and then, by concentrating most of its potassium channels in its endfeet that abut the vitreous, the cell can siphon off excess potassium into the vitreous (Newman, 1986, 1987).

Another critical function of the Müller cell is to regenerate a *cis*-form of the visual pigment 11-*cis*-retinal, which the cone can convert to 11-*cis*-retinol for use in transduction (Mata et al., 2002). This reaction within the Müller cell, relative to the alternate pathway for regenerating retinol within the pigment epithelial cells, is 20-fold faster (to match the cone’s high rate of bleaching). Rods cannot convert retinal to retinol, so they rely exclusively on the slower regenerating pathway within the pigment epithelial cells. Because rods are 20-fold more numerous than cones, this critically conserves the active form for use by cones.

CELL POPULATIONS

Spatial Density of Receptors. Cones and rods pack densely, occupying 90% of the two-dimensional receptor sheet with a residual extracellular space of about 10% (Fig. 6.10) (Packer et al., 1989). Animals active in both day and night, such as human, macaque, cat, and rabbit, assign about 5% of their receptors to cones and the rest to rods. If this seems counterintuitive, simply recall that the photon flux in daytime is many orders of



Fig. 6.9. Two types of amacrine cell in tangential view. **A:** Medium-field, “starburst” amacrine cells. Processes from adjacent cells associate to form a planar network with input from cone bipolar ribbon synapses and output to motion-sensitive ganglion cells, including the alpha and directionally selective ganglion cells. **B:** Wide-field amacrine cell whose proximal dendrites (spiny) emit multiple axons (arrowheads). **C:** Same cell at lower magnification. Cell fires transient burst of action potentials (inset) to ON and OFF of a stimulus to receptive field center (black disc) which corresponds to the dendritic field; action potentials travel centrifugally from the cell in all directions. [A from Tauchi and Masland, 1984; B and C from Stafford and Dacey, 1997.]

magnitude greater than that at night. Therefore, in daytime, the retina can operate effectively on a fraction of the photons striking the receptor sheet, whereas from dusk to dawn, every photon counts.

Cone density always peaks in central retina. Species whose lifestyle requires high spatial acuity, such as raptors scanning for prey from great heights or primates foraging for fine morsels at close range, pack cones so densely at the center (*fovea*) that rods are completely excluded (see Fig. 6.10). Each cone connects to a private (*midget*) bipolar cell followed by a midget ganglion cell, and this provides a neural image at the output as fine as the *grain* of the cone array. In human fovea, cone density reaches nearly 200,000/mm², providing 120 cones/degree, which is adequate to create a neu-

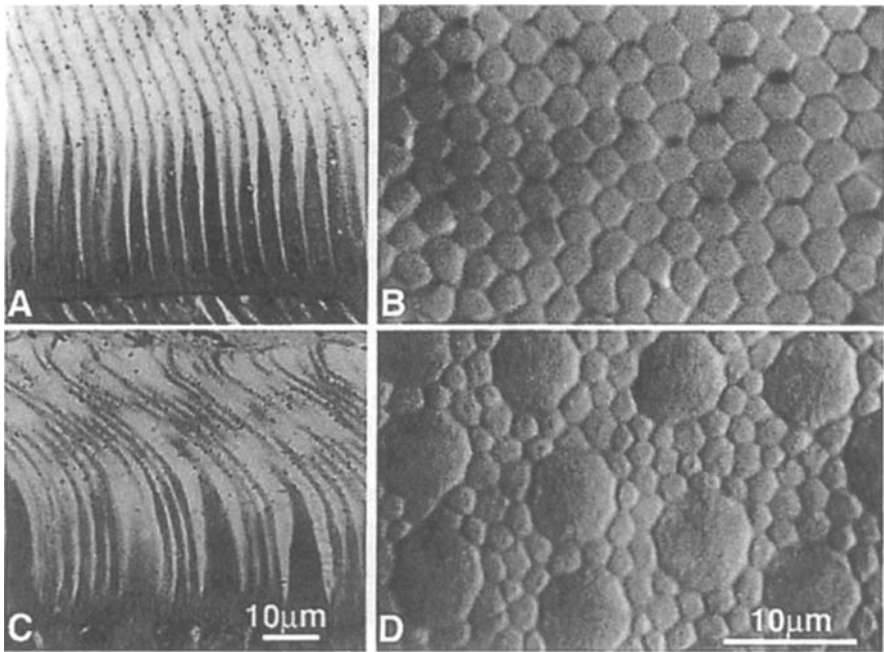


Fig. 6.10. Mosaic of photoreceptors (human). **A:** Fovea: radial section shows cone inner segments to be narrow and gently tapered, and the outer segments to be long and fine. **B:** Fovea: tangential section through base of inner segments shows hexagonal packing. Thus, fovea provides fine spatial sampling in daylight, but absence of rods renders it useless in twilight and starlight. **C:** Periphery: vertical section shows cone inner segments to be squatter but still tapered and surrounded by rod inner segments that are much finer and untapered. **D:** Periphery: tangential view shows about 10 rods per cone, which can boost the cone signal in twilight (see text). Although cones comprise only 10% of the mosaic, their apertures occupy 40% of available collecting area. This is advantageous in daylight when the cones need photons. Then the pupil narrows to accept only photons arriving parallel to the optical axis. These are efficiently captured by the cone's wave-guide mechanism. But the system also works at night, when the rods need photons. Now the pupil dilates to admit photons over a wide range of angles. These are poorly captured by the cone's wave-guide and thus escape to neighboring rods. [Light micrographs from Curcio et al., 1990.]

ral image of a grating as fine as 60 cycles/degree (Fig. 6.10; Curcio et al., 1990; Williams, 1992; Smallman et al., 1996). In the eagle's fovea, cone density and spatial acuity are about double this, apparently reaching a biophysical limit. A higher cone density would require a still finer inner segment, with a wave-guide mechanism that could no longer prevent photons from escaping to a neighboring cone (Reymond, 1985).

Naturally once light intensity falls below cone threshold, the fovea, lacking rods, becomes a blind spot. It is easy to convince yourself of this. At dusk, just as your perception of color fades completely, note that you have also lost the ability to read fine print (as in *The New York Times*). Now hold your thumb at arm's length and, as your gaze steadies upon it, watch it disappear. At this distance, the thumb subtends about 1 degree on the retina, corresponding to the fovea's rod-free region. Thus, while your eyes are free to move, vision seems entirely normal and you do not suspect that 10^6 cones (and consequently about one quarter of your striate cortex) have been silenced (Baseler et al., 2002). Species that can accept somewhat coarser vision in daylight but need central acuity at night reduce cone density at the center to accommodate rods. Thus, cat cone density is almost 10-fold lower than human's in the central area ($30,000/\text{mm}^2$), and this allows for rods at $200,000/\text{mm}^2$ (Williams et al., 1993b). Rod density commonly peaks at about 15–25 degrees from the center (Packer et al., 1989; Curcio et al., 1990; Young and Vaney, 1991; Williams et al., 1993b).

Toward the periphery receptor density declines, but receptor diameter generally increases. For example, in macaque retina (20–80 degrees) rod collecting increases about 2-fold, so that the total photon collecting area remains about constant; the same is true for cones (see Fig. 6.10D; Packer et al., 1989). This would make sense if the optical light gathering efficiency declines toward the periphery, because then a larger receptor could still collect enough light to fill its dynamic range. Such factors must be considered in comparing densities. For example, peak rod density is about 2-fold greater in cat than in human ($400,000/\text{mm}^2$ vs. $175,000/\text{mm}^2$; e.g., Curcio et al., 1990; Williams, et al., 1993b), but the cat rod's collecting area is smaller by about the same factor. Thus, in terms of photon collecting area, these densities may be equivalent. One reason to make the cat rod finer is that the cat's eye collects more light (larger pupil, reflecting tapetum, etc.); therefore, a finer cross section allows the rod to serve as a single photon detector over a wider intensity range.

Spatial density of different cone types also varies with retinal location. For example, the very center of human retina, termed *foveola*, includes M and L, but not S, cones (Williams et al., 1981; Curcio et al., 1990). This makes functional sense because, when middle and long wavelengths are in sharp focus, short wavelengths are strongly blurred (Williams et al., 1993a). Therefore, to provide maximum spatial acuity, the foveola sacrifices trichromacy. In guinea pig and rabbit, S cones distribute sparsely in superior retina but densely in inferior retina, presumably because inferior retina views the sky (Röhlich et al., 1994). In mouse, there may be only a single cone type that co-expresses both a UV pigment and a middle wavelength (M) pigment (Lyubarsky et al., 1999; Applebury et al., 2000). Cones in inferior retina express mostly UV pigment, whereas those in superior retina express mostly M pigment (Szél et al., 1992; Applebury et al., 2000).

That photoreceptor density is so finely sculpted across the retina implies an efficient postreceptoral circuitry. Such local sculpting could evolve only if the small trades of

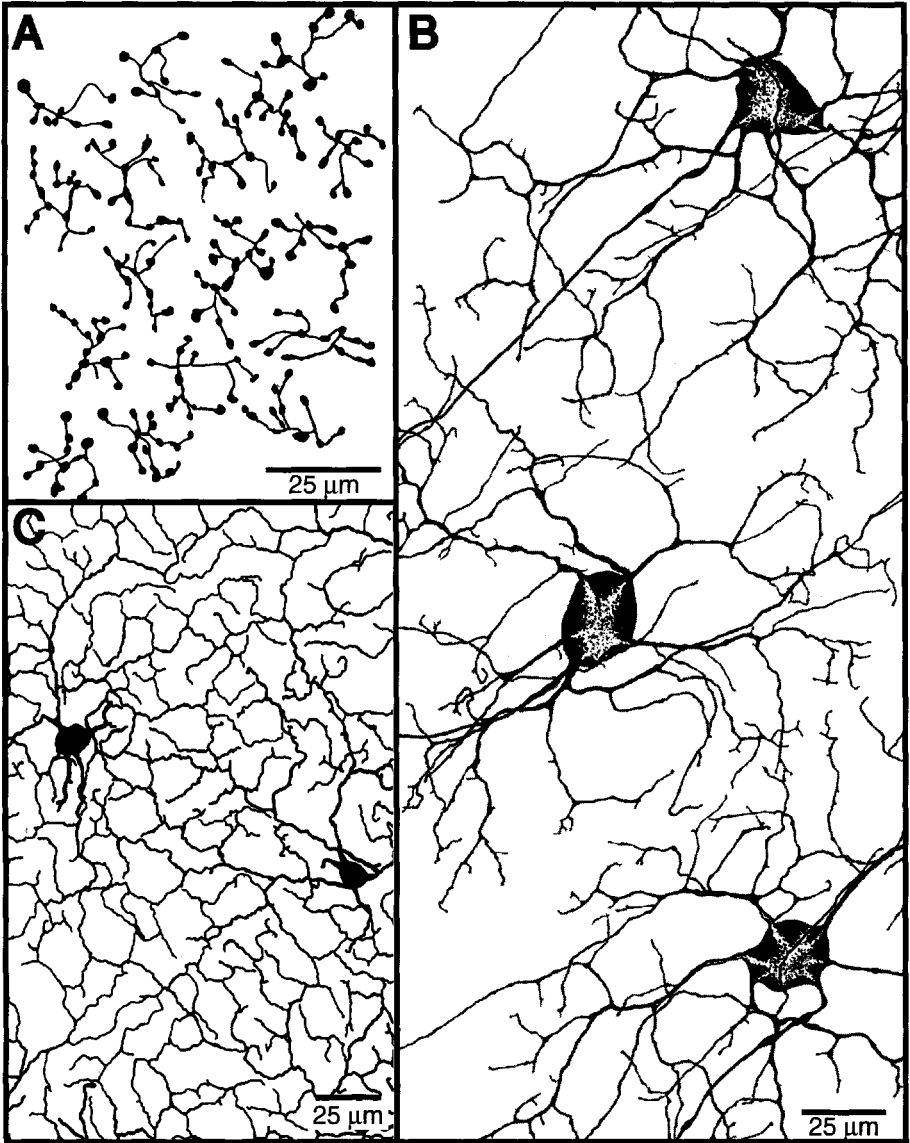


Fig. 6.11. **A:** Array of OFF midget bipolar terminals (macaque) in tangential view. Drawn from tissue immunostained for recoverin, about 10 mm beyond the fovea. The terminals “tile” the plane without overlap. **B:** Array of ON midget ganglion cells (human) in tangential view. Cells injected individually with neurobiotin, about 12 mm beyond fovea. The dendrites tile the plane without overlap and would collect input from many axons in the midget bipolar array shown in **A**. **C:** Array of directionally selective ganglion cells (only the OFF dendrites of the ON/OFF type are shown). One cell was injected with neurobiotin which then spread to adjacent cells. Note the characteristic “loopy” dendrites that tile the plane without overlap. Such tiling behavior holds for all ganglion cells studied so far, with one exception discussed in the text. [A from Wässle et al., 1991; B from Dacey, 1993; C from D. Vaney after Vaney, 1994.]

collecting area between rods and cones at each locus offered a selective advantage. For any such trade, the effect on signal-to-noise (S/N) ratio for photon capture would be proportional to the square root of the fractional change in area (Rose, 1973). For example, a 2-fold increase in cone collecting area would improve S/N for the cone system by at most 1.4-fold. But if subsequent neural stages that process these signals added noise by this factor or more, then any potential advantage of such a difference would be swamped. This alerts one to identify in the postreceptoral circuitry the key contribution to efficient (non-noisy) processing (see Functional Circuits, later).

Spatial Density of Postreceptoral Neurons. Postreceptoral cell types also distribute with characteristic spatial density (Wässle and Riemann, 1978). This has been determined by standard histological methods, by reconstruction from electron micrographs (e.g., Sterling et al., 1988; Cohen and Sterling, 1990b), and by immunostaining for a particular protein or epitope that fortuitously selects a particular type and stains the whole array. Thus, antibody to protein kinase C reveals the complete rod bipolar cell array (see Fig. 6.5; Young and Vaney, 1991); anti-Go_α shows the ON cone bipolar cells (Vardi, 1998), anti-recoverin shows OFF midget bipolar cells (Fig. 6.11A) (Milam et al., 1993; Wässle et al., 1994); anti-CCK shows S cone bipolars (Kouyama and Marshak, 1992); anti-calbindin shows the wide-field horizontal cells in cat and rabbit (Röhrenbeck et al., 1989); and anti-calretinin shows the AII amacrine cells (Wässle et al., 1995; for a review, see Hendry and Calkins, 1998). Also, because many cell types couple to their neighbors in the array, intracellular injection of a small tracer molecule, such as neurobiotin, has been used to establish the spatial densities (Figs. 6.11C and 6.12).

The spatial density of postreceptoral neurons follows the photoreceptors in peaking centrally and declining toward the periphery. As spatial density falls, a cell's dendritic tree expands to compensate, so "tiling," or a specific degree of overlap (see later), is maintained (see, e.g., Wässle et al., 1978b, 1981a,c). However, the number of neurons

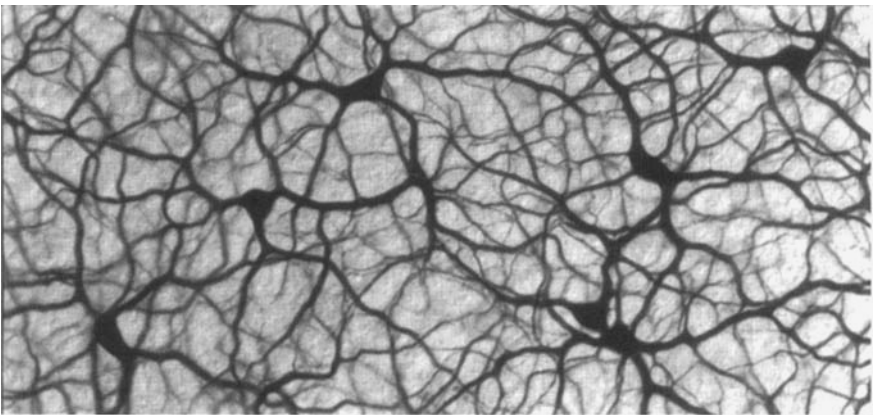


Fig. 6.12. Array of type A horizontal cells (rabbit) in tangential view. One cell was injected with neurobiotin, which then spread through gap junctions to reveal the whole array. Note the characteristic of this array: stout cables, strong coupling, and extensive overlap (cf. Fig. 6.12). [From S. Mills, after Mills and Massey, 1994.]

converging upon a particular cell type may increase or remain constant. For example, rods converging onto the rod bipolar cell increase from about 15 in macaque central retina to about 60 in the periphery, whereas the number of cones converging upon a given type of cone bipolar cell remains constant at 5–10 (Grünert et al., 1994). Photoreceptors converging upon a ganglion cell increase linearly. For example, about 35 cones converge upon a central beta cell, but 180 cones converge on a peripheral beta cell (Tsukamoto et al., 1990).

The Finest Ganglion Cell Array Sets Visual Acuity. Spatial resolution is set by the finest sampling array at the retinal output. To discriminate the fine lines of a grating from a homogeneous field requires one ganglion cell for each dark or bright line (Tsukamoto and Sterling, 1991; reviewed in Wässle and Boycott, 1991; Smallman et al., 1996). In the fovea, because a midget ganglion cell connects to only one cone, resolution corresponds to the cone sampling frequency. But outside the fovea, many cones converge on a midget ganglion cell (see Fig. 6.11B; Dacey, 1993), so resolution is set by the midget cell array. Similarly in cat, resolution is set by the beta cell array. Because pairs of ON and OFF of the same cell class (e.g., midget, beta) sample the same territory (see Fig. 6.15), resolution is set by the density of one of these arrays but not by their combined density (reviewed in Wässle and Boycott, 1991).

Tiling vs. Overlap of Neuronal Arbors. Along the forward pathways from cones, the neuronal arbors of a given type do not overlap. Instead they show mutual avoidance, also termed “territoriality” (Wässle et al., 1981a,b,c). Consequently, their fields tend to tile the plane of the retina, forming a quasi-regular meshwork (Panico and Sterling, 1995). This rule holds for dendrites of each cone bipolar type and for their axon terminals (see Fig. 6.11A; Cohen and Sterling, 1990a,b; Boycott and Wässle, 1991).

Ganglion cell dendritic fields also tile. This has been shown for the alpha cell and delta cell in cat (Dann et al., 1988; Dacey, 1989b), for the ON-OFF directionally selective ganglion cell in rabbit (see Fig. 6.11C; Vaney, 1994b), and for parasol and midget ganglion cells in primate (see Fig. 6.11B; Dacey and Brace, 1992; Dacey, 1993). The lattice structures formed by presynaptic cone bipolar axon arbors complement the postsynaptic ganglion cell dendritic arbors (cf. Fig. 6.11A vs. Fig. 6.11B). This connects the two arrays reliably while minimizing cost in materials and the volume occupied by the lattices (Panico and Sterling, 1995).

Overall, a cone terminal, being narrower than the bipolar dendritic field, contributes most of its synapses to one member of each bipolar array and a few synapses to some neighbors (Sterling, et al., 1988; Cohen and Sterling, 1990a). Similarly the cone bipolar axon arbor is narrower than the ganglion cell dendritic field so each bipolar contributes most of its synapses to one ganglion cell (cf. Fig. 6.6A vs. Fig. 6.6B; Fig. 6.11A vs. Fig. 6.11B). Consequently, a cone signal diverges very little on its course toward the retinal output, so each cone contributes most of its synaptic output to one member of a ganglion cell array (Sterling et al., 1988).

Along the forward pathways from rods, certain neural arbors *do* overlap. Thus, dendrites of neighboring rod bipolars overlap enough that every rod synapse, although approximating a point in the plane of the retina, contacts at least two bipolar cells (see Fig. 6.5; Sterling et al., 1988; Young and Vaney, 1991). Similarly, the AII cell’s col-

lecting arbor in the inner plexiform layer overlaps more extensively, by 2- to 3-fold in central retina of cat, rabbit, and monkey and up to 10-fold in peripheral retina of rabbit (Vaney, 1985; Sterling et al., 1988; Vaney et al., 1991; Wässle et al., 1995). Thus, although the rod bipolar axon arbors tile without overlap (see Fig. 6.5; Sterling et al., 1988; Young and Vaney, 1991), the circuit leading from one rod diverges markedly (Sterling et al., 1988; Vardi and Smith, 1996).

Along *lateral pathways*, a given cell type does not show simple territorial behavior; instead, it overlaps with its neighbors, and sometimes they actually associate. Horizontal cell processes overlap enough that each retinal locus is “covered” by the arbors of 3–8 cells (Wässle et al., 1978a; Röhrenbeck et al., 1989). Furthermore, where horizontal cell processes of a given type cross each other, they form gap junctions and thus couple electrically. This holds for both the wide-field and narrow-field horizontal cells that connect with cones and for the axon arbors that connect to rods; thus, using both chemical and electrical synapses, these systems diverge extensively. Experimentally, this is convenient because a small tracer molecule injected into one neuron can reveal much of the network (see Fig. 6.12; Mills and Massey, 1994; Vaney, 1994a).

Wide-field amacrine cells behave similarly: their processes cross each other extensively and couple. Thus, although their somas distribute sparsely, their processes and synapses distribute densely, forming a rather fine meshwork (Masland, 1986; Dacey, 1989a; Vaney, 1990). Certain narrow-field amacrine cells are labeled by neurobiotin injected into an alpha or a parasol ganglion cell (Dacey and Brace, 1992; Vaney, 1994a; Xin and Bloomfield, 1997). Thus, coupling in lateral pathways is not limited to wide-field types, nor invariably to members of the same type.

The massive evidence of extensive cytoplasmic coupling between neurons is sobering in historical perspective. One hundred years ago, debate was fierce as to whether neurons were coupled (“reticularism”) or entirely separate (“neuronism”). The two schools, led respectively by Camillo Golgi and Santiago Ramon y Cajal, heaped scorn upon each other and refused to consider seriously each other’s observations. For about 50 years, it seemed that Cajal and the “neurone doctrine” had triumphed. But now it is clear that Cajal jumped to conclusions well beyond the resolution of the light microscope. Further, the drawings by reticularists, such as Dogiel (see Vaney, 2002), of apparently coupled ganglion cells may well have reflected spread of tracer (methylene blue) between coupled cells.

The starburst amacrine cell (both ON and OFF types) forms a different and distinctive pattern. The spatial densities are intermediate and their arbors are medium-field, so each retinal locus is covered by about 80 arbors. Yet, the individual processes do not cross each other but instead associate in bundles, thus forming a coarse, quasi-regular meshwork (see Fig. 6.9A).

Foveal Architecture Implies “Pursuit” Eye Movements. The foregoing aspects of retinal architecture reflect the broad central nervous system strategy for sensory surfaces: specialize one region to “sample” finely and assign a relatively large volume of brain to analyze the data. Concurrently, render the specialized surface mobile and evolve “attentional” mechanisms to allow the organism to select which region of the environment to analyze. In the primate retina, about half of the cones and ganglion cells are concentrated in the fovea, and a quarter of striate cortex is devoted to the fovea (re-

viewed in van Essen et al., 1992; Baseler et al., 2002). Apparently the fovea occupies only its fair share of cortex, i.e., in proportion to the ganglion cells that it contributes (Schein, 1988; Wässle et al., 1989). Although this has been disputed (Azzopardi and Cowey, 1993), it seems parsimonious to think that the brain allots computational space proportional to the information content of the input. Therefore, to devote more space than warranted purely by ganglion cell density would seem, *prima facie*, a poor investment.

The strategy of using the central retina for fine spatial sampling requires “smooth pursuit” eye movements to stabilize an object of interest upon the center. This minimizes motion in the image, reducing the need for central ganglion cells to code temporal information. But however, conversely, this strategy *maximizes* image motion seen by peripheral ganglion cells (Eckert and Buchsbaum, 1993a,b). Thus, within a given cell type response properties should vary with retinal location. A cat beta cell or primate midget cell that fires tonically to stabilized stimuli in central retina should fire more transiently to moving stimuli in peripheral retina. This has been found experimentally (Cleland et al., 1971; de Monasterio, 1978) and may in part explain why peripheral ganglion cells collect from more cones (Tsukamoto et al., 1990)—the better to measure transient signals.

Spatial Density of Müller Cells (Glia). The peripheral primate retina contains two Müller cells for each cone; however, the fovea contains one Müller cell for each cone (Burris et al., 2002). Processes of several Müller cells coat the lateral surfaces of each foveal cone synaptic terminal, but these sheets form small windows to permit gap junctions between the pedicles and avoid the basal surface of the pedicle (Fig. 6.13) (Tsukamoto et al., 1992; Burris et al., 2002). Müller cell processes express at high density transporters for glutamate, GABA, etc. Consequently, their three-dimensional relationship to the synapse is important—either for *facilitating* “spillover” at the base of the cone terminal (Haverkamp and Wässle, 2000) or for *preventing* spillover between adjacent terminals (Burris et al., 2002).

SYNAPTIC CONNECTIONS

OUTER PLEXIFORM LAYER

Ribbon Synapse. The photoreceptor’s chemical synapse employs a synaptic ribbon. This is a flat organelle whose long axis anchors near the presynaptic membrane (see Fig. 6.13). Synaptic vesicles tether to both faces of the ribbon via short filaments, so vesicles along the ribbon’s basal edge touch the presynaptic membrane. Here they appear to “dock” ready for release. This occurs when the photoreceptor depolarizes, admitting calcium through channels in the presynaptic membrane all along the region where the ribbon anchors (reviewed in Matthews, 1996; Morgans, 2001; Wässle, 2003). The elongated active zone docks about 5- to 10-fold more vesicles than at a conventional synapse, and, because a vesicle need move only 30 nm on the ribbon to reach an emptied docking site, the ribbon has long suggested a mechanism for rapid “reloading” (Rao-Mirotznik et al., 1995).

This idea is now supported by capacitance measurements on isolated cells and terminals. A vesicle fusing to the presynaptic membrane increases the capacitance by

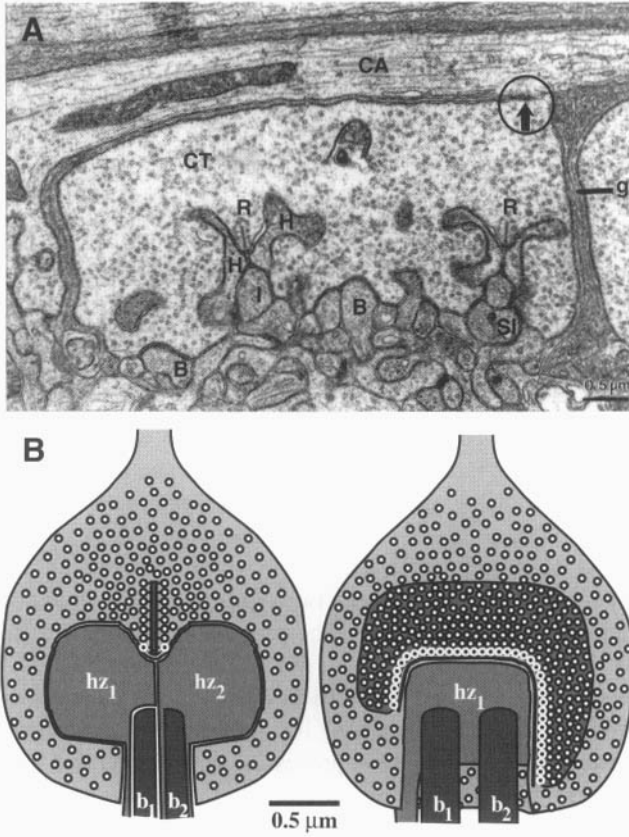


Fig. 6.13. **A**: Cone terminal in radial section (electron micrograph, macaque fovea). Two “triads” are present, each with a synaptic ribbon (*r*) pointing between two horizontal cell processes (*H*) toward an invaginating bipolar dendrite (*IB*). There are also “basal contacts” onto bipolar dendrites distant from the ribbon (*B*), and a gap junction (*G*) with the adjacent cone axon (*CA*). The complete terminal contains about 20 ribbon synapses. **B**: Rod terminal in orthogonal views (from three-dimensional reconstruction, cat central area). One ribbon points between two horizontal cell processes (*hz*) toward two rod bipolar dendrites (*b*). Note that bipolar dendrites are hundreds of nanometers distant from docked vesicles at base of ribbon. [**A** from Tsukamoto et al., 1992; **B** from Rao-Mirotznik et al., 1995.]

about 26 attoFarads (von Gersdorff and Matthews, 1994; von Gersdorff et al., 1996). When synchronous fusion of many vesicles is induced by a step depolarization, the increase in capacitance becomes measurable. Where the number of ribbon synapses is known, the peak fusion rate has been calculated at about 500 vesicles/ribbon/s (Parsons et al., 1994; von Gersdorff et al., 1996). Furthermore, the capacitance jump corresponds to the total number of vesicles tethered on all the ribbons in a terminal (von Gersdorff et al., 1996). These maximum evoked rates appear to represent the peak of the operating range, so normal rates may be more like 20–100 vesicles/ribbon/s (Rao et al., 1994b; Freed, 2000a,b). Indeed, a milder stimulus, raising intracellular calcium by 2 μM , fuses 400 vesicles/s in salamander rod, or about 50/s/ribbon (Townes-

Anderson et al., 1985; Rieke and Schwartz, 1996). A ribbon synapse outperforms a conventional synapse in both peak and sustained rates. A conventional synapse attains a peak rate of 150 vesicles/s (Borges et al., 1995) and a sustained rate of 20 vesicles/s (Borges et al., 1995; Stevens and Tsujimoto, 1995). The ribbon synapse appears to be present in all cases where transmitter release is modulated by graded potentials rather than spikes, probably because graded potentials permit much higher rates of information transfer (de Ruyter and Laughlin, 1996).

How the ribbon facilitates rapid exocytosis is uncertain. The ribbon might serve as a “conveyor belt” along which vesicles move by a cytoplasmic motor. Indeed, such a motor, *kinesin*, is present on the ribbon (Muresan et al., 1999). But microtubules, the “tracks” for the kinesin motor, do not associate with the ribbon. Furthermore, the pool of vesicles equivalent to the number tethered to all the ribbons can be completely released when the patch electrode contains an ATP analog that is not hydrolyzed by kinesin (Heidelberger et al., 2002). Conceivably, vesicles might move rapidly on the ribbon by passive diffusion—or simply be held in place and release their contents rapidly via “compound fusion,” a mechanism used by certain neuroendocrine cells (Parsons and Sterling, 2003).

The rod terminal employs a single active zone with one ribbon and one invagination (see Fig. 6.13B). The invagination houses two types of postsynaptic process: horizontal cell spines and bipolar dendritic tips. The paired spines from overlapping horizontal cell axons penetrate deeply to place their glutamate receptors near the vesicle release site, within about 16 nm. The dendritic tips from two or more cells also penetrate but end quite far from the release sites, about 100–600 nm. In cross section, the invagination often seems to contain only three processes, so it was termed a “triad,” but now we know that the invagination contains at least four processes (see Fig. 6.13B; Rao-Mirotnik et al., 1995). The crescent shape of the rod ribbon, its size (600 tethered vesicles), and the length of the active zone (130 docked vesicles) are all conserved across mammalian species.

The cone terminal employs multiple active zones, each with a ribbon and an invagination (see Fig. 6.13A). There are about 20 active zones per terminal in the fovea and 40 or more per terminal in the periphery (Ahnelt et al., 1990; Calkins and Sterling, 1996; Chun et al., 1996). Each invagination houses paired horizontal cell processes, one from a wide-field, the other from a narrow-field cell, and these penetrate deeply to end near the cone terminal’s release sites (Fig. 6.13A; Kolb, 1970, 1974). One or two bipolar dendrites also invaginate at each active zone but less deeply, terminating 100–200 nm from the release sites (Fig. 6.13A; Kolb, 1970; Calkins and Sterling, 1996; Chun et al., 1996). The external, basal surface of the cone terminal forms symmetrical junctions termed *flat* or *basal* contacts with the tips of bipolar dendrites (Kolb, 1970; Calkins and Sterling, 1996; Haverkamp et al., 2000). All of the invaginating positions are occupied by ON bipolar dendrites, and many of the basal positions are occupied by OFF bipolar dendrites. The cone terminal membrane at the basal contacts bears neither a ribbon nor a conventional cluster of docked vesicles. Therefore, it was widely thought that ribbon synapses serve the ON dendrites by exocytosis and that basal synapses serve the OFF dendrites by some transmitter release mechanism yet to be identified (e.g., Kolb, 1994).

However, this simple rule does not hold. Many ON bipolar dendrites also receive basal contacts (Calkins and Sterling, 1996; Chun et al., 1996), and it becomes appar-

ent that the key functional difference between OFF and ON dendrites depends not on the junctional morphology but on which type of glutamate receptor they express. OFF bipolar cells express ionotropic glutamate receptors (iGluR), AMPA for one cell type and kainate for two other types (DeVries and Schwartz, 1999; Haverkamp et al., 2001a; Gruenert et al., 2002). ON bipolar cells express the metabotropic glutamate receptor, mGluR6 (Masu et al., 1995; Vardi et al., 2000a). Because iGluRs *open* a cation channel, whereas mGluR6 *closes* a cation channel, glutamate drives the membrane potentials of these cell classes in opposite directions. Despite the relatively huge distance from the vesicle release site to invaginating and flat bipolar dendrites (hundreds of nanometers), a single vesicle can still deliver pulses of transmitter in the 10 μM range by simple diffusion (Rao-Mirotnik et al., 1998). This concentration, which would be sustained for several milliseconds, corresponds to the effective concentrations for ON and OFF bipolar dendritic tips (de la Villa et al., 1995; Sasaki and Kaneko, 1996). Thus, a vesicle released at the ribbon synapse probably serves both invaginating and basal dendrites.

Nonribbon Synapses. Horizontal cell processes contain some small vesicles and in one case (human rod) clearly form conventional synapses onto the photoreceptor (Linberg and Fisher, 1988). However, this is the only known case, so it is uncertain whether GABA is released from horizontal cells via conventional vesicular mechanism or via a calcium-independent mechanism, such as a GABA transporter (Schwartz, 1987). The vesicular GABA transporter (vGAT) has been localized near the plasma membrane, suggesting a role in releasing GABA (Cueva et al., 2002; Jellali et al., 2002). In cold-blooded species the photoreceptor terminal is sensitive to GABA (e.g., Tachibana and Kaneko, 1984; reviewed in Piccolino, 1995), so one expects this as well in mammals. This has yet to be confirmed by physiology or immunocytochemistry, because antibodies to various subunits of GABA_A and GABA_C receptors do not stain the terminals. Cone bipolar dendrites do stain strongly for GABA_A receptor just outside the invagination (Vardi and Sterling, 1994), and rod bipolar dendrites stain for GABA_C receptor (Vardi and Sterling, 1994; Enz et al., 1996; Haverkamp et al., 2000). Physiologically, cone and rod bipolar dendrites express both a GABA_A and a GABA_C current, with a GABA_A-to-GABA_C ratio of $\approx 4:1$ (Shields et al., 2000). Therefore, horizontal cells may release transmitter diffusely along the interface between bipolar dendrites and photoreceptor terminals.

A few conventional synapses are present in the OPL. Mostly these are from GABAergic interplexiform processes onto bipolar dendrites (McGuire et al., 1984; Cohen and Sterling, 1990b). However, other transmitters may affect the OPL without benefit of conventional synapses. For example, the dopamine-containing processes ascending from the amacrine cell layer meander through the OPL without making conventional contacts. D₁ receptors are present in OPL (Veruki and Wässle, 1996; Nguyen et al., 1997; Koulen, 1999), and dopamine potently uncouples horizontal cell gap junctions (DeVries and Schwartz, 1989; Hampson et al., 1994; Xin and Bloomfield, 1999; He et al., 2000; reviewed in Weiler et al., 2000). In short, there is ample evidence here for “paracrine” effects of a transmitter (Witkovsky et al., 1993).

Gap Junctions. Electrical synapses (gap junctions) are present at three critical sites in the OPL. First, each cone terminal couples to its immediate neighbors via relatively

small junctions (see Fig. 6.13A). For example, each terminal in primate fovea is estimated to have 10–100 connexons (the multimeric channel that forms the junction) with its neighbors (Raviola and Gilula, 1973; Tsukamoto et al., 1990; DeVries et al., 2002). Second, each rod terminal forms a gap junction with each of two neighboring cone terminals (Kolb, 1977; Smith et al., 1986). Because there are about 20 rods for every cone, a cone must couple to about 40 rods (Sterling et al., 1988). These junctions feed rod signals into the cone terminal (Nelson, 1977; Schneeweis and Schnapf, 1995, 1999). Third, there are numerous, extensive gap junctions between horizontal cells. Wide-field cells couple and narrow-field cells couple, but the two types do not cross-couple (Mills and Massey, 1994; Vaney, 1994a).

INNER PLEXIFORM LAYER

The sole input to this layer derives from bipolar axon terminals. These form ribbon synapses, but the ribbons are generally smaller and more numerous than in a photoreceptor terminal. For example, compared with a rod ribbon's 600 vesicles with 130 docked, a rod bipolar terminal has relatively few vesicles—only 100 with 20 docked (Rao and Sterling, 1991). The rod bipolar terminal (cat) contains about 30 ribbons, whereas a cone bipolar terminal can contain more than 100 ribbons. The number of ribbons is distinctive for a given cell type at a given eccentricity and is highly regular, varying at most by 10% (McGuire et al., 1984; Cohen and Sterling, 1990b; Calkins et al., 1994; Tsukamoto et al., 2001).

The bipolar terminal does not invaginate, so one ribbon synapse cannot accommodate many postsynaptic processes. Instead, two postsynaptic processes align on either side of the linear active zone, forming a *dyad* (Fig. 6.14) (Dowling and Boycott, 1966). The postsynaptic elements at a dyad can be two ganglion cell dendrites, two amacrine processes, or one of each. Often, the amacrine process feeds back a conventional synapse onto the bipolar axon, in which case it is called a *reciprocal* synapse (e.g., Calkins and Sterling, 1996; Freed et al., 2003). Each bipolar type expresses a specific pattern. For example, the rod bipolar dyad always includes one process from an AII amacrine and another from a small subset of different amacrine types. The AII *never* gives a reciprocal synapse at the rod bipolar dyad, but the other amacrine types *always* do. Beta ganglion cell dendrites are *never* found at the rod bipolar dyad, but alpha cell dendrites are present at about 1 dyad of 30 (McGuire et al., 1984; Freed et al., 1987; Freed and Sterling, 1988).

Lateral connections in the IPL use conventional chemical synapses and gap junctions. Amacrine cells are the sole source of conventional synapses (Dowling and Boycott, 1966). Synaptic vesicles are invariably round, and presynaptic and postsynaptic densities show symmetrical thickening. Therefore, synapses cannot be classified as excitatory or inhibitory based on morphology. Commonly in cold-blooded (small-brained) animals, conventional synapses are arranged such that adjacent processes contact each other serially in long sequences (Dubin, 1976). These sequences might perform complex, local computations. However, the underlying circuits have not yet been worked out, and their actual function is unknown.

An electrical synapse is present at five classes of connection in the IPL. First, it interconnects certain types of cone bipolar cell, both homotypically (b_4 – b_4) and heterotypically (b_3 – b_4 ; Cohen and Sterling, 1990b). Second, it couples particular types of amacrine cell homotypically, such as the AII and wide-field types (Vaney, 1994b). Third,

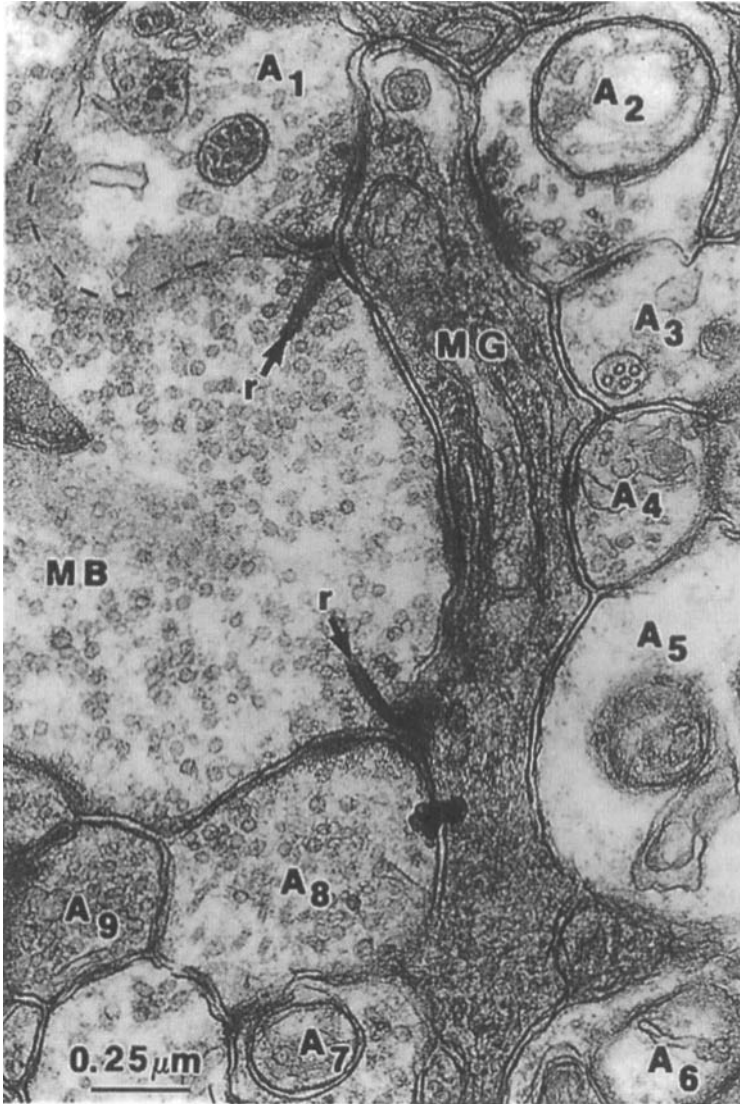


Fig. 6.14. Midget bipolar terminal (MB) in radial section (electron micrograph, macaque fovea). Two “dyads” are present, each with a presynaptic ribbon. The ribbon points between two post-synaptic processes, the dendrite of a midget ganglion cell (MG) and an amacrine process (A_1 , A_8) that feeds back onto the bipolar terminal and forward onto the ganglion cell (A_8). Many other amacrine processes also contact the ganglion cell. [From Calkins and Sterling, 1996.]

it couples particular amacrine types to bipolar cells. For example, the largest electrical synapse in IPL couples an AII amacrine dendrite to an ON cone bipolar axon terminal (Kolb and Famiglietti, 1974; Sterling et al., 1988; Strettoi et al., 1990). This connection is apparently critical for vision under starlight, as is discussed later. Fourth, certain narrow-field amacrine cells couple to particular types of ganglion cell (alpha,

parasol; Dacey and Brace, 1992; Vaney, 1994b). Finally, certain types of ganglion cell couple homotypically without amacrine participation, e.g., the directionally sensitive ganglion cell (see Fig. 6.11C; Vaney, 1994a,b).

The ganglion cell differs from “output” cells in other brain regions. The cell is a relatively small, 10–25 μm soma, compared with 50–80 μm for the motoneuron and Purkinje cell. And ganglion cell dendrites typically extend for only 20–200 μm , compared with 1000 μm for the motoneuron. Correspondingly, the ganglion cell collects relatively few synapses: 60–100 for a central midget cell, 200 for a central beta cell, and 3000 for a peripheral beta and a central alpha cell (Freed and Sterling, 1988; Cohen and Sterling, 1992; Kier et al., 1995; Calkins et al., 1996). In contrast, a spinal alpha motoneuron collects about 10,000 synapses, and cerebellar Purkinje cell collects more than 100,000 synapses! Another difference: a ganglion cell collects synapses exclusively on dendrites and not the soma. By contrast, the motoneuron is encrusted with synapses over its entire surface (see Chap. 3), and the very design of the Purkinje cell seems to hinge on an antagonism between excitatory inputs to the dendritic tree and inhibitory inputs to the soma (see Chap. 7).

DEVELOPMENT

Understanding of how retinal circuits develop is rather fragmentary at present, so rather than attempt a synthesis, we note some current lines of investigation. A key effort is to identify mechanisms that generate the plethora of retinal cell types. This seems to involve specific transcription factors. For example, the Brn-3 family of POU domain transcription factors are expressed in subsets of retinal ganglion cells. These proteins first appear in ganglion cell precursors migrating from the zone of dividing neuroblasts to the future ganglion cell layer. Targeted disruption of the *Brn-3b* gene causes selective loss of 70% of ganglion cells but not other types (Gan et al., 1996); also, transgene expression of *Brn-3* members labels various types of amacrine and ganglion cells but not other types (Xiang et al., 1996). Still another POU-domain protein, RPF-1, is expressed in neuroblasts destined to become ganglion and amacrine cells (Zhou et al., 1996).

Another effort concerns the mechanisms that regulate cell number (Williams and Herrup, 1988). As is generally the case, excess cells are produced and then “pruned” by cell death (“apoptosis”). Thus, in cat by embryonic day 39, about 700,000 ganglion cells send axons into the optic nerve. They connect centrally and fire action potentials that drive geniculate neurons (Katz and Shatz, 1996). Nevertheless, by birth only 270,000 axons remain, and by 6 weeks postnatally, there are only about 180,000, which is the adult number (Williams et al., 1986). Why certain ganglion cells live while others die remains to be established, but the current best guess is that the process involves competition for a specific neurotrophin (reviewed in Katz and Shatz, 1996).

Prenatal firing of optic axons shapes geniculate development because blocking these action potentials prevents segregation of eye-specific geniculate layers (Penn et al., 1998). The activity may also help establish orderly two-dimensional maps of retina in central structures (Katz and Shatz, 1996; Katz and Crowley, 2002). This spontaneous ganglion cell firing is not random but rather sweeps across the retina in waves, so that adjacent cells fire together (Meister et al., 1991). The waves of firing are also associ-

ated with waves of intracellular calcium fluctuation in amacrine and ganglion cells that may be triggered by cholinergic amacrine cells (Zhou, 2001b). The waves may also be coordinated via electrical coupling and shared levels of extracellular potassium (Burgi and Grzywacz, 1994; Penn et al., 1994; Singer et al., 2001). Because “neurons that fire together, wire together,” these waves of correlated activity may contribute to the orderly relationships at the far end of the optic nerve (Katz and Shatz, 1996). The need to generate these early waves of activity may explain why the earliest synaptic connections in the retina involve lateral rather than forward elements (Maslim and Stone, 1986).

In this early period, GABA and glycine excite ganglion cells and only later switch over to their more standard inhibitory actions (Fischer et al., 1998; Zhou, 2001a). For GABA and glycine to excite, the chloride equilibrium potential must be positive to the resting potential, implying that intracellular chloride concentration is higher during development than in the adult. Consistent with this prediction, the chloride transporter NKCC (which raises intracellular chloride) is high in early development and declines relative to KCC2 (which lowers intracellular chloride) about the time that GABA becomes inhibitory (Vu et al., 2000; Zhang et al., 2003).

At birth, the main ganglion cells in cat (alpha, beta, etc.) are easily recognized (Dann et al., 1988; Ramoa et al., 1988). But they are not yet connected to their intraretinal circuits because the photoreceptors are still proliferating, and the bipolar axons are just descending toward the IPL. As the eyes open (6–10 days postnatal), synaptogenesis enters high gear and is nearly complete by 4 weeks (Vogel, 1978; Maslim and Stone, 1986). Each cell type probably has its own programmed period and rate of synaptogenesis, and there is no simple way to characterize the sequence. Thus, it proceeds neither strictly centrifugally (ganglion cell → bipolar → receptor) nor vice versa (McArdle et al., 1977; cf. Nishimura and Rakic, 1987). Further, the genesis of retinal wiring, despite its coincidence with eye opening, appears to follow a genetic program and to be little affected by light or patterned stimulation. Thus, neither dark rearing nor occlusion by lid suture (which prevents patterned stimulation) much affects adult retinal morphology or physiology, even though such procedures profoundly alter the structure and function of the visual cortex (Daw and Wyatt, 1974; Hubel and Wiesel, 1977). However, ON and OFF ganglion cells express distinct firing properties during development, which may allow postsynaptic thalamic cells to distinguish between them and segregate their output into separate ON and OFF sublaminae (Stryker and Zahs, 1983; Wong and Oakley, 1996). Thus, developmental changes in retinal circuitry influence developmental changes in ganglion cell axon targeting.

Perinatal alpha and beta ganglion cells display immature dendritic arbors with excessive branches and spines, and their ON/OFF dendritic stratification is incomplete (Dann et al., 1988; Ramoa et al., 1988). Pruning of the ganglion dendritic arbors proceeds almost normally in the presence of TTX. Therefore, action potentials, which crucially shape the axon arbor, hardly affect the dendritic arbor (Wong et al., 1991). On the other hand, bipolar input (insensitive to TTX) apparently *does* shape the dendritic arbors. Thus, tonically hyperpolarizing ON bipolar cells during eye opening (by intraocular application of the mGluR6 agonist APB) arrests the normal progress of stratification (Bodnarenko et al., 1995). Furthermore, during synaptogenesis, a retinal ganglion cell’s dendritic tree expands and contracts locally, bringing postsynaptic den-

dritic membrane into contact with presynaptic amacrine and bipolar cell release sites. Such dendritic remodeling depends on nicotinic acetylcholine receptors and local Ca^{2+} release from internal stores in the ganglion cell (Lohmann et al., 2002).

The synaptic connections in adult mammalian retina appear not to be “plastic.” But in lower vertebrates (such as fish and amphibia), the retina continues to grow throughout life, adding nerve cells in concentric rings at the periphery to all three layers. The optic tectum, the main target of the fish and amphibian optic nerve, also continues to add neurons but in concentric crescents rather than in complete rings. This creates a topological mismatch between the retina and its map on the tectum. Consequently, the map requires continuous readjustment. This is accomplished by the continuous retraction of old retinotectal synapses, growth of the optic axons across the tectum, and the formation of new synapses (Easter and Stuermer, 1984; Reh and Constantine-Paton, 1984). If the neural retina is totally removed from the eye of a fish or amphibian, cells from the pigment epithelium de-differentiate, divide, and regenerate a whole new neural retina whose ganglion cell axons find their way to the brain and reconnect properly (Stone, 1950; Saito, 1999).

Another fascinating developmental plasticity is the shift in retinal wiring that in certain organisms accompanies changes in lifestyle. For example, the adult frog eats flies and has a type of ganglion cell tuned by specific circuits to “fly-like” stimuli (Barlow, 1953; Maturana et al., 1960). However, the tadpole eats algae and lacks this cell type. The fly-detecting ganglion cell and its neural circuitry develop as part of the many complex changes that accompany metamorphosis (Frank and Hollyfield, 1987). However, it seems fairly certain that its emergence is directed by a genetic program that operates whether or not the frog is ever confronted with a fly.

VISUAL TRANSDUCTION

Rods and cones share the same transduction mechanism (Fig. 6.15). The outer segment bears numerous cation channels permeable to Na^+ and Ca^{2+} . A channel flickers open upon binding four molecules of cGMP, and in the dark the intracellular concentration of cGMP is high. Therefore, at any instant about 10^6 channels are open. The result in darkness is a continuous inward sodium current at the outer segment, which is balanced by an outward potassium current at the inner segment. This circulating dark current depolarizes the receptor to about -40 mV. The cell’s ionic balance is maintained by an active sodium/potassium exchanger operating continuously at the inner segment, which explains the large energy demand at this site and thus its need for densely packed mitochondria (see Fig. 6.4; reviewed in Yau, 1994; Pugh and Lamb, 1993, 2000).

The optical image focuses at the level of the *inner* segments (see Figs. 6.4 and 6.10). A photon contributing to this image penetrates the plasma membrane to enter the inner segment. Entering a rod, the photon may simply pass through, continuing on until it is finally trapped in a neighboring receptor. Which rod captures a given photon does not matter because at night the optical image is poor and subsequent pooling of rod signals is great. However, if a photon enters a *cone* inner segment roughly parallel to its long axis, it is trapped due to the densely packed and longitudinally oriented mitochondria that raise the refractive index. Thus, the cone inner segment’s “wave-guide”

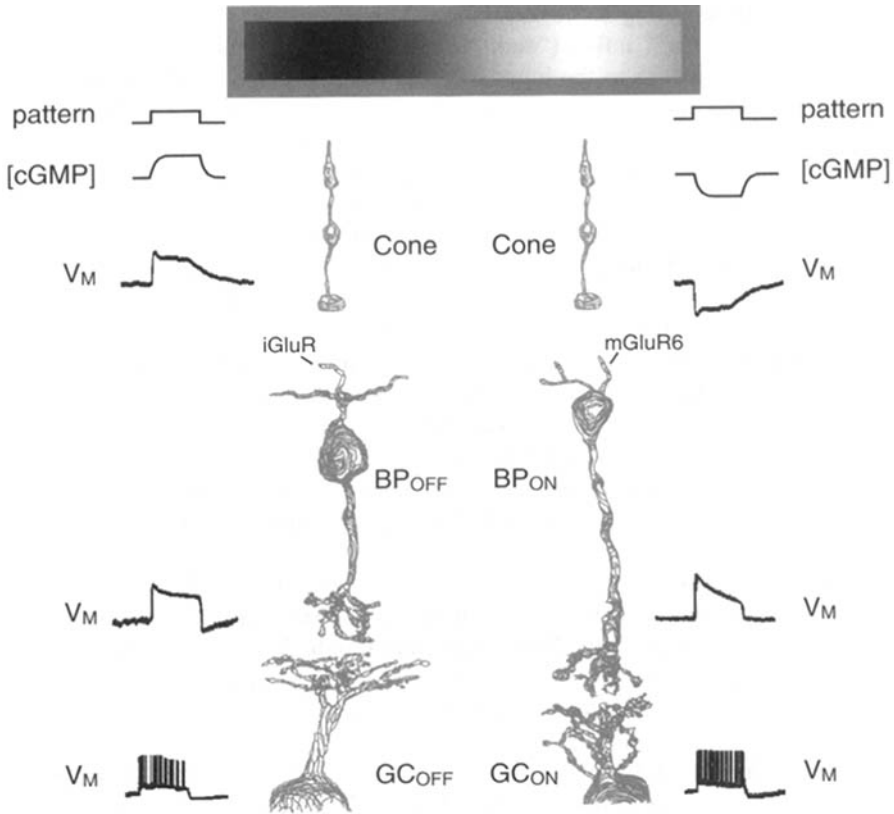


Fig. 6.15. Basics of transduction and forward signal transfer. One cycle of a dark/bright grating flashes briefly on a steady background. Light *decrement* for the left cone allows guanyl cyclase to raise [cGMP], thus opening cation channels in the outer segment and depolarizing the cone membrane potential (V_m). The cone terminal increases its discharge of glutamate onto ionotropic receptors (iGluR), depolarizing the OFF bipolar cell, thus releasing glutamate onto the OFF ganglion cell and causing it to spike. Light *increment* for the right cone isomerizes rhodopsin, triggering the G protein cascade that lowers [cGMP], thus closing cation channels in the outer segment and hyperpolarizing the cone membrane potential. The cone terminal ceases its tonic release of glutamate onto metabotropic (mGluR6) receptors, depolarizing the ON bipolar cell, thus releasing glutamate onto the ON ganglion cell and causing it to spike. This key step at the cone terminal, use of paired neurons to separately encode light decrement and increment, carries forward to the ganglion cells that feed the geniculostriate pathway, doubling the total dynamic range.

funnels photons toward the outer segment to preserve the correspondence between the optical image and the transduced image (Enoch, 1981).

A photon reaching the outer segment penetrates the stacked membrane discs (see Fig. 6.4) until it encounters a molecule of photopigment (rhodopsin) and transfers its energy. This isomerizes the vitamin A group attached to the opsin protein, activates the molecule, and causes it to activate several hundred molecules of the G-protein transducin. Transducin then activates hundreds of phosphodiesterase molecules that rapidly

hydrolyze cGMP, lowering its concentration. This closes the cation channels and reduces the Na^+ and Ca^{2+} influx (“dark current”), thus hyperpolarizing the outer segment. This signal spreads to the inner segment where voltage-gated channels further shape it temporally and boost its amplitude (reviewed in Pugh and Lamb, 1993; Yau, 1994) before sending it down the axon (Hsu et al., 1998).

The rod achieves the ultimate sensitivity: one photon isomerizes one rhodopsin molecule (Rh^*), which lowers the cGMP concentration enough to suppress about 4% of the dark current. This gives a ≈ 0.7 pA signal with a signal/noise ratio of about 3.5 (Baylor et al., 1984). Although the rhodopsin molecule is quite stable, it does isomerize without a photon—by thermal agitation—producing ≈ 0.006 $\text{Rh}^*/\text{rod/s}$. Because the next stage cannot distinguish a photic isomerization from a thermal one, this rate of “dark light” helps set the lower limit of visual sensitivity (reviewed in Barlow, 1982).

The rod sums linearly up to about 20 Rh^* delivered as a flash, saturating completely to 100 Rh^*/flash (Baylor et al., 1984). But to a background that steadily evokes 100 Rh^* per integration time (corresponding to twilight), the rod can reduce its sensitivity and thus avoid saturation when the cone signal is declining toward its threshold. Complete saturation occurs at about 1000 Rh^* per integration time (Tamura et al., 1989, 1991).

Rod adaptation arises from multiple mechanisms that affect individual steps of the phototransduction cascade, and many of these mechanisms depend on the intracellular level of Ca^{2+} (Pugh and Lamb, 2000; Burns and Lamb, 2003). An additional mechanism for adaptation, observed *in vivo*, involves the light-induced movement of the G-protein transducin from the rod outer segment to compartments in the inner segment and soma (Sokolov et al., 2002).

The cone is less sensitive by nearly 70-fold: 1 Rh^* suppresses only about 0.06% of the dark current, but this response is buried by random fluctuations of the membrane current and so is undetectable. The cone signal first rises above the noise when about 100 Rh^* arrive within its integration time; thus its threshold for signaling uses about the same fraction of the dark current as the rod (Schnapf et al., 1990). The cone signal turns on at the same rate as the rod, but turns off much faster, which is key to its shorter integration time and greater temporal resolution (Pugh and Lamb, 1993; Tachibanaki et al., 2001). As light intensity rises, several mechanisms turn down cone sensitivity to retain a linear response, and even in the brightest light the response does not saturate completely (Burkhardt, 1994). The mechanisms that arrest transduction and turn down its sensitivity involve feedback control by calcium at many levels of the cascade but are as yet incompletely understood (reviewed in Yau, 1994; Burns and Lamb, 2003).

DENDRITIC AND AXONAL PROPERTIES

PATTERNS OF FUNCTIONAL POLARIZATION

Classically, “dendritic” has implied passive current flow toward the soma and axon hillock. “Axonal” has implied active propagation away from the soma toward the presynaptic terminal. But in retina as elsewhere (see Chaps. 1 and 2), these simple definitions tend to dissolve. True, the forward “relay” neurons do display typical polarity. Indeed, the sequence: photoreceptor \rightarrow bipolar cell \rightarrow ganglion cell was Cajal’s pri-

mary exemplar (together with the olfactory bulb's mitral cell; see Chap. 5) for his "law" of polarized conduction. However, photoreceptor and bipolar axons do not normally spike; rather they are passive, releasing transmitter upon graded depolarization (von Gersdorff and Matthews, 1994; Rieke and Schwartz, 1996). Also, these axon terminals receive modulatory inputs. Both points violate classical theory.

The lateral elements break *all* the classical rules (Piccolino, 1986). In fact, their designs seem almost *ad hoc*, each suited to accomplish a particular task. Thus, a horizontal cell collects input all along its processes and gives output at the same sites. Furthermore, because horizontal cells are strongly coupled, they present essentially a continuous sheet, passively integrating inputs and modulating outputs rather widely in space and time (Smith, 1995). A narrow or medium-field amacrine cell is also non-polarized because its input and output tend to be near each other (Famiglietti, 1991; Calkins and Sterling, 1996). However, these amacrine processes are quite fine caliber, are not coupled, and may be passive. Consequently the output of such a cell may create a local feedback circuit for temporal sharpening (Freed et al., 2003).

The starburst amacrine cell, with dendrites like spokes of a wagon wheel (see Fig. 6.9), collects excitatory input uniformly along each branch but provides output only at the distal segments. Consequently, light stimulus sweeping across this cell proximo \rightarrow distally excites the output more effectively than a stimulus moving disto \rightarrow proximally (Euler et al., 2002). This effect, coupled with the starburst cell's asymmetrical connections to the directionally selective ganglion cell (Fried et al., 2002), may explain the mechanism for directional selectivity identified long ago (Barlow and Levick, 1965).

The wide-field amacrine cells present a bizarre twist to the theme of polarized conduction. As noted, these cells collect input conventionally via a dendritic tree that funnels PSPs toward the soma. Action potentials also arise conventionally, at an axon hillock, and propagate for millimeters across the retina (see Fig. 6.9). Unconventionally, though, each primary dendrite emits its own axon; thus, although the cell segregates its passive dendrites and spiking axons, the latter broadcast spikes radially in two dimensions.

The AII amacrine cell represents still another twist to the theme of functional polarity and active versus passive membrane. The cell collects its key input from rod bipolar synapses on its main arbor in the ON layer of the IPL and uses gap junctions with cone bipolar axon terminals as a local excitatory output. Because the AII collecting arbor is narrow-field, it should not require active membrane to propagate its signal, yet the cell produces large, fast depolarizations that are sensitive to TTX (Nelson, 1982; Boos, et al., 1993). Here, a voltage-sensitive membrane, rather than spreading signals beyond where passive conduction could take them, seems to provide a "thresholding" mechanism that amplifies nonlinearly to separate small signals from noise (Freed et al., 1987; Smith and Vardi, 1995).

Neighboring AII cells couple to one another with a conductance of about 700 pS, which promotes synchronous spiking in the network (Veruki and Hartveit, 2002). The importance of AII spiking for the ganglion cell response remains unclear because in dark-adapted retina (where the AII carries the rod signal), robust ganglion cell responses are recorded even when AII spikes are blocked with TTX (Taylor, 1999). The AII's response properties and the extent of AII-AII coupling depend strongly on the degree of light adaptation (Bloomfield et al., 1997; Xin and Bloomfield, 1999). Only a few of the 40 amacrine types have been studied, so further surprises are to be expected.

INDIVIDUAL RETINAL NEURONS ARE ELECTROTONICALLY COMPACT

The axons and main dendrites of feedforward neurons are relatively short and thick. Thus rod and cone axons, respectively, 0.5 and 1.6 μm diameter, range from 20 to 400 μm long (Hsu et al., 1998). Bipolar dendrites and axons are about the same thickness as photoreceptor axons but even shorter. Ganglion cell dendrites (beta and alpha) are also about 0.5–1.5 μm in diameter, and the arbors range from about 30 to 250 μm across. Consequently, all synapses onto these cells are calculated to be well within one space constant of the soma. Electrotonic considerations indicate that photovoltages transmitted to rod and cone terminals and EPSPs transmitted from distal dendrites to the ganglion cell soma are little attenuated (Koch et al., 1982; Freed et al., 1992; Kier et al., 1995; Hsu et al., 1998). Ganglion cells in the periphery (alpha, parasol) and certain cell types all across the retina are much larger than 250 μm , reaching up to 1 mm diameter (Berson et al., 1998; Peterson and Dacey, 1999). In these cells, active mechanisms, such as dendritic Na^+ channels, may allow transmission from distal dendrite to soma (Velte and Masland, 1999).

NEUROTRANSMITTERS AND POSTSYNAPTIC RECEPTORS

Essentially all of the transmitters identified elsewhere in the brain exist also in the retina. A transmitter can be assigned to a cell type upon immunocytochemical detection of (1) the endogenous transmitter, (2) its synthetic enzyme, and (3) transmitter receptors on postsynaptic cells. When no antibody is available, *in situ* hybridization for mRNA of the appropriate molecule also provides a clue, but the conclusion remains tentative because the mRNA may not be expressed. Commonly, a neuron that uses a particular transmitter also expresses a transporter molecule on its surface that binds the transmitter in the extracellular space and actively pumps its back into the cell. Müller cells are not known to release glutamate, but they do express receptors for amino acid transmitters and also transporters for both GABA and glutamate (reviewed in Newman and Reichenbach, 1996). Most recently, they are shown to release ATP, which activates A_1 adenosine receptors on ganglion cells and inhibits them, probably by modulating a GIRK (G-protein-regulated K^+ channel; Newman, 2003).

PHOTORECEPTORS TO HORIZONTAL AND BIPOLAR CELLS

Photoreceptors contain the excitatory amino acid glutamate and release it when depolarized. Two experimental *tours de force* seem conclusive. First, a turtle rod was sucked by its outer segment into a micropipette through which it could be electrically stimulated. The tip of a second pipette, bearing a patch of neuronal membrane ripped from a cultured hippocampal neuron, was moved close to the rod axon terminal. The membrane patch, which was “outside out” (see Chap. 2), contained the NMDA type of glutamate receptor. Electrically depolarized, the rod released a transmitter onto this “sniffer” patch, opening ion channels gated by the NMDA receptor (Copenhagen and Jahr, 1989). Second, the rod axon terminal was sucked into a pipette containing glutamate dehydrogenase plus NAD; then release of glutamate was measured directly by an increase in fluorescence due to the formation of NADH_2 (Ayoub et al., 1989).

Postsynaptic to photoreceptors, horizontal cells express iGluRs (AMPA and kainate) that open a cation channel with a reversal potential near zero (Haverkamp et al., 2000, 2001a,b). Thus, as the photoreceptor depolarizes to dark stimuli and releases glutamate

(see earlier and Fig. 6.15), the horizontal cell depolarizes. The OFF bipolar cell dendrites also express iGluRs and thus also depolarize to dark stimuli. Although horizontal and OFF bipolar cells express the same broad class of receptor (iGluRs), the particular combinations of receptor subunits differ (DeVries, 2000). This could explain how the effective concentration for a half-maximal response (EC_{50}) could be 0.5 mM for the horizontal cell and 10 μ M for the bipolar cell (Sasaki and Kaneko, 1996). This sensitivity difference seems key to assembling multiple postsynaptic processes into a complex where they can all be activated by the same point source of glutamate (see Fig 6.13; Rao-Mirotnik et al., 1998).

The ON bipolar dendrites express a *metabotropic* glutamate receptor, mGluR6 (see Fig. 6.15A; Nomura et al., 1994). This receptor, highly localized to the tips of rod bipolar and ON cone bipolar dendrites, couples to a second messenger system requiring the G-protein, G_o (Vardi and Morigiwa, 1997; Dhingra et al., 2000, 2002). Glutamate binds this receptor to *close* an ion channel with reversal potential near zero and thus hyperpolarizes the cell. Light suppresses the photoreceptor's glutamate release to open this cation channel and depolarize the cell. This synapse has been termed "sign-reversing" and "inhibitory" because glutamate's action is to hyperpolarize, but the reversal potential is positive (i.e., excitatory). Therefore, it may be simplest to consider the ON bipolar cell as excited by bright stimuli and the OFF bipolar cell as excited by dark stimuli (both relative to the local mean intensity level).

By using two different receptors for the same transmitter, OFF and ON cone bipolar cells double the dynamic range for encoding intensity differences across a natural scene (see Fig. 6.18). Half of the bipolar cells carry signals greater than the local mean, and half carry signals less than the local mean. Their ganglion cells and corresponding cells in the lateral geniculate nucleus follow suit. Finally, at the level of simple cells in striate cortex, these signals recombine. The receptive field of a cortical "simple cell" comprises elongated ON and OFF subregions. Within an ON subregion firing is evoked by increased excitation from ON geniculate cells and decreased inhibition from OFF geniculate cells; conversely, within an OFF subregion firing is evoked by increased excitation from OFF geniculate cells and decreased inhibition from ON ganglion cells (Palmer and Davis, 1981; Ferster, 1988). Thus, each subregion, wired in "push-pull" fashion, uses the full dynamic range that was initially divided at the cone synapse. An important lesson here is that to understand the reason for a particular encoding procedure at one synapse, one may need to look ahead another four or five stages!

It was thought initially that the ON bipolar cell's mGluR6 couples to a G-protein that activates phosphodiesterase (PDE) to hydrolyze cGMP and close a cation channel, i.e., mimicking the mechanism for phototransduction (Nawy and Jahr, 1990; Shiells and Falk, 1990). But $G_{o\alpha 1}$, the protein coupled to mGluR6, although crucial to the ON light response, is not linked to PDE or cGMP hydrolysis, and thus the link between activation of $G_{o\alpha 1}$ and the closing of the cation channel remains a mystery (Vardi, 1998; Nawy, 1999; Dhingra et al., 2000, 2002).

HORIZONTAL TO PHOTORECEPTOR AND BIPOLAR CELLS

Horizontal cells use GABA. Although mammalian horizontal cells do not demonstrably accumulate exogenous GABA, they do contain it (Chun and Wässle, 1989). They

also express the GABA-synthetic enzyme glutamic acid decarboxylase (GAD) in one of two isoforms, GAD₆₅ or GAD₆₇ (Vardi and Sterling, 1994; Johnson and Vardi, 1998). Further, GABA_A and GABA_C receptors are expressed by cone bipolar and rod bipolar dendrites, implying a local source of GABA, presumably horizontal cells (Vardi et al., 1992; Vardi and Sterling, 1994; Enz et al., 1996; Shields et al., 2000). The cone axon terminal hyperpolarizes to ionophoresis of GABA, suggesting GABA feedback onto it (e.g., Tachibana and Kaneko, 1984; Wu, 1992; Pattnaik et al., 2000).

BIPOLAR TO GANGLION AND AMACRINE CELLS

Bipolar neurons use glutamate as a transmitter. Here the evidence rests mainly on the responsiveness of ganglion and amacrine cells to ionophoresed glutamate and its various agonists and antagonists. iGluRs are both expressed by ganglion cells and specific amacrine types (Cohen et al., 1994; reviewed in Wilson, 2003). Many different subunits of each receptor type are present (Vardi and Morigiwa, 1997; Qin and Pourcho, 1999a,b; Fletcher et al., 2000; Pourcho et al., 2001). However, in general amacrine cells express kainate receptors, whereas ganglion cells express AMPA and NMDA receptors (Grunert et al., 2002). Furthermore, various processes in the inner plexiform layer, including bipolar terminals, express metabotropic glutamate receptors (Hartveit et al., 1995; Brandstätter et al., 1996; Awatramani and Slaughter, 2001; Higgs et al., 2002).

Certain bipolar neurons contain glycine and appear to accumulate it from the extracellular medium (Cohen and Sterling, 1986; Pourcho and Goebel, 1987). Furthermore, some ganglion cells bear glycine receptors and respond to ionophoretic glycine with an increased Cl⁻ conductance that is blocked specifically by strychnine (Bolz et al., 1985; Koulen et al., 1996). However, it now appears that glycine enters the bipolar terminal via the gap junctions with the AII amacrine cell that accumulates it via a glycine transporter (Cohen and Sterling, 1986; Vaney et al., 1998). Thus, although bipolar cells contain glycine and apparently provide a glycine reservoir for the AII cell, they probably do not release it.

One striking complication is that certain bipolar cells contain endogenous GABA and express GAD (Wässle and Chun, 1988; Vardi and Auerbach, 1995). These cells represent two distinct types with axons in the OFF layer of the IPL (Kao et al., 2003). These cells express the vesicular transporters of both glutamate and GABA, and thus probably do release both transmitters (Kao et al., 2003). If so, a differential arrangement of postsynaptic receptors would permit this synapse to excite one member of its postsynaptic dyad (ganglion cell) while simultaneously inhibiting the other (AII amacrine cell).

AMACRINE CELLS

About half of all amacrine somas contain glycine and half contain GABA plus GAD (Vardi and Auerbach, 1995). However, GABA is expressed by many amacrine types that also express other transmitters. For example, the starburst amacrine cells that synthesize acetylcholine also synthesize GABA using both isoforms of GAD (Brecha et al., 1988; Kosaka et al., 1988; Vaney and Young, 1988; Vardi and Auerbach, 1995).

Other GABA amacrine cells contain dopamine, indoleamines, or neuropeptides such as somatostatin, vasoactive intestinal polypeptide, and substance P (Sagar, 1987; Vaney et al., 1989b; White et al., 1990; reviewed in Vaney, 1990, 2003; Casini and Brecha,

1992). Still other amacrine cells contain NADPH diaphorase, which synthesizes nitric oxide, so conceivably GABA in amacrine cells is never the sole transmitter (Sandell, 1985; Sagar, 1987). It remains unclear whether any cell co-releases GABA with its other transmitter/modulator, whether they are released at different spatial loci, or in response to different electrical or chemical signals (O'Malley et al., 1994).

Processes postsynaptic at amacrine synapses bear the standard receptor molecules. Thus, where glycine is presynaptic, there are postsynaptic glycine receptors (Freed and Sterling, 1988; Pourcho and Owczarzak, 1991; Sassoè-Pognetto et al., 1994); where GABA is presynaptic, there are postsynaptic GABA_A or GABA_C receptors (Vardi and Sterling, 1994; Enz et al., 1996). Bipolar terminals express both GABA_A and GABA_C receptors, whereas ganglion cells express mainly GABA_A (Shields et al., 2000). GABA_A currents are more transient than GABA_C currents, and thus the relative expression of these two receptors will temporally shape light-evoked inhibition (Shields et al., 2000).

Unlike GABA, dopamine can act in a "paracrine" fashion, reaching postsynaptic targets tens of microns beyond its site of release. Thus, the D₁ receptors distribute much more widely than the conventional dopaminergic synapses (Witkovsky et al., 1993; Veruki and Wässle, 1996). Neuropeptide receptors tend to have many subtypes. For example, for somatostatin there are five types, one of which, SSRT2a, has been localized in retina to the rod bipolar terminal (Reisine and Bell, 1995; Vasilaki et al., 1996). Acetylcholine released by the starburst amacrine cell also must have different receptors because the direction selective cell is affected by nicotinic blockers (ionotropic), whereas alpha and beta cells are also affected by muscarinic agonists (metabotropic) (Schmidt et al., 1987).

Matters already seem complicated by multiple presynaptic transmitters and multiple subtypes of postsynaptic receptor. But they are profoundly more so because many postsynaptic receptors, including those for glutamate, GABA, dopamine, indoleamines, and peptides, couple to various G-proteins, and these trigger a variety of "second messenger" systems. For example, G_{olf} is expressed by wide-field horizontal cells and ganglion cells in the IPL; G_o is expressed by ON bipolar cells and by certain amacrine processes in IPL (Vardi et al., 1993). Because a given G-protein can couple to more than one type of downstream effector, the possible signaling pathways must be very large. Thus, one senses an underlying neurochemical network at least as complex as the network of anatomical connections.

FUNCTIONAL CIRCUITS

HOW EFFICIENT IS THE RETINA?

Having described the main types of retinal neuron and their connections, transmitters, etc., we are nearly ready to consider how the anatomical wiring serves function. But first we should ask how well does the retina perform? The first steps of phototransduction are inefficient: only about one-third of the photons striking the retina are absorbed by a rhodopsin molecule, and only half of these cause isomerization (reviewed in Sterling et al., 1987). Yet once activated, an Rh* projects this information through subsequent stages with remarkable reliability. Thus, a single Rh* activates several hundred transducin (G-protein) molecules and thence a comparable number of PDE cat-

alytic subunits (Leskov et al., 2000), leading reliably to two or three spikes in several ON ganglion cells and to suppression of two or three spikes in several OFF ganglion cells (Barlow et al., 1971; Mastrorarde, 1983; Vardi and Smith, 1996).

Once a single photon signal reaches a ganglion cell, to be useful it must sum efficiently with other such signals. If noise were added along the way, e.g., due to random release of synaptic vesicles, or if the signal were to saturate some stage along the transmission pathway, information would be lost and the image would be degraded. Yet we discriminate stimuli near threshold with very little information loss along neural circuits. The evidence stems from “ideal observer” computer models that perform any specified discrimination simply based on the number of photons counted. The models take account of losses due to optics, photoreceptor sampling, and transduction. But thereafter, they operate ideally, i.e., with no further information loss due to neural mechanisms (Geisler, 1989). It turns out that for a suitable stimulus we approach the sensitivity of an ideal observer to within a factor of 2–3 in both dim and bright light (Crowell and Banks, 1988; Savage and Banks, 1992). Therefore, the sum of all stages—from transduction to the ultimate site of discrimination—must not lose any more information than this. Thus retinal circuits must be extremely efficient—as implied by the fine sculpting of the receptor mosaic (described earlier). This alerts us to circuit mechanisms that prevent noise and saturation.

CIRCUITS FOR GANGLION CELL RECEPTIVE FIELD

Center. The center circuit turns out to be fairly simple: the cones co-spatial with the ganglion cell dendritic field modulate glutamate release onto dendrites of cone bipolar cells whose axons contact the ganglion cell dendritic tree. Brightening these cones depolarizes the ON bipolar cells and delivers glutamate to ON ganglion cell dendrites; dimming these cones depolarizes the OFF bipolar cells and delivers glutamate to OFF ganglion cell dendrites (see Fig. 6.15A). Thus, the “center” circuit is purely excitatory.

The number of cones that connect directly to a ganglion cell dendritic arbor depends on species, retinal location, and ganglion cell type. For example, in cat, about 35 cones overlie a central beta cell dendritic field and employ about 15 bipolar cells to contact it with nearly 200 synapses (Fig. 6.16) (Cohen and Sterling, 1992). About 625 cones overlie a central alpha cell and use about 150 bipolar cells with nearly 450 synapses (Fig. 6.16; Freed and Sterling, 1988). In these respects, a peripheral beta cell resembles a central alpha cell (Kolb and Nelson, 1993; Kier et al., 1995).

In primates, the receptive field centers are much smaller. For example, in the fovea a single cone contacts a pair of “midget” bipolar cells (ON and OFF) that in turn contact, respectively, ON and OFF “midget” ganglion cells. This 1:1 bipolar-to-ganglion cell connection is accomplished with only about 50 synapses (Calkins et al., 1994). In the periphery, e.g., 20 degrees, about 10 cones overlie the midget ganglion cell. Here, although each cone still contacts its own private midget bipolar cell, several of these converge onto a midget ganglion cell (Dacey, 1996; Goodchild et al., 1996b). The wider-field ganglion cells in primate fovea, “parasol” and “garland” cells, collect on the order of 30–50 cones (Calkins and Sterling, 2003).

What explains the alpha cell’s transient response to a steady center stimulus versus the beta cell’s sustained response (see Fig. 6.7)? Multiple mechanisms cooperate: (1) only one type of bipolar cell contacts the alpha cell, and it has a large transient re-

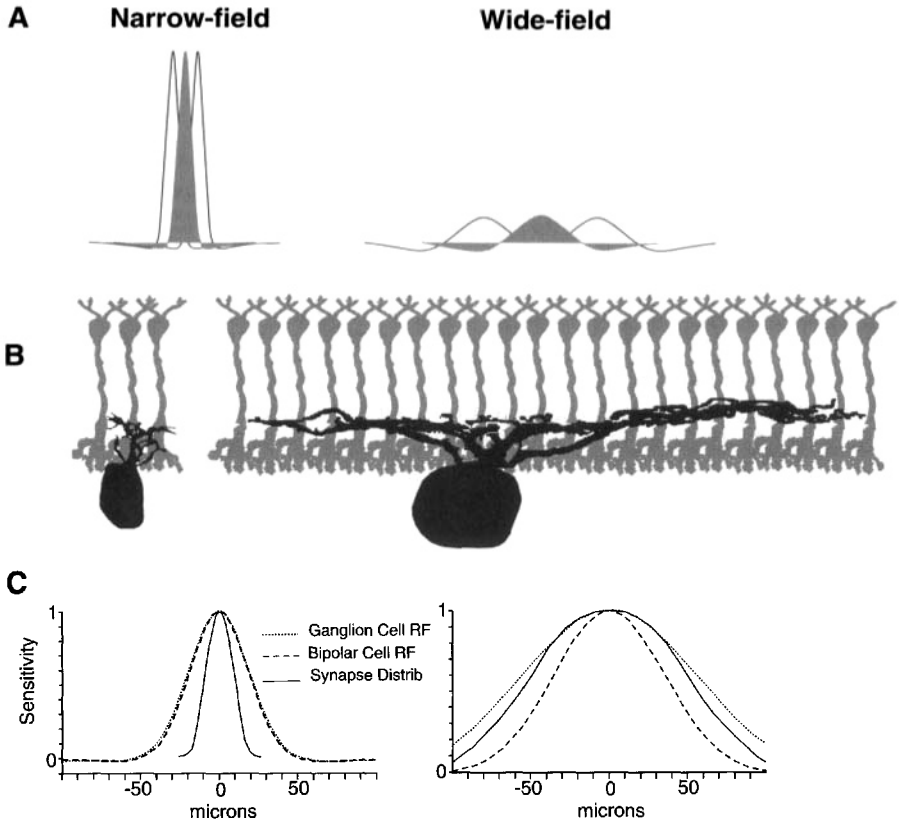


Fig. 6.16. Circuits for the ganglion cell receptive field center. **A:** Sensitivity profiles of central beta and alpha cell receptive fields. Beta cell is 8-fold more sensitive than an alpha cell to a small spot (just covering the beta center). Beta centers are narrow and closely spaced; alpha centers are broader and coarsely spaced. **B:** Beta cell collects about 80 synapses from the b_1 bipolar array, whereas the alpha cell collects 450 b_1 synapses. **C:** Beta gaussian sensitivity profile is shaped mainly by the bipolar receptive field center, which is broad due to optical blur and cone coupling (see Fig. 6.17); the synapse distribution across the narrow beta dendritic tree hardly matters. Alpha gaussian sensitivity profile is shaped partly by the bipolar centers, but more importantly by the dome-like distribution of synapses across the dendritic tree. The beta cell's greater peak sensitivity is due to its greater density of synapses/retinal area. [After Freed and Sterling, 1988; Freed et al., 1992.]

sponse, whereas three types of bipolar cell contact the beta cell and carry sustained as well as transient responses (see Fig. 6.6B; Nelson and Kolb, 1983; Freed and Sterling, 1988; Cohen and Sterling, 1992; Freed, 2000a,b). (2) Starburst amacrine processes, coplanar with the alpha dendritic arbor, associate with it, whereas starburst processes have access to only a small fraction of the beta dendritic arbor (Vardi et al., 1989; Luo et al., 1996). (3) Bipolar input to the starburst cell, mediated by kainate receptors, transiently releases acetylcholine onto ganglion cell dendrites (Famiglietti, 1991; Linn et al., 1991). (4) Nicotinic receptors so activated depolarize but rapidly desensitize

(Kaneda et al., 1995). (5) Glycinergic amacrine synapses from narrow-field amacrine cells provide many synapses to the alpha cell and may antagonize the center excitation (Freed and Sterling, 1988). (6) Voltage-gated sodium channels for the alpha cell action potential inactivate rapidly (Kaneda and Kaneko, 1991). (7) Alpha cells have very low impedance, which may contribute to a faster time constant (Cohen, 2001; O'Brien et al., 2002). In short, this key physiological difference between the alpha and beta cell types arises partly from differences at the *intercellular* level (wiring) and partly from differences at the *intracellular* level (different receptors and channels).

Surround. The inhibitory surround arises first at the cone terminal (Fig. 6.17) (e.g., Baylor et al., 1971; Smith and Sterling, 1990). Whereas a bright spot hyperpolarizes a central cone, a bright annulus hyperpolarizes surrounding cones. This suppresses their tonic excitation of horizontal cells, reducing GABA released onto the central cone and causing it to *depolarize*, in antagonism to its light response (Fig. 6.17D; Leeper and Charlton, 1985). Illuminating a small patch of cones, corresponding to the ganglion cell center, hardly affects horizontal cells because the patch constitutes at most a few

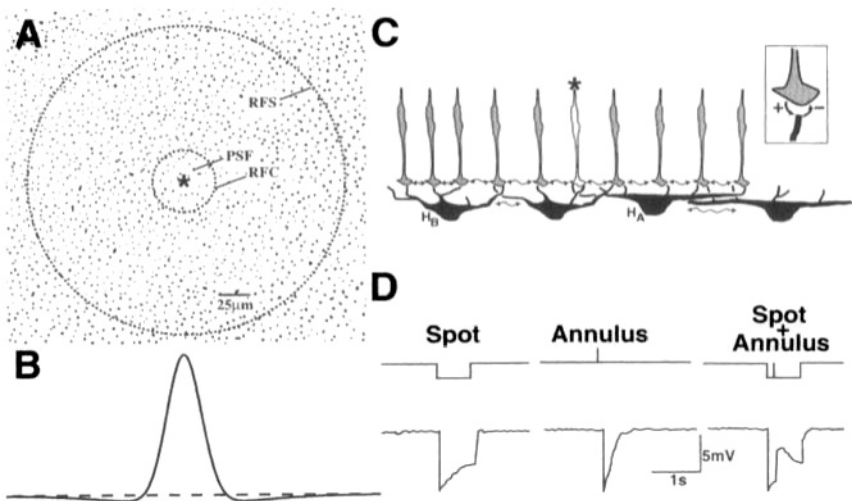


Fig. 6.17. **A:** Cone array in cat central area ($24,000/\text{mm}^2$). A point of light striking the cornea spreads, due to optical blur, to stimulate about 10 cones (PSF = point spread function). The signal spreads farther, due to coupling at cone terminals, to create a receptive field center (RFC) for one cone (*) that encompasses about 50 cones. Inhibitory feedback via horizontal cells causes a receptive field surround (RFS) encompassing about 1200 cones. **B:** Sensitivity profile (difference-of-Gaussians) calculated for the cone receptive field. **C:** Neural circuit thought to shape the cone sensitivity profile: center shaped by optics plus coupling; surround shaped by inhibitory feedback (inset): its narrow, deep region set by narrow, weakly coupled H_B cell; its broad, shallow region set by broad, strongly coupled H_A cell. **D:** Intracellular recordings from turtle cone demonstrate its center-surround receptive field: a spot hyperpolarizes the center cone (*); an annulus causes a brief hyperpolarization by scattering light onto the center; the annulus plus the spot demonstrates the surround's depolarizing effect. [A-C from Smith, 1995; D from Ger-schenfeld et al., 1980.]

percent of the horizontal cell input. But covering a wide field of cones (50–80 times as many cones as the center) is effective. Experiments suggest that the electrical effect of modulating a hemi-gap junction at the tip of the horizontal cell spine might contribute to modulating the cone terminal (Kamermans et al., 2001).

The bipolar cell, by summing center-surround receptive fields of 5–10 converging cones, begins at the OPL to establish its own center-surround receptive field (Werblin and Dowling, 1969; Kaneko, 1970; Dacey et al., 2000). Another contribution to the bipolar cell's surround comes from horizontal cell release of GABA onto GABA_A receptors on the bipolar dendrite (Vardi et al., 1992; Vardi and Sterling, 1994; Haverkamp and Wässle, 2000). Cone glutamate release drives ON and OFF bipolar cells in opposite directions depending on their glutamate receptor (mGluR for ON, iGluR for OFF).

Horizontal cell GABA release also drives ON and OFF bipolar cells in opposite directions, but does so using only one class of receptor: GABA-gated chloride channels. So, how might this work? The two bipolar classes express different chloride transporters on their dendrites—NKCC, (a chloride accumulator) for ON cells, and KCC2 (a chloride extruder) for OFF cells (Vardi et al., 2000b). Therefore, one idea is that NKCC sets the ON cell's chloride reversal potential positive to rest and that KCC2 sets the OFF cell's chloride reversal negative to rest (Vardi et al., 2000b). However, the ON bipolar axon terminal also expresses GABA-gated chloride reversal potentials that appear to be hyperpolarizing (E_{Cl} negative to rest). This would imply an intracellular gradient of chloride, which has not been found (Sato et al., 2001; Billups and Attwell, 2002). The puzzle remains.

The bipolar response pattern carries forward via excitatory synapses onto the ganglion cell. Consequently, when a beta cell sums 100 excitatory cone signals in its center, it also sums the antagonism of their surrounds; when an alpha cell sums 625 cone signals for its center, it likewise sums their antagonism. Because the alpha surround represents many more cone surrounds than the beta surround, it is noticeably stronger (see Fig. 6.16; Freed and Sterling, 1988; Smith and Sterling, 1990). The efficacy of this lateral inhibitory circuit was demonstrated by injecting current into a horizontal cell and observing its suppression of light-evoked firing in ganglion cells (Mangel, 1991).

Lateral circuits of the IPL also contribute to the ganglion cell surround. Bipolar axons beyond the ganglion cell dendritic field excite amacrine arbors and spread signals toward the ganglion cell where they release glycine or GABA onto presynaptic bipolar terminals and ganglion cell dendrites (Pourcho and Owczarzak, 1989; Grünert and Wässle, 1990; Crooks and Kolb, 1992; Vardi and Sterling, 1994; Calkins and Sterling, 1996; Cook and McReynolds, 1998; Taylor, 1999; Flores-Herr et al., 2001; Roska and Werblin, 2001). Correspondingly, inhibitory conductances are recorded in the ganglion cell to broad stimuli but not to narrow ones (Freed and Nelson, 1994; Flores-Herr et al., 2001).

HOW RETINAL CIRCUITS SERVE VISION

NATURAL SCENES CONTAIN FINE DETAIL AT LOW CONTRAST

To appreciate how retinal circuitry serves visual performance, consider a scene from nature: a sheep among cottonwoods as viewed by a predator (wildcat) at 10 meters

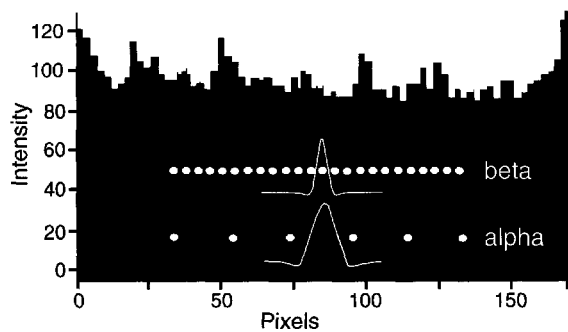
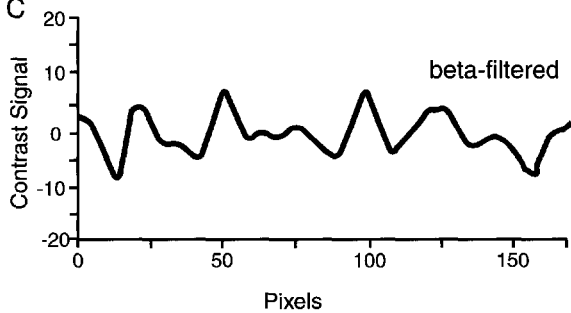
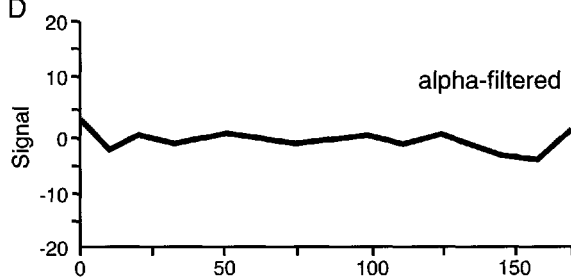
(Fig. 6.18A). At this distance the retinal image contains detail that is fine with respect to the grain of the ganglion cell mosaic. For example, the dark tip of the sheep's nose projected onto the cat's retina fills a beta cell's receptive field center. But the detail in this scene differs from that in an eye chart or a newspaper where the contrast is high (white/black = 100/10). In nature, the contrast tends to be low, more like 100/90 and even 100/99, and this is apparent in the photometer reading across the scene (Fig. 6.18B; Srinivasan et al., 1982).

To create the optical *image* of a low-contrast *scene* requires lots of light. You can verify this simply by viewing fine detail at a distance where it begins to blur. Decrease the intensity, either by dimming the light or by viewing through a dark glass, and the detail is utterly lost. Increase the intensity, and further detail emerges until the light is very bright. This can hardly be news, for who is unaware that visual acuity deteriorates after sunset? But why? Consider the explanation by Albert Rose, a pioneer in video engineering.

Rose (1973) likens the retina to a black canvas on which photons paint a scene in the pointillist style. To render one picture element (pixel) black and the others white (high contrast) requires at least $N - 1$ photons, where N is the number of pixels in the array. However, to render this pixel *gray*, say an intensity 99% of the surrounding white pixels, requires the gray pixel to receive 99 photons while the others receive 100. Thus, the number of photons needed to render this scene is $100N - 1$; more generally, the lower the contrast in a scene, the more light is needed to represent it in an image.

There is an additional fact of physics to consider: photons arrive at a given point randomly in time. Their temporal fluctuation causes uncertainty regarding the true intensity at this point and is thus termed *photon noise*. As for all random processes that follow Poisson distribution, this noise (i.e., standard deviation) is proportional to the square root of the mean. Consequently, to paint a pixel pale gray (1% dimmer than its neighbors) using random photons requires not 100 photons per pixel, as with the determinate dots of a pointillist, but the *square* of 100, i.e., 10,000 photons! To represent for an instant (≈ 50 ms) in gray the finest detail that human optics can project onto the retinal canvas would require a single cone to register about 10,000 photons—and that is about what is available in strong daylight. In short, to register fine detail at low contrast, every possible photon must be transduced to minimize photon noise. This

Fig. 6.18. How narrow-field and wide-field arrays “filter” the transduced image of a natural scene. **A:** Photograph of a bighorn sheep among the cottonwoods. Spatial detail is represented as peaks and troughs of intensity around some mean level. **B:** Photometer scan across the middle of the image (between the arrows). Much discernible structure, e.g., fine branches, differs from the mean by only a few percent. Were this scene viewed by a mountain lion at 10 meters, one pixel would correspond roughly to one cone, and the intensity axis would correspond roughly to the signal amplitude across the cone array. Dimensions and spacings of the narrow-field and wide-field receptive fields are also indicated. **C:** Signal amplitude after filtering by narrow-field cell array. Subtraction by the surrounds of the shared signal component has reset the mean to zero; pooling by the centers has reduced the noisy fluctuations. **D:** Signal amplitude after filtering by the wide-field cell array. Again, a zero mean, but the broad pooling and sparse sampling has removed all but the coarsest spatial detail, thereby clearing the wide-field cell's dynamic range to efficiently encode motion. [Photograph by A. Pearlman; computations for B–D by R. Rao-Mirotnik and M. Eckert.]

A**B****C****D**

explains why baseball players tracking a white flyball (subtending only a few cones) against a bright sky do not wear sunglasses (Sterling et al., 1992).

TO TRANSMIT A LOW-CONTRAST NEURAL IMAGE
REQUIRES MANY SIGNALING EVENTS

One problem is that photon fluctuation in the optical image carries forward into the neural image at the level of the cones. Here, there are additional sources of noise because each step in transduction depends on random processes whose noise levels follow the same “square-root law” as photons. For example, cation channels in the cone outer segment flicker open and shut as they bind and release molecules of cGMP. The closing of a given channel at any instant does not represent a fall in the concentration of cGMP (any more than a single bump of a gas molecule on the wall of a container represents pressure) and therefore does not represent a transduction event. Only a fall in the *average* number of open channels signifies transduction; so again, the S/N ratio is N/\sqrt{N} . To represent at the first neural stage a 1% difference in the optical image requires 10,000 photosuppressible channels—and that is about 10% of what is available at any instant in one cone (Yau, 1994).

The next problem is that a synapse can transmit only a limited number of intensity levels. This is determined by the number of synaptic vesicles that it can modulate over its modest integration time. For example, a cone terminal has been calculated to release 100 vesicles/s at each of 20 ribbon synapses (Rao et al., 1994a), but over its integration time of about 50 ms, this is only 100 vesicles. Assuming that vesicle release is temporally random, the terminal could transmit at most 10 levels ($\sqrt{100}$). This may be somewhat fewer levels than a cone outer segment could encode given that a threshold stimulus uses 5% of its photosuppressible conductance. So how can the cone terminal match the information content at its output to the number of vesicles available for transmission? The question applies equally to the ganglion cell—which fires hundreds of spikes/s (Kuffler, 1953), but over its 100-ms integration time, only 10–20 spikes are fired. So broadly, the question is how to transfer a low-contrast signal using noisy elements of limited information capacity.

EFFICIENT CODING STRATEGIES

It is well known in the fields of information theory and image processing that a channel’s capacity to transmit information increases logarithmically with S/N ratio and linearly with temporal bandwidth (Shannon and Weaver, 1949; Attick and Redlich, 1992; van Hateren, 1992; reviewed in Laughlin, 1994). So given a neural channel’s limited capacity, circuits should use this capacity efficiently by maximizing the S/N ratio, removing redundancy, and subdividing the signal to segment the spatial and temporal bandwidths.

Center Mechanisms Improve the S/N Ratio. First, wherever possible, a circuit should reduce accumulated noise *before* transmitting the signal forward. This prevents noise from occupying precious channel capacity needed for the signal; it also prevents noise from being amplified, which would make its removal at a later stage more difficult. To reduce photon noise and transduction noise, adjacent cone terminals pool their signals by electrical coupling. This little reduces their amplitudes because signals in adjacent

cones are similar (“correlated”). However, it strongly attenuates noise because random fluctuations in adjacent cones are *uncorrelated*. Consequently, the ratio of signal to noise improves (Lamb and Simon, 1976). Pooling loses the very finest detail in the optical image (cf. Fig. 6.18B vs. Fig. 6.18C). However, some of what seems to be “fine detail” in this static image is simply photon fluctuation captured over the brief integration time of the photographic exposure. Coupling human foveal cones blurs the neural image less than the eye blurs the optical image, yet coupling improves the S/N ratio for middle spatial frequencies by about 77% (DeVries et al., 2002).

Further pooling of cone signals occurs by convergence of cones onto bipolar cells and bipolar cells onto the ganglion cell (see Fig. 6.16). Thus, the final weighting of cone signals across the ganglion cell center is the combination of many factors: optical blur, cone-coupling, cone-to-bipolar-to-ganglion cell convergence, and the domed distribution of bipolar synapses across the ganglion cell dendritic field (see Fig. 6.16C; Freed et al., 1992; Kier et al., 1995). The net effect is a Gaussian weighting (Rodieck, 1965; Enroth-Cugell and Robson, 1966; Linsenmeier et al., 1982). This seems to be no accident but rather occurs to express another computational strategy. Such a dome-like weighting for summing partially correlated signals optimally improves the beta ganglion cell S/N ratio compared with a single cone by about 5-fold (Tsukamoto et al., 1990). As a consequence of all the preceding mechanisms to improve the S/N ratio in the ganglion cell, it can detect an optimal center spot when the contrast is less than 1% (Derrington and Lennie, 1982; Linsenmeier et al., 1982; Dhingra et al., 2003). This is just what is needed to transmit the low-contrast features in a natural scene (see Fig. 6.18).

“Surround” Mechanism Reduces Redundancy. The second image-processing strategy is to strip each cone’s signal of information that is also carried by the neighbors. What they share, essentially, is the *mean* intensity across the a small region of the scene (see Fig. 6.18B). This signal component, being redundant, can be removed without loss of the essential news that a given cone (or patch of cones) is dimmer or brighter than the mean. This strategy is executed by horizontal cells: they pool signals from thousands of cone and effectively measure the local mean; then they subtract it from the cone terminal via the circuit mechanisms already noted. By transmitting forward along the excitatory pathway, only the *difference between the local signal and the mean*, the proportion of the dynamic range devoted to differences is increased, and this improves the fineness with which small differences can be transferred.

Note that the ganglion cell surround seems not concerned, as commonly suggested, with “edge detection” or “image sharpening.” Rather, it reflects a widely used image-processing strategy, termed *predictive coding* (Srinivasan et al., 1982). A signal averaged over some region “predicts” a value for the center; then only the difference between the predicted value and the actual value is propagated. The best theoretical prediction “weights” the values near the center most strongly because they best predict the center value. The theory also suggests that in dim light the surround should become broader and shallower to get the best prediction, and indeed this occurs in ganglion cells (Derrington and Lennie, 1982; Srinivasan et al., 1982; van Hateren, 1993).

There is computational value in giving the surround a precise shape and adjusting it for different intensities: it gives the optimal “prediction.” This may explain why there are two types of horizontal cell with different degrees of coupling and the ability to

vary it. A large-scale compartmental model shows that when wide-field horizontal cells alone feed back onto the cone, the surround is too broad and shallow, and when narrow-field horizontal cells alone feed back, the surround is too narrow and deep. But when both feed back, the cone surround has the proper shape (Smith, 1995). Stronger coupling broadens and flattens the modeled cone surround. This suggests one reason to reduce dopamine in darkness—to increase horizontal cell coupling and thereby optimize predictive coding of an image as it becomes progressively noisier.

Parallel Circuits Expand Dynamic Range and Divide Spatiotemporal Bandwidth. The third image-processing strategy is to use multiple, parallel circuits, each specialized for a different aspect of the image. This permits a given circuit to devote its full channel capacity to a small component of the original signal and transmit that component efficiently. The ON and OFF cone bipolar cells provide a good example: predictive coding at the cone terminals effectively subtracts the background, thus allowing small signals to fluctuate about a mean of zero (see Fig. 6.18C). Further, circuits that excite ON bipolar cells carry signals above the mean and circuits that excite OFF bipolar cells carry signals below the mean, allowing each bipolar group to encode only half of the total deviation—with a consequent doubling of the dynamic range. This also permits the corresponding ganglion cells to use high spike rates to signal decrements as well as increments, which improves their transfer. Predictably, blocking the ON bipolar circuits with an mGluR6 agonist reduces behavioral sensitivity to light increments but not decrements (Schiller et al., 1986).

Beta and alpha cells represent another key example of parallel processing strategy to achieve efficient coding. The beta cell's narrow center and fine sampling array render it sensitive to fine spatial detail at low contrast but *insensitive* to coarser structure; thus, the beta cell's contrast sensitivity declines at low spatial frequencies (Derrington and Lennie, 1982). The alpha cell fills this gap. Although its broad center and sparse sampling array render it insensitive to fine stationary detail, these same properties improve its sensitivity to lower spatial frequencies. It is as though the two arrays view the world through screens of different mesh (see Fig. 6.18C).

And there is another advantage: the alpha cell can do for fine temporal correlations in the visual scene what the beta cell does for fine spatial correlations. A low-contrast spot moving rapidly across the cone mosaic adds to each cone only modest numbers of extra photons. It would be impossible, by examining the output of any single cone, to distinguish this signal from photon fluctuation. However, the S/N ratio could be improved by summing the temporally correlated signals from a sequence of cones. In this case the most valuable information in the signal is that which is most sharply demarcated in time—that is, the transient. Furthermore, the larger the region that can be devoted to temporal averaging, the greater is the sensitivity to high velocity. Thus, both major features of the alpha cell—its large receptive field center and its transient response—suit it to extend the range of motion detection beyond what the beta cell can do.

Because a channel's information capacity depends linearly on temporal bandwidth and only on the log of the S/N ratio, retinal circuits could transmit more information by segmenting the temporal bandwidth than by incrementally improving S/N ratio. This might explain why ON and OFF classes of cone bipolar cell both comprise *four* different types. Because each bipolar type collects from the same set of cones, they are

bombarded by synaptic vesicles at the same rate and should have similar S/N ratios. However, by expressing different ion channels, different glutamate receptors, etc., they could carry different temporal bandwidths from the cone (Cohen and Sterling, 1990a,b). Some observations from fish support this (Saito et al., 1985), and studies of OFF bipolar cells in ground squirrel confirm it: one morphological type of bipolar cell senses cone glutamate release with fast-adapting AMPA receptors and responds transiently, whereas two other types sense the same glutamate with slow-adapting kainate receptors and respond more slowly and sustainedly (DeVries and Schwartz, 1999; DeVries, 2000). Different types of bipolar cell also vary their output, releasing glutamate quanta of different sizes and at different rates. For example, the transient ON bipolar cell in cat releases about two quanta/synapse/s to steady illumination, rising 10-fold to a flash, whereas the sustained ON bipolar cells release up to 50 quanta/synapse/s, and these quanta are much smaller than those from the transient cell (Freed, 2000a,b). Bipolar responses may be further shaped by different GABA-mediated conductances at the axon terminal (Euler and Masland, 2000; Shields et al., 2000; Freed et al., 2003). Finally, bipolar responses are shaped by intrinsic mechanisms, such as voltage-dependent potassium currents (Hu and Pan, 2002).

Ribbon Synapses Transfer Information at High Rates. When noise has been reduced by spatial pooling, when redundant information has been stripped by predictive coding, and when different temporal bandwidths have been assigned to different bipolar types, there remains another problem: how to transfer signals to the ganglion cell? Assuming vesicle release to be temporally random (reviewed in Korn and Faber, 1991; Frerking and Wilson, 1996), a ganglion cell would require many vesicles to signal a small change within the receptive field center. An alpha cell responds to a spot on the receptive field center at contrasts as low as 1% (Dhingra et al., 2003). If coding were accomplished simply by Poisson release, a 1% contrast would require at least 10,000 vesicles over the ganglion cell's integration time (100 ms). For an alpha ganglion cell bearing about 1000 bipolar (ribbon) synapses, this would require 100 vesicles/synapse/s. Smaller beta cells in cat central retina and midget ganglion cells in primate fovea, which collect 10- to 40-fold fewer synapses, are far noisier and do not respond to such low contrasts (Lee et al., 1990; Croner and Kaplan, 1995).

Additional Strategies and Circuits Needed to Optimize Signal Transfer. The retina needs additional strategies (and circuits) to optimize information transfer. For example, one expects an efficient computational strategy and corresponding circuits for color (Buchsbaum and Gottschalk, 1983; reviewed in Calkins and Sterling, 1999). Also, there may be mechanisms to reduce randomness in the timing of transmitter release (Freed et al., 2003) and mechanisms to generate strong temporal correlations in firing by adjacent ganglion cells (Meister and Berry, 1999)—both of which could improve coding efficiency. To prevent response saturation, which as noted would reduce efficiency (i.e., lose information), there needs to be mechanisms to adjust local sensitivity, i.e., mechanisms for adaptation/gain control. For example, an ON ganglion cell's sensitivity to a steady, bright stimulus to its center resets downward within about 100 ms (Cleland and Freeman, 1988). This adaptation occurs in small "subunits" across the ganglion cell center, so it cannot be due to horizontal cells, whose fields are broader than the center. Possi-

bly, the subunit represents a bipolar cell that adapts or a narrow-field amacrine cell that responds focally and feeds back negatively onto the bipolar axon terminal (see Fig. 6.14; Dong and Werblin, 1998; Roska et al., 1998; Shiells and Falk, 1999).

Beyond adapting to a first-order property, such as intensity, ganglion cells adapt to second-order properties, such as contrast (Shapley and Victor, 1978; Victor, 1987). When contrast increases, a ganglion cell adapts by (1) rapidly reducing response sensitivity, (2) shortening integration time, and (3) increasing firing rate. The decreased sensitivity and shortened integration time persist while high contrast remains, whereas the increased firing rate declines slowly (over tens of seconds; Smirnakis et al., 1997; Chander and Chichilnisky, 2001; Baccus and Meister, 2002). Adaptations of sensitivity and integration time depend in part on intrinsic properties of bipolar and ganglion cells (Kim and Rieke, 2001; Rieke, 2001). Contrast adaptation also occurs over different spatial scales: over <1 mm (scale of the classic center-surround) and over several millimeters (well beyond classical receptive field; Enroth-Cugell and Jakiela, 1980; Brown and Masland, 2001). The adapting signal is transferred over several millimeters by long-range, spiking amacrine cells of the sort shown in Fig. 6.9 (Cook et al., 1998; Demb et al., 1999).

These different expressions of contrast adaptation may serve slightly different functions (Demb, 2002). Shorter integration time reduces sensitivity to low temporal frequencies, which contain partially redundant components of the visual scene that can be eliminated when the signal is strong. Lower sensitivity avoids response saturation. Rapidly increasing spike rate usefully signals the new (high contrast) environment, but prolonging the high spike rate is expensive metabolically (Attwell and Laughlin, 2001). Thus, the subsequent slow reduction in spike rate would conserve energy.

Another strategy to improve signal transfer is “nonlinear spatial summation,” the signature property of alpha (Y) cells (Enroth-Cugell and Robson, 1966; Hochstein and Shapley, 1976a,b; Victor et al., 1977). An alpha cell can be excited by a small spot of appropriate contrast (i.e., bright for an ON cell) placed anywhere in the receptive field center, and because spatial summation is nonlinear, the response is not “vetoed” by a similar spot of opposite contrast elsewhere in the receptive field. This renders the cell sensitive to small objects and fine patterns (i.e., high spatial frequencies) and also to “second-order” motion defined by spatiotemporal changes in contrast on a fine scale (Baker, 1999; Demb et al., 2001b). Nonlinear summation occurs because transmitter release from bipolar cells onto an alpha cell is rectified; i.e., release can increase above a basal level more than it can decrease below that level (Demb et al., 2001a; Fig. 6.19). Nonlinear responses can be evoked from the far periphery of the receptive field where they are driven by spiking amacrine cells (McIlwain, 1964, 1966; Derrington et al., 1979; Demb et al., 1999).

CIRCUITS FOR DAYLIGHT, TWILIGHT, AND STARLIGHT

Over the course of the day, intensity shifts by *ten billion-fold*, but a ganglion cell’s spike rate can vary only by 100-fold (Sakmann and Creutzfeldt, 1969). To cover the huge intensity range, two fundamentally different circuits are required: a *cone bipolar circuit* for graded photoreceptor signals (see Fig. 6.15) and a *rod bipolar circuit* for binary signals (Fig. 6.20). By using gap junctions as neural switches, the two circuits can share key components (Fig. 6.21).

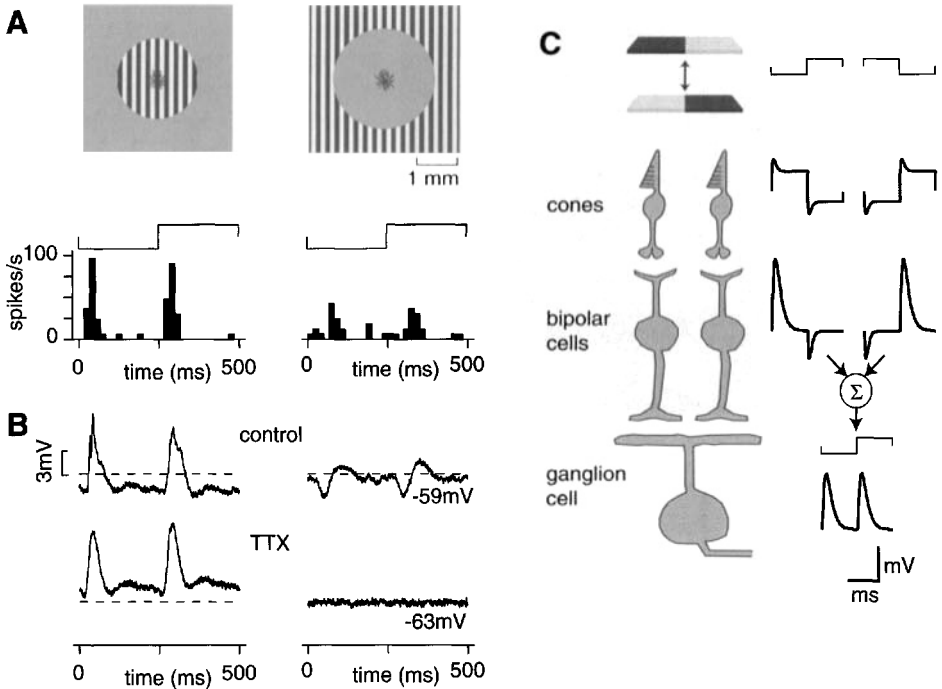


Fig. 6.19. Nonlinear subunits in the Y cell receptive field. **A**: A fine grating (≈ 100 micron bars) reversed contrast over the receptive field center and near surround (left) or over the far surround (right). At each reversal, a Y-type (α) ganglion cell fired a burst of spikes. The burst to the peripheral grating was slightly delayed relative to the burst to the central grating. [Data from Demb et al., 2001a.] **B**: Control traces show the membrane potential (spikes clipped; same cell as in A). At each reversal, the central grating caused a tonic hyperpolarization plus transient depolarizations; whereas the peripheral grating caused a transient hyperpolarization followed by a depolarization. When the spikes were blocked with bath-applied tetrodotoxin, the response to the central grating was little affected, but the response to the peripheral grating was abolished. This implies that the peripheral response is driven by an amacrine cell that fires TTX-sensitive spikes. (Dashed line indicates resting potential to a gray field of mean luminance.) **C**: Circuit diagram to explain the response to a central contrast-reversing grating. A cone responds linearly (equal but opposite responses to a dark and light bar); whereas a bipolar responds nonlinearly (large depolarization to a dark bar and small hyperpolarization to a light bar). A ganglion cell that sums the output of two bipolar cells, responding out-of-phase, generates a frequency-doubled response. This model ganglion cell response approximates the voltage response in **B**. Some of the nonlinearity in the bipolar cell may arise in the cone response. [Hennig et al., 2002.]

Daylight, of course, activates the cone bipolar circuit, whose key features for efficiently transferring graded signals will be recalled: coupling of cone terminals (reduce noise), negative feedback (reduce redundancy), and multiple ribbon synapses at both synaptic stages (high vesicle rates encode finely graded signals). At twilight, when ambient light intensity falls below cone threshold (100 photons cone $^{-1}$ integration time $^{-1}$), this circuit fails. However, rods are now desaturating. Because there are 20 rods per cone and because a rod integrates for about 6-fold longer, signals are available from 12,000 photons transduced by rods. The 40 rod terminals immediately surrounding each

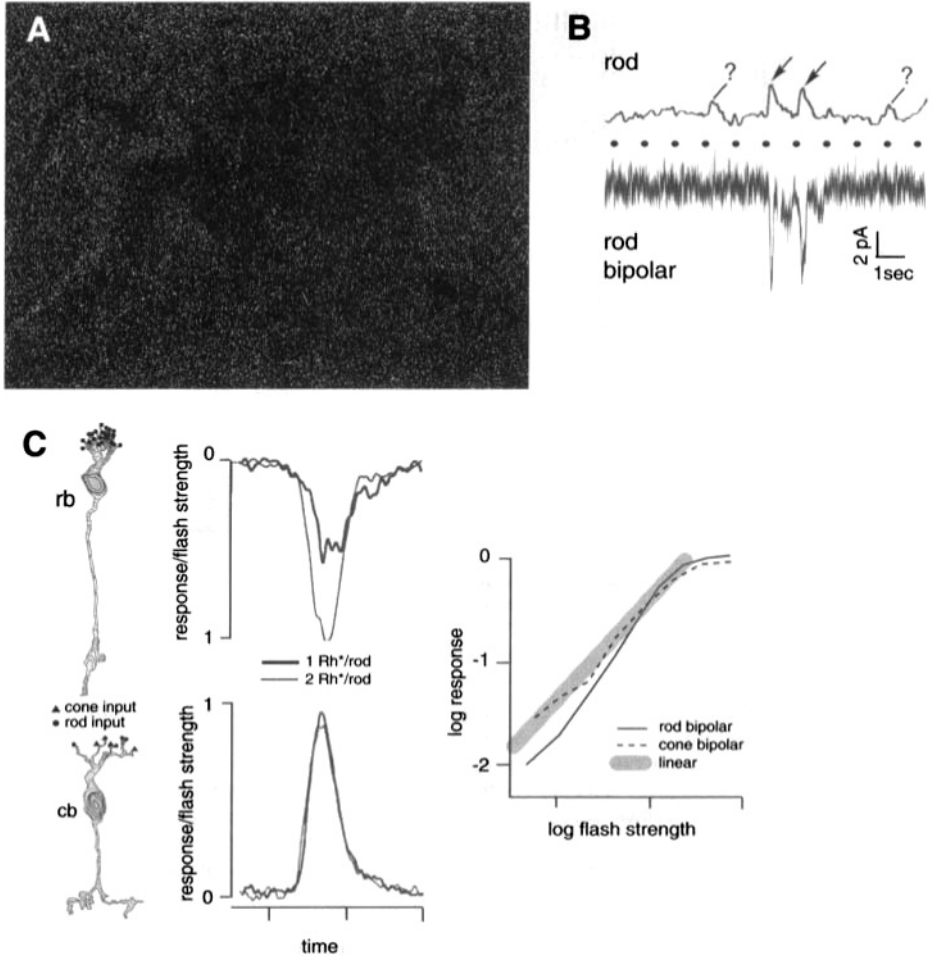


Fig. 6.20. **A**: Faint image of a baboon in starlight painted by photons in “pointillist” fashion. Probability of each pixel receiving a photon was governed by Poisson distribution whose mean corresponded roughly to the intensities used by Field and Rieke (2002). **B**: Single-photon event in a rod (mouse) rises clearly above the continuous noise (arrows) only when it is considerably larger than average. Same event in the rod bipolar is faster with much improved signal-to-noise. Dotted trace represents flash timing. **C**: Left: rod bipolar cell collects chemical synapses from 20 rods and cone bipolar cell from only a few rods. However, each rod probably pools signals from neighboring rods via gap junctions. Middle: Response amplitudes normalized for flash intensity. Cone bipolar response doubles for twice the intensity, but rod bipolar response more than doubles. Right: Input/output curve for cone bipolar is essentially linear, but for rod bipolar it is clearly nonlinear. [Image, courtesy of A. Hsu and R. Smith; neurons, reprinted from Tsukamoto et al., 2001; responses replotted from Field and Rieke, 2002.]

cone terminal couple to it via gap junctions and thus inject this graded signal to be carried forward by the cone bipolar circuit (Kolb, 1977; Nelson, 1977; Smith et al., 1986; Sterling et al., 1988; DeVries and Baylor, 1995; Schneeweis and Schnapf, 1995).

When ambient intensity falls to one photon/rod/integration time, photons are spread too thinly to provide a graded signal. Thus, the cone bipolar circuit is not needed and,

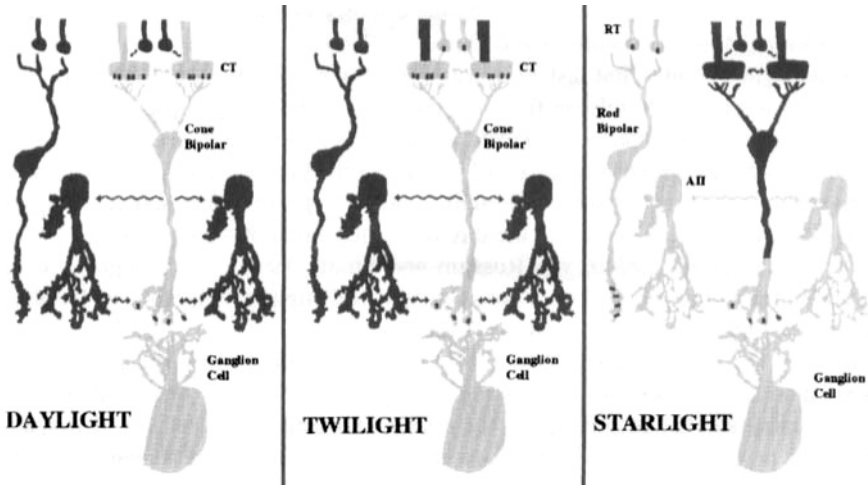


Fig. 6.21. To convey the full range of environmental intensities efficiently (i.e., minimizing neural noise and retinal thickness) requires three different circuits that partially overlap, plus three sets of gap junctions ($\sim\sim$) to switch between them. In *daylight*, cone signals are graded and thus require many ribbon synapses for transfer (both at OPL and IPL). In *twilight*, rod signals are graded and thus also require many ribbon synapses. Rods obtain access to these by turning on their gap junctions to cone terminals, in effect “parasitizing” the multiple ribbon synapses available at both stages of the cone bipolar circuit. In *starlight*, rod signals are binary and thus require only one ribbon synapse (see Fig. 6.13). The single-photon response cannot transfer via coupling to the cone terminal because the many rods lacking a photon add too much noise. Therefore, the rod-cone junction turns off, and the binary signal transfers via the rod’s single ribbon synapse to the rod bipolar cell. The latter’s response will be coarsely graded over some part of the intensity range (due to rod convergence) and thus will require multiple ribbon synapses—which are present in the rod bipolar terminal. The AII cell’s response will be more finely graded (due to rod bipolar convergence) and thus will require yet more ribbon synapses. The AII cell obtains access to these by turning on its gap junctions with cone bipolar terminals. Coupling the AII cells, indirectly via the cone bipolar terminals and also directly via AII–AII junctions, spreads current widely enough to enlarge the ganglion cell’s summation area well beyond its dendritic tree. This improves the signal/noise ratio in very dim light but would degrade acuity in brighter light. Therefore, both sets of junction are regulated and presumably uncouple in twilight and daylight. See text.

worse, the coupling of many receptors that lack photons to one rod that does capture a photon would inject continuous “dark noise” from the transduction cascade. Noise in this rod would increase by the square root of the number of noisy rods coupled to it (i.e., ≈ 6 -fold), and this would obliterate its single Rh^* response. To protect the Rh^* response from noise and to preserve its amplitude, the rod-cone gap junctions should uncouple at very low intensities and switch over to the rod bipolar circuit (Smith et al., 1986). Although rod-cone uncoupling has not been demonstrated directly, two rod pathways have been demonstrated psychophysically: a fast one for middle intensities (twilight) and a slower one for lowest intensities (starlight). Because their intensity ranges overlap for certain rates of a flickering stimulus, they can be made to cancel (Stockman et al., 1995). Presumably these pathways correspond, respectively, to the rod-

driven cone bipolar circuit and the rod bipolar circuit (see Fig. 6.21; reviewed in Sharpe and Stockman, 1999; Bloomfield and Dacheux, 2001).

The starlight circuit's first task is to transfer a binary signal: 0 or 1 Rh*. "0" is represented by tonic vesicle release from the rod's single ribbon synapse, and "1" is represented by a pause in release. However, assuming release is temporally random, some extra-long intervals between quanta will occur that the bipolar cell might "mistake" for a pause. The release rate should be high enough to prevent this source of spurious single-photon signals. A model of the circuit suggests that 50–100 vesicles/s might be sufficient (Rao et al., 1994b; van Rossum and Smith, 1998). This roughly fits measured rates for ribbon synapses (as noted earlier) and suggests why the rod bipolar circuit requires only one ribbon synapse at the first stage.

However, at the next stage, 20 to 120 rods converge on a rod bipolar cell, and this exposes another problem for processing starlight signals. Only one of these rods is likely to carry an Rh* response, but the others will carry noise, which, if transferred to the rod bipolar cell, would increase its noise (again, as the square root of the convergence)—and swamp the single Rh* response in the bipolar cell. To prevent this, the rod synapse acts nonlinearly, amplifying large signals more than small ones (see Fig. 6.20). This removes the small, noisy events by thresholding (van Rossum and Smith, 1998; Field and Rieke, 2002). But the Rh* events in a rod vary in amplitude, many hardly rising above the noise. Thresholding removes the noise but also these small photon signals, a process that has been vividly termed "throwing out the smaller babies with the bath" (Wilson, 2002). You might think that discarding photon events in dim light would be a bad strategy. But because small events are much more likely to be noise than photons, it actually proves to be an excellent computational bet, improving S/N by more than 350-fold (Field and Rieke, 2002)! At higher intensities, where every rod captures at least one photon, linear amplification is a better bet, and indeed a direct pathway from rods to OFF bipolar cells acts linearly (Soucy et al., 1998; Hack et al., 1999; Tsukamoto et al., 2001; Field and Rieke, 2002).

At all except the lowest intensities, the rod bipolar cell's large convergence gives it, not a binary signal, but a coarsely graded one. Consistent with this, instead of using one ribbon (as at the rod output), the rod bipolar axon uses 30 ribbon synapses at its output (Sterling et al., 1988). The AII cell collecting from about 30 rod bipolar cells needs to transfer a more finely graded signal, and for this it couples electrically to cone bipolar terminals that contribute 150–2000 synapses to a ganglion cell. Thus, the overall pattern of the rod bipolar circuit is a stepwise expansion in number of ribbon synapses to match the stepwise increase in signal pooling. The rod bipolar circuit's "parasitic" use of the cone bipolar terminals as final input to ganglion cells saves space, which, in a tissue constrained to be thin ($\leq 250 \mu\text{m}$), is at a premium.

Tuning the Circuits. Rod circuits, like the cone circuit, are also tuned for efficiency at different intensities by modulated coupling (reviewed in Sterling, 1995; Demb and Pugh, 2002). In twilight, to preserve spatial acuity, ganglion cell receptive field centers should be narrow. But if cone bipolar axons were coupled to AII cells, cone signals would spread laterally in the AII network and degrade spatial acuity (Sterling, 1983). Therefore, the cone bipolar–AII junctions might remain uncoupled until starlight, when the noisy optical image can be transmitted most efficiently by expanding the gan-

gion cell center (Barlow et al., 1957). Indeed, AII–cone bipolar junctions *do* uncouple when cGMP rises within the bipolar cell in response to nitric oxide production (Mills and Massey, 1995), and this mechanism may serve the transition to starlight intensities. Also in starlight, as noted, rods should uncouple from cones, but whether they do is not established (Schneeweis and Schnapf, 1999).

Finally, in starlight, the AII–AII junctions should couple, but to a variable degree. This coupling reduces noise by signal averaging, and also interacts with the AII cell's voltage-sensitive mechanism (Nelson, 1982; Boos et al., 1993; Veruki and Hartveit, 2002). This mechanism, by “thresholding,” may remove noise that would otherwise swamp the Rh* signals when 30 rod bipolar cells converge on an AII cell (Freed et al., 1987; Smith and Vardi, 1995). However, it could also spread spurious spikes through the AII network. A computational model suggests that by matching coupling to the noise level (which shifts with light intensity), the circuit can maximize thresholding and minimize spurious spiking (Smith and Vardi, 1995). Dopaminergic synapses on the AII soma (Pourcho, 1982; Voight and Wässle, 1987) uncouple AII–AII junctions (Hampson et al., 1992), and because retinal dopamine declines in darkness, AII coupling should rise. Of course, once neuromodulators of coupling are identified, such as NO and dopamine, the question arises: What signals and effectors modulate the modulators? These are concerns for the future.

CONCLUDING REMARKS

We have noted that once photons are transduced, most of their information reaches the brain. Retinal circuits achieve this astonishing efficiency in part by finely dividing responsibility. Thus, we have distinguished circuits that (1) divide the dynamic range around the local mean intensity (ON and OFF), (2) divide the spatiotemporal bandwidth (beta vs. alpha, P vs. M), (3) divide the color spectrum (blue-yellow, red-green), and (4) divide vast diurnal shifts in intensity (cone bipolar vs. rod bipolar). Also key to efficient forward transfer are the ribbon synapses that can fuse vesicles and reload at very high rates, and also contributing are various linear mechanisms that reduce noise at each stage of summation by spatial averaging and optimal weighting.

Several *nonlinear* mechanisms were noted: “thresholding” for the single Rh* signal at the rod output (Field and Rieke, 2002); thresholding of the multi-Rh* signal by the AII cell (Smith and Vardi, 1995); rectification by the cone bipolar cells, which produces “nonlinear subunits”; and mechanisms for fast and slower “contrast gain control” (reviewed in Demb, 2002). Intuitively, nonlinear mechanisms should involve amacrine cells—with their many different types, their rich possibilities for chemical signaling, and their spiking behavior. So far we know little about amacrine synaptic circuits *between* cells or about their second-messenger circuits *within* cells. These are puzzles for the future. However, rapid technical advances in unraveling the retina's synaptic organization, new methods for *in vitro* recording, and molecular biology lead one to think that the future is near.

This page intentionally left blank

CEREBELLUM

RODOLFO R. LLINÁS, KERRY D. WALTON,
AND ERIC J. LANG

The *cerebellum*, a very distinct region of the brain, derives its name as a diminutive of the word “cerebrum.” To the ancient anatomists, this was a second, smaller brain in its own right. This is particularly explicit in the German language, where *Kleinhirn* (“cerebellum”) translates literally into “small brain.” It occupies, in all vertebrates, a position immediately behind the tectal plate and straddles the midline as a bridge over the fourth ventricle. In addition, it is the only region of the nervous system to span the midline without interruption.

The cerebellum has undergone an enormous elaboration throughout evolution, in fact, more so than any other region of the central nervous system (CNS), including the cerebrum. On the other hand, the cerebellum has maintained its initial neuronal structure, almost invariant, throughout vertebrate evolution. Thus, its size but not its wiring has changed in evolution. As an example, the cerebellar cortex in a frog has an area approximately 12 mm²; that is, 4 mm wide (in the mediolateral direction) and 3 mm long (in the rostrocaudal direction). In humans, the cerebellar cortex is a single continuous sheet with an area of 50,000 cm² (1,000 mm wide and an average of 50 mm long). This is 4×10^3 times more extensive than that of a frog (Braitenberg and Atwood, 1958). This cortex folds into very deep folia (Fig. 7.1), allowing this enormous surface to be packed into a volume of 6 cm \times 5 cm \times 10 cm. Because the cerebellar cortex is very long in the rostrocaudal direction, most of the foldings occur in that direction.

The basic functional design of the cerebellum is that of an interaction between two sets of quite different neuronal elements: those of the *cortex* and those in the centrally located *cerebellar nuclei*. The cerebellar cortex receives two types of afferents, the climbing fibers and the mossy fibers, and generates a single output system, the axons of Purkinje cells (Cajal, 1904). The cerebellar nuclei receive collaterals from the climbing and mossy fibers (Bloedel and Courville, 1981; Shinoda et al., 1992) and are the main targets for the Purkinje cell axons. The cerebellum as a whole is connected to the rest of the central nervous system by three large fiber bundles, the cerebellar peduncles.

The function of the cerebellum must be considered within the context of the rest of the nervous system because it is not a primary way station for sensory or motor function; that is, its destruction does not produce sensory deficits or paralysis. Neverthe-

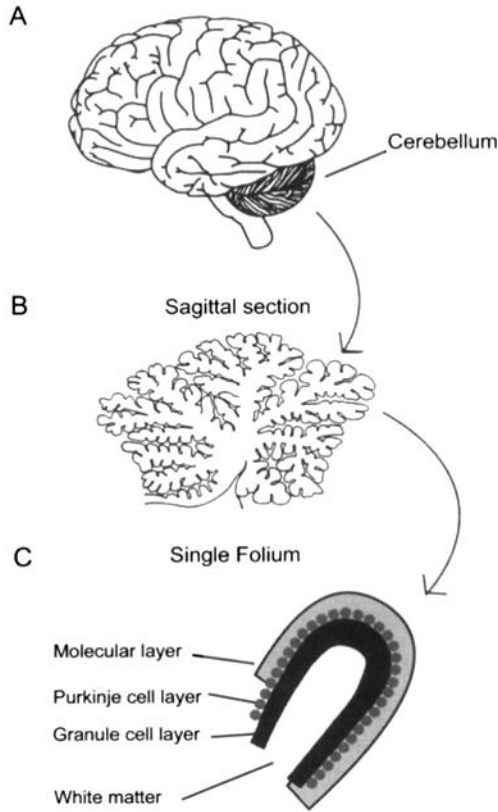


Fig. 7.1. **A:** Drawing of the lateral view of the human brain showing the cerebellum. **B:** Mid-sagittal section of the cerebellum. **C:** Drawing of a single folium, showing the three layers of cerebellar cortex and the white matter.

less, lesions of the cerebellum are accompanied by well-defined and often devastating changes in the ability of the rest of the nervous system to generate even the simplest motor sequences used to attain motor goals. Indeed, the cerebellum is essential to the execution of specific movements as well as to placing motor sequences in the context of the total motor state of the individual at a given instant. Such a function is called *motor coordination* and relates to many different levels of brain function. It is not surprising then that the cerebellum has a complex neuronal organization and that it is vigorously connected with the rest of the brain. The enormous Purkinje cells are the sole link between the cerebellar cortex and the cerebellar nuclei. These neurons are the largest neuronal elements in the brain with respect to the number of synapses they receive and probably also with regard to the complexity of their integrative properties. In this chapter, we show how the role of the cerebellum in motor coordination arises from an interplay between the intrinsic excitability of the Purkinje and cerebellar nuclear cell membranes and from the crystal-like organization of the synaptic connectivity in the cerebellar cortex (Fig. 7.2).

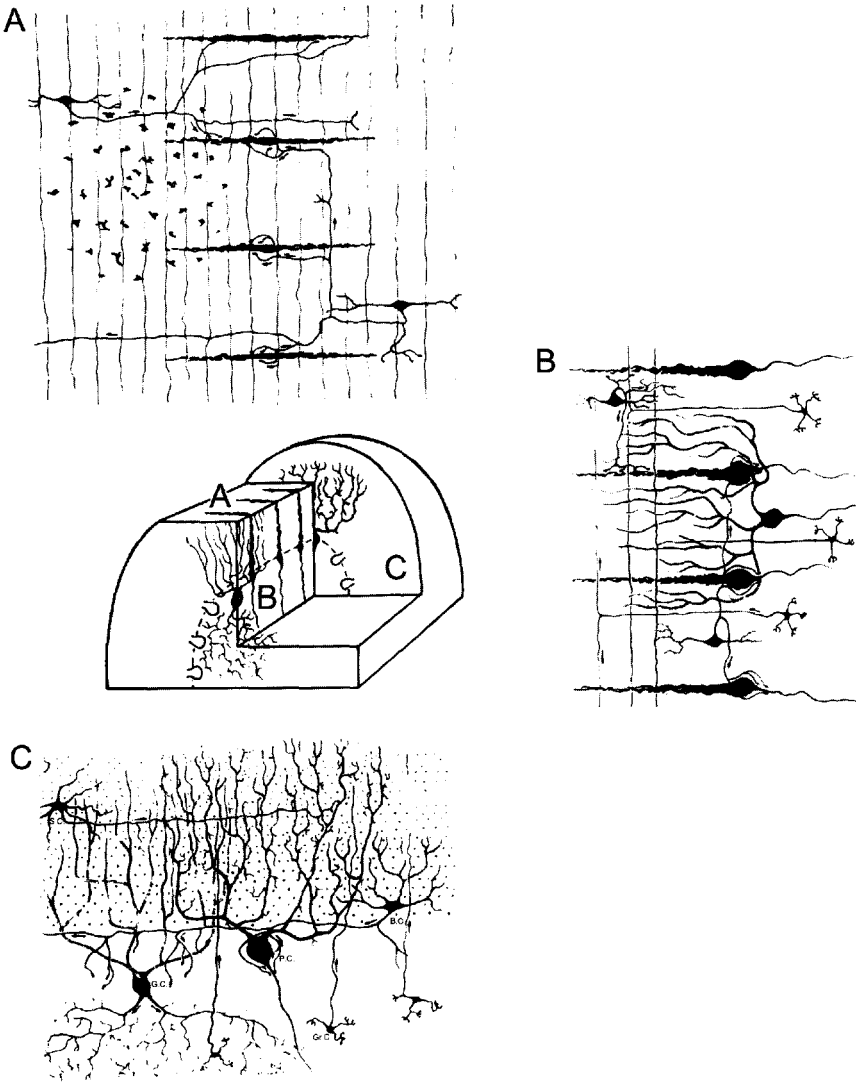


Fig. 7.2. Geometric organization of the neuronal elements of the cerebellar cortex. Three planes of section through a cerebellar folium. **A:** Tangential plane (looking down on the cortical surface). **B:** Transverse (medial-to-lateral) plane. **C:** Sagittal (anterior-to-posterior) plane.

NEURONAL ELEMENTS

The cerebellar cortex is one of the least variable of CNS structures with respect to its neuronal elements (Cajal, 1904; Palay and Chan-Palay, 1974). In fact, a basic circuit present in all vertebrates is now well recognized as being composed of the Purkinje cell, the single output system of the cortex, and two inputs: (1) a monosynaptic input to the Purkinje cell, the climbing fiber, and (2) a disynaptic input, the mossy fiber–granule cell–Purkinje cell system.

Because the Purkinje cell bodies are arranged in a single sheet, the Purkinje cell layer, the cerebellar cortex is divided into two main strata: (1) the level peripheral to the Purkinje cell layer, known as the *molecular layer*, and (2) the layer deep to the Purkinje cells (i.e., toward the white matter), the *granular layer*. Central to the granular layer is the white matter formed by the input and output nerve-fiber systems of this cortex (see Fig. 7.1B,C).

INPUT ELEMENTS

Climbing Fibers. The two types of cerebellar afferents, the climbing fibers and the mossy fibers, represent opposite extremes among the afferents in the CNS. The climbing fibers originate from only one brainstem nucleus, the inferior olive. The main inputs to the inferior olive originate in the spinal cord, brainstem, cerebellar nuclei, and motor cortex. Olivary axons are long, fine (1–3 μm in diameter), and myelinated. They cross the brainstem at the level of the inferior olive, after which they course rostrally to enter the cerebellum primarily via the inferior cerebellar peduncle (a small contingent from the caudal portion of the inferior olive enters via the superior peduncle). Upon entering the cerebellar mass, they give off collaterals to the cerebellar nuclei and proceed toward the cerebellar cortex after branching into several fine fibers. The fibers lose their myelin as they penetrate through the granular layer before meeting with the Purkinje cell dendrites in the molecular layer (Fig. 7.3, CF). Each fiber branches repeatedly to “climb” along the entire Purkinje cell dendritic tree; thus, they were named *climbing fibers* by Ramón y Cajal. Each Purkinje cell receives only one climbing fiber. However, a given inferior olivary cell axon branches to form several climbing fibers. On average, about 10 climbing fibers are generated by a single inferior olivary cell.

Mossy Fiber–Parallel Fiber Pathway. The other cerebellar afferents, the mossy fibers, originate from many CNS regions. Chief among these are the vestibular nerve and nuclei, spinal cord, reticular formation, cerebellar nuclei, and basilar pontine nuclei. The pontine nuclei receive input from much of the neocortex, making the cortico-ponto-cerebellar pathway one of the most massive in the brain. Mossy fibers enter through all three cerebellar peduncles (inferior, middle, and superior) and send collaterals to the deep cerebellar nuclei before branching in the white matter and synapsing on the granule cells (Chan-Palay, 1977; Shinoda et al., 1992). Thus, unlike the climbing fibers, mossy fibers do not synapse directly on Purkinje cells but rather on the small granule cells lying directly below them (Fig. 7.3B). This connectivity increases the number of Purkinje cells ultimately stimulated by one mossy fiber axon. Also, because mossy fibers branch profusely in the white matter, a given mossy fiber innervates several folia. The synapses between mossy fibers and granule cells occur as the fine branches of the mossy fibers twine through the granular layer. The contacts are made as the mossy fiber enlarges and generates tight knottings along its length. These portions of contact are called *mossy fiber rosettes*. One mossy fiber may have 20–30 rosettes (see Fig. 7.5B).

An integral part of the mossy-fiber input pathway is the granule cell axon, which completes the disynaptic input connection to the Purkinje cells. The axon of the granule cell, usually nonmyelinated, projects upward, past the Purkinje cell layer, into the molecular layer. On its way, it may form synapses with the dendritic trunk of Purkinje cells. In the molecular layer, the axon splits into two branches which take diametrically opposite directions, forming the shape of an uppercase “T” (see Fig. 7.3B). Fibers forming the hor-

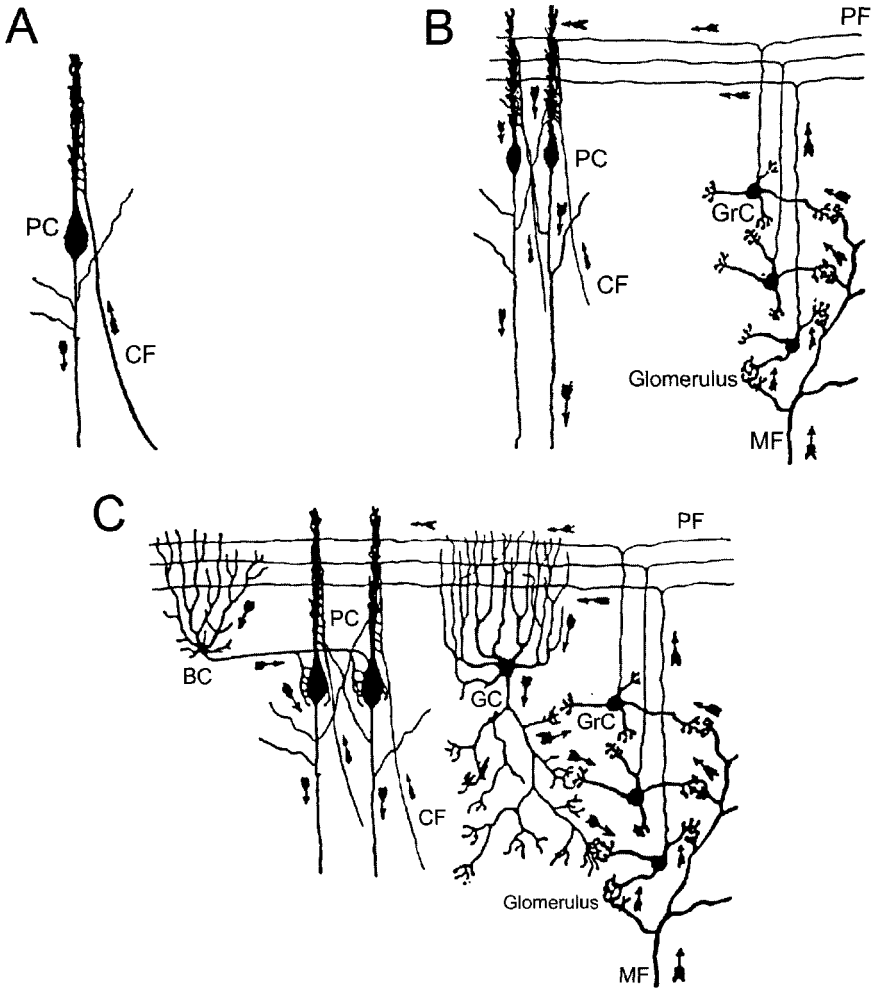


Fig. 7.3. Drawing of the cerebellar afferent circuits and intrinsic neurons. **A:** The climbing fiber–Purkinje cell circuit. A fine branch of an axon from the inferior olivary nucleus (CF) climbs over the extensive arborization of the Purkinje cell (PC) dendritic tree; note the axon collaterals of the Purkinje cell axon. The Purkinje cell is viewed in profile here since it is drawn from a coronal section of the cerebellar cortex. **B:** In the glomeruli, activity in the mossy fibers (MF) excites granule cells (GrC), whose axons project toward the surface of the cortex where they bifurcate to form parallel fibers (PF); these in turn pass through many Purkinje cell dendrites with which they form excitatory synapses. **C:** In this drawing, the two afferent systems shown in A and B are combined and the two main types of intrinsic neurons are depicted: (1) the Golgi cells (GC), with cell bodies just below the Purkinje cell layer; and (2) the basket cells (BC), with cell bodies in the molecular layer. [Modified from Cajal, 1904, with permission.]

horizontal part of the T are found in all depths of the molecular layer. Because these fibers are precisely arrayed parallel to each other along the length of a folia, they have been named *parallel fibers*. These are perpendicular to the plane of the Purkinje cell dendrites (Fig. 7.3B), so that each Purkinje cell dendritic tree in humans may be intersected by as many as 200,000 parallel fibers (Braitenberg and Atwood, 1958).

OUTPUT ELEMENTS

Purkinje Cells. As stated earlier, Purkinje cell axons provide the only output of the cerebellar cortex. These cells, which reach numbers as high as 15×10^6 in humans, were among the first neurons recognized in the nervous system (Purkinje, 1837) (Fig. 7.4A). Each cell has a large and extensive dendritic arborization, a single primary dendrite, a sphere-like soma ($20\text{--}40 \mu\text{m}$), and a long, slender axon that is myelinated when it leaves the granular layer. As the main Purkinje cell axon leaves the cortex, it gives off recurrent collaterals that ascend back through the granular layer to form plexi above and below the Purkinje somata and ultimately form synapses with Golgi and basket cells.

The Purkinje cell dendrites extend densely above the Purkinje cell layer through the molecular layer toward the boundary of the cortex. The unusual arrangement of the Purkinje cell dendrites makes them at once the most conspicuous structural element in the cerebellar cortex and provides an important clue to its functional organization. The

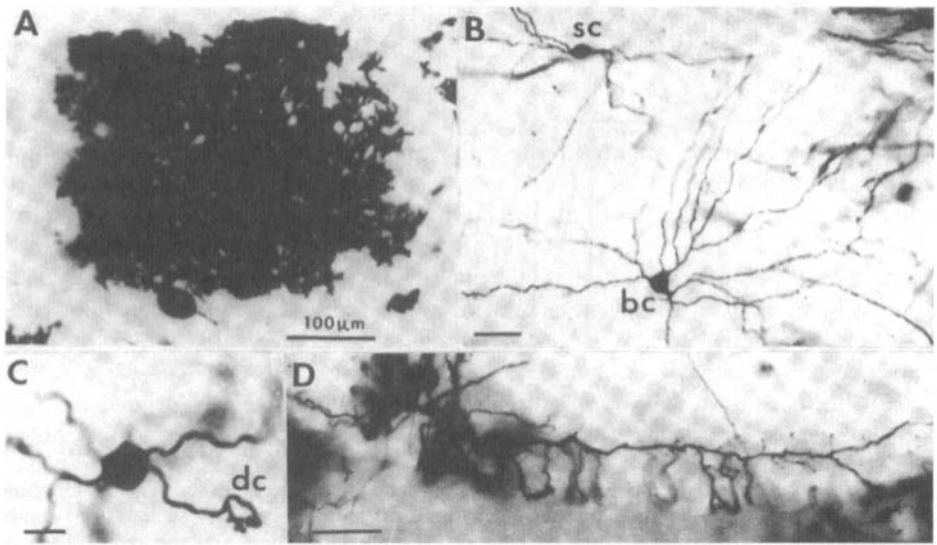


Fig. 7.4. Golgi preparations of cerebellar neurons. **A:** Purkinje cell soma, axonic initial segment, and dendritic arbor in a sagittal plane of section. The extent of the dendritic tree is from the Purkinje cell layer and spreads rostrocaudally to reach the cerebellar surface. **B:** Molecular layer interneurons and stellate (sc) and basket (bc) cells. The stellate cell is found in the upper three-fourths of the molecular layer. Their dendrites have few branching points and project in the same plane as the Purkinje cell dendrites. Basket cells are found deeper in the cortex, their dendrites project horizontally subtending over 180° of arc. The interneuron axons (not shown) project horizontally to the Purkinje cell layer where they contact Purkinje cell dendrites (see **D** below). **C:** Granule cell showing a soma with five emerging dendrites. Note that the dendrite ends in the form of a claw (dc) for contact with a mossy fiber and Golgi cell axons. **D:** Basket cell axon projects horizontally above and along the Purkinje cell layer in the same plane as Purkinje cell dendrites. Short projections of the basket axon descend about $30 \mu\text{m}$ into the Purkinje cell layer and each clasps a Purkinje cell soma. Scale: A = $100 \mu\text{m}$; B = $20 \mu\text{m}$; C = $5 \mu\text{m}$; D = $50 \mu\text{m}$. [Micrographs courtesy of Dean Hillman.]

entire mass of tangled, repeatedly bifurcating branches is confined to a single plane, very much like a pressed leaf. Moreover, the planes of all the Purkinje cell dendrites in a given region are parallel, so that the dendritic arrays of the cells stack up in neat ranks; adjacent cells in a single plane form equally neat, but overlapping, files (see Fig. 7.2A). To a large extent, this orderly array determines the nature and number of contacts made with other types of cells. Thus, parallel fibers running perpendicular to the plane of the dendrites can intersect a great many Purkinje cells. Conversely, the dendrites of a typical human Purkinje cell may form as many as 200,000 synapses with afferent fibers—more than any other cell in the CNS.

The Purkinje cell is not merely a transmitter or repeater of information originating elsewhere. As we shall see, its output is determined by its synaptic interactions with other neurons, by their interactions with one another, and by its quite complex intrinsic membrane properties.

INTRINSIC ELEMENTS

The basic circuit common to all cerebella contains only one excitatory intrinsic neuron, the granule cell (Fig. 7.3C, GrC). This basic circuit is augmented by three types of inhibitory interneurons: the Golgi cells of the granular layer (see Fig. 7.3C, GC) and the basket (see Fig. 7.3C, BC) and stellate cells of the molecular layer, which are elaborated progressively in evolution. We begin with the granule cells.

Granule Cells. These are the smallest cells in the cerebellum, with an oval or a round soma 5–8 μm in diameter. They are densely packed in the granule cell layer, which occupies about one-third of the cerebellar mass. In fact, these cells are the most numerous in the CNS; there are about 5×10^{10} cerebellar granule cells in the human brain. Each cell has four or five short dendrites (each less than 30 μm long) that end in an expansion called a dendritic claw (Fig. 7.4C). Their thin (0.1–0.2 μm in diameter), ascending axon has varicosities where synapses are formed, before it bifurcates to form the parallel fibers (see earlier). After bifurcating, the parallel fiber may run for 6 mm (3 mm on each side) before coming to an end (see Fig. 7.3C).

Golgi Cells. There are two sizes of Golgi cells: (1) large ones (somata 9–16 μm in diameter), which are found mainly in the upper part of the granular cell layer, and (2) smaller ones (somata 6–11 μm in diameter), which are found in the lower half of the granular layer. They have extensive radial dendritic trees (Fig. 7.2A) that extend through all layers of the cortex (Fig. 7.3C). They receive input from the parallel fibers in the molecular layer and from climbing and mossy fiber collaterals in the granular layer. Their axons branch repeatedly in the granular layer, where they terminate on granule cell dendrites in the cerebellar glomeruli (see later). There are approximately as many Golgi cells as Purkinje cells.

Basket and Stellate Cells. These are both found in the molecular layer, receive input from parallel fibers, and may be considered to be members of a single class. The processes of both cell types are oriented transversely to the long axis of the folia (see Fig. 7.3C, BC).

Basket cells are found in the deep parts of the molecular layer, near the Purkinje cell layer. Their dendrites ascend into the molecular layer, in some instances as far as $300\ \mu\text{m}$ (Fig. 7.4). Their axons extend along the Purkinje cell layer at right angles to the direction of the parallel fibers. They may spread over a distance equal to 20 Purkinje cell widths and 6 deep and may contact as many as 150 Purkinje cell bodies. During its course, the horizontal segment of a basket cell axon sends off groups of collaterals that descend and embrace the Purkinje cell soma and initial segment (see Figs. 7.3C and 7.4D; see also later). As many as 50 different basket cells are thought to wrap their axon terminals around each Purkinje cell soma, forming a basket-like meshwork resembling that on a Chianti bottle (Hámori and Szentágothai, 1966). Basket cell axons also ascend to contact the Purkinje cell dendritic tree. There are about six times as many basket cells as Purkinje cells.

The stellate cells are generally found in the outer two-thirds of the molecular layer. The smallest stellate cells, in the most superficial regions of the molecular layer, have 5- to $9\text{-}\mu\text{m}$ -diameter somata, a few radial dendrites, and a short axon (see Fig. 7.4B, sc). Deeper stellate cells are larger, have more elaborate dendritic arborizations that radiate in all directions, and have varicose axons that can extend parallel to the Purkinje cell dendritic plane as far as $450\ \mu\text{m}$. There are about 16 times as many small stellate cells as Purkinje cells.

CEREBELLAR NUCLEI

There are three cerebellar nuclei on each side of the midline; each receives input via Purkinje cell axons from the region of cortex directly above it and projects to specific brain regions. The most medial nucleus, the *fastigial*, receives input from the midline region of the cerebellar cortex, the *vermis*. It projects caudally to the pons, medulla, vestibular nuclei, and spinal cord and rostrally to the ventral thalamic nuclei. Lateral to the vermis are the newer parts of the cerebellar cortex, the *paravermis*, which projects to the interpositus nucleus (which itself is divided into anterior and posterior divisions), and the *hemispheres*, which project to the convoluted dentate nucleus. The latter two cerebellar nuclei project rostrally to the red nucleus and ventral thalamic nuclei and caudally to the pons, medulla, cervical spinal cord, and reticular formation. There is a pattern of innervation of the cerebellar nuclei within this broad radial organization whereby the rostrocaudal and mediolateral groups of Purkinje cell axons parcel each cerebellar nucleus into well-defined territories (Voogd and Bigaré, 1980).

The cells of the cerebellar nuclei are not uniform in size: cells of small, medium, and even large diameter ($\approx 35\ \mu\text{m}$) are found. The large cells have 10–12 long dendrites ($\approx 400\ \mu\text{m}$ long) that radiate to encompass a sphere. There are a few small cells with short axons, but the majority have long axons that leave the nuclei. It is also useful to distinguish cerebellar nuclear cells according to whether they are GABAergic. Only the smaller cerebellar nuclear neurons are GABAergic and virtually all of these neurons project to the inferior olive, whereas almost no non-GABAergic neurons do so (De Zeeuw et al., 1989; Fredette and Mugnaini, 1991). The non-GABAergic neurons project to the other targets of the cerebellum, as described earlier. Thus, the non-GABAergic neurons carry cerebellar influences to the rest of the brain, whereas the GABAergic neurons provide feedback to the inferior olive,

one of the principal afferent sources to the cerebellum. We take up the function of this feedback circuit in Functional Circuits.

The cerebellar nuclei are not simply “throughput” stations; rather, the synaptic integration that takes place here is a fulcrum for cerebellum function. Indeed, it is here that information from the cerebellar cortex is integrated with direct input from the mossy and climbing fibers. (This is discussed in Basic Circuits.)

As in Purkinje cells, the intrinsic properties of the nuclear neurons are very important to their function (see Intrinsic Membrane Properties).

SYNAPTIC CONNECTIONS

Over 100 years ago, Ramón y Cajal (1888) published his description of the cerebellum. In this study of Golgi-stained material, the synaptic connections were already indicated, as shown in Fig. 7.2, as were the directions of flow of impulses in this cortex. Electron microscopic studies have provided additional information about the type of synaptic connections and their fine structure (cf. Palay and Chan-Palay, 1974) and confirmed Cajal’s initial description. The synaptic connections among the elements in the cerebellum are discussed by layer, not by cell type, to highlight the local circuits at each level of the cerebellum. We begin with the granular layer.

GRANULAR LAYER

Two cell types receive input here: the granule cells and the Golgi cells. The synapses onto granule cells take place in the cerebellar “glomeruli.” The rosettes, which occur along the fine branches at the terminals of mossy fibers, form the core of each glomerulus. Excitatory synapses (Gray’s type 1) are made between the rosettes and the interdigitating dendrites from as many as 20 granule cells. This can be seen in the electron micrograph in Fig. 7.5B, where a large mossy fiber presynaptic terminal (mf) is seen to be surrounded by several granular cell dendritic claws (dc). The presynaptic terminal contains spherical presynaptic vesicles of about 450 Å in diameter. Golgi cell axon terminals surround the rosettes, where they make inhibitory (Gray’s type 2) synapses onto the granule cell dendrites (Fig. 7.5B, ga). All are encapsulated by a glial lamella that marks the border of each glomerulus.

In the granular layer, Golgi cells receive excitatory (type 1) input from the mossy fibers. These synapses are formed on the Golgi cell dendrites and somata. Thus, mossy fiber volleys excite Golgi and granule cells. Climbing fibers also contact Golgi cells in the granular cell layer. Finally, Purkinje-cell recurrent axon-collateral varicosities and terminals make inhibitory (type 2) synapses on Golgi-cell dendritic trunks and primary branches.

PURKINJE CELL LAYER

The synapse formed in this region is between the basket-cell axon terminal and the Purkinje-cell soma and initial segment. As many as 50 basket-cell axon branches make intricate arborizations surrounding the somata, which form many axosomatic synapses; the electron micrograph in Fig. 7.5C illustrates basket cell axon (ba) contacts on the soma and initial segment of a Purkinje cell. Even though basket cell terminals cover

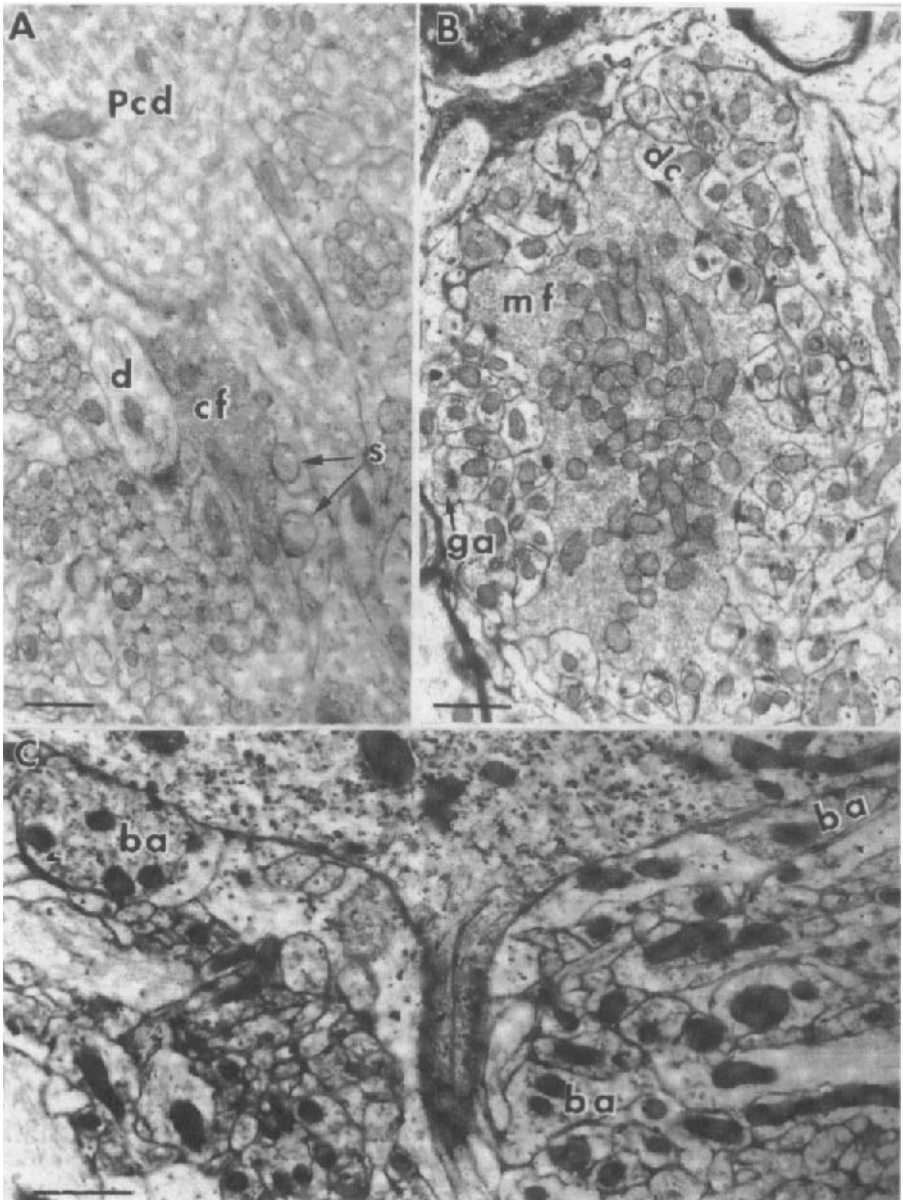


Fig. 7.5. Electron micrographs of parallel fiber and basket axon synaptic relationships. **A:** Climbing fiber (cf) synapse with spines from a large adjacent Purkinje cell dendrite (Pcd). The contact is made on Purkinje cell spines (s) as the climbing fiber follows the main Purkinje cell dendrite. Note that glial projections surround the dendrite and synaptic spines. A stellate cell or Golgi cell dendrite is adjacent to the climbing fiber and is contacted by a parallel fiber. **B:** A mossy fiber rosette (mf) filled with synaptic vesicles and mitochondria. Surrounding the mossy fiber axon are numerous profiles from dendritic claws (dc) making synaptic contacts. Golgi axon boutons (ga) contact the dendritic claws. **C:** Initial axonal segment of Purkinje cell. The base of the soma has basket axonal contacts (ba). Basket axons are separated from the Purkinje axon by glia but contact each other forming the pinneau of contacts between axons at their tips below this region. Scale: A = 5 μm ; B = 3 μm ; C = 1 μm . [Micrographs courtesy of Dean Hillman and Suzanne Chen.]

both the soma and the axon hillock of the Purkinje cells, only a few synapses with the typical structure of Gray's type 2 (see Chap. 1) have been observed at the axon hillock level; however, a rather impressive morphological structure known as the *pinso terminale* may be found at this level (Cajal, 1888). This terminal portion is not a chemical synapse but is similar to the electrical inhibitory synapse in Mauthner cells. These synapses very effectively shut down the output of the cortex.

MOLECULAR LAYER

Climbing Fiber–Purkinje Cell Connection. Among the afferent systems of central neurons, none is more remarkable in extent and power than the climbing fiber junction with Purkinje cells. This junction is unusual not only for its large coverage of a considerable portion of the Purkinje cell dendritic tree but also because, as we have seen, only one climbing fiber afferent contacts each Purkinje cell. The synapses are made between varicosities (2 μm across) on the climbing fiber and stubby spines on the soma and main dendrites of the Purkinje cell; as many as 300 synaptic contacts may be made between a climbing fiber and its Purkinje cell. Each climbing fiber varicosity may synapse with one to six spines. A climbing fiber terminal (cf) contacting a Purkinje cell spine(s) near a dendrite (Pcd) is shown in Fig. 7.5A. A dendrite (d) from a Golgi or stellate cell is adjacent to the climbing fiber terminal. The presynaptic vesicles are round and 440–590 \AA in diameter. Morphologically, the presence of a climbing fiber synapse seems to exclude nearby parallel fiber–Purkinje cell contacts. The Purkinje cell dendrites can thus be divided into a central area covered by the climbing fibers and the more peripheral, spiny dendritic portion that is contacted by parallel fibers.

Parallel Fiber Connections. In contrast to the climbing fibers, which mainly contact Purkinje cell dendrites, the parallel fibers terminate on the dendrites of all the neuronal elements in the cerebellar cortex, except for the granule cells. Thus, parallel fibers contact the dendrites of Purkinje cells, basket cells, stellate cells, and Golgi cells. On the Purkinje cells, parallel fibers synapse with the spines on the terminal regions of the Purkinje cell dendrites, called *spiny branchlets*. These are shown in Fig. 7.6A, where an antibody against calbindin has been used to reveal the great density of spines on the dendritic trees of two Purkinje cells. The synaptic junction is formed between the head of a spine and a globular expansion of the parallel fiber; the spine penetrates the swollen part of the fiber. The electron micrograph in Fig. 7.6B illustrates a Purkinje cell spiny branchlet (sb) with at least three spines (one is marked). A synapse with a parallel fiber is clearly seen on each of the three right-hand spines. The synaptic vesicles are spherical and 260–440 \AA in diameter. A parallel fiber forms synapses with one of every three to five Purkinje cells that it traverses. Thus, most of the parallel fibers passing through the dendritic tree of a Purkinje cell will not form synapses. Nevertheless, there is such a large number of parallel fibers that as many as 200,000 synapses on one Purkinje cell dendrite may be formed in humans, by far the largest number of synaptic inputs to any central neuron. In addition, the ascending portion of the granule cell axon has varicosities that are presynaptic to spines on the lower dendrites of Purkinje cells.

Golgi cell dendrites receive excitatory synapses from the parallel fibers. These axodendritic synapses are by far the largest number of synapses onto Golgi cells. An

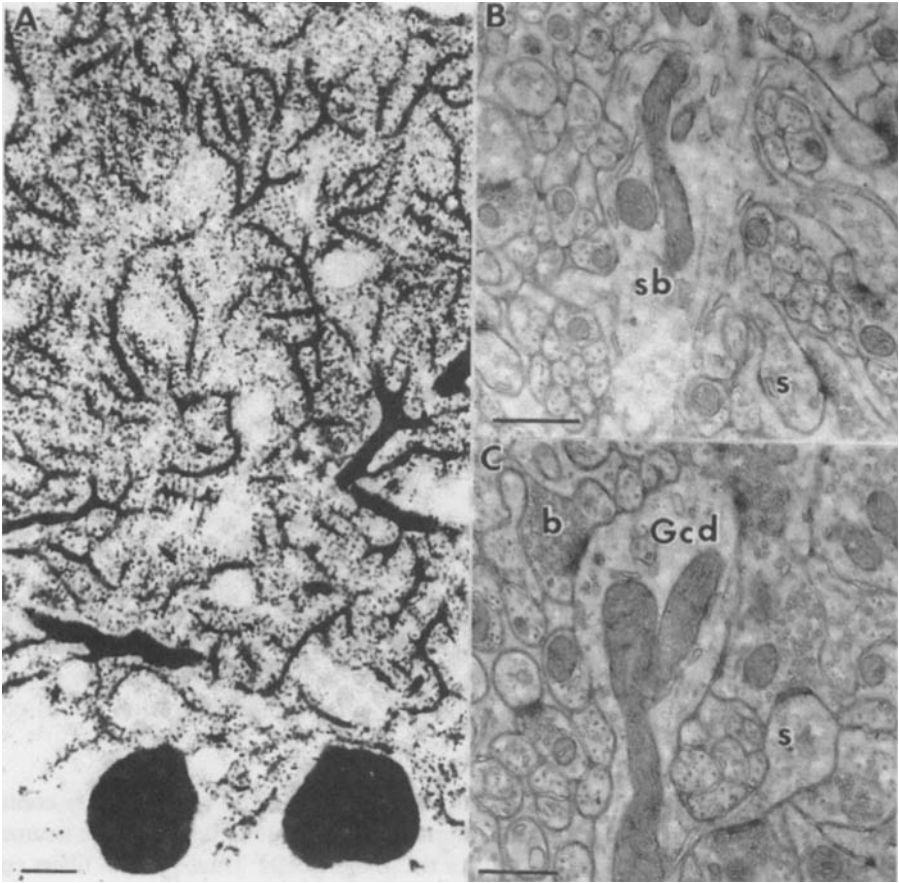


Fig. 7.6. Cerebellar molecular layer synaptic relationships of parallel fibers (granule cell axons) with Purkinje cells and interneurons. **A:** Immunoreaction of a Purkinje cell showing the detail of spine density on spiny branchlets (calbindin antibody on a 1- μm plastic section). The profiles of two Purkinje cell somata are seen with segments of the main dendritic arbor and numerous spiny branchlets. Emerging spines and profiles of spine heads dot the field, revealing the high density of Purkinje cell spine synapses with parallel fibers. Longitudinal sections of spiny branchlets show that the interspace interval of spines along the dendrite is near the diameter of the spine head. Note that the larger main branches have few spines. **B:** Electron micrograph of a Purkinje cell spiny branchlet (sb) that is longitudinally sectioned and has spines (s) emerging from the dendritic shaft in contact with a parallel fiber bouton. Bergmann glial projections shroud the spine shaft and junctional site. **C:** Golgi cell dendrite (Gcd) with parallel fiber (b) synapses. Spine (s) emerges from the dendritic shaft with parallel fiber synapse on the head and the shaft. Parallel fiber boutons (b) synapse directly on the dendrite. Scale: A = 10 μm ; B = 1 μm ; C = 1 μm . [Micrographs courtesy of Dean Hillman and Suzanne Chen.]

example is shown in Fig. 7.6C, where parallel fiber boutons (b) synapse directly onto a Golgi cell dendrite (Gcd) as well as with the head and shaft its dendritic spine(s).

Plasticity of Purkinje Cell Connectivity. In the Purkinje cell dendritic tree, the climbing fiber input is normally proximal to the parallel fiber input (Fox et al., 1967). When damage to the climbing fibers occurs in the adult animal, however, spines proliferate in large numbers on Purkinje cell smooth dendrites. These are promptly invaded by newly formed parallel fiber contacts (Sotelo et al., 1975), indicating a tug of war or a territoriality between the two systems. Also, destruction of the parallel fibers promotes multiple climbing fiber innervation (Mariani et al., 1977), indicating that a true competition for a Purkinje cell dendritic tree exists between parallel and climbing fiber afferents and even between climbing fiber afferents themselves. It also indicates that a single climbing fiber cannot provide all of the necessary input, because Purkinje cells become multiply innervated by climbing fibers after parallel fiber damage.

Quantitative studies have been made of the changes in the parallel fiber–Purkinje cell synapse localization after lesioning of the parallel fiber input. In one set of experiments, the parallel fibers were sectioned and the molecular layer was undercut (to destroy the granule cells) (Hillman and Chen, 1984). The number, size, and average contact area of the parallel fiber–Purkinje cell synapses were evaluated 2–3 weeks after the lesion and compared with control values from unlesioned animals. It was found that the number of parallel fibers contacting a Purkinje cell was reduced in relation to the extent of the lesion but that the area of synaptic contact of the surviving synapses was proportionately increased. Thus, there was a change in the position and size of the synapses in response to perturbations, but the total area of synaptic contact remained stable. Change in the size of the presynaptic boutons was not accompanied by a change in the presynaptic grid densities or the number of synaptic vesicles (Hillman and Chen, 1985a). This suggests that as the size of the boutons increased, there was a parallel increase in the morphological correlates of the neurotransmitter release machinery. Stabilization of the total synaptic area has also been seen in other areas of the CNS (see Hillman and Chen, 1985b).

Other Connectivity in the Molecular Layer. In addition to Purkinje cells, the dendrites of stellate, basket, and Golgi cells receive inputs in the molecular layer (see Fig. 7.3C). Parallel fiber swellings make excitatory synapses onto stellate cell dendritic spines. The stellate cells in turn make inhibitory synapses into Purkinje cell dendritic shafts. The basket cells receive excitatory synaptic connections from climbing fibers and parallel fibers and are inhibited by Purkinje cell axon collaterals. Parallel and climbing fibers make the same *en passant* synapses with basket cell dendrites as with Purkinje cell dendrites.

CEREBELLAR NUCLEI

Five different types of synaptic terminals have been distinguished on the basis of the characteristics of their membrane attachment and shape of synaptic vesicles. Both axosomatic and axodendritic synapses are found. The presynaptic terminals are made by collaterals of the mossy and climbing fibers and by Purkinje cell axons (Palkovits et al., 1977). Purkinje cell axons have two or three branches that arborize extensively in the nucleus, describing a narrow cone. Synapses are formed at the terminals and at *en passant* thickenings along the length of the axon. Synapses are usually formed with

dendritic thorns or spines of nuclear cells, although some synapses are axosomatic. The thickenings and terminals have dispersed ovoid vesicles, which are usually found where they contact the dendrites of nuclear neurons.

There is both significant divergence and convergence in the Purkinje cell–cerebellar nuclei projection (Palkovits et al., 1977). For example, in cats, individual Purkinje cells are estimated to contact as many as 35 nuclear cells; however, the bulk of the synapses are made with only 3–6 nuclear cells. Conversely, there are about 26 Purkinje cells for each nuclear cell, and each Purkinje cell axon branches extensively. As a result, each nuclear cell may receive input from up to 860 different Purkinje cells.

Complex synaptic combinations such as serial and triadic synapses are found in the cerebellar nuclei (Hámori and Mezey, 1977), as is also seen in the retina (see Chap. 6) and thalamic nuclei (see Chap. 8). These synaptic arrangements imply a quite complex interaction between the afferents and nuclear cells. In these synapses, the first presynaptic element may be a Purkinje cell axon terminal, a brainstem afferent terminal (collateral of a climbing or mossy fiber), or an axon terminal that is probably from a collateral of a cerebellar nuclear projection cell. The second terminal in the sequence is from either an axon collateral of a projection neuron or a Golgi type II interneuron and is both postsynaptic to the first element and presynaptic to the third element. The third element of the triad is a dendrite of a cerebellar nuclear neuron, which receives synaptic input from the other two elements. Although such triadic synapses are a regular feature of the nuclei, they do not form as large a percentage of synapses as in some sensory systems.

BASIC CIRCUIT ORGANIZATION

There are three main circuits in the cerebellum: two circuits in the cortex, which include afferent fibers as shown in Fig. 7.3, and one circuit in the deep nuclei. They are diagrammed in Fig. 7.7.

MOSSY FIBER CIRCUIT

The sequence of events that follows the stimulation of mossy fibers was first suggested by János Szentágothai at the Semmelweis University School of Medicine in Budapest: the stimulation of a small number of mossy fibers activates, through the granule cells and their parallel fibers, an extensive array of Purkinje cells and all three types of inhibitory interneurons. Subsequent interactions of the neurons tend to limit the extent and duration of the response. The activation of Purkinje cells through the parallel fibers is soon inhibited by the basket cells and the stellate cells, which are activated by the same parallel fibers. Because the axons of the basket and stellate cells run at right angles to the parallel fibers, the inhibition is not confined to the activated Purkinje cells; those on each side of the beam or column of stimulated Purkinje cells are also subject to strong inhibition. The effect of the inhibitory neurons is therefore to sharpen the boundary and increase the contrast between those cells that have been activated and those that have not.

At the same time, the parallel fibers and the mossy fibers activate the Golgi cells in the granular layer. The Golgi cells exert their inhibitory effect on the granule cells and thereby quench any further activity in the parallel fibers. This mechanism is one of negative feedback: through the Golgi cells, the parallel fiber extinguishes its own stimulus (see Fig. 7.7A). The net result of these interactions is the brief firing of a relatively large but sharply defined population of Purkinje cells.

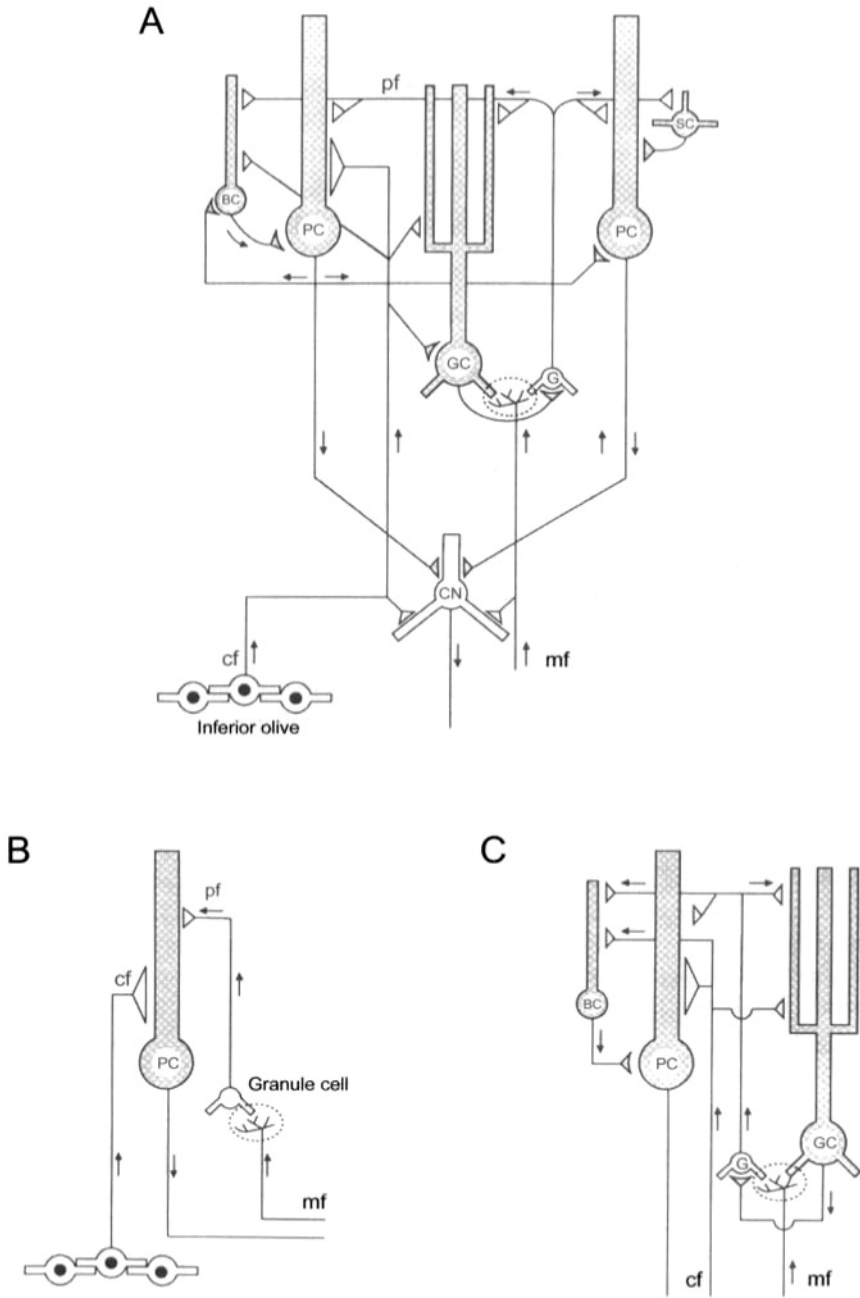


Fig. 7.7. Diagram of the basic circuit in the mammalian cerebellum. **A:** This circuit includes all the elements making specific synaptic connections in the cerebellar cortex and nuclei. **B and C:** Simplified diagrams of cerebellar cortex showing the afferent circuits (**B**) and the intrinsic neurons (**C**). Abbreviations: BC, basket cell; cf, climbing fiber; CN, cerebellar nuclear cell; G, granule cell; GC, Golgi cell; mf, mossy fiber; PC, Purkinje cell; pf, parallel fiber; SC, stellate cell.

CLIMBING FIBER CIRCUIT

In the normal adult cerebellum, a one-to-one relationship exists between a climbing fiber and a given Purkinje cell (i.e., each Purkinje cell receives one climbing fiber); however, each olivary axon branches to provide climbing fibers to approximately 10 Purkinje cells. The branching patterns of olivocerebellar axons are not random, but rather the branches of an individual axon predominantly remain within a relatively narrow plane that is aligned to the rostrocaudal axis (Sugihara et al., 2001). Moreover, neurons from the same region of the inferior olive tend to project to the same rostrocaudally oriented strip of cerebellar cortex. Thus, the projection pattern of the olivocerebellar pathway divides the cerebellar cortex into a series of parasagittally oriented zones. Interestingly, the projection pattern of the olivocerebellar pathway is largely in register with corticonuclear (Purkinje cell axons to deep cerebellar nuclei) and cerebellar nucleo-olivary projections, such that a series of reentrant loops are formed. For example, climbing fibers from the principal nucleus of the inferior olive project to the lateral part of the cerebellar hemisphere and also send collaterals to the dentate nucleus. In turn, the dentate is targeted by Purkinje cells of the lateral part of the hemisphere, and its GABAergic cells project back to the principal olivary nucleus.

Although climbing fibers have Purkinje cells as their primary targets, they also activate other neurons of the cerebellar cortex. For example, they activate Golgi cells, which will inhibit the input through the mossy fibers (see Fig. 7.7A). Thus, when climbing fibers fire, their Purkinje cells are dominated by this input. The climbing fiber input to basket and stellate cells sharpens the area of activated Purkinje cells.

An additional feature of the anatomy of the olivocerebellar system is of particular note with regard to its action on the cerebellum: olivary neurons are electrotonically coupled by gap junctions (Llinás et al., 1974; Sotelo et al., 1974; Llinás and Yarom, 1981). In fact, immunofluorescence and mRNA studies indicate that the inferior olive has one of the highest densities of connexin 36 (Condorelli et al., 1998; Belluardo et al., 2000), the protein from which neuronal gap junctions are usually formed (Rash et al., 2000). This electrotonic coupling is thought to allow olivary neurons to synchronize their activity. Interestingly, most of these gap junctions occur between dendritic spines that are part of complex synaptic arrangements known as *glomeruli*. Olivary glomeruli, in addition to the gap-junction-coupled dendritic spines, contain presynaptic terminals, whose function is thought to be to control the efficacy of the electrotonic coupling.

CEREBELLAR CORTEX-DEEP NUCLEI CIRCUIT

Electrical activation of mossy fiber inputs to the cerebellar system generates an early excitation in the cerebellar nuclei because the collaterals terminate directly on the cerebellar nuclear cells (see Fig. 7.7A). The same information then proceeds to the cerebellar cortex, which in turn produces an early excitation of Purkinje cells to be translated into inhibition at the cerebellar nucleus. This inhibition is followed by a prolonged increase in excitability of the cerebellar nuclear cells. The increased excitability is the result of two actions: (1) disinhibition due to reduced Purkinje cell activity, which in turn results from the inhibitory action of basket and stellate cells after the initial activation of Purkinje cells, and (2) cerebellar nuclear cell intrinsic properties (see later). The Purkinje cell inhibition is also due indirectly to the inhibitory action of the Golgi

interneuron, which, by preventing the mossy fiber input from reaching the molecular layer, reduces the excitatory drive to Purkinje cells. The cerebellar nuclear projection neurons themselves send axon collaterals to cortical inhibitory interneurons including basket cells, which thus provide recurrent inhibition of the cerebellar nuclear neurons, as seen in spinal motoneurons (see Chap. 3).

INTRINSIC MEMBRANE PROPERTIES

In Chap. 2, it was emphasized that the functional characteristics of a neuron are the outcome of a complex interplay between its intrinsic membrane properties and its synaptic interactions. In no part of the brain is this exemplified more vividly than in the cerebellum. Indeed, as already mentioned in Chap. 2, the Purkinje cell is one of the best known models for demonstrating these properties. Because of this importance, we consider the intrinsic membrane properties separately in this section before addressing the synaptic actions of the system.

PURKINJE CELLS

The intrinsic membrane properties of cells may be considered independent of synaptic input, although interaction of synaptic potentials with intrinsic membrane properties shapes the activity of the cell. Intrinsic properties are usually studied by determining the response to direct activation, that is, to depolarizing or hyperpolarizing current injected into the cell, usually into the soma. Purkinje cell electrical activity may be recorded under *in vivo* or *in vitro* conditions; however, because the most reliable recordings are obtained *in vitro*, our understanding of the electrical properties of the mammalian Purkinje cell membrane has come mainly from studies of cerebellar slices (Llinás and Sugimori, 1978, 1980a,b). Antidromic activation of a Purkinje cell is characterized by a large spike having an initial segment–soma dendritic (IS-SD) break that is in many ways similar to that obtained *in vivo* from motoneurons and other central neurons.

Direct stimulation of Purkinje soma via the recording microelectrode demonstrates that these cells fire in a way that is quite different from that seen in other neurons. Indeed, square current pulses lasting about 1 sec (Fig. 7.8A) produce, at just threshold depolarization, a repetitive activation of the cell. That is, with long pulses, the neuron fires, but a single isolated spike cannot be generated by this type of stimulation. This burst of activity is produced by a low-threshold, sodium-dependent conductance that does not inactivate within several seconds and serves to trigger the fast action potentials. This sodium conductance is different from that responsible for the fast action potentials seen in virtually all nerve cells: it is activated at a lower voltage and does not inactivate. With increased stimulation, the onset of the repetitive firing moves earlier. Also at the end of the initial pulse of firing, a reduction in the amplitude of the spikes is followed by a rhythmic bursting, as marked by arrows in Fig. 7.8B.

Pharmacological studies in cerebellar slices have shown that the fast action potentials and the bursting responses have different ionic mechanisms. Removal of extracellular sodium or the application of tetrodotoxin (TTX, a sodium-conductance blocker) to the bath causes a complete abolition of the fast action potentials seen in Fig. 7.8A and B but leaves a late, slow-rising burst potential intact, as shown in Fig. 7.8C. This slow bursting of Purkinje cells has been found to be generated by a voltage-activated

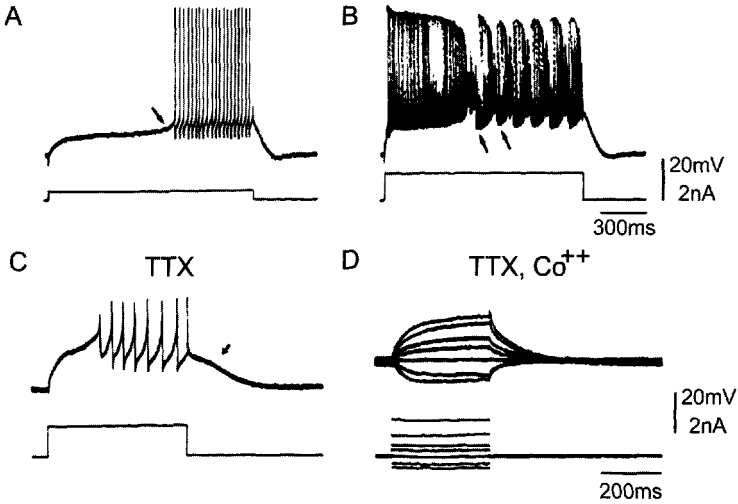


Fig. 7.8. Intrinsic properties of mammalian Purkinje cells recorded *in vitro*. **A:** A prolonged, threshold current pulse injected into the soma of a Purkinje cell elicits a train of action potentials after an initial local response (arrow). **B:** Increased current strength elicits high-frequency firing and oscillatory behavior (arrows). **C:** After addition of TTX to the bath, the fast action potentials are blocked, and the slowly rising action potentials underlying the oscillations seen in **B** are revealed. A slow afterdepolarization may also be seen. **D:** Addition of cobalt chloride (Co^{2+}) to the TTX perfusate removes all electroresponsiveness, indicating that the slow action potentials in **C** were calcium dependent. [Modified from Llinás and Sugimori, 1980a, with permission.]

calcium conductance followed by a calcium-dependent potassium conductance increase. We know the spikes are calcium dependent because they are seen in the absence of sodium and because they are blocked by the removal of calcium from the extracellular medium or by ions that block the slow calcium conductance (cobalt, cadmium, manganese), as shown in Fig. 7.8D. When the calcium in the bathing solution is replaced by barium, the afterhyperpolarization is reduced and the bursting response is converted into a prolonged single action potential. This demonstrates the presence of a calcium-activated potassium conductance, because it is known that barium does not activate the calcium-activated potassium conductance. All electroresponsiveness is gone after calcium and sodium blockade, as shown by the application of both TTX and cobalt to the extracellular medium (see Fig. 7.8D). Thus, at the somatic level, Purkinje cells have not one, but three, main mechanisms for spike generation: (1) a sodium-dependent spike similar to that seen in other cells, which is blocked by the absence of extracellular sodium or by the application of TTX; (2) a low-threshold, noninactivating sodium spike; and (3) a calcium-dependent action potential, which has a slow rising time and a rather rapid return to baseline.

The distribution and properties of voltage-gated channels in the dendrites are discussed later (see Dendritic Properties).

CEREBELLAR NUCLEAR CELLS

The electrical properties of cerebellar nuclear neurons were first studied in detail in *in vitro* preparations (Jahnsen, 1986a,b; Llinás and Mühlethaler, 1988b). Like Purkinje

cells, cerebellar nuclear cells have a collection of ionic conductances that give them complex firing abilities. Cerebellar nuclear cells have a noninactivating sodium conductance similar to that described in Purkinje cells, in addition to the usual sodium- and potassium-dependent conductances that generate fast action potentials. The firing of cerebellar nuclear cells depends on their resting potential. If a cell is depolarized with a current pulse from the resting potential, as in Fig. 7.9A, the cell fires a train of

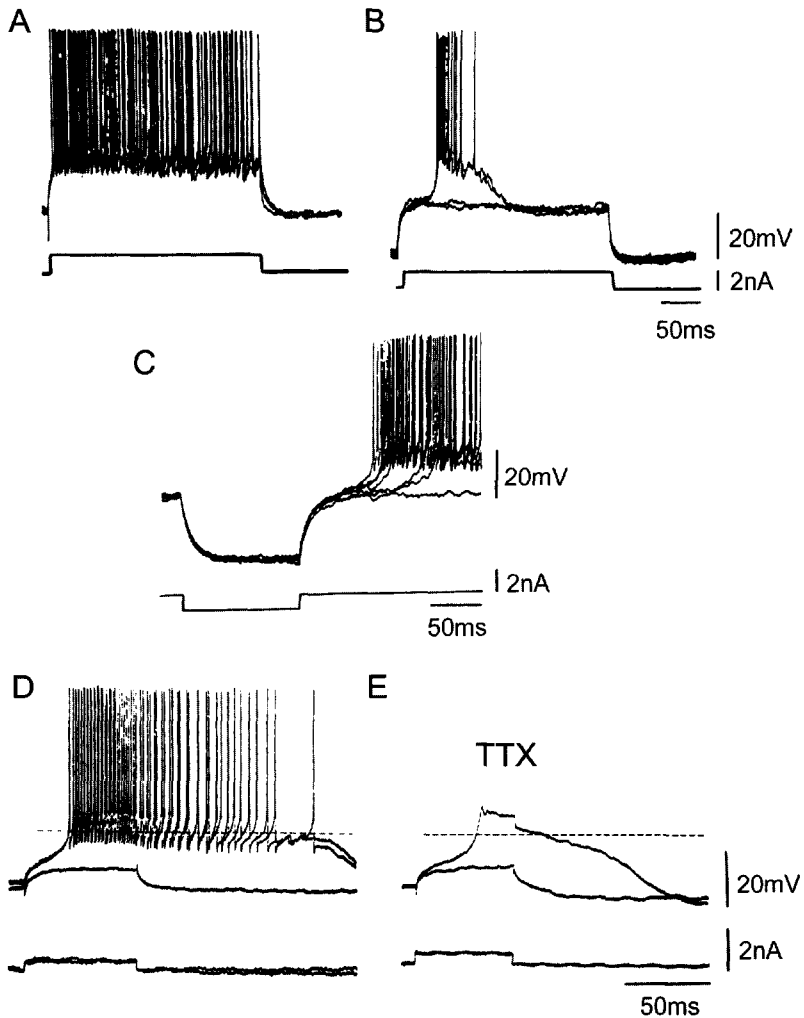


Fig. 7.9. Intrinsic properties of cerebellar nuclear neurons. **A:** A depolarizing current injection from resting potential elicits tonic firing. **B:** When the same strength current pulse is delivered from a hyperpolarized membrane level, an all-or-none burst response is elicited. **C:** Hyperpolarizing current injection from the resting potential elicits a strong rebound burst of action potentials from a slow depolarization. **D:** Response to current injection from a hyperpolarized level (resting potential marked by broken line). **E:** Addition of TTX to the perfusate blocked the fast action potentials, revealing a slowly rising, prolonged depolarization and afterdepolarization; these responses were then blocked by addition of Co^{2+} to the bath. [Modified from Llinás and Muhlethaler, 1988b, with permission.]

action potentials. However, if the same current pulse is injected when the cell is held hyperpolarized from the resting potential, all-or-nothing bursts are seen, as shown in Fig. 7.9B and D. Also, if a hyperpolarizing current pulse is injected into a cerebellar nuclear neuron, a burst of action potentials is seen at the end of the current injection (Fig. 7.9C).

This "rebound response" following hyperpolarization is important in cerebellar nuclear cell function. This is easily understood because Purkinje cells are inhibitory and generate inhibitory postsynaptic potentials (IPSPs) in cerebellar nuclear cells. The ionic basis for these burst responses was determined by pharmacological studies. Thus, after eliminating the fast sodium conductance by the application of TTX, the fast action potentials seen in Fig. 7.9D are blocked and a slowly rising spike is elicited from the hyperpolarized membrane potential (Fig. 7.9E). The threshold for these spikes is lower than that for the fast sodium-dependent action potentials; they are therefore called low-threshold spikes (LTSs). They are calcium dependent because they are blocked after the addition of cobalt or the removal of calcium from the bath and are insensitive to TTX. The presence of an LTS is probably of major functional significance in cerebellar nuclear neurons because following climbing fiber activation of Purkinje cells, such bursts can easily be elicited following the powerful IPSPs produced by this input (see Fig. 7.18; Llinás and Mühlethaler, 1988b).

SYNAPTIC ACTIONS

CLIMBING FIBER ACTION ON PURKINJE CELLS

One of the most powerful synaptic junctions in the CNS is that between the climbing fiber afferent and the dendrites of a Purkinje cell. It has been called a *distributed synapse* because a single presynaptic fiber makes contact with the postsynaptic cell at many points (≈ 300) throughout the Purkinje cell dendritic tree, and thus the synapse is distributed over a large surface area. This is in contrast to more typical synapses, such as between a Ia terminal and motoneuron, where there are only a few, relatively localized points of contact (see Chap. 3). Eccles et al. (1966a) demonstrated electrophysiologically that stimulation of the inferior olive produces a powerful activation of the Purkinje cell. This synaptic excitation is characterized by an all-or-nothing burst of spikes that shows little variability from one activation to the next. These are called *complex spikes*. Several complex spikes recorded from an isolated preparation are superimposed in Fig. 7.10A and B. It is now known that the spikes on the broad EPSP are produced in the dendrites by a voltage-activated calcium conductance (see later) and at the somatic and axonic levels by the usual Hodgkin-Huxley sodium and potassium conductances (Llinás and Sugimori, 1978, 1980b).

Climbing fiber responses in Purkinje cells may be elicited by placing a stimulating electrode in the white matter near the midline. This "juxtastigial" stimulation activates inferior olivary axons in the white matter. Following a juxtastigial stimulus, climbing fiber synapses are activated simultaneously and produce a very large unitary EPSP in the postsynaptic dendrite. This unitary synaptic potential usually has an amplitude of 40 mV and lasts 20 msec. The all-or-nothing character of the climbing fiber-evoked EPSP contrasts with the usual graded nature of EPSPs within the CNS and reflects the singular climbing fiber innervation of a Purkinje cell. If the Purkinje

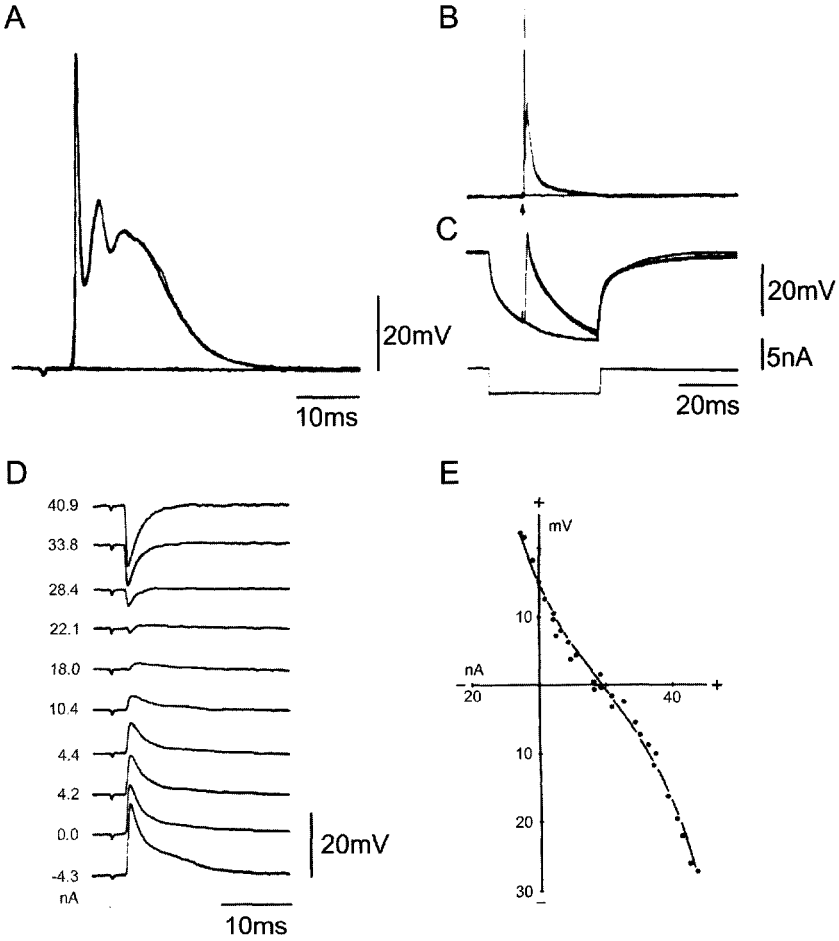


Fig. 7.10. Climbing fiber activation of mammalian Purkinje cells *in vitro*. **A:** All-or-none complex spikes in a Purkinje cell evoked by white matter stimulation are superimposed. **B:** In another Purkinje cell, five threshold white-matter stimuli (arrow) evoke very uniform complex spikes on four occasions. **C:** If threshold stimuli are delivered when the cell is hyperpolarized (to prevent action potential firing), the all-or-none climbing fiber EPSP may be seen. **D:** Reversal of climbing fiber EPSP. Notice that, as expected in a distributed synapse, the reversal is biphasic, with the early portion of the potential reversing at lower levels of injected current than the late part; this may be seen at 18, 22, and 28 nA. **E:** Plot of the voltage current relation for the EPSP reversal shown in **D**. [Modified from Llinás and Nicholson, 1976, and Llinás and Mühlethaler, 1988a, with permission.]

cells are hyperpolarized far enough to prevent the cell from spiking, the all-or-nothing character of the EPSPs may be seen (see Fig. 7.10C).

Under conditions in which the sodium- and calcium-dependent spikes are prevented, the chemical nature of the synapse may be studied in detail and its distributed character clearly demonstrated. Depolarization of the soma or dendrite can produce a reduction in amplitude and an actual reversal of the sign of the climbing fiber EPSP, as shown

in Fig. 7.10D. A large increase in the EPSP amplitude is seen when the membrane potential is moved in the hyperpolarizing direction (lower traces in D). The reversal in sign (shown in Fig. 7.10D, 22.1 nA) is then the necessary and sufficient evidence to indicate that a synaptic junction is chemical in nature (see Chap. 2).

The fact that different parts of the EPSP (the peak and falling phase) reverse at different levels of depolarization (see biphasic reversal at 22.1 nA in Fig. 7.10D) indicates that the synapse occurs at multiple sites with different distances from the site of recording in the soma (Llinás and Nicholson, 1976). Because a current point source, a microelectrode, is used to change the membrane potential, the potential change along the dendrite is maximum near the site of impalement and decreases with distance. Because the synapses closest to the site of recording generate most of the rising phase of the recorded EPSP, this component is the first to reverse. Those synapses located at a distance generate the slowest components (owing to the cable properties of the dendrites) and are less affected by the current injection. Recordings similar to those obtained *in vitro* can also be obtained *in vivo*.

Activation of the climbing fiber afferents generates a burst of action potentials at the Purkinje cell axon. The frequency of this response is high, generally 500/sec. Indeed, it is higher normally than that seen after parallel fiber stimulation, suggesting that one of the possible functions of the climbing fiber system is to produce a discharge of distinct bursts of action potentials. As discussed later, climbing fiber activation also produces very sharp IPSPs in the target neurons of Purkinje cells.

PARALLEL FIBER ACTION ON PURKINJE CELLS

As discussed earlier, mossy fiber inputs activate Purkinje cells via the parallel fiber–Purkinje cell synapse (Eccles et al., 1966b). Early investigators named these responses *simple spikes*. Purkinje cell responses to spontaneous activity in the parallel fibers are illustrated in Fig. 7.11A; notice that during this recording period, two complex spikes were also recorded. This circuit can be activated by direct parallel fiber stimulation of the cerebellar surface or via the mossy fiber–granule cell–parallel fiber pathway from white matter stimulation. Both types of stimulation generate short-latency EPSPs in Purkinje cells.

This postsynaptic potential differs from that generated by the climbing fiber in two ways. First, it is graded as shown by the response to juxtastigial stimuli of increasing intensity (Fig. 7.11B, C). Second, it is generally followed by an IPSP (see trace, Fig. 7.11B). The IPSP is generated by activation of the inhibitory interneurons of the molecular layer. The parallel fiber synaptic depolarization can generate action potentials at the somatic level as well as dendritic calcium spikes if the stimulus is large enough (see later). Because parallel fiber activation of Purkinje cells is followed by a disynaptic inhibition, this synaptic sequence is reviewed in detail in conjunction with the inhibitory systems in the next section.

INHIBITORY SYNAPSES IN THE CORTEX

Inhibitory neurons are organized in the cerebellar cortex into two main categories: those that reside in the molecular layer (basket and stellate cells), and those that reside in the granular layer (Golgi cells).

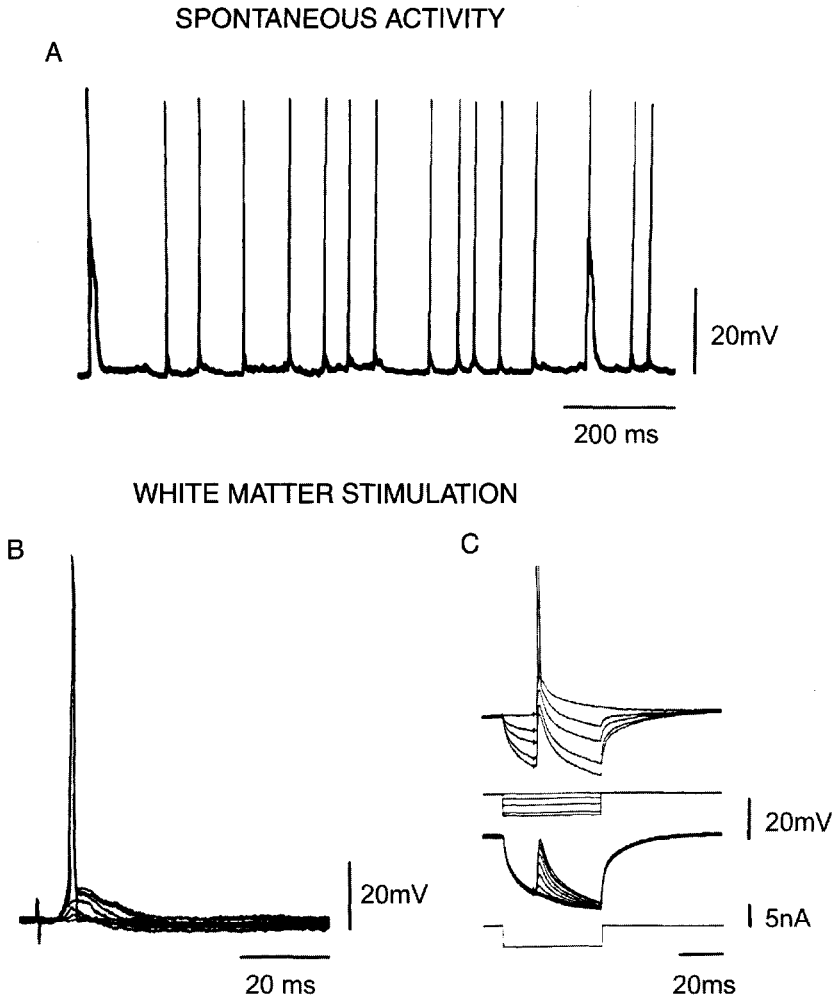


Fig. 7.11. Mossy fiber activation of mammalian Purkinje cells *in vitro*. **A:** Spontaneous activity in the mossy fiber–parallel fiber system gives rise to fast, simple spikes in Purkinje cells, which are in contrast to the two broad, climbing fiber–evoked complex spikes in the trace. **B:** White matter stimulation of increasing strength evoked graded EPSP–IPSP sequences due to mossy fiber–parallel fiber activation. **C:** When such stimulation is delivered during hyperpolarizing pulses of increasing amplitude (middle trace), the parallel fiber–mediated EPSP may be seen (top trace); the bottom trace illustrates the graded nature of the synaptic potential. [Modified from Llinás and Mühlethaler, 1988a, with permission.]

Granular Layer. In the granular layer, the main inhibitory system is the Golgi cell axonic plexus. This plexus releases GABA, inhibiting granule cell dendrites within the granule cell glomerulus. Indeed, while mossy fibers activate the terminal dendritic claws of the granule cells, the Golgi cell axons also distribute their contacts on the dendrites of the granule cells and act to counter the synaptic action of the mossy fibers by the

release of GABA. The inhibition that ensues is so powerful as to totally block parallel fiber activity in the cerebellar cortex (Eccles et al., 1966d).

Molecular Layer. In the molecular layer, inputs from climbing fibers and parallel fibers represent the two types of excitatory afferents terminating on a Purkinje cell. The Purkinje cell also receives input from three inhibitory systems: the basket cell, the stellate cell, and the catecholamine system, which arises from the locus coeruleus (Bloom et al., 1971; Pickel et al., 1974). Activation of the *basket cells* generates a graded inhibition at each side of the activated bundle of parallel fibers (Andersen et al., 1964; Eccles et al., 1966b,c). This can be seen clearly when recordings are made lateral to the beam of stimulated parallel fibers. In this case, at low stimulus intensity, only the IPSP is seen; however, if the stimulus intensity is increased, more Purkinje cells are excited by the parallel fibers and an EPSP–IPSP sequence is seen (Fig. 7.12A). The basket cell IPSP is generated by a membrane conductance increase to chloride, most probably by the release of GABA (see later). The second inhibitory system is that represented by the *stellate cells*, which synapse mainly on Purkinje cell dendrites. Electrophysiologically, they have the same pattern of inhibition as that of basket cells.

Monoaminergic Inhibition. The third inhibitory system in the molecular layer is that of the locus coeruleus; its catecholamine-mediated inhibition generates a large, prolonged hyperpolarization in Purkinje cells (Hoffer et al., 1973). Although intriguing questions arise about the function of this system, it is possible (because of its rather widespread character) that it is related to the general state of wakefulness of the animal rather than to specific cerebellar functions. Indeed, morphologically, the system consists of rather thin filamentous afferents that reach the cerebellar cortex and bifurcate widely to cover not only the neuronal elements but probably also the vascular system (Bloom et al., 1971).

PURKINJE CELL ACTION ON CEREBELLAR NUCLEAR CELLS

Perhaps one of the most surprising findings in the physiology of the cerebellum is the fact that the only output of the cerebellar cortex, the Purkinje cells, exercises an inhibitory input onto the cerebellar nuclear neurons (Ito et al., 1964). This finding indicates that the cerebellar cortex is the most sophisticated inhibitory system in the brain, not only because of its refinement of connectivity and the integrative ability of these neurons but also because of the extent of information reaching the cerebellar cortex. Indeed, there are as many neurons in the cortex ($\approx 5 \times 10^{10}$) as there are neurons in the rest of the brain. The powerful GABAergic inhibition of the Purkinje cells on the cerebellar nuclei also demonstrates the rich biochemistry of the system (Obata et al., 1967). The Purkinje cells project in a radial pattern onto the nuclei as discussed previously (see Neuronal Elements).

Electrical stimulation of the cerebellar white matter can elicit quite complex sequences of EPSPs and IPSPs in cerebellar nuclear cells. Here, we consider the simplest case—where white matter stimulation is limited to the Purkinje cell axons. In this case, only IPSPs are recorded. The records shown in Fig. 7.12B were made from a cerebellar nuclear cell in a cerebellum-brainstem preparation isolated from adult guinea pig (Llinás and Mühlethaler, 1988b). In the example shown in Fig. 7.12C, several

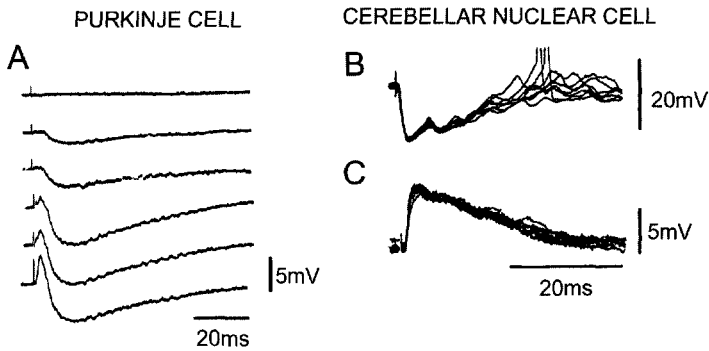


Fig. 7.12. Inhibitory synaptic potentials in Purkinje cells and cerebellar nuclear cells. **A:** Here, the stimulating electrode was placed on the cerebellar surface lateral to the recorded Purkinje cell because under such conditions, powerful IPSPs could be recorded in the Purkinje cell. As the stimulus intensity was increased (lower traces), the band of activated parallel fibers became wider, and finally the parallel fibers synapsing on the recorded Purkinje cell were themselves activated; thus an EPSP preceded the IPSP. **B:** IPSPs recorded in a cerebellar nuclear cell. Stimulation of the white matter between the cerebellar cortex and nuclei may elicit graded EPSPs and IPSPs. For particular locations and amplitudes of stimulation, IPSPs may be elicited in the absence of an early EPSP, as shown here. These IPSPs are very regular, often triggering rebound firing of the cell, as seen here. **C:** That these large potentials are synaptic potentials is shown by their reversal upon injection of a hyperpolarizing current.

IPSPs were elicited; it can be seen that their onset and amplitude are very reliable (four traces are superimposed) and that they can be easily reversed in sign by current injection, as in this example. The response of cerebellar nuclear cells to white matter stimulation is not always so straightforward, as is discussed later (see Functional Circuits).

MODULATION OF EXCITATORY SYNAPSES

In addition to the excitatory action of climbing and parallel fibers on Purkinje cells (see earlier) and their intrinsic roles in Purkinje cell integration, other functions related to their temporal interaction have been proposed. Ito et al. (1982) reported that simultaneous low-frequency activation (1–4 Hz) of these two inputs such that climbing fibers precede parallel fiber activation (induction) reduces subsequent parallel fiber action on Purkinje cells when both inputs are again stimulated (expression). Thus, following such pairing, the parallel fiber EPSP or EPSC amplitude is reduced by 20%–50%; this effect is maximal after 5–10 min. It lasts as long as it has been studied, usually 1–2 hr, and is called *long-term depression* (LTD). Comparable phenomena induced by low-frequency stimulation have been found in other regions of the brain (cf. Chaps. 10–12).

The order and temporal sequence for the generation of this depression were initially proposed on theoretical grounds by Albus (1971) as the basis for his hypothesis that the cerebellar cortex may be the seat of motor learning. Ito et al. (1982) interpreted their results as a confirmation of Albus's theory, but this is a matter of controversy. The phenomenon has since been studied largely in cerebellar slices, dispersed Purkinje cells, and more reduced preparations (Narasimhan and Linden, 1996). With these *in vitro* preparations, the cellular mechanism underlying this form of “memory” has become

an area of active research (Linden and Connor, 1993) and discussion (Llinás and Welsh, 1993).

An important issue with LTD has been its apparent specificity. Because climbing fiber activation stimulates the entire dendritic tree, the specificity is determined by the parallel fiber synapses. That is, only Purkinje cells that respond to those parallel fibers that were coactivated with climbing fiber input during the induction phase would presumably show a decrease in parallel fiber activation. This would mean that the input from a small group of granule cells would be selectively depressed, modifying the "computational" power of each Purkinje cell.

However, it has been shown that the opposite order of stimulation—parallel fiber activation preceding climbing fiber activation of Purkinje cells—can also lead to LTD (Chen and Thompson, 1995) and that parallel fibers in their own right can also activate such a process (Hartell, 1996). Indeed, parallel fibers alone can activate calcium entry on the spines of Purkinje cells (Denk et al., 1995). Thus, a new hypothesis as to how LTD may relate to motor function must be developed because Albus' learning hypothesis was quite specific on the nature and order of climbing fiber–parallel fiber interaction.

From a molecular biological point of view, it has been proposed that LTD induction is associated with activation of voltage-gated calcium channels following climbing fiber activity and of metabotropic glutamate receptors (mGluR1) and AMPA glutamate receptors following parallel fiber activity. Climbing fiber activation of Purkinje cells leads to the opening of voltage-gated calcium channels and the generation of calcium spikes in the dendrites. The resulting increased intracellular concentration of calcium is necessary for LTD induction. Direct Purkinje cell depolarization can be substituted for climbing fiber activation. Activation of the metabotropic glutamate channels leads to phospholipase C-mediated production of diacylglycerol and inositol-1,4,5-triphosphate. The AMPA receptors are linked to Na^+ -selective channels and sodium entry through the AMPA channels is necessary for the induction of LTD (Linden et al., 1993). Ionophoresis of glutamate can be substituted for parallel fiber stimulation. The ultimate expression of LTD is thought to be due to desensitization of AMPA receptor function (Linden, 1994). Finally, another issue has come up; LTD may in fact be a neuroprotective mechanism to control possible damage of the Purkinje cell dendritic tree by excess calcium entry during high-level activation (Llinás et al., 1997).

We can summarize what is known about the induction of LTD in the cerebellar cortex as follows. (1) Climbing fiber stimulation leads to increased intracellular concentration of calcium through voltage-gated channels and to increased cGMP, possibly through nitric oxide and guanylate cyclase. Parallel fibers also increase, in their own right, calcium concentration in these dendrites. (2) Parallel fiber activation leads to activation of metabotropic glutamate receptor-linked channels, which in turn leads to increased diacylglycerol and inositol-1,4,5-triphosphate. (3) Parallel fiber activation leads to activation of glutamate receptors and inflow of sodium and calcium via the ligand-dependent channels and of calcium via voltage-gated channels. (4) The expression of LTD is through desensitization of specific, parallel fiber-activated Purkinje cell AMPA receptors. The physiological role of LTD and its mode of generation remain matters of debate. Indeed, placing LTD in the context of cerebellar function awaits further studies carried out under physiological conditions.

NEUROTRANSMITTERS

GLUTAMATE

In the cerebellar cortex, as is the case throughout most of the CNS, glutamate appears to be the major excitatory transmitter. Supporting its role as a neurotransmitter in the cerebellum, its release is dependent on calcium, antagonized by increases in magnesium, and stimulated by membrane depolarization caused by elevated levels of potassium (Sandoval and Cotman, 1978).

There is strong evidence that glutamate is the neurotransmitter of granule cells. Glutamate depolarizes Purkinje cells when applied ionophoretically to the dendrites (Krnjevic and Phillis, 1963; Curtis and Johnston, 1974; Sugimori and Llinás, 1981). Further, naturally occurring L-glutamate is more potent than the D-glutamate isomer (Chujo et al., 1975; Crepel et al., 1982). In frog Purkinje cells, the reversal potential of the glutamate-elicited EPSP is close to that for parallel fiber-evoked EPSPs (Hackett et al., 1979). Moreover, neurochemical studies have shown that the glutamate content is lower than normal in cerebella in which the number of granular cells has been reduced by X-irradiation (Valcana et al., 1972; McBride et al., 1976), virus infection (Young et al., 1974), or mutation (Hudson et al., 1976; Roffler-Tarlov and Turey, 1982). Also, compared with control values, glutamate uptake is reduced in synaptosomal preparations from cerebella in which the granule cell number has been reduced (Young et al., 1974; Rohde et al., 1979). Immunocytochemical studies have demonstrated high levels of glutamate immunoreactivity in parallel fiber terminals (Somogyi et al., 1986), which decrease under conditions that induce transmitter release (Ottersen et al., 1990a; Ottersen and Laake, 1992). Last, glutamate receptors are found on Purkinje cell dendrites as well as on other cells (basket, stellate, and Golgi) whose dendrites are contacted by parallel fibers (Petralia and Wenthold, 1992).

Glutamate also appears to be the neurotransmitter of the large majority of mossy fibers (Ottersen, 1993). Mossy fiber terminals are enriched in glutamate (Somogyi et al., 1986), and glutamate receptors are present on the postsynaptic granule cells (Gallo et al., 1992; Petralia and Wenthold, 1992). Moreover, CNQX, an AMPA antagonist, blocks granule cell responses to mossy fiber stimulation (Garthwaite and Brodbelt, 1989). However, mossy fibers originate from a number of brain regions, and at least some mossy fibers may use transmitters other than or in addition to glutamate (see Mossy Fiber).

There has been considerable debate regarding the neurotransmitter of the climbing fibers. Early biochemical results suggested that aspartate rather than glutamate was the neurotransmitter (Wiklund et al., 1982). Homocysteate was also put forward as a candidate because selective lesion of the climbing fibers abolished its release from cerebellar slices (Vollenweider et al., 1990). However, climbing fiber terminals show high immunoreactivity for glutamate but not for aspartate or homocysteate (Zhang et al., 1990; Zhang and Ottersen, 1993). Furthermore, homocysteate staining in the cerebellar molecular layer has been localized to the glial processes surrounding the Purkinje cell dendrites (Grandes et al., 1991). Thus, the evidence to date points to glutamate being the transmitter of the climbing fibers.

GABA

GABA is the major inhibitory neurotransmitter of the cerebellum. In the cortex, it is utilized by Purkinje cells and all three local inhibitory interneurons (basket, stellate,

and Golgi cells). In the cerebellar nuclei, the cells that give rise to the nucleo-olivary projection are GABAergic (De Zeeuw et al., 1989; Fredette and Mugnaini, 1991).

The inhibitory nature of Purkinje cells was first demonstrated in Deiters' nucleus. Ionophoretic application of GABA hyperpolarizes Deiters' neurons (Obata et al., 1967), a target of Purkinje cell axons. IPSPs following Purkinje cell activation, as well as GABA-induced potentials, reverse near the same membrane potential and are mediated by an increased conductance to chlorine (Obata et al., 1970; ten Bruggencate and Engberg, 1971). Picrotoxin, which blocks the chloride channel associated with the GABA-A receptor, blocks both Purkinje cell IPSPs and GABA potentials in Deiters' neurons. A reduction in the GABA-synthesizing enzyme glutamic acid dehydrogenase (GAD) in the interpositus nucleus is associated with destruction of the cerebellar hemisphere of the same side. Immunocytochemical studies have associated GAD activity with Purkinje cell axon terminals (Fonnum et al., 1970). In fact, GAD activity in Purkinje cell axon terminals is very high; 350–1,000 mM GABA can be synthesized per hour (Fonnum and Walberg, 1973).

Basket cell inhibition of Purkinje cell electrical activity is blocked by the application of agents known to block GABA receptors, such as bicuculline or picrotoxin. This effect has been demonstrated in several ways, involving a reduction in the ability of basket cell activation to (1) depress Purkinje cell spontaneous firing (Curtis and Felix, 1971), (2) depress Purkinje cell antidromic field potentials (Bisti et al., 1971), or (3) elicit IPSPs in Purkinje cells (Dupont et al., 1979). Also, ionophoretic application of GABA inhibits Purkinje cell spontaneous activity (Kawamura and Provini, 1970; Okamoto et al., 1976; Okamoto and Sakai, 1981). Moreover, basket cells take up radioactive GABA (Sotelo et al., 1972; Ljungdahl et al., 1978). Immunocytochemical studies have demonstrated the presence of GAD in basket cell terminals around Purkinje cell somata (McLaughlin et al., 1974; Chan-Palay et al., 1979; Oertel et al., 1981). Antibodies against GABA itself also strongly stain basket cells (Ottersen, 1993).

Stellate cells produce IPSPs in Purkinje cells that reverse around -75 mV and are blocked by bicuculline and picrotoxin, suggesting that they are mediated by GABA-A receptors (Midtgaard, 1992). However, these results by themselves do not exclude taurine as the neurotransmitter, for which there also is some evidence (Frederickson et al., 1978). However, immunocytochemical studies have directly demonstrated the presence of GABA in stellate cells, as well as a GABA reuptake system (Ottersen, 1993).

Antibodies against GAD or GABA label Golgi cells, including their synaptic terminals, indicating their GABAergic nature (Ottersen, 1993). However, most Golgi cells ($\approx 70\%$) are also labeled by glycine, and the labeling for both GABA and glycine is reduced following induction of synaptic activity with elevated potassium concentrations (Ottersen et al., 1990b). Moreover, granule cells, the targets of Golgi cell axons, have both GABA and glycine receptors (Triller et al., 1987; Somogyi et al., 1989).

MONOAMINERGIC AFFERENTS

In addition to the inhibition produced by local circuit neurons, elements of the cerebellar cortex (in particular, the Purkinje cells) may be inhibited by release of norepinephrine following activation of the locus coeruleus (see Foote et al., 1983). This form of inhibition, first demonstrated by Bloom and collaborators (Siggins et al., 1971b), suggests that Purkinje cell excitability may be depressed for protracted periods by the

release of norepinephrine from terminals arising from the brainstem neurons. Rather than synapsing at specific points, the terminals seem to be widespread within the cortex. Their activation apparently produces a widespread release of catecholamines that hyperpolarize the Purkinje cells. Such hyperpolarization seems to be mimicked by application of cyclic adenosine-3',5'-monophosphate (cAMP) (Siggins et al., 1971a,c), and norepinephrine may function via the activation of an electrogenic sodium pump similar to those in other central neurons (Phillis and Wu, 1981). Indeed, the possibility that an electrogenic sodium pump may be activated by norepinephrine is indicated, because the hyperpolarization is accompanied by a decreased ionic conductance change (Siggins et al., 1971c).

There is also evidence for dopaminergic cerebellar afferents projecting to the cerebellar nuclei and to the Purkinje and granular cell layers of the cortex (Simon et al., 1979). The raphe nuclei, which synthesize and release serotonin, project fibers to all parts of the cerebellar nuclei and cortex (Takeuchi et al., 1982). These terminate at mossy fiber rosettes diffusely throughout the granular layer; in the molecular layer, they bifurcate like parallel fibers and synapse with the intrinsic neurons (Chan-Palay, 1977). In the molecular and granular layers, beaded fibers with fine varicosities have been labeled with serotonin-specific antibodies (Takeuchi et al., 1982).

MOSSY FIBERS

Although the majority of mossy fibers appear to use glutamate as a neurotransmitter, some mossy fibers appear to use other neurotransmitters. For example, among the peptides, somatostatin-immunoreactive fibers have been shown to enter the cerebellum (Inagaki et al., 1982); these probably end as mossy fibers. Acetylcholine (ACh) is present in some mossy fiber terminals isolated as synaptosomes (Israel and Whittaker, 1965), and some mossy fibers contain acetylcholinesterase (Phillis, 1968). Choline acetyltransferase (ChAT), the enzyme for ACh synthesis, has been demonstrated in mossy fibers and glomeruli through immunocytochemical methods (Kan et al., 1978, 1980). Subsequent labeling studies have suggested that ChAT-positive mossy fibers may be largely restricted to cerebellar regions that receive vestibular input (Barmack et al., 1992). However, a role for ACh as a transmitter has not been supported by pharmacological or physiological studies, which have shown that while cholinergic antagonists fail to block mossy fiber evoked activity, glutamate blockers are effective, even in the vestibular-related areas of the cerebellum (Crepel and Dhanjal, 1982; Rossi et al., 1995).

DENDRITIC PROPERTIES

MICROELECTRODE RECORDINGS

That dendrites are capable of electroresponsive activity and are not simple, passive cables was first shown in Purkinje cells. The earliest recordings indicating that the dendrites are active were made from alligator cerebellum. Here, intradendritic recordings revealed large dendritic spikes in response to parallel fiber stimulation (Llinás and Nicholson, 1971). The injection of hyperpolarizing current allowed these spikes to be dissected into several all-or-none components. From these early studies, it was proposed that there are several "hot spots" in the dendrites that are capable of spike gen-

eration and that dendritic spikes travel toward the soma in a discontinuous manner. Subsequent intradendritic recordings from pigeon Purkinje cells showed that dendritic spikes are calcium dependent (Llinás and Hess, 1976). It was not until cerebellar slice preparation was used, however, that the dendritic properties of Purkinje cells were revealed in all their complexity.

The types of spontaneous action potentials that may be seen at different levels in a mammalian Purkinje cell soma and dendrites are illustrated for an *in vitro* experiment in Fig. 7.13. Typical bursts, consisting of fast sodium spikes and a terminal, slower rising calcium spike, are seen at the somatic level (Fig. 7.13B). Recordings obtained at different levels in the dendritic tree are shown in Fig. 7.13C–E. The decrease in amplitude of the fast spike that occurs as recordings are made farther from the soma indicates clearly that the fast sodium action potentials seen at the soma do not actively invade the dendrites. Rather, they are electrotonically conducted and can be detected only to about mid-dendritic level, their amplitude decrements rather quickly with distance from the soma.

The bursting calcium-dependent spike, on the other hand, is large and rather prominent in the upper dendrites, indicating a differential distribution for sodium and cal-

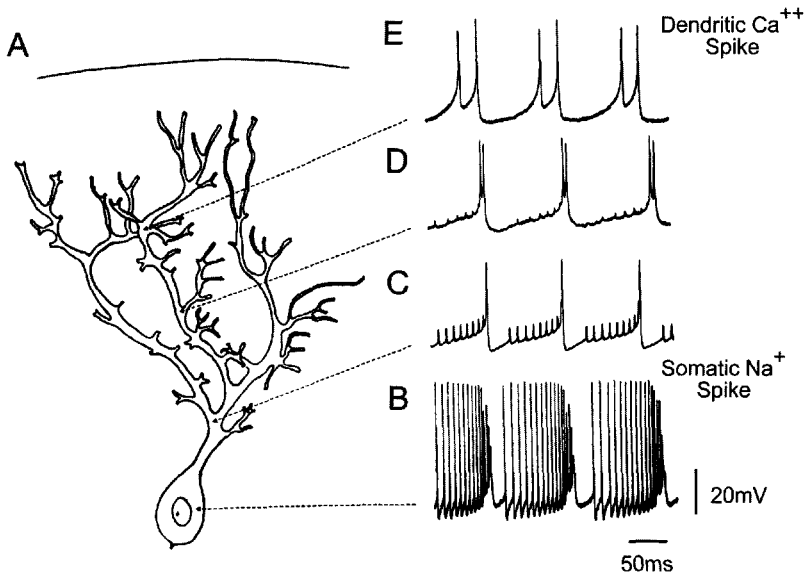


Fig. 7.13. Composite illustration of recordings made from different regions of a Purkinje cell *in vitro*. **A:** Drawing of typical mammalian Purkinje cell. **B:** Fast action potentials dominate this recording, with slower membrane oscillations. **C–E:** As the electrode moves away from the soma, (1) the amplitude of the fast, Na-dependent action potentials progressively decreases until they are not seen in the most distal branches; and (2) the slow, prolonged, Ca²⁺-dependent action potentials increase in amplitude and become distinct in the distal branches. Although the dendritic spikes are discontinuously propagated toward the soma, the somatic spikes do not actively invade the dendrites. [Modified from Llinás and Sugimori, 1980a, with permission.]

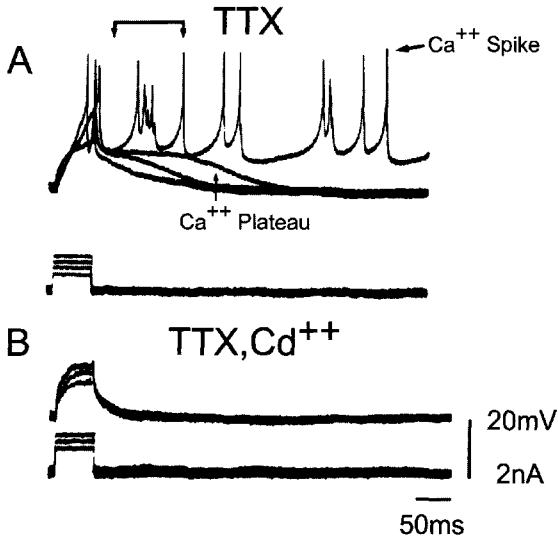


Fig. 7.14. Purkinje cell dendritic recording in the presence of TTX. Short depolarizing pulses elicit Ca-dependent plateau potentials and Ca²⁺ spikes. As the current amplitude is increased, the plateau responses increase in duration, and full spike bursts are generated. **B**: The calcium dependence of both the plateau and the spike bursts is demonstrated by their complete abolition after Cd²⁺ has been added to the TTX bathing solution.

cium conductances. Furthermore, direct stimulation of dendrites after the application of TTX, as shown in Fig. 7.14A, produces two types of calcium-dependent electroresponsiveness. A small stimulus can generate a plateau-like response and a burst of action potentials. Because both responses can be blocked by cobalt, cadmium, or D600 (see Fig. 7.14B), it must be concluded that the dendrites of the Purkinje cell are capable of generating calcium-dependent spikes, which may be of either a prolonged plateau form or clear, all-or-nothing action potentials.

The Purkinje cells thus demonstrate the following set of voltage-dependent ionic conductances. As discussed earlier, in the soma there are (1) a rapid, inactivating Hodgkin-Huxley sodium current that generates a fast spike; (2) a fast voltage-activated potassium current that generates the afterhyperpolarization following a fast spike; (3) a calcium-activated potassium conductance, and (4) a noninactivating, voltage-activated sodium conductance capable of generating repetitive firing of the Purkinje cell following prolonged depolarization. At the dendritic level, on the other hand, excitability seems to be due mainly to a voltage-activated calcium conductance increase. This conductance may generate a low plateau potential or calcium spikes (Fig. 7.14A), and the spikes may be followed by an increase in both voltage-activated and calcium-activated potassium conductances.

It is therefore clear that the complex electrical responses observed in these cells after direct stimulation or activation of climbing or parallel fibers are largely due to the electroresponsive properties of the Purkinje cells themselves.

OPTICAL RECORDING

Optical probes have been used to mark the spatial distribution of voltage-sensitive ionic channels in Purkinje cells. The sodium conductance is restricted to the soma and axon as visualized by using fluorescently labeled TTX (Sugimori et al., 1986).

Mapping of the distribution of an increase in intracellular calcium concentration ($[Ca^{2+}]_i$) during spontaneous and evoked Purkinje cell activity allows visualization of the probable location of calcium channels in the somatodendritic membrane. This has been done in experiments using Arsenazo III absorption (Ross and Werman, 1987) and Fura-2 as a calcium indicator. Experiments using the fluorescent Ca^{2+} indicator Fura-2 have shown that during spontaneous bursting, the $[Ca^{2+}]_i$ increases first in the fine dendritic branches, where the increase is also the largest (Tank et al., 1988). The $[Ca^{2+}]_i$ is later seen to increase in the dendritic trunk, and by this time it has begun to subside in the fine dendrites. The $[Ca^{2+}]_i$ in the soma increases very little. This temporal sequence of increased calcium activity, first in the distal and then in the proximal dendrites, supports the electrophysiological description of the two calcium conductances—the low-threshold plateau and all-or-none calcium-dependent dendritic spikes (see Fig. 7.13). The presence of voltage-activated calcium channels in the spiny branchlets provides a mechanism whereby parallel fiber EPSPs can be enhanced by slow local increases in calcium conductance. In contrast, when the synaptic activity is in the larger dendritic branches, full calcium-dependent dendritic spikes can be generated in the main dendritic tree. Climbing fiber synapses tend to depolarize the main dendritic tree, producing full dendritic spikes. If a cell loaded with Fura-2 is depolarized by somatic current injection, the increased $[Ca^{2+}]_i$ in the dendrites is not uniform. Rather, there are well-localized areas of marked increases, supporting the earlier hypothesis of “hot spots” of calcium influx (Llinás and Nicholson, 1971). Thus, the distribution of calcium channels over the dendritic tree is a critical element in the fine tuning of the electrophysiological sophistication of this most remarkable cell.

Unlike the climbing fiber input, which produces a widespread activation of the Purkinje cell dendritic tree, parallel fibers have the ability to excite small compartments of the dendritic tree. Given the complexity of its dendritic tree, the Purkinje cell has tremendous computational power when activated by the parallel fiber system. Indeed, the actual number of possible functional states will depend on the nature and, therefore, on the number of independent dendritic compartments activated. *In vitro* experiments with the calcium-sensitive dye Calcium Green have suggested that the smallest functional units of neuronal integration may in fact be the individual spines (Denk et al., 1995). Figure 7.15 shows an example of independent activation of single spines in a Purkinje cell following parallel fiber activation. The cell was filled with Calcium Green using a whole-cell patch electrode and imaged using two-photon fluorescence laser scanning microscopy. At low magnification the complete dendritic tree is shown (Fig. 7.15A), whereas at higher magnifications the individual spines of the spiny branchlets are clearly resolved (Fig. 7.15B–D). Trains of electrical microstimulation pulses applied to a restricted parallel fiber group evoked well-resolved EPSCs recorded at the soma by the patch electrode (Fig. 7.15E) and produced activation of individual dendritic spines, as measured by taking the difference in fluorescence intensity between the resting and stimulated conditions (Fig. 7.15F). Because there are approximately 10^7

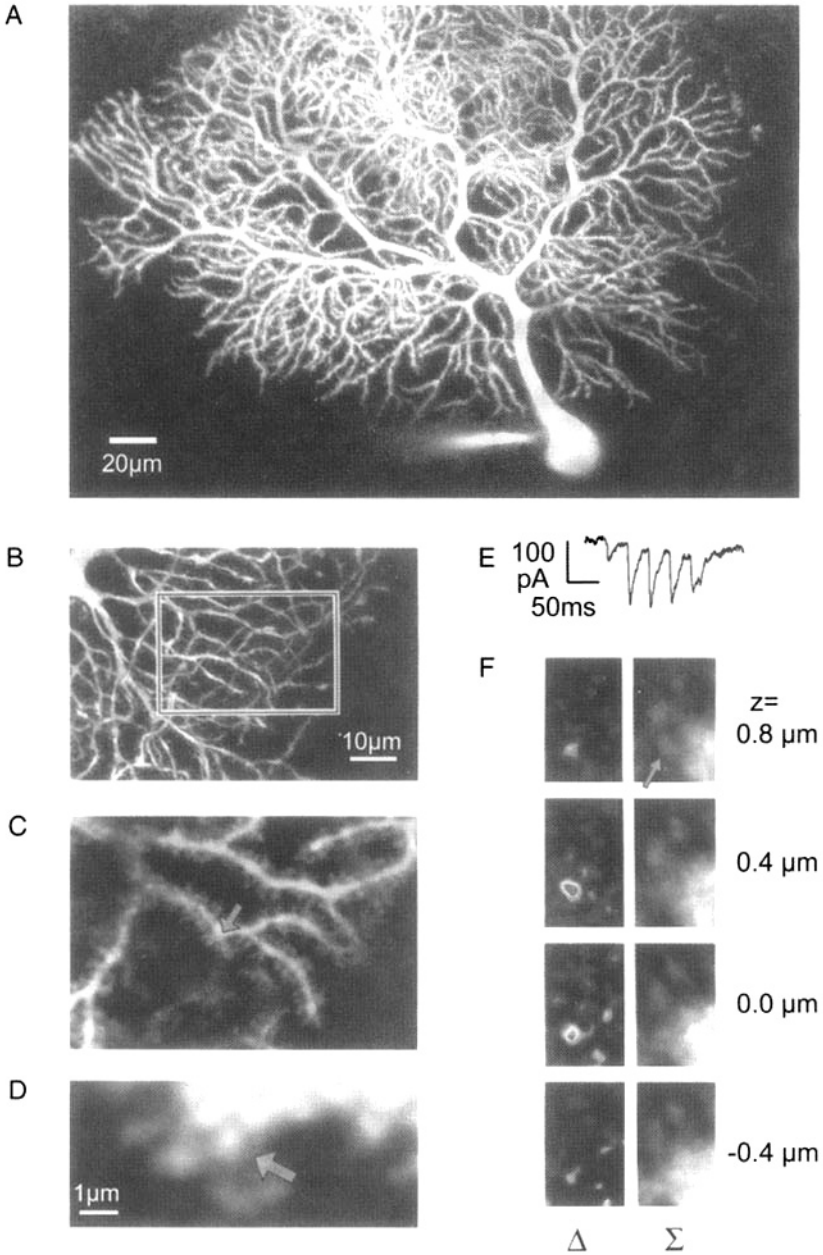


Fig. 7.15. Single spine activation via parallel fiber stimulation. After Calcium Green diffusion from the patch electrode, a complete Purkinje cell dendritic tree (A) is shown. Functional imaging was performed in a different cell, which is shown at three magnifications (B–D). Note that single spines are well resolved. A–D: Maximal value projections of a stack of optical sections. In (C) and (D), the spine activated in E is indicated by arrows. A train of low-amplitude parallel fiber stimuli generated small subthreshold synaptic currents (E) at the soma. In (F), difference images (stimulated minus resting; Δ) and the resting fluorescence level (Σ) taken at four different depths show the single spine calcium response produced by the parallel fiber stimuli. [Modified from Denk et al., 1995.]

Purkinje cells in humans, each of which has over 100,000 spines, the number of computational events implementable from a neuronal point of view for the output layer of the cerebellar cortex exceeds 10^{12} .

FUNCTIONAL CIRCUITS

We have seen that the climbing fiber and the mossy fiber–granule cell–parallel fiber pathways are the two main types of afferents to the cerebellum as a whole and to the Purkinje cells in particular. These afferent systems differ dramatically in their interactions with the Purkinje cells. For example, the Purkinje cell and its climbing fiber afferent have a one-to-one relationship, whereas the relationship between the Purkinje cell and the mossy fiber–parallel fiber system can be characterized as many-to-many. Moreover, the directionality of the parallel fibers imparts a mediolateral orientation to Purkinje cell activation by the mossy fiber–parallel fiber system, whereas the climbing fiber system, as we shall see, is organized to produce synchronous activation of specific groupings of Purkinje cells, groupings that often have a rostrocaudal orientation. Their electrophysiological and anatomical differences lead to distinct functional roles for these two systems, which we discuss later.

Let us first consider the climbing fiber system. As a result of the electrotonic coupling between inferior olivary neurons and the topography of the olivocerebellar projection, this system generates synchronous (on a millisecond time scale) complex spike activity in rostrocaudal bands of Purkinje cells (Fig. 7.16B). These bands are normally only about 250 μm wide in the mediolateral direction but can be several millimeters long in the rostrocaudal direction and may extend down the walls of the cerebellar folia and across several lobules (Sugihara et al., 1993; Yamamoto et al., 2001). It is important to realize that the banding structure shown in Fig. 7.16B is an average from a long (20-min) recording and that the moment-to-moment synchrony distribution is dynamically controlled by afferents to the inferior olive (Llinás, 1974). In fact, instead of providing the primary drive for activity in the olivocerebellar system, the major role of olivary afferents may be to determine the pattern of “effective” electronic coupling between olivary neurons and thereby the distribution of synchronous complex spike activity across the cerebellar cortex. This idea is supported by results showing that spontaneous climbing spike activity persists following the block of glutamatergic and GABAergic input to the inferior olive (Lang, 2001, 2002).

The role of GABAergic and glutamatergic olivary afferents in shaping the patterns of olivocerebellar synchrony has been investigated using multiple electrode recordings of complex spike activity (Llinás and Sasaki, 1989; Lang et al., 1996; Lang, 2001, 2002) and voltage-sensitive dye imaging of inferior olivary activity (Leznik et al., 2002). The effect of neurotransmitter release within olivary glomeruli was proposed to increase the conductance of the membrane adjacent to the gap junctions. This would shunt any current flowing between olivary cells, thus decoupling their activity (Llinás, 1974). Evidence supporting this hypothesis was obtained by making multiple electrode recordings of complex spike activity and comparing the patterns of synchrony before and after elimination of GABAergic activity in the inferior olive (Lang et al., 1996). GABAergic activity was blocked either with microinjections of picrotoxin into the inferior olive or by destroying the cerebellar nuclei, the source of the GABAergic pro-

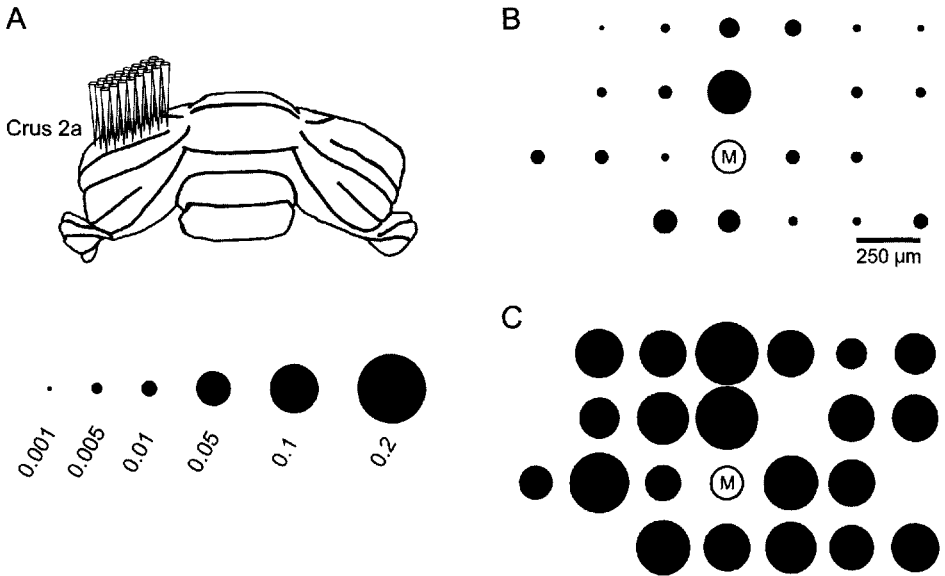


Fig. 7.16. Complex spike synchrony patterns revealed by multiple electrode recording. **A:** (Top) Schematic of rat cerebellum showing the placement of an array of microelectrodes on lobule crus 2a. Each electrode records the complex spikes from a single Purkinje cell. (Bottom) Synchrony scale for plots in **B** and **C**. **B:** Distribution of synchronous complex spike activity with respect to the activity of reference cell **M** under control conditions. Each circle represents the location of an electrode in the recording array, where left and right correspond to lateral and medial on crus 2a and top and bottom correspond to rostral and caudal. The area of a circle is proportional to the level of synchronous activity between the cell at that location and the selected reference cell **M**. Synchrony is defined as the normalized cross correlation coefficient at 0 ms time lag as calculated from the spike trains of the two cells using a time bin of 1 ms. Note how cells showing high levels of synchrony with cell **M** form a column or band that roughly runs from the top to the bottom of the plot (i.e., rostral to caudal). Scale bar indicates the spacing of the electrodes. **C:** Distribution of synchronous complex spike activity after a lesion the cerebellar nuclei and therefore loss of GABAergic activity within the inferior olive. Note the higher synchrony level compared with **B** and the more uniform distribution.

jection. Figure 7.16C shows the widespread distribution of synchronous complex spike activity that follows the loss of GABAergic input to the inferior olive. Note that the banding pattern seen under control conditions has been replaced by a uniform distribution. In contrast, it was shown that blocking glutamatergic input to the inferior olive actually accentuates the banding pattern (Lang, 2001). Thus, GABAergic and glutamatergic olivary afferents act in a complementary fashion to shape the exact pattern of synchronous complex spike activity across the cerebellum.

Optical recordings from *in vitro* inferior olivary slices treated with voltage-sensitive dyes have provided direct visualization of the GABAergic modulation of inferior olivary cell coupling. As shown in Fig. 7.17A, B (Control), an electrical stimulus delivered to the surrounding white matter results in coherent oscillatory activity in small, discrete clusters of inferior olivary neurons. This is presumably a result of electrotonic coupling via gap junctions. After the application of picrotoxin, an identical stimulus

generated a much stronger optical signal (Fig. 7.17A, B, Picrotoxin). This enhanced signal is not due to an increase in the responses of individual cells to the stimulus. Indeed, intracellular recordings show that the responses of individual cells before and after picrotoxin application are similar (Fig. 7.17C). Rather, the large increase in the dye signal reflects a more coherent population response, as a result of the greater efficacy of electrotonic coupling after blocking GABAergic synapses with picrotoxin. These examples show that pharmacological manipulations can dramatically alter the patterns of synchronous activity in the olivocerebellar system. Changes in synchrony patterns have also been demonstrated to be associated with movements made by animals performing a motor task (Welsh et al., 1995), which points to their significance for normal cerebellar function.

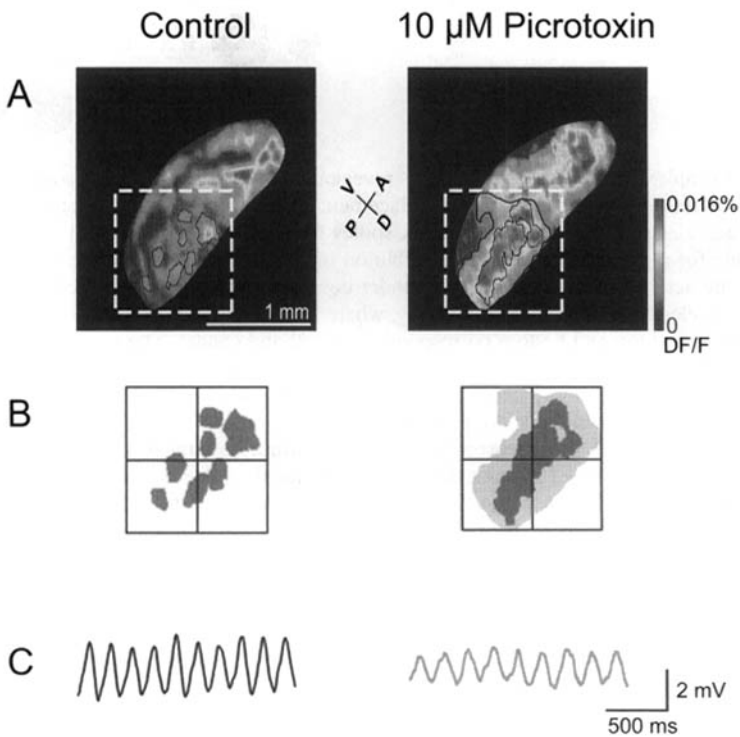


Fig. 7.17. Effects of picrotoxin on intracellularly and optically recorded oscillations in the inferior olive measured using a voltage-sensitive dye. **A:** A frame of imaged ensemble neuronal oscillating clusters in control conditions (left) and after addition of $20\ \mu\text{M}$ picrotoxin (right) to block GABAergic activity. In the control condition, several representative clusters in the bottom right of the inferior olive are outlined in black. The clusters were defined as areas with pixels above a selected threshold value (0.007%). After picrotoxin an additional threshold level (0.014%) was added to delineate the areas with the highest response. **B:** Higher magnification view of boxed areas in A. Note how picrotoxin significantly increased the size of the clusters by merging several smaller discrete areas into a continuous larger area. **C:** Intracellular recording from an inferior olivary neuron showing spontaneous subthreshold oscillations before (left) and after (right) bath application of $20\ \mu\text{M}$ picrotoxin. [Modified from Leznick et al., 2002.]

To understand more fully the functional significance of the olivocerebellar circuit, we must consider what effect this activity has on the cerebellar nuclear cells. This is the case because the ultimate role of the cortex is to help determine the firing of cerebellar nuclear cells. We consider this below and then finish by adding the mossy fiber–granule cell–parallel fiber circuitry to the picture.

The activity of the cerebellar nuclei is regulated in three ways: (1) by excitatory input from collaterals of the cerebellar afferent systems, (2) by inhibitory inputs from Purkinje cells activated over the mossy fiber pathways, and (3) by inputs from Purkinje cells activated by the climbing fiber system. The effect of these inputs on cerebellar nuclear cells is shown by the intracellular recording of the response of these neurons to white matter stimulation (Fig. 7.18, right). The stimulus activates a variety of axons that are running through the white matter (Fig. 7.18, left), and as a result the response of these cells has five parts as shown in the figure: (1) an initial EPSP due to antidromic activation of the mossy fiber collaterals to the nuclear cell (1 in Fig. 7.18); (2) an IPSP, which results from direct excitation of Purkinje axons projecting to the nuclear cell (2 in Fig. 7.18); and (3 and 4) a second EPSP–IPSP sequence (3 and 4 in Fig. 7.18) with a latency of 3–4.5 msec. The EPSP results from climbing fiber collateral activation of the cerebellar nuclear cells, and the IPSP is generated as a result of climbing fiber activation of Purkinje cells that in turn project onto the cerebellar nucleus. Finally, (5) the second IPSP is terminated by a rebound response, which is due to the intrinsic membrane properties of the cerebellar nuclear cells themselves

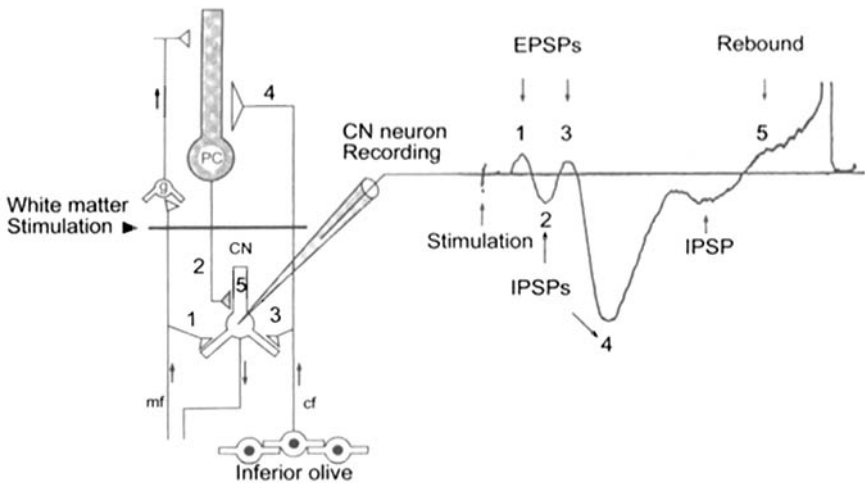


Fig. 7.18. Response of cerebellar nuclear cells to white matter stimulation. **A:** Drawing of elements activated after white matter stimulation. **B:** White matter stimulation activates mossy fibers, climbing fibers, and Purkinje cell (PC) axons. The first response (1), a graded EPSP, is due to activation of the mossy fiber collaterals; the second (2), a small IPSP, is due to direct stimulation of Purkinje cell axons. The third response (3), a graded EPSP, is due to activation of climbing fiber collaterals. Finally (4), the powerful IPSP and smaller IPSPs follow climbing fiber activation of Purkinje cells. Although the cell is at the resting potential, the hyperpolarization is often sufficient to elicit a rebound response in the cerebellar nuclear cell (5).

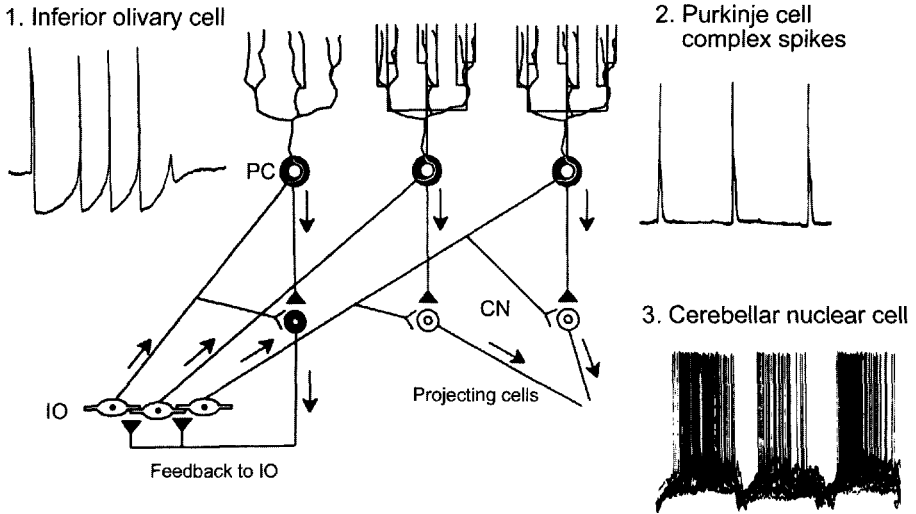


Fig. 7.19. Diagram of the circuit involved in the production of rhythmic activity in the olivocerebellar system. (1) Rhythmic activity in the inferior olivary neurons is transmitted to the Purkinje cells (PC), where it is transformed to complex spikes (2) to the cerebellar nuclear projecting cells (white somata) and inhibitory cells (filled soma) eliciting EPSPs. Complex spikes trigger high-frequency firing of Purkinje cell axons that impinge on the cerebellar nuclear cells with powerful IPSPs and rebound firing (3). Thus bursts of spikes are transmitted to the rest of the nervous system including the cerebellum (as mossy fibers). The cerebellar nuclear cells projecting to the inferior olive (IO) are inhibitory and synapse in the glomeruli. (Filled synaptic terminals are inhibitory, and open synaptic terminals are excitatory.)

(Fig. 7.18). Thus, the response in Fig. 7.18 is a combination of the properties of the synaptic circuit and the intrinsic properties of the Purkinje and cerebellar nuclear cells.

We can now consider the effect of synchronous olivocerebellar activity on the output of the cerebellar nuclei. In this regard, it is of particular interest that punctate and rather powerful synaptic EPSP-IPSP sequences are often followed by a rebound spike burst, as is seen in Fig. 7.18 (right), because this type of EPSP-IPSP sequence is likely to occur as a result of synchronous olivocerebellar activity. (Remember that there is a large convergence of Purkinje axons onto individual cerebellar nuclear cells.) This means that if a sufficient number of inferior olivary neurons, having a common rhythmicity, are activated synchronously, a large and equally synchronous activation of Purkinje cells will occur. This should in turn produce a large IPSP followed by a rebound burst response in the cerebellar nuclear cells. In fact, this is what occurs when harmaline, a tremorigenic agent known to act directly on the inferior olive (de Montigny and Lamarre, 1973; Llinás and Volkind, 1973; Llinás and Yarom, 1986), is administered. Harmaline activation of the inferior olive produces alternating inhibition and rebound activation in cerebellar nuclear cells (Fig. 7.19). This activity has been demonstrated *in vitro* and probably occurs *in vivo*, as indicated by the increased rhythmicity and synchrony of complex spike activity observed in multiple electrode recordings following systemic harmaline injection (Llinás, 1985; Llinás and Sasaki, 1989;

Yamamoto et al., 2001). The behavioral consequence of these synchronous bursts from the cerebellar nuclei is a phase-locked tremor.

In contrast to the punctate nature of cerebellar activation by the olivocerebellar system, the mossy fiber–parallel fiber system provides a continuous and very delicate regulation of the excitability of the cerebellar nuclei, brought about by the tonic activation of simple spikes in Purkinje cells, which ultimately generates the fine control of movement known as motor coordination. The fact that the mossy fibers inform the cerebellar cortex of both ascending and descending messages to and from the motor centers in the spinal cord and brainstem gives us an idea of the ultimate role of the mossy fiber system: it informs the cortex of the place and rate of movement of limbs and puts the motor intentions generated by the brain into the context of the status of the body at the time the movement is to be executed. Moreover, through its effects on the inhibitory GABAergic cerebellar nuclear cells, which project back to the inferior olive, it helps shape the pattern of coupling among olivary cells and hence the synchrony distribution in the upcoming olivocerebellar discharge.

This page intentionally left blank

THALAMUS

S. MURRAY SHERMAN AND R. W. GUILLERY

The thalamus is the largest part of the diencephalon, one of the major subdivisions of the brain. Each of these subdivisions of the brain—the *telencephalon*, *diencephalon*, *mesencephalon*, and *rhombencephalon*—forms around one of the major ventricular spaces, and each has a distinctive structure, determined at early developmental stages by regulatory genes that produce distinct patterns of regional specification (Rubenstein et al., 1994, 1998). The diencephalon itself is further subdivided into several distinct parts, which are the *epithalamus*, *dorsal thalamus*, *ventral thalamus*, *subthalamus*, and *hypothalamus*. In this chapter we are concerned with the dorsal thalamus, commonly, as in this chapter, referred to simply as the *thalamus*, and with a part of the ventral thalamus called the *thalamic reticular nucleus*. Each of these parts of the diencephalon develops a distinctive structure. Particularly for the dorsal thalamus, which is, as we shall see, divided into many different subdivisions, or “nuclei,” the common developmental origin has produced a common structural pattern, and this allows us to look at some parts and arrive at generalizations that to a great extent apply to all of the parts.

The dorsal and the ventral thalamus are the two parts of the diencephalon that play a role in transmitting the messages going to the neocortex from the periphery and from the rest of the brain, and it is the organization of the connections with the neocortex that forms the focus of this chapter. There are other pathways that connect parts of the thalamus with the striatum (see Chap. 9) and with the amygdaloid complex (LeDoux et al., 1985), concerned with movement control and affective responses, respectively, but these are not considered further here.

The thalamus provides the major route for afferents to the neocortex (Jones, 1985; Sherman and Guillery, 2001). Essentially no messages can reach the neocortex without first passing through the thalamus. Messages from many different sources pass through the thalamus on the way to the neocortex, including messages from peripheral sense organs (such as vision, hearing, touch, temperature, pain, taste, olfaction), other regions of the brain (such as the cerebellum and the mamillary bodies), and the neocortex itself. In general, each functionally distinct group of messages passes through a distinct part of the thalamus, identifiable as a well defined cell group or thalamic “nucleus.” One finds the same arrangement of inputs, outputs, and synaptic relationships in each of these nuclei, although, as we shall see, there are some differences in the details. We will treat the visual relay in the lateral geniculate nucleus as a prototype of

thalamic nuclei. We know that many features demonstrable in the lateral geniculate nucleus are also seen in other nuclei, and the amount of information about the functional organization of the lateral geniculate nucleus is significantly more detailed than that for any other thalamic nucleus.

THE GENERAL ORGANIZATION OF THE THALAMUS

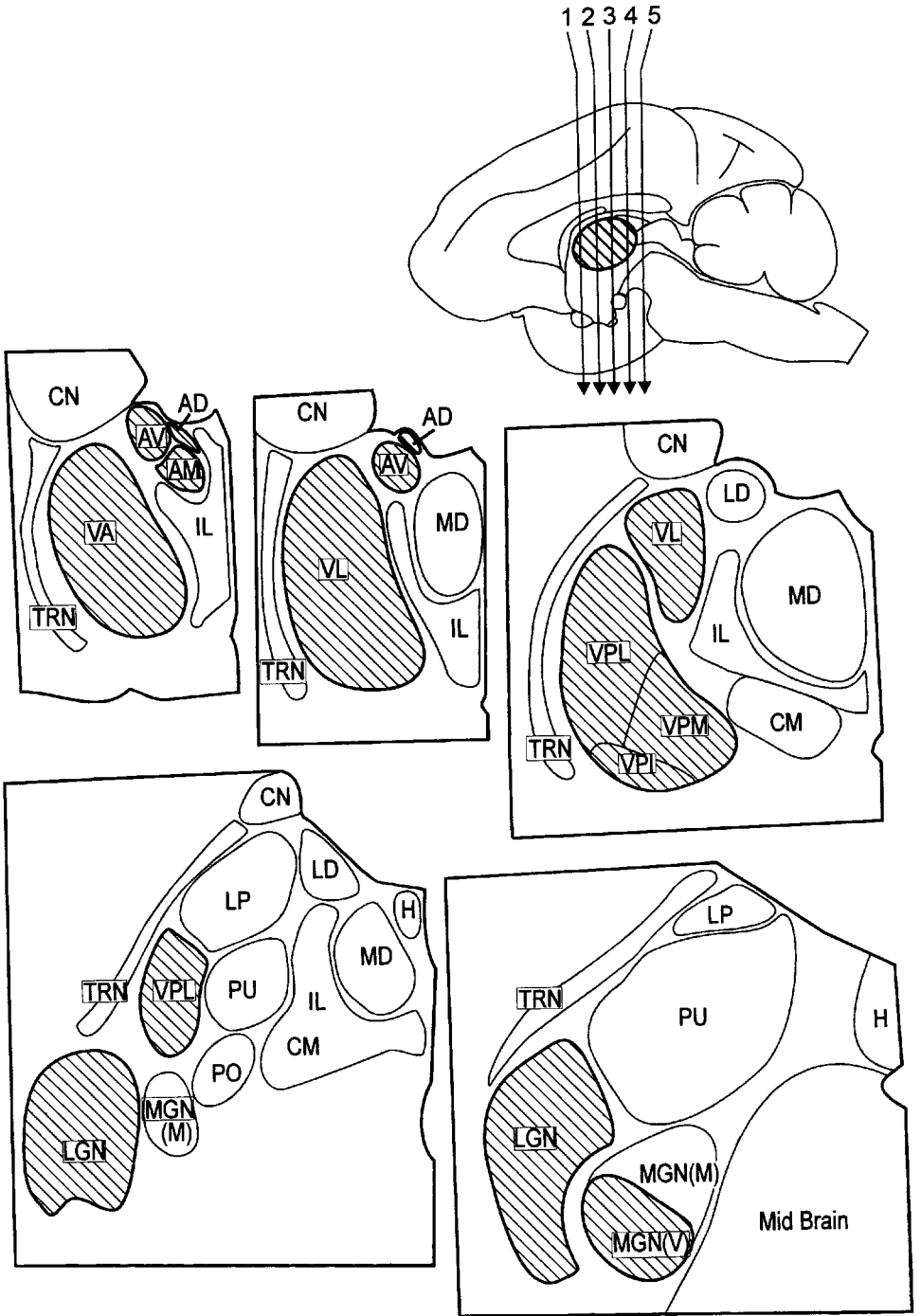
THE MAJOR THALAMIC NUCLEAR GROUPS

The major thalamic nuclear groups of a primate like the macaque monkey are shown schematically in Fig. 8.1.

Two functionally distinct types of nucleus are shown. The first, shown shaded, contain *first order relays* to the cerebral cortex. These carry messages from the periphery or from lower brain centers to the neocortex. They are the thalamic nuclei about which we know the most, but they represent less than one-half of the volume of the thalamus in a primate brain. In order, from rostral to caudal levels, these are as follows: the *anterior thalamic nuclei*, which receive afferents from the mamillary bodies and from the postcommissural fornix and send efferents to the cingulate and retrosplenial cortex; the *ventral anterior and ventral lateral thalamic nuclei*, which receive afferents from the deep cerebellar nuclei and send efferents to the motor and premotor cortex; the *ventral posterior thalamic nuclei*, which have an inferior, a lateral, and a medial part and receive afferents from the medial lemniscus, concerned with limb position, tactile, and deep pressure receptors, and from the anterolateral pathways, concerned with thermal and nociceptive afferents from all parts of the body; the *ventral part of the medial geniculate nucleus*, which receives auditory afferents from the inferior colliculus and sends efferents to the auditory cortex; and the *lateral geniculate nucleus*, which receives afferents from the retina and sends efferents to the visual cortex.

The nuclei that are unshaded in Fig. 8.1 all represent nuclei that contain *higher order relays*; that is, they all receive incoming messages from the cortex itself and relay these messages from one cortical area to another. These nuclei include the *mediodorsal nucleus*, which, in addition to inputs from olfactory cortex and from the amygdaloid complex, receives afferents from frontal cortex and sends efferents to the frontal cortex, linking one part of frontal cortex to another; the *laterodorsal nucleus*, which probably receives afferents from cingulate cortex and sends efferents back to cingulate

Fig. 8.1. Schematic view of five sections (1 at top left through 5 at bottom right) through monkey thalamus cut in the coronal planes indicated by the numbered arrows in the upper midsagittal view of a right hemisphere. The major thalamic nuclei for a generalized primate are shown. The nuclei outlined by a heavier line and filled by hatching are largely or entirely first order relays, receiving their driving afferents from ascending pathways. The other nuclei are primarily or entirely higher order relays (further details in text), receiving many or all of their driving afferents from layer 5 cells of neocortex. Abbreviations: AD, anterodorsal nucleus; AM, anteromedial nucleus; AV, anteroventral nucleus; CM, centre median nucleus; CN, caudate nucleus; H, habenular nucleus; IL, intralaminar (and midline) nuclei; LD, lateral dorsal nucleus; LGN, lateral geniculate nucleus; MGN(M) and MGN(V), magnocellular and ventral divisions, respectively, of medial geniculate nucleus; PO, posterior nucleus; PU, pulvinar; TRN, thalamic reticular nucleus; VA, ventral anterior nucleus; VL, ventral lateral nucleus; VPI, VPL, VPM, inferior, lateral, and medial parts of the ventral posterior nucleus. [From Sherman and Guillery, 2001.]



cortex, again serving to link one cortical area to another; the *pulvinar region* (we use this term to include the lateral posterior nucleus and the pulvinar in the cat), which serves to link cortical areas of occipital and temporal lobes, and the *intralaminar nuclei*, which represent a mixed group of cells, with some receiving ascending afferents from the anterolateral system (and thus first order) and others receiving afferents from motor cortex and sending their axons to cortex and also to the striatum.

THE MAJOR TYPES OF AFFERENT TO A THALAMIC NUCLEUS

In later parts of this chapter (in Drivers and Modulators), we provide functional and morphological details that distinguish afferents that are *drivers* from those that are *modulators* (for details, see Sherman and Guillery, 1998, 2001). The significance of this distinction can be illustrated for the visual relay in the lateral geniculate nucleus. Here we find that fewer than 10% of the synapses on the *relay cells* (the cells concerned with sending messages on to the visual cortex) are formed by axons that come from the retina. The other 90% of the synapses come from visual cortex, from the brainstem, from cells in the thalamic reticular nucleus, and from local, geniculate interneurons. It is clear for this relay that the crucial information conveyed to the visual cortex is the visual information that comes from the retina. Because the lateral geniculate nucleus is demonstrably concerned with transmitting visual information, we can recognize that the retinal afferents must be the drivers. The characteristic response properties of these thalamic cells are lost following loss or silencing of the drivers. Comparable arguments allow us to recognize the lemniscal and anterolateral afferents as the drivers for the ventral posterior nucleus and the afferents from the inferior colliculus as the drivers for the medial geniculate nucleus. The axons that represent these drivers are all similar in their light and electron microscopic appearance, and all establish similar synaptic patterns in the thalamus and share certain functional properties; these patterns are distinct from those formed by all of the other afferents, which are all regarded as modulators (see details in Drivers and Modulators). Silencing a driver to a nucleus abolishes the characteristic receptive field properties of the cells in that nucleus. The modulators, in contrast to the drivers, do not bring the characteristic receptive field properties to a nucleus but, instead, modify the nature of the transmission to the cortex. The degree to which the modulators outnumber the drivers is surprising at first sight but can probably be seen as representing the complexity of the modulation that is possible at the thalamic relay, a complexity that is only partially understood at present.

For nuclei other than the medial and lateral geniculate nuclei and the ventral posterior nucleus, it is less easy to identify the drivers on purely functional grounds. However, we know that the mamillothalamic afferents to the anterior thalamic nuclei and the cerebellar afferents to the ventral anterior and ventral lateral nuclei also closely resemble, in their structure and in their synaptic relationships (see below in The Electron Microscopic Appearance of the Neuronal Elements), the identifiable drivers. Therefore, we regard them as the drivers of these first order nuclei. Similarly, the nuclei shown in Fig. 8.1 as containing higher order relays receive afferents from layer 5 of cortex that resemble the known visual, auditory, and somatosensory drivers (see details in First Order and Higher Order Relays). Whereas the cortex sends modulatory afferents from cells in cortical layer 6 to every thalamic nucleus, only the higher order

relays receive the functionally and morphologically characteristic drivers from cortical layer 5. For some of these higher order drivers, coming from somatosensory or visual cortex, we know that they must be drivers because, when they are silenced, the relevant higher order thalamic relay loses its receptive field properties (Bender, 1983; Chalupa, 1991; Diamond et al., 1992); for others, the critical functional evidence is not available but the morphological relationships provide a strong clue that they, indeed, are drivers (Mathers, 1972; Schwartz et al., 1991).

It has to be stressed that, for many thalamic nuclei, defining the specific properties of the drivers for that nucleus is yet not possible. This is true for many higher order relays and is also true for the cells of the intralaminar nuclei and for the cells that receive cerebellar (and pallidal) afferents. For the anterior thalamic nuclei, there is evidence that they receive messages concerned with head direction in space and with spatial maps from the mamillary bodies (Taube, 1995; Van Groen et al., 2002).

PARALLEL PROCESSING

For the visual and somatosensory pathways, there are functionally distinct parallel driver pathways running through, respectively, the lateral geniculate nucleus and the ventral posterior nucleus. For instance, the retinal ganglion cells that innervate the lateral geniculate nucleus fall into several distinct morphological and functional classes that provide parallel streams with minimal interaction through thalamus to cortex (Sherman, 1985). Thus, each of these ganglion cell classes innervates a unique relay cell class in the lateral geniculate nucleus. In the cat, these retino-geniculo-cortical streams are known as the W, X, and Y pathways, and a comparable set of koniocellular (K), parvocellular (P), and magnocellular (M) pathways exists in the monkey (see Chap. 6 for a fuller account of these and other retinal ganglion cell classes; see also Sherman and Spear, 1982; Rodieck and Brening, 1983; Stone, 1983; Shapley and Lennie, 1985; Sherman, 1985). There is evidence that the somatosensory first order relay is also involved in analogous parallel processing in the sense that each submodality or receptor type is represented by parallel neuronal streams through thalamus (Dykes, 1983). The important point is that in each relay, these parallel pathways show little or no interaction with each other. This may represent an important aspect of thalamic function generally. That is, functionally distinct driver pathways, even where they are intimately intermingled in a thalamic nucleus or a subdivision of a thalamic nucleus, may show no sign of integrative interactions. Although we have little relevant evidence for other thalamic relays, the shared common organizational plan seen throughout the thalamus suggests that this may prove to be a general rule. Certainly, as a general proposition about the thalamus, the hypothesis that there are no significant interactions between driver afferents in the thalamus bears serious consideration and experimental study.

MAPS IN THE THALAMUS

It is well established that the drivers concerned with visual, somatosensory, and auditory afferents are mapped. That is, within each of these first order relays, the relevant sensory surface is mapped. Correspondingly, the thalamocortical outputs from these relays are also mapped, so that for the visual pathways one can recognize a map of the retina (or of the visual field) in the lateral geniculate nucleus and also in the visual cortex that receives the geniculate input. The fact that there are maps in the thalamus looks

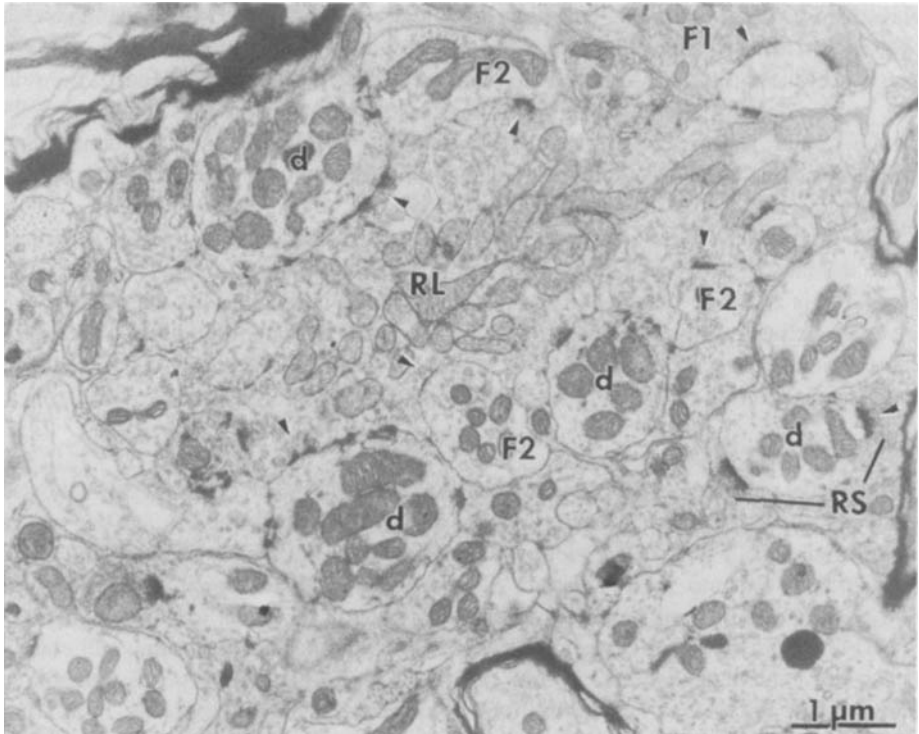


Fig. 8.2. Electron micrograph of a glomerulus from the A layers of the lateral geniculate nucleus of a cat with a centrally located RL terminal. Some of the synaptic junctions are identified by arrowheads. The major types of axon terminal are present and labeled F1, F2, RL, and RS (see text); "d" identifies some of the dendritic profiles (see Fig. 8.3). [From Sherman and Guillery, 2001.]

like another general principle that can be applied to all thalamic nuclei, because there is good evidence for an orderly pattern of organization between the thalamus and the cortex for most thalamic nuclei (Cowan and Powell, 1954; Frost and Caviness, 1980). However, for many of the thalamic nuclei we have no clear idea of what functional feature is mapped. This may prove to be an important point for future studies. For example, in the higher order relays concerned with vision (the pulvinar region), it is possible to define maps of the visual field, but they are less precise than the maps in the lateral geniculate nucleus, and as the connections are traced further beyond the first order geniculocortical relay, so the maps become less well defined. It is likely that the thalamocortical connections may then be concerned with mapping some other functional features, but at the present we have no evidence about the nature of these features.

NEURONAL ELEMENTS OF THE THALAMUS

The neuronal elements of the thalamus can be divided into three components: the extrinsic afferent inputs to the relay nuclei, the relay cells (or principal neurons) that proj-

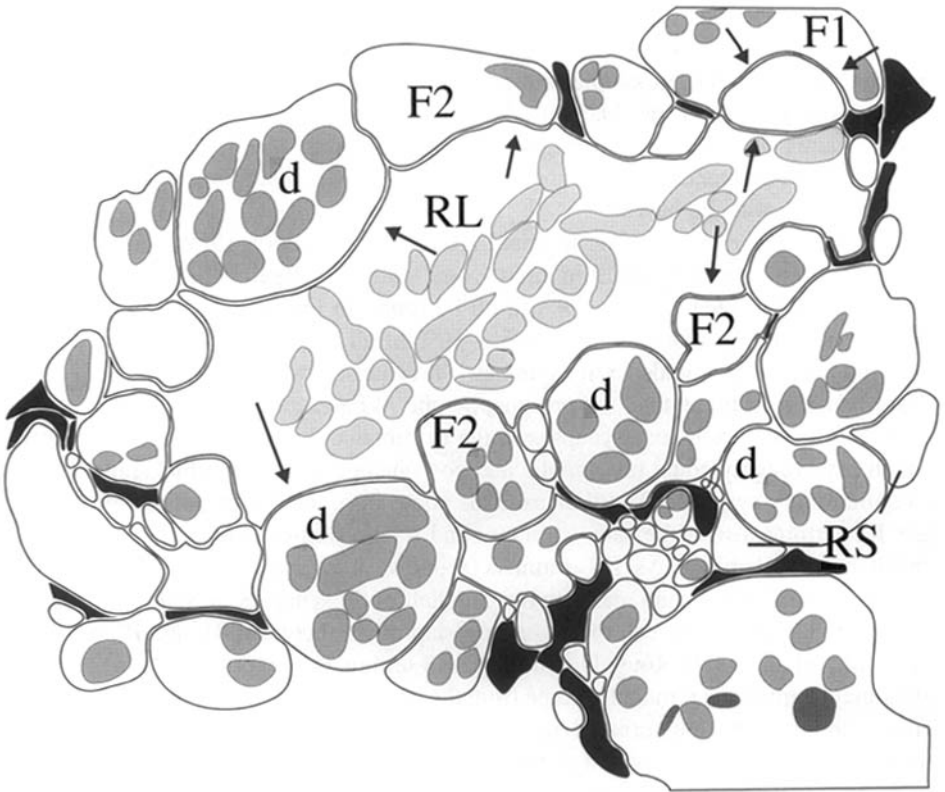


Fig. 8.3. Schematic interpretation of the major profiles shown in Fig. 8.2. [From Sherman and Guillery, 2001.]

ect to cortex (or other parts of the telencephalon; see earlier), and the interneurons (or intrinsic neurons). These structures have all been identified with light microscopic studies, and their synaptic relationships have been defined on the basis of electron microscopic studies that have over many years been closely related to studies involving the selective degeneration or labeling of specific axonal groups. Details can be found for a number of thalamic relays: the lateral geniculate nucleus (Guillery, 1969a,b; Wilson et al., 1984; Hamos et al., 1985; Jones, 1985; Montero, 1987), the ventral posterior nucleus (Jones and Powell, 1969; Ralston, 1969), the medial geniculate nucleus (Jones and Rockel, 1971; Morest, 1975), the ventral lateral nucleus (Harding, 1973; Ilinsky and Kultas-Ilinsky, 1990), the pulvinar region (Feig and Harting, 1998; Patel et al., 1999; Carden and Bickford, 2002; Wang et al., 2002a), and the anterior thalamic nuclei (Somogyi et al., 1978).

THE ELECTRON MICROSCOPIC APPEARANCE OF THE NEURONAL ELEMENTS

Figures 8.2 and 8.3 show the profiles that can be seen in an electron microscopic section through the lateral geniculate nucleus of the cat. The organization that is seen here is characteristic of most of the thalamic nuclei of most species. Because most of the

thalamic nuclei of the rat and mouse contain very few or no interneurons (see also Interneurons), the thalamus of these species is unusual and the relationships between the profiles are somewhat simpler but apart from that one can expect to see the same structures anywhere in the thalamus. Identifying these structures and understanding their synaptic relationships are important for the sections that follow, because these represent the fundamental connectional patterns upon which our understanding of thalamic function must be based.

Four major types of synaptic terminal are present (Guillery, 1969a), and their origins have been defined by electron microscopic studies of degenerating or labeled thalamic neuronal elements. Examples can all be found in Fig. 8.2. *RL* terminals (round vesicles and large profiles) contribute 5%–10% of all synaptic contacts (Van Horn et al., 2001). These terminals form asymmetrical synapses, with more thickening of the postsynaptic membrane than the presynaptic one. Whereas asymmetrical synapses are a feature of most excitatory synapses in the mammalian brain, symmetrical synapses, which have roughly equal presynaptic and postsynaptic membrane thickenings, typify most inhibitory synapses. The *RL* terminals come from the retina and are glutamatergic. *RL* terminals with the same structure and relationships are also the driver terminals in other thalamic relays. *RS* terminals (round vesicles and small profiles) also form asymmetrical synapses and make up roughly half of all synapses present. In the lateral geniculate nucleus of the cat, there is no overlap in size between *RL* and *RS* terminals (Van Horn et al., 2000). Roughly half of the *RS* terminals are corticothalamic and they are glutamatergic; the remainder come from the brainstem. Most of the latter are cholinergic, although some are noradrenergic or serotonergic. *F* terminals (flattened vesicles) form symmetrical synapses and make roughly one quarter of the synaptic contacts; these are GABAergic. Two subtypes, *F1* and *F2*, have been recognized. Although a constellation of features can distinguish them, the most salient are that *F1* terminals are axonal and are strictly presynaptic, whereas *F2* terminals are dendritic in origin and are both presynaptic and postsynaptic. *F1* terminals arise from axons of reticular cells, interneurons, and, in the lateral geniculate nucleus, axons of cells of the nucleus of the optic tract; *F2* terminals are the dendritic processes of interneurons.

An overview (Erişir et al., 1997b; Van Horn et al., 2000) shows that the *RL* terminals form only 5%–10% of the synaptic profiles onto relay cells in the lateral geniculate nucleus, which is often seen as a surprisingly low number for driver inputs; for the remaining modulatory synaptic inputs to relay cells, roughly one-third come from local GABAergic sources (*F1* and *F2* terminals), one-third come from layer 6 of cortex (*RS* terminals), and one-third come from brainstem (*RS* terminals).

Dendrites of relay cells are postsynaptic to all of these terminals, and dendrites of interneurons are postsynaptic to all of these terminals except for *F2* terminals. The *F2* terminals are postsynaptic to *RL* terminals or *RS* terminals from brainstem; *F1* terminals are also occasionally presynaptic to *F2* terminals. The glomeruli, illustrated in Figs. 8.2 and 8.3 and described in more detail later, contain *RL* (driver) terminals, *F* terminals (both *F1* and *F2*), and *RS* terminals from brainstem. Cortical *RS* terminals rarely, if ever, innervate glomeruli.

One feature seen in Figs. 8.2 and 8.3, which is rare in most parts of the brain but is commonly seen where many thalamic synapses are closely interrelated, is that there is

little or no astrocytic cytoplasm between the synaptic profiles. Such regions have been called *glomeruli*. A glomerulus is a complex synaptic structure (see also Fig. 8.4), where interneuronal dendrites relate to driver terminals, relay cell dendrites, and other processes. As shown in Figs. 8.2, 8.3, and 8.4, the astrocytic processes tend to form around the glomeruli; their absence from among the synapses in the glomeruli suggests that here the functional relationships between synapses and astrocytes, which commonly involve transport of potassium ions and transmitter uptake mechanisms, are weak or absent. A comparable situation in the cerebellar glomeruli, which also lack astrocytic cytoplasm, has been studied in greater detail than have the thalamic glomeruli (see DiGregorio et al., 2002). The rat's ventral posterior lateral nucleus, which lacks interneurons (see Interneurons, earlier), also lacks glomeruli (Ralston, 1983), demonstrating that the typical glomerular structure depends on interneurons.

The retinal or driver terminal usually contacts several F2 terminals within a glomerulus, and these interneuronal F2 terminals in turn are presynaptic at symmetrical contacts to the *same* relay cell dendritic appendage or shaft that is contacted by the retinal terminal. Because three terminal types are involved, this special neuronal circuit within the glomerulus is known as a *triad* (for a detailed hypothesis concerning the role of

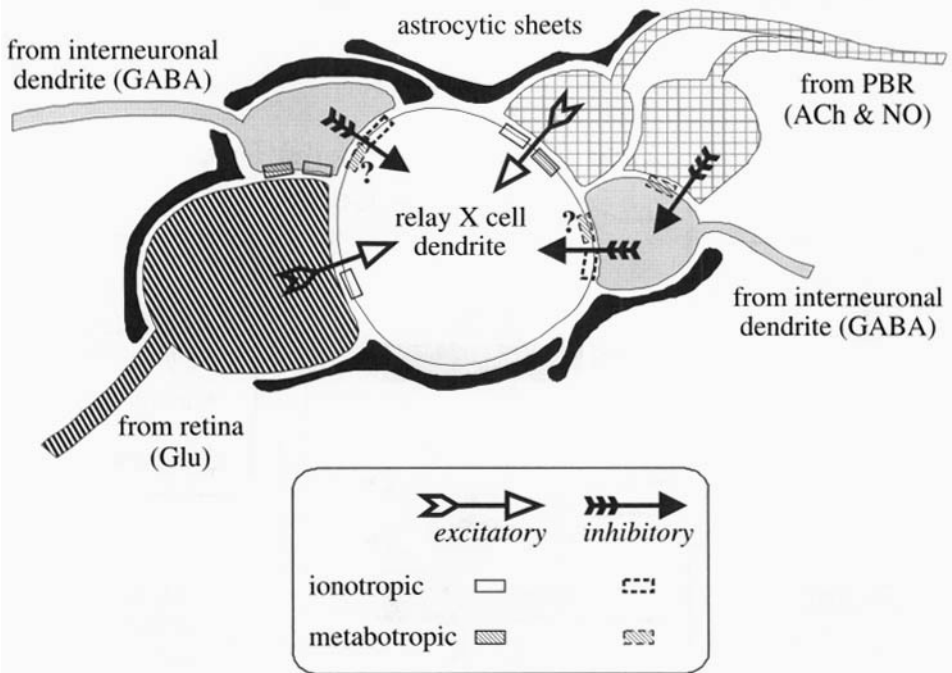


Fig. 8.4. Schematic view of a small glomerulus showing synaptic triadic arrangements. Arrows indicate direction of synaptic function, pointing from presynaptic to postsynaptic elements. The question marks postsynaptic to the dendritic terminals of interneurons indicate that it is not clear whether metabotropic ($GABA_B$) receptors exist there. Abbreviation: PBR, parabrachial region.

these triadic circuits, see Koch, 1985); because the extrinsic input to this complex is retinal, this is called a *retinal triad*. A triad involving RL and F2 terminals and a dendritic appendage of a relay X cell is shown (see Fig. 8.8). A slightly different form of triad is the *parabrachial triad*. This involves two terminals from one parabrachial axon: one of the parabrachial terminals contacts an interneuronal dendritic terminal, and the other contacts a relay cell dendrite, with the dendritic terminal contacting the same relay cell dendrite (see Figs. 8.2 to 8.4).

INPUTS

Figure 8.5 schematically illustrates the major afferents for a typical dorsal thalamic nucleus. As indicated earlier, we can divide the inputs into two broad classes: driving and modulatory. The driving input represents the primary information to be relayed to cortex, such as retinal input to the lateral geniculate nucleus or cortical layer 5 input to a higher order relay. All of the other inputs are modulatory, and these serve to modulate or control the relay of information from the driving input to cortex. Modulatory inputs come from several different sources. Local inhibitory inputs come from interneurons and from cells in the thalamic reticular nucleus. Other modulatory inputs also come from layer 6 of cortex and from the brainstem. In addition to these, some other, potentially modulatory, inputs to some particular thalamic relays also exist, such as inputs from the tuberomammillary nucleus of the hypothalamus to the lateral geniculate nucleus and pulvinar region (Manning et al., 1996), from the pretectum to the lateral

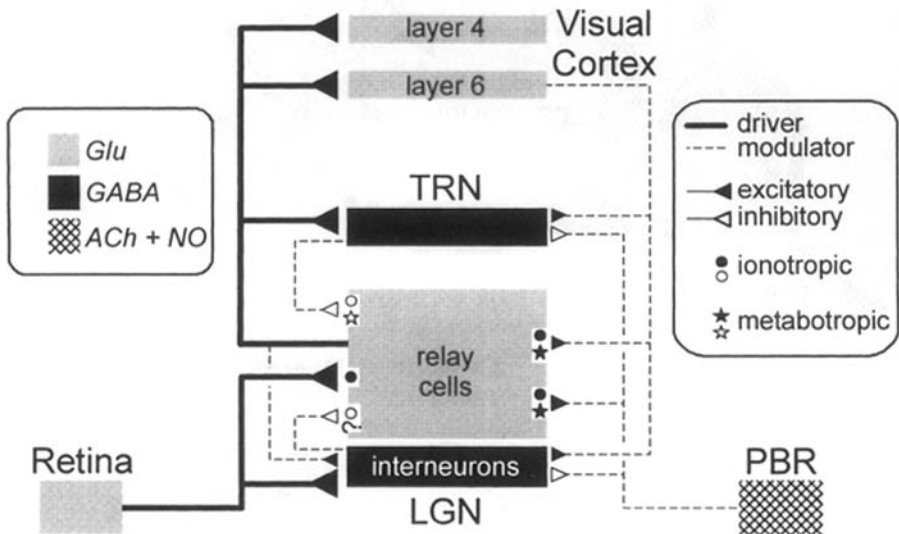


Fig. 8.5. Schematic view of details of the main connections of the lateral geniculate nucleus. Indicated are the inhibitory or excitatory nature of the synapses, the postsynaptic receptors activated by each input on relay cells, and the neurotransmitters involved. Abbreviations: LGN, lateral geniculate nucleus; PBR, parabrachial region; TRN, thalamic reticular nucleus.

geniculate nucleus (Cucchiari et al., 1991a), and from the basal ganglia to the ventral anterior nucleus (Ilinsky et al., 1997). Seen in this perspective, driving afferents to relay cells are one class among several and, in terms of number of synapses formed on relay cells, are a minority input (Guillery, 1969a,b; Liu et al., 1995; Van Horn et al., 2000).

Driving Afferents. The driving input from the retina to the lateral geniculate nucleus is the best characterized input to a dorsal thalamic nucleus. This input comes from the ganglion cells of the retina, whose axons travel in the *optic nerve* and *tract* to the lateral geniculate nucleus and also go to the superior colliculus, pretectum, and ventral lateral geniculate nucleus. The geniculate input is glutamatergic (Salt, 1988; Scharfman et al., 1990; Kwon et al., 1991). Comparable driving inputs to the ventral posterior and medial geniculate nuclei come from the *medial lemniscus* and inferior colliculus, respectively. We have seen that these afferents have a characteristic fine structural appearance and synaptic organization. Light microscopically, they are also readily identifiable, regardless of whether they are ascending afferents to a first order relay or axons from cortical layer 5 going to a higher order nucleus. The structural distinction between the drivers and the corticothalamic modulators that come from layer 6 is always clear in all thalamic nuclei, and this is illustrated in Fig. 8.6.

Cortical Afferents. There are a great many corticothalamic afferents that arise from pyramidal cells in layer 6 of all cortical areas, and all thalamic nuclei receive such axons. For the visual pathways, there is at least an order of magnitude more corticothalamic axons than thalamocortical ones (Sherman and Koch, 1986). For the lateral geniculate nucleus and for all of the first order relays, all of the cortical afferents come from layer 6. Cortical afferents to higher order relays from layer 5 are considered separately. Each cortical axon innervates many thalamic neurons, thereby establishing considerable divergence and convergence in the corticothalamic pathway. Like retinal (or other driving) axons, these cortical axons from layer 6 are excitatory and appear to be glutamatergic (Giuffrida and Rustioni, 1988; McCormick and Von Krosigk, 1992; Montero, 1994). Strong reciprocity exists in thalamocortical connections, because the cortical input for each thalamic nucleus generally, but not always, originates from the same cortical area that is innervated by the thalamic nucleus in question. Thus, for the lateral geniculate nucleus, this cortical pathway comes from visual cortex (mostly areas 17, 18, and 19), and likewise, somatosensory and auditory cortex project back, respectively, to the ventral posterior lateral and medial geniculate nuclei.

One implication of this reciprocity is that the corticothalamic pathway faithfully adheres to the map established in the thalamic nucleus. For instance, the corticogeniculate pathway conforms to the retinotopic map in the lateral geniculate nucleus. However, there is some question as to the extent to which the maps match at the cellular level. This is based on evidence that, in the cat (Murphy and Sillito, 1996), the spread of an individual corticogeniculate axon arbor can be quite extensive, reaching well beyond the region within which receptive fields that match those of the cortical axon can be recorded. The corticogeniculate terminals have a maximal extent of 1.5 mm compared with the spread of a typical retinogeniculate arbor of only about 0.2–0.4 mm (Bowling and Michael, 1984; Sur et al., 1987). The retinogeniculate arbor's expanse roughly

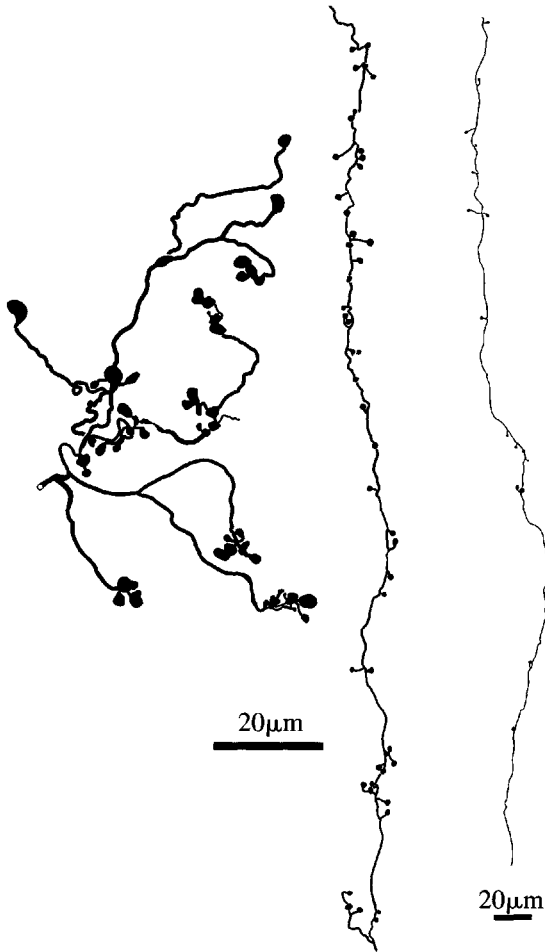


Fig. 8.6. Tracings of partial terminal arbors of three corticothalamic axons in the pulvinar region labeled by biotinylated dextran amine. The axon on the left, a type 2 axon (Guillery, 1966), displays driver morphology from cortical layer 5, and the two on the right, type 1 axons (Guillery, 1966), display modulator morphology from layer 6. [From Sherman and Guillery, 2001.]

corresponds to the size of a geniculate receptive field, implying that the corticogeniculate axonal arbor can contribute to subtle effects on relay responses beyond the “classic” receptive field. However, the majority of the corticothalamic terminals lie in a central core that roughly corresponds to the classical receptive field.

In visual cortex, only a subset of pyramidal cells in layer 6 actually sends axons into the corticothalamic pathway, with the remainder either innervating the claustrum or not projecting out of cortex, and the corticothalamic cells tend to be located in the top half of layer 6 (Lund et al., 1975; Katz, 1987; Usrey and Fitzpatrick, 1996). These layer 6 corticothalamic cells also project into that part of layer 4 that is supplied by geniculocortical input (Lund et al., 1975), implying that these layer 6 cells not only modulate the relay of information through the lateral geniculate nucleus but may also modulate

the flow of geniculate input into cortex. This layer 6 projection to layer 4, unlike some other intrinsic cortical circuits, is very limited in horizontal extent (Katz, 1987), thereby limiting the retinotopic spread of effect.

Finally, corticothalamic neurons are heterogeneous and probably represent several functional classes identifiable on the basis of axonal conduction velocities and receptive field properties (Tsumoto and Suda, 1980) or on the basis of their dendritic and intracortical axonal arbors (Katz, 1987). For somatosensory cortex of the rat, Zhang and Deschênes (1997) have distinguished corticothalamic cells that project to a first order nucleus (ventral posterior) from those that project to a higher order relay (the posterior group). They differ in their intracortical axonal and dendritic arbors; the former lie in the more superficial parts of layer 6, and the latter, in the deeper parts. It is not clear exactly how the several different cell types relate to the relay functions of the thalamus, but it is important to stress that the variety of these cortical cells suggests a corresponding variety of modulatory functions in the thalamus that are still largely unexplored.

Inputs From the Thalamic Reticular Nucleus. Other inputs to each dorsal thalamic nucleus come from the thalamic reticular nucleus (Ohara and Lieberman, 1985; Jones, 1985; Cox et al., 1996; Sherman and Guillery, 2001). This nucleus forms a thin shell of cells lateral to the dorsal thalamus (lying in the path of the thalamocortical and corticothalamic axons; see Fig. 8.1). Generally, functionally related groups of dorsal thalamic nuclei (e.g., visual, auditory, somatosensory) form reciprocal connections with a sector of the reticular nucleus (Jones, 1985; Sherman and Guillery, 1996, 2001; Guillery et al., 1998). That is, relay cell axons on their way to cortex pass through the appropriate reticular sector and give off branches with terminals in that sector, and the reticular cells in turn send axons back into the same part of the dorsal thalamic nucleus. It is worth noting that the functionally related corticothalamic axons from layer 6 also pass through the appropriate reticular sector as they go to their thalamic destination, and these axons also provide collateral innervation to these reticular cells. The cortical and thalamic inputs to the reticular nucleus are mapped (Crabtree and Killackey, 1989; Crabtree, 1996, 1998; Conley and Diamond, 1990; Conley et al., 1991), and this relatively accurate mapping stands in sharp contrast to earlier views of the reticular nucleus as diffusely organized. Finally, the thalamic reticular nucleus is also innervated by the same regions of brainstem that innervate the dorsal thalamus. The reticular cells are GABAergic and inhibit their dorsal thalamic targets, which are nearly exclusively relay cells rather than interneurons (Cucchiari et al., 1991b; Wang et al., 2001).

Brainstem Afferents. A final extrinsic source of innervation to the thalamus comes from various brainstem sources. The mix and relative strength of these brainstem inputs can vary both with species as well as with specific thalamic nuclei (Fitzpatrick et al., 1989). Afferents from the pons and midbrain (see Fig. 8.5) include cholinergic neurons (i.e., using acetylcholine as a neurotransmitter) of the *parabrachial region* (the cells of origin are located near the brachium conjunctivum; this is also known as the *pedunculo-pontine tegmental nucleus*), noradrenergic neurons (i.e., using noradrenaline, also known as norepinephrine) of the *locus coeruleus* and parabrachial region (i.e., most cells there are cholinergic, but some are noradrenergic), and serotonergic neurons of

the *dorsal raphé nucleus*. These inputs can either excite or inhibit thalamic neurons (see Chapter 2 and below). By far the most numerous of these inputs to the lateral geniculate nucleus is the cholinergic input, representing perhaps 90% of the brainstem input in the cat (Smith et al., 1988; Bickford et al., 1993) and 100% in the monkey (Bickford et al., 2000). However, there may be considerable variability in the relative distribution of these various brainstem inputs to different thalamic nuclei (Fitzpatrick et al., 1989).

Figure 8.3 shows the main inputs to thalamus, but other modulatory inputs that vary across nuclei also exist, and these have been most closely studied for the lateral geniculate nucleus (Harting et al., 1986; Fitzpatrick et al., 1988a; Cucchiari et al., 1991a, 1993; Uhlrich et al., 1993; Bickford et al., 1994). The *tuberomammillary nucleus* of the hypothalamus provides a histaminergic input. A GABAergic input exists from the *basal forebrain* to the thalamic reticular nucleus, and while this input does not directly innervate dorsal thalamus, it can influence relay properties indirectly via reticular inputs to relay cells described in the previous section. Finally, the lateral geniculate nucleus receives additional, although sparse, brainstem inputs that may be unique to the visual pathways, and these are also omitted from Fig. 8.5. These include afferents from the *superior colliculus* and *parabigeminal nucleus* of the midbrain and from the *pretectal nucleus of the optic tract*. The parabigeminal input is cholinergic, that from the pretectum is GABAergic, and that from the superior colliculus is thought to be glutamatergic. There is evidence that the GABAergic input from the nucleus of the optic tract does not innervate relay cells directly but instead innervates reticular cells and interneurons, which would presumably disinhibit relay cells (Cucchiari et al., 1993; Wang et al., 2002b).

Although modulatory inputs other than those shown in Fig. 8.3 have not been much explored in other thalamic relays, one that is particularly interesting to consider is that from the basal ganglia to the ventral anterior and lateral nuclei. This is a GABAergic, inhibitory pathway, and it is notable, because in many textbooks (e.g., Purves et al., 1997; Kandel et al., 2000) this pathway is treated as though it were a driver, functionally comparable to the retinal, lemniscal, or cerebellar inputs, which are either known drivers or have the morphological characteristics of a driver and use the same transmitter. However, there is reason to believe that inhibitory inputs are unlikely to be drivers (Smith and Sherman, 2002). This is because inhibitory inputs are effective only when they cancel postsynaptic spikes, whereas excitatory inputs work by adding spikes; spike cancellation can occur only within a limited temporal window during which a spike and inhibitory input coincide, whereas excitatory inputs can add spikes during virtually any period in the postsynaptic spike train as long as the background firing rates are not near saturation levels. At physiological rates of spontaneous activity (say, ≤ 30 – 50 spikes/sec), excitatory inputs are far more effective in altering the spike train than are inhibitory ones (Smith and Sherman, 2002). Thus we suspect that this is a modulatory input. Driver inputs to these nuclei appear to come from cerebellum and from cortical layer 5 (see also Chap. 9).

RELAY NEURONS

Relay neurons are the only output of a dorsal thalamic nucleus. Their axons go predominantly to the neocortex, with some (from the intralaminar nuclei) going to the

striatum and others also going to the amygdaloid complex. Many, possibly all, of these axons send a branch to the thalamic reticular nucleus (see Fig. 8.1).

Classes of Relay Cell. We have indicated (see Parallel Processing) that there are three parallel pathways connecting the retina through the lateral geniculate nucleus to the visual cortex. Two of them connect through the A layers of the cat's lateral geniculate nucleus. Figure 8.7A,B shows examples of these relay cells and shows that they are morphologically distinct: Y cells have cruciate arbors that radiate symmetrically from the soma and are mostly devoid of complex appendages; X cells tend to be elongated along projection lines and usually have complex appendages near primary branch points. These appendages mark the postsynaptic location of retinal inputs involved in the glomeruli and triads, in accordance with the observation that X cells participate in triads, whereas Y cells do not (Wilson et al., 1984; Hamos et al., 1987; but see

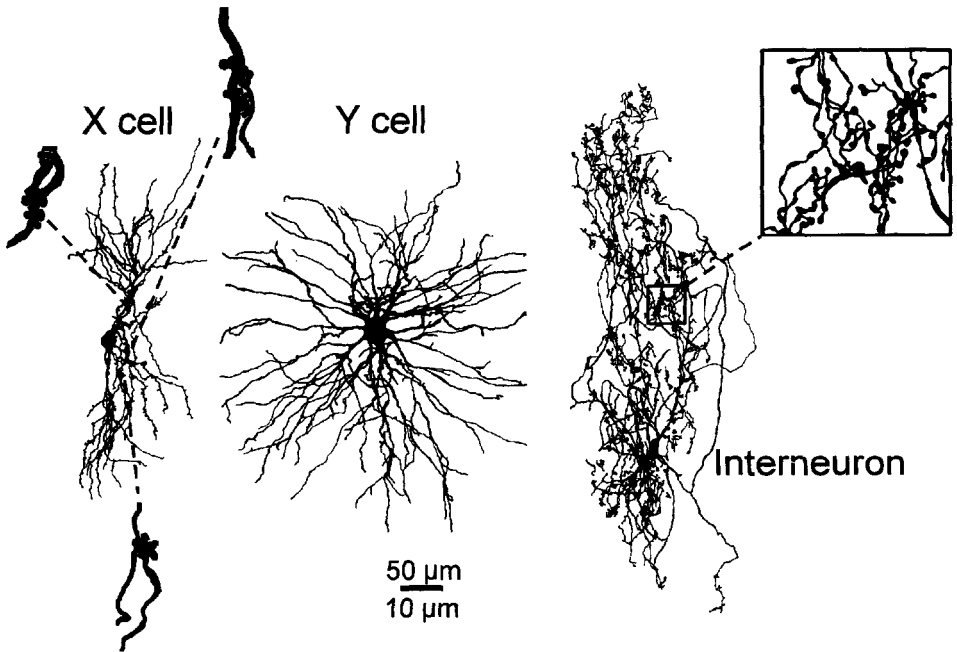


Fig. 8.7. Tracings of a relay X and Y cell and interneuron from the A layers of the cat's lateral geniculate nucleus. These were all physiologically identified during *in vivo* recording and filled intracellularly with horseradish peroxidase for morphological analysis (Friedlander et al., 1981; Hamos et al., 1985). The dendritic arbor of the X cell is tufted and elongated, oriented perpendicular to the plane of the layers, whereas the Y cell dendrites show a stellate distribution with an approximately spherical arbor. The X cell also has prominent clusters of dendritic appendages near proximal branch points. These are hard to see in the cell reconstructions, so three examples are shown at greater magnification, with dashed lines indicating their dendritic locations (the scale is $50\ \mu\text{m}$ for the cell reconstructions and $10\ \mu\text{m}$ for the dendritic appendage examples). The interneuron is also elongated in a direction perpendicular to the layers and has richly branched, thin dendrites with an axoniform appearance. The upper inset shows an enlarged view of the dendritic terminals (the scale, again, is $10\ \mu\text{m}$ for this). [Redrawn from Sherman and Guillery, 2001.]

Datskovskaia et al., 2001; Dankowski and Bickford, 2003). Comparable morphological distinctions between two types of relay cell have been described in several other thalamic nuclei (Kölliker, 1896; Morest, 1964; Pearson and Haines, 1980; Bartlett et al., 2000). Although the functional properties of the pathways through these relays are not as clear as they are in the lateral geniculate nucleus, it is important to stress that most thalamic nuclei have RL terminals related to triads in glomeruli as well as RL terminals that relate more simply to dendritic stems. That is, pathways comparable to the X and Y pathways of the cat's lateral geniculate nucleus are to be expected in all thalamic nuclei that have significant numbers of interneurons. The cortical axon terminals of the geniculate relay cells distribute primarily to layer 4 of the cortical target area, with a smaller terminal zone in layer 6 and some in more superficial layers.

Calcium Binding Proteins. A different classification of relay cells has been proposed by Jones (1998). This is based on two different calcium binding proteins that characterize the relay cells. Larger cells that generally dominate in first order nuclei are immunoreactive for parvalbumin. Smaller cells are immunoreactive for calbindin, and these are more densely distributed in parts of the thalamus other than the first order nuclei. Jones describes the parvalbumin-positive cells as forming a core of thalamic cells and the calbindin-positive cells as forming a matrix. The core cells project to layers 3 and 4 of cortex and carry well-mapped projections to cortex. Matrix cells are more likely to project to layer 1 of cortex, and their axons are more widely (diffusely) distributed to the cortex. That is, Jones regards the core as concerned with sending specific, well localized messages, whereas the matrix conveys more diffuse messages to cortex concerned with controlling the rhythmic discharges of cortical cells that have been proposed as playing a role in perceptual binding (Singer and Gray, 1995; Singer, 1999). This categorization applies primarily to the monkey thalamus; the calcium binding proteins do not show the same patterns in other mammals (Ichida et al., 2000).

It should be stressed that although matrix cells are more common in parts of the thalamus that contain higher order relays, the higher order relays from, for example, the pulvinar region connect to layer 3 of cortex and should not be thought of as contributing to a diffuse system. The first order/higher order distinction described here does not correspond to the core/matrix distinction proposed by Jones.

From the point of view of the lateral geniculate nucleus itself, the parvalbumin/calbindin distinction as representative of a functional core/matrix difference is somewhat problematical. The koniocellular system in the monkey is calbindin positive, whereas the parvocellular and magnocellular layers are parvalbumin positive. The koniocellular layers project to layer 3, and there is no evidence that would suggest that they represent a diffuse system.

INTERNEURONS

Roughly 20%–25% of the cells in most thalamic nuclei of most species are local interneurons (Arcelli et al., 1997). The figure is comparable for the lateral geniculate nucleus of the rat and mouse. Oddly, other thalamic nuclei in the rat and mouse, but not in other rodents, have practically no interneurons (Arcelli et al., 1997). Thus analogous nuclei in the same animal (e.g., the rat's lateral geniculate and ventral posterior lateral

nuclei) can vary in this regard, as can homologous nuclei across species (e.g., the ventral lateral posterior nuclei of cats and rats).

The most intensively studied interneurons are those found in the A layers of the cat's lateral geniculate nucleus (see Fig. 8.7), but they are basically similar in other thalamic nuclei (Guillery, 1966, 1969a,b; Ralston, 1971; Morest, 1971; Hamos et al., 1985; Carden and Bickford, 2002). These geniculate interneurons have small cell bodies with long, thin, and sinuous dendrites (Fig. 8.7C). The dendrites are notable for giving rise to bulbous appendages connected to the stem dendrite by long ($\geq 10 \mu\text{m}$), thin (usually $< 0.1 \mu\text{m}$ in diameter) processes; these appendages usually occur in clusters. Overall, the dendrites with their bulbous appendages look like the terminal arbors of axons, and thus Guillery (1966) referred to these dendrites as "axoniform" in appearance. In fact, these bulbous appendages represent the F2 terminals described earlier, which are both presynaptic and postsynaptic to other elements in the lateral geniculate nucleus (Guillery, 1969a,b; Morest, 1971; Ralston, 1971; Famiglietti and Peters, 1972; Hamos et al., 1985; Ralston, et al., 1988). Most of the synapses from interneurons are thus dendritic in origin.

These interneurons usually have a conventional axon that arborizes locally, typically within the dendritic arbor (Hamos et al., 1985; Montero, 1987), although axonless interneurons may exist (Ralston et al., 1988). Inputs to these interneurons in the lateral geniculate nucleus include many from retina, exclusively or nearly so from X axons (Sherman and Friedlander, 1988). Their dendritic outputs contact mostly only relay X cells in triadic arrangements within glomeruli associated with proximal dendrites of the target cell (Hamos et al., 1985, 1987; but see Datskovskaia et al., 2001; Dankowski and Bickford, 2003). Evidence for interneuronal influences on relay Y cells also exists (Lindström, 1982), and this probably reflects the axonal output. All interneurons are GABAergic, and both their dendritic and axonal outputs inhibit their postsynaptic targets.

There is clear evidence that other types of interneuron exist. The interneurons described in the preceding paragraphs lack the enzyme brain nitric oxide synthase (BNOS), but other interneurons do contain BNOS and they are morphologically distinguishable (Meng et al., 1996; Carden and Bickford, 2002). In the cat's pulvinar region and in the C layers of the cat's lateral geniculate nucleus, the interneurons with BNOS have larger cell bodies and dendrites that radiate in all directions over a larger distance than do those of the other interneurons (Bickford et al., 1999; Carden and Bickford, 2002). Also, these latter interneurons have different input/output characteristics than do those without BNOS (Carden and Bickford, 2002): they receive no inputs from terminals with driver morphology, and although both make dendrodendritic contacts (and, indeed, those with BNOS have no detectable axon), they contact relay cells on distal dendrites, outside glomeruli).

A potentially different type of interneuron is one found in the interlaminar zones of the ferret's lateral geniculate nucleus (Sanchez-Vives et al., 1996). These have been described as a displaced part of the thalamic reticular nucleus, in part because they lack a direct driver (retinal) innervation. This is similar to the interneurons with BNOS in the pulvinar region, but, unfortunately, there is as yet no description of their BNOS content.

Clearly, we need a more complete survey of the various types of interneuron found in thalamus and we need to define each type in terms of the details of its contribution to thalamic circuitry.

CELLS OF THE THALAMIC RETICULAR NUCLEUS

As noted earlier, the thalamic reticular nucleus is a source of modulatory afferents to the dorsal thalamus. The axons of reticular cells do not go beyond the thalamus; instead they provide local, GABAergic, inhibitory input to thalamic relay cells. They are thus functionally similar in some ways to interneurons, and many investigators group them with interneurons as local inhibitory cells. However, two clear differences between interneurons and reticular cells are that only the former have dendritic appendages that are presynaptic to relay cells and that reticular cells receive no synaptic contacts from the driver afferents to thalamic relay cells.

SYNAPTIC CONNECTIONS

INPUTS TO RELAY CELLS

Reconstructions from electron micrographs show that thalamic relay cells receive roughly 4000–5000 synapses, nearly all onto their dendrites, with rare contacts on the cell bodies (Wilson et al., 1984; Liu et al., 1995). Figure 8.8 schematically summarizes the distribution of various types of synaptic input on the dendritic arbors of relay X and Y cells of the cat's lateral geniculate nucleus. Relay cells in other thalamic nuclei probably have a comparable pattern of synaptic inputs (Wilson et al., 1984; Liu et al.,

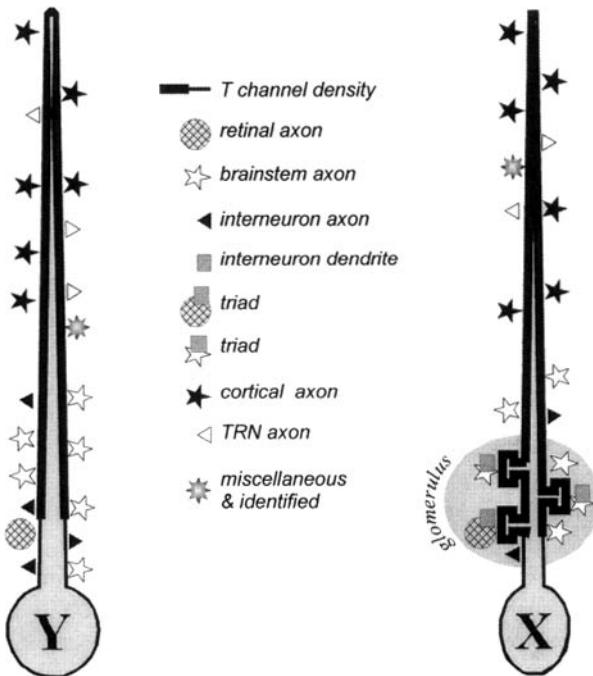


Fig. 8.8. Schematic view of synaptic inputs onto an X cell and a Y cell of the lateral geniculate nucleus of the cat. The T channels are also shown. They are found throughout the cell body and dendritic membranes but are denser on the dendrites than on the cell body. Note that retinal, interneuronal, and parabrachial inputs contact proximal dendrites, whereas cortical and reticular inputs are concentrated on peripheral dendrites. [Redrawn from Sherman and Guillery, 2001.]

1995). For both relay X and Y cells, inputs from retinal terminals concentrate in the proximal region of the dendritic arbor, whereas cortical RS input dominates distal dendrites, and there is little or no overlap of these zones. Parabrachial RS terminals are found proximally, among retinal terminals. F terminals are found all along the dendritic arbor but are more numerous proximally. Interestingly, among the F1 terminals, those from reticular cells are mostly located distally, among cortical RS terminals (Wang et al., 2001). The remaining F1 terminals are found proximally, and these, by a process of elimination, must derive mostly from axons of interneurons.

However, major differences between relay X and Y cells exist in the types of F terminal present and in the detailed nature of the retinal input. In particular, the innervation of X cells heavily involves triads and glomeruli, but that of Y cells does not. That is, the vast majority of retinal inputs to relay X cells are filtered through the complicated circuitry of the glomerulus. Retinal input to relay Y cells is simpler and involves conventional asymmetrical synapses onto proximal dendritic shafts (Wilson et al., 1984; Sherman, 1988). F2 terminals are nearly always limited to glomeruli, and the lack of glomeruli associated with the Y pathway results in very few such terminals contacting relay Y cells (but see Datskovaia et al., 2001; Dankowski and Bickford, 2003). More than 90% of the F input to these cells is of the F1 variety, whereas roughly two-thirds of F input onto relay X cells is of the F2 variety.

INPUTS TO INTERNEURONS

As with our previous examples, most of our detailed knowledge of interneurons stems from studies of the lateral geniculate nucleus, but comparable studies in other thalamic nuclei, especially the ventral posterior lateral nucleus, reveal basically similar properties for thalamic interneurons (Ralston et al., 1988). In the lateral geniculate nucleus, many retinal, RS, and F1 terminals contact interneurons (Hamos et al., 1985). RS terminals include cortical (from layer 6) and parabrachial sources, as for relay cells, but relay cells themselves also innervate interneurons via local collaterals (Cox and Sherman, 2003), and it is likely that these terminals are also of the RS type. Much of this input is focused onto the dendritic appendages, which are the presynaptic F2 terminals. Input is also formed onto dendritic shafts and cell bodies, and these are the only geniculate neurons that seem to receive significant retinal input onto their cell bodies.

BASIC NEURONAL CIRCUIT

Enough is known about the cat's lateral geniculate nucleus to provide a schematic circuit diagram, including a fair estimate of the numbers of neuronal elements present. Of course, many of the specific features of this diagram remain somewhat uncertain, but the broad outlines are clear. It is likely that these broad outlines apply as well to other thalamic nuclei.

COMPONENT POPULATIONS

As noted earlier, roughly three-fourths of the neurons in the A-laminae are relay cells, and the rest are interneurons. The interneurons have two outputs, the major one being the dendritic F2 terminals and the minor one being the axonal F1 terminals (see Figs. 8.2, 8.3, and 8.4). The dendritic output of interneurons targets relay X cells nearly exclusively (but see Datskovaia et al., 2001; Dankowski and Bickford, 2003), and the

axons target both X and Y cells. Relay X cells somewhat outnumber relay Y cells (Sherman, 1985). These geniculate neurons are specifically innervated by appropriate retinogeniculate axons—X to X and Y to Y—but the details of how other axons (from cortex, brainstem, and local GABAergic sources) innervate relay X and Y cells or interneurons are not yet clear. We also still lack estimates for the number of afferent axons from the thalamic reticular nucleus and various brainstem sites, and such estimates are only in part available for other species.

INTRINSIC CIRCUITRY

The basic organization of major inputs to the cat's lateral geniculate nucleus is summarized schematically in Fig. 8.9. Many of the details of this circuit, including the differences between the X and Y pathways, were described earlier. These relay cells also receive input from cortex and from the brainstem. Major inhibitory input comes from local GABAergic cells, which are the interneurons and reticular cells. Both of these GABAergic cells are innervated by cortex and by the brainstem parabrachial region. In addition, interneurons and reticular cells are innervated by axon collaterals from the relay cells, and interneurons also receive input from retinal X axons. Reticular cells also receive a GABAergic input from the basal forebrain. Not included, for simplicity, are lesser known and probably smaller inputs described earlier from the hypothalamus

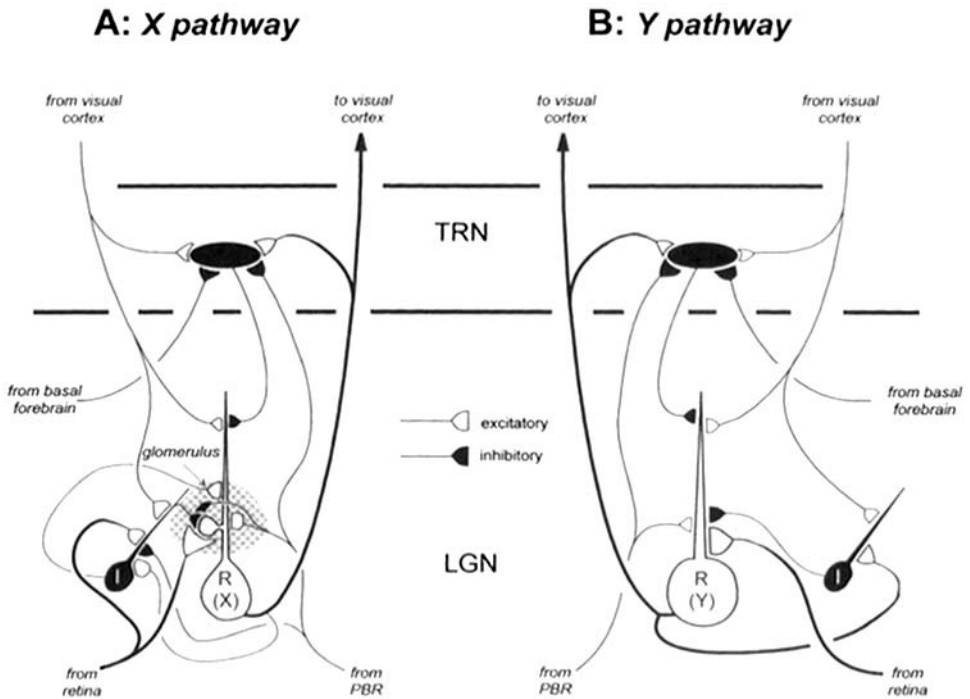


Fig. 8.9. Detailed circuitry related to X and Y relay cells of the lateral geniculate nucleus of the cat. Abbreviations: I, interneuron; LGN, lateral geniculate nucleus; PBR, parabrachial region; R, relay cell; TRN, thalamic reticular nucleus.

(histaminergic), pretectum (GABAergic), the parabrachial region or locus coeruleus (noradrenergic), and the dorsal raphe nucleus (serotonergic).

Although much of the circuitry outlined in Fig. 8.9 is sketchy, the following conclusions can be tentatively drawn. Much of this repeats earlier points, but it is offered here as a concise summary. Relay cells receive retinal input onto proximal dendrites in close association with some GABAergic and parabrachial input. The proximal GABAergic input, both axonal (F1) and dendritic (F2), derives from interneurons. Distal dendrites are dominated by cortical input, and, at least for geniculate relay cells, these inputs are limited to dendritic locations more distal than those of retinal inputs (Guillery, 1969a,b; Wilson et al., 1984; Erişir et al., 1997a). Some GABAergic inputs can also be seen on distal dendrites, and these derive from reticular cells. However, the electrotonic compactness of relay cells implies that even the distal inputs can be quite important functionally (see also Dendritic Cable Properties).

Figure 8.9 also summarizes some differences between the X and Y pathways, and perhaps this can be taken as a reflection of the kinds of variation present throughout thalamic circuitry. Three main differences exist: the nature of retinal input, the presence of glomeruli, and the role of interneurons. Retinal input to relay Y cells is fairly straightforward, innervating proximal dendritic shafts in simple contact zones. Retinal input to relay X cells is much more elaborate, because it involves complicated triadic relationships that include dendritic terminals of interneurons. Glomeruli are also a major feature of X, but not Y, circuitry, and the glomerulus may be viewed as a major filter of retinogeniculate transmission (see The Electron Microscopic Appearance of the Neuronal Elements). Finally, interneuronal dendritic outputs also seem to be intimately related to X, but not Y, circuitry. The axonal targets of interneurons appear to innervate both X and Y cells proximally, and those of reticular cells, distally.

It should be emphasized that the circuit schematically represented in Fig. 8.9 is preliminary and greatly simplified. Many questions still remain. For example, what is the interrelated pattern of innervation involving single cortical axons, reticular cells (or interneurons), and relay cells? The implication of this last question is illustrated in Fig. 8.10A,B showing two extremes of possible functional circuits involving inputs to relay cells and the local, GABAergic inhibitory cells. This reflects our superficial knowledge of interconnections among these cell populations and makes the point that in many cases we still cannot even determine if activation of these circuits excites or inhibits relay cells. For instance, Fig. 8.10A shows a true feedback inhibitory circuit in which an axon collateral from a relay cell (*cell b*) excites a reticular cell (*cell 2*) that in turn inhibits this same relay cell. In Fig. 8.10B, there is a very different relationship: now relay *cell b* excites reticular *cells 1* and *3*, but not *cell 2*, and reticular *cells 1* and *3* do not inhibit relay *cell b* but rather inhibit its neighbors (*cells a* and *c*). Because *cells a* and *c* excite the reticular cell (*cell 2*) that inhibits relay *cell b*, the net result of the circuit depicted in Fig. 8.10B is that activity in relay *cell b* results in its further disinhibition, which is precisely the opposite of the feedback inhibition resulting from Fig. 8.10A. Likewise, the circuits shown in Fig. 8.10C,D have opposite effects when the corticogeniculate axon is activated: that in Fig. 8.10C results in feedforward inhibition of relay *cell b*, whereas that in Fig. 8.10D results in feedforward disinhibition of this same cell. The message here is that the details count, particularly for connections of

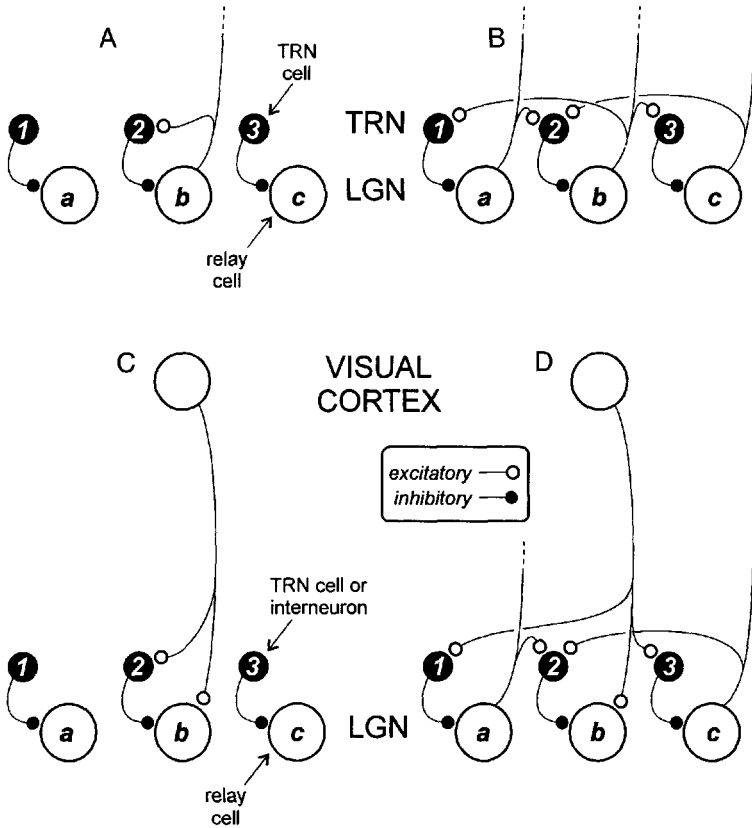


Fig. 8.10. Schematic view of different possible circuits involving the thalamic reticular nucleus that have quite different effects on relay cells. See text for details. [From Sherman and Guillery, 2001.]

individual neurons, and we are not yet sufficiently certain of many of the details to determine the final effect on relay cells of activating certain inputs or local circuits. It should be noted that the circuits depicted here are probably extreme examples, and combinations of each type may well exist.

DENDRITIC CABLE PROPERTIES

RELAY CELLS

Both X and Y classes of relay cell are electrically rather compact, with dendritic arbors extending for roughly one length constant (Bloomfield et al., 1987; Bloomfield and Sherman, 1989). In practice, this means that even the most distally located synaptic input can have significant effects on the soma and axon, with attenuation of post-synaptic potentials never exceeding one-third to one-half (Fig. 8.11). One of the reasons for the electrotonically restricted dendritic arbors of relay X and Y cells is the nature

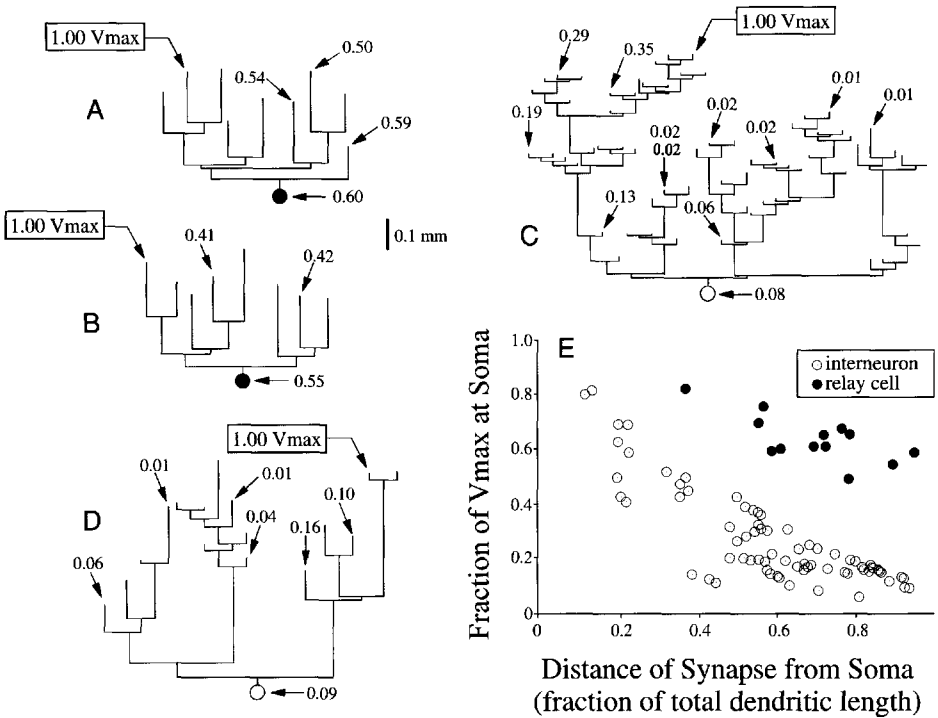


Fig. 8.11. **A–D:** Cable modeling of the voltage attenuation occurring within the dendritic arbors of two relay cells (**A** and **B**) and two interneurons (**C** and **D**) from the cat's lateral geniculate nucleus following a single voltage injection to mimic the activation of a single synapse. The cells were labeled by intracellular injection of horseradish peroxidase *in vivo*, and the stick figures schematically represent one primary dendrite from each cell with all of its progeny branches. Each branch length is proportional to its calculated electrotonic length. The site of voltage injection is indicated by the boxed value labeled 1.00 V_{max} (maximum voltage). Attenuated voltage levels at various terminal endings within the arbor and soma are indicated by arrows and given as fractions of V_{max}. **E:** Attenuation at soma of single voltage injection placed at different terminal endings within the dendritic arbor as function of anatomical distance of the voltage injection from the soma. The abscissa represents relative anatomical distances normalized to the greatest extent of each arbor, and the plotted points represent values from the four cells shown in **A–D**. [From Bloomfield and Sherman, 1989.]

of their dendritic branches. These branches closely adhere to Rall's "3/2 branching rule" (Bloomfield et al., 1987). This states that the diameters of the daughter dendrites each raised to the 3/2 power and summed equals the diameter of the parent dendrite raised to the 3/2 power (Rall, 1977). Such branching matches impedance on both sides of the branch point and permits efficient current flow across these branches in *both* directions. This maximizes the transmission of distal postsynaptic potentials to the soma. This also implies that a potential generated anywhere in the dendritic arbor or at the soma will be efficiently transmitted throughout the dendritic arbor. Among other things, this means that the discharge of an action potential will depolarize the entire dendritic

arbor by tens of millivolts, and this could have significant effects on voltage-dependent processes in the dendrites (see Membrane Properties).

INTERNEURONS

Unlike relay cells, interneurons are not electrotonically compact (Bloomfield and Sherman, 1989). This is in part because their dendrites are thinner and longer than those of relay cells. More importantly, the dendritic branch points of interneurons violate the “3/2 branching rule,” because daughter branches tend to be too thin. This limits the current flowing across these branch points. As a result, *providing that there are no major active conductances in the dendritic arbor of interneurons*, much of the synaptic circuitry in distal dendrites, including that involving the F2 terminals, would be functionally isolated from the soma and axon (see Fig. 8.11). We emphasize the proviso here concerning the assumption of no significant Ca^{2+} and Na^{+} conductances in the dendrites, and this attribute remains unknown. Ralston (1971) proposed some time ago that synaptic input onto the axoniform dendritic (F2) terminals of interneurons in the cat’s ventral posterior lateral nucleus would also be isolated from the soma. Other examples of this property are found in the olfactory bulb (see Chap. 5) and retina (see Chap. 6).

Computational modeling based on these observations and with the assumption of passive cable properties suggests an interesting mode of operation for these interneurons (Sherman, 1988; Bloomfield and Sherman, 1989), shown schematically in Fig. 8.12. Clusters of dendritic appendages, which are major sites of input and output, represent local circuits whose computations are largely independent of activity in other clusters and in the soma. In contrast, the axonal output is controlled in a more orthodox manner by input to the soma and proximal dendrites. This output appears to be mediated by conventional action potentials (Sherman and Friedlander, 1988). Also, although the dendritic F2 outputs innervate relay X cells through glomeruli, the axon forms F1 terminals that innervate dendritic shafts outside of glomeruli of relay X and Y cells (Hamos et al., 1985; Montero, 1987; Sherman and Friedlander, 1988; Wang et al., 2001). This suggests that the interneuron simultaneously does double duty: integration of the axonal F1 outputs via action potentials depends on one set of proximal inputs and involves one type of postsynaptic target, whereas integration of the dendritic F2 outputs depends on local inputs and involves different postsynaptic targets.

MEMBRANE PROPERTIES

The integrative characteristics of neurons are heavily dependent on their intrinsic electrophysiological properties (see Chap. 2). We can no longer view a thalamic cell as being a simple response element that linearly sums its synaptic inputs to determine its axonal output. Thus cable modeling as described earlier is only a beginning toward explaining how a neuron responds to various synaptic inputs. In reality, these cells have a variety of active membrane conductances. Many of these are controlled by ligand binding of neurotransmitters, including effects of second messenger pathways activated by metabotropic receptors, but some are controlled by membrane voltage and others are controlled by concentration levels of certain ions, such as Ca^{2+} .

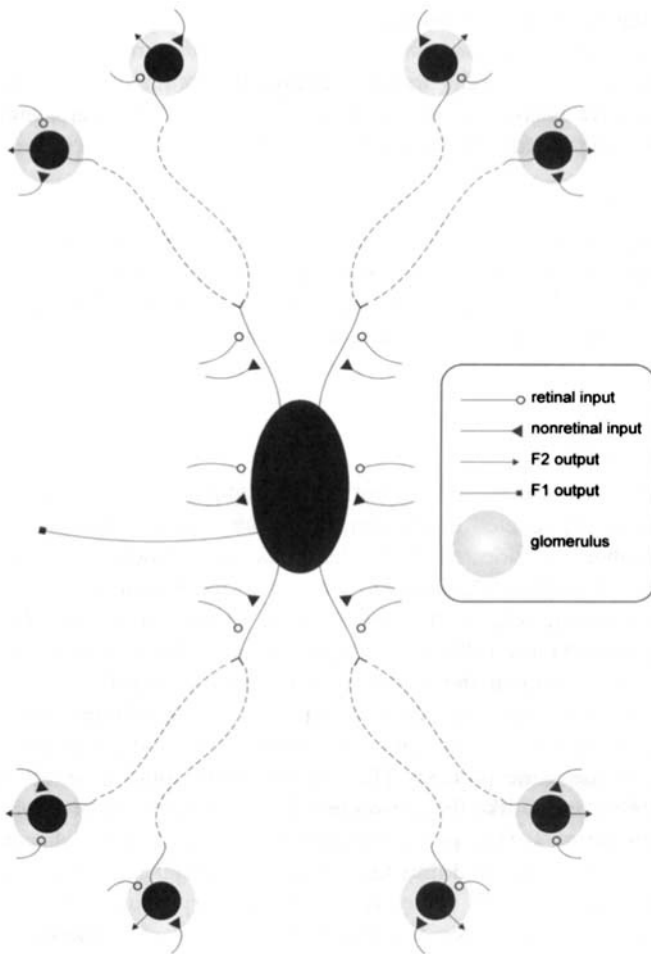


Fig. 8.12. Schematic view of hypothesis for functioning of interneurons in the lateral geniculate nucleus of the cat. Retinal and nonretinal inputs are shown both to the distal dendrites, associated with glomeruli, as well as to the proximal dendrites and soma. The glomerular inputs lead to F2 outputs from the dendrites, whereas the inputs to the proximal dendrites and soma lead to F1 outputs from the axon. The dashed lines indicate the electrotonic isolation between glomeruli and the proximal dendrites plus soma. This isolation suggests that the two sets of synaptic computations, peripheral for the glomerular F2 outputs and proximal for the axonal F1 outputs, transpire in parallel and independently of one another. Most glomeruli are also functionally isolated from one other. [Redrawn from Sherman and Guillery, 2001.]

Both *in vitro* and *in vivo* experiments of different thalamic nuclei across several mammalian species have revealed a surprising plethora of intrinsic membrane conductances present in *all* thalamic neurons, both in the dorsal thalamus nuclei and within reticular neurons (Steriade et al., 1987; Steriade and Llinás, 1988; Huguenard and McCormick, 1992; McCormick and Huguenard, 1992). These conductances all lead to currents that alter the membrane potential. The number of active conductances de-

scribed for thalamic neurons continues to grow. Which conductances are active can greatly affect how a thalamic neuron's input is relayed to cortex. Conductances found in thalamic neurons are generally found in many other brain cells as well, and for the most part these have been described in detail in Chap. 2. The major and best understood ones operating in thalamic neurons are listed below (see also Chap. 2).

Na⁺ CONDUCTANCES

Two voltage-dependent Na⁺ conductances have been described. The fast, inactivating Na⁺ conductance, similar to the one described by Hodgkin and Huxley (1952) for the squid giant axon, is voltage dependent and subserves the conventional action potential. The other Na⁺ conductance is persistent and noninactivating. This creates a plateau depolarization that serves to inactivate certain currents, such as I_A and I_T (see next paragraphs).

Ca²⁺ CONDUCTANCES

There are at least two voltage-dependent Ca²⁺ conductances. One has a high threshold and is most likely located in the dendrites; rather little is known about this conductance. The other, also located in the dendrites, has a lower threshold and plays a dramatic role in retinogeniculate transmission (and the transmission of other driving inputs in other thalamic relays). It is often known as the *low threshold Ca²⁺ conductance* and is described more fully here. It operates via T (for transient)-type Ca²⁺ channels. When the channels open, the resultant conductance leads to Ca²⁺ entry, represented by an inward current known as I_T, thereby depolarizing the cell and producing the *low threshold spike*. Thus the low threshold Ca²⁺ conductance, the low threshold spike, and I_T are all part of the same process. The low threshold spike is an all-or-none spike (Zhan et al., 1999), much like the conventional action potential, propagating throughout the dendritic arbor. It is important to note that this channel is absent in appreciable numbers from the axon, and thus the low threshold spike is not propagated up the axon to cortex. Low threshold spikes are found in every relay cell of every thalamic nucleus of every mammalian species so far studied (reviewed in Sherman and Guillery, 1996). These spikes also occur in cells of the thalamic reticular nucleus and interneurons, although their prevalence in interneurons remains controversial (see K⁺ Conductances).

Apart from those underlying the generation of conventional action potentials, the low threshold Ca²⁺ conductance is probably the most important conductance for relay cells. Details of its properties can be found elsewhere (Jahnsen and Llinás, 1984a,b; McCormick and Feese, 1990; Huguenard and McCormick, 1992; McCormick and Huguenard, 1992) and are summarized here. Figure 8.13 shows the voltage dependence of the T channels and those of K⁺ channels, which are also involved in the generation of the low threshold spikes. The T channels have two voltage-sensitive gates, an activation gate and an inactivation gate, and both must be open for Ca²⁺ to flow into the cell to generate I_T. At relatively hyperpolarized resting membrane potentials (Fig. 8.13,1), the activation gate is closed but the inactivation gate is open, so I_T is *de-inactivated*. The single gate of the K⁺ channel is closed at this membrane potential. If the cell is now sufficiently depolarized (e.g., by an EPSP), the activation gate opens, and Ca²⁺ flows into the cell, generating I_T and providing the upswing of the low threshold spike (Fig. 8.13,2). However, depolarization eventually closes the inactivation gate af-

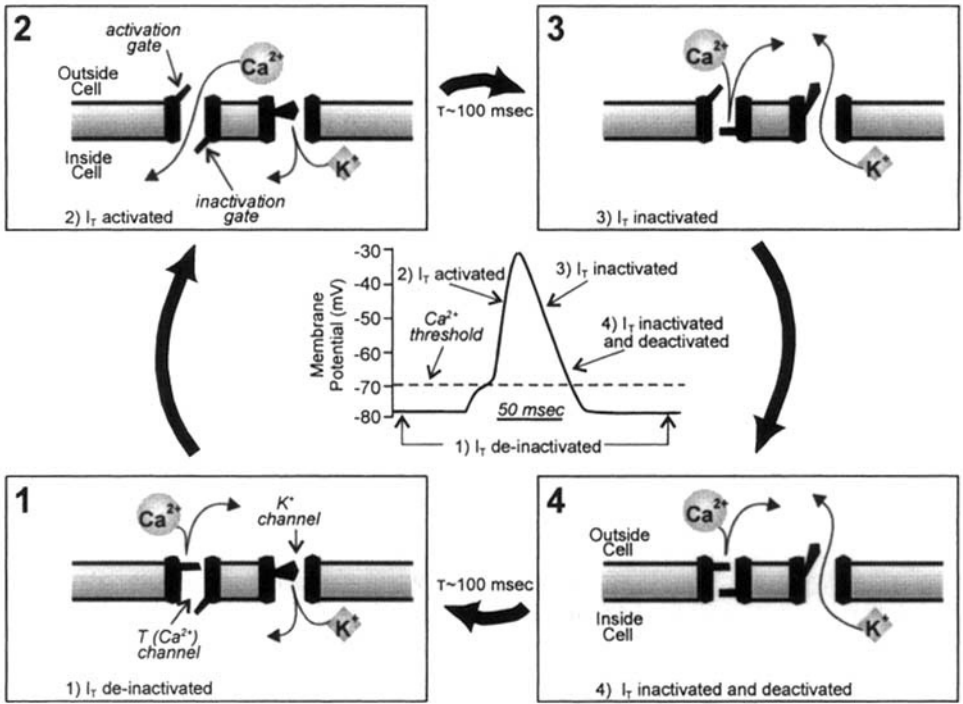
The Low Threshold Ca^{2+} Spike

Fig. 8.13. Schematized view of actions of voltage-dependent T (Ca^{2+}) and K^+ channels underlying low threshold Ca^{2+} spike. The four numbered panels show the sequence of channel events, and the central graph shows the effects on membrane potential. The T channel has two voltage-dependent gates: an *activation* gate that opens with depolarization and closes at hyperpolarized levels and an *inactivation* gate that shows the opposite voltage dependency. The K^+ channel shown is really a conglomeration of several such channels that have only a single gate that opens during depolarization; thus, these channels do not inactivate. (1) At a relatively hyperpolarized resting membrane potential (≈ -70 mV), the activation gate of the T channel is closed, but the inactivation gate is open, and so the T channel is de-inactivated. The single gate for the K^+ channel is closed. (2) With sufficient depolarization to reach its threshold, the activation gate of the T channel opens, and Ca^{2+} flows into the cell. This further depolarizes the cell, providing the rise of the low threshold spike. (3) The inactivation gate of the T channel closes after being depolarized for roughly 100 msec ("roughly" because closing of the channel is a complex function of voltage and time), and the K^+ channel also opens. These actions repolarize the cell. When the inactivation gate of the T channel is closed, the channel is inactivated. (4) Even though the initial resting potential is reached, the T channel remains inactivated, because it takes roughly 100 msec ("roughly" having the same meaning as before) of hyperpolarization to de-inactivate it; it also takes a bit of time for the various K^+ channels to close. Note that the behavior of the T channel is qualitatively exactly like the Na^+ channel involved with the action potential but with several quantitative differences: the T channel is slower to inactivate and de-inactivate, and it operates in a more hyperpolarized regime.

ter ≈ 100 msec (Fig. 8.13,3). Actually, the opening or closing of the inactivation gate is a complex function of voltage and time (Jahnsen and Llinás, 1984a,b) so that the more depolarized (or hyperpolarized), the more quickly the gate closes (or opens), but the important point is that under normal conditions, ≈ 100 msec is required for these actions. Thus I_T is *inactivated*. The single gate of the voltage- and Ca^{2+} -dependent K^+

channel also opens, and the combined inactivation of I_T and activation of the K^+ channels repolarizes the cell (Fig. 8.13,4). Although the membrane is repolarized to its initial potential, I_T remains inactivated, because it takes ≈ 100 msec of this hyperpolarization to remove the inactivation of I_T (and thus I_T is *de-inactivated*), after which, the initial conditions are re-established (Fig. 8.13,1). To reiterate: when the cell is sufficiently hyperpolarized for more than about ≈ 100 msec, I_T is de-inactivated; if de-inactivated, a suitable depolarization can then activate I_T , but continued depolarization for more than ≈ 100 msec will inactivate it; the inactivation can then be removed by suitable hyperpolarization for more than about 100 msec.

Note that the voltage-dependent properties of the T channels are qualitatively identical to those of the Na^+ channels underlying the action potential, but there are important quantitative differences: (1) the T channels are found in the soma and dendrites, but not in the axon, and thus the low threshold spike can be propagated through the dendrites and soma, but not along the axon to cortex. Nonetheless, the T channels can affect the message reaching cortex by the effect of the low threshold spike on action potential generation (see Burst and Tonic Relay Response Modes). (2) Opening or closing of the inactivation gate is roughly two orders of magnitude faster for the Na^+ channel. (3) The T channels operate in a somewhat more hyperpolarized regime.

Figure 8.14 shows some of the functional consequences of I_T in recordings from relay cells of the cat's lateral geniculate nucleus. When the membrane is more depolarized than roughly -60 to -65 mV for $>\approx 100$ msec, I_T becomes inactivated (Fig. 8.14A), and activation by a depolarizing pulse evokes a steady stream of unitary action potentials that lasts for the duration of the stimulus: this is the *tonic mode* of firing, which prevails when I_T is inactivated.

"Tonic" used in this sense refers to a response mode of a thalamic relay cell, and here it is paired with "burst." All thalamic relay cells, including the X and Y cells in the A-laminae of the cat's lateral geniculate nucleus, display both response modes. However, for a functional categorization of the X and Y cells, "tonic" X cells are often contrasted with "phasic" Y cells. This is an entirely different use of "tonic," and the two should not be confused. Throughout this account, we shall use "tonic" only to refer to response mode, not to cell type.

When the membrane is more hyperpolarized than about -65 to -70 mV for $>\approx 100$ msec (see Fig. 8.14B), I_T becomes de-inactivated. The identical depolarizing pulse now activates I_T , leading to a low threshold spike, which in turn activates a burst of several action potentials: this is the *burst mode* of firing, which prevails when I_T is de-inactivated and then activated.

K^+ CONDUCTANCES

A number of voltage- and Ca^{2+} -dependent K^+ conductances exist that give rise to various membrane currents (see Chap. 2). The best known is the *delayed rectifier* (I_K), which is part of the action potential and repolarizes the neuron following the Na^+ conductance. Several others (I_A , I_C , and possibly I_{AHP}) hyperpolarize the neuron for varying lengths of time following a conventional action potential. The amount of this hyperpolarization determines the cell's relative refractory period, which limits its maximum firing rate. Finally, thalamic cells exhibit a variable, voltage-independent K^+ "leak" current, which, in addition to other such "leak" currents for Na^+ , Cl^- , etc., determine the resting membrane potential.

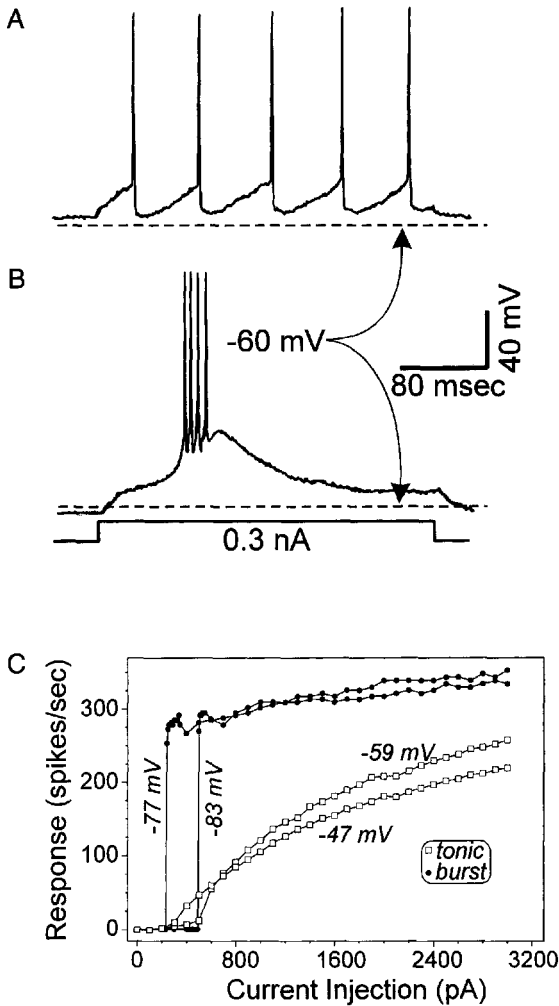


Fig. 8.14. Properties of burst and tonic firing for relay cells of the cat's lateral geniculate nucleus recorded intracellularly *in vitro*. **A** and **B**: Voltage dependency of the low threshold spike for one cell. Responses are shown to the same depolarizing current pulse administered intracellularly but from two different initial holding potentials. I_T is inactivated with relative depolarization (**A**), and the response is a succession of unitary action potentials for the duration of the suprathreshold stimulus. This is the *tonic mode* of firing. I_T is de-inactivated with relative hyperpolarization (**B**), and the response is a low threshold spike with 4 action potentials riding its crest. This is the *burst mode* of firing. **C**: Input-output relationship for another cell. The abscissa plots the amplitude of the depolarizing current pulse, and the ordinate plots the evoked firing frequency based on the first 6 action potentials of the response, because this cell usually exhibited 6 action potentials per burst in this experiment. The initial holding potentials are shown: -47 mV and -59 mV reflect tonic mode, whereas -77 mV and -83 mV reflect burst mode. [Redrawn from Sherman and Guillery, 2001.]

I_A and its relationship with I_T is particularly interesting. The voltage dependencies of these two currents are generally similar in that both are inactive at depolarized V_m and can be activated by depolarization from relatively hyperpolarized V_m . However, although I_T leads to depolarization due to Ca^{2+} entry, I_A leads to hyperpolarization due to K^+ leaving the cell. Because I_A is activated by depolarization, this means that it will oppose that depolarization, making it smaller and slowing it down. However, for most relay cells, the activation and inactivation curves of I_T are offset by at least 10 mV in the hyperpolarized direction with respect to those of I_A (Pape et al., 1994). This means that, when a relay cell is hyperpolarized sufficiently to de-inactivate both currents and then is depolarized, I_T will activate before I_A , and the resultant spike-like depolarization will rapidly inactivate I_A before it has a chance to develop. It may thus be uncommon to activate I_A in relay cells under most conditions. However, there is a narrow window of V_m in which I_T is largely inactivated and I_A is largely de-inactivated, and depolarization that occurs within this limited membrane voltage range will activate I_A but not I_T .

There is evidence that this pattern is different in interneurons (Pape et al., 1994), because the voltage dependencies of I_T and I_A largely overlap. Thus I_A and I_T will tend to be activated together, but the effect of I_A in offsetting and slowing the depolarization will prevent full expression of I_T . The result is that interneurons should rarely express I_T (Pape et al., 1994). However, Zhu et al. (1999) have shown that bursting from low threshold spikes can be elicited in interneurons if a larger activating pulse is given sufficient to overcome I_A .

HYPERPOLARIZATION-ACTIVATED CONDUCTANCE

A conductance that is activated by membrane hyperpolarization and inactivated by depolarization is often associated with the low threshold Ca^{2+} conductance. This *hyperpolarization-activated cation conductance*, leads, via influx of cations, to a depolarizing current, which is called I_h (McCormick and Pape, 1990b). Activation is slow, with a time constant of >200 msec. The combination of I_T , the above mentioned K^+ conductances, and I_h helps to support rhythmic bursting, typically at 3–10 Hz for the low threshold spikes, which is often seen in recordings from *in vitro* slice preparations of thalamus. Hyperpolarizing a cell will activate I_h , but so slowly that I_T fully de-inactivates. Once I_h is activated, it will depolarize the cell, thereby activating I_T . This in turn inactivates both I_h and I_T while activating K^+ conductances, resulting in repolarization. The cycle then repeats. This leads to prolonged rhythmic bursting. This bursting can be interrupted only by a sufficiently strong and prolonged depolarization to produce tonic firing, and appropriate membrane voltage shifts can effectively switch the cell between rhythmic bursting and tonic firing. The significance of these different response modes in thalamic function is considered more fully later.

SYNAPTIC TRANSMISSION

IONOTROPIC AND METABOTROPIC RECEPTORS

Inputs to thalamus operate via conventional chemical synapses, and these in turn influence their postsynaptic targets through transmitter interactions with postsynaptic receptors. As discussed in Chap. 2, these receptors can be divided into two basic types:

ionotropic and *metabotropic*, and both types are found in thalamus (see Fig. 8.3). Although many differences between these receptor types exist, only a few concern us here (for details, see Chap. 2). Ionotropic receptors include AMPA ($[\pm]$ - α -amino-3-hydroxy-5-methylisoxazole-4-propionic acid) and NMDA (*N*-methyl-D-aspartate) receptors for glutamate, GABA_A, and nicotinic receptors for acetylcholine, and these are directly linked to specific ion channels. Transmitter binding leads to a rapid conformational change that opens an ionic channel and produces a postsynaptic potential that is fast, with a short latency (<1 msec) and a brief duration (few tens of milliseconds). Metabotropic receptors include various metabotropic glutamate receptors, GABA_B, and various muscarinic receptors for acetylcholine. These are not directly linked to ion channels. Instead, transmitter binding produces a series of biochemical reactions that ultimately leads to the opening or closing of an ion channel, which, for thalamic cells, is usually a K⁺ channel; when opened, this produces an IPSP as K⁺ flows out of the cell and, when closed, produces an EPSP as K⁺ leakage is reduced. These postsynaptic responses are slow, with a long latency (≥ 10 msec) and a prolonged duration (hundreds of milliseconds or more).

The time course of receptor activation is important with regard to control of I_T and other voltage- and time-dependent processes. Recall that inactivation or de-inactivation of I_T requires that a depolarization or hyperpolarization, respectively, be maintained for $\approx > 100$ msec. This means that the short-lived postsynaptic potentials of ionotropic receptors are ill suited to control the inactivation state of I_T . In contrast, the sustained responses associated with metabotropic receptors are ideally suited for this. That is, EPSPs from activation of metabotropic glutamate or muscarinic receptors are sufficiently sustained to inactivate I_T , and IPSPs from activation of GABA_B receptors are sufficiently sustained to de-inactivate I_T .

Fig. 8.3 shows the transmitters and associated receptor types for the various inputs to thalamus.

GLUTAMATERGIC INPUTS

The retinal and cortical inputs to thalamus are both glutamatergic.

Retinogeniculate (and Other Driving) Inputs. Retinogeniculate axons innervating relay cells (and driving inputs innervating relay cells in other nuclei) activate ionotropic receptors only, not metabotropic ones (Salt and Eaton, 1991; McCormick and Von Krosigk, 1992; Eaton and Salt, 1996; Godwin et al., 1996a), and both AMPA and NMDA receptors are involved. As explained in Chap. 2, for an EPSP to be generated via an NMDA receptor, two events must occur simultaneously: the presynaptic presence of a glutamate-like neurotransmitter coupled with a postsynaptic depolarization sufficient to unblock the channel. As pointed out in Chap. 1, this enables the NMDA receptor complex to act as a sort of molecular *AND* gate (Koch, 1987).

Studies of the lateral geniculate nucleus *in vitro* suggest that the retinogeniculate EPSP controlling action potentials in interneurons also involves only ionotropic glutamate receptors (Pape and McCormick, 1995). However, as noted earlier, this input may be limited to retinal synapses onto relatively proximal dendrites, because the retinal inputs to F2 terminals located in the distal dendritic arbor may have little influence on the soma and spike generating region of the axon hillock. Indeed, evidence indicates

that the retinal input onto dendritic terminals of interneurons activates metabotropic glutamate receptors and possibly also AMPA receptors (Godwin et al., 1996a; Cox and Sherman, 2000).

Corticogeniculate Inputs From Layer 6. Corticogeniculate axons from layer 6 synapsing onto relay cells appear to activate the same types of ionotropic receptors as do retinogeniculate axons. However, in addition to these, the axons from cortex also activate a *metabotropic* glutamate receptor on relay cells (McCormick and Von Krosigk, 1992; Eaton and Salt, 1996; Godwin et al., 1996a; Golshani et al., 1998).

Indirect evidence suggests that layer 6 cortical inputs to interneurons also activate only ionotropic glutamate receptors. That is, the application of metabotropic glutamate agonists does not affect the firing of interneurons (Pape and McCormick, 1995; Cox and Sherman, 2000), suggesting that there are no metabotropic glutamate receptors on proximal dendrites, and this is consistent with immunocytochemical evidence (Godwin et al., 1996a). Also, cortical inputs do not innervate F2 terminals, where metabotropic glutamate receptors are found and are apparently postsynaptic to retinal and cholinergic brainstem inputs (Godwin et al., 1996a; Erişir et al., 1997a; Cox and Sherman, 2000).

Both ionotropic and metabotropic receptors are found on reticular cells (Cox and Sherman, 1999), but it is not clear whether the two main glutamatergic inputs—from cortical layer 6 and thalamic relay cells—each activates one or both types of receptor.

GABAERGIC INPUTS

Thalamic relay cells receive an inhibitory, GABAergic input from cells of the thalamic reticular nucleus and from interneurons. The postsynaptic response to these inputs involves both GABA_A (ionotropic) and GABA_B (metabotropic) receptors (see Chap. 2 for details of IPSPs related to these receptor types).

As noted earlier, reticular cells can respond in both tonic and burst modes. However, on the relay cell, the postsynaptic effect of these modes can be quite different, because tonic firing primarily activates only GABA_A receptors, whereas burst firing often activates GABA_B receptors (Kim et al., 1997; Kim and McCormick, 1998). This is because a cluster of high frequency action potentials in an input is often required to activate metabotropic receptors, whereas single action potentials can often activate ionotropic receptors alone. The difference in the postsynaptic effect in relay cells is that tonic firing of reticular cells will presumably evoke a series of fast and brief IPSPs in the relay cells, but burst firing will evoke slow, prolonged IPSPs. The additional importance of this for firing mode in relay cells is considered in Control of Response Mode.

The functional significance of interneuronal activity is more complicated for two reasons. First, as noted earlier, the question of how common it is for interneurons to fire in burst mode remains controversial. Second, most synaptic outputs of interneurons are dendritic. Clearly, the axonal outputs will follow the firing of the interneuron, but it is not clear what relationship exists between cell firing and the dendritic, F2 terminal activity. If these are electrically isolated from the soma, as has been suggested (Bloomfield and Sherman, 1989; Cox and Sherman, 2000), then there might be no relationship. These F2 terminals might then be controlled solely by local inputs that do not reflect those controlling firing in the cell body and axon hillock. However, it is possible that action potentials in the soma do affect the F2 outputs; for instance, it is

not known whether backpropagation of the action potential exists throughout the dendrites. Thus we are far from understanding how an interneuron's firing affects relay cells.

BRAINSTEM INPUTS

Parabrachial Inputs. In cats, most of the input to the lateral geniculate nucleus from the brainstem derives from the parabrachial region and is cholinergic (de Lima et al., 1985; de Lima and Singer, 1987; Fitzpatrick et al., 1988b, 1989; Raczkowski and Fitzpatrick, 1989; Bickford et al., 1993). Activation of this input in relay cells produces an excitatory postsynaptic potential due primarily to activation of two different receptors (McCormick and Prince, 1987; McCormick, 1989, 1992). The first is a nicotinic (ionotropic) receptor that produces a fast excitatory postsynaptic potential by permitting influx of cations. The second is an M1 muscarinic (metabotropic) receptor that triggers a slow, long lasting excitatory postsynaptic potential. It seems remarkably similar to the metabotropic glutamate response seen from activation of corticogeniculate input (see Corticogeniculate Inputs From Layer 6), and the possibility exists that both metabotropic receptors may be linked to the same second messenger pathway and K^+ channels.

Activation of the cholinergic inputs from the parabrachial region generally inhibits interneurons and reticular cells (Dingledine and Kelly, 1977; Ahlsén et al., 1984; McCormick and Prince, 1987; McCormick and Pape, 1988). This is interesting, because individual parabrachial axons branch to innervate both of these cell groups as well as relay cells and, as noted earlier, these axons excite relay cells. This is accomplished by yet another type of muscarinic receptor, M2, that dominates on these GABAergic targets (McCormick and Prince, 1987; Hu et al., 1989; McCormick, 1989, 1992). Activation of this receptor increases a K^+ conductance, leading to hyperpolarization. The M2 receptor on interneurons is found both on proximal dendrites, allowing parabrachial inputs to affect action potential generation (Plummer et al., 1999; Carden and Bickford, 1999), and on the F2 terminal, which inhibits release of GABA there (Cox and Sherman, 2000). Cells of the thalamic reticular nucleus also respond to this cholinergic input with another, nicotinic receptor that leads to fast depolarization (Lee and McCormick, 1995). Nonetheless, the main effect of cholinergic stimulation of these cells seems to be dominated by the muscarinic, inhibitory response (Dingledine and Kelly, 1977; Ahlsén et al., 1984; McCormick and Prince, 1987; McCormick and Pape, 1988). Because these interneurons and reticular cells inhibit relay cells, activation of this cholinergic pathway thus disinhibits relay cells (see Fig. 8.10).

In addition to acetylcholine (ACh), these axon terminals appear to co-localize nitric oxide (Bickford et al., 1993; Erişir et al., 1997a), a neurotransmitter or neuromodulator with a widespread distribution in the brain (Schuman and Madison, 1991, 1994; Snyder, 1992; Bredt and Snyder, 1992). Relatively little is known concerning the action of nitric oxide in the thalamus, but studies suggest that its release from parabrachial terminals serves two possible roles in the lateral geniculate nucleus: to switch response mode from burst to tonic (Pape and Mager, 1992), perhaps complementing the role of ACh in this regard; and to promote the generation of NMDA responses from retinal inputs (Cudeiro et al., 1994a,b, 1996). Nothing is as yet known about the action of nitric oxide on interneurons or reticular cells.

Other Brainstem Inputs. Other less well understood brainstem inputs to thalamus include noradrenergic axons from cells in the parabrachial region, serotonergic axons from cells in the dorsal raphe nucleus, and histaminergic axons from cells in the tuberomammillary nucleus of the hypothalamus; other inputs unique to specific thalamic nuclei may also occur, such as the GABAergic input from cells from the pretectum to the lateral geniculate nucleus and from the basal ganglia to the ventral anterior nucleus.

Noradrenaline has two very different effects on relay cells, and these effects act through two metabotropic receptors. One effect, via activation of the α_1 adrenoreceptors, produces a long slow EPSP, which promotes tonic firing, much like activation of metabotropic glutamate or M1 muscarinic receptors. The other effect, which operates through the β adrenoreceptors, changes the voltage dependency of I_h in such a way as to increase this depolarizing, voltage-dependent current.

In vitro studies suggest that application of serotonin has no conventional inhibitory or excitatory effect on relay cells (McCormick and Pape, 1990a). However, by operating through an unknown but probably metabotropic receptor, serotonin has the same effect on I_h as that described earlier for noradrenaline (McCormick and Pape, 1990a).

The application of histamine to geniculate relay cells has nearly identical effects to noradrenergic application (McCormick and Williamson, 1991). One effect, operating through an H1 metabotropic receptor, produces a long slow EPSP that also promotes tonic firing (see also Uhlrich et al., 2002). The other effect, which operates through an H2 metabotropic receptor, changes I_h in the same way as do noradrenaline and serotonin.

GATING AND OTHER TRANSFORMATIONS IN THE THALAMIC RELAY

The rich array of membrane properties of thalamic relay cells plus their complex ensemble of inputs from various sources suggests that the relay of peripheral information to cortex is not a simple, or trivial, affair. Instead, it is a complex process that we are just beginning to understand. This is a marked change from earlier views of, for instance, the lateral geniculate nucleus, which was thought to provide a simple, machine-like relay of retinal information to cortex with minor processing added. This will be considered in more depth here both in terms of the different burst and tonic response modes introduced earlier and the role they play in the thalamic relay and also in terms of what we are just beginning to learn about the role of cortical and brainstem inputs in this relay.

BURST AND TONIC RELAY RESPONSE MODES

Signal Transmission During Burst and Tonic Firing. Burst and tonic modes clearly represent two very different types of response to afferent input and thus two very different forms of thalamic relay. In fact, earlier studies suggested that tonic firing represented the only true relay mode and that burst firing, when it occurred, was always characterized by *rhythmic* bursting that was synchronized across large regions of thalamus. This functionally disconnected the relay cell from its primary afferent input, thereby interrupting the relay (Steriade and Llinás, 1988; McCormick and Feeser, 1990; Steriade and McCarley, 1990; Le Masson et al., 2002). The idea was that switching between these modes was accomplished by inputs that changed V_m . Rhythmic bursting was of-

ten seen *in vitro*, and the first *in vivo* studies of the response modes in cats demonstrated that, when the animal entered quiet or non-REM sleep, thalamic relay cells began to burst rhythmically, and that such rhythmic bursting was not seen during awake, alert states (Livingstone and Hubel, 1981; Steriade and Llinás, 1988; Steriade and McCarley, 1990; Steriade et al., 1990, 1993; Steriade and Contreras, 1995).

However, more recent data in lightly anesthetized and awake, behaving animals, including awake humans (reviewed in Sherman, 2001), makes it clear that relay cells can burst arrhythmically and asynchronously in these states and that relay cells in the lateral geniculate nucleus and ventral posterior lateral and medial nuclei still respond in burst mode to sensory stimulation (Fanselow et al., 2001; Swadlow and Gusev, 2001; Nicolelis and Fanselow, 2002). The best examples of such burst responses come from geniculate cells. During spontaneous activity, the cells may often discharge a low threshold spike with a burst response, but these burst discharges occur irregularly. When the cell is then stimulated visually, the cell may produce a burst in response to each presentation of the stimulus, and the bursting under these conditions clearly reflects the external stimulus rather than any intrinsic pacemaker (Guido et al., 1992, 1995; Guido and Weyand, 1995; Mukherjee and Kaplan, 1995; Godwin et al., 1996b; Sherman, 1996, 2001; Ramcharan et al., 2000).

There are thus three different recognizable response modes: rhythmic bursting, arrhythmic bursting, and tonic firing. The first occurs during quiet or non-REM sleep and might also occur during epileptic episodes (Steriade and Llinás, 1988; Steriade and McCarley, 1990); this seems to be associated with an interruption of the relay through thalamus.

The last two occur during the awake state, including drowsiness and fully alert conditions, meaning that both burst and tonic modes can be effective relay modes. However, they differ in the nature of the information relayed. This can be seen with respect to the linearity and signal detectability of the messages relayed to cortex.

Linearity. Note in Fig. 8.14A,B that the very same excitatory stimulus produces two very different signals relayed to cortex, and the difference depends on initial membrane potential of the relay cell, because this determines the inactivation state of I_T . The stimulus in this example is a current pulse, but the same would apply to a sufficiently large EPSP. Because, as noted earlier, the low threshold spike is activated in an all-or-none manner, a larger EPSP will not produce a larger low threshold spike and thus will not produce a larger burst of action potentials (Zhan et al., 2000). This underlies an important difference in input/output relationships between burst and tonic firing, as shown in Fig. 8.14C. This relationship is fairly linear for tonic firing but highly nonlinear for burst firing.

This linearity difference is also seen in the responses of geniculate relay cells to visual stimuli. A clear example is shown in Fig. 8.15A,B, which shows the responses to a drifting sinusoidal grating of a relay cell recorded *in vivo* in an anesthetized cat. When in tonic mode, the cell responds to the grating with a sinusoidal profile (Fig. 8.15D, lower). This means that the response level closely matches the changes in contrast, indicating a very linear relay of this input to cortex. However, when the same stimulus is applied to the same cell, but now in burst mode, the response no longer looks sinusoidal (Fig. 8.15B, lower), indicating considerable nonlinear distortion in the relay.

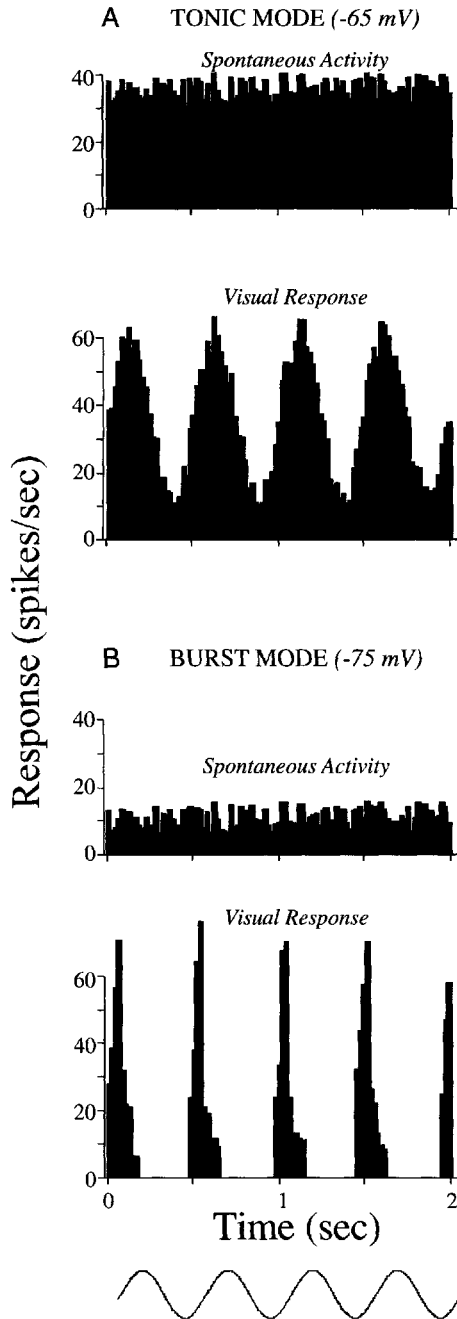


Fig. 8.15. Properties of burst and tonic firing for a relay cell of the cat's lateral geniculate nucleus recorded intracellularly *in vivo*. **A** and **B**: Tonic and burst responses to visual stimulation. Shown in each condition are average response histograms during spontaneous activity (upper) and to four cycles of a drifting sinusoidal grating (lower). The sinusoidal contrast changes resulting from the drifting grating are shown below the histograms. Current injected through the recording electrode was used to bias membrane potential to more depolarized (-65 mV), producing tonic firing (**A**), or more hyperpolarized (-75 mV), producing burst firing (**B**). [Redrawn from Sherman and Guillery, 2001.]

Thus tonic mode is better at preserving linearity in the relay of information to cortex (Sherman, 1996, 2001).

Detectability. The upper histograms of Fig. 8.15A,B show further that spontaneous activity is lower during burst than during tonic firing. Higher spontaneous activity helps to preserve response linearity, because it minimizes rectification of the response to inhibitory phases of visual stimulation, and rectification is a nonlinearity. Perhaps more interesting is the notion that spontaneous activity represents firing without a visual stimulus and can thus be considered a noisy background against which the signal—the response to the visual stimulus—must be detected. Therefore, the signal-to-noise ratio is higher during burst firing, and a higher signal-to-noise ratio implies greater stimulus detectability. This has been confirmed through the use of a method from signal detection theory involving the calculation of *receiver operating characteristic* curves (Green and Swets, 1966; Macmillan and Creelman, 1991) showing that stimulus detectability is improved during burst firing compared with tonic firing (Sherman, 1996, 2001).

Bursting as a “Wake-up Call.” These differences in firing modes concerning linearity and detectability suggest the following hypothesis (Sherman, 1996, 2001). The tonic mode is better for an accurate and faithful relay, because it minimizes the nonlinear distortions created during burst firing. However, the burst mode is better for initial stimulus detectability. As one example, it might be useful during drowsiness to have geniculate relay cells in burst mode to maximize detection of a novel visual stimulus, and after detection, the relay can be switched to tonic firing for more faithful stimulus analysis (for details of this hypothesis, see Sherman, 1996, 2001). Indeed, bursting is more common during drowsiness than during fully alert behavior (Ramcharan et al., 2000; Swadlow and Gusev, 2001), perhaps to maximize the chance of detecting a novel stimulus. Also consistent with this is evidence from studies of the somatosensory thalamus of awake, behaving rabbits that relay cells in burst mode are much more likely to activate their cortical target cells and produce a larger pattern of active cells in cortex than when these relay cells fire in tonic mode (Swadlow and Gusev, 2001; Swadlow et al., 2002). Nonetheless, this notion of bursting as a “wake-up call” remains a hypothesis requiring further testing.

Control of Response Mode. Part of this hypothesis requires thalamic circuitry capable of controlling firing mode, and the circuitry shown in Fig. 8.5 provides this requirement. As noted earlier, to switch between response modes means changing the inactivation state of I_T , and this requires a change in membrane voltage that must be sustained for ≥ 100 msec. Thus a sustained depolarization inactivates I_T , switching the response mode from burst to tonic, and a sustained hyperpolarization de-inactivates I_T , switching the response mode from tonic to burst. Inputs that activate only ionotropic receptors (i.e., driver inputs) produce mainly fast PSPs poorly suited to this task, because without extensive temporal summation, the evoked changes in membrane polarization would be too transient to affect the inactivation state of I_T significantly. However, inputs that activate metabotropic receptors (e.g., all of the modulatory inputs) produce sufficiently sustained PSPs. Thus activation of metabotropic glutamate receptors from cortex or muscarinic receptors from the parabrachial region produces a sustained EPSP that inactivates I_T and switches the firing mode from burst to tonic. Likewise, activa-

tion of GABA_B receptors, from reticular and/or interneuronal inputs, produces a sustained IPSP that de-inactivates I_T and switches the firing mode from tonic to burst (for details, see Sherman and Guillery, 1996, 2001). Evidence indeed exists that activating these various modulatory inputs has these effects on response mode.

Note that the cortical and parabrachial inputs ultimately control firing mode via their direct inputs to relay cells, which promote tonic firing, and their indirect inputs, via reticular and/or interneuron inputs, which promote burst firing. Cortical and parabrachial inputs may have the same cellular effects, but the corticothalamic pathway as well as its reticular and interneuronal relay is topographic and purely unimodal (i.e., visual for the lateral geniculate nucleus, somatosensory for the ventral posterior nucleus, etc.), so that this pathway presumably controls firing mode for discrete thalamic relay cell populations based on such properties as different locations or different class (i.e., X or Y). The parabrachial input is diffusely organized, suggesting more dispersed effects, such as would be relevant for overall levels of attention.

Anatomical Relationship of Modulator Inputs to T Channels. Figure 8.8 shows how the various modulator inputs that control I_T distribute on the dendrites of relay cells. The T channels that underlie I_T are found throughout the cell body and dendritic membranes but are more numerous and denser on dendrites, including peripheral dendrites (Zhou et al., 1997; Destexhe et al., 1998). Thus brainstem and interneuronal inputs, which are located proximally near retinal inputs, can influence membrane voltage there, which not only affect nearby T channels but are also close enough to retinal inputs to directly influence the establishment of retinal EPSPs. In contrast, cortical and reticular inputs are so distally located that they are likely to have less direct influence on retinal inputs (see Fig. 8.11). Instead, they may mainly affect the postsynaptic cell by controlling membrane voltage where voltage-sensitive ion channels, such as T channels, are localized.

OTHER EFFECTS OF NONRETINAL OR MODULATORY INPUTS ON THE THALAMIC RELAY

Although we have focused so far on the role of brainstem and cortical afferents to thalamus in terms of their ability to affect response mode, other roles may be played by these and other inputs regarding thalamic relay properties.

Inputs From the Thalamic Reticular Nucleus. Although thalamic neurons may switch between relay and burst modes at any time during awake, alert behavioral states, the burst mode is more common during less alert periods, including drowsiness and quiet or non-REM sleep (McCarley et al., 1983; Steriade and Llinás, 1988; Steriade and McCarley, 1990; Steriade et al., 1990, 1993; Steriade and Contreras, 1995). During such inattentive periods, the EEG in all mammals, including humans, becomes highly synchronized, and fast, rhythmic spike-like electrical phenomena known as *spindles* can be seen (Fig. 8.16). These spindles have a frequency of 7–14 Hz.

This dominant feature of the synchronized EEG is generated in the thalamus (Steriade and Llinás, 1988). Studies of thalamic neurons have shown that all cells of the thalamic reticular nucleus can spontaneously generate rhythmic discharges at a rate of ≈ 10 Hz. The low threshold spike appears to be a key feature of this endogenous bursting behavior, and the oscillations can be generated within individual reticular cells.

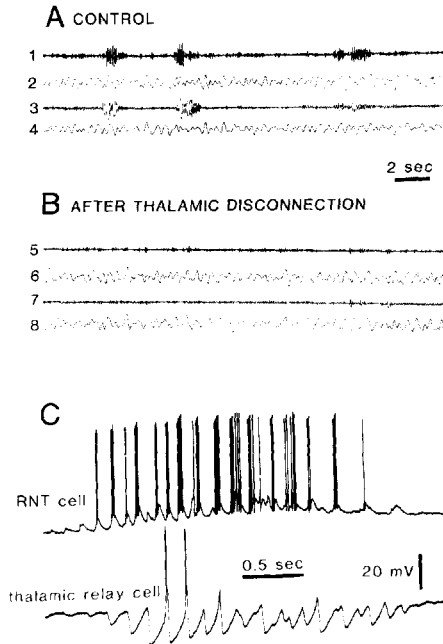


Fig. 8.16. Relationship of thalamus to spindle activity in the cortical electroencephalogram (EEG) of cats. **A** and **B**: Effect on the EEG of rostral thalamic transections that disconnect the thalamus from the cortex. The numbering of traces is as follows: 1 and 5, higher frequency EEG (7–14 Hz) for right hemisphere; 2 and 6, lower frequency EEG (0.5–4 Hz) for right hemisphere; 3 and 7, higher frequency EEG (7–14 Hz) for left hemisphere; 4 and 8, lower frequency EEG (0.5–4 Hz) for left hemisphere. Normally (**A**, before transection), each hemisphere shows activity in both the higher (7–14 Hz) and lower (0.5–4 Hz) filtered traces. After transection (**B**), the higher frequencies are selectively eliminated from the EEG. [Revised from Steriade et al., 1987.] **C**: Activity of thalamic neurons during an EEG spindle. During the spindle, the TRN neuron (top) undergoes a long-lasting, slow depolarization that elevates its firing rate. In contrast, a thalamic relay cell (bottom) is hyperpolarized rhythmically, and the rebound from these hyperpolarizations often lead to low threshold Ca^{2+} spikes. The elevated firing in the TRN cell seems to cause the rhythmic hyperpolarizations in the relay cell. [A and B revised from Steriade et al., 1987; C revised from Steriade and Llinás, 1988.]

Also, groups of deafferented reticular neurons can generate such synchronized oscillatory activity in the absence of external input (Steriade et al., 1987; Steriade and Llinás, 1988). Reticular neurons are connected to other reticular cells via collaterals of the axon that innervates dorsal thalamus and by electrical contacts (Landisman et al., 2002), and these connections could serve to synchronize entire reticular regions; dendrodendritic synapses may also exist among reticular neurons to further synchronize these cells (Steriade et al., 1987; Steriade and Llinás, 1988; Pinault et al., 1997).

Because reticular neurons provide an inhibitory, GABAergic input to thalamic relay cells, the thalamic reticular nucleus entrains its oscillatory activity onto these relay cells. That is, the synchronized bursts of reticular activity would lead to waves of hyperpolarization among relay cells; this would de-inactivate low threshold spikes in the relay cells, and they would synchronously enter the burst mode. By themselves, neu-

rons in the lateral geniculate or in other thalamic nuclei do not spontaneously generate spindle rhythmicity; disconnecting the projection cells from the reticular nucleus by surgical or chemical means abolishes the oscillations (Steriade et al., 1987; Steriade and Llinás, 1988). Thus this feature of synchronized, rhythmic bursting among relay cells, which is associated with inattentive and unconscious states and interruption of the thalamic relay, depends critically on the reticular nucleus.

Brainstem Inputs. Non-REM sleep and spindle activity is associated with quiescence among many of the cholinergic inputs to the thalamus from the parabrachial region (Steriade and Contreras, 1995). It thus seems plausible that increasing activity of these inputs will serve to terminate the synchronized, rhythmic activity and restore relay cell responses to tonic or arrhythmic burst firing. Indeed, there is ample evidence that activity in brainstem afferents is associated with more alert behavioral states. More to the point, modulatory inputs to the thalamic reticular nucleus from the parabrachial region can inhibit reticular cells and thereby break their hold on relay cells, halting the synchronized, rhythmic bursting and restoring functional relay properties (Le Masson et al., 2002).

There is also evidence that eye movements can affect the geniculate relay (Büttner and Fuchs, 1973; Noda, 1975; Bartlett et al., 1976; Lal and Friedlander, 1989; Guido and Weyand, 1995; Ramcharan et al., 2001). Both saccades and passive movement of the eye can have such effects. Although the details for this have yet to be worked out, it seems likely that these effects are accomplished via brainstem afferents to thalamus.

Cortical Inputs From Layer 6. As noted earlier, the corticogeniculate input is both massive and heterogeneous. It is thus plausible that it subserves several distinct functions. Perhaps this is why earlier attempts to identify any *single* function for this “feedback” pathway have led to confusing and conflicting conclusions. For instance, some studies suggest that the corticogeniculate pathway facilitates relay cell firing, whereas others suggest the opposite (Kalil and Chase, 1970; Baker and Malpeli, 1977; Schmielau and Singer, 1977; Geisert et al., 1981; McClurkin and Marrocco, 1984; McClurkin et al., 1994). The large number of layer 6 inputs suggests that this feedback could be highly specific to receptive field location, orientation, direction of motion, and ocularity. Mumford (1994) has developed a detailed framework, based on ideas from machine vision, in which the detection of weak or incomplete stimuli under noisy conditions (think of a gray mouse at dusk viewed by a cat) would be enhanced by such feedback. In this context, it should be pointed out that the vast majority of experiments carried out in the lateral geniculate nucleus have involved anesthetized animals stimulated with single bars or gratings on a blank background, not a situation that might be expected to activate the type of feedback function suggested by Mumford (1994).

Schmielau and Singer (1977) have proposed that corticogeniculate input is important to binocular functions, such as stereopsis. Several studies have identified a role for the corticogeniculate input in controlling inhibitory surrounds of geniculate relay cells (reviewed in Sillito and Jones, 2002). More recent studies have suggested that the pathway affects temporal properties of relay cell discharges (McClurkin et al., 1994) or establishes correlated firing among nearby relay cells with similar receptive field properties (Sillito et al., 1994). Earlier we suggested that this input serves to control

response mode, tonic or burst, of the relay cells. Given the likelihood that the cortico-geniculate pathway is heterogeneous, these different suggestions for its function are not incompatible, and more functions may yet emerge.

A recent study suggests an additional possible role for layer 6 cortical input. When fairly balanced excitatory and inhibitory modulatory inputs increase, there is no major net effect on membrane potential, but the increasing synaptic conductance will lower neuronal input resistance and render driver inputs less effective; this is a form of gain modulation (Chance et al., 2002). That is, the lower input resistance due to the increased synaptic conductance would mean that driver EPSP amplitudes were reduced. Because activation of cortical axons can in many cases lead to a conjoint increase in excitation (through direct inputs) and inhibition (through activation of reticular cells or interneuron), the corticothalamic pathway may also play such a role in gain modulation. If this were the case, the effect would be that increasing activity in the corticothalamic axons would lead to reduced synaptic efficacy of driver inputs to relay cells.

An example of how this might operate comes again from the lateral geniculate nucleus; this would serve as a mechanism for contrast gain control. Higher contrast in the retinal image leads to increased firing of retinal axons, and this in turn leads to increased firing levels in geniculate relay cells. If the firing becomes too high and approaches saturation, the relay becomes nonlinear and can no longer signal further increases in input firing levels. However, this very increase in firing of relay cells could plausibly lead to increased activity in the target cortical area, including the cortico-geniculate feedback. The increased firing in the feedback would serve, as indicated in the preceding paragraph, to reduce the gain of the retinogeniculate synapse, thereby down-regulating the sensitivity of the relay and keeping it in its linear range.

DRIVERS AND MODULATORS

It is clear when we look at the innervation of relay cells that a wide variety of inputs is present, and they represent quite different functions. This is clearest for relay cells of the lateral geniculate nucleus, and we will look at this nucleus to explore part of the functional significance of these different inputs. We know that the function of geniculate relay cells is to transfer retinal information to cortex, yet retinal input represents only a small fraction of all synapses found on these relay cells. If retinal input is what is being relayed, and can be set apart, what are the other inputs doing?

One of the main reasons that we know retinal input is being relayed is that it is necessary and sufficient for the receptive fields of geniculate relay cells, and these receptive fields indicate the sort of information being relayed to cortex. There are two parts to this. First, the receptive fields of retinal ganglion cells innervating the lateral geniculate nucleus are virtually the same as those of the relay cells (reviewed in Lennie, 1980; Sherman, 1985), which in turn are quite unlike the receptive fields of nonretinal inputs, such as those from cortex or brainstem (e.g., Gilbert, 1977; Murphy et al., 1999). Second, removing cortical (Gilbert, 1977; Murphy et al., 1999) or brainstem (Meulders and Godfraind, 1969; Wróbel, 1981) inputs to relay cells has only quite subtle effects on geniculate receptive fields, whereas removing retina necessarily obliterates them. We have referred to the input to thalamus that brings the information to be relayed as the *driver* input, and all others as *modulatory* input, with the latter serving to

modulate thalamic transmission of driver input. Drivers and, by elimination, modulators can also be readily recognized for the main somatosensory and auditory thalamic relays on the basis of functional arguments parallel to those presented for the visual pathways, and also on the basis of the common light and electron microscopic structures and relationships of these several drivers.

However, assignment of various inputs to these classes in many thalamic relays is less clear and must be based on incomplete evidence. One approach here is to look at other differences between drivers and modulators in the lateral geniculate nucleus and, where known, also in the ventral posterior nuclei and ventral portion of the medial geniculate nucleus. These are as follows (for details, see Sherman and Guillery, 1998):

1. Driver (retinal) inputs to relay cells provide the main receptive field properties and are necessary for the existence of the receptive fields, whereas modulator inputs induce only subtle changes in receptive field properties.
2. Driver inputs end in RL terminals, which, as noted earlier, are by far the largest in the neuropil, and each typically provides several different contact zones onto the same postsynaptic profile. This might help explain the great synaptic strength of drivers. The smaller modulator terminals seldom have more than one synaptic contact zone each. Driver inputs vary in their relationships to interneurons but otherwise show essentially the same structure throughout the thalamus.
3. Despite the small number of driver synapses, driver EPSPs are relatively large, suggesting relatively strong synapses.
4. Driver inputs provide a minority of synapses to relay cells (only 5%–10% come from retina).
5. Driver terminals are limited to proximal dendrites and often form triadic synaptic arrangements in glomeruli, whereas modulator terminals can be found anywhere on the dendritic arbor.
6. As a general rule, inhibitory inputs make poor drivers (Smith and Sherman, 2002), and thus drivers are all likely to be excitatory (and probably glutamatergic).
7. Driver inputs activate only ionotropic glutamate receptors, whereas modulator inputs can activate metabotropic receptors and often also ionotropic receptors; this means that drivers do not act slowly, a point elaborated later.
8. There is relatively little convergence of driver inputs, so that, for instance, geniculate relay cells receive most retinal synapses from one to three axons, whereas the number of corticogeniculate axons converging onto a relay cell is at least an order of magnitude greater and probably very much greater than that.
9. As a result of many of these points, the *cross-correlogram* (the probability of a spike in the postsynaptic cell for each spike in the presynaptic axon) has a relatively sharp, narrow peak for driver inputs but not for modulator inputs.
10. Driver inputs do not innervate the thalamic reticular nucleus, whereas modulator inputs do.

These criteria cannot usually be applied to all thalamic relays: for instance, it is not clear how the receptive field criterion might be applied to nonsensory relays. However, other criteria, such as the size of afferent terminals, the location of terminals in the dendritic arbor, whether the thalamic reticular nucleus is innervated by collaterals, and

the nature of associated postsynaptic receptors, can give clues as to which set of afferents to a thalamic relay might be the drivers.

The fact that driver inputs activate only ionotropic receptors has several important functional implications. Consider retinal inputs, for example. They will activate only ionotropic glutamate receptors, ensuring a relatively fast, short duration EPSP. This permits fast changes in the spike pattern of the retinal afferents to be encoded in the pattern of EPSPs. If, instead, retinal axons were to activate metabotropic glutamate receptors, the sustained EPSP would serve to obscure fast changes in the afferent firing rate, acting like a low pass temporal filter that eliminates higher frequency information. Thus the lack of metabotropic glutamate receptors at the retinogeniculate synapse helps to ensure a wider range of temporal information in the relay to cortex. However, this also means that the fast EPSPs evoked would not serve well to control neuronal voltage-dependent properties with longer time courses, such as I_T underlying the burst firing mode; as noted earlier, such properties are better controlled by modulators and their activation of metabotropic receptors.

Another important point in this distinction between drivers and modulators can be seen in numbers. The relatively small numbers of drivers means that it does not require the large synaptic numbers characteristic of a thalamic relay to convey the basic information carried by a sensory or other driver pathway. However, the large number of modulator synapses is in keeping with the many forms of subtle modulation of thalamic relays these inputs perform. Furthermore, there is a lesson here that numbers alone can be misleading. That is, if only the anatomical numbers of inputs to geniculate relay cells were known, the roughly one-third that come from the parabrachial region would seem huge compared with the 5%–10% from retina, with the likely result that one would be tempted to conclude that the lateral geniculate nucleus relays parabrachial, and not retinal, information to cortex. The point is that it is not the quantity of the input that counts but rather its nature, particularly with regard to driver versus modulator function.

Finally, this driver/modulator distinction may apply beyond thalamus and perhaps into cortical circuitry as well. For instance, the geniculocortical synapse has many of the above features of a driver (Ahmed et al., 1994, 1997; Reid and Alonso, 1995, 1996; Stratford et al., 1996): large axons and terminals; small synaptic numbers (only 6% of synapses on layer 4 cells derive from geniculate axons, a number suspiciously close to the contribution of retinal inputs to the synapses on geniculate relay cells); synaptic location on proximal dendrites; large EPSPs, relatively little convergence, and cross-correlograms with a sharp, narrow peak. This is considered further in the next section.

FIRST ORDER AND HIGHER ORDER RELAYS

We indicated in the introduction that there is a basic distinction between first order and higher order relays. Higher order relays receive driving afferents from cells in layer 5 of the cerebral cortex, whereas first order relays receive their driving afferents from a variety of noncortical sources. Figure 8-1 shows the thalamic nuclei that represent first order relays and those that are entirely or predominantly higher order. Two points should be noted. One is that this classification applies to specific thalamic relays, rather than to thalamic nuclei. Although there are nuclei like the lateral geniculate nucleus or the

ventral part of the medial geniculate nucleus that are essentially pure first order relays, there are also reasons for believing that in many nuclei one will find a mixture of first and higher order relays. The second point is that "first order" refers to the fact that these relays transmit information that is on its way to the cortex for the first time. We have used "higher order" rather than "second order" because many of the corticothalamic drivers that innervate the higher order relays will be representing loops that are bringing messages for a third or fourth or higher order re-presentation to cortex.

The nuclei that are not shaded in Fig. 8-1 were long regarded as "association nuclei." This was not because anyone had traced pathways that might serve to provide the implied sensory associative functions; it was camouflage for ignorance. No one knew what sort of messages these nuclei might be transmitting to cortex, even though for most of them the general details of the thalamocortical projection pattern had been well defined (e.g., Walker, 1938). The first indication that the driving afferents to these nuclei might be coming from cortex rather than from other diencephalic centers came from the demonstration that in the monkey pulvinar region the RL terminals, which correspond to the drivers in first order nuclei (see *The Electron Microscopic Appearance of the Neuronal Elements*) degenerated after lesions of visual cortex (Mathers, 1972). Further autoradiographic and degeneration studies confirmed this for the pulvinar region (Robson and Hall, 1977; Ogren and Hendrickson, 1979) and also for a pathway from frontal cortex to the mediodorsal nucleus in monkey (Schwartz et al., 1991). More evidence came from an electrophysiological demonstration of a corticocortical pathway linking visual cortical areas through the lateral posterior nucleus of the cat (Kato, 1990). Light microscopic evidence about the structure of the driver afferents to higher order relays did not become available until it was possible to fill single axons, or small groups of axons, and identify the structure of the terminals in the thalamus, thus distinguishing type 1 from type 2 axons (see Fig. 8.6). It then appeared that injections of cells in layer 5 of cortex produced labeled axons having the appearance of type 2 axons (Hoogland et al., 1991; Deschênes et al., 1994; Ojima, 1994; Rockland, 1996), whereas injections in layer 6 produced labeled axons having the appearance of type 1 axons. The former match the structure of the (ascending) drivers of first order relays and do not go to first order relay nuclei like the lateral geniculate nucleus, whereas the latter correspond to the corticothalamic modulators found in first order relays and are represented in all thalamic nuclei. It is important to note that in many instances the type 2 axons from layer 5 have a strictly localized thalamic terminal distribution, showing a far more limited terminal field than the type 1 axons coming from layer 6 of the same cortical column (Bourassa et al., 1995; Darian-Smith et al., 1999; Guillery et al., 2001). This is in contrast to a recent claim that the layer 5 afferents have diffuse thalamic terminals (Jones, 2002).

The evidence about the origin of the layer 5 and layer 6 corticothalamic axons was in accord with observations of retrogradely transported label. That is, injections of the first order relays marked cortical cells in layer 6 only but marked cells in layers 5 and 6 after injections into higher order relays (Gilbert and Kelly, 1975; Abramson and Chalupa, 1985).

Apart from the details of their synaptic organization that were considered earlier, there are two further telling parallels between the ascending drivers to first order nuclei and the corticothalamic drivers to higher order nuclei. Neither has branches with

terminals in the thalamic reticular nucleus, and both very commonly have branches that innervate lower levels of the brain stem or spinal cord (see *How Does the Thalamus Relate to Motor Outputs?*).

We have indicated that one important distinction between drivers and modulators is that silencing the drivers abolishes the characteristic receptive fields of thalamic relay neurons, whereas silencing the modulators does not. That is, for the lateral geniculate nucleus, destruction or silencing of visual cortex produces subtle changes in receptive field properties, but the visual receptive fields survive. This is in contrast to silencing retinal ganglion cells, which produces a complete loss of geniculate receptive fields. The same argument can be applied to higher order nuclei. Recordings from thalamic relay cells in two higher order relays (the pulvinar region of the monkey and the posterior nucleus of the rat) have demonstrated that lesions of the cortical areas that provide layer 5 (type 2) afferents to the relay cells produce a loss of receptive fields, comparable to the loss seen in first order relays after removal of the ascending driver afferents (Bender, 1983; Chalupa, 1991; Diamond et al., 1992).

The receptive field properties that have been reported for cells in the pulvinar region resemble those of cells in layer 5 of visual cortex, further supporting the idea that the layer 5 cells provide the driving input to the pulvinar cells. However, the situation is complicated because there are several separate cortical areas that provide driving afferents to any one small area of the pulvinar region (Guillery et al., 2001), and it is reasonable to expect each area to provide somewhat different functional properties to the pulvinar cells. That is, cells in the pulvinar region receiving from layer 5 inputs that come from different cortical areas and have distinct functions are likely to be intermingled, as are X cells and Y cells in the A layers of the cat's lateral geniculate nucleus. For anesthetized animals, there are reports of cells with receptive field properties resembling those of area 17 (Chalupa and Abramson, 1989; Merabet et al., 1998; Casanova et al., 2001) or of cortical area MT (Merabet et al., 1998). For awake behaving monkeys, there are reports of cells resembling cells in cortical area 5a that respond for reaching movements of the hand (Cudeiro et al., 1989; Acuña et al., 1990). Tellingly, in the relevant part of the pulvinar only about 16% show this property, indicating that there are other cells with different properties in the same region, and suggesting that, perhaps, if each functionally distinct class represents only about 16% of the cells, then there is room for a significant number of functionally distinct classes. The issue of whether there is any interaction among pathways in the pulvinar region, involving elaboration of receptive field properties, or whether, like the lateral geniculate nucleus, the pulvinar cells provide independent straight through pathways to cortex remains to be defined.

The recognition of corticothalamic driver afferents to higher order relays has vitally important implications for our understanding of thalamocortical and corticocortical relationships and functions (Guillery, 1995; Sherman and Guillery, 1998, 2001, 2002; Guillery and Sherman, 2002a). The thalamus is no longer seen as essentially just a relay for ascending messages to reach the cortex, with all subsequent cortical processing carried out by a complex array of hierarchical and parallel corticocortical pathways as shown in Fig. 8.17A (Felleman and Van Essen, 1991; Van Essen et al., 1992; Purves et al., 1997; Kandel et al., 2000). Instead, recognition of transthalamic corticocortical pathways through higher order thalamic relays introduces an array of novel connec-

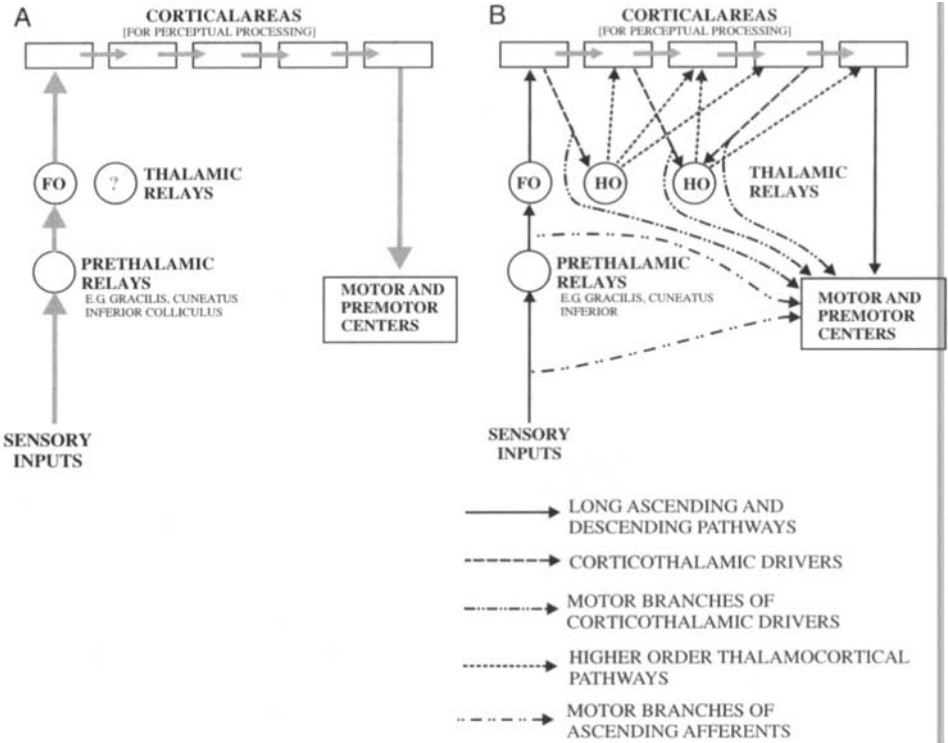


Fig. 8.17. Schematic representation of thalamocortical relationships. **A:** Conventional view of thalamocortical processing in relation to motor outputs. **B:** Connections documented here, showing the transthalamic corticocortical pathways and the connections to motor centers at all levels of the classic sensory pathways. Abbreviations: FO, first order relay; HO, higher order relay. Further details in the text.

tions through which one cortical area can communicate with another (Fig. 8.17B). Each of these transthalamic corticocortical pathways will be subject to the modulatory influences that play such a dominant role in the synaptic organization of thalamic relays. That is, for each transthalamic corticocortical pathway, there will be opportunities for cortical and for brainstem modulatory influences as well as for local inhibitory influences to act.

Every area of neocortex receives afferents from the thalamus. For primary receiving areas like visual, auditory, or somatosensory cortex, we can claim a fair understanding of the nature of the thalamic inputs, and it is easy to appreciate that the dominant, or only, function of these cortical areas is the processing of information that comes from the thalamus. The possibility that the same holds for other cortical areas has not been explored. In fact the thalamic inputs to these other areas are generally ignored as experiments that concern perceptual processing or movement control are studied.

HOW DOES THE THALAMUS RELATE TO MOTOR OUTPUTS?

The relationship of the thalamus to sensory mechanisms at first sight looks relatively straightforward. Messages from each of the major classes of sensory receptor pass through the first order thalamic relays and onto primary receiving areas of the cortex, being exposed to the modulatory inputs discussed earlier. From there, on the view of intracortical perceptual processing discussed earlier (see Fig 8.17A), the sensory messages are passed through a hierarchical series of cortical areas with no further thalamic modulation and then are passed to areas concerned with motor outputs. On the transthalamic view of perceptual processing, the messages are passed to other cortical areas through one or more higher order thalamic relays and are subject to modulatory influences at each pass through the thalamus. The transthalamic pathways also introduce an important link between sensory and motor pathways that is not represented in the intracortical pathways. This link is provided by the driver afferents to thalamus that come from layer 5 of cortex, because, as we have seen, these afferents also have long descending axons, and these innervate motor or premotor structures. There are two ways of viewing this link. One is that at each stage of the transthalamic pathway the motor system receives inputs that relate to the ongoing perceptual processing. A second is that the transthalamic pathway for perceptual processing is based on corticothalamic driver messages from layer 5 that represent copies of motor instructions. These are not mutually exclusive mechanisms; they are alternative ways of interpreting the same close functional links between the sensory and the motor systems.

These links not only can be seen in the higher order thalamic relays involved in the transthalamic corticocortical pathways but are also well represented in the first order thalamic relays that carry messages to primary receiving areas of cortex. The evidence concerning the motor links of driving afferents to the thalamus, which was reviewed in detail (Guillery and Sherman, 2002b), will be briefly summarized, first for first order thalamic relays and then for the higher order relays.

MOTOR LINKS OF FIRST ORDER AFFERENT DRIVERS

These are well illustrated by the visual pathways, where one finds that most or all of the retinal afferents that go to the lateral geniculate nucleus also send a branch to the superior colliculus or the pretectum. For rodents and rabbits, the evidence that all of the retinogeniculate axons are branches of axons that also go the midbrain is strong (Chalupa and Thompson, 1980; Vaney et al., 1981; Jhaveri et al., 1991). For the cat, there is wide agreement that the Y cells and W cells all send branches to the midbrain (Fukuda and Stone, 1974; Wässle and Illing, 1980; Leventhal et al., 1985), but the branching pattern of the X cells has proved somewhat more difficult to demonstrate because these cells send quite thin branches to the pretectum, which have been demonstrated by intracellular injections of relatively small tracer molecules (Tamamaki et al., 1994). These studies of the retinopretectal branches of X cells in the cat lead to two important conclusions. One is that in the cat all retinogeniculate axons are likely to be branches of axons that also innervate the midbrain, and the second is that negative evidence about the presence of a branch cannot be interpreted as evidence for the absence of such a branch. The methods that are available, whether anatomical or phys-

iological, are not sufficiently robust to allow any interpretation of a negative result (see also Lu and Willis, 1999). The evidence for the monkey shows that the magnocellular and koniocellular pathways have branches that go to the midbrain. The evidence for the parvocellular pathways is less clear, although the occasional report of a midbrain connection suggests that these may be like the cat's X cell axons—present but thin and difficult to demonstrate.

In the past the retinotectal branches were often viewed as an alternative, extrageniculate pathway to the cerebral cortex, reaching extrastriate cortical areas along tectopulvinocortical connections (Sprague, 1966, 1972; Schneider, 1969; Sprague et al., 1970; Diamond, 1973). This view of the tectal connections cannot be entirely ruled out, but it is relevant that receptive fields of cells in the pulvinar region are lost after lesions of visual cortex but are not lost after lesions of the tectum. That is, the cortical inputs to the pulvinar region are more likely to be the drivers than are the tectal inputs. No matter what may be the action of the tectal pathway on the pulvinar cells, the input to the superior colliculus and pretectum must produce some change in these motor centers themselves, and that is the point that is relevant for appreciating that activity in the retinogeniculate pathway will almost invariably be accompanied by activity in the pathways to the midbrain.

Evidence for other first order relays also shows that many of the axons going to the thalamus have branches going to lower, motor centers, or else the cells that give rise to these axons are innervated by axons that have such branches. The anterolateral pathways concerned with pain and temperature give off many branches at the level of the spinal cord and play a significant role in spinal reflexes before they reach the thalamus (Lu and Willis, 1999). The axons of the dorsal roots that enter the posterior columns and contribute to the spinal levels of the lemniscal pathways similarly have many intraspinal branches. At the next synaptic relay in the posterior columns and lateral cervical nucleus, there are many cells that contribute to centers other than the thalamus, several of them doing so via branches of the axons that also go to the thalamus (Berkley, 1975; Craig and Burton, 1979; Feldman and Kruger, 1980; Djouhri et al., 1997). Similarly, there is evidence that axons going from the deep cerebellar nuclei to the ventrolateral nucleus also send branches to the brain stem (Cajal, 1911; Tsukahara et al., 1967; Shinoda et al., 1988), and the axons that come from the mamillary bodies and innervate the anterior thalamic nuclei also have branches that travel in the mamillothalamic tract to regions of the brain concerned with eye movement control and vestibular mechanisms (Kölliker, 1896; Cajal, 1911; Guillery, 1961; Torigoe et al., 1986). There is only limited information about the details of branching patterns in the auditory pathways, but it is relevant to note that the inferior colliculus, which sends driver afferents to the medial geniculate nucleus, also sends afferents to the superior colliculus (Harting and Van Lieshout, 2000).

MOTOR LINKS OF HIGHER ORDER AFFERENT DRIVERS

Evidence that corticothalamic axons from layer 5 pyramids that innervate higher order thalamic relays are branches of axons that also pass to lower centers in the brainstem comes from injections that label single cortical cells or small groups of cortical cells and that allow the individual axons to be traced through the thalamus. Several studies, including studies in cat, rat, and monkey, of pathways involving visual and so-

matosensory systems (Bourassa et al., 1995; Bourassa and Deschênes, 1995; Rockland, 1996) have demonstrated that the axons from layer 5 have thalamic branches with characteristic well localized thalamic terminals that look essentially like retinal or lemniscal terminals. Like these other driver afferents, they do not send branches to the thalamic reticular nucleus, but they commonly, possibly always (Guillery et al., 2001), have long descending branches that go to the midbrain or pons or farther caudally. Currently, we know very little about the functional properties of the cells that come from layer 5, especially in regard to the possible actions of the long descending pathways. It is possible that knowledge about the role of these long descending axons would help to illuminate the nature of the message that is being sent to the higher order relays in the thalamus.

RELATIONSHIPS OF SENSORY PERCEPTION TO MECHANISMS OF MOTOR CONTROL

The axons that provide driver afferents for the thalamus from the cerebral cortex or from lower centers cannot be considered as providing a dedicated *sensory* line from periphery or from cortex to the appropriate thalamic nucleus. Instead, they all, or almost all, represent a system that is concurrently feeding the same information to the thalamic relay and to one or another center concerned with *movement control*. When the thalamic pathways are viewed in this light, the messages passing through the thalamus to cortex for perceptual processing can be seen as providing information to cortex about how the body is currently being prepared to react to sensory inputs. The information that is classically treated as “sensory” information, providing the cortex with information about what is really out there in the perceived world, is also information that is serving to control the organism’s immediate responses, and this may be of primary relevance for the survival of the organism (Guillery, 2003).

SUMMARY

It has long been clear that the thalamus plays a crucial role in information transfer to cortex. Evidence shows that, in addition, it is an important part of ongoing communications between cortical areas. This puts the thalamus at the very core of cortical processing. Furthermore, the information, whether ascending or corticocortical, is not relayed through the thalamus in a simple, passive, machine-like manner, but rather is a complex process that keeps the nature and extent of information transfer under dynamic control. The complexity is evident in the fact that a vast majority of synaptic inputs to relay cells do not come from the drivers, the main source of information to be relayed to cortex, but from modulatory sources, including, among others, inputs from local GABAergic cells, inputs from cortex, and inputs from the brainstem. Further, there is increasing evidence that for most, possibly all, thalamic relays, the message that is relayed, whether from the periphery through a first order thalamic relay or from one cortical area to another through a higher order relay, comes from a branching axon that is concurrently sending the same message to motor centers. This in turn suggests that all thalamocortical relays, even the classic “sensory” relays like the lateral geniculate nucleus, function to provide to the cortex not so much a picture of the world that is thought to be represented in the sensory pathways but rather a constant updating of motor commands that are currently being issued at many different levels in response to the sensory inputs.

This page intentionally left blank

BASAL GANGLIA

CHARLES J. WILSON

The basal ganglia are a richly interconnected set of brain nuclei found in the forebrain and midbrain of mammals, birds, and reptiles. In many species, including most mammals, the forebrain nuclei of the basal ganglia are the most prominent subcortical telencephalic structures. The large size of these nuclei, and their similarity in structure in such a wide range of species, make it likely that they contribute some very essential function to the basic organizational plan of the brain of the terrestrial vertebrates. However, the assignment of a specific functional role for the basal ganglia has been difficult, as it has for other brain structures that have no direct connections with either the sensory or motor organs.

The most widely accepted views of basal ganglia function are based on observations of humans afflicted with degenerative diseases that attack these structures. In all cases these diseases produce severe deficits of movement. None of the movement deficits is simple, however, or easily described. In some, such as Parkinson's disease, movements become more difficult to make, as if the body were somehow made rigid and resistive to changes in position. In others, such as Huntington's disease, useless and unintended movements interfere with the execution of useful and intended ones. In general, these symptoms affect only voluntary, purposive movements, with reflexive movements being relatively unaffected. These observations have led most clinical investigators to view the basal ganglia as components of a system that is somehow involved in the generation of goal-directed voluntary movement but in complex and subtle aspects of that process. Current views based on experimental studies suggest a more general role for the basal ganglia in selection among candidate movements, goals, strategies, and interpretations of sensory information. In such views, the basal ganglia make these selections based on the past history of success under similar circumstances.

The anatomical connections of the basal ganglia link it to elements of the sensory, motor, cognitive, and motivational apparatus of the brain. These connections are best appreciated within the context of the arrangement of the several nuclei that make up the basal ganglia. A diagram showing the arrangement of the most prominent of these nuclei as they appear in a frontal section of the human brain is shown in Fig. 9.1. The major structures are the caudate nucleus, putamen, globus pallidus (GP), substantia nigra, and subthalamic nucleus. Also seen in the diagram are the two largest sources of input to the basal ganglia: the cerebral cortex and the thalamus.

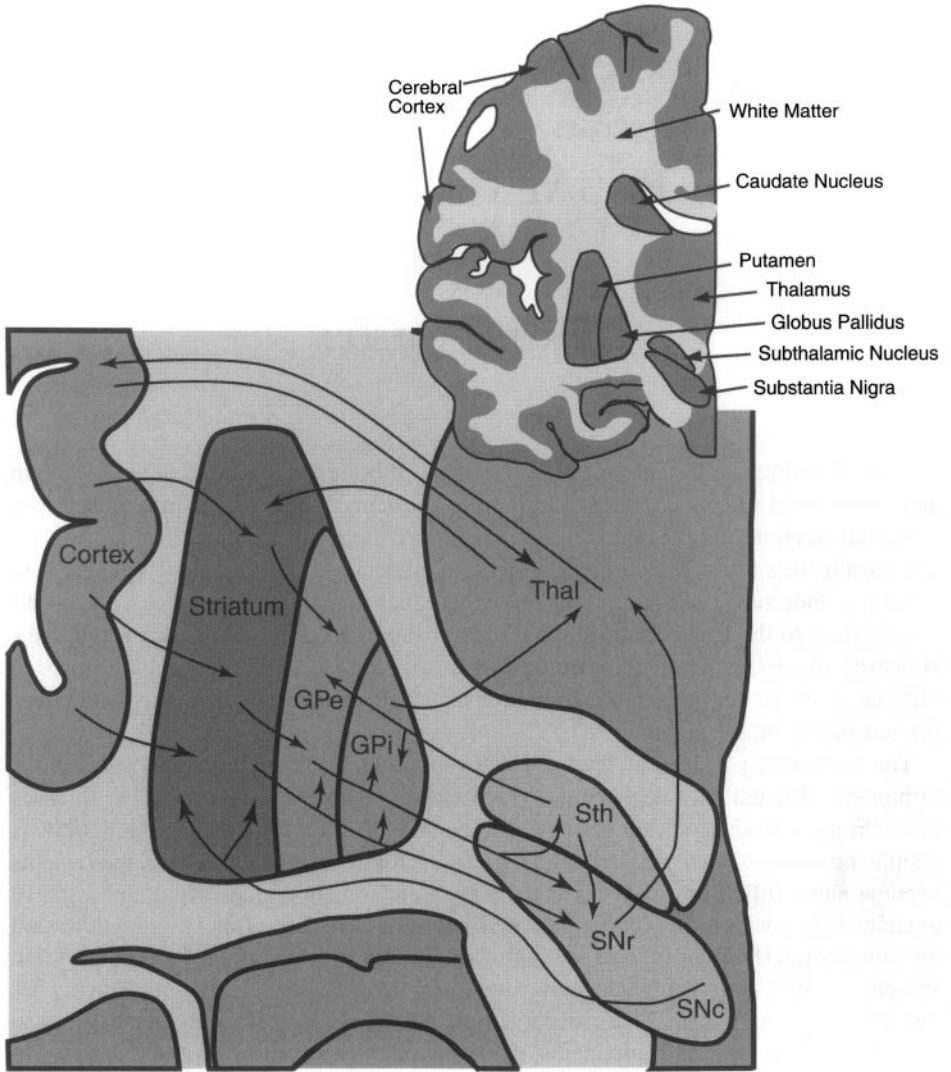


Fig. 9.1. Schematic representation of a transverse section through a human brain hemisphere showing the sizes and locations of several important components of the basal ganglia, and connections among them. Abbreviations: GPe, globus pallidus, external segment; GPi, globus pallidus, internal segment; Thal, thalamus; Sth, subthalamic nucleus; SNr, substantia nigra, pars reticulata; SNc, substantia nigra, pars compacta.

Several of the major connections between these structures are shown in Fig. 9.1. In dealing with this complexity, it is helpful to focus on the overall direction of information flow. Most of the input to the basal ganglia from other brain structures arrives in the *neostriatum*, which consists of the caudate nucleus, putamen, and nucleus accumbens. Within the caudate nucleus and the putamen, inputs from sensory, motor, and association *cortical* areas converge with inputs from the *thalamic* intralaminar nuclei,

dopaminergic inputs from the *substantia nigra pars compacta* (SNc), and serotonergic inputs from the *dorsal raphe* nucleus (not shown). Not shown are analogous connections arising from the limbic cortex and hippocampus, dopaminergic inputs from the ventral tegmental area, converging in a third striatal structure, the nucleus accumbens. These three input structures of the basal ganglia (caudate nucleus, putamen, and nucleus accumbens) are very similar in their internal structure. In the connectational diagram in Fig. 9.1, the putamen has been used to represent the entire neostriatum.

The output from the neostriatum projects exclusively to other basal ganglia structures. The main targets of these axons are three nuclei: the *external segment* of the *globus pallidus* (GPe), the *internal segment* of the *globus pallidus* (GPi), and the *pars reticulata* of the *substantia nigra* (SNr). These three structures are very similar in their cellular organization. Two of them, the GPi and the SNr, project to structures outside the basal ganglia and provide the main output pathways for the results of neuronal operations performed within the nuclei. Their targets are primarily in the *thalamus* (mostly in the ventral tier thalamic nuclei that project to frontal areas of the cortex), *lateral habenular nucleus*, and deep layers of the *superior colliculus*. For simplicity, only the thalamic projections are shown in Fig. 9.1. Basal ganglia connections to all of the target structures are inhibitory and must act by modulating transmission through other circuits. In the thalamus, for example, the basal ganglia inputs act mainly to modify activity in cortico-thalamo-cortical pathways (see Chap. 8). The GPe projects mainly to the *subthalamic nucleus*. The subthalamic nucleus is a small but important component of the basal ganglia that, like the neostriatum, receives input from the frontal regions of the cortex (not shown) and projects to the GP (both segments) and the *substantia nigra*.

Several overall features of these connections should be recognized. First, although inputs from outside the basal ganglia can enter the system at several points, including the subthalamic nucleus, *substantia nigra*, and GP, by far most inputs enter at the level of the neostriatum. The neostriatum has reciprocal projections with the *substantia nigra* but not with its other major sources of afferents; that is, there are no direct projections of the neostriatum back to the cortex or the thalamus. Second, the projections of the neostriatum form two major pathways through the basal ganglia. One of these, called the *direct pathway*, is formed by neurons that have direct projections to the GPi or to *substantia nigra* (as well as to the GPe), and so gain immediate access to the output of the basal ganglia. The other neostriatal efferent pathway, called the *indirect pathway*, is formed by neurons projecting no farther than the GPe. These neurons can affect the basal ganglia output only by way of the subthalamic nucleus and its projections to the GPi and the *substantia nigra*, or by the projections of the GPe to the output neurons. Of course, there are a variety of even more indirect pathways and loops, but this distinction between the direct and indirect pathway is important because it emphasizes the dual nature of the neostriatal output. Third, within the basal ganglia there are several reciprocal connected pairs of structures, like the one involving the GPe and subthalamic nucleus. Finally, the neostriatum is the natural focus of our attention in the basal ganglia, being the largest of its structures, the recipient of most of its afferent input, and the origin of the two major pathways through the basal ganglia. Thus, it has been the object of most basal ganglia research, and its organization is the main topic of this chapter.

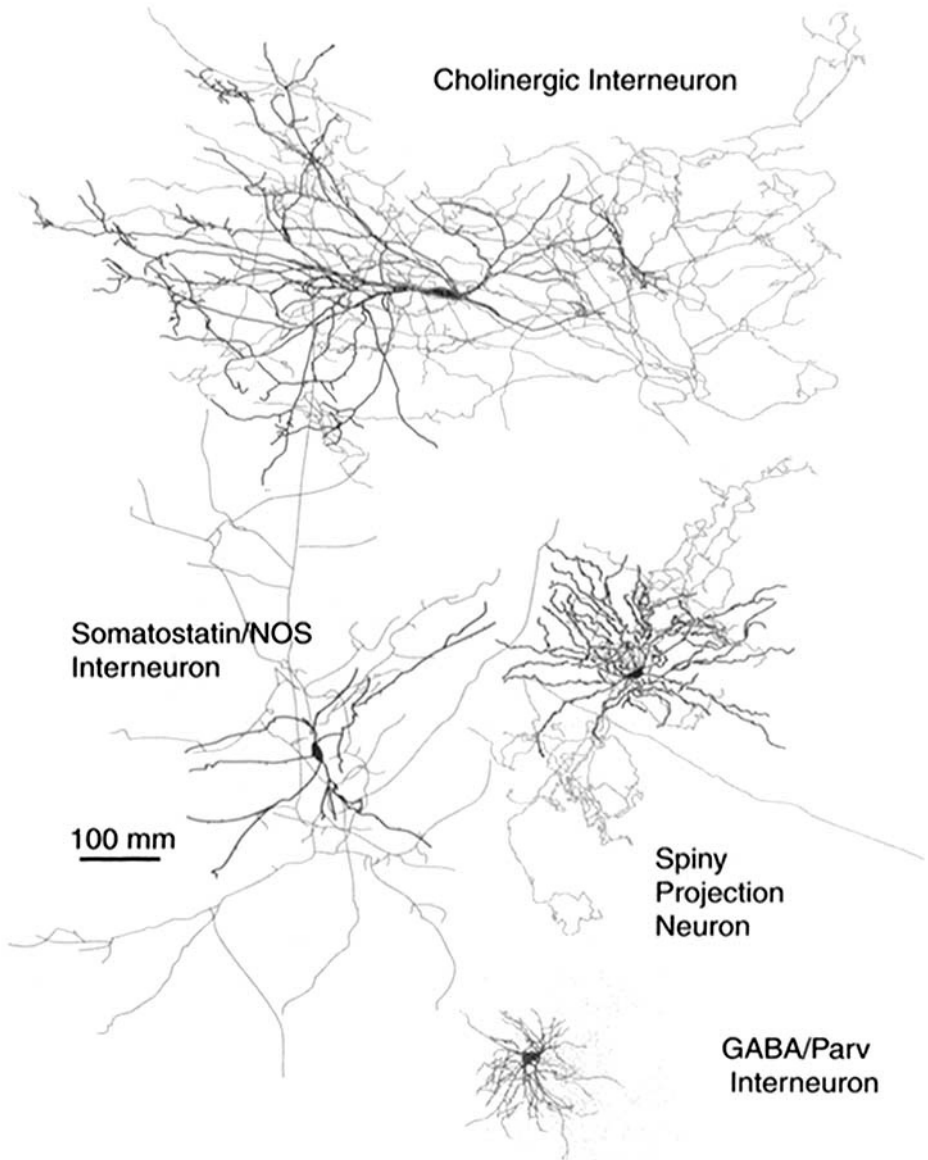


Fig. 9.2. The afferent fibers and neuron types of the neostriatum, shown at the standard scale. [The Somatostatin/NOS neuron is modified from Kawaguchi, 1993b, with permission. The GABA/Parv. neuron drawing is modified from Koós and Tepper, 1999, with permission.]

NEURONAL ELEMENTS

The neostriatum consists mainly of the principal neurons and the afferent fibers. Despite the numerical preponderance of principal neurons, however, the interneurons of the neostriatum are rich in variety and complexity. The major neuronal elements are shown in Fig. 9.2, in the standard scale to facilitate comparison with other brain regions. Afferent axons are shown at reduced scale in Fig. 9.3.

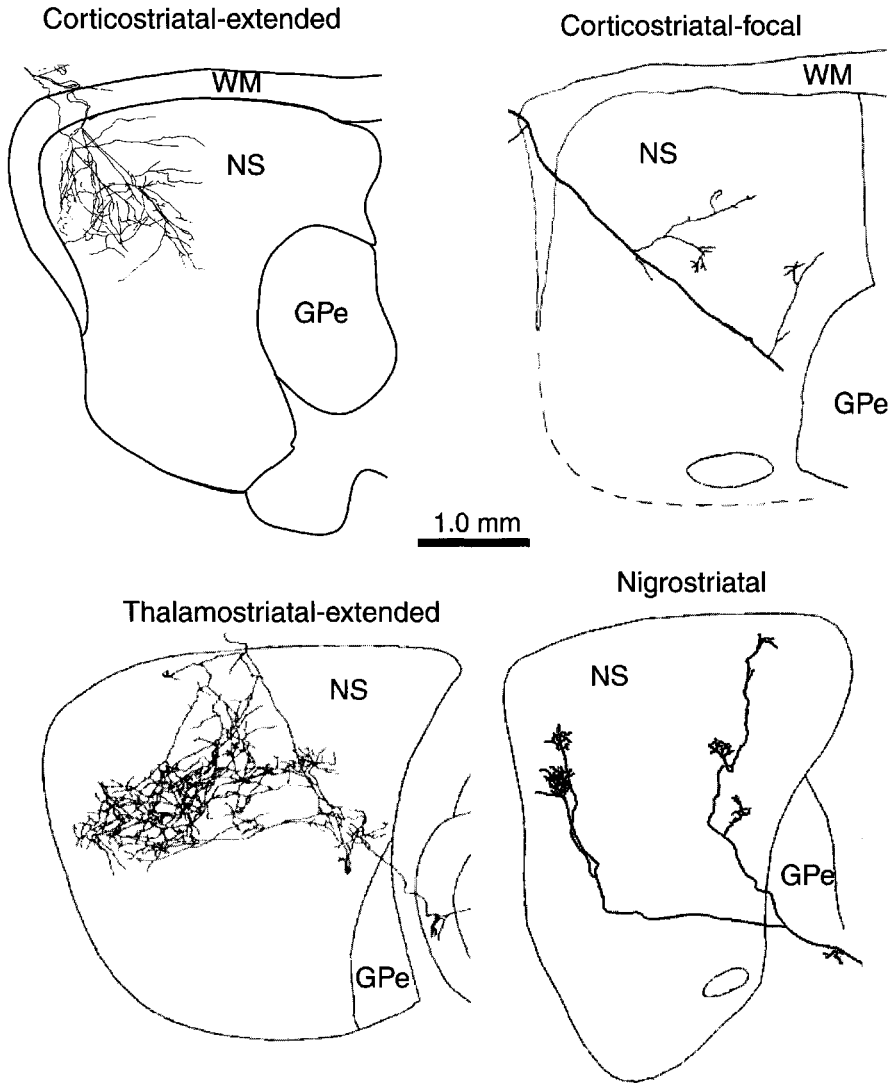


Fig. 9.3. Camera lucida drawings of afferent axons to the striatum in rats, drawn at a scale that accommodates them. [The corticostriatal axons are both modified from Cowan and Wilson, 1994. The thalamostriatal axon is modified from Deschenes et al., 1996, with permission. The nigrostriatal axon is modified from Prensa and Parent, 2001, with permission.]

INPUTS

Input fibers to the neostriatum arise primarily from the cerebral cortex, the intralaminar nuclei of the thalamus, the dopaminergic neurons of the SNc, the serotonergic neurons of the dorsal raphé nucleus, and the basolateral nucleus of the amygdala. Less numerous inputs also arise from the GPe and from the SNr (see review by Gerfen and Wilson, 1996).

Cortical and Thalamic Afferents. Golgi studies showed that afferent fibers to the neostriatum arborize mostly in the pattern described by Cajal as *cruciform axodendritic* (Fox et al., 1971). *Cruciform axodendritic* means that the fibers take a relatively straight course through the tissue, crossing over dendrites and making synapses with them *en passant*. The implication of this kind of arborization pattern is that individual fibers cross the dendritic fields of many neurons but do not make many synapses with any given cell. Conversely, neostriatal neurons can be expected to receive inputs from a large number of afferent fibers but not to receive many synapses from any one of them. The reader will recognize that these are the same rules that govern the input connections in several other regions: from granule cell parallel axons to cartwheel and pyramidal cells in the dorsal cochlear nucleus (Chap. 4); from parallel fibers to Purkinje cells (Chap. 7), and from lateral olfactory tract fibers to olfactory pyramidal neurons (Chap. 10). However, studies using single axonal staining have shown that cortical and thalamic fibers do not all arborize in a highly extended fashion. Axons from the parafascicular nucleus of the thalamus (Deschenes et al., 1996) and a subset of corticostriatal axons (Cowan and Wilson, 1994) arborize by forming several small and separate focal arborizations. These two kinds of axonal arborizations are illustrated in the drawings of Fig. 9.3. It should also be noted that the cells that give rise to both the corticostriatal and thalamostriatal projections do not project exclusively to the basal ganglia. Corticostriatal fibers arise from collaterals of cortical efferents projecting to a variety of other structures, including other regions of the cortex, thalamus, brainstem, and spinal cord. Thalamostriatal neurons project to the cortex as well as the striatum.

Even in the focal arborizations, the density of synaptic contacts from any one axon is small compared with the overall density of synaptic inputs from the cortex or thalamus. Thus, at the level of single neurons, the convergence of many different axons seems to be the dominant pattern of axonal arborization in the neostriatum. It is therefore fundamental to know the distribution of neurons in the cortex and elsewhere that converge onto a single neostriatal neuron, and most theories of basal ganglia organization can be reduced to statements about the functional patterns formed by the convergence of afferents. So far there is no experimental method for specifically staining all the cells that make synaptic contact on one neuron. Instead, investigators have attempted to infer features of axonal convergence, especially that of cortical fibers, from studies of the spatial patterns formed by axonal arborizations. Studies using the classic population axonal tracing methods have established that the projections arising from even a very small region of the cerebral cortex may extend through a large region of the neostriatum, being especially extensive in the rostrocaudal direction (e.g., Selemon and Goldman-Rakic, 1985; Flaherty and Graybiel, 1994). Intracellular staining has shown that single cortical afferent fibers correspondingly extend over large portions of the neostriatum (e.g., Zheng and Wilson, 2002). Thus it is geometrically necessary that inputs from wide areas of the cortex would have access to a common pool of neostriatal neurons and that no cortical area could exercise exclusive control of any

neostriatal neuron. This scheme suggests a sort of combinatorial logic circuit in the neostriatum, in which a striatal neuron may be excited only if there is convergent input from the correct combination of cortical (and perhaps other) pathways.

If this is even approximately correct, it becomes very important to learn which areas of the cortex send axons to each area of the neostriatum. One particularly wants to know if some cortical areas overlap greatly in their projections to the neostriatum, whereas fibers from other cortical areas never converge. Initial studies of the arborization patterns of selected cortical areas yielded the provocative suggestion that cortical regions interconnected by strong corticocortical connections (and therefore likely to be functionally related) project to similar, perhaps overlapping portions in the neostriatum, whereas functionally unrelated cortical areas had nonoverlapping domains in the neostriatum (Yeterian and Van Hoesen, 1978). Subsequent more detailed examination of the axonal projection patterns, however, revealed that the axonal arborizations possess a rich internal patterning (e.g., Flaherty and Graybiel, 1994). Within the rather large general area of neostriatum occupied by fibers from a specific cortical region, there are areas of relative concentration and rarefaction of inputs. Another cortical area projecting to this same region may exhibit either a similar or a complementary pattern of fiber arborization. These experiments have concluded that the organization of cortical axons to the striatum is not a map of the cortex in the simple sense. That is, nearby cortical regions do not necessarily project to nearby regions in the striatum. Instead, the striatum appears to contain a functional re-mapping of the cortex, in which functionally similar cortical regions have overlapping innervations independent of spatial proximity. For example, the motor and sensory cortical representations of a single body part specifically converge on a particular region of the striatum (Flaherty and Graybiel, 1991).

In the study of axonal innervation patterns, it is often forgotten that the postsynaptic neurons have dendrites that can reach across the domains created by the axonal arborizations and sample from more than one of them. This introduces still more complicated possibilities for the convergence of synaptic inputs. It is typical of brain organization that some cells restrict their dendritic fields to correspond to the geometry of axonal arborizations, whereas others create a higher order level of organization by reaching out to receive combinations of nonoverlapping but adjacent inputs. The possible input combinations are determined by both the pattern of axonal arborizations and the patterns of dendritic branching. It is therefore of importance not only which axons actually overlap with others in the target zone but also which are neighbors and which never are. Axonal domains that are not adjacent are unlikely to converge on any cells, regardless of their dendritic fields, whereas neighboring axonal arborizations are likely to converge on some cells even if they do not overlap.

Nigrostriatal Afferents. The distribution of dopaminergic axons from the substantia nigra is important, as this modulator has been shown to be essential for synaptic plasticity in the neostriatum. Arborizations of nigrostriatal axons have been described by Prensa and Parent (2001). These axons, one of which is shown in Fig. 9.3, formed sparse arborizations, usually composed of several focal sub-arborizations, similar to those of the focal-type axons from the cortex and thalamus. This is in contrast to the previously held view of the dopaminergic projection as a diffuse system with little spatial organization and suggests that any local region of the neostriatum may receive its dopaminergic innervation from a relatively small number of dopaminergic neurons.

PRINCIPAL NEURON

Most of the neurons in the neostriatum are principal neurons. This resembles the arrangement in the thalamus and neocortex (Chaps. 8 and 12) but stands in contrast to brain structures such as the retina (Chap. 6) or cerebellar cortex (Chap. 7), where the principal neurons are few in comparison to interneurons. The neostriatal principal neurons are called *spiny neurons* because of the large numbers of dendritic spines that cover their dendrites (e.g., DiFiglia et al., 1976; Wilson and Groves, 1980). As shown in Fig. 9.4, the cell bodies of these cells range from 12 to 20 μm in diameter, and they give rise to a small number of dendritic trunks with diameters of 2–3 μm . The cell bodies and the initial dendritic trunks are usually free of spines. The smooth trunks divide within 10–30 μm of their origins to give rise to spiny secondary dendrites, which may branch one or two more times. A spiny neuron generally has 25–30 dendritic terminal branches, which radiate in all directions from the cell body to fill a roughly spherical volume with a radius of 0.3–0.5 mm (300–500 μm). The density of dendritic spines increases rapidly from the first appearance of spines at about 20 μm from the soma to a peak at a distance of about 80 μm from the soma. The peak spine density can be as high as 4–6 per 1 μm of dendritic length, making the neostriatal principal neuron one of the most spine-laden cells in the brain (in density, not in total spine number). The spiny dendrites taper gradually in diameter from about 1.5 μm to only 0.25 μm at the tips, and the spine density likewise tapers gradually, reaching about half the peak value at the dendritic tips (Wilson et al., 1983). The total numbers of spines, and the implications of spines for the function of the spiny neuron, are discussed later.

The axon of the spiny cell arises from a well-defined initial segment on the soma or a proximal dendritic trunk. The main axon emits several collaterals before leaving the vicinity of the cell body, and these give rise to a local collateral arborization. The local axonal arborizations of spiny neurons are so rich that many earlier investigators using the Golgi method concluded that these cells must be interneurons. The spiny cells were among the first cells to be studied by intracellular injection of horseradish peroxidase (HRP) (see Kitai et al., 1976a), which revealed that their collateral axonal arborizations were much more elaborate even than that visualized using the Golgi method. A photomicrograph of an intracellularly stained spiny neuron from the rat is shown in Fig. 9.4. The spiny cells were identified as projection cells in the 1970s, and their axonal arborizations within the striatum and without have been studied using intracellular staining (Chang et al., 1981; Kawaguchi et al., 1990; Parent et al., 1995). These experiments have shown that spiny neurons fall into two general classes depending upon their axonal targets. One class of spiny neurons (approximately half) forms the origin of the *indirect pathway*, projecting to the GPe and to no other target, whereas the remaining spiny neurons have highly collateralized axons, projecting to some combination of striatal targets, the internal and external segments of the GP, and substantia nigra. These neurons form the *direct pathway* from the neostriatum.

INTERNEURONS

Golgi studies of the neostriatum have revealed a great diversity of interneuron morphology. The number of cell types that can be described on morphological grounds may be as high as eight or nine, and in most schemes there are still neurons that cannot be categorized (e.g., Chang et al., 1982). Together these cells account for only a small proportion of the cells in the neostriatum, and it is not at all clear what the existence of so

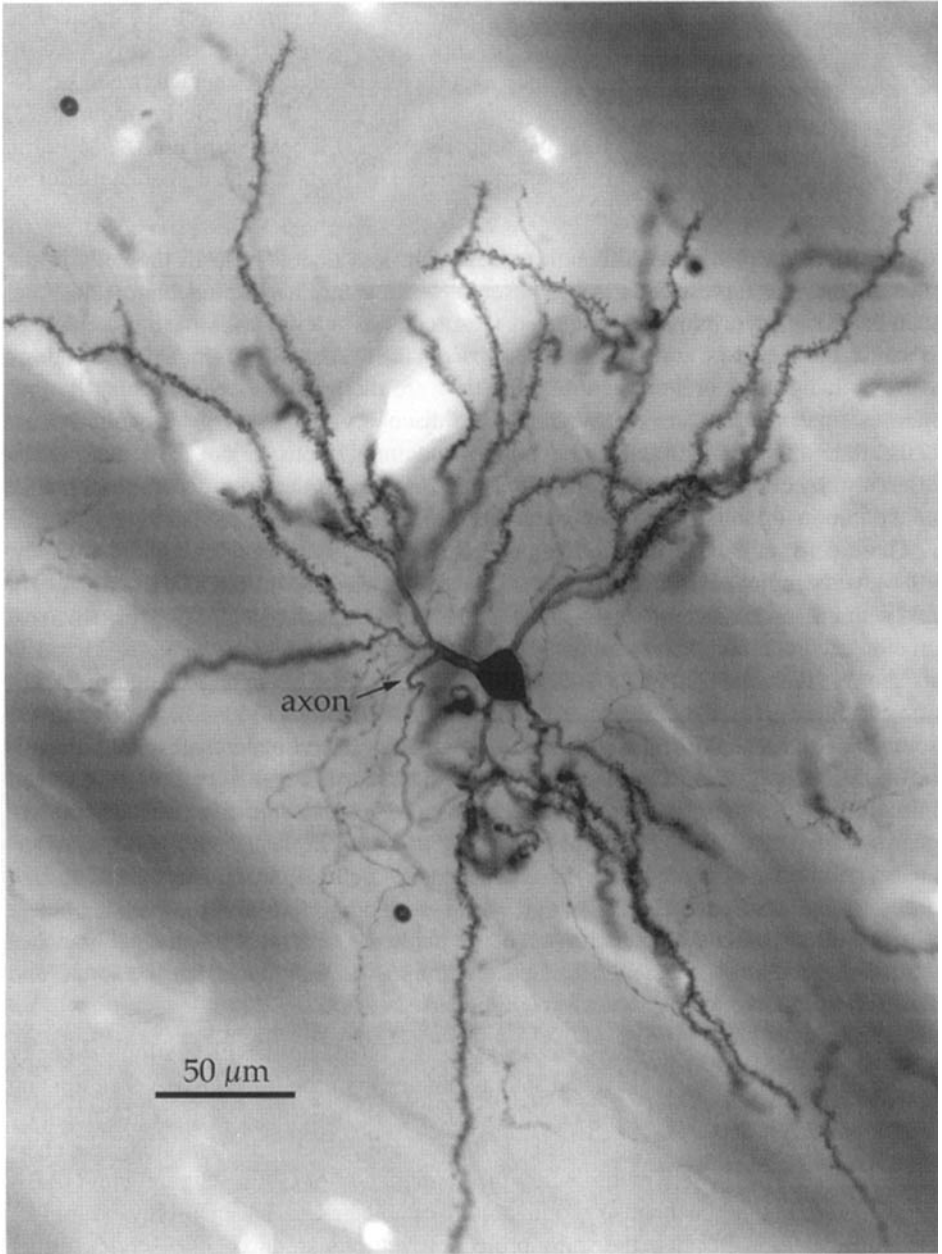


Fig. 9.4. A photomicrograph of a spiny projection neuron. Dendritic spines can be seen on all but the most proximal portions of the dendrites. The axon initial segment is indicated by the arrow, and some fine branches of the local axonal arborization are visible. [From Wilson and Kawaguchi, 1996.]

many different kinds of rare interneurons could mean. For purposes of this discussion, as for most other practical purposes at this time, it is enough to describe only three interneuron types that have been examined in sufficient detail to be characterized as functionally and structurally separate categories: (1) the giant cholinergic interneuron, (2) the GABA/parvalbumin-containing basket cells, and (3) the somatostatin (SOM)/nitric oxide synthetase (NOS)-containing interneurons. The morphological characteristics of these cells are shown in Fig. 9.2.

Cholinergic Interneurons. Although representing less than 2% of all the cells in the neostriatum, the largest cells in the tissue have long fascinated students of the basal ganglia. Kölliker originally recognized these cells as interneurons in the late 1800s. Because they are few and large, many subsequent investigators assumed (by analogy with so many other brain structures) that they are the principal cells and that the numerous small neurons are interneurons. The discovery that most or all of the largest cells are cholinergic and that acetylcholine-containing axons do not participate in the efferent projections to GP and substantia nigra eventually led to a general acceptance of the interneuronal status of the giant cell of Kölliker.

These cells have been described in Golgi-stained sections (e.g., DiFiglia and Carey, 1986), with immunocytochemistry for cholinacetyltransferase (e.g., Bolam et al., 1984), and with intracellular staining (Wilson et al., 1990; Kawaguchi, 1992). They usually have an elongated cell body, up to 50 or 60 μm in length, but commonly only 15–25 μm in its shortest diameter. A few stout dendrites arise from the soma and branch in a radiating fashion, with some dendrites extending 0.5–0.75 mm (500–750 μm) from the soma. The distal dendrites exhibit some irregularly shaped appendages and varicosities. The axons of these neurons arise from dendritic trunks. They may be myelinated initially but lose their myelin in the reductions of axonal diameter that occur in repeated bifurcations. The axon branches many times in the fashion classically associated with interneurons, i.e., with daughter branches being approximately equal in size and forming approximately 120° angles with each other and with the parent branch. The resulting arborization consists of a dense plexus of extremely fine axonal branches that fill the region of the dendritic field (commonly up to 1 mm from the soma) and sometimes go beyond but do not leave the neostriatum.

GABA/Parvalbumin-Containing Interneurons. An interneuron with a strong capacity for uptake of exogenous GABA, and staining intensely for both the GABA-synthesizing enzyme glutamate decarboxylase and for GABA itself, was characterized in studies by Bolam and his collaborators in the 1980s (Bolam et al., 1983). The morphological characteristics of the cell were identified by the combination of Golgi staining with GABA uptake or immunocytochemistry, and it was established to be an aspiny neuron of medium diameter. Because the spiny projection neurons are also GABAergic, further studies of these cells awaited the discovery that they can be identified by the presence of the calcium binding protein parvalbumin (Gerfen et al., 1987; Cowan et al., 1990; Kita et al., 1990). Most parvalbumin-containing cells are medium sized, that is, with somata about the same size as the spiny neurons; some cells are larger than this but smaller than the giant cell of Kölliker. They have round somata, smooth, often varicose dendrites, and an intensely branching axonal arborization that often forms baskets on the somata of the spiny neurons. Thus, they are close relatives of the GABA

and parvalbumin-containing basket cells of the hippocampus and cerebral cortex, which they also resemble in their firing pattern and physiological properties (see later). These cells represent only 3%–5% of the total cell number in the neostriatum and so are usually widely spaced apart, but their dendrites are connected together by gap junctions; therefore, they may interact electrically to form a network larger than a single neuron's dendritic and axonal tree (Kita et al., 1990; Koós and Tepper, 1999). Intracellular staining studies (Kawaguchi, 1993) have shown that the cells can be divided into two subgroups according to whether their dendrites and axons ramify strictly locally (within 100–150 μm of the soma) or are more extended (up to 300 μm).

SOM/NOS-Containing Interneurons. A second group of medium-sized aspiny interneurons identified on the basis of their neurotransmitter content was first recognized as positive in the histochemical reaction for NADPH-diaphorase. At the time the significance of this enzymatic activity was unknown, but a small subset of neurons were seen to be diffusely and beautifully stained (Vincent et al., 1983). Subsequently, this enzymatic activity has been shown to be due to a neuronal form of NOS, the enzyme that produces the neuromodulator nitric oxide. In addition, the neurons staining for NADPH-diaphorase and NOS have been shown to be identical to those staining for two other known striatal neuromodulators: SOM and neuropeptide-Y. These neurons represent 1%–2% of the total population of neurons and are medium sized with longer and less-branched dendrites and a more-extended axonal field than the GABA/parvalbumin interneurons (Kawaguchi et al., 1995). The axons of these cells do not make pericellular baskets around the spiny neurons. Although the somata of these neurons are not intensely stained for GABA or GAD, their axon terminals contain GABA, and it is likely that they, too, are GABAergic interneurons (Kubota and Kawaguchi, 2000).

A third group of aspiny GABAergic interneurons contain the calcium binding protein calretinin (Bennett and Bolam, 1993). These cells have not yet been studied in intracellular staining experiments, so their morphology is not known in detail, and they are not shown in Fig. 9.2.

EFFERENT AXONS

The axons of spiny neostriatal neurons are gathered into small fiber fascicles that perforate the gray matter of the neostriatum, giving it the striated appearance for which it is named. Although these axons form a major fiber system of the forebrain, they are not large or heavily myelinated. The two subpopulations of spiny neurons that give rise to the direct and indirect pathways are both GABAergic, forming GABA-containing synapses in the neostriatum, GP, and substantia nigra. In addition to GABA, these axons contain peptide neurotransmitters, with indirect pathway axons containing enkephalin, whereas the axons of the direct pathway contain substance P and dynorphin (e.g., Gerfen and Young, 1988; Flaherty and Graybiel, 1994).

In the GP and substantia nigra, the axons of neostriatal spiny neurons arborize in a very characteristic *longitudinal axodendritic* pattern. This pattern, which contrasts sharply with that of afferent fibers in the neostriatum, is characterized by individual neostriatal efferent axons running parallel to dendrites of the pallidal and nigral target neurons, making multiple synaptic contacts that almost completely ensheath the dendrites of the postsynaptic cells (e.g., DiFiglia and Rafols, 1988).

CELL POPULATIONS

According to studies of Nissl-stained sections that show all cell bodies, there are approximately 100 million neurons in the neostriatum of the human (Fox and Rafols, 1976). There are approximately 540,000 neurons in the lateral segment of the GP and 170,000 cells in the internal segment. These numbers, of course, are not derived from exhaustive counting of every neuron but by estimating the total from the density of cells in a small sample and extrapolating this result to the entire volume. The methods for doing this have improved dramatically in the time since the above-cited results were obtained. We can have confidence in recent estimates of the number of cells in the various basal ganglia nuclei of the rat by Oorschot (1996), who used modern unbiased stereological measurement techniques. According to her account, there are about 2,800,000 neurons in the neostriatum, 46,000 cells in the GPe, 3,200 cells in the entopeduncular nucleus (GPi homologue), 14,000 cells in the subthalamic nucleus, 26,000 cells in the SNr, and 7,200 cells in the SNc in each hemisphere of the brain of rats. The absolute number of cells is much smaller than in humans, of course, but by less than would be expected from the volume difference; this is because the density of cells in the human nuclei is much lower than that in rats. In the neostriatum, for example, the cell density is $11,000/\text{mm}^3$ in humans vs. $84,000/\text{mm}^3$ in rats (Oorschot, 1996). The difference is presumably because of the need to allocate more volume for axons in larger brains, as the dendritic trees of human and rat spiny neurons are similar in size (Graveland and DiFiglia, 1985b). The ratio of striatal to pallidal neurons is also different. The human measurements suggest a ratio of striatal to GPe cells of over 200, with the same ratio in rats being about 60. This implies more convergence of inputs from the striatum, as well as more neurons, in the human brain. But in either case there must be an impressive convergence of inputs from the neostriatum onto the output cells to both segments of the GP. Principal neurons make up the largest population, representing over 90% of cells in rats (Graveland and DiFiglia, 1985a). Approximately half of neostriatal projection neurons project exclusively to the GP. The other half also make some synaptic contacts, but in only considering those that project exclusively to GPe, there would be about 1,260,000 neostriatal spiny neurons contributing to the innervation of 46,000 cells in the GPe and a minimal convergence ratio of 30:1.

Of course, this convergence does not imply a random mixing of neostriatal information in the GP and substantia nigra, and it does not imply that all GP neurons receive the same inputs. In fact, this convergence ensures that in principle each neuron of the GP could receive a unique combination of neostriatal inputs. Extracellular recording studies have shown that correlations among the neurons of GP are few in awake behaving animals, suggesting that even nearby cells do not tend to fire together, which they probably would if they shared a large proportion of their sources of input (Nini et al., 1995). Anatomical data using transneuronal axonal tracing with viruses also show that the spatial arrangement of inputs in these structures is very specific and that spatial patterns of activity in the neostriatum may be expected to be preserved in the output structures (Hoover and Strick, 1993).

The principal neurons of the striatum receive convergent cortical and thalamic input. The density of such afferent synapses has been estimated in rat to be 920,000,000 per cubic millimeter (Ingham et al., 1998). Of these, nearly all are formed on dendritic

spines of spiny neurons. The density of principal cells is 84,000 per cubic millimeter, giving a ratio of about 11,000 afferent synapses per principal cell, which agrees with direct counts of dendritic spines (Wilson et al., 1983). This means that every spiny neuron receives about 11,000 synaptic contacts from cortical and thalamic axons, but how many different axons contribute to this innervation? Knowing this requires a count of the average number of synapses each axon will make on a spiny neuron. There is not currently a direct way to make this measurement, but an upper limit on the number can be obtained from the number of synapses each axon makes in the volume of a spiny cell's dendritic tree. Kincaid et al. (1998) measured this upper limit for corticostriatal axons. Within the volume of a single spiny cell's dendritic tree, each cortical axon makes at most 40 boutons. The volume of a spiny cell's dendritic tree is about 0.033 cubic millimeter (from the volume of a 0.4-mm-diameter sphere), and so in that volume there should be about $31,000,000$ afferent-type synapses formed by cortical and thalamic axons ($0.43 * \pi / 6 * 920,000,000$). Each cortical axon (and probably thalamic axon, as they are similar) makes at most 40 synapses, so there must be at least $775,000$ axons innervating the spiny neurons in that volume. This is a surprisingly large number. Within the volume of one striatal spiny cell's dendritic tree, there are about $2,800$ other spiny neurons' somata ($0.43 * \pi / 6 * 84,000$). On average, if each axon made synapses with all spiny neurons non-preferentially, the probability of making more than one synapse on any one spiny neuron would be extremely small, and each axon would innervate at most 40 of the $2,800$ neurons in the volume. At the other extreme, if each axon somehow sought out and made all of its synapses on only one neuron in the volume, it would make at most 40, which would still be a small part (0.4%) of the total innervation of the cell. Despite our ignorance of whether axons make multiple contacts on striatal neurons, it can safely be concluded that each striatal neuron receives its innervation from a large number of different neurons in the cortex and thalamus. Because the axonal arborization size is larger than the volume of the spiny neuron's dendritic field (see Fig. 9.3), each cortical neuron also contacts a relatively large number of widely distributed spiny neurons within a large volume. Single cortical axons can innervate from 1% to 15% of the total volume of the striatum, even though the number of cortical axons is about 17 million (Zheng and Wilson, 2002).

This extremely sparse connectivity in the afferent synaptic pathways has the additional implication that nearby striatal neurons do not necessarily have inputs in common. In fact, because the density of synapses made by one axon is so low, the fact that the axon makes a synapse with one striatal neuron substantially reduces the chances of a nearby neuron receiving a synapse from the same axon. Striatal neurons with nonoverlapping dendritic fields actually have a higher chance of sharing input from a common set of axons. If axons were to make multiple contacts with striatal neurons, this would be even truer. In the case of nonpreferential synaptic connections, spiny neurons within the diameter of a cortical axonal arborization (regardless of how close together they are within that) will have about 75 cortical inputs in common. That is, any pair of spiny cells selected at random will have 75 shared cortical axons, although it will be a different 75 axons for each pair of neurons. This is a surprising result, because it predicts that each spiny neuron has a truly unique set of inputs, with very few inputs in common with other cells, and that nearby neurons (with overlapping dendritic trees) will not share more inputs than more separated neurons (Kincaid et al., 1998; Zheng and Wilson, 2002).

It is remarkable, in view of this large and diverse excitatory innervation, that most spiny neurons are electrophysiologically silent most of the time. How this comes about requires analysis of the functional organization of the spiny neuron and its dendritic tree (see later).

SYNAPTIC CONNECTIONS

The typical synaptic connections of the neostriatum are shown in Fig. 9.5. We describe briefly each of the main types of connections.

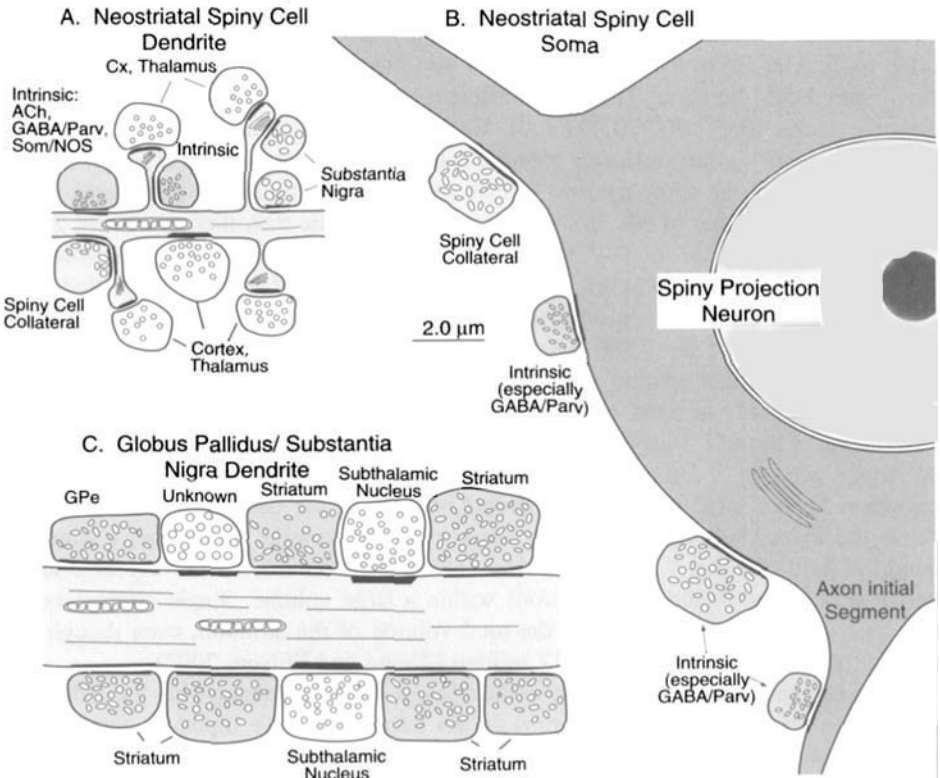


Fig. 9.5. The major synaptic types of the neostriatal spiny neuron and the neurons in the substantia nigra and globus pallidus that receive input from it. **A:** The distal spiny dendrites of the spiny neurons. Inputs with round synaptic vesicles form asymmetrical inputs primarily on dendritic spines, but occasionally on the shafts of the dendrites. These arise mostly from afferent fibers, especially from the cerebral cortex (Cx) and thalamus. Spiny cell collaterals, TH-staining axons from the substantia nigra and intrinsic intrastriatal connections (from aspiny neurons) form symmetrical synapses with pleomorphic and flattened vesicles on the stalks of dendritic spines, on the proximal part of the spine heads, and on dendritic shafts. Axodendritic synapses are overrepresented so that all the synapse types could be shown. Most of the surface of the dendritic shaft is free of synaptic input. **B:** The inputs to the proximal surface of the spiny neurons are primarily intrinsic to the neostriatum, arising from the axons of interneurons and from the collateral arborizations of the spiny neurons. They form symmetrical synapses with pleomorphic or flattened synaptic vesicles and are present at very low density on the aspiny initial portion of the dendrites, the somata, and the axon initial segments. **C:** Synaptic types observed in dendrites in the GP and SNr.

CORTICAL AND THALAMIC CONNECTIONS

The most noticeable feature of the neostriatum as seen in the electron microscope is the large number of small axons forming asymmetrical synapses (Gray's type I; see Chap. 1) on the heads of dendritic spines. This kind of synapse accounts for about 80% of all synapses in the neostriatum (Ingham et al., 1998). It is the characteristic synaptic type formed by afferents from cerebral cortex, and from parts of the intralaminar nuclei of the thalamus (e.g., Kemp and Powell, 1971). The axons from the cerebral cortex and thalamus are similar in morphology, with both exhibiting small round synaptic vesicles. A smaller number of cortical afferent synapses are made onto dendritic shafts and somata of neostriatal neurons. Some of these are formed on dendritic shafts of spiny projection neurons, and others are formed on the somata and dendrites of the aspiny neurons. The intralaminar thalamic nuclei (such as the central lateral nucleus) make synapses on spines, similar to the corticostriatal synapses. Another region of the thalamus (the parafascicular nucleus) has been shown to form preferentially axodendritic rather than axospinous synapses, although almost half of the synapses on those cells are still formed onto dendritic spines (Dubé et al., 1988; Xu et al., 1991).

SUBSTANTIA NIGRA CONNECTIONS

The dopaminergic neurons of the nigrostriatal pathway have a very large complement of the enzyme tyrosine hydroxylase (TH), which is essential for the synthesis of dopamine. Immunocytochemistry using antibodies to TH is therefore an excellent way to demonstrate which axons are from the substantia nigra. If the TH method is used to label axons forming synapses in the neostriatum, they are seen to contain larger, more variably shaped synaptic vesicles and to form symmetrical synapses on dendritic shafts, somata, and the stalks of dendritic spines (e.g., Freund et al., 1984). It is often emphasized that dopaminergic synapses share dendritic spines with cortical neurons, but dopaminergic synapses are not preferentially located on spines. Only about half of TH-positive synapses are formed on spines, whereas over 90% of cortical inputs go to dendritic spines. About half of the surface area of the spiny dendrites is occupied by spines (see later). Thus having half of all dopaminergic synapses on spines is what is expected if they showed no preference for any part of the cell surface. It should also be noted that although the dopaminergic input is very important functionally, it is not comparable to the cortical and thalamic projections in size. Dopaminergic synapses are symmetrical, and only 20% of all striatal synapses are symmetrical. It is not easy to count dopaminergic synapses, because the synapses are not made preferentially at varicosities along the axon (Freund et al., 1984; Groves et al., 1994). Thus counting varicosities in the light microscope does not provide an accurate count of synapses. Roberts et al. (2002) used electron microscopic stereological techniques to measure the density of TH-positive symmetrical synapses in the striatum. They report the density to be $0.03/\mu\text{m}^3$, which is about 3% of the total synaptic density and about 13% of the total number of asymmetrical synapses. If dopaminergic synapses are formed on spiny neurons in proportion to their incidence in the striatum at large, each spiny neuron will receive on average about 300 dopaminergic synapses, only half of which are on dendritic spines. Ingham et al. (1998) report that 15% of striatal dendritic spines receive a second (symmetrical) synapse (1500/neuron). Dopaminergic synapses account for only about 20% of that number, with the rest arising from the axons of striatal neurons.

AXON COLLATERAL CONNECTIONS

The boutons that arise from the local collaterals of spiny neurons contain large synaptic vesicles of variable shape and form symmetrical synapses onto the stalks of dendritic spines, dendritic shafts, somata and initial segments of axons (Wilson and Groves, 1980; Somogyi et al., 1981). These synapses are similar in appearance to those stained positively with TH. Like the TH synapses, about half of local spiny cell collateral synapses are formed onto spines, and those that end on dendritic spines share that spine with some other input, often a cortical fiber. Some of the terminals of spiny cell axons synapse with dendrites, somata, and initial axonal segments of other spiny neurons, but some synapses are made with these portions of the aspiny cells, including the cholinergic interneuron (Bolam et al., 1986).

INTERNEURON CONNECTIONS

Synapses formed by the axons of the cholinergic interneuron and those of the other interneuron types (Bolam et al., 1984; Phelps et al., 1985; Kubota and Kawaguchi, 2000) contribute to a third major morphological synaptic type in the neostriatum. These synapses have small, flattened vesicles and form symmetrical synapses on the stalks of dendritic spines, dendritic shafts, somata, and initial segments; they therefore fall into Gray's type II (see Chap. 1). They are common on spiny neurons, and axons from both cholinergic interneurons and both types of GABAergic interneurons have been shown to terminate in this way on identified spiny cells. Terminals of this type, and the terminals with large pleomorphic synaptic vesicles, form the primary synaptic types found on the somata and proximal dendritic surface of the spiny cell.

Inputs to the cholinergic interneuron are of the same three major morphological types, but they do not show the specific localization on the cell surface that is observed on the spiny neurons (Chang and Kitai, 1982; DiFiglia and Carey, 1986). Boutons with small round vesicles form asymmetrical synapses on dendrites of all sizes and even on the somata of aspiny neurons. Likewise, symmetrical synapses formed by boutons with large pleomorphic vesicles and by boutons with small, flattened synaptic vesicles are seen on all parts of these cells. The synaptic density on the cholinergic neuron is much lower as well, with large parts of the surface area of the cell being free of synapses. It is likely that despite its large size, the giant interneuron receives fewer synaptic contacts than the spiny cell. Cortical inputs to the cholinergic interneuron are restricted to the distal dendrites, whereas the thalamic input makes easily demonstrable synaptic contacts on cholinergic cells (Lapper and Bolam, 1992; Thomas et al., 2000). This preference for thalamic input by the cholinergic cell may contribute to the differences in the activity of these cells during natural behavior (see later).

OUTPUT CONNECTIONS

The output axons of the spiny neurons form synapses in the substantia nigra and GP that are similar in morphology to the synapses formed by their local axonal terminals (Chang et al., 1981). In both the GP and substantia nigra, the dendrites of most neurons are completely encased in a quilt-work of synaptic terminals. The majority of those terminals are derived from the neostriatal efferent fibers. A second kind of terminal found on these dendrites, containing small, round vesicles and forming asymmetrical contacts, is derived from the subthalamic nucleus (Kita and Kitai, 1987). The GPe pro-

jects to the GPi and SNr and has recurrent local synaptic projections, which are all inhibitory. The GPe also receives some inputs from the cerebral cortex and the thalamus. The subthalamic neurons receive excitatory glutamatergic inputs from the cerebral cortex and inhibitory GABAergic connections from the external pallidal segment.

BASIC CIRCUIT

The known connections between elements in the neostriatum are summarized in Fig. 9.6. Although this diagram is no doubt incomplete, especially in its portrayal of the connections of interneurons, it does show the most well established connections among the cells. Two identical spiny cells are shown in the diagram, to represent the neurons of the direct and indirect pathways. Both kinds of spiny neurons receive input from every element in the neostriatum, including each other (although this connection between spiny cells is not shown). A GABA/parvalbumin interneuron and a GABA/SOM/NOS neuron are shown as intrinsic inhibitory elements, making synapses primarily with the principal cells. The SOM/NOS neurons presumably release SOM, neuropeptide-Y, and nitric oxide as co-transmitters, in addition to GABA, and their functions cannot be characterized as simply excitatory or inhibitory (see later). Both the GABA/parvalbumin neurons and cholinergic interneurons have been shown to make synaptic contacts with striatal spiny neurons (Izzo and Bolam, 1988; Kita et al., 1990; Bennett and Bolam, 1994). The former interneuron is a powerful inhibitory influence in the striatum (Koós and Tepper, 1999), whereas the postsynaptic effect of acetylcholine on spiny neurons in the neostriatum is primarily modulatory (see later) and cannot be characterized as excitatory or inhibitory. To indicate this modulatory nature of the synapses made by the giant aspiny interneurons, as for dopaminergic inputs (see later), they are shown in gray. It is a key observation about the striatum that so many synapse types are shown gray.

Afferent inputs go to all of the neostriatal cell types, where most make excitatory synapses predominantly on the dendritic spines of the spiny neurons. Included in this category are inputs from cerebral cortex, some of the thalamic nuclei, amygdala, and hippocampus (in n. accumbens). The TH-containing axons are shown separately in Fig. 9.6. These axons end upon spine stalks and dendritic shafts, rather than spine heads, and do not make the classic Gray's type I synapse formed by other neostriatal afferent fibers. Their synapses resemble those of intrinsic cells. The neostriatum is unusual in that the principal neurons, as well as many of the interneurons, are inhibitory. In this regard it is similar to the cerebellar cortex (Chap. 7). The next neurons in the output pathway, the principal neurons of the GPe, and the internal segment of the GP and substantia nigra, are also shown in Fig. 9.6, and these cells are inhibited by the neostriatal input. Both of these sets of neurons receive an excitatory input from the subthalamic nucleus (and pedunculopontine nucleus of the brainstem and thalamic nuclei not shown). The GPe inhibits the GPi and SNr, which are the output nuclei of the basal ganglia. The subthalamic nucleus neurons receive a large inhibitory input from the external pallidal segment and excitatory input from regions of the motor cortex and thalamus (not shown).

Appreciation of the operation of this mostly inhibitory circuit requires knowledge of the firing patterns of the neurons involved. This is described in a later section, but

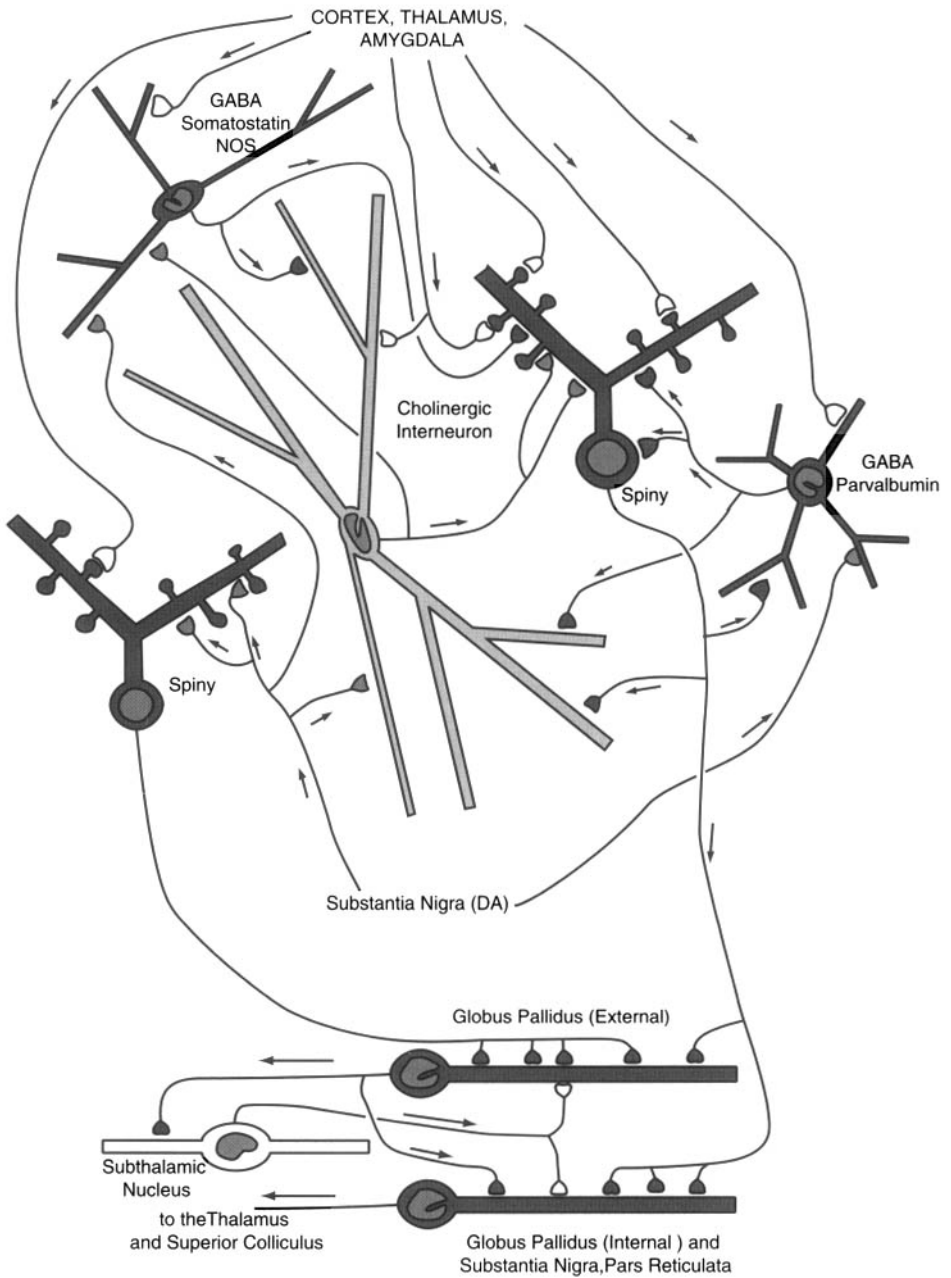


Fig. 9.6. Simplified basic circuit of the neostriatum and its outputs. Excitatory afferent input from several sources is received by all cell types. Because of their large numbers and heavy afferent innervation, most of these are formed on spiny neurons. Spiny cells contribute inhibitory input to all cell types. The interneurons regulate activity through the pathway consisting of the afferent fibers and the spiny projection neurons. The output of the spiny neurons converges on the dendrites of target cells in the substantia nigra and globus pallidus, which themselves project to the thalamus and superior colliculus.

for the present purposes it is important to understand that neostriatal spiny cells fire very rarely and in episodes that last for only about 0.1–3 sec. Thus tonic intrinsic inhibitory interactions between the projection neurons are probably not important contributors to the membrane potential of the spiny neuron under resting conditions but rather limit firing during episodes of excitation that arise because of activity in excitatory inputs. The cells in the GP and substantia nigra, on the other hand, fire tonically at very high rates. Their tonic firing produces a constant inhibition of neurons in the thalamus and superior colliculus. The firing of spiny neostriatal neurons can cause a transient pause in that tonic inhibition, releasing thalamic and superior colliculus neurons to respond to excitatory inputs that would otherwise be subthreshold. Thus the neostriatum acts to disinhibit neurons in thalamus and superior colliculus in response to excitation by its afferent fibers, and the interneurons of the neostriatum help to regulate the duration, strength, and spatial pattern of that disinhibition.

MOSAIC ORGANIZATION OF THE NEOSTRIATUM

In the human neostriatum and in the neostriatum of some primates, the neurons are clustered into groups of high density separated by areas of lower cell density (Goldman-Rakic, 1982). Despite the apparent cell clusters of primates, the neostriatum has long been believed to be structurally homogeneous. This stood in contrast the cerebral and cerebellar cortices, olfactory bulb, and other brain structures that possess a prominent layered organization.

It is now evident that the clusters of cells in the primate neostriatum, originally called cell islands, represent a fundamental feature of the organization of this structure and are present in a less visible form in all mammals. Unlike layered structures, this mosaic organizational plan does not separate the tissue into many compartments but rather only two, with the equivalent of the cell islands usually called *striosomes* or sometimes just *patches* (Graybiel et al., 1981; Herkenham and Pert, 1981), and the area between them is called the *matrix*. A very important finding for the interpretation of this organization was the observation that afferent fibers, particularly fibers of cortical origin, observe these tissue compartment boundaries (e.g., Ragsdale and Graybiel, 1981; Gerfen, 1989). Certain cortical areas project preferentially to the matrix, whereas other areas project preferentially to the striosomes (e.g., Gerfen, 1984; Eblen and Graybiel, 1995). This preferential projection is not absolute but reflects areal differences in the distribution of various types of corticostriatal neurons (Gerfen, 1989). Many cortical areas in the rat have been shown to project to both patches and matrix, with projections from more deeply situated neurons providing the input to the patches and more superficial ones projecting to the matrix.

In addition to their different inputs, the striosomes and matrix have different output targets, at least for their projections to the substantia nigra. The striosomes project preferentially to the SNc, where the dopaminergic nigrostriatal neurons are located, whereas the matrix projects to SNr, where nondopaminergic neurons projecting to the thalamus and superior colliculus are found (Gerfen, 1985; Jimenez-Castellanos and Graybiel, 1989). These observations indicate that the most direct pathway through the neostriatum, going from afferent fibers to the principal neurons and out to the target structures, consists of two parallel and independent pathways—one from the striosomes and one from the matrix (Fig. 9.7). This dichotomy is not to be confused with the direct and

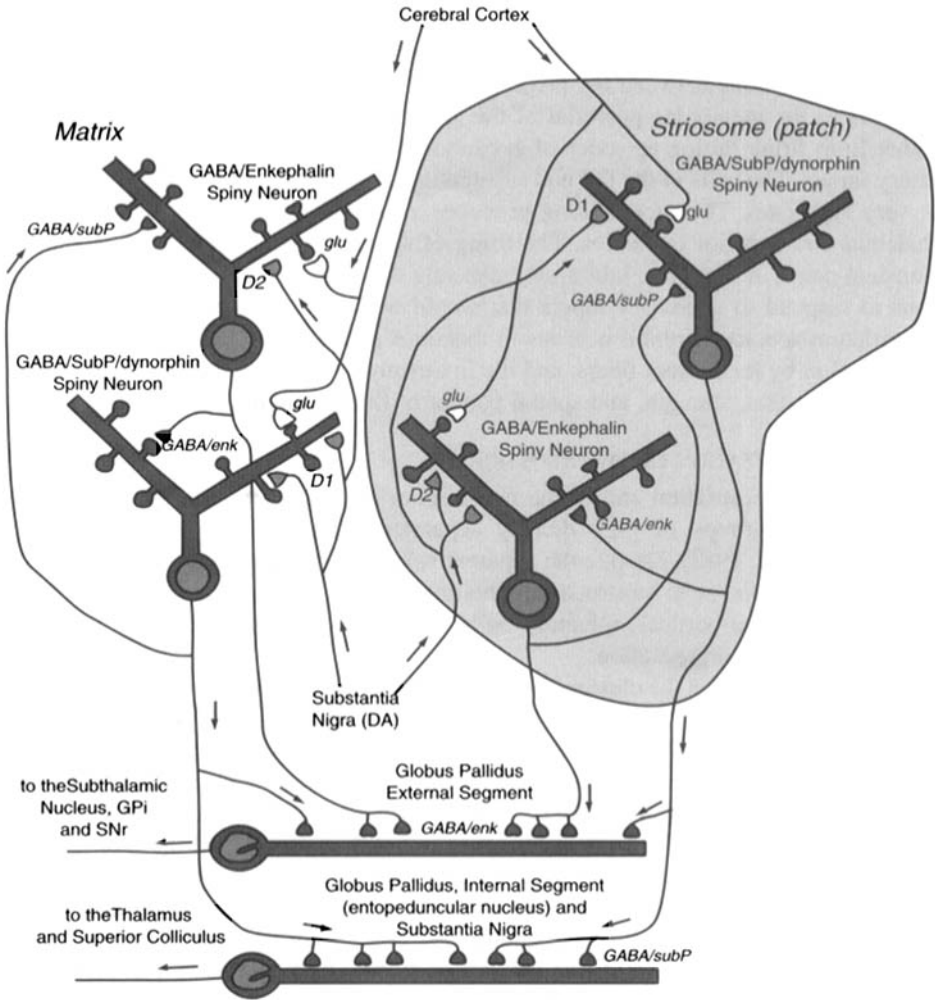


Fig. 9.7. The direct and indirect pathways, arising from both the striosomal and matrix compartments. These consist of separate sets of GABAergic spiny neurons, with the indirect pathway neurons containing the co-transmitter enkephalin, whereas the direct pathway neurons contain substance P and dynorphin. Separate dopaminergic axons innervate the striosomes and matrix, but the direct and indirect pathway neurons in each compartment express different dopamine receptors. Although indirect pathway spiny neurons innervate only the external pallidal segment, the direct pathway neurons project both to the external segment, and either the internal pallidal segment, substantia nigra pars reticulata, or both.

indirect pathways, which are present in both compartments (see later). Communication between compartments may be a major role of the interneurons in the neostriatum.

A particularly exciting development has been the discovery that neostriatal compartments can be distinguished on the basis of their cytochemical characteristics (e.g., Graybiel et al., 1981). Cells in the striosomes and matrix, although similar in many re-

spects, are sufficiently different biochemically to allow demonstration of the compartments using many standard cytochemical methods. For example, the μ opiate receptor is present in much higher concentration in the neuropil of the striosomes (e.g., Herkenham and Pert, 1981). The peptides met-enkephalin and substance P, both very abundant in the neostriatum, are also differentially localized but in a more complex way. In some parts of the neostriatum, the striosomes are richer in these substances, whereas other parts preferentially express them in the matrix.

DIRECT AND INDIRECT PATHWAYS

The use of the peptides enkephalin and substance P as cytochemical markers to distinguish the striosomal and matrix compartments of the neostriatum was instrumental in the discovery of another major organizational principle of the basal ganglia, the direct and indirect neostriatal efferent pathways. In early intracellular staining studies in rats, it was shown that about half of spiny neurons had dense and elaborate projections to the GPe and that these cells did not project to the substantia nigra, as assessed using antidromic stimulation (Chang et al., 1981). Double retrograde tracing studies later showed that neurons heavily labeled by injections of tracers in the substantia nigra or GPi were rarely heavily labeled by injection in the GPe (e.g., Parent et al., 1984). At the same time, studies of the cellular localization of the peptides enkephalin and substance P showed that these were specific markers for mostly nonoverlapping subpopulations of striatal spiny projection neurons (e.g., Penny et al., 1986). GABA, on the other hand, coexists with these peptides, being present in all subclasses of spiny neurons (Kita and Kitai, 1988). Moreover, the external pallidal segment was found to contain many striatal axon terminals staining for enkephalin, whereas substance P was common in neostriatal axons terminating in the internal pallidal segment and the substantia nigra. Subsequent intracellular staining studies have confirmed that about half of spiny neurons project to the GPe and nowhere else, whereas the remaining half of the cells have smaller collateral projections to the external pallidal segment but primarily project to the internal pallidal segment, the substantia nigra, or both (Kawaguchi et al., 1990). These two populations of neurons and their connections are seen superimposed upon the mosaic organization of the neostriatum in Fig. 9.7. Direct and indirect pathway spiny neurons are intermingled throughout both compartments and in all regions of the neostriatum (Gerfen and Young, 1988). Spiny neurons of the direct and indirect pathways also make direct synaptic connections among each other, as well as within each subgroup (Yung et al., 1996), but their axons do not cross striosomal boundaries (Kawaguchi et al., 1989).

Morphologically, the spiny neurons forming the direct and indirect pathways are very similar, except for the difference in their axonal projections (see earlier). This explains why the distinction between them was not apparent using the Golgi method; axons of spiny cells are not well stained by that method. Studies employing cytochemical methods have revealed a number of other differences between direct and indirect pathway neurons. One of these that may be of particular importance is a difference in the dopamine receptors expressed on the surfaces of the two groups of cells. Although there are a number of different dopamine receptor subtypes present in the neostriatum and elsewhere, they can be generally grouped into two classes: the D1 class and the D2 class. The most common of the D1 class in the neostriatum, D1a, is preferentially ex-

pressed by the substance P-containing cells of the direct pathway, whereas the D2 receptor is specifically expressed on enkephalin-containing spiny neurons (e.g., Gerfen, 1992; Surmeier et al., 1996).

DENDRITIC MEMBRANE PROPERTIES

Spiny Neurons. The properties of dendrites constitute a theme running through most of the chapters of this book, and perhaps nowhere are they more important than in the spiny neurons of the neostriatum. In the analysis of the linear properties of dendrites, three electrophysiological parameters are particularly important: the input resistance (R_N), the membrane time constant (τ), and the electrotonic length of the dendritic tree (L). We will discuss how the spiny neuron has served as a case study for the experimental determination of these properties. This will give the student a greater appreciation for the crucial importance of the dendrites in determining the input-output characteristics of the spiny neuron.

For many neurons, one observes much higher input resistances when the cells are recorded in tissue slices than when recorded in intact animals. Two reasons are usually presented to explain this fact. First, tonic synaptic activity, which is generally lost in the preparation of the slices, will act to lower the apparent input resistance by the opening of synaptic ionic conductance channels. Second, the damage done by the microelectrode is probably somewhat less under the mechanically more stable conditions of the *in vitro* recording chamber.

In the case of neostriatal spiny neurons, the input resistance recorded in slices is 20–60 Mohm, which in fact matches very well with that obtained *in vivo* (Sugimori et al., 1978; Kita et al., 1984; Bargas et al., 1988). This is probably because the most important influence on input resistance in spiny neurons is neither damage done by the electrode nor synaptic activity. The biggest determinant is instead the action of a fast anomalous rectification. This rectification can be seen by passage of current pulses of different amplitudes through the spiny neuron (Fig. 9.8). If the cell were to show no rectification, the input resistance (the ratio between the size of the voltage shift and the amplitude of the injected current that causes it) would remain constant regardless of the size of the current pulse (dotted line in the graph on the right in Fig. 9.8), i.e., increasing the size of the current pulse in constant steps would produce voltage deflections that also increase by constant steps. In contrast, the usual behavior of spiny neurons is illustrated by the curve shown on the right in Fig. 9.8. These cells show a marked anomalous rectification over their entire subthreshold range of membrane potentials. In anomalous rectification, input resistance decreases with increasing membrane polarization. In the voltage range near the resting potential and going more negative, the rectification is due to the action of a potassium conductance called g_{IRK} , which increases as the cell is hyperpolarized. Anomalous rectification also is apparent with current injections that move the membrane potential in the depolarizing direction, and in this case it appears as a slowly developing depolarization (arrow in Fig. 9.8) superimposed upon the linear charging curve to depolarizing currents.

This ramp-like depolarizing response is due to a combination of the slow inactivation of a voltage-dependent potassium conductance that is turned on as the cell is depolarized and of the activation of sodium conductance I_{Na} near spike threshold

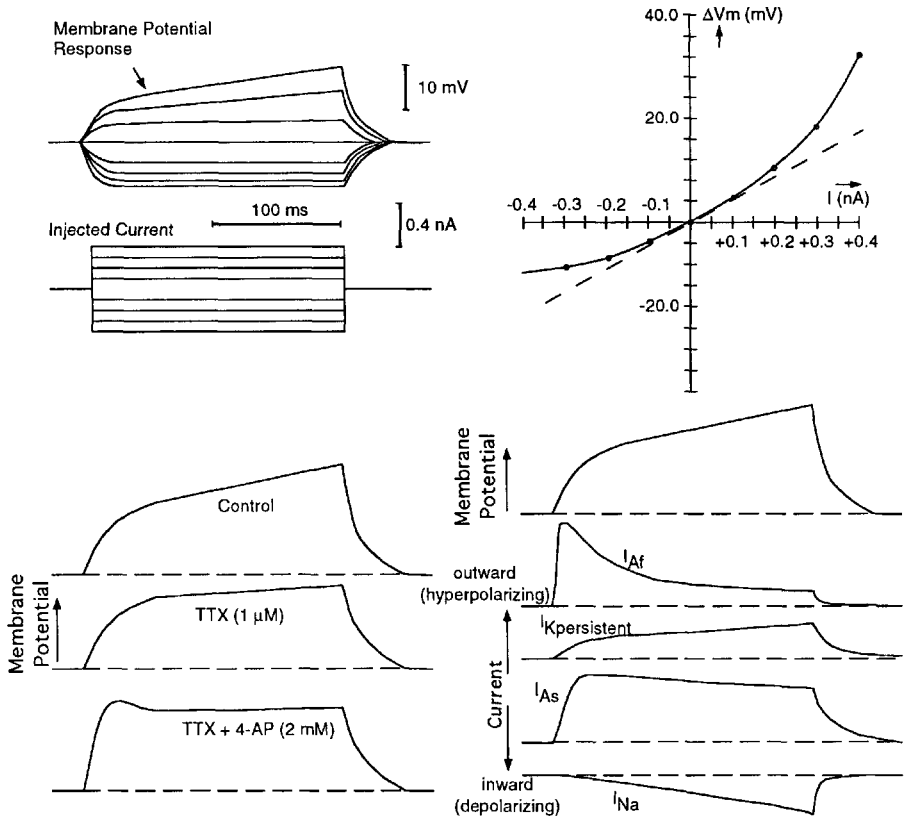


Fig. 9.8. The response of the neostriatal neuron to application of transmembrane current pulses through an intracellular microelectrode. At top left, are shown the membrane potential response and injected current waveforms for current pulses of eight different but equally spaced intensities. The arrow in the largest response indicates the onset of the slow depolarizing membrane response, which is superimposed upon the linear portion of the response to depolarizing currents. At top right, a steady state current–voltage relationship is shown. The dotted line indicates the behavior that would be expected of a linear neuron. The deviations from this line, both in the depolarizing and hyperpolarizing directions, are typical of that seen in neostriatal spiny neurons. At lower left are responses to large depolarizing currents, comparing control responses with those after poisoning of sodium channels with tetrodotoxin (TTX) and a combination of TTX and a selective blockade of inactivating depolarization-activated potassium currents using 4-amino pyridine (4-AP). At lower right are represented the time courses of currents activated by a depolarizing current pulse in the absence of blockers.

(Nisenbaum and Wilson, 1995). This can be seen in intracellular recording experiments using the ion channel poison TTX, which poisons sodium channels, and 4-aminopyridine (4-AP), which poisons the inactivating potassium channels found in spiny neurons. The effects of these drugs on the ramp-like depolarization are shown in Fig. 9.8 (bottom trace). TTX greatly reduces the ramp, indicating that a portion of the ramp current is carried by sodium channels (Chap. 2). A residual ramp-like response to depolarization is retained even when all sodium channels are blocked. Blockade of potas-

sium channels with 4-AP totally blocks the ramp-like depolarization, whether it is given alone or in the presence of TTX. In addition, however, the early part of the response to depolarizing current is enhanced by 4-AP, and a distinct sag in the response is observed (see Fig. 9.8). There are at least three voltage-dependent potassium conductances contributing to the subthreshold response of spiny neurons to depolarizing currents (Nisenbaum et al., 1996). They differ in their voltage dependence and also in their time courses. One of the most important differences is their rate of inactivation. Two of the conductances, called g_{As} and g_{Af} , are transient in nature due to inactivation. These two differ in the rate of inactivation, with g_{Af} inactivating rapidly (tens of milliseconds) and g_{As} inactivating slowly (hundreds of milliseconds). The other conductances (called $g_{Kpersistent}$) are persistent, either not inactivating or inactivating with a time course of several seconds. As a group they activate during depolarization, and they work together to cause the membrane resistance to decrease again as the cell approaches spike threshold. The currents flowing through each of the conductances in response to a constant current pulse (as seen in computer simulations) are shown at the bottom right in Fig. 9.8. Because some of these conductances inactivate, the membrane resistance decreases gradually over time after the cell is depolarized. This inactivation causes the gradual ramp-like depolarization seen with depolarizing current pulses. Thus the inactivation of the potassium conductance is the *cause* of the ramp depolarization, but most of the charge is carried by the sodium current, which is beginning to turn on in this same voltage range. Thus the rectification in the depolarizing direction is not apparent immediately after the onset of the current injection but increases with time. In fact, the responses in the depolarizing direction do not really achieve steady state but grow gradually until the neuron fires an action potential. In the hyperpolarizing direction, the onset of anomalous rectification in neostriatal spiny neurons is fast relative to the time constant of the neuron, so it affects the entire time course of the charging curve. (Anomalous rectification is not really an anomaly. It is actually quite common. It is called anomalous because it was not expected on the basis of an early biophysical theory of membranes.)

It is difficult to apply the linear cable theory to such a nonlinear cell. Certainly, the time constant of the cell cannot be a constant if the membrane resistivity is altered by any shift in membrane potential. It is therefore perhaps not surprising that there has been some disagreement about the time constants of the cells. Experiments in tissue slices using small current pulses (to minimize the effects of anomalous rectification) have yielded values near 5 ms for the time constant under these circumstances. It is quite possible to increase the time constant to 10 or 15 ms by depolarizing the cells slightly (Nisenbaum and Wilson, 1995), and longer time constants have been obtained with small changes in the extracellular potassium concentration (Bargas et al., 1988).

Again using small current pulses in cells recorded *in vitro*, the electrotonic length of the equivalent cylinder of the dendrites has been measured to be about 1.5–1.8 length constants. This electrotonic length seems very long, and it is especially surprising in view of the relatively short dendrites of these cells (about 200 μm). However, this result is predicted by cable theory, because of the spiny nature of the dendrites. The dendritic spines create a very large surface area. Measurement of this area is made difficult by the small dimensions of the spines. These structures cannot be accurately measured in the light microscope (remember that the resolution of the light microscope allows

measurements to the nearest $0.25 \mu\text{m}$ or thereabouts, while the stalks of dendritic spines can be as small as $0.1 \mu\text{m}$).

Estimation of the surface areas of neostriatal spiny neurons has been accomplished using a combination of reconstruction of serial sections from electron micrographs and high-voltage electron microscopy (HVEM) of thick ($5\text{-}\mu\text{m}$) sections (Wilson, 1992). These measurements have shown that the dendritic field of spiny neurons cannot be approximated as a cylinder, or even a tapered cylinder. Its surface area is dominated by the dendritic spines, being greatest at about $80 \mu\text{m}$ from the soma, where the dendritic spine density is highest, and tapering off slowly to the tips of the dendrites. This distribution of surface area is shown in Fig. 9.9. Because the dendritic diameter does not change in proportion to the surface area, the leakage of current from the dendrites of the spiny neuron and thus the low pass filtering effect of the dendrites are both increased dramatically by the presence of spines. After this is taken into account for the neostriatal spiny neurons, the measurements of time constant (t), electrotonic length (L), and input resistance (R_N) of the cells can be seen to agree on a membrane resistivity (R_M) ranging from about $5,000$ to $15,000 \text{ ohm-cm}^2$, depending upon the state of the anomalous rectification (which itself depends upon membrane potential).

We are now in a position to pull together these considerations of dendritic properties and understand how they contribute to the input–output operations of the spiny neuron. The small amplitudes of individual synaptic responses on spiny neurons are probably due to their placement on dendritic spines and on the electrotonically long dendrites. The electrotonic length of the dendrites is actually not constant, but variable due to the action of the voltage-sensitive conductances. When the cell is very hyperpolarized, the membrane conductance is dominated by the fast inwardly rectifying potassium conductance g_{IRK} . The membrane resistance is low due to this conductance, and as a result the electrotonic length of the dendrites is long. In computer simulations of the spiny neuron, isolated synaptic inputs have little effect at the soma under these circumstances (Wilson, 1992). This is called the Down state of the spiny neuron

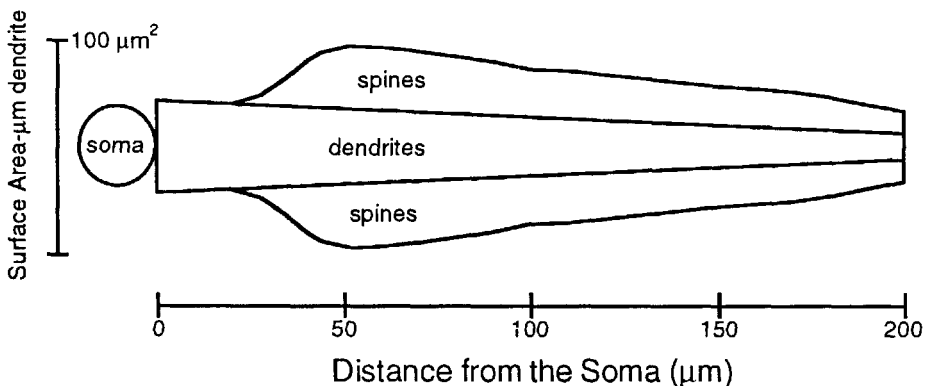


Fig. 9.9. The distribution of membrane on the neostriatal spiny neuron as a function of distance from the soma. The total somatic membrane is represented by the diameter of the circle marked soma. The remaining membrane area is shown as a density ($\mu\text{m}^2/\mu\text{m}$ of linear distance from the soma), and the contributions of the spines and dendrites are indicated. [From Wilson, 1986b.]

(Wilson and Kawaguchi, 1996). When large numbers of synapses depolarize the neuron, the hyperpolarization-activated potassium current turns off, raising the membrane resistance. The effect of this will be to shorten the dendrites electrotonically and to make the cell more sensitive to subsequent inputs, which will cooperate to depolarize the cell more, until the cell membrane escapes the influence of the hyperpolarization-activated potassium current by depolarizing beyond its activation range. As the membrane potential leaves the range dominated by g_{IRK} , it enters the membrane potential range in which the depolarization-activated potassium conductances turn on. The electrotonic length of the dendrites will increase again as the membrane potential approaches threshold, and the effects of individual synapses decrease. This depolarized high conductance state of the neuron is called the Up state (Wilson and Kawaguchi, 1996).

These changes in electrotonic length and membrane potential during an episode of synaptic excitation are shown schematically in Fig. 9.10. Near the resting potential (Down state), the cell is dominated by a hyperpolarization-activated potassium channel. The dendrites are electrotonically long, but the neurons are extremely sensitive to

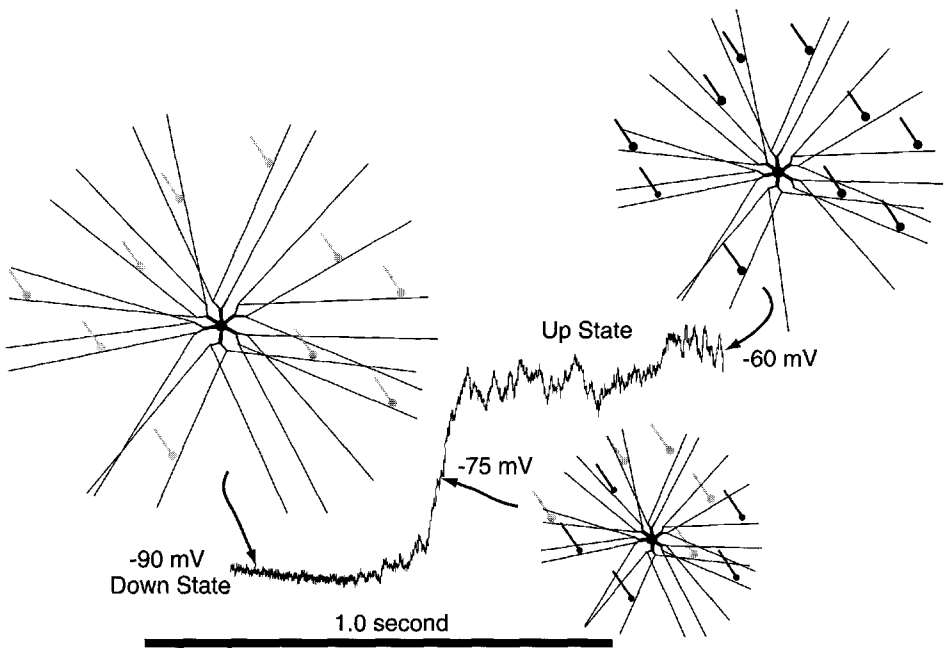


Fig. 9.10. Electrotonic expansion and contraction of the spiny cell dendritic tree during the course of synaptic excitation. During periods of relative synaptic quiescence, the electrotonic structure of the cell is extended due to the action of anomalous rectification. In the course of excitatory input, depolarization deactivates the rectification, causing an electrotonic collapse of the cell and a resulting increase in synaptic effectiveness. As the cell depolarizes rapidly, depolarization-activated potassium conductances cause the electrotonic structure of the cell to expand, and the cell achieves a relatively constant membrane potential at a level determined by the equilibrium between synaptic currents and the resulting potassium currents. This equilibrium point is on average below the spike threshold.

depolarizing inputs if they are large and sustained enough to overcome the low membrane resistance and short length constant and escape the effects of the potassium conductance. Because of the electrotonic contraction that results from depolarization in this membrane potential range, all synaptic inputs placed more distal to a powerful input will be enhanced in importance. However, once the membrane potential begins to approach the spike threshold, depolarization-activated potassium conductances will be engaged, which cause another electrotonic expansion and tend to stabilize the membrane potential in the Up state. In that state, synaptic current is balanced by the potassium current, and the membrane potential is determined by the voltage sensitivity and strength of the potassium conductance and by the strength of the synaptic excitation.

Cholinergic Interneurons. The small number of these cells impeded physiological studies of all striatal interneurons for many years. Intracellular recording studies both *in vivo* and *in slices* long depended upon chance encounters between the microelectrode and a cell, and so the chances of obtaining an intracellular recording of a striatal interneuron were less than 10%, even assuming all the cells were equally resistant to the damaging effects of microelectrode impalement. The chances of recording from striatal interneurons were reduced further because the numerous spiny cells are especially hardy, and experimenters setting out to record from interneurons were almost always distracted by a particularly nice recording from a spiny cell that could not be resisted. Despite two decades of intracellular recording in the striatum, there were practically no intracellular recording studies of the cholinergic interneurons before 1990. With the advent of visualized recording in slices, which allows visual targeting of neurons on the basis of their somatic sizes and shapes, this situation changed rapidly. Because they are so large, the cholinergic interneurons are the most identifiable cells in the striatum in the slice. There has been an explosion of new information about their properties, starting with the work of Kawaguchi (1993), who demonstrated that cholinergic cells could be reliably identified by their appearance in slices and described their basic physiological properties.

An example showing the appearance of a cholinergic cell in a visualized slice, and typical characteristics of the cell in intracellular recordings are shown in Fig. 9.11. Characteristic features of the neurons are their long-duration action potential and spontaneous activity. Unlike the spiny neurons, which require large numbers of convergent synaptic inputs to bring them to threshold for action potential, the cholinergic interneurons fire action potentials all the time, even in the absence of any synaptic input (Bennett and Wilson, 1999). Many of the cells fire in a simple rhythmic single spiking pattern, but other cholinergic interneurons exhibit rhythmic bursting, or even irregular and aperiodic activity in the absence of synaptic input. This puts the cells in the category of pacemaker neurons (see Chap. 2). The ionic conductances responsible for simple rhythmic pace making by cholinergic interneurons have been described (Bennett et al., 2000). Pacemaking in cholinergic interneurons is ensured by the presence of a negative conductance region in the cell's steady-state voltage-current relationship in the subthreshold range. What this means is that the cell has no stable resting membrane potential. Regardless of the starting voltage, the intrinsic properties of the cell will tend to move the membrane potential toward the action potential threshold, leading to an action potential. The sequence of ionic currents giving rise to pacemaking

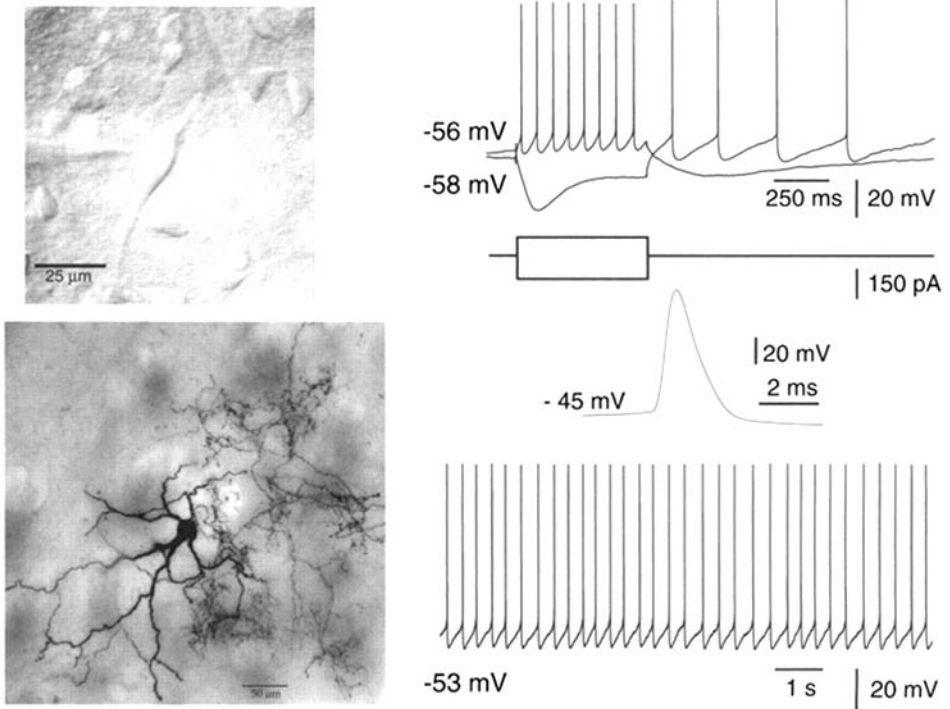


Fig. 9.11. Striatal cholinergic interneurons. At the left is the appearance of the cholinergic neuron at the time of visualization for intracellular recording, showing identification of the cell in slices by its size (top), and the appearance of the dendritic and axonal tree after staining with biocytin (bottom). At the right are recordings from the cell. At the top, passing depolarizing and hyperpolarizing currents shows the nonlinearity of the cholinergic neuron. Note the prominent sag in the response to hyperpolarizing current, caused primarily by the activation of I_H . The middle trace shows an action potential waveform, demonstrating the long duration of the action potential. At the bottom right is spontaneous rhythmic single spiking activity recorded in the slice, in the absence of synaptic input.

in cholinergic cells is shown in Fig. 9.12. During the action potential, high-voltage-activated calcium currents are activated, which cause the action potential to be prolonged and which cause an influx of calcium into the cell. Calcium currents are slow to turn off, so they continue to flow for a short time after the action potential is over. Calcium enters the cell during this current and builds up in the cytoplasm, where it can interact with calcium-dependent potassium current (I_{AHP}), which produces a long-lasting spike afterhyperpolarization. At the hyperpolarized potential that is enforced by the calcium-dependent potassium current, the hyperpolarization-activated cation current (I_H , Chap. 2) is activated. As the cell disposes of the calcium that entered during the action potential, the calcium-dependent potassium current is reduced, and I_H tends to depolarize the cell. As I_H is turning off (around -60 mV), persistent sodium current ($I_{Na,p}$, see Chap. 2) begins to be activated, which continues the depolarization of the cell. In the voltage range between this and spike threshold, the cell has a negative slope conductance because depolarization of the cell causes increased activation of $I_{Na,p}$.

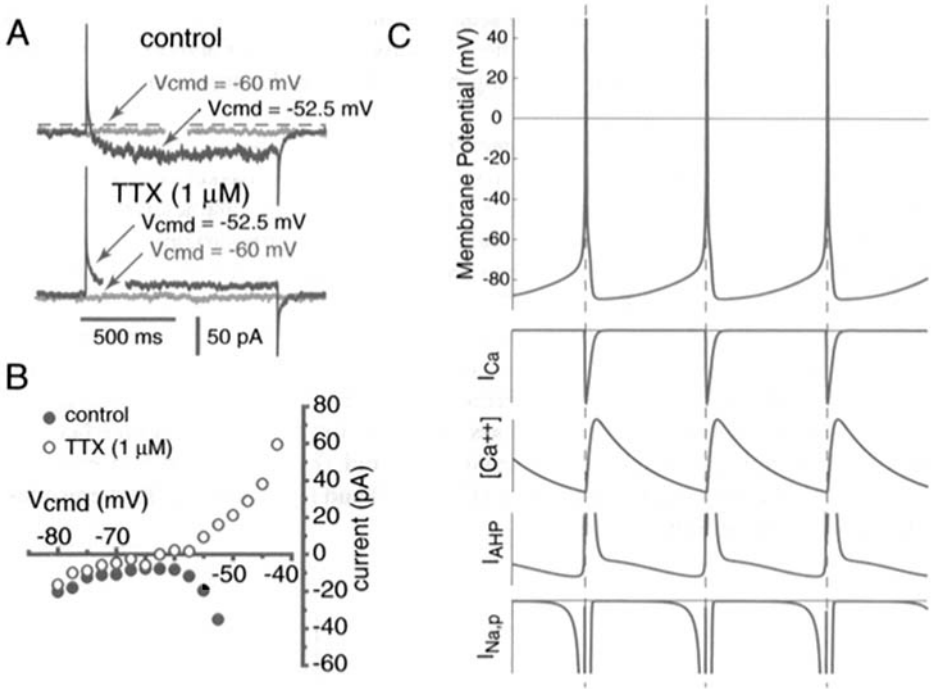


Fig. 9.12. Mechanism of pacemaking by cholinergic neurons. **A** and **B**: Voltage-clamp demonstration of the presence of a persistent sodium conductance in cholinergic cells in slices. [Modified from Bennett et al., 2000.] **A**: In control solution, a small depolarizing voltage step from -60 mV evokes an inward current that lasts for the duration of the voltage pulse. Blockade of sodium currents with TTX abolishes the inward current and reveals a small outward current in its place. **B**: Repeating the experiment in **A** with a range of voltage steps reveals a TTX-sensitive noninactivating inward current starting at about -65 and increasing up to spike threshold, which is near -50 mV. The negative slope of the current-voltage curve indicates that the cell will undergo regenerative depolarization above -65 mV and will have no stable membrane potential (which would be indicated by a crossing of the abscissa). After TTX treatment, this negative slope region is gone and a stable resting potential occurs at about -60 mV. **C**: Simulation of rhythmic spiking in a cholinergic cell and its underlying currents. The persistent sodium current ($I_{Na,p}$) increases gradually during the depolarizing cycle of the oscillation and is abruptly terminated by the afterhyperpolarization that follows each action potential. Action potentials trigger a calcium current (I_{Ca}) that results in an increase in calcium concentration $[Ca^{2+}]$ and produces a powerful and long-lasting potassium current (I_{AHP}) that must wear off before the sodium current can again depolarize the neuron to threshold.

which depolarizes the cell further. Thus the slope of the voltage-current curve is negative, and the cell is under the influence of depolarizing positive feedback. This proceeds slowly because the net inward current is small, and the slow explosion of membrane potential is terminated when the cell reaches spike threshold, upon which it begins the cycle again.

Although this mechanism is sufficient to explain the rhythmic single spiking mode of the cholinergic interneuron, it does not explain the irregular and rhythmic bursting

firing modes of the cell, which are also seen in synaptically isolated cells in slices (as well as in the intact animal, see later). The mechanism of irregular activity is especially interesting, because it gives rise to a firing pattern that has the appearance of noise.

GABA/Parvalbumin Fast Spiking Interneurons. The fast spiking interneuron in the striatum is similar to the GABAergic, parvalbumin-positive basket cells in the hippocampus and cerebral cortex (Chaps. 11 and 12). They are characterized by their very short-duration action potentials, short spike afterhyperpolarizations, and ability to maintain firing at high rates (up to about 200 spikes/sec) without much adaptation (Kawaguchi, 1993; Koós and Tepper, 1999). The ionic currents in the fast spiking interneurons have not been studied in detail, but these cells express a kind of potassium current with a high threshold and rapid activation and deactivation, needed for high-frequency sustained firing. These cells do not fire spontaneously in slices and have relatively linear responses to current over the voltage range between the resting membrane potential and spike threshold (Fig. 9.13). With stimuli just above threshold, they fire intermittently (Fig. 9.13) and sometimes in short episodes, interrupted with periods of silence.

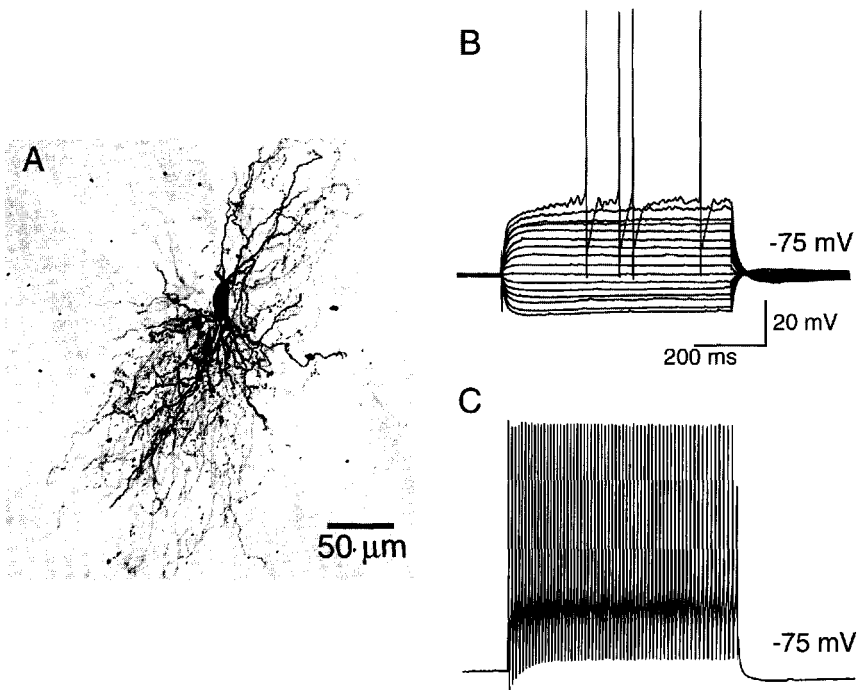


Fig. 9.13. Fast-spiking interneuron. **A:** Intracellularly stained fast-spiking neuron filled with biocytin *in vivo*. [Contributed by Ed Stern.] The region around the soma and dendritic tree are crowded with fine axonal branches. **B:** Responses of a fast-spiking neuron to current pulses, showing the relatively linear current–voltage relationship. **C:** Response to a large current pulse showing high-frequency firing with little spike-frequency adaptation. [Modified from Bennett and Wilson, 1998b.]

GABA/SOM/NO Interneurons. The interneurons containing GABA and SOM, NO, and neuropeptide Y have been resistant to physiological study in slices because they are difficult to identify by their somatic appearance. In the most thorough report on these cells, Kawaguchi (1993) used immunocytochemical identification of the neurons after intracellular staining. These cells exhibited powerful postinhibitory rebounds that were self-sustaining. That is, after a prolonged inhibition, the rebound depolarizations and associated firing of the cells could long outlast the stimulus.

SYNAPTIC ACTIONS

INPUT FIBERS

A variety of evidence indicates that the neurotransmitter in the corticostriatal pathway is glutamate (e.g., McGeer et al., 1977). The thalamostriatal pathway is less clear but is likely to be glutamate as well, because virtually all excitatory responses evoked in spiny neurons by local stimulation are abolished by application of excitatory amino acid receptor blockers (Jiang and North, 1991, Kita, 1996). The nigrostriatal projection is almost entirely dopaminergic, and the input from the raphé contains serotonin.

Because the neostriatum is a central structure, several synaptic relays removed from the direct sensory input pathways, it is not possible to analyze its synaptic actions by natural stimulation, as in so many other regions considered in this book. Analysis of synaptic actions therefore must rely on activation of neostriatal input and output pathways by electrical stimulation. We shall summarize the evidence for the main types of excitatory and inhibitory actions that control the activity of the striatal neurons as revealed by this experimental approach.

ACTIONS OF CORTICAL AND THALAMIC INPUTS

Stimulation of the cerebral cortex in intact animals sets up a synchronous volley of impulses in a subset of the corticostriatal axons, which evokes large-amplitude EPSPs in the spiny neurons of the neostriatum (e.g., Wilson, 1986). The latency of this EPSP matches that of the fastest corticostriatal axons and shows a constant latency despite changes in stimulus intensity or frequency, as expected for a monosynaptic EPSP. The behavior of this EPSP suggests that it represents the action of many synapses, each of whose effect at the soma is very weak. Its amplitude is finely graded with stimulus intensity. That is, very small changes in stimulus intensity produce correspondingly small changes in EPSP amplitude. Likewise, the EPSP shows no minimal threshold amplitude. Thus the synaptic potential components contributed by individual axons are too small to detect in a conventional intracellular recording, and the EPSP that is recorded must be composed of many such small EPSPs.

This initial EPSP is followed by a long-lasting hyperpolarization and, upon its termination, by a period of depolarization and increased synaptic conductance. These components of the response are illustrated in Fig. 9.14Aa. Among these late components of the response we should find the effects of recurrent collaterals of the spiny neurons that fired action potentials in response to the initial EPSP and the effects of interneurons excited by the stimulus.

Stimulation of the thalamus in intact animals produces effects that are very similar to those of cortical stimulation (e.g., Wilson et al., 1983a). It is important to note in

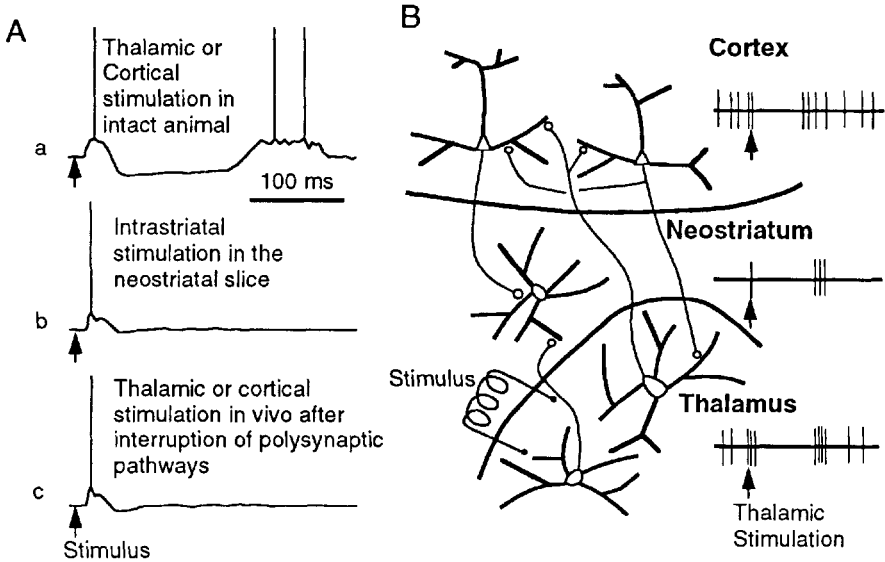


Fig. 9.14. Synaptic potentials evoked in spiny neurons by stimulation of the cerebral cortex and the thalamus, and their interpretation. **A:** Synaptic potentials in three different preparations. The trace shown in a shows the response evoked by stimulation of the cortex or thalamus (the response is the same for either site) in an intact animal. There is an initial large EPSP, which can trigger an action potential, followed by a long period of membrane hyperpolarization and inhibition of synaptic responses. This period is followed by a period of rebound excitation. The trace labeled (b) shows the response evoked by local stimulation in neostriatal slices, part of which is probably due to stimulation of cortical and thalamic afferents. The trace labeled (c) shows the response to cortical or thalamic stimulation in an animal in which the polysynaptic pathways shown in **B** have been interrupted experimentally. **B:** A diagram showing some of the synaptic connections between the cerebral cortex, thalamus, and neostriatum that contribute to the long-lasting inhibition and rebound excitation observed in spiny neostriatal neurons after cortical or thalamic stimulation. Typical responses of a cortical, striatal, and thalamic neuron upon stimulation of the thalamus are illustrated at the right. Stimulation of the cortex produces similar responses, due to activation of the same circuits.

such experiments that when stimulating one area, we are often engaging the activity of many structures indirectly. This is illustrated for the thalamo-cortico-striatal system in Fig. 9.14B. One cannot stimulate thalamostriatal cells without also stimulating thalamic neurons that project to cortex, and the stimulation of these thalamocortical fibers has profound effects on cortical activity. Also, some cortical neurons projecting to the thalamus are stimulated antidromically, and their recurrent collaterals in the cortex are activated. It is important to attempt to separate these polysynaptic effects from the direct response to stimulation by experimentally interrupting the polysynaptic pathways. When such experiments are performed, the cortical and thalamic responses are greatly simplified and display almost identical EPSPs. Although it is usually assumed that the corticostriatal input is more powerful than the thalamic one, there is no indication of this in a comparison of the sizes of the responses that can be produced by stimulation of the two structures. Their maximal EPSP amplitudes are approximately equal.

The results of the experiments described here indicate that the late components of the responses seen in intact animals are not due to the action of intrastriatal circuits. If the long-lasting hyperpolarization and late depolarization components of the response are not due to intrastriatal circuitry, then to what could they be due?

Measurement of the effect of hyperpolarizing and depolarizing currents, and of conductance changes that accompany the membrane potential change, can help to provide an answer. The long-lasting hyperpolarization is slightly increased in amplitude when the cell is hyperpolarized and decreased with membrane depolarization. The effect is approximately equal in magnitude to the effect of the same manipulation on the EPSP. This suggests that the ionic currents responsible for the long-lasting hyperpolarization resemble those responsible for the EPSP. In addition, measurement of whole cell input resistance (R_N) during the long-lasting hyperpolarization shows that the cell has a net increase in resistance during this time. This measurement is difficult because of the large anomalous rectification of spiny neurons in this voltage range (see later) that has to be compensated out of the analysis. When this is done, the long-lasting hyperpolarization is seen to be accompanied by a decrease in conductance (increase in the resistance) of the cell. This is what would be expected if the long-lasting hyperpolarization were a disfacilitation, that is, the removal of an excitatory input.

This interpretation is strengthened by examination of the behavior of neurons in the cerebral cortex and thalamus after stimulation of either structure. It has long been known that stimulation of the thalamus produces an initial excitatory effect in the cerebral cortex, which is followed by a long-lasting inhibitory period. The inhibitory period is itself followed by a "rebound" excitation (see Chaps. 8 and 12). A similar pattern of excitation and inhibition is observed in both the cortex and the thalamus after the application of a stimulus to the cortex. This pattern is precisely what is required if the long-lasting hyperpolarization and subsequent excitatory period in the neostriatum were due to a removal and subsequent reassertion of tonic excitatory influences from the cortex and thalamus.

The complexity of the response observed in the *in vivo* preparation suggests that it would be useful to carry out further analysis in a simplified preparation, such as slices of neostriatum. Such experiments have not usually been performed using cortical stimulation because it is difficult to get any significant piece of the corticostriatal pathway intact in a slice. They have instead used intrastriatal stimulation or stimulation of the subcortical white matter. Because of the nature of current spread from stimulation sites, these two kinds of stimulation are probably the same thing. They stimulate not only the corticostriatal fibers but also all afferent fibers, the axons of spiny neurons, and striatal interneurons. Nonetheless, the response to this kind of stimulation is very informative. As shown in Fig. 9.14Ab, excitatory inputs *in vitro* never produce the pronounced long-lasting inhibition or rebound excitation seen in the intact animal. Instead, the EPSP, which looks similar to that observed *in vivo*, is followed by only a small and short-lasting IPSP. Similar results have been obtained using cortical stimulation in a slice prepared to maintain the integrity of a portion of the corticostriatal projection (Kawaguchi et al., 1989). The IPSP component seen after cortical or local stimulation in slices probably is not due to recurrent axon collaterals of the spiny neurons but rather to inhibitory interneurons excited by the stimulus (Kita, 1993).

The short-duration monosynaptic component of the corticostriatal EPSP to a single stimulus is mediated by glutamate, and primarily by glutamate acting at non-NMDA receptors (e.g., Calabresi et al., 1996; Kita, 1996). However, neostriatal spiny neurons possess NMDA receptors in abundance, but in most experimental preparations their contribution to evoked EPSPs is prevented by the voltage-dependent magnesium block of the NMDA ion channel. When spiny neurons are depolarized by passage of transmembrane current or the block is relieved by removal of extracellular magnesium or the stimulus is repeated at high frequencies, an NMDA component of the EPSP is readily demonstrated (Kita, 1996).

SYNAPTIC PLASTICITY

Like most glutamate-mediated synapses, those on neostriatal spiny neurons can undergo long-lasting changes in effectiveness after tetanic stimulation. Tetanic local stimulation in striatal slices under experimental conditions that minimize NMDA receptor activation lead to long-term depression (LTD) of glutamatergic synaptic transmission. The same stimulation, applied in the absence of extracellular Mg^{2+} , so that the block of NMDA receptors is removed, will give rise to long-term potentiation (LTP) (Calabresi et al., 1992b). Because reliable induction of LTP in slices often requires unphysiologically low extracellular Mg^{2+} , it might be considered an artifact of the experimental treatment, but LTP has been observed *in vivo* using cortical stimulation at physiological frequencies (Charpier et al., 1999; Reynolds and Wickens, 2000). This relative ease at inducing LTP *in vivo* may result from the background of depolarizing synaptic activity seen in the spiny neurons *in vivo*. That background activity can depolarize the cells to the point of relief of the Mg^{2+} block of the NMDA channel. Thus both LTP and LTD should be considered mechanisms present at corticostriatal synapses under normal conditions. Both LTP and LTD are induced by trains of high-frequency stimulation, so it is worth asking what might normally determine whether use would increase or decrease the strength of glutamate synapses on spiny neurons. This has been a very fruitful line of research, and it has revealed a complex dependency on striatal neuromodulators.

The neuromodulatory conditions important for induction of LTP and LTD are shown in Fig. 9.15. Induction of LTD in the striatum depends upon the presence of dopamine, being prevented by blockade of either D1 or D2 receptors (Calabresi et al., 1992a). In addition, LTD requires activation of group I metabotropic glutamate receptors (Sung et al., 2001). AMPA receptor activation is not necessary, but depolarization is required, and normally AMPA receptor activation is mainly responsible for the depolarizing synaptic potential at striatal glutamatergic synapses. The effect of depolarization is probably to trigger calcium influx through L-type channels, as LTD induction is also prevented by L-type calcium channel blockers (Choi and Lovinger, 1997). Finally, it is prevented by the inhibition of nitric oxide synthesis or by inhibition of soluble guanylyl cyclase, a cGMP-synthesizing enzyme whose activation is promoted by NO (Calabresi et al., 1999a). Thus LTD requires a large number of conditions for its induction in the striatum, including dopaminergic activation, release of NO (presumably by the GABA/SOM/NO interneurons), postsynaptic depolarization and activation of L-channels, and release of glutamate by axons to act at metabotropic glutamate receptors. Once established, LTD reduces the probability of release of glutamate by presynaptic terminals on the spiny neuron (Choi and Lovinger, 1997).

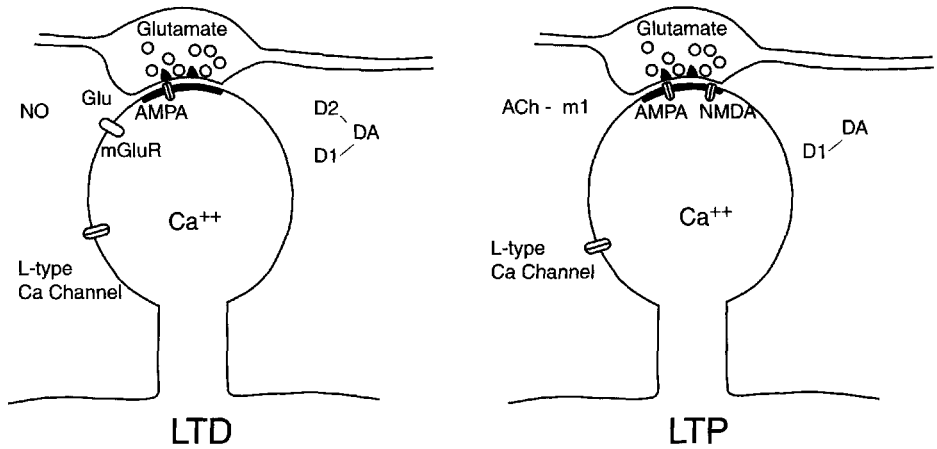


Fig. 9.15. Conditions for induction of LTD and LTP in striatal spiny neurons. The postsynaptic spiny neuron is represented by the dendritic spine, upon which a modifiable glutamatergic synapse is made. For repetitive stimulation of the synapse to induce LTD, depolarization and calcium entry through L-type Ca^{2+} channels are required and occur via activation of AMPA receptors. In addition, glutamate activation of metabotropic glutamate receptors and dopaminergic activation of both D1 and D2 receptors are required, as is release of nitric oxide. Similar stimulation can produce LTP if it is accompanied by activation of NMDA receptors and activation of m1 acetylcholine receptors. D1, but not D2, dopaminergic activation is required for LTP induction.

LTP of glutamatergic synapses on spiny neurons likewise requires much more than simply conjunction of presynaptic and postsynaptic activity and NMDA receptor activation, although those are necessary. Release of dopamine is also necessary, although only D1 receptors are apparently involved (Kerr and Wickens, 2001). Although NO release from interneurons is not involved, acetylcholine acting on m1 muscarinic receptors is required for induction of LTP (Calabresi, 1999b). LTP induction is favored when dopamine is applied directly to the cell under study at the time of tetanic stimulation, even under conditions that would otherwise produce LTD instead (Wickens et al., 1996).

It is important to recognize that the sites of action of some of the modulators are not known. It is tempting to assume that the dopamine and m1-acetylcholine receptors involved are on dendritic spines of the spiny cells, but this has not yet been established and there are other possibilities.

These results highlight the conditional nature of synaptic plasticity on the striatal neuron. Synaptic connections from excitatory inputs are not simply strengthened or weakened according to their ability to evoke action potentials in the spiny cells. The determination of which synapses are made stronger and weaker also depends upon the timing of dopamine release and on the activity of striatal interneurons at the time of their activation. It also helps us to understand the function of neuromodulators in the striatum. Dopamine, NO, and acetylcholine are all released in the striatum at synapses on the spiny neuron but do not evoke synaptic potentials there (see later). The role of these substances in creating the context for synaptic plasticity may help to explain their presence in striatal neurons and synapses on spiny cells. The dependence of both LTP and LTD on dopamine emphasizes the importance of that substance in synaptic plasticity in the striatum.

It should also be noted that the glutamate synapses undergoing LTD and LTP in the experiments described earlier may arise from more than one source. Most authors have claimed to be studying plasticity of corticostriatal synapses but have used stimuli that would excite activity in more than one afferent pathway. Many experiments have employed local stimulation in the striatum, which of course directly stimulates every kind of element in the tissue. However, stimuli placed in the white matter overlying the striatum, and even in the cerebral cortex itself, will not evoke specifically corticostriatal responses. Thalamic axons that make up the thalamostriatal pathway often also make large arborizations in the cortex, and the stimulation of their synapses is included in all studies of plasticity at glutamatergic synapses. Likewise, it should be kept in mind that in electrical stimulation experiments, cholinergic neurons and other interneurons, and dopaminergic axons, are almost always excited by the stimulus used to evoke glutamatergic responses. This can happen simply because they are included within the (usually unknown) region of action of the electrical stimulus or because they are stimulated synaptically by some axon that is directly stimulated. Under more natural conditions of stimulation, some kinds of interneurons may be activated while others are not, so the balance of neuromodulators responsible for LTP and LTD may be sculpted in subtle ways to build up the strength of some synapses while reducing that of others.

Cortical and Thalamic Inputs to Striatal Interneurons. Although most of the synapses formed by cortical and thalamic axons are on spiny neurons, most interneurons receive synapses from afferent fibers. The physiological effects of these inputs are of increasing interest because of the roles of interneurons in synaptic plasticity in the striatum, as well as for their classic role in the circuit.

Giant aspiny cholinergic cells are directly excited by cortical and thalamic stimulation (Wilson et al., 1990) and fast EPSCs in response to local stimulation in slices (Kawaguchi, 1993; Bennett and Wilson, 1998). These cells exhibit simple EPSPs, with fast rise times and little or no late response components. The maximal amplitudes of the EPSPs are much smaller than they are for the spiny neurons (see later). It is possible, however, to detect discrete components in the EPSPs in these neurons, especially with low-intensity stimuli. Thus the EPSPs evoked in the aspiny neurons appear to consist of the action of fewer axons than those in the spiny neurons, with each synaptic contact creating a larger EPSP as observed from the soma. These properties are consistent with there being relatively fewer excitatory afferent synapses on these neurons and (for thalamic inputs) their placement on relatively proximal dendritic shafts and even somata.

In vivo intracellular recordings of the responses of a cell that is probably the GABA/parvalbumin neuron have been reported by Kita (1993). These cells responded to cortical stimulation with a very powerful EPSP that gave rise to a burst of action potentials. In slices, GABA/parvalbumin neurons respond with an EPSP capable of evoking one or a burst of action potentials (Kawaguchi, 1993).

Synaptic activation of the SOM/NOS neurons by local stimulation in slices can trigger a regenerative calcium-dependent low-threshold response (LTS), which can develop into a self-sustained plateau potential, greatly out-lasting the synaptic conductance. During the plateau potential, the cells are capable of generating repetitive fast action

potentials. Thus, unlike any of the other neostriatal cells, these neurons have the capacity to set up a long-lasting response to relatively brief synaptic inputs (Kawaguchi, 1993).

ACTIONS OF SUBSTANTIA NIGRA INPUTS

Responses of spiny neurons to stimulation of the nigrostriatal afferents have been difficult to characterize. The nigrostriatal fibers are notoriously resistant to electrical stimulation, and they lie very close to other fiber systems that can produce large excitatory responses in the neostriatum (e.g., cortical efferent fibers in the cerebral peduncle and internal capsule). Simple stimulation of the nigrostriatal pathway therefore produces results that are difficult to interpret.

Early studies employing stimulation of substantia nigra yielded mixed results. In extracellular recordings, both excitatory and inhibitory responses were observed. It was difficult to prove in these studies that the responses observed in extracellular recording experiments were really due to the direct effect of the nigrostriatal axons rather than indirect polysynaptic pathways within the neostriatum and between the neostriatum and related structures. Intracellular recordings were more consistent in showing excitation (see review in Kitai, 1981). Intracellular recordings provide a more direct measurement of the effect of stimulation, because they allow visualization of sub-threshold responses and a more direct view of the response to synaptic activation. The latency of the responses is also more accurately measured, because the synaptic responses are directly visible rather than inferred from the latency of action potentials that may follow them by a variable additional delay. In these ways the results of the intracellular recording experiments were more reliable, but when the antidromic conduction time of nigrostriatal neurons was measured, it was discovered to be much longer than the latency of the EPSP observed in striatal neurons after stimulation of the substantia nigra. Further analysis of the EPSPs observed in the intracellular recordings of nigrostriatal responses revealed that a large proportion of these were actually due to activation of fibers of passage (Wilson et al., 1982). This is shown schematically in Fig. 9.16A and B. Stimulation of the substantia nigra excites cortical axons passing through and near that region. Some of these give off collaterals in the striatum, producing a monosynaptic excitation when excited, and they can also excite other corticostriatal neurons, giving rise to a polysynaptic excitation of the neostriatal neurons. The polysynaptic excitation is removed if the cortex is removed acutely, but the direct axon collateral remains. Thus one can get a very simple monosynaptic response in the neostriatum upon substantia nigra stimulation in the acutely decorticate animal, but it is caused by corticostriatal, rather than nigrostriatal, axons. Chronic decortication, allowing several days for all cortical axons to degenerate, allows stimulation of the nigrostriatal axons without the complication of cortical axons. Under these conditions (Fig. 9.16Cc), usually no clear synaptic response is seen. Thus a synaptic response due purely to the nigrostriatal pathway is difficult to demonstrate in an unambiguous way, even after removal of the confounding fibers of passage.

In parallel with these efforts to understand the nigrostriatal input, other investigators were performing experiments using iontophoretic application of dopamine and dopamine agonists to neostriatal neurons *in vivo*. These likewise produced mixed results. In most experiments, changes in firing rate due to dopamine application were recorded

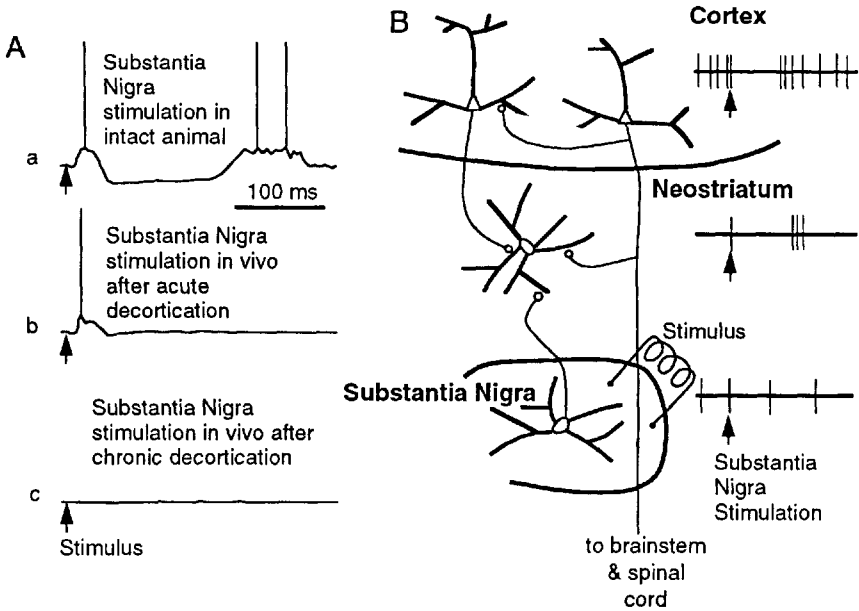


Fig. 9.16. Synaptic potentials evoked in spiny neurons by stimulation of the substantia nigra. **A:** Synaptic potentials in three different preparations. The trace in (a) shows the response evoked in intact animals, which resembles the response to cortical or thalamic stimulation. Immediately after removal or deactivation of cortical polysynaptic circuits, substantia nigra stimulation no longer evokes the late components of the response. After loss of cortical axons by degeneration after chronic cortical lesions, no reliable PSP response to substantia nigra stimulation is seen. **B:** The arrangement of cortical axons explains the responses in **B**. Substantia nigra stimulation evokes a monosynaptic excitation via axon collaterals of cortical neurons projecting to the brainstem and inadvertently excited by substantia nigra stimulation. These cells also evoke polysynaptic responses via their intracortical connections. The nigrostriatal projection axons, while present, produce no PSP in the striatal spiny neurons.

extracellularly, and the effect of dopamine on the cell was inferred from the firing rate changes. In these studies, some neurons increased their firing rate, whereas others decreased. In a small number of experiments, the effects of dopamine were observed more directly by intracellular recording. These experiments (Kitai et al., 1976b; Herrling and Hull, 1980) usually revealed depolarizations, but they were often accompanied by a decrease in neuronal excitability and a decrease in firing rate. Understanding such unusual responses requires an analysis of the ionic mechanisms underlying them, and this analysis cannot be performed in the *in vivo* preparation.

For this reason, studies of the effects of the nigrostriatal input onto neostriatal neurons have become concentrated on the direct application of dopamine or dopaminergic agonists onto striatal neurons *in vitro*. These studies have not revealed an ionic conductance in spiny neurons that can be directly gated by dopamine. Even the D2 receptor, which in dopaminergic neurons of the substantia nigra can be shown to mediate a fast IPSP due to a potassium conductance increase (Lacey et al., 1987), has no

such direct effects on spiny neurons (of the indirect pathway), which possess the D2 receptor. Instead, dopamine receptors, like muscarinic receptors on spiny neurons, act indirectly by altering the voltage-gated ion channels that are responsible for action potentials and for the dendritic properties of the cells. These effects do not lead to fast changes in membrane potential (hence the absence of PSPs in response to substantia nigra stimulation), and they are often not easily categorized as either excitatory or inhibitory. For example, D1 receptor activation raises the threshold for action potentials on spiny neurons (of the direct pathway) that possess this receptor by altering the availability of sodium channels responsible for action potentials (Surmeier et al., 1992). Because this will cause the cell to be less likely to fire action potentials, it could be considered to be a kind of inhibition. Similarly, D1 agonists suppress several P-, N-, and Q-type high-voltage-activated calcium currents. However, D1 agonists also enhance L-type calcium currents and so should have a net excitatory effect (for a review, see Nicola et al., 2000). D2 receptor agonists can enhance or depress voltage-dependent sodium channels (through different intracellular pathways) and suppress N-, P-, and Q-type calcium channels (Nicola et al., 2000).

This diversity of effects is quite different from the direct effects of neurotransmitter-gated conductances that are generally thought to be associated with fast synaptic transmission. Two general points about these neuromodulatory effects of dopamine should be emphasized. First, the diversity of the neuromodulatory effects of dopamine produces a computationally rich kind of intercellular communication. There is no requirement that all of the effects of any one dopamine receptor should combine to create a simple net increase or decrease in excitability. Instead, this mechanism is capable of producing conditional changes in excitability that depend upon the presence of another input or the past history of synaptic excitation and inhibition. Second, it should be noted that this diversity is possible because these effects of dopamine are indirect, being mediated by intracellular signaling pathways (e.g., cyclic AMP and phospholipase C) that can interact with a variety of ion channels and other molecules, including the receptors for other neurotransmitters (Nicola et al., 2000).

These effects of dopamine on striatal spiny neurons are not consistent with the often-stated view that dopamine excites direct pathway spiny neurons via D1 receptors and inhibits indirect pathway cells via D2 receptors. Although that view of dopamine's effects seems helpful in explaining some of the behavioral effects of dopamine depletion and Parkinson's disease, it is not supported by studies of dopamine's actions at the cellular level. Resolution of the views of dopamine action developed at these two different levels remains a task for the future.

Dopaminergic synapses are also formed on striatal interneurons. The inhibitory effects of dopamine on acetylcholine turnover in the striatum have been studied for decades. More recent studies have shown that the inhibitory effect of dopamine on acetylcholine release is mediated by D2 receptors (see Abercrombie and DeBoer, 1997). D2 receptors may exert their effects on cholinergic neurons by means of modulation of high-voltage-activated calcium channels, which control the release of acetylcholine at the axon terminals (Yan and Surmeier, 1996). In addition to D2 receptors, cholinergic neurons express a D1-class receptor that has been reported to cause slow depolarizations of the cholinergic cell (Aosaki et al., 1998). The D1 class receptor has been

suggested to affect spike afterhyperpolarizations in cholinergic cells (Bennett and Wilson, 1998). Dopamine also affects the excitability of cholinergic neurons by altering the effectiveness of synaptic inhibition, primarily from the GABAergic interneurons of the striatum.

Dopaminergic axons also make synapses on GABA/parvalbumin fast-spiking neurons, and their effects have been studied indirectly, from changes in inhibition of other striatal neurons. Dopamine, acting via D2 receptors linked to N-type calcium channels, reduced the amplitudes of GABAergic IPSCs recorded from cholinergic cells (Momiya and Koga, 2000; Pisani et al., 2000). More direct measurements from the fast-spiking neurons themselves indicate D1-class receptor-mediated depolarization associated with a decrease in membrane conductance (Bracci et al., 2002). Fast spiking neurons inhibit each other, and that inhibition is also reduced by the D1-mediated mechanism described for their effects on cholinergic interneurons. This suggests that the effect on GABA/parvalbumin cell-mediated inhibition via N-type calcium current modulation may be located at the axon terminals of the GABAergic interneurons.

INTRINSIC CONNECTIONS

Spiny Neuron. The neurotransmitter of the spiny neuron has long been believed to be GABA. At their target neurons in the substantia nigra and GP, the spiny neurons have a powerful inhibitory effect, mediated by GABA acting mainly at GABA_A receptors (e.g., Precht and Yoshida, 1971). By analogy, it has long been assumed that the spiny neurons powerfully inhibit each other. A large proportion of the synapses made by the collaterals of spiny neurons is made on dendritic spines or can otherwise be identified as having a spiny neuron as the postsynaptic element (Wilson and Groves, 1980; Yung et al., 1996). Thus the network of the spiny neurons and their recurrent collaterals has the appearance of a mutually inhibitory network of principal neurons, and many influential theories of the neostriatum have been based upon the assumption that the spiny cells exert a powerful mutual inhibition.

It was thus surprising when attempts to demonstrate a powerful mutual inhibition among spiny neurons failed (Jaeger et al., 1994). This test used two different techniques. In the first, spiny neurons were antidromically activated, by electrical stimulation of either the substantia nigra or the GPe. The stimulation was set near the threshold for antidromic action potential generation for a single neuron recorded intracellularly. This means that there was an antidromic action potential in response to the stimulus about half of the time, and about half of the time the stimulus failed to evoke an antidromic action potential. Under these circumstances, it is expected that about half of the spiny neurons are antidromically activated in response to any stimulus presentation. Even on the trials in which there was no antidromic activation of the recorded neuron, about half of the neighboring spiny neurons can be expected to respond to the stimulus. If the spiny neurons strongly inhibited their neighbors, a powerful (half-maximal) IPSP should be generated in the recorded neuron in response to this stimulus, even upon those stimulus presentations in which there was no antidromic action potential to mask the synaptic response. This is the method that was used to demonstrate the powerful Renshaw inhibition of motoneurons in the spinal cord (see Chap. 3). When used in the neostriatum, no IPSP could be detected. In the second method, pairs of nearby spiny neurons were recorded intracellularly in slices. In no case could

action potentials generated in one of the neurons by the injection of depolarizing current produce any detectable synaptic potential in the other spiny cell.

These experiments do not rule out synaptic inhibition among spiny neurons. In fact, a weak IPSP evoked by action potentials in nearby spiny neurons has been detected, using paired recording in slices but averaging hundreds of trials to reveal the small effect of the spiny neurons on each other (Tunstall et al., 2002). These results point out a weakness in qualitative approaches to the study of synaptic circuitry. Because synapses could be observed to occur among spiny neurons and because the axon collaterals of spiny neurons are a prominent feature of their morphology, it was assumed that mutual inhibition was much stronger than it proved to be. Nothing in the morphological literature allowed an estimate of the number of synapses formed by a spiny neuron upon its neighbors, and even now there is no quantitative estimate of the connectivity of spiny neurons. However, despite these negative results, GABAergic inhibition is demonstrable in the neostriatum, and the weakness of feedback inhibition via the output neurons has drawn attention to the role of feedforward interneurons.

Interneurons. With the exception of the cholinergic interneuron, all of the well-studied interneurons in the neostriatum contain GABA and presumably release it as a synaptic neurotransmitter. Like the subtypes of spiny neurons, the various interneuron subtypes can be distinguished by the presence or absence of peptides also believed to be involved in neurotransmission. One class of spiny interneurons that has not been shown to contain any co-transmitter is the GABA/parvalbumin neuron. These neurons are easily distinguished from the spiny cells by their especially high concentration of GABA, which causes them to stand out from other GABAergic neurons in immunocytochemical studies (Bolam et al., 1983), and their content of the calcium-buffering protein parvalbumin (Cowan et al., 1990; Kita et al., 1990). Parvalbumin is present in some, but not all, classes of GABAergic neurons in various parts of the brain, including the cerebral cortex, hippocampus, and thalamus. In the basal ganglia, it is found in the GABAergic principal cells of the substantia nigra and GP, as well as in the strongly GABA-positive spiny interneurons in the neostriatum. In all cases, it appears to be concentrated in cells that are capable of maintaining high rates of firing.

The GABA/parvalbumin interneurons receive powerful excitation from the cerebral cortex (Kita, 1993). Paired recording studies by Koós and Tepper (1999) allowed direct visualization of the IPSPs generated in spiny projection neurons by these cells. Single action potentials in a single interneuron produced large IPSPs in 25% of projection neurons located within 250 μm of the interneuron and were strong enough to delay action potential generation in a spiny cell made to fire repetitively by current injection. The IPSPs were mediated by GABA_A receptors. The dendritic and axonal fields of these neurons are compact, but the presence of gap junctions connecting these neurons together suggests the possibility that the inhibitory effects of these cells may spread over a wider area than that of the excitation. Koós and Tepper (1999) were able to directly demonstrate the electrical connections between fast-spiking interneurons in paired recordings. As already described, these interneurons also make synapses with each other and with cholinergic interneurons. Much of the inhibition observed in the aftermath of cortical excitation in the neostriatum is probably attributable to these neurons.

The SOM/NOS interneuron likewise contains (and presumably releases) GABA, but unlike the GABA/parvalbumin neuron, its soma does not stain heavily for GABA or its synthetic enzyme, GAD. This neuron has been thought not to be GABAergic, in fact, which set it apart from similar neurons in the cerebral cortex and hippocampus that were known to contain GABA as well as SOM. After treatment of the neostriatum with colchicine, which blocks axonal transport, SOM-containing striatal interneurons were shown to become GABA and GAD positive, suggesting that these substances may not be present in the soma and dendrites because they are efficiently transported into the axons of the cells (Kubota et al., 1993). However, the possibility that this treatment was actually inducing expression of GAD could not be eliminated. Subsequently, electron microscopic immunocytochemical studies of the axon terminals of these neurons have shown that they contain GABA as well as SOM in the absence of any colchicine treatment (Kawaguchi et al., 1995). These cells probably represent another GABAergic interneuron in the neostriatum. These cells also release SOM, neuropeptide Y, and NO. The effects of these substances on striatal neurons can be expected to attract intense study in the next few years. NO, which can diffuse across cell membranes, has already been shown to have profound effects on the release of glutamate, GABA, acetylcholine, and dopamine by axons in the neostriatum (Kawaguchi et al., 1995) and is essential for LTD at glutamatergic synapses in the striatum (see earlier).

Although cholinergic neurons are few in number, their axonal arborizations are very large and dense, and they provide a very rich cholinergic innervation to the neostriatum. This is another good example of the error that is committed if we judge the importance of a cell type purely by its number. The cholinergic neurons of the neostriatum and the system of cholinergic synapses that they give rise to in the neostriatal neuropil are known to exert a powerful influence on the firing of the spiny neurons and the final output of the neostriatum. Pharmacological treatments for many human disorders, including Huntington's disease, Parkinson's disease, and even schizophrenia, often rely upon manipulation of transmission at cholinergic synapses in the neostriatum.

Multiple acetylcholine receptors are known to exist in the neostriatum. Nicotinic receptors are located primarily on the axons of dopaminergic inputs to the striatum and on the GABA/parvalbumin fast-spiking interneurons. Nicotinic agonists excite these neurons directly (Koós and Tepper, 2002), presumably at synapses formed by cholinergic interneurons on the axodendritic membrane of the interneuron. At dopaminergic axons, nicotinic receptors enhance dopamine release (Zhou et al., 2001). In this situation, the acetylcholine is acting at extrasynaptic receptors, as these axons are not postsynaptic to cholinergic neurons (Jones et al., 2001).

On spiny neurons, the effects of cholinergic synapses are mediated by muscarinic receptors with neuromodulatory effects. Like dopaminergic receptors, muscarinic receptors are categorized into two major classes: the m1 and m2 classes. This terminology is somewhat confusing, because m1 is also the name of one of the m1 class receptors and likewise for the m2 class. The receptors within each class have signaling pathways in common. The m1 class receptors stimulate phospholipase C, whereas m2 class receptors inhibit adenylate cyclase. Spiny neurons express one of the m1 class receptors (m1 itself) and one of the m2 class receptors (m4) (Bernard et al., 1992; Yan et al., 2001). Although m1 receptors are present on nearly all spiny neurons, m2 class re-

ceptors are common only on cells of the indirect pathway. M2 receptors are especially enriched on cholinergic interneurons themselves (Thomas et al., 2000).

In spiny neurons in slices, m1 receptor activation results in an increase in input resistance and depolarization due to closure of potassium channels open at the normal resting membrane potentials of these cells (Hsu et al., 1996; Galarraga et al., 1999). This is a direct effect and not due to changes in tonic synaptic inputs, as it is unaffected by treatment with TTX. The potassium current inhibited in these studies is almost certainly the inwardly rectifying one that makes striatal neurons insensitive to small and unsustained inputs (see earlier), so its blockade, although not a classic transmitter action, will make the cells much less selective and more easily excited. The other key set of potassium currents governing the subthreshold sensitivity of spiny neurons is also modulated by muscarinic agonists. Muscarinic stimulation enhances inactivation of slowly inactivating potassium currents that are critical in determining the potential of the Up state of the striatal neurons (Gabel and Nisenbaum, 1999), and the inactivating potassium current I_{AF} that is critical in the transition between the Down and Up state (Adkins et al., 1990).

Muscarinic receptors also mediate effects of ACh on high voltage activate calcium channels of striatal spiny neurons. M1 receptors inhibit N-, P-, and L-type calcium channels in spiny cells (Howe and Surmeier, 1995), which may make them less excitable but may also indirectly increase their responsiveness by reducing calcium entry, and so the spike afterhyperpolarizations of striatal spiny cells (Pineta et al., 1992).

In addition to these diverse effects on ion channels, acetylcholine increases the responses of spiny neurons to glutamatergic excitation, specifically by enhancing NMDA receptor sensitivity (Calabresi et al., 1998) and is important in the mechanism of LTP at glutamatergic synapses (as already described).

M2 muscarinic mechanisms produce a decrease in synaptic transmission at glutamate and GABA synapses, due to action of acetylcholine at extrasynaptic receptors on axon terminals (e.g., Koós and Tepper, 2002).

FUNCTIONAL OPERATIONS

NATURAL FIRING PATTERNS

Neostriatal spiny neurons exhibit a very characteristic firing pattern. Even in unanesthetized and behaving animals, the cells are usually silent. Occasionally, the cells fire a train of several action potentials that lasts from 0.1 to 2.0 sec and then become silent once again. The train of action potentials is not really stereotyped enough to be called a burst. The discharge rate during the episode of firing usually does not become greater than 40/sec, and the cells usually do not fire rhythmically during the episode (suggesting that firing rate is not limited by spike afterpotentials). In behaving animals, these episodes of firing are sometimes locked to the onset of movements (e.g., DeLong, 1973; Kimura et al., 1984). An example showing an intracellular recording of a spiny neuron in an anesthetized rat and the task-related firing of a presumed spiny neuron during a learned movement is shown in Fig. 9.17.

Why are the cells silent so much of the time? The answer to this question evaded investigators using extracellular recording but was readily obtained when intracellular recordings *in vivo* became routinely available. Intracellular recording experiments show

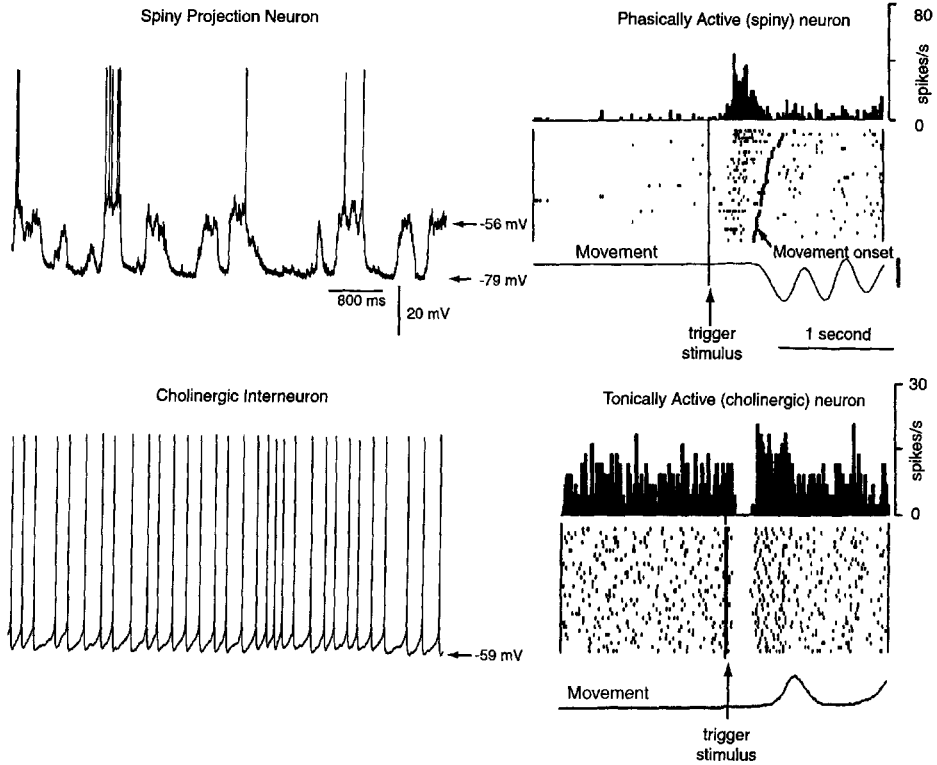


Fig. 9.17. Representative firing patterns of projection neurons and cholinergic interneurons. Intracellular recordings from rats are on the left. On the right are typical data collected during extracellular recording in awake primates. For each neuron, there is a peri-event time histogram (top), a spike raster (middle), and measure of the movement. Each line of the raster represents one trial during the task. The horizontal axis is time, and each dot represents one action potential in the neuron. Activity to the left of the vertical line marked trigger stimulus is spontaneous activity of the neuron. The trigger stimulus is the instruction to the animal to move. The phasically active neurons, which are the spiny cells, show an episode of activity during the task. [From Kimura, 1990, with permission.] This activity is more closely locked to the time of the movement than to presentation of the trigger stimulus. The dark spots labeled *Movement Onset* indicate the time of movement onset for each trial. The peri-event histogram represents the cumulative firing rate across all trials. The low spontaneous activity and episodic nature of the response match the spontaneous firing pattern of the spiny neuron. The cholinergic neuron (from Aosaki et al., 1995, with permission), in contrast, shows tonic spontaneous firing due to its pacemaker properties. Its response during a learned movement usually consists of a pause in firing that is best aligned to the trigger stimulus rather than to the movement onset. Movement onset is not shown in the figure. In some cholinergic cells, the pause in firing is preceded by a brief period of increased firing probability (not shown).

that when spiny neurons do fire, the train of action potentials arises from a prolonged episode of depolarization (the Up state) accompanied by an increased synaptic noise (Wilson and Groves, 1981). The depolarizing episodes also show several other revealing characteristics. They cannot be triggered by depolarizing current pulses; they cannot be terminated by hyperpolarizing current pulses; and they do not disappear when

the cell is hyperpolarized below spike threshold by passage of current into the soma. In anesthetized animals, and perhaps also in waking animals, there must be episodes of local corticostriatal and thalamostriatal synchrony, that is, correlations in firing of small converging subsets of corticostriatal and thalamostriatal neurons that may be important for shaping the firing patterns of the cells.

In vivo intracellular recording experiments have revealed that the membrane potential achieved during the Up state of the depolarizing episodes is not simply the envelope of converging synaptic input (Wilson and Kawaguchi, 1996). Blocking depolarization-activated potassium channels by intracellular injection of cesium caused the membrane potential during the depolarizing episodes to approach 0 mV (near the reversal potential for corticostriatal synapses). The membrane potential in the Down state was almost unaffected. Of course, it was necessary to poison both sodium and calcium currents in the recorded neuron using intracellularly applied blockers, to prevent action potentials from interfering with the measurements. These treatments did not prevent the occurrence of Up states. In the absence of subthreshold voltage-dependent potassium currents, it was possible to measure the decrease in input resistance due to synaptic input during the depolarizing episodes. This showed that the Up state was due to a very powerful synaptic input and that the Down states were periods of little or no synaptic input (either excitation or inhibition). The membrane potential during the Up state is held below spike threshold (on the average) by the potassium currents generated by synaptic excitation, rather than by synaptic inhibition. The mean subthreshold value of the membrane potential explains why the spiny neurons do not fire rhythmically during the depolarizations. Action potentials occur due to threshold crossings that occur at unpredictable times during the depolarizations, and so interspike intervals in the depolarized state are highly variable. Still, although the membrane potential achieved and the firing rate maintained during the episodes of excitation do not accurately reflect the strength of the synaptic input, the timing and duration of the episodes of excitation are determined almost totally by the pattern of converging synaptic excitation on the spiny neurons.

Most neostriatal neurons are spiny cells, and nearly all recordings of single neurons that are obtained from the neostriatum are from spiny cells. It is therefore not always necessary to obtain anatomical verification of the cell type associated with responses that are common to most neurons. On the other hand, identification of firing patterns and synaptic responses of interneurons requires intracellular staining for the determination of cell type. The firing patterns of cholinergic neurons have been studied in anesthetized animals and slices using intracellular recording (Wilson et al., 1990; Bennett et al., 2000) and using extracellular recording in awake behaving animals (e.g., Aosaki et al., 1995). They are pacemaker cells that fire sometimes regularly, sometimes irregularly, with average rates less than 20 Hz. Synaptic potentials superimposed on the pacemaker activity act by perturbing the pacemaker mechanism, rather than by summing to cause a spike threshold crossing, as in more linear neurons (e.g., Bennett and Wilson, 1998). In extracellular recordings from the motor regions of the striatum of behaving monkeys, neurons with firing patterns like that of the giant aspiny neuron have been reported to show a unique kind of response during execution of learned movements. Unlike the spiny neurons, which fire in relation to execution of the movement, tonically firing neurons fire in relation to the sensory cue that triggers the move-

ment (Kimura et al., 1984). This is not to say that the tonically active neurons are sensory cells. They do not respond to the same stimulus when it is not a signal for initiation of a movement, and the responses of these cells develop gradually during the acquisition of a learned movement (Graybiel et al., 1994). This firing pattern is also largely determined by the membrane properties of the neuron. Cholinergic neurons have resting membrane potentials (in the absence of input) within a few millivolts of the action potential threshold (Jiang and North, 1991; Kawaguchi, 1992). The firing pattern of a cholinergic interneuron and the firing of a tonically active neuron during a learned movement are shown in Fig. 9.17.

Data on the firing patterns of the other interneurons *in vivo* are sparse. In slices, the GABA/parvalbumin interneuron has been shown to fire short-duration action potentials, to have powerful but short-lasting spike afterhyperpolarizations, and to fire at high frequencies with little spike frequency adaptation in response to depolarization (Kawaguchi, 1993). The other interneuron, the SOM/NOS neuron, has not been studied *in vivo*. The identification of these cells in *in vivo* recordings and the description of their natural firing patterns, especially in behaving animals, are challenges for future work.

The end result of activity in the neostriatum must be expressed as a change in the activity of neurons in the GP and substantia nigra that receive an input from the neostriatum. Although the spiny neurons contain many peptides and other substances, physiological studies indicate that the primary fast effect of activity in spiny neurons is a GABAergic inhibition of the target cells. The cells in GP and in SNr that are the target of this inhibition have very high rates of tonic activity. These cells are also pacemakers and usually fire rhythmically at a rate determined primarily by their own membrane characteristics (Nakanishi et al., 1991; Nambu and Llinas, 1994; Cooper and Stanford, 2000). They are driven by pacemaker cells in the subthalamic nucleus (Bevan and Wilson, 1999), so the neurons of the output nuclei are almost all spontaneously active pacemakers that can maintain an output of the basal ganglia, even in the absence of any input from the cortex or thalamus (Terman et al., 2002).

COMPLEX INTEGRATIVE TASKS

In the past two decades, our understanding even of difficult regions of the brain like the striatum has increased enormously. Research on the anatomical, physiological, and pharmacological details of the operation of the basal ganglia has led to new concepts of their function, not only in disease but also in the healthy brain. One idea that arose from anatomical considerations, and which may be obvious to the reader, is that the basal ganglia is part of a loop that supports thalamocortical interactions by positive feedback. This idea is based on the disinhibition hypothesis advanced by Deniau and Chevalier (1985). It was already embedded in the influential review by Penney and Young (1983) and has been elaborated by anatomical studies of parallel pathways through the striatum forming separate loops for various functionally distinguished cortical systems (Alexander et al., 1986). The basis of the idea as currently advanced is that striatal neurons are detectors of specific distributed patterns of cortical activity that represent candidate movements, goals, strategies, or interpretations of sensory patterns (e.g., Graybiel, 1998). As seen from the study of their cellular properties (see earlier), striatal spiny neurons fire rarely, and an episode of firing in those neurons signals con-

vergent input of many cells distributed in a variety of distant but functionally related regions of the cortex and thalamus. When a group of striatal neurons projecting to the same cells in the GP and substantia nigra undergo an episode of firing, they should inhibit the pallidal cells to which they project. Pallidal and nigral basal ganglia output neurons fire spontaneously at high rates, so the result of activity in the striatum is expected to be a pause in the otherwise constant inhibition exerted in the thalamus by these cells. The net effect (in this hypothetical scheme) is cortico-striato-pallido-thalamic disinhibition. When the striatal cells fire, they release some thalamocortical interaction from inhibition. These ideas have emerged from the bottom up. That is, they arise from the study of the anatomy and physiology of the neurons and circuits without any a priori knowledge of the psychological functions of the basal ganglia. They present an image of the corticobasal ganglia-thalamic loop as a kind of filter, in which the basal ganglia identify some cellular activity patterns in the cortex and release some other (or the same) pattern of activity in the cortex via the thalamus.

The problem with testing this idea is that one does not know the specific nature of the pattern of activity in the corticostriatal pathway, or the thalamocortical pattern that it releases. Must we know how the thalamocortical system works in detail before we can understand the function of the basal ganglia? Perhaps not, as another output of the basal ganglia, to the superior colliculus, is analogous in nearly every way but controls a different pathway whose function is much better understood. The superior colliculus is a central point of integration of signals from the retina, cerebral cortex, and brainstem pathways that have information about the position of the head and eyes relative to visual stimuli. The main pathway for generating eye movements does not involve the basal ganglia. Basal ganglia output neurons in the SNr exert a tonic inhibition on the neurons of the deep layers of the superior colliculus that carry the output of the that structure to the cells that perform eye movements. When the substantia nigra cells pause, it does not cause an eye movement, but it favors movement of the eyes to the particular target associated with the disinhibited neurons (Hikosaka et al., 2000). Studies of the activity of neurons projecting from the substantia nigra to the superior colliculus have shown those cells acquire both increases and decreases in activity during various phases of eye movement as predicted by the disinhibition hypothesis.

What kinds of patterns are identified by the basal ganglia, and what does it contribute to eye movements or anything else? The convergence of cortical and thalamic inputs from widespread areas in a pattern based upon functional similarity rather than spatial proximity suggests that the striatum is looking for the convergence of polysensory, motor, and cognitive streams of processing. How do these get associated in the striatum? Perhaps the striatum is a kind of adaptive neural network, which associates streams of processing all over the cortex, and uses a learning rule of some kind to form the associations. If it followed a simple Hebb associative learning rule, as has been proposed for the hippocampus (see Chap. 11), then patterns of cortical neurons would come to be encoded by the striatum according to how often they occurred. The statistical structure of cortical patterns would be represented in the striatum. This might allow a more efficient recoding of the cortical pattern, but it would not really add anything, and it is hard to understand why that would be useful as feedback to enhance activity in the cortex. A breakthrough in our understanding of the nature of the associations that might form in the striatum occurred with the combination of two discov-

eries. One was the discovery that LTP and LTD in the striatum were dependent upon dopamine (as already described). The second was the discovery that dopaminergic neurons fire in a very special way during learning.

Early studies of dopaminergic neuron firing in animals during performance of learned tasks suggested that firing of those cells was not closely related to any phase of a learned task. This was disappointing, because direct stimulation of the dopaminergic pathway acts as a powerful reinforcer of behavior, so it seemed possible that they may play an important role in operant behavior (see review in Berridge and Robinson, 1998). However, experiments that followed the responses of dopaminergic cells throughout the learning process produced a very different result. The fundamental discovery, made in the laboratory of Wolfram Schultz (for a review, see Schultz, 1998), is that dopaminergic neurons fire in response to the resolution of uncertainty about the prospects for reward. That is, they fire at the moment when the animal recognizes the opportunity to begin a behavioral sequence that will end with a reward. Experimental examination of these responses of the dopaminergic neuron showed that they were encoding a kind of error signal, representing a change in expectation of reward. Examples of experimental data from Schultz and his collaborators are shown in Fig. 9.18. For exam-

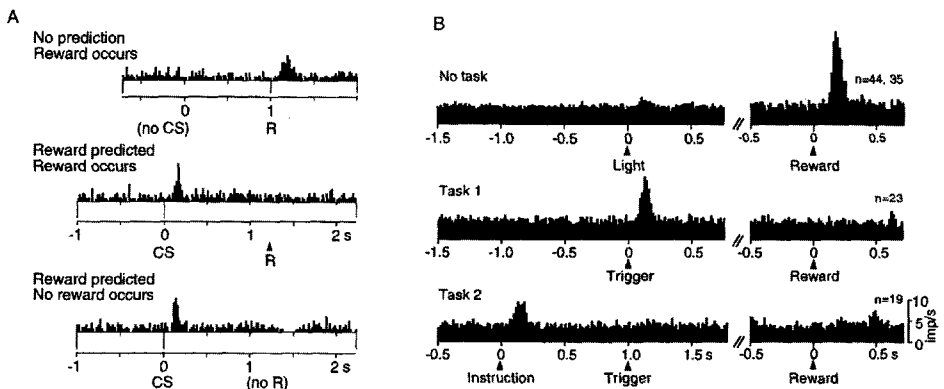


Fig. 9.18. Reward-prediction-related responses of dopaminergic neurons. **A:** Histograms of responses of a single dopaminergic neuron collected across a set of trials. When a rewarding stimulus is presented unpredictably (in the absence of a predictive conditioned stimulus), the cell responds with a brief increase in firing rate. When the rewarding stimulus has been paired with presentation of a CS, the dopaminergic neuron fires in relation to the reward predictor, and not to the subsequent reward. If the reward is withheld unexpectedly, the dopaminergic neuron responds to the CS, and a pause occurs at the moment when the reward was expected to occur. [Reproduced from Schultz et al., 1997, with permission.] **B:** Transfer of the dopamine cell's response to an earlier predictor. In this figure, the histograms are represent the collective responses of a sample of neurons (indicated by n). Presentation of a light that has not yet been paired to a reward evokes no response from dopaminergic cells, but the cells do respond to the unexpected reward (no task). A trigger stimulus that has been paired with the reward acquires the response of the dopaminergic cells, and its presence as a predictor suppresses the response to the reward (task 1). Subsequently, repeated presentation of the light before the trigger stimulus and reward causes the light to acquire the response, and the previous CS becomes ineffective. The dopamine cells' response occurs to the earliest stimulus that is a reliable predictor of the reward. [From Schultz et al., 1995, with permission.]

ple, an unexpected reward is a good stimulus for dopaminergic neurons and will elicit a brief period of higher-than-normal firing rate. The absence of a reward at the time one was expected (e.g., an unrewarded trial in a learned behavioral task that normally ends with reward) results in a pause in the ongoing pacemaker activity of the dopaminergic neuron (Fig. 9.18A). This sounds a lot like simply a neural representation of reward, until one notices that if the reward was expected (e.g., at the end of a rewarded trial in a learned task that normally ends in reward), there is no response from the dopaminergic cell. Sometime between the first trial during learning (when the reward was unexpected and the subject accidentally did the right thing and received the reward) and the time that the task is fully learned, the dopaminergic cells' activity disappeared. What happened to it? Schultz's work showed that the response of the dopaminergic neuron was gradually transferred to earlier and earlier phases of the learned task. Stimuli that were not intrinsically rewarding but were good predictors of an upcoming reward acquired the ability to evoke an increase in firing of the dopaminergic cells. This process shifts the dopaminergic cell's response earlier and earlier in time, corresponding to the animal's increasing knowledge about the nature of the rewarded sequence of events. This process is demonstrated in Fig. 9.18B. The existence of neurons that encode reward-prediction error is required for a kind of learning process called *reinforcement learning*.

Reinforcement learning is different from the usual control theory-inspired notions of motor learning that dominate most of the motor systems field. In those, a feedback signal not only evaluates performance of the task but also instructs the controller on the direction and degree of alteration required to improve performance. Likewise, it differs from the usual supervised learning ideas in neural networks, in which evaluation of performance of the network has specific suggestions for improvement of the network embedded within it. In reinforcement learning, behavior is simply rewarded to the extent that it succeeds. There is no instruction on how to make it better. Intrinsic variations in behavior lead to chance improvements, and the reinforcement signal acts to increase the probability of recurrence of whatever behavior preceded success. Thus, like evolution, it operates on a principle of selection rather than instruction.

A simple reward pathway, which when activated increased the synaptic strengths of neurons firing just before the reward, might sound sufficient for the operation of this process, but it is not. Such a system would increase the probability of the last step in a behavior that leads to reward but nothing more. Interesting and useful behavior patterns usually involve a sequence of unrewarded steps that lead to a reward at the end. One way to teach a network the entire sequence would be to move the neural representation of the reward to earlier and earlier steps in the sequence over trials. For example, once one learns that a particular final move in chess will win the game, it should become rewarding to see that there is a move that will put the board in the configuration that allows that final move. Success at chess requires learning to place a value on all possible configurations of the pieces. That is, the player must be able to estimate the probability of a successful outcome from any arrangement of the chessboard. One then may play the early phases of the game for the reward of seeing an improvement in the value placed on the board. For this to occur, the value of the board must be learned over trials from the end of the game (where primary rewards occur) toward the beginning. A neural representation of reward must move backward in time toward the

beginning of the rewarded sequence. The firing of dopaminergic neurons, in the experiments by Schultz and coworkers, does exactly that. As learning proceeds, the dopaminergic neurons fire earlier in the sequence, so that activity is detected at the earliest time that the animal recognizes the opportunity to complete a sequence of behavior associated with the reward. This explains why the response is acquired by earlier phases in the sequence, but why should the dopaminergic neuron quit firing at the later stages of the sequence? The sensory, motor, and internal synaptic signals associated with the last step in the sequence of events leading to reward need be rewarded only if they are part of the step in the rewarded sequence currently being acquired. Imagine a situation in which some simple behavior led immediately to firing of neurons representing reward. An animal or a human operating on the reinforcement learning principle would simply repeat that simple behavior over and over at the expense of all others. The cellular mechanisms that inhibit the dopamine cells' response to the primary reward prevent this automatic repetition of simple appetitive behaviors and allow them to be incorporated into more complex sequences. The reader will recognize that when simple behaviors are made capable of directly stimulating dopamine release, e.g., self-stimulation of the dopaminergic pathway or self-administration of indirect dopamine agonists like amphetamine or cocaine, this can cause repetition of those acts at the expense of more complex and useful behavioral sequences.

What does this view of the basal ganglia predict for the striatum? Because striatal neurons undergo synaptic plasticity conditional on the release of dopamine, some investigators have speculated that the striatum is an associative network in which each neuron is learning to recognize the conjoint activation of a number of its inputs using a synaptic strength-altering learning rule (Houk et al., 1995; Wickens and Kötter, 1995). If the learning is only permitted when dopaminergic neurons projecting to that neuron fire, what will the striatal cells learn? They will learn which combinations of their inputs are associated with an unexpected improvement in the predicted success of ongoing behavior. Thus the dopaminergic neurons teach the striatal neurons to filter cortical and thalamic input patterns on the basis of their value in behavior. If this is true, the striatum is learning to predict the value of various patterns of cortical activity for success in sequences of actions that may not be rewarded until some future time. This advice on future success is then integrated into corticothalamic interactions, or to specific neurons of the superior colliculus, to increase the likelihood of the highest valued strategy.

This idea is an exciting one, but it raises a number of questions that have not yet been answered. For example, if the prediction proves wrong, then the advice of the last set of striatal neurons in the process should be devalued. In this situation, the studies of dopaminergic cell activity say that dopaminergic neurons will respond with a pause in activity at the time the reward should occur. This will place the blame on the neurons representing the last phase of the sequence, not those predicting reward at the beginning (when dopaminergic cells fired as if a reward was coming). It would be interesting to see if during extinction of a learned sequence, the pause response would propagate back to the beginning of the sequence, as the increase in firing does. But even if it does, how can the pause in dopaminergic neurons devalue the association of synaptic activity that precedes it, given that reduction in dopamine release in the striatum does not lead to LTD but rather to disabling of both LTD and LTP? The

dopamine-contingent learning rule in the striatum seems to leave no room for learning from failure, only success.

What can be the contribution of the striatal interneurons in this scheme? The GABA/parvalbumin interneuron seems to have a traditional circuit role in the basal ganglia, but the cholinergic interneuron and the GABA/SOM/NO cells do not. We do not know what the GABA/SOM/NO cells do during learning, but we do know about the cholinergic cells because they are recognizable by their tonic activity in extracellular recording experiments. Cholinergic interneurons do not respond in relation to learned tasks in the beginning but acquire a response during the acquisition of learned behavior. Like the dopaminergic neuron, their response moves to earlier and earlier stages in the sequence (Apicella et al., 1998). The pause responses of cholinergic neurons are also dependent upon dopamine, as loss of dopaminergic input blocks the acquired pauses to trigger stimuli (Aosaki et al., 1994a). However, their responses are not as related to reward, because cholinergic cells also respond to noxious stimuli and to unexpected stimuli regardless of their reward value. Also, their response usually does not consist of an increase but rather of a decrease in firing rate. As we have already noted, cholinergic neurons are pacemaker cells that fire continuously even in the absence of synaptic input. Most cells respond with a pause in activity, often followed by a rebound increase in firing. However, some cells also exhibit a brief increase in firing just before the pause (Aosaki et al., 1994b, 1995). The pause responses for a learned task are shown in Fig. 9.17. We should also note that unlike dopamine, which is required for both LTP and LTD, acetylcholine is required only for LTP. If dopamine and acetylcholine are both present, LTP is enabled, whereas if dopamine is present and acetylcholine is not, the balance in synaptic plasticity is shifted in favor of LTD (Centzone et al., 1999). A background level of dopamine and acetylcholine is maintained by the spontaneous tonic activity of these two cell types. During the acquisition of a new task, dopaminergic and some cholinergic cells will respond together, and over the course of learning, more cholinergic cells will be recruited in the task, until pause responses are observed in widespread regions of the striatum (Aosaki et al., 1995). In the vicinity of many fewer cholinergic cells that respond with an initial increase in firing (followed by a pause), synaptic strengths of active cortical and perhaps thalamic inputs may be increased by LTP, whereas in the regions innervated by the much larger group of cholinergic cells responding with only a pause in firing, associations among concurrently firing afferents may be weakened by LTD. This mechanism may act to limit the extent of the striatum that is engaged in the learning of a specific task.

This scheme puts a lot of responsibility on the dopaminergic neurons. How do they come to be able to predict the reward value of events at a particular moment? There are a number of possible avenues. Some authors think that connections from the amygdala or frontal cortex may carry this information, and the dopaminergic neurons may be only relays for these structures. These ideas pass the responsibility onto other brain areas. One especially clever idea of this kind is that of Houk and his associates (Houk et al., 1995). It is based upon the observation that spiny striatal projection neurons in the striosomes project specifically to the dopaminergic neurons, rather than to the basal ganglia output nuclei. Remember that the cellular organization of the striosomes was the same as that of the matrix, but its input and output were different, with striosomes receiving input from associational and limbic regions that had corticostriatal

neurons in deeper layers. According to Houk et al., these inputs may contain the fragments of cortical information required to make a reward prediction, and they are associated by striatal neurons, which learn to predict rewards using the same dopamine-dependent learning rule used in the matrix. While in the matrix, striatal neurons are learning to identify which strategies, goals, movements, or sensory interpretations have been most associated with rewarded behavioral sequences in the past, the striosomes are learning which cortical inputs have been best able to predict the value of particular situations. The striatal neurons in striosomes use dopaminergic signals based on current knowledge to learn how to make more accurately predicting dopaminergic signals. This idea, which is illustrated in Fig. 9.19, has the advantage of applying the same mechanism to controlling the dopaminergic neuron, and it is based on known anatomical and physiological relationships. It has not been subjected to direct experimental test, so it remains only an attractive idea. One prediction is that striatal spiny neurons in the striosomes would not fire in relation to execution, like most spiny cells, but would show reward, and reward-predicting signals somehow related to those

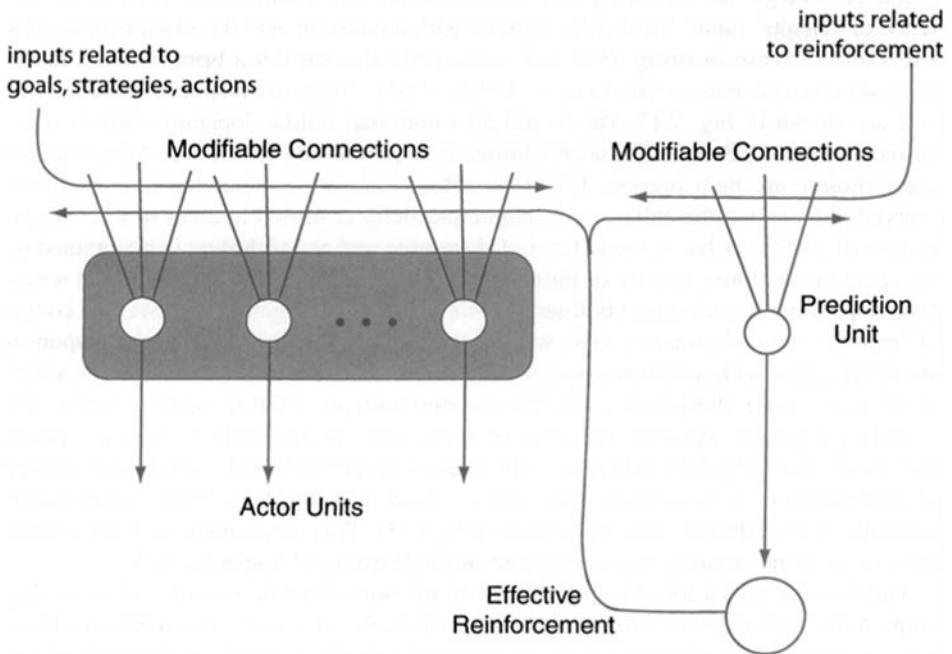


Fig. 9.19. Diagram of the actor critic model, as applied to the striatum by Houk et al. (1995). Striatal neurons are of two kinds—one labeled *actor units* and one labeled *prediction units*. These receive modifiable synaptic connections, whose modification is dependent upon dopamine release from the dopaminergic cells, labeled *Effective Reinforcement*. The learning rule is the same in both sets of units, but the actor units receive inputs related to movements, goals, or interpretations of sensory information, whereas the prediction units receive inputs that may be useful in predicting future reinforcement. The role of the predictor unit is to improve the prediction of rewards, improving the usefulness of the effective reinforcement signal. [Modified from Barto, 1995, with permission.]

of the dopaminergic cells. Although identifying striosomal vs. matrix neurons has not been possible in experiments on behaving animals so far, there are reports of a minority of spiny neurons that show reward-related responses (Hassani et al., 2001; Takikawa et al., 2002).

A thorough test for these ideas may not first come from studies of mammals. Reptiles and birds also have basal ganglia, and studies of bird song learning have helped elucidate the role of the basal ganglia in learning complex sequential tasks (e.g., Brainard and Doupe, 2000). The song of a songbird is a complex sequence of syllables, each of which must be enunciated and which have to be placed in order. Songbirds are not born knowing their species-specific song but must learn it by copying the song of an adult bird. Lesions of the basal ganglia in songbirds disrupt the learning process and prevent a juvenile bird from learning its correct song, even when the auditory and motor cortical pathways are intact. If the same lesion is produced in an adult who has learned the song, there is no immediate effect on performance of the song. If a bird is deafened in adulthood, its song will gradually deteriorate. If the basal ganglia are destroyed in a deafened adult, the song will not deteriorate but will remain stable. Thus the deterioration of the song of the deaf bird is interpreted as an active process. The adult bird varies its motor patterns but cannot correctly evaluate the value of those alterations because sensory feedback is disrupted. The accumulating errors associated with these alterations are responsible for the deterioration of the behavior sequence. This suggests that the basal ganglia may be required not only for the evaluation of candidate modifications to operant tasks but also for the generation of the variations in behavior required for reinforcement learning to work.

This page intentionally left blank

OLFACTORY CORTEX

KEVIN R. NEVILLE AND LEWIS B. HABERLY

Three different types of cerebral cortex can be distinguished: the *neocortex*, which forms the large convoluted mantle of the human brain, and two phylogenetically older types, the *olfactory cortex*, or *paleocortex*, and the *hippocampal formation*, or *archicortex*. Although the olfactory cortex and hippocampus have a simpler architecture than the neocortex and are usually described in terms of three layers rather than six, all three types of cortex display many common features at the level of synaptic organization. In the following chapters it will become apparent that there are striking similarities in cellular morphology, physiology, neurochemistry, synaptic relationships, and local circuitry. These similarities have allowed the phylogenetically old types of cortex, with their easily analyzed, precise laminar organizations, to serve as model systems for the analysis of questions of general interest regarding cortical function. The olfactory cortex, with which our account of cerebral cortex begins, is well suited for the analysis of questions related to mechanisms of sensory discrimination, including learning-related plasticity. With a comparatively simple structure, it is able to process the complex spatial and temporal patterns of neuronal activity that constitute the olfactory code (see Chap. 5). The olfactory system is also unusual in its shallow processing depth—information from receptors reaches central structures such as the entorhinal cortex, prefrontal cortex, and amygdala in relatively few synapses without an obligatory relay in the thalamus. Other aspects of the olfactory cortex that have attracted interest are its similarity in architecture and other features to artificial “neural networks” with brain-like capabilities, the presence of prominent oscillations, and its susceptibility to epileptogenesis.

Olfactory cortex is usually defined as those areas that receive direct synaptic input from the olfactory bulb (Fig. 10.1A) (Price, 1973). As in other types of cerebral cortex, many different olfactory cortical areas can be distinguished on the basis of anatomical differences (Switzer et al., 1985; Price, 1987; Carmichael et al., 1994; Ekstrand et al., 2001a; Haberly, 2001). The largest olfactory area, on which this chapter will focus, is the *piriform cortex* (also termed the *pyriform* or *prepiriform cortex*). Other cortical regions that receive direct olfactory bulb input include the *olfactory tubercle*, *entorhinal cortex*, and *agranular insula*, cortical areas associated with the *amygdala*, and small cortical areas within the olfactory peduncle (anterior olfactory “nucleus,” *tenia tecta*, and dorsal peduncular cortex). Because the traditional designation of the

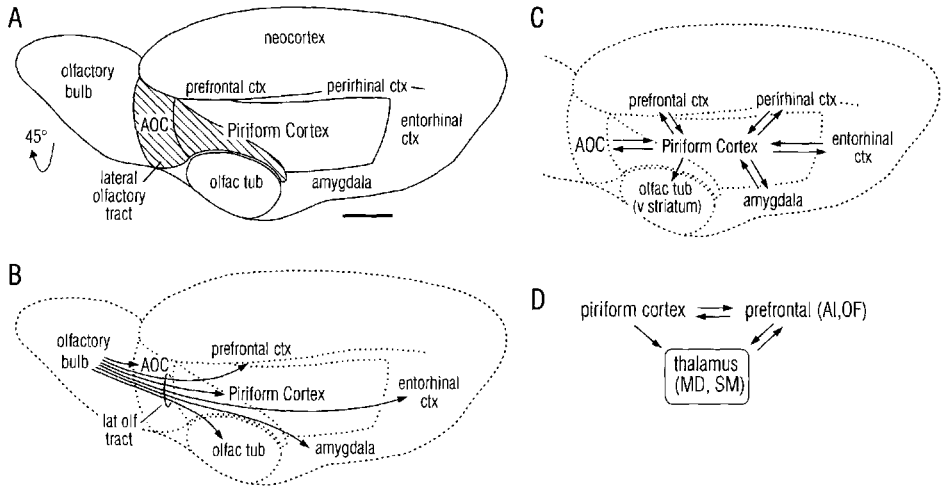


Fig. 10.1. Olfactory cortical areas and connections. **A:** Ventrolateral view of rat brain. The hatched area is the lateral olfactory tract (LOT), which carries afferents from the olfactory bulb to piriform cortex and other olfactory cortical areas. Scale bar: 2 mm. **B:** Areas that receive afferent input from the olfactory bulb. AOC, anterior olfactory cortex (equivalent to the misnamed anterior olfactory “nucleus”). **C:** Associational (corticocortical) connections of piriform cortex. Note the direct reciprocal connections with high order cortical areas and unidirectional projection to the olfactory tubercle (olfac tub). **D:** Parallel projections from piriform cortex to two regions of prefrontal cortex: agranular insula (AI) and orbitofrontal cortex (OF). There are heavy direct associational (corticocortical) projections to prefrontal cortex from pyramidal cells in piriform cortex and a sparse projection from deep multipolar cells that relays in two “high order” thalamic nuclei, the mediodorsal (MD) and submedial (SM).

anterior olfactory nucleus is misleading (it is actually pyramidal cell-based cortex), we will refer to this region as the *anterior olfactory cortex* (AOC in Fig. 10.1). Also note that although the agranular insula and entorhinal cortex are olfactory cortex by virtue of olfactory bulb input, these areas are not paleocortex. They have a more highly laminated structure and are considered to be transitional in form between neocortex and paleocortex (Krettek and Price, 1977).

NEURONAL ELEMENTS

CYTOARCHITECTURE

The laminar organization and prominent cell types are illustrated for piriform cortex in Figs. 10.2 and 10.3.

Layer I is a superficial plexiform layer that contains dendrites, fiber systems, and a small number of neurons. It has been divided into a superficial part, *layer Ia*, that receives afferent fibers from the olfactory bulb by way of the *lateral olfactory tract* (LOT) (Fig. 10.1A) and a deep part, *layer Ib*, that receives association (corticocortical) fibers from other parts of the piriform cortex and other olfactory cortical areas (Figs. 10.1C see later) (Price, 1973).

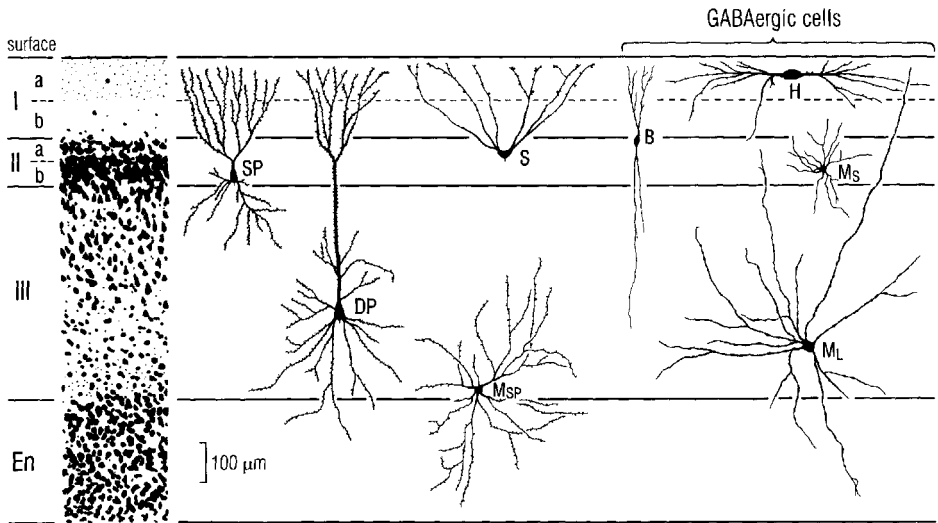


Fig. 10.2. Cytoarchitecture and major cell types of piriform cortex. Excitatory neurons include superficial pyramidal cells (SP), deep pyramidal cells (DP), semilunar cells (S) (pyramidal-type neurons without basal dendrites), multipolar cell with spiny dendrites (M_{SP}) in deep layer III and the endopiriform nucleus (En). Inhibitory GABAergic cells include large multipolar cells with long, sparsely spiny dendrites (M_L); small multipolar cells with thin dendrites (M_S); small bipolar/bitufted cells with long, thin ascending and descending dendrites (B); and large horizontal cells in layer I (H).

Layer II is a compact layer of cell bodies. It can be divided into a superficial part, *layer IIa*, in which *semilunar cells* (cell S in Fig. 10.2) are concentrated, and a more densely packed deep part, *layer IIb*, which is dominated by cell bodies of *superficial pyramidal cells* (SP in Fig. 10.2) (Haberly and Price, 1978a).

Layer III displays a gradient in structure from superficial to deep (Cajal, 1955; Valverde, 1965; Haberly, 1983). Its superficial part contains a moderately high density of *deep pyramidal cells* (DP in Fig. 10.2; Fig. 10.3) and a much lower density of large multipolar cells (M_L in Fig. 10.2). With increasing depth, cell density falls and the proportion of nonpyramidal cells increases. Like layer Ib, layer III contains a high density of associational axons that synapse on pyramidal cell dendrites and other neuronal elements.

Deep to layer III is the *endopiriform nucleus*, which is interconnected with the overlying cortex (Behan and Haberly, 1999). This nucleus has also been termed *layer IV* of the piriform cortex (O'Leary, 1937; Valverde, 1965). The predominant cell type in the endopiriform nucleus is a spiny multipolar neuron (M_{SP} in Fig. 10.2), also found in smaller numbers in the deep part of layer III (Tseng and Haberly, 1989a).

SUBDIVISIONS OF PIRIFORM CORTEX

Although the entire piriform cortex has the same basic three-layer organization, it is not homogeneous in structure. Many differences in both axonal connections and cytoarchitecture of different regions of piriform cortex have been described (Rose, 1928;

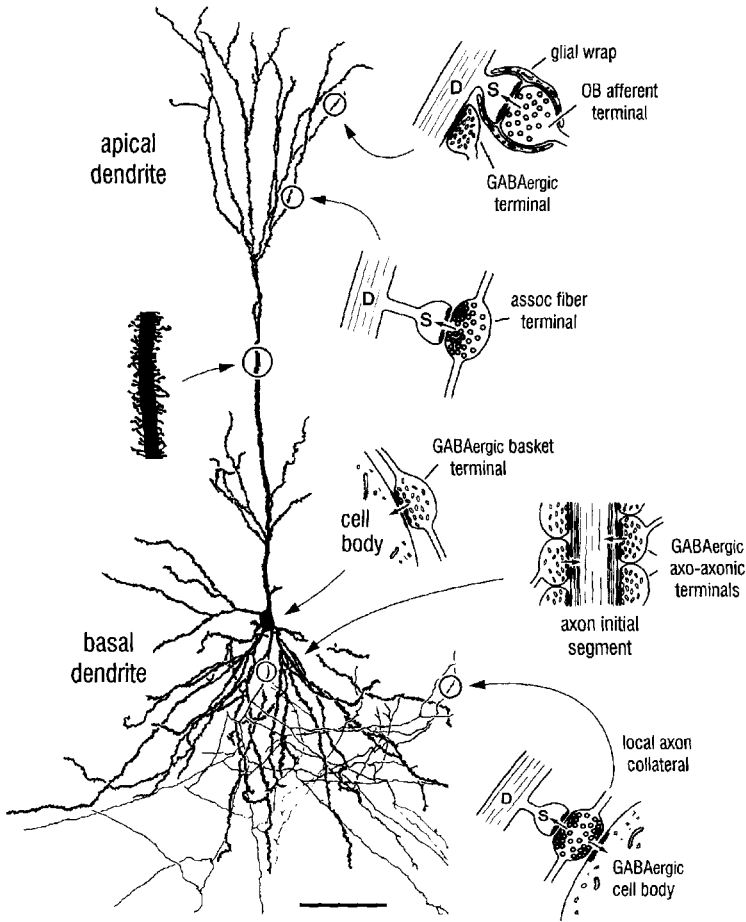


Fig. 10.3. Deep pyramidal cell in layer III of rat piriform cortex stained by intracellular dye injection. Fine processes are axon collaterals. Inset at left is segment of apical dendrite showing dendritic spines. Insets at right show synaptic relationships revealed by electron microscopy. Abbreviations: D, dendritic shaft; S, dendritic spine. Scale bar: 100 μm . [Modified from Tseng and Haberly, 1989a, with permission.]

Haberly, 1973; Price, 1973; Haberly and Price, 1978a; Carmichael et al., 1994; Behan et al., 1995; Ekstrand et al., 2001a). Although six or more regions could be differentiated on anatomical grounds, for the present account it will be divided into two primary divisions, the *anterior piriform cortex (APC)* and *posterior piriform cortex (PPC)*, and the APC will be divided into dorsal (APC_D) and ventral (APC_V) subdivisions (Fig. 10.4). PPC is posterior to the LOT and recognizable by a well-developed layer III, APC_V is deep to the LOT and has a thick layer Ia and thin layer III, and APC_D is dorsal to the LOT with a cytoarchitecture that is somewhat intermediate between APC_V and PPC. These differences in structure are believed to reflect differences in functional roles (Kaas, 1990; Ekstrand et al., 2001a).

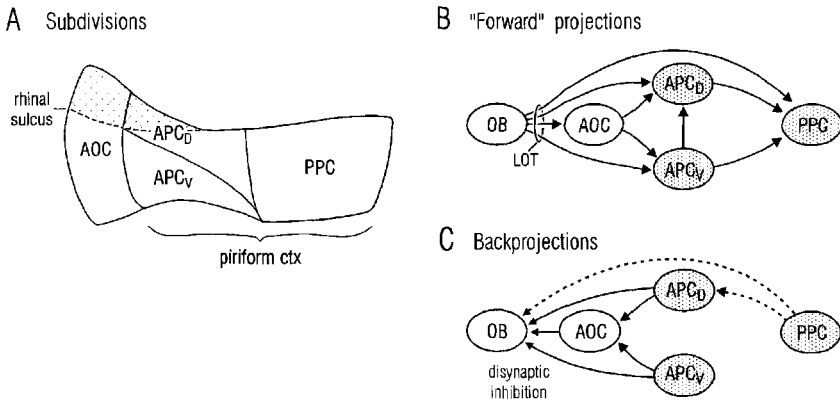


Fig. 10.4. Subdivisions of piriform cortex and their connections with the olfactory bulb and anterior olfactory cortex (AOC). **A:** Posterior piriform cortex (PPC), and ventral and dorsal subdivisions of anterior piriform cortex (APC_V and APC_D). The crosshatched regions of AOC and APC_D are buried in the rhinal sulcus. **B:** Afferent and associational fiber systems that constitute the "forward" pathway that extends from the olfactory bulb (OB) through the AOC and subdivisions of piriform cortex. **C:** Backprojections from subdivisions of piriform cortex that extend directly, and indirectly via the AOC, to the olfactory bulb where they contact granule cells that are inhibitory onto mitral and tufted cells (the principal neurons that project to olfactory cortex). The dashed lines are comparatively weak projections.

AFFERENT INPUT

Mitral cells in the olfactory bulb are the primary source of afferent input to the piriform cortex (see Chap. 5). Cortical areas in the olfactory peduncle and the olfactory tubercle also receive heavy projections from tufted cells in the olfactory bulb, but this projection extends to only a small region in the anteroventral part of piriform cortex (Haberly and Price, 1977; Skeen and Hall, 1977; Wouterlood and Härtig, 1995; Ekstrand et al., 2001a). Axons of mitral and tufted cells reach the piriform cortex and other olfactory areas by way of the LOT, which extends over the surface of the APC_V (hatched area in Fig. 10.1A). Axons in this tract are predominantly myelinated but small in diameter (mean of 1.3 μm in the rat) (Price and Sprich, 1975). Each LOT axon gives rise to many thin collaterals. These leave the LOT throughout its length and spread obliquely across the entire surface of the piriform cortex and all other olfactory areas (see Fig. 10.1B) (Devor, 1976). This mode of afferent input via tangentially spreading superficial fibers is shared by portions of the hippocampal formation but contrasts with the mammalian neocortex where axons from thalamic relay nuclei enter from the deep white matter and ascend vertically to terminate within "columns" (see Chap. 12). However, in the dorsal cortex of reptiles, which may be homologous to the neocortex of mammals, afferent input fibers spread tangentially in a superficial subzone of layer I, just as in the olfactory cortex (Hall and Ebner, 1970; Haberly, 1989).

NEUROMODULATORY INPUTS

Like other parts of the cerebral cortex, the piriform cortex receives diffusely distributed neuromodulatory inputs from cholinergic, noradrenergic, serotonergic, dopami-

nergic, and histaminergic cells. These cell groups are located in the basal forebrain, brainstem, and hypothalamus (see Neurotransmitters).

CONNECTIONS BETWEEN OLFACTORY CORTICAL AREAS

As detailed below (see Basic Circuit), there are extensive connections between olfactory cortical areas on the ipsilateral side that will be termed *associational* (see Fig. 10.1C). The olfactory tubercle is the only olfactory cortical area that does not give rise to associational projections (Haberly and Price, 1978a). *Commissural* connections between olfactory areas on opposite sides are lighter and involve fewer areas than associational connections (de Olmos et al., 1978; Haberly and Price, 1978a,b; Luskin and Price, 1983b) but are sufficient to allow odors to drive unitary activity in the piriform cortex on the contralateral side (Wilson, 1997). A potential functional role for these commissural projections was recently demonstrated in the human: olfactory learning acquired from stimuli delivered to a single nostril generalizes to stimulation through the contralateral nostril (Mainland et al., 2002).

RETURN PROJECTIONS FROM OLFACTORY CORTEX TO OLFACTORY BULB

The piriform cortex and other olfactory cortical areas send projections back to the olfactory bulb (Fig. 10.4C) (de Olmos et al., 1978; Haberly and Price, 1978a,b; Luskin and Price, 1983b). Numbers are not available, but like the return projections from sensory neocortex to thalamic relay nuclei (see Chap. 8), the projection from piriform cortex back to the olfactory bulb is much heavier than the forward projection. This projection terminates on granule cells that are inhibitory to mitral and tufted cells (see Chap. 5). Reversible cryogenic blockade of the peduncle, which blocks this centrifugal system, alters the form of oscillatory activity in the olfactory bulb (Gray and Skinner, 1988), but the functional role of this system is unknown.

OUTPUTS

Many output pathways from the piriform cortex have been identified (Tanabe et al., 1975; Luskin and Price, 1983b; Price, 1985; Switzer et al., 1985; Takagi, 1986; Price et al., 1991; Carmichael et al., 1994; Shipley et al., 1995; Shipley and Ennis, 1996). The dominant pathways are direct projections from pyramidal cells to other cortical areas (see Fig. 10.1C). Cortical targets of these projections can be loosely grouped as areas implicated in associative memory (entorhinal cortex and perirhinal cortex) (see Chap. 11), prefrontal areas thought to be involved in mediating complex discriminative/behavioral processes (orbital and insular cortex) (Schoenbaum and Eichenbaum, 1995), amygdaloid areas that play a central role in emotion and visceral functions (Schoenbaum et al., 1999), and the olfactory tubercle that is considered to be part of the ventral striatum (Switzer et al., 1982). The piriform cortex and other olfactory cortical areas also project to the hypothalamus (Price et al., 1991) and indirectly to other areas associated with autonomic and endocrine functions (Shipley et al., 1995).

Although afferent input to olfactory cortex does not relay in the thalamus as in other sensory systems, olfactory cortical areas do project to the thalamus (see Fig. 10.1D). Input to the thalamus originates from a relatively small number of cells in a loosely defined band that extends through deep layers in the piriform cortex, olfactory tubercle, and anterior olfactory cortex (Price, 1985, 1987). An intriguing feature is that

piriform cortex projects by way of “high order” thalamic nuclei (mediodorsal and submedial) to the same prefrontal areas to which it projects directly (Ray and Price, 1992; Ekstrand et al., 2001a). This pathway may be analogous to connections between areas in neocortex that are both direct by way of corticocortical projections and indirect by way of high order thalamic nuclei (see Chap. 8) (Sherman and Guillery, 2001). A light return projection from the thalamus originates in nucleus reuniens (Datiche et al., 1995).

PRINCIPAL NEURON

Pyramidal cells are considered to be the principal neurons in all three types of cerebral cortex by virtue of their extensive dendritic trees and axons that project to other areas. As in the neocortex (see Chap. 12) and hippocampus (see Chap. 11), pyramidal cells in the piriform cortex and other olfactory cortical areas have several distinctive features, as shown in Fig. 10.3 (Haberly, 1983; Haberly and Feig, 1983; Tseng and Haberly, 1989a). At the light microscopic level, these include an *apical* dendritic tree that is directed toward the cortical surface, a *basal* tree that radiates from the cell body, a profusion of small *dendritic spines* (inset at left in Fig. 10.3), and a myelinated axon that is deep-directed at its point of origin. Pyramidal cells in all three types of cerebral cortex also display similar synaptic relationships, pharmacology, and physiological features.

Two populations of pyramidal cells can be distinguished in the piriform cortex: *superficial pyramidal cells*, whose cell bodies are tightly packed in layer IIb, and *deep pyramidal cells*, whose cell bodies are found in layer III at progressively lower density with increasing depth from layer II (see Fig. 10.2). Morphologically, these two populations are virtually indistinguishable except for the lengths of their apical dendritic trunks. Physiologically, however, they display differences in membrane properties and synaptic responses (see Synaptic Actions).

The apical dendrites of most superficial and deep pyramidal cells arborize into secondary branches near the border between layers I and II and extend through the afferent fiber termination zone in layer Ia. Most deep pyramidal cells have single long apical trunks (cell DP in Fig. 10.2; see also Fig. 10.3), whereas superficial pyramidal cells have short apical trunks or secondary dendrites that extend directly from cell bodies (cell SP in Fig. 10.2), as in layer II of the neocortex (Peters and Kaiserman-Abramof, 1970; Ghosh et al., 1988). Basal dendrites of both superficial and deep pyramidal cells have long deep-directed branches. The primary axons of pyramidal cells give rise to thin collaterals that synapse in the vicinity of parent cells as well as at greater distances (Figs. 10.3 and 10.6) (Johnson et al., 2000).

At the superficial border of layer II, there is a population of “pyramidal-type” neurons that resemble granule cells in the dentate gyrus (see Chap. 11) and phylogenetically primitive pyramidal cells (Sanides and Sanides, 1972) by virtue of apical but no basal dendrites (Calleja, 1893). Somata of these *semilunar cells* are concentrated in layer IIa (see Fig. 10.2) (Haberly and Price, 1978a). Ultrastructurally, these neurons resemble pyramidal cells (Haberly and Feig, 1983), and like pyramidal cells they have spiny dendrites and deep-directed axons. Also in common with pyramidal cells, semilunar cells give rise to extensive associational projections, but in marked contrast to pyramidal cells, they do not project back to the olfactory bulb (Haberly and Price, 1978a). An intriguing feature is that they die within 24 hours following removal of the olfactory bulb (Heimer and Kalil, 1978).

NONPYRAMIDAL NEURONS

Before the development of methods that now allow the full extents of axons to be visualized, the term *interneuron* or *intrinsic neuron* was applied to cells in the cerebral cortex whose axons were believed to arborize exclusively within the area of origin. In recent years, however, it has become apparent that many neurons that were once thought to be of this form actually have long axon branches in addition to local arbors (Zaborszky et al., 1986). Furthermore, many pyramidal cells have axons that arborize extensively within the area of origin (see Fig. 10.6). As a result, we will follow the now-common convention of grouping all neurons that lack the distinctive somatodendritic features of pyramidal cells as *nonpyramidal* cells.

As in all parts of the cerebral cortex, studies with Golgi, immunocytochemical, and intracellularly injected stains in the piriform cortex have revealed many different morphologically distinguishable types of nonpyramidal neurons (see Fig. 10.2) (O'Leary, 1937; Cajal, 1955; Valverde, 1965; Haberly, 1983; Ekstrand et al., 2001; Frassoni et al., 2002; Protopapas and Bower, 2002). Although nonpyramidal neurons in piriform cortex have received much less study than those in the neocortex or hippocampus, many of the distinctive forms previously defined by morphology and neurochemical markers in these other areas (see Freund and Buzsáki, 1996) also can be recognized in piriform cortex.

Most nonpyramidal cells in the piriform cortex, as in the hippocampus and neocortex, use GABA as neurotransmitter and are inhibitory in action. These are considered in some detail later (see Inhibitory Circuitry and Synaptic Actions). A prominent exception is a population of large multipolar cells with pyramidal-like spiny dendrites (cell M_{SP} in Fig. 10.2) to which physiological studies have attributed an excitatory action with glutamate as neurotransmitter (Hoffman and Haberly, 1993). These neurons are the predominant cell type in the endopiriform nucleus but are also found in the deep part of layer III (Tseng and Haberly, 1989a). There are also nonpyramidal neurons in layer II of piriform cortex that stain for the calcium binding protein calretinin but not for GABA and therefore may mediate an excitatory action (Frassoni et al., 1998).

NUMBERS

The number of pyramidal cells in the piriform cortex has not been determined but clearly exceeds the number of mitral cells ($\approx 5 \times 10^4$), from which they receive afferent sensory input, by at least an order of magnitude. In view of the highly branched nature of mitral cell axons (Scott, 1981; Luskin and Price, 1982; Ojima et al., 1984), each mitral cell provides synaptic input to a very large number of pyramidal cells, although, again, there has been no quantitative analysis. This situation contrasts sharply with the olfactory receptor input to the olfactory bulb where large numbers of receptor neurons converge onto a much smaller number of principal cells (see Functional Operations and Chap. 5).

SYNAPTIC CONNECTIONS

In general, synaptic relationships in the piriform cortex (see Fig. 10.3) resemble those in both the hippocampus and neocortex. As in these other areas, two major categories of synapses can be distinguished: those with *asymmetrical* contacts with associated

spherical vesicles, many of which use glutamate as an excitatory neurotransmitter (afferent and association fiber terminals in Fig. 10.3), and those with *symmetrical* contacts with associated pleomorphic vesicles, many of which mediate inhibition (basket and axo-axonic terminals in Fig. 10.3). On pyramidal cells, asymmetrical synapses are concentrated on dendritic spines (S in Fig. 10.3) and excluded from cell bodies and axon initial segments (Haberly and Feig, 1983; Haberly and Presto, 1986). Symmetrical synapses are found at high density on axon initial segments and at lower densities on cell bodies and the shafts of dendrites out to their distal ends (Westrum, 1970; Haberly and Feig, 1983; Haberly and Presto, 1986). Despite the relatively low density of symmetrical synapses on dendritic membrane, the total number on dendrites is much higher than on cell bodies and initial segments.

BASIC CIRCUIT

EXCITATORY CIRCUITRY

Laminar Organization. A feature of piriform cortex that is largely responsible for the relative ease with which its circuitry can be analyzed is a segregation of fiber systems and postsynaptic elements over depth. This is especially apparent in layer I where afferent fibers and different association fiber systems terminate in different sublayers (Fig. 10.5). Afferent axons arriving in the LOT synapse exclusively in layer Ia; association fiber systems from the piriform cortex synapse exclusively in layer Ib (Price, 1973). The sharply defined boundary between these two sublayers can be visualized with the Timm stain, which stains zinc in synaptic terminals of association fibers (Friedman and Price, 1984).

Afferent axons excite superficial and deep pyramidal cells through synapses on distal segments of their apical dendrites, and association axons excite the same pyramidal cells through synapses on proximal and middle segments (Fig. 10.5) (Haberly and Bower, 1984; Haberly, 1985; Tseng and Haberly, 1989a). Both afferent and association fibers also excite GABAergic cells in layer I, as well as certain GABAergic cells

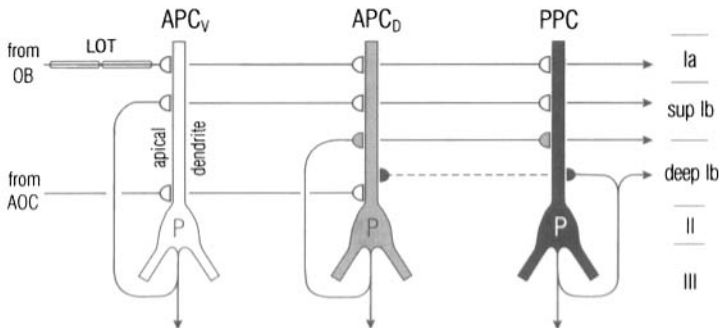


Fig. 10.5. Organization of excitatory inputs to pyramidal cell apical dendrites. Each schematic cell (P) represents the entire population of superficial pyramidal cells in the three subdivisions defined in Fig. 10.4. Half-circles represent excitatory synapses; the dashed line is a comparatively weak projection.

in layer III that have long ascending dendrites (M_L in Fig. 10.2) (see Inhibitory Circuitry). Semilunar cells are excited by afferent and associational inputs to their apical dendrites (J. J. Ekstrand and L. B. Haberly, unpublished observations).

Within layer Ib there is a further laminar organization: association fibers from pyramidal cells in different parts of the piriform cortex synapse at different depths (Fig. 10.5) (Luskin and Price, 1983a,b). These association fibers also synapse in layer III and, to a lesser extent, layer II. Projections to piriform cortex from outside areas also have distinctive laminar patterns of termination (Luskin and Price, 1983a,b). Unlike the intrinsic associational connections of piriform cortex that are all concentrated in layers Ib and III, these projections can extend across the layer Ia–Ib border or be concentrated in layer II.

The myelinated axons of pyramidal cells in piriform cortex typically give rise to many unmyelinated collaterals within a few hundred microns of their origin (Fig. 10.6). These collaterals radiate through layer III, establishing a large number of synapses in the vicinity of the parent neuron. Electron microscopic observations on intracellularly stained neurons have revealed that these synapses are on dendritic spines of pyramidal cells, particularly in the superficial part of layer III, and on dendritic shafts of non-pyramidal neurons (Fig. 10.3) (Haberly and Presto, 1986).

Semilunar cells (S in Fig. 10.2) also give rise to long associational projections (Haberly and Price, 1978a), but they do not project to the opposite hemisphere or to the olfactory bulb.

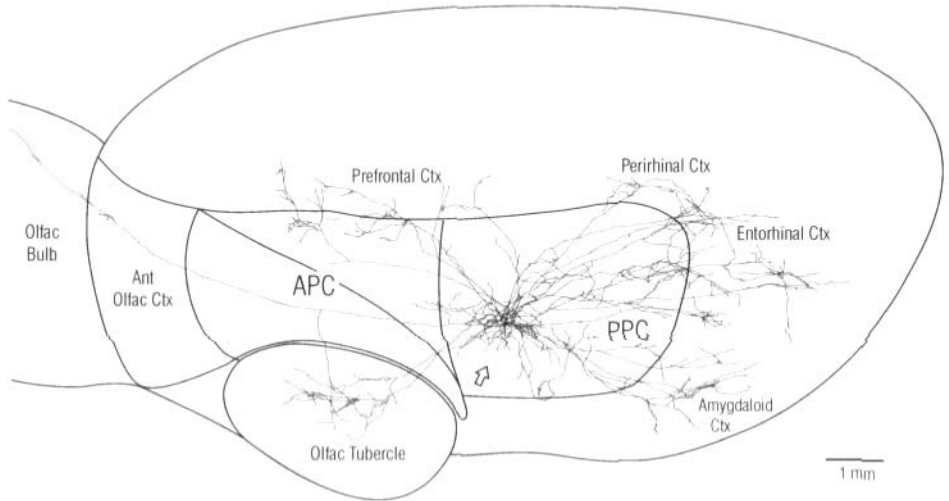


Fig. 10.6. Pyramidal cells in posterior piriform cortex give rise to axons that branch into fine unmyelinated collaterals that synapse extensively in the subdivision of origin, other subdivisions of piriform cortex, the olfactory bulb, anterior olfactory cortex, and multiple high order cortical areas. The illustrated axons originated from two nearby superficial pyramidal cells (open arrow) in posterior piriform cortex (PPC) whose cell bodies were injected with dye. [Modified from Johnson et al., 2001, with permission.]

Horizontal Organization of Afferent System. In contrast to their precise restriction over depth in layer I, afferent fibers are highly distributed in the horizontal dimension (parallel to the cortical surface). Rather than a systematic point to point topographical ordering as observed in the afferent input to sensory areas of neocortex (see Chap. 12), single mitral cells in the olfactory bulb project to broad regions of the olfactory cortex. However, the distribution of afferents is not uniform as revealed by studies with injected axonal tracers (Haberly and Price, 1977; Scott et al., 1980; Ojima et al., 1984; Buonviso et al., 1991) and a new “genetic tracing” method (Zou et al., 2001). The new method allows label to be visualized in pyramidal cells in piriform cortex that has been transneuronally transported through the olfactory bulb from the olfactory receptor neurons expressing a particular olfactory receptor gene. Although this method has thus far been applied to only two receptors, the results, together with findings from studies with conventional tracers, provide evidence that projections from single “receptor qualities” (see Chap. 5) are concentrated in well-defined patches in the APC (Fig. 10.7). However, in marked contrast to primary visual cortex (see Chap. 12) where different stimulus features are represented in very large numbers of patches with little overlap, the patches observed in APC are sufficiently large ($\approx 5\%$ of total area) that input from the full complement of olfactory receptors (≈ 1000) must be highly overlapping. Although input to the PPC as visualized by conventional and genetic tracing techniques is not spatially uniform, it is much more broadly distributed than that to APC (Fig. 10.7).

Horizontal Organization of Association Fiber Systems. Like afferent fibers from the olfactory bulb, associational fiber systems in piriform cortex are segregated in depth but remarkably distributed in the horizontal dimension (see Fig. 10.6). Small injections of anterogradely transported axon tracers placed at any location in piriform cortex stain axons and synaptic terminals over broad areas (Luskin and Price, 1983b; Johnson et al., 2000) with no hint of a systematic point-to-point “mapping” like that observed in certain areas in the neocortex (see Chap. 12). However, as in the case of the afferent input, there appears to be a broadly defined order in these systems. Although the distribution of associational connections within individual subdivisions does appear to be rather uniform, those between subdivisions are not (Haberly and Price, 1978a,b; Luskin and Price, 1983a,b; Datiche et al., 1996; Ekstrand et al., 2001). Projections from different subdivisions are concentrated in different areas and at different depths, and dis-

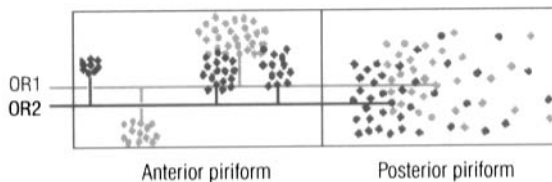


Fig. 10.7. Patterns of afferent fiber distribution to piriform cortex as revealed by “genetic tracing.” This new technique allows label that is selectively introduced into the olfactory receptor neurons that express particular olfactory receptors to be traced transneuronally to the olfactory cortex where it is taken up by pyramidal cells. Label from the two receptors that were studied (OR1, OR2) was concentrated in well-defined but comparatively large patches in APC but widely distributed in PPC. [Modified from Zou et al., 2001, with permission.]

play different laminar patterns of termination. Although many details are lacking and some of the supporting evidence is preliminary, the following principles of organization can be tentatively proposed:

First, the extent over depth in layer I that is occupied by association fibers (layer Ib) relative to afferent fibers (layer Ia) differs substantially in different parts of the piriform cortex (Schwob and Price, 1978; Friedman and Price, 1984). The thickness of layer Ib relative to Ia increases from anterior to posterior divisions of piriform cortex, and from ventral to dorsal subdivisions of APC.

Second, the laminar pattern of termination of association fibers in piriform cortex reflects the area of origin, not the area of termination. For example, the associational projection from APC_V is concentrated in the superficial part of layer Ib throughout APC_V, APC_D, PPC, and all other olfactory cortical areas to which it projects (Behan et al., 1995).

Third, there is an intriguing order in the depth of termination from the different subdivisions (Haberly and Price, 1978a; Luskin and Price, 1983a; Haberly, 2001). This order appears to follow the sequence of activation. As summarized in Fig. 10.5, associational fibers from APC_V—the area that is activated first—synapse in a superficial subzone of layer Ib, adjacent to the afferent input in layer Ia. The associational input from APC_D, which is activated immediately following APC_V, is concentrated in a middle zone in layer Ib, with a lighter component in layer III. Finally, association fibers from PPC terminate even further from the afferent zone: they are concentrated in layer III with a lighter component in deep Ib. From the laminar arrangement of pyramidal cell dendrites and findings from current source–density analysis (see Synaptic Actions), it appears that successively activated subdivisions provide input to dendritic segments that are progressively further removed from the site of afferent input on the distalmost apical segments (see Fig. 10.5).

Fourth, associational connections between the subdivisions of piriform cortex display a marked asymmetry. Although all three subdivisions have extensive *intrinsic associational* connections (i.e., projections to “themselves”), the associational projections from APC to PPC and from APC_V to APC_D are predominantly one-way projections (see Figs. 10.4 and 10.5). Commissural connections in piriform cortex also exhibit a marked asymmetry: the PPC receives commissural input from the opposite APC, and the APC receives commissural input from the opposite anterior olfactory cortex (Haberly and Price, 1978a).

Finally, individual pyramidal cells in piriform cortex project to many widely separated olfactory and nonolfactory areas. Studies with extracellularly injected anatomical tracers and direct visualization by intracellular injection have revealed that individual cells can give rise to both associational and commissural fibers (Haberly and Price, 1978a) and that associational projections from single cells can extend in both anterior and posterior directions and terminate in piriform cortex, other olfactory cortical areas, and the olfactory bulb (see Fig. 10.6) (Johnson et al., 2000). Particularly intriguing from a functional standpoint is the presence of direct projections, as well as return projections, to many high order areas (see Comparisons With Other Cortical Systems).

INHIBITORY CIRCUITRY

Physiological studies have shown that synaptically mediated inhibitory processes in the piriform cortex, as in the other types of cerebral cortex, are complex and diverse (see

Synaptic Actions). This state of affairs stems both from the diverse actions of GABA by way of different receptors and different postsynaptic locations and from a large repertoire of inhibitory neurons that can be distinguished by morphological features, particularly as revealed by immunocytochemically detected markers.

Of particular importance from a functional standpoint are the synaptic relationships of inhibitory cells to principal cells: *feedforward* inhibitory neurons are directly excited by afferent fibers in parallel with principal cells, whereas *feedback* neurons inhibit the principal cells that excite them (Fig. 10.8). A feedforward relationship allows inhibition to be mediated at the shortest-possible latency and with an independence from principal cell firing (output). This configuration provides the potential for inhibitory shaping of the timecourse and other characteristics of EPSPs (see later). In contrast,

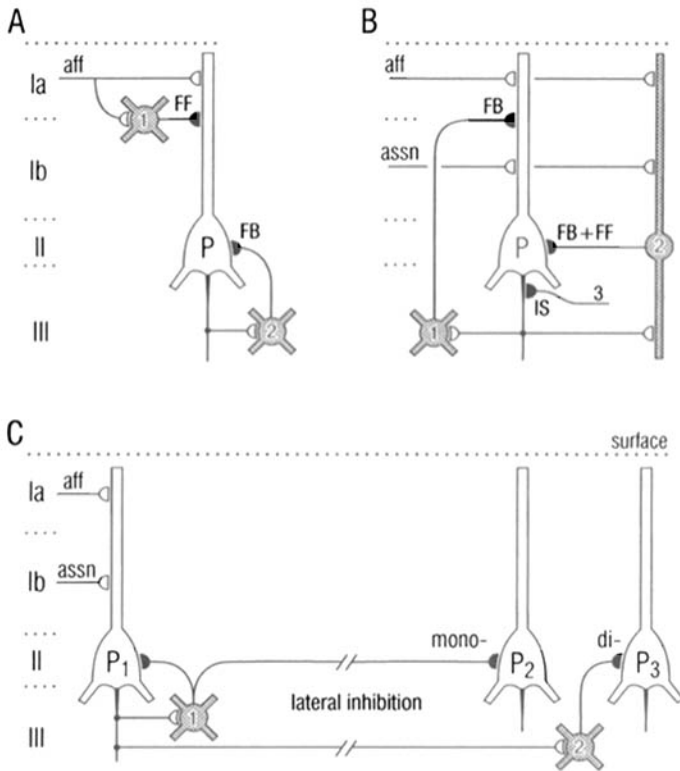


Fig. 10.8. Basic inhibitory circuitry in piriform cortex. **A:** Feedforward (FF) inhibition onto pyramidal cell (P) dendrite from superficial GABAergic cell (*cell 1*), and feedback (FB) inhibition onto cell body of pyramidal neuron from basket endings of deep GABAergic neuron (*cell 2*). Solid half-circles are inhibitory synapses; open are excitatory. **B:** Deep GABAergic cell with long ascending axon (*cell 1*) that mediates feedback inhibition onto pyramidal cell apical dendrite; bipolar/bitufted basket cell (*cell 2*) in both feedback and feedforward relationship to a pyramidal cell; and axo-axonic input to axon initial segments (IS) of pyramidal cells from unidentified neurons (*cell 3*). **C:** Two pathways for lateral inhibition: by way of long axon branch from basket cell (*cell 1*) that also mediates local FB inhibition, and through long axon branch from pyramidal cell that terminate on basket cell (*cell 2*).

inhibition mediated by feedback neurons appears only when principal cells fire. This configuration allows pyramidal cells to be extensively interconnected by excitatory associational fibers without being subject to regenerative positive feedback (seizure activity) that would otherwise develop. Such excitatory interconnections are thought to provide the substrate for complex discrimination and learning processes in piriform cortex and other cortical areas (see Role in Olfactory Discrimination and Memory).

An intriguing feature of inhibitory cells in piriform cortex as in other types of cerebral cortex is the exceedingly large number of structurally distinguishable forms. Although a few well-defined populations can be distinguished on the basis of individual structural features (e.g., shapes of dendritic trees), attempts to categorize inhibitory cells on the basis of all available structural features have been foiled by a “combinatorial explosion” that results from the relative lack of correlation between different features. A long-standing explanation for this phenomenon is that structural phenotypes of inhibitory neurons are highly variable and only loosely related to function and that the number of functionally distinguishable forms is comparatively small. However, attempts to incorporate physiological features into categorization schemes have resulted in a further explosion rather than the reduction that would be expected from the traditional explanation (Parra et al., 1998). The profusion of forms may actually reflect a very large number of functional roles for inhibition in the cerebral cortex—a conclusion that has been reached by modelers attempting realistic computer simulations of cortical processes (see Ekstrand et al., 2001b). Rather subtle differences in structural features such as dendritic specializations, or in the repertoire of membrane channels expressed at different locations, may serve to optimize the neuronal substrate to meet these many needs.

Studies with antisera to GABA and GAD (synthetic enzyme for GABA) have revealed diverse populations of inhibitory cells in the piriform cortex despite a restriction of staining to the somatic region and synaptic terminals (Haberly et al., 1987; Westenbroek et al., 1987; Frassoni et al., 1998; Kubota and Jones, 1992; Ekstrand et al., 2001b). However, for an increasing number of these populations, it has been possible to visualize dendritic and axonal details by staining for certain calcium binding proteins and neuropeptides that co-localize with GABA (Sanides-Kohlrausch and Wahle, 1990; Cho and Takagi, 1993; Ekstrand et al., 2001b). Neuronal structure visualized in this fashion can be sufficiently detailed to provide insight into functional roles (see Fig. 10.8).

Four populations of morphologically distinct GABAergic neurons that have been distinguished in piriform cortex are illustrated in Fig. 10.2. Most numerous are *large multipolar cells* that are found in layer II and all depths in layer III but concentrated in superficial III (M_L in Fig. 10.2). These cells have long sparsely spiny dendrites and myelinated axons that branch into widespread arbors. Many of these neurons are *basket cells*, i.e., their axons terminate in basket-like arbors around cell bodies of pyramidal cells and other neuron populations including GABAergic cells. Large multipolar cells are believed to be the primary source of the strong feedback inhibition that has been widely demonstrated in pyramidal cells in piriform cortex (Biedenbach and Stevens, 1969; Scholfield, 1978; Satou et al., 1983; Tseng and Haberly, 1988; Gellman and Aghajanian, 1993) and may correspond to the monoamine-response cells that have been extensively studied by Aghajanian and colleagues (see Neurotransmitters). Axons

from these cells can give rise to long branches that span subdivisions (Ekstrand et al., 1998), providing a potential substrate for the *lateral inhibition* (see Fig. 10.8) for which evidence has been obtained by imaging with an activity-inducible immediate early gene (Illig and Haberly, 2002).

A recent finding is that much smaller neurons, termed *bipolar* or *bitufted cells*, that have long thin surface- and deep-directed dendrites are an additional source of basket endings on pyramidal cells (Sanides-Kohlrausch and Wahle, 1990; Cho and Takagi, 1993; Ekstrand et al., 2001a). An important feature of these small cells (Sanides-Kohlrausch and Wahle, 1990; Cho and Takagi, 1993; Ekstrand et al., 2001a), that also has been demonstrated for large multipolar cells (Cho and Takagi, 1993), is the presence of dendritic branches that extend into layer Ia. This would allow these cells to function in both feedback and feedforward capacities. This configuration would be expected provide a fast-onset component whose strength is proportional to the strength of both afferent and association fiber inputs, as well as a component whose strength is tied to pyramidal cell firing (see Fig. 10.8B).

From evidence from Golgi staining (Somogyi et al., 1982), electron microscopy (Haberly and Presto, 1986), and immunocytochemical staining (Ekstrand et al., 2001b), it is now clear that GABAergic inhibition is also generated in the axon initial segments of pyramidal cells in piriform cortex. Two features of these *axo-axonic* terminals with potential functional consequences are the presence of GAT-1, a GABA transporter that is not observed in basket endings, and GAD-67 rather than GAD-65, which is found in basket endings (see Ekstrand et al., 2001a). Based on morphological parallels these endings are believed to originate from *chandelier cells* like those in the neocortex and hippocampus (Somogyi et al., 1982), but the cell bodies of origin have not been identified in piriform cortex. The functional roles of this inhibitory system remain a matter of speculation (see Ekstrand et al., 2001a).

Although inhibitory input to pyramidal cells was long thought to be largely restricted to the somatic region, it is now clear that there is also extensive inhibitory input to dendrites. A striking feature of piriform cortex is the very high density of GABAergic synaptic terminals in layer I, particularly layer Ia. Electron microscopic observations suggest that many of these synapses are on distal dendrites of pyramidal cells (Haberly and Feig, 1983; unpublished observations). Preliminary morphological and physiological evidence (Haberly et al., 1987; Ekstrand and Haberly, 1995; Ekstrand et al., 1996) suggests that the large *horizontal* and *small multipolar* cells in layer I (see Fig. 10.2) are one source of these synapses. Dendrites of many of these cells are concentrated in layer Ia, suggesting that they contribute to the feedforward inhibition that has been observed in pyramidal cells (Tseng and Haberly, 1988). However, because these cells can have dendrites that extend into deeper layers and large numbers of GABA-positive axons ascend from layer III and arborize in layer I (M. E. Domroese and L. B. Haberly, unpublished observations), dendritic inhibition must have both feedforward and feedback components.

Finally, physiological evidence indicates that inhibitory interneurons synapse on other inhibitory interneurons in addition to pyramidal cells (Satou et al., 1982). Symmetrical synapses and GABA-containing boutons also have been observed on somata and proximal dendrites of GABAergic cells (Haberly et al., 1987).

SYNAPTIC ACTIONS

SYNAPTIC POTENTIALS AND CURRENTS

In all three types of cerebral cortex, shock stimulation of excitatory pathways evokes an excitatory postsynaptic potential (EPSP) followed by Cl^- -mediated and slow K^+ -mediated inhibitory postsynaptic potentials (IPSPs) in pyramidal cells. Figure 10.9 illustrates this sequence for an SP cell in the piriform cortex. Because the Cl^- -mediated IPSP is depolarizing at resting membrane potential in superficial pyramidal cells (Scholfield, 1978b; Tseng and Haberly, 1988), it cannot be distinguished from the EPSP in intracellularly recorded voltage records under resting conditions (Fig. 10.9A, upper trace). However, its presence can be revealed by reversing the driving force on Cl^- by shifting the cell's membrane potential in the depolarizing direction (Fig. 10.9A, lower trace) or by measuring input resistance to reveal its associated conductance increase (Fig. 10.9B). This depolarizing IPSP opposes spike generation by a concomitantly occurring EPSP (Scholfield, 1978b). This is a consequence of the increased conductance to Cl^- , which has an equilibrium potential below the threshold for spike generation. Thus, an inward current, which would otherwise depolarize the membrane potential to threshold, will be opposed by an inward flow of Cl^- ions—a phenomenon known as *shunting inhibition*. In DP and multipolar cells, the resting membrane potential is more depolarized than in SP cells, and the Cl^- -mediated IPSP is hyperpolarizing at rest (Tseng and Haberly, 1989a). The EPSP, Cl^- -mediated IPSP, and slow K^+ -mediated IPSP can be evoked by stimulation of either the afferent or association fiber systems.

The slow K^+ -mediated IPSP is generated in dendrites by the action of GABA on GABA_B receptors (Tseng and Haberly, 1988). The Cl^- -mediated IPSP is generated in

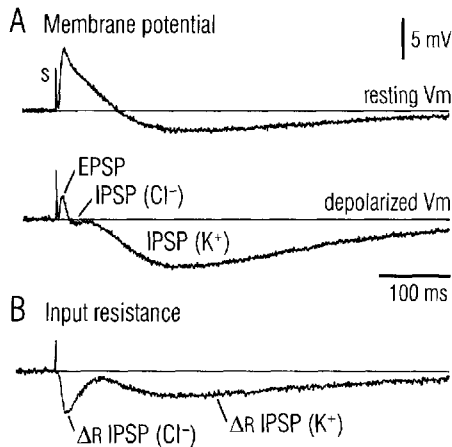


Fig. 10.9. Intracellularly recorded responses of a superficial pyramidal cell in a slice preparation of piriform cortex to current pulse stimulation of association fibers. **A:** Response at resting membrane potential (upper trace) and at a depolarized membrane potential induced by current injection (lower trace). S, stimulus artifact. **B:** Approximate timecourse of the change in input resistance that accompanied the response in A. The response consists of an EPSP followed by a Cl^- -mediated IPSP that is depolarizing at resting potential and a slow K^+ -mediated IPSP. [Modified from Tseng and Haberly, 1988, with permission.]

both cell bodies and dendrites by GABA_A receptors (see Fig. 10.8; Kanter et al., 1996; Kapur et al. 1997a). Studies with voltage-clamp recordings have demonstrated that, as in the hippocampus (Pearce, 1993), GABA_A-mediated inhibitory postsynaptic currents (IPSCs) in piriform cortex have fast and slow components, termed GABA_{A,fast} and GABA_{A,slow}, with time constants of decay on the order of 10 and 50 ms (Kapur et al., 1997a). The GABA_A-mediated IPSC is slower in the distal apical dendrites than in the cell body as a consequence of a higher proportion of GABA_{A,slow}.

VISUALIZATION OF DENDRITIC PROCESSES BY CURRENT SOURCE-DENSITY ANALYSIS

A problem with the direct recording of membrane potentials and currents is that, for most neurons, whole-cell and intracellular recordings can be made only at cell bodies and proximal dendrites. As a result, the power of direct recording is rather limited for the study of dendritic processes. Fortunately, in highly ordered neuronal systems such as the piriform cortex, a technique termed *current source-density* (CSD) analysis allows spatial and temporal sequences of membrane currents in dendrites to be visualized (Mitzdorf, 1985). This information can be combined with data derived from direct recordings in the somatic region to generate a detailed picture of the operation of integrative processes in dendrites.

CSD analysis begins with a set of extracellular *field potential* recordings, spaced over depth at small increments. Figure 10.10A illustrates the field potentials evoked in

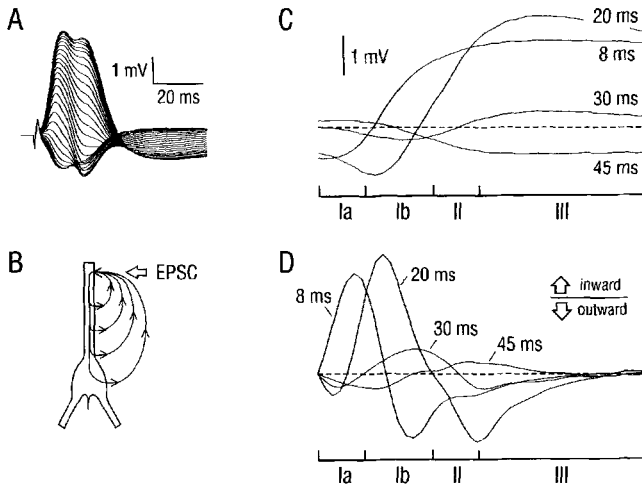


Fig. 10.10. Current source-density (CSD) method used in subsequent figures. **A:** CSD analysis was carried out on sets of shock-evoked field potentials recorded at small increments through the depth of piriform cortex. The illustrated responses were evoked by pulse stimulation of afferent fibers *in vivo*; note that responses invert over depth. **B:** Current flow during an excitatory postsynaptic current (EPSC) evoked in a distal apical dendrite. **C:** Voltage as a function of depth at a series of latencies that correspond to major response components (see Fig. 10.11). **D:** Net membrane current as a function of depth, computed as the unscaled second derivative (curvature) of the potential profiles in C. [Modified from Ketchum and Haberly, 1993a.]

PPC by current pulse stimulation of the LOT. These potentials are generated by current passing through the extracellular space that links “active” current through membrane channels with passive “return” current (Fig. 10.10B). At each time point, the voltage is plotted as a function of recording depth (Fig. 10.10C). In systems like piriform cortex where current flow is largely constrained to the vertical dimension, the net membrane current is computed from the second derivative of this function and plotted as a function of depth (Fig. 10.10D) (see Mitzdorf, 1985). This process is repeated for each time point to compute the net membrane current as a function of depth and time (Fig. 10.11). In the piriform cortex, where different neuronal elements are segregated in depth, these net membrane currents can be interpreted in terms of sequences of synaptically mediated processes in specific dendritic segments and cell bodies of pyramidal cells (Haberly and Shepherd, 1973; Ketchum and Haberly, 1993a,b; Biella and de Curtis, 1995).

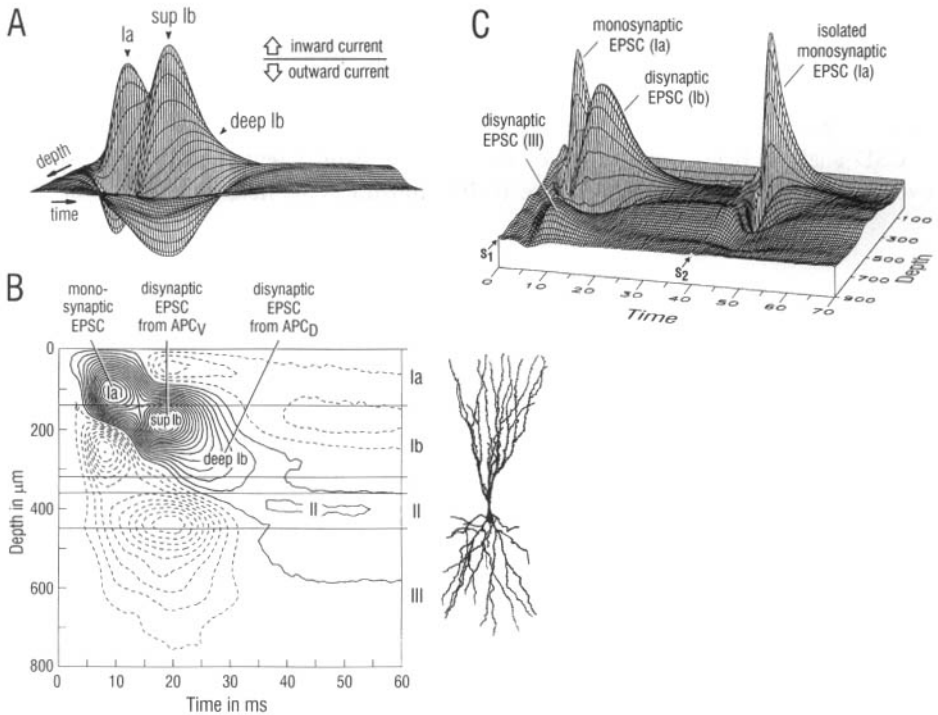


Fig. 10.11. Synaptic events evoked by afferent-fiber stimulation in rat piriform cortex *in vivo* as revealed by CSD analysis. **A:** Surface plot of net membrane current as a function of time and depth in PPC; inward current is upward. **B:** Same response as a contour plot with net inward current indicated by solid lines. Cortical lamination is indicated at the right; superficial pyramidal cell is aligned in depth. Response components are identified by the layers in which they are maximal (Ia, superficial Ib, deep Ib, and II) and by the underlying synaptic events (e.g., monosynaptic EPSC). **C:** Response evoked in APC by paired stimulation of afferent fibers. The response to the second shock (S_2) is an isolated monosynaptic EPSC (disynaptic components are blocked when the IPSC evoked by S_1 prevents generation of action potentials by S_2). [Modified from Ketchum and Haberly, 1993a, with permission.]

AFFERENT STIMULATION EVOKES AN ORDERED SERIES OF POSTSYNAPTIC CURRENTS

Figure 10.11 illustrates the net membrane currents derived by CSD analysis in the PPC in response to current pulse stimulation of the LOT. Inward current is represented as upward deflections in the surface plots (Fig. 10.11A,C) and as solid lines in the contour plot (Fig. 10.11B). The response includes three peaks of inward current that have been identified as excitatory postsynaptic currents (EPSCs): the large peak in layer Ia is the monosynaptic EPSC in distal apical dendrites, the large peak in superficial Ib is the disynaptic EPSC in mid-apical segments mediated by association fibers from APC_V, and the small peak in deep Ib is the disynaptic EPSC in proximal dendritic segments mediated by association fibers that originate in APC_D and other areas (see Fig. 10.5). In the APC, an EPSC in basal dendrites in layer III can also be visualized (Fig. 10.11C). This EPSC is obscured in the PPC by the outward return currents (downward deflections and dashed lines in Fig. 10.11A,B) associated with the large EPSCs in layer I.

Current associated with inhibitory processes overlaps in time with EPSCs and contributes comparatively little to net membrane current in responses to strong afferent stimulation. The portion of the Cl⁻-mediated IPSC that remains following decay of the monosynaptic and disynaptic EPSCs can be seen as a small net inward current focused in layer II (II in Fig. 10.11B) that is coupled with outward current in layer I.

As illustrated in Fig. 10.11C, monosynaptic and disynaptic EPSCs can be separated by delivering a pair of shocks. The GABA_A-mediated IPSC evoked by the first shock blocks the generation of action potentials in response to the second shock, thereby preventing disynaptic EPSCs and resulting in an isolation of the monosynaptic EPSC.

Following LOT stimulation, the APC is activated nearly synchronously. This is a consequence of the high conduction velocity of the myelinated LOT fibers that pass over its surface. By contrast, the PPC, which receives its afferent input via long collaterals from the LOT, is activated from rostral to caudal at a rate that is slow relative to synaptic processes (Ketchum and Haberly, 1993a,b). This is clearly seen when the isolated monosynaptic EPSC is recorded at a series of distances from the caudal end of the LOT (Fig. 10.12). The monosynaptic EPSC in the PPC also increases in duration with increasing distance from the LOT (Fig. 10.12). This is due to a spectrum of axon diameters that disperses the arrival times of action potentials (Fig. 10.12, inset).

TEMPORAL PATTERNS OF ACTIVITY IN PIRIFORM CORTEX

Neural activity in the olfactory system is structured into distinct temporal patterns. In the piriform cortex, these patterns take the form of fast oscillations and slower respiratory-linked modulations of firing rate. The temporal structure of activity has implications for the integration of neural signals and the plasticity of synaptic connections.

Respiratory Modulation and Odor-Induced Slow Temporal Patterning of Afferent Input. A 3- to 8-Hz wave is apparent in field potential recordings in piriform cortex, corresponding to the respiration of the animal (Fig. 10.13A) (Freeman, 1959). Observations in olfactory bulb indicate that the firing rate of many mitral and tufted cells is modulated over the respiratory cycle (Macrides and Chorover, 1972; Chaput et al., 1992). When an odor is present, many mitral and tufted cells change their pattern of

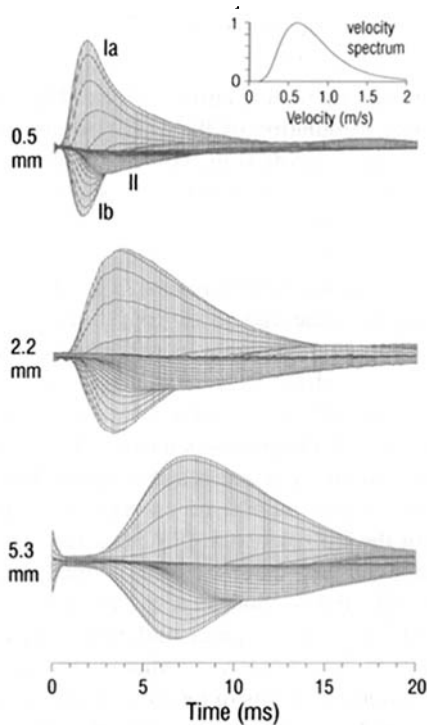


Fig. 10.12. “Dispersive propagation” of afferent-evoked response in PPC that results from a distribution in conduction velocity of afferent axons. Illustrated responses are surface plots of net membrane current as a function of time, at three locations at the indicated distances from the caudal end of the LOT. Amplitudes are normalized to emphasize the slowing of time course over distance. *Inset*, distribution of conduction velocities that allowed a computer simulation to reproduce the experimental data. [Reproduced from Ketchum and Haberly, 1993b, with permission.]

modulation in a way that depends on the identity and concentration of the odorant (Macrides and Chorover, 1972; Wellis et al., 1989; Chaput et al., 1992). Thus, the ensemble of active mitral cells evolves over the course of a few hundred milliseconds during an odor response. In the zebrafish olfactory bulb, similar odorants initially activate largely overlapping ensembles of mitral cells. However, as ensemble activity evolves over the course of the odor response, the degree of overlap becomes much less (Friedrich and Laurent, 2001). If a similar process occurs in the mammals, the slow temporal patterning of mitral cell responses may serve to decorrelate the inputs to olfactory cortex. This is especially intriguing in light of the hypothesis that piriform cortex acts as an associative memory system, with parallels to artificial neural networks designed for pattern storage and recognition (Haberly, 2001). Such artificial networks often perform poorly when presented with highly correlated input patterns (Hertz et al., 1991). It is thus tempting to speculate that the olfactory bulb is “preprocessing” the input signal by decorrelating the patterns of afferent activity, in a way that will improve the associative memory capabilities of the olfactory cortex.

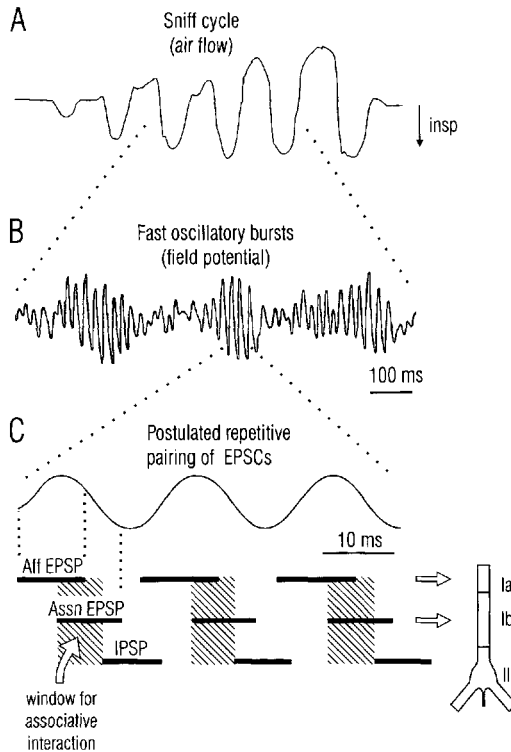


Fig. 10.13. Fast and slow oscillatory rhythms evoked by odor. **A:** Airflow through the nasal cavity of a rat during sniffing behavior elicited by odor. Note the slow (4–8 Hz) oscillatory rhythm. [Modified from Youngentob et al., 1987, with permission.] **B:** Field potential recorded from piriform cortex of an unanesthetized rat during odor-evoked sniffing. Each inspiratory cycle evokes an envelope of gamma frequency (50 Hz) oscillation. [Modified from Woolley and Timiras, 1965, with permission.] **C:** Illustration of hypothesis, derived from the results of CSD analysis, that monosynaptic and disynaptic EPSPs generated in adjacent dendritic segments are repetitively paired at 50 Hz during the gamma oscillation. The hatched area represents the time period when EPSPs overlap before onset of the IPSC.

In some circumstances, sniffing is synchronized with the hippocampal theta oscillation (Macrides et al., 1982). This may serve to coordinate stimulus acquisition with limbic processing.

The Gamma Oscillation (50–100 Hz). Early descriptions of field potentials in olfactory cortex emphasized a fast oscillation associated with general behavioral arousal, which occurs in bursts at the crest of the inspiratory phase of the respiratory cycle (see Fig. 10.13B) (Freeman, 1959, 1960). This fast oscillation has a typical frequency of 40 Hz in cats and 50 Hz or faster in rabbits and smaller mammals including rats (Bressler and Freeman, 1980), and thus has been designated a *gamma oscillation*. It can be observed in both the olfactory bulb and olfactory cortex, with a high degree of coherence both within and between these structures (Freeman, 1978; Bressler, 1984; Boeijinga and Lopes da Silva, 1988; Kay and Freeman, 1998). The gamma oscillation appears to

originate in the olfactory bulb (see Chap. 5)—it is abolished in the piriform cortex following removal of the olfactory bulb (Becker and Freeman, 1968) and preserved in the olfactory bulb when transmission through the olfactory peduncle is blocked (Gray and Skinner, 1988) or the LOT is surgically interrupted (Neville and Haberly, in preparation). The amplitude is much reduced in PPC compared with APC (Freeman, 1959; Boejinga and Lopes da Silva, 1988).

Unit activity in both the olfactory bulb and piriform cortex is restricted to a particular phase of the gamma oscillation (Eeckman and Freeman, 1990). The observation that mitral cell action potentials arrive as a series of synchronous volleys has led to the hypothesis that the sequence of synaptic events which results from strong shock stimulation of the LOT may be repeated within each cycle of the gamma oscillation (Ketchum and Haberly, 1993c). In particular, afferent and associative EPSCs would occur with the temporal relationship described previously, followed by fast GABA_A-mediated inhibition (Fig. 10.13C). This hypothesis has not yet been tested for the odor-evoked gamma oscillation. However, a single *weak* shock delivered to the LOT in an anesthetized rat results in a ≈ 50 -Hz damped oscillatory response (Fig. 10.14A). The

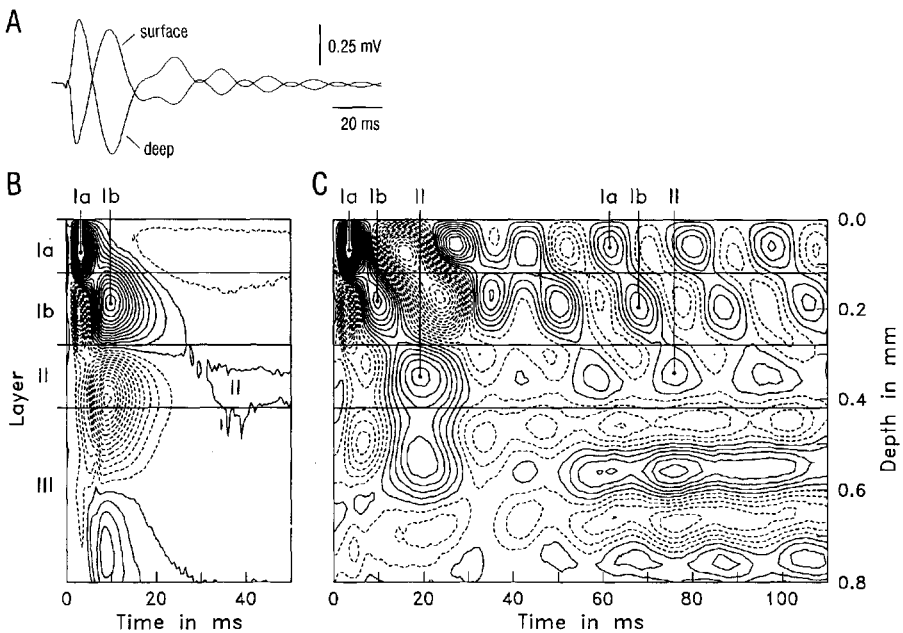


Fig. 10.14. CSD analysis of gamma oscillation evoked by afferent fiber stimulation in piriform cortex. **A:** Oscillatory field potentials recorded at surface and deep sites in PPC *in vivo* in response to weak shock stimulation of afferent fibers. **B:** Contour plot of net membrane currents derived by CSD analysis of the nonoscillatory response to a strong current pulse (comparable to Fig. 10.11B). **C:** CSD of oscillatory response to weak pulse, illustrated in A, reveals that a series of synaptic events repeats within each cycle of the gamma oscillation. Note that the events within each cycle resemble those in the response to the strong stimulus. Also note that the monosynaptic EPSC (solid contours in layer Ia) is paired with the disynaptic association fiber evoked EPSC (solid contours in layer Ib) within each cycle of the oscillation. Each cycle ends with an inward current in layer II that is believed to be the Cl⁻-mediated IPSC. [Reproduced from Ketchum and Haberly, 1993c, with permission.]

frequency of this evoked oscillatory potential suggests that the weak shock may initiate the same reverberatory circuitry that sustains the gamma oscillation. CSD analysis reveals that within each cycle of the fast oscillation initiated by a single weak shock, there is a monosynaptic EPSC in layer Ia, followed by a large disynaptic EPSC in layer Ib, as observed in response to strong shocks (compare B and C in Fig. 10.14). These EPSCs are followed by an inward membrane current in layer II that has been tentatively identified as the IPSC that generates the depolarizing, Cl^- -mediated IPSP (II in Fig. 10.14). The results of this experiment suggest that there is a stereotyped spatial and temporal ordering of synaptic input to pyramidal cells during each cycle of the gamma oscillation. The repetitive pairing of EPSCs at this frequency might contribute to the induction of long-term potentiation (see later). The Cl^- -mediated IPSC might limit the integration of monosynaptic and disynaptic EPSCs to a recurring time window as illustrated in Fig. 10.13C.

The Beta Oscillation (15–40 Hz). Early recordings from piriform cortex note the presence of an oscillation at approximately half the frequency of the gamma oscillation (Freeman, 1959). A 14- to 20-Hz oscillation was observed following the surgical isolation of piriform cortex in cats (Becker and Freeman, 1968). A 15- to 35-Hz component of the EEG was noted to be more prevalent in the piriform cortex than the olfactory bulb (Bressler, 1984). More recently, specific odorants, including some organic solvents and components of predator secretions, have been shown to elicit a 15- to 35-Hz oscillation in the olfactory bulb, piriform cortex, entorhinal cortex, and dentate gyrus (Vanderwolf, 1992; Zibrowski and Vanderwolf, 1997; Chapman et al., 1998; Zibrowski et al., 1998).

The mechanism of generation of this *beta oscillation* is unclear. Some reports suggest that it may originate in piriform cortex or entorhinal cortex and propagate centrifugally to the olfactory bulb (Bressler, 1984; Kay and Freeman, 1998). Other authors, however, report that the oscillation propagates caudally from the olfactory bulb, through piriform cortex, and to entorhinal cortex with a velocity that matches that of electrically evoked responses (Chapman et al., 1998). In urethane-anesthetized rats, it is abolished in the olfactory bulb by surgical interruption of the LOT, implicating cortex in its generation (Neville and Haberly, unpublished observations). It is also abolished by scopolamine, suggesting a role for cholinergic modulation in supporting its generation (Heale and Vanderwolf, 1995).

The functional significance of the beta oscillation is also unclear. Considering the coherence of beta waves throughout the olfactory system and extending to the dentate gyrus (Chapman et al., 1998), this population rhythm may serve to organize olfactory information for processing by hippocampal circuitry.

SYNAPTIC PLASTICITY AND ITS REGULATION IN PIRIFORM CORTEX

NMDA-Dependent Homosynaptic LTP. A key question with regard to the operation of piriform cortex is whether it is involved in the learning of olfactory discriminations and associations and, if it is, what are the underlying mechanisms. There is growing evidence from behavioral studies that a form of activity-induced synaptic plasticity that requires the activation of NMDA receptors, termed NMDA-dependent *long-term potentiation* (LTP), plays a role in a number of different learning processes including the acquisition of olfactory discriminations (Staubli et al., 1989). Demonstrations of this

form of synaptic plasticity in piriform cortex therefore support the involvement of this system in olfactory learning. NMDA-dependent LTP has been demonstrated in both afferent and association fiber systems in slices of piriform cortex (Fig. 10.15) (Jung et al., 1990a; Kanter and Haberly, 1990; Carpenter et al., 1994; Collins, 1994). As in the CA1 region of hippocampus, expression is primarily in the AMPA component of the EPSP (Jung and Larson, 1994), protein kinases are required for both induction and maintenance (Collins, 1994), and activation of metabotropic glutamate receptors in addition to NMDA receptors may be required for induction (Collins, 1994). This LTP can be induced by the “theta-burst” paradigm that consists of brief, high-frequency trains of shock stimuli repeated at the frequency of the theta rhythm (4–8 Hz). Because odor-induced sniffing in the rat occurs in the same frequency range as the theta rhythm (see Fig. 10.13A) and a burst of gamma-frequency oscillatory activity is evoked during each sniff cycle (Fig. 10.13B), this paradigm resembles naturally patterned activity in the olfactory system.

In contrast to these results *in vitro*, homosynaptic LTP of afferent synapses has been difficult to demonstrate in anesthetized animals. Potentiation of these synapses occurs

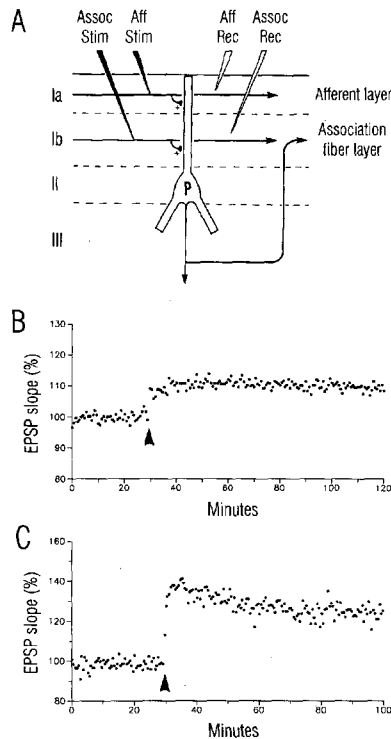


Fig. 10.15. Long-term potentiation (LTP) in a slice preparation of piriform cortex. **A**: Schematic showing positions of stimulating (Stim) and recording (Rec) electrodes in afferent (Aff) and association (Assoc) fiber layers. **B**: Slope of the rising phase of the extracellularly recorded “population EPSP” evoked by stimulation of afferent fibers. At the arrow, a strong “theta-burst” stimulus applied to afferent fibers elicited a sustained potentiation. **C**: Same as **B** but from stimulation of association fibers. [Modified from Kanter and Haberly, 1990, with permission.]

but decays quickly (Kapur and Haberly, 1998). A different phenomenon is seen following high-frequency stimulation of the association fiber system. A late component of the field potential response is potentiated in both olfactory bulb and piriform cortex (Stripling et al., 1988, 1991; Stripling and Patneau, 1999). Potential contributors to this effect include LTP at association fiber synapses, a persistent potentiation that has been observed following epileptiform activity (Racine et al., 1991; Kapur and Haberly, 1998), and increased excitability and bursting in deep cells of layer III and the endopiriform nucleus (Hoffman and Haberly, 1989, 1991).

In awake-behaving animals, an innovative set of experiments has demonstrated the link between olfactory learning and LTP. Rats were trained on a series of two-odor discriminations, after which patterned electrical stimulation of the LOT was used as the discriminative cue. Following learning, the evoked response in piriform cortex was potentiated for stimulation delivered through an electrode that had been used as the “positive” or “negative” cue, but not through a control electrode (Roman et al., 1987). The patterned electrical stimulation did not induce LTP in a naïve animal, outside the context of olfactory learning. Furthermore, the development of potentiation was gradual and highly correlated with the acquisition of the discrimination (Roman et al., 1987, 1993). These experiments provide some of the most convincing evidence connecting LTP to behaviorally measured learning.

Associative LTP. An intriguing feature of NMDA-dependent LTP is that it provides a potential mechanism for various forms of associative learning. This capacity stems from the requirement of both neurotransmitter release and postsynaptic depolarization for activation of NMDA-mediated responses. As a result of this requirement, synaptic reinforcement can be restricted to simultaneously activated convergent inputs. The evidence that afferent and association fiber-evoked EPSCs are repetitively paired on adjacent dendritic segments during fast oscillations (see Fig. 10.14) suggests that this pairing may play a role in the induction of *associative LTP*. The same process could allow the reinforcement of simultaneously activated synapses of association fibers that originate from more than one location in piriform cortex or from other cortical areas.

The hypothesis that NMDA-dependent associative LTP occurs in the piriform cortex has been tested with the “weak-strong” paradigm developed in studies in hippocampus, where a weakly stimulated input is only potentiated during concomitant strong activation of an independent fiber system that terminates nearby (Levy and Steward, 1979; Barrionuevo and Brown, 1983). The results of similar experiments in the piriform cortex have confirmed that NMDA-dependent associative LTP can be induced in either direction between afferent and association fiber inputs to pyramidal cells (Kanter and Haberly, 1993). The same result has also been obtained when two independent sets of association fibers are stimulated (Jung and Larson, 1994).

Because spatial proximity of the termination zones of different fiber systems is a key determinant of the capacity for associative LTP (White et al., 1990), predictions can be made concerning the extent to which the different excitatory systems in piriform cortex can interact in this fashion. As discussed earlier, it would be expected that the afferent fiber system would strongly interact with the association fiber system that originates in APC_V because these two systems terminate on adjacent apical dendritic segments, but would interact less with the systems from APC_D and PPC that synapse

at greater distances from the afferent termination zone (see Fig. 10.5). Likewise, association fiber systems that terminate on adjacent segments of pyramidal cells would have a greater propensity for plastic interaction. For example, association fiber synapses from APC_V in superficial Ib would be expected to strongly interact with those from APC_D in deep Ib but not with those from PPC that are concentrated on basal dendrites in layer III.

Another form of associative LTP is based on a close temporal relationship between a synaptic input and the generation of a postsynaptic action potential, a phenomenon termed *spike-timing dependent synaptic plasticity*. In hippocampus and neocortex, the timing requirements are quite precise, with potentiation occurring only when the postsynaptic spike follows the synaptic input within ~20 ms (Magee and Johnston, 1997; Markram et al., 1997; Sjostrom and Nelson, 2002). The ability of a postsynaptic spike to increase Ca²⁺ influx through NMDA channels depends on its “backpropagation” into the dendritic tree, which relies on dendritic ion channels (Johnston et al., 1999; Neville and Lytton, 1999). In piriform cortex, the fast oscillations control the arrival times of various inputs (see Fig. 10.14), and the spiking of pyramidal cells is restricted to specific time windows (Eeckman and Freeman, 1990). Therefore, these temporal patterns can be expected to determine the nature of associative LTP. The precise timing of these interactions has not yet been investigated in sufficient detail to make specific predictions about plasticity during the beta and gamma oscillations.

Regulation of LTP. Given the evidence that LTP plays a role in learning and memory (Roman et al., 1987, 1993), its occurrence or persistence must be regulated to avoid saturation of synaptic efficacies. One process that has been shown to regulate LTP in piriform cortex is the GABA_A-mediated IPSC (del Cerro et al., 1992; Kanter and Haberly, 1993; Collins, 1994). As described earlier (see Synaptic Actions), this IPSC is mediated in dendritic and somatic regions by different interneurons. Because of its location and slower time course (Kapur et al., 1997a), the dendritic IPSC has a much stronger action than the somatic IPSC on the NMDA component of afferent-evoked EPSCs (Fig. 10.16) (Kanter et al., 1996; Kapur et al., 1997b). If centrifugal fiber systems were to selectively modulate this dendritic IPSC, synaptic plasticity could be regulated without compromising the somatic-region IPSC. Preservation of negative feedback onto the somatic region would allow compensatory adjustments in system excitability, without which epileptiform bursting can develop.

Consistent with a role for GABAergic regulation of LTP, activation of the muscarinic cholinergic system with carbachol, which has been shown to reduce the IPSP that follows association fiber stimulation (Patil et al., 1999), enables associative LTP of an association fiber input that is paired with a strong afferent input (Patil et al., 1998). Finally, slices taken from rats trained in an olfactory discrimination task show reduced susceptibility to monosynaptic LTP of the association fiber system, compared with naïve or pseudo-trained controls (Lebel et al., 2001). Furthermore, a long train of low-frequency stimulation leads to a *long-term depression* (LTD) of this synapse in these slices. These results suggest that synaptic strength is maintained within a defined range, and synapses that have been strengthened by learning are more easily depotentiated than potentiated further.

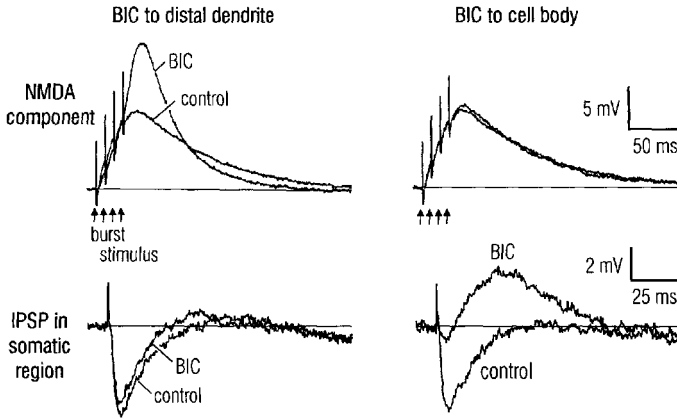


Fig. 10.16. The NMDA component of the EPSP evoked by burst stimulation of afferent fibers is enhanced by blockade of dendritic but not somatic GABA_A-mediated inhibition. Responses are from a superficial pyramidal cell in a slice preparation of piriform cortex with the AMPA component of the EPSP blocked by DNQX. Traces in the top row are intracellularly recorded responses to burst stimulation of afferent fibers. The NMDA component is enhanced after local application of the GABA_A antagonist bicuculline (BIC) to the apical dendrite (top left) but not to the cell body (top right). Traces in the bottom row are intracellularly recorded responses to a nearby current pulse stimulus that evokes an IPSP in the somatic region (membrane potential was depolarized by current injection to make the IPSP hyperpolarizing). This IPSP is blocked by application of bicuculline to the cell body (bottom right) but not to the apical dendrite (bottom left). [Modified from Kanter et al., 1996, with permission.]

NEUROTRANSMITTERS

GLUTAMATE

Findings with specific antagonists and a variety of other methods (reviewed by Haberly, 1990b) indicate that glutamate is the primary excitatory neurotransmitter in the piriform cortex as it is in the hippocampus (see Chap. 11) and neocortex (see Chap. 12). This is true for afferent and association fiber systems in piriform cortex (Jung et al., 1990b), as well as for intrinsic connections in the endopiriform nucleus (Hoffman and Haberly, 1993). As in the hippocampus and neocortex, glutamate mediates EPSCs via AMPA and NMDA receptors (Jung et al., 1990b). The AMPA receptor mediates a fast EPSC via a nonspecific increase in cationic conductance with a reversal potential near 0 mV. The NMDA receptor mediates an EPSC with a similar reversal potential, but with a higher proportion of current carried by Ca²⁺, a slower time course, and a requirement of postsynaptic depolarization to remove blockade by extracellular Mg²⁺. As described earlier, activation of these receptors is required for the induction of LTP in piriform cortex.

In addition to acting on AMPA and NMDA receptors that have integral channels, glutamate also acts on metabotropic receptors whose actions are mediated by way of second-messenger pathways (see Chap. 2). The application of selective agonists for the metabotropic receptor evokes a long-lasting depolarization with accompanying spike discharge, and results in a long afterdepolarization following large depolarizing pulses

(Constanti and Libri, 1992; Libri et al., 1997). Metabotropic agonists have also been reported to induce a long-lasting increase in the afferent-evoked NMDA component (Collins, 1993).

GABA

Inhibitory processes in the piriform cortex also closely resemble those in hippocampus (see Chap. 11) and neocortex (see Chap. 12). Studies with a variety of methods have revealed that GABA is the predominant inhibitory neurotransmitter (reviewed in Haberly, 1990b). Its action is on postsynaptic GABA_A receptors, and on GABA_B receptors on both postsynaptic and presynaptic membranes. As described earlier (see Synaptic Actions), GABA_A receptors mediate an IPSC in pyramidal cell bodies and dendrites through an increase in Cl⁻ conductance (see Fig. 10.9). Postsynaptic GABA_B receptors mediate a slowly developing, long-lasting IPSP in dendrites (Fig. 10.9).

GABA_B receptors are also present presynaptically, where they mediate inhibition of both excitatory (Tang and Hasselmo, 1994) and inhibitory (Kapur and Haberly, 1997a) inputs to pyramidal cells. This effect is much stronger for the association fiber-mediated EPSP than for the afferent-mediated EPSP (Tang and Hasselmo, 1994), and for the GABA_{A,slow} component of inhibition than for the GABA_{A,fast} (Kapur and Haberly, 1997a). Because inhibitory synapses onto synaptic terminals are absent in the piriform cortex (Haberly and Feig, 1983), presynaptic inhibition is mediated by the action of GABA on extrasynaptic "autoreceptors" located on inhibitory synaptic terminals (GABA_B receptors on the terminals from which GABA is released) and by diffusion of GABA through the extracellular space to excitatory synaptic terminals with GABA_B receptors. In other cortical systems, there is evidence that presynaptic GABA_B-mediated inhibition of GABA release plays a key role in the mediation of synaptic plasticity (Davies et al., 1991; Mott and Lewis, 1991).

ACETYLCHOLINE

As in other types of cerebral cortex, the piriform cortex and other olfactory cortical areas receive input from cholinergic cells in the basal forebrain (Haberly and Price, 1978a; Luskin and Price, 1982; Gaykema et al., 1990). Both nicotinic and muscarinic receptors are present, although the cellular and dendritic locations of these receptors are not known (Shiple and Ennis, 1996).

Cholinergic agonists have been shown to exert a number of different actions at the cellular and synaptic level (reviewed in Linster and Hasselmo, 2001). In pyramidal cells, these include a depolarization of the membrane potential, which may result in spike discharge (Tseng and Haberly, 1989b; Constanti et al., 1993; Barkai and Hasselmo, 1994; Libri et al., 1994), a block of I_{AHP} and suppression of the spike frequency adaptation to which it contributes (Tseng and Haberly, 1989b; Barkai and Hasselmo, 1994), and a block of I_M (Constanti and Sim, 1987a). Excitatory synaptic transmission is suppressed (Williams and Constanti, 1988; Hasselmo and Bower, 1992; Linster et al., 1999), as is inhibitory synaptic transmission (Patil and Hasselmo, 1999). At the same time, LTP is enhanced (Patil et al., 1998).

These cellular and synaptic changes have been incorporated into network models of cortical associative memory function, in which the cellular and synaptic effects of acetylcholine serve to improve the network's ability to store distributed and overlapping input patterns (see Functional Operations).

MONOAMINES

The piriform cortex receives projections from norepinephrine-, serotonin-, and dopamine-containing neurons in the brainstem, and histaminergic cells in the hypothalamus, as do most other cortical areas. Evidence includes the presence of axons containing these monoamines (Bjorklund and Lindvall, 1984; Moore and Card, 1984; Inagaki et al., 1988; Datiche et al., 1996; Datiche and Hasselmo, 1996) and retrogradely labeled cells in the appropriate cell groups from injections of anatomical tracer in the piriform cortex and other olfactory cortical areas (Haberly and Price, 1978a; Datiche and Hasselmo, 1996). Receptor types and their distributions are described by Shipley and Ennis (1996).

A role for these neurotransmitters is suspected in many different functions; these include the regulation of learning, sleep, and emotions. In the piriform cortex, as in the hippocampal formation, much of the analysis of mechanisms of action of monoamines has focused on their modulatory effects on inhibitory processes. In a series of studies, Aghajanian and collaborators have examined the actions of monoamines on a population of "fast-spiking" cells concentrated in the superficial part of layer III that appear to mediate GABAergic IPSPs in pyramidal cells; serotonin, norepinephrine, and dopamine directly excite many of these interneurons with a concomitant increase in IPSPs in pyramidal cells (Sheldon and Aghajanian, 1990; Gellman and Aghajanian, 1993; Marek and Aghajanian, 1996). This action of serotonin has been shown to be mediated by 5-HT_{2A} receptors (Marek and Aghajanian, 1994). This system has been used to study the mechanism of action of antipsychotic agents (Gellman and Aghajanian, 1994).

PEPTIDES

Many neuropeptides, mRNAs for their synthesis, and neuropeptide receptors have been demonstrated in the piriform cortex and other olfactory areas (Shipley and Ennis, 1996). Most of these neuropeptides are co-localized with GABA, and they have provided a powerful means of distinguishing and visualizing different populations of inhibitory neurons in piriform cortex and other cortical areas (see Inhibitory Circuitry). However, there is little understanding of their functional roles.

MEMBRANE AND DENDRITIC PROPERTIES

ELECTROTONIC STRUCTURE

The only detailed electrotonic analysis in the piriform cortex has been on superficial pyramidal cells. Parameters obtained by whole-cell patch recording and application of the method of Holmes and Rall (1992) to these data indicate that these cells are similar to pyramidal cells in the CA1 region of the hippocampus (Kapur et al., 1997b). Both cell types are electrotonically compact with a similar membrane time constant

(≈ 20 ms), input resistance (≈ 100 M Ω), and membrane resistivity ($\approx 2 \times 10^4$ Ω -cm 2) (Kapur et al., 1997b).

VOLTAGE-DEPENDENT PROCESSES

Channels whose conductance is determined by voltage play a role in the integration of EPSCs and IPSCs in all parts of cerebral cortex. As described in Chap. 2, there are many types of such voltage-dependent channels. To further complicate the analysis of their functional roles, different neurons display different mixtures of types, and many types are differentially distributed on the different elements of individual neurons.

As a result of voltage-dependent channels, the relationship between intracellularly injected current and the resulting voltage (I-V relationship; Fig. 10.17) displays nonlinearities in both depolarizing and hyperpolarizing directions for the three types of cells that have been examined in the piriform cortex: SP, DP, and deep multipolar cells (M_L in Fig. 10.2) (Scholfield, 1978a; Constanti and Galvan, 1983a; Tseng and Haberly, 1989b; Sciancalepore and Constanti, 1998; Protopapas and Bower, 2000). Voltage-sensitive Ca^{2+} , Na^+ , and K^+ channels shape these current-voltage curves. In the hyperpolarizing direction, at least two currents contribute to the observed nonlinearities: an M current (I_M) (Constanti and Galvan, 1983b) and a fast inward rectifier (I_{IR}) (Constanti and Galvan, 1983a). Although I_{IR} may be of limited significance within the normal physiological range of potential and extracellular environment, I_M is tonically active at resting membrane potential and may contribute to accommodation of firing. In the depolarizing direction, transient low-threshold (I_T) and long-lasting high-threshold Ca^{2+} currents and a "slow" Na^+ current appear to contribute to current-voltage nonlinearities (Halliwell and Scholfield, 1984; Constanti et al., 1985; Tseng and Haberly, 1989b; Magistretti and de Curtis, 1998; Magistretti et al., 1999, 2000; Brevi et al., 2001). The

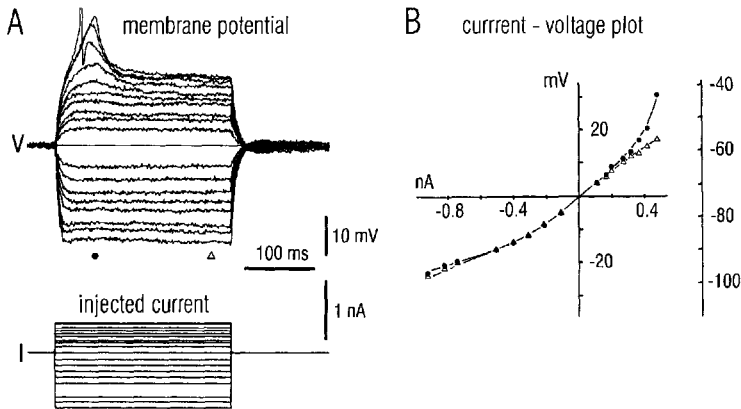


Fig. 10.17. Current-voltage relationship for a deep pyramidal cell in piriform cortex. **A:** Voltage (V) responses to depolarizing (up) and hyperpolarizing (down) square pulses of intracellularly injected current (I). **B:** Plot of voltage as a function of current at the times indicated by the solid circle and open triangle in A. The ordinate is potential relative to resting membrane potential; the scale at the right is absolute membrane potential. Note the nonlinear relationship that results from the opening and closing of voltage-sensitive channels. [Modified from Tseng and Haberly, 1989b, with permission.]

low-threshold I_T Ca^{2+} current is preferentially expressed in cells of layer III and the endopiriform nucleus and contributes to the generation of low-threshold Ca^{2+} spikes (Tseng and Haberly, 1989b; Magistretti and de Curtis, 1998).

A transient K^+ current (I_A) has been identified that appears to contribute to the observed differences in response properties of SP and deep multipolar cells (Banks et al., 1996). In cells in the endopiriform nucleus, the steady-state inactivation curve for I_A (degree to which channels are inactivated as a function of membrane potential) is shifted by 10 mV in the depolarizing direction relative to SP cells. Modeling analysis suggests that this difference is sufficient to explain the more depolarized membrane potential of deep cells and results in a 2-fold decrease in latency of the first spike evoked by depolarizing steps (Banks et al., 1996). Both of these factors could contribute to the greater susceptibility of the endopiriform nucleus to epileptogenesis.

There are also channels in pyramidal cells in piriform cortex that are activated by action potentials. These include fast and slow, and depolarizing and hyperpolarizing spike afterpotentials (Constanti and Sim, 1987b; Tseng and Haberly, 1988, 1989b). The most prominent of these is a K^+ current activated by Ca^{2+} influx (I_{AHP}). This current, which is substantial in most deep pyramidal and multipolar cells (Tseng and Haberly, 1989b), generates hyperpolarizing potentials that last for several seconds. In deep pyramidal and multipolar cells, I_{AHP} contributes to the rapid adaptation of firing that is observed during sustained depolarization. In SP cells, both I_{AHP} and I_M are weak at resting membrane potential in slices (Tseng and Haberly, 1988) but substantial at more depolarized potentials (Constanti and Sim, 1987a). The afterhyperpolarization current in SP cells is reduced in slices taken from rats trained in an olfactory discrimination task (Saar et al., 1998, 2001), an effect that occludes the normal reduction of I_{AHP} by application of the muscarinic agonist carbachol (Saar et al., 2001). These results suggest that high levels of acetylcholine may serve to reduce I_{AHP} during the learning process.

The analysis of membrane properties of nonpyramidal cells in piriform cortex is at an early stage (Protopapas and Bower, 2000; Eckstrand and Haberly, unpublished observations).

INTEGRATIVE PROCESSES

The ease with which synaptically evoked membrane currents can be visualized as a function of time and depth by CSD analysis has afforded the opportunity for a detailed analysis of integrative processes in pyramidal cells in piriform cortex. This analysis has been carried out with a computer model for which the key parameters were well constrained by available morphological and physiological data (Ketchum and Haberly, 1993b). With this model, the sequence of net membrane current computed by CSD analysis was dissected into synaptic, capacitative, and resistive components, and membrane potential was computed as a function of time and dendritic location. Results of this analysis are presented in Fig. 10.18 for the isolated monosynaptic EPSC.

Passive Return Current and the Electrotonic Spread of EPSPs. One of the more intriguing findings with this model was the complex nature of the passive components of the net membrane current. The EPSCs in pyramidal cell dendrites are sufficiently fast that most of the return current passes through the membrane capacitance rather

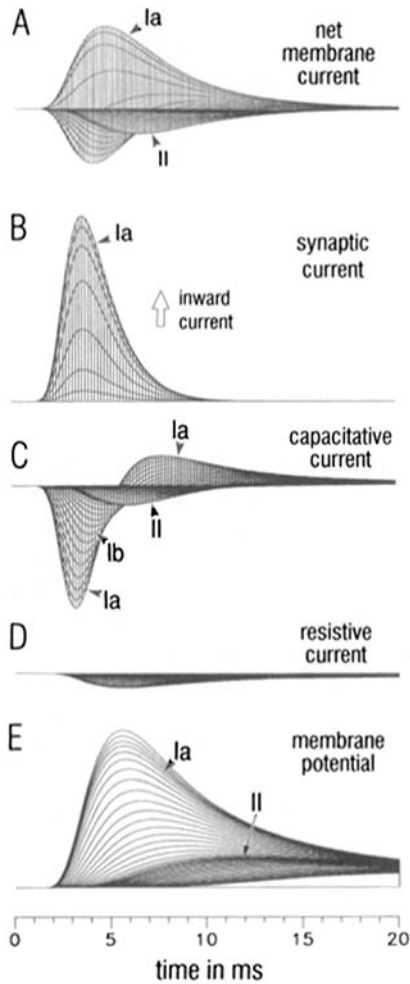


Fig. 10.18. Membrane current components associated with an afferent fiber-evoked EPSC in superficial pyramidal cells in piriform cortex. All panels are “side views” of three-dimensional plots of current or potential as a function of time and depth (compressed in the Z-dimension). Response components were computed from CSD data using a cable representation of the pyramidal cell population. **A:** Net membrane current determined by CSD analysis of monosynaptic component isolated as illustrated in Fig. 10.11C. **B:** Synaptic current (monosynaptic EPSC). Note that the EPSC is faster and larger than net membrane current. **C:** Capacitive component of the passive “return” current associated with the EPSC. **D:** Resistive component of return current. **E:** Membrane potential. Depths of selected components are indicated by the arrowheads. [Modified from Ketchum and Haberly, 1993b, with permission.]

than resistive channels (compare C and D in Fig. 10.18). This outward capacitive current is carried by the removal of the hyperpolarizing charge on the resting membrane, and it accounts for the depolarization of the membrane potential both at the site of synaptic input and at distant locations. As seen in Fig. 10.18C, the outward capacitive current falls off over distance so that the electrotonic spread of the EPSP that it drives is

strongly decremental within the apical dendritic tree (Fig. 10.18E). In simulations with the full sequence of monosynaptic and disynaptic EPSCs, peak amplitude of the monosynaptic EPSP at the cell body was $\approx 25\%$ of that in the distal dendrite, compared with 50% and 80% of peak amplitude, respectively, for the disynaptic EPSPs generated in superficial and deep parts of layer Ib. It follows from this analysis that despite the small amplitude of the EPSC in deep Ib (see Fig. 10.11), the EPSP it generates has an effect on output comparable to that from the much larger inputs at more distal sites.

A surprising result was that, as the synaptic current decays over time, the capacitative current becomes inward with a depth profile that approximates that of the synaptic current (Fig. 10.18C). This inward current is associated with the *equalization* of potential in different parts of the neuron that follows the termination of active currents (Ketchum and Haberly, 1993b). This redistribution of charge serves to repolarize the membrane at the site of synaptic input more quickly than would be predicted from the cell's membrane time constant. Another consequence of this inward tail of capacitative current, together with the outward capacitative current at a shorter latency, is that the net inward membrane current computed with the CSD method is substantially slower and smaller than the synaptic current (compare A and B in Fig. 10.18). The discrepancy in time course between field potentials and the underlying synaptic currents can be even greater (see Fig. 7 in Ketchum and Haberly, 1993a).

Integration of EPSPs. The time course of electrotonic spread of the monosynaptic EPSP accounts for the delay of approximately 6 ms between peak depolarization at the afferent input zone in layer Ia and peak depolarization at the soma (Fig. 10.18E). The disynaptic EPSCs occur at a substantial latency following the monosynaptic EPSC in response to strong shock stimulation of the LOT (see Fig. 10.11) and during each cycle of the fast oscillation evoked by weak shock stimulation of the LOT (see Fig. 10.14). The CSD-derived model was used to investigate the consequences of this ordering of synaptic inputs. When all three EPSCs were applied simultaneously, peak potential at the cell body was only 2% greater than the peak potential generated by the largest EPSC alone. However, when the three EPSCs were presented in the natural sequence, peak depolarization at the soma increased to 50% greater than that for the largest individual EPSC. The delay between the monosynaptic and disynaptic EPSCs thus serves to increase the extent of summation of the resulting EPSPs at the soma. This increase in summation is primarily a consequence of the delay in disynaptic EPSCs until the peak depolarization from the monosynaptic EPSC is achieved at the cell-body layer (compare Fig. 10.18E with Fig. 10.11). In the isolated *in vitro* guinea pig brain, simultaneous activation of two independent sets of association fibers results in nearly linear summation of the resulting EPSCs (Biella et al., 1996).

FUNCTIONAL OPERATIONS

RESPONSES TO ODOR STIMULATION

Several experimental techniques have been applied to study the responses of olfactory cortex to odors. These include visualizing the activity-related spatial patterns in the uptake of 2-deoxyglucose (2-DG) and the induction of the immediate early gene *c-fos*, electrical recording of field potentials and single units, and visualization of blood flow

with functional magnetic resonance imaging (fMRI). Together, these studies imply that activity is distributed broadly, odorant stimuli are encoded by overlapping ensembles of cells, and the activity of many cells is strongly modulated by the animal's behavior.

In the olfactory bulb, visualization of odor-induced activity by 2-DG uptake, *in situ* hybridization of *c-fos* mRNA, or immunocytochemical detection of Fos protein reveals discreet foci corresponding to specific glomeruli, which are activated in an odor-specific way (see Chap. 5). In the olfactory cortex, however, activity appears to be much more widely distributed, as measured by 2-DG uptake (Sharp et al., 1977; Cattarelli et al., 1988; Hamrick et al., 1993), *c-fos* mRNA expression (Hess et al., 1995), and Fos protein expression (Datiche et al., 2001; Illig and Haberly, 2002). Although broad, overlapping bands of Fos staining have recently been described in APC, they do not appear to represent odorant quality and may stem from differences in properties of APC subdivisions (Illig and Haberly, 2002). Interestingly, *c-fos* levels in the piriform cortex of rats were substantially higher after exploration of a novel environment than after performance of a well-learned olfactory discrimination task (Hess et al., 1995).

As described earlier (see Temporal Patterns of Activity in Piriform Cortex), field potentials in piriform cortex reflect the respiration of the animal, and also oscillate at the beta and gamma frequencies. The strength of these fast oscillations is modulated by the behavior of the animal (Freeman, 1960; Boeijinga and Lopes da Silva, 1989; Zibrowski and Vanderwolf, 1997; Kay and Freeman 1998; Neville and Haberly, unpublished observations). However, their spatial distribution does not appear to reflect the olfactory stimulus (Freeman, 1978; Bressler, 1988).

The responses of single units to olfactory stimulation have been recorded in both anesthetized and awake animals. Common findings include a low baseline firing rate and a greater proportion of excitatory responses to odor stimulation than inhibitory ones. In urethane-anesthetized rats, many cells seem to be broadly responsive to multiple odorants, such that any particular odorant evokes a phasic firing rate increase in a substantial fraction of the population of cells (Nemitz and Goldberg, 1983; Wilson, 1998a, 2000a, 2001a). In intracellular recordings, pyramidal cells commonly had depolarizing responses, which could be brief or sustained; hyperpolarizing responses were also observed, although less frequently (Nemitz and Goldberg, 1983; Wilson, 1998a).

Cortical firing rates decline rapidly when odor is present continuously or when two second odor pulses are repeatedly presented at 30-second intervals (Wilson, 1998a, 2000a,b; reviewed in Wilson, 2001a). This response habituation is greater and more rapid for cortical cells than for the mitral/tufted cells of the olfactory bulb (Fig. 10.19A) (Wilson, 1998a, 2000b), a difference that can be at least in part accounted for by depression of the afferent synapses within the piriform (Wilson, 1998b). Habituation is specific to the presented odor (Wilson, 1998a, 2000a,b, 2001a). The degree of specificity has been tested and compared with the specificity of habituation in the bulb using a set of homologous alkanes that differ only in carbon chain length. Remarkably, habituation was found to be more specific in the cortex than in the bulb; for example, if pentane was used as the habituating odor, the cortex responded to a test pulse of heptane or nonane at nearly prehabituation levels, even though the responses of mitral cells were substantially suppressed by cross-habituation (Fig. 10.19B) (Wilson, 2000b, 2001a). Topical application of the muscarinic antagonist scopolamine reduced the specificity of cortical habituation, such that cortical cross-habituation to alkanes of differ-

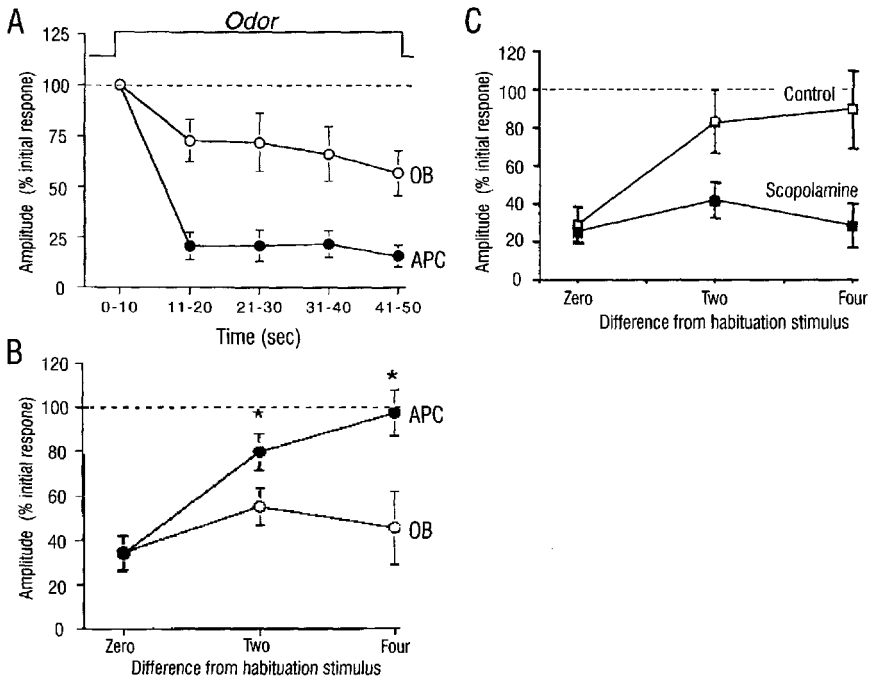


Fig. 10.19. Habituation of single-unit responses to odor in the olfactory bulb and APC of urethane-anesthetized rats. **A:** Time course of habituation in the olfactory bulb and APC during a 50-sec odor presentation. Note that habituation is much stronger in the APC than in the olfactory bulb. **B:** Extent to which habituation to one odorant generalizes to a structurally related odorant. The rat was exposed to a straight-chain alkane for 50 sec as illustrated in **A**, and then tested for responsiveness to the same alkane or an alkane that differed in length by two or four carbons. The response in APC was significantly reduced only for the habituated odor despite strong cross-habituation in the olfactory bulb. **C:** Scopolamine applied to the cortical surface reduced the specificity of habituation in the APC to a level comparable to that in the olfactory bulb. [**A** and **B** from Wilson, 2000b; **C** from Wilson, 2001b; reproduced with permission].

ent lengths resembled that in the bulb (Fig. 10.19C) (Wilson, 2001b). The rapid habituation of the cortical response may allow the cortex to filter out maintained background stimuli, whereas the specificity of this habituation would preserve responsiveness to similar, novel odors or change (Wilson 2000b, 2001a).

In awake animals, many cells in piriform cortex are responsive to odorant presentation (Tanabe et al., 1975; McCollum et al., 1991; Schoenbaum and Eichenbaum, 1995; Zinyuk et al., 2001). In controlled behavioral experiments in which the animal performed a stereotyped sequence of actions, the firing of many cells could also be related to other components of the trial, such as entry into an odor port or a reward port, or consumption of the reward (Schoenbaum and Eichenbaum, 1995; Zinyuk et al., 2001). Cells in piriform cortex responded to all of the trial events to which orbitofrontal cells responded, with only modest differences between the two areas in the fraction of cells in each class (Schoenbaum and Eichenbaum, 1995). It remains to be determined, however, to what extent this altered activity represents the encoding of these non-

factory events, and to what extent it is a consequence of altered respiratory/sniffing activity (and therefore altered afferent input) associated with the performance of different motor actions.

Most recently, fMRI has been applied to humans during olfactory stimulation (Sobel et al., 1998, 2000). These studies confirm the rapid adaptation of odor responses in piriform cortex (Sobel et al., 2000) and also suggest that the somatosensory stimulation associated with sniffing may cause increased activity in piriform cortex (Sobel et al., 1998).

The different experimental approaches described above all address the question of the nature of the “olfactory code” within the piriform cortex. An abundance of recent research has greatly clarified our understanding of the manner in which odors are represented at the level of the olfactory receptor neurons and the olfactory bulb (Fig. 10.20) (see Chap. 5). A typical odorant activates a large number of olfactory receptors, and the olfactory receptor neurons (ORNs) expressing a particular receptor converge onto a few specific glomeruli in the bulb. Thus, an odor is represented by a “spot code,” consisting of the subset of activated glomeruli. Mitral cells are excited by input from a single glomerulus, but their output to olfactory cortex is also shaped by inhibitory processes (Yokoi et al., 1995), and their firing is constrained to specific time windows by the gamma oscillation (Eeckman and Freeman, 1990). Within the APC, some broad topography exists in the distribution of afferent inputs (Buonviso et al., 1991; Zou et al., 2001). However, markers of cellular activity and analysis of oscillatory field potentials suggest that the excitatory response to an odor in piriform cortex is highly distributed spatially. This result is consistent with the large size of the afferent patches, the activation of many olfactory receptors by typical odorants, and the extensive excitatory interconnections between pyramidal cells in piriform cortex. The odorant specificity of individual cells has also been studied with single-unit recordings. Most of these studies have concluded that cortical cells are broadly tuned (i.e., responsive to a variety of odorants). The principal exception is the study of McCollum et al. (1991), in which most cells responded to the first few presentations of an odorant but only a

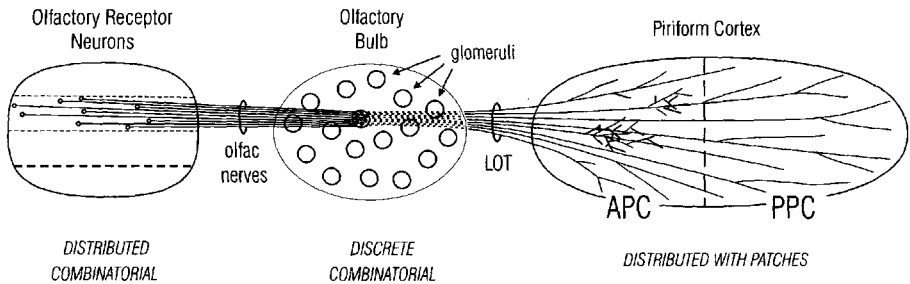


Fig. 10.20. Patterns of connectivity in the olfactory system. Olfactory receptor neurons expressing a particular receptor are widely distributed in one of four zones of the olfactory epithelium. Their axons converge to a few discrete glomeruli in the olfactory bulb. An odor is thus represented by a combinatorial “spot code” in the olfactory bulb according to the olfactory receptors that it activates. Recent evidence suggests that axons from the mitral cells that receive input from a glomerulus have terminations that are concentrated in large patches in APC but broadly distributed in PPC. [Reproduced from Haberly, 2001, with permission.]

small fraction of cells maintained their responsiveness over repeated trials. The reasons for this discrepancy are unclear but may include differences in recording site (sub-division) or in the definition of a “response.” The lack of responses on later trials may also reflect habituation due to the short intertrial interval used in this study. Collectively, studies of the patterns of cellular activity and oscillatory field potentials, together with studies of the response properties of single cells, suggest that piriform cortex uses spatially distributed overlapping ensembles of active cells to represent odors.

ROLE IN OLFACTORY DISCRIMINATION AND MEMORY

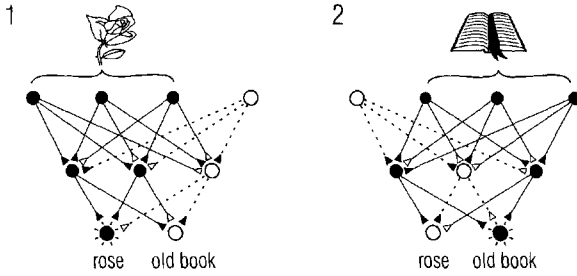
Sensory discrimination and memory processes cannot be easily dissociated—a discrimination task presumes memory for the stimuli to be discriminated, whereas a memory task presumes the ability to discriminate between stimuli. Olfactory cortex is an excellent system in which to study cortical mechanisms of discrimination and memory. Not only does it possess comparatively simple circuitry and cytoarchitecture, and direct interconnections with high-order brain areas, but also olfaction seems to be a preferred sensory modality for rodents, the mammals of choice for many researchers. Rats learn olfactory discriminations very rapidly, remember them for long periods of time, and are capable of using olfactory information flexibly and in complex tasks (Otto and Eichenbaum, 1992).

Studies of the effects of lesions have confirmed that the piriform cortex participates in the discrimination and learning of odorants. In general, rats with piriform cortex lesions or transections of the posterior LOT are able to learn and perform odor discriminations, but they show deficits in the initial acquisition of the task (Staubli et al., 1987) or fail to learn discriminations involving complex odor cues (Staubli et al., 1987) or long intertrial intervals (Thanos and Slotnick, 1997).

Two types of artificial “neural network” models have influenced ideas about the nature of computation in olfactory cortex. First, feedforward networks (also called *perceptrons*) can be used to learn and recognize input patterns (Fig. 10.21A) (Hertz et al., 1991). When these networks contain multiple layers, the response properties of units in successive layers can become increasingly complex. This type of network architecture, in which information flows in one direction and units are described by their response properties, has been very influential in theories of the visual system. This model leads to a description of the olfactory system in which each olfactory receptor responds to a particular “feature” of odorant molecules. An odor is represented at the level of the olfactory bulb by the set of glomeruli responsive to the features of that odor. Cortical cells then respond, not to individual features but rather to collections of features, as represented by patterns of active mitral cells. This view of olfactory processing is a prominent feature of a computer simulation of piriform cortex (Ambros-Ingerson et al., 1990) and has been used to account for the greater specificity of habituation in piriform cortex, compared with olfactory bulb (Wilson, 2000b).

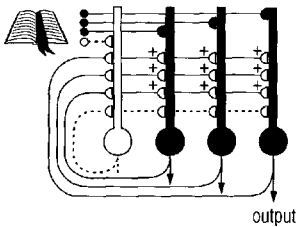
Second, recurrent networks (of which the *Hopfield network* is the best known) can store input patterns by strengthening the connections between simultaneously active units (Hertz et al., 1991). When the network is then presented with a degraded version of one of these patterns, these strengthened connections serve to recruit the appropriate units to complete the stored pattern (Fig. 10.21B). In olfactory cortex, this type of pattern completion could be used to correctly identify and recall an odor when activa-

A Feedforward network



B Associative network

1 Learning



2 Recall

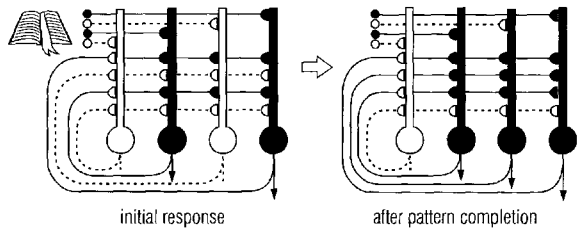


Fig. 10.21. Artificial “neural networks” that can learn and recognize patterns. **A:** A multilayer feedforward network. Filled circles and solid lines represent active “neurons,” whereas open circles and dotted lines represent inactive units. Filled terminals represent connections that have been previously strengthened. Thresholds are set so that each neuron in the middle and output layers becomes active if two or more strengthened synapses onto it are active. Connection strengths are set so that the activation of three input cells by the rose (1) leads to activation of one of the output cells, whereas activation of an overlapping set of inputs by the book (2) leads to activation of the other output cell. Note that individual neurons and connections participate in the coding of multiple patterns; one neuron in the middle layer is activated by both input patterns. **B:** A recurrent network with connectivity reminiscent of piriform cortex. Filled cells and solid lines represent active cells, whereas open cells and dotted lines represent inactive cells. Open terminals are inactive; filled terminals are active. During learning, associative connections between active cells are strengthened (+). When a degraded or altered version of the learned pattern is presented in the recall phase, only a subset of the cells from the full pattern are initially activated. The associative connections that were strengthened in the learning phase serve to recruit the remaining cells and restore the original output. Networks such as this are capable of storing and recalling multiple overlapping patterns (i.e., where the same synapses and neurons participate in the storage of many patterns). [Modified from Haberly, 2001, with permission.]

tion of the olfactory bulb is weak or noisy. Associations between olfactory cues and nonolfactory information could also be stored and retrieved in this manner. The computer modeling studies of Hasselmo and colleagues (Hasselmo et al., 1990, 1992; Barkai et al., 1994; Hasselmo and Barkai, 1995) are based on this view of olfactory cortex as a recurrent network. They demonstrate that biologically inspired models can store and recall multiple input patterns. They also highlight the importance of suppression of the strength of associative synapses (e.g., by cholinergic mechanisms) during learning.

Without this regulation, inappropriate connections become strengthened, and the capacity of the network to store multiple patterns is diminished (Fig. 10.22). A computer model by Chover and colleagues (2001) further suggests that sparsely interconnected networks may perform better if they employ a set of unpotentiated (possibly NMDA receptor-mediated) associative synapses during learning and then switch to the potentiated (presumably AMPA receptor-mediated) synapses during recall.

In fact, the architecture of the olfactory cortex suggests that a combination of feedforward and recurrent processing may be employed (Haberly, 2001; see also Chap. 1). Anterior olfactory cortex, the subdivisions of piriform cortex, and some cortical areas to which piriform cortex projects are connected in series and parallel along the afferent pathway from the olfactory bulb. Each of these structure receives feedforward input from the olfactory bulb and preceding cortical areas and a varying amount of recurrent input (local association fibers) and backprojections from downstream areas (see Fig. 10.5). Thus, olfactory information is processed in both a feedforward manner, as it is relayed from area to area, and in a recurrent manner, through activation of the association fiber systems within each area.

COMPARISONS WITH OTHER CORTICAL SYSTEMS

Piriform cortex has been compared with the hippocampus for its circuitry and to inferotemporal visual cortex for its extrinsic connectivity. Findings from these other systems may contribute to our understanding of olfactory cortical function, and vice versa (Haberly, 2001; see also Chap. 1).

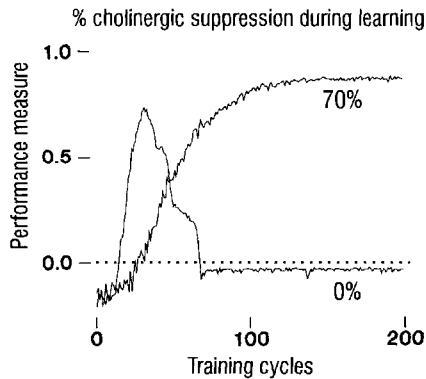


Fig. 10.22. Performance of a recurrent network model of piriform cortex is improved by suppression of association fiber synapses during the learning phase. A network of 30 “neurons” was trained on a set of five overlapping patterns. Performance was assessed by the overlap between the model output and the learned patterns, when degraded versions of those patterns were presented as input. Without suppression of associative connections during the learning phase, network performance initially improved but then became very poor. This occurred because overlap between the stored patterns and the currently presented pattern caused cells from those stored patterns to become active, and thus a large number of connections were strengthened inappropriately. With a 70% reduction in the strength of the association connections during learning (presumed to be by a cholinergic mechanism; see Neurotransmitters), the network was able to store the overlapping patterns in a stable manner. [Reproduced from Hasselmo et al., 1992, with permission.]

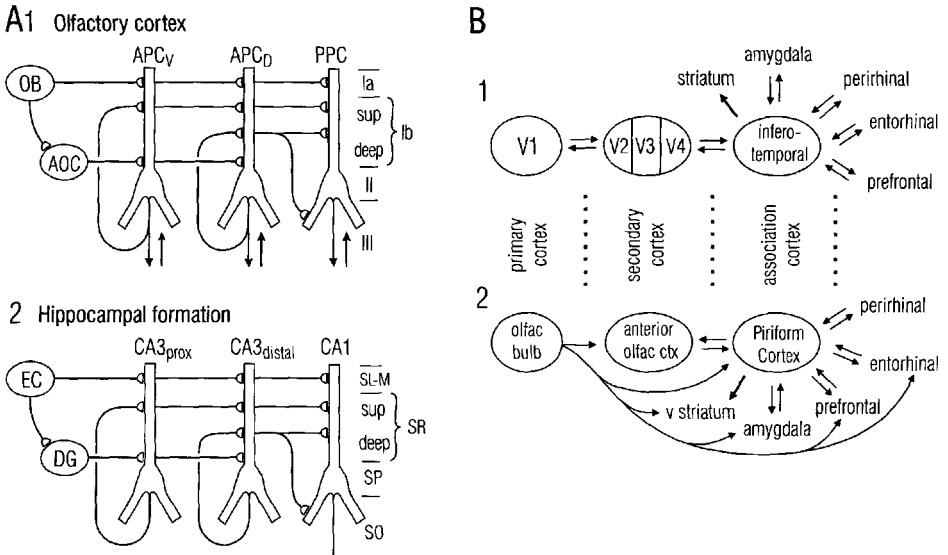


Fig. 10.23. Comparisons between the olfactory system and other cortical systems. **A**: Similarities in the neuronal circuitry of olfactory cortex and the hippocampal formation. Note the parallels in both the horizontal dimension (connections between subdivisions) and the vertical dimension (laminar organization of fiber systems according to their areas of origin). **B**: Comparison of olfactory and visual cortical pathways. Note that the piriform cortex resembles inferotemporal cortex by virtue of direct connections with “high order” cortical areas involved in emotion, cognition, associative learning, and movement. [Reproduced from Haberly, 2001, with permission.]

The neuronal circuitry of the olfactory system has strong parallels with that of the entorhinal-hippocampal system (Fig. 10.23A). Both three-layer cortical systems consist of multiple divisions and subdivisions, which are interconnected by feedforward, recurrent, and backprojecting connections. Afferent input (from the olfactory bulb and entorhinal cortex) reaches all areas of the respective systems and is confined to the most superficial sublayer. Additional parallels are apparent in the organization of association fiber systems, both in the pattern of connections between subdivisions and in the laminar arrangement of fiber systems according to their areas of origin. These intriguing similarities in neuronal circuitry suggest that the two systems operate on similar functional principles (see Haberly, 2001, and Chap. 11 for further discussion).

The olfactory system has also been compared with the visual system (see Fig. 10.23B). Although the term *primary olfactory cortex* is applied to all cortical areas that receive afferent input from the olfactory bulb, piriform cortex more closely resembles inferotemporal cortex, a high-order “association” area, on the basis of its extrinsic connections (Johnson et al., 2000; Haberly, 2001). Like inferotemporal cortex, piriform cortex has direct bidirectional connections with entorhinal, perirhinal, amygdaloid, and prefrontal cortical areas and unidirectional projections to the striatum. Under this comparison, the olfactory bulb and AOC fulfill the roles of primary and secondary sensory cortex, respectively. It is also intriguing to note that faces (Rolls, 2000) and complex objects (Ishai et al., 1999) appear to be represented by spatially distributed overlapping ensembles in inferotemporal cortex, as odors are in piriform cortex.

HIPPOCAMPUS

DANIEL JOHNSTON AND DAVID G. AMARAL

The hippocampus is one of the most thoroughly studied areas of the mammalian central nervous system. There are two main reasons for this. First, it has a distinctive and readily identifiable structure at both the gross and histological levels. The unusual shape of the human hippocampus resembles that of a sea horse, which is what led to its most common name (in Greek, *hippo* means "horse" and *kampos* means "sea monster"). The hippocampus is also sometimes called Ammon's horn due to its resemblance to a ram's horn (the Egyptian god Ammon had ram's horns). It is the histology of the hippocampus, however, that makes it so seductive to neuroscientists. The hippocampus is beautifully laminated; both the neuronal cell bodies and the zones of connectivity are arranged in orderly layers. The hippocampus is one of a group of structures within the limbic system typically called the *hippocampal formation*, which includes the dentate gyrus, hippocampus, subiculum, presubiculum and parasubiculum, and entorhinal cortex. The dentate gyrus, hippocampus, and subiculum have a single cell layer with less-cellular or acellular layers located above and below it. The other parts of the hippocampal formation have several cellular layers. The highly laminar nature of the dentate gyrus and hippocampus lends them to neuroanatomical and electrophysiological studies.

A second reason for the interest in the hippocampus is that since the early 1950s, it has been recognized to play a fundamental role in some forms of learning and memory. In a landmark paper, Scoville and Milner (1957) reported the neuropsychological findings from a patient known by his initials, H.M., who underwent bilateral hippocampal removal for the treatment of intractable epilepsy. H.M., who is probably the most thoroughly studied neuropsychological subject in memory research, experienced a permanent loss of the ability to encode new information into long-term memory. This anterograde memory impairment has been seen in other patients with bilateral damage restricted to the hippocampus (Zola-Morgan et al., 1986). The intense interest in understanding the brain mechanisms involved in learning and memory have helped foster research at the neuroanatomical, physiological, and behavior levels of analysis in the hippocampus. These studies have forged a strong theoretical link between the hippocampus and certain forms of memory (see Functional Synthesis). The hippocampal formation is also of interest because of its high seizure susceptibility. It has the lowest seizure threshold of any brain region (Green, 1964). Most patients with epilepsy

have seizures that involve the hippocampus, and these seizures are often the most difficult to control medically. Portions of the hippocampal formation, particularly the entorhinal cortex, also appear to be prime targets for the pathology associated with Alzheimer's disease, and the hippocampus is very vulnerable to the effects of ischemia and anoxia.

The anatomical and functional organization of the hippocampus is of particular relevance to this text on the synaptic organization of the brain because in many ways the hippocampus has become a model system for studies of other cortical structures. Much of what is currently known about the physiology and pharmacology of synaptic transmission in the central nervous system has come from studies of the hippocampus, although such studies using tissue from neocortical areas have increased dramatically during the past 5 years (see Chap. 12). Because the largest portion of the physiological literature on the hippocampal formation deals with either the dentate gyrus or the

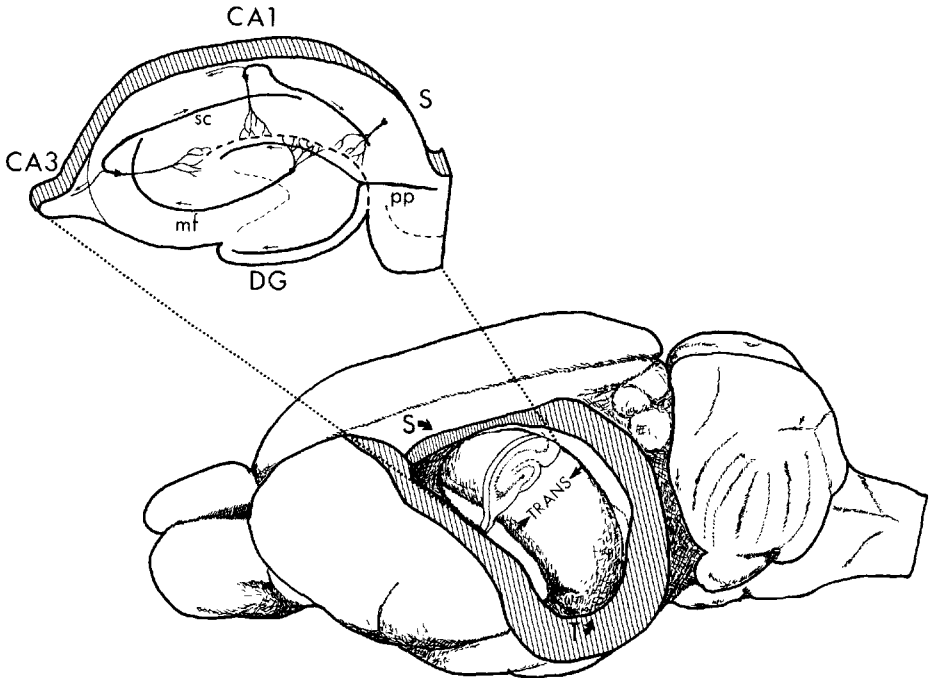


Fig. 11.1. Line drawing of a lateral cutaway view of the rat brain showing the location of the hippocampal formation (rostral is to the left and caudal is to the right). The hippocampus is a banana-shaped structure that extends from the septal nuclei rostrally to the temporal cortex, caudally. The long axis is called the *septotemporal axis* (indicated by S-T) and the orthogonal axis is the *transverse axis* (TRANS). A slice cut perpendicular to the long axis of the hippocampus (above left) shows several fields of the hippocampal formation and several of the intrinsic connections. Slices of this type are typically used for *in vitro* electrophysiological analyses of the hippocampus. Abbreviations: DG, dentate gyrus; CA3, CA1, fields of the hippocampus; S, subiculum; pp, perforant path fibers from the entorhinal cortex; mf, mossy fibers from the granule cells; sc, Schaffer collateral connections from CA3 to CA1. [From Amaral and Witter, 1989, with permission.]

hippocampus, we devote most of our coverage to these structures and focus mainly on the organization of the rat hippocampus.

NEURONAL ELEMENTS

THREE-DIMENSIONAL POSITION AND LAYERS OF THE RAT HIPPOCAMPUS

The three-dimensional position of the rat hippocampal formation in the brain is shown in Fig. 11.1. It appears grossly as an elongated, banana-shaped structure with its long axis extending in a “C”-shaped fashion from the septal nuclei rostrally, over and behind the diencephalon, into the temporal lobe caudally and ventrally. The long axis of the hippocampus is referred to as the *septotemporal axis*, and the orthogonal axis is referred to as the *transverse axis*.

The various fields and layers of the hippocampal formation are shown in Fig. 11.2. The dentate gyrus consists of three layers: the principal, or granule cell, layer; the largely acellular molecular layer that is located above the granule cell layer; and the

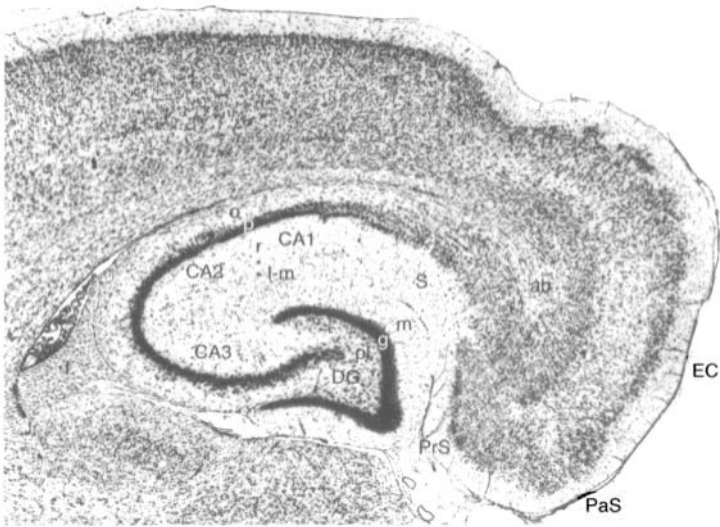


Fig. 11.2. A Nissl-stained horizontal section through the rat hippocampal formation showing all of its cytoarchitectonic divisions. (Caudal is to the right, rostral is to the left, and lateral is to the top.) The dark layers contain stained cell bodies. The acellular regions contain dendrites of the hippocampal neurons and axons from intrinsic and extrinsic sources. The dentate gyrus (DG) has three layers: the molecular layer (m); the granule cell layer (g) and the polymorphic cell layer (pl). The hippocampus is divided into CA3, CA2, and CA1 regions. In all hippocampal fields, the surface is formed by the alveus, a thin sheet of outgoing and incoming fibers. The layer occupied by basal dendrites of the pyramidal cells is stratum oriens (o) followed by the pyramidal cell layer (p) where the cell bodies of the pyramidal cells are located. Superficial to the pyramidal cell layer is stratum radiatum (r) and stratum lacunosum-moleculare (l-m) where the apical dendrites of the pyramidal cells are located. The subiculum (S), presubiculum (PrS), parasubiculum (PaS) and entorhinal cortex (EC) are also illustrated. A major input-output fiber bundle is the fimbria (f). The angular bundle (ab) is a fiber region in which the perforant path fibers travel from the entorhinal cortex to the other fields of the hippocampal formation.

diffusely cellular polymorphic cell layer (also called the hilus) that is located below the granule cell layer. The hippocampus also has a principal cell layer called the *pyramidal cell layer*. The regions above and below the pyramidal cell layer are divided into a number of strata that we describe in due course.

PRINCIPAL NEURONS

The principal neurons in the dentate gyrus are the *granule cells*, and in the hippocampus they are the *pyramidal neurons*. The pyramidal cell layer of the hippocampus has been divided into three regions designated CA1, CA2, and CA3 (Lorente de N6, 1934) based on the size and appearance of the neurons.

The granule cells have small (about 10 mm in diameter), spherical cell bodies that are arranged four to six cells thick in the granule cell layer. In rodents, the granule cell layer is shaped like the letter "V" or "U," depending on the septotemporal level (Fig. 11.3). The granule cell dendrites extend perpendicularly to the granule cell layer, into the overlying molecular layer where they receive synaptic connections from several sources. Because the dendrites emerge only from the top or apical portion of the cell body, granule cells are considered to be monopolar neurons. The axons of the granule cells are called *mossy fibers* because of the peculiar appearance of their synaptic ter-

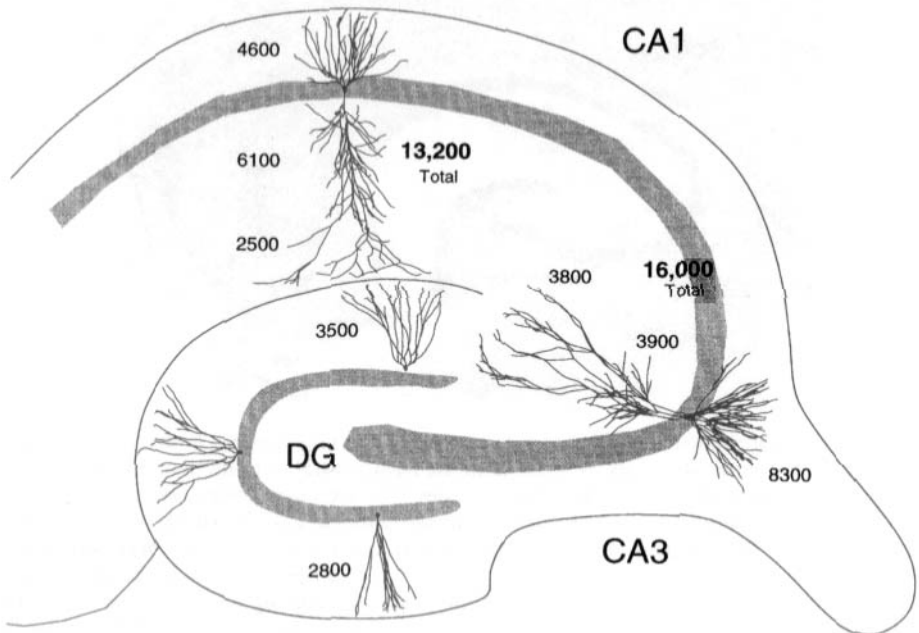


Fig. 11.3. Line drawing showing the shape and size of the principal neurons in the dentate gyrus (DG) and hippocampus (CA3 and CA1). Numbers indicate the total dendritic length of granule cells and of the portions of the dendritic trees located in stratum lacunosum-moleculare, radiatum, and oriens of the hippocampus. For the hippocampal cells, the total dendritic lengths are also given.

minals. They typically originate from the basal portion of the cell body, i.e., opposite to where the dendrites originate, and extend into the polymorphic cell layer (also called the hilus). The mossy fibers synapse onto some of the neurons, such as mossy cells, in the polymorphic cell layer before coalescing into a bundle of fibers that exits the hilus and enters stratum lucidum of CA3. The polymorphic cells are, as the name implies, of various types but they only project to other parts of the dentate gyrus.

The cell bodies of the hippocampal pyramidal neurons are arranged, three to six cells deep, in an orderly layer called the *pyramidal cell layer*. These neurons have elaborate dendritic trees extending perpendicularly to the cell layer in both directions and are thus considered to be multipolar neurons but more typically called pyramidal cells. The apical dendrites are longer than the basal and extend from the apex of the pyramidal cell body toward the center of the hippocampus, i.e., toward the dentate gyrus (see Fig. 11.3). The apical dendrites of CA3 pyramidal cells traverse three strata: stratum lucidum, stratum radiatum, and stratum lacunosum-moleculare. The dendrites receive different types of synaptic contacts in each one of these strata. The basal dendrites extend from the base of the pyramidal cell body into stratum oriens.

The hippocampus can clearly be divided into two major regions: a large-celled region closer to the dentate gyrus and a smaller-celled distal region. Ramon y Cajal (1911) called these two regions *regio inferior* and *regio superior*, respectively. However, as noted earlier, Lorente de N6 (1934) divided the hippocampus into three fields (CA3, CA2, and CA1). He also used the term *CA4*, although this referred to the region occupied by the polymorphic layer of the dentate gyrus; CA4 is typically no longer used. His CA3 and CA2 fields are equivalent to the large-celled *regio inferior* of Ramon y Cajal and his CA1 is equivalent to *regio superior*. In addition to differences in the size of the pyramidal cells in CA3 and CA1, there is a clear-cut connective difference. The CA3 pyramidal cells receive a mossy fiber input from the dentate gyrus and the CA2 and CA1 pyramidal cells do not.

The CA2 field has been a matter of some controversy. As originally defined by Lorente de N6, it was a narrow zone of cells interposed between CA3 and CA1, which had large cell bodies like CA3 but did not receive mossy fiber innervation like CA1 cells. The bulk of available evidence indicates that there is, indeed, a narrow CA2 that has both connective and perhaps even functional differences with the other hippocampal fields. CA2, for example, appears to be more resistant to epileptic cell death than CA3 or CA1 and is sometimes referred to as the resistant sector (Corsellis and Bruton, 1983).

The dendrites of the pyramidal neurons are covered with spines onto which most excitatory synapses terminate. Some of the largest spines in the nervous system are the thorny excrescences, which are located on the proximal dendrites of CA3 and receive the synapses of the mossy fibers. The thorny excrescences are complex branched spines engulfed by a single mossy fiber bouton (Hamlyn, 1962; see later). The remainder of the dendritic tree of CA3 pyramidal cells and the entire CA1 pyramidal cell dendritic tree have standard "cortical-like" spines on which excitatory, asymmetrical synapses are formed.

Quantitative analyses of the dendritic organization of hippocampal pyramidal cells indicate that the CA3 neurons have quite variable dendritic lengths (Ishizuka et al., 1995). Those located closer to the dentate gyrus tend to have shorter total dendritic

lengths, whereas those located closer to CA1 have longer dendrites. The dendritic trees of CA1 neurons, in contrast, are quite regular and the total dendritic length averages approximately 12,000–13,000 μm (Ishizuka et al., 1995; Megias et al., 2001). Megias et al. (2001) estimated that a typical CA1 pyramidal neuron may have as many as 30,000 excitatory inputs and 1700 inhibitory inputs. The proximal apical dendritic shaft is heavily innervated by inhibitory synapses (Papp et al., 2001).

Although neurons located in layers other than the pyramidal cell layers are presumed to be forms of interneurons, this may not always be the case. Gulyas et al. (1998), for example, observed a very large neuronal cell type in stratum radiatum of the CA1 field that had spiny dendrites characteristic of principal neurons and a thick, myelinated axon that was directed toward the fimbria. They concluded that this “stratum radiatum giant cell” was actually a projection neuron rather than an interneuron.

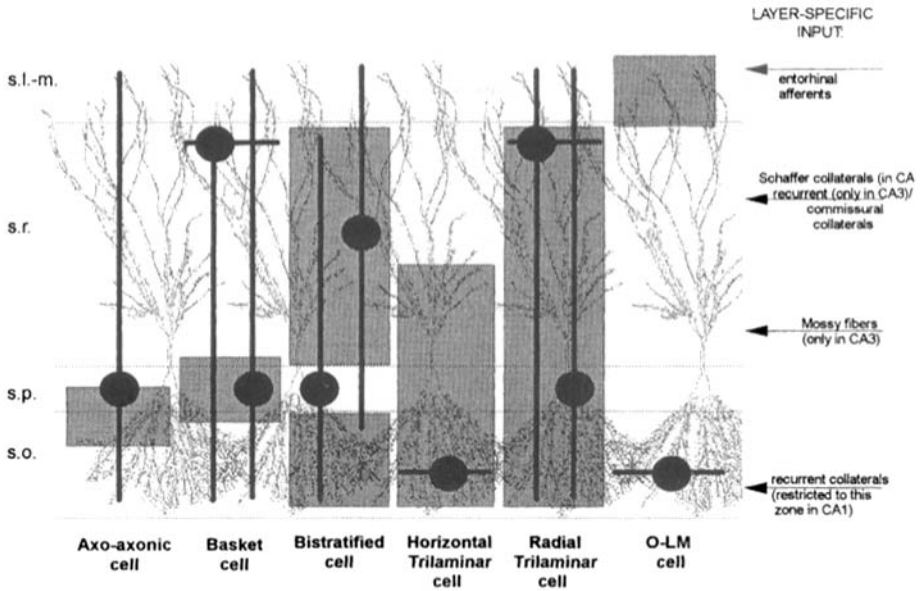
INTERNEURONS

Intrinsic neurons, or interneurons, have traditionally been defined as neurons with a locally restricted axon plexus that lack spines and release γ -aminobutyric acid (GABA). With advances in cell labeling, staining, and recording, interneurons have been found to be much more diverse than previously thought, and exceptions to all of these traditional views have been described (Buckmaster and Soltesz, 1996).

The vast majority of interneurons in the dentate gyrus and hippocampus (Fig. 11.4) do indeed have locally restricted target regions, lack spines, and are GABAergic (Freund and Buzsaki, 1996). In the dentate gyrus, the most prominent class of interneurons is called the pyramidal basket cell, and the cell bodies of these neurons are typically located at the border between the granule cell layer and the polymorphic cell layer. Axons from these neurons innervate the cell bodies of granule cells. There are at least five different types of these basket cells (Ribak and Seress, 1983). There are also interneurons in the molecular layer. Perhaps the most interesting of these is an axo-axonic cell that terminates on the axon initial segments of granule cells (Kosaka, 1983; Freund and Buzsaki, 1996). There also is a variety of interneurons located in the polymorphic cell layer. Some of these have axons that remain within the polymorphic cell layer while others innervate the granule and molecular layers (Freund and Buzsaki, 1996). There is a class of neurons in the polymorphic layer that are called *mossy cells* (Amaral, 1978). These are excitatory neurons that nonetheless project only to the molecular layer of the dentate gyrus both ipsilaterally and contralaterally. Although some investigators have called these *excitatory interneurons*, the fact that they project their axons for long distances on both sides of the hippocampus would seem to preclude the use of the term *interneuron*. In fact, these neurons tend not to project locally but rather to distant septotemporal levels of the dentate gyrus. These types of neurons would then form an exception to the traditional definitions of interneurons and principal neurons.

Hippocampal interneurons with cell bodies in or near the pyramidal cell layer can be classified into three groups on the basis of their synaptic targets: axo-axonic cells, basket cells, and bistratified cells. As the name implies, *axo-axonic cells* synapse onto the initial segments of pyramidal neurons and thus exert a strong control over action potential initiation. *Basket cells* synapse onto the somata of pyramidal neurons. Each basket cell can make multiple contacts onto a pyramidal neuron, forming what looks like a “basket” into which the soma sits. Finally, *bistratified cells* make synaptic

Hippocampus



Dentate gyrus

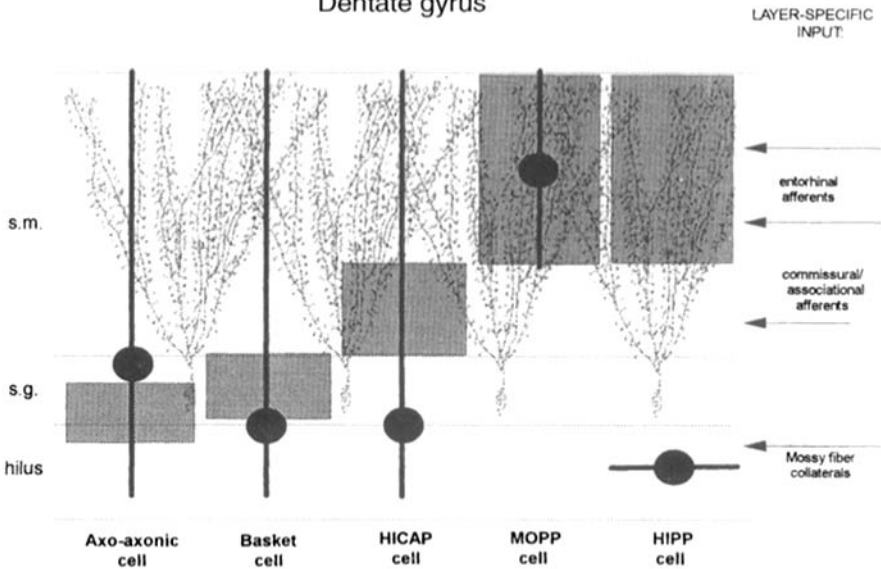


Fig. 11.4. A summary diagram of the various interneurons in the hippocampus and dentate gyrus. Most of the interneurons use GABA as their transmitter. Light profiles in the background show pyramidal cells (in the hippocampus) and granule cells (in the dentate gyrus). The interneurons innervate different portions of these principal neurons. For the interneurons, the locations of the cell bodies are marked with circles. The dark lines emanating from the circles represent the orientation and the laminar location of the major dendrites. The hatched area marks the regions where the axons from each interneuron typically arborizes. The laminar distribution of several of the excitatory inputs to these fields are indicated at right. [From Freund and Buzsaki, 1996, with permission.]

contacts onto apical and basal dendrites of pyramidal neurons. Although there is very little overlap among their target regions, the dendrites of all three cell types project into stratum radiatum and stratum oriens and thus may receive excitatory inputs from Schaffer collaterals, commissural-associational fibers, and feedback synapses from pyramidal neurons in the local region of the interneurons (Buhl et al., 1996; Halasy et al., 1996). There are also mutual inhibitory connections among these interneurons. The mutual inhibitory connections are thought to synchronize the interneurons producing oscillations at various frequencies, including theta (5 Hz) and gamma (40 Hz) frequencies (Jefferys et al., 1996). Many GABAergic interneurons also contain and release neuroactive peptides (see Freund and Buzsaki, 1996, for review).

There are also GABAergic interneurons in stratum radiatum and stratum lacunosum-moleculare that receive excitatory inputs from Schaffer collaterals and perforant path fibers, respectively, and synapse onto pyramidal neuron dendrites in various regions. Among interneurons whose properties and connections are less well known are putative excitatory interneurons in stratum lucidum that receive input from mossy fibers and synapse onto CA3 pyramidal neurons (Soriano and Frotscher, 1993) and interneurons whose postsynaptic targets are exclusively other interneurons (Freund and Buzsaki, 1996).

BASIC CIRCUITS

The basic circuitry of the hippocampal formation has been known since the time of Ramon y Cajal (1911), although details worked out by modern neuroanatomists have contributed to our current understanding, which is illustrated schematically in Fig. 11.5.

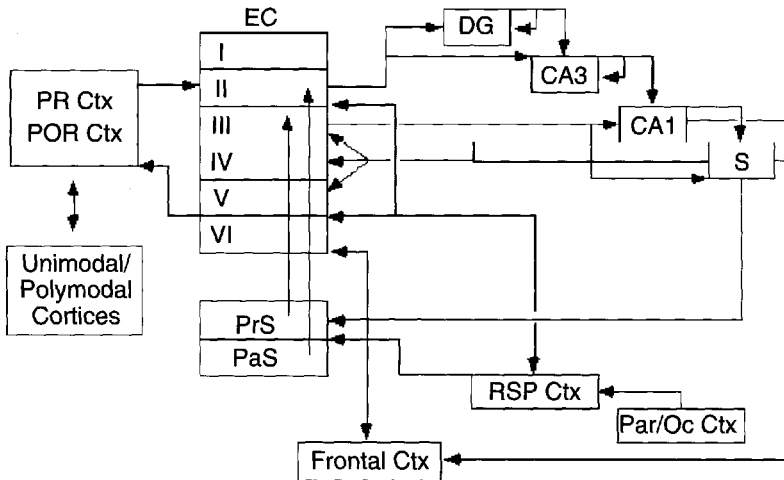


Fig. 11.5. Summary diagram of the major intrinsic connections of the rat hippocampal formation and several of the extrinsic cortical inputs. This diagram emphasizes the serial and parallel aspects of the intrinsic hippocampal circuitry. See text. Abbreviations: DG, dentate gyrus; CA3, CA1 fields of the hippocampus; EC, entorhinal cortex; PR, perirhinal; POR, postrhinal; PrS, presubiculum; PaS, parasubiculum; Par/Oc Ctx, parietal occipital cortices; RSP Ctx, retrosplenial cortex.

Andersen and colleagues (1971) emphasized the unique unidirectional progression of excitatory pathways that linked each region of the hippocampal formation and coined the term *trisynaptic circuit*. For simplicity, the entorhinal cortex is considered to be the starting point of the circuit because much of the sensory information that reaches the hippocampus enters through the entorhinal cortex. Most of the sensory information to the hippocampal formation arises in two adjacent cortical areas: the perirhinal and postrhinal (parahippocampal in the primate) cortices. These relay high-level, polysensory information to the entorhinal cortex (Burwell, 2000). This input to the entorhinal cortex is generally excitatory (Martina et al., 2001). The other major source of sensory information is the retrosplenial cortex (van Groen and Wyss, 1992; Wyss and van Groen, 1992).

Neurons located in layer II of the entorhinal cortex give rise to a pathway, the perforant path, that projects through (perforates) the subiculum and terminates both in the dentate gyrus and in the CA3 field of the hippocampus. Cells in the medial entorhinal cortex contribute axons that terminate in a highly restricted fashion within the middle portion of the molecular layer of the dentate gyrus, and those from the lateral entorhinal cortex terminate in the outer third of the molecular layer. These two components of the perforant path also end in a laminar pattern in the stratum lacunosum-moleculare of CA3 and CA2. Neurons located in layer III of the entorhinal cortex do not project to the dentate gyrus or CA3 but do project to CA1 and the subiculum. In this case, the projection is not organized in a laminar fashion but rather in a topographic fashion. Axons originating from neurons in the lateral entorhinal cortex terminate in that portion of stratum lacunosum-moleculare located at the border of CA1 with the subiculum. Projections arising from the medial entorhinal cortex terminate in that portion of stratum lacunosum-moleculare of CA1 that is located close to CA3 and in the molecular layer of the subiculum located close to the presubiculum.

The dentate gyrus is the next step in the progression of connections, and it gives rise to the mossy fibers that terminate on the proximal dendrites of the CA3 pyramidal cells. The granule cells also synapse on cells of the polymorphic layer, the mossy cells, which provides associational connections to other levels of the dentate gyrus. The CA3 pyramidal cells, in turn, project heavily to other levels of CA3 as well as to CA1. The projection to CA1 is typically called the *Schaffer collateral projection*. CA1 pyramidal cells give rise to connections both to the subiculum and to the deep layers of the entorhinal cortex. The subiculum also originates a projection to the deep layers of the entorhinal cortex. The deep layers of the entorhinal cortex, in turn, originate projections to many of the same cortical areas that originally projected to the entorhinal cortex. Thus, information entering the entorhinal cortex from a particular cortical area can traverse the entire hippocampal circuit through the excitatory pathways just described and ultimately be returned to the cortical area from which it originated. The transformations that take place through this traversal are presumably essential for enabling the information to be stored as long-term memories.

Now that the basic framework of the connectivity of the hippocampal formation has been laid out, we delve more deeply into the synaptic organization of the dentate gyrus and hippocampus.

SYNAPTIC CONNECTIONS

SYNAPTIC CONNECTIONS OF THE DENTATE GYRUS

The dentate granule cells give rise to the distinctive unmyelinated axons called mossy fibers (Fig. 11.6). Each mossy fiber gives rise to about seven thinner collaterals within the polymorphic layer before entering the CA3 field of the hippocampus (Claiborne et al., 1986). Within the polymorphic layer, the mossy fiber collaterals have two types of synaptic varicosities. There are about 160 small ($0.5\text{--}2\ \mu\text{m}$) varicosities that form contacts on spines and dendritic shafts of polymorphic layer neurons (Claiborne et al., 1986). At the ends of each of the collateral branches there are usually single, larger ($3\text{--}5\ \mu\text{m}$), irregularly shaped varicosities that resemble the mossy fiber terminals found in the CA3 field. These large mossy fiber terminals in the polymorphic layer establish contacts with the proximal dendrites of the mossy cells, the basal dendrites of the pyramidal basket cells, and other polymorphic layer cells (Ribak and Seress, 1983; Ribak et al., 1985; Scharfman et al., 1990a). Acsady and colleagues (1998) demonstrated that single mossy fiber axons innervate 7–12 mossy cells. More striking was the finding that the vast majority of the smaller synapses that arise from the filipodia associated with mossy fiber boutons or from thin collateral fibers preferentially synapse on interneurons! Thus, a typical mossy fiber axon synapses on more inhibitory neurons than excitatory neurons. In fact, as many as 95% of the excitatory synapses to the parvalbumin immunoreactive interneurons in the dentate gyrus and CA3 field of the hippocampus come from granule cell axons (Seress et al., 2001).

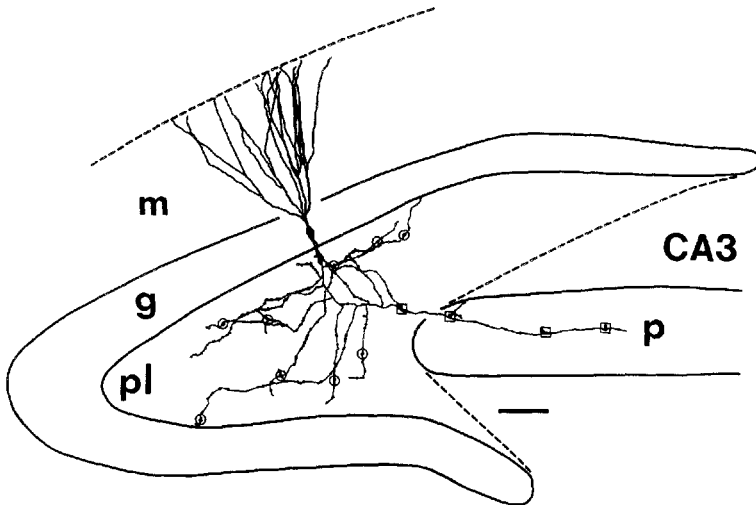


Fig. 11.6. Line drawing of a dentate granule cell and its mossy fiber axonal plexus. The axon originates from the cell body and descends into the polymorphic layer (pl) where it collateralizes. Each collateral has many small synaptic varicosities (small dots) and usually one larger presynaptic terminal (circles) that resemble the mossy fiber expansions found in stratum lucidum. The main mossy fiber axon enters CA3 and demonstrates several en passant and very large ($3\text{--}8\ \mu\text{m}$) expansions (boxes) as it transverse the entire CA3 field before entering stratum lucidum. Abbreviations: m, molecular layer; g, granule cell layer; p, pyramidal cell layer, pl, polymorphic layer.

As noted previously, there is a variety of basket cells located close to the granule cell layer. These all appear to contribute to the very dense terminal plexus that is confined to the granule cell layer. The terminals in this basket plexus are GABAergic and form symmetric, presumably inhibitory, contacts primarily on the cell bodies and shafts of apical dendrites of the granule cells (Kosaka et al., 1984). GABAergic neurons in the polymorphic layer are themselves innervated by GABAergic terminals (Misgeld and Frotscher, 1986). How widespread is the influence of a single basket cell? Analysis of Golgi-stained axonal plexuses from single basket cells (Struble et al., 1978) indicates that they extend on average 400 μm in the transverse axis and at least 1.1 μm in the septotemporal axis. It is conceivable, therefore, that a single basket cell has influence over a very large number of granule cells.

A second inhibitory input to granule cells originates from the axo-axonic or "chandelier-type" cells located in the molecular layer (Kosaka, 1983; Soriano and Frotscher, 1989). These form symmetrical contacts exclusively with the axon initial segment of granule cells. Another intrinsic projection within the dentate gyrus arises from a population of somatostatin immunoreactive neurons scattered throughout the polymorphic layer (Morrison et al., 1982; Bakst et al., 1986). These somatostatin cells, located in the polymorphic layer, colocalize GABA and contribute a plexus of fibers and terminals to the outer portions of the molecular layer. This system of fibers, which forms contacts on the distal dendrites of the granule cells, provides a third means for inhibitory control over granule cell activity (Freund and Buzsaki, 1996). The somatostatin-positive neurons of the dentate gyrus appear to terminate on a variety of cell types that include principal cells (76%) and many other forms of interneurons (Katona et al., 1999).

The inner third of the molecular layer of the dentate gyrus receives a projection that originates exclusively from cells in the polymorphic layer (Blackstad, 1956; Laurberg and Sorensen, 1981). Because this projection originates on both the ipsilateral and contralateral sides, it has been called the *ipsilateral associational-commissural projection*. The ipsilateral associational and commissural projections appear to originate as collaterals from axons of the mossy cells of the hilus (Laurberg and Sorensen, 1981). Most terminals of this pathway form asymmetrical, presumably excitatory synaptic terminals on spines of the granule cell dendrites (Laatsch and Cowan, 1967; Kishi et al., 1980). Because the mossy cells are immunoreactive for glutamate (Soriano and Frotscher, 1993), it is likely that they release this excitatory transmitter substance at their terminals within the ipsilateral associational-commissural zone of the molecular layer.

Because the mossy cells are densely innervated by the granule cells, they provide the substrate for a potential feedback loop via their axons to the proximal dendrites of the granule cells. A few facts temper the way in which we think about this feedback loop, however. The granule cells innervate mossy cells at the same septotemporal level at which their cell bodies are located. Further, the mossy cells project not to the same level that their cell bodies are located but rather to distant levels located both septally and temporally from the level of the cell body. Thus, it would appear that the mossy cells pass on the collective output of granule cells from one septotemporal level to granule cells located at distant levels of the dentate gyrus. The functional significance of the longitudinal distribution of the associational projection cannot be fully appreci-

ated without one further piece of information. In addition to contacting the spines of dentate granule cells, the associational fibers also contact the dendritic shafts of GABAergic basket cells (Frotscher and Zimmer, 1983; Seress and Ribak, 1984). Thus, the associational and commissural projections may function both as a feedforward excitatory pathway and as a disinaptic feedforward inhibitory pathway. A final fact that contributes to this discussion is that the somatostatin/GABA pathway described earlier (which originates from cells in the polymorphic layer) has a more local and limited terminal distribution. Thus, mossy fiber collaterals terminating on GABA/somatostatin cells in the polymorphic layer may lead predominantly to direct inhibition of granule cells at the same septotemporal level and to either inhibition or excitation (via the ipsilateral associational connection) at more distant levels of the dentate gyrus. The fact that the ipsilateral associational connection appears to be organized primarily to influence cells some distance away from the cell bodies of origin is a significant contradiction to the notion that the hippocampus processes information exclusively in a lamellar fashion, i.e., within slices of the hippocampal banana (Amaral and Witter, 1989).

Synaptic Connections From the Entorhinal Cortex. The major input to the dentate gyrus is from the entorhinal cortex. The major organizational features of this projection have already been described. The projection to the dentate gyrus arises mainly from layer II of the entorhinal cortex (Steward and Scoville, 1976; Schwartz and Coleman, 1981; Ruth et al., 1982, 1988). A minor component of the projection also comes from the deep layers (IV–VI) of the entorhinal cortex (Köhler, 1985). In the molecular layer of the dentate gyrus, the terminals of the perforant path fibers are strictly confined to the outer or superficial two-thirds, where they form asymmetrical synapses (Nafstad, 1967). These occur most frequently on the dendritic spines of dentate granule cells, although a small proportion of perforant path fibers terminate on the basket pyramidal interneurons (Zipp et al., 1989). Within the outer two-thirds of the molecular layer, perforant path synapses make up at least 85% of the total synaptic population (Nafstad, 1967). The perforant path is most likely glutamatergic (Fonnum et al., 1979). At least for the projection to the dentate gyrus, the terminals of the lateral perforant pathway are enkephalin immunoreactive, whereas those of the medial pathway are immunoreactive for CCK (Fredens et al., 1984).

Extrinsic Inputs to the Dentate Gyrus. The remainder of this section will deal with the subcortical inputs to the dentate gyrus, which originate mainly from the septal nuclei, supramammillary region of the posterior hypothalamus, and several monoaminergic nuclei in the brainstem, especially the locus coeruleus and raphe nuclei.

The septal projection arises from cells of the medial septal nucleus and the nucleus of the diagonal band of Broca and travels to the hippocampal formation via four routes—the fimbria, dorsal fornix, supracallosal stria—and via a ventral route through and around the amygdaloid complex (Mosko et al., 1973; Swanson, 1978; Amaral and Kurz, 1985). Septal fibers heavily innervate the polymorphic layer, particularly in a narrow band just below the granule cell layer and terminate more lightly in the molecular layer. From 30% to 50% of the cells in the medial septal nucleus and 50%–75% of the cells in the nucleus of the diagonal band that project to the hippocampal formation are cholin-

ergic (Amaral and Kurz, 1985; Wainer et al., 1985). A number of cell types are presumed to receive cholinergic innervation from these cells, although electron microscopic verification of this is still limited. Deller et al. (1999) have demonstrated that mossy cells are innervated by cholinergic terminals, however. Many of the other septal cells that project to the dentate gyrus, however, contain glutamic acid decarboxylase and are presumably GABAergic (Köhler et al., 1984); they terminate in the dentate gyrus and have an apparent preference for terminating on the GABAergic nonpyramidal cells (Freund and Antal, 1988). The septal GABAergic projection provides a striking example of long, projection neurons (not interneurons) that use GABA as their transmitter.

There is only one major hypothalamic projection to the dentate gyrus and this arises from the supramammillary area (Wyss et al., 1979a,b; Dent et al., 1983; Haglund et al., 1984). The supramammillary projection terminates heavily in a narrow zone of the molecular layer located just superficial to the granule cell layer; there is only light innervation of the polymorphic or molecular layers.

The dentate gyrus receives a particularly prominent noradrenergic input primarily from the locus coeruleus (Pickel et al., 1974; Swanson and Hartman, 1975), and the noradrenergic fibers terminate mainly in the polymorphic layer of the dentate gyrus. The serotonergic projection, which originates from the raphe nuclei, also terminates most heavily in the polymorphic layer, but the projection tends to be limited to an immediately subgranular portion of the layer (Conrad et al., 1974). Freund and colleagues (Halasy et al., 1991) have shown that the serotonergic fibers preferentially terminate on a class of interneurons in the dentate gyrus that primarily innervate the distal dendrites of the granule cells. As with the cholinergic projection, many of the cells in the raphe nuclei that project to the hippocampal formation appear to be nonserotonergic (Köhler and Steinbusch, 1982). The dentate gyrus receives a lighter and diffusely distributed dopaminergic projection that arises mainly from cells located in the ventral tegmental area (Swanson, 1982).

Outputs of the Dentate Gyrus. The dentate gyrus does not project to other brain regions. Within the hippocampal formation, it only projects to CA3 via the mossy fibers. Once the mossy fibers leave the hilus and enter the CA3 region, they have few collaterals. The mossy fibers tend to fasciculate as they extend in stratum lucidum throughout the CA3 field, where they demonstrate the large (3–6 μm in diameter), presynaptic varicosities characteristic of mossy fiber–CA3 pyramidal cell contacts (Claiborne et al., 1986). These large, presynaptic expansions are distributed at approximately 140- μm intervals along the course of the mossy fiber axons. In the part of CA3 located closest to the dentate gyrus, some mossy fibers extend deep to the pyramidal cell layer in what has been called the infrapyramidal bundle. In this region, the mossy fibers terminate on large thorny excrescences that are located both on the proximal apical and basal dendrites of the pyramidal cells.

The mossy fiber presynaptic expansion forms a unique synaptic complex with an equally intricate postsynaptic process called the thorny excrescence (Fig. 11.7). These spine-like processes are large, multilobulated entities (with as many as 16 branches) that are surrounded by a single mossy fiber expansion. A single mossy fiber expansion can make as many as 37 synaptic contacts with a single CA3 pyramidal-cell dendrite

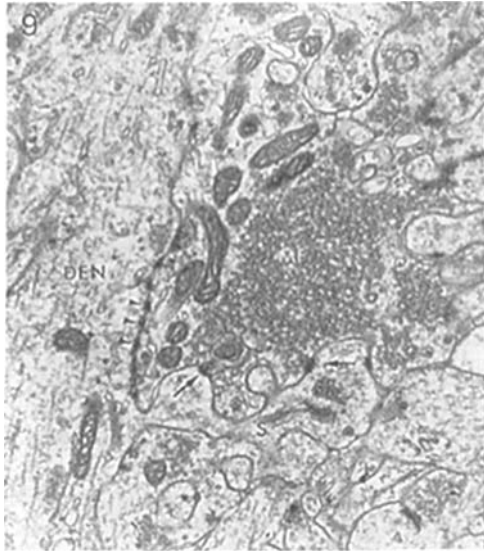


Fig. 11.7. Electron micrograph of a mossy fiber expansion (MF) that makes contact with a pyramidal cell dendrite (DEN). A large, complex thorny excrescence (S) is shown penetrating the expansion. There are several symmetrical contacts between the dendritic shaft and the expansion (arrowheads) which are nonsynaptic puncta adhaerentia. There are also several asymmetric synapses between the expansions and the complex spine (arrows). Note that the small, round synaptic vesicles are only associated with the spine specializations. [From Amaral and Dent, 1981, with permission.]

(Chicurel and Harris, 1992). Because of the large size and proximal dendritic location of the mossy fiber synapse, the granule cells are in a unique position to influence the activity of hippocampal pyramidal cells. However, mossy fibers contact relatively few pyramidal cells, perhaps no more than 14 throughout their entire trajectory (Claiborne et al., 1986; Acsady et al., 1998). Each pyramidal cell receives contacts from approximately 50 dentate granule cells.

The mossy fibers remain at approximately the same septotemporal level as their cells of origin (Gaarskjaer, 1978a,b; Swanson et al., 1978; Claiborne et al., 1986). In this respect, they are different from the organization of the ipsilateral associational connection in the dentate gyrus and the connections of the hippocampus, which tend to have much more extensive septotemporal distributions. Near the CA3–CA2 border, however, the mossy fibers make an abrupt turn temporally and extend for 1 mm or more toward the temporal pole of the hippocampus. The functional significance of this component of the mossy fibers has never been understood.

The mossy fibers are thought to use glutamate (Storm-Mathisen and Fonnum, 1972) as their primary transmitter substance, but some mossy fibers harbor opiate peptides such as dynorphin and enkephalin (Gall et al., 1981; Gall, 1984; van Daal et al., 1989). More recently, mossy fibers have also been shown to be immunoreactive for GABA (Sloviter et al., 1996). However, it is not clear whether this is involved in synaptic transmission or has a more general metabolic role.

SYNAPTIC CONNECTIONS OF CA3

The CA3 pyramidal cells give rise to highly collateralized axons that distribute fibers both within the hippocampus (to CA3, CA2, and CA1), to the same fields in the contralateral hippocampus (the commissural projections), and subcortically to the lateral septal nucleus. CA3 cells, especially those located proximally in the field, and CA2 cells contribute a small number of collaterals that innervate the polymorphic layer of the dentate gyrus.

All of the CA3 and CA2 pyramidal cells give rise to highly divergent projections to all portions of the hippocampus (Ishizuka et al., 1990). The projections to CA3 and CA2 are typically called the *associational connections*, and the CA3 projections to the CA1 field are called the *Schaffer collaterals*. There is a highly ordered and spatially distributed pattern of projections from CA3 to CA3 and from CA3 to CA1 (Ishizuka et al., 1990). The essential elements of the organization of these connections include the following.

All portions of CA3 and CA2 project to CA1, but the distribution of terminations in CA1 depends on the transverse location of the CA3/CA2 cells of origin. The older notion that a typical CA3 pyramidal cell sends a single axon to CA1 that extends linearly through the field with equal contact probability at all regions within CA1 is clearly incorrect. The topographic organization of projections from CA3 to CA1 determines a network in which certain CA3 cells are more likely to contact certain CA1 cells. CA3 cells located close to the dentate gyrus, while projecting both septally and temporally for substantial distances, tend to project more heavily to levels of CA1 located septal to their location. CA3 cells located closer to CA1, in contrast, project more heavily to levels of CA1 located temporally. At or close to the septotemporal level of the cells of origin, those cells located proximally in CA3 give rise to collaterals that tend to terminate superficially in stratum radiatum. Conversely, cells of origin located more distally in CA3 give rise to projections that terminate deeper in stratum radiatum and in stratum oriens. At or close to the septotemporal level of origin, CA3 pyramidal cells located near the dentate gyrus tend to project somewhat more heavily to distal portions of CA1 (near the subicular border), whereas CA3 projections arising from cells located distally in CA3 terminate more heavily in portions of CA1 located closer to the CA2 border.

Regardless of the septotemporal or transverse origin of a projection, the highest density of terminal and fiber labeling in CA1 shifts to deeper parts of stratum radiatum and stratum oriens at levels septal to the cells of origin and shifts out of stratum oriens and into superficial parts of stratum radiatum at levels temporal to the origin. Moreover, the highest density of fiber and terminal labeling in CA1 shifts proximally (toward CA3) at levels septal to the origin and distally (toward the subiculum) at levels temporal to the origin. Although Schaffer collaterals are often illustrated as extending only through stratum radiatum, it should be emphasized that both stratum radiatum and stratum oriens of CA1 are heavily innervated by CA3 axons. Thus, the Schaffer collaterals are as highly associated with the apical dendrites of CA1 cells in stratum radiatum as they are with the basal dendrites in stratum oriens. Moreover, some Schaffer collaterals that are initially in stratum radiatum ultimately extend into stratum oriens, and thus these axons may terminate on the apical dendrites of some pyramidal cells

and the basal dendrites of other pyramidal cells. Although it has been implicit in our discussion of these connections, it should be emphasized that each CA3 neuron makes contacts with many CA1 pyramidal cells. It has been estimated, for example, that a single CA1 neuron may be innervated by more than 5,000 ipsilateral CA3 pyramidal cells (Amaral et al., 1990). The projections from CA3 to CA1 terminate as asymmetrical, axospinous synapses located on the apical and basal dendrites of the CA1 pyramidal cells (Fig. 11.8). The sizes and shapes of the spines and presynaptic profiles in this region are quite variable and may be related to the physiological efficacy of the synapses in CA1. Shepherd and Harris (1998) have carried out the laborious task of analyzing 75 segments of Shaffer collaterals with electron microscopy. They found that synapses occur at intervals of approximately $2.7 \mu\text{m}$. Most of these synapses (68%) had one postsynaptic density, whereas 19% had two to four and 13% had none (the synapse was defined as having an accumulation of synaptic vesicles).

The associational projections from CA3 to CA3 are also organized in a highly systematic fashion and again terminate throughout stratum radiatum and oriens. One somewhat idiosyncratic facet of this projection is that cells located proximally in CA3 communicate only with other cells in the proximal portion of CA3 of the same and adjacent septotemporal levels. Associational projections arising from mid and distal portions of CA3, however, project throughout much of the transverse extent of CA3 and also project much more extensively along the septotemporal axis.

An important feature of the CA3-to-CA3 associational and CA3-to-CA1 Schaffer collateral projections is that they are both divergently distributed along the septotemporal axis. Single CA3 and CA2 pyramidal cells give rise to highly arborized axonal plexuses that distribute to as much as 75% of the septotemporal extent of the ipsilateral and contralateral CA1 fields (Tamamaki et al., 1984, 1988). Using intracellular techniques, Li et al. (1994) have found that the total length of the axonal plexus from single CA3 neurons can be as long as 150–300 mm and that a single CA3 cell may contact as many as 30,000–60,000 neurons in the ipsilateral hippocampus!

In the rat, but not in the monkey (Amaral et al., 1984; Demeter et al., 1985), the CA3 pyramidal cells give rise to commissural projections to the CA3, CA2, and CA1 regions of the contralateral hippocampal formation (Swanson et al., 1978). The same CA3 cells give rise both to ipsilateral and commissural projections (Swanson et al., 1980). Although the commissural projections roughly follow the same topographic organization and generally terminate in homologous regions on both sides, there are minor differences in the distribution of terminals. If a projection is heavier to stratum oriens on the ipsilateral side, for example, it may be heavier in stratum radiatum on the contralateral side (Swanson et al., 1978). As with the commissural projections from the dentate gyrus, CA3 fibers to the contralateral hippocampus form asymmetrical synapses on the spines of pyramidal cells in CA3 and CA1 (Gottlieb and Cowan, 1972) but also terminate on the smooth dendrites of interneurons (Frotscher and Zimmer, 1983).

Projections to Other Brain Regions. Until the mid-1970s, it was commonly assumed that the hippocampal fields (CA1–CA3) gave rise to all of the subcortical connections to the basal forebrain and diencephalon. Swanson and Cowan (1975), however, demonstrated that most of these projections actually originate from the subiculum. The only

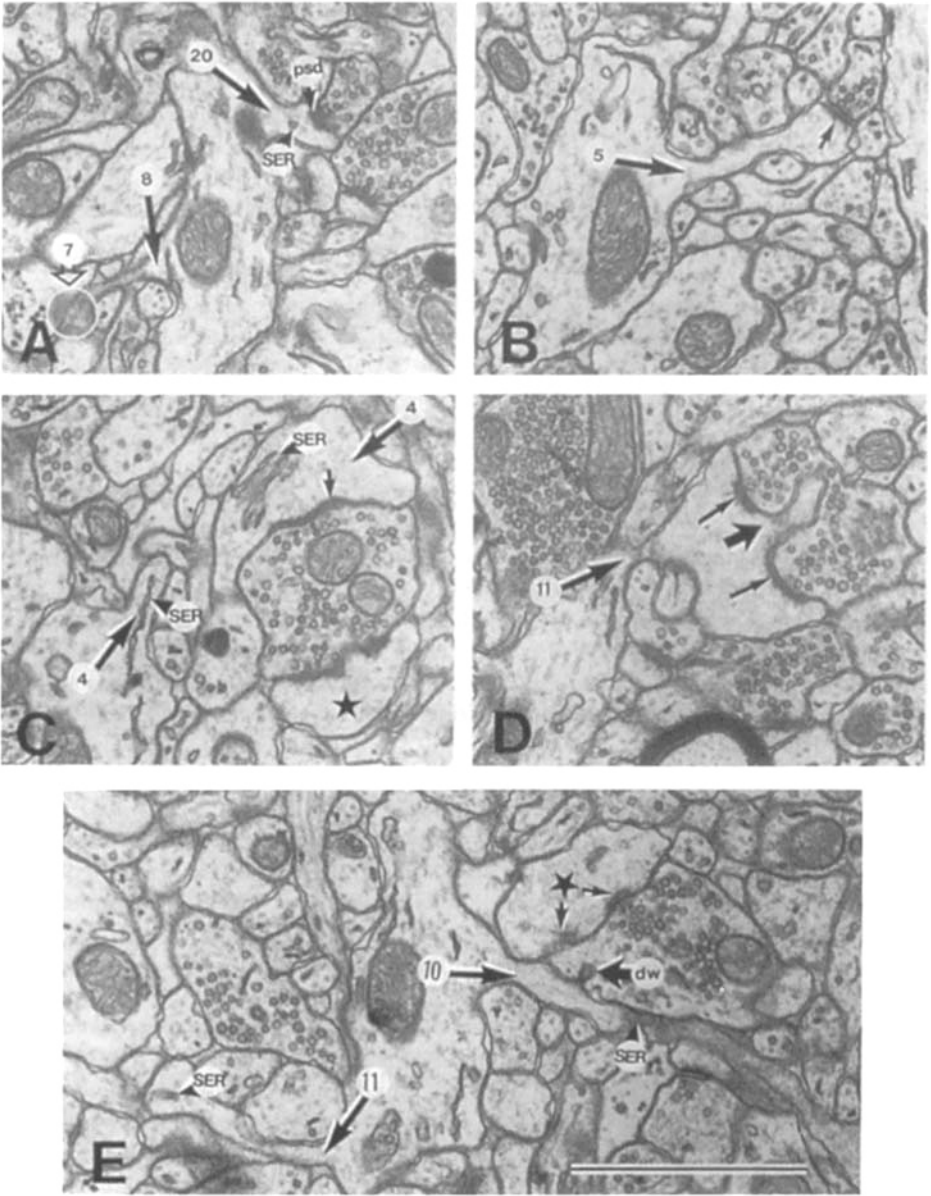


Fig. 11.8. Electron micrographs of axospinous synapses in the CA1 region of the rat hippocampus. **A:** A stubby spine (20) is identified and shows a postsynaptic density (psd). A cistern of smooth endoplasmic reticulum (ser) is in the spine. **B:** A typical thin spine with asymmetrical synapse on its head. **C:** Spine with large spine head making contact with axonal terminal. **D:** Perforated synapse. The spinule (large arrow) perforates the postsynaptic density which forms two patches (small arrows). **E:** Two very thin spine necks (10 and 11). [From Harris and Stevens, 1989, with permission.]

sizable subcortical projection from CA3 is to the lateral septal nucleus (Swanson and Cowan, 1977). The CA3 projection to the septal complex is distinct from other hippocampal projections to the septal region in that it is bilateral. Some CA3 fibers cross in the ventral hippocampal commissure to innervate the homologous region of the contralateral lateral septal nucleus. Interestingly, essentially all of the CA3 cells give rise to projections both to CA1 and to the lateral septal nucleus (Swanson et al., 1980). It should be noted that at least some of the hippocampal neurons that project to the septal region are GABAergic (Toth and Freund, 1992).

The septal nucleus also provides the major subcortical input to CA3. As with the dentate gyrus, the septal projection originates mainly in the medial septal nucleus and nucleus of the diagonal band of Broca. The projection appears to terminate most heavily in stratum oriens and, to a lesser extent, in stratum radiatum (Nyakas et al., 1987; Gaykema et al., 1990). As in the dentate gyrus, the GABAergic component of the septal projection to the CA3 field terminates mainly on GABAergic interneurons (Freund and Antal, 1988; Gulyas et al., 1990).

The CA3 field also receives inputs from the noradrenergic nucleus locus coeruleus. Noradrenergic fibers and terminals are most densely distributed in the stratum lucidum and in the most superficial portion of stratum lacunosum-moleculare. A much thinner plexus of noradrenergic axons is distributed throughout the other layers of CA3. Serotonergic fibers are diffusely and sparsely distributed in CA3, and there are few, if any, dopaminergic fibers in this field (Swanson et al., 1987). As in the dentate gyrus, the serotonergic fibers, although diffusely distributed, nonetheless appear to terminate preferentially on interneurons (Freund et al., 1990) with axons that innervate the distal dendrites of pyramidal cells.

SYNAPTIC CONNECTIONS OF CA2

The CA2 field is relatively narrow and is located distal to the end of the mossy fiber projection; it is typically no wider than approximately 250 μm . It is made up of large, darkly staining pyramidal cells, like those of CA3. However, the CA2 pyramidal cells lack the thorny excrescences that are characteristic of CA3 pyramidal cells (Lorente de N6, 1934; Tamamaki et al., 1988). A number of immunohistochemical studies have also demonstrated differential labeling of CA2. This region demonstrates denser acetylcholinesterase staining and much denser labeling for the calcium-binding protein parvalbumin than adjacent regions of CA3 or CA1 (Bainbridge and Miller, 1982). This is of interest because the calcium-binding proteins are considered to be protective of ischemic or excitotoxic cell death, and the CA2 region is purported to be the "resistant sector" described in the human epilepsy literature (Corsellis and Bruton, 1983).

The intrahippocampal connections of CA2 resemble, in part, those of the distal portions of CA3, but there are also some distinguishing characteristics. Like CA3, the CA2 cells give rise to a projection to CA1 (Ishizuka et al., 1990). The projection is rather sparse and diffuse, however, and does not clearly follow the gradient rules established by the CA3-to-CA1 projection. Interestingly, more collaterals from CA2 are distributed to the polymorphic layer of the dentate gyrus than from any portion of CA3.

There has been little work dealing specifically with the extrinsic inputs and outputs of CA2. In general, CA2 appears to share the connections of CA3. However, CA2 ap-

pears to receive a particularly prominent innervation from the supramammillary area (Haglund et al., 1984) and from the tuberomammillary nucleus (Köhler et al., 1985).

SYNAPTIC CONNECTIONS OF CA1

Unlike the CA3 field, pyramidal cells in CA1 do not appear to give rise to a major set of collaterals that distribute within CA1 (Tamamaki et al., 1987; Amaral et al., 1991), i.e., they have few associational connections. As the CA1 axons extend in the alveus or in stratum oriens toward the subiculum, occasional collaterals do arise and appear to enter stratum oriens and the pyramidal cell layer. It is likely that these collaterals terminate on the basal dendrites of other CA1 cells (Deuchars and Thomson, 1996). What is clear, however, is that the massive associational network that is so apparent in CA3 is largely missing in CA1. It was thought that the CA1 field gave rise to no commissural connections (Swanson et al., 1978), but it now appears that a small number of CA1 neurons may project to the contralateral CA1 (van Groen and Wyss, 1990).

The CA1 field receives a similar but substantially lighter septal projection than CA3 (Nyakas et al., 1987). As with CA3, the CA1 field receives light noradrenergic and serotonergic projections. The distal portion of CA1 receives a fairly substantial input from the amygdaloid complex (Krettek and Price, 1977b; Pitkanen et al., 2000). Fibers originating in the basolateral nucleus terminate in stratum lacunosum-moleculare of the CA1 field; this input from the amygdala appears to be restricted to the temporal third of CA1.

The thalamic inputs to the hippocampal formation have received relatively little attention. It has been known for some time that the anterior thalamic complex is intimately interconnected with the subiculum and the presubiculum. Herkenham (1978) demonstrated fairly prominent projections from midline (or nonspecific) regions of thalamus to several fields of the hippocampal formation. In particular, the small midline nucleus reuniens gives rise to a prominent projection to the stratum lacunosum-moleculare of CA1. Wouterlood and colleagues (1990; Dolleman-Van der Weel and Witter, 1992) found that the nucleus reuniens projections travel to the CA1 field via the internal capsule and cingulum bundle rather than through the fimbria/fornix. The nucleus reuniens projection terminates massively in stratum lacunosum-moleculare and innervates all septotemporal fields. Electron microscopic analysis indicates that the nucleus reuniens fibers terminate with asymmetric synapses on spines and thin dendritic shafts in stratum lacunosum-moleculare.

The CA1 field gives rise to two intrahippocampal projections. The first is a topographically organized projection to the adjacent subiculum (Amaral et al., 1991). The second is to the deep layers of the entorhinal cortex (Naber et al., 2001).

Axons of CA1 pyramidal cells descend into stratum oriens or the alveus and bend sharply toward the subiculum (Finch et al., 1983; Tamamaki et al., 1988; Amaral et al., 1991). The fibers re-enter the pyramidal cell layer of the subiculum and ramify profusely in the pyramidal cell layer and in the deep portion of the molecular layer. Unlike the CA3 to CA1 projection, which distributes throughout CA1 in a gradient fashion, the CA1 projection ends in a columnar fashion in the subiculum. CA1 cells located proximally in the field project to the distal third of the subiculum, whereas CA1 cells located distally in the field project just across the border into the proximal portion of the subiculum; the mid-portion of CA1 projects to the mid-portion of the subiculum

(Amaral et al., 1991). Tamamaki et al. (1988) injected single CA1 pyramidal cells with horseradish peroxidase and demonstrated that individual axonal plexuses distribute to about one-third the width of the subicular pyramidal cell layer. Thus, the CA1-to-subiculum projection segments these structures roughly into thirds.

CA1 is the first hippocampal field that originates a return projection to the entorhinal cortex and thus is different from the dentate gyrus and fields, CA3/CA2 in this respect. Projections from CA1 to the entorhinal cortex originate from the full septo-temporal and transverse extent of CA1 and appear to terminate most densely in the medial entorhinal cortex, although projections also reach the lateral entorhinal cortex. The CA1 projections to the entorhinal cortex terminate predominantly in layer V (Swanson and Cowan, 1977; Finch and Babb, 1980, 1981; van Groen and Wyss, 1990).

SYNAPTIC CONNECTIONS OF THE SUBICULUM

Although the main regions of interest in this chapter are the dentate gyrus and hippocampus, because the subiculum is such an important component of the output of the hippocampal formation, it is prudent to at least highlight some recent research on this region. There is far less known about the principal neurons of the subiculum, the pyramidal cells (Harris et al., 2001). It appears that their axons form a dense local collateral plexus that nonetheless retains the columnar organization of the subiculum. The subiculum projects to several subcortical regions, including the nucleus accumbens, the anterior thalamic nuclei, the medial mammillary nucleus, and the lateral septal nucleus, as well as the presubiculum and entorhinal cortex. As noted earlier, the CA1 projections to the subiculum appear to produce a transversely oriented columnar organization. Interestingly, the outputs to the various cortical and subcortical regions appear to respect this organization (Naber and Witter, 1998; Ishizuka, 2001), although the exact organization of these columns is still being worked out. Ishizuka (2001) has demonstrated that the neurons that give rise to different subcortical regions have different somal diameters: those projecting to the anterior thalamus are smallest, those to the nucleus accumbens are intermediate, and those to the medial mammillary nucleus are largest. The synaptic organization of the subiculum and adjacent presubiculum and parasubiculum will undoubtedly be areas of increased interest in the years to come.

PHYSIOLOGICAL AND PHARMACOLOGICAL PROPERTIES

GENERAL PROPERTIES

Basic Response. As mentioned in previous sections, the highly structured and organized arrangement of synaptic pathways makes the hippocampus ideal for studying synaptic actions *in vivo* or *in vitro* (Andersen et al., 1971). Single-shock electrical stimulations to the perforant path, mossy fibers, or Schaffer collaterals result in a characteristic sequence of excitation followed by inhibition in the appropriate target neurons. The excitation typically precedes the inhibition by a few milliseconds but otherwise they overlap in time (Barrionuevo et al., 1986). The inhibition arises from the feedforward and feedback (recurrent) connections described earlier and often has two phases: a fast and a slow phase (see later). Some of the first recordings of synaptic actions in the hippocampus were made by Andersen and colleagues using electrical field recordings *in vivo* (see Langmoen and Andersen, 1981).

Extracellular Responses. Electrical field recordings represent the summed responses from a number of neurons in the vicinity of the recording electrode. Because of the orderly arrangement of pyramidal neurons and their dendrites, the electrical fields generated by active neurons have symmetry along the septal-temporal and cell-layer dimensions and asymmetry along the dendritic-somatic axis. This two-dimensional symmetry and one-dimensional asymmetry make electrical field recordings in hippocampus quite informative. For example, it can be shown that under appropriate conditions, the time course of the field potential is approximately equal to the time course of the underlying synaptic current (see Johnston and Wu, 1995). Furthermore, if multiple recordings are made at different sites along the dendritic axis, it is possible to localize the approximate site of generation of the electrical response using a technique called CSD analysis (Haberly and Shepherd, 1973; Richardson et al., 1987).

Because current flows into the dendrites during excitatory synaptic activity, a field-recording electrode in stratum radiatum records, first, a brief negative-going transient that results from the volley of action potentials in the presynaptic fibers (called the *fiber volley*), followed by a slower negative-going potential with a time course similar to that of the underlying excitatory synaptic currents (Fig. 11.9). This latter waveform is called a *population excitatory postsynaptic potential*, or pEPSP, to signify that the measured potential results from the summed activity across a population of neurons. The current flowing into the dendrites during this pEPSP will exit the neurons near the cell body layer so that a field electrode in stratum pyramidale will record a positive-going potential during this same synaptic event. If the intensity of the synaptic input is sufficient to evoke action potentials in the neurons, then the field electrode in stratum pyramidale will also record a negative-going potential (called a *pspike*) resulting

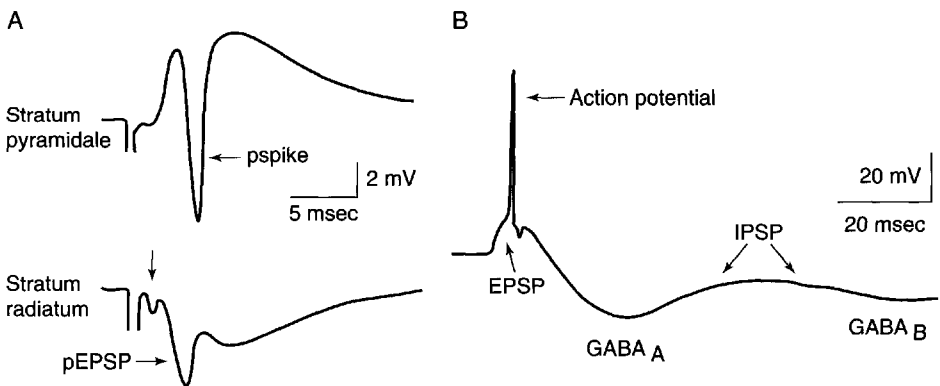


Fig. 11.9. Synaptic responses in hippocampus. **A:** Extracellular recordings from stratum pyramidale (SP) and stratum radiatum (SR) of CA1 in response to stimulation of Schaffer collaterals. The initial positivity from stratum pyramidale corresponds to the large negativity in stratum radiatum and results from synaptic current into the dendrites. This is the pEPSP and can be measured in either stratum pyramidale or stratum radiatum. The large negativity in stratum pyramidale is the pspike. It can be seen as a small positivity in stratum radiatum. The arrow in the stratum radiatum recording indicates the fiber volley. See text. [Modified from Alger et al., 1984, with permission.] **B:** Intracellular response in a CA1 neuron to Schaffer collateral stimulation. The initial EPSP triggers an action potential. The EPSP is followed by an IPSP with fast (GABA_A) and slow (GABA_B) phases. [Modified from Schwartzkroin, 1986, with permission.]

from the inward current during the postsynaptic action potentials. Measurements of the initial slope of the pEPSP measured in either stratum radiatum or stratum pyramidale provide a reliable estimate of the intensity of synaptic activity, whereas a measure of the amplitude of the pspike provides an estimate of the number of neurons reaching threshold from this synaptic input. The amplitude of the fiber volley is proportional to the number of presynaptic axons being activated by the electrical stimulus. These field potentials can be easily recorded from *in vitro* preparations for many hours and have provided a wealth of information about the physiology and pharmacology of synaptic transmission in the hippocampus.

Intracellular Responses. The electrophysiological behavior of the different neurons in the hippocampus is variable. Dentate granule and CA1 pyramidal neurons can fire repetitively at up to several hundred Hertz (Schwartzkroin, 1975, 1977), whereas CA3 pyramidal neurons tend to fire in short bursts of 5–10 action potentials (Wong and Prince, 1978; Hablitz and Johnston, 1981) (Fig. 11.10). The bursting properties of CA3 were first noticed by Kandel and Spencer (1961a) in their landmark study of hippocampal neurons *in vivo* and are thought to be important for explaining the seizure susceptibility of the hippocampus (Kandel and Spencer, 1961b; Traub and Llinas, 1979; Traub and Wong, 1981). Another prominent feature of hippocampal neurons firing repetitively is that the frequency of action potentials declines or accommodates during the train, and there is a slow afterhyperpolarization (AHP) at the end of the train. Both the frequency accommodation and the slow AHP result in part from the activation of potassium channels by the influx of calcium ions during the train.

Intracellular recordings during electrical stimulation of an afferent pathway reveal the excitation–inhibition (EPSP–IPSP) sequence illustrated in Fig. 11.9B. These recordings can be made with sharp microelectrodes or with whole-cell patch electrodes. With advances in the visualization of single neurons in brain slices using infrared video-

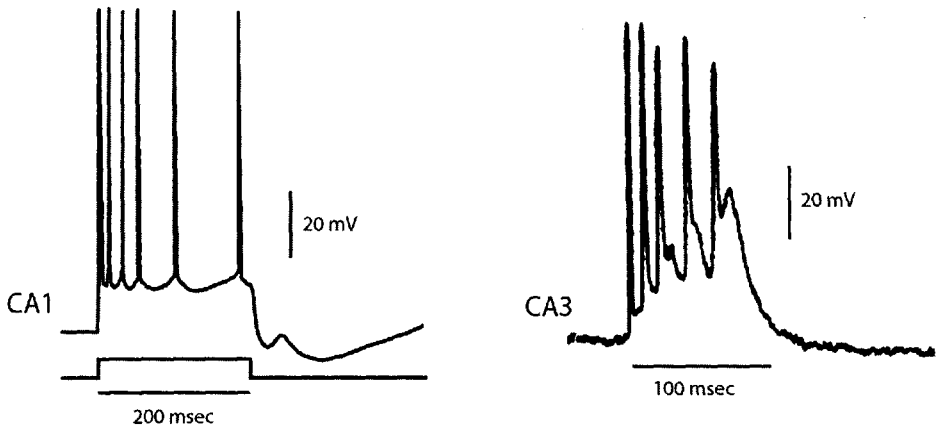


Fig. 11.10. Firing properties of CA1 and CA3 pyramidal neurons. CA1 neurons fire repetitively but show accommodation and fast and slow afterhyperpolarizations. CA3 neurons tend to fire in bursts of action potentials with declining amplitudes. [From Johnston and Wu, 1995; Johnston and Brown, 1984b.]

microscopy (Stuart et al., 1993), the whole-cell patch method is the technique of choice for most studies. The amplitudes of the electrically evoked EPSPs can range from less than 1 mV to several 10s of mV, whereas the IPSPs, if present, are in the range of 1–10 mV. The EPSP rise times (usually measured from 10% to 90% of the peak) are on the order of 5 ms, and if not accompanied by an IPSP, the EPSP decays as a function of the membrane time constant, which is about 50 ms (Spruston and Johnston, 1992). IPSPs evoked by stimulation of afferent pathways are typically much slower than EPSPs and are characterized by two components. The fast component peaks in about 20–50 ms from the stimulus and decays nonexponentially in 100–500 ms. The slow component peaks in about 100 ms and can take more than 1 sec to decay. Dendritic IPSPs are typically slower than somatic IPSPs and more closely follow the time course of NMDA receptor-mediated responses (see later; Pearce, 1993).

If the afferent stimulation is of sufficient intensity, the EPSP will evoke one or more action potentials. These action potentials are usually initiated first in the axon and then propagate into the soma and dendrites as well as down the axon to the synaptic terminals. The threshold for initiating an action potential in the soma of CA1 pyramidal cells is about 20–25 mV depolarized from the usual resting potential of –65 mV. The threshold, however, is not a fixed value and will vary according to the prior history of the membrane potential. For example, threshold will be lowered following a prolonged (>100 ms) hyperpolarization. In addition to evoked synaptic activity, there is a high rate of spontaneous synaptic potentials that can be recorded from hippocampal neurons both in vivo and in vitro. These spontaneous synaptic potentials result from random firings of presynaptic neurons and from the quantal release of neurotransmitter from synaptic terminals (Brown et al., 1979; Brown and Johnston, 1984a; Cossart et al., 2002).

Physiology and Biophysics of Synaptic Actions. Many of the basic hypotheses for synaptic transmission that were first derived from studies of invertebrate preparations have been tested in hippocampal neurons. Presynaptic mechanisms, including the quantal hypothesis for transmitter release and the role of presynaptic calcium, have been studied directly at both mossy fiber and Schaffer collateral synapses (Jonas et al., 1993; Stevens and Wang, 1994; Xiang et al., 1994; Bekkers and Stevens, 1995; Stricker et al., 1996; see also Johnston and Wu, 1995). As for postsynaptic mechanisms, the properties of conductance-increase and conductance-decrease PSPs have been explored in hippocampal neurons (Barrionuevo et al., 1986; Magee and Cook, 2000). Because excitatory synapses and some inhibitory synapses terminate on the dendrites, the study of the physiology and biophysics of synaptic transmission is complicated by the properties of dendrites, and thus an entire section is devoted here to dendritic properties.

The basic sequence of synaptic transmission begins with an action potential in the presynaptic axon that elicits Ca^{2+} influx into the bouton, and neurotransmitter is then released into the cleft from transmitter-containing vesicles in the presynaptic terminal (see Chaps. 1 and 2). The transmitter molecules diffuse across the synaptic cleft and bind to specific receptors on the postsynaptic neuron opening ion channels. The unit response from a single vesicle is called a *quantum*. Single boutons may have as few as one active zone in some Schaffer collateral boutons to as many as 37 active zones on some of the largest mossy fiber terminals (Chicurel and Harris, 1992). A prominent

theory is that one vesicle per action potential is released at each active zone with a mean probability of about one release every fourth action potential (Korn and Faber, 1991; Allen and Stevens, 1994; Stevens and Wang, 1994). Recent results, however, strongly suggest that multiquantal release can occur from at least mossy fiber hippocampal synapses (Henze et al., 2002).

INHIBITORY SYNAPSES

Although in general less is known about transmission at inhibitory synapses in the hippocampus, this situation is changing rapidly. Much new information about inhibitory synaptic transmission is available (Lambert and Wilson, 1994; McMahon and Kauer, 1997; Ouardouz and Lacaille, 1997; Bartos et al., 2001; Bertrand and Lacaille, 2001; McBain and Fisahn, 2001). The quantal nature of transmission at inhibitory synapses appears similar except that each synapse may have multiple release sites and a high probability of release (Kraushaar and Jonas, 2000; see also Miles and Wong, 1984; Miles, 1990; Ropert et al., 1990). Another important difference is that inhibitory neurons can fire repetitively at rates much higher than is typical for excitatory neurons (Schwartzkroin and Mathers, 1978). This means that excitatory input to inhibitory interneurons may trigger a high-frequency train of action potentials in the interneurons, leading to longer-lasting transmitter release and a longer-lasting inhibition of the postsynaptic neuron than from the excitatory response. Examples of firing patterns of some hippocampal interneurons are illustrated in Fig. 11.11.

NEUROTRANSMITTER RECEPTORS

EXCITATORY NEUROTRANSMITTERS

The major excitatory neurotransmitter in the hippocampus is glutamate (Storm-Mathison, 1977; Roberts et al., 1981). Glutamate is released from the perforant path, mossy fibers, commissural-associational fibers, Schaffer collaterals, and the several types of excitatory interneurons described elsewhere. The action of glutamate is on two main types of receptors: ionotropic and metabotropic (Hicks et al., 1987). The

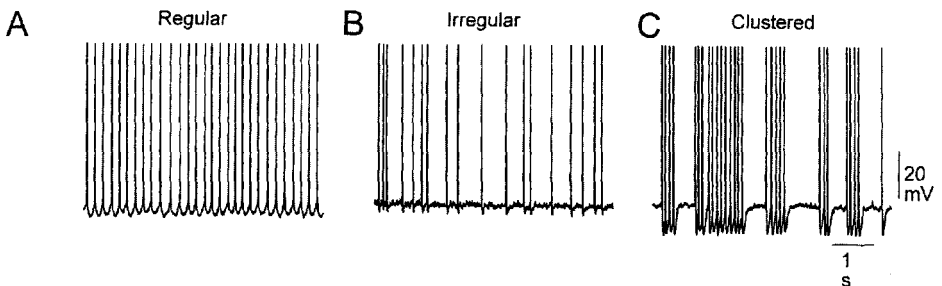


Fig. 11.11. Spontaneous firing patterns of hippocampal interneurons. Interneurons located in stratum radiatum, stratum oriens, and stratum lacunosum-moleculare can fire in regular, irregular, or clustered patterns. There is no particular classification or correlation of interneurons based on location and firing pattern. Interneurons with these firing patterns can be found in all locations. [From Parra et al., 1998.]

ionotropic receptors directly gate ion channels that are part of the receptor–molecule complex, whereas the metabotropic receptors mediate their actions through intermediary G-proteins that either gate ion channels or activate second messenger molecules. There are large families of receptor molecules within each of these classes (Hollmann and Heineman, 1994) (see Chap. 2). The ionotropic glutamate receptors consist primarily of AMPA, kainate, and NMDA receptors, all named for the particular ligand used to characterize them. AMPA and kainate receptors mediate fast EPSPs, whereas NMDA receptors mediate slower-rising and slower-decaying EPSPs. The molecular components of these receptors have been cloned (Jonas and Monyer 1999; Hollmann and Heineman 1994). AMPA receptors consist of subunits GluR1–GluR4; KA receptors contain subunits GluR5–GluR7 and KA1–KA2; and NMDA receptors contain subunits NMDAR1 and NMDAR2A–NMDAR2D. Each of the receptors is thought to be composed of four subunits from a given class in either a homomeric or heteromeric complex (Hollman, 1999).

Various combinations of AMPA, kainate, and NMDA receptors are present at all of the excitatory pathways of the hippocampus, although there may be variations at individual synapses. For example, there are fewer NMDA receptors at mossy fiber synapses (Monaghan et al., 1983). Also, it has been proposed that some Schaffer collateral synapses, especially at early stages of development, contain only NMDA receptors (Isaac et al., 1995; Liao et al., 1995).

The metabotropic glutamate receptors are also present at glutamatergic synapses, at both the presynaptic and postsynaptic side of the synapse (Shigemoto et al., 1997). They coexist in different combinations with ionotropic receptors postsynaptically and modulate transmitter release presynaptically (Schoepp and Conn, 1993). The molecular subunits of metabotropic receptors are mGluR1–mGluR8, and these are further subdivided into group I (mGluR1 and mGluR5), group II (mGluR2 and mGluR3), and group III (mGluR4 and mGluR6–mGluR8). The classification is based on sequence homology, coupling to second messenger systems, and agonist selectivity (Conn and Pin, 1997). Group I mGluRs increase phosphoinositide and can lead to activation of protein kinase C; group II mGluRs inhibit adenylyl-cyclase and can lead to a decrease in cAMP and protein kinase A activity; and group III mGluRs also negatively couple to adenylyl-cyclase. Group I receptors are primarily postsynaptic, whereas groups II and III are primarily presynaptic (Alagarsamy et al., 2001).

All of the ionotropic glutamate receptors open channels that are nonselective for the monovalent cations Na^+ and K^+ (Mayer and Westbrook, 1987). Some of the AMPA and kainate receptors and all of the NMDA receptors are also permeable to Ca^{2+} (MacDermott et al., 1986). In addition to Ca^{2+} permeability, the NMDA receptors have a unique voltage dependency. At membrane potentials near rest, the channel is blocked by Mg^{2+} from the extracellular side but becomes unblocked at more depolarized potentials (Mayer et al., 1984). The NMDA receptor plays an important role in the induction of certain forms of long-term plasticity (Collingridge and Watkins, 1994) (see later).

The AMPA-mediated response to glutamate is fast in comparison to that for NMDA (Fig. 11.12). Synapses containing both AMPA and NMDA receptors will have a mixture of fast and slow responses, depending on the membrane potential and whether the NMDA receptors are blocked by Mg^{2+} .

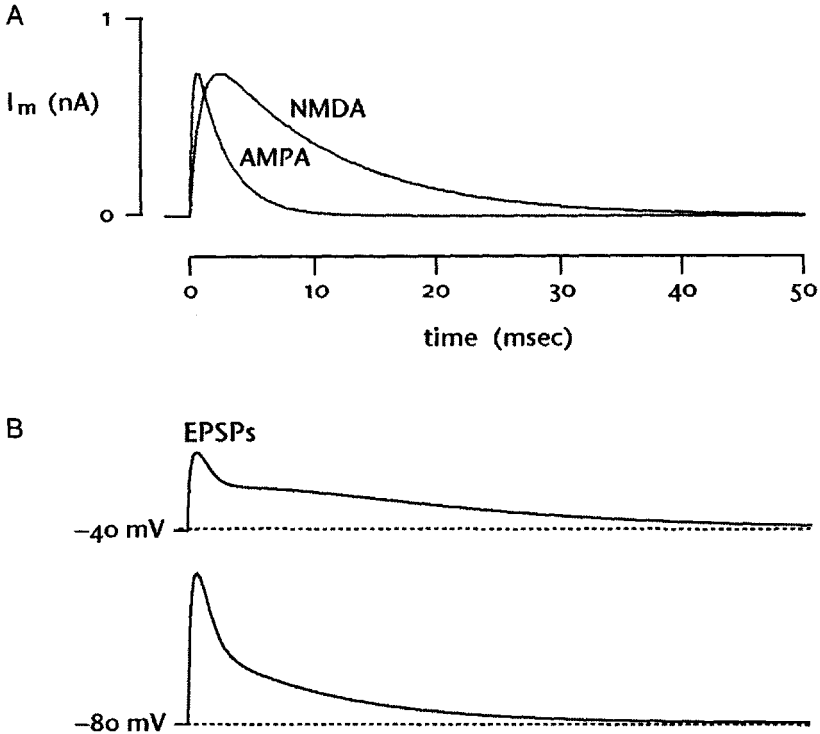


Fig. 11.12. AMPA and NMDA components of synaptic responses. **A:** The time courses of individual AMPA and NMDA currents are indicated and compared. The AMPA current has relatively fast rise and decay times compared with those of the NMDA current. **B:** Mixed AMPA/NMDA EPSPs. The EPSPs recorded at -40 mV are composed of a fast-rising AMPA component and a slow-decaying NMDA component. At -80 mV, the NMDA component is much smaller so the EPSP is primarily due to the AMPA component. [Modified from Johnston and Wu, 1995, with permission.]

Another prominent excitatory transmitter in the hippocampus is acetylcholine (ACh). As with glutamate, ACh acts on both ionotropic and metabotropic receptors. The ionotropic receptors are the nicotinic receptors, whereas the metabotropic receptors are muscarinic. Nicotinic receptors are present presynaptically and can modulate glutamate release from excitatory synapses (Gray et al., 1996; McGehee and Role, 1996; MacDermott et al., 1999). They are also on inhibitory interneurons and can modulate inhibition. Muscarinic receptors have been described at both presynaptic and postsynaptic sites in the hippocampus (Williams and Johnston, 1993). Their presynaptic effects are to decrease glutamate release and thus could be considered inhibitory. Their postsynaptic effects are to decrease a potassium conductance (Brown and Adams, 1980; Brown et al., 1990; Storm, 1990), which in turn produces a depolarization of the postsynaptic neuron, making it more likely to fire an action potential (Halliwell and Adams, 1982). Muscarinic receptor activation also reduces the slow, potassium-mediated AHP following a train of action potentials (Madison et al., 1987) (see the sAHP in Fig. 11.10). These latter two actions are strongly excitatory, because not only is the

neuron depolarized by the action of ACh on muscarinic receptors, but also the decrease in potassium conductances increases the input resistance, making other concomitant excitatory inputs more likely to fire the neuron.

There are also many other putative excitatory neurotransmitters (see Frotscher et al., 1988), but so far most are believed to be metabotropic and act indirectly through G-proteins; these include norepinephrine, dopamine, serotonin, and a number of neuroactive peptides. With their indirect actions through G-proteins, it is sometimes difficult to classify them as excitatory or inhibitory because their actions often depend on the state of the neuron. They may thus be more accurately described as neuromodulatory (Kaczmarek and Levitan, 1987).

INHIBITORY NEUROTRANSMITTERS

The major inhibitory neurotransmitter in the hippocampus is GABA (Roberts et al., 1976). Although glycine is a prominent inhibitory neurotransmitter in the spinal cord and in some brain regions (see Chaps. 3 and 5), it plays little role as a classic neurotransmitter in the hippocampus. It does act as a coagonist at the NMDA receptor, however (Johnson and Ascher, 1987).

Once again, GABA receptors can be divided into ionotropic and metabotropic. The ionotropic receptors (GABA_A) open channels permeable to Cl⁻ and are blocked by picrotoxin and bicuculline. Because the Nernst potential for Cl⁻ in most adult hippocampal neurons is negative to the resting potential, the opening of these channels results in a hyperpolarization. The opening of these GABA-gated channels also decreases the input resistance of the postsynaptic neurons and can thus reduce the effectiveness of concomitant excitatory inputs. The action of GABA on ionotropic receptors is therefore both a hyperpolarization and a reduction of excitation, each of which can be considered inhibitory.

The metabotropic GABA receptor is called the GABA_B receptor, and its action is mediated through G-proteins that open K⁺ channels on both the presynaptic and postsynaptic sides of the synapse (Dutar and Nicoll, 1988a,b; Thalmann, 1988). In the postsynaptic cell, this also leads to a hyperpolarization of the membrane potential, but the hyperpolarization has a slower onset and slower decay than the GABA_A response (see Fig. 11.9B). In the presynaptic terminal, activation of GABA_B receptors reduces transmitter release at both glutamatergic and GABAergic synapses.

It was once believed that inhibitory synapses were primarily on the cell bodies of pyramidal neurons (Andersen et al., 1964). There is much evidence that GABAergic synapses occur both on the cell bodies and throughout the dendritic tree. The GABA_B responses are primarily dendritic in origin (Miles et al., 1996), but the GABA_A responses are distributed throughout the neuron. Whether GABA_A and GABA_B receptors coexist at the same synapses is not clear, and some have proposed that the responses are mediated through different interneurons and that GABA_B receptors are outside the active zone of the synapse (Mody et al. 1994).

Another ionotropic neurotransmitter in the hippocampus is serotonin acting through 5-HT₃ receptors (Jackson and Yakel, 1995). These receptors directly gate nonselective cation channels and produce a depolarization. They often occur on inhibitory neurons, however, so that their overall effect is mostly inhibitory. There are also neuromodulatory neurotransmitters acting presynaptically and/or postsynaptically that under some

conditions can be considered inhibitory. These include norepinephrine, serotonin (through non-5-HT₃ receptors), dopamine, and neuroactive peptides (Frotscher et al., 1988).

SPECIFIC PATHWAYS

Perforant Pathway. As described previously, the perforant pathway can be separated into two groups of fibers—the lateral and medial perforant paths—depending on the neurons of origin in the entorhinal cortex and the termination zone in the different target regions (Steward, 1976; Yeckel and Berger, 1990, 1995). Both pathways produce glutamatergic EPSPs in the dendrites, although the lateral perforant path also co-releases opioid peptides when there is high-frequency activity of the presynaptic neurons (Gall et al., 1981). It has been reported that opioid peptides influence the induction of long-term potentiation (see later) in the lateral perforant path (Bramham et al., 1988; Breindl et al., 1994; Xie and Lewis, 1995).

Hilar Pathways. The physiology of the hilar region is poorly understood, compared with the rest of the hippocampus. As with other regions, there are inhibitory interneurons or basket cells forming feedforward and feedback inhibition to dentate granule cells. The mossy cells (Scharfman and Schwartzkroin, 1988) receive excitatory inputs from the mossy fibers (see later) and send feedback excitation via glutamatergic synapses to the granule cells (Scharfman, 1995; Jackson and Scharfman, 1996). The functional significance of this pathway is not clear, although it seems to be prominently involved in certain seizure models (Scharfman, 1994).

Mossy Fibers. Mossy fiber boutons are among the largest synapses of the mammalian central nervous system, surpassed only by certain synapses in the cochlear nucleus (see Chap. 4). At each bouton, there are multiple active zones (up to 37) resulting in multiple release sites for neurotransmitter (Chicurel and Harris, 1992). The boutons contain large amounts of Zn²⁺ and opioid peptides that are co-released with the main neurotransmitter glutamate (Stengaard-Pedersen et al., 1981; Howell et al., 1984; Aniksztejn et al., 1987). As with most peptides, the opioids are generally co-released only with high-frequency stimulation (McGinty et al., 1983; Hökfelt et al., 1989). It has been suggested that the mossy fibers also co-release GABA (Walker et al., 2001). As summarized previously, the mossy fibers terminate on the proximal dendrites of CA3 pyramidal cells. This proximal termination site has important practical and functional significance.

Despite these idiosyncratic features, the physiology of mossy-fiber synaptic transmission is nonetheless conventional in many respects. Mossy fiber activity produces fast glutamatergic EPSPs in CA3 neurons. Because of the multiple release sites, however, the EPSPs produced by a single mossy fiber are larger than, for example, those from a single Schaffer collateral. Furthermore, because of the proximal location of the synapses on the dendrites, the EPSPs are less attenuated by the dendrites (see Dendritic Properties). It thus takes fewer active mossy fibers to fire a CA3 neuron than for other types of synapses. The function of the co-released Zn²⁺ and opioid peptides (and perhaps GABA) is not clear, but in part the opioids may play a role in the induction of long-term potentiation at mossy fiber synapses (Derrick and Martinez, 1996; Williams and Johnston, 1996).

One of the practical advantages for the proximal location of the mossy fibers is that better voltage control of the subsynaptic membrane can be achieved from a voltage clamp applied to the soma than for synapses more distally located on the dendritic tree (Johnston and Brown, 1983). Rather detailed studies of synaptic currents and the underlying conductances have been made for mossy fiber synapses (Brown and Johnston, 1983; Jonas et al., 1993). These studies reveal unitary synaptic conductances of around 1 nS and quantal conductances of 100–200 nS. This suggests that each bouton normally releases about 5–10 quanta. The quantal events, when measured with a voltage clamp, have rise times of <1 ms and decay time constants of about 5 ms. These values are close to those derived from the kinetics of the underlying glutamate channels, which suggests that the voltage-clamp measurements are fairly accurate.

The large size of the mossy fiber synapses has also permitted patch clamping and Ca^{2+} imaging of single synapses (Geiger and Jonas, 2000; Bischofberger et al., 2002; Liang et al., 2002; Regehr et al., 1994). Jonas and colleagues have characterized the types of Ca^{2+} and other channels present in the boutons and the activity-dependent changes in action potential waveform that could alter neurotransmitter release (Bischofberger et al., 2002). In addition to Ca^{2+} influx through voltage-gated Ca^{2+} channels, there may also be Ca^{2+} -induced release of Ca^{2+} from internal stores under certain conditions (Liang et al., 2002).

Along with the mossy fibers, stratum lucidum also contains interneurons (Spruston et al., 1997) that receive input from the mossy fibers and come in two varieties: spiny and aspiny. The aspiny neurons are believed to be GABAergic and mediate feedforward inhibition to the pyramidal neurons. In contrast, the spiny neurons are thought to be glutamatergic and mediate feedforward excitation to pyramidal neurons and thus represent another type of excitatory interneuron. The function of these neurons is not known.

Recurrent Pathways. One of the hallmarks of the CA3 region is the prominent, recurrent excitatory connections among the pyramidal neurons (MacVicar and Dudek, 1980; Miles and Wong, 1986). This recurrent pathway is glutamatergic and excitatory and represents a form of positive feedback that makes the CA3 region inherently unstable. In combination with the intrinsic bursting properties of CA3 neurons, subtle increases in the ratio of excitation to inhibition in this region can result in epileptiform activity, which is characterized by spontaneous and synchronous, rhythmic firing among large numbers of neurons (Traub and Miles, 1991). The epileptiform activity in the CA3 region can then spread into CA1 and beyond. Many forms of epilepsy are believed to develop in this manner—that is, from subtle alterations in the balance between excitation and inhibition in areas like CA3 where there is strong, positive synaptic feedback among neurons.

The recurrent connections are also responsible for the “sharp wave” activity (see Functional Synthesis), which is probably the result of a synchronous burst of a small group of CA3 neurons. These sharp waves occur during quiet wakefulness and slow-wave sleep and may be associated with memory formation (Buzsaki, 1989). In fact, the feedback nature of the recurrent pathways has been suggested to provide the substrate for autoassociative memories (see Kohonen, 1978). Direct support for the “pattern completion” hypothesis for the recurrent collaterals came from a recent study in which NMDA receptors were genetically deleted specifically from CA3 pyramidal neu-

rons. The resulting animals were found to have very specific memory deficits, as predicted by this hypothesis and the autoassociative memory function of the CA3 region (Nakazawa et al., 2002).

Schaffer Collaterals. The Schaffer collaterals are probably the best-studied synaptic pathway in the hippocampus. Each Schaffer collateral axon synapses onto thousands of CA1 pyramidal neurons but usually with only one or two synaptic contacts per neuron (Sorra and Harris, 1993). The Schaffer collateral pathway has been studied extensively because of interest in the various forms of synaptic plasticity occurring at this synapse. Electrical stimulation of the Schaffer collaterals in stratum radiatum results in the sequence of excitation–inhibition described earlier. The axons of the CA1 pyramidal neurons also form a recurrent excitatory pathway that synapses back onto other CA1 neurons (Radpour and Thomson, 1991), although it is much sparser and weaker than that in CA3.

SYNAPTIC PLASTICITY

Most of the excitatory synapses in the hippocampus exhibit various forms of use- or activity-dependent synaptic plasticity. These are generally defined as changes in the amplitudes of synaptic potentials that are dependent on the prior activity of the synapse. The different forms are generally distinguished on the basis of their duration or time course and are briefly described below.

SHORT-TERM PLASTICITIES

The short-term plasticities are facilitation, post-tetanic potentiation (PTP), and depression. They range in duration from hundreds of milliseconds to several minutes.

FACILITATION

Facilitation was first described at the frog neuromuscular junction by Bernard Katz and colleagues (del Castillo and Katz, 1954), but it has also been studied in some detail in the motoneuron (see Chap. 3) and hippocampus (McNaughton, 1982; Debanne et al., 1996; Dittman et al., 2000; Kim and Alger, 2001). It is more commonly referred to as *paired-pulse facilitation* (PPF), because it is usually studied by giving a pair of pulses (stimuli) to a synaptic pathway and comparing the amplitude of the second EPSP in the pair with that of the first EPSP (Schulz et al., 1994; Kim and Alger, 2001). The amount of PPF depends on the interval between stimuli. At intervals of about 50 ms, PPF can produce a several hundred percent increase in the EPSP. PPF decreases with increasing intervals between stimuli. This decay in PPF with time between the pair of pulses is roughly exponential, with a time constant of 100–200 ms.

POST-TETANIC POTENTIATION

PTP represents a transient increase in the amplitude of a synaptic response after a brief train of stimuli. The increase in amplitude can again be several hundred percent immediately following the train and decay over the time course of several minutes after the train. PTP often has two components—a component with a decay time of 5–10 sec, called *augmentation*, and a slower-decaying component, called PTP (see Johnston and

Wu, 1995). PPF and both phases of PTP result from increases in the probability of transmitter release from the presynaptic terminal triggered by an increase in intraterminal Ca^{2+} . They represent important forms of synaptic plasticity and are highly reproducible from trial to trial and preparation to preparation.

DEPRESSION

Depression of a synaptic response can have many forms. After repetitive activity of a synapse, there can be a short-term depression due to depletion of readily releasable transmitter from the presynaptic terminal. The duration of this depression can be quite variable depending on the amount of transmitter released, but it can range from hundreds of milliseconds to a few minutes. Depression can also occur on a very short time-scale (<10 ms), but this is due to desensitization of the postsynaptic transmitter receptor molecules after repeatedly binding neurotransmitter (Stevens and Wang, 1995; Wang and Kelly, 1996).

LONG-TERM PLASTICITIES

There are several forms of synaptic plasticities at glutamatergic, excitatory synapses in hippocampus that have durations from 30 min to hours, days, or weeks. They typically occur after repetitive trains of synaptic activity, or with specific pairings of presynaptic and postsynaptic firings, and are thought to contribute to the learning and memory functions of the hippocampus (see later). They are collectively called *long-term potentiation* and *depression* (LTP and LTD), terms that each encompass several mechanistically separate processes.

LONG-TERM POTENTIATION

LTP was first described by Bliss and colleagues (Bliss and Gardner-Medwin, 1973; Bliss and Lømo, 1973) and is probably the most intensely studied of all the synaptic plasticities because of its presumed role in learning and memory (Bliss and Collingridge, 1993; Malenka and Nicoll, 1999; Bennett, 2000; Martin et al., 2000). Although details of the mechanisms underlying LTP are hotly debated and are far from certain, there are a number of general features of LTP that can be described. LTP can be induced by giving one or more high-frequency (25–200 Hz) stimulus trains to a synaptic pathway, such as the perforant path, mossy fibers, or Schaffer collaterals. This period of high-frequency stimulation is called the *induction phase*. Following the induction phase is the expression phase and during this period, the amplitude of the EPSP from a test stimulus is increased some 50%–200% above control. One of the characteristics of LTP is that the expression phase lasts much longer than the induction phase. For example, the induction phase can be a few seconds to 1 min in duration, whereas the expression phase may last up to several days. The maximum duration of expression is difficult to study, but LTP in hippocampus is unlikely to be permanent.

LTP can also be induced by giving short, repetitive trains of synaptic stimulation. The hippocampus of awake-behaving animals exhibits a rhythmic EEG pattern called *theta*, which is in the range of 5–10 Hz. LTP can be induced by giving brief trains or a burst of synaptic stimulation within this same frequency range (usually 5 Hz) in what is called *theta burst stimulation* or *theta burst pairing* (Magee and Johnston, 1997; Thomas et al., 1998) (Fig. 11.13). The latter refers to specific *pairing* of presynaptic

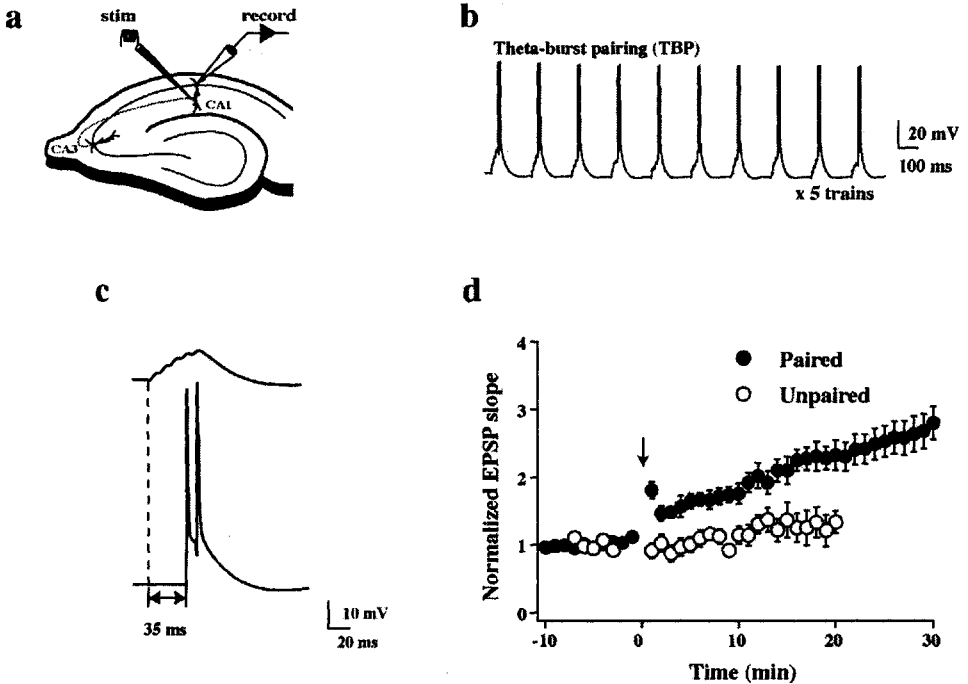


Fig. 11.13. LTP induced with a theta-burst pairing paradigm. **a:** Schematic of a hippocampal slice showing stimulating and recording sites. **b:** A sample of the theta burst pairing protocol. **c:** Representative traces of subthreshold EPSPs (train of 5 at 100 Hz) and two postsynaptic action potentials timed to occur on the last two EPSPs in the train. **d:** Time course and magnitude of the test EPSP before and after the theta burst pairing (TBP) procedure (arrow) and for similar but unpaired stimulation. [From Watanabe et al., 2002.]

and postsynaptic stimulation at theta frequencies. The use of theta-like stimulation to induce LTP is thought to be more physiological, because it falls within activity patterns that are known to occur in a behaving animal.

Finally, research has shown that repetitive pairing of single presynaptic and postsynaptic action potentials can induce either LTP or LTD depending on the relative timing between the two. For example, if the postsynaptic action potential precedes the presynaptic action potential within the interval of about 0–100 ms, LTD is induced. If instead the postsynaptic action potential follows the presynaptic action potential within the interval of about 0–20 ms, LTP is induced. This paradigm has been called *spike timing dependent plasticity* (STDP) (reviewed in Bi and Poo, 2001) (Fig. 11.14).

An important feature of LTP (and all of the long-term plasticities described in this section) is that they are generally synapse specific (see also Hoffman et al., 2002). In other words, the changes in the synaptic response are usually confined to the synapses receiving the high-frequency, theta burst, or paired stimulation. LTP also has so-called associative properties in that synapses may exhibit LTP only when they are active at the same time as other synapses. These and other properties (see reviews in Bliss and

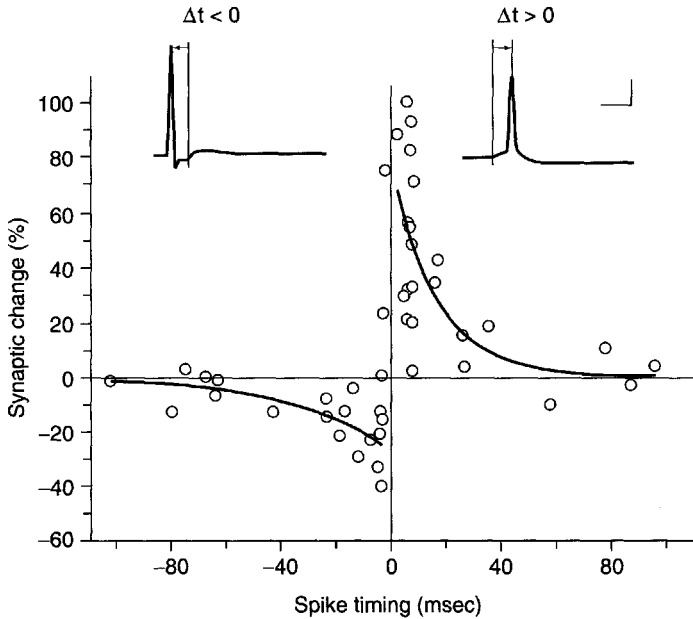


Fig. 11.14. Spike-timing dependent plasticity. LTP/LTD were induced depending on the relative timing of presynaptic and postsynaptic action potentials (APs). LTP is represented by a positive synaptic change on the ordinate; LTD by a negative synaptic change. Negative time on the abscissa is when the postsynaptic AP preceded the presynaptic AP, whereas positive time is when the presynaptic AP preceded the postsynaptic AP. [From Bi and Poo 2001.]

Lynch, 1988; Madison et al., 1991; Teyler et al., 1994; Brown et al., 2002) make LTP an attractive candidate mnemonic device.

LONG-TERM DEPRESSION

The flip side of LTP is LTD. LTD represents a long-term depression of a synaptic response (Dudek and Bear, 1992; Mulkey and Malenka, 1992; Bear and Abraham, 1996; Christie et al., 1994, 1996; Goda and Stevens, 1996). It is often induced by giving low-frequency stimulation (1–5 Hz) to a synaptic pathway for several minutes or by using the STDP paradigm described earlier; the expression of LTD can last from 30 min to 1 hour or more. A similar, but perhaps mechanistically separate, phenomenon called *depotentiation* occurs when low-frequency stimulation is given to a synaptic pathway that has already been potentiated and is expressing LTP (Levy and Steward, 1979; Wagner and Alger, 1996; Zhuo et al., 1999). Most theories for learning involve strengthening of specific synaptic pathways at the expense of others, and thus the existence of an LTD-like phenomenon has long been theorized.

At many synapses, LTP and LTD are dependent on the activation of NMDA receptors. A requirement for the induction of LTP is that there must be a sufficient increase in the intracellular Ca^{2+} concentration near the stimulated synapses. This occurs by the influx of Ca^{2+} ions through NMDA receptors and/or voltage-gated Ca^{2+} channels (Johnston et al., 1992; Teyler et al., 1994; Morgan and Teyler, 1999). At mossy fiber

synapses, LTP is not dependent on the activation of NMDA receptors, and thus many of the features of LTP at this synapse are different from those at other synapses in the hippocampus. For a variety of reasons this synapse has been difficult to study, and therefore some of the mechanisms for LTP remain controversial (Nicoll and Malenka, 1995; Yeckel et al., 1999).

DENDRITIC PROPERTIES

Hippocampal dendrites are beautiful, tree-like structures that receive all of the excitatory and much of the inhibitory synaptic input to the neuron. Approximately 90%–95% of the total surface area of a neuron (excluding the axon) is made up of dendrites. A neuron therefore expends a tremendous amount of energy growing and maintaining its dendritic tree. Nevertheless, the function of dendrites has always been somewhat of an enigma. The size and complexity of the dendritic arbor appear to increase during development (Rihn and Claiborne, 1990) and, in particular, when animals are reared in complex sensory environments (Greenough, 1975). These data suggest that dendritic size and branching patterns are important features of normal development and normal function. This conclusion is further supported by data in which dendritic structure was found altered in specific ways in patients with certain neurological and psychiatric disorders (Scheibel and Scheibel, 1973; Purpura, 1974; Mehraein et al., 1975; Abede et al., 1991; Scheibel and Conrad, 1993).

A typical CA3 hippocampal pyramidal neuron has a total dendritic length of approximately 16 mm (see Fig. 11.3) and receives approximately 25,000 excitatory synapses and fewer inhibitory synapses (Ishizuka et al., 1995). Most of these synapses terminate on dendrites, and it is assumed that dendrites somehow integrate (i.e., coordinate and blend into a unified whole) these myriad inputs to produce an output of the neuron in a process called *synaptic integration*. The output of the neuron is usually, but not always, in the form of an action potential. The properties of dendrites that provide this integrative function, as well as the nature of the integration itself, are poorly understood. For many years there have been two somewhat conflicting opinions about dendritic properties: dendrites were considered to be either passive or active.

This distinction concerns the manner in which electrical potentials spread from one point to another in the dendrites. Passive propagation of electrical potentials means that there is no involvement of voltage-gated ion channels and that electrical potentials decrement as they spread because of the so-called cable or electrotonic properties of the neuron (reviewed in Jack et al., 1975; Johnston and Wu, 1995; Segev et al., 1995). The active propagation of signals involves the opening of voltage-gated channels to help propel potentials from one point to another with little or no attenuation. For example, the action potential traveling down an axon results from the active properties of the axon. Hippocampal dendrites function in a combined way that includes both passive and active spread of potentials. Some of the functional consequences of this will be presented in the sections below (see also Spruston et al., 1994; Johnston and Wu, 1995; Johnston et al., 1996; Yuste and Tauk, 1996; Stuart et al., 1997, 1999; Magee et al., 1998).

PASSIVE PROPERTIES

A number of studies have explored the passive electrotonic properties of hippocampal neurons, including dentate granule cells, CA1 and CA3 pyramidal neurons, and interneurons (Brown et al., 1981; Spruston and Johnston, 1992; Thurbon et al., 1994). The overall conclusions from these studies is that the length constants are quite long (about 2 mm), and the membrane time constants are slow (about 50 ms). The long length constant suggests that there is very little decay of steady-state potentials through the dendrites, whereas the time constants determine the rate of decay of synaptic potentials with time and the amount of attenuation of the peak amplitude of synaptic potentials with distance. For example, EPSPs at their site of origin decay approximately monoexponentially with a time constant of about 50 ms. At sites distant from the synapse, however, the EPSP has a much longer total duration and the peak amplitude is less. In other words, the EPSP gets “filtered” by the dendrites in accordance with the membrane time constant and geometrical factors associated with the shape and branching of the dendritic tree. In fact, an EPSP spreading to the soma from the distal half of the dendritic tree may attenuate to one-fifth or less of its original peak amplitude.

Action potentials are also “filtered” by the passive properties of dendrites to an even greater extent than EPSPs. Action potentials spreading into dendrites that do not have active properties decay in amplitude very quickly with distance. One of the functions of active properties (see later) may be to reduce the filtering of EPSPs and to permit active propagation of action potentials in dendrites.

Because of this strong filtering and attenuation of EPSPs as they spread from the dendrites to the soma, it has been a mystery as to how distal synapses could have much affect on the firing properties of a neuron (which they do). At least a piece of this puzzle was found when it was discovered that the local strength of distal synapses is greater than proximal ones, probably because of a higher density of AMPA receptors at the distal inputs (Andrasfalvy and Magee, 2001). This has been called *synaptic scaling* or *synaptic normalization* (Magee and Cook, 2000) (Fig. 11.15). Briefly, the local synaptic signal (EPSP) is larger for distal vs. proximal synapses so that when the distal EPSP decays as it spreads to the soma it ends up with a very similar amplitude as the more proximal EPSP. This is a rather remarkable biological compensation for the passive properties of the dendrites.

ACTIVE PROPERTIES

It has been known for some time that action potentials can propagate at least part way into the dendrites of hippocampal neurons and perhaps, under certain conditions, even be initiated in the dendrites (Wong et al., 1979; Golding and Spruston, 1998; also see Johnston et al., 1996). Dendrites therefore must contain certain voltage-gated ion channels such as Na^+ , Ca^{2+} , and K^+ channels. The types, distribution, and function of these channels in dendrites, however, have only recently been explored, and in so doing, the full complexity of dendritic integration of synaptic potentials is just beginning to be appreciated.

Voltage-gated Na^+ channels have been recorded in the axon, soma, and distal dendrites of CA1 pyramidal neurons (Magee and Johnston, 1995a; Colbert and Johnston

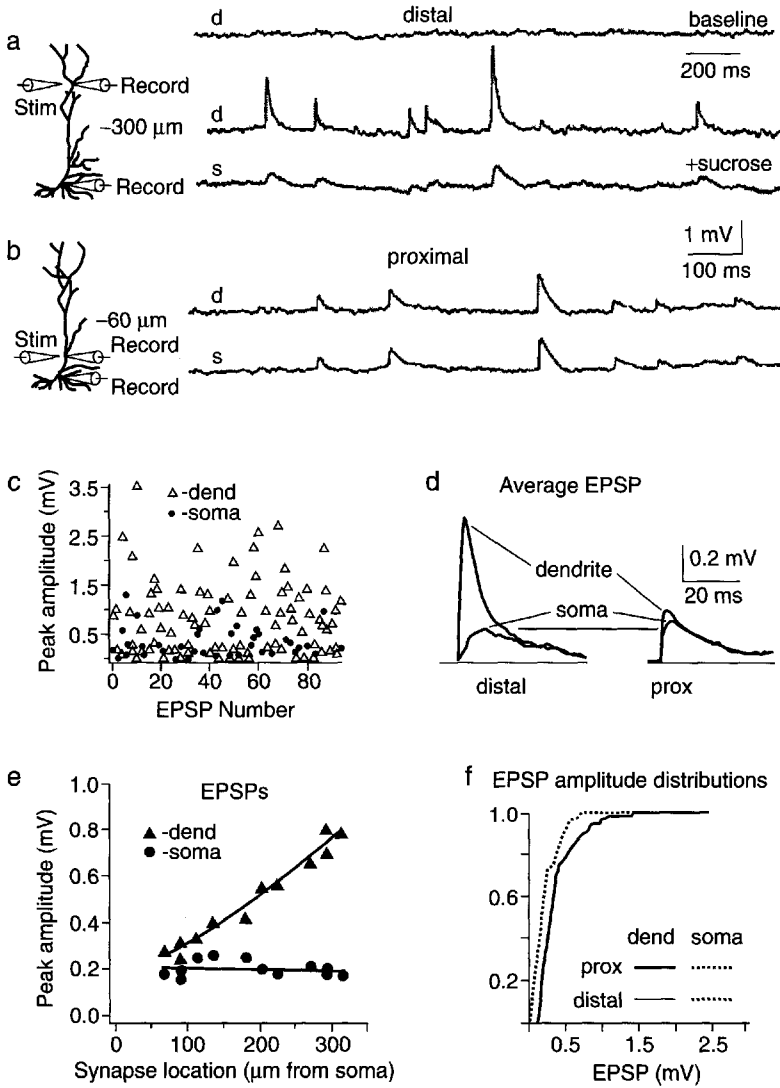


Fig. 11.15. [From Magee and Cook, 2000.]

1996). The density of these channels is approximately the same throughout the dendrites, soma, and the first 30 μm of the axon (Fig. 11.16). Beyond this point in the axon, perhaps at the first node of Ranvier, there is a high density of Na⁺ channels, and it is believed that the action potential is normally initiated here (Colbert and Johnston, 1996). Once initiated, however, it actively propagates into the soma and at least part way into the dendrites by way of these Na⁺ channels. This is an extremely important difference from the classic view, which stated that action potentials propagate only in the orthograde (from soma to synapse) direction. In fact, we now know that action potentials, once initiated in the axon, also propagate in the retrograde direction through

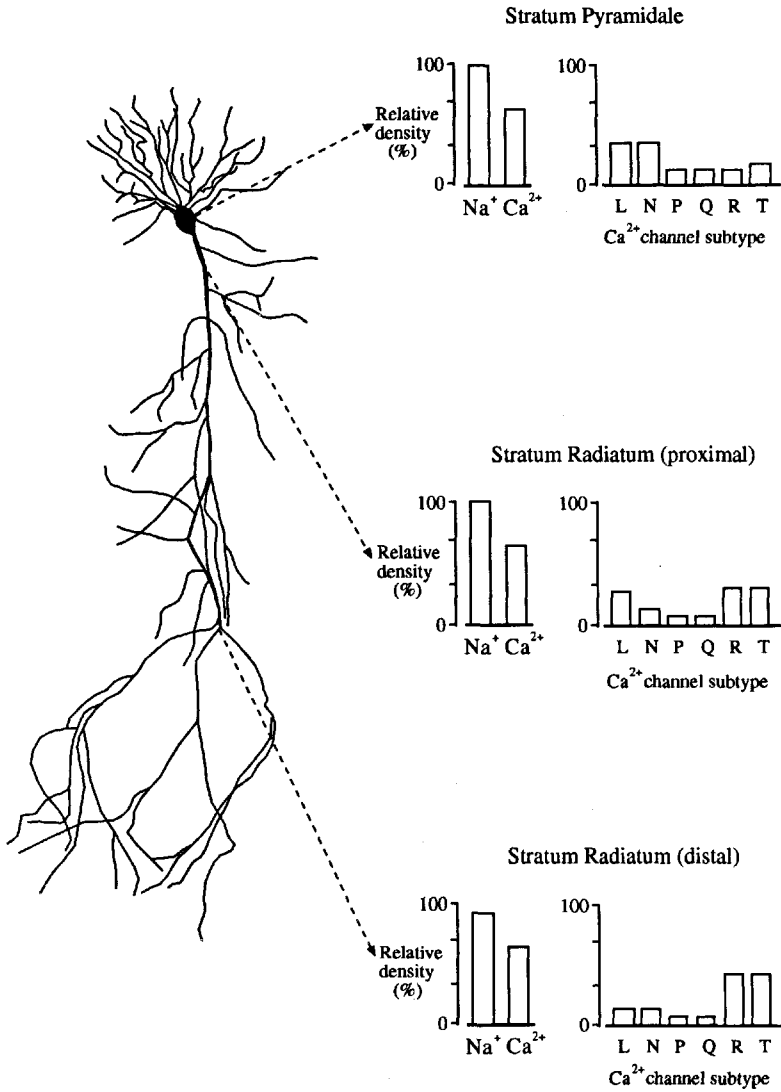


Fig. 11.16. Hypothesized distribution of voltage-gated Na⁺ and Ca²⁺ channels in CA1 pyramidal neurons. The bar graphs represent the approximate relative density of the channels in the soma and proximal and distal apical dendrites based on fluorescence imaging and dendritic patch clamping. L, N, P, Q, R, and T represent the different types of Ca²⁺ channels that occur in these neurons. [From Johnston et al., 1996, with permission.]

the soma and into the dendrites (Fig. 11.17). This has been called *back-propagation* and is an important new concept for the functioning of hippocampal neurons (Stuart et al., 1997) (see Chap. 1). This back-propagating action potential is not “all or none,” like an action potential in an axon. The amplitude of the action potential decrements as it propagates into the dendrites (Turner et al., 1991; Yuan et al., 2002). This decrease in amplitude appears to be due to an increasing density of transient K⁺ channels so

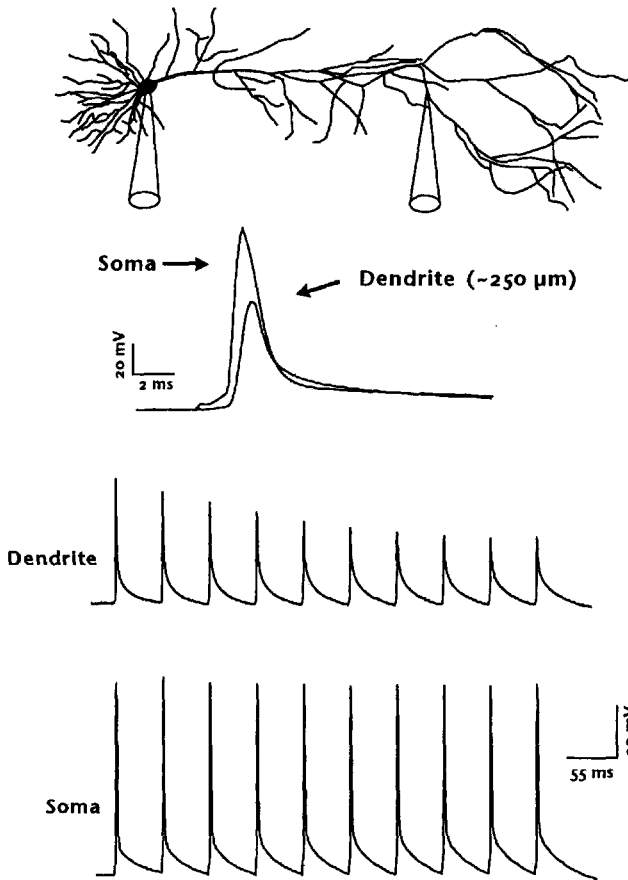


Fig. 11.17. Back-propagation of action potentials. At the top is a diagram of a CA1 neuron with two whole-cell recordings, one in the soma and one in the dendrites about $250 \mu\text{m}$ from the soma. An action potential is initiated by current injection in the soma. It begins in the axon and then propagates into the soma and dendrites. The action potential in the dendrites is smaller than in the soma because of a high density of A-type K^+ channels. It is delayed from that in the soma because of the conduction time (the conduction velocity of back-propagation is about 0.3 m/sec). The bottom part of the diagram shows the response in the soma and dendrites to a train of action potentials. The action potentials in the soma are all approximately the same amplitude, whereas those in the dendrites undergo a frequency-dependent decline in amplitude because of slow inactivation of Na^+ channels and the high density of K^+ channels. See text.

that the action potential is not able to reach its full height in the dendrites (Hoffman et al., 1997). Also, the amplitudes of back-propagating action potentials decrease successively during a train (Spruston et al., 1995; Callaway and Ross, 1995). For example, in the middle of stratum radiatum, a single action potential may be 60 mV in amplitude compared with 100 mV in the soma (Fig. 11.17). For a train of about 10 action potentials, however, the last one in the train might be 30 mV compared with 60 mV for the first. This decline in amplitude during a train is both frequency and distance-from-the-soma dependent and is due, in part, to a slow inactivation of Na^+

channels (Colbert et al., 1997; Mickus et al., 1999). At dendritic branch points, action potentials may fail to invade one or the other of the branches. This is particularly true for the more distal locations where the action potential at the branch point is small (Spruston et al., 1995; Magee and Johnston, 1997; Magee et al., 1998). EPSPs that are too small to trigger a full action potential in the axon may also open some Na^+ channels in the dendrites (Magee and Johnston, 1995b). The opening of these channels provides additional inward current that helps overcome the normal filtering of EPSPs by the passive properties. In this way, EPSPs originating on distal branches may be amplified or boosted by Na^+ channels during their spread to the soma.

In addition to Na^+ channels, voltage-gated Ca^{2+} channels have also been described in hippocampal dendrites (Christie et al., 1995; Magee and Johnston, 1995a). There are many different types of Ca^{2+} channels, some that open with small depolarizations from rest and others that require large depolarizations before opening (Tsien et al., 1988). The distribution of these different Ca^{2+} channels is not homogeneous throughout the neuron (Westenbroek et al., 1990) (see Fig. 11.16). There are different channels in dendrites from the soma. For example, the Ca^{2+} channels that open near the resting potential appear to have a higher density in dendrites than in the cell body.

When a back-propagating action potential invades the dendrites, many of these voltage-gated Ca^{2+} channels are activated and produce a significant rise in the concentration of intracellular Ca^{2+} (Jaffe et al., 1992; Miyakawa et al., 1992; Regehr and Tank, 1992; Christie et al., 1995). The change in $[\text{Ca}^{2+}]_i$ contributes to the induction of some of the long-term forms of synaptic plasticity discussed earlier. Furthermore, changes in $[\text{Ca}^{2+}]_i$ can activate a number of second-messenger systems that can have myriad effects on the neuron (Kennedy, 1989). Increases in $[\text{Ca}^{2+}]_i$ also occur with EPSPs that are too small to trigger action potentials (Magee et al., 1995, 1996). These sub-threshold EPSPs activate the Ca^{2+} channels that are opened near the resting potential. This rise in $[\text{Ca}^{2+}]_i$ from small EPSPs may also contribute to various forms of synaptic plasticity.

DENDRITIC INTEGRATION OF SYNAPTIC AND ACTION POTENTIALS

The active properties of dendrites can produce highly nonlinear interactions among EPSPs, IPSPs, and action potentials and have powerful influences over neuronal function. The two principal functions of neurons are, first, to decode incoming synaptic input and produce an appropriate output, and, second, to alter the weights or strengths of specific synaptic connections so that certain inputs will, in the future, have more or less control over the neuron's output.

As mentioned earlier, the opening of Na^+ and Ca^{2+} channels by EPSPs may, under certain conditions, lead to an amplification or boosting of distal synaptic events. This would reduce the location-dependent variability among inputs spread across the dendrites in terms of their ability to influence neuronal firing (Cook and Johnston, 1997). This has important consequences for increasing the memory storage ability of the hippocampus and is an example of how active dendrites may play a role in processing synaptic information.

In 1949, neuropsychologist Donald Hebb proposed what has become *Hebb's postulate for learning* (Stent, 1973). It states that "when an axon of cell A is near enough to excite cell B or repeatedly or consistently takes part in firing it, some growth pro-

cess or metabolic changes take place in one or both cells such that A's efficiency, as one of the cells firing B, is increased." Hebb's postulate is really a synaptic modification rule-relating strengthening of a synaptic connection to some type of correlated firing of presynaptic and postsynaptic elements (see Brown et al., 1990). It is one of the most influential learning theories in all of neuroscience.

LTP (see earlier) is considered to be the synaptic implementation of Hebb's postulate. A number of studies have shown that simultaneous presynaptic activity and postsynaptic depolarization are required for the induction of LTP (Kelso et al., 1986; Malinow and Miller, 1986; Wigstrom et al., 1986). Under physiological conditions, the postsynaptic depolarization may be the back-propagating action potential (Magee and Johnston, 1997; Markram et al., 1997) (see Fig. 11.18). It thus can provide the feedback signal from the axon to the synaptic input region that an output of the neuron has occurred. The signal may be the amplitude of the action potential that unblocks NMDA receptors or opens Ca^{2+} channels. Either way, an increase in $[\text{Ca}^{2+}]_i$ in the spine and dendrites occurs and leads to LTP of the active synapses. The amplitude of the back-propagating action potential is controlled by local IPSPs and EPSPs (Tsubokawa and Ross, 1996). IPSPs on specific dendritic branches will either reduce the amplitude of the action potential or prevent it from fully propagating into those dendrites. On the other hand, EPSPs will increase the amplitude of back-propagating action potentials and facilitate the propagation of the action potential into specific branches (Hoffman et al., 1997; Magee and Johnston, 1997). In this way, local EPSPs and IPSPs can control and guide the back-propagating action potential into different regions of the dendrites and thus control Hebbian learning. None of this would be possible without the active properties of dendrites.

FUNCTIONAL SYNTHESIS

LEARNING AND MEMORY

Perhaps the most widely accepted and long-lived proposal about hippocampal function relates to its role in memory (Eichenbaum, 1994, 2000; Milner et al., 1998). It has been known for nearly a century that damage to certain brain regions can result in an enduring amnesic syndrome that is characterized by a complete, or near-complete, anterograde amnesia. Affected patients are incapable of recreating a record of everyday events and facts. It is now clear that damage isolated to the human hippocampal formation is sufficient to produce this form of memory impairment.

The most famous example of this is the patient mentioned earlier, H.M. As a young man, H.M. experienced epilepsy that was so severe that it was life threatening. In 1953, H.M. underwent a neurosurgical procedure in which the hippocampal formation and surrounding brain tissue on both sides of his brain were removed. Although this surgery substantially reduced his seizures, there was a dramatic side effect. From the time of his surgery until the present day, H.M. has not been able to store any new information into his long-term memory. In all other respects, however, H.M.'s cognitive functions appear normal.

More recently, a number of other patients with bilateral damage confined to the hippocampus have been described. Patient R.B. was reported by Zola-Morgan and colleagues (1986). R.B. became ischemic following coronary bypass surgery and was

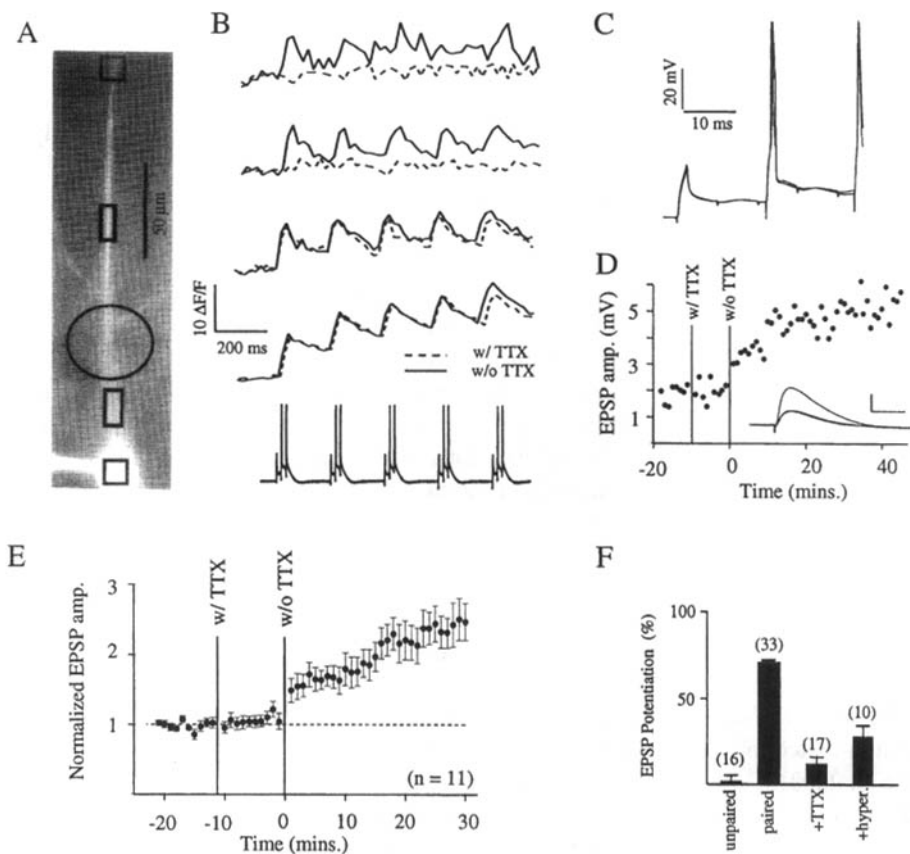


Fig. 11.18. Back-propagating action potentials paired with EPSPs induce LTP. **A:** Fura-filled CA1 pyramidal neuron with somatic electrode. Approximate area of TTX application shown by oval. **B:** Superimposed optical recordings of changes in fura-2 fluorescence from regions of the neuron delimited by the boxes in **A**. An increase in $[Ca^{2+}]_i$ is represented by an increase in $\Delta F/F$. Traces are from progressively more proximal regions moving down the column in **B**. Dashed lines are average $\Delta F/F$ during pairing protocol given along with a transient application of $10 \mu M$ TTX to the dendrite. Solid lines are average $\Delta F/F$ during pairing protocol given without TTX application (approximately 11 min later). The rise in $[Ca^{2+}]_i$ is similar in regions of the neuron proximal to the TTX application and significantly reduced in those regions distal to TTX application site. Lower trace is somatic voltage during paired train. **C:** Expanded somatic voltage recordings during the first burst of paired stimuli for trains with the TTX application and without it. No appreciable differences are observable. First current injection was subthreshold in all traces, so only two action potentials were evoked during each individual burst. **D:** Plot of EPSP amplitude for the same neuron showing that paired stimuli without back-propagating action potentials do not modify EPSP amplitude, whereas subsequent paired stimuli with back-propagating action potentials do result in a long-term, large-magnitude increase in EPSP amplitude. Average EPSPs for last 2 min of each period shown in inset (control, +TTX, -TTX). **E:** Grouped data showing normalized EPSP amplitude after paired stimulation with and without TTX application. **F:** Summary of mean LTP amplitude under various experimental conditions. Plot shows the amount of EPSP potentiation, plotted as percent of control, for all cells under each condition. Potentiation was calculated by dividing the average EPSP amplitude at 10–15 min poststimulation by the average control EPSP amplitude. [From Magee and Johnston, 1997, with permission.]

neuropsychologically evaluated for 5 years after the incident. Like H.M., R.B. demonstrated a substantial anterograde memory impairment with little or no loss of memories formed before his surgery. R.B.'s brain was subjected to postmortem analysis, and the only pathology that could be associated with his memory defect was a bilateral, complete loss of the CA1 field of the hippocampus. Because his amnesia was less severe than that of H.M., it has been proposed that the severity of the memory impairment may depend on the amount of the hippocampal formation or adjacent cortex that is included in the lesion. It is clear, however, that damage confined to the human hippocampus is sufficient to produce a clinically significant amnesic syndrome.

Although the types of tasks that are used to assess memory in animal models are typically quite different from those used in humans, like in humans, damage confined to the hippocampal formation of rats produces a severe memory impairment. One standard task of spatial memory is called the Morris water maze. In this task, rats are placed to swim in a small pool of milky water. Somewhere in the pool is a submerged platform that the animals cannot see but that provides a means for them to get out of the water. The rat ultimately learns the location of the platform through its position relative to spatial cues that exist in the testing room and exhibits rapid swimming from the starting point to the platform. Animals with lesions of the hippocampus are dramatically impaired in this task and never really learn the position of the platform.

Other tasks that have come into increasing favor among experimentalists interested in the memory function of the hippocampus include contextual fear conditioning, delay non-match to sample (DNMS), and spatial alternation T-maze (Eichenbaum, 2000; Sweatt, 2003). Contextual fear conditioning is a pavlovian or classic conditioning paradigm in which an animal learns to associate contextual or environmental cues with a mild aversive shock. This is a very simple task that may have less behavioral variables than the swim test (for example, swimming ability or motivation to swim). The DNMS task requires the subject to remember a stimulus such as a particular object or odor over a variable delay period and has been used effectively to assess memory function across a wide range of species, including humans. The T-maze has been used to assess sequential events in a memory by requiring an animal to alternate left-right choices in the maze and measuring the activity of neurons that precede the left-right choice. All of these behavioral tasks require the hippocampus, and, in particular, the DNMS and T-maze tasks have demonstrated that the hippocampus is critical for remembering the sequence of events (Lisman, 1999; Fortin et al., 2002).

Electrophysiological studies have demonstrated that neurons in the hippocampus are preferentially activated by certain stimuli located in the environment. If one records the neural activity of single hippocampal cells while a rat is running around in a maze, for example, the cell might be activated when the rat travels through a certain location of the maze (called *place cells*). Data of this type have prompted the suggestion that the hippocampus can form a "cognitive map" of the outside world (Okeefe, 1979). In a more general sense, it might be thought that the neurons of the hippocampal formation, acting as an assembly of differentially activated units, can form a representation of ongoing experience. Perhaps the interaction of this hippocampal representation of experience with the more detailed information of the experience located in the neocortex is the route through which long-term memories are formed (Wilson and McNaughton, 1993, 1994; McHugh et al., 1996). One implication of the electrophysio-

logical data is that neurons in the hippocampal formation are not uniquely sensitive to certain types of information. Rather, neurons in the hippocampal formation may act as a short-term memory buffer that records a representation of all behavioral events. This representation can then be replayed later to facilitate the longer-term and slower memory formation in the neocortex (Eichenbaum, 2001; Haist et al., 2001). The replay of behavioral events by the hippocampus has been suggested to occur during slow-wave sleep (Hoffman and McNaughton, 2002).

The hippocampus displays very characteristic brain-wave activity that may be associated with learning and memory. When animals are exploring their environment, electroencephalographic (EEG) activity of 5- to 10-Hz frequencies (theta) are recorded (O'Keefe, 1979; Buzsaki, 1989, 2002). When the animal stops exploring and is in a period of quiet wakefulness, the theta frequencies cease and are replaced by sharp-wave activity consisting of large-amplitude, irregularly occurring waveforms. These two types of EEG patterns are mutually exclusive. One theory holds that during theta (exploratory) activity, the hippocampus is acquiring a new representation of its environment (Huerta et al., 2000; Mehta et al., 2000), whereas during sharp-wave (quiet) activity (and also during slow-wave sleep), the hippocampus is facilitating the consolidation of this information in the form of long-term memories elsewhere in the cortex (Sutherland and McNaughton, 2000; Jarosiewicz et al., 2002).

DISEASES OF THE HIPPOCAMPUS

The hippocampus has been implicated in a number of neurological and psychiatric disorders, including epilepsy, Alzheimer's disease, and schizophrenia. As mentioned at the beginning of this chapter, the hippocampus has the lowest seizure threshold in the brain. In animal models of epilepsy, much of the electrical activity associated with seizures can be recorded from the hippocampus either *in vivo* or *in vitro* (Traub et al., 1989) (see Fig. 11.19). The epileptiform activity so recorded is characterized by large, synchronous discharges that occur rhythmically and are often initiated in the CA2 or CA3 regions (Johnston and Brown, 1981, 1984, 1986). The propensity for the hippocampus to exhibit this epileptiform activity has been attributed to the recurrent excitatory connections among pyramidal neurons and the tendency for CA3 neurons to fire in bursts of action potentials. Under normal conditions, the strong inhibition mediated by the various GABAergic interneurons described above prevents this abnormal activity from manifesting itself. Subtle changes in the firing properties of neurons or in the balance between excitation and inhibition, however, can permit a breakthrough of this hyperexcitable state leading to seizures.

An early and devastating feature of the onset of Alzheimer's disease is the inability to form new memories. Ultimately, even old memories weaken and fail. Because of the important role of the hippocampus in learning and memory, it is not surprising that the hippocampus is heavily damaged in Alzheimer's disease. In fact, it has been suggested that the hippocampus is functionally disconnected from the rest of the brain in this disease (Hyman et al., 1984). Moreover, there is evidence that the entorhinal cortex may be one of the first brain regions in which Alzheimer's pathology becomes apparent. Although other parts of the brain are also affected, the ability of the hippocampus to process new information is seriously impaired in Alzheimer's disease. The hippocampus is also particularly vulnerable to ischemia and anoxia. In many patients who sustain

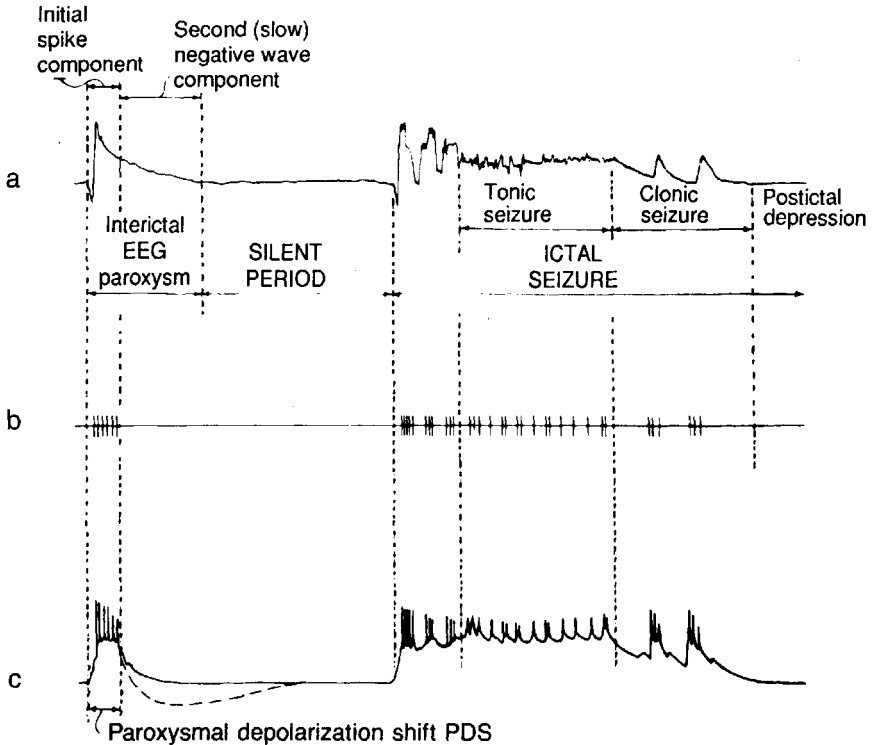


Fig. 11.19. Relationship between (a) cortical EEG and (b) extracellular and (c) intracellular discharges from a penicillin-induced, spontaneous epileptiform discharge in a cat. [From Ayala et al., 1970, with permission.]

these conditions, the hippocampus is one of only a few brain regions in which neuronal loss is observed. It appears that this loss is due to an excitotoxicity that may be mediated through the NMDA receptor. Some have proposed that the price the hippocampus pays for being able to rapidly encode new information is that it is inherently unstable and thus prone to a number of metabolic stressors. Finally, the link between schizophrenia and the hippocampus is not so clear. The principal finding is that the hippocampus is significantly smaller and has altered morphology in patients with schizophrenia (Luchins, 1990). Why these alterations should lead to the hallucinations and other altered mentation associated with schizophrenia is not known.

NEOCORTEX

RODNEY DOUGLAS, HENRY MARKRAM,
AND KEVAN MARTIN

Many of the brain regions discussed in this volume are examples of cortical (“bark-like”) structures. Taking its place alongside the *archicortex* (hippocampus) and *paleocortex* (olfactory bulb and olfactory cortex) is the *neocortex*, which is the most recent arrival in evolutionary history and arguably the most impressive example of the genre. It has certainly impressed paleontologists, whose research on the fossil record of hominids has demonstrated that the size of the hominid brain has trebled over the past 3 million years. Endocasts of the fossil hominid skulls indicate that this increase in size is largely due to the expansion of the neocortex and its connections. The massive and rapid changes in the size of the neocortex are paralleled in the phylogenetic differences we see in contemporary mammalian brains (Fig. 12.1). Of land mammals, the primates have the largest brains in proportion to their body weight. However, the human brain is three times as large as might be expected for a primate of equivalent weight (Passingham, 1982). Furthermore, the human brain is not simply a scaled-up version of our closest primate relatives, i.e., the chimpanzee. The greatest expansion is in the cortical structures, particularly the cerebellum and neocortex. Within the neocortex itself, the expansion is uneven. In comparison with nonhuman primates of equivalent body weight, the association and premotor areas have expanded relative to the sensory areas. When added together, the neocortex and its connections form a massive 80% by volume of the human brain (Passingham, 1982).

In all mammals, the neocortex consists of a sheet of cells, about 2 mm thick. Conventionally it is divided into six layers, but in many regions more than six laminae are in evidence (Fig. 12.2). Each cubic millimeter of cortex contains approximately 50,000 neurons. The study of the laminar organization of these cells in the neocortex began in the early part of the 20th century and became known as *cytoarchitectonics*. In conjunction with studies of the organization of myelinated fibers, called *myeloarchitectonics*, cytoarchitectonics was applied by Campbell in England and by Vogt and Brodmann in Germany, to divide the neocortex into about 20 different regions. Although many more areas have since been identified, there are three major cytoarchitectural divisions of the neocortex. The *koniocortex*, or granular cortex, of the sensory areas contains small densely packed neurons in the middle layers. These small neurons are largely absent in the *agranular* cortex of the motor and premotor cortical areas.

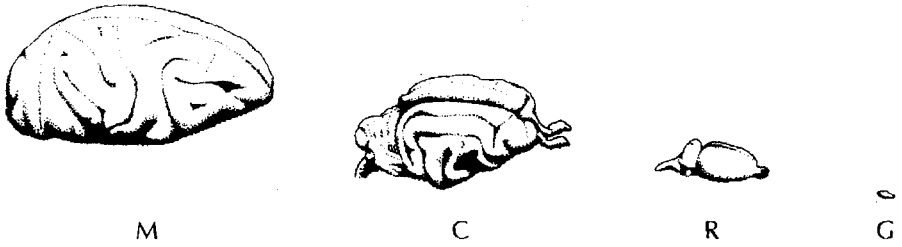


Fig. 12.1. Brains of modern vertebrates: goldfish (G), rat (R), cat (C), and Old World monkey (M). Scaled to body weight, the neocortex and its connections form an increasingly greater proportion of the brain volume. The neocortex in monkey completely envelops all other brain structures.

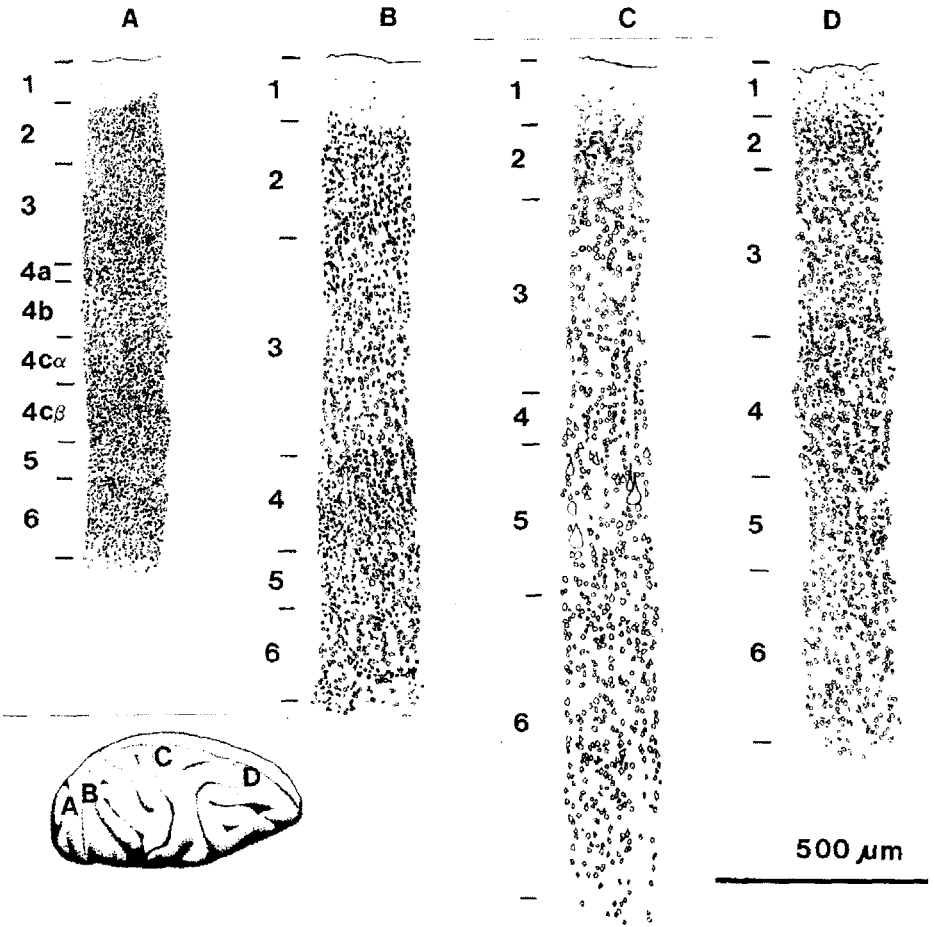


Fig. 12.2. The laminar organization of neurons in different cortical areas of the macaque monkey cortex (inset). **A:** Area 17 (striate visual cortex). **B:** Area 18 (extrastriate cortex). **C:** Area 4 (motor cortex). **D:** Area 9 (frontal cortex). A basic six-layer structure can be identified in all areas. The pia covers layer 1; the white matter is below layer 6. Note the marked difference in cell size and density among the different areas, but additional layers are apparent in some areas (e.g., area 17). The giant neurons in layer 5 of area 4 are the Betz cells. (Celloidin-embedded brain, cut in 40- μ m-thick parasagittal sections, stained for Nissl substance, uncorrected for shrinkage.)

The third type of cortex has varying populations of granule cells and is called *eulaminate*, or *homotypical*, cortex. It includes much of “association cortex,” which is a convenient description for cortex whose function has yet to be discovered (Fig. 12.2). Within each of these areas are many subdivisions, both functional and anatomical. Some are clearly delimited by their cytoarchitectonic structure, as in the case of area 17, the primary visual cortex, or by myeloarchitectonics, as in the case of the middle temporal visual area (MT). Other areas, such as area 18 in the monkey, can only be subdivided by more elaborate immunochemical, histological, or physiological methods.

In a planar view, the map of these architectonically defined areas looks like a patchwork quilt. The functional properties and subdivisions of these have been mapped most extensively in the monkey cortical areas concerned with vision. The exponential growth of functional imaging studies in humans means that increasingly more is becoming known about the equivalent subdivisions of the human brain. In addition to the basic sensory and motor functions, the cortex appears to be particularly involved in high-level functions, such as speech production and comprehension. Indeed, the concept of cortical localization of function derives from studies in the early 1900s that correlated damage of specific areas of human cortex with specific deficits in speech production. Similar modern case studies of aphasias have become celebrated in the popular culture of books, television, and films. With the advent of functional imaging studies with positron emission tomography (PET), functional magnetic resonance imaging (fMRI), and electroencephalography (EEG), there has been a rapid increase in our knowledge of the functional and anatomical map of human cortex. These techniques do not attempt to identify the mechanisms or neuronal circuits responsible for these functions. Thus, the challenge is to discover what is actually happening when different regions of the cortex are activated under different sensory or behavioral tasks. Fundamental to this central endeavor is an understanding of the structure and function of the microcircuits of the neocortex and their components.

EMBRYONIC DEVELOPMENT

The cerebral cortex develops in the walls of the telencephalic vesicles of the reptilian and mammalian forebrain (Fig. 12.3). It develops from the cortical plate that is itself embedded in the primordial cortical preplate. The preplate “pioneer” neurons regulate neuronal migration of the cortical plate neurons, and form the first axonal connections. As the cortical plate expands, it splits the preplate into a superficial layer or marginal zone, and a subplate that lies beneath the cortical plate at its boundary with the white matter. Eventually, the cortical plate differentiates into cortical layers II–VI. The marginal zone becomes layer I, and the subplate transforms into layer VIb, or vanishes (see Supér and Uylings, 2001).

Most postmitotic neurons are generated by the neuroblasts of the ventricular zone (VZ) beneath the region of the cortical plate they will finally occupy. However, some fraction of the GABAergic neurons are generated in the subventricular zone (SVZ), or in the ganglionic eminence, which lies some distance from their final location in the cortical plate.

The ventricular cells have two modes of division. Symmetrical division gives rise to two daughter cells that both maintain their proliferative properties, and so increases the

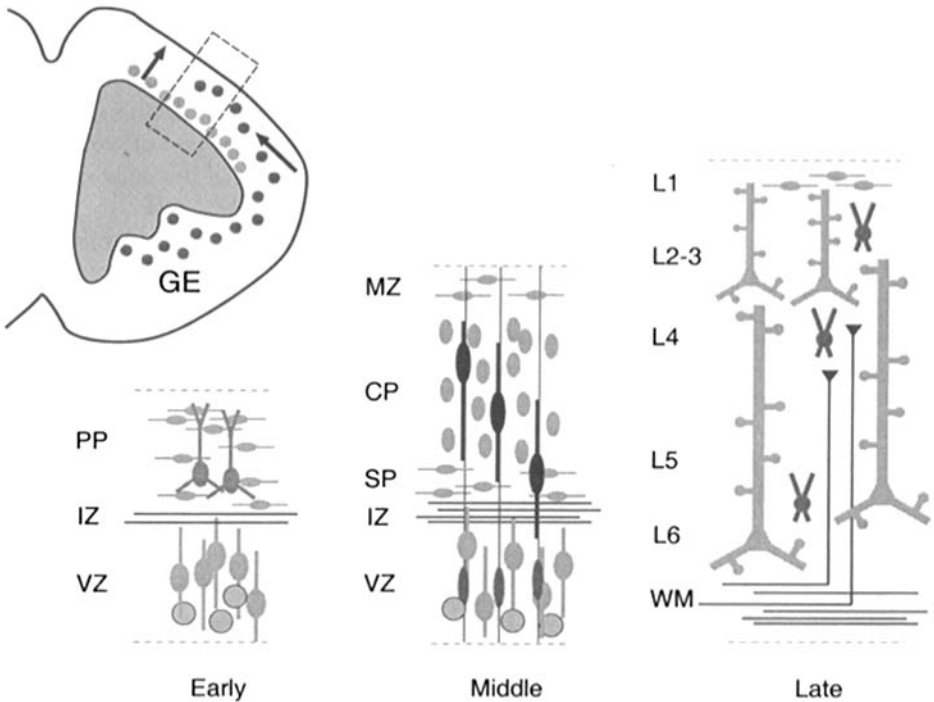


Fig. 12.3. The embryonic cerebral cortex develops in the wall of the bilateral telencephalic vesicles (one vesicle, with shaded ventricle, is shown in the schematic anatomical coronal cross section at top left). The construction sequence of increasing cortical organization in a typical region of the telencephalic wall (dashed rectangle) is shown for the early, middle, and late phases of embryonic development. All the spiny neurons and some smooth neurons arise (radial arrow in anatomical cross section) from the neuroblasts of the ventricular zone (VZ, light filled circles in cross section, cross-hatched circles in diagrams below). The majority of GABAergic neurons arise in the VZ of the ganglionic eminences (GE) and then migrate tangentially (tangential arrow in anatomical cross section) along the telencephalic wall at about the level of the intermediate zone (IZ), before taking up position in the cortical plate (CP) where they complete their differentiation (dark vertical bipolar cells in "Late" phase). The preplate (PP, "Early" phase) is the earliest structure generated by the neuroblasts of the ventricular zone. Postmitotic neurons migrate vertically (black vertically elongated cells in "Middle" phase) into the PP guided by a scaffolding of radial glial cells (dark vertical lines with elongated somata in "Middle" phase), which extend from the ventricular wall to the outer surface of the telencephalon. These neurons form the cortical plate (CP) within the preplate, so splitting the preplate into a superficial marginal zone (MZ) and a deep subplate (SP). The cortical plate neurons are assembled in inside-out order. During this phase afferent axons advance tangentially in the intermediate zone, before turning vertically to make contact with their targets in the CP. Cortical plate neurons, derived from radial migration from VZ and tangential migration from GE, differentiate into the spiny and smooth neurons that compose layers 2–6 of neocortex ("Late" phase). [From Parnavelas, 2000.]

pool of neuroblasts. Asymmetrical division gives rise to one proliferative cell (so conserving the pool of neuroblasts) and one postmitotic cell. The postmitotic cells migrate radially upward through the subplate, into the neocortical plate (Rakic, 1971). The migration is an inside-out stacking process, whereby the earliest migrators settle in the deepest layers and subsequent migrators pass through the previously settled layers and

finally come to rest in the outer layers. This radial migration of cortical neurons is supported by a transient scaffolding of radial glial cells; it is controlled by preplate pioneer cells, such as the Cajal-Retzius cells (Ogawa et al., 1995). Radial migration has two phases. Initially, the entire neuron migrates. Later, migration is dominated by translocation of the nucleus within the radially extended cell to the layer location where the soma will finally be established.

Afferents growing into the mammalian neocortex advance tangentially beneath the cortical plate in the subplate and intermediate zone. Then they turn radially and ascend vertically through the subplate to reach their target neurons within the plate. The subplate plays a major role in the organization of the afferent connections with the newly settled cortical neurons. Its thickness is proportional to the complexity of the mammal's behavior. It is always very thin in rodents, but in humans it transiently attains a thickness nearly six times that of the cortical plate it serves (Supér and Uylings, 2001).

This uniform two-dimensional radial construction mechanism could provide a simple explanation for the more than 1000-fold increase in the cortical area without a comparable increase in its thickness. A simple mutation of a regulatory gene (or genes) that control the rate and duration and the mode (symmetrical/asymmetrical) of cell division in the proliferative zone, coupled with constraints in the radial distribution of migrating neurons, could create an expanded cortical plate with enhanced capacity for establishing new patterns of connectivity that are validated through natural selection (Rakic, 1995). This simple picture has been complicated by the discovery that significant numbers (at least 75% in mice) of the GABAergic neurons migrate along distinct pathways from the ganglionic eminence, probably along corticofugal fibres (Parnavelas, 2000). They travel close to the VZ and then turn to migrate radially. They appear first in the marginal zone, some in the form of Cajal-Retzius cells, which are thought to influence the migration of pyramidal neurons generated in the VZ. Later, they appear in the intermediate zone and cortical plate. The second population of GABAergic neurons, generated in the SVZ, form themselves into chains, which they use as a scaffold for their own radial migration. The GABAergic neurons exhibit a great morphological diversity, which may also be due to their exposure to different differentiating factors in the course of their various migrations from different sources. One of the major fascinations of cortical anatomists has been to discover how the different pieces of the cortical jigsaw fit together to form functional circuits of such evident sophistication.

NEURONAL ELEMENTS

Nearly 100 years ago, Ramon y Cajal outlined the basic approach to studying the elementary organization of cortical connectivity (Cajal, 1911). The method is to reveal the complete structure of neurons, including their axons, and then piece together these components in a jigsaw puzzle fashion to produce circuits. He, and many since, studied the morphology and circuitry of the neocortex with the silver impregnation technique discovered by Golgi. Although this technique has been superseded by much more sophisticated modern techniques, the basic classes of neurons revealed by the Golgi technique used by Ramon y Cajal have remained largely unaltered. All three cytoarchitectural divisions of the neocortex contain the same two basic types of neurons: those whose dendrites bear spines (the stellate and pyramidal neurons, e.g., see Fig. 12.5) and those whose dendrites are smooth (smooth cells, e.g., see Fig. 12.7). Occa-

sionally, “sparsely” spiny cells have been described, but these neurons form a very small subclass of cortical neurons.

The proximal shafts of the dendrites of the spiny cell types are nearly devoid of spines. The spine density varies considerably between different types of neurons. At one extreme is the “sparsely spiny” neuron, which may bear fewer than 100 spines over the entire dendritic tree. These neurons form a small subclass of the inhibitory neuron population. At another extreme are neurons such as the Betz cell, a large pyramidal neuron that is found in the motor cortex (area 4) and bears about 10,000 spines. Each spine forms a Type 1 (see later and Chap. 1) synapse with a presynaptic bouton. Thus, simply counting spines gives a lower limit on the number of Type 1 synapses. However, because not all type 1 synapses are formed on spines, the degree of underestimation can only be determined by quantitative electron microscopy of the dendrites of identified neurons. Due to this methodological bottleneck, accurate estimates of the number and positions of synapses onto particular neuronal types are, unfortunately, extremely rare.

Modern electron microscopic and immunochemical techniques have been used to determine the proportion of the different types in the different regions of cortex. These studies have shown that although the different types may be differentially distributed between laminae within a single cortical area, the overall proportions of a given neuronal type remain approximately constant between different areas. The pyramidal neurons form about 70% of the neurons (Sloper et al., 1979; Powell, 1981) and the smooth cells form about 20% of the neurons (Gabbott and Somogyi, 1986) in all cortical areas. These morphological differences in the dendritic structure are only one of many differences between these two basic types. For example, the spiny neurons are excitatory, whereas the smooth neurons are inhibitory. Spiny neurons use quite different neurotransmitters from smooth neurons; their respective synapses are associated with a quite different set of receptors, and this is reflected in the morphology of the synapses.

SPINY NEURONS

Spiny neurons are called such because their dendrites bear small processes called *spines*. Spines are usually club-shaped, with a head of about 1 μm diameter and a shaft or “neck” of about 0.1 μm diameter (see electron micrograph in Fig. 1.7). The length of the neck varies greatly, from virtually nothing as in “stubby” spines, in which the head attaches directly to the dendritic shaft, to necks that are several micrometers long (Jones and Powell, 1969). At the high magnifications achieved with the electron microscope, spines can be distinguished from other dendritic elements in the neuropil by the presence of a characteristic “spine apparatus,” composed of calcium-binding proteins, and this has been an important marker for spines in quantitative electron microscopic studies (cf., for example, Chap. 7, Fig. 7.5A).

Spiny neurons are usually defined according to the lamina in which their soma is located. However, many types can be distinguished on the basis of their dendritic morphology. The clearest distinction is that some spiny neurons have an apical dendrite (pyramidal neurons) and some do not (spiny stellate cells).

Pyramidal Neurons. The major subtype of spiny neuron is the pyramidal neurons (Figs. 12.4 and 12.5), which constitute about two-thirds of the neurons in the neocortex. Pyra-



Fig. 12.4. Pyramidal neuron of layer 3. Note characteristic apical dendrite extending to layer 1. Many collateral branches arise from the main axon before it leaves the cortex. Labeled intracellularly *in vivo* with horseradish peroxidase. Cortical layers are as indicated. Bars = 100 μm .

midal neurons are found in all cortical layers except layer 1. Their most prominent feature is an apical dendrite that may extend through all the layers of the cortex above the soma. Pyramidal cells are the major output neurons of the neocortex. They participate both in connections between the different cortical areas and to subcortical structures such as the thalamus and superior colliculus. However, they are also a major provider of excitatory input to the area in which they are found: each pyramidal neuron has a rich collateral network that forms part of the local cortical circuitry.

Many subgroups of the pyramidal neurons can be distinguished on the basis of their morphology or functional characteristics, and in each layer pyramidal neurons can be found whose morphology and axonal projections are exclusive to that layer. For example, in layer 4, Lorente de No identified “star” pyramids, which are so-called because of their symmetrical and radially orientated basal dendrites. The most prominent pyramidal neurons in the neocortex are the Betz cells of area 4, the “motor” cortex. The Betz cells are very large pyramidal neurons located in layer 5 (see Fig. 12.5). Their axons form part of the pyramidal tract that descends to the spinal cord. The primary visual cortex also has a distinct set of exceptionally large pyramidal neurons, called the *solitary cells of Meynert*. These pyramidal neurons, which are found in the deep layers (5 or 6 depending on the species), project to other cortical areas and down to the midbrain structures such as the superior colliculus and the pons.



Fig. 12.5. Pyramidal neuron of layer 5. Note the very rich axon collateral arbor in the superficial layers. This neuron did not project out of area 17. Labeled intracellularly *in vivo* with horseradish peroxidase. Cortical layers are as indicated. Bars = 100 μm .

Within layer 5 in the visual cortex, two distinct types of pyramidal cells have been distinguished on the basis of a correlated structure–function relationship. One type has a thick apical dendrite that ascends to layer 1, where it forms a terminal tuft. These neurons have a bursting discharge of action potentials in response to a depolarizing current. The other type has a regular discharge, and their apical dendrite is thin and terminates without branching in layer 2 (Chagnac-Amitai et al., 1990; Mason and Larkman, 1990). This observation has led to theoretical work suggesting that the shape of the dendritic tree itself is a major factor in controlling the pattern of spike output from the neurons (Mainen and Sejnowski, 1996). Of course, the distribution of ion channels over the surface of the neuronal membrane also is a significant factor in determining the biophysical responses of the neuron, especially in the case of the tufted layer 5 pyramidal neuron (see later).

Pyramidal neurons can also be distinguished by their extra-areal efferent connections. For example, the thin untufted pyramids of layer 5 tend to project to the opposite hemisphere, whereas the thick tufted pyramids provide most of the output to subcortical areas. The thick tufted pyramids can be further subdivided according to the precise subcortical structure to which they project (Rumberger et al., 1998).

Spiny Stellate Neurons. A second group of spiny neurons, the spiny stellate neurons (Fig. 12.6, are found exclusively in layer 4 of the granular cortex (Cajal 1911). These



Fig. 12.6. Spiny stellate neurons of layer 4 from cat visual cortex. Labeled intracellularly *in vivo* with horseradish peroxidase. Cortical layers are as indicated. Bars = 100 μm .

also have spiny dendrites, but they do not have the apical dendrite that is characteristic of the pyramidal neurons. Instead, dendrites of approximately equal lengths radiate out from the soma and give these neurons a star-like appearance—hence their name. Occasionally, these neurons project to other areas, but most have axonal projections confined to the area in which they occur. It has been proposed that these neurons are simply pyramidal neurons without an apical dendrite. However, they differ in a number of important respects from pyramidal neurons, e.g., they have much lower spine densities and many more excitatory synapses on their dendritic tree. They should be considered as a distinct cell type confined to layer 4 of sensory cortex. Previously, the spiny stellate cells were thought to be the sole recipients of the thalamic input to the sensory cortices, but it is clear that although they probably are the major recipient, thalamic neurons also connect to the pyramidal neurons and smooth cells (Hersch and White, 1981; Hornung and Garey, 1981; Freund et al., 1985; Ahmed et al., 1994).

SMOOTH NEURONS

The class of neurons with spine-free dendrites is frequently referred to as smooth stellates, but because their dendritic morphology is rarely stellate, a more accurate term is simply *smooth neurons*. They tend to have elongated dendritic trees, in both the radial and the tangential dimension. Their dendritic morphologies have been described as multipolar, bipolar, bitufted, and stellate, but the most useful discriminator of the different types has been the axonal arbor. At least 19 different types of smooth neurons

have been described (Szentágothai, 1978; Peters and Regidor, 1981). These smooth neurons do not just have morphologically distinct axonal arbors; they also form quite specific synaptic connections, as described later.

The most prominent smooth neuron is the cortical *basket cell*, which was first described by Ramón y Cajal. As with basket cells in the cerebellum (see Chap. 7) and hippocampus (see Chap. 11), the convergence of multiple axons of the basket cells forms nests or baskets around the somata of their targets, usually pyramidal cells. Modern studies, however, have shown that basket cell boutons form most of their synapses on the dendrites and spines of pyramidal neurons. In superficial and deep layers, the main feature of the basket cell axonal arborization is the lateral extension of the axon (Fig. 12.7). However, deep basket cells often also have an arborization in the superficial layers vertically above their soma (Kisvárdy et al., 1987). Similarly, superficial basket cells can have an arborization in deep layers beneath their soma.

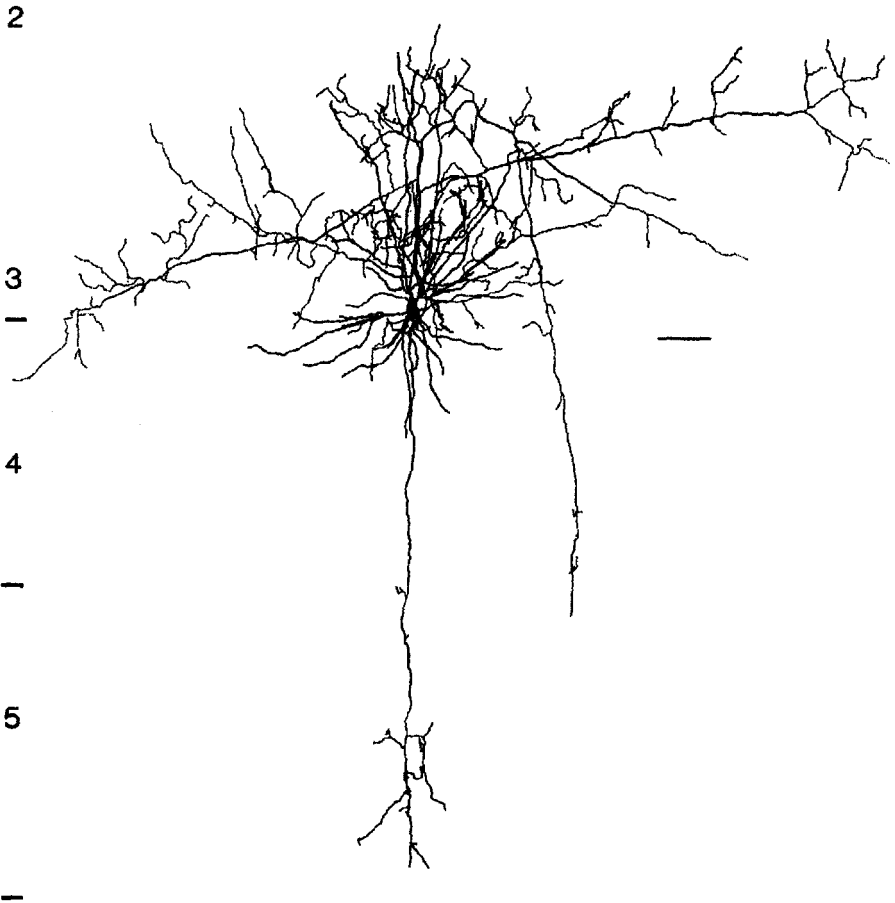


Fig. 12.7. Large basket smooth neuron from cat visual cortex. Cortical layers are as indicated. Bar = 100 μm .

In the middle layers, the basket cells have much more compact axonal arbors (Fig. 12.8). As with the well-studied pattern of thalamic afferents to the visual cortex (see later), which underlie the functional ocular dominance columns, these differences in the axonal arborizations most probably relate to the functional architecture of the piece of cortex in which they are located.

As with the spiny cells, some morphological types of smooth neurons are found only in particular layers. Layer 1, for example, has two types that are not found in other lay-

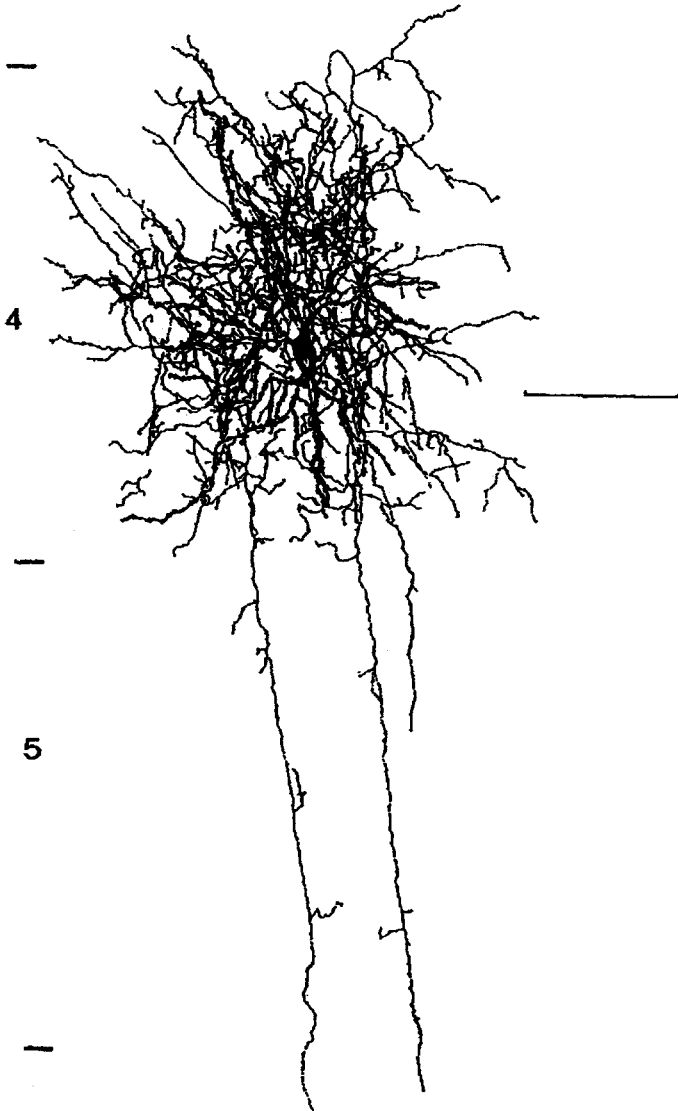


Fig. 12.8. Small basket smooth neuron from layer 4 of cat visual cortex. The major portion of the axon arbor is confined to layer 4. Cortical layers are as indicated. Bar = 100 μm .

ers: the *Retzius-Cajal neuron*, which has a horizontally elongated dendritic tree, and the *small neuron of layer 1*, which has a highly localized dendritic and axonal arbor. Many of the smooth types have descending or ascending axon collaterals in addition to their lateral extensions. Most notable of these is the *double bouquet cell* of Ramón y Cajal (Fig. 12.9), which is characterized by elongated dendrites extending radially above and below the somata and an axon that forms a cascade of vertically oriented collaterals. Another neuron with a vertical organization is the *Martinotti cell*. Originally, the Martinotti cell was described as a multipolar or bitufted neuron, with compact dendrite, that is located mainly in the deep cortical layers and whose defining axon arose from the upper

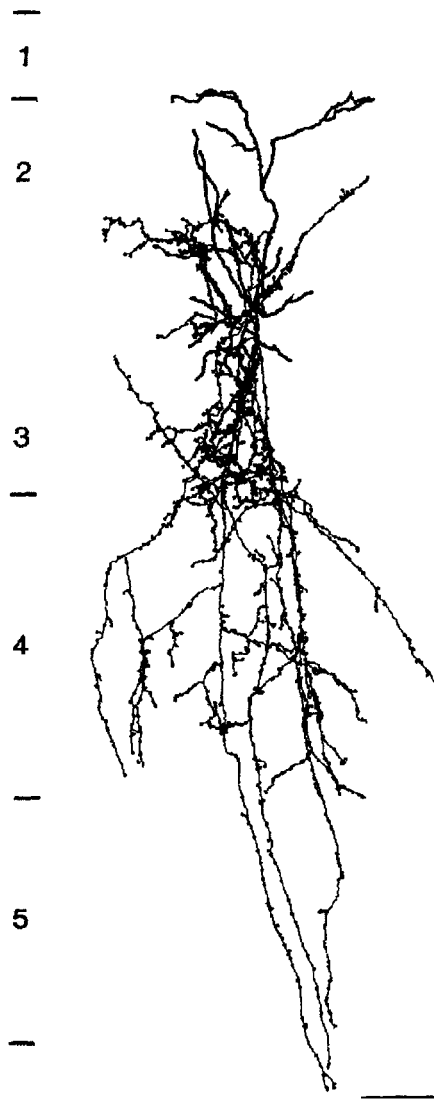


Fig. 12.9. Double bouquet smooth neuron from layer 4 of cat visual cortex. The axon collaterals run vertically. Cortical layers are as indicated. Bar = 100 μm .

cell body or dendrites and ran vertically to layer 1, where it arborized (Faireñ et al., 1984). More recently, the arborization is thought to span all layers (Faireñ et al., 1984; Wahle, 1993). Martinotti cells are frequently observed in immature animals, but many degenerate during the early early postnatal period (Wahle, 1993).

Perhaps the most evocative description of a smooth cell was given by Szentágothai to the *chandelier cell*, so-named because its axonal boutons are arranged in a series of vertical “candles” that give the whole axonal arborization the appearance of a chandelier (Fig. 12.10).

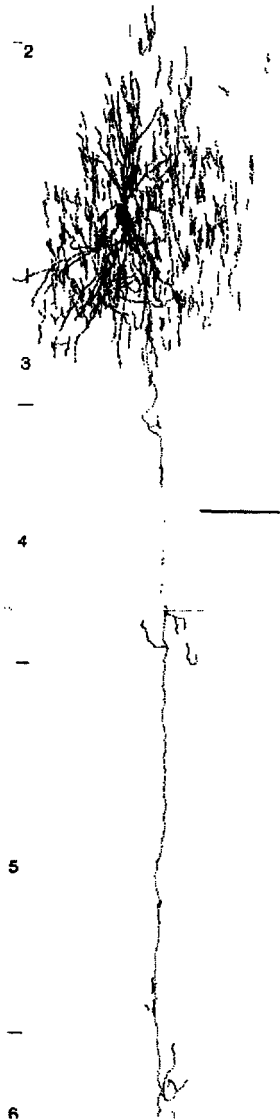


Fig. 12.10. Chandelier smooth neuron from cat visual cortex. Cortical layers are as indicated. Bar = 100 μm .

Histochemical methods have revealed the existence of an additional smooth neuronal type, which is sparse in the gray matter but forms a distinct monolayer at the border of the gray and white matter. These neurons stain positively for the enzyme NADPH-diaphorase, which is a synthetic enzyme for nitric oxide gas. Although they are few in number, their axonal ramifications are immense and provide a rich plexus of axons throughout the gray matter.

There is a striking variety of smooth neuron morphological types by comparison with stellate neurons (Wang et al., 2002). The functional significance of this difference is not clear. However, the various types do show some preference for forming synapses on particular regions of their postsynaptic targets. Some types target the proximal soma and dendrite (e.g., basket cells), mid-field dendrites (e.g., bitufted, double bouquet, bipolar, neurogliaform), and distal dendritic inhibition (e.g., Martinotti cells), yet others target the axon initial segment (e.g., chandelier cells). This distinction in target regions suggests that the various inhibitory cell types might participate in different functional subsystems. For example, distal inhibition could influence local dendritic integration and modulate local synaptic modification for learning; more proximal inhibition is well placed to control overall neuronal signal gain and thresholding, and inhibition of the axon initial segment could affect the detailed timing of action potentials. Similar considerations apply to a variety of inhibitory interneurons in other regions (see especially hippocampus, Chap. 11).

AFFERENTS

Thalamus. The thalamus projects to all cortical areas and provides input to most layers of the cortex. The densest projections are to the middle layers, where they form about 5%–10% of the synapses in those layers (LeVay and Gilbert, 1976; White, 1989; Ahmed et al., 1994). The main feature of this input is that it is highly ordered. The sensory inputs are represented centrally in a way that their topographic arrangement in the periphery is preserved. This mapping is achieved by preserving the nearest-neighbor relationships of the arrangements of the sensory or motor elements in the periphery. Such topographic projections are a ubiquitous feature of the cortex. The precision of the mapping does vary between areas, however. The primary sensory and motor areas usually preserve the highest detail of the topography, which degrades progressively through secondary and tertiary and higher order areas of cortex.

An important transform in the topography from the periphery to the center is that the regions of highest sensory receptor density have the largest representation in the cortex. This transformation is described as the *magnification factor* of the projection (Daniel and Whitteridge, 1961). In the visual system of the primate, the fovea of the retina contains the highest density of photoreceptors, and the primary visual cortex represents this by devoting cortex in the ratio of 30 mm/degree of visual field to this representation. In the far periphery of the visual field, the ratio falls off to about 0.01 mm/degree of visual field. In the somatosensory system, the hand and face have high densities of touch receptors, and these parts have a magnified representation in the primary somatosensory cortex. One of the most remarkable cortical representations is that of the whiskers of rats and mice. Each whisker has a separate representation in the cortex, which has a barrel-like form when viewed in a tangential section of the somatosensory cortex (Woolsey and Van der Loos, 1970). The centers of the barrels are

formed by clusters of thalamic afferents that convey input from each whisker. The cortical map of the whiskers forms a representation that is topologically equivalent to the arrangement of whiskers on the face of the rat or mouse. This whisker map dominates the representation of the sensory surface of the rodent.

In the cat visual cortex, the terminal arbors of each individual thalamic afferent may extend over 1–5 mm of the cortical surface (Fig. 12.11) so that each point in layer 4 is covered by the arbors of at least 1000 separate thalamic relay cells. Thus, the dendritic tree of an average layer 4 neuron, which extends for 200–300 μm , could receive input from many more thalamic afferents. However, the connections are not made randomly between the geniculate afferents and the cortical neurons. Selectivity is expressed in several ways. For example, there is a high degree of precision in the visuotopic map recorded in the first-order cortical neurons in the input layer, i.e., those receiving monosynaptic activation by the thalamic afferents. This clustering is made according to the eye preference of the arbors. The afferents of those thalamic relay neurons that are driven by the right eye cluster together in regions about 0.5 mm in diameter and are partially segregated from the afferents that are driven by the left eye. This segregation forms the basis of ocular dominance columns. In addition, there is some clustering of the afferents according to whether they are ON or OFF center. This clustering of inputs forms the basis of the ON and OFF subfields of the simple cells. In the somato-

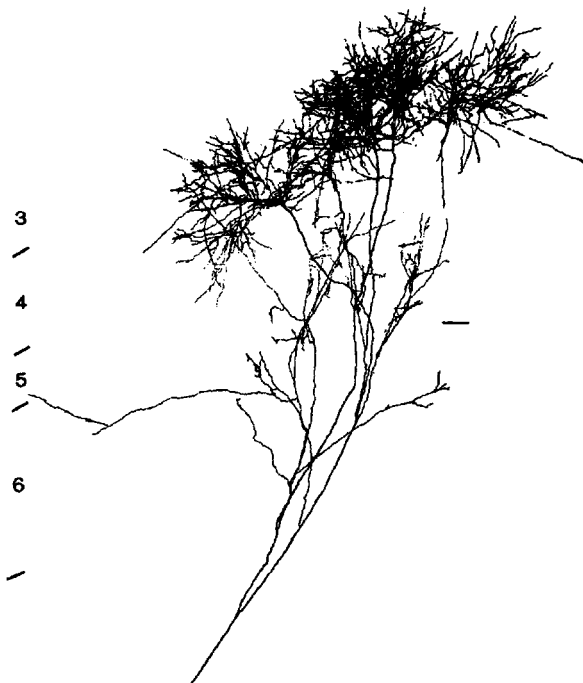


Fig. 12.11. Y-type thalamic afferent from cat visual cortex. Note extensive but patchy arbor in layer 4. This axon formed over 8000 boutons. Labeled intracellularly *in vivo* with horseradish peroxidase. Cortical layers are as indicated. Bars = 100 μm .

sensory pathway, there are segregations according to the modality of the sensory information, e.g., light touch is segregated from deep pressure, and so on.

Other Subcortical Regions. Although the thalamus is a major source of input to the neocortex, it is not the only one. More than 20 different subcortical structures projecting to the neocortex have been identified (Tigges and Tigges, 1985). These structures include the claustrum, locus coeruleus, basal forebrain, the dorsal and median raphe, and the pontine reticular system. As has been pointed out in other chapters, these pathways have distinct neurochemical signatures, which has made the analysis of their cortical targets more tractable. The contributions of these different pathways vary from one cortical area to the next and among species for a homologous cortical area. There are also wide differences in the laminar projections of the terminals of these neurons between areas, and in very few cases have the synaptic targets of these projections been identified. Thus, it is as yet not possible to offer a simple schematic of these pathways, but there are a few whose role in plasticity and development have been examined.

Monoamines. Because of their relative ease of identification, the monoaminergic innervation of the cerebral cortex has been studied most intensively. These systems are generally thought to be diffuse and nonspecific, both in terms of the information they carry and in terms of their lack of spatial specificity and anatomical organization. Physiological examinations of these neurons are rare, but closer examinations of the anatomy have generally revealed a higher degree of specificity (Parnevelas and Papadopoulos, 1989). Three main types of monoamine-containing cortical afferents have been described: the dopamine-positive axons arising from the rostral mesencephalon, the axons containing norepinephrine (also called noradrenaline) originating from the locus coeruleus, and the serotonin (5-hydroxytryptamine [5-HT]) axons that originate from the mesencephalic raphe nuclei. There has been some doubt as to the mode of release of the transmitter, because early studies failed to find clear ultrastructural evidence of synapses. This was consistent with an older concept of the brain as a complex neuroendocrine organ where neurosecretion was the means by which brain activity was modulated. However, it is now clear that monoaminergic axons in the neocortex do form conventional synapses and can show a high degree of anatomical specificity, both for particular cortical areas and for particular laminae within a single cortical area.

Norepinephrine (Noradrenaline). The projections of the locus coeruleus, which lies in the dorsal pons, have been relatively well studied. The nucleus is small, but it projects to most of the neocortex in a roughly topographic arrangement (Waterhouse et al., 1983). Neurons in the dorsal portion project to posterior regions of the neocortex, such as the visual regions, whereas neurons in the ventral portion project to frontal cortical areas. In primates, the strongest projections are to the primary motor and somatosensory cortices and their related association areas in frontal and parietal lobes (Tigges and Tigges, 1985). The fine, unmyelinated axons ramify horizontally, most prominently in layer 6, and form synapses with spine shafts and somata (Papadopoulos et al., 1987). The neurons synthesize norepinephrine, which is thought to be involved in the development and plasticity of thalamocortical projections in the visual cortex. These fibers develop early, and their removal by neurotoxins prevents plasticity of the columns

formed by the thalamic afferents arbors driven by left and right eye (Pettigrew, 1982; Daw et al., 1983). Activity in locus coeruleus neurons correlate with changes in the EEG, which suggests that it is involved in the arousal response induced by sensory stimuli.

Serotonin. The raphe nuclei and pontine reticular formation are a complex of nuclei that contain the highest density of neurons that synthesize serotonin. These neurons project to all cortical areas with varying degrees of laminar specificity (Tigges and Tigges, 1985; Mulligan and Tork, 1988). There are clear differences between projections to the homologous areas in different species that make generalizations impossible, e.g., the strongest projections in the monkey are to the thalamorecipient layers of area 17, whereas these layers are relatively poorly innervated in the adult cat. In the kitten, however, there is a transient surge of serotonergic innervation of the thalamorecipient layer 4, which may indicate a relationship to the critical period (Gu et al., 1990).

Dopamine. The third monoamine projection to cortex is the dopaminergic pathway. It has been suggested that a dysfunction of the dopaminergic innervation of the prefrontal cortex is one of the factors in the pathogenesis of schizophrenia. The dopaminergic projection to the frontal cortex originates from ventral tegmental area, the rostral mesencephalic groups, and the nucleus linearis. They form symmetrical synapses with the dendrites of pyramidal neurons and with GABAergic smooth neurons. All layers except layer 4 receive dopaminergic input. Dopaminergic projections are strongest to the rostral cortical areas, especially the prefrontal cortex. Here, they target pyramidal neurons, particularly spines, which they share with an excitatory synapse (Goldman-Rakic et al., 2000).

Acetylcholine. Although there are intrinsic sources of acetylcholine (ACh) from neurons within the cortex, the major sources of the cholinergic fibers in the cortex are extrinsic. These fibers originate from the nucleus basalis of Meynert and the diagonal band of Broca, which constitute the nuclei of the basal forebrain. These cholinergic projections to the neocortex have been of particular interest because of their possible involvement in the pathology of Alzheimer's disease. The terminals of the acetylcholinergic fibers distribute through all cortical layers, with the most dense innervation in layer 1 and relatively sparse innervation of the deep layers (De Lima and Singer, 1986; Aoki and Kabak, 1992). They form synapses with dendritic shaft and spines but show some bias for the GABAergic neurons.

GABA. Although it was previously thought that all GABAergic synapses were derived from intrinsic sources in the cortex, it has been demonstrated that there are GABAergic projections from subcortical nuclei to the cortex. These afferents arise from the basal forebrain, the ventral tegmental area, and the zona incerta. The GABAergic neurons of the zona incerta project to sensory and motor cortex but not to the frontal cortex. As with the acetylcholinergic fibers from the same source, the GABAergic neurons of the visual cortex are a major target of the GABAergic afferents of the basal forebrain (Beaulieu and Somogyi, 1991).

Clastrum. The claustrum is also a nucleus of the basal forebrain. It connects reciprocally and topographically with the cerebral cortex (LeVay and Sherk, 1981; Tigges and Tigges, 1985). However, the reciprocal connections do not form a single continuous map but are segregated into function-specific divisions. Thus, the claustrum is not strictly multimodal, although it contains representations of visual, auditory, somatosensory, limbic, and perhaps motor functions. These functions are represented separately in the nuclear mass of the claustrum, and there is no evidence of integration of the different modalities. In this respect, the claustrum follows the principle of separate representation of these modalities adopted by the neocortex and thalamus. In the case of the visual system, it is clear that many, perhaps all, of the retinotopically organized visual areas converge on the claustrum, and it in turn projects divergently back to them. In the primary visual cortex the projection to the claustrum arises from a subset of the layer 6 pyramidal neurons. The claustrum sends a sparse projection back to all layers of visual cortex, where it forms excitatory connections mainly with the spines of excitatory neurons, except in layer 4, where synapses with dendritic shafts form about half the targets (LeVay and Sherk, 1981).

Corticocortical Connections. Although anatomists have emphasized the long fiber tracts between the neocortex and their subcortical targets and suppliers, the major input to any cortical area is from other cortical areas. Braitenberg and Schüz (1991) have calculated that only 1 in 100 or even 1000 fibers in the white matter is involved in subcortical projection; the majority of the fibers in the white matter are involved in the intrahemispheric connections and interhemispheric connections. Since the 1980s, these connections have been intensively studied, particularly in the primate visual cortex. The pattern that has emerged is that the pyramidal neurons of the superficial layers project to the middle layers (principally layer 4) of their cortical target area, whereas the deep layer pyramids project outside the middle layers to superficial and deep layers. These patterns have been used to classify connections as feedforward (projecting to layer 4) or feedback (projecting outside layer 4) (Felleman and Van Essen, 1991). All cortical areas are reciprocally connected by these “feedforward” and “feedback” pathways. In the face of multiple parallel pathways projecting to and from cortical and subcortical areas, such simple classifications of feedforward and feedback may not translate into functional significance. However, it is clear that the substantial majority of the neuronal targets of these corticocortical connections are pyramidal neurons.

CONSIDERATIONS OF CORTICAL WIRING

One of the most important principles of a cortical circuit is the need to save “wire,” i.e., to reduce the length of the axons that interconnect neurons (Mead, 1990; Mitchison, 1992). The dimensions of this problem are evident in the statistics of the amount of wire involved. Each cubic millimeter of white matter contains about 9 m of axon, and an equal volume of gray matter contains about 3 km of axon. The volume occupied by axons would be greatly increased if each neuron had to connect to every other neuron in a given area or if every neuron were involved in long distance connections between cortical areas. Instead, the design principles of cortex are that neurons are sparsely connected, that most connections are local, and that only restricted subsets of neurons are involved in long distance connections.

The constraint on volume can also lead to multiple cortical areas. If separate areas are fused into a single area that preserves the total cortical thickness of 2 mm, then the components of the original areas must spread over a larger area (Mitchison, 1992). The original connections between neurons now have to span larger distances and so contribute to a larger volume for the same number of neurons. Mitchison has shown that fusing 100 cortical areas leads to a 10-fold increase in the cortical volume. Of course, if all the cortical areas are fused into one area, then much of the white matter can be eliminated. However, the increase in the volume of the *intra*-areal axons far exceeds the reduction of the *interareal* axons. Similar arguments can be raised for the patchiness of connections within a cortical area that are a cardinal feature of cortical organization. A given cluster of neurons projects to a number of sites within a given cortical area. These clusters tend to link areas of common functional properties. The size of the clusters—about 400 μm —is remarkably uniform between cortical areas. This size is similar to the spread of the dendritic arbor. Malach (1992) has shown theoretically that such an organization increased the diversity of sampling across a cortical area that has a nonuniform distribution of functional properties.

SYNAPTIC CONNECTIONS

TYPES

As discussed in Chap. 1, there are two basic types of synapses in the neocortex, which Gray called type 1 and type 2 (Gray, 1959). The synapses made by the vast majority of the cortical spiny neurons and by some of the subcortical projections such as the thalamic and claustral afferents are type 1. Type 2 synapses are made by smooth neurons and some of the subcortical projections such as the noradrenergic fibers.

Both types of synapses are found throughout the cortex in approximately constant proportions. In each cubic millimeter of neocortex, there are 2.78×10^8 synapses, of which 84% are type 1 and 16% are type 2 synapses (Beaulieu and Colonnier, 1985). Both types are found on all cortical neurons, but their locations on the dendritic trees of the different types differ (see Fig. 12.12; Gray, 1959; Szentágothai, 1978; White and Rock, 1980; Beaulieu and Colonnier, 1985; White, 1989). Pyramidal neurons receive few type 1 synapses on their dendritic shafts and none at all on their somata or initial segment of the axon. Conversely, type 2 synapses are found on the proximal dendritic shafts, on the somata, and on the axon initial segment of pyramidal cells. Nearly every spine of pyramidal neurons forms a type 1 synapse, but only about 7% of spines form an additional type 2 synapse. Similar distributions have been reported for the spiny stellate cells of the mouse somatosensory cortex, but the pattern for the spiny stellate cells in layer 4 of the primary visual cortex is different. About 60% of the type 1 synapses are formed with the proximal and distal dendritic shafts; the remainder are formed on the heads of the dendritic spines. Type 2 synapses are found on the somata, but synapses are rarely found on the axon initial segment. Although the type 2 synapses are clustered in higher density on the proximal dendrites, about 40% of the type 2 synapses are on distal portions of the dendrites (i.e., more than 50 μm from the soma).

The smooth neurons by definition do not bear spines, so both type 1 and type 2 synapses are formed on the beaded dendrites that are a characteristic feature of smooth neurons (Fig. 12.13). The beads themselves are the sites of clusters of synaptic inputs.

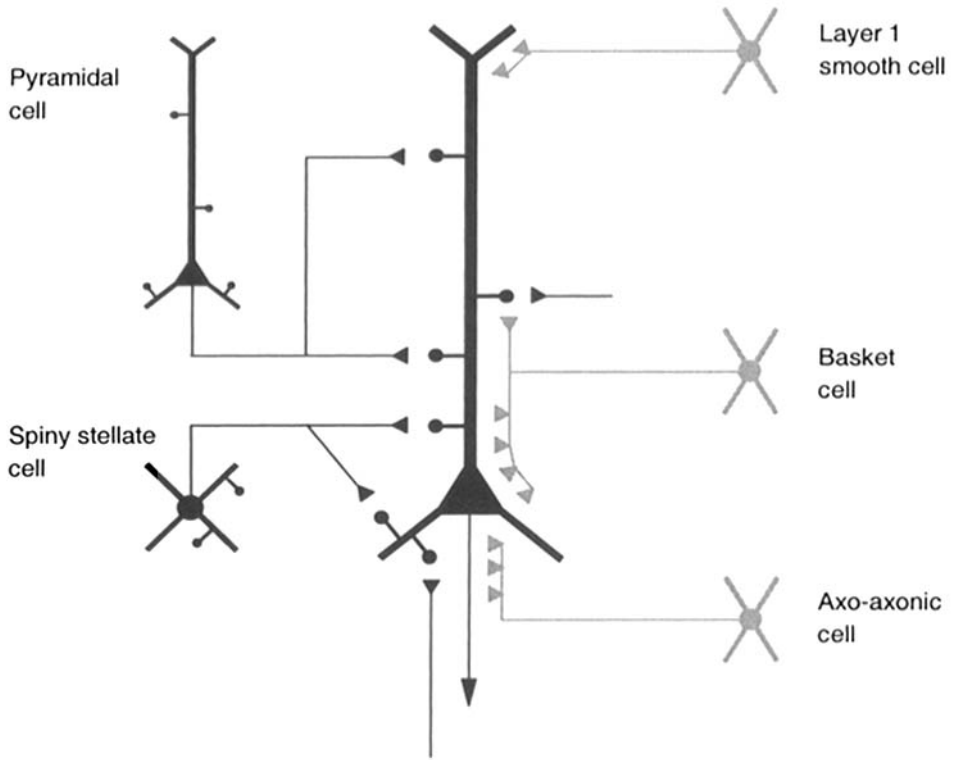


Fig. 12.12. Synaptic connections in neocortex. Configurations of excitatory and inhibitory connections made onto a typical pyramidal neuron. The excitatory (spiny) cells (black, left) and thalamic afferents (black, bottom) form synapses with the spines of the target pyramidal neuron. Layer 6 pyramidal neurons (not shown) are the exception to this rule. They form synapses mainly with the dendritic shafts of target spiny cells. There are a number of different classes of inhibitory (smooth) cells (gray, right), each with a characteristic pattern of connection to the pyramidal neuron. Examples of three of the many classes of inhibitory neurons are shown. Each inhibitory cell makes multiple contacts with its target. The superficial smooth cell forms synapses with the apical tuft. The basket cell forms synapses with the soma, dendritic trunk, and dendritic spines. The chandelier cell forms synapses with the initial segment of the axon.

The pattern of input to the smooth neurons is quite different from that of the spiny neurons: both types of synapses cluster on the proximal dendrites and somata at about 2–3 times the density found for spiny dendrites. The type 2 synapses are rarely found on the distal regions of the dendritic tree, and the density of type 1 synapses on the distal dendrites is less than that on the proximal dendrites. The initial segment of the axon of smooth neurons does not form synapses.

Gap junctions have been observed between smooth neurons in an electron microscope study of primate neocortex (Sloper, 1972). Later electrophysiological studies established that there are electrical synapses in the neocortex created by low-resistance pathways, or gap junctions, between dendrites or between dendrites and somata of particular GABAergic neurons, which contain parvalbumin or somatostatin (Galarreta and



Fig. 12.13. Reconstruction of serial electron microscopic sections showing the complete synaptic input to the dendrite of a small basket cell (top) and the proximal dendrite of a spiny stellate cell (bottom). The leftmost end is connected to the cell body. Both were located in layer 4 of cat visual cortex. The dark shapes are presynaptic boutons that formed asymmetrical (excitatory) synapses, and the open shapes indicate boutons that formed symmetrical (inhibitory) synapses. Scale bar is 10 μm .

Hestrin, 2001). These voltage-dependent gap junctions are formed by a class of proteins called *connexins*. The electrical synapses act as low pass filters. However, because spikes are transmitted through the gap junctions, a spike in one neuron can lead to a fast depolarization in coupled cells, thus providing a means of synchronizing a network of GABAergic neurons (Galarreta and Hestrin, 1999; Gibson et al., 1999). This interpretation is supported by experiments showing that electrical coupling is virtually absent when connexin36 was knocked out, leading to a reduction in gamma frequency synchronization (Gibson et al., 2001).

SPINY NEURONS

The axons of the spiny neurons form the vast majority of the synapses in the cortex. The synapses they form are type 1 in morphology, and almost all are on spines (80%–90% of targets) (Sloper and Powell, 1979a; Martin, 1988). One type of spiny neuron, a layer 6 pyramidal neuron, is the exception to this general rule: it forms most of its synapses preferentially with the shafts of spiny neurons in layer 4 (see White, 1989). The axonal boutons come in two basic types. One is like a bead on the axon; these are called *en passant* boutons. The other bouton looks like a small drumstick and in appearance and dimension closely resembles a dendritic spine. These are called boutons *terminaux*. Some synapses of the spiny stellate or pyramidal neurons are formed with dendrites or somata of smooth neurons, but these constitute only about 10% of their output. A feature of the output of the spiny neurons is that they contribute only a few synapses to any individual postsynaptic target. Conversely, any single neuron must receive its excitatory input from the convergence of many thousands of neurons, most of which are in the same cortical area. The thalamic afferents, which provide the principal sensory input to cortex, form about 10% or less of the synapses in layer 4, the main thalamorecipient layer (White, 1989; Ahmed et al., 1994) (Fig. 12.14).

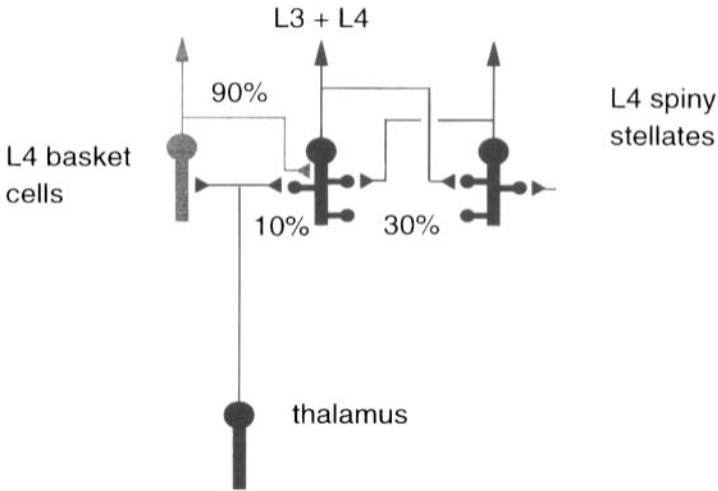


Fig. 12.14. Fractions of synaptic connections onto spiny stellate neurons in layer 4 of cat striate cortex. [From Ahmed et al., 1994.] Only about 10% of the excitatory synapses are derived from the lateral geniculate nucleus. Thirty percent arise from other spiny stellate neurons in layer 4, and an additional 40% arise from the layer 6 pyramidal neurons (not shown). Ninety percent of the inhibitory inputs arise from layer 4 GABAergic neurons, like the basket cells (gray).

SMOOTH NEURONS

The synaptic connections of the smooth neurons differ in a number of significant respects from the spiny neurons. Their axons are less extensive than the spiny neurons, and they make multiple synapses on their targets. This means they contact many fewer targets on average than do spiny neurons. Although the spiny neurons generally form synapses with dendritic spines and shafts, the smooth neurons target these and the soma and axon initial segment. In addition, different smooth neuron types form synapses specifically with different portions of the neuron (see Fig. 12.12). The major output of the smooth neurons, however, is to spiny neurons. The smooth neurons form no more than 15% of the targets of the spiny neurons.

These neurons again fall into several characteristic classes: large basket cells, small basket cells (clutch cells), chandelier cells, double bouquet cells, bipolar cells, neuroglialform cells, Martinotti cells, and Cajal Retzius cells. Smooth neurons use GABA as a transmitter and hence act to inhibit those neurons to which they connect.

Basket cells (see Fig. 12.7) are the most frequently encountered smooth neuron in Golgi preparations and in intracellular physiological studies *in vivo*. Kisvárdy (1992) has estimated that they form at least 20% of all GABAergic neurons. They have a very characteristic axon that forms the most extensive lateral connections of any of the smooth cell types. The basket cells of the superficial and deep layers have axons that radiate from the soma up to distances of 1–2 mm. In layer 4, the small basket cell (see Fig. 12.8) axon is more localized and extends about 0.5 mm laterally in most cases (Mates and Lund, 1983; Kisvárdy et al., 1985). Each basket cell forms multiple synapses with about 300–500 target neurons and makes about 10 synapses on average

with each target. Ramón y Cajal originally provided the descriptive name *basket cells* because in the Golgi preparations the axons of the basket cells form pericellular *nests*, or baskets, around the soma of the pyramidal neurons (Cajal, 1911). Modern light and electron microscopic studies on the axonal boutons of intracellularly labeled basket cells has revealed, as noted earlier, that the major targets of the basket cell axons are the dendritic shafts and spines of pyramidal and spiny stellate cells (Somogyi et al., 1983; Kisvárdy, 1992). The “basket” seen by Ramón y Cajal is formed by the convergence of about 10–30 basket cells, each contributing a twiglet to the perisomatic nest. Superficial and deep basket cells and clutch cells make about 20%–40% of their synapses with spines, 20%–40% with dendritic shafts, and the remainder with somata.

Chandelier cells (see Fig. 12.10) are rarely encountered in Golgi preparation and in intracellular recordings *in vitro* and *in vivo*. However, they have been a focus of interest because their sole output is to the initial segment of the axons of pyramidal neurons. Such specificity is not seen with any other neocortical cell, although it is common elsewhere in the brain (see earlier chapters). The chandelier cells seem to be found only in the superficial layers and layer 4, but some have a descending axon collateral that innervates the deep layer pyramidal neurons. Correspondingly, electron microscopic examination of the initial segments of the pyramidal neurons has indicated that there are about 3 times as many synapses along the initial segment of the axon of superficial layer pyramidal neurons as in deep layer pyramidal cells (Somogyi, 1977; Sloper et al., 1979; Peters, 1984). In the superficial layers, the axon initial segment forms about 40 type 2 synapses with the boutons of the chandelier cell. Each pyramidal neuron receives input from three to five chandelier cells, and each chandelier cell forms synapses with about 300 pyramidal neurons over a surface of about 200–400 μm (Somogyi et al., 1982; Peters, 1984).

Double bouquet neurons (see Fig. 12.9) are smooth neurons that are found in the superficial layers and have a “bitufted” axonal system that spans several layers (Cajal, 1911; Somogyi and Cowey, 1981). In contrast to the laterally directed axons of the basket cell, the predominant orientation of the double bouquet cell’s axon is vertical. For this reason it was originally thought that the vertically oriented apical dendrites of the pyramidal neurons were the major target of multiple synapses from the pallisades of double bouquet axons. There is no clear evidence of multiple synapses between double bouquet axons and apical dendrites, but the pyramidal neurons are nevertheless major targets. In the cat, about 70% of the type 2 synapses of double bouquet cells are formed with dendritic spines, and most of the remainder are formed with dendritic shafts (Tamas et al., 1998).

The synaptic connections formed by the axons of layer 1 neurons have been studied rarely. The small neurons of layer 1 have as their major target the spines and dendritic shafts of pyramidal neurons apical dendritic tufts that form most of the neuropil of layer 1. The connections made by the Cajal-Retzius cells are unknown. Similarly, the connections made by other smooth neurons of the neocortex have yet to be determined.

Many GABAergic cells are immunoreactive to one or more of the calcium binding proteins parvalbumin, calbindin, and calretinin, as well as to neuropeptides such as cholecystokinin, somatostatin (SSt), vasoactive intestinal polypeptide (VIP), neuropeptide Y, and corticotropin-releasing factor (Demeulemeester et al., 1988, 1991). The profile of immunoreactivity expressed by a neuron depends on its laminar location and

morphological type. There is considerable overlap between cell types, and the profile also depends on the cortex's state of embryological development. Nevertheless, these provide a useful basis for the classification of smooth cell subtypes (Wang et al., 2002). Some spiny neurons also express immunoreactivity for calbindin, cholecystokinin, and SST. However, their reactivity for these molecules is weaker, particularly in more mature animals.

BASIC CIRCUIT

An article of faith among neuroanatomists from the beginning of the study of the cortical circuits was that there was an elementary pattern of cortical organization. Anatomists studying Golgi-stained material were generally convinced that there were structural details that remained constant despite variations in cell number, form, size, and type of neurons. This constant, according to Lorente de Nó, was the "arrangement of the plexuses of dendrites and axonal branches," by which he meant the synaptic connections between cortical neurons. However, subsequent examination of the details of cortical circuitry still leave considerable leeway in interpretation of the pattern of connections. Any attempt to suggest a common basic pattern of connections necessarily will be open to the criticism that such models are based on the intensive study of a very small number of areas, mainly primary sensory areas (White, 1989). Nevertheless, the great advantage of having some hypothetical circuit is that it focuses ideas and gives form to otherwise simply descriptive accounts of cells and connections within a given area that have been the standard works in the anatomical field.

Most modern models of cortical circuits are derived from functional studies. In contradistinction to the great diversity of cell types and interconnections that characterize the anatomical descriptions, the circuits derived from physiological experiments strip off all of the embellishment and detail: simple circuits of excitatory cells make up the core of these models. The Hubel-Wiesel models of the local circuits of visual cortex are the best known examples (Hubel and Wiesel, 1977). In these circuits, the inhibitory neurons are added as a means of providing the lateral inhibition that is such a feature of sensory processing at all levels. Two basic designs have emerged. In the dominant model, the processing is strictly serial: input arrives in the cortical circuit, it is fed forward through a short chain of two or three neurons within the local area, and then is transmitted to other areas by the output neurons. This feedforward model follows from the simple idea that sensory input must pass through several processing stages in the neocortex before it arrives at a motor output.

An alternative view was first given form by Lorente de Nó (1949). He supposed that the rich interconnections between the different cortical layers made the cortical circuit a unitary system, with no clear basis for a distinction between input, association, and output layers. In his view, impulses circulate through these recurrent circuits, and the activity in the cortical circuit is modified by the action of the association fibers arriving at critical points within the circuit. In turn, the effect of the incoming input depends on the activity in the circuit at that point in time.

Both the feedforward and the recurrent model agree, however, that the processing that occurs in the neocortex is essentially local and vertical. In this arrangement, the anatomy and the physiology agree. In most cortical areas, the function being repre-

sented is laid out topographically, as in the retinotopic maps of the visual cortex or the motor maps in the motor cortex. For example, portions of the sensory surface that will receive related input are nearest neighbors in their cortical representation. The vertical connectivity within the cortex is similarly local. The axons of cortical neurons do not extend more than a few millimeters laterally in any area; thus, the monosynaptic connections at least are local. This corresponds with the physiological findings of Mountcastle, Hubel, Wiesel, and others who discovered that neurons with similar functional properties are organized in “columns” that extend for the cortical surface to the white matter (Powell and Mountcastle, 1959; Hubel and Wiesel, 1977).

In fact, with few exceptions, most arrangements of neurons are only strictly columnar when viewed with the one-dimensional tool of the microelectrode. The clearest view arises from optical imaging in which the activity of large numbers of nerve cells can be viewed by optical imaging (Sengpiel and Bonhoeffer, 2002) and fMRI (Duong et al., 2001). Such imaging techniques have been used to show that in the lateral dimension, the different functional maps take the form of slabs or pinwheels. The widths of the slabs vary according to the particular property being mapped but are of the order of 0.5 mm in the case of the best-studied system—the ocular dominance system of the primary visual cortex. In this system, the afferents of the lateral geniculate nucleus representing the left and right eye map into a series of parallel slabs that look like a zebra’s stripes when viewed from the surface. Such segregation and patchiness are seen at the level of single axonal arbors and appear to be the means by which the cortex maps multiple processes into a single area. In the few cases in which it has been examined, the rule of connectivity between patches is that “like connects to like.” For example, a number of different functional dimensions are represented within the retinotopic map of the primary visual cortex of primates. These dimensions are seen physically in the ocular dominance, the orientation slabs, and the cytochrome oxidase columns, which are called *blobs* because of their appearance when viewed in tangentially cut sections of the cortex (Hendrickson et al., 1981; Horton and Hubel, 1981; Wong-Riley and Carroll, 1984). In each of these systems, neurons of like function interconnect.

CORTICAL OUTPUT

All projection neurons have recurrent collaterals that participate in local cortical circuits, so there are no layers that have exclusively output functions. The output neurons from the cortex are generally pyramidal neurons. These same cells, however, may also be *input* neurons in that they may receive direct input from the thalamus. There is a laminar-specific organization of the output according to the location of their targets. A simplified view of the laminar organization is provided in the summary diagram in Fig. 12.15. The general rule of thumb is that corticocortical connections arise mainly from the superficial cortical layers and the subcortical projections arise from the deep layers. Within the deep layers, there is an output to regions that have a motor-related function, e.g., the superior colliculus, basal ganglia, brainstem nuclei, and spinal cord. These regions receive their cortical output from a relatively small number of layer 5 pyramidal neurons. There is also an output to the subcortical relay nuclei in the thalamus, which are the source of the primary sensory input to the cortex. This corticothalamic projection generally arises from the layer 6 pyramidal neurons. However,

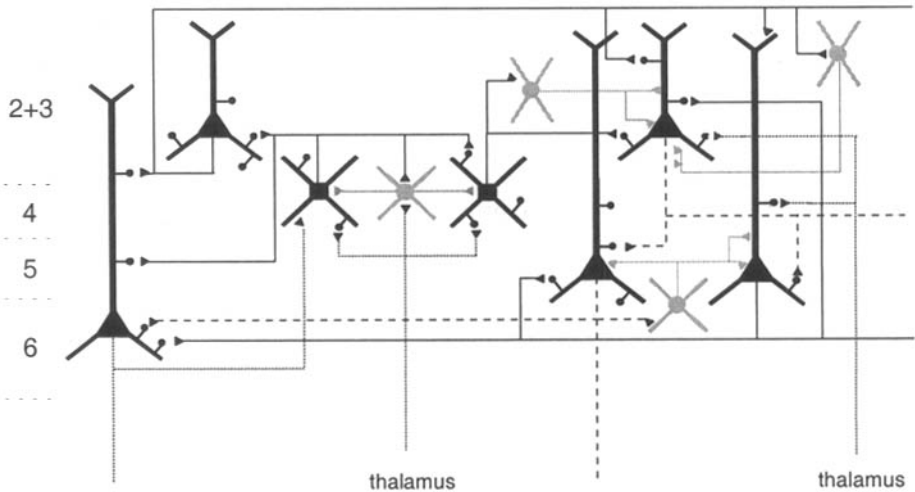


Fig. 12.15. Basic circuit for visual cortex. Smooth, GABAergic neurons and their connections are indicated in gray. Spiny neurons and their connections are indicated in black. Cortical layers as indicated.

there are clear exceptions to this rule of thumb. In area 4 the projections that form the pyramidal tract, which supplies the spinal cord and cerebellum, arise from both layer 5 and layer 3 pyramidal cells. The corticocortical connections may also arise from neurons in the deep layers. However, the simplifications are not extreme and offer a useful constraint on the connections that can be made within the basic circuits. For example, if a circuit in cat visual cortex requires an output to the eye-movement maps of the superior colliculus, then it necessarily will have to connect to the output pyramidal neurons of layer 5. Although particular laminae are the source of the outputs to these different cortical and subcortical regions, the set of output neurons within a given lamina may not be uniform. Thus, within layer 6, the pyramidal neurons that give rise to the corticothalamic projection are morphologically different from those that give rise to the corticoclaustral projection (Katz, 1987). These two groups of pyramidal neurons also have different local projection patterns: the corticothalamic pyramidal neurons have a rich projection to layer 4, whereas the corticoclaustral cells project within layer 6 itself. The receptive fields of the corticothalamic neurons are significantly smaller than those of the corticoclaustral neurons (Grieve and Sillito, 1995).

As with the local intra-areal connectivity, the output neurons that project to other cortical areas also appear to be organized in patchy systems. One of the most elaborate discovered so far is the output from primary (V1) to the secondary visual area (V2), which arises from at least three specific subgroups of neurons in V1. These neurons project to a stripe system in area V2 in the monkey. These pathways may be visualized by the pattern of cytochrome oxidase staining (Gilbert and Kelly, 1975; Gilbert and Wiesel, 1979). Neurons located in the cytochrome oxidase blobs in V1 project to a series of thin cytochrome oxidase blobs in V2. The neurons in layer 3 outside the blobs project to pale stripe (interstripes) in V2, whereas the third group of projection neurons located in layer 4B of V1 project to a series of thick cytochrome stripes in V2.

The stripes formed by these projections themselves reveal the organization of output from V2 to other cortical areas: the thin cytochrome stripes project to visual area 4 (V4), the interstripes to V3 and V4, and the thick stripes to area MT.

SYNAPTIC ACTIONS

Release of neurotransmitter at synapses is triggered by the membrane depolarization associated with the arrival of an action potential. Consequently, the pattern of arrival of action potentials at the synaptic bouton is one of the fundamental factors governing the interaction of presynaptic and postsynaptic neurons. It is usually assumed that the pattern of action potentials seen by the presynaptic terminal is exactly the pattern that was generated at the beginning of the presynaptic axon. That is, we assume that the axon acts as a simple transmission line for action potentials and that there are no factors that selectively alter its transmission characteristics over moderate time intervals. The presynaptic axon begins at the initial segment, which is also the site at which the axonal action potential transmission begins. The initial segment is electrotonically close to the soma, and therefore we assume the electrical events of the initial segment can be recorded from the soma, which is where most intracellular recordings are made with patch or sharp pipettes. Most of our knowledge about interneuronal communication rests on interpretations of electrical events in the soma and in particular on the assumption that the action potentials that we observe in the soma will ultimately affect postsynaptic targets.

NEURONAL EXCITABILITY

In considering the action of synapses, there are two key issues. One is the effect of the synapses on the neuron at the site of the synapse; the other, the response of the whole neuron to these local synaptic actions. The former issue includes the attributes of the synapse such as the kinetics of a single synaptic response and the dynamics of a series of synaptic transmissions, whereas the latter includes the attributes of the neuron such as its membrane properties, the ionic currents involved, and the shape and cable properties of the neuron.

Sodium Currents. Action potential generation entails regenerative depolarization followed by a restorative repolarization. In cortical neurons, as in most other neurons, these two phases are mediated by a fast, voltage-dependent, inactivating sodium current (Connors et al., 1982) and a delayed, voltage-dependent potassium current (Prince and Huguenard, 1988), respectively. In addition to the inactivating sodium current, cortical neurons also exhibit a noninactivating, voltage-dependent sodium current (Stafstrom et al., 1982, 1984) similar to that observed in cerebellar Purkinje cells (Llinas and Sugimori, 1980a,b) (see Chap. 7) and hippocampal pyramidal neurons (Hotson et al., 1979; Connors et al., 1982) (see Chap. 11) and analogous to the slow inward calcium current (I_i) seen in spinal motoneurons (Schwindt and Crill, 1980) (see Chap. 3). In cortical neurons, this "persistent" sodium current ($I_{Na,P}$) is activated about 10–20 mV positive to the resting potential and attains steady state conductance within about 4 ms. It remains persistent and large up to at least 50 mV above resting potential (Stafstrom et al., 1984). These properties suggest that $I_{Na,P}$ can be activated by EPSPs and that $I_{Na,P}$ acts as a current

amplifier for depolarizing inputs. Indeed, $I_{Na,P}$ can itself provide regenerative depolarization that is able to drive the membrane to the level where the larger spike-generating sodium current is activated (Stafstrom et al., 1982). The difference in kinetics between these two regenerative sodium currents is probably responsible for the indistinct transition between the subthreshold rise of membrane potential and the rapid initial rise of the action potential (Stafstrom et al., 1984). On the other hand, the deactivation of $I_{Na,P}$ during an IPSP removes its contribution to regeneration and thereby enhances the effect of inhibition when the cell is relatively depolarized.

By recording directly from the apical dendrites of the pyramidal neurons (Stuart and Sakmann, 1994; Stuart et al., 1997), it has been shown that the dendrites contain active sodium conductances. This permits the action potential to propagate back along the apical dendrite. However, the dendritic sodium conductances appear to be at a much lower density than at the soma or axon initial segment, which has the highest density and is the main site of initiation of the action potential as was originally proposed from recordings from the motoneuron (Eccles, 1957; Fuortes et al., 1957) (but see Colbert, 2001) in hippocampus.

One effect of the dendritic sodium conductances is that they support propagation of the action potential from the soma backward into the dendritic tree. However, because their concentration is relatively low in the dendrites, the gain for depolarization there is not necessarily regenerative, and so the back propagation into the dendrites is passive. This renders the dendritic action potential a graded action potential, the amplitude of which depends on the local input resistance, which can, for example, be reduced by dendritic inhibition. Such local changes in the gain for depolarization may be crucial for controlling the amount of calcium influx evoked by the action potential into the dendrites, and thereby scale the degree of synaptic plasticity induced at a synapse as a function of background dendritic activity.

Potassium Currents. The inward sodium currents that accompany spike depolarization are opposed by an increase in outward potassium currents, and these currents ultimately restore the neuronal membrane to its resting level. The classic action potential mechanism provides a restorative outward current by just one delayed voltage-dependent potassium conductance, but the restorative outward current of cortical neurons is enhanced by several additional potassium currents. These currents affect the dynamics of membrane during postspike recovery and also during the subthreshold response to depolarizing inputs. Consequently, they affect the neuron's repetitive discharge behavior.

In the simplest case, a suprathreshold sustained depolarizing input current will evoke a train of action potentials. Each action potential ends with a repolarization that drives the membrane potential below threshold. The subsequent interspike interval will depend on the rate of postspike depolarization, because this will determine the interval to the next threshold crossing. If the time constants of the membrane currents are all short (i.e., of the order of an action potential duration), then the interspike intervals will be of equal duration and the neuron will exhibit sustained regular discharge. But some of the potassium conductances have much longer time constants, so their outward currents can be active throughout successive interspike intervals.

Because these outward potassium currents oppose the depolarizing input currents, they retard threshold crossing and so increase the interspike interval. These interactions

are the basis of adaptation, often referred to as “spike frequency adaptation,” the progressive lengthening of interspike interval that occurs during a sustained depolarizing input to some cortical neurons. The process of adaptation in cortical cells is interesting because it imposes an intrinsic restriction on their discharge. It is calcium dependent, it can be modified by neurotransmission, and adaptation characteristics correlate with morphological cell type.

The outward potassium currents that underly the impulse afterhyperpolarizations (AHPs) are seen in cortical neurons both *in vivo* and *in vitro* (Connors et al., 1982). Three separate AHPs have been identified in layer 5 neurons of sensorimotor cortex: fast, medium, and slow (Schwindt et al., 1988). The fast AHP has a duration of milliseconds and follows spike repolarization. It is often followed by a transient delayed afterdepolarization (ADP). The medium AHP follows a brief train of spikes. It has a duration of tens of milliseconds, and its amplitude and duration are increased by the frequency and number of spikes in the train. The slow AHP is evoked by sustained discharge and has a duration of seconds. All three hyperpolarizations are sensitive to extracellular potassium concentration, but they have different sensitivities to divalent ion substitutions and pharmacological manipulations (Schwindt et al., 1988). This suggests that they are mediated by at least three distinct potassium conductances. However, the individual potassium conductances have not been identified completely. This is partly because of the difficulty in comparing the characteristics of the many potassium conductance types found in various excitable cells, the many different regimens of investigation, and inconsistent nomenclature.

There is evidence that neocortical cells have at least four potassium conductances: (1) a delayed rectifier, (2) a fast transient voltage-dependent (A-like) current, (3) a slow calcium-mediated (APH-like) current, and (4) a slow receptor-modulated voltage-dependent (M-like, mAHP) current (Connors et al., 1982; Schwindt et al., 1988). Thus, the potassium currents of neocortical neurons appear qualitatively similar to those reported in hippocampal neurons of archicortex (see Chap. 11). However, the situation is rather more complicated than this, as the following examples illustrate. The transient fast current of cortex is TEA sensitive (Schwindt et al., 1988). The mAHP current is due to a calcium-mediated potassium conductance and so is superficially similar to AHP currents seen in hippocampal neurons, but the cortical conductance mechanism is not sensitive to TEA, whereas the hippocampal current is. The cortical conductance is sensitive to apamin, whereas the hippocampal current is not (Schwindt et al., 1988). Muscarine and beta-adrenergic agonists abolish the sAHP but have no effect on the mAHP (Schwindt et al., 1988), whereas in hippocampus acetylcholine affects both the M and AHP currents (Madison and Nicoll, 1984). These and other conductance differences may be due to important functional constraints on the discharge of neocortical neurons that are different from the discharge requirements of hippocampal neurons. An alternative view is that the differences have less to do with unique discharge requirements than with the variations of parallel evolution.

Some outward current conductances can be modulated by neurotransmitters (see Chap. 2). The outward potassium M current of cortical pyramids is reduced by activation of muscarinic receptors (McCormick and Prince, 1985; Brown, 1988). Because the outward current is reduced, the effect of depolarizing currents is enhanced. The slow Ca^{++} -activated potassium (AHP) current of cortical pyramids is also decreased

by ACh (McCormick and Prince, 1986a). These modulations of slow outward currents are the means whereby ACh enhances discharge frequency and decreases adaptation. Similar effects have been noted in hippocampal neurons (Benardo and Prince, 1982; Cole and Nicoll, 1984; Madison and Nicoll, 1984). Neurotransmitters may also modulate currents that interact with the slow hyperpolarizing potassium currents. Schwindt et al. (1988) have shown that low concentrations of muscarine abolish the sAHP, but at higher concentrations the sAHP is replaced by an sADP that is not potassium sensitive, nor is it sensitive to the sodium channel blocker TTX. The mechanism of the sADP is unknown.

In addition to these effects, acetylcholine also evokes a transient early inhibition of pyramidal neurons. However, two findings indicate that this inhibition is probably an indirect effect of the excitation of inhibitory interneurons. First, the inhibition is mediated by a chloride conductance similar to that activated by GABA. Second, ACh has a rapid excitatory effect on the fast-spiking (presumably GABAergic) cortical neurons (McCormick and Prince, 1986a,b), and smooth cells are known to have cholinergic afferents (Houser et al., 1985).

Calcium Conductances. Calcium currents also contribute to the dynamics of cortical neurons. For example, depolarization of the dendrites, by dendritic action potentials, can evoke calcium influx through multiple calcium channels (Yuste et al., 1994; Markram et al., 1995; Schiller et al., 1995). These calcium currents may affect the dynamics directly by contributing to the electrical behavior of the membrane or indirectly by changing the internal calcium concentration, which in turn affects potassium conductance (described earlier) and also by regulating multiple intracellular metabolic pathways and receptor kinetics, as well as synaptic plasticity.

Somatic recordings from antidromically activated pyramidal tract neurons *in vivo* indicated the existence of fast prepotentials (Deschenês, 1981). Blocking the sodium channel blocker with QX-314 left these prepotentials intact, suggesting they were mediated by calcium channels in the dendrites (Hirsch et al., 1995). Where calcium currents are voltage dependent, they operate as sodium currents do and so could contribute to spike generation. However, the calcium currents appear to be relatively small in cortical neurons and must be unmasked by both blocking the sodium currents and depressing the potassium currents. Under these conditions, a Ca^{2+} spike can be elicited from some cortical neurons (Connors et al., 1982; Stafstrom et al., 1985). The threshold for this spike is about 30–40 mV positive to the resting potential and therefore well above the activation thresholds for the sodium currents, $I_{\text{Na,P}}$ and I_{Na} .

Calcium spikes have been observed in hippocampal pyramidal neurons (see Chap. 11) and elsewhere, and in these cases they can be evoked after blockade of the sodium currents alone (Schwartzkroin and Slawsky, 1977; Wong et al., 1979). To initiate a calcium spike, the conductance for calcium must be much larger than that for potassium. Presumably, g_{K} is large in cortical cells and must be depressed to obtain a conductance ratio favorable for calcium spike initiation. Therefore, the need to depress the potassium conductance in cortical cells implies either that g_{K} is larger in cortical neurons than other calcium-spiking cells or that the calcium conductance is smaller. An alternative explanation is that the site of the calcium conductance is located in the dendrites, electronically distant from the soma. In this case, a depolarization large enough

to drive the distant site to the activation threshold of the calcium conductance would also strongly activate the more proximal voltage-dependent potassium conductances. The resulting increase in potassium conductance would shunt depolarizing current injected into the soma, and so prevent the dendritic membrane from reaching the threshold for calcium current activation.

Stafstrom et al. (1985) suggest that there are two calcium conductances in cortical neurons and that these are distributed along the soma-dendrite. The somatic calcium conductance is slow and small and has a high threshold. The dendritic conductance is both faster and larger than its somatic counterpart. Its threshold is also high, but this may be partly due to electrotonic distance from the soma, which makes it relatively difficult to activate from an electrode in the soma. Both somatic and dendritic currents contribute to the calcium spike. Somatic depolarization activates the somatic calcium current, and that in turn activates the more distal dendritic calcium conductance that powers the calcium spike. Both currents are probably persistent, so they require activation of an outward current to effect the recovery phase of the spike. This outward current is provided by the slow potassium (AHP) current that is activated by the influx of calcium in cortical (Hotson and Prince, 1980) and hippocampal (Lancaster and Adams, 1986; Madison and Nicoll, 1984) neurons.

Direct evidence for the existence of dendritic voltage-sensitive calcium channels has come from membrane patches of apical dendrites (Huguenard et al., 1989) and by calcium imaging of the dendrites (Yuste et al., 1994). The imaging studies showed that the dendritic accumulation of calcium took place immediately after calcium spikes were triggered, followed by a slower diffusion of intracellular calcium. Confocal and two-photon microscopic imaging of calcium has revealed the sites of calcium channels in the dendritic shaft (Markram and Sakmann, 1994) and in spine heads (Yuste and Denk, 1995; Holthoff et al., 2002). It appears that calcium channels are distributed over the whole dendritic tree, but the distribution has hot spots where activation can be regenerative. For example, in the tuft of the layer 5 pyramidal neurons, the sodium-dependent action potential can propagate back into the terminal tuft of layer 5 pyramidal neurons and evoke a calcium-dependent action potential, which then propagates forward toward the soma (Schiller et al., 1997). This is due to a spatially restricted low-threshold zone on the apical dendrite, located 550–900 μm from the soma, at which calcium-dependent action potentials can be evoked. This zone appears to be active *in vivo* during synaptic stimulation (Larkum and Zhu, 2002).

The issue of the role of spines in the compartmentalization of calcium has also been addressed by a number of studies. The first studies that used optical methods to image the spines in hippocampal pyramidal neurons indicated that individual spines could have quite different calcium dynamics to their parent dendrites (Guthrie et al., 1991; Muller and Connor, 1991). However, further studies in the hippocampal pyramids in which two-photon microscopy was used to image the spines of hippocampal pyramidal neurons loaded with a calcium-sensitive dye indicate that individual spines are only activated under subthreshold conditions. If the neuron fires an action potential, then calcium enters the spines (Denk et al., 1996). In cortical pyramidal cells, the spine calcium kinetics are controlled by the diameter of the parent dendrites, the length of the spine neck, and the strength of the spine calcium pumps. The importance of the spine neck is that it is motile and thus the calcium dynamics of the spine can be regulated

by rapid spine motility (Majewska et al., 2000). The morphological constraints also mean that the calcium dynamics of spines depends on their location on the dendritic tree (Holthoff et al., 2002). Theoretically, the restriction of calcium in the spine during subthreshold synaptic activation could serve to segregate the potential that occurs on spines during coactivation of presynaptic and postsynaptic neuron (Rall, 1974a).

Repetitive Discharge. The repetitive discharge properties of neocortical cells has been investigated both *in vivo* (e.g., Calvin and Sypert, 1976) and *in vitro* (e.g., Ogawa et al., 1981). McCormick et al. (1985) originally reported three electrophysiological cell types in neocortex: fast-spiking, regular spiking, and bursting cells. The fast-spiking cells were sparsely spiny or aspiny neurons. These “smooth cells” are the GABA-containing, inhibitory neurons of cortex. The regular and bursting cells were both pyramidal neurons. “Regular firing,” which is somewhat of a misnomer, refers to the adapting pattern of discharge in response to an injection of constant current into the soma. This was the predominant behavior of most pyramidal neurons. Only a small percentage of these pyramidal neurons exhibited a bursting discharge, and they were located mainly in the deep cortical layers (Connors and Gutnick, 1990). However, it is now clear that there are exceptions to the general function–structure relationships described, and smooth neurons are found that have the adapting pattern that was thought to be a characteristic of pyramidal neurons. Kawaguchi (1995), for example, has found chandelier cells, double bouquet cells, and neurogliaform cells with adapting patterns of discharge that are more commonly associated with spiny neurons.

The discharge of regular spiking neurons showed various degrees of adaptation, and the presence of both AHP and M currents could be demonstrated in these cells. A transient fast voltage-dependent (A) current is present in pyramids, and this may contribute to their adaptation (Schwindt et al., 1988). The structure–function correlations of the burst/nonburst firing pyramidal neurons of layer 5 have been determined (Chagnac-Amitai et al., 1990; Connors and Gutnick, 1990; Mason and Larkman, 1990; Kim and Connors, 1993). The regular firing pyramids have thin apical dendrites that do not branch extensively in layer 1. The burst-firing pyramids, by contrast, have thick apical dendrites and an extensive tuft in layer 1. Multipolar and bitufted neurons with bursting patterns have been described by Kawaguchi (1995), who called them “low-threshold spike” cells. These neurons would respond with a burst of action potentials when the neuron was depolarized from a hyperpolarized potential. Their dendrites had few spines.

Bursting neurons (Connors et al., 1982; McCormick et al., 1985; Kawaguchi, 1995) respond to depolarization by generating a short burst of about three spikes. McCormick and Gray (1996) have reported another class of bursting cell, which they called a “chattering cell.” This fast-spiking spiny cell produces a rhythmic series of high-frequency bursts during sustained depolarization. The exact mechanism of bursting in cortical neurons is unknown, but it has been explained by various mechanisms including the activation of low- and high-threshold calcium currents (McCormick et al., 1985; Jahnsen, 1986; McCormick, 1996), by a calcium-dependent potassium current (Berman et al., 1989), and by the distribution of sodium channels in the dendritic tree (Mainen and Sejnowski, 1996). In theory, it is possible to achieve a short burst in a neuron that has limited fast outward current and a dominant AHP current (Berman et al., 1989).

The reduced fast outward current encourages a short interspike interval and consequently a rapid discharge. The discharge would be terminated by the growing AHP current. Thus, variations in the parameters of the same outward current conductances could determine whether a pyramidal neuron discharges in regular or burst mode. In the model of Mainen and Sejnowski (1996), the dendritic sodium conductances promote propagation of the somatic action potential back into the dendrites. When the soma has repolarized, current returns from the dendrites to produce a late depolarization and some maintained action potential discharge. This effect was enhanced by high-threshold voltage-gated Ca^{2+} channels. Schwindt et al. (1988) have shown that reduction of the transient fast potassium conductance converts normal firing into burst firing, whereas specific reduction of mAHP increases the instantaneous discharge rate but does not affect adaptation.

The “fast spiking” cells encompass a variety of smooth neuron types (Kawaguchi, 1995) (Fig. 12.16). The action potentials of fast-spiking cells are brief by comparison with pyramidal neurons. The repolarization phase of the action potential is rapid and followed by a significant undershoot. This indicates the presence of an unusually large and fast repolarizing potassium current. Indeed, Hamill et al. (1991) were able to demonstrate that fast-spiking cells have a higher density of “delayed rectifier” potassium currents than do pyramidal neurons. The spike repolarization is fol-

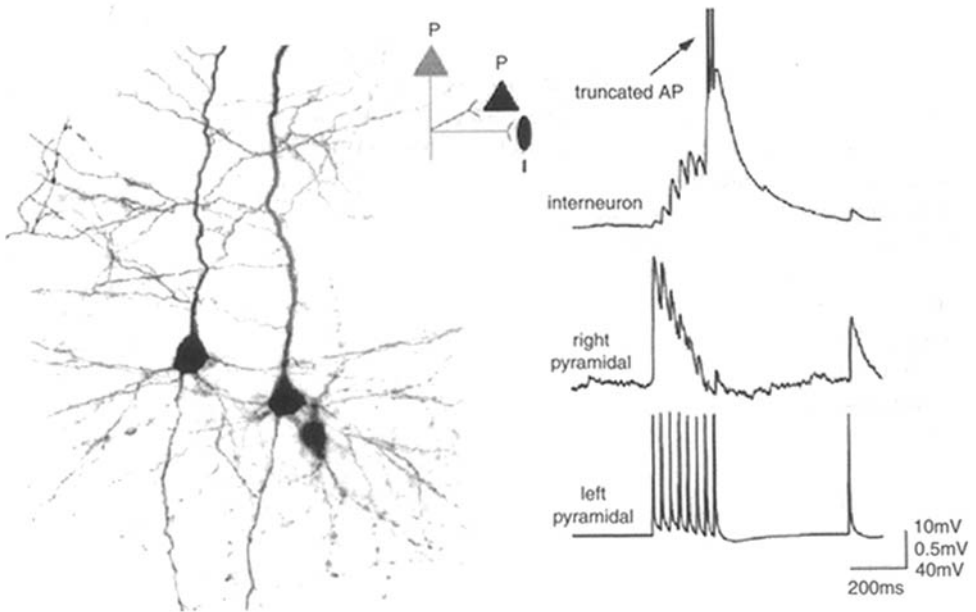


Fig. 12.16. An example of differential facilitation and depression, in a network of three biocytin-labeled cortical neurons (two pyramidal neurons and an interneuron) that were recorded simultaneously using the whole-cell patch-clamp technique. Trains of action potentials evoked in the right most pyramidal neuron by direct current injection elicited a facilitating synaptic response in the interneuron (upper voltage trace) but a depressing synaptic response in the neighboring pyramidal neuron (lower voltage trace).

lowed by a transient afterhyperpolarization. These cells showed little adaptation. The initial slopes of their current–discharge relation were steeper, and their maximum discharge frequencies were higher than those of pyramidal neurons. There was no evidence of either the AHP or M potassium currents in these neurons, and the absence of these longer time-constant outward currents in fast-spiking cells would explain their lack of adaptation.

Studies have attempted to classify the different electrical properties of interneurons in more detail. Five main classes have been identified; adapting, nonadapting, stuttering, irregular spiking, and bursting (Kawaguchi and Kubota, 1993; Kawaguchi, 1995; Porter et al., 1998; Gupta et al., 2000). Different behaviors at the onset of a depolarizing pulse have also been reported: delayed discharge, transient bursting, or no special onset response.

SYNAPTIC DYNAMICS

The effect of a presynaptic action potential on a particular postsynaptic target is complex, and depends on a functional context in both the presynaptic and postsynaptic components of the synapse which the action potential excites. This context is governed by many time-scales, from milliseconds to years.

Transient Changes in Effect. The arrival of an action potential at a presynaptic terminal triggers an increase in the intracellular concentration of calcium. This rise in Ca^{2+} enables a process whereby transmitter-laden vesicles fuse with the synaptic membrane and release their contents into the synaptic cleft. A precondition for release is that the vesicles be docked at a restricted number of sites on the presynaptic membrane. However, not every vesicle releases its contents in response to an action potential. Some sites are refractory following previous release; of all of the n vesicles that are primed to release their contents, any particular vesicle will react to a given action potential with probability P , as discussed in Chap. 1. This probability varies from less than 0.01 at specific pyramidal neuron–interneuron connections (Thomson et al., 1995) to 0.3–0.6 for typical pyramidal–pyramidal neuron connections (Markram et al., 1998; Thomson and Bannister, 1999). The value for thalamic synapses is even higher, perhaps as much as 1.0 (Stratford et al., 1996). The value of P depends also on the prevailing synaptic calcium dynamics.

Because the overall amount of transmitter released by an action potential depends on prevailing n and P and they depend on the evolving state of the synapse, the effect of a given action potential depends on its temporal relationship to preceding spikes. Consequently, the precise dynamics of transmission displayed at a synapse depends on the probability of release, time constants of recovery from synaptic facilitation, and synaptic depression (Markram et al., 1998).

If P is high, then the synapse will exhibit depression: The first action potential of a sufficiently closely spaced train will exhaust the synapse so that subsequent spikes in a train of action potentials will evoke successively smaller effects. If P is low, then the synapse will exhibit facilitation: the first action potential will release only a few of the available vesicles and will prime the others by increasing the intracellular calcium concentrations. Subsequent spikes in a train will evoke successively larger effects until a steady-state effect is reached (Thomson, 2000).

Long-Term Potentiation. Unlike the short time-scale of facilitation and depression, longer tetanic stimulation potentiates synapses in hippocampal excitatory synapses for many hours (Bliss and Lomo, 1973). The mechanisms of this process have been intensively studied in the hippocampus (see Chap. 11) and the same processes are found in neocortical neurons. Homosynaptic (specific to the stimulated pathway) long-term potentiation (LTP) was first seen in neocortex *in vivo*, along with the converse phenomenon of heterosynaptic (affecting nonstimulated pathways) long-term depression (LTD) in which the synapses become weaker (Tsumoto and Suda, 1979). Subsequent investigation *in vitro* confirmed the presence of both LTP and LTD in neocortical neurons of young rats and kittens (Komatsu et al., 1981; Artola and Singer, 1987; Bindman et al., 1988; Artola et al., 1990; Aroniadou and Teyler, 1992). However, although LTP could be readily induced in neocortical neurons that showed bursting behavior (Artola and Singer, 1987), LTP was only induced in other cortical neurons in the presence of bicuculline, the GABA_A antagonist (Artola and Singer, 1987).

Artola et al. (1990) provided evidence that identical stimulations could produce either LTD or LTP, depending on the level of depolarization of the postsynaptic neurons. They suggested that if the EPSPs produced a depolarization that exceeds a certain level but remains below the threshold for activation of the NMDA receptor, then LTD results. If, however, the threshold for the NMDA receptor is reached, then LTP results. This is essentially an experimental verification of the theoretical model of Bienenstock et al. (1982). Kimura et al. (1990) found that tetanic stimulation that would otherwise produce LTP will produce LTD if postsynaptic calcium ions are chelated. This indicates that the prevailing calcium concentration may be important for the production of LTP or LTD.

Kirkwood et al. (1993) showed that one of the most effective means of producing LTD is by low frequency (1 Hz) stimulation and that the induction of LTD was dependent on NMDA receptors. This suggests that the actual level of calcium might be critical for determining whether LTP (high postsynaptic calcium) or LTD (low postsynaptic calcium) is induced.

Recent studies have refined the conditions for inducing LTP/LTD by showing that relative millisecond timing of presynaptic and postsynaptic activity determines whether LTP or LTD is induced (Markram et al., 1997a). When the presynaptic input arrives to assist the postsynaptic neuron to discharge action potentials, LTP is observed, and when the presynaptic input arrives after the postsynaptic neuron discharges, LTD is induced, revealing a causal-reward/acausal-punishment. This form of plasticity is referred to as spike-time-dependent plasticity (STDP) and has also been reported in several other brain regions, indicating that it is not unique to neocortical synapses (see Abbot, 2001).

Recent studies indicate that the form of modification of synapses between pyramidal neurons in the neocortex, which are typically depressing, is not a uniform change but rather a redistribution of synaptic efficacy that is caused when the probability of release is increased (Markram and Tsodyks, 1996). This observation introduces a new notion of the plasticity of synaptic dynamics, as opposed to the plasticity of simple synaptic gain.

LTP of inhibitory synapses has also been observed in the visual cortex of developing rat (Komatsu and Iwakiri, 1993). Tetanic stimulation of an inhibitory pathway onto layer 5 pyramidal neurons leads to a long (more than 1 hr) potentiation of the IPSPs.

Weaker stimuli led to a short-term potentiation. The effects were specific to the stimulated pathway. Relative timing of presynaptic and postsynaptic activity determines the direction of synaptic modification also at inhibitory synapses (Holmgren and Zilberter, 2001).

The precise roles of LTP and LTD in general and plasticity of synaptic gain and synaptic dynamics in particular remain a matter of speculation—the widely held belief that they have something to do with memory remains the central dogma. The existence of a clear “critical period” of development in the sensory cortex, in particular, has led to the obvious hypothesis that these synaptic processes are part of the cascade that leads to the formation and modification by experience of nerve connections. Investigations of mouse barrel cortex and rat visual cortex have indicated that LTP, induced without the aid of GABA antagonists, has a critical period. For example, in barrel cortex, it was possible to potentiate the thalamocortical synapses during the first week of life but not the second (Crair and Malenka, 1995). This matches approximately the time course of structural plasticity of the thalamocortical afferents (Schlaggar et al., 1993). The LTP was dependent on NMDA-receptor activation and on increases in postsynaptic calcium.

In rat visual cortex, Kirkwood et al. (1995) also demonstrated that there is a critical period for LTP that corresponds to the falling phase for the plasticity of left and right eye inputs to cortex (ocular dominance plasticity). LTP was evoked in layer 3 by tetanic stimulation in the white matter. Unlike in adult rat cortex (described earlier), the LTP could be induced without blocking the GABA_A receptors. LTP could, however, be preserved beyond the normal end of the critical period by dark-rearing the pups. This procedure is known to delay the critical period in cats (Cynader and Mitchell, 1980) and appears to have some effect in rats. This dark-rearing paradigm has also been used to study the model of Bienenstock et al. (1982), which predicts that synapses that are used a lot will be more prone to LTD, whereas synapses that are used less will potentiate more readily. The history of synapse use therefore is an important factor in deciding whether a particular stimulation will lead to LTD or LTP. Kirkwood et al. (1996) found that in dark-reared rats, LTP was enhanced, whereas LTD was hard to evoke. The effect was reversed after dark-reared rats were exposed to light after just 2 days.

Understanding the function of synaptic plasticity may also require considering differences in synapses within local microcircuits, between cortical areas, and between neocortex and subcortical regions. The processes of LTP and LTD have been studied in a number of different cortical areas and for thalamocortical fibers. In the motor cortex (area 5a) of young adult cats, brief tetanic stimulation of the same area or area 1 and 2 could evoke LTP (Keller et al., 1990). This study was one of few to examine the phenomenon *in vivo* and to identify the neurons being recorded. They found that LTP could be evoked in both spiny (pyramidal neurons) and smooth neurons. However, LTP was induced only in those neurons that produced monosynaptic EPSPs in response to stimulation. Thalamic input to the motor cortex could also be potentiated *in vivo* by co-activation with the corticocortical pathway (Iriki et al., 1991). Tetanic stimulation of the ventrobasal thalamus alone did not produce LTP.

There are, however, some differences in the plasticity seen in rat sensory (granular) cortex and motor (agranular) cortex *in vitro* (Castro-Alamancos et al., 1995). Although both cortical areas could reliably generate homosynaptic LTD, LTP was more reliably generated in sensory cortex than in motor cortex, unless inhibition was reduced by ap-

plication of GABA receptor antagonists. In both areas, the application of NMDA antagonists blocked the induction of both LTP and LTD. However, the kainate/AMPA receptor-mediated responses are also potentiated (Aroniadou and Keller, 1995) in rat motor cortex *in vitro*.

Homeostatic Plasticity. Development and learning mold cortical neuronal circuits by changing the number and strength of synapses. During this process, individual neurons change their morphology, synapses and the profile of their dendrosomatic ion channels. Nevertheless, the functional expression of the neurons and networks remain relatively stable.

In cultured cortical neurons, the strength of excitatory synaptic connections between pyramidal neurons scales as a function of firing rate. The scaling is due to changes in the quantal amplitude of AMPA receptor-mediated excitatory neurotransmission (Turrigiano et al., 1998). The changes are mediated by brain derived neurotrophic factor (BDNF), which is produced by pyramidal neurons and acts on a high-affinity receptor, *trkB*, found on both pyramidal and nonpyramidal neurons. BDNF has opposite effects on pyramidal neurons and interneurons. It reduces the strength of pyramidal-pyramidal connections but increases the strength of inhibitory interneuron to pyramidal neuron connections. Thus, increases in network pyramidal activity that enhance BDNF secretion are followed by a compensatory reduction in interpyramidal connection strength and increase in pyramidal neuron inhibition (Turrigiano, 1999).

EXCITATORY SYNAPSES

In the neocortex, the main excitatory neurotransmitter is the amino acid glutamate. The postsynaptic membrane of glutamate synapses contains a collection of different receptor types. The amino-acid sequences of many of these receptor proteins have now been identified and specific antibodies have been raised that recognize subunits of the receptors (see Chap. 2). Although additional species of glutamate receptor may well be identified, the immediate goal is to discover the role of these different receptor subtypes in the different cortical circuits.

Glutamate Receptors. As discussed in Chap. 2, the glutamate receptors have been divided into three major types: AMPA/kainate receptor, NMDA receptor, and metabotropic.

In the neocortex, studies of the action of metabotropic receptors in the neocortex are in their infancy and have mainly addressed issues of development and plasticity. Few have considered their functional roles. The direct action of the mGluR on pyramidal neurons, after blocking AMPA and NMDA receptors, was to produce a slow depolarization after evoked spikes (Greene et al., 1994). In burst-firing neurons that project to the superior colliculus or pons, application of mGluR agonists inhibited the burst firing and changed the neurons to a tonic mode of firing (McCormick et al., 1993; Wang and McCormick, 1993). This effect is mediated by a decrease in a potassium conductance. In isolated neocortical neurons, Sayer et al. (1992) found that mGluR activation reduced the high-threshold Ca^{2+} current mediated by L-type calcium channels.

In slices of frontal cortex of immature rats, Burke and Hablitz (1995) provided evidence that mGlu receptors are located on both presynaptic and postsynaptic terminals. It appeared from their pharmacological dissection that different receptor subtypes

were localized at the presynaptic and postsynaptic sites. When GABA_A receptors were blocked, mGluR agonists increased epileptiform discharges, whereas the antagonist *RS- α -methyl-4-carboxyphenylglycine* (MCPG) suppressed epileptiform activity. Ionotophoretic application of mGluR agonists in rat barrel cortex *in vivo* produced disinhibition in response to natural stimulation of the vibrissae, whereas application of the antagonists reversed these disinhibitory effects (Wan and Cahusac, 1995). The effect might be mediated by a presynaptic receptor that depresses the release of GABA.

Locations of Excitatory Synapses. The major fraction (65%–85%) of excitatory synapses made on pyramidal cells are on their spines, with the remainder being on dendritic shafts. No excitatory synapses are made on the somata of pyramidal neurons. It was previously supposed that spiny stellate cells followed the pattern of innervation of pyramidal neurons. This is true for spiny stellate cells of the mouse barrel cortex (White, 1989), but it is not true for spiny stellates of layer 4a in area 17 of the cat (Ahmed et al., 1994). It also may not be true for monkey spiny stellates. In the cat, about 60% of the excitatory input arrives on shafts of dendrites. The excitatory inputs to smooth neurons are onto both the dendritic shafts and the soma. In the case of the cat, at least some of the layer 4 smooth neurons form somatic synapses with the thalamic afferents (see Synaptic Connections).

The strength of the excitatory synaptic coupling between excitatory neurons has been studied in a variety of cortical areas in rat and cat. Mason et al. (1991) made the first recordings from pairs of pyramidal neurons in the superficial layers of the rat visual cortex. They reported that the synapses produced small-amplitude EPSPs, about 0.1–0.4 mV as recorded in the soma. Thomson et al. (1993) studied the connections between pyramidal neurons in the deep layers of the rat's motor cortex. They found that synaptic transmission was mediated by both NMDA and non-NMDA glutamate receptors. These synapses produce an EPSP with an amplitude of 1–2 mV, recorded in the soma, which was depressed by repetitive stimulation. Similar findings have been made by Markram and Tsodyks (1996), recording from pairs of neighboring layer 5 pyramidal neurons in rat somatosensory cortex.

Stratford et al. (1996) examined the excitatory input to spiny stellate neurons in layer 4 of cat visual cortex. The advantage of the spiny stellate neuron for these studies is that its dendritic tree is symmetrical and electrotonically compact. Thus, variations in amplitude and time course of the epsps are largely due to synaptic properties rather than to the cable properties of the dendrites. The sources of excitation were spiny stellate neurons similar to the target, as well as layer 6 pyramidal neurons. These two types of cortical neuron had very different synaptic physiologies. The spiny stellate to spiny stellate synapse produced EPSPs with an amplitude recorded in the soma of about 1.5 mV, which depressed slightly with repetitive stimulation. The layer 6 pyramid synapses produced comparatively small amplitude EPSPs (0.4 mV), which showed strong facilitation with repetitive stimulation. In addition, they were able to demonstrate large-amplitude (2.0 mV) EPSPs from putative single thalamic fiber inputs to these same spiny stellate cells. Unlike the EPSPs of cortical origin, these putative thalamic EPSPs showed remarkably little variance in amplitude from trial to trial and only slight depression with repetitive stimulation. Thus, the excitatory synapses formed with a single type of neuron can show a variety of static and dynamic properties, according to their source.

INHIBITORY SYNAPSES

The existence of inhibition in the cortex has been demonstrated repeatedly using intracellular recording. The first recordings were made in the Betz cells of the cat motor cortex *in vivo* (Phillips, 1959). By antidromically activating the pyramidal tract neurons, Phillips demonstrated the presence of a recurrent inhibitory pathway in the cortex. Later studies were made in visual cortex (Li et al., 1960; Creutzfeldt et al., 1966; Pollen and Lux, 1966; Krnjévić and Schwartz, 1967; Toyama et al., 1974). These confirmed Phillips' (1959) observation that every neuron received an inhibitory input. Electrical stimulation of either the subcortical thalamic nuclei or local cortical stimulation produced a long-lasting (100–200 msec) IPSP. The role and mode of operation of inhibition in generating the stimulus-specific responses of neurons in the visual cortex remain questions of intense interest (Douglas et al., 1995; Somers et al., 1995; Ferster et al., 1996).

A number of chemical substances have inhibitory effects on cortical neurons, but the most dominant inhibitor appears to be GABA. Krnjévić and Schwartz (1967) performed a direct comparison between the membrane effects of GABA and naturally occurring IPSPs in mammalian cortex. They used surface stimulation to evoke IPSPs in neurons of pericruciate cortex and recorded IPSPs that reached peaks at about 20–30 ms, had durations of 200–300 ms, and had amplitudes of about -10 mV at the resting membrane potential. These IPSPs could be reversed by current injection or intracellular Cl^- injection (Krnjévić and Schwartz, 1967; Dreifuss et al., 1969). Application of GABA usually hyperpolarized the cells and reduced the amplitude of the IPSPs (Krnjévić and Schwartz, 1967). The reduction in IPSP amplitude was dependent on the GABA ejection current. The highest ejection currents flattened the IPSP (Krnjévić and Schwartz, 1967) and sometimes slightly inverted them (Dreifuss et al., 1969). The applied GABA increased the input conductance, whose time course was similar to that of the IPSP voltage response and decayed with a time constant of about 50 ms. Direct application of GABA also gave a marked increase in input conductance, together with hyperpolarization in most instances. The reversal potentials for the direct GABA effect and the IPSP were similar; Dreifuss et al. (1969) therefore concluded that GABA was the source of the cortical IPSP. The development of a specific GABA receptor antagonist, bicuculline, confirmed that cortical inhibitory processes were GABA mediated and had an important functional role in shaping cortical responses (Sillito, 1975; Tsumoto et al., 1979). Subsequent identification of the structure of the GABA receptor (Barnard et al., 1987) has allowed specific antibodies to be developed for the GABA receptor subunits and so enabled the regional distribution of GABA receptor subunits to be mapped (Fritschy and Mohler, 1995).

Receptor Types. In their original paper on the heterogeneity of hippocampal responses to GABA, Alger and Nicoll (1982) proposed that there were two different mechanisms mediating GABA inhibition and that these two mechanisms were activated by two different GABA receptor types. However, the details of their hypothesis differed considerably from current models of GABA action in hippocampus. Alger and Nicoll (1982) suggested that there was only one hyperpolarizing mechanism and that it was distributed throughout both soma and dendrites. This hyperpolarization was Cl^- dependent. Their second mechanism was depolarizing. They were uncertain of the ion conduc-

tance involved, but it was slightly sensitive to chloride. However, the presence of both hyperpolarizing and depolarizing responses on the dendrite, and both sensitive to chloride, did not seem attractive! A solution to this paradox is the notion that the chloride transporters (chloride/bicarbonate exchangers, $\text{Na}^+/\text{K}^+/\text{Cl}^-$ cotransporters, and an ATP-driven chloride pump) are unevenly distributed between soma and dendrites, resulting in a gradient of chloride concentration (Hara et al., 1992). This gradient would shift the reversal potential of the GABA_A synapse according to its location (Staley, 1995).

GABA_A . In early studies it was found that the conductance changes, reversal potential, and sensitivity to chloride of GABA ionophoresis and IPSPs were similar (Eccles, 1964), suggesting that they were both mediated by chloride channels. The GABA receptor associated with the chloride conductance is now known as the GABA_A receptor. It is the receptor that also binds benzodiazepine and barbiturate (see Matsumoto, 1989). The GABA_A receptor is selectively blocked by bicuculline. There are 16 known GABA_A receptor subunits that may assemble in various combinations of 5 (pentamers) that form the functional chloride channels (Barnard et al., 1987; Nayeem et al., 1994). The beta subunit contains the GABA_A receptor site, whereas the alpha subunit contains the benzodiazepine receptor site. Benzodiazepines increase the effect of GABA by increasing the frequency of channel opening in the presence of GABA. Picrotoxin acts by interference with the chloride ionophore (Barker et al., 1983). At low concentrations, barbiturates prolong the duration of GABA_A channel opening without affecting conductance, and at concentrations of the order $50 \mu\text{m}$, they directly activate chloride channels (Study and Barker, 1981). Alphaxalone has similar effects (Cottrell et al., 1987). The GABA_A receptor sensitivity is reduced in the presence of the raised intracellular calcium associated with the calcium spike (Inoue et al., 1986).

GABA_B . The failure of the specific GABA_A -receptor antagonist bicuculline to block the long-duration IPSP in cortex (Curtis et al., 1970; Godfraind et al., 1970; Curtis and Felix, 1971) indicated the presence of another GABA-mediated response. Bowery and colleagues (Hill and Bowery, 1981; Bowery et al., 1987) discovered a second class of GABA receptor, which was not sensitive to barbiturates or benzodiazepine (Alger and Nicoll, 1982; Blaxter et al., 1986; Bormann, 1988). These GABA_B receptors are activated by the antispastic drug baclofen, which is ineffective at GABA_A receptors (Bowery et al., 1984). The GABA_B receptor, which was cloned in 1997 (Kaupmann et al., 1997), forms part of the G-protein-coupled receptor superfamily (Bowery, 1993). The GABA_B receptor is indirectly coupled to calcium and potassium channels via GTP-binding proteins and perhaps protein kinase C (Dolphin and Scott, 1986; Dutar and Nicoll, 1988). In frontal cortex, G-proteins are involved in the postsynaptic response, and the short latency of the GABA_B IPSPs suggests a close coupling between receptor and ionophore (Hablitz and Thalmann, 1987). The GABA_B receptors are also found presynaptically, where they activate potassium channels or inhibit calcium conductances. This may reduce the GABA released and reduce the overall level of GABA-mediated inhibition. On excitatory terminals, the GABA_B receptors may also reduce the release of excitatory neurotransmitter (Thomson et al., 1993). Connors et al. (1988) showed in cortical slices that baclofen, the GABA_B agonist, activated a long time course

hyperpolarization with a reversal potential around the potassium reversal potential, and similar observations were made in cat visual cortex *in vivo* by Douglas et al. (1988) and Douglas and Martin (1991).

Two low-potency GABA_B antagonists, phaclofen and saclophen, have been used as GABA_B receptor blockers (Kerr et al., 1987, 1988). They block the long-duration late component of the IPSPs *in vitro* in frontal cortex (Karlsson et al., 1988) and in visual cortex (Connors et al., 1988; Hirsch and Gilbert, 1991). Due to the low potency of phaclofen, its effects on orientation and direction selectivity of visual cortical neurons *in vivo* have proved to be inconclusive (Baumfalk and Albus, 1988), whereas blocking GABA_A receptors with *n-m*-bicuculline produces a marked reduction in the selectivity of visual cortical neurons to visual stimuli (Sillito, 1975).

In addition to their role in postsynaptic inhibitory process, GABA_B receptors inhibit transmitter release in neocortical neurons via a presynaptic mechanism (Deisz and Prince, 1989). The mechanism is probably by reducing the entry of calcium into the presynaptic terminal and thus lowering the probability of transmitter release. Phaclofen is ineffective at the presynaptic GABA_B sites (Dutar and Nicoll, 1988).

Neocortical GABAergic synapses also display frequency-dependent dynamics (Thomson and Deuchars, 1994). Three classes of synapses have been defined according to the relative amount of facilitation and depression they exhibit (Gupta et al., 2000). The type of synapse deployed at an inhibitory connection depends on the nature of the presynaptic interneuron and its target neuron.

ELECTRICAL PROPERTIES OF THE IPSP

Responses to GABA. There are at least three distinct responses to direct GABA applications to cortical neurons *in vitro* (Scharfman and Sarvey, 1987). The first response is a fast hyperpolarization; this predominated when the GABA was ejected close to the soma. It produced a large increase in the input conductance. The second was a longer-lasting depolarization, which was evoked most readily by application of GABA to the distal dendrites. It was associated with a moderate increase in the input conductance. The third was a slow hyperpolarization that appeared on the trailing edge of the depolarization. It was a prolonged response that decayed over many seconds and was associated with a moderate increase in the input conductance. The three components are often mixed. For example, ejection in the vicinity of soma may show early somatic (hyperpolarizing response) followed by a relatively late depolarization (as GABA diffuses onto dendrites and evokes a dendritic response). GABA ejected in the vicinity of proximal dendrites evokes both a somatic and a dendritic response.

The somatic response had a reversal potential of -65 mV, was chloride dependent, and was blocked by bicuculline (Scharfman and Sarvey, 1987; Connors et al., 1988). The dendritic depolarization is probably also mediated by GABA_A receptors because it is blocked by bicuculline and picrotoxin and is potentiated by benzodiazepines (Blaxter and Cottrell, 1985). The differences in the response between somatic and dendritic activation of the same receptor have been explained by possible differences in the chloride concentrations in dendrites and soma (Thomson et al., 1988). Lambert et al. (1991) have proposed that the GABA_A receptors in the hippocampus mediate their dendritic responses via a different ionophore. By contrast, the dendritic hyperpolarization evoked by GABA is mimicked by baclofen, the specific GABA_B agonist. This hyperpolariza-

tion reverses at -90 mV (Ogawa et al., 1986; Scharfman and Sarvey, 1987; Connors et al., 1988). The GABA hyperpolarization is potassium dependent and can be evoked alone by small doses of GABA applied to the dendrites (Wong and Watkins, 1982) or by blocking the depolarizing component with bicuculline (Inoue et al., 1985a,b). This dendritic hyperpolarization is blocked by phaclofen and thus is probably mediated by the GABA_B receptor (Dutar and Nicoll, 1988).

In neocortical slices, long and short IPSPs have been observed (Ogawa et al., 1981; Connors et al., 1982). The stimulus threshold for the late, long IPSPs mediated by the GABA_B receptor is higher than that for the early, short IPSPs, which are mediated by the GABA_A receptors (Connors et al., 1982). In most neurons, the early IPSPs were depolarizing because the resting potential of the cortical neurons was more negative than the reversal potential of chloride (Connors et al., 1982; McCormick et al., 1985).

Sites of Action of Inhibitory Synapses. The soma or the proximal dendrites are the regions where anatomical and immunocytochemical studies have revealed the major concentration of symmetrical (Gray type II), GABAergic synapses (LeVay, 1973; Ribak, 1978; White and Rock, 1980; Freund et al., 1983; Peters, 1987). In brain slice preparations, large conductance changes occur only transiently at the onset of an electrically evoked IPSP and last for 15–25 ms. The long phase of the IPSP is associated with a small conductance change (Ogawa et al., 1981). Intracellular recordings from visual cortical neurons *in vivo* revealed hyperpolarization during a long period of visually evoked inhibition (Douglas et al., 1988; Ferster, 1988; Ferster and Jagadeesh, 1992). Large conductance changes have been observed *in vitro* studies and have been reported in cat visual cortex (Borg-Graham et al., 1998) in response to natural stimulation. A more distal location would enhance the shunting effect of the synapse (see “shunting synapses” in Chaps. 1 and 2), because the input conductance of the trunk dendrite decreases relative to the active conductance of the inhibitory synapse. Inputs to the apical dendrite of large layer 5 pyramidal neurons in the rat from a single inhibitory neuron are strong enough to block the dendritic Ca²⁺ action potential (Larkum et al., 1999).

An extreme example of dendritic inhibition is where the shunting inhibitory synapse is located on the spine head or neck. Under these circumstances, a large increase in conductance evoked in the spine head would provide very specific shunting of an excitatory synapse on the spine head, but the conductance change would be masked from the soma by the high axial resistance of the spine neck. However, the present neuroanatomical data suggest that relatively few excitatory synapses could be influenced in this way: only 7% of spines have both synaptic types (Beaulieu and Colonnier, 1985). Even if this figure is an underestimate, there remain a large number of spines without inhibitory input. Because the major excitatory input to pyramidal neurons is thought to arrive on spines (Colonnier, 1968; LeVay, 1973; Szentágothai, 1973; Peters, 1987), most of this input could not be selectively inhibited.

NEUROTRANSMITTERS

AMINO-ACID TRANSMITTERS

The establishment of the identity of cortical neurotransmitters has been one of the most tortuous activities of the past 40 years.

Glutamate. The failure of the specific Hayashi (1954) first proposed the amino acids L-glutamate and L-aspartate as candidates for the excitatory neurotransmitters in the cerebral cortex. This was supported by Krnjévić and Phillis (1963) and by the superfusion studies of Jasper et al. (1965), who found that glutamate, aspartate, glycine, and taurine were released during activation of the cortex. Clark and Collins (1976) showed that the release of glutamate, aspartate, and GABA were calcium dependent. However, resistance to accepting glutamate as a neurotransmitter was strong because glutamate is distributed throughout the brain in high concentrations, a quite different picture from the restricted location and lower concentrations of acknowledged neurotransmitters such as ACh and catecholamines.

Other amino acids also exert an excitatory effect of neurons. Some of these are more potent than the endogenous amino acids. The D-isomer of N-methyl aspartate is much more potent than L-glutamate (Curtis and Watkins, 1963). The extraction of kainate and quisqualate from plants provided more agents that had stronger excitatory effects on neurons than L-glutamate (Shinozaki and Konishi, 1970). An antagonist, L-glutamic acid diethylester (GDEE) proved to be more effective against L-glutamate than other excitatory amino acids and indicated that there may be more than one type of excitatory amino acid receptor (Haldeman et al., 1972; Haldeman and McLennan, 1972). With the recent effort devoted to the characterization of receptor subunits L-glutamate has emerged as the major excitatory amino acid transmitter of the cerebral cortex.

GABA. The acceptance of the amino acid GABA as the major inhibitory neurotransmitter has been as slow as that for glutamate. This occurred despite the demonstration by Krnjévić and Schwartz (1967) that ionophoretically applied GABA profoundly inhibited cortical neurons and the evidence that GABA was released from active cortical synapses (Iversen et al., 1971). Application of *n-m*-bicuculline, the GABA's receptor antagonist, has a marked effect on the receptive field structure of visual cortical cells (Sillito, 1975; Tsumoto et al., 1979) and on the shape of the electrically evoked IPSP (Connors et al., 1988; Douglas et al., 1989). Antibodies directed against the synthetic enzyme for GABA, glutamate decarboxylase, or against the amino acid itself, indicate that about 20% of the neocortical neurons synthesize and contain GABA (Naegele and Barnstable, 1989).

Acetylcholine. Ionophoretic application of ACh modifies the response to visual stimulation of most neurons in the cat visual cortex (Sillito and Kemp, 1983). The effect is usually facilitatory and seems to enhance the signal-to-noise ratio, rather than being generally excitatory. In deep layer pyramidal neurons, ACh induces a depolarization accompanied by an increase in resistance. The reversal potential is above that for potassium, suggesting that the action of ACh is to decrease the conductance for potassium (Krnjévić et al., 1971) by modulation of the slow outward potassium M current. The ACh response is mediated by a muscarinic receptor. The slow depolarization is preceded by a short-latency hyperpolarization and a decrease in resistance that is probably due to the rapid muscarinic excitation of the inhibitory neurons (McCormick and Prince, 1985, 1986a). The inhibitory neurons are innervated by cholinergic afferents (Houser et al., 1985).

The onset of the depolarizing muscarinic excitation is slow and the response is sustained for many seconds. Some of the effects of ACh are mediated by second mes-

sengers (Stone and Taylor, 1977). Low concentrations of muscarine abolish the sAHP, but at higher concentrations the sAHP is replaced by a slow afterdepolarization (sADP) that is not mediated by potassium or sodium (Schwindt et al., 1988). ACh-induced excitation can be enhanced selectively by SSt, although SSt itself inhibits spontaneous firing (Mancillas et al., 1986).

Biogenic Amines. Norepinephrine depresses the spontaneous extracellular activity of most cortical neurons (Reader et al., 1979; Armstrong-James and Fox, 1983). Some cortical cells in the deep layers are excited by low concentration of norepinephrine but inhibited by higher concentrations (Armstrong-James and Fox, 1983). Waterhouse et al. (1990) found that visual cortical cells in the rat showed enhanced responses to visual stimuli during iontophoresis of norepinephrine but depressed responses during serotonin iontophoresis.

Neuropeptides. The GABAergic neurons of the neocortex co-localize various peptides, including SSt, cholecystokinin, neuropeptide Y, VIP, and substance P (Hendry et al., 1984; Schmechel et al., 1984; Somogyi et al., 1984; Demeulemeester et al., 1988). VIP and substance P are also associated with cholinergic axons (Vincent et al., 1983; Eckenstein and Baughman, 1984).

The physiological role of neuropeptides remains obscure. Salt and Sillito (1984) showed that SSt could inhibit or excite cortical neurons. They were unable to demonstrate a modulatory effect on either GABAergic or cholinergic transmission. Mancillas et al. (1986) found that SSt inhibited rat cortical neurons. Cholecystokinin and VIP (Grieve et al., 1985a,b) produce mild excitation in some neurons. The difficulty in detecting effects, and the variety of effects produced, suggests that the role of these peptides is not primarily neurotransmission. Possibly they are part of some cascade of effects acting over time-courses of many hours or days, rather than 1 hour or so for conventional experiments that require receptive field mapping.

DENDRITES

The surface area of the dendrites is one to two orders of magnitude larger than that of the soma, and the dendrites receive the vast majority of the synaptic inputs to the neuron, as has been shown for most other neurons in preceding chapters. This arrangement suggests that the role of the dendrites is to integrate synaptic input, the result of which the neuron then expresses as the discharge activity of the soma. Unfortunately, in most cases the diameters of the dendrites of typical cortical neurons are too small to obtain stable recordings using available electrophysiological techniques, so most of our understanding of their electrical behavior is derived indirectly, from recordings made from the somata and apical dendrites (Stuart and Sakmann, 1994) (see Fig. 1.9B). These methods are now being supplemented by sophisticated imaging techniques such as calcium imaging and two-photon microscopy (Denk et al., 1995).

The simplest electrical model of a dendrite is the passive electrotonic structure (Rall, 1977, 1989; Johnston and Wu, 1995; Segev et al., 1995). In this *cable model*, the dendrites are composed of cylindrical segments of membrane that are linked in a tree-like structure. The membranous walls of the cylinders have capacitance and linear con-

ductance, and the interior of the cylinders present a linear axial conductance to the longitudinal passage of current. Such cylinders are electrically distributed (nonisopotential) structures, and an input current injected at a point will establish voltage gradients along the dendrite. For simple cylindrical dendrites, the voltages at any point along their length is specified by the *cable equation* (see Jack et al., 1975). The solution of this equation, and so the voltage profile, depends on the boundary conditions at the ends of the dendritic cylinder. These boundaries are usually approximated as either an infinite cable, a cut (short circuit) end, or sealed (open circuit) end. Rall (1959) showed that the cable equation could also be solved for branching cylindrical dendrites, provided that there was a “3/2 power” relationship between the parent and daughter branch diameters. When this relationship and a few other restrictions hold, then the entire dendrite can be reduced to a single equivalent cable of constant diameter.

In real neurons, the synaptic voltages attenuate more rapidly toward the soma than toward the dendritic terminations. The electrical asymmetry of the dendritic tree arises because the terminations are sealed ends and little synaptic current is lost from them, whereas the somatic end has many other dendrites attached and so presents a large conductance load to the source synapse located on one of the dendrites. The voltage attenuation from dendrites to soma may be as much as a few hundred-fold. This implies that a number of EPSPs must occur within a membrane time constant to displace the somatic potential across a 10- to 20-mV threshold. If the effect of a synapse depended only on its peak voltage, then the response of the neuron would be very sensitive to the displacement along the dendrite of the synapse. But, if the entire EPSP is considered, the situation is different. The passive dendrite behaves as a low-pass filter, and so the temporal form of the synaptic potentials become significantly broader as they spread from distal synaptic sites toward the soma. Although the *peak* synaptic voltages are attenuated, the attenuation of the time integral of the EPSP at the soma is smaller and not much affected by synaptic location. This is also true of the integral of the synaptic current at the soma (synaptic charge delivery). Because the synapses exert their effect collectively, by sustained depolarization of the somatic membrane, it is the charge delivery to the soma that best expresses synaptic efficacy (Bernander et al., 1994).

The broadening of the EPSP as it spreads centripetally has the effect of delaying the signal and makes the response at the soma sensitive to the temporal order of synaptic events applied in the dendrites. This means that the dendrite can usefully compute functions such as direction of motion (Rall, 1964; Koch et al., 1982). Passive dendrites can also act on different time-scales. For example, extensively branched distal dendrites provide a large area for charge equilibration, so the time constant for synaptic integration is much shorter (about $0.1 \tau_m$) there than closer to the soma. The briefer synaptic events in the distal arbors interact as coincidence detectors, whereas the longer events closer to the soma integrate (Agmon-Snir and Segev, 1992).

The morphology of the dendritic tree is important, at least in so far as it affects the passive spread of currents from the synapses to the initial segment (Mainen and Sejnowski, 1996). Most cortical neurons are electronically compact, whether measured electrophysiologically (Stafstrom et al., 1985) or anatomically (Douglas and Martin, 1992). However, the apical dendrite of the pyramidal neurons is a special case. The electrotonic length of the apical dendrite is about 2–3 times greater than that of the basal dendrites, and the synaptic inputs injected into the “apical tuft” at the distal end of

the apical dendrite are greatly attenuated en route to the soma (Bernander et al., 1994). This apparent ineffectiveness of the distal apical input is counterintuitive. Important interareal projections make their synapses there, and there has been no phylogenetic trend to dispense with apical dendrites (with the possible exception of layer 4 spiny neurons). One possibility is that the apical dendrite makes use of active currents to enhance selectively signal transmission to the soma (Bernander et al., 1994). Where the dendrites are long and narrow, and so electrotonically short, the dendrite can decompose into electrotonically separate subunits, each of which can compute a relatively independent function (Koch et al., 1982). It is unlikely that such conditions exist in cortical neurons, except possibly in the apical tufts.

ACTIVE PROPERTIES

The cable model has been extremely useful in obtaining qualitative insights into the behavior of quiescent dendrites. However, it has two significant failings that limit its application to cortical neurons. First, the approximation to a cable across the branches in a dendrite requires that a particular relationship of diameters hold between the parent and daughter segments of the branch. This relationship is only rarely true across the dendritic branches of cortical neurons. Second, it is clear that the majority of cortical neurons have many active conductances in their dendrites (Stuart and Sakmann, 1994), so the linear cable approximation is only useful under very restricted conditions. Active dendritic conductances include voltage-dependent sodium, potassium, and calcium currents (Stuart and Sakmann, 1994; Markram and Sakmann, 1994; Johnston et al., 1996). When the nonlinearities due to the active conductances are included, the dendritic models have mathematical descriptions that cannot be solved analytically. The models must then be investigated by numerical simulations of compartmental approximations to the dendrites.

The active conductances are able to generate a variety of subthreshold nonlinearities and may cross the thresholds for calcium or sodium action potentials. The exact interactions of the various active dendritic conductances are unknown, but they support a number of interesting functions. In the case of subthreshold synaptic potentials, the apical tuft of the layer 5 pyramidal neuron has a high potassium channel (I_h) density that increases the attenuation of EPSPs, and could uncouple the apical tuft dendrites from their basal counterparts, by decreasing the somatopetal length constant (Berger et al., 2001). However, action potentials initiated in the somata of layer 5 pyramidal neurons are able to propagate actively backward into their dendritic tree. This retrograde propagation is probably due partly to the amplification of depolarizing currents by the relatively high density of sodium channels found in the dendrites of those neurons (Stuart et al., 1997). The action potential propagates more reliably centrifugally than it does centripetally, because in the latter case the branching dendritic tree presents a large impedance load to the small action potential currents generated in the narrow peripheral dendrites. On the other hand, the degree and pattern of back propagation can be affected by the spatiotemporal conductance profile of the dendritic tree due to activation of intrinsic conductances or high conductance synaptic inputs.

The retrograde spikes could provide a signal to Hebbian synapses that the postsynaptic cell is active, and so trigger synaptic changes mediating learning. For example, Yuste and Denk (1995) used two-photon microscopy of hippocampal pyramidal neu-

rons to show that the centrifugal action potential invades the dendritic spines and leads to a local rise in their calcium ion concentration. The increase in calcium concentration can induce synaptic plasticity, modify NMDA receptor responses, and modify the conductance profile of the dendritic tree by activating dendritic potassium conductance (Stuart et al., 1997; Koch, 1999). The relative timing of a presynaptic spike and the retrograde postsynaptic spike can be used to drive causal associative learning (Gerstner, 1999).

The introduction of active conductances in the apical dendrite could also support anterograde signal transmission by providing amplification and linearization of synaptic inputs to the apical tuft (Bernander et al., 1994), by decomposing the dendritic tree into a number of distinct multiplicative subunits (Mel, 1993), or by supporting localized dendritic action potentials (Stuart et al., 1997). The active conductances could also amplify selective combinations of input by nonlinear multiplicative interactions (Mel, 1993). Because these effects are usually associated with increases in conductance, increasing stimulation will cause the multiplicative and subregion effects to become more localized in space and time (Mel, 1993).

Dendrites with slow active currents that are partly decoupled from the fast spike generating currents at the soma can produce a wide repertoire of temporal patterns of output spikes, including bursting (Pinsky and Rinzel, 1994; Mainen and Sejnowski, 1996). Activation of dendritic potassium conductances could also offset large dendritic input currents, so providing an adaptive mechanism to keep the dendrite in a favorable operating range (Bernander et al., 1991, 1994).

SPINES

One of the most prominent features of cortical neurons are their dendritic spines (reviewed in Chap. 1). They are the major recipients of excitatory input and play an important role in activity-dependent modification of synaptic efficacy such as LTD and LTP (for a review, see Shepherd, 1996). Although these structures have been extensively examined by light and electron microscopy, physiological data have been more difficult to obtain because of their tiny dimensions, and so their functional role is still not entirely understood. Fortunately, recent advances in imaging techniques are making it possible to measure calcium dynamics in individual spines with high time resolution (Denk et al., 1996).

The simplest views of spine function were mechanical. They were thought to be convenient physical connections whereby *en passant* axonal boutons could more easily connect to dendrites (Peters and Kaiserman-Abramof, 1970; Swindale, 1981; Anderson and Martin, 2001). More elaborate views have considered the electrical and chemical properties of the spinous connection.

ELECTRICAL MODELS

The membrane area of the spine neck is very small, and consequently little synaptic current flows through the neck membrane; most of the synaptic current injected into the spine head reaches the trunk dendrite via the spine neck. Nevertheless, the resistance to current flow through the neck is high, on the order of 100 M Ω or more (Segev and Rall, 1988). This is roughly the input resistance of a typical spiny dendrite about

half a length-constant from the soma. Therefore, the spine neck will attenuate by about half of the voltage applied at the spine head. Thus, the neck resistance could be used to control the efficacy of the synapse (Rall, 1962) and so provide a basis for synaptic plasticity (Fifkova and Anderson, 1981). The resistance could be changed by modifying the neck diameter or length (Rall, 1974a,b) or by partial occlusion of the neck by the spine apparatus (Rall and Segev, 1987).

The “twitching spine” hypothesis of Crick (1982) proposed that a change in spine length could be achieved quickly, through calcium activation of myosin and actin localized in the spine neck (Fifkova and Delay, 1982; Markham and Fifkova, 1986). In theory, a burst discharge of the excitatory afferent could raise the free calcium concentration in a spine to the level required to activate the actin (Gamble and Koch, 1987). Although it has now been shown with modern imaging methods that spines are motile on very short (seconds) time-scales (Fischer et al., 1998; Dunaevsky et al., 1999), the function of this motility is still not clear.

As discussed earlier, the calcium dynamics between spine and dendritic shaft are certainly affected by changes in spine neck dimensions (Majewska et al., 2000). Attempts to correlate changes in spine dimensions in relation to, for example, LTP induction have indicated that spines become larger but do not increase in number (Fifkova and van Harrevel, 1977; Andersen et al., 1987; Desmond and Levy, 1990). More recent studies of “on-line” imaging of spines have shown that new spines appear about 30 min after the induction of LTP (Yuste and Bonhoeffer, 2001).

Saturating Spines. The flow of synaptic current through the spine input resistance will shift the spine head potential toward the EPSP reversal potential and reduce the driving potential for the synaptic current. For small synaptic conductances, the synaptic current increases approximately linearly, but for larger synaptic conductances, the synaptic current saturates. This interdependence gives rise to a sigmoidal relationship between synaptic conductance and synaptic current. We do not know exactly where on this relationship the operating range of the neocortical synapse lies.

The spines generally receive only one excitatory synapse can be interpreted in two opposing ways, in this context. It may reflect the need to avoid saturating the synapse, or it may indicate that a single synapse on a spine always saturates the synapse, so that additional inputs would be redundant. If the synapse is driven into saturation, then the spine potential will be relatively insensitive to the exact amount of neurotransmitter delivered to the synapse. The spine head will simply turn on to a repeatable voltage level. Moreover, because the spine neck resistance is at least as large as that of the parent dendritic trunk, the spine approximates a constant current source attached to the dendrite. The synapse on the spine head is less susceptible to changes in the dendritic input resistance than is a synapse located on the dendritic trunk.

Spine Action Potentials. A special case of saturation behavior arises if the spine head membrane contains active conductances that could amplify the synaptic signal (Jack et al., 1975; Miller et al., 1985; Perkel and Perkel, 1985; Rall and Segev, 1987; Segev and Rall, 1988). Shepherd et al. (1985) and others (Rall and Segev, 1987; Baer and Rinzel, 1991) have suggested that this amplification could lead to spinous action potentials. The saltatory transmission of these action potentials from spine to spine, con-

ditional on their synaptic input, could form the basis of Boolean algebraic-like processing along the dendrite. Although these notions are attractive, the experimental evidence consistent with spiking spines has been obtained only in cerebellar Purkinje neurons (Denk et al., 1995).

Nonsaturating Spines. If the synapse on the spine is not driven into saturation but operates instead within its linear range of sensitivity, then the synapse will be particularly susceptible to nonlinear interactions with other spines. Because the resistance of the spine head membrane is much greater than the axial resistance of the neck, the dendritic potential is transferred to the spine head with little attenuation. Consequently, a depolarization of the dendritic trunk will reduce the driving potential of the spine synapse and mediate nonlinear interactions between neighboring spines. These interactions are only possible if the spines operate in their linear range. If the spines operate in saturation, then their synapse will be insensitive to modulations of local driving potential.

Inhibition on Spines. A small proportion (about 10%) of neocortical spines receive input from a type 2 (GABAergic) synapse in addition to the type 1 (excitatory) synapse (Jones and Powell, 1969; Peters and Kaiserman-Abramof, 1970; Sloper and Powell, 1979b; Somogyi et al., 1983; Beaulieu and Colonnier, 1985; Dehay et al., 1991). This arrangement raises the possibility that some excitatory inputs receive selective inhibition. Nonlinear inhibition of excitatory inputs on the same spine can be large and are essentially limited to the affected spine (Koch and Poggio, 1983). The large series resistance of the spine neck masks changes that occur in the head from the trunk dendrite and so may effectively restrict the inhibitory control to the affected spine. This specific effect has attracted much theoretical interest (Koch and Poggio, 1983; Segev and Rall, 1988) because of its computational possibilities, but only a small percentage of the excitatory input onto a single neuron could be gated in this way. It is possible that all of the spines that are controlled by an inhibitory synapse receive input from a strategically important class of afferents, such as the thalamocortical inputs for example. However, Dehay et al. (1991) have shown that this selective inhibition does not occur.

Less selective locations of inhibitory synapses may also permit strong nonlinear effects. For example, inhibitory synapses on the trunk dendrite would reduce interspine communication and could control saltatory conduction between spines (Shepherd and Brayton, 1987). This raises the possibility of enabling or disabling selected branches of dendrites. However, logical computations in spines do not necessitate inhibitory inputs. Triggering an action potential could also be conditioned by activation of the spine head synapse (e.g., the NMDA receptor is voltage dependent only if gated by neurotransmitter). If saltatory conduction were conditional on excitatory input, then this arrangement would provide an elegant means of signal gating that depends on the coincidence of excitatory inputs, rather than the interaction of excitatory and inhibitory inputs.

BIOCHEMICAL COMPARTMENTS

The strong role of calcium in synaptic plasticity and the need to localize plasticity to the activated synapse have led to the suggestion that the spines provide the necessary isolated biochemical compartment (Koch and Zador, 1993; Zador and Koch, 1994).

The spine neck limits the diffusion of calcium between the head and the dendrite. It is proposed that restriction in calcium movement through the neck arises from the calcium sink created by the calcium pumps in the neck membrane. Their activity has the effect of shortening the calcium space constant in the neck, leading to significant calcium attenuation across the neck.

Calcium could enter the head through NMDA channels, voltage-dependent calcium channels, and second-messenger channels. Studies in hippocampal neurons have provided evidence that calcium levels in the spine head are to some extent uncoupled from those in the parent dendrite (Guthrie et al., 1991; Muller and Connor, 1991; Yuste and Denk, 1995; Yuste et al., 2000). In neocortical pyramidal neurons, the decay kinetics of calcium in spines are controlled by calcium pumps in the spine and by diffusion through the neck of the spine (see earlier) (Majewska et al., 2000).

FUNCTIONAL OPERATIONS

SINGLE NEURONS OR NEURAL NETWORKS

The history of ideas of cortical function makes a fascinating account of the interplay of hypothesis and experiment (Martin, 1988). In particular, the experimental results from microelectrode recordings from single cortical units (neurons) have had a deep influence on our ideas of cortical function. Much of the motivation for studying the functional properties of single units in the cortex in such detail arises from the fact that the activities of cortical neurons are thought to describe the world and so to reflect our subjective experiences. However, the nature of the encoding used by the neurons to represent the world is still a matter of intense and interesting debate.

The encoding problem is important because it determines to a large extent the success with which the nervous system can interact with the world. It is clear that the attributes of the world must be encoded in the variables of the nervous system. If the neural encoding is suitable, then the nervous system will be able to well represent the world, and the efficiency interactions with the physical world will be enhanced. For example, in artificial neural networks, learning and generalization improve with the quality of data representation.

One central question is whether the nervous system uses a data representation in which the encoding of objects is distributed across many neurons or whether the representation is localized. This debate is usually couched in the domain of perception. There the question is whether the discharge of a combination of neurons, or the discharge of just one neuron, reflects the experience of a percept. These opposing views of the operation of cortex have a long and distinguished history. Sherrington (1941), for example, contrasted the notion of “one ultimate pontifical nerve-cell . . . [as] the climax of the whole system of integration [with the concept of mind as] a million-fold democracy, whose each unit is a cell.”

The case for localized encoding has been formalized in the *neuron doctrine* proposed by Barlow (1972). He proposed five dogmas that encapsulate the powerful idea that percepts are the product of the activity of certain individual cortical neurons, rather than by some more complex (and obscure) properties of the combinatorial rules of the usage of nerve cells. The force of Barlow’s thesis in molding our ideas is evident in most textbooks of psychology and neurobiology, which are well stocked with illustra-

tions showing how the specificity of neurons arises from a hierarchical sequence of processing through the cortical circuits.

Recently, the pendulum has begun to swing back. The antithetical proposition that perceptual processing occurs through the collective properties of parallel cortical networks rather than through the activity of single units has been receiving close attention from theoreticians working on *neural networks* or *connectionist* models of cortical function. Results obtained from computer simulations of these hypothetical nerve circuits have led to a model of cortical function that is quite different from that proposed in the neuron doctrine.

The dialectic of the one versus many neurons is best considered in the context of the visual system, where the physiology and anatomy are known in greatest detail and where the behavioral performance is well established.

SINGLE NEURONS OR NEURAL NETWORKS?

It is evident that visual perception is a complex task. We need not only to determine the form, movement, and position in space of the objects we encounter but also to recognize them as being particular objects. Solving this key problem was central to Barlow's development of the neuron doctrine. He proposed that the primary visual cortex dealt only with the elemental building blocks of perception, the detection of orientated line segments, or the local motion of these segments, for example. To build these responses into neurons that were selective for a cat, chair, or grandmother, he proposed a hierarchical sequence of processing within single cortical areas and through the many visual areas. Thus, the *grandmother* cell scheme is essentially a classification network in which the input is classified according to which output neuron is activated. In nervous systems, the classification occurs in a hierarchical network. The neurons at each stage of the hierarchy become progressively more selective to the attributes of the stimulus, so that while the neurons in the primary visual cortex would respond to many objects, neurons at the highest level of the hierarchy would respond only to particular objects. Barlow (1972) suggested that the activity of about 1000 of these high-level *cardinal* neurons would be sufficient to represent a single visual scene. Because the number of possible percepts is very large, however, the total number of cardinal cells would have to be a substantial fraction of the 10^{10} cells of the human brain (Barlow, 1972).

The single neuron representation faces two major difficulties: poor generalization and limited encoding capacity. If individual objects are very specifically encoded by single neurons, then it is difficult for the neurons to generalize their classification to novel intermediate cases. For example, given only a "red apple" neuron and a "green apple" neuron, how does the nervous system respond to a yellow apple? Either it must quickly recruit a new neuron with very similar connections and assign it to yellow apples, or the yellow apple percept must arise from some combination of the activity of the "red" and "green" neurons, in which case the single cell-encoding hypothesis is weakened. Moreover, if new neurons must be recruited for each new feature (such as yellow) that is added to the classification scheme, then the number of neurons required to encode selectively the various combinations of features increases explosively and soon exceeds the number of neurons available.

Despite these difficulties, selective encoding representation has remained a popular implicit hypothesis in experimental neuroscience. Since 1972, many of the visual areas

beyond area 17 have been explored in some detail. Efforts to discover whether cardinal cells reside in these visual areas have met with mixed success. In most areas, the stimulus requirements for activating neurons are not very different in quality from those for area 17. If anything, the requirements are less restrictive, in that only a single property of the stimulus might be important, such as its direction of motion, or color, or depth in visual space. Only in the primate inferotemporal region of cortex have neurons with higher-order properties been found (Gross et al., 1972). These neurons respond preferentially to parts of the body, especially faces, although they respond to other visual stimuli as well (Gross et al., 1972; Bruce et al., 1981; Richmond et al., 1983; Young and Yamane, 1992). Other cells in the inferotemporal region have large receptive fields that respond quite specifically to complex shapes, but close neighbors tend to respond to similar features (Miyashita, 1988; Miyashita and Chang, 1988; Tanaka et al., 1991; Fujita et al., 1992). Neurons in these areas appear to “learn” specific complex stimuli.

Direct examination of neuronal responses involved in the perceptual foundation of a decision process (Salzman and Newsome, 1994; Shadlen and Newsome, 1996) have also brought some support for the cardinal cell view. It appears that in the motion discrimination task, the reliability of the animal’s decision is not much better than that of a single observed neuron, which argues against the view that the animal bases its decision on an average across many neurons.

Nevertheless, the general conclusion from the many studies that have examined encoding is that individual neurons do not respond completely selectively to single *trigger features*. Instead, each neuron is sensitive to a number of different stimulus characteristics, such as contrast, dimension, depth, and orientation. Single cortical neurons appear unable to signal unambiguously the presence of a particular stimulus, and therefore cannot act as cardinal cells. An important reason why such cardinal cells are not found may lie in the basic organization of the cortical circuitry, which expresses much stronger lateral and recurrent interactions between neurons than is expected of a feedforward classification network.

NEW DESIGNS FOR THE VISUAL CIRCUITS

When Barlow proposed his neuron doctrine in 1972, the modern study of cortical microcircuitry was in its infancy. Anatomical studies had emphasized the vertical, columnar structure of cortex. This view was reinforced by many electrophysiological studies, which showed vertical functional columns. Technical advances since the late 1970s have resulted in a wealth of new information about the cortical microcircuitry. The technique of intracellular labeling of neurons has revealed an extensive system of horizontal connections within the cortex. Certain markers such as horseradish peroxidase or biocytin fill the entire axonal arborization, including the boutons, and so estimates of the number and spatial distribution of the synapses made by a single neuron are now evident for the first time. The horizontal spread of connections means that each point in cortex is covered by axons of a very large number of neurons. For example, estimates for the number of geniculate X cells (see Chap. 8) that provide input to any point in cat area 17 range from 400 to 800 (Freund et al., 1985), whereas the figure for Y cells may be even higher. The geniculate axons form less than 10% of the excitatory synapses on spiny stellate neurons in layer 4 (Ahmed et al., 1994) (see Synaptic Con-

nections), so the number of cortical neurons providing the input to a single point must be considerably higher. Because one cortical neuron supplies only a few synapses to any other cortical neuron, each neuron can potentially be activated by hundreds of other neurons. It is this highly divergent and convergent connectivity that is the feature of neocortex, and it differs considerably from that of the lateral geniculate nucleus (see Chap. 8), where there is a much tighter coupling between neurons.

The widespread and rich connections of the thalamic afferents ensure that even the smallest detectable disturbance of the retinal receptor layer—for example, that induced by a dim flash of light—alters the probability of firing of thousands of cortical neurons in the primary visual cortex. The signal is then amplified by the divergent axonal arbors of the cortical neurons, which ensure that many thousands more neurons are activated both within area 17 and in the other cortical areas to which these neurons project. Thus, although there certainly is the convergence of many inputs that is required to create the cardinal cells, the considerable divergence of the connections of each neuron ensures the simultaneous activation of many neurons. In such a context it is difficult to see that the activity of any single neuron can be completely isolated from that of its companions to signal a unique percept. Instead, the combined activity of large numbers of cortical neurons seems more likely to be the basis of our perceptual experience. However, distributed representations have problems of their own, such as the ambiguity of interpretation when a particular neuron is permitted to respond in more than a single context. For example, many neurons may implement the distributed encoding of apples, and some common fraction of these will be activated by particular red, yellow, and green apples. If this common fraction is activated in a number of different contexts, what is the unique neural object that defines a particular apple? von der Malsburg (1981) has proposed that the population of neurons activated by the stimuli of a particular physical object are bound together transiently by a common physiological process. One possibility is that the 40-Hz oscillation of discharge observed in cortical neurons reflects such a binding process (Gray and Singer, 1989; Crick and Koch, 1992; Singer, 1994).

PARALLEL PROCESSING IN NEURAL NETWORKS

It is evident from the preceding discussion that normal vision involves the activity of very large numbers of cortical neurons. These large numbers do not simply reflect redundancy, which an efficient coding must avoid, but rather are a necessary part of perception. This is evident in the example of color vision, where both behavioral and theoretical studies show that the relative stability of the perceived color of objects in the face of changing illumination (e.g., moving from indoors to outdoors) requires the comparison of the reflected wavelengths over a large region of the visual field (Jameson and Hurvich, 1959; Land, 1959a,b; Land, 1983). This phenomenon of color constancy necessarily involves the coordinated activity of large numbers of cortical neurons. Similar considerations apply in the case of binocular vision, where two slightly different views of the same complex scene must be fused to produce a single vision and stereopsis. Attempts to replicate this performance have shown that it is a difficult task (Marr and Poggio, 1979; Mahowald, 1994), yet we fuse the image and extract the exact three-dimensional information effortlessly and far more rapidly than can any computer. One reason for this difference is that the strict hierarchy of serial processing used

by computers with von Neumann architecture is slow. In the cerebral cortex, by contrast, the higher degree of divergence in the connections makes it likely that much of the processing occurs simultaneously through parallel pathways. Of course, computers have transistors that can generate digital impulses at very high rates and transmit them at the speed of light to perform their computations. By comparison, neurons generate impulses at very low rates and transmit them at speeds of meters per second. However, the neocortex makes many connections to and from each neuron, whereas the limitations of size and thickness mean that silicon components have limited connectivity. Thus, advantages of speed are offset against limited connectivity.

The increase in speed offered by parallel processing has been exploited in a number of models of visual processing based on feedforward artificial neural networks. The most common form of feedforward network is composed of three layers of highly abstract neurons whose activity typically varies between 0 and 1. A first layer, or *input layer*, connects extensively to units of a second, *hidden layer*, which in turn sends its output to the third, *output layer*. The sensory input is applied via the input layer. The responses of units in the hidden and output layers are determined by summing activities of all the units in the previous layer. The effect of each of the inputs is governed by a synaptic *weight*, which may be positive (excitatory) or negative (inhibitory). The values of these weights determine what functions of the input the network can compute, and so what overall task the network performs. These weights may be specified directly, but more often they are organized by a learning algorithm, such as *back propagation* (Rumelhart and McClelland, 1986; Anderson, 1995; Hertz et al., 1991). Such networks turn out to be powerful and are capable of solving some of the perceptual problems of depth, form, and motion perception (Lehky and Sejnowski, 1988; Zipser and Andersen, 1988).

ARE NEURAL NETWORKS LIKE CORTICAL CIRCUITS?

The neural network models, besides being functionally successful, have a strong appeal because of their superficial resemblance to the structure of the cortex: they are layered and have highly interconnected units. However, this superficial resemblance should be examined more critically in the light of our knowledge of the structure of area 17. The basic circuit of Fig. 12.18 illustrates some of the main neuronal components and their connections within area 17. Comparing this figure with the feedforward neural network of Fig. 12.17 shows a number of similarities. The first layer in the neural network corresponds to the map of the geniculate terminals, the second layer units to the neurons in layer 4 that project to the superficial layers, and the third to the pyramidal neurons projecting from cortical layers 2 and 3. In respect of this laminar organization, the pattern of the model corresponds to that of cortex in that very few neurons of layer 4 provide an output to other cortical areas, whereas a large proportion (70%) of the pyramidal neurons in layers 2 and 3 do project to other areas. However, it is evident at a glance that the organization of cortex shown in Fig. 12.18 is in many important respects different from the neural network circuit of Fig. 12.17.

Unlike the neural network, the primate visual cortex receives at least two physiologically and anatomically distinct inputs from the thalamus, which are laminar specific. The cortex has twice as many or more layers, particularly if the subdivisions of the six basic layers are taken into account. This may be a requirement of the cortex to

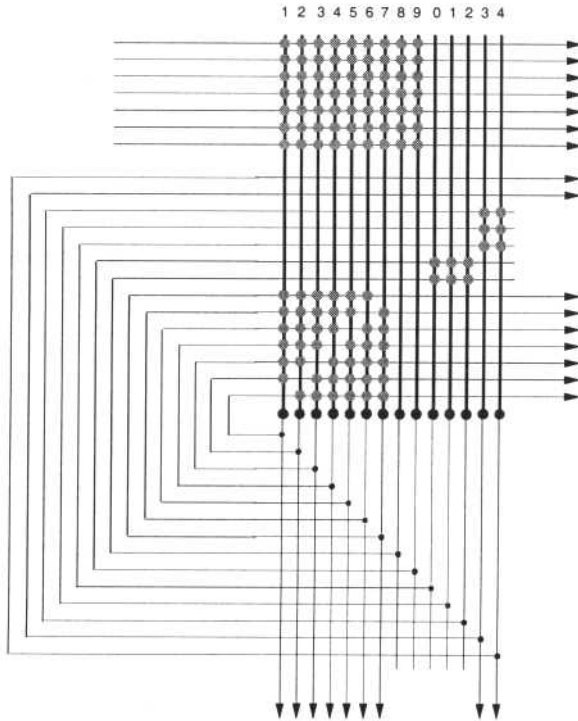


Fig. 12.17. A hypothetical cortical neuronal network composed of two subnetworks; one feedforward and the other feedback. Neurons of the network (black) receive input synapses (gray circles) onto their dendrites (thick black vertical lines). The effects of these neurons are integrated into the neuronal somata (black circles), and their outputs are transmitted along their axons (thin black lines). Branch points of the axons are indicated as small black dots on the axons. The neurons are numbered from 1 to 14. Feedforward inputs enter via the seven horizontal axons above. Feedforward network: the feedforward inputs synapse with the first layer of cortical neurons (8 and 9), which project to the second layer (10–12) and thence to the final layer (13 and 14) whose outputs project out of this region of cortex. The intermediate computations of this entirely feedforward network are unaffected by connections between cells in the same layer or by backward projections from later layers. Feedback network: The feedforward inputs synapse with the distal dendrites of the recurrently connected population of neurons (1–7). Their axons synapse with all other members of their population (but not with themselves). In this case, the evolving response of each neuron comes to influence the computations of its fellows. The overall computation is iterative in quality and finds a solution that is, in some sense, a consensus among the cooperating neurons. The state of the population is transmitted out of this region of cortex.

divide its output destinations (“addresses”) into laminar specific zones. However, the internal connectivity and physiology differ in different layers, indicating that there may be important differences in the processing within layers. In contrast to the units within a single layer of the neural network, there are extensive lateral connections within a single lamina or sublamina of cortex. Thus, the local connectivity of cortical neurons resembles that of a “Hopfield” recurrent network, but with the notable difference that synaptic interactions between two neurons are not symmetrical as required for a pure

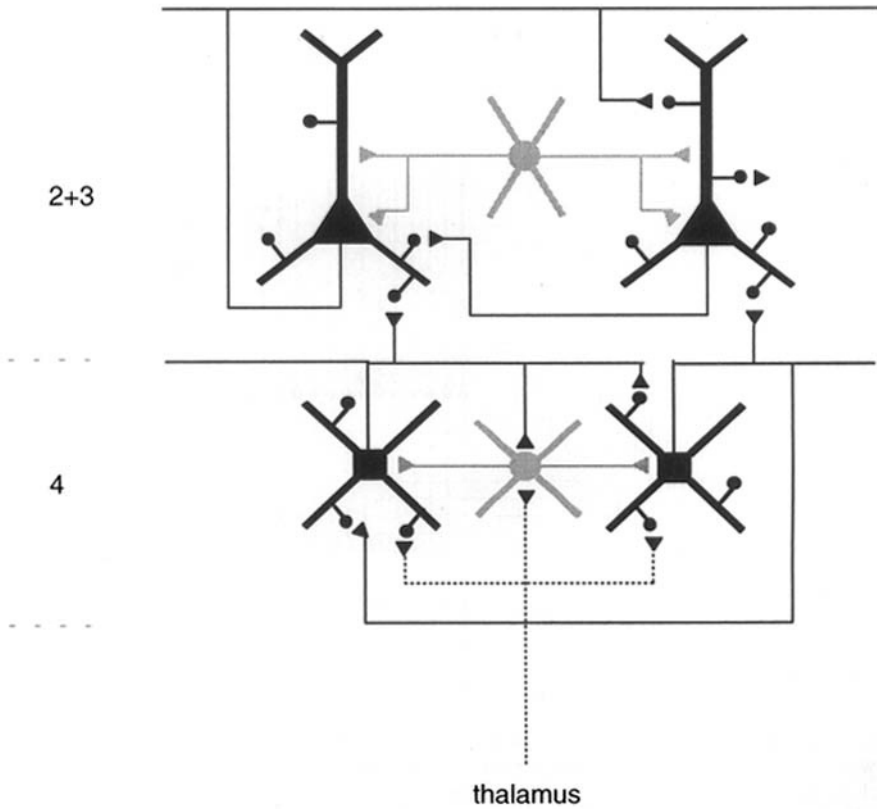


Fig. 12.18. Possible recurrent connections in neocortex. This figure is an elaboration of Figs. 12.15 and 12.14. The feedforward thalamic inputs synapse with spiny stellate neurons and a small basket cell in layer 4. Some of the spiny stellate connections are recurrent to other spiny stellates. They also synapse onto superficial pyramidal neurons that in turn have recurrent connections with one another.

Hopfield network (Hopfield, 1982, 1984). This similarity of cortical networks to artificial recurrent networks is useful, because it offers a partial explanation for how cortical circuits could interpret their inputs. The model shows how output patterns can be stored as the dynamical attractors of the network by setting the strengths of all the network connections appropriately. External input initializes the network dynamics, which then retrieves a stored memory by converging to the attractor that most nearly matches the pattern of external input.

Unlike typical recurrent artificial neural networks the cortical ones are not fully connected. Instead, they are quite sparsely connected. Similarly, the interconnections between cortical laminae are highly specific and do not simply connect adjacent layers as in the units of the neural network. Both the vertical and the lateral connections in the cortex are clustered, focusing on discrete zones. This columnar structure is a feature of cortical organization, but it is the exception rather than the rule to incorporate such horizontal organization within network models.

STATIC AND DYNAMIC CONNECTIVITY

Both the neuroanatomical diagram shown in Fig. 12.18 and the neural network circuit of Fig. 12.17 depict the static connectivity between neurons in the respective networks. It is clear from the above discussions of the physiology of the various cortical neuronal types and their synapses that the static connectivity only sets the most fundamental constraint on what kinds of interactions are *possible* within the network. The dynamic, functional connectivity of the network may differ very significantly from its static counterpart. These dynamic circuit changes have important consequences for signal processing.

For example, the spike discharge gain of a neuron with respect to a presynaptic neuron depends not only on its intrinsic feedforward gain but also on feedback activation that it receives from the network in which it is embedded. If the feedback signal is well correlated with the input, then the presynaptic signal can be strongly amplified. Thus, the neurons response to presynaptic input depends on a context offered by the embedding network. Even if all synaptic strengths between neurons of the network are kept fixed, the effective strength of feedback is variable. The variation arises because the neurons of the network are partitioned into two disjoint sets: those that are above threshold and active and those that are below threshold and inactive. The effective strength of feedback depends only on the synaptic connections between active neurons, as only they participate in feedback loops (Hahnloser et al., 2000). However, the synaptic strengths of active neurons are not fixed: dynamic synapses transmit different aspects of presynaptic activity depending on the pattern of activity and synaptic parameters (Markram, 1998; Tsodyks et al., 1998; Tarczy-Hornoch et al., 1998). Thus, the effective connectivity of the network changes with time, because individual neurons fall beneath an inhibitory threshold and so no longer activate their group output synapses, and also because the effect of an individual activated synapse depends also on the pattern of its past activations (Fig. 12.19). Novel network scale activity detection methods with high temporal and spatial resolution will be required to characterize the relationship between the static and dynamic connectivity.

It is somewhat surprising, given the intensity of cortical research, that the rules of even the static connectivity for neocortex have still to be discovered. At this stage we know that the different types of neurons connect with some degree of specificity to particular regions of other neurons, e.g., dendritic shafts or spines, but whether single neuron-to-single neuron connections are specified is still quite unclear. At this stage it seems likely that neurons do not connect on a point-to-point basis. Rather, they connect on a point-to-zone basis, targeting particular subsets of neurons within a zone.

The point is readily made that these and other differences show that the artificial neural networks are different in important respects from the cerebral cortex. Finally, artificial *neural* networks are not really very neural. They are just networks operating according to a specific algorithm, and it would be rash to press their analogy to cortical circuits too far. Nevertheless, the potential usefulness of network models that are biologically based cannot be overestimated. The major problem lies in trying to bridge the gap between experimental data and theory. Our knowledge of the structure of the cortical microcircuitry outstrips our understanding of the function of these circuits. This disparity, together with the sheer complexity of the cortical circuits, is a significant barrier to moving from networks that are simply *neurally inspired* to those that actually

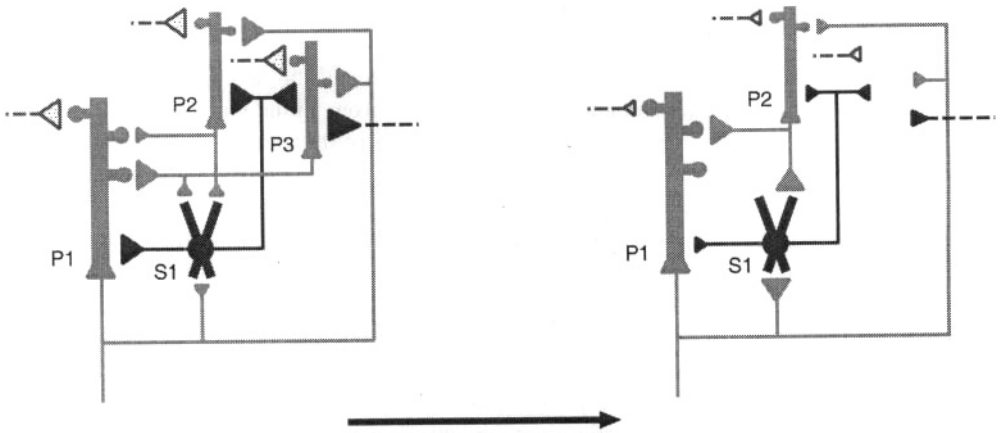


Fig. 12.19. Simplified schematic representation of dynamical changes in the functional connectivity of a hypothetical cortical network, showing how a circuit might reconfigure itself during processing. P1–3, pyramidal neurons; S1, smooth neuron. Left initial state; right, final state, later in time. The size of a synapse represents its strength. Input is delivered via the three stippled synapses, which depress over time. The connections between neuron P1 and its pyramidal targets (P2, P3) also depress, whereas its synapse with the smooth neuron S1 facilitates. P3 is similar to P1. However, the combination of local and external inhibition drive this neuron below threshold, and so it no longer participates in the circuit. P2 is an example of a pyramidal neuron whose P-to-P synapse facilitates. In this example, all of the smooth cell synapses depress.

incorporate basic features of the biology. To achieve this step, the cortical connections shown in Fig. 12.15, and their associated physiology, have to be simplified. Given the outline of the preceding sections, one such simplification can now be suggested (Fig. 12.20). The form of this “canonical” circuit was arrived at from an analysis of the structure and function of local circuits in the visual cortex (Douglas et al., 1989, 1995; Douglas and Martin, 1991). However, an analysis of the circuits of other cortical structures such as the olfactory cortex (paleocortex) and hippocampus (archicortex) reveals that they, too, bear many resemblances to the circuits of the neocortex (Shepherd, 1988b,a). Thus, it is tempting to suppose that there may be some common basic principles that underly the organization and operation of all cortical circuits, reflecting the principles of synaptic circuit design outlined in Chap. 1.

A CANONICAL CORTICAL CIRCUIT

From the anatomy, several components and connections seem to dominate in most cortical areas (see Fig. 12.20). Any realistic model must separate inhibitory (GABAergic) and excitatory neurons into distinct populations. The excitatory group (80% of the cortical neurons) can be subdivided into two major pools, one being found in the granular and supragranular layers (layers 2–4), and the other in the deep layers (layers 5 and 6). Although these groups are extensively interconnected, this division is made because their outputs are distinct, and because inhibition appears to be stronger in the deep layers (Douglas et al., 1989). The different types of GABAergic smooth neurons cannot

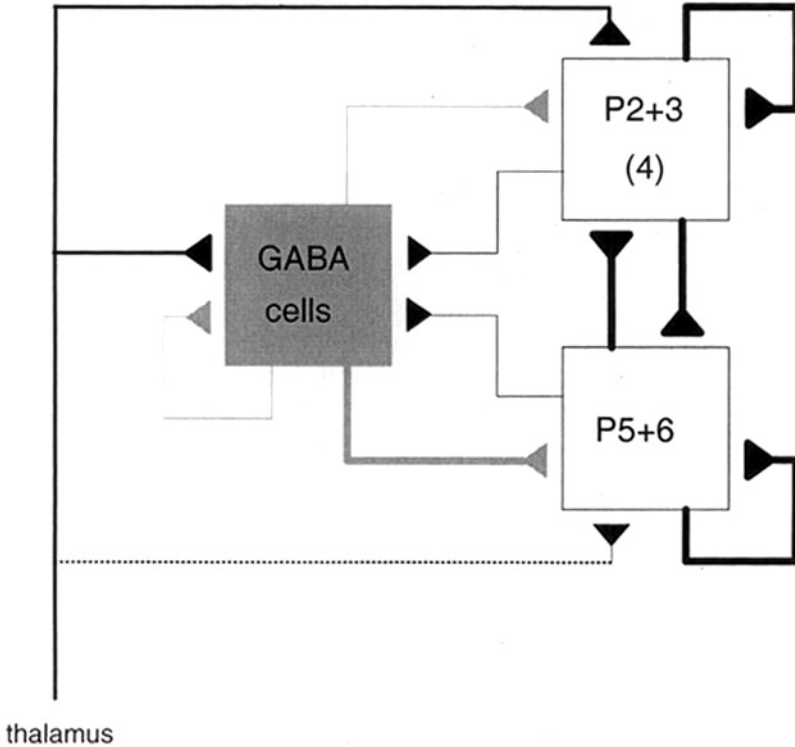


Fig. 12.20. The canonical microcircuit for striate cortex. Three populations of neurons interact with one another: One population is inhibitory (GABAergic cells, gray synapses), and two are excitatory (black synapses) representing superficial (P2 + 3) and deep (P5 + 6) pyramidal neurons. The properties of layer 4 stellates (4), which contribute 10% of neurons in granular cortex (less elsewhere), are similar to those of the superficial pyramids. The thickness of the connecting lines indicates the functional strength of the input. Note that the dominant connection is between excitatory neurons, so that a relatively weak thalamic input can be greatly amplified by the recurrent excitation of the spiny neurons.

yet be distinguished on functional grounds; they are therefore represented in the diagram of Fig. 12.20 by a single population.

Neurons within each division form connections with other members of that division. The dominant interlaminar connections are between the superficial and deep layer groups of spiny neurons, whereas the inhibitory neurons connect across the laminae to both groups of spiny neurons. All three groups receive direct activation from the thalamic afferents, but because the thalamic input provides only about 10% of the excitatory input, 90% of the excitation is provided here by intracortical connections between pyramidal neurons. This recurrent excitation may provide selective amplification of geniculate input (Douglas et al., 1989, 1995). Such intracortical amplification provides the basis for a number of recent models of cortical computation (Mahowald, 1994; Ben-Yishai et al., 1995; Douglas et al., 1995; Somers et al., 1995; Suarez et al., 1995).

Inhibition acts by modulating the recurrent excitation and so is effective even though it may be relatively weak (Douglas et al., 1995).

The excitatory neurotransmitters act on two major receptor types, the NMDA and non-NMDA receptors. The inhibitory neurotransmitter GABA acts via the GABA_A and the GABA_B receptors. These distinctions are made because the receptor types have distinctly different kinetics. The biophysical characteristics of the cortical neurons, as outlined in the previous sections, also need to be incorporated to give the appropriate response characteristics.

This recurrent excitation model provides the minimum specifications that seem necessary for basic cortical circuits, based on our present level of knowledge. The form of this simplified model is sufficiently general that it can be applied equally well to visual cortex as to motor cortex, and as such has the properties of a canonical circuit. This circuit forms only a basic building block. Obviously, each cortical area has individual features that need to be incorporated. However, simplicity encourages the convergence of theory and biology through common models, and such convergence is imperative if we are to understand how the synaptic organization of the neocortex produces the complexity of cortical function.

REFERENCES

- Abbot, L. 2001. The timing game. *Nat. Neurosci.* 2: 115–116.
- Abbott, L.F., Varela, J.A., Sen, K., and Nelson, S.B. 1997. Synaptic depression and cortical gain control. *Science* 275: 220–224.
- Abercrombie, E.D., and DeBoer, P. 1997. Substantia nigra D1 receptors and stimulation of striatal cholinergic interneurons by dopamine: a proposed circuit mechanism. *J. Neurosci.* 17: 8498–8505.
- Abramson, B.P., and Chalupa, L.M. 1985. The laminar distribution of cortical connections with the tecto- and cortico-recipient zones in the cat's lateral posterior nucleus. *Neuroscience* 15: 81–95.
- Ache, B.W. 1994. Towards a common strategy for transducing olfactory information. *Semin. Cell Biol.* 5: 55–64.
- Acsady, L., Kamondi, A., Sik, A., Freund, T., and Buzsaki, G. 1998. GABAergic cells are the major postsynaptic targets of mossy fibers in the rat hippocampus. *J. Neurosci.* 18: 3386–3403.
- Acuña, C., Cudeiro, J., Gonzalez, F., Alonso, J.M., and Perez, R. 1990. Lateral-posterior and pulvinar reaching cells—comparison with parietal area 5a: a study in behaving *Macaca nemestrina* monkeys. *Exp. Brain Res.* 82: 158–166.
- Adams, J.C. 1976. Single unit studies on the dorsal and intermediate acoustic striae. *J. Comp. Neurol.* 170: 97–106.
- Adams, J.C. 1979. Ascending projections to the inferior colliculus. *J. Comp. Neurol.* 183: 519–538.
- Adams, J.C. 1983. Multipolar cells in the ventral cochlear nucleus project to the dorsal cochlear nucleus and the inferior colliculus. *Neurosci. Lett.* 37: 205–208.
- Adams, J.C. 1997. Projections from octopus cells of the posteroventral cochlear nucleus to the ventral nucleus of the lateral lemniscus in cat and human. *Auditory Neurosci.* 3: 335–350.
- Adams, P. 1982. Voltage-dependent conductances of vertebrate neurones. *Trends Neurosci.* 2: 116–119.
- Adams, P.R., and Galvan, M. 1986. Voltage-dependent currents of vertebrate neurons and their role in membrane excitability. *Adv. Neurol.* 44: 137–170.
- Adkins, P.T., Surmeier, D.J., and Kitai, S.T. 1990. Muscarinic modulation of a transient K⁺ conductance in rat neostriatal neurons. *Nature* 344: 240–242.
- Adrian, E.D. 1942. Olfactory reactions in the brain of the hedgehog. *J. Physiol. (Lond.)* 100: 459–473.
- Adrian, E.D. 1950. The electrical activity of the mammalian olfactory bulb. *Electroencephalogr. Clin. Neurophysiol.* 2: 377–388.
- Adrian, E.D. 1953. Sensory messages and sensation. The response of the olfactory organ to different smells. *Acta Physiol. Scand.* 29: 5–14.
- Aghajanian, G.K. 1985. Modulation of a transient outward current in serotonergic neurones by alpha₁-adrenoceptors. *Nature* 315: 501–503.
- Agmon-Snir, H., and Segev, I. 1992. Signal delay and propagation velocity in passive dendritic structures. *J. Neurophysiol.* 70: 2066–2085.
- Ahlsén, G., Lindström, S., and Lo, F.-S. 1984. Inhibition from the brainstem of inhibitory interneurons of the cat's dorsal lateral geniculate nucleus. *J. Physiol. (Lond.)* 347: 539–609.
- Ahmed, B., Anderson, J.C., Douglas, R.J., Martin, K.A.C., and Nelson, J.C. 1994. Polyneuronal innervation of spiny stellate neurons in cat visual cortex. *J. Comp. Neurol.* 341: 39–49.

- Ahmed, B., Anderson, J.C., Martin, K.A.C., and Nelson, J.C. 1997. Map of the synapses onto layer 4 basket cells of the primary visual cortex of the cat. *J. Comp. Neurol.* 380: 230–242.
- Ahnelt, P., Keri, C., and Kolb, H. 1990. Identification of pedicles of putative blue-sensitive cones in the human retina. *J. Comp. Neurol.* 293: 39–53.
- Alagarsamy, S., Sorensen, S.D., and Conn, P.J. 2001. Coordinate regulation of metabotropic glutamate receptors. *Curr. Opin. Neurobiol.* 11: 357–362.
- Albuquerque, E.X., Peieira, E.F., Castro, N.G., and Alkondon, M. 1995. Nicotinic receptor function in the mammalian central nervous system. *Ann. N.Y. Acad. Sci.* 757: 48–72.
- Albus, J.S. 1971. A theory of cerebellar function. *Math. Biosci.* 10: 25–61.
- Alexander, G.E., DeLong, M.R., and Strick, P.L. 1986. Parallel organization of functionally segregated circuits linking basal ganglia and cortex. *Ann. Rev. Neurosci.* 9: 357–381.
- Alger, B.E., Dhanjal, S.S., Dingledine, R., Garthwaite, J., Henderson, G., King, G.L., Lipton, P., North, A., Schwartzkroin, P.A., Sears, T.A. et al. 1984. Brain slice methods. In: *Brain Slices* (Dingledine, R., ed.) New York: Plenum Press, pp. 381–437.
- Alger, B.E., and Nicoll, R. 1982. Feed-forward dendritic inhibition in rat hippocampal pyramidal cells studied in vitro. *J. Physiol. (Lond.)* 328: 105–123.
- Alibardi, L. 1998. Ultrastructural and immunocytochemical characterization of neurons in the rat ventral cochlear nucleus projecting to the inferior colliculus. *Ann. Anat.* 180: 415–426.
- Allen, C., and Stevens, C.F. 1994. An evaluation of causes for unreliability of synaptic transmission. *Proc. Natl. Acad. Sci. U.S.A.* 91: 10380–10383.
- Allison, A.C. 1953. The morphology of the olfactory system in the vertebrates. *Biol. Rev.* 28: 195–244.
- Altschuler, R.A., Betz, H., Parakkal, M.H., Reeks, K.A., and Wenthold, R.J. 1986. Identification of glycinergic synapses in the cochlear nucleus through immunocytochemical localization of the postsynaptic receptor. *Brain Res.* 369: 316–320.
- Alvarez, F., Dewey, D.E., Harrington, D.A., and Fyffe, R.E.W. 1997. Cell-type specific organization of glycine receptor clusters in the mammalian spinal cord. *J. Comp. Neurol.* 379: 150–170.
- Alvarez, F., Dewey, D.E., McMillan, P., and Fyffe, R.E.W. 1999. Distribution of cholinergic contacts on Renshaw cells in the rat spinal cord: a light microscopic study. *J. Physiol. (Lond.)* 515: 787–797.
- Alvarez, F., Pearson, D., Harrington, D., Dewey, D., Torbeck, L., and Fyffe, R. 1998. Distribution of 5-hydroxytryptamine-immunoreactive boutons on α -motoneurons in the lumbar spinal cord of adult cats. *J. Comp. Neurol.* 393: 69–83.
- Alvarez, V.A., Chow, C.C., Van Bockstaele, E.J., and Williams, J.T. 2002. Frequency-dependent synchrony in locus ceruleus: role of electrotonic coupling. *Proc. Natl. Acad. Sci. U.S.A.* 99: 4032–4036.
- Alvarez-Leefmans, F., Nani, A., and Marquez, S. 1998. Chloride transport, osmotic balance and presynaptic inhibition. In: *Presynaptic Inhibition and Neural Control*. (Rudomin, P., Romo, R., and Mendell, L., eds.) New York: Oxford University Press, pp. 50–79.
- Amaral, D.G. 1978. A Golgi study of the cell types in the hilar region of the hippocampus in the rat. *J. Comp. Neurol.* 182: 851–914.
- Amaral, D.G. 1979. Synaptic extensions from mossy fibers of fascia dentata. *Anat. Embryol.* 155: 241–251.
- Amaral, D.G. 1993. Emerging principles of intrinsic hippocampal organization. *Curr. Opin. Neurobiol.* 3: 225–229.
- Amaral, D.G., and Dent, J.A. 1981. Development of the mossy fibers of the dentate gyrus: I. A light and electron microscopic study of the mossy fibers and their expansions. *J. Comp. Neurol.* 195: 51–86.
- Amaral, D.G., Dolorfo, C., and Alvarez-Royo, P. 1991. Organization of CA1 projections to the subiculum: a PHA-L analysis in the rat. *Hippocampus* 1: 415–436.

- Amaral, D.G., Insausti, R., and Cowan, W.M. 1984. The commissural connections of the monkey hippocampal formation. *J. Comp. Neurol.* 224: 307–336.
- Amaral, D.G., Ishizuka, N., and Claiborne, B. 1990. Neurons, numbers and the hippocampal network. In: *Progress in Brain Research, Understanding the Brain Through the Hippocampus: The Hippocampal Region as a Model for Studying Structure and Function* (Storm-Mathisen, J., Zimmer, J., and Ottersen, O.P., eds.) Amsterdam: Elsevier, pp. 1–11.
- Amaral, D.G., and Kurz, J. 1985. An analysis of the origins of the cholinergic and noncholinergic septal projections to the hippocampal formation of the rat. *J. Comp. Neurol.* 240: 37–59.
- Amaral, D.G., and Witter, M. 1995. Hippocampal formation. In: *The Rat Nervous System* (Paxinos, G., ed.) San Diego: Academic Press, pp. 443–493.
- Amaral, D.G., and Witter, M.P. 1989. The three dimensional organization of the hippocampal formation: a review of anatomical data. *Neuroscience* 31: 571–591.
- Ambros-Ingerson, J., Granger, R., and Lynch, G. 1990. Simulation of paleocortex performs hierarchical clustering. *Science* 247: 1344–1348.
- Amthor, F.R., and Grzywacz, N.M. 1993. Directional selectivity in vertebrate retinal ganglion cells. *Rev. Oculomot. Res.* 5: 79–100.
- Amthor, F.R., Takahashi, E.S., and Oyster, C.W. 1989a. Morphologies of rabbit retinal ganglion cells with concentric receptive fields. *J. Comp. Neurol.* 280: 72–96.
- Amthor, F.R., Takahashi, E.S., and Oyster, C.W. 1989b. Morphologies of rabbit retinal ganglion cells with complex receptive fields. *J. Comp. Neurol.* 280: 97–121.
- Andersen, P., Eccles, J.C., and Voorhoeve, P.E., 1964. Postsynaptic inhibition of cerebellar Purkinje cells. *J. Neurophysiol.* 27: 1138–1153.
- Andersen, J.P., and Bittar, E.E. 1998. Ion pumps. *Adv. Mol. Cell Biol.* 23.
- Andersen, P., Blackstad, T., Hulleberg, G., and Al, E. 1987. Changes in spine morphology associated with LTP in rat dentate granule cells. *Proc. Physiol. Soc.* 50: 288.
- Andersen, P., Bliss, T.V.P., and Skrede, K. 1971. Lamellar organization of hippocampal excitatory pathways. *Exp. Brain Res.* 13: 222–238.
- Andersen, P., Eccles, J.C., and Loynig, Y. 1964a. Location of postsynaptic inhibitory synapses on hippocampal pyramids. *J. Neurophysiol.* 27: 592–607.
- Andersen, P., Eccles, J.C., and Voorhoeve, P.E. 1964b. Postsynaptic inhibition of cerebellar Purkinje cells. *J. Neurophysiol.* 27: 1139–1153.
- Anderson, A.J. 1995. *An Introduction to Neural Networks*. Cambridge, MA: Bradford Books.
- Anderson, J., and Martin, K. 2001. Does bouton morphology optimize axon length? *Nat. Neurosci.* 4: 1166–1167.
- Anderson, J.A. 1970. Two models for memory organization using interacting traces. *Math. Biosci.* 8: 137–160.
- Anderson, J.A. 1972. A simple network generating an interactive memory. *Math. Biosci.* 14: 197–220.
- Anderson, J.A. 1995. *An Introduction to Neural Networks*. Cambridge, MA: Bradford Books.
- Anderson, J.C., Douglas, R., Martin, K.A.C., Nelson, C., and Whitteridge, D. 1994. Synaptic output of physiologically identified spiny neurons in cat visual cortex. *J. Comp. Neurol.* 341: 16–24.
- Anderson, O.S., and Koeppe, R.E.I. 1992. Molecular determinants of channel function. *Physiol. Rev.* 72 (Suppl.): S89–S158.
- Andrasfalvy, B.K., and Magee, J.C. 2001. Distance-dependent increases in AMPA receptor number in the dendrites of adult hippocampal CA1 pyramidal neurons. *J. Neurosci.* 21: 9151–9159.
- Andres, K. 1965. Der Feinbau des Bulbus Olfactorius der Ratte unter besonderer Berücksichtigung der Synaptischen Verbindungen. *Z. Zellforsch. Mikrosk. Anat.* 65: 530–561.
- Angel, M.J., Guertin, P., Jiminez, I., and McCrea, D.A. 1996. Group I extensor afferents evoke

- disynaptic EPSPs in cat hindlimb extensor motoneurons during fictive locomotion. *J. Physiol. (Lond.)* 494: 851–861.
- Aniksztejn, L., Charton, G., and Ben-Ari, Y. 1987. Selective release of endogenous zinc from the hippocampal mossy fibers in situ. *Brain Res.* 404: 58–64.
- Aoki, C., and Kabak, S. 1992. Cholinergic terminals in the cat visual cortex: ultrastructural basis for interaction with glutamate-immunoreactive neurons and other cells. *Vis. Neurosci.* 8: 177–191.
- Aosaki, T., Graybiel, A.M., and Kimura, M. 1994a. Effect of the nigrostriatal dopamine system on acquired neural responses in the striatum of behaving monkeys. *Science* 265: 412–415.
- Aosaki, T., Tsubokawa, H., Watanabe, K., Graybiel, A.M., and Kimura, M. 1994b. Responses of tonically active neurons in the primate's striatum undergo systematic changes during behavioral sensory-motor conditioning. *J. Neurosci.* 14: 3969–3984.
- Aosaki, T., Kimura, M., and Graybiel, A.M. 1995. Temporal and spatial characteristics of tonically active neurons in the primate's striatum. *J. Neurophysiol.* 73: 1234–1252.
- Aosaki, T., Kiuchi, K., and Kawaguchi, Y. 1998. Dopamine D1-like receptor activation excites rat striatal large aspiny neurons in vitro. *J. Neurosci.* 18: 5180–5190.
- Apicella, P., Ravel, S., and Legaller, E. 1998. Influence of predictive information on responses of tonically active neurons in the monkey striatum. *J. Neurophysiol.* 80: 3341–3344.
- Applebury, M.L., Antoch, M.P., Baxter, L.C., Chun, L.L., Falk, J.D., Farhangfar, F., Kage, K., Krzystolik, M.G., Lyass, L.A., and Robbins, J.T. 2000. The murine cone photoreceptor: a single cone type expresses both S and M opsins with retinal spatial patterning. *Neuron* 27: 513–523.
- Arcelli, P., Frassoni, C., Regondi, M.C., De Biasi, S., and Spreafico, R. 1997. GABAergic neurons in mammalian thalamus: a marker of thalamic complexity? *Brain Res. Bull.* 42: 27–37.
- Arle, J.E., and Kim, D.O. 1991. Neural modeling of intrinsic and spike-discharge properties of cochlear nucleus neurons. *Biol. Cybernet.* 64: 273–283.
- Armstrong, D.M. 1974. Functional significance of connections of the inferior olive. *Physiol. Rev.* 54: 358–417.
- Armstrong-James, M., and Fox, K. 1983. Effects of iontophoretically applied noradrenaline on the spontaneous activity of neurons in rat primary somatosensory cortex. *J. Physiol. (Lond.)* 335: 427–447.
- Armstrong-James, M., Welker, I., and Callahan, C. 1993. The contribution of NMDA and non-NMDA receptors to fast and slow transmission of sensory information in the rat SI barrel cortex. *J. Neurosci.* 13: 2149–2160.
- Aroniadou, V., and Keller, A. 1995. Mechanisms of long term potentiation induction in rat motor cortex in vitro. *Cereb. Cortex* 5: 353–362.
- Aroniadou, V., and Teyler, T. 1992. Induction of NMDA receptor independent long-term potentiation of LTP in visual cortex of adult rats. *Brain Res.* 584: 169–173.
- Aroniadou-Anderjaska, V., Ennis, M., and Shipley, M.T. 1999a. Current-source density analysis in the rat olfactory bulb: laminar distribution of kainate/AMPA- and NMDA-receptor-mediated currents. *J. Neurophysiol.* 81: 15–28.
- Aroniadou-Anderjaska, V., Ennis, M., and Shipley, M.T. 1999b. Dendrodendritic recurrent excitation in mitral cells of the rat olfactory bulb. *J. Neurophysiol.* 82: 489–494.
- Artola, A., and Singer, W. 1987. Long-term potentiation and NMDA receptors in rat visual cortex. *Nature* 330: 649–652.
- Artola, A., Brocher, S., and Singer, W. 1990. Different voltage-dependent thresholds for inducing long-term depression and long-term potentiation in slices of rat visual cortex. *Nature* 347: 69–72.
- Artola, P., and Singer, L. 1987. Long-term potentiation and NMDA receptors in rat visual cortex. *Nature* 330, 649–652.
- Arvidsson, U., Cullheim, S., Ulfhake, B., Bennett, G.W., Fone, K.C.F., Cuello, A.C., Verhofstad,

- A.A.J., Visser, T.J., and Hökfelt, T. 1990. 5-Hydroxytryptamine, substance P, and thyrotropin-releasing hormone in the adult spinal cord segment L7: Immunohistochemical and chemical studies. *Synapse* 6: 237–270.
- Ascher, P., and Nowak, L. 1987. Electrophysiological studies of NMDA receptors. *Trends Neurosci.* 10: 284–287.
- Atick, J.J., and Redlich, A.N. 1992. What does the retina know about natural scenes? *Neural Comp.* 4: 196–210.
- Attwell, D. 1986. Ion channels and signal processing in the outer retina. *Q. J. Exp. Physiol.* 71: 497–536.
- Attwell, D., and Laughlin, S. 2001. An energy budget for signaling in the grey matter of the brain. *J. Cereb. Blood Flow Metab.* 21: 1133–1145.
- Au, W.W., Treloar, H.B., and Greer, C.A. 2002. Sublaminar organization of the mouse olfactory bulb nerve layer. *J. Comp. Neurol.* 446: 68–80.
- Awatramani, G.B., and Slaughter, M.M. 2001. Intensity-dependent, rapid activation of presynaptic metabotropic glutamate receptors at a central synapse. *J. Neurosci.* 21: 741–749.
- Ayala, G.F., Matsumoto, H., and Gumnit, R.J. 1970. Excitability changes and inhibitory mechanisms in neocortical neurons during seizures. *J. Neurophysiol.* 33: 73–85.
- Ayoub, G.S., Korenbrot, J.I., and Copenhagen, D.R. 1989. The release of endogenous glutamate from isolated cone photoreceptors of the lizard. *Neurosci. Res. (Suppl.)* 10: 547–556.
- Azzopardi, P., and Cowey, A. 1993. Preferential representation of the fovea in the primary visual cortex. *Nature* 361: 719–721.
- Baccus, S.A., and Meister, M. 2002. Fast and slow contrast adaptation in retinal circuitry. *Neuron* 36: 909–919.
- Baer, S., and Rinzel, J. 1991. Propagation of dendritic spikes mediated by excitable spines: a continuum theory. *J. Neurophysiol.* 65: 874–890.
- Bailey, M.S., Puche, A.C., and Shipley, M.T. 1999. Development of the olfactory bulb: evidence for glia-neuron interactions in glomerular formation. *J. Comp. Neurol.* 415: 423–448.
- Bainbridge, K.G., and Miller, J.J. 1982. Immunohistochemical localization of calcium-binding protein in the cerebellum, hippocampal formation and olfactory bulb of the rat. *Brain Res.* 245: 223–229.
- Baker, F.H., and Malpeli, J.G. 1977. Effects of cryogenic blockade of visual cortex on the responses of lateral geniculate neurons in the monkey. *Exp. Brain. Res.* 29: 433–444.
- Baker, H. 1988. Neurotransmitter plasticity in the juxtglomerular cells of the olfactory bulb. In: *Molecular Neurobiology of the Olfactory System* (Margolis, F.L., and Getchell, T.V., eds.) New York: Plenum Press, pp. 185–216.
- Baker, H., Cummings, D.M., Munger, S.D., Margolis, J.W., Franzen, L., Reed, R.R., and Margolis, F.L. 1999. Targeted deletion of a cyclic nucleotide-gated channel subunit (OCNC1): biochemical and morphological consequences in adult mice. *J. Neurosci.* 19: 9313–9321.
- Baker, H., Kwano, T., Margolis, F.L., and Joh, T.H. 1983. Transneuronal regulation of tyrosine hydroxylase expression in olfactory bulb of mouse and rat. *J. Neurosci.* 3: 69–78.
- Baker, H., Liu, N., Chun, H.S., Saino, S., Berlin, R., Volpe, B., and Son, J.H. 2001. Phenotypic differentiation during migration of dopaminergic progenitor cells to the olfactory bulb. *J. Neurosci.* 21: 8505–8513.
- Baker, L.P., Nielson, M.D., Impey, S., Hacker, B.M., Poser, S.W., Chan, M.Y.M., and Storm, D.R. 1999. Regulation and immunohistochemical localization of betagamma-stimulated adenylyl cyclases in mouse hippocampus. *J. Neurosci.* 19: 180–192.
- Bakst, I., Avendano, C., Morrison, J.H., and Amaral, D.G. 1986. An experimental analysis of the origins of somatostatin-like immunoreactivity in the dentate gyrus of the rat. *J. Neurosci.* 6: 1452–1462.
- Bal, R., and Oertel, D. 2000. Hyperpolarization-activated, mixed-cation current (I_h) in octopus cells of the mammalian cochlear nucleus. *J. Neurophysiol.* 84: 806–817.

- Bal, R., and Oertel, D. 2001. Potassium currents in octopus cells of the mammalian cochlear nucleus. *J. Neurophysiol.* 86: 2299–2311.
- Baldissera, F., and Gustafsson, B. 1974. Firing behavior of a neurone model based on the afterhyperpolarization conductance time course. First interval firing. *Acta Physiol. Scand.* 91: 528–544.
- Baldissera, F., and Gustafsson, B. 1971. Regulation of repetitive firing in motoneurons by the afterhyperpolarization conductance. *Brain Res.* 30: 431–434.
- Baldissera, F., Hultborn, H., and Illert, M. 1981. Integration in spinal neuronal systems In: *Handbook of Spinal Cord: Ventral Horn Physiology. Section 1: The Nervous System. Vol. III. Motor Control, Part 1.* (Brooks, V.B., ed.) Washington, DC: American Physiological Society, pp. 509–595.
- Balfour, D.J., Wright, A.E., Benwell, M.E., and Birrell, C.E. 2000. The putative role of extrasynaptic mesolimbic dopamine in the neurobiology of nicotine dependence. *Behav. Brain Res.* 114: 73–83.
- Banks, M.I., Haberly, L.B., and Jackson, M.B. 1996. Layer-specific properties of the transient K current (I_A) in piriform cortex. *J. Neurosci.* 16: 3862–3876.
- Banks, M.I., and Sachs, M.B. 1991. Regularity analysis in a compartmental model of chopper units in the anterodorsal cochlear nucleus. *J. Neurophysiol.* 65: 606–629.
- Barber, P.C., and Lindsay, R.M. 1982. Schwann cells of the olfactory nerves contain glial fibrillary acidic protein and resemble astrocytes. *Neuroscience* 7: 2687–2695.
- Bargas, J., Galarraga, E., and Aceves, J. 1988. Electrotonic properties of neostriatal neurons are modulated by extracellular potassium. *Exp. Brain Res.* 72: 390–398.
- Barkai, E., and Hasselmo, M.E. 1994. Modulation of the input/output function of rat piriform cortex pyramidal cells. *J. Neurophysiol.* 72: 664–658.
- Barkai, E., Bergman, R.E., Horwitz, G., and Hasselmo, M.E. 1994. Modulation of associative memory function in a biophysical simulation of rat piriform cortex. *J. Neurophysiol.* 72: 659–677.
- Barker, J., McBurney, R., and Mathers, D. 1983. Convulsant induced depression of aminoacid responses in cultured mouse spinal neurons studied under voltage clamp. *Br. J. Pharmacol.* 80: 619–629.
- Barlow, H.B. 1953. Summation and inhibition in the frog's retina. *J. Physiol. (Lond.)* 119: 69–88.
- Barlow, B.H. 1972. Single units and sensation: a neuron doctrine for perceptual psychology? *Perception* 1: 371–394.
- Barlow, H.B. 1982. General principles: The senses considered as physical instruments. In: *The Senses.* (Barlow, H.B., and Mollon, J.D., eds.) Cambridge, UK: Cambridge University Press, pp. 1–33.
- Barlow, H.B., Fitzhugh, B.R., and Kuffler, S.W. 1957. Change of organization in the receptive fields of the cat's retina during dark adaptation. *J. Physiol. (Lond.)* 137: 338–354.
- Barlow, H.B., and Levick, W.R. 1965. The mechanism of directionally selective units in rabbit's retina. *J. Physiol.* 178: 477–504.
- Barlow, H.B., Levick, W.R., and Yoon, M. 1971. Responses to single quanta of light in retinal ganglion cells of the cat. *Vision Res.* S3: 87–101.
- Barnack, N.H., Baughman, R.W., and Eckenstein, F.P. 1992. Cholinergic innervation of the cerebellum of rat, rabbit, cat, and monkey as revealed by choline acetyltransferase activity and immunohistochemistry. *J. Comp. Neurol.* 317: 233–249.
- Barnard, E., Darlison, M., and Seeburg, P. 1987. Molecular biology of the GABA_A receptor: the receptor/channel superfamily. *Trends Neurosci.* 10: 502–509.
- Barnes, J.M., and Henley, J.M. 1992. Molecular characteristics of excitatory amino acid receptors. *Prog. Neurobiol.* 39: 113–133.
- Barrett, E.F., and Barrett, J.N. 1976. Separation of two voltage-sensitive potassium currents, and

- demonstration of a tetrodotoxin-resistant calcium current in frog motoneurons. *J. Physiol. (Lond.)* 255: 737–774.
- Barrett, E.F., Barrett, J.N., and Crill, W.E. 1980. Voltage-sensitive outward currents in cat motoneurons. *J. Physiol. (Lond.)* 304: 251–276.
- Barrett, E.F., and Magleby, K.L. 1976. Physiology of cholinergic transmission. In: *Biology of Cholinergic Function* (Goldberg, A.M., and Hanin, E., eds.) New York: Raven Press, pp. 29–100.
- Barrett, J.N., and Crill, W.E. 1974. Specific membrane properties of cat motoneurons. *J. Physiol. (Lond.)* 239: 301–324.
- Barrionuevo, G., and Brown, T.H. 1983. Associative long-term potentiation in hippocampal slices. *Proc. Natl. Acad. Sci. U.S.A.* 80: 7347–7351.
- Barrionuevo, G., Kelso, S.R., Johnston, D., and Brown, T.H. 1986. Conductance mechanism responsible for long-term potentiation in monosynaptic and isolated excitatory synaptic inputs to hippocampus. *J. Neurophysiol.* 55: 540–550.
- Bartlett, E.L., Stark, J.M. Guillery, R.W., and Smith, P.H. 2000. Comparison of the fine structure of cortical and collicular terminals in the rat medial geniculate body. *Neuroscience* 100: 811–828.
- Bartlett, J.R., Doty, R.W., Sr., Lee, B.B., and Sakakura, H. 1976. Influence of saccadic eye movements on geniculostriate excitability in normal monkeys. *Exp. Brain Res.* 25: 487–509.
- Barto, A.G. 1995. Adaptive critics and the basal ganglia. In: *Models of Information Processing in the Basal Ganglia* (J.C. Houk, J.L. Davis and D.G. Beiser, eds.) Cambridge, MA: MIT Press, pp. 215–232.
- Bartolomei, J.C., and Greer, C.A. 1998. The organization of piriform cortex and the lateral olfactory tract following the loss of mitral cells in PCD mice. *Exp. Neurol.* 154: 537–550.
- Bartos, M., Vida, I., Frotscher, M., Geiger, J.R., and Jonas, P. 2001. Rapid signaling at inhibitory synapses in a dentate gyrus interneuron network. *J. Neurosci.* 21: 2687–98.
- Baseler, H.A., Brewer, A.A., Sharpe, L.T., Moreland, A.B., Jagle, H., and Wandell, B.A. 2002. Reorganization of human cortical maps caused by inherited photoreceptor abnormalities. *Nat. Neurosci.* 5: 364–370.
- Bassett, J.L., Shipley, M.T., and Foote, S.L. 1992. Localization of corticotropin-releasing factor-like immunoreactivity in monkey olfactory bulb and secondary olfactory areas. *J. Comp. Neurol.* 316: 348–362.
- Baumfalk, U., and Albus, K. 1988. Phaclofen antagonizes baclofen-induced suppression of visually evoked responses in the cats striate cortex. *Brain Res.* 463: 398–402.
- Baylor, D.A., Fuortes, M.G.F., and O'Bryan, P.M. 1971. Receptive fields of cones in the retina of the turtle. *J. Physiol. (Lond.)* 214: 265–294.
- Baylor, D.A., Nunn, B.J., and Schnapf, J.L. 1984. The photocurrent, noise and spectral sensitivity of rods of the monkey *Macaca fascicularis*. *J. Physiol. (Lond.)* 357: 575–607.
- Bean, B.P. 1989. Classes of calcium channels in vertebrate cells. *Annu. Rev. Physiol.* 51: 367–384.
- Bear, M.F., and Abraham, W.C. 1996. Long-term depression in hippocampus. *Annu. Rev. Neurosci.* 19: 437–462.
- Beaulieu, C., and Colonnier, M. 1983. The number of neurons in the different laminae of the binocular and monocular regions of area 17 in the cat. *J. Comp. Neurol.* 217: 337–344.
- Beaulieu, C., and Colonnier, M. 1985. A laminar analysis of the the number of round-asymmetrical and flat-symmetrical synapses on spines, dendritic trunks, and cell bodies in area 17 of the cat. *J. Comp. Neurol.* 231: 180–189.
- Beaulieu, C., and Somogyi, P. 1991. Enrichment of cholinergic synaptic terminals on GABAergic neurons and coexistence of immunoreactive GABA and choline acetyltransferase in the same synaptic terminals in the striate cortex of the cat. *J. Comp. Neurol.* 304: 666–680.

- Becker, C.J., and Freeman, W.J. 1968. Prepyriform electrical activity after loss of peripheral or central input, or both. *Physiol. Behav.* 3: 597–599.
- Beckstead, R.M. 1979. An autoradiographic examination of corticocortical and subcortical projections of the mediodorsal-projection (prefrontal) cortex in the rat. *J. Comp. Neurol.* 184: 43–62.
- Behan, M., and Haberly, L.B. 1999. Intrinsic and efferent connections of the endopiriform nucleus in rat. *J. Comp. Neurol.* 408: 548.
- Behan, M., Johnson, D.M.G., Feig, S.L., and Haberly, L.B. 1995. A new anatomically and physiologically distinct subdivision of the piriform (olfactory) cortex. *Soc. Neurosci. Abstr.* 21: 1186.
- Beierlein, M., Gibson, J.R., and Connors, B.W. 2000. A network of electrically coupled interneurons drives synchronized inhibition in neocortex. *Nat. Neurosci.* 3: 904–910.
- Bekkers, J.M., and Stevens, C.F. 1995. Quantal analysis of EPSPs recorded from small numbers of synapses in hippocampal cultures. *J. Neurophysiol.* 73: 1145–1156.
- Bell, C., Bodznick, D., Montgomery, J., and Bastian, J. 1997. The generation and subtraction of sensory expectations within cerebellum-like structures. *Brain Behav. Evol.* 50: 17–31.
- Bell, C.C. 2002. Evolution of cerebellum-like structures. *Brain Behav. Evol.* 59: 312–326.
- Bellingham, M.C., Lim, R., and Walmsley, B. 1998. Developmental changes in EPSC quantal size and quantal content at a central glutamatergic synapse in rat. *J. Physiol. (Lond.)* 511: 861–869.
- Belluardo, N., Muddò, G., Travato-Salinaro, A., Le Gurun, S., Charollais, A., Serre-Beinier, V., Amato, G., Haefliger, J.-A., Meda, P., and Condorelli, D.F. 2000. Expression of connexin36 in the adult and developing rat brain. *Brain Res.* 865: 121–138.
- Belluscio, L., and Katz, L.C. 2001. Symmetry, stereotypy, and topography of odorant representations in mouse olfactory bulbs. *J. Neurosci.* 21: 2113–2122.
- Belluscio, L., Lodovichi, C., Feinstein, P., Mombaerts, P., and Katz, L.C. 2002. Odorant receptors instruct functional circuitry in the mouse olfactory bulb. *Nature* 419: 296–300.
- Benardo, L., and Prince, D. 1982. Cholinergic excitation of hippocampal pyramidal cells. *Brain Res.* 249: 315–333.
- Bender, D.B. 1983. Visual activation of neurons in the primate pulvinar depends on cortex but not colliculus. *Brain Res.* 279: 258–261.
- Bennett, B.D., and Bolam, J.P. 1993. Characterization of calretinin-immunoreactive structures in the striatum of the rat. *Brain Res.* 609: 137–148.
- Bennett, B.D., and Bolam, J.P. 1994. Synaptic input and output of parvalbumin-immunoreactive neurons in the neostriatum of the rat. *Neuroscience* 62: 707–719.
- Bennett, B.D., and Wilson, C.J. 1998. Synaptic regulation of action potential timing in neostriatal cholinergic interneurons. *J. Neurosci.* 18: 8539–8549.
- Bennett, B.D., and Wilson, C.J. 1999. Spontaneous activity of neostriatal cholinergic interneurons in vitro. *J. Neurosci.* 19: 5586–5596.
- Bennett, B.D., Callaway, J.C., and Wilson, C.J. 2000. Intrinsic membrane properties underlying spontaneous tonic firing in neostriatal cholinergic interneurons. *J. Neuroscience* 20: 8493–8503.
- Bennett, M.R. 2000. The concept of long term potentiation of transmission at synapses. *Prog. Neurobiol.* 60: 109–137.
- Bennett, M.V.L. 1977. Electrical transmission: a functional analysis and comparison to chemical transmission. In: *Handbook of Physiology, Section 1: The Nervous System, Vol. I. Cellular Biology of Neurons, Part 1* (Kandel, E.R., ed.) Washington, DC: American Physiological Society, pp. 357–416.
- Benson, T.E., Berglund, A.M., and Brown, M.C. 1996. Synaptic input to cochlear nucleus dendrites that receive medial olivocochlear synapses. *J. Comp. Neurol.* 365: 27–41.
- Benson, T.E., and Brown, M.C. 1990. Synapses formed by olivocochlear axon branches in the mouse cochlear nucleus. *J. Comp. Neurol.* 294: 52–70.

- Benson, T.E., Burd, G.D., Greer, C.A., Landis, D.M., and Shepherd, G.M. 1985. High-resolution 2-deoxyglucose autoradiography in quick-frozen slabs of neonatal rat olfactory bulb. *Brain Res.* 339: 67–78.
- Benson, T.E., Ryugo, D., and Hinds, J. 1984. Effects of sensory deprivation on developing mouse olfactory system. *J. Neurosci.* 4: 638–653.
- Ben-Yishai, R., Lev Bar-Or, R., and Sompolinsky, H. 1995. Theory of orientation tuning in visual cortex. *Proc. Natl. Acad. Sci. U.S.A.* 92: 3844–3848.
- Berg, H.C. 1993. *Random Walks in Biology*. Princeton, NJ: Princeton University Press.
- Berger, T., Larkum, M., and Luscher, H. 2001. High I_h channel density in the distal apical dendrite of layer v pyramidal cells increases bidirectional attenuation of EPSPS. *Nature* 85: 855–865.
- Berkley, K.J. 1975. Different targets of different neurons in nucleus gracilis of the cat. *J. Comp. Neurol.* 163: 285–303.
- Berkowicz, D.A., and Trombley, P.Q. 2000. Dopaminergic modulation at the olfactory nerve synapse. *Brain Res.* 855: 90–99.
- Berkowicz, D.A., Trombley, P.Q., and Shepherd, G.M. 1994. Evidence for glutamate as the olfactory receptor cell neurotransmitter. *J. Neurophysiol.* 71: 2557–2561.
- Berman, N., Bush, P., and Douglas, R. 1989. Adaptation and bursting may be controlled by a single fast potassium current. *Q. J. Exp. Physiol.* 74: 223–226.
- Bernander, O., Douglas, R., and Koch, C. 1994. Amplification and linearization of synaptic input to the apical dendrites of cortical pyramidal neurons. *J. Neurophysiol.* 72: 2743–2753.
- Bernander, O., Douglas, R., Martin, K., and Koch, C. 1991. Synaptic background activity influences spatiotemporal integration in single pyramidal cells. *Proc. Natl. Acad. Sci. U.S.A.* 88: 11569–11573.
- Bernard, V., Normand, E., and Bloch, B. 1992. Phenotypical characterization of the rat striatal neurons expressing muscarinic receptor genes. *J. Neurosci.* 12: 3591–3600.
- Berrebi, A.S., Morgan, J.I., and Mugnaini, E. 1990. The Purkinje cell class may extend beyond the cerebellum. *J. Neurocytol.* 19: 643–654.
- Berrebi, A.S., and Mugnaini, E. 1991. Distribution and targets of the cartwheel cell axon in the dorsal cochlear nucleus of the guinea pig. *Anat. Embryol.* 183: 427–454.
- Berridge, K.C., and Robinson, T.E. 1998. What is the role of dopamine in reward: hedonic impact, reward learning, or incentive salience. *Brain Res. Rev.* 28: 309–369.
- Berson, D.M., and Graybiel, A.M. 1983. Organization of the striate-recipient zone of the cat's lateralis posterior-pulvinar complex and its relations with the geniculostriate system. *Neuroscience* 9: 337–372.
- Berson, D.M., Dunn, F.A., and Takao, M. 2002. Phototransduction by retinal ganglion cells that set the circadian clock. *Science* 295: 1070–1073.
- Berson, D.M., Isayama, T., and Pu, M. 1999. The eta ganglion cell type of cat retina. *J. Comp. Neurol.* 408: 204–219.
- Berson, D.M., Pu, M., and Famiglietti, E.V. 1998. The zeta cell: a new ganglion cell type in cat retina. *J. Comp. Neurol.* 399: 269–288.
- Berson, D.M., Pu, M., and Isayama, T. 1997. The eta cell: a new ganglion cell type in cat retina. *Invest. Ophthalmol. Vis. Sci. Abstr.* 38: S51.
- Bertrand, S., and Lacaille, J.C. 2001. Unitary synaptic currents between lacunosum-moleculare interneurons and pyramidal cells in rat hippocampus. *J. Physiol. (Lond.)* 532: 369–384.
- Bessou, P., Emonet-Denand, F., and Laporte, Y. 1965. Motor fibres innervating extrafusal and intrafusal muscle fibres in the cat. *J. Physiol. (Lond.)* 180: 649–672.
- Betz, H. 1991. Glycine receptors: heterogeneous and widespread in the mammalian brain. *Trends. Neurosci.* 14: 458–461.
- Bevan, M.D., and Wilson, C.J. 1999. Mechanisms underlying spontaneous oscillation and rhythmic firing in rat subthalamic neurons. *J. Neurosci.* 19: 7617–7628.

- Bhalla, U.S., and Bower, J.M. 1993. Exploring parameter space in detailed single neuron models: simulations of the mitral and granule cells of the olfactory bulb. *J. Neurophysiol.* 69: 1948–1965.
- Bi, G., and Poo, M. 2001. Synaptic modification by correlated activity: Hebb's postulate revisited. *Annu. Rev. Neurosci.* 24: 139–66.
- Bickford, M.E., Carden, W.B., and Patel, N.C. 1999. Two types of interneurons in the cat visual thalamus are distinguished by morphology, synaptic connections, and nitric oxide synthase content. *J. Comp. Neurol.* 413: 83–100.
- Bickford, M.E., Günlük, A.E., Guido, W., and Sherman, S.M. 1993. Evidence that cholinergic axons from the parabrachial region of the brainstem are the exclusive source of nitric oxide in the lateral geniculate nucleus of the cat. *J. Comp. Neurol.* 334: 410–430.
- Bickford, M.E., Günlük, A.E., Van Horn, S.C., and Sherman, S.M. 1994. GABAergic projection from the basal forebrain to the visual sector of the thalamic reticular nucleus in the cat. *J. Comp. Neurol.* 348: 481–510.
- Bickford, M.E., Ramcharan, E., Godwin, D.W., Erişir, A., Gnadt, J., and Sherman, S.M. 2000. Neurotransmitters contained in the subcortical extraretinal inputs to the monkey lateral geniculate nucleus. *J. Comp. Neurol.* 424: 701–717.
- Biedenbach, M.A., and Stevens, C.F. 1969. Synaptic organization of the cat olfactory cortex as revealed by intracellular recording. *J. Neurophysiol.* 32: 204–214.
- Biella, G., and de Curtis, M. 1995. Associative synaptic potentials in the piriform cortex of the isolated guinea-pig brain in vitro. *Eur. J. Neurosci.* 7: 54–64.
- Biella, G., Panzica, F., and de Curtis, M. 1996. Interactions between associative synaptic potentials in the piriform cortex of the in vitro isolated guinea pig brain. *Eur. J. Neurosci.* 8: 1350–1357.
- Bienenstock, E.L., Cooper, L.N., and Munro, P.W. 1982. Theory for the development of neuron selectivity: orientation specificity and binocular interaction in visual cortex. *J. Neurosci.* 2: 32–48.
- Billups, D., and Attwell, D. 2002. Control of intracellular chloride concentration and GABA response polarity in rat retinal ON bipolar cells. *J. Physiol.* 545: 183–198.
- Binder, M., Heckman, C., and Powers, R. 1996. The physiological control of motoneuron activity. In: *Handbook of Physiology. Section 12: Exercise: Regulation and Integration of Multiple Systems.* (Rowell, L., and Shepherd, J., eds.) New York: Oxford University Press/American Physiological Society, pp. 3–53.
- Binder, M.D., Heckman, C.J., and Powers, R.K. 1993. How different inputs control motoneuron discharge and the output of the motoneuron pool. *Curr. Opin. Neurobiol.* 3: 1028–1034.
- Bindman, L., Meyer, T., and Prince, C. 1988. Comparison of the electrical properties of neocortical neurones in slices in vitro and in the anaesthetized rat. *Brain Res.* 68: 489–496.
- Birbaumer, L., Campbell, K.P., Catterall, W.A., Harpold, M.M., Hofmann, F., Horne, W.A., Mori, Y., Schwartz, A., Snutch, T.P., Tanabe, T., et al. 1994. The naming of voltage-gated calcium channels. *Neuron* 13: 505–506.
- Bischofberger, J., Geiger, J.R., and Jonas, P. 2002. Timing and efficacy of Ca²⁺ channel activation in hippocampal mossy fiber boutons. *J. Neurosci.* 22: 10593–10602.
- Bischofberger, J., and Jonas, P. 1997. Action potential propagation into the presynaptic dendrites of rat mitral cells. *J. Physiol. (Lond.)* 504: 359–365.
- Bishop, G.A., Chang, H.T., and Kitai. 1982. Morphological and physiological properties of neostriatal neurons: an intracellular horseradish peroxidase study in the rat. *Neuroscience* 7: 179–191.
- Bisti, S., Iosif, G., Marchesi, G.F., and Strata, P. 1971. Pharmacological properties of inhibitions in the cerebellar cortex. *Exp. Brain Res.* 14: 24–37.
- Björklund, A., and Lindvall, O. 1984. Dopamine-containing systems in the CNS. In: *Handbook*

- of Chemical Neuroanatomy. Volume 2: Classical Transmitters in the CNS Part I (Björklund, A., and Hokfelt, T., eds.) Amsterdam: Elsevier, pp. 55–122.
- Blackburn, C.C., and Sachs, M.B. 1989. Classification of unit types in the anteroventral cochlear nucleus: PST histograms and regularity analysis. *J. Neurophysiol.* 62: 1303–1329.
- Blackburn, C.C., and Sachs, M.B. 1990. The representation of the steady-state vowel sound /e/ in the discharge patterns of cat anteroventral cochlear nucleus neurons. *J. Neurophysiol.* 63: 1191–1212.
- Blackburn, C.C., and Sachs, M.B. 1992. Effects of off-BF tones on responses of chopper units in ventral cochlear nucleus. I. Regularity and temporal adaptation patterns. *J. Neurophysiol.* 68: 124–143.
- Blackstad, T.W. 1956. Commissural connections of the hippocampal region in the rat, with special reference to their mode of termination. *J. Comp. Neurol.* 105: 417–537.
- Blackstad, T.W., and Kjaerheim, A. 1961. Special axo-dendritic synapses in the hippocampal cortex electron and light microscopic studies on the layer of mossy fibers. *J. Comp. Neurol.* 117: 133–159.
- Blackstad, T.W., Osen, K.K., and Mugnaini, E. 1984. Pyramidal neurones of the dorsal cochlear nucleus: a Golgi and computer reconstruction study in cat. *Neuroscience* 13: 827–854.
- Blaxter, T., and Cottrell, G. 1985. Actions of GABA and ethylenediamine on CA1 pyramidal neurones in the rat hippocampus. *Q. J. Exp. Physiol.* 70: 75–93.
- Blaxter, T., Carlen, P., Davies, M., and Kujitan, P. 1986. γ -Aminobutyric acid hyperpolarizes rat hippocampal pyramidal cells through a calcium-dependent potassium conductance. *J. Physiol. (Lond.)* 373: 181–194.
- Bliss, T.V.P., and Collingridge, G.L. 1993. A synaptic model of memory long-term potentiation in the hippocampus. *Nature* 361: 31–39.
- Bliss, T.V.P., and Gardner-Medwin, A.R. 1973. Long-lasting potentiation of synaptic transmission in the dentate area of the unanaesthetized rabbit following stimulation of the perforant path. *J. Physiol. (Lond.)* 232: 357–374.
- Bliss, T.V.P., and Lomo, T. 1973. Long-lasting potentiation of synaptic transmission in the dentate area of the unanaesthetized rabbit following stimulation of the perforant path. *J. Physiol. (Lond.)* 232: 331–356.
- Bliss, T.V.P., and Lynch, M.A. 1988. Long-term potentiation of synaptic transmission in the hippocampus: properties and mechanisms. In: *Long-Term Potentiation. From Biophysics to Behavior* (Landfield, P.W., and Deadwyle, S.A., eds.) New York: Alan R. Liss, pp. 3–72.
- Bliss, T.V.P., and Rosenburg, M. 1979. Activity-dependent changes on conduction velocity in the olfactory nerve of the tortoise. *Pflügers Arch.* 381: 209–216.
- Bloedel, J.R., and Courville, J. 1981. Cerebellar afferent systems In: *Handbook of Physiology. Section I. The Nervous System. Vol. II, Motor Control, Part 2* (Brooks, V.B., ed.) Bethesda, MD: American Physiological Society, pp. 735–829.
- Bloom, F.E., Hoffer, B.J., and Siggins, G.R. 1971. Studies on norepinephrine-containing afferents to Purkinje cells of rat cerebellum. I. Localization of the fibers and their synapses. *Brain Res.* 25: 501–521.
- Bloomfield, S.A. 1992. Relationship between receptive and dendritic field size of amacrine cells in the rabbit retina. *J. Neurophysiol.* 68: 711–725.
- Bloomfield, S.A., and Dacheux, R.F. 2001. Rod vision: pathways and processing in the mammalian retina. *Prog. Ret. Eye Res.* 20: 351–384.
- Bloomfield, S.A., Hamos, J.E., and Sherman, S.M. 1987. Passive cable properties and morphological correlates of neurones in the lateral geniculate nucleus of the cat. *J. Physiol. (Lond.)* 383: 653–692.
- Bloomfield, S.A., and Sherman, S.M. 1989. Dendritic current flow in relay cells and interneurons of the cat's lateral geniculate nucleus. *Proc. Natl. Acad. Sci. U.S.A.* 86: 3911–3914.

- Bloomfield, S.A., Xin, D., and Osborne, T. 1997. Light-induced modulation of coupling between AII amacrine cells in the rabbit retina. *Vis. Neurosci.* 14: 565–576.
- Boahen, K.A. 1996. Retinomorphic vision systems: reverse engineering the vertebrate retina. Ph.D. Thesis, California Institute of Technology.
- Bodnarenko, S.R., Jeyarasasingam, G., and Chalupa, L. 1995. Development and regulation of dendritic stratification in retinal ganglion cells by glutamate-mediated afferent activity. *J. Neurosci.* 15: 7037–7045.
- Boeijinga, P.H., and Lopes da Silva, F.H. 1988. Differential distribution of beta and theta EEG activity in the entorhinal cortex of the cat. *Brain Res.* 448: 272–286.
- Boeijinga, P.H., and Lopes da Silva, F.H. 1989. Modulations of EEG activity in the entorhinal cortex and forebrain olfactory areas during odour sampling. *Brain Res.* 478: 257–268.
- Bogan, N., Brecha, N., Gall, C., and Karten, H.J. 1982. Distribution of enkephalin-like immunoreactivity in the rat main olfactory bulb. *Neuroscience* 7: 895–906.
- Bolam, J.P., Clarke, D.J., Smith, A.D., and Somogyi, P. 1983. A type of aspiny neuron in the neostriatum accumulates [³H]gamma-aminobutyric acid: combination of Golgi-staining, autoradiography, and electron microscopy. *J. Comp. Neurol.* 213: 121–134.
- Bolam, J.P., Ingham, C.A., Izzo, P.N., Levey, A.I., Rye, D.B., Smith, A.D., and Wainer, B.H. 1986. Substance P-containing terminals in synaptic contact with cholinergic neurons in the neostriatum and basal forebrain: a double immunocytochemical study in the rat. *Brain Res.* 397: 279–289.
- Bolam, J.P., Somogyi, P., Totterdell, S., and Smith, A.D. 1981. A second-type of striatonigral neuron: a comparison between retrogradely labelled and Golgi-stained neurons at the light and electron microscopic levels. *Neuroscience* 6: 2141–2157.
- Bolam, J.P., Wainer, B.H., and Smith, A.D. 1984. Characterization of cholinergic neurons in the rat neostriatum. A combination of choline acetyltransferase immunocytochemistry, Golgi-impregnation and electron microscopy. *Neuroscience* 12: 711–718.
- Bolz, J., Thier, P., Voight, T., and Wässle, H. 1985. Action and localization of glycine and taurine in the cat retina. *J. Physiol. (Lond.)* 362: 395–413.
- Boos, R., Schneider, H., and Wässle, H. 1993. Voltage- and transmitter-gated currents of AII-amacrine cells in a slice preparation of the rat retina. *J. Neurosci.* 13: 2874–2888.
- Borges, S., Gleason, E., Turelli, M., and Wilson, M. 1995. The kinetics of quantal transmitter release from retinal amacrine cells. *Proc. Natl. Acad. Sci. U.S.A.* 92: 6896–6900.
- Borg-Graham, L., Monier, C., and Fregnac, Y. 1998. Visual input evokes transient and strong shunting inhibition in visual cortical neurons. *Nature* 393: 369–373.
- Bormann, J. 1988. Electrophysiology of GABAA and GABAB receptor subtypes. *Trends Neurosci.* 11: 112–116.
- Bormann, J., and Feigenspan, A. 1995. GABAC receptors. *Trends Pharmacol. Sci.* 18: 515–519.
- Bosco, G., and Poppele, R. 2001. Proprioception from a spinocerebellar perspective. *Physiol. Rev.* 81: 539–568.
- Boudreau, J.C., and Tsuchitani, C. 1970. Cat superior olive S-segment cell discharge to tonal stimulation. *Contrib. Sens. Physiol.* 4: 143–213.
- Bourassa, J., and Deschênes, M. 1995. Corticothalamic projections from the primary visual cortex in rats: a single fiber study using biocytin as an anterograde tracer. *Neuroscience* 66: 253–263.
- Bourassa, J., Pinault, D., and Deschênes M. 1995. Corticothalamic projections from the cortical barrel field to the somatosensory thalamus in rats: a single-fibre study using biocytin as an anterograde tracer. *Eur. J. Neurosci.* 7: 19–30.
- Bourk, T.R. 1976. Electrical responses of neural units in the anteroventral cochlear nucleus of the cat. Ph.D. Thesis, Massachusetts Institute of Technology, Cambridge, MA.
- Bourk, T.R., Mielcarz, J.P., and Norris, B.E. 1981. Tonotopic organization of the anteroventral cochlear nucleus of the cat. *Hearing Res.* 4: 215–241.

- Bowery, N. 1993. GABAB receptor pharmacology. *Annu. Rev. Pharmacol. Toxicol.* 33: 109–147.
- Bowery, N., Hudson, A., and Price, G. 1987. GABA-A and GABA-B receptor site distribution in the rat central nervous system. *Neuroscience* 20: 365–383.
- Bowery, N., Price, G., Hudson, A., Hill, D., Wilkin, G., and Turnbull, M. 1984. GABA receptor multiplicity: visualization of different receptor types in the mammalian CNS. *Neuropharmacology* 23: 219–231.
- Bowery, N.G., Bettler, B., Froestl, E., Gallagher, J.P., Marshall, F., Raiteri, M., Bonner, T.I., and Enna, S.J. 2002. International Union of Pharmacology. XXXIII. Mammalian γ -aminobutyric acid_B receptors: structure and function. *Pharmacol. Rev.* 54: 247–264.
- Bowling, D.B., and Michael, C.R. 1984. Terminal patterns of single, physiologically characterized optic tract fibers in the cat's lateral geniculate nucleus. *J. Neurosci.* 4: 198–216.
- Bowmaker, J.K., Govardovskii, V.I., Shukolyukov, S.A., Zueva, L.V., Hunt, D.M., Sideleva, V.G., and Smirnova, O.G. 1994. Visual pigments and the photic environment: the cottoid fish of Lake Baikal. *Vision Res.* 34: 591–605.
- Boycott, B.B., and Dowling, J.E. 1969. Organization of the primate retina: Light microscopy. *Phil. Trans. R. Soc. Lond. B* 255: 109–184.
- Boycott, B.B., and Kolb, H. 1973. The connections between bipolar cells and photoreceptors in the retina of the domestic cat. *J. Comp. Neurol.* 148: 91–114.
- Boycott, B.B., and Wässle, H. 1974. The morphological types of ganglion cells of the domestic cat's retina. *J. Physiol. (Lond.)* 240: 397–419.
- Boycott, B.B., and Wässle, H. 1991. Morphological classification of bipolar cells of the primate retina. *Eur. J. Neurosci.* 3: 1069–1088.
- Boyd, I.A., and Davey, M.R. 1968. *Composition of Peripheral Nerves*. Edinburgh: E. & S. Livingstone.
- Bracci, E., Centonze, D., Bernardi, G., and Calabresi, P. 2002. Dopamine excites fast-spiking interneurons in the striatum. *J. Neurophysiol.* 87: 2190–2194.
- Brainard, M.S., and Doupe, A.J. 2000. Interruption of a basal ganglia-forebrain circuit prevents plasticity of learned vocalizations. *Nature* 404: 762–766.
- Brainard, D.H., Roorda, A., Yamauchi, Y., Calderone, J.B., Metha, A., Neitz, M., Neitz, J., Williams, D.R., and Jacobs, G.H. 2000. Functional consequences of the relative numbers of L and M cones. *J. Opt. Soc. Am. A* 17: 607–614.
- Braitenberg, V., and Atwood, R.P. 1958. Morphological observations on the cerebellar cortex. *J. Comp. Neurol.* 109: 1–33.
- Braitenberg, V., and Schuz, A. 1991. *Anatomy of the Cortex: Statistics and Geometry*. New York: Springer Verlag.
- Bramham, C.R., Errington, M.L., and Bliss, T.V.P. 1988. Naloxone blocks the induction of long-term potentiation in the lateral but not in the medial perforant pathway in the anesthetized rat. *Brain Res.* 449: 352–356.
- Brand, A., Behrend, O., Marquardt, T., McAlpine, D., and Grothe, B. 2002. Precise inhibition is essential for microsecond interaural time difference coding. *Nature* 417: 543–547.
- Brandstätter, J.H., Koulen, P., Kuhn, R., van der Putten, H., and Wässle, H. 1996. Compartmental localization of a metabotropic glutamate receptor (mGluR7): two different active sites at a retinal synapse. *J. Neurosci.* 16: 4749–4756.
- Brännström, T. 1993. Quantitative synaptology of functionally different types of cat medial gastrocnemius alpha-motoneurons. *J. Comp. Neurol.* 330: 439–454.
- Brawer, J.R., and Morest, D.K. 1975. Relations between auditory nerve endings and cell types in the cat's anteroventral cochlear nucleus seen with the Golgi method and Nomarski optics. *J. Comp. Neurol.* 160: 491–506.
- Brawer, J.R., Morest, D.K., and Kane, E.C. 1974. The neuronal architecture of the cochlear nucleus of the cat. *J. Comp. Neurol.* 155: 251–300.
- Brazier, M.A.B. 1960. The historical development of neurophysiology In: *Handbook of Physi-*

- ology, Section 1: Neurophysiology, Vol. I (Magoun, H.W., ed.) Bethesda: American Physiological Society, pp. 1–58.
- Brecha, N., Johnson, D., Peichl, L., and Wässle, H. 1988. Cholinergic amacrine cells of the rabbit retina contain glutamate decarboxylase and gamma-aminobutyrate immunoreactivity. *Proc. Natl. Acad. Sci. U.S.A.* 85: 6187–6191.
- Bredt, D.S., Glatt, C.E., Hwang, P.M., Fotuhi, M., Dawson, T.M., and Snyder, S.H. 1991. Nitric oxide synthase protein and mRNA are discretely localized in neuronal populations of the mammalian CNS together with NADPH diaphorase. *Neuron* 7: 615–624.
- Bredt, D.S., Hwang, P.M., and Snyder, S.H. 1990. Localization of nitric oxide synthase indicating a neural role for nitric oxide. *Nature* 347: 768–770.
- Bredt, D.S., and Snyder, S.H. 1992. Nitric oxide, a novel neuronal messenger. *Neuron* 8: 3–11.
- Breer, H. 1994. Odor recognition and second messenger signaling in olfactory receptor neurons. *Semin. Cell Biol.* 5: 25–32.
- Breer, H., and Shepherd, G.M. 1993. Implications of the NO/cGMP system for olfaction. *Trends Neurosci.* 16: 5–9.
- Breindl, A., Derrick, B.E., Rodriguez, S.B., and Martinez, J.L.J. 1994. Opioid receptor-dependent long-term potentiation at the lateral perforant path-CA3 synapse in rat hippocampus. *Brain Res. Bull.* 33: 17–24.
- Brenowitz, S., David, J., and Trussell, L.O. 1998. Enhancement of synaptic efficacy by presynaptic GABA(B) receptors. *Neuron* 20: 135–141.
- Brenowitz, S., and Trussell, L.O. 2001. Maturation of synaptic transmission at end-bulb synapses of the cochlear nucleus. *J. Neurosci.* 21: 9487–9498.
- Bressler, S.L. 1984. Spatial organization of EEGs from olfactory bulb and cortex. *Electroencephalogr. Clin. Neurophysiol.* 57: 270–276.
- Bressler, S.L. 1988. Changes in electrical activity of rabbit olfactory bulb and cortex to conditioned odor stimulation. *Behav. Neurosci.* 102: 740–747.
- Bressler, S.L., and Freeman, W.J. 1980. Frequency analysis of olfactory system EEG in cat, rabbit, and rat. *Electroencephalogr. Clin. Neurophysiol.* 50: 19–24.
- Brevi, S., de Curtis, M., and Magistretti, J. 2001. Pharmacological and biophysical characterization of voltage-gated calcium currents in the endopiriform nucleus of the guinea pig. *J. Neurophysiol.* 85: 2076–2087.
- Brock, L.G., Coombs, J.S., and Eccles, J.C. 1952. The recording of potentials from motoneurons with an intracellular electrode. *J. Physiol. (Lond.)* 117: 431–460.
- Brodal, A. 1981. *Neurological Anatomy*. Oxford: Oxford University Press.
- Brown, A.G. 1981. *Organization in the Spinal Cord: The Anatomy and Physiology of Identified Neurones*. Berlin: Springer-Verlag.
- Brown, A.G., and Fyffe, R.E.W. 1981. Direct observations on the contacts made between Ia afferents and a-motoneurons in the cat's lumbosacral spinal cord. *J. Physiol. (Lond.)* 313: 121–140.
- Brown, A.G., Rose, P.K., and Snow, P.J. 1977. The morphology of spinocervical tract neurones revealed by intracellular injection of horseradish peroxidase. *J. Physiol. (Lond.)* 270: 747–764.
- Brown, D.A. 1988. M-currents: an update. *Trends Neurosci.* 44: 294–299.
- Brown, D.A., and Adams, P.R. 1980. Muscarinic suppression of a novel voltage-sensitive K1 current in a vertebrate neurone. *Nature* 283: 673–676.
- Brown, D.A., and Kukulka, C.G. 1993. Human flexor reflex modulation during cycling. *J. Neurophysiol.* 69: 1212–1224.
- Brown, D.A., Gahwiler, B.H., Griffith, W.H., and Halliwell, J.V. 1990a. Membrane currents in hippocampal neurons. *Prog. Brain Res.* 83: 141–160.
- Brown, M.C., Berglund, A.M., Kiang, N.Y.S., and Ryugo, D.K. 1988a. Central trajectories of type II spiral ganglion neurons. *J. Comp. Neurol.* 278: 581–590.

- Brown, M.C., and Ledwith, J.V. 1990. Projections of thin (type-II) and thick (type-I) auditory-nerve fibers into the cochlear nucleus of the mouse. *Hearing Res.* 49: 105–118.
- Brown, M.C., Liberman, M.C., Benson, T.E., and Ryugo, D.K. 1988b. Brainstem branches from olivocochlear axons in cats and rodents. *J. Comp. Neurol.* 278: 591–603.
- Brown, S.P., and Masland, R.H. 2001. Spatial scale and cellular substrate of contrast adaptation by retinal ganglion cells. *Nat. Neurosci.* 4: 44–51.
- Brown, T.H., and Johnston, D. 1983. Voltage-clamp analysis of mossy fiber synaptic input to hippocampal neurons. *J. Neurophysiol.* 50: 487–507.
- Brown, T.H., Fricke, R.A., and Perkel, D.H. 1981. Passive electrical constants in three classes of hippocampal neurons. *J. Neurophysiol.* 46: 812–827.
- Brown, T.H., Kairiss, E.W., and Keenan, C.L. 1990. Hebbian synapses: biophysical mechanisms and algorithms. *Annu. Rev. Neurosci.* 13: 475–511.
- Brown, T.H., Lindquist, D., and Teyler, T. Learning and memory: basic mechanisms of long-term synaptic potentiation and depression. In: *Cellular and Molecular Neuroscience*. (Byrne, J.H., and Roberts, J.L., eds.) New York: Academic Press.
- Brown, T.H., Wong, R.K.S., and Prince, D.A. 1979. Spontaneous miniature synaptic potentials in hippocampal neurons. *Brain Res.* 177: 194–199.
- Brownstone, R.M., Gossard, J.P., and Hultborn, H. 1994. Voltage-dependent excitation of motoneurons from spinal locomotor centers in the cat. *Exp. Brain Res.* 102: 34–44.
- Bruce, C., Desimone, R., and Gross, C. 1981. Visual properties of neurons in a polysensory area in superior temporal sulcus of the macaque. *J. Neurophysiol.* 46: 369–384.
- Bruce, H.M. 1959. An exteroceptive block to pregnancy in the mouse. *Nature* 184: 105.
- Brughera, A.R., Stutman, E.R., Carney, L.H., and Colburn, H.S. 1996. A model with excitation and inhibition for cells in the medial superior olive. *Auditory Neurosci.* 2: 219–233.
- Brunjes, P.C. 1994. Unilateral naris closure and olfactory system development. *Brain Res. Revs.* 19: 146–160.
- Brunso-Bechtold, J.K., Thompson, G.C., and Masterton, R.B. 1981. HRP study of the organization of auditory afferents ascending to central nucleus of inferior colliculus in cat. *J. Comp. Neurol.* 197: 705–722.
- Buchsbaum, G., and Gottschalk, A. 1983. Trichromacy, opponent colours coding and optimum colour information transmission in the retina. *Proc. R. Soc. Lond. B* 220: 89–113.
- Buck, L.B. 2000. The molecular architecture of odor and pheromone sensing in mammals. *Cell* 100: 611–618.
- Buck, L.D., and Axel, R. 1991. A novel multigene family may encode odorant receptors: a molecular basis for odorant recognition. *Cell* 65: 175–187.
- Buckmaster, P.S., and Soltesz, I. 1996. Neurobiology of hippocampal interneurons: a workshop review. *Hippocampus* 6: 330–339.
- Buckmaster, P.S., Wenzel, J.H., Kunkel, D.D., and Schwartzkroin, P.A. 1996. Axon arbors and synaptic connections of hippocampal mossy cells in the rat in vivo. *J. Comp. Neurol.* 366: 270–292.
- Buhl, E.H., Szilagy, T., Halasy, K., and Somogyi, P. 1996. Physiological properties of anatomically identified basket and bistratified cells in the CA1 area of the rat hippocampus in vitro. *Hippocampus* 6: 294–305.
- Bührle, C.P., and Sonnhof, U. 1985. The ionic basis of postsynaptic inhibition of motoneurons of the frog spinal cord. *Neuroscience* 14: 581–592.
- Buonviso, N., and Chaput, M.A. 1990. Response similarity to odors in olfactory bulb output cells presumed to be connected to the same glomerulus: electrophysiological study using simultaneous single unit recordings. *J. Neurophysiol.* 63: 447–454.
- Buonviso, N., Revial, M.F., and Jourdan, F. 1991. The projections of mitral cells from small local regions of the olfactory bulb: an anterograde tracing study using PHA-L (*Phaseolus vulgaris leucoagglutinin*). *Eur. J. Neurosci.* 3: 493–500.

- Burd, G. 1980. Myelinated dendrites and neuronal perikarya in the olfactory bulb of the mouse. *Brain Res.* 181: 450–454.
- Burgi, P.-Y., and Grzywacz, N.M. 1994. Model for the pharmacological basis of spontaneous synchronous activity in developing retinas. *J. Neurosci.* 14: 7426–7439.
- Burian, M., and Gestöettner, W. 1988. Projection of primary vestibular afferent fibres to the cochlear nucleus in the guinea pig. *Neurosci. Lett.* 84: 13–17.
- Burke, J., and Hablitz, J. 1995. Modulation of epileptiform activity by metabotropic glutamate receptors in immature rat neocortex. *J. Neurophysiol.* 73: 205–217.
- Burke, R.E. 1967. The composite nature of the monosynaptic excitatory postsynaptic potential. *J. Neurophysiol.* 30: 1114–1137.
- Burke, R.E. 1968. Firing patterns of gastrocnemius motor units in the decerebrate cat. *J. Physiol. (Lond.)* 196: 631–645.
- Burke, R.E. 1981. Motor Units: Anatomy, Physiology and Functional Organization. In: *Handbook of Physiology, Section 1: The Nervous System, Vol. II. Motor Control, Part 1* (Brooks, V.B., ed.) Washington, DC: American Physiological Society, pp. 345–422.
- Burke, R.E. 1991. Selective recruitment of motor units. In: *Motor Control: Concepts and Issues* (Humphrey, D.R., and Freund, H.-J., eds.) Chichester: John Wiley & Sons, pp. 5–21.
- Burke, R.E. 1998. Presynaptic inhibition and the anatomy of group Ia afferents in the cat spinal cord. In: *Presynaptic Inhibition and Neural Control Mechanisms* (Rudomin, P., Romo, R., and Mendell, L., eds.) New York: Oxford University Press, pp. 245–258.
- Burke, R.E. 1999a. Revisiting the notion of ‘motor unit types.’ In: *Peripheral and Spinal Mechanisms in the Neural Control of Movement. Progress in Brain Research, Vol. 123* (Binder, M., ed.) Amsterdam: Elsevier, pp. 167–175.
- Burke, R.E. 1999b. The use of state-dependent modulation of spinal reflexes as a tool to investigate the organization of spinal interneurons. *Exp. Brain Res.* 128: 263–277.
- Burke, R.E. 2000. Comparison of alternative designs for reducing complex neurons to equivalent cables. *J. Comp. Neurosci.* 9: 31–47.
- Burke, R.E. 2002. Some unresolved issues in motor unit research. In: *Sensorimotor Control of Movement and Posture (Advances in Experimental Medicine and Biology)* (Gandevia, S., Proske, U., and Stuart, D., eds.) New York: Kluwer Academic/Plenum Publishers, pp. 171–178.
- Burke, R.E., Degtyarenko, A.M., and Simon, E.S. 2001. Patterns of locomotor drive to motoneurons and last order interneurons: clues to the structure of the CPG. *J. Neurophysiol.* 86: 447–462.
- Burke, R.E., Dum, R.P., Fleshman, J.W., Glenn, L.L., Lev-Tov, A., O’Donovan, M.J., and Pinter, M.J. 1982. An HRP study of the relation between cell size and motor unit type in cat ankle extensor motoneurons. *J. Comp. Neurol.* 209: 17–28.
- Burke, R.E., Fedina, L., and Lundberg, A. 1971. Spatial synaptic distribution of recurrent and group Ia inhibitory systems in cat spinal motoneurons. *J. Physiol. (Lond.)* 214: 305–326.
- Burke, R.E., Fyffe, R.E.W., and Moschovakis, A.K. 1994. Electrotonic architecture of cat gamma motoneurons. *J. Neurophysiol.* 72: 2302–2316.
- Burke, R.E., and Glenn, L.L. 1996. Horseradish peroxidase study of the spatial and electrotonic distribution of group Ia synapses on type-identified ankle extensor motoneurons of the cat. *J. Comp. Neurol.* 372: 465–485.
- Burke, R.E., Jankowska, E., and ten Bruggencate, G. 1970a. A comparison of peripheral and rubrospinal synaptic input to slow and fast twitch motor units of triceps surae. *J. Physiol. (Lond.)* 207: 709–732.
- Burke, R.E., Levine, D.N., Tsairis, P., and Zajac, F.E. 1973a. Physiological types and histochemical profiles in motor units of the cat gastrocnemius. *J. Physiol. (Lond.)* 234: 723–748.
- Burke, R.E., and Nelson, P.G. 1971. Accommodation to current ramps in motoneurons of fast and slow twitch motor units. *Int. J. Neurosci.* 1: 347–356.

- Burke, R.E., and Rudomin, P. 1977. Spinal neurons and synapses. In: *Handbook of Physiology, Section 1: The Nervous System, Vol. I: The Cellular Biology of Neurons, Part 2.* (Kandel, E.R., ed.) Bethesda, MD: American Physiological Society, pp. 877–944.
- Burke, R.E., Rudomin, P., and Zajac, F.E. 1970b. Catch property in single mammalian motor units. *Science* 168: 122–124.
- Burke, R.E., Rudomin, P., and Zajac, F.E. 1976a. The effect of activation history on tension production by individual muscle units. *Brain Res.* 109: 515–529.
- Burke, R.E., Rymer, W.Z., and Walsh, J.V. 1973b. Functional specialization in the motor unit population of cat medial gastrocnemius muscle. In: *Control of Posture and Locomotion.* (Stein, R.B., Pearson, K.B., Smith, R.S., and Redford, J.B., ed.) New York: Plenum, pp. 29–44.
- Burke, R.E., Rymer, W.Z., and Walsh, J.V. 1976b. Relative strength of synaptic input from short latency pathways to motor units of defined type in cat medial gastrocnemius. *J. Neurophysiol.* 39: 447–458.
- Burke, R.E., Strick, P.L., Kanda, K., Kim, C.C., and Walmsley, B. 1977. Anatomy of medial gastrocnemius and soleus motor nuclei in cat spinal cord. *J. Neurophysiol.* 40: 667–680.
- Burke, R.E., and Tsairis, P. 1977. Histochemical and physiological profile of a skeletofusimotor (beta) unit in cat soleus muscle. *Brain Res.* 129: 341–345.
- Burkhardt, D.A. 1994. Light adaptation and photopigment bleaching in cone photoreceptors in situ in the retina of the turtle. *J. Neurosci.* 14: 1091–1105.
- Burns, M.E., and Lamb, T.D. 2003. Visual transduction by rod and cone photoreceptors. In: *Visual Neurosciences.* (Chalupa, L., and Werner, J.S., eds.) Cambridge MA: MIT Press.
- Burriss, C., Klug, K., Ngo, I.-T., Sterling, P., and Schein, S. 2002. How Müller glial cells in macaque fovea coat and isolate the synaptic terminals of cone photoreceptors. *J. Comp. Neurol.* 453: 100–111.
- Burwell, R.D. 2000. The parahippocampal region: corticocortical connectivity. *Ann. NY Acad. Sci.* 911: 25–42.
- Büttner, U., and Fuchs, A.F. 1973. Influence of saccadic eye movements on unit activity in simian lateral geniculate and perigeniculate nuclei. *J. Neurophysiol.* 36: 127–141.
- Buzsáki, G. 1989. Two-stage model of memory trace formation: a role for “noisy” brain states. *Neuroscience* 31: 551–570.
- Buzsáki, G. 2002. Theta oscillations in the hippocampus. *Neuron* 33, 325–40.
- Caggiano, M., Kauer, J.S., and Hunter, D.D. 1994. Globose basal cells are neuronal progenitors in the olfactory epithelium: a lineage analysis using a replication-incompetent retrovirus. *Neuron* 13: 339–352.
- Cai, Y., McGee, J., and Walsh, E.J. 2000. Contributions of ion conductances to the onset responses of octopus cells in the ventral cochlear nucleus: simulation results. *J. Neurophysiol.* 83: 301–314.
- Caicedo, A., and Herbert, H. 1993. Topography of descending projections from the inferior colliculus to auditory brainstem nuclei in the rat. *J. Comp. Neurol.* 328: 377–392.
- Cajal, S. Ramon y. 1904. *La Textura del Sistema Nervioso del Hombre y los Vertebrados.* Madrid: Moya.
- Cajal, S. Ramon y. 1911. *Histologie du Système Nerveux de l’Homme et des Vertèbres, Vol. II.* (L. Azoulay, trans.) Paris, Maloine.
- Cajal, S. Ramón y. 1955. *Studies on the cerebral cortex (limbic structures).* (Kraft, L.M., trans.) London: Loyd-Luke.
- Cajal, S. Ramon y. 1972. *The Structure of the Retina.* Springfield, IL: Charles C Thomas.
- Cajal, S. Ramón y., 1888. Estructura de los centros nerviosos de los aves. *Rev. Trimestr. Histol. Normal Patol.* 1, 305–315.
- Calabresi, P., Lacey, M.G., and North, R.A. 1989. Nicotinic excitation of rat ventral tegmental neurones in vitro studied by intracellular recording. *Br. J. Pharmacol.* 98: 135–140.

- Calabresi, P., Maj, R., Pisani, A., Mercuri, N.B., and Bernardi, G. 1992a. Long term synaptic depression in the striatum: physiological and pharmacological characterization. *J. Neurosci.* 12: 4224–4233.
- Calabresi, P., Pisani, A., Mercuri, N.B., and Bernardi, G. 1992b. Long-term potentiation in the striatum is unmasked by removing the voltage dependent blockade of NMDA receptor channel. *Eur. J. Neurosci.* 4: 929–935.
- Calabresi, P., Mercuri, N.B., and Bernardi, G. 1993. Chemical modulation of synaptic transmission in the striatum. In: *Chemical Signalling in the Basal Ganglia.* (Arbuthnott, G., and Emson, P.C., eds.) *Prog. Brain Res.* 99: 299–308.
- Calabresi, P., Pisani, A., Mercuri, N.B., and Bernardi, G. 1996. The corticostriatal projection: from synaptic plasticity to dysfunctions of the basal ganglia. *Trends Neurosci.* 19: 19–24.
- Calabresi, P., Centonze, D., Gubellini, P., Pisani, A., and Bernardi, G. 1998. Endogenous ACh enhances striatal NMDA-responses via M1-like muscarinic receptors and PKC activation. *Eur. J. Neurosci.* 10: 2887–2895.
- Calabresi, P., Gubellini, P., Centonze, D., Sancesario, G., Morello, M., Giorgi, M., Pisani, A., and Bernardi, G. 1999a. A critical role of the NO/cGMP pathway in corticostriatal long-term depression. *J. Neurosci.* 19: 2489–2499.
- Calabresi, P., Centonze, D., Gubellini, P., and Bernardi, G. 1999b. Activation of M1-like muscarinic receptors is required for the induction of corticostriatal LTP. *Neuropharm.* 38: 323–326.
- Calancie, B., and Bawa, P. 1990. Motor unit recruitment in humans. In: *The Segmental Motor System* (Binder, M., and Mendell, L., eds.) New York: Oxford University Press, pp. 75–95.
- Calancie, B., Needham-Shropshire, B., Jacobs, P., Willer, K., Zych, G., and Green, B.A. 1994. Involuntary stepping after chronic spinal cord injury. Evidence for a central rhythm generator for locomotion in man. *Brain* 117: 1143–1159.
- Calkins, D.J., Schein, S., Tsukamoto, Y., and Sterling, P. 1994. M and L cones in macaque fovea connect to midget ganglion cells via different numbers of excitatory synapses. *Nature* 371: 70–72.
- Calkins, D.J., and Sterling, P. 1996. Absence of spectrally specific lateral inputs to midget ganglion cells in primate retina. *Nature* 381: 613–615.
- Calkins, D.J., and Sterling, P. 1997a. Microcircuitry of the primate blue/yellow ganglion cell. *J. Neurosci.* 18: 3373–3385.
- Calkins, D.J., and Sterling, P. 1997b. Midget (P) ganglion cells in retina of trichromatic primates are not wired for color opponency. *J. Neurosci.* 18: 3386–3395.
- Calkins, D.J., and Sterling, P. 1999. Evidence that circuits for spatial and color vision segregate at the first retinal synapse. *Neuron* 24: 313–321.
- Calkins, D., and Sterling, P. 2003. Synaptic connections of OFF parasol ganglion cells in primate fovea.
- Calkins, D.J., Tsukamoto, Y., and Sterling, P. 1996. Foveal cones form basal as well as invaginating contacts with diffuse ON bipolar cells. *Vision Res.* 36: 3373–3381.
- Callaway, J.C., and Ross, W.N. 1995. Frequency dependent propagation of sodium action potentials in dendrites of hippocampal CA1 pyramidal neurons. *J. Neurophysiol.* 74: 1395–1403.
- Calleja, C. 1893. *La Region Olfactoria del Cerebro.* Madrid: Moya.
- Calvin, W.H., and Schwindt, P.C. 1972. Steps in the production of motoneuron spikes during rhythmic firing. *J. Neurophysiol.* 35: 297–310.
- Calvin, W.H., and Sybert, G. 1976. Fast and slow pyramidal tract neurons: an intracellular analysis of their contrasting repetitive firing properties in the cat. *J. Neurophysiol.* 39: 420–434.
- Cant, N.B. 1981. The fine structure of two types of stellate cells in the anterior division of the anteroventral cochlear nucleus of the cat. *Neuroscience* 6: 2643–2655.

- Cant, N.B. 1982. Identification of cell types in the anteroventral cochlear nucleus that project to the inferior colliculus. *Neurosci. Lett.* 32: 241–246.
- Cant, N.B. 1992. The cochlear nucleus: neuronal types and their synaptic organization. In: *The Mammalian Auditory Pathway: Neuroanatomy.* (Webster, D.B., Popper, A.N., and Fay, R.R., eds.) Berlin: Springer-Verlag, pp. 66–116.
- Cant, N.B. 1993. The synaptic organization of the ventral cochlear nucleus of the cat: the peripheral cap of small cells. In: *The Mammalian Cochlear Nuclei* (Merchán, M.A., Juiz, J.M., Godfrey, D.A., and Mugnaini, E., eds.) New York: Plenum, pp. 91–105.
- Cant, N.B., and Gaston, K.C. 1982. Pathways connecting the right and left cochlear nuclei. *J. Comp. Neurol.* 212: 313–326.
- Cant, N.B., and Hyson, R.L. 1992. Projections from the lateral nucleus of the trapezoid body to the medial superior olivary nucleus in the gerbil. *Hearing Res.* 58: 26–34.
- Cant, N.B., and Morest, D.K. 1979a. Organization of the neurons in the anterior division of the anteroventral cochlear nucleus of the cat. Light-microscopic observations. *Neuroscience* 4: 1909–1923.
- Cant, N.B., and Morest, D.K. 1979b. The bushy cells in the anteroventral cochlear nucleus of the cat. A study with the electron microscope. *Neuroscience* 4: 1925–1945.
- Cant, N.B., and Morest, D.K. 1984. The structural basis for stimulus coding in the cochlear nucleus of the cat. In: *Hearing Science, Recent Advances* (Berlin, C.I., ed.) San Diego: College-Hill Press, pp. 371–421.
- Carbonne, E., and Lux, H.D. 1984. A low voltage-activated calcium conductance in embryonic chick sensory neurons. *Biophys. J.* 46: 413–418.
- Carden, W.B., and Bickford, M.E. 1999. Location of muscarinic type 2 receptors within the synaptic circuitry of the cat visual thalamus. *J. Comp. Neurol.* 410: 431–443.
- Carden, W.B., and Bickford, M.E. 2002. Synaptic inputs of class III and class V interneurons in the cat pulvinar nucleus: differential integration of RS and RL inputs. *Vis. Neurosci.* 19: 51–59.
- Carlin, K., Jones, K.E., Jiang, Z., Jordan, L., and Brownstone, R. 2000. Dendritic L-type calcium currents in mouse spinal motoneurons: implications for bistability. *Eur. J. Neurosci.* 12: 1635–1646.
- Carlson, G.C., Shipley, M.T., and Keller, A. 2000. Long-lasting depolarizations in mitral cells of the rat olfactory bulb. *J. Neurosci.* 20: 2011–2021.
- Carlson-Kuhta, P., Trank, T.V., and Smith, J.L. 1998. Forms of forward quadrupedal locomotion. II. A comparison of posture, hindlimb kinematics, and motor patterns for upslope and level walking. *J. Neurophysiol.* 79: 1687–1701.
- Carmichael, S.T., Clugnet, M.-C., and Price, J.L. 1994. Central olfactory connections in the macaque monkey. *J. Comp. Neurol.* 346: 403–434.
- Carnevale, N.T., Tsai, K.Y., Claiborne, B.J., and Brown, T.H. 1997. Comparative electronic analysis of 3 classes of rat hippocampal neurons. *J. Neurophysiol.* 78: 703–720.
- Carpenter, D.O., Matthews, M.R., Parsons, P.J., and Hori, N. 1994. Long-term potentiation in the piriform cortex is blocked by lead. *Cell. Mol. Neurobiol.* 14: 723–733.
- Casagrande, V.A., and Norton, T.T. 1996. Lateral geniculate nucleus: A review of its physiology and function. In: *The Neural Basis of Visual Function* (Leventhal, A.G., ed.) London: MacMillan, pp. 41–84.
- Casanova, C., Merabet, L., Desautels, A., and Minville, K. 2001. Higher-order motion processing in the pulvinar. *Prog. Brain Res.* 134: 71–82.
- Casini, G., and Brecha, N.C. 1992. Colocalization of vasoactive intestinal polypeptide and GABA immunoreactivities in a population of wide-field amacrine cells in the rabbit retina. *Vis. Neurosci.* 8: 373–378.
- Caspary, D.M., Backoff, P.M., Finlayson, P.G., and Palombi, P.S. 1994. Inhibitory inputs mod-

- ulate discharge rate within frequency receptive fields of anteroventral cochlear nucleus neurons. *J. Neurophysiol.* 72: 2124–2133.
- Caspary, D.M., Pazara, K.E., Kossel, M., and Faingold, C.L. 1987. Strychnine alters the fusiform cell output from the dorsal cochlear nucleus. *Brain Res.* 417: 273–282.
- Castillo, J.D., and Katz, B. 1954. Statistical factors involved in neuromuscular facilitation and depression. *J. Physiol. (Lond.)* 124: 574–585.
- Castillo, P.E., Carleton, A., Vincent, J.D., and Lledo, P.M. 1999. Multiple and opposing roles of cholinergic transmission in the main olfactory bulb. *J. Neurosci.* 19: 9180–9191.
- Castro-Alamancos, M., Donoghue, J., and Connors, B. 1995. Different forms of synaptic plasticity in somatosensory and motor areas of the neocortex. *J. Neurosci.* 15: 5324–5333.
- Cattarelli, M., Astic, L., and Kauer, J.S. 1988. Metabolic mapping of 2-deoxyglucose uptake in the rat piriform cortex using computerized image processing. *Brain Res.* 442: 180–184.
- Catterall, W.A. 1988. Structure and function of voltage-sensitive ion channels. *Science* 242: 50–61.
- Catterall, W.A. 1992. Cellular and molecular biology of voltage-gated sodium channels. *Physiol. Rev.* 72 (Suppl. 4): 515–548.
- Catterall, W.A. 1995. Structure and function of voltage-gated ion channels. *Annu. Rev. Biochem.* 64: 493–531.
- Catterall, W.A. 2000a. Structure and regulation of voltage-gated Ca^{2+} channels. *Annu. Rev. Cell Dev. Biol.* 16: 521–555.
- Catterall, W.A. 2000b. From ionic currents to molecular mechanisms: the structure and function of voltage-gated sodium channels. *Neuron* 26: 13–25.
- Centonze, D., Gubellini, P., Bernardi, G., and Calabresi, P. 1999. Permissive role of interneurons in corticostriatal synaptic plasticity. *Brain Res. Rev.* 31: 1–5.
- Chagnac-Amitai, Y., Luhmann, H., and Prince, D. 1990. Burst-generating and regular spiking layer 5 pyramidal neurons of rat neocortex have different morphological features. *J. Comp. Neurol.* 296: 598–613.
- Chalupa, L.M. 1991. Visual function of the pulvinar. In: *The Neural Basis of Visual Function* (Leventhal, A.G., ed.) Boca Raton, FL: CRC Press, pp. 140–159.
- Chalupa, L.M., and Abramson, B.P. 1989. Visual receptive fields in the striate-recipient zone of the lateral posterior-pulvinar complex. *J. Neurosci.* 9: 347–357.
- Chalupa, L.M., and Thompson, I.D. 1980. Retinal ganglion cell projections to the superior colliculus of the hamster demonstrated by the horseradish peroxidase technique. *Neurosci. Lett.* 19: 13–19.
- Chance, F.S., Abbott, L.F., and Reyes, A. 2002. Gain modulation from background synaptic input. *Neuron* 35: 773–782.
- Chander, D., and Chichilnisky, E.J. 2001. Adaptation to temporal contrast in primate and salamander retina. *J. Neurosci.* 21: 9904–9916.
- Chandy, K.G., and Gutman, G.A. 1995. Voltage-gated potassium channel genes. In: *Ligand- and Voltage-Gated Channels* (North, A., ed.) Boca Raton, FL: CRC Press, pp. 1–71.
- Chang, H.T., and Kitai, S.T. 1982. Large neostriatal neurons in the rat: an electron microscopic study of gold-toned Golgi-stained cells. *Brain Res. Bull.* 8: 631–643.
- Chang, H.T., Wilson, C.J., and Kitai, S.T. 1981. Single neostriatal efferent axons in the globus pallidus: a light and electron microscopic study. *Science* 213: 915–918.
- Chang, H.T., Wilson, C.J., and Kitai, S.T. 1982. A Golgi study of rat neostriatal neurons: light microscopic analysis. *J. Comp. Neurol.* 208: 107–126.
- Chan-Palay, V. 1977. *Cerebellar Dentate Nucleus. Organization, Cytology and Transmitters.* Springer-Verlag, New York.
- Chan-Palay, V., Palay, S.L., and Wu, J.Y. 1979. Gamma-aminobutyric acid pathways in the cerebellum studied by retrograde and anterograde transport of glutamic acid decarboxylase antibody after in vivo injections. *Anat. Embryol.* 157: 1–14.

- Chapman, C.A., Xu, Y., Haykin, S., and Racine, R.J. 1998. Beta-frequency (15–35 Hz) electroencephalogram activities elicited by toluene and electrical stimulation in the behaving rat. *Neuroscience* 86: 1307–1319.
- Chaput, M.A., Buonviso, N., and Berthommier, F. 1992. Temporal patterns in spontaneous and odour-evoked mitral cell discharges recorded in anaesthetized freely breathing animals. *Eur. J. Neurosci.* 4: 813–822.
- Chaprik, S., Gähwiler, B.H., Do, K.Q., and Knopfel, T. 1990. Potassium conductances in hippocampal neurons blocked by excitatory amino-acid transmitters. *Nature* 347: 765–767.
- Chaprik, S., Mertz, J., Beaupaire, E., Moreaux, L., and Delaney, K. 2001. Odor-evoked calcium signals in dendrites of rat mitral cells. *Proc. Natl. Acad. Sci. U.S.A.* 98: 1230–1234.
- Charpier, S, Mahon, S., and Deniau, J.-M. 1999. In vivo induction of striatal long-term potentiation by low-frequency stimulation of the cerebral cortex. *Neuroscience* 91: 1209–1222.
- Chen, C., and Thompson, R. 1995. Temporal specificity of long-term depression in parallel fiber–Purkinje synapses in rat cerebellar slice. *Learn. Memory* 2: 185–198.
- Chen, W.R., Midtgaard, J., and Shepherd, G.M. 1997. Forward and backward propagation of dendritic impulses and their synaptic control in mitral cells. *Science* 278: 463–467.
- Chen, W.R., Shen, G.Y., Shepherd, G.M., Hines, M.L., and Midtgaard, J. 2002. Multiple modes of action potential initiation and propagation in mitral cell primary dendrite. *J. Neurophysiol.* 88: 2755–2764.
- Chen, W.R., and Shepherd, G.M. 1997. Membrane and synaptic properties of mitral cells in slices of rat olfactory bulb. *Brain Res.* 745: 189–196.
- Chen, W.R., and Shepherd, G.M. 1998. Activation of olfactory dendrodendritic reciprocal synapses through NMDA receptors and its dependence on action potential propagation in the mitral cell secondary dendrites. *Am. Chem. Soc. Abstr.* 20: 274.
- Chen, W.R., Xiong, W., and Shepherd, G.M. 2000. Analysis of relations between NMDA receptors and GABA release at olfactory bulb reciprocal synapses. *Neuron* 25: 625–633.
- Chesselet, M.F., and Graybiel, A.M. 1986. Striatal neurons expressing somatostatin-like immunoreactivity evidence for a peptidergic interneuronal system in the cat. *Neuroscience* 17: 547–571.
- Chicurel, M.E., and Harris, K.M. 1992. Three-dimensional analysis of the structure and composition of CA3 branched dendritic spines and their synaptic relationships with mossy fiber boutons in the rat hippocampus. *J. Comp. Neurol.* 325: 169–182.
- Chiu, K., and Greer, C.A. 1996. Immunocytochemical analyses of astrocyte development in the olfactory bulb. *Dev. Brain Res.* 95: 28–37.
- Cho, H.J., and Takagi, H. 1993. Cholecystokinin (CCK)-8-immunoreactivity in the piriform cortex of the rat with special reference to its fine structures. *Osaka City Med. J.* 39: 75–92.
- Choi, S., and Lovinger, D.M. 1997. Decreased probability of neurotransmitter release underlies striatal long-term depression and postnatal development of corticostriatal synapses. *Proc. Natl. Acad. Sci. USA* 94: 2665–2670.
- Choi, W.S., Kim, M.O., Lee, B.J., Kim, J.H., Sun, W., Seong, J.Y., and Kim, K. 1994. Presence of gonadotropin-releasing hormone mRNA in the rat olfactory piriform cortex. *Brain Res.* 648: 148–151.
- Chover, J., Haberly, L.B., and Lytton, W.W. 2001. Alternating dominance of NMDA and AMPA for learning and recall: a computer model. *Neuroreport* 12: 2503–2507.
- Christensen, T.A., Heinbockel, T., and Hildebrand, J.G. 1996. Olfactory information processing in the brain: encoding chemical and temporal features of odors. *J. Neurobiol.* 30: 82–91.
- Christensen, T.A., and Hildebrand, J.G. 1987. Male-specific, sex pheromone-selective projection neurons in the antennal lobes of the moth *Manduca sexta*. *J. Comp. Physiol. A* 160: 553–569.
- Christensen, T.A., Waldrop, B.R., Harrow, I.D., and Hildebrand, J.G. 1993. Local interneurons

- and information processing in the olfactory glomeruli of the moth *Manduca sexta*. *J. Comp. Physiol. A* 173: 385–99.
- Christie, B.R., Eliot, L.S., Ito, K.I., Miyakawa, H., and Johnston, D. 1995. Different Ca^{2+} channels in soma and dendrites of hippocampal pyramidal neurons mediate spike-induced Ca^{2+} influx. *J. Neurophysiol.* 73: 2553–2557.
- Christie, B.R., Kerr, D.S., and Abraham, W.C. 1994. Flip side of synaptic plasticity long-term depression mechanisms in the hippocampus. *Hippocampus* 4: 127–135.
- Christie, B.R., Magee, J.C., and Johnston, D. 1996. The role of dendritic action potentials and Ca^{2+} influx in the induction of homosynaptic long-term depression in hippocampal CA1 pyramidal neurons. *Learn. Memory* 3: 160–169.
- Christie, J.M., Schoppa, N.E., and Westbrook, G.L. 2001. Tufted cell dendrodendritic inhibition in the olfactory bulb is dependent on NMDA receptor activity. *J. Neurophysiol.* 85: 169–173.
- Chujo T., Yamada Y., and Yamamoto C., 1975. Sensitivity of Purkinje cell dendrites to glutamic acid. *Exp. Brain Res.* 23: 293–300.
- Chun, M.-H., Grünert, U., Martin, P.R., and Wässle, H. 1996. The synaptic complex of cones in the fovea and in the periphery of the macaque monkey retina. *Vis. Res.* 36: 3383–3395.
- Chun, M.-H., and Wässle, H. 1989. GABA-like immunoreactivity in the cat retina: electron microscopy. *J. Comp. Neurol.* 279: 55–67.
- Cinelli, A.R., and Kauer, J.S. 1994. Voltage-sensitive dyes and functional activity in the olfactory pathway. *Annu. Rev. Neurosci.* 15: 321–351.
- Claiborne, B.J., Amaral, D.G., and Cowan, W.M. 1986. A light and electron microscopic analysis of the mossy fibers of the rat dentate gyrus. *J. Comp. Neurol.* 246: 435–458.
- Claiborne, B.J., Amaral, D.G., and Cowan, W.M. 1990. A quantitative three-dimensional analysis of granule cell dendrites in the rat dentate gyrus. *J. Comp. Neurol.* 302: 206–219.
- Clark, R., and Collins, G. 1976. The release of endogenous amino acids from the rat visual cortex. *J. Physiol. (Lond.)* 263: 383–400.
- Clark, W.E. 1957. Inquiries into the anatomical basis of olfactory discrimination. *Proc. R. Soc. Lond. B Biol. Sci.* 146: 299–319.
- Cleland, B.G., Dubin, M.W., and Levick, W.R. 1971. Sustained and transient neurones in the cat's retina and lateral geniculate nucleus. *J. Physiol. (Lond.)* 217: 473–496.
- Cleland, B.G., and Freeman, A.W. 1988. Visual adaptation is highly localized in the cat's retina. *J. Physiol. (Lond.)* 404: 591–611.
- Cleland, B.G., and Levick, W.R. 1974a. Brisk and sluggish concentrically organized ganglion cells in the cat's retina. *J. Physiol. (Lond.)* 240: 421–456.
- Cleland, B.G., and Levick, W.R. 1974b. Properties of rarely encountered types of ganglion cells in the cat's retina and an overall classification. *J. Physiol. (Lond.)* 240: 457–492.
- Clements, J., and Redman, S. 1989. Cable properties of cat spinal motoneurons measured by combining voltage clamp, current clamp and intracellular staining. *J. Physiol. (Lond.)* 409: 63–87.
- Cline, H. 1999. Development of dendrites. In: *Dendrites* (Stuart, G.J., Spruston, N., and Häusser, M., eds.) New York: Oxford University Press, pp. 35–67.
- Clough, J., Kernell, D., and Phillips, C. 1968. The distribution of monosynaptic excitation from the pyramidal tract and from primary spindle afferents to motoneurons of the baboon's hand and forearm. *J. Physiol. (Lond.)* 198: 145–166.
- Cohen, E., and Sterling, P. 1986. Accumulation of [3H] glycine by cone bipolar neurons in the cat retina. *J. Comp. Neurol.* 250: 1–7.
- Cohen, E., and Sterling, P. 1990a. Demonstration of cell types among cone bipolar neurons of cat retina. *Philos. Trans. R. Soc. (Lond.) B* 330: 305–321.
- Cohen, E., and Sterling, P. 1990b. Convergence and divergence of cones onto bipolar cells in the central area of cat retina. *Philos. Trans. R. Soc. (Lond.) B* 330: 323–328.

- Cohen, E., and Sterling, P. 1992. Parallel circuits from cones to the ON-beta ganglion cell. *Eur. J. Neurosci.* 4: 506–520.
- Cohen, E.D. 2001. Synaptic mechanisms shaping the light-response in retinal ganglion cells. *Prog. Brain Res.* 131: 215–228.
- Cohen, E.D., Zhou, Z.J., and Fain, G.L. 1994. Ligand-gated currents of alpha and beta ganglion cells in the cat retinal slice. *J. Neurophysiol.* 72: 1260–1269.
- Colbert, C. 2001. Back-propagating action potentials in pyramidal neurons: a putative signaling mechanism for the induction of hebbian synaptic plasticity. *Restor. Neurol. Neurosci.* 19: 199–211.
- Colbert, C.M., and Johnston, D. 1996. Axonal action-potential initiation and Na⁺ channel densities in the soma and axon initial segment of subicular pyramidal neurons. *J. Neurosci.* 16: 6676–6686.
- Colbert, C.M., Magee, J.C., Hoffman, D., and Johnston, D. 1997. Slow recovery from inactivation of Na⁺ channels underlies the activity-dependent attenuation of dendritic action potentials in hippocampal Ca1 pyramidal neurons. *J. Neurosci.* 17: 6512–6521.
- Cole, A., and Nicoll, R. 1984. Characterization of a slow cholinergic postsynaptic potential recorded in vitro from rat hippocampal pyramidal cells. *J. Physiol. (Lond.)* 352: 173–188.
- Cole, K.S. 1968. *Membrane, Ions and Impulses. A Chapter of Classical Biophysics.* Berkeley, CA: University of California Press.
- Collingridge, G.L., and Bliss, T.V.P. 1987. NMDA receptors—Their role in long-term potentiation. *Trends Neurosci.* 10: 288–293.
- Collingridge, G.L., Herron, C., and Lester, R. 1988a. Frequency-dependent N-methyl-D-aspartate receptor-mediated synaptic transmission in rat hippocampus. *J. Physiol. (Lond.)* 399: 301–312.
- Collingridge, G.L., Herron, C., and Lester, R. 1988b. Synaptic activation of N-methyl-D-aspartate receptors in the Schaffer collateral-commissural pathway of rat hippocampus. *J. Physiol. (Lond.)* 399: 283–300.
- Collingridge, G.L., and Watkins, J.C. (eds.) 1994. *The NMDA Receptor.* New York: Oxford University Press.
- Collins, G.G. 1993. Actions of agonists of metabotropic glutamate receptors on synaptic transmission and transmitter release in the olfactory cortex. *Br. J. Pharmacol.* 108: 422–430.
- Collins, G.G.S. 1994. The characteristics and pharmacology of olfactory cortical LTP induced by theta-burst high frequency stimulation and 1S,3R-ACPD. *Neuropharmacology* 33: 87–95.
- Colonnier, M. 1968. Synaptic patterns on different cell types in the different laminae of the cat visual cortex. An electron microscope study. *Brain Res.* 9: 268–287.
- Condorelli, D.F., Parenti, R., Spinella, F., Salinaro, A.T., Belluardo, N., Cardile, V., and Cicirata, F. 1998. Cloning of a new gap junction gene (Cx36) highly expressed in mammalian brain neurons. *Eur. J. Neurosci.* 10: 1202–1208.
- Conley, M., and Diamond, I.T. 1990. Organization of the visual sector of the thalamic reticular nucleus in *Galago*. *Eur. J. Neurosci.* 3: 211–226.
- Conley, M., Kupersmith, A.C., and Diamond, I.T. 1991. The organization of projections from subdivisions of the auditory cortex and thalamus to the auditory sector of the thalamic reticular nucleus in *Galago*. *Eur. J. Neurosci.* 3: 1089–1103.
- Conn, P.J., and Pin, J.P. 1997. Pharmacology and functions of metabotropic glutamate receptors. *Annu. Rev. Pharmacol. Toxicol.* 37: 205–237.
- Connor, J.A., and Stevens, C.F. 1971. Voltage clamp studies of a transient outward membrane current in gastropod neural somata. *J. Physiol. (Lond.)* 213: 21–30.
- Connors, B.W., and Gutnick, M.J. 1990. Intrinsic firing patterns of diverse neocortical neurons. *Trends Neurosci.* 13: 99–104.

- Connors, B.W., Gutnick, M.J., and Prince, D.A. 1982. Electrophysiological properties of neocortical neurons in vitro. *J. Neurophysiol.* 48: 1302–1320.
- Connors, B.W., Malenka, R., and Silva, L. 1988. Two inhibitory postsynaptic potentials, and GABA_A and GABA_B receptor-mediated responses in neocortex of rat and cat. *J. Physiol. (Lond.)* 406: 443–468.
- Conrad, L.C.A., Leonard, C.M., and Pfaff, D.W. 1974. Connections of the median and dorsal raphe nuclei in the rat: an autoradiographic and degeneration study. *J. Comp. Neurol.* 156: 179–206.
- Conradi, S., Cullheim, S., Gollnik, L., and Kellerth, J.-O. 1983. Electron microscopic observations on the synaptic contacts of group Ia and muscle spindle afferents in the cat lumbosacral spinal cord. *Brain Res.* 265: 31–40.
- Conradi, S., Kellerth, J.-O., and Berthold, C.-H. 1979. Electron microscopic studies of cat spinal motoneurons: II. A method for the description of neuronal architecture and synaptology from serial sections through the cell body and proximal dendritic segments. *J. Comp. Neurol.* 184: 741–754.
- Constanti, A., Bagegta, G., and Libri, V. 1993. Persistent muscarinic excitation in guinea-pig olfactory cortex neurons: involvement of a slow post-stimulus afterdepolarizing current. *Neuroscience* 56: 887–904.
- Constanti, A., and Galvan, M. 1983a. Fast inward-rectifying current accounts for anomalous rectification in olfactory cortex neurones. *J. Physiol.* 335: 153–178.
- Constanti, A., and Galvan, M. 1983b. M-current in voltage-clamped olfactory cortex neurones. *Neurosci. Lett.* 39: 65–70.
- Constanti, A., Galvan, M., Franz, P., and Sim, J.A. 1985. Calcium-dependent inward currents in voltage-clamped guinea-pig olfactory cortex neurones. *Pflügers Arch.* 404: 259–265.
- Constanti, A., and Libri, V. 1992. Trans-ACPD induces a slow post-stimulus inward tail current (I_{ADP}) in guinea-pig olfactory cortex neurones in vitro. *Eur. J. Pharmacol.* 216: 463–464.
- Constanti, A., and Sim, J.A. 1987a. Calcium-dependent potassium conductance in guinea-pig olfactory cortex neurones in vitro. *J. Physiol.* 387: 173–194.
- Constanti, A., and Sim, J.A. 1987b. Muscarinic receptors mediating suppression of the M-current in guinea-pig olfactory cortex neurones may be of the M2-subtype. *Br. J. Pharmacol.* 90: 3–5.
- Conway, B., Hultborn, H., Kiehn, O., and Mintz, I.M. 1988. Plateau potentials in alpha-motoneurons induced by intravenous injection of L-dopa and clonidine in the spinal cat. *J. Physiol. (Lond.)* 405: 369–384.
- Cook, E.P., and Johnston, D. 1997. Active dendrites reduce location-dependent variability of synaptic input trains. *J. Neurophysiol.* 78: 2116–2128.
- Cook, P.B., and McReynolds, J.S. 1998. Modulation of sustained and transient lateral inhibitory mechanisms in the mudpuppy retina during light adaptation. *J. Neurophysiol.* 79: 197–204.
- Cook, P.B., Lukaszewicz, P.D., and McReynolds, J.S. 1998. Action potentials are required for the lateral transmission of glycinergic transient inhibition in the amphibian retina. *J. Neurosci.* 18: 2301–2308.
- Cook, P.B., and Werblin, F.S. 1994. Spike initiation and propagation in wide field transient amacrine cells of the salamander retina. *J. Neurosci.* 14: 3852–3861.
- Coombs, J.S., Eccles, J.C., and Fatt, P. 1955a. Excitatory synaptic actions in motoneurons. *J. Physiol. (Lond.)* 130: 374–395.
- Coombs, J.S., Eccles, J.C., and Fatt, P. 1955b. The specific ionic conductances and the ionic movements across the motoneuronal membrane that produce the inhibitory post-synaptic potential. *J. Physiol. (Lond.)* 130: 326–373.
- Cooper, A.J., and Stanford, I.M. 2000. Electrophysiological and morphological characteristics of three subtypes of rat globus pallidus neurone in vitro. *J. Physiol. (Lond.)* 527: 291–304.

- Cooper, J.R., Bloom, F.E., and Roth, R.H. 1987. *The Biochemical Basis of Neuropharmacology*, 5th ed. New York: Oxford University Press.
- Cope, T., and Pinter, M. 1995. The size principle: still working after all these years. *News Physiol. Sci.* 10: 280–286.
- Cope, T.C., and Sokoloff, A.J. 1999. Orderly recruitment tested across muscle boundaries. In: *Peripheral and Spinal Mechanisms in the Neural Control of Movement*. Progress in Brain Research, Vol. 123. (Binder, M.D., ed.) Amsterdam: Elsevier, pp. 177–190.
- Copenhagen, D.R., and Jahr, C.E. 1989. Release of endogenous excitatory amino acids from turtle photoreceptors. *Nature* 341: 536–539.
- Corsellis, J.A.N., and Bruton, C.J. 1983. Neuropathology of status epilepticus in humans. *Adv. Neurol.* 34: 129–139.
- Coskun, V., and Luskin, M.B. 2002. Intrinsic and extrinsic regulation of the proliferation and differentiation of cells in the rodent rostral migratory stream. *J. Neurosci. Res.* 69: 795–802.
- Cossart, R., Tyzio, R., Dinocourt, C., Esclapez, M., Hirsch, J.C., Ben-Ari, Y., and Bernard, C. 2001. Presynaptic kainate receptors that enhance the release of GABA on CA1 hippocampal interneurons. *Neuron* 29: 497–508.
- Cotman, C.W., Monaghan, D.T., Ottersen, O.P., and Storm-Mathisen, J. 1987. Anatomical organization of excitatory amino acid receptors and their pathways. *Trends Neurosci.* 10:273–280.
- Cottrell, G., Lambert, J., and Peters, J. 1987. Modulation of GABA_A receptor activity by alopaxalone. *Br. J. Pharmacol.* 90: 491–500.
- Coulter, D.A., Huguenard, J.R., and Prince, D.A. 1990. Differential effects of petit mal anti-convulsants and convulsants on thalamic neurones: calcium current reduction. *Br. J. Pharmacol.* 100: 800–806.
- Cowan, W.M., and Powell, T.P.S. 1954. An experimental study of the relation between the medial mamillary nucleus and the cingulate cortex. *Proc. R. Soc. Lond. B* 143: 114–125.
- Cowan, R.L., and Wilson, C.J. 1994. Spontaneous firing patterns and axonal projections of single corticostriatal neurons in the rat medial agranular cortex. *J. Neurophysiol.* 71: 17–32.
- Cowan, R.L., Wilson, C.J., Emson, P.C., and Heizmann, C.W. 1990. Parvalbumin-containing GABAergic interneurons in the rat neostriatum. *J. Comp. Neurol.* 302: 198–205.
- Cowan, W.M., Sudhof, T.C., and Stevens, C.F. *Synapses*. Baltimore: Johns Hopkins University Press.
- Cox, C.L., Huguenard, J.R., and Prince, D.A. 1996. Heterogeneous axonal arborizations of rat thalamic reticular neurons in the ventrobasal nucleus. *J. Comp. Neurol.* 366: 416–430.
- Cox, J.F., and Rowe, M.H. 1996. Linear and nonlinear contributions to step responses in cat retinal ganglion cells. *Vis. Res.* 36: 2047–2060.
- Cox, C.L., and Sherman, S.M. 1999. Glutamate inhibits thalamic reticular neurons. *J. Neurosci.* 19: 6694–6699.
- Cox, C.L., and Sherman, S.M. 2000. Control of dendritic outputs of inhibitory interneurons in the lateral geniculate nucleus. *Neuron* 27: 597–610.
- Cox, C.L., and Sherman, S.M. 2003. Functional synaptic contacts by intranuclear axon collaterals of thalamic relay neurons. *J. Neurosci.* 23:7642–7646.
- Crabtree, J.W., and Killackey, H.P. 1989. The topographical organization of the axis of projection within the visual sector of the rabbit's thalamic reticular nucleus. *Eur. J. Neurosci.* 1:94–109.
- Crabtree, J.W. 1996. Organization in the somatosensory sector of the cat's thalamic reticular nucleus. *J. Comp. Neurol.* 366: 207–222.
- Crabtree, J.W. 1998. Organization in the auditory sector of the cat's thalamic reticular nucleus. *J. Comp. Neurol.* 390: 167–182.
- Crabtree, J.W., and Killackey, H.P. 1989. The topographical organization of the axis of projection within the visual sector of the rabbit's thalamic reticular nucleus. *Eur. J. Neurosci.* 1: 94–109.

- Craig, A.D., and Burton, H. 1979. The lateral cervical nucleus of the cat; anatomic organization of cervicothalamic neurons. *J. Comp. Neurol.* 185: 329–346.
- Crair, M., and Malenka, R. 1995. A critical period for long-term potentiation at thalamocortical synapses. *Nature* 375: 325–328.
- Creed, R.S., Denny-Brown, D., Eccles, J.C., Liddell, E.G.T., and Sherrington, C.S. 1932. *Reflex Activity of the Spinal Cord*. London: Oxford University Press.
- Crepel, F., and Dhanjal, S.S. 1982. Cholinergic mechanisms and neurotransmission in the cerebellum of the rat. An *in vitro* study. *Brain Res.* 244, 59–68.
- Crepel, F., and Jaillaes, D. 1990. Protein kinases, nitric oxide and long-term depression of synapses in the cerebellum. *NeuroReport* 1: 133–136.
- Crepel, F., and Penit-Soria, J. 1986. Inward rectification and low threshold calcium conductance in rat cerebellar Purkinje cells. An *in vitro* study. *J. Physiol. (Lond.)* 372: 1–23.
- Crepel, F., Daniel, H., Hemart, N., and Jaillard, D. 1993. Mechanisms of synaptic plasticity in the cerebellum. In: *Long-Term Potentiation: A Debate of Current Issues*. (Baudry, M., and Davis, J., eds.) Cambridge, MA: MIT Press, pp. 145–150.
- Crepel, F., Dhanjal, S.S., and Sears, T.A., 1982. Effect of glutamate, aspartate and related derivatives on cerebellar Purkinje cell dendrites: an *in vitro* study. *J. Physiol. (Lond.)* 329: 297–317.
- Creutzfeldt, O., Lux, D., and Watanabe, S. 1966. Electrophysiology of cortical cells. In: *The Thalamus*. (Purpura, D., and Yuhr, Y., eds.) New York: Columbia University Press, pp. 209–235.
- Crick, F. 1982. Do dendritic spines twitch? *Trends Neurosci.* 5: 44–46.
- Crick, F. 1984. Function of the thalamic reticular complex: the searchlight hypothesis. *Proc. Natl. Acad. Sci. U.S.A.* 81: 4586–4590.
- Crick, F., and Koch, C. 1992. The problem of consciousness. *Sci. Am.* 267: 152–159.
- Crill, W. 1996. Persistent sodium current in mammalian central neurons. *Annu. Rev. Physiol.* 58: 349–362.
- Crone, C., Hultborn, H., Kiehn, O., Mazieres, L., and Wigström, H. 1988. Maintained changes in motoneuronal excitability by short-lasting synaptic inputs in the decerebrate cat. *J. Physiol. (Lond.)* 405: 321–343.
- Croner, L.J., and Kaplan, E. 1995. Receptive fields of P and M ganglion cells across the primate retina. *Vision Res.* 35: 7–24.
- Crooks, J., and Kolb, H. 1992. Localization of GABA, glycine, glutamate and tyrosine hydroxylase in the human retina. *J. Comp. Neurol.* 315: 287–302.
- Crowell, J.A., and Banks, M.S. 1988. Physical limits of grating visibility: fovea and periphery. *Invest. Ophthalmol. Vis. Sci.* 29: 139.
- Crunelli, V., Forda, S., and Kelly, J. 1984. The reversal potential of excitatory amino acid action on granule cells of the rat dentate gyrus. *J. Physiol. (Lond.)* 351: 327–342.
- Crunelli, V., Lightowler, S., and Pollard, C.E. 1989. A T-type Ca^{2+} current underlies low-threshold Ca^{2+} potentials in cells of the cat and rat lateral geniculate nucleus. *J. Physiol. (Lond.)* 413: 543–561.
- Cucchiario, J.B., Bickford, M.E., and Sherman, S.M. 1991. A GABAergic projection from the pretectum to the dorsal lateral geniculate nucleus in the cat. *Neuroscience* 41: 213–226.
- Cucchiario, J.B., Uhlrich, D.J., and Sherman, S.M. 1991. Electron-microscopic analysis of synaptic input from the perigeniculate nucleus to the A-laminae of the lateral geniculate nucleus in cats. *J. Comp. Neurol.* 310: 316–336.
- Cucchiario, J.B., Uhlrich, D.J., and Sherman, S.M. 1993. Ultrastructure of synapses from the pretectum in the A-laminae of the cat's lateral geniculate nucleus. *J. Comp. Neurol.* 334: 618–630.
- Cudeiro, J., Gonzalez, F., Perez, R., Alonso, J.M., and Acuna, C. 1989. Does the pulvinar-LP complex contribute to motor programming? *Brain Res.* 484: 367–370.

- Cudeiro, J., Grieve, K.L., Rivadulla, C., Rodríguez, R., Martínez-Conde, S., and Acuña, C. 1994a. The role of nitric oxide in the transformation of visual information within the dorsal lateral geniculate nucleus of the cat. *Neuropharmacology* 33: 1413–1418.
- Cudeiro, J., Rivadulla, C., Rodríguez, R., Martínez-Conde, S., Acuña, C., and Alonso, J.M. 1994. Modulatory influence of putative inhibitors of nitric oxide synthesis on visual processing in the cat lateral geniculate nucleus. *J. Neurophysiol.* 71: 146–149.
- Cudeiro, J., Rivadulla, C., Rodríguez, R., Martínez-Conde, S., Martínez, L., Grieve, K.L., and Acuña, C. 1996. Further observations on the role of nitric oxide in the feline lateral geniculate nucleus. *Eur. J. Neurosci.* 8: 144–152.
- Cudeiro, J., and Sillito, A.M. 1996. Spatial frequency tuning of orientation-discontinuity-sensitive corticofugal feedback to the cat lateral geniculate nucleus. *J. Physiol. (Lond.)* 490: 481–492.
- Cueva, J.G., Haverkamp, S., Reimer, R.J., Edwards, R., Wässle, H., and Brecha, N.C. 2002. Vesicular gamma-aminobutyric acid transporter expression in amacrine and horizontal cells. *J. Comp. Neurol.* 445: 227–237.
- Cull-Candy, S.G., and Usowicz, M.M. 1987. Multiple-conductance channels activated by excitatory amino acids in cerebellar neurons. *Nature* 325: 525–528.
- Cullheim, S., and Kellerth, J.-O. 1978a. A morphological study of the axons and recurrent axon collaterals of cat α -motoneurons supplying different functional types of muscle unit. *J. Physiol. (Lond.)* 281: 301–313.
- Cullheim, S., and Kellerth, J.-O. 1978b. A morphological study of the axons and recurrent axon collaterals of cat α -motoneurons supplying different hind-limb muscles. *J. Physiol. (Lond.)* 281: 285–299.
- Cullheim, S., and Kellerth, J.-O. 1981. Two kinds of recurrent inhibition of cat spinal α -motoneurons as differentiated pharmacologically. *J. Physiol. (Lond.)* 312: 209–224.
- Cullheim, S., Fleshman, J.W., Glenn, L.L., and Burke, R.E. 1987. Membrane area and dendritic structure in type-identified triceps surae alpha-motoneurons. *J. Comp. Neurol.* 255: 68–81.
- Cullheim, S., Kellerth, J., and Conradi, S. 1977. Evidence for direct synaptic interconnections between cat spinal α -motoneurons via the recurrent axon collaterals: a morphological study using intracellular injection of horseradish peroxidase. *Brain Res.* 132: 1–10.
- Curcio, C.A., Allen, K.A., Sloan, K.R., Lerea, C.L., Hurlley, J.B., Klock, I.B., and Milam, A.H. 1991. Distribution and morphology of human cone photoreceptors stained with anti-blue opsin. *J. Comp. Neurol.* 312: 610–624.
- Curcio, C.A., Sloan, K.R., Kalina, R.E., and Hendrickson, A.E. 1990. Human photoreceptor topography. *J. Comp. Neurol.* 292: 497–523.
- Curtis, D.R., and Eccles, J.C. 1960. Synaptic action during and after repetitive stimulation. *J. Physiol.* 150: 374–398.
- Curtis, D.R., and Felix, D. 1971. The effect of bicuculline upon synaptic inhibition in the cerebral and cerebellar cortices of the cat. *Brain Res.* 34: 301–321.
- Curtis, D.R., and Johnston, G.A.R. 1974. Amino acid transmitters in the mammalian central nervous system. *Ergeb. Physiol.* 69: 98–188.
- Curtis, D.R., and Watkins, J. 1963. Acidic amino acids with strong excitatory actions on mammalian neurones. *J. Physiol. (Lond.)* 166: 1–14.
- Curtis, D.R., Duggan, A., Felix, D., and Johnston, G. 1970. GABA, bicuculline and central inhibition. *Nature* 226: 1222–1224.
- Curtis, D.R., Gynther, B.D., Beattie, D.T., and Lacey, G. 1995. An in vivo electrophysiological investigation of group Ia afferent fibres and ventral horn terminations in the cat spinal cord. *Exp. Brain Res.* 106: 403–417.
- Curtis, D.R., Lodge, D., Bornstein, J.C., and Peet, M.J. 1981. Selective effects of (–) baclofen on spinal synaptic transmission in the cat. *Exp. Brain Res.* 42: 158–170.

- Cynader, M., and Mitchell, D. 1980. Prolonged sensitivity to monocular deprivation in dark reared cats. *J. Neurophysiol.* 43: 1041–1054.
- Czarkowska, J., Jankowska, E., and Sybirska, E. 1981. Common interneurons in reflex pathways from group Ia and Ib afferents of knee flexors and extensors in the cat. *J. Physiol. (Lond.)* 319: 367–380.
- Dacey, D., Packer, O.S., Diller, L., Branard, D., Peterson, B., and Lee, B. 2000. Center surround receptive field structure of cone bipolar cells in primate retina. *Vis. Res.* 40: 1801–1811.
- Dacey, D.M. 1989a. Axon-bearing amacrine cells of the macaque monkey retina. *J. Comp. Neurol.* 284: 275–293.
- Dacey, D.M. 1989b. Monoamine-accumulating ganglion cell type of the cat's retina. *J. Comp. Neurol.* 288: 59–80.
- Dacey, D.M. 1990. The dopaminergic amacrine cell. *J. Comp. Neurol.* 301: 461–489.
- Dacey, D.M. 1993. The mosaic of midget ganglion cells in the human retina. *J. Neurosci.* 13: 5334–5355.
- Dacey, D.M. 1996. Circuitry for color coding in the primate retina. *Proc. Natl. Acad. Sci. U.S.A.* 93: 582–588.
- Dacey, D.M., and Brace, S. 1992. A coupled network for parasol but not midget ganglion cells in the primate retina. *Vis. Neurosci.* 9: 279–290.
- Dacey, D.M., and Lee, B.B. 1994. The 'blue-on' opponent pathway in primate retina originates from a distinct bistratified ganglion cell type. *Nature* 367: 731–735.
- Dacey, D.M., Lee, B.B., Stafford, D.K., Pokorny, J., and Smith, V.C. 1996. Horizontal cells of the primate retina: cone specificity without spectral opponency. *Science* 271: 656–659.
- Dacheux, R.F., and Raviola, E. 1986. The rod pathway in the rabbit retina: a depolarizing bipolar and amacrine cell. *J. Neurosci.* 6: 331–345.
- Dacheux, R.F., and Raviola, E. 1995. Light responses from one type of ON-OFF amacrine cells in the rabbit retina. *J. Neurophysiol.* 74: 2460–2467.
- Dale, H.H. 1935. Pharmacology and nerve endings. *Proc. R. Soc. Med.* 28: 319–332.
- Daniel, H., Hemart, N., Jaillard, D., and Crepel, F. 1993. Long-term depression requires nitric oxide and guanosine 3'-5' cyclic monophosphate production in cerebellar Purkinje cells. *Eur. J. Neurosci.* 5: 1079–1082.
- Daniel, P., and Whitteridge, D. 1961. The representation of the visual field on the cerebral cortex in monkeys. *J. Physiol. (Lond.)* 159: 203–221.
- Dankowski, A., and Bickford, M.E. 2003. Inhibitory circuitry involving Y cells and Y retinal terminals in the C laminae of the cat dorsal lateral geniculate nucleus. *J. Comp. Neurol.* 460: 368–379.
- Dann, J.F., Buhl, E.H., and Peichl, L. 1988. Postnatal dendritic maturation of alpha and beta ganglion cells in cat retina. *J. Neurosci.* 8: 1485–1499.
- Darian-Smith, C., Tan, A., and Edwards, S. 1999. Comparing thalamocortical and corticothalamic microstructure and spatial reciprocity in the macaque ventral posterolateral nucleus (VPLc) and medial pulvinar. *J. Comp. Neurol.* 410: 211–234.
- Darian-Smith, I. 1984. The sense of touch: performance and peripheral neural processes In: *Handbook of Physiology, Section 1: The Nervous System. Vol. III. Sensory Processes, Part 2* (Darian-Smith, I., ed.) Bethesda: American Physiological Society, pp. 739–788.
- Datiche, F., and Cattarelli, M. 1996. Catecholamine innervation of the piriform cortex: a tracing and immunohistochemical study in the rat. *Brain Res.* 710: 69–78.
- Datiche, F., Litaudon, P., and Cattarelli, M. 1996a. Intrinsic association fiber system of the piriform cortex: a quantitative study based on a cholera toxin B subunit tracing in the rat. *J. Comp. Neurol.* 376: 265–277.
- Datiche, F., Luppi, P.-H., and Cattarelli, M. 1995. Projection from nucleus reuniens thalami to piriform cortex: a tracing study in the rat. *Brain Res. Bull.* 38: 87–92.
- Datiche, F., Luppi, P.-H., and Cattarelli, M. 1996b. Serotonergic and non-serotonergic projec-

- tions from the raphe nuclei to the piriform cortex in the rat: a cholera toxin B subunit (CTb) and 5-HT immunohistochemical study. *Brain Res.* 671: 27–37.
- Datiche, F., Rouillet, F., and Cattarelli, M. 2001. Expression of Fos in the piriform cortex after acquisition of olfactory learning: an immunohistochemical study in the rat. *Brain Res. Bull.* 55: 95–99.
- Datskovskaia, A., Carden, W.B., and Bickford, M.E. 2001. Y retinal terminals contact interneurons in the cat dorsal lateral geniculate nucleus. *J. Comp. Neurol.* 430: 85–100.
- Datta, A.K., and Stephens, J.A. 1981. The effects of digital nerve stimulation on the firing of motor units in human first dorsal interosseous muscle. *J. Physiol. (Lond.)* 318: 501–510.
- Davies, C.H., Starkey, S.J., Pozza, M.F., and Collingridge, G.L. 1991. GABA_B autoreceptors regulate the induction of LTP. *Nature* 349: 609–611.
- Davis, B.J., Burd, G.D., and Macrides, F. 1982. Localization of methionine-enkephalin, substance P and somatostatin immunoreactivities in the main olfactory bulb of the hamster. *J. Comp. Neurol.* 204: 377–383.
- Davis, K.A., Ding, J., Benson, T.E., and Voigt, H.F. 1996b. Response properties of units in the dorsal cochlear nucleus of unanesthetized decerebrate gerbil. *J. Neurophysiol.* 75: 1411–1431.
- Davis, K.A., Miller, R.L., and Young, E.D. 1996a. Effects of somatosensory and parallel-fiber stimulation on neurons in dorsal cochlear nucleus. *J. Neurophysiol.* 76: 3012–3024.
- Davis, K.A., and Voigt, H.F. 1997. Evidence of stimulus-dependent correlated activity in the dorsal cochlear nucleus of decerebrate gerbils. *J. Neurophysiol.* 78: 229–247.
- Davis, K.A., and Young, E.D. 1997. Granule cell activation of complex-spiking neurons in dorsal cochlear nucleus. *J. Neurosci.* 17: 6798–6806.
- Davis, K.A., and Young, E.D. 2000. Pharmacological evidence of inhibitory and disinhibitory neural circuits in dorsal cochlear nucleus. *J. Neurophysiol.* 83: 926–940.
- Daw, N., Rader, R., Robertson, T., and Ariel, M. 1983. Effects of 6-hydroxydopamine on visual deprivation in the kitten striate cortex. *J. Neurosci.* 3: 907–914.
- Daw, N.W., and Wyatt, H.J. 1974. Raising rabbits in a moving visual environment: An attempt to modify directional sensitivity in the retina. *J. Physiol. (Lond.)* 240: 309–330.
- de Curtis, M., Biella, G., and Forti, M. 1996. Epileptiform activity in the piriform cortex of the in vitro isolated guinea pig brain preparation. *Epilepsy Res.* 26: 75–80.
- de la Villa, P., Kurahashi, T., and Kaneko, A. 1995. L-glutamate-induced responses and cGMP-activated channels in retinal bipolar cells dissociated from the cat. *J. Neurosci.* 15: 3571–3582.
- de Lima, A.D., Montero, V.M., and Singer, W. 1985. The cholinergic innervation of the visual thalamus: an EM immunocytochemical study. *Exp. Brain Res.* 59: 206–212.
- de Lima, A., and Singer, W. 1986. Cholinergic innervation of the cat striate cortex: a choline acetyltransferase immunocytochemical analysis. *J. Comp. Neurol.* 250: 324–338.
- de Lima, A.D., and Singer, W. 1987. The brainstem projection to the lateral geniculate nucleus in the cat: identification of cholinergic and monoaminergic elements. *J. Comp. Neurol.* 259: 92–121.
- de Monasterio, F.M. 1978. Properties of concentrically organized X and Y ganglion cells of macaque retina. *J. Neurophysiol.* 41: 1394–1417.
- de Monasterio, F.M., Schein, S.J., and McCrane, E.P. 1981. Staining of blue-sensitive cones of the macaque retina by a fluorescent dye. *Science* 213: 1278–1281.
- de Montigny, C., and Lamarre, Y. 1974. Rhythmic activity induced by harmaline in the olivocerebellar-bulbar systems of the cat. *Brain Res.* 53: 81–95.
- de Olmos, J., Hardy, H., and Heimer, L. 1978. The afferent connections of the main and the accessory olfactory bulb formations in the rat: an experimental HRP-study. *J. Comp. Neurol.* 181: 213–244.
- De Quidt, M.E., and Emson, P.C. 1986. Distribution of neuropeptide Y-like immunoreactivity

- in the rat central nervous system. II. Immunocytochemical analysis. *Neuroscience* 18: 545–618.
- de Ruyter van Steveninck, R., and Laughlin, S.B. 1996. The rate of information transfer at graded-potential synapses. *Nature* 379: 642–645.
- De Zeeuw, C.I., Holstege, J.C., Ruigrok, T.J.H., and Voogd, J., 1989. Ultrastructural study of the GABAergic, cerebellar, and mesodiencephalic innervation of the cat medial accessory olive: anterograde tracing combined with immunocytochemistry. *J. Comp. Neurol.* 284: 12–35.
- Deacon, T.W., Eichenbaum, H., Rosenberg, P., and Eckmann, K.W. 1983. Afferent connections of the perirhinal cortex in the rat. *J. Comp. Neurol.* 220: 168–190.
- Debanne, D., Guèrineau, N.C., Gähwiler, B.H., and Thompson, S.M. 1996. Paired-pulse facilitation and depression at unitary synapses in rat hippocampus: Quantal fluctuation affects subsequent release. *J. Physiol. (Lond.)* 491: 163–176.
- Degtyarenko, A.M., Simon, E.S., and Burke, R.E. 1996. Differential modulation of disinaptic cutaneous inhibition and excitation in ankle flexor motoneurons during fictive locomotion. *J. Neurophysiol.* 76: 2972–2985.
- Degtyarenko, A.M., Simon, E.S., Norden-Krichmar, T., and Burke, R.E. 1998. Modulation of oligosynaptic cutaneous and muscle afferent reflex pathways during fictive locomotion and scratching in the cat. *J. Neurophysiol.* 79: 447–63.
- Dehay, C., Douglas, R., Martin, K., and Nelson, C. 1991. Excitation by geniculocortical synapses is not “vetoed” at the level of dendritic spines in cat visual cortex. *J. Physiol. (Lond.)* 440: 723–734.
- Deisz, R., and Prince, D. 1989. Frequency-dependent depression of inhibition in the guinea-pig neocortex in vitro by GABAB receptor feed-back on GABA release. *J. Physiol. (Lond.)* 412: 513–542.
- del Cerro, S., Jung, M., and Lynch, G. 1992. Benzodiazepines block long-term potentiation in slices of hippocampus and piriform cortex. *Neuroscience* 49: 1–6.
- Del Punta, K., Puche, A., Adams, N.C., Rodriguez, I., and Mombaerts, P. 2002. A divergent pattern of sensory axonal projections is rendered convergent by second-order neurons in the accessory olfactory bulb. *Neuron* 35: 1057–1066.
- Delgado-Lezama, R., and Hounsgaard, J. 1999. Adapting motoneurons for motor behavior. In: *Peripheral and Spinal Mechanisms in the Neural Control of Movement. Progress in Brain Research*, Vol. 123. (Binder, M.D., ed.) Amsterdam: Elsevier, pp. 57–63.
- Delgutte, B., Hammond, B.M., and Cariani, P.A. 1998. Neural coding of the temporal envelope of speech: relation to modulation transfer functions. In: *Psychophysical and Physiological Advances in Hearing* (Palmer, A.R., Rees, A., Summerfield, A.Q., and Meddis, R., eds.) London: Whurr Publ. Inc., pp. 595–603.
- Deller, T., Katona, I., Cozzari, C., Frotscher, M., and Freund, T.F. 1999. Cholinergic innervation of mossy cells in the rat fascia dentata. *Hippocampus* 9: 314–320.
- DeLong, M.R. 1973. Putamen: activity of single units during slow and rapid arm movements. *Science* 179: 1240–1242.
- Demb, J.B. 2002. Multiple mechanisms for contrast adaptation in the retina. *Neuron* 36: 781–783.
- Demb, J.B., and Pugh, E.N. 2002. Connexin 36 forms synapses essential for night vision. *Neuron* 36: 551–553.
- Demb, J.B., Haarsma, L., Freed, M.A., and Sterling, P. 1999. Functional circuitry of the retinal ganglion cell’s nonlinear receptive field. *J. Neurosci.* 19: 9756–9767.
- Demb, J.B., Zaghoul, K., Haarsma, L., and Sterling, P. 2001a. Bipolar cells contribute to nonlinear spatial summation in the brisk transient (Y) ganglion cell in mammalian retina. *J. Neurosci.* 21: 7447–7454.
- Demb, J.B., Zaghoul, K., and Sterling, P. 2001b. Cellular basis for the response to second-order motion cues in Y retinal ganglion cells. *Neuron* 32: 711–721.

- Dembner, J.M., and Greer, C.A. 1994. Topological distribution of olfactory receptor cell axons in olfactory bulb glomeruli: a confocal microscopic analysis of DiI staining. *Assoc. Chemorecep. Sci. Abstr.* 16: 333.
- Demeter, S., Rosene, D.L., and Van Hoesen, G.W. 1985. Interhemispheric pathways of the hippocampal formation, presubiculum and entorhinal and posterior parahippocampal cortices in the rhesus monkey: the structure and organization of the hippocampal commissures. *J. Comp. Neurol.* 233: 30–47.
- Demeulemeester, H., Arckens, L., Vandasande, F., Orban, G., Heizmann, C.W., and Pochet, R. 1991. Calcium binding proteins and neuropeptides as molecular markers of GABAergic interneurons in the cat visual cortex. *Exp. Brain Res.* 84: 538–544.
- Demeulemeester, H., Vandesande, F.A.G., Orban, G., Brandon, C., and Vanderhaegen, J.J. 1988. Heterogeneity of GABAergic cells in cat visual cortex. *J. Neurosci.* 8: 988–1000.
- Deniau, J.M., and Chevalier, G. 1985. Disinhibition as a basic process in the expression of striatal functions. II. The striato-nigral influence on thalamocortical cells of the ventromedial thalamic nucleus. *Brain Res.* 334: 227–233.
- Denk, W., Sugimori, M., and Llinas, R. 1995. Two types of calcium response limited to single spines in cerebellar Purkinje cells. *Proc. Natl. Acad. Sci. U.S.A.* 92: 8279–8282.
- Denk, W., Yuste, R., Svoboda, K., and Tank, D. 1996. Imaging calcium dynamics in dendritic spines. *Curr. Opin. Neurobiol.* 6: 372–378.
- Denny-Brown, D. 1929. On the nature of postural reflexes. *Proc. R. Soc. Lond. B Biol. Sci.* 104: 252–301.
- Denny-Brown, D. 1949. Interpretation of the electromyogram. *Arch. Neurol. Psychiatry* 61: 99–128.
- Dent, J.A., Galvin, N.J., Stanfield, B.B., and Cowan, W.M. 1983. The mode of termination of the hypothalamic projection to the dentate gyrus: an EM autoradiographic study. *Brain Res.* 258: 1–10.
- Derrick, B.E., and Martinez, J.L. 1996. Associative, bidirectional modifications at the hippocampal mossy fibre-CA3 synapse. *Nature* 381: 429–434.
- Derrick, B.E., Rodriguez, S.B., Lieberman, D.N., and Martinez, J. 1992. Mu opioid receptors are associated with the induction of hippocampal mossy fiber long-term potentiation. *J. Pharmacol. Exp. Ther.* 263: 725–733.
- Derrington, A.M., and Lennie, P. 1982. The influence of temporal frequency and adaptation level on receptive field organization of retinal ganglion cells in cat. *J. Physiol. (Lond.)* 333: 343–366.
- Derrington, A.M., Lennie, P., and Wright, M.J. 1979. The mechanism of peripherally evoked responses in retinal ganglion cells. *J. Physiol. (Lond.)* 289: 299–310.
- Deschênes, M. 1981. Dendritic spikes induced in fast pyramidal tract neurons by thalamic stimulation. *Exp. Brain Res.* 43: 304–308.
- Deschênes, M., Bourassa, J., Doan, V.D., and Parent, A. 1996. A single-cell study of the axonal projections arising from the posterior intralaminar thalamic nuclei in the rat. *Eur. J. Neurosci.* 8: 329–343.
- Deschênes, M., Bourassa, J., and Parent, A. 1996. Striatal and cortical projections of single neurons from the central lateral thalamic nucleus in the rat. *Neuroscience* 72: 679–687.
- Deschênes, M., Bourassa, J., and Pinault, D. 1994. Corticothalamic projections from layer V cells in rat are collaterals of long-range corticofugal axons. *Brain Res.* 664: 215–219.
- Desmedt, J.E., and Godaux, E. 1977. Ballistic contractions in man: Characteristic recruitment pattern of single motor units of the tibialis anterior muscle. *J. Physiol. (Lond.)* 264: 673–694.
- Desmond, N., and Levy, W. 1990. Morphological correlates of long-term potentiation imply the modification of existing synapses, not synaptogenesis, in the hippocampal dentate gyrus. *Synapse* 5: 139–143.

- Destexhe, A., Neubig, M., Ulrich, D., and Huguenard, J. 1998. Dendritic low-threshold calcium currents in thalamic relay cells. *J. Neuroscience* 18: 3574–3588.
- Destombes, J., Horcholle-Bossavit, G., Simon, M., and Thiesson, D. 1996. Gaba-like immunoreactive terminals on lumbar motoneurons of the adult cat. A quantitative ultrastructural study. *Neurosci. Res.* 24: 123–130.
- Destombes, J., Horcholle-Bossavit, G., and Thiesson, D. 1992. Distribution of glycinergic terminals on lumbar motoneurons of the adult cat—an ultrastructural study. *Brain Res.* 599: 353–360.
- Deuchars, J., and Thomson, A.M. 1996. CA1 pyramid-pyramid connections in rat hippocampus in vitro: dual intracellular recordings with biocytin filling. *Neuroscience* 74: 1009–1018.
- Devor, M. 1976. Fiber trajectories of olfactory bulb efferents in the hamster. *J. Comp. Neurol.* 166: 31–48.
- DeVries, S.H. 2000. Bipolar cells use kainate and AMPA receptors to filter visual information into separate channels. *Neuron* 28: 847–856.
- DeVries, S.H., and Baylor, D.A. 1995. An alternative pathway for signal flow from rod photoreceptors to ganglion cells in mammalian retina. *Proc. Natl. Acad. Sci. U.S.A.* 92: 10658–10662.
- DeVries, S.H., and Schwartz, E.A. 1989. Modulation of an electrical synapse between solitary pairs of catfish horizontal cells by dopamine and second messengers. *J. Physiol.* 414: 351–375.
- DeVries, S.H., and Schwartz, E.A. 1999. Kainate receptors mediate synaptic transmission between cones and ‘Off’ bipolar cells in a mammalian retina. *Nature* 397: 157–160.
- DeVries, S.H., Qi, X., Smith, R.G., Makous, W., and Sterling, P. 2002. Electrical coupling between mammalian cones. *Curr. Biol.* 12: 1900–1907.
- DeYoe, E.A., Felleman, D.J., Van Essen, D.C., and McClendon, E. 1994. Multiple processing streams in occipitotemporal visual cortex. *Nature* 371: 151–154.
- Dhingra, A., Jiang, M., Wang, T.-L., Lyubarsky, A., Savchenko, A., Bar-Yehuda, T., Sterling, P., Birnbaumer, L., and Vardi, N. 2002. Light response of retinal ON bipolar cells requires a specific splice variant of Galpha(o). *J. Neurosci.* 22: 4878–4884.
- Dhingra, A., Lyubarsky, A., Jiang, M., Pugh Jr., E.N., Birnbaumer, L., Sterling, P., and Vardi, N. 2000. The light response of ON bipolar neurons requires Galpha(o). *J. Neurosci.* 20: 9053–9058.
- Dhingra, N.K., Kao, Y.-H., Sterling, P., and Smith, R.G. 2003. Contrast threshold of a brisk-transient ganglion cell in vitro. *J. Neurophysiol.* (in press).
- Diamond, I.T. 1973. The evolution of the tectal-pulvinar system in mammals: structural and behavioral studies of the visual system. *Symp. Zool. Soc. Lond.* 33: 205–233.
- Diamond, M.E., Armstrong-James, M., Budway, M.J., and Ebner, F.F. 1992. Somatic sensory responses in the rostral sector of the posterior group (POm) and in the ventral posterior medial nucleus (VPM) of the rat thalamus: dependence on the barrel field cortex. *J. Comp. Neurol.* 319: 66–84.
- DiFiglia, M., and Aronin, N. 1982. Ultrastructural features of immunoreactive somatostatin neurons in the rat caudate nucleus. *J. Neurosci.* 2: 1267–1274.
- DiFiglia, M., and Carey, J. 1986. Large neurons in the primate neostriatum examined with the combined Golgi-electron microscopic method. *J. Comp. Neurol.* 244: 36–52.
- DiFiglia, M., and Rafols, J.A. 1988. Synaptic organization of the globus pallidus. *J. Electron Microsc. Tech.* 10: 247–263.
- DiFiglia, M., Pasik, P., and Pasik, T. 1976. A Golgi study of neuronal types in the neostriatum of monkeys. *Brain Res.* 114: 245–256.
- DiFrancesco, D. 1985. The cardiac hyperpolarization-activated current I_f : Origins and developments. *Prog. Biophys. Mol. Biol.* 46: 163–183.

- DiGregorio, D.A., Nusser, Z., and Silver, R.A. 2002. Spillover of glutamate onto synaptic AMPA receptors enhances fast transmission at a cerebellar synapse. *Neuron* 35: 521–533.
- Dinerman, J.L., Dawson, T.M., Schell, M.J., Snowman, A., and Snyder, S.H. 1994. Endothelial nitric oxide synthase localized to hippocampal pyramidal cells: implications for synaptic plasticity. *Proc. Natl. Acad. Sci. U.S.A.* 91: 4214–4218.
- Dingledine, R., and Kelly, J.S. 1977. Brain stem stimulation and the acetylcholine-evoked inhibition of neurones in the feline nucleus reticularis thalami. *J. Physiol. (Lond.)* 271: 135–154.
- Dittman, J.S., Kreitzer, A.C., and Regehr, W.G. 2000. Interplay between facilitation, depression, and residual calcium at three presynaptic terminals. *J. Neurosci.* 20: 1374–85.
- Djoughri, L., Meng, Z., Brown, A.G., and Short, A.D. 1997. Electrophysiological evidence that spinomesencephalic neurons in the cat may be excited via spinocervical tract collaterals. *Exp. Brain Res.* 116: 477–484.
- Dodge, F.A. 1979. The nonuniform excitability of central neurons as exemplified by a model of the spinal motoneuron. In: *The Neurosciences: Fourth Study Program.* (Schmitt, F.O., ed.) Cambridge: MIT Press, pp. 439–455.
- Doty, H.U., and Misgeld, U. 1986. Muscarinic slow excitation and muscarinic inhibition of synaptic transmission in the rat neostriatum. *J. Physiol. (Lond.)* 380: 593–608.
- Doetsch, F., Garcia-Verdugo, J.M., and Alvarez-Buylla, A. 1997. Cellular composition and three-dimensional organization of the subventricular germinal zone in the adult mammalian brain. *J. Neurosci.* 17: 5046–5061.
- Dolleman-Van der Weel, M.J., and Witter, M.P. 1992. Organization of nucleus reuniens thalami projections to the hippocampal region, studied by multiple retrograde tracing in the rat. *Eur. J. Neurosci. Suppl.* 5: 69.
- Dolphin, A., and Scott, R. 1986. Inhibition of calcium currents in dorsal root ganglion neurones by baclofen. *Br. J. Pharmacol.* 88: 213–220.
- Domroese, M.E., and Haberly, L.B. 1995. NMDA-dependent induction of epileptiform activity in piriform cortex in vitro does not involve kinases that are required for LTP. *Soc. Neurosci. Abstr.* 21: 982.
- Domroese, M.E., and Haberly, L.B. 1996. Dual origin of slow regenerative potentials in the endopiriform nucleus. *Soc. Neurosci. Abstr.* 22: 2103.
- Dong, C.-J., and Werblin, F.S. 1998. Temporal contrast enhancement via GABAC feedback at bipolar terminals in the tiger salamander retina. *J. Neurophysiol.* 79: 2171–2180.
- Doucet, J.R., Ross, A.T., Gillespie, M.B., and Ryugo, D.K. 1999. Glycine immunoreactivity of multipolar neurons in the ventral cochlear nucleus which project to the dorsal cochlear nucleus. *J. Comp. Neurol.* 408: 515–531.
- Doucet, J.R., and Ryugo, D.K. 1997. Projections from the ventral cochlear nucleus to the dorsal cochlear nucleus in rats. *J. Comp. Neurol.* 385: 245–264.
- Doucette, R. 1993. Glial cells in the nerve fiber layer of the main olfactory bulb of embryonic and adult mammals. *Microsc. Res. Tech.* 24: 113–130.
- Douglas, R., and Martin, K.A.C. 1993. Exploring cortical microcircuits: a combined anatomical, physiological, computational approach. In: *Single Neuron Computation.* (McKenna, J.D.T., and Zornetzer, S., eds.) Orlando, FL: Academic Press, pp. 381–412.
- Douglas, R., Koch, C., Mahowald, M., Martin, K.A.C., and Suarez, H.H. 1995. Recurrent excitation in neocortical circuits. *Science* 269: 981–985.
- Douglas, R., Martin, K.A.C., and Whitteridge, D. 1988. Selective responses of visual cortical cells do not depend on shunting inhibition. *Nature* 332: 642–644.
- Douglas, R., Martin, K.A.C., and Whitteridge, D. 1989. A canonical microcircuit for neocortex. *Neural Comput.* 1: 480–488.
- Douglas, R.G., and Martin, K.A.C. 1991. A functional microcircuit for cat visual cortex. *J. Physiol. (Lond.)* 440: 735–769.

- Dowling, J.E. 1986. Dopamine: a retinal neuromodulator? *Trends Neurosci.* 9: 236–240.
- Dowling, J.E., and Boycott, B.B. 1965. Neural connections of the retina: fine structure of the inner plexiform layer. *Cold Spring Harb. Symp. Quant. Biol.* 30: 393–402.
- Dowling, J.E., and Boycott, B.B. 1966. Organization of the primate retina: electron microscopy. *Proc. R. Soc. Lond. B Biol. Sci.* 166: 80–111.
- Dowling, J.E., and Cowan, W.M. 1966. An electron microscope study of normal and degenerating centrifugal fiber terminals in the pigeon retina. *Z. Zellforsch. Mikrosk. Anat.* 71: 14–28.
- Dreifuss, J., Kelly, J., and Krnjevic, K. 1969. Cortical inhibition and g-aminobutyric acid. *Exp. Brain Res.* 9: 137–154.
- Dubé, L., Smith, A.D., and Bolam, J.P. 1988. Identification of synaptic terminals of thalamic or cortical origin in contact with distinct medium-size spiny neurons in the rat neostriatum. *J. Comp. Neurol.* 267: 455–471.
- Dubin, H. 1976. The inner plexiform layer of the vertebrate retina: a quantitative and comparative electron microscopic analysis. *J. Comp. Neurol.* 140: 479–506.
- Dudek, S.M., and Bear, M.F. 1992. Homosynaptic long-term depression in area CA1 of hippocampus and effects of N-methyl-D-aspartate receptor blockade. *Proc. Natl. Acad. Sci. U.S.A.* 89: 4363–4367.
- Dulac, C., and Axel, R. 1995. A novel family of genes encoding putative pheromone receptors in mammals. *Cell* 83: 195–206.
- Dunaevsky, A., Tashiro, A., Majewska, A., Mason, C., and Yuste, R. 1999. Developmental regulation of spine motility in mammalian CNS. *Nature* 96: 13438–13443.
- Dunlap, K., and Fischbach, G.D. 1981. Neurotransmitters decrease the calcium conductance activated by depolarization of embryonic chick sensory neurons. *J. Physiol. (Lond.)* 317: 519–535.
- Duong, T.Q., Kim, D.S., Ugurbil, K., and Kim, S.G. 2001. Localized cerebral blood flow response at submillimeter columnar resolution. *Proc. Natl. Acad. Sci. U.S.A.* 98: 10904–10909.
- Dupont, J.L., Crepel, F., and Delhay-Bouchaud, N. 1979. Influence of bicuculline and picrotoxin on reversal properties of excitatory synaptic potentials in cerebellar Purkinje cells of the rat. *Brain Res.* 173: 577–580.
- Durand, D. 1984. The somatic shunt cable model for neurons. *Biophys. J.* 46: 645–653.
- Dutar, P., and Nicoll, R.A. 1988a. A physiological role for GABAB receptors in the central nervous system. *Nature* 332: 156–158.
- Dutar, P., and Nicoll, R.A. 1988b. Pre- and postsynaptic GABAB receptors in the hippocampus have different pharmacological properties. *Neuron* 1: 585–591.
- Duysens, J., Trippel, M., Horstmann, G.A., and Dietz, V. Gating and reversal of reflexes in ankle muscles during human walking. *Exp. Brain Res.* 82: 351–358, 1990.
- Dykes, R.W. 1983. Parallel processing of somatosensory information: a theory. *Brain Res. Rev.* 6: 47–115.
- Easter, S.S., and Stuermer, C. 1984. An evaluation of the hypothesis of shifting terminals in goldfish optic tectum. *J. Neurosci.* 4: 1052–1063.
- Eaton, S.A., and Salt, T.E. 1996. Role of N-methyl-D-aspartate and metabotropic glutamate receptors in corticothalamic excitatory postsynaptic potentials *in vivo*. *Neuroscience* 73: 1–5.
- Eblen, F., and Graybiel, A.M. 1995. Highly restricted origin of prefrontal cortical inputs to striosomes in the macaque monkey. *J. Neurosci.* 15: 5999–6013.
- Eccles, J.C., Schmidt, R.F., and Willis, W.D. 1963. Pharmacological studies on presynaptic inhibition. *J. Physiol. (Lond.)* 168: 500–530.
- Eccles, J.C. 1957. *The Physiology of Nerve Cells*. Baltimore: Johns Hopkins University Press.
- Eccles, J.C. 1964. *The Physiology of Synapses*. Berlin: Springer.

- Eccles, J.C., Eccles, R.M., and Lundberg, A. 1957. The convergence of monosynaptic excitatory afferents onto many different species of alpha-motoneurons. *J. Physiol. (Lond.)* 137: 22–50.
- Eccles, J.C., Eccles, R.M., and Lundberg, A. 1960. Types of neurone in and around the intermediate nucleus of the lumbosacral cord. *J. Physiol. (Lond.)* 154: 89–114.
- Eccles, J.C., Fatt, P., and Koketsu, K. 1954. Cholinergic and inhibitory synapses in a pathway from motor-axon collaterals to motoneurons. *J. Physiol. (Lond.)* 126: 524–562.
- Eccles, J.C., Fatt, P., and Landgren, S. 1956. The central pathway for the direct inhibitory action of impulses in the largest afferent fibers to muscle. *J. Neurophysiol.* 19: 75–98.
- Eccles, J.C., Llinás R., and Sasaki, K., 1966. The mossy fibre-granule cell relay of the cerebellum and its inhibitory control by Golgi cells. *Exp. Brain Res.* 1: 82–101.
- Eccles, J.C., Llinás, R., and Sasaki, K., 1966. The inhibitory interneurons within the cerebellar cortex. *Exp. Brain Res.* 1: 1–16.
- Eccles, J.C., Llinás, R., and Sasaki, K. 1966. Parallel fiber stimulation and the responses induced thereby in the Purkinje cells of the cerebellum. *Exp. Brain Res.* 1: 17–39.
- Eccles, J.C., Llinás, R., and Sasaki, K. 1966. The excitatory synaptic action of climbing fibers on the Purkinje cells of the cerebellum. *J. Physiol. (Lond.)* 182: 268–296.
- Eccles, R.M., and Lundberg, A. 1958. Integrative pattern of Ia synaptic actions on motoneurons of hip and knee muscles. *J. Physiol. (Lond.)* 144: 271–298.
- Eccles, R.M., and Lundberg, A. 1959. Synaptic action in motoneurons by afferents which may evoke the flexion reflex. *Arch. Ital. Biol.* 97: 199–221.
- Eckenstein, F., and Baughman, R. 1984. Two types of cholinergic innervation in the cortex, one co-localised with vasoactive intestinal polypeptide. *Nature* 309: 153–155.
- Eckert, M.P., and Buchsbaum, G. 1993a. Efficient coding of natural time varying images in the early visual system. *Phil. Trans. R. Soc. (Lond.) B* 339: 385–395.
- Eckert, M.P., and Buchsbaum, G. 1993b. Effect of tracking strategies on the velocity structure of two-dimensional image sequences. *J. Opt. Soc. Am.* 10: 1582–1585.
- Edwards, C., and Ottoson, D. 1958. The site of impulse initiation in a nerve cell of a crustacean stretch receptor. *J. Physiol. (Lond.)* 143: 138–148.
- Edwards, F.R., Redman, S.J., and Walmsley, B. 1976. Statistical fluctuations in charge transfer at Ia synapses on spinal motoneurons. *J. Physiol. (Lond.)* 259: 665–688.
- Eeckman, F.H., and Freeman, W.J. 1990. Correlations between unit firing and EEG in the rat olfactory system. *Brain Res.* 528: 238–244.
- Eguibar, J., Quevedo, J., and Rudomin, P. 1997. Selective cortical and segmental control of primary afferent depolarization of single muscle afferents in the cat spinal cord. *Exp. Brain Res.* 113: 411–430.
- Eichenbaum, H. 1994. The hippocampal system and the declarative memory in humans and animals: experimental analysis and historical origins. In: *Memory Systems.* (Schacter, D.L., and Tulving, E., eds.) Cambridge, MA: MIT Press, pp. 147–201.
- Eichenbaum, H. 2000. A cortical-hippocampal system for declarative memory. *Nat. Rev. Neurosci.* 1: 41–50.
- Ekstrand, J.J., Domroese, M.E., Feig, S.L., Illig, K.R., and Haberly, L.B. 2001a. Immunocytochemical analysis of basket cells in rat piriform cortex. *J. Comp. Neurol.* 434: 308–328.
- Ekstrand, J.J., Domroese, M.E., and Haberly, L.B. 1998. Basket interneurons in rat piriform (olfactory) cortex. *Soc. Neurosci. Abstr.* 24: 2142.
- Ekstrand, J.J., Domroese, M.E., Johnson, D.M.G., Feig, S.L., Knodel, S.M., Behan, M., and Haberly, L.B. 2001b. A new subdivision of anterior piriform cortex and associated deep nucleus with novel features of interest for olfaction and epilepsy. *J. Comp. Neurol.* 434: 289–307.
- Ekstrand, J.J., and Haberly, L.B. 1995. GABAergic neurons in the molecular layer of piriform (olfactory) cortex have lamina-specific axonal arbors. *Soc. Neurosci. Abstr.* 21: 1186.

- Ekstrand, J.J., Johnson, D.M.G., Feig, S.L., and Haberly, L.B. 1996. Cajal-Retzius cells in anterior piriform cortex mediate fast feedforward inhibition in a large area of the piriform cortex, anterior olfactory nucleus, and olfactory tubercle. *Soc. Neurosci. Abstr.* 22: 1824.
- Emonet-Denand, F., Jami, L., and Laporte, Y. 1975. Skeletofusimotor axons in hind-limb muscles of the cat. *J. Physiol. (Lond.)* 249: 153–166.
- Eng, D.L., and Kocsis, J.D. 1987. Activity dependent changes in extracellular potassium and excitability in turtle olfactory nerve. *J. Neurophysiol.* 57: 740–754.
- Engberg, I., and Marshall, K.C. 1979. Reversal potentials for Ia excitatory post synaptic potentials in spinal motoneurons of cats. *Neuroscience* 4: 1583–1591.
- Ennis, M., Linster, C., Aroniadou-Anderjaska, V., Ciombor, K., and Shipley, M.T. 1998. Glutamate and synaptic plasticity at mammalian primary olfactory synapses. *Ann. NY Acad. Sci.* 855: 457–466.
- Ennis, M., Zhou, F.M., Ciombor, K.J., Aroniadou-Anderjaska, V., Hayar, A., Borrelli, E., Zimmer, L.A., Margolis, F., and Shipley, M.T. 2001. Dopamine D2 receptor-mediated presynaptic inhibition of olfactory nerve terminals. *J. Neurophysiol.* 86: 2986–2997.
- Ennis, M., Zimmer, L.A., and Shipley, M.T. 1996. Olfactory nerve stimulation activates rat mitral cells via NMDA and non-NMDA receptors in vitro. *NeuroReport* 7: 989–992.
- Enoch, J.M. 1981. Retinal receptor orientation and photoreceptor optics. In: *Vertebrate Photoreceptor Optics* (Enoch, J.M., and Tobey, F.L.J., eds.) Berlin: Springer-Verlag, pp. 127–168.
- Enroth-Cugell, C., and Jakiela, H.G. 1980. Suppression of cat retinal ganglion cell responses by moving patterns. *J. Physiol. (Lond.)* 302: 49–72.
- Enroth-Cugell, C., and Robson, J.G. 1966. The contrast sensitivity of retinal ganglion cells of the cat. *J. Physiol. (Lond.)* 187: 517–552.
- Enz, R., Brandstätter, J.H., Wässle, H., and Bormann, J. 1996. Immunocytochemical localization of GABAC receptor rho subunits in the mammalian retina. *J. Neurosci.* 16: 4479–4490.
- Erisir, A., Van Horn, S.C., Bickford, M.E., and Sherman, S.M. 1997a. Immunocytochemistry and distribution of parabrachial terminals in the lateral geniculate nucleus of the cat: a comparison with corticogeniculate terminals. *J. Comp. Neurol.* 377: 535–549.
- Erisir, A., Van Horn, S.C., and Sherman, S.M. 1977b. Relative numbers of cortical and brainstem inputs to the lateral geniculate nucleus. *Proc. Natl. Acad. Sci. U.S.A.* 94: 1517–1520.
- Ertel, E.A., Campbell, K.P., Harpold, M.M., Hofmann, F., Mori, Y., Perez-Reyes, E., Schwartz, A., Snutch, T.P., Tanabe, T., Birnbaumer, L., Tsien, R.W., and Caterall, W.A. 2000. Nomenclature of voltage-gated calcium currents. *Neuron* 25: 533–535.
- Esclapez, M., Tillakaratne, N.J.K., Tobin, A.J., and Houser, C.R. 1993. Comparative localization of mRNAs encoding two forms of glutamic acid decarboxylase with nonradioactive in situ hybridization methods. *J. Comp. Neurol.* 331: 339–362.
- Euler, T., and Masland, R.H. 2000. Light-evoked responses of bipolar cells in a mammalian retina. *J. Neurophysiol.* 83: 1817–1829.
- Euler, T., Detwiler, P.B., and Denk, W. 2002. Directionally selective calcium signals in dendrites of starburst amacrine cells. *Nature* 418: 845–852.
- Euler, T., Schneider, H., and Wässle, H. 1996. Glutamate responses of bipolar cells in a slice preparation of the rat retina. *J. Neurosci.* 16: 2934–2944.
- Evans, E.F., and Nelson, P.G. 1973. The responses of single neurons in the cochlear nucleus of the cat as a function of their location and the anaesthetic state. *Exp. Brain Res.* 17: 402–427.
- Evans, E.F., and Zhao, W. 1993. Varieties of inhibition in the processing and control of processing in the mammalian cochlear nucleus. *Prog. Brain Res.* 97: 117–126.
- Ezeh, P.I., Davis, L.M., and Scott, J.W. 1995. Regional distribution of rat electroolfactogram. *J. Neurophysiol.* 73: 2207–2220.
- Faber, D., Korn, H., Redman, S., Thompson, S., and Altman, J. 1998. *Central Synapses: Quantal Mechanisms and Plasticity*. Strasbourg: Human Frontier Science Program.

- Fadiga, E., and Brookhart, J.M. 1960. Monosynaptic activation of different portions of the motor neuron membrane. *Am. J. Physiol.* 198: 693–703.
- Fahrenbach, W.H. 1985. Anatomical circuitry of lateral inhibition in the eye of the horseshoe crab, *Limulus polyphemus*. *Proc. R. Soc. Lond. B* 225: 219–249.
- Fairen, A., De Felipe, J., and Regidor, J. 1984. Nonpyramidal neurons: general account. In: *Cerebral Cortex: Cellular Components of the Cerebral Cortex*, Vol. 1, Chap. 6. (Peters, A., and Jones, E., eds.) New York: Plenum Press, pp. 201–253.
- Fallon, J.H., and Leslie, F.M. 1986. Distribution of dynorphin and enkephalin peptides in the rat brain. *J. Comp. Neurol.* 249: 293–336.
- Famiglietti, E.V. 1991. Synaptic organization of starburst amacrine cells in rabbit retina: analysis of serial thin sections by electron microscopy and graphic reconstruction. *J. Comp. Neurol.* 309: 40–70.
- Famiglietti, E.V. 1992a. Dendritic co-stratification of ON and ON-OFF directionally selective ganglion cells with starburst amacrine cells in rabbit retina. *J. Comp. Neurol.* 324: 322–335.
- Famiglietti, E.V. 1992b. Polyaxonal amacrine cells of rabbit retina: size and distribution of PA1 cells. *J. Comp. Neurol.* 316: 406–421.
- Famiglietti, E.V., and Kolb, H. 1976. Structural basis for ON- and OFF-center responses in retinal ganglion cells. *Science* 194: 193–195.
- Famiglietti, E.V., Jr., and Peters, A. 1972. The synaptic glomerulus and the intrinsic neuron in the dorsal lateral geniculate nucleus of the cat. *J. Comp. Neurol.* 144: 285–334.
- Fanselow, E.E., Sameshima, K., Baccala, L.A., and Nicolelis, M.A. 2001. Thalamic bursting in rats during different awake behavioral states. *Proc. Natl. Acad. Sci. U.S.A.* 98: 15330–15335.
- Farbman, A.I. 1986. Prenatal development of mammalian olfactory receptor cells. *Chem. Senses* 11: 3–18.
- Farbman, A.I. 1994. Developmental biology of olfactory sensory neurons. *Semin. Cell Biol.* 5: 3–10.
- Fatt, P. 1957. Sequence of events in synaptic activation of a motoneurone. *J. Neurophysiol.* 20: 61–80.
- Fatt, P., and Katz, B. 1953. The effect of inhibitory nerve impulses on a crustacean muscle fibre. *J. Physiol. (Lond.)* 121: 374–389.
- Feig, S., and Harting, J.K. 1998. Corticocortical communication via the thalamus: ultrastructural studies of corticothalamic projections from area 17 to the lateral posterior nucleus of the cat and inferior pulvinar nucleus of the owl monkey. *J. Comp. Neurol.* 395: 281–295.
- Fekete, D.M., Rouiller, E.M., Liberman, M.C., and Ryugo, D.K. 1984. The central projections of intracellularly labeled auditory nerve fibers in cats. *J. Comp. Neurol.* 229: 432–450.
- Feldman, A., and Orlovsky, G. 1975. Activity of interneurons mediating reciprocal Ia inhibition during locomotion. *Brain Res.* 84: 181–194.
- Feldman, M.L. 1984. Morphology of the neocortical pyramidal neuron. In: *Cerebral Cortex*, Vol. 1: Cellular Components of the Cerebral Cortex (Peters, A., and Jones, E.G., eds.) New York: Plenum Press, pp. 123–200.
- Feldman, S.G., and Kruger, L. 1980. An axonal transport study of the ascending projection of medial lemniscal neurons in the rat. *J. Comp. Neurol.* 192: 427–454.
- Feliciano, M., Saldaña, E., and Mugnaini, E. 1995. Direct projections from the rat primary auditory neocortex to nucleus salgulum, paralemniscal regions, superior olivary complex and cochlear nucleus. *Auditory Neurosci.* 1: 287–308.
- Felleman, J.D., and Van Essen, C.D. 1991. Distributed hierarchical processing in the primate cerebral cortex. *Cereb. Cortex* 1: 1–47.
- Feller, M.B., Wellis, D.P., Stellwagen, D., Werblin, F.S., and Shatz, C.J. 1996. Requirement of cholinergic synaptic transmission in the propagation of spontaneous retinal waves. *Science* 272: 1182–1187.

- Feng, J.J., Kuwada, S., Ostapoff, E.M., Batra, R., and Morest, D.K. 1994. A physiological and structural study of neuron types in the cochlear nucleus. I. Intracellular responses to acoustic stimulation and current injection. *J. Comp. Neurol.* 346: 1–18.
- Fernandez, C., and Karapas, F. 1967. The course and termination of the striae of Monakow and Held in the cat. *J. Comp. Neurol.* 131: 371–386.
- Ferragamo, M.J., and Oertel, D. 2002. Octopus cells of the mammalian ventral cochlear nucleus sense the rate of depolarization. *J. Neurophysiol.* 87: 2262–2270.
- Ferragamo, M.J., Golding, N.L., Gardner, S.M., and Oertel, D. 1998b. Golgi cells in the superficial granule cell domain overlying the ventral cochlear nucleus: morphology and electrophysiology in slices. *J. Comp. Neurol.* 400: 519–528.
- Ferragamo, M.J., Golding, N.L., and Oertel, D. 1998a. Synaptic inputs to stellate cells in the ventral cochlear nucleus. *J. Neurophysiol.* 79: 51–63.
- Ferster, D. 1988. Spatially opponent excitation and inhibition in simple cells of the cat visual cortex. *J. Neurosci.* 8: 1172–1180.
- Ferster, D., Chung, S., and Wheat, H. 1996. Orientation selectivity of thalamic input to simple cells of cat visual cortex. *Nature* 380: 249–252.
- Ferster, D., and Jagadeesh, B. 1992. EPSP-IPSP interactions in cat visual cortex studied with in vivo whole-cell patch recording. *J. Neurosci.* 12: 1262–1274.
- Ferster, D., and Koch, C. 1987. Neuronal connections underlying orientation selectivity in cat visual cortex. *Trends Neurosci.* 10: 487–492.
- Fetcho, J.R. 1987. A review of the organization and evolution of motoneurons innervating the axial musculature of vertebrates. *Brain Res. Rev.* 12: 243–280.
- Field, G.D., and Rieke, F. 2002. Nonlinear signal transfer from mouse rods to bipolar cells and implications for visual sensitivity. *Neuron* 34: 773–785.
- Fifkova, E., and Anderson, C. 1981. Stimulation induced changes in the dimensions of stalks of dendritic spines in the dentate molecular layer. *Exp. Neurol.* 74: 621–627.
- Fifkova, E., and Delay, R. 1982. Cytoplasmic actin in dendritic spines as possible mediator of synaptic plasticity. *J. Cell Biol.* 95: 345–350.
- Fifkova, E.F., and van Harrevel, A. 1977. Long-lasting morphological changes in the dendritic spines of dentate granular cells following stimulation of the entorhinal area. *J. Neurocytol.* 6: 211–230.
- Finch, D.M., and Babb, T.L. 1980. Inhibition in subicular and entorhinal principal neurons in response to electrical stimulation of the fornix and hippocampus. *Brain Res.* 196: 89–98.
- Finch, D.M., and Babb, T.L. 1981. Demonstration of caudally directed hippocampal efferents in the rat by intracellular injection of horseradish peroxidase. *Brain Res.* 214: 405–410.
- Finch, D.M., Nowlin, N.L., and Babb, T.L. 1983. Demonstration of axonal projections of neurons in the rat hippocampus and subiculum by intracellular injection of HRP. *Brain Res.* 271: 201–216.
- Finkel, A.S., and Redman, S.J. 1983. The synaptic current evoked in cat spinal motoneurons by impulses in single group Ia axons. *J. Physiol. (Lond.)* 342: 615–632.
- Fischer, K.F., Lukasiewicz, P.D., and Wong, R.O.L. 1998. Age-dependent and cell class-specific modulation of retinal ganglion cell bursting activity by GABA. *J. Neurosci.* 18: 3767–3778.
- Fischer, M., Kaech, S., Knutti, D., and Matus, A. 1998. Rapid actin-based plasticity in dendritic spine. *Neuron* 20: 847–854.
- Fisher, S.K., and Boycott, B.B. 1974. Synaptic connexions made by horizontal cells within the outer plexiform layer of the retina of the cat and the rabbit. *Proc. R. Soc. Lond. B* 186: 317–331.
- Fitzpatrick, D., Conley, M., Luppino, G., Matelli, M., and Diamond, I.T. 1988. Cholinergic projections from the midbrain reticular formation and the parabrachial nucleus to the lateral geniculate nucleus in the tree shrew. *J. Comp. Neurol.* 272: 43–67.

- Fitzpatrick, D., Conley, M., Luppino, G., Matelli, M., and Diamond, I.T. 1988. Cholinergic projections to the lateral geniculate nucleus in the tree shrew. In: *Cellular Thalamic Mechanisms* (Bentivoglio, M., and Spreafico, R., eds.) New York: Elsevier, pp. 399–415.
- Fitzpatrick, D., Diamond, I.T., and Raczkowski, D. 1989. Cholinergic and monoaminergic innervation of the cat's thalamus: comparison of the lateral geniculate nucleus with other principal sensory nuclei. *J. Comp. Neurol.* 288: 647–675.
- Fitzpatrick, D., Lund, J.S., Schmechel, D.E., and Towles, A.C. 1987. Distribution of GABAergic neurons and axon terminals in the macaque striate cortex. *J. Comp. Neurol.* 264: 73–91.
- Fitzpatrick, D., Penny, G.R., and Schmechel, D.E. 1984. Glutamic acid decarboxylase-immunoreactive neurons and terminals in the lateral geniculate nucleus of the cat. *J. Neurosci.* 4: 1809–1829.
- Flaherty, A.W., and Graybiel, A.M. 1991. Corticostriatal transformations in the primate somatosensory system. Projections from physiologically mapped body-part representations. *J. Neurophysiol.* 66: 1249–1263.
- Flaherty, A.W., and Graybiel, A.M. 1994. Input-output organization of the sensorimotor striatum in the squirrel monkey. *J. Neurosci.* 14: 599–610.
- Fleshman, J.W., Lev-Tov, A., and Burke, R.E. 1984. Peripheral and central control of flexor digitorum longus and flexor hallucis longus motoneurons: the synaptic basis of functional diversity. *Exp. Brain Res.* 54: 133–149.
- Fleshman, J.W., Munson, J.B., and Sybert, G.W. 1981a. Homonymous projection of individual group Ia-fibers to physiologically characterized medial gastrocnemius motoneurons in the cat. *J. Neurophysiol.* 46: 1339–1348.
- Fleshman, J.W., Munson, J.B., Sybert, G.W., and Friedman, W.A. 1981b. Rheobase, input resistance, and motor-unit type in medial gastrocnemius motoneurons in the cat. *J. Neurophysiol.* 46: 1326–1338.
- Fleshman, J.W., Rudomin, P., and Burke, R.E. 1988a. Supraspinal control of a short-latency cutaneous pathway to hindlimb motoneurons. *Exp. Brain Res.* 69: 449–459.
- Fleshman, J.W., Segev, I., and Burke, R.E. 1988. Electrotonic architecture of type-identified alpha-motoneurons in the cat spinal cord. *J. Neurophysiol.* 60: 60–85.
- Fletcher, E.L., Hack, I., Brandstätter, J.H., and Wässle, H. 2000. Synaptic localization of NMDA receptor subunits in the rat retina. *J. Comp. Neurol.* 420: 98–112.
- Flores-Herr, N., Protti, D.A., and Wässle, H. 2001. Synaptic currents generating the inhibitory surround of ganglion cells in the mammalian retina. *J. Neurosci.* 21: 4852–4863.
- Floris, A., Diño, M., Jacobowitz, D.M., and Mugnaini, E. 1994. The unipolar brush cells of the rat cerebellar cortex and cochlear nucleus are calretinin-positive: a study by light and electron microscopic immunocytochemistry. *Anat. Embryol.* 189: 495–520.
- Fonnum, F., and Walberg F., 1973. An estimation of the concentration of γ -aminobutyric acid and glutamate decarboxylase in the inhibitory Purkinje axon terminals in the cat. *Brain Res.* 54: 115–127.
- Fonnum, F., Karlsen, R.L., Malthe-Sorensen, D., Skrede, K.K., and Walaas, I. 1979. Localization of neurotransmitters, particularly glutamate, in hippocampus, septum, nucleus accumbens and superior colliculus. *Prog. Brain Res.* 51: 167–191.
- Fonnum, F., Storm-Mathisen, J., and Walberg, F. 1970. Glutamate decarboxylase in inhibitory neurons. A study of the enzyme in Purkinje cells axons and boutons in the cat. *Brain Res.* 20: 259–270.
- Foote, S.L., Bloom, F.E., and Aston-Jones, G. 1983. Nucleus locus ceruleus: new evidence of anatomical and physiological specificity. *Physiol. Rev.* 63: 844–914.
- Forsberg, H. 1979. Stumbling corrective reaction: a phase-dependent compensatory reaction during locomotion. *J. Neurophysiol.* 42: 936–953.
- Fortin, N.J., Agster, K.L., and Eichenbaum, H.B. 2002. Critical role of the hippocampus in memory for sequences of events. *Nat. Neurosci.* 5: 458–62.

- Fox, C.A., Andrade, A.N., Hillman, D.E., and Schwyn, R.C. 1971. The spiny neurons in the primate striatum: a Golgi and electron microscopic study. *J. Hirnforsch.* 13: 181–201.
- Fox, C.A., Hillman, D.E., Siegesmund, K.A., and Dutta, C.R. 1967. The primate cerebellar cortex: a Golgi study and electron microscopical study. *Prog. Brain Res.* 25: 174–225.
- Fox, C.A., and Rafols, J.A. 1976. The striatal efferents in the globus pallidus and in the substantia nigra. In: *The Basal Ganglia* (Yahr, M.D., ed.) New York: Raven Press, pp. 37–55.
- Fox, K., Sato, H., and Daw, N. 1990. The effect of varying stimulus intensity on NMDA-receptor activity in cat visual cortex. *J. Neurophysiol.* 64: 1413–1429.
- Fox, S., Krnjevic, K., Morris, M.E., Puil, E., and Werman, R. 1978. Action of baclofen on mammalian synaptic transmission. *Neuroscience* 3: 495–515.
- Frank, B.D., and Hollyfield, J.G. 1987. Retinal ganglion cell morphology in the frog, *Rana pipiens*. *J. Comp. Neurol.* 266: 413–434.
- Frank, K. 1959. Basic mechanisms of synaptic transmission in the central nervous system. *IRE Trans. Med. Electr.* ME-6: 85–88.
- Frank, K., and Fuortes, M.G.F. 1956. Stimulation of motoneurons with intracellular electrodes. *J. Physiol. (Lond.)* 134: 451–460.
- Frank, K., and Fuortes, M.G.F. 1957. Presynaptic and postsynaptic inhibition of monosynaptic reflexes. *Fed. Proc.* 16: 39–40.
- Frassoni, C., Radici, C., Spreafico, R., and de Curtis, M. 1998. Calcium-binding protein immunoreactivity in the piriform cortex of the guinea-pig: selective staining of subsets of non-GABAergic neurons by calretinin. *Neuroscience* 83: 229–237.
- Frazier-Cierpial, L., and Brunjes, P.C. 1989. Early postnatal cellular proliferation and survival in the olfactory bulb rostral migratory stream of normal and unilateral odor-deprived rats. *J. Comp. Neurol.* 289: 481–492.
- Fredens, K., Steengaard-Pedersen, K., and Larsson, L.I. 1984. Localization of enkephalin and cholecystokinin immunoreactivities in the perforant path terminal fields of the rat hippocampal formation. *Brain Res.* 304: 255–263.
- Frederickson, R.C.A., Neuss, M., Morzorati, S.L., and McBride, W.J. 1978. A comparison of inhibitory effects of taurine and GABA on identified Purkinje cells and other neurons in the cerebellar cortex of the rat. *Brain Res.* 145: 117–126.
- Fredette, B.J., and Mugnaini, E. 1991. The GABAergic cerebello-olivary projection in the rat. *Anat. Embryol.* 184: 225–243.
- Freed, M.A. 1992. GABAergic circuits in the mammalian retina. In: *Progress in Brain Research* (Mize, R.R., Marc, R.E., and Sillito, A.M., eds.) Philadelphia: Elsevier Science Publishers.
- Freed, M.A. 2000a. Parallel cone bipolar pathways to ganglion cell use different rates and amplitudes of quantal excitation. *J. Neurosci.* 20: 3956–3963.
- Freed, M.A. 2000b. Rate of quantal excitation to a retinal ganglion cell evoked by sensory input. *J. Neurophysiol.* 83: 2956–2966.
- Freed, M.A., and Nelson, R. 1994. Conductances evoked by light in the ON-beta ganglion cell of the cat retina. *Vis. Neurosci.* 11: 261–269.
- Freed, M.A., and Sterling, P. 1988. The ON-alpha ganglion cell of the cat retina and its presynaptic cell types. *J. Neurosci.* 8: 2303–2320.
- Freed, M.A., Pflug, R., Kolb, H., and Nelson, R. 1996. ON-OFF amacrine cells in cat retina. *J. Comp. Neurol.* 364: 556–566.
- Freed, M.A., Smith, R.G., and Sterling, P. 1992. Computational model of the ON-alpha ganglion cell receptive field based on bipolar circuitry. *Proc. Natl. Acad. Sci. U.S.A.* 89: 236–240.
- Freed, M.A., Smith, R.G., and Sterling, P. 1987. Rod bipolar array in the cat retina: pattern of input from rods and GABA-accumulating amacrine cells. *J. Comp. Neurol.* 266: 445–455.
- Freeman, W.J. 1959. Distribution in time and space of prepyriform electrical activity. *J. Neurophysiol.* 22: 644–665.

- Freeman, W.J. 1960. Correlation of electrical activity of prepyriform cortex and behavior in cat. *J. Neurophysiol.* 23: 111–131.
- Freeman, W.J. 1974. Relation of glomerular neuronal activity to glomerular transmission attenuation. *Brain Res.* 65: 91–107.
- Freeman, W.J. 1975. *Mass Action in the Nervous System*. New York: Academic Press.
- Freeman, W.J. 1978. Spatial properties of an EEG event in the olfactory bulb and cortex. *Electroencephalogr. Clin. Neurophysiol.* 44: 586–605.
- Freeman, W.J. 1983. Dynamics of image formation by nerve cell assemblies. In: *Synergetics of the Brain*. Berlin: Springer.
- Freeman, W.J., and Grajski, K.A. 1987. Relation of olfactory EEG to behavior factor analysis. *Behav. Neurosci.* 101: 766–777.
- Frerking, M., and Wilson, M. 1996. Effects of variance in mini amplitude on stimulus-evoked release: a comparison of two models. *Biophys. J.* 70: 2078–2091.
- Freund, T.F., and Antal M., 1988. GABA-containing neurons in the septum control inhibitory interneurons in the hippocampus. *Nature* 336: 170–173.
- Freund, T.F., and Buzsáki, G. 1996. Interneurons of the hippocampus. *Hippocampus* 6: 345–470.
- Freund, T.F., Gulyás, A.I., Acsády, L., Görcs, T., and Tóth, K. 1990. Serotonergic control of the hippocampus via local inhibitory interneurons. *Proc. Natl. Acad. Sci. U.S.A.* 87: 8501–8505.
- Freund, T.F., Martin, K.A.C., Smith, A.D., and Somogyi, P. 1983. Glutamate decarboxylase-immunoreactive terminals of Golgi impregnated axo-axonic neurons and of presumed basket neurons in synaptic contact with pyramidal neurons of the cat's visual cortex. *J. Comp. Neurol.* 221: 263–278.
- Freund, T.F., Martin, K.A.C., Somogyi, P., and Whitteridge, D. 1985. Innervation of cat visual areas 17 and 18 by physiologically identified α - and γ -type thalamic afferents. II. Identification of postsynaptic targets by GABA immunocytochemistry and Golgi impregnation. *J. Comp. Neurol.* 242: 275–291.
- Freund, T.F., Powell, J.F., and Smith, A.D. 1984. Tyrosine hydroxylase-immunoreactive boutons in synaptic contact with identified striatonigral neurons, with particular reference to dendritic spines. *Neuroscience* 13: 1189–1215.
- Fried, S.I., Münch, T.A., and Werblin, F.S. 2002. Mechanisms and circuitry underlying directional selectivity in the retina. *Nature* 420: 411–414.
- Friedlander, M.J., Lin, C.-S., Stanford, L.R., and Sherman, S.M. 1981. Morphology of functionally identified neurons in lateral geniculate nucleus of the cat. *J. Neurophysiol.* 46: 80–129.
- Friedman, B., and Price, J.L. 1984. Fiber systems in the olfactory bulb and cortex: a study in adult and developing rats, using the Timm method with the light and electron microscope. *J. Comp. Neurol.* 223: 88–109.
- Friedman, D., and Strowbridge, B.W. 2000. Functional role of NMDA autoreceptors in olfactory mitral cells. *J. Neurophysiol.* 84: 39–50.
- Friedman, W.A., Sypert, G.W., Munson, J.B., and Fleshman, J.W. 1981. Recurrent inhibition in type-identified motoneurons. *J. Neurophysiol.* 46: 1349–1359.
- Friedrich, R., and Korsching, S.I. 1996. Representation of odorant information by spatial afferent activity patterns in the zebrafish olfactory bulb. *Soc. Neurosci. Abstr.* 22: 1072.
- Friedrich, R.W., and Korsching, S.I. 1997. Combinatorial and chemotopic odorant coding in the zebrafish olfactory bulb visualized by optical imaging. *Neuron* 18: 737–752.
- Friedrich, R.W., and Laurent, G. 2001. Dynamic optimization of odor representations by slow temporal patterning of mitral cell activity. *Science* 291: 889–894.
- Frisina, R.D. 2001. Subcortical neural coding mechanisms for auditory temporal processing. *Hear. Res.* 158: 1–27.

- Frisina, R.D., Smith, R.L., and Chamberlain, S.C. 1990. Encoding of amplitude modulation in the gerbil cochlear nucleus: I. A hierarchy of enhancement. *Hear. Res.* 44: 99–122.
- Fritschy, J.-M., and Mohler, H. 1995. GABAA-receptor heterogeneity in the adult rat brain: differential regional and cellular distribution of seven major subunits. *J. Comp. Neurol.* 359: 154–194.
- Frost, D.O., and Caviness, V.S. 1980. Radial organization of thalamic projections to the neocortex in the mouse. *J. Comp. Neurol.* 194: 369–393.
- Frotscher, M., Kugler, P., Misgeld, U., and Zilles, K. 1988. Neurotransmission in the hippocampus. In: *Advances in Anatomy, Embryology, and Cell Biology.* (Beck, F., Hild, W., Kriz, W., Ortman, R., Pauly, J.E., and Schiebler, T.H., eds.) Berlin: Springer-Verlag.
- Frotscher, M., and Leranth, C. 1985. Cholinergic innervation of the rat hippocampus as revealed by choline acetyltransferase immunocytochemistry. *J. Comp. Neurol.* 239: 237–246.
- Frotscher, M., and Zimmer, J. 1983. Commissural fibers terminated on non-pyramidal neurons in the guinea pig hippocampus—a combined Golgi/EM degeneration study. *Brain Res.* 265: 289–293.
- Fujino, K., and Oertel, D. 2001. Cholinergic modulation of stellate cells in the mammalian ventral cochlear nucleus. *J. Neurosci.* 21: 7372–7383.
- Fujino, K., and Oertel, D. 2003. Bidirectional synaptic plasticity in the cerebellum-like mammalian dorsal cochlear nucleus. *Proc. Natl. Acad. Sci. U.S.A.* 100: 265–270.
- Fujita, I., Tanaka, K., Ito, M., and Cheng, K. 1992. Columns for visual features in monkey inferotemporal cortex. *Nature* 360: 343–346.
- Fukuda, Y., and Stone, J. 1974. Retinal distribution and central projections of Y-, X-, and W-cells of the cat's retina. *J. Neurophysiol.* 37: 749–772.
- Fünfschilling, U., and Reichardt, L.F. 2002. Cre-mediated recombination in rhombic lip derivatives. *Genesis* 33: 160–169.
- Funke, K., Pape, H.-C., and Eysel, U.T. 1993. Noradrenergic modulation of retinogeniculate transmission in the cat. *J. Physiol. (Lond.)* 463: 169–191.
- Fuortes, M., Frank, K., and Becker, M. 1957. Steps in the production of motoneuron spikes. *J. Gen. Physiol.* 40: 735–752.
- Fuster, J.M. 1985. The prefrontal cortex and temporal integration. In: *Cerebral Cortex* (Jones, E.G., and Peters, A., eds.) New York: Plenum, pp. 151–177.
- Fyffe, R.E.W. 1984. Afferent fibers. In: *Handbook of the Spinal Cord, Vol. 1: Physiology.* (Davidoff, R.E., ed.) New York: Marcel Dekker, pp. 79–136.
- Fyffe, R.E.W. 1990. Evidence for separate morphological classes of Renshaw cells in the cat's spinal cord. *Brain Res.* 536: 301–304.
- Fyffe, R.E.W. 1991a. Glycine-like immunoreactivity in synaptic boutons of identified inhibitory interneurons in the mammalian spinal cord. *Brain Res.* 547: 175–179.
- Fyffe, R.E.W. 1991b. Spatial distribution of recurrent inhibitory synapses on spinal motoneurons in the cat. *J. Neurophysiol.* 65: 1134–1149.
- Fyffe, R.E.W., and Light, A.R. 1984. The ultrastructure of group Ia afferent fiber synapses in the lumbosacral spinal cord of the cat. *Brain Res.* 300: 201–209.
- Gaarskjaer, F.B. 1978. Organization of the mossy fiber system of the rat studied in extended hippocampi. I. Terminal area related to number of granule and pyramidal cells. *J. Comp. Neurol.* 178: 49–72.
- Gaarskjaer, F.B. 1978. Organization of the mossy fiber system of the rat studied in extended hippocampi. II. Experimental analysis of fiber distribution with silver impregnation methods. *J. Comp. Neurol.* 178: 73–88.
- Gabbott, P., and Somogyi, P. 1986. Quantitative distribution of GABA-immunoreactive neurons in the visual cortex (area 17) of the cat. *Exp. Brain Res.* 61: 323–331.
- Gabel, L.A., and Nisenbaum, E.S. 1999. Muscarinic receptors differentially modulate the per-

- sistent potassium current in striatal spiny projection neurons. *J. Neurophysiol* 81: 1418–1423.
- Galarraga, E., Hernandez-Lopez, S., Reyes, A., Miranda, I., Bermudez-Rattoni, F. Vilchis, C. and Bargas, J. 1999. Cholinergic modulation of neostriatal output: A functional antagonism between different types of muscarinic receptors. *J. Neurosci.* 19: 3629–3638.
- Galarreta, M., and Hestrin, S. 1999. A network of fast-spiking cells in the neocortex connected by electrical synapses. *Nature* 402: 72–75.
- Galarreta, M., and Hestrin, S. 2001. Electrical synapses between GABA-releasing interneurons. *Nat. Rev. Neurosci.* 2: 425–433.
- Gall, C. 1984. Ontogeny of dynorphin-like immunoreactivity in the hippocampal formation of the rat. *Brain Res.* 307: 327–331.
- Gall, C., Brecha, N., Karten, H.J., and Chang, K.J. 1981. Localization of enkephalin-like immunoreactivity to identified axonal and neuronal populations of the rat hippocampus. *J. Comp. Neurol.* 198: 335–350.
- Gallo, V., Upson, L.M., Hayes, W.P., Vyklicky, L.J., Winters, C.A., and Buonanno, A., 1992. Molecular cloning and development analysis of a new glutamate receptor subunit isoform in cerebellum. *J. Neurosci.* 12: 1010–1023.
- Galupo, M.P., and Stripling, J.S. 1995. All-or-none threshold for expression of LTP in the olfactory bulb and piriform cortex: modulation by behavioral state. *Soc. Neurosci. Abstr.* 21: 1185.
- Gamble, E., and Koch, C. 1987. The dynamics of free calcium in dendritic spines in response to repetitive synaptic input. *Science* 236: 1311–1315.
- Gan, L., Xiang, M., Zhou, L., Wagner, D.S., Klein, W.H., and Nathans, J. 1996. POU domain factor Brn-3b is required for the development of a large set of retinal ganglion cells. *Proc. Natl. Acad. Sci. U.S.A.* 93: 3920–3925.
- Gardner, S.M., Trussell, L.O., and Oertel, D. 1999. Time course and permeation of synaptic AMPA receptors in cochlear nuclear neurons correlate with input. *J. Neurosci.* 19: 8721–8729.
- Gardner, S.M., Trussell, L.O., and Oertel, D. 2001. Correlation of AMPA receptor subunit composition with synaptic input in the mammalian cochlear nuclei. *J. Neurosci.* 21: 7428–7437.
- Garnett, R., and Stephens, J.A. 1981. Changes in the recruitment threshold of motor units produced by cutaneous stimulation in man. *J. Physiol. (Lond.)* 311: 463–473.
- Garthwaite J., and Brodbelt, A.R. 1989. Synaptic activation of N-methyl-D-aspartate and non-N-methyl-D-aspartate receptors in the mossy fibre pathway in adult and immature rat cerebellar slices. *Neuroscience* 29: 401–412.
- Gaykema, R.P.A., Luiten, P.G.M., Nyakas, C., and Traber, J. 1990. Cortical projection patterns of the medial septum-diagonal band complex. *J. Comp. Neurol.* 293: 103–124.
- Geiger, J.R., and Jonas, P. 2000. Dynamic control of presynaptic Ca(2+) inflow by fast-inactivating K(+) channels in hippocampal mossy fiber boutons. *Neuron* 28: 927–939.
- Geisert, E.E., Langsetmo, A., and Spear, P.D. 1981. Influence of the cortico-geniculate pathway on response properties of cat lateral geniculate neurons. *Brain Res.* 208: 409–415.
- Geisler, W.S. 1989. Sequential ideal-observer analysis of visual discriminations. *Psychol. Rev.* 96: 267–314.
- Gellman, R.L., and Aghajanian, G.K. 1993. Pyramidal cells in piriform cortex receive a convergence of inputs from monoamine activated GABAergic interneurons. *Brain Res.* 60: 63–73.
- Gellman, R.L., and Aghajanian, G.K. 1994. 5-HT₂-receptor mediated excitation of interneurons in piriform cortex antagonism by atypical antipsychotic drugs. *Neuroscience* 58: 515–525.
- Gerfen, C.R. 1984. The neostriatal mosaic. Compartmentalization of corticostriatal input and striatonigral output systems. *Nature* 311: 461–464.

- Gerfen, C.R. 1985. The neostriatal mosaic. I. Compartmental organization of projections of the striatonigral system in the rat. *J. Comp. Neurol.* 236: 454–476.
- Gerfen, C.R. 1989. The neostriatal mosaic. Striatal patch-matrix organization is related to cortical lamination. *Science* 246: 385–388.
- Gerfen, C.R. 1992. The neostriatal mosaic: multiple levels of compartmental organization in the basal ganglia. *Annu Rev Neurosci.* 15: 285–320.
- Gerfen, C.R., Baimbridge, K.G., and Thibault, J. 1987. The neostriatal mosaic. III. Biochemical and developmental dissociation of patch-matrix mesostriatal systems. *J. Neurosci.* 7: 3935–3944.
- Gerfen, C.R., Engber, T.M., Mahan, L.C., Susel, Z., Chase, T.N., Monsma, F.J., and Sibley, D.R. 1990. D1 and D2 dopamine receptor-regulated gene expression of striatonigral and striatopallidal neurons. *Science* 250: 1492–1432.
- Gerfen, C.R. and Wilson, C.J. 1996. The basal ganglia. In: *Handbook of Chemical Neuroanatomy, Vol 12: Integrated systems of the CNS, Part III* (Swanson L.W., Björklund A. and Hökfelt T., eds.), pp. 371–468.
- Gerfen, C.R., and Young, W.S. 1988. Distribution of striatonigral and striatopallidal peptidergic neurons in both patch and matrix compartments: an in situ hybridization histochemistry and fluorescent retrograde tracing study. *Brain Res.* 460: 161–167.
- Gerschenfeld, H.M., Piccolino, M., and Neyton, J. 1980. Feed-back modulation of cone synapses by L-horizontal cells of turtle retina. *J. Exp. Biol.* 89: 177–192.
- Gerstner, W. 1999. Spiking neurons. In: *Pulsed Neural Networks*. (Maass, W., and Bishop, C.M., eds.) Cambridge: MIT Press, pp. 3–54.
- Gesteland, R.C. 1986. Speculation on receptor cells as analyzers and filters. *Experientia* 42: 287–291.
- Getchell, T.V., and Shepherd, G.M. 1975a. Short-axon cells in the olfactory bulb: dendrodendritic synaptic interactions. *J. Physiol. (Lond.)* 251: 523–548.
- Getchell, T.V., and Shepherd, G.M. 1975b. Synaptic actions on mitral and tufted cells elicited by olfactory nerve volleys in the rabbit. *J. Physiol. (Lond.)* 251: 497–522.
- Ghosh, S., Fyffe, R.E.W., and Porter, R. 1988. Morphology of neurons in area 4 gamma of the cat's cortex studied with intracellular injection of HRP. *J. Comp. Neurol.* 269: 290–312.
- Gibson, J., Beierlein, M., and Connors, B. 1999. Two networks of electrically coupled inhibitory neurons in neocortex. *Nature* 402: 75–79.
- Gibson, J., Sellitto, C., Connors, B., and Paul, D. 2001. Synchronous activity of inhibitory networks in neocortex requires electrical synapses containing connexin36. *Neuron* 31: 477–485.
- Gilbert, C., and Kelly, J. 1975. The projection of cells in the different layers of the cat's visual cortex. *J. Comp. Neurol.* 163: 81–106.
- Gilbert, C., and Wiesel, T. 1979. Morphology and intracortical projections of functionally characterized neurons in the cat visual cortex. *Nature* 280: 120–125.
- Gilbert, C.D. 1977. Laminar differences in receptive field properties of cells in cat primary visual cortex. *J. Physiol. (Lond.)* 268: 391–421.
- Giuffrida, R., and Rustioni, A. 1988. Glutamate and aspartate immunoreactivity in corticothalamic neurons of rats. In: *Cellular Thalamic Mechanisms* (Bentivoglio, M., and Spreafico, R., eds.) Amsterdam: Elsevier, pp. 311–320.
- Giustetto, M., Bovolín, P., Fasolo, A., Bonino, M., Cantino, D., and Sassoe-Pognetto, M. 1997. Glutamate receptors in the olfactory bulb synaptic circuitry: heterogeneity and synaptic localization of N-methyl-D-aspartate receptor subunit 1 and AMPA receptor subunit 1. *Neuroscience* 76: 787–798.
- Gladden, M., Jankowska, E., and Czarkowska-Bauch, J. 1998. New observations of coupling between group II muscle afferents and feline g-motoneurons. *J. Physiol. (Lond.)* 512: 507–520.

- Glitsch, H.G. 2001. Electrophysiology of the sodium-potassium ATPase in cardiac cells. *Physiol. Rev.* 81: 1791–1826.
- Gobel, S., Falls, W.M., Bennett, G.J., Abheloumoune, M., Hayashi, H., and Humphrey, E. 1980. An EM analysis of the synaptic connections of horseradish peroxidase-filled stalked cells and islet cells in the substantia gelatinosa of adult cat spinal cord. *J. Comp. Neurol.* 194: 781–807.
- Goda, Y., and Stevens, C.F. 1996. Long-term depression properties in a simple system. *Neuron* 16: 103–111.
- Godfraind, J., Krnjevic, K., and Pumain, R. 1970. Doubtful value of bicuculline as a specific antagonist of GABA. *Nature* 228: 675–670.
- Godfrey, D.A., Kiang, N.Y.S., and Norris, B.E. 1975a. Single unit activity in the posteroventral cochlear nucleus of the cat. *J. Comp. Neurol.* 162: 247–268.
- Godfrey, D.A., Kiang, N.Y.S., and Norris, B.E. 1975b. Single unit activity in the dorsal cochlear nucleus of the cat. *J. Comp. Neurol.* 162: 269–284.
- Godwin, D.W., Van Horn, S.C., Erişir, A., Sesma M., Romano, C., and Sherman, S.M. 1996. Ultrastructural localization suggests that retinal and cortical inputs access different metabotropic glutamate receptors in the lateral geniculate nucleus. *J. Neurosci.* 16: 8181–8192.
- Godwin, D.W., Vaughan, J.W., and Sherman, S.M. 1996b. Metabotropic glutamate receptors switch visual response mode of lateral geniculate nucleus cells from burst to tonic. *J. Neurophysiol.* 76: 1800–1816.
- Godwin, D.W., Zhou, Q., and Sherman, S.M. 1996b. Evidence for activation of feedforward GABAergic circuitry in cat LGN via a specific metabotropic glutamate receptor. *Soc. Neurosci. Abstr.* 22: 1606.
- Gogan, P., Gueritaud, J.P., Horchelle-Bossavit, G., and Tyc-Dumont, S. 1977. Direct excitatory interactions between spinal motoneurons of the cat. *J. Physiol. (Lond.)* 272: 755–767.
- Goldberg, J.M., and Brown, P.B. 1969. Response of binaural neurons of dog superior olivary complex to dichotic tonal stimuli: Some physiological mechanisms of sound localization. *J. Neurophysiol.* 32: 613–636.
- Goldberg, J.M., and Brownell, W.E. 1973. Discharge characteristics of neurons in anteroventral and dorsal cochlear nuclei of cat. *Brain Res.* 64: 35–54.
- Golding, N.L., Ferragamo, M.J., and Oertel, D. 1999. Role of intrinsic conductances underlying responses to transients in octopus cells of the cochlear nucleus. *J. Neurosci.* 19: 2897–2905.
- Golding, N.L., and Oertel, D. 1996. Context-dependent synaptic action of glycinergic and GABAergic inputs in the dorsal cochlear nucleus. *J. Neurosci.* 16: 2208–2219.
- Golding, N.L., and Oertel, D. 1997. Physiological identification of the targets of cartwheel cells in the dorsal cochlear nucleus. *J. Neurophysiol.* 78: 248–60.
- Golding, N.L., Robertson, D., and Oertel, D. 1995. Recordings from slices indicate that octopus cells of the cochlear nucleus detect coincident firing of auditory nerve fibers with temporal precision. *J. Neurosci.* 15: 3138–3153.
- Golding, N.L., and Spruston, N. 1998. Dendritic sodium spikes are variable triggers of axonal action potentials in hippocampal CA1 pyramidal neurons. *Neuron* 21: 1189–1200.
- Goldman, D.E. 1943. Potential, impedance, and rectification in membranes. *J. Gen. Physiol.* 27: 37–60.
- Goldman, P.S., and Nauta, W.J.H. 1977. An intricately patterned prefronto-caudate projection in the rhesus monkey. *J. Comp. Neurol.* 171: 369–385.
- Goldman-Rakic, P.S., Muly, E., and Williams, G. 2000. D(1) receptors in prefrontal cells and circuits. *Brain Res. Rev.* 31: 355–364.
- Goldman-Rakic, P.S. 1982. Cytoarchitectonic heterogeneity of the primate neostriatum—subdivision into island and matrix cellular compartments. *J. Comp. Neurol.* 205: 398–413.
- Goldman-Rakic, P.S. 1987. Circuitry of primate prefrontal cortex and regulation of behavior by representational memory. In: *Handbook of Physiology, The Nervous System, Higher Func-*

- tions of the Brain (Plum, F., and Mountcastle, V.B., eds.) Bethesda: American Physiology Society, pp. 373–417.
- Golgi, C. 1886. *Sulla fina Anatomia degli Organi Centrali del Sistema Nervoso*. Milano: Hoepli.
- Golshani, P., Warren, R.A., Jones, E.G. 1998. Progression of change in NMDA, non-NMDA, and metabotropic glutamate receptor function at the developing corticothalamic synapse. *J. Neurophysiol.* 80: 143–154.
- Gong, Q., and Shipley, M.T. 1995. Evidence that pioneer olfactory axons regulate telencephalon cell cycle kinetics to induce the formation of the olfactory bulb. *Neuron* 14: 91–101.
- Gonzalez, M.L., Malemud, C.J., and Silver, J. 1993. Role of astroglial extracellular matrix in the formation of rat olfactory bulb glomeruli. *Exp. Neurol.* 123: 91–105.
- Goodchild, A.K., Chan, T.L., and Grünert, U. 1996a. Horizontal cell connections with short-wavelength-sensitive cones in macaque monkey retina. *Vis. Neurosci.* 13: 833–845.
- Goodchild, A.K., Ghosh, K.K., and Martin, P.R. 1996b. Comparison of photoreceptor spatial density and ganglion cell morphology in the retina of human, macaque monkey, cat, and the marmoset *Callithrix jacchus*. *J. Comp. Neurol.* 366: 55–75.
- Gossard, J. P. 1996. Control of transmission in muscle group IA afferents during fictive locomotion in the cat. *J. Neurophysiol.* 76: 4104–4112.
- Gossard, J.-P., Floeter, M.K., Kawai, Y., Burke, R.E., Chang, T., and Schiff, S.J. 1994. Fluctuations of excitability in the monosynaptic reflex pathway to lumbar motoneurons in the cat. *J. Neurophysiol.* 72: 1227–1239.
- Gottlieb, D.I., and Cowan, W.M. 1972. On the distribution of axonal terminals containing spheroidal and flattened synaptic vesicles in the hippocampus and dentate gyrus of the rat and cat. *Z. Zellforsch. Mikrosk. Anat.* 129: 413–429.
- Graham, B., and Redman, S. 1994. A simulation of action-potentials in synaptic boutons during presynaptic inhibition. *J. Neurophysiol.* 71: 538–549.
- Grandes P., Do K.Q., Morino P., Cuenod M., and Streit P. 1991. Homocysteate, an excitatory transmitter candidate localized in glia. *Eur. J. Neurosci.* 3: 1370–1373.
- Granger, R., Ambros-Ingerson, J., and Lynch, G. 1988. Derivation of encoding characteristics of layer II cerebral cortex. *J. Cogn. Neurosci.* 1: 61–87.
- Graveland, G.A., and DiFiglia, M. 1985a. The frequency and distribution of medium-sized neurons with indented nuclei in the primate and rodent neostriatum. *Brain Res.* 327: 308–311.
- Graveland, G.A., and DiFiglia, M. 1985b. A Golgi study of the human neostriatum—neurons and afferent fibers. *J. Comp. Neurol.* 234: 317–333.
- Gray, C.M., and McCormick, D.A. 1996. Chattering cells: superficial pyramidal neurons contributing to the generation of synchronous oscillations in the visual cortex. *Science* 274: 109–112.
- Gray, C.M., and Singer, W. 1989. Stimulus-specific neuronal oscillations in orientation columns of cat visual cortex. *Proc. Natl. Acad. Sci. U.S.A.* 86: 1698–1702.
- Gray, C.M., and Skinner, J.E. 1988. Centrifugal regulation of neuronal activity in the olfactory bulb of the waking rabbit as revealed by reversible cryogenic blockade. *Exp. Brain Res.* 69: 378–386.
- Gray, E.G. 1959. Axo-somatic and axo-dendritic synapses of the cerebral cortex: an electron-microscopic study. *J. Anat.* 93: 420–433.
- Gray, R., Rajan, A.S., Radcliffe, K.A., Yakehiro, M., and Dani, J.A. 1996. Hippocampal synaptic transmission enhanced by low concentrations of nicotine. *Nature* 383: 713–716.
- Graybiel, A.M. 1998. The basal ganglia and chunking of action repertoires. *Neurobiol. Learn Mem.* 70: 119–136.
- Graybiel, A.M., Aosaki, T., Flaherty, A.W., and Kimura, M. 1994. The basal ganglia and adaptive motor control. *Science* 265: 1826–1831.
- Graybiel, A.M., Baughman, R.W., and Eckenstein, F. 1986. Cholinergic neuropil of the striatum observes striosomal boundaries. *Nature* 323: 625–627.

- Graybiel, A.M., and Ragsdale, C.W., Jr. 1983. Biochemical anatomy of the striatum. In: *Chemical Neuroanatomy* (Emson, P.C., ed.) New York: Raven Press, pp. 427–503.
- Graybiel, A.M., Ragsdale, C.W., Jr., Yoneoka, E.S., and Elde, R.P. 1981. An immunohistochemical study of enkephalin and other neuropeptides in the striatum of the cat with evidence that opiate peptides are arranged to form mosaic patterns in register with striosomal compartments visible by acetylcholinesterase staining. *Neuroscience* 6: 377–397.
- Graziadei, P.P.C., and Monti-Graziadei, G.A. 1979. Neurogenesis and neuron regeneration in the olfactory system of mammals. I. Morphological aspects of differentiation and structural organization of the olfactory sensory neurons. *J. Neurocytol.* 8: 1–18.
- Green, D.M., and Swets, J.A. 1966. *Signal Detection Theory and Psychophysics*. New York: Wiley.
- Green, J.D. 1964. The hippocampus. *Physiol. Rev.* 44: 561–608.
- Greene, C., Schwindt, P., and Crill, W. 1994. Properties and ionic mechanisms of a metabotropic glutamate receptor-mediated slow after depolarization in neocortical neurons. *J. Neurophysiol.* 72: 693–704.
- Greenough, W.T. 1975. Experimental modification of the developing brain. *Sci. Am.* 63: 37–46.
- Greer, C.A. 1984. A Golgi analysis of granule cell development in the neonatal rat olfactory bulb. *Soc. Neurosci. Abstr.* 10: 531.
- Greer, C.A. 1987. Golgi analyses of dendritic organization among denervated olfactory bulb granule cells. *J. Comp. Neurol.* 257: 442–452.
- Greer, C.A. 1988. High voltage electromicroscopic analyses of olfactory bulb granule cell spine geometry. *J. Comp. Neurol.* 257: 442–452.
- Greer, C.A., and Halasz, N. 1987. Plasticity of dendrodendritic microcircuits following mitral cell loss in the olfactory bulb of the murine mutant PCD. *J. Comp. Neurol.* 256: 284–298.
- Greer, C.A., Kaliszewski, C.K., and Cameron, H.A. 1989. Ultrastructural analyses of local circuits in the olfactory system. *Proc. EMSA* 47: 790–791.
- Greer, C.A., and Shepherd, G.M. 1982. Mitral cell degeneration and sensory function in the neurological mutant mouse Purkinje cell degeneration (PCD). *Brain Res.* 235: 156–161.
- Greer, C.A., Stewart, W.B., Teicher, M.H., and Shepherd, G.M. 1982. Functional development of the olfactory bulb and a unique glomerular complex in the neonatal rat. *J. Neurosci.* 2: 1744–1759.
- Grieve, K., Murphy, P., and Sillito, A. 1985a. The actions of VIP and ACh on the visual responses of neurons in the striate cortex. *Br. J. Pharmacol.* [Suppl.] 85: 253.
- Grieve, K., Murphy, P., and Sillito, A. 1985b. An evaluation of the role of CCK and VIP in the cat visual cortex. *J. Physiol. (Lond.)* 365: 42P.
- Grieve, K., and Sillito, A. 1995. Differential properties of cells in the feline primary visual cortex providing the corticofugal feedback to the lateral geniculate nucleus and visual claustrum. *J. Neurosci.* 15: 4868–4874.
- Grill, S., and Rymer, W. 1987. Reflex actions of muscle afferents on fusimotor innervation in decerebrated cats: an assessment of beta contributions. *J. Neurophysiol.* 57: 574–595.
- Grillner, S. 1981. Control of locomotion in bipeds, tetrapods and fish. In: *Handbook of Physiology, Section 1: The Nervous System, Vol. II: Motor Control, Part 2* (Brooks, V.P., ed.) Bethesda: American Physiological Society, pp. 1179–1236.
- Gross, C., Rocha-Miranda, C., and Bender, D. 1972. Visual properties of neurons in inferotemporal cortex of the macaque. *J. Neurophysiol.* 35: 96–111.
- Groves, P.M., Linder, J.C., and Young, S.J. 1994. 5-hydroxydopamine-labeled dopaminergic axons: three-dimensional reconstructions of axons, synapses and postsynaptic targets in rat neostriatum. *Neuroscience* 58: 593–604.
- Grünert, U., Haverkamp, S., Fletcher, E.L., and Wässle, H. 2002. Synaptic distribution of ionotropic glutamate receptors in the inner plexiform layer of the primate retina. *J. Comp. Neurol.* 447: 138–151.

- Grünert, U., Martin, P.R., and Wässle, H. 1994. Immunocytochemical analysis of bipolar cells in the macaque monkey retina. *J. Comp. Neurol.* 348: 607–627.
- Grünert, U., and Wässle, H. 1990. GABA-like immunoreactivity in the macaque monkey retina: a light and electron microscopic study. *J. Comp. Neurol.* 297: 509–524.
- Gu, Q., Patel, B., and Singer, W. 1990. The laminar distribution and postnatal development of serotonin-immunoreactive axons in the cat primary visual cortex. *Exp. Brain Res.* 81: 257–266.
- Guido, W., Lu, S.-M., and Sherman, S.M. 1992. Relative contributions of burst and tonic responses to the receptive field properties of lateral geniculate neurons in the cat. *J. Neurophysiol.* 68: 2199–2211.
- Guido, W., Lu, S.-M., Vaughan, J.W., Godwin, D.W., Sherman, S.M. 1995. Receiver operating characteristic (ROC) analysis of neurons in the cat's lateral geniculate nucleus during tonic and burst response mode. *Vis. Neurosci.* 12: 723–741.
- Guido, W., and Weyand, T. 1995. Burst responses in thalamic relay cells of the awake behaving cat. *J. Neurophysiol.* 74: 1782–1786.
- Guillery, R.W. 1961 Fibre degeneration in the efferent mamillary tracts of the cat. In: *Cytology of Nervous Tissue*. London: Taylor and Francis, pp. 64–67.
- Guillery, R.W. 1966. A study of Golgi preparations from the dorsal lateral geniculate nucleus of the adult cat. *J. Comp. Neurol.* 128: 21–50.
- Guillery, R.W. 1969a. A quantitative study of synaptic interconnections in the dorsal lateral geniculate nucleus of the cat. *Z. Zellforsch.* 96: 39–48.
- Guillery, R.W. 1969b. The organization of synaptic interconnections in the laminae of the dorsal lateral geniculate nucleus of the cat. *Z. Zellforsch.* 96: 1–38.
- Guillery, R.W. 1995. Anatomical evidence concerning the role of the thalamus in corticocortical communication: a brief review. *J. Anat.* 187: 583–592.
- Guillery, R.W., Feig, S.L., Lozsádi, D.A. 1998. Paying attention to the thalamic reticular nucleus. *Trends Neurosci.* 21: 28–32.
- Guillery, R.W., Feig, S.L., Van Lieshout, D.P. 2001. Connections of higher order visual relays in the thalamus: a study of corticothalamic pathways in cats. *J. Comp. Neurol.* 438: 66–85.
- Guillery, R.W., and Sherman, S.M. 2002a. Thalamic relay functions and their role in corticocortical communication: generalizations from the visual system. *Neuron* 33: 1–20.
- Guillery, R. W., and Sherman, S. M. 2002b. Thalamocortical pathways as monitors of ongoing motor instructions. *Phil. Trans. R. Soc. Lond. B Biol. Sci.* 357: 1809–1821.
- Guillery, R.W. 2003. Branching thalamic afferents link action and perception. *J. Neurophysiol.* 90: 539–548.
- Guinan, J.J. 1996. Physiology of olivocochlear efferents. In: *The Cochlea* (Dallos, P., Popper, A.N., and Fay, R.R., eds.) New York: Springer, pp. 435–502.
- Guinan, J.J., and Li, R.Y.-S. 1990. Signal processing in brainstem auditory neurons which receive giant endings (calyces of Held) in the medial nucleus of the trapezoid body of the cat. *Hearing Res.* 49: 321–334.
- Gulyas, A.I., Göröcs, T.J., and Freund, T.F. 1990. Innervation of different peptide-containing neurons in the hippocampus by GABAergic septal afferents. *Neuroscience* 37: 31–44.
- Gulyas, A.I., Toth, K., McBain, C.J., and Freund, T.F. 1998. Stratum radiatum giant cells: a type of principal cell in the rat hippocampus. *Eur. J. Neurosci.* 10: 3813–3822.
- Gupta, A., Wang, Y., and Markram, H. 2000. Organizing principles for a diversity of gabaergic interneurons and synapses in the neocortex. *Science* 287: 273–278.
- Gustafsson, B., and Pinter, M.J. 1984. Relations among passive electrical properties of lumbar a-motoneurons of the cat. *J. Physiol. (Lond.)* 356: 401–431.
- Guthrie, K.M., Anderson, A.J., Leon, M., and Gall, C. 1993. Odor-induced increases in c-fos mRNA expression reveal an anatomical 'unit' for odor processing in olfactory bulb. *Proc. Natl. Acad. Sci. U.S.A.* 90: 3329–3333.

- Guthrie, K.M., and Gall, C.M. 1995. Odors increase Fos in olfactory bulb neurons including dopaminergic cells. *NeuroReport* 6: 2145–2149.
- Guthrie, P., Segal, M., and Kater, S. 1991. Independent regulation of calcium revealed by imaging dendritic spines. *Nature* 354: 76–80.
- Haberly, L.B. 1973. Unitary analysis of opossum prepyriform cortex. *J. Neurophysiol.* 36: 762–774.
- Haberly, L.B. 1983. Structure of the piriform cortex of the opossum. I. Description of neuron types with Golgi methods. *J. Comp. Neurol.* 213: 163–187.
- Haberly, L.B. 1985. Neuronal circuitry in olfactory cortex. Anatomy and functional implications. *Chem. Senses* 10: 219–238.
- Haberly, L.B. 1990a. Comparative aspects of olfactory cortex. In: *Cerebral Cortex*, Vol. 8. (Jones, E.G., and Peters, A., eds.) New York: Plenum, pp. 137–166.
- Haberly, L.B. 1990b. Olfactory cortex. In: *Synaptic Organization of the Brain*, 3rd ed. (Shepherd, G.M., ed.) New York: Oxford University Press, pp. 317–345.
- Haberly, L.B. 2001. Parallel-distributed processing in olfactory cortex: new insights from morphological and physiological analysis of neuronal circuitry. *Chem. Senses* 26: 551–576.
- Haberly, L.B., and Bower, J.M. 1982. Graphical methods for three-dimensional rotation of complex axonal arborizations. *J. Neurosci. Methods* 6: 75–84.
- Haberly, L.B., and Bower, J.M. 1984. Analysis of association fiber system in piriform cortex with intracellular recording and staining methods. *J. Neurophysiol.* 51: 90–112.
- Haberly, L.B., and Bower, J.M. 1989. Olfactory cortex. Model circuit for study of associative memory? *Trends Neurosci.* 12: 258–264.
- Haberly, L.B., and Feig, S. 1983. Structure of the piriform cortex of the opossum. II. Fine structure of cell bodies and neuropil. *J. Comp. Neurol.* 216: 69–98.
- Haberly, L.B., Hansen, D.J., Feig, S.L., and Presto, S. 1987. Distribution and ultrastructure of neurons in opossum displaying immunoreactivity to GABA and GAD and high affinity tritiated GABA uptake. *J. Comp. Neurol.* 266: 269–290.
- Haberly, L.B., and Presto, S. 1986. Ultrastructural analysis of synaptic relationships of intracellularly stained pyramidal cell axons in piriform cortex. *J. Comp. Neurol.* 248: 464–474.
- Haberly, L.B., and Price, J.L. 1977. The axonal projection patterns of the mitral and tufted cells of the olfactory bulb in the rat. *Brain Res.* 129: 152–157.
- Haberly, L.B., and Price, J.L. 1978a. Association and commissural fiber systems of the olfactory cortex of the rat. I. Systems originating in the piriform cortex and adjacent areas. *J. Comp. Neurol.* 178: 711–740.
- Haberly, L.B., and Price, J.L. 1978b. Association and commissural fiber systems of the olfactory cortex of the rat. II. Systems originating in the olfactory peduncle. *J. Comp. Neurol.* 181: 781–808.
- Haberly, L.B., and Shepherd, G.M. 1973. Current-density analysis of summed evoked potentials in opossum prepyriform cortex. *J. Neurophysiol.* 36: 789–802.
- Hablitz, J., and Langmoen, I. 1982. Excitation of hippocampal pyramidal cells by glutamate in the guinea-pig and rat. *J. Physiol. (Lond.)* 325: 317–331.
- Hablitz, J., and Thalmann, R. 1987. Conductance changes underlying a late synaptic hyperpolarization in hippocampal neurons. *J. Neurophysiol.* 58: 160–179.
- Hablitz, J.J., and Johnston, D. 1981. Endogenous nature of spontaneous bursts in hippocampal neurons. *Cell. Mol. Neurobiol.* 1: 325–334.
- Hack, I., Peichl, L., and Brandstätter, J.H. 1999. An alternative pathway for rod signals in the rodent retina: rod photoreceptors, cone bipolar cells, and the localization of glutamate receptors. *Proc. Natl. Acad. Sci. U.S.A.* 96: 14130–14135.
- Hackett, J.T., Hou, S.M., and Cochran, S.L. 1979. Glutamate and synaptic depolarization of Purkinje cells evoked by climbing fibers. *Brain Res.* 170: 377–380.

- Hackney, C.M., Osen, K.K., Ottersen, O.P., Storm-Mathisen, J., and Manjaly, G. 1996. Immunocytochemical evidence that glutamate is a neurotransmitter in the cochlear nerve: a quantitative study in the guinea-pig anteroventral cochlear nucleus. *Eur. J. Neurosci.* 8: 79–91.
- Haglund, L., Swanson, L.W., and Köhler, C. 1984. The projection of the supramammillary nucleus to the hippocampal formation: an immunohistochemical and anterograde transport study with the lectin PHA-L in the rat. *J. Comp. Neurol.* 229: 171–185.
- Hahnloser, R., Sarpeshkar, R., Mahowald, M., Douglas, R., and Seung, H. 2000. Neural networks with dynamic synapses. *Nature* 405: 947–951.
- Haist, F., Gore, J. B., and Mao, H. 2001 Consolidation of human memory over decades revealed by functional magnetic resonance imaging. *Nat. Neurosci.* 4: 1139–1145.
- Halabisky, B., Friedman, D., Radojicic, M., and Strowbridge, B.W. 2000. Calcium influx through NMDA receptors directly evokes GABA release in olfactory bulb granule cells. *J. Neurosci.* 20: 5124–5134.
- Halasy, K., Buhl, E.H., Lorinczi, Z., Tamas, G., and Somogyi, P. 1996. Synaptic target selectivity and input of GABAergic basket and bistratified interneurons in the CA1 area of the rat hippocampus. *Hippocampus* 6: 306–329.
- Halasy, K., Miettinen, R., Szabat, E., and Freund, T.F. 1991. GABAergic interneurons are the major postsynaptic targets of median raphe afferents in the rat dentate gyrus. *Eur. J. Neurosci.* 4: 144–153.
- Halasz, N., and Greer, C.A. 1993. Terminal arborizations of olfactory nerve fibers in the glomeruli of the olfactory bulb. *J. Comp. Neurol.* 337: 307–316.
- Halasz, N., and Shepherd, G.M. 1983. Neurochemistry of the vertebrate olfactory bulb. *Neuroscience* 10: 579–619.
- Halasz, N., Ljungdahl, A., Hokfelt, T., Johannsson, O., Goldstein, M., Park, D., and Biberfeld, P. 1977. Transmitter histochemistry of the rat olfactory bulb. I. Immunohistochemical localization of monoamine-synthesizing enzymes. *Brain Res.* 455–474.
- Halasz, N., Ljungdahl, A., and Hökfelt, T. 1978. Transmitter histochemistry of the rat olfactory bulb. II. Fluorescence histochemical, autoradiographic and electron microscopic localization of monoamines. *Brain Res.* 154: 253–271.
- Haldeman, S., Huffman, R., Marshall, K., and McLennan, H. 1972. The antagonism of the glutamate induced and synaptic excitations of the thalamic neurons. *Brain Res.* 39: 419–425.
- Haldeman, S., and McLennan, H. 1972. The antagonistic action of glutamic acid diethylester toward amino-acid-induced and synaptic excitations of central neurons. *Brain Res.* 45: 393–400.
- Hall, W.C., and Ebner, F.F. 1970. Thalamo-telencephalic projections in the turtle (*Pseudemys scripta*). *J. Comp. Neurol.* 14: 101–122.
- Halliwel, J.V., and Adams, P.R. 1982. Voltage-clamp analysis of muscarinic excitation in hippocampal neurons. *Brain Res.* 250: 71–92.
- Halliwel, J.V., and Scholfield, C.N. 1984. Somatically recorded Ca-currents in guinea-pig hippocampal and olfactory cortex neurones are resistant to adenosine action. *Neurosci. Lett.* 50: 13–18.
- Hamassaki-Britto, D.E., Hermans-Borgmeyer, I., Heinemann, S., and Hughes, T.E. 1993. Expression of glutamate receptor genes in the mammalian retina: the localization of GluR1 through GluR7 mRNAs. *J. Neurosci.* 13: 1888–1898.
- Hamill, O.P., Huguenard, J., and Prince, D. 1991. Patch-clamp studies of voltage-gated currents in identified neurons of the rat cerebral cortex. *Cereb. Cortex* 1: 48–61.
- Hamill, O.P., Bormann, J., and Sakmann, B. 1983. Activation of multiple-conductance state chloride channels in spinal neurones by glycine and GABA. *Nature* 305: 805–808.
- Hamill, O.P., Marty, A., Neher, E., Sakmann, B., and Sigworth, F.J. 1981. Improved patch-clamp techniques for high-resolution current recordings from cells and cell-free membrane patches. *Pflügers Arch.* 391: 85–100.

- Hamilton, K.A., and Kauer, J.S. 1985. Intracellular potentials of salamander mitral/tufted neurons in response to odor stimulation. *Brain Res* 338: 181–185.
- Hamilton, K.A., and Kauer, J.S. 1988. Responses of mitral/tufted cells to orthodromic and antidromic electrical stimulation in the olfactory bulb of the tiger salamander. *J. Neurophysiol.* 59: 1736–1755.
- Hamilton, K.A., and Kauer, J.S. 1989. Patterns of intracellular potentials in salamander mitral/tufted cells in response to odor stimulation. *J. Neurophysiol.* 62: 609–625.
- Hamlyn, L.H. 1962. The fine structure of the mossy fibre endings in the hippocampus of the rabbit. *J. Anat.* 96: 112–120.
- Hámori J., and Mezey E., 1977. Serial and triadic synapses in the cerebellar nuclei of the cat. *Exp. Brain Res.* 30, 259–273.
- Hamori, J., and Szentagothai, J. 1966. Identification under the electron microscope of climbing fibers and their synaptic contacts. *Exp. Brain Res.* 1: 65–81.
- Hamos, J.E., Van Horn, S.C., Raczkowski, D., and Sherman, S.M. 1987. Synaptic circuits involving an individual retinogeniculate axon in the cat. *J. Comp. Neurol.* 259: 165–192.
- Hamos, J.E., Van Horn, S.C., Raczkowski, D., Uhlrich, D.J., and Sherman, S.M. 1985. Synaptic connectivity of a local circuit neurone in lateral geniculate nucleus of the cat. *Nature* 317: 618–621.
- Hampson, E.C., Vaney, D.I., and Weiler, R. 1992. Dopaminergic modulation of gap junction permeability between amacrine cells in mammalian retina. *J. Neurosci.* 12: 4911–4922.
- Hampson, E.C.G.M., Weiler, R., and Vaney, D.I. 1994. pH-gated dopaminergic modulation of horizontal cell gap junctions in mammalian retina. *Proc. Roy. Soc. Lond. B* 255: 67–72.
- Hamrick, W.D., Wilson, D.A., and Sullivan, R.M. 1993. Neural correlates of memory for odor detection conditioning in adult rats. *Neurosci. Lett.* 163: 36–40.
- Hara, M., Inoue, M., Yasukura, T., Ohnishi, S., Mikami, Y., and Inagaki, C. 1992. Uneven distribution of intracellular Cl^- in rat hippocampal neurons. *Neurosci. Lett.* 143: 135–138.
- Harding, B.N. 1973. An ultrastructural study of the termination of afferent fibres within the ventrolateral and centre median nuclei of the monkey thalamus. *Brain Res.* 54: 341–346.
- Harlan, R.E., Shivers, B.D., Romano, G.J., Howells, R.D., and Pfaff, D.W. 1987. Localization of preproenkephalin mRNA in the rat brain and spinal cord by in situ hybridization. *J. Comp. Neurol.* 258: 159–184.
- Harris, E., Witter, M.P., Weinstein, G., and Stewart, M. 2001. Intrinsic connectivity of the rat subiculum: I. Dendritic morphology and patterns of axonal arborization by pyramidal neurons. *J. Compl. Neurol.* 435: 490–505.
- Harris, K.M. 1999. Structure, development, and plasticity of dendritic spines. *Curr. Opin. Neurobiol.* 9: 343–348.
- Harris, K.M., Jensen, F.E., and Tsao, B.H. 1989. Ultrastructure, development, and plasticity of dendritic spine synapses in area CA1 of the rat hippocampus: Extending our vision with serial electron microscopy and three-dimensional analyses. In: *The Hippocampus—New Vistas* (Chan-Palay, V., and Köhler, C., eds.) New York: Alan R. Liss, pp. 33–52.
- Harris, K.M., and Kater, S.B. 1994. Dendritic spines: cellular specializations imparting both stability and flexibility to synaptic function. *Annu. Rev. Neurosci.* 17: 341–371.
- Harris, K.M., and Stevens, J.K. 1988. Dendritic spines of rat cerebellar Purkinje cells: serial electron microscopy with reference to their biophysical characteristics. *J. Neurosci.* 8: 4455–4469.
- Harris, K.M., and Stevens, J.K. 1989. Dendritic spines of CA1 pyramidal cells in the rat hippocampus: serial electron microscopy with reference to their biophysical characteristics. *J. Neurosci.* 9: 2982–2997.
- Hartell, N. 1994. cGMP acts within cerebellar Purkinje cells to produce long-term depression via mechanisms involving PKC and PKG. *NeuroReport* 5: 833–836.

- Hartell, N. 1996. Strong activation of parallel fibers produces localized calcium transients and a form of LTD that spreads to distant synapses. *Neuron* 16: 601–610.
- Harting, J.K., Hashikawa, T., and Van Lieshout, D. 1986. Laminar distribution of tectal, parabrachial and pretectal inputs to the primate dorsal lateral geniculate nucleus: connectional studies in *Galago crassicaudatus*. *Brain Res.* 366: 358–363.
- Harting, J.K., Van Lieshout, D.P. 2000. Projections from the rostral pole of the inferior colliculus to the cat superior colliculus. *Brain Res* 881: 244–247.
- Hartveit, E., Brandstätter, J.H., Enz, R., and Wässle, H. 1995. Expression of the mRNA of seven metabotropic glutamate receptors (mGluR1 to 7) in the rat retina. An *in situ* hybridization study on tissue sections and isolated cells. *Eur. J. Neurosci.* 7: 1472–1483.
- Harty, T.P., and Manis, P.B. 1996. Glycine-evoked currents in acutely dissociated neurons of the guinea pig ventral cochlear nucleus. *J. Neurophysiol.* 75: 2300–2311.
- Hartzell, H.C. 1981. Mechanisms of slow postsynaptic potentials. *Nature* 291: 539–544.
- Hasan, Z., and Stuart, D.G. 1984. Mammalian muscle receptors In: *Handbook of the Spinal Cord, Vol. 1: Physiology* (Davidoff, R.E., ed.) New York: Marcel Dekker, pp. 559–608.
- Hassani, O.K., Cromwell, H.C., and Schultz, W. 2001. Influence of expectation of different rewards on behavior-related neuronal activity in the striatum. *J. Neurophysiol.* 85: 2477–2489.
- Hasselmo, M.E. 1994. Neuromodulation and cortical function. Modeling the physiological basis of behavior. *Behav. Brain Res.* 67: 1–27.
- Hasselmo, M.E., Anderson, B.P., and Bower, J.M. 1992. Cholinergic modulation of cortical associative memory function. *J. Neurophysiol.* 67: 1230–1246.
- Hasselmo, M.E., and Barkai, E. 1995. Cholinergic modulation of activity-dependent synaptic plasticity in the piriform cortex and associative memory function in a network biophysical simulation. *J. Neurosci.* 15: 6592–6604.
- Hasselmo, M.E., and Bower, J.M. 1992. Cholinergic suppression specific to intrinsic not afferent fiber synapses in rat piriform (olfactory) cortex. *J. Neurophysiol.* 67: 1222–1229.
- Hasselmo, M.E., Wilson, M.A., Anderson, B.P., and Bower, J.M. 1990. Associative memory function in piriform (olfactory) cortex: computational modeling and neuropharmacology. *Cold Spring Harbor Symp. Quant. Biol.* 60: 599–609.
- Hattar, S., Liao, H.-W., Takao, M., Berson, D.M., and Yau, K.-W. 2002. Melanopsin-containing retinal ganglion cells: architecture, projections, and intrinsic photosensitivity. *Science* 295: 1065–1070.
- Hattori, T., Fibiger, H.C., McGeer, P.L., and Maller, L. 1973. Analysis of the fine structure of the dopaminergic nigrostriatal projection by electron microscopy. *Exp. Neurol.* 41: 599–611.
- Hausser, M., Spruston, N., and Stuart, G.J. 2000. Diversity and dynamics of dendritic signaling. *Science* 290: 739–744.
- Haverkamp, S., Grünert, U., and Wässle, H. 2000. The cone pedicle, a complex synapse in the retina. *Neuron* 27: 85–95.
- Haverkamp, S., Grünert, U., and Wässle, H. 2001a. Localization of kainate receptors at the cone pedicles of the primate retina. *J. Comp. Neurol.* 436: 471–486.
- Haverkamp, S., Grünert, U., and Wässle, H. 2001b. The synaptic architecture of AMPA receptors at the cone pedicle of the primate retina. *J. Neurosci.* 21: 2488–2500.
- Haverkamp, S., and Wässle, H. 2000. Immunocytochemical analysis of the mouse retina. *J. Comp. Neurol.* 424: 1–23.
- Hayar, A., Heyward, P.M., Heinbockel, T., Shipley, M.T., and Ennis, M. 2001. Direct excitation of mitral cells via activation of alpha1-noradrenergic receptors in rat olfactory bulb slices. *J. Neurophysiol.* 86: 2173–2182.
- Hayashi, T. 1954. Effects of sodium glutamate on the nervous system. *Keio J. Med.* 302: 183–192.
- He, S., Weiler, R., and Vaney, D.I. 2000. Endogenous dopaminergic regulation of horizontal cell coupling in the mammalian retina. *J. Comp. Neurol.* 418: 33–40.

- Heale, V.R., and Vanderwolf, C.H. 1995. Scopolamine blocks olfaction-induced fast waves but not olfactory evoked potentials in the dentate gyrus. *Behav. Brain Res.* 68: 57–64.
- Hebb, D.O. 1949. *The Organization of Behavior*. New York: John Wiley & Sons.
- Heckman, C.J., and Binder, M.D. 1988. Analysis of effective synaptic currents generated by homonymous Ia afferent fibers in motoneurons of the cat. *J. Neurophysiol.* 60: 1946–1966.
- Heckman, C.J., and Binder, M.D. 1993. Computer simulations of motoneuron firing rate modulation. *J. Neurophysiol.* 69: 1005–1008.
- Heggelund, P. 1981. Receptive field organization of simple cells in cat striate cortex. *Exp. Brain Res.* 42: 89–98.
- Heggelund, P., and Hartveit, E. 1990. Neurotransmitter receptors mediating excitatory input to cells in the cat lateral geniculate nucleus. I. Lagged cells. *J. Neurophysiol.* 63: 1347–1360.
- Heidelberger, R., Sterling, P., and Matthews, G. 2002. Roles of ATP in depletion and replenishment of the releasable pool of synaptic vesicles. *J. Neurophysiol.* 88: 98–106.
- Heimer, L., and Kalil, R. 1978. Rapid transneuronal degeneration and death of cortical neurons following removal of the olfactory bulb in adult rats. *J. Comp. Neurol.* 178: 559–619.
- Hellstrom, J., Arvidsson, U., Elde, R., Cullheim, S., and Meister, B. 1999. Differential expression of nerve terminal protein in VAcHT-containing varicosities of the spinal cord ventral horn. *J. Comp. Neurol.* 411: 578–590.
- Hendrickson, A., Hunt, S., and J.-Wu, Y. 1981. Immunocytochemical localization of glutamic acid decarboxylase in monkey striate cortex. *Nature* 292: 605.
- Hendry, A., Jones, E., DeFelipe, J., Schmechel, D., Brandon, C., and Emson, P. 1984. Neuropeptide-containing neurons of the cerebral cortex are also GABA-ergic. *Proc. Natl. Acad. Sci. U.S.A.* 81: 6526–6530.
- Hendry, S.H.C., and Calkins, D.J. 1998. Neuronal chemistry and functional organization in the primate visual system. *Trends Neurosci.* 21: 344–349.
- Hendry, S.H.C., and Yoshioka, T. 1994. A neurochemically distinct third channel in the macaque dorsal lateral geniculate nucleus. *Science* 264: 575–577.
- Henneman, E., Clamann, H.P., Gillies, J.D., and Skinner, R.D. 1974. Rank order of motoneurons within a pool: law of combination. *J. Neurophysiol.* 37: 1338–1349.
- Henneman, E., Lüscher, H.-R., and Mathis, J. 1984. Simultaneously active and inactive synapses of single Ia fibres on cat spinal motoneurons. *J. Physiol. (Lond.)* 352: 147–161.
- Henneman, E., and Mendell, L.M. 1981. Functional organization of motoneuron pool and its inputs. In: *Handbook of Physiology*. Section I. The Nervous System. Vol. II, Part 1 (Brooks, V.B., ed.) Bethesda, MD: American Physiological Society, pp. 423–507.
- Henneman, E., and Olson, C.B. 1965. Relations between structure and function in the design of skeletal muscles. *J. Neurophysiol.* 28: 581–598.
- Henneman, E., Somjen, G., and Carpenter, D.O. 1965. Excitability and inhibibility of motoneurons of different sizes. *J. Neurophysiol.* 28: 599–620.
- Hennig, M.H., Funke, K., and Worgotter, F. 2002. The influence of different retinal subcircuits on the nonlinearity of ganglion cell behavior. *J. Neurosci.* 22: 8726–8738.
- Henze, D.A., McMahon, D.B., Harris, K.M., and Barrionuevo, G. 2002. Giant miniature EPSCs at the hippocampal mossy fiber to CA3 pyramidal cell synapse are monoquantal. *J. Neurophysiol.* 87: 15–29.
- Herkenham, M. 1978. The connections of the nucleus reuniens thalami: evidence for a direct thalamo-hippocampal pathway in the rat. *J. Comp. Neurol.* 177: 589–610.
- Herkenham, M., and Pert, C.B. 1981. Mosaic distribution of opiate receptors, parafascicular projections and acetylcholinesterase in the rat striatum. *Nature* 291: 415–418.
- Herraras, O. 1990. Propagating dendritic actium potential mediates synaptic transmission in CA1 pyramidal cells in situ. *J. Neurophysiol.* 64: 1429–1441.

- Herrling, P.L., and Hull, C.D. 1980. Iontophoretically applied dopamine depolarizes and hyperpolarizes the membrane of cat caudate neurons. *Brain Res.* 192: 441–462.
- Hersch, S., and White, E. 1981. Quantification of synapses formed with apical dendrites of Golgi-impregnated pyramidal cells: variability in thalamocortical inputs, but consistence in the ratios of asymmetrical to symmetrical synapses. *J. Neurosci.* 6: 1043–1051.
- Hertz, J., Krogh, A., and Palmer, R.G. 1991. *Introduction to the Theory of Neural Computation.* Redwood City, CA: Addison-Wesley.
- Hewitt, M.J., and Meddis, R. 1993. Regularity of cochlear nucleus stellate cells: a computational modeling study. *J. Acoust. Soc. Am.* 93: 3390–3399.
- Hewitt, M.J., and Meddis, R. 1995. A computer model of dorsal cochlear nucleus pyramidal cells: intrinsic membrane properties. *J. Acoust. Soc. Am.* 97: 2405–2413.
- Hicks, T.P., Lodge, D., and McLennan, H. eds. 1987. *Excitatory Amino Acid Transmission.* New York: Alan R. Liss.
- Higgs, M.H., Romano, C., and Lukasiewicz, P.D. 2002. Presynaptic effects of group III metabotropic glutamate receptors on excitatory synaptic transmission in the retina. *Neuroscience* 115: 163–172.
- Hikosaka, O., and Wurtz, R.H. 1983. Visual and oculomotor functions of monkey substantia nigra pars reticulata. III. Memory-contingent visual and saccade responses. *J. Neurophysiol.* 49: 1268–1284.
- Hikosaka, O., Takikawa, Y., and Kawagoe, R. 2000. Role of the basal ganglia in the control of purposive saccadic eye movements. *Physiol Rev.* 80: 953–978.
- Hildebrand, J.G. 1995. Analysis of chemical signals by nervous systems. *Proc. Natl. Acad. Sci. U.S.A.* 92: 67–74.
- Hildebrand, J.G. 1996. Olfactory control of behavior in moths: Central processing of odor information and the functional significance of olfactory glomeruli. *J. Comp. Physiol. A* 178: 5–19.
- Hildebrand, J.G., and Shepherd, G.M. 1997. Molecular mechanisms of olfactory discrimination: converging evidence for common principles across phyla. *Annu. Rev. Neurosci.* 20: 595–631.
- Hill, D., and Bowery, N. 1981. 3H-baclofen and H-GABA bind to bicuculline-insensitive GABA_B sites in rat brain. *Nature* 290: 149–152.
- Hille, B. 2001. *Ionic Channels of Excitable Membranes.* 3rd edition. Sunderland, MA: Sinauer Associates.
- Hillman, D.E., and Chen, S. 1984. Reciprocal relationship between size of postsynaptic densities and their number: constancy in contact area. *Brain Res.* 295: 325–343.
- Hillman, D.E., and Chen, S. 1985a. Compensation in the number of presynaptic dense projections and synaptic vesicles in remaining parallel fibres following cerebellar lesions. *J. Neurocytol.* 14: 673–687.
- Hillman, D.E., and Chen, S., 1985b. Plasticity in the size of presynaptic and postsynaptic membrane specializations. In: *Synaptic Plasticity* (C.W. Cotman, ed.) New York: The Guilford Press, pp. 39–76.
- Hinds, J.W. 1970. Reciprocal and serial dendrodendritic synapses in the glomerular layer of the rat olfactory bulb. *Brain Res.* 17: 530–534.
- Hinds, J.W., and Hinds, P.L. 1976. Synapse formation in the mouse olfactory bulb. I. Quantitative studies. *J. Comp. Neurol.* 169: 15–40.
- Hinds, J.W., and Hinds, P.L. 1976. Synapse formation in the mouse olfactory bulb. II. Morphogenesis. *J. Comp. Neurol.* 169: 41–61.
- Hirata, Y. 1964. Some observations on the fine structure of synapses in the olfactory bulb of the mouse, with particular reference to the atypical synaptic configurations. *Arch. Histol. Jpn.* 24: 303–317.

- Hirsch, J., Alonso, J., and Reid, R.C. 1995. Visually evoked calcium action potentials in cat striate cortex. *Nature* 378: 612–616.
- Hirsch, J., and Gilbert, C. 1991. Synaptic connections of horizontal connections in the cat's visual cortex. *J. Neurosci.* 11: 1800–1809.
- Hirsch, J.A., and Oertel, D. 1988. Intrinsic properties of neurones in the dorsal cochlear nucleus of mice, *in vitro*. *J. Physiol. (Lond.)* 396: 535–548.
- Hirsch, J.C., Fourment, A., and Marc, M.E. 1983. Sleep-related variations of membrane potential in the lateral geniculate body relay neurons of the cat. *Brain Res.* 259: 308–312.
- Hjorth-Simonsen, A., and Jeune, B. 1972. Origin and termination of the hippocampal perforant path in the rat studied by silver impregnation. *J. Comp. Neurol.* 144: 215–232.
- Hochstein, S., and Shapley, R.M. 1976a. Linear and nonlinear spatial subunits in Y cat retinal ganglion cells. *J. Physiol. (Lond.)* 262: 265–284.
- Hochstein, S., and Shapley, R.M. 1976b. Quantitative analysis of retinal ganglion cell classifications. *J. Physiol.* 262: 237–264.
- Hodgkin, A.L., and Huxley, A.F. 1952a. Currents carried by sodium and potassium ions through the membrane of the giant axon of *Loligo*. *J. Physiol. (Lond.)* 116: 449–472.
- Hodgkin, A.L., and Huxley, A.F. 1952b. The components of membrane conductance in the giant axon of *Loligo*. *J. Physiol. (Lond.)* 116: 473–496.
- Hodgkin, A.L., and Huxley, A.F. 1952c. The dual effect of membrane potential and sodium conductance in the giant axon of *Loligo*. *J. Physiol. (Lond.)* 116: 497–506.
- Hodgkin, A.L., and Huxley, A.F. 1952d. A quantitative description of membrane current and its application to conduction and excitation in nerve. *J. Physiol. (Lond.)* 117: 500–544.
- Hodgkin, A.L., and Katz, B. 1949. The effect of sodium ions on the electrical activity of the giant axon of the squid. *J. Physiol. (Lond.)* 108: 37–77.
- Hoffer, B.J., Siggins, G.R., Oliver, A.P., and Bloom, F.E. 1973. Activation of the pathway from locus coeruleus to rat cerebellar Purkinje neurons. Pharmacological evidence of noradrenergic central inhibition. *J. Pharmacol. Exp. Ther.* 184: 553–569.
- Hoffman, D., Magee, J.C., Colbert, C.M., and Johnston, D. 1997. K^+ channel regulation of signal propagation in dendrites of hippocampal pyramidal neurons. *Nature* 387: 869–875.
- Hoffman, K.L., and McNaughton, B.L. 2002. Sleep on it: cortical reorganization after-the-fact. *Trends Neurosci.* 25: 1–2.
- Hoffman, W.H., and Haberly, L.B. 1989. Bursting induces persistent all-or-none EPSPs by an NMDA-dependent process in piriform cortex. *J. Neurosci.* 9: 206–215.
- Hoffman, W.H., and Haberly, L.B. 1991. Bursting-induced epileptiform EPSPs in slices of piriform cortex are generated by deep cells. *J. Neurosci.* 11: 2021–2031.
- Hoffman, W.H., and Haberly, L.B. 1993. Role of synaptic excitation in the generation of bursting-induced epileptiform potentials in the endopiriform nucleus and piriform cortex. *J. Neurophysiol.* 70: 2550–2561.
- Hökfelt, T., Millhorn, D., Seroogy, K., Tsuruo, Y., Ceccatelli, S., Lindh, B., Meister, B., Melander, T., Schalling, M., and Bartfai, T. 1989. Coexistence of peptides with classical neurotransmitters. *Experientia* 56: 154–179.
- Hollmann, M. 1999. Structure of Ionotropic Glutamate Receptors. In: *Ionotropic Glutamate Receptors in the CNS* (Jonas, P., and Monyer, H., eds.) Heidelberg: Springer, pp. 3–98.
- Hollmann, M., and Heinemann, S. 1994. Cloned glutamate receptors. *Annu. Rev. Neurosci.* 17: 31–108.
- Holmes, W.R., and Rall, W. 1992. Estimating the electrotonic structure of neurons with compartmental models. *J. Neurophysiol.* 68: 1438–1452.
- Holmgren, C., and Zilberter, Y. 2001. Coincident spiking activity induces long-term changes in inhibition of neocortical pyramidal cells. *J. Neurosci.* 21: 8270–8277.

- Holthoff, K., Tsay, D., and Yuste, R. 2002. Calcium dynamics depend on their dendritic location. *Neuron* 33: 425–437.
- Hongo, T., Jankowska, E., Ohno, T., Sasaki, S., Yamashita, M., and Yoshida, K. 1983. The same interneurons mediate inhibition of dorsal spinocerebellar tract cells and lumbar motoneurons in the cat. *J. Physiol. (Lond.)* 342: 161–180.
- Honig, M.G., Collins, W.F., and Mendell, L.M. 1983. α -Motoneuron EPSPs exhibit different frequency sensitivities to single Ia-afferent fiber stimulation. *J. Neurophysiol.* 49: 886–901.
- Hoogland, P., Wouterlood, F.G., Welker, E., and van der Loos, H. 1991. Ultrastructure of giant and small thalamic terminals of cortical origin: a study of the projections from the barrel cortex in mice using *Phaseolus vulgaris* leuco-agglutinin (PHA-L). *Exp. Brain Res.* 87: 159–172.
- Hoover, J.E., and Strick, P.L. 1993. Multiple output channels in the basal ganglia. *Science* 259: 819–821.
- Hopfield, J.J. 1982. Neural networks and physical systems with emergent collective computational abilities. *Proc. Natl. Acad. Sci. U.S.A.* 79: 2554–2558.
- Hopfield, J.J. 1984. Neurons with graded response have collective properties like those of two-state neurons. *Proc. Natl. Acad. Sci. U.S.A.* 81: 3088–3092.
- Horikawa, K., and Armstrong, W.E. 1988. A versatile means of intracellular labeling injection of biocytin and its detection with avidin conjugates. *J. Neurosci. Methods* 25: 1–11.
- Hornung, J., and Garey, L. 1981. The thalamic projection to cat visual cortex: ultrastructure of neurons identified by Golgi impregnation or retrograde horseradish peroxidase transport. *Neuroscience* 6: 1053–1068.
- Horton, J., and Hubel, D. 1981. A regular patchy distribution of cytochrome oxidase staining in primary visual cortex of the macaque monkey. *Nature* 292: 762–764.
- Horvath, M., Kraus, K.S., and Illing, R.B. 2000. Olivocochlear neurons sending axon collaterals into the ventral cochlear nucleus of the rat. *J. Comp. Neurol.* 422: 95–105.
- Hotson, J.R., and Prince, D.A. 1980. A calcium-activated hyperpolarization follows repetitive firing in hippocampal neurons. *J. Neurophysiol.* 43: 409–419.
- Hotson, J.R., Prince, D.A., and Schwartzkroin, P.A. 1979. Anomalous rectification in hippocampal neurons. *J. Neurophysiol.* 42: 889–895.
- Houk, J.C., Adams, J.L., and Barto, A.G. 1995. A model of how the basal ganglia generate and use neural signals that predict reinforcement. In: *Models of Information Processing in the Basal Ganglia* (J.C. Houk, J.L. Davis and D.G. Beiser, eds.) Cambridge, MA, MIT Press, pp. 229–270.
- Houk, J.C., and Rymer, W.Z. 1981. Neural control of muscle length and tension In: *Handbook of Physiology. Section I. The Nervous System. Vol. II, Motor Control, Part 1* (Brooks, V.B., ed.) Bethesda, MD: American Physiological Society, pp. 257–323.
- Hounsgaard, J., Hultborn, H., Jespersen, B., and Kiehn, O. 1988. Bistability of α -motoneurons in the decerebrate cat and in the acute spinal cat after intravenous 5-hydroxytryptophane. *J. Physiol. (Lond.)* 405: 345–367.
- Hounsgaard, J., and Kiehn, O. 1989. Serotonin-induced bistability of turtle motoneurons caused by a nifedipine-sensitive calcium plateau potential. *J. Physiol. (Lond.)* 414: 265–282.
- Houser, C., Crawford, G., Salvaterra, P., and Vaughn, J. 1985. Immunocytochemical localization of choline acetyltransferase in rat cerebral cortex: a study of cholinergic neurons and synapses. *J. Comp. Neurol.* 234: 17–34.
- Howe, A.R., and Surmeier, D.J. 1995. Muscarinic receptors modulate N-, P- and L-type Ca^{2+} currents in rat striatal neurons through parallel pathways. *J. Neurosci.* 15: 458–469.
- Howell, G.A., Welch, M.G., and Frederickson, C.J. 1984. Simulation-induced uptake and release of zinc in hippocampal slices. *Nature* 308: 736–738.

- Hsia, A.Y., Vincent, J.D., and Lledo, P.M. 1999. Dopamine depresses synaptic inputs into the olfactory bulb. *J. Neurophysiol.* 82: 1082–1085.
- Hsu, A., Tsukamoto, Y., Smith, R.G., and Sterling, P. 1998. Functional architecture of primate rod and cone axons. *Vision Res.* 38: 2539–2549.
- Hsu, A.C.C. 1998. Optimal transfer of form and color information through the primate retina.
- Hsu, K.S., Yang, C.H., Huang, C.C., and Gean, P.W. 1996. Carbachol induces inward current in neostriatal neurons through M1-like muscarinic receptors. *Neuroscience* 73: 751–760.
- Hu, B., Steriade, M., and Deschênes, M. 1989a. The effects of brainstem peribrachial stimulation on neurons of the lateral geniculate nucleus. *Neuroscience* 31: 13–24.
- Hu, B., Steriade, M., and Deschênes, M. 1989b. The cellular mechanism of thalamic pontogeniculo-occipital waves. *Neuroscience* 31: 25–35.
- Hu, H., Tomasiewicz, H., Magnuson, T., and Rutishauser, U. 1996. The role of polysialic acid in migration of olfactory bulb interneuron precursors in the subventricular zone. *Neuron* 16: 735–743.
- Hu, H.J., and Pan, Z.H. 2002. Differential expression of K^+ currents in mammalian retinal bipolar cells. *Vis. Neurosci.* 19: 163–173.
- Huang, A.Y., and May, B.J. 1996. Sound orientation behavior in cats. II. Mid-frequency spectral cues for sound localization. *J. Acoust. Soc. Am.* 100: 1070–1080.
- Hubel, D.H., and Wiesel, T.N. 1962. Receptive fields, binocular interaction and functional architecture in the cat's visual cortex. *J. Physiol. (Lond.)* 160: 106–154.
- Hubel, D.H., and Wiesel, T.N. 1977. The functional architecture of the macaque visual cortex. *Proc. R. Soc. Lond. B* 198: 1–59.
- Hudson, D.B., Valcana, T., Bean, G., and Timiras, P.S. 1976. Glutamic acid: a strong candidate as the neurotransmitter of the cerebellar granule cell. *Neurochem. Res.* 1: 73–81.
- Huerta, P. T., Sun, L. D., Wilson, M. A., and Tonegawa, S. 2000. Formation of temporal memory requires NMDA receptors within CA1 pyramidal neurons. *Neuron* 25: 473–80.
- Huettnner, J.E., and Baughman, R.W. 1988. The pharmacology of synapses formed by identified corticocollicular neurons in primary cultures of rat visual cortex. *J. Neurosci.* 8: 160–175.
- Huguenard, J., Hamill, O., and Prince, D. 1989. Sodium channels in dendrites of rat cortical pyramidal neurons. *Proc. Natl. Acad. Sci. U.S.A.* 86: 2473–2477.
- Huguenard, J.R., and McCormick, D.A. 1992. Simulation of the currents involved in rhythmic oscillations in thalamic relay neurons. *J. Neurophysiol.* 68: 1373–1383.
- Huguenard, J.R., and McCormick, D.A. 1994. *Electrophysiology of the Neuron*. New York: Oxford University Press.
- Hultborn, H., Jankowska, E., and Lindström, S. 1971. Recurrent inhibition from motor axon collaterals of transmission in the Ia inhibitory pathway to motoneurons. *J. Physiol. (Lond.)* 215: 591–612.
- Hultborn, H., Katz, R., and Mackel, R. 1988a. Distribution of recurrent inhibition within a motor nucleus. II. Amount of recurrent inhibition in motoneurons to fast and slow units. *Acta Physiol. Scand.* 134: 363–374.
- Hultborn, H., Lipski, J., Mackel, R., and Wigström, H. 1988b. Distribution of recurrent inhibition within a motor nucleus. I. Contribution from slow and fast motor units to the excitation of Renshaw cells. *Acta Physiol. Scand.* 134: 347–361.
- Humphrey, A.L., and Weller, R.E. 1988. Functionally distinct groups of X-cells in the lateral geniculate nucleus of the cat. *J. Comp. Neurol.* 268: 429–447.
- Hunter, C., Petralia, R.S., Vu, T., and Wenthold, R.J. 1993. Expression of AMPA-selective glutamate receptor subunits in morphologically defined neurons of the mammalian cochlear nucleus. *J. Neurosci.* 13: 1932–1946.
- Hyman, B.T., Van Hoesen, G.W., Damasio, A.R., and Barnes, C.L. 1984. Alzheimer's disease: cell-specific pathology isolates the hippocampal formation. *Science* 225: 1168–1171.

- Iansek, R., and Redman, S.J. 1973. An analysis of the cable properties of spinal motoneurons using a brief intracellular current pulse. *J. Physiol. (Lond.)* 234: 613–636.
- Ichida, J.M., Rosa, M.G.P., and Casagrande, V.A. 2000. Does the visual system of the flying fox resemble that of primates? The distribution of calcium-binding proteins in the primary visual pathway of *Pteropus poliocephalus*. *J. Comp. Neurol.* 417: 73–87.
- Ilinsky, I.A., and Kultas-Ilinsky, K. 1990. Fine structure of the magnocellular subdivision of the ventral anterior thalamic nucleus (VAmc) of *Macaca mulatta*: I. Cell types and synaptology. *J. Comp. Neurol.* 294: 455–478.
- Ilinsky, I.A., Yi, H., and Kultas-Ilinsky, K. 1997. Mode of termination of pallidal afferents to the thalamus: a light and electron microscopic study with anterograde tracers and immunocytochemistry in *Macaca mulatta*. *J. Comp. Neurol.* 386: 601–612.
- Illert, M., Lundberg, A., and Tanaka, R. 1976. Integration in descending motor pathways controlling the forelimb in the cat. 2. Convergence on neurones mediating disynaptic cortico-motoneuronal excitation. *Exp. Brain Res.* 26: 521–540.
- Illig, K.R., and Haberly, L.B. 2002. Odor-evoked activity is spatially distributed in piriform cortex. *J. Comp. Neurol.*
- Inagaki, N., Yamatodani, A., Ando-Yamamoto, M., Tohyama, M., Watanabe, T., and Wada, H. 1988. Organization of histaminergic fibers in the rat brain. *J. Comp. Neurol.* 273: 283–300.
- Inagaki, S., Kubota, Y., Shinoda, K., Kawai, Y., and Tohyama, M. 1983. Neurotensin-containing pathway from the endopiriform nucleus and the adjacent prepiriform cortex to the dorso-medial nucleus in the rat. *Brain Res.* 260: 143–146.
- Inagaki, S., Shiosaka, S., Takatsuki, K., Iida, H., Sakanaka, M., Senba, E., Hara, Y., Matsuzuki, T., Kawai, Y., and Tohyama, M. 1982. Ontogeny of somatostatin-containing neuron system of the rat cerebellum including its fiber connections: an experimental and immunohistochemical analysis. *Dev. Brain Res.* 3: 509–527.
- Ingham, C.A., Hood, S.H., Taggart, P., and Arbuthnott, G.W. 1998. Plasticity of synapses in the rat neostriatum after unilateral lesion of the nigrostriatal dopaminergic pathway. *J. Neurosci.* 18: 4732–4743.
- Inoue, M., Matsuo, T., and Ogata, N. 1985a. Characterisation of pre- and postsynaptic actions of (–)baclofen in the guinea-pig hippocampus in vitro. *Br. J. Pharmacol.* 84: 843–853.
- Inoue, M., Matsuo, T., and Ogata, N. 1985b. Possible involvement of K^+ conductance in action of gamma-aminobutyric acid in the guinea-pig hippocampus. *Br. J. Pharmacol.* 86: 515–524.
- Inoue, M., Oomara, Y., Yakushiji, T., and Akaike, N. 1986. Intracellular calcium ions decrease the affinity of the GABA receptor. *Nature* 324: 156–158.
- Iriki, A., Pavlides, C., Keller, A., and Asanuma, H. 1991. Long-term potentiation of thalamic input to the motor cortex induced by co-activation of thalamo-cortical afferents. *J. Neurophysiol.* 65: 1435–1441.
- Irvin, G.E., Casagrande, V.A., and Norton, T.T. 1993. Center/surround relationships of magnocellular, parvocellular, and koniocellular relay cells in primate lateral geniculate nucleus. *Vis. Neurosci.* 10: 363–373.
- Irvine, D.R.F. 1986. *The Auditory Brainstem*. Berlin: Springer-Verlag.
- Isaac, J.T.R., Nicoll, R.A., and Malenka, R.C. 1995. Evidence for silent synapses: implications for the expression of LTP. *Neuron* 15: 427–434.
- Isaacson, J.S. 1999. Glutamate spillover mediates excitatory transmission in the rat olfactory bulb. *Neuron* 23: 377–384.
- Isaacson, J.S., and Strowbridge, B.W. 1998. Olfactory reciprocal synapses: dendritic signaling in the CNS. *Neuron* 20: 749–761.
- Isaacson, J.S., and Walmsley, B. 1995. Counting quanta: direct measurements of transmitter release at a central synapse. *Neuron* 15: 875–884.
- Isayama, T., Berson, D.M., and Pu, M. 2000. Theta ganglion cell type of cat retina. *J. Comp. Neurol.* 417: 32–48.

- Ishai, A., Ungerleider, L.G., Martin, A., Schouten, J.L., and Haxby, J.V. 1999. Distributed representation of objects in the human ventral visual pathway. *Proc. Natl. Acad. Sci. U.S.A.* 96: 9379–9384.
- Ishizuka, N. 2001. Laminar organization of the pyramidal cell layer of the subiculum in the rat. *J. Comp. Neurol.* 435: 89–110.
- Ishizuka, N., Cowan, W.M., and Amaral, D.G. 1995. A quantitative analysis of the dendritic organization of pyramidal cells in the rat hippocampus. *J. Comp. Neurol.* 362: 17–45.
- Ishizuka, N., Mannen, H., Hongo, T., and Sasaki, S. 1979. Trajectory of group Ia afferent fibers stained with horseradish peroxidase in the lumbosacral spinal cord of the cat: three-dimensional reconstructions from serial sections. *J. Comp. Neurol.* 186: 189–211.
- Ishizuka, N., Weber, J., and Amaral, D.G. 1990. Organization of intrahippocampal projections originating from CA3 pyramidal cells in the rat. *J. Comp. Neurol.* 295: 580–623.
- Israel, M., and Whittaker, V.P. 1965. The isolation of mossy fiber endings from the granular layer of the cerebellar cortex. *Experientia* 21: 325–326.
- Ito, M., Sakurai M., and Tongroach P., 1982. Climbing fibre induced depression of both mossy fibre responsiveness and glutamate sensitivity of cerebellar Purkinje cells. *J. Physiol. (Lond.)* 324: 113–134.
- Ito, M., Yoshida, M., and Obata K., 1964. Monosynaptic inhibition of the intracerebellar nuclei induced from the cerebellar cortex. *Experientia.* 20: 575–576.
- Itoh, K., Kamiya, H., Mitani, A., Yasui, Y., Takada, M., and Mizuno, N. 1987. Direct projection from the dorsal column nuclei and the spinal trigeminal nuclei to the cochlear nuclei in the cat. *Brain Res.* 400: 145–150.
- Iversen, L., Mitchell, J., and Srinivasan, V. 1971. The release of gamma-aminobutyric acid during inhibition in the cat visual cortex. *J. Physiol. (Lond.)* 212: 519–534.
- Izzo, P.N., and Bolam, J.P. 1988. Cholinergic synaptic input to different parts of spiny striatonigral neurons in the rat. *J. Comp. Neurol.* 269: 219–234.
- Jack, J.J.B. 1979. Introduction to linear cable theory. In: *The Neurosciences: Fourth Study Program* (Schmitt, F.O., and Worden, F.G., eds.) Cambridge, MA: MIT Press, pp. 423–437.
- Jack, J.J.B., Miller, S., Porter, R., and Redman, S.J. 1971. The time course of minimal excitatory post-synaptic potentials evoked in spinal motoneurons by group Ia afferent fibres. *J. Physiol. (Lond.)* 215: 353–380.
- Jack, J.J.B., Noble, D., and Tsien, R.W. 1975. *Electric Current Flow in Excitable Cells.* Oxford: Oxford University Press.
- Jack, J.J.B., Redman, S.J., and Wong, K. 1981a. The components of synaptic potentials evoked in cat spinal motoneurons by impulses in single group Ia afferents. *J. Physiol. (Lond.)* 321: 65–96.
- Jack, J.J.B., Redman, S.J., and Wong, K. 1981b. Modifications to synaptic transmission at group Ia synapses on cat spinal motoneurons by 4-aminopyridine. *J. Physiol. (Lond.)* 321: 111–126.
- Jackowski, A., Parnevalas, J.G., and Lieberman, A.R. 1978. The reciprocal synapse in the external plexiform layer of the mammalian olfactory bulb. *Brain Res.* 195: 17–28.
- Jackson, M.B., and Scharfman, H.E. 1996. Positive feedback from hilar mossy cells to granule cells in the dentate gyrus revealed by voltage-sensitive dye and microelectrode recording. *J. Neurophysiol.* 76: 601–616.
- Jackson, M.B., and Yakel, J.L. 1995. The 5-HT₃ receptor channel. *Annu. Rev. Physiol.* 57: 447–468.
- Jacobs, G.H. 1993. The distribution and nature of colour vision among the mammals. *Biol. Rev.* 68: 413–471.
- Jacobson, M. 1978. *Developmental Neurobiology.* 2nd edition. New York: Plenum Press.
- Jacoby, R., Stafford, D., Kouyama, N., and Marshak, D. 1996. Synaptic inputs to ON parasol ganglion cells in the primate retina. *J. Neurosci.* 16: 8041–8056.

- Jaeger, D., Kita, H., and Wilson, C.J. 1994. Surround inhibition among projection neurons is weak or nonexistent in the rat neostriatum. *J. Neurophysiol.* 72: 2555–2558.
- Jaffe, D.B., Johnston, D., Lasser-Ross, N., Lisman, J.E., Miyakawa, H., and Ross, W.N. 1992. The spread of Na⁺ spikes determines the pattern of dendritic Ca²⁺ entry into hippocampal neurons. *Nature* 357: 244–246.
- Jahnsen, H. 1986a. Responses of neurons in isolated preparations of the mammalian central nervous system. *Prog. Neurobiol.* 27: 351–372.
- Jahnsen H., 1986b. Electrophysiological characteristics of neurones in the guinea-pig deep cerebellar nuclei *in vitro*. *J. Physiol. Lond.* 372, 129–147.
- Jahnsen, H., and Llinás, R. 1984a. Electrophysiological properties of guinea-pig thalamic neurones: an *in vitro* study. *J. Physiol. (Lond.)* 349: 205–226.
- Jahnsen, H., and Llinás, R. 1984b. Ionic basis for the electroresponsiveness and oscillatory properties of guinea-pig thalamic neurones *in vitro*. *J. Physiol. (Lond.)* 349: 227–247.
- Jahr, C.E., and Nicoll, R.A. 1982a. An intracellular analysis of dendrodendritic inhibition in the turtle *in vitro* olfactory bulb. *J. Physiol. (Lond.)* 326: 213–34.
- Jahr, C.E., and Nicoll, R.A. 1982b. Noradrenergic modulation of dendrodendritic inhibition in the olfactory bulb. *Nature* 297: 227–229.
- Jahr, C.E., and Stevens, C.F. 1987. Glutamate activates multiple single channels conductances in hippocampal neurons. *Nature* 325: 522–525.
- Jahr, C.E., and Yoshioka, K. 1986. Ia afferent excitation of motoneurons in the *in vitro* newborn rat spinal cord is selectively antagonized by kynurenate. *J. Physiol. (Lond.)* 370: 515–530.
- Jameson, D., and Hurvich, L. 1959. Perceived color and its dependence on focal surrounding and preceding stimulus variables. *J. Opt. Soc. Am.* 49: 890–898.
- Jami, L., Murthy, K.S.K., and Petit, J. 1982. A quantitative study of skeletofusimotor innervation on the cat peroneus tertius muscle. *J. Physiol. (Lond.)* 325: 125–144.
- Jan, L.Y., and Jan, Y.N. 1990. How might the diversity of potassium channels be generated? *Trends Neurosci.* 13: 415–419.
- Jankowska, E. 1992. Interneuronal relay in spinal pathways from proprioceptors. *Prog. Neurobiol.* 38: 335–378.
- Jankowska, E., and Lindström, S. 1972. Morphology of interneurons mediating Ia reciprocal inhibition of motoneurons in the spinal cord of the cat. *J. Physiol. (Lond.)* 226: 805–823.
- Jankowska, E., and Lundberg, A. 1981. Interneurons in the spinal cord. *Trends Neurosci.* 4: 230–233.
- Jankowska, E., Lundberg, A., Rudomin, P., and Sykova, E. 1977. Effects of 4-aminopyridine on transmission in excitatory and inhibitory synapses in the spinal cord. *Brain Res.* 136: 387–392.
- Jankowska, E., and Roberts, W.J. 1972a. An electrophysiological demonstration of the axonal projections of single spinal interneurons in the cat. *J. Physiol. (Lond.)* 222: 597–622.
- Jankowska, E., and Roberts, W.J. 1972b. Synaptic actions of single interneurons mediating reciprocal Ia inhibition of motoneurons. *J. Physiol. (Lond.)* 222: 623–642.
- Jankowska, E., and Smith, D.O. 1973. Antidromic activation of Renshaw cells and their axonal projections. *Acta Physiol. Scand.* 88: 198–214.
- Jansen, J. 1969. On cerebellar evolution and organization from the point of view of a morphologist. In: *Neurobiology of Cerebellar Evolution and Development* (Llinás, R., ed.) Chicago: American Medical Association, pp. 881–893.
- Jardemark, K., Nilsson, M., Muyderman, H., and Jacobson, I. 1997. Ca²⁺ ion permeability properties of (R,S) alpha-amino-3-hydroxy-5-methyl-4-isoxazolepropionate (AMPA) receptors in isolated interneurons from the olfactory bulb of the rat. *J. Neurophysiol.* 77: 702–708.
- Jarosiewicz, B., McNaughton, B. L., and Skaggs, W. E. 2002. Hippocampal population activity during the small-amplitude irregular activity state in the rat. *J. Neurosci.* 22: 1373–1384.

- Jasper, H., Khan, R., and Elliot, K. 1965. Amino acids released from the cerebral cortex in relation to its state of activation. *Science* 147: 1448–1449.
- Jefferys, J.G. 1995. Nonsynaptic modulation of neuronal activity in the brain: electric currents and extracellular ions. *Physiol. Rev.* 75: 689–723.
- Jefferys, J.G.R., Traub, R.D., and Whittington, M.A. 1996. Neuronal networks for induced ‘40Hz’ rhythms. *Trends Neurosci.* 19: 202–208.
- Jellali, A., Stussi-Garaud, C., Gasmier, B., Rendon, A., Sahel, J.A., Dreyfus, H., and Picaud, S. 2002. Cellular localization of the vesicular inhibitory amino acid transporter in the mouse and human retina. *J. Comp. Neurol.* 449: 76–87.
- Jensen, R.J. 1995. Receptive-field properties of displaced starburst amacrine cells change following axotomy-induced degeneration of ganglion cells. *Vis. Neurosci.* 12: 177–184.
- Jentsch, T.J. 2000. Neuronal KCNQ potassium channels: physiology and role in disease. *Nat. Rev. Neurosci.* 1: 21–30.
- Jentsch, T.J. 2002. Molecular structure and physiological function of chloride channels. *Physiol. Rev.* 82: 503–568.
- Jessell, T.M., and Kandel, E.R. 1993. Synaptic transmission: a bidirectional and self-modifiable form of cell–cell communication. *Neuron* 10: 1–30.
- Jhaveri, S., Edwards, M.A., and Schneider, G.E. 1991. Initial stages of retinofugal axon development in the hamster: evidence for two distinct modes of growth. *Exp. Brain Res.* 87: 371–382.
- Jiang, D., Palmer, A.R., and Winter, I.M. 1996. Frequency extent of two-tone facilitation in onset units in the ventral cochlear nucleus. *J. Neurophysiol.* 75: 380–395.
- Jiang, Y., Lee, A., Cadene, M., Chait, B.T., and MacKinnon, R. 2002b. The open pore conformation of potassium channels. *Nature* 417: 523–526.
- Jiang, Y., Lee, A., Chen, J., Cadene, M., Chait, B.T., and MacKinnon, R. 2002a. Crystal structure and mechanism of calcium-gated potassium channel. *Nature* 417: 515–522.
- Jiang, Z.G., and North, R.A. 1991. Membrane properties and synaptic responses of rat striatal neurones in vitro. *J. Physiol. (Lond.)* 443: 533–553.
- Jimenez-Catellanos, J., and Graybiel, A.M. 1989. Compartmental origin of striatal efferent projections in the cat. *Neuroscience* 32: 297–321.
- Johnson, D.H. 1980. The relationship between spike rate and synchrony in responses of auditory-nerve fibers to single tones. *J. Acoust. Soc. Am.* 68: 1115–1122.
- Johnson, D.M., Illig, K.R., Behan, M., and Haberly, L.B. 2000. New features of connectivity in piriform cortex visualized by intracellular injection of pyramidal cells suggest that “primary” olfactory cortex functions like “association” cortex in other sensory systems. *J. Neurosci.* 20: 6974–6982.
- Johnson, J.W., and Ascher, P. 1987. Glycine potentiates the NMDA response in cultured mouse brain neurons. *Nature* 325: 529–531.
- Johnson, M.A., and Vardi, N. 1998. Regional differences in GABA and GAD immunoreactivity in rabbit horizontal cells. *Vis. Neurosci.* 15: 743–753.
- Johnston, D., and Brown, T.H. 1981. Giant synaptic potential hypothesis for epileptiform activity. *Science* 211: 294–297.
- Johnston, D., and Brown, T.H. 1983. Interpretation of voltage-clamp measurements in hippocampal neurons. *J. Neurophysiol.* 50: 464–486.
- Johnston, D., and Brown, T.H. 1984a. Biophysics and microphysiology of synaptic transmission in hippocampus. In: *Brain Slices* (Dingledine, R., ed.) New York: Plenum Press, pp. 51–86.
- Johnston, D., and Brown, T.H. 1984b. The synaptic nature of the paroxysmal depolarizing shift in hippocampal neurons. *Ann. Neurol.* 16: S65–S71.
- Johnston, D., and Brown, T.H. 1984c. Mechanisms of neuronal burst generation. In: *Electrophysiology of Epilepsy* (Schwartzkroin, P.A., and Wheal, H., eds.) London: Academic Press, pp. 277–301.

- Johnston, D., and Brown, T.H. 1986. Control theory applied to neural networks illuminates synaptic basis of interictal epileptiform activity. In: *Basic Mechanisms of the Epilepsies Molecular and Cellular Approaches* (Delgado-Escueta, A.V., Ward, A., Woodbury, D.M., and Porter, R.J., eds.) New York: Raven Press, pp. 263–274.
- Johnston, D., Hoffman, D.A., Colbert, C.M., and Magee, J.C. 1999. Regulation of back-propagating action potentials in hippocampal neurons. *Curr. Opin. Neurobiol.* 9: 288–292.
- Johnston, D., Magee, J.C., Colbert, C.M., and Christie, B. 1996. Active properties of neuronal dendrites. *Annu. Rev. Neurosci.* 19: 165–186.
- Johnston, D., Williams, S., Jaffe, D., and Gray, R. 1992. NMDA-receptor-independent long-term potentiation. *Annu. Rev. Physiol.* 54: 489–505.
- Johnston, D., and Wu, S. 1995. *Foundations of Cellular Neurophysiology*. Cambridge, Massachusetts: MIT.
- Jonas, P., and Monyer, H. 1999. Ionotropic Glutamate Receptors in the CNS. *Handbook of Experimental Pharmacology*. Vol. 141. New York: Springer-Verlag.
- Jonas, P., Major, G., and Sakmann, B. 1993. Quantal components of unitary EPSCs at the mossy fibre synapse on CA3 pyramidal cells of rat hippocampus. *J. Physiol. (Lond.)* 472: 615–663.
- Jones, E.G. 1985. *The Thalamus*. New York: Plenum Press.
- Jones, E. G. 1998. Viewpoint: the core and matrix of thalamic organization. *Neuroscience* 85: 331–345.
- Jones, E. G. 2002. Thalamic circuitry and thalamo-cortical synchrony. *Phil. Trans. Roy. Soc. Lond. B* 357: 1659–1673.
- Jones, E.G., and Powell, T.P. 1968. The projection of the somatic sensory cortex upon the thalamus in the cat. *Brain Res.* 10: 369–391.
- Jones, E.G., and Powell, T.P.S. 1969a. Electron microscopy of synaptic glomeruli in the thalamic relay nuclei of the cat. *Proc. R. Soc. Lond. B Biol. Sci.* 172: 153–171.
- Jones, E.G., and Powell, T.P.S. 1969b. An electron microscopic study of the mode of termination of cortico-thalamic fibres within the sensory relay nuclei of the thalamus. *Proc. R. Soc. Lond. B Biol. Sci.* 172: 173–185.
- Jones, E.G., and Powell, T.P.S. 1969c. Morphological variations in the dendritic spines of the neocortex. *J. Cell Sci.* 5: 495–507.
- Jones, E.G., and Rockel, A.J. 1971. The synaptic organization in the medial geniculate body of afferent fibres ascending from the inferior colliculus. *Z. Zellforsch.* 113: 44–66.
- Jones, I.W., Bolam, J.P., and Wonnacott, S. 2001. Presynaptic localization of the nicotinic acetylcholine receptor $\beta 2$ subunit immunoreactivity in rat nigrostriatal dopaminergic neurons. *J. Comp. Neurol.* 439: 235–247.
- Jordan, L.M. 1983. Factors determining motoneuron rhythmicity during fictive locomotion. *Symp. Soc. Exp. Biol.* 37: 423–44.
- Joris, P.X., Carney, L.H., Smith, P.H., and Yin, T.C.T. 1994a. Enhancement of neural synchronization in the anteroventral cochlear nucleus. I: Responses to tones at the characteristic frequency. *J. Neurophysiol.* 71: 1022–1036.
- Joris, P.X., Carney, L.H., Smith, P.H., and Yin, T.C.T. 1994b. Enhancement of neural synchronization in the anteroventral cochlear nucleus. II: Responses in the tuning curve tail. *J. Neurophysiol.* 71: 1037–1051.
- Jourdan, F. 1975. Ultrastructure de l'épithélium olfactif du rat: polymorphisme des récepteurs. *C.R. Séances Acad. Sci. [III]* 280: 443–446.
- Jourdan, F. 1982. Spatial dimension in olfactory coding: a representation of the 2-deoxyglucose patterns of glomerular labeling in the olfactory bulb. *Brain Res.* 240: 341–344.
- Juilfs, D.M., Fulle, H.J., Zhao, A.Z., Houslay, M.D., Garbers, D.L., and Beavo, J.A. 1997. A subset of olfactory neurons that selectively express cGMP-stimulated phosphodiesterase (PDE2) and guanylyl cyclase-D define a unique olfactory signal transduction pathway. *Proc. Natl. Acad. Sci. U.S.A.* 94: 3388–3395.

- Juiz, J.M., Helfert, R.H., Bonneau, J.M., Campos, M.L., and Altschuler, R.A. 1996. Distribution of glycine and GABA immunoreactivities in the cochlear nucleus: quantitative patterns of putative inhibitory inputs on three cell types. *J. Hirnforsch.* 37: 561–574.
- Jung, M.W., and Larson, J. 1994. Further characteristics of long-term potentiation in piriform cortex. *Synapse* 18: 298–306.
- Jung, M.W., Larson, J., and Lynch, G. 1990a. Long-term potentiation of monosynaptic EPSPs in rat piriform cortex *in vitro*. *Synapse* 6: 279–283.
- Jung, M.W., Larson, J., and Lynch, G. 1990b. Role of NMDA and non-NMDA receptors in synaptic transmission in rat piriform cortex. *Synapse* 82: 451–455.
- Kaas, J.H. 1978. The organization of visual cortex in primates. In: *Sensory Systems of Primates* (Noback, C.R., ed.) New York: Plenum Press, pp. 151–179.
- Kaas, J.H. 1990. How sensory cortex is subdivided in mammals: implications for studies of prefrontal cortex. *Progr. Brain Res.* 85: 3–11.
- Kaba, H., Hayashi, Y., Higuchi, T., and Nakanishi, S. 1994. Induction of an olfactory memory by the activation of a metabotropic glutamate receptor. *Science* 265: 262–264.
- Kaczmarek, L.K., and Levitan, I.B. 1987. *Neuromodulation: The Biochemical Control of Neuronal Excitability*. New York: Oxford University Press.
- Kafitz, K.W., and Greer, C.A. 1997. Role of laminin in axonal extension from olfactory receptor cells. *J. Neurobiol.* 32: 298–310.
- Kalil, R.E., and Chase, R. 1970. Corticofugal influence on activity of lateral geniculate neurons in the cat. *J. Neurophysiol.* 33: 459–474.
- Kamermans, M., Fahrenfort, I., Schultz, K., Janssen-Bienhold, U., Sjoerdsma, T., and Weiler, R. 2001. Hemichannel-mediated inhibition in the outer retina. *Science* 292: 1178–1180.
- Kan, K.S.K., Chao, L.P., and Eng, L.F. 1978. Immunohistochemical localization of choline acetyltransferase in rabbit spinal cord and cerebellum. *Brain Res.* 146: 221–229.
- Kan, K.S.K., Chao, L.P., and Forno, L.S. 1980. Immuno-histochemical localization of choline acetyltransferase in the human cerebellum. *Brain Res.* 193: 165–171.
- Kanda, K., Burke, R.E., and Walmsley, B. 1977. Differential control of fast and slow twitch motor units in the decerebrate cat. *Exp. Brain Res.* 29: 57–74.
- Kandel, E.R., Schwartz, J.H., and Jessell, T.M. 2000. *Principles of Neural Science*. New York: McGraw-Hill.
- Kandel, E.R., and Spencer, W.A. 1961a. Electrophysiology of hippocampal neurons. II. Afterpotentials and repetitive firing. *J. Neurophysiol.* 24: 243–259.
- Kandel, E.R., and Spencer, W.A. 1961b. Excitation and inhibition of single pyramidal cells during hippocampal seizure. *Exp. Neurol.* 4: 162–179.
- Kane, E.C. 1973. Octopus cells in the cochlear nucleus of the cat: heterotypic synapses upon homotypic neurons. *Int. J. Neurosci.* 5: 251–279.
- Kane, E.C. 1974. Synaptic organization in the dorsal cochlear nucleus of the cat: a light and electron microscopic study. *J. Comp. Neurol.* 155: 301–329.
- Kane, E.S., Puglisi, S.G., and Gordon, B.S. 1981. Neuronal types in the deep dorsal cochlear nucleus of the cat: I. Giant neurons. *J. Comp. Neurol.* 198: 483–513.
- Kaneda, M., Hashimoto, M., and Kaneko, A. 1995. Neuronal nicotinic acetylcholine receptors of ganglion cells in the cat retina. *Jpn. J. Physiol.* 45: 491–508.
- Kaneda, M., and Kaneko, A. 1991. Voltage-gated sodium currents in isolated retinal ganglion cells of the cat: relation between the inactivation kinetics and the cell type. *Neurosci. Res.* 11: 261–275.
- Kaneko, A. 1970. Physiological and morphological identification of horizontal, bipolar and amacrine cells in goldfish retina. *J. Physiol. (Lond.)* 207: 623–633.
- Kanold, P.O., and Manis, P.B. 1999. Transient potassium currents regulate the discharge patterns of dorsal cochlear nucleus pyramidal cells. *J. Neurosci.* 19: 2195–2208.
- Kanold, P.O., and Manis, P.B. 2001. A physiologically based model of discharge pattern regu-

- lation by transient K^+ currents in cochlear nucleus pyramidal cells. *J. Neurophysiol.* 85: 523–538.
- Kanold, P.O., and Young, E.D. 2001. Proprioceptive information from the pinna provides somatosensory input to cat dorsal cochlear nucleus. *J. Neurosci.* 21: 7848–7858.
- Kanter, E.D., and Haberly, L.B. 1990. NMDA-dependent induction of long-term potentiation in afferent and association fiber systems of piriform cortex in vitro. *Brain Res.* 525: 175–179.
- Kanter, E.D., and Haberly, L.B. 1993. Associative long-term potentiation in piriform cortex slices requires GABA_A blockade. *J. Neurosci.* 13: 2477–2482.
- Kanter, E.D., Kapur, A., and Haberly, L.B. 1996. A dendritic GABAA-mediated IPSP regulates facilitation of NMDA-mediated responses to burst stimulation of afferent fibers in piriform cortex. *J. Neurosci.* 16: 307–312.
- Kao, Y.-H., Lassová, L., Sterling, P., and Vardi, N. 2003. Evidence that two types of retinal bipolar cell use both glutamate and GABA. (Submitted).
- Kaplan, E., Lee, B.B., and Shapley, R.M. 1990. New views of primate retinal function. In: *Progress in Retinal Research* (Osborne, N., and Chader, J., eds.) Oxford: Pergamon, pp. 273–336.
- Kaplan, E., and Shapley, R.M. 1982. X and Y cells in the lateral geniculate nucleus of macaque monkeys. *J. Physiol. (Lond.)* 330: 125–143.
- Kapur, A., and Haberly, L.B. 1998. Duration of NMDA-dependent synaptic potentiation in piriform cortex in vivo is increased after epileptiform bursting. *J. Neurophysiol.* 80: 1623–1629.
- Kapur, A., Lytton, W.W., Ketchum, K.L., and Haberly, L.B. 1997a. Regulation of the NMDA component of EPSPs by different components of postsynaptic GABAergic inhibition: computer simulation analysis in piriform cortex. *J. Neurophysiol.* 78: 2546–2559.
- Kapur, A., Pearce, R.A., Lytton, W.W., and Haberly, L.B. 1997b. GABAA-mediated IPSCs in piriform cortex have fast and slow components with different properties and locations on pyramidal cells. *J. Neurophysiol.* 78: 2531–2545.
- Karlsson, G., Pozzo, M., and Olpe, H.-R. 1988. Phaclofen: a GABAB blocker reduces long-duration inhibition in the neocortex. *Eur. J. Pharmacol.* 148: 485–486.
- Kashiwadani, H., Sasaki, Y.F., Uchida, N., and Mori, K. 1999. Synchronized oscillatory discharges of mitral/tufted cells with different molecular receptive ranges in the rabbit olfactory bulb. *J. Neurophysiol.* 82: 1786–1792.
- Kasowski, H.J., Kim, H., and Greer, C.A. 1999. Compartmental organization of the olfactory bulb glomerulus. *J. Comp. Neurol.* 407: 261–274.
- Kato, N. 1990. Cortico-thalamo-cortical projection between visual cortices. *Brain Res.* 509: 150–152.
- Katona, I., Acsady, L., and Freund, T.F. 1999. Postsynaptic targets of somatostatin-immunoreactive interneurons in the rat hippocampus. *Neuroscience* 88: 37–55.
- Katz, B. 1966. *Nerve, Muscle, and Synapse*. New York: McGraw-Hill. McGraw-Hill Series in the New Biology.
- Katz, L.C. 1987. Local circuitry of identified projection neurons in cat primary visual cortex brain slices. *J. Neurosci.* 7: 1223–1249.
- Katz, L.C., and Crowley, J.C. 2002. Development of cortical circuits: lessons from ocular dominance columns. *Nat. Rev. Neurosci.* 3: 34–42.
- Katz, L.C., and Shatz, C.J. 1996. Synaptic activity and the construction of cortical circuits. *Science* 274: 1133–1138.
- Kauer, J.S. 1974. Response patterns of amphibian olfactory bulb neurones to odour stimulation. *J. Physiol. (Lond.)* 243: 695–715.
- Kauer, J.S., and Cinelli, A.R. 1993. Are there structural and functional modules in the vertebrate olfactory bulb? *Microsc. Res. Tech.* 24: 154–167.
- Kauer, J.S., and Moulton, D.G. 1974. Responses of olfactory bulb neurones to odour stimulation of small nasal areas in the salamander. *J. Physiol. (Lond.)* 243: 717–737.

- Kauer, J.S., Neff, S.R., Hamilston, K.A., and Cinelli, A.R. 1993. The salamander olfactory pathway: visualizing and modeling circuit activity. In: *Olfaction: A Model for Computational Neuroscience* (Eichenbaum, H., and Davis, J.L., eds.) Cambridge, MA: MIT Press, pp. 43–68.
- Kauer, J.S., and Shepherd, G.M. 1977. Analysis of the onset phase of olfactory bulb unit responses to odour pulses in the salamander. *J. Physiol. (Lond.)* 272: 495–516.
- Kaupmann, K., Huggel, K., Heid, J., Flor, P.J., Mickel, Bischoff, S., McMaster, G., Angst, C., Bittiger, H., Froestl, W., and Bettler, B. 1997. Expression cloning of GABAB receptors uncovers similarity to metabotropic glutamate receptors. *Nature* 386: 239–246.
- Kawaguchi, Y. 1992. Large aspiny cells in the matrix of the rat neostriatum in vitro—physiological identification, relation to the compartments and excitatory postsynaptic currents. *J. Neurophysiol.* 67: 1669–1682.
- Kawaguchi, Y. 1993. Groupings of nonpyramidal and pyramidal cells with specific physiological and morphological characteristics in layer II/III of rat frontal cortex. *J. Neurosci.* 69: 416–431.
- Kawaguchi, Y. 1995. Physiological subgroups of nonpyramidal cells with specific morphological characteristics in layer II/III of rat frontal cortex. *J. Neurosci.* 15: 2638–2655.
- Kawaguchi, Y., and Kubota, Y. 1993. Correlation of physiological subgroupings of nonpyramidal cells with parvalbumin- and calbindin d28k-immunoreactive neurons in layer V of rat frontal cortex. *J. Neurophysiol.* 70: 387–396.
- Kawaguchi, Y., Wilson, C.J., Augood, S.J., and Emson, P.C. 1995. Striatal interneurons—chemical, physiological and morphological characterization. *Trends Neurosci.* 18: 527–535.
- Kawaguchi, Y., Wilson, C.J., and Emson, P.C. 1989. Intracellular recording of identified neostriatal patch and matrix spiny cells in a slice preparation preserving cortical inputs. *J. Neurophysiol.* 62: 1052–1068.
- Kawaguchi, Y., Wilson, C.J., and Emson, P.C. 1990. Projection subtypes of rat neostriatal matrix cells revealed by intracellular injection of biocytin. *J. Neurosci.* 10: 3421–3438.
- Kawamura, H., and Provini, K. 1970. Depression of cerebellar Purkinje cells by microiontophoretic application of GABA and related amino acids. *Brain Res.* 24: 293–304.
- Kay, L.M., and Freeman, W.J. 1998. Bidirectional processing in the olfactory-limbic axis during olfactory behavior. *Behav. Neurosci.* 112: 541–553.
- Keller, A., Iriki, A., and Asanuma, H. 1990. Identification of neurons producing long-term potentiation in the cat motor cortex: intracellular recordings and labelling. *J. Comp. Neurol.* 300: 47–60.
- Kelso, S.R., Ganong, A.H., and Brown, T.H. 1986. Hebbian synapses in hippocampus. *Proc. Natl. Acad. Sci. U.S.A.* 83: 5326–5330.
- Kemp, J.A., and Sillito, A.M. 1982. The nature of the excitatory transmitter mediating X and Y cell inputs to the cat dorsal lateral geniculate nucleus. *J. Physiol. (Lond.)* 323: 377–391.
- Kemp, J.M., and Powell, T.P.S. 1971. The site of termination of afferent fibers in the caudate nucleus. *Philos. Trans. Soc. Lond. B* 262: 413–427.
- Kennedy, H., Meissirel, C., and Dehay, C. 1991. Callosal pathways and their compliancy to general rules governing the organization of cortical connectivity. In: *Vision and Visual Dysfunction, Vol. 3: Neuroanatomy of the Visual Pathways and Their Development* (Dreher, B., and Robinson, S., eds.) London: Macmillan, pp. 324–359.
- Kennedy, M.B. 1989. Regulation of neuronal function by calcium. *Trends Neurosci.* 12: 417–420.
- Kernell, D. 1965. The limits of firing frequency in cat lumbosacral motoneurons possessing different time course of afterhyperpolarization. *Acta Physiol. Scand.* 65: 87–100.
- Kernell, D. 1965a. The adaptation and the relation between discharge frequency and current strength of cat lumbosacral motoneurons stimulated by long-lasting injected currents. *Acta Physiol. Scand.* 65: 65–73.

- Kernell, D. 1965b. The limits of firing frequency in cat lumbosacral motoneurons possessing different time course of afterhyperpolarization. *Acta Physiol. Scand.* 65: 87–100.
- Kernell, D. 1992. Organized variability in the neuromuscular system: a survey of task-related adaptations. *Arch. Ital. Biol.* 130: 19–66.
- Kerr, D., Ong, J., Johnston, G., Abbenante, J., and Prager, R. 1988. 2-Hydroxy-saclofen: an improved antagonist at central and peripheral GABAB receptors. *Neurosci. Lett.* 92.
- Kerr, D., Ong, J., Prager, R., Gynther, B., and Curtis, D. 1987. Phaclophen: a peripheral and central baclophen antagonist. *Brain Res.* 405: 150–154.
- Kerr, J.N.D., and Wickens, J.R. 2001. Dopamine D-1/D-5 receptor activation is required for long-term potentiation in the rat neostriatum in vitro. *J. Neurophysiol.* 85: 117–124.
- Ketchum, K.L., and Haberly, L.B. 1991. Fast oscillations and dispersive propagation in olfactory cortex and other cortical areas: a functional hypothesis. In: *Olfaction. A Model System for Computational Neuroscience* (Davis, J.L., and Eichenbaum, H., eds.) Cambridge, MA: MIT Press, pp. 69–100.
- Ketchum, K.L., and Haberly, L.B. 1993a. Synaptic events that generate fast oscillations in piriform cortex. *J. Neurosci.* 13: 3980–3985.
- Ketchum, K.L., and Haberly, L.B. 1993b. Membrane currents evoked by afferent fiber stimulation in rat piriform cortex. I. Current source-density analysis. *J. Neurophysiol.* 69: 248–260.
- Ketchum, K.L., and Haberly, L.B. 1993c. Membrane currents evoked by afferent fiber stimulation in rat piriform cortex. II. Analysis with a system model. *J. Neurophysiol.* 69: 261–281.
- Keverne, E.B. 1995. Olfactory learning. *Curr. Opin. Neurobiol.* 5: 482–488.
- Kevetter, G.A., and Perachio, A.A. 1989. Projections from the sacculus to the cochlear nuclei in the Mongolian gerbil. *Brain Behav. Evol.* 34: 193–200.
- Key, B., and St. John, J. 2002. Axon navigation in the mammalian primary olfactory pathway: where to next? *Chem. Senses* 27: 245–260.
- Kiang, N.Y.S., Morest, D.K., Godfrey, D.A., Guinan, J.J., and Kane, E.C. 1973. Stimulus coding at caudal levels of the cat's auditory nervous system: I. Response characteristics of single units. In: *Basic Mechanisms in Hearing* (Møller, A.R., and Boston, P., eds.) New York: Academic, pp. 455–478.
- Kiang, N.Y.S., Rho, J.M., Northrop, C.C., Liberman, M.C., and Ryugo, D.K. 1982. Hair-cell innervation by spiral ganglion cells in adult cats. *Science* 217: 175–177.
- Kier, C.K., Buchsbaum, G., and Sterling, P. 1995. How retinal microcircuits scale for ganglion cells of different size. *J. Neurosci.* 15: 7673–7683.
- Kim, D.O., Ghoshal, S., Khant, S.L., and Parham, K. 1994. A computational model with ionic conductances for the fusiform cell of the dorsal cochlear nucleus. *J. Acoust. Soc. Am.* 96: 1501–1514.
- Kim, H., and Connors, B. 1993. Apical dendrites of the neocortex: Correlation between sodium- and calcium-dependent spiking and pyramidal cell morphology. *J. Neurosci.* 13: 5301–5311.
- Kim, H., and Greer, C.A. 2000. The emergence of compartmental organization in olfactory bulb glomeruli during postnatal development. *J. Comp. Neurol.* 422: 297–311.
- Kim, J., and Alger, B. E. 2001. Random response fluctuations lead to spurious paired-pulse facilitation. *J. Neurosci.* 21: 9608–9618.
- Kim, K.J., and Rieke, F. 2001. Temporal contrast adaptation in the input and output signals of salamander retinal ganglion cells. *J. Neurosci.* 21: 287–299.
- Kim, U., and McCormick, D.A. 1998. The functional influence of burst and tonic firing mode on synaptic interactions in the thalamus. *J. Neurosci.* 18: 9500–9516.
- Kim, U., Sanchez-Vives, M.V., and McCormick, D.A. 1997. Functional dynamics of GABAergic inhibition in the thalamus. *Science* 278: 130–133.
- Kimura, F., Tsunoto, T., Nishigori, A., and Yoshimura, Y. 1990. Long-term depression but not potentiation is induced in Ca²⁺-chelated visual cortex neurons. *Neurosci. Rep.* 1: 65–68.

- Kimura, M. 1990. Behaviorally contingent property of movement-related activity of the primate putamen. *J. Neurophysiol.* 63: 1277–1296.
- Kincaid, A.E., Zheng, T., and Wilson, C.J. 1998. Connectivity and convergence of single corticostriatal axons. *J. Neurosci.* 18: 4722–4731.
- Kingston, P.A., Zufall, F., and Barnstable, C.J. 1996. Widespread expression of olfactory cyclic nucleotide-gated channel genes in rat brain: implications for neuronal signalling. *Synapse* 32: 1–12.
- Kirkwood, A., Dudek, S., Gold, J., Aisenman, C., and Bear, M. 1993. Common forms of synaptic plasticity in hippocampus and neocortex *in vitro*. *Science* 260: 1518–1521.
- Kirkwood, A., Lee, H.-K., and Bear, M. 1995. Co-regulation of long-term potentiation and experience-dependent synaptic plasticity in visual cortex by age and experience. *Nature* 375: 328–331.
- Kirkwood, A., Riutt, M., and Bear, M. 1996. Experience-dependent modification of synaptic plasticity in visual cortex. *Nature* 381: 526–528.
- Kirkwood, P., Ford, T., Donga, R., Saywell, S., and Holstege, G. 1999. Assessing the strengths of motoneuron inputs: different anatomical and physiological approaches compared. In: *Peripheral and Spinal Mechanisms on the Neural Control of Movement* (Binder, M., ed.) Amsterdam: Elsevier, pp. 67–82.
- Kishi, K. 1987. Golgi studies on the development of granule cells of the rat olfactory bulb with reference to migration in the subependymal layer. *J. Comp. Neurol.* 258: 112–124.
- Kishi, K., Mori, K., and Ojima, H. 1984. Distribution of local axon collaterals of mitral, displaced mitral and tufted cells in the rabbit olfactory bulb. *J. Comp. Neurol.* 225: 511–526.
- Kishi, K., Stanfield, B.B., and Cowan, W.M. 1980. A quantitative EM autoradiographic study of the commissural and associational connections of the dentate gyrus in the rat. *Anat. Embryol.* 160: 173–186.
- Kisvárdy, Z. 1992. GABAergic networks of basket cells in the visual cortex. *Prog. Brain Res.* 90: 385–405.
- Kisvárdy, Z., Martin, K.A.C., Friedlander, M., and Somogyi, P. 1987. Evidence for interlaminar inhibitory circuits in the striate cortex of the cat. *J. Comp. Neurol.* 260: 1–19.
- Kisvárdy, Z., Martin, K.A.C., Whitteridge, D., and Somogyi, P. 1985. Synaptic connections of intracellularly filled clutch neurons, a type of small basket neuron in the visual cortex of the cat. *J. Comp. Neurol.* 241: 111–137.
- Kita, H. 1993. GABAergic circuits of the striatum. In: *Chemical Signalling in the Basal Ganglia* (G.W. Arbuthnott and P.C. Emson, eds.). *Prog. Brain Res.* 99: 51–72.
- Kita, H. 1996. Glutamatergic and GABAergic postsynaptic responses of striatal spiny neurons to intrastriatal and cortical stimulation recorded in slice preparations. *Neuroscience* 70: 925–940.
- Kita, T., Kita, H., and Kitai, S.T. 1984. Passive electrical membrane properties of rat neostriatal neurons in an *in vitro* slice preparation. *Brain Res.* 300: 129–139.
- Kita, H., and Kitai, S.T. 1987. Efferent projections of the subthalamic nucleus in the rat—light and electron microscopic analysis with the PHA-L method. *J. Comp. Neurol.* 260: 435–452.
- Kita, H., and Kitai, S.T. 1988. Glutamate decarboxylase immunoreactive neurons in rat neostriatum: their morphological types and populations. *Brain Res.* 447: 346–352.
- Kita, H., Kosaka, T., and Heizmann, C.W. 1990. Parvalbumin-immunoreactive neurons in the rat neostriatum: a light and electron microscopic study. *Brain Res.* 536: 1–15.
- Kitai, S.T. 1981. Electrophysiology of the corpus striatum and brain stem integrating systems. In: *Section 1: The Nervous System, Vol. II: Motor Control, Part I: Handbook of Physiology* (Brooks, V.B., ed.) Bethesda: American Physiological Society, pp. 997–1015.
- Kitai, S.T., Kocsis, J.D., Preston, R.J., and Sugimori, M. 1976a. Monosynaptic inputs to caudate

- neurons identified by intracellular injection of horseradish peroxidase. *Brain Res.* 109: 601–606.
- Kitai, S.T., Sugimori, M., and Kocsis, J.D. 1976b. Excitatory nature of dopamine in the nigro-caudate pathway. *Exp. Brain Res.* 24: 351–363.
- Kleinfeld, D. 1986. Sequential state generation by model neural networks. *Proc. Natl. Acad. Sci. U.S.A.* 83: 9469–9473.
- Klenoff, J.R., and Greer, C.A. 1998. Postnatal development of olfactory receptor cell axonal arbors. *J. Comp. Neurol.* 390: 256–267.
- Klug, K., Herr, S., Esfahani, P., and Schein, S. 1997. Distribution of different cell types in a small region of the macaque fovea.
- Knierim, J.J., and Van Essen, D.C. 1992. Visual cortex cartography, connectivity, and concurrent processing. *Curr. Opin. Neurobiol.* 2: 150–155.
- Koch, C. 1985. Understanding the intrinsic circuitry of the cat's LGN electrical properties of the spine-triad arrangement. *Proc. R. Soc. Lond. B* 225: 365–390.
- Koch, C. 1987. The action of the corticofugal pathway on sensory thalamic nuclei: a hypothesis. *Neuroscience* 23: 399–406.
- Koch, C. 1997. Computation and the single neuron. *Nature* 385: 207–210.
- Koch, C. 1999. *Biophysics of Computation*. Oxford University Press, New York.
- Koch, C., and Poggio, T. 1983. A theoretical analysis of electrical properties of spines. *Proc. R. Soc. Lond. B Biol. Sci.* 218: 455–477.
- Koch, C., and Poggio, T. 1987. *Biophysics of computation: Neurons, synapses and membranes*. In: *Synaptic Function* (Gall, W.E., and Cowan, W.M., eds.) New York: John Wiley, pp. 637–697.
- Koch, C., Poggio, T., and Torre, V. 1982. Retinal ganglion cells: a functional interpretation of dendritic morphology. *Phil. Trans. R. Soc. Lond. B* 298: 227–264.
- Koch, C., Poggio, T., and Torre, V. 1983. Nonlinear interactions in a dendritic tree: Localization, timing, and role of information processing. *Proc. Natl. Acad. Sci. U.S.A.* 80: 2799–802.
- Koch, C., and Zador, A. 1993. The function of dendritic spines: devices subserving biochemical rather than electrical compartmentalization. *J. Neurosci.* 13: 413–422.
- Kocsis, J.D., Sugimori, M., and Kitai, S.T. 1976. Convergence of excitatory synaptic inputs to caudate spiny neurons. *Brain Res.* 124: 403–413.
- Koerber, H.R., Druzinsky, R.E., and Mendell, L.M. 1988. Properties of somata of spinal dorsal root ganglion cells differ according to peripheral receptor innervated. *J. Neurophysiol.* 60: 1584–1596.
- Kohler, C. 1985. A projection from the deep layers of the entorhinal area to the hippocampal formation in the rat brain. *Neurosci. Lett.* 56: 13–19.
- Kohler, C., Chan-Palay, V., and Wu, J.Y. 1984. Septal neurons containing glutamic acid decarboxylase immuno-reactivity project to the hippocampal region in the rat brain. *Anat. Embryol.* 169: 41–44.
- Kohler, C., and Steinbusch, H. 1982. Identification of serotonin and non-serotonin-containing neurons of the mid-brain raphe projecting to the entorhinal area and the hippocampal formation. A combined immunohistochemical and fluorescent retrograde tracing. *Neuroscience* 7: 951–975.
- Kohler, C., Swanson, L.W., Haglund, L., and Wu, Y.Y. 1985. The cytoarchitecture, histochemistry, and projections of the tuberomammillary nucleus in the rat. *Neuroscience* 16: 85–110.
- Kohonen, T. 1978. *Associative Memory*. Berlin: Springer-Verlag.
- Kohonen, T., Lehtio, P., Hyvarinen, J., Bry, K., and Vainio, L. 1977. A principal of neural associative memory. *Neuroscience* 2: 1065–1076.
- Kolb, H. 1970. Organization of the outer plexiform layer of the primate retina: electron microscopy of Golgi-impregnated cells. *Phil. Trans. Roy. Soc. Lond. B* 258: 261–283.

- Kolb, H. 1974. The connections between horizontal cells and photoreceptors in the retina of the cat: electron microscopy of golgi preparations. *J. Comp. Neurol.* 155: 1–14.
- Kolb, H. 1977. The organization of the outer plexiform layer in the retina of the cat: electron microscopic observations. *J. Neurocytol.* 6: 131–153.
- Kolb, H. 1994. The architecture of functional neural circuits in the vertebrate retina. *Invest. Ophthalmol. Vis. Sci.* 35: 2385–2404.
- Kolb, H., and Dekorver, L. 1991. Midget ganglion cells of the parafovea of the human retina: a study by electron microscopy and serial section reconstructions. *J. Comp. Neurol.* 303: 617–636.
- Kolb, H., and Famiglietti, E.V. 1974. Rod and cone pathways in the inner plexiform layer of cat retina. *Science* 186: 47–49.
- Kolb, H., and Nelson, R. 1993. OFF-alpha and OFF-beta ganglion cells in cat retina: II. Neural circuitry as revealed by electron microscopy of HRP stains. *J. Comp. Neurol.* 329: 85–110.
- Kolb, H., and West, R.W. 1977. Synaptic connections of the interplexiform cell in the retina of the cat. *J. Neurocytol.* 6: 155–170.
- Kolb, H., Nelson, R., and Mariani, A. 1981. Amacrine cells, bipolar cells and ganglion cells of the cat retina: a Golgi study. *Vision Res.* 21: 1081–1114.
- Kölliker, A. 1896. *Handbuch der Gewebelehre des Menschen. Nervensystemen des Menschen und der Thiere.* Leipzig: Engelmann.
- Kolston, J., Osen, K.K., Hackney, C.M., Ottersen, O.P., and Storm-Mathisen, J. 1992. An atlas of glycine- and GABA-like immunoreactivity and colocalization in the cochlear nuclear complex of the guinea pig. *Anat. Embryol.* 186: 443–465.
- Komatsu, Y., and Iwakiri, M. 1993. Long-term modification of inhibitory synaptic transmission in developing visual cortex. *Neurosci. Rep.* 7: 907–910.
- Komatsu, Y., Toyama, K., Maeda, J., and Sakaguchi, H. 1981. Long-term potentiation investigated in a slice preparation of striate cortex of young kittens. *Neurosci. Lett.* 26: 269–274.
- Koós, T., and Tepper, J.M. 1999. Inhibitory control of neostriatal projection neurons by GABAergic interneurons. *Nature Neurosci.* 2: 467–472.
- Koós T., and Tepper, J.M. 2002. Dual cholinergic control of fast-spiking interneurons in the neostriatum. *J. Neurosci.* 22: 529–535.
- Kopp-Scheinpflug, C., Lippe, W.R., Dörrscheidt, G.J., and Rübsamen, R. 2002. The medial nucleus of the trapezoid body in the gerbil is more than a relay: comparison of pre- and post-synaptic activity. *J. Assoc. Res. Otolaryngol.* 4: 1–23.
- Korn, H., and Faber, D.S. 1987. Regulation and significance of probabilistic release mechanisms at central synapses. In: *Synaptic Functions* (Edelman, G.M., Gall, W.E., and Cowan, W.M., eds.) New York: John Wiley, pp. 57–108.
- Korn, H., and Faber, D.S. 1991. Quantal analysis and synaptic efficacy in the CNS. *Trends Neurosci.* 14: 439–445.
- Kosaka, T. 1983. Axon initial segments of the granule cell in the rat dentate gyrus: synaptic contacts on bundles of axon initial segments. *Brain Res.* 274: 129–134.
- Kosaka, K., Aika, Y., Toida, K., and Kosaka, T. 2001. Structure of intraglomerular dendritic tufts of mitral cells and their contacts with olfactory nerve terminals and calbindin-immunoreactive type 2 periglomerular neurons. *J. Comp. Neurol.* 440: 219–235.
- Kosaka, T., Hama, K., and Wu, J.Y. 1984. GABAergic synaptic boutons in the granule cell layer of rat dentate gyrus. *Brain Res.* 293: 353–359.
- Kosaka, T., Tauchi, M., and Dahl, J.L. 1988. Cholinergic neurons containing GABA-like and/or glutamic acid decarboxylase-like immunoreactivities in various brain regions of the rat. *Exp. Brain Res.* 70: 605–617.
- Kosaka, K., Toida, K., Aika, Y., and Kosaka T. 1998. How simple is the organization of the olfactory glomerulus? The heterogeneity of so-called periglomerular cells. *Neurosci. Res.* 30: 101–110.

- Kosel, K.C., Van Hoesen, G. W., and Rosene, D. L. (1983) A direct projection from the perirhinal cortex (area 35) to the subiculum in the rat. *Brain Res.* 269: 347–351.
- Koulen, P. 1999. Postnatal development of GABAA receptor beta 1, beta 2/3, and gamma2 immunoreactivity in the rat retina. *J. Neurosci. Res.* 57: 185–194.
- Koulen, P., Sassoè-Pognetto, M., Grünert, U., and Wässle, H. 1996. Selective clustering of GABAA and glycine receptors in the mammalian retina. *J. Neurosci.* 16: 2127–2140.
- Kouyama, N., and Marshak, D.W. 1992. Bipolar cells specific for blue cones in the Macaque retina. *J. Neurosci.* 12: 1233–1252.
- Kraushaar, U., and Jonas, P. 2000. Efficacy and stability of quantal GABA release at a hippocampal interneuron-principal neuron synapse. *J. Neurosci.* 20: 5594–5607.
- Krettek, J.E., and Price, J.L. 1977a. Projections from the amygdaloid complex to the cerebral cortex and thalamus in the rat and cat. *J. Comp. Neurol.* 172: 687–722.
- Krettek, J.E., and Price, J.L. 1977b. Projections from the amygdaloid complex and adjacent olfactory structures to the entorhinal cortex and to the subiculum in the rat and cat. *J. Comp. Neurol.* 172: 723–752.
- Krettek, J.E., and Price, J.L. 1978. A description of the amygdaloid complex in the rat and cat, with observations on intra-amygdaloid axonal connections. *J. Comp. Neurol.* 178: 255–280.
- Kriegstein, A.R., and Connors, B.W. 1986. Cellular physiology of the turtle visual cortex: synaptic properties and intrinsic circuitry. *J. Neurosci.* 6: 178–191.
- Krnjevic, K. 1981. Transmitters in motor systems. In: *Handbook of Physiology, Section I: The Nervous System, Vol. II: Motor Control, Part 1* (Brooks, V.B., ed.) Bethesda: American Physiological Society, pp. 107–154.
- Krnjevic, K., and Phillis, J.W. 1963. Acetylcholine sensitive cells in the cerebellar cortex. *J. Physiol. (Lond.)* 166: 296–327.
- Krnjevic, K., Pumain, R., and Renaud, L. 1971. The mechanism of excitation by acetylcholine in the cerebral cortex. *J. Physiol. (Lond.)* 215: 247–268.
- Krnjevic, K., and Schwartz, S. 1967. The action of gamma-aminobutyric acid on cortical neurones. *Exp. Brain Res.* 3: 320–336.
- Kröllner, J., and Grüsser, O.-J. 1983. Convergence of muscle spindle afferents on single neurons of the cat dorsal spino-cerebellar tract and their synaptic efficacy. *Brain Res.* 253: 65–80.
- Kros, C.J. 1996. Physiology of mammalian cochlear hair cells. In: *The Cochlea* (Dallos, P., Popper, A.N., and Fay, R.R., eds.) New York: Springer, pp. 318–385.
- Kubek, M.J., Knoblach, S.M., Sharif, N.A., Burt, D.R., Buterbaugh, G.G., and Fuson, K.S. 1993. Thyrotropin-releasing hormone gene expression and receptors are differentially modified in limbic foci by seizures. *Ann. Neurol.* 33: 70–76.
- Kubota, Y., and Jones, E.G. 1992. Co-localization of two calcium binding proteins in GABA cells of rat piriform cortex. *Brain Res.* 600: 339–344.
- Kubota, Y., and Kawaguchi, Y. 2000. Dependence of GABAergic synaptic areas on the interneuron type and target size. *J. Neurosci.* 20: 375–386.
- Kubota, Y., Mikawa, S., and Mikawa, S. 1993. Neostriatal GABAergic interneurons contain NOS, calretinin or parvalbumin. *NeuroReport* 5: 205–208.
- Kuffler, S.W. 1953. Discharge patterns and functional organization of mammalian retina. *J. Neurophysiol.* 16: 37–68.
- Kuhse, J., Becker, C.M., Schmieden, V., Hoch, W., Pribilla, I., Langosch, D., Malosio, M.L., Muntz, M., and Betz, H. 1991. Heterogeneity of the inhibitory glycine receptor. *Ann. N.Y. Acad. Sci.* 625: 129–135.
- Kuhse, J., Betz, H., and Kirsch, J. 1995. The inhibitory glycine receptor: architecture, synaptic localization and molecular pathology of a postsynaptic ion-channel complex. *Curr. Opin. Neurobiol.* 5: 318–323.

- Kullmann, D.M., and Asztely, F. 1998. Extrasynaptic glutamate spillover in the hippocampus: evidence and implications. *Trends Neurosci.* 21: 8–14.
- Kuno, M. 1964. Quantal components of excitatory synaptic potentials in spinal motoneurons. *J. Physiol. (Lond.)* 175: 81–99.
- Kunzle, H. 1976. Thalamic projections from the precentral motor cortex in *Macaca fascicularis*. *Brain Res.* 105: 253–267.
- Kwon, Y.H., Esguerra, M., and Sur, M. 1991. NMDA and non-NMDA receptors mediate visual responses of neurons in the cat's lateral geniculate nucleus. *J. Neurophysiol.* 66: 414–428.
- Laatsch, R.H., and Cowan, W.M. 1967. Electron microscopic studies of the dentate gyrus of the rat. II. Degeneration of commissural afferents. *J. Comp. Neurol.* 130: 241–262.
- Lacy, M.C., Mercuri, N.B., and North, R.A. 1987. Dopamine acts on D2 receptors to increase potassium conductance in neurons of the rat substantia nigra zona compacta. *J. Physiol. (Lond.)* 392: 397–416.
- Lagerbäck, P., and Kellerth, J.-O. 1985. Light microscopic observations on cat Renshaw cells after intracellular staining with horseradish peroxidase. I. The axonal system. *J. Comp. Neurol.* 240: 359–367.
- Lai, Y.C., Winslow, R.L., and Sachs, M.B. 1994. A model of selective processing of auditory-nerve inputs by stellate cells of the antero-ventral cochlear nucleus. *J. Comp. Neurosci.* 1: 167–194.
- Lal, R., and Friedlander, M.J. 1989. Gating of retinal transmission by afferent eye position and movement signals. *Science* 243: 93–96.
- Lamb, T.D., and Pugh, E.N.J. 1992. G-protein cascades: gain and kinetics. *Trends Neurosci.* 15: 291–298.
- Lamb, T.D., and Simon, E.J. 1976. The relation between intercellular coupling and electrical noise in turtle photoreceptors. *J. Physiol. (Lond.)*. 263: 257–286.
- Lambert, N., Borroni, A., Grover, L., and Teyler, T. 1991. Hyperpolarizing and depolarizing GABAA receptor mediated dendritic inhibition in area CA1 of the rat hippocampus. *J. Neurophysiol.* 66: 1538–1548.
- Lambert, N.A., and Wilson, W.A. 1994. Temporally distinct mechanisms of use-dependent depression at inhibitory synapses in the rat hippocampus in vitro. *J. Neurophysiol.* 72: 121–130.
- Lancaster, B., and Adams, P.R. 1986. Calcium-dependent current generating the afterhyperpolarization of hippocampal neurons. *J. Neurophysiol.* 55: 1268–1282.
- Lancet, D., Greer, C.A., Kauer, J.S., and Shepherd, G.M. 1982. Mapping of odor-related neuronal activity in the olfactory bulb by high-resolution 2-deoxyglucose autoradiography. *Proc. Natl. Acad. Sci. U.S.A.* 79: 670–674.
- Land, E. 1959a. Color vision and the natural image. Part I. *Proc. Natl. Acad. Sci. U.S.A.* 45: 115–129.
- Land, E. 1959b. Color vision and the natural image. Part II. *Proc. Natl. Acad. Sci. U.S.A.* 46: 636–644.
- Land, E. 1983. Recent advances in retinex theory and some implications for cortical computations: color vision and the natural image. *Proc. Natl. Acad. Sci. U.S.A.* 80: 5163–5169.
- Land, L.J., and Shepherd, G.M. 1974. Autoradiographic analysis of olfactory receptor projections in the rabbit. *Brain Res.* 70: 506–10.
- Land, L.J., Eager, R.P., and Shepherd, G.M. 1970. Olfactory nerve projections to the olfactory bulb in rabbit: demonstration by means of a simplified ammoniacal silver degeneration method. *Brain Res.* 23: 250–254.
- Landis, D.M.D., and Reese, T.S. 1983. Cytoplasmic organization in cerebellar dendritic spines. *J. Cell. Biol.* 97: 1169–1178.
- Landisman, C.E., Long, M.A., Beierlein, M., Deans, M.R., Paul, D.L., and Connors, B.W. 2002. Electrical synapses in the thalamic reticular nucleus. *J. Neurosci.* 22: 1002–1009.

- Landmesser, L. 1978. The distribution of motoneurons supplying chick hind limb muscles. *J. Physiol. (Lond.)* 264: 371–389.
- Lang, E.J. 2001. Organization of olivocerebellar activity in the absence of excitatory glutamatergic input. *J. Neurosci.* 21: 1663–1675.
- Lang, E.J. 2002. GABAergic and glutamatergic modulation of spontaneous and motor-cortex-evoked complex spike activity. *J. Neurophysiol.* 87: 1993–2008.
- Lang, E.J., Sugihara I., and Llinás R. 1996. GABAergic modulation of complex spike activity by the cerebellar nucleoolivary pathway in rat. *J. Neurophysiol.* 76: 255–275.
- Langer, L.F., and Graybiel, A.M. 1989. Distinct nigrostriatal projection systems innervate striosomes and matrix in the primate striatum. *Brain Res.* 498: 344–350.
- Langmoen, I.A., and Andersen, P. 1981. The hippocampal slice in vitro. A description of the technique and some examples of the opportunities it offers. In: *Electrophysiology of Isolated Mammalian CNS Preparations* (Kerkut, G.A., and Wheal, H.V., eds.) London: Academic Press, pp. 51–105.
- Langner, G. 1992. Periodicity coding in the auditory system. *Hear. Res.* 60: 115–142.
- Lankheet, M.J.M., Rowe, M.H., van Wezel, R.J.A., and van de Grind, W.A. 1996. Horizontal cell sensitivity in the cat retina during prolonged dark adaptation. *Vis. Neurosci.* 13: 885–896.
- Lapper, S.R., and Bolam, J.P. 1992. Input from the frontal cortex and the parafascicular nucleus to cholinergic interneurons in the dorsal striatum of the rat. *Neuroscience* 51: 533–545.
- Larkum, M., and Zhu, J. 2002. Signaling of layer 1 and whisker-evoked Ca^{++} and Na^{+} action potentials in distal and terminal dendrites of rat neocortical pyramidal neurons in vitro and in vivo. *J. Neurosci.* 22: 6991–7005.
- Larkum, M.E., Kaiser, K.M., and Sakmann, B. 1999. Calcium electrogenesis in distal apical dendrites of layer 5 pyramidal cells at a critical frequency of back-propagating action potentials. *Proc. Natl. Acad. Sci. U.S.A.* 96: 14600–14604.
- Larkum, M.E., Rioult, M.G., and Lüscher, H.-R. 1996. Propagation of action potentials in the dendrites of neurons from rat spinal cord slice cultures. *J. Neurophysiol.* 75:
- Läuger, P. 1991. *Electrogenic Ion Pumps*. Sunderland, MA: Sinauer.
- Laughlin, S.B. 1994. Matching coding, circuits, cells, and molecules to signals: general principles of retinal design in the fly's eye. *Prog. Retina Eye Res.* 13: 165–196.
- Laughlin, S.B., Howard, J., and Blakeslee, B. 1987. Synaptic limitations to contrast coding in the retina of the blowfly *Calliphora*. *Proc. R. Soc. Lond. B* 231: 437–467.
- Laurberg, S., and Sorensen, K.E. 1981. Associational and commissural collaterals of neurons in the hippocampal formation (hilus fasciae dentate and subfield CA3). *Brain Res.* 212: 287–300.
- Laurent, G., Stopfer, M., Friedrich, R.W., Rabinovich, M.I., Volkovskii, A., and Abarbanel, H.D. 2001. Odor encoding as an active, dynamical process: experiments, computation, and theory. *Annu. Rev. Neurosci.* 24: 263–97.
- Laurent, G., Wehr, M., and Davidowitz, H. 1996. Temporal representations of odors in an olfactory network. *J. Neurosci.* 16: 3837–3847.
- Lawrence, D.G., Porter, R., and Redman, S.J. 1985. Corticomotoneuronal synapses in the monkey: light microscopic localization upon motoneurons of intrinsic muscles of the hand. *J. Comp. Neurol.* 232: 499–510.
- Le Masson, G., Renaud-Le Masson, S., Debay, D., and Bal, T. 2002. Feedback inhibition controls spike transfer in hybrid thalamic circuits. *Nature* 417: 854–858.
- Lebel, D., Grossman, Y., and Barkai, E. 2001. Olfactory learning modifies predisposition for long-term potentiation and long-term depression induction in the rat piriform (olfactory) cortex. *Cereb. Cortex* 11: 485–489.
- LeDoux, J.E., Ruggiero, D.A., and Reis, D.J. 1985. Projections to the subcortical forebrain from

- anatomically defined regions of the medial geniculate body in the rat. *J. Comp. Neurol.* 242: 182–213.
- Lee, B.B., Pokorny, J., Smith, V.C., Martin, P.R., and Valberg, A. 1990. Luminance and chromatic modulation sensitivity of macaque ganglion cells and human observers. *J. Opt. Soc. Am. A* 7: 2223–2236.
- Lee, K.H., and McCormick, D.A. 1995. Acetylcholine excites GABAergic neurons of the ferret perigeniculate nucleus through nicotinic receptors. *J. Neurophysiol.* 73: 2123–2127.
- Lee, R., and Heckman, C. 1998. Bistability in spinal motoneurons *in vivo*: systematic variations in rhythmic firing patterns. *J. Neurophysiol.* 80: 572–582.
- Lee, R., and Heckman, C. 2000. Adjustable amplification of synaptic input in the dendrites of spinal motoneurons *in vivo*. *J. Neurosci.* 20: 6734–6740.
- Leeper, H.F., and Charlton, J.S. 1985. Response properties of horizontal cells and photoreceptor cells in the retina of the tree squirrel, *Sciurus carolinensis*. *J. Neurophysiol.* 54: 1157–1166.
- Lehky, S., and Sejnowski, T. 1988. Network model of shape from shading: neural function arises from both receptive and projective fields. *Nature* 333: 452–454.
- Lenn, N.J., and Reese, T.S. 1966. The fine structure of nerve endings in the nucleus of the trapezoid body and the ventral cochlear nucleus. *Am. J. Anat.* 118: 375–390.
- Lennie, P. 1980. Perceptual signs of parallel pathways. *Phil. Trans. R. Soc. Lond. B* 290: 23–37.
- Leskov, I.B., Klenchin, V.A., Handy, J.W., Whitlock, G.G., Govardovskii, V.I., Bownds, M.D., Lamb, T.D., Pugh Jr., E.N., and Arshavsky, V.Y. 2000. The gain of rod phototransduction: reconciliation of biochemical and electrophysiological measurements. *Neuron* 27: 525–537.
- LeVay, S. 1973. Synaptic patterns in the visual cortex of the cat and monkey. Electron microscopy of Golgi preparations. *J. Comp. Neurol.* 150: 53–86.
- LeVay, S., and Gilbert, C. 1976. Laminar patterns of geniculocortical projection in the cat. *Brain Res.* 113: 1–19.
- LeVay, S., and Sherk, H. 1981. The visual claustrum of the cat. *J. Neurosci.* 1: 956–980.
- Leventhal, A.G., Rodieck, R.W., and Dreher, B. 1985. Central projections of cat retinal ganglion cells. *J. Comp. Neurol.* 237: 216–226.
- Leveteau, J., and MacLeod, P. 1966. Olfactory discrimination in the rabbit olfactory glomerulus. *Science* 175: 170–178.
- Levey, A.I., Hallanger, A.E., and Wainer, B.H. 1987. Choline acetyltransferase immunoreactivity in the rat thalamus. *J. Comp. Neurol.* 257: 317–332.
- Levine, M.S., Cepeda, C., Day, M., Altemus, K.L., and Li, Z. 1995. Dopaminergic modulation of responses evoked by activation of excitatory amino acid receptors in the neostriatum is dependent upon specific receptor subtypes. In: *Molecular and Cellular Mechanisms of Neostriatal Function* (Ariano, M.A., and Surmeier, D.J., eds.) Austin: R.G. Landes, pp. 217–228.
- Lev-Tov, A., Fleshman, J.W., and Burke, R.E. 1983a. Primary afferent depolarization and presynaptic inhibition of monosynaptic group Ia EPSPs during post-tetanic potentiation. *J. Neurophysiol.* 50: 413–427.
- Lev-Tov, A., Meyers, D.E.R., and Burke, R.E. 1988. Activation of type B γ -amino-butyric acid receptors in the intact mammalian spinal cord mimics the effects of reduced presynaptic Ca^{2+} influx. *Proc. Nat. Acad. Sci. U.S.A.* 85: 5330–5334.
- Lev-Tov, A., Pinter, M.J., and Burke, R.E. 1983b. Post-tetanic potentiation of group Ia EPSPs: possible mechanisms for differential distribution in the MG motor nucleus. *J. Neurophysiol.* 50: 379–398.
- Levy, W.B., and Steward, O. 1979. Synapses as associative memory elements in the hippocampal formation. *Brain Res.* 175: 233–245.
- Leznik E., Makarenko V., and Llinás R. 2002. Electrotonically mediated oscillatory patterns in neuronal ensembles: an *in vitro* voltage-dependent dye-imaging study in the inferior olive. *J. Neurosci.* 22: 2804–2815.

- Li, C.-L., Ortiz, A., Galvin, Chon, S., and Howard, S. 1960. Cortical intracellular potentials in response to stimulation of lateral geniculate body. *J. Neurophysiol.* 29: 367–381.
- Li, W., Zhang, J., and Massey, S.C. 2002. Coupling pattern of S1 and S2 amacrine cells in the rabbit retina. *Vis. Neurosci.* 19: 119–131.
- Li, X.-G., Somogyi, P., Ylinen, A., and Buzsaki, G. 1994. The hippocampal CA3 network: an *in vivo* intracellular labeling study. *J. Comp. Neurol.* 339: 181–208.
- Li, Y., and Burke, R. 2001. Short-term synaptic depression in the neonatal mouse spinal cord: effects of calcium and temperature. *J. Neurophysiol.* 85: 2047–2062.
- Liang, Y., Yuan, L. L., Johnston, D., and Gray, R. 2002. Calcium signaling at single mossy fiber presynaptic terminals in the rat hippocampus. *J. Neurophysiol.* 87: 1132–1137.
- Liao, D., Hessler, N., and Malinow, R. 1995. Activation of postsynaptically silent synapses during pairing-induced LTP in CA1 region of hippocampal slice. *Nature* 375: 400–404.
- Lieberman, M.C. 1982. The cochlear frequency map for the cat: labelling auditory-nerve fibers of known characteristic frequency. *J. Acoust. Soc. Am.* 72: 1441–1449.
- Lieberman, M.C. 1991. Central projections of auditory-nerve fibers of differing spontaneous rate. I: anteroventral cochlear nucleus. *J. Comp. Neurol.* 313: 240–258.
- Lieberman, M.C. 1993. Central projections of auditory nerve fibers of differing spontaneous rate. II: posteroventral and dorsal cochlear nuclei. *J. Comp. Neurol.* 327: 17–36.
- Libri, V., Constanti, A., Calaminici, M., and Nistico, G. 1994. A comparison of the muscarinic response and morphological properties of identified cells in the guinea-pig olfactory cortex *in vitro*. *Neuroscience* 59: 331–347.
- Libri, V., Constanti, A., Zibetti, M., and Postlethwaite, M. 1997. Metabotropic glutamate receptor subtypes mediating slow inward tail current (I_{ADP}) induction and inhibition of synaptic transmission in olfactory cortical neurones. *Br. J. Pharmacol.* 12: 1083–1095.
- Liddell, E.G.T., and Sherrington, C.S. 1925. Recruitment and some other factors of reflex inhibition. *Proc. R. Soc. Lond. B Biol. Sci.* 97: 488–518.
- Liesi, P. 1985. Laminin-immunoreactive glia distinguish regenerative adult CNS systems from non-regenerative ones. *EMBO J.* 4: 2505–2511.
- Lim, R., Alvarez, F.J., and Walmsley, B. 2000. GABA mediates presynaptic inhibition at glycinergic synapses in a rat auditory brainstem nucleus. *J. Physiol. (Lond.)* 525: 447–459.
- Lin, D.M., Wang, F., Lowe, G., Gold, G.H., Axel, R., Ngai, J., and Brunet, L. 2000. Formation of precise connections in the olfactory bulb occurs in the absence of odorant-evoked neuronal activity. *Neuron* 26: 69–80.
- Linberg, K.A., and Fisher, S.K. 1988. Ultrastructural evidence that horizontal cell axon terminals are presynaptic in the human retina. *J. Comp. Neurol.* 268: 281–297.
- Linden, D.J. 1994. Long-term synaptic depression in the mammalian brain. *Neuron* 12: 457–472.
- Linden, D.J., and Connor, J.A. 1991. Participation of postsynaptic PKC in cerebellar long-term depression in culture. *Science* 254: 1656–1659.
- Linden, D.J., and Connor, J.A. 1993. Cellular mechanisms of long-term depression in the cerebellum. *Curr. Opin. Neurobiol.* 3: 401–406.
- Linden, D.J., and Connor, J.A. 1995. Long-term synaptic depression. *Annu. Rev. Neurosci.* 18: 319–57.
- Linden, D.J., Dawson, T.M., and Dawson, V.L. 1995. An evaluation of the nitric oxide/cGMP/cGMP-dependent protein kinase cascade in the induction of cerebellar long-term depression in culture. *J. Neurosci.* 15: 5098–5105.
- Linden, D.J., Smeyne, M., and Connor, J.A., 1993. Induction of cerebellar long-term depression in culture requires postsynaptic action of sodium ions. *Neuron* 11: 1093–1100.
- Lindsay, A., and Binder, M. 1991. Distribution of effective synaptic currents underlying recurrent inhibition in cat triceps surae motoneurons. *J. Neurophysiol.* 65: 168–177.

- Lindström, S. 1982. Synaptic organization of inhibitory pathways to principal cells in the lateral geniculate nucleus of the cat. *Brain Res.* 234: 447–453.
- Linn, D.M., Blazynski, C., Redburn, D.A., and Massey, S.C. 1991. Acetylcholine release from the rabbit retina mediated by kainate receptors. *J. Neurosci.* 11: 111–122.
- Linsenmeier, R.A., Frishman, L.J., Jakiela, H.G., and Enroth-Cugell, C. 1982. Receptive field properties of X and Y cells in the rat retina derived from contrast sensitivity measurements. *Vis. Res.* 22: 1173–1183.
- Linster, C., and Hasselmo, M.E. 2001. Neuromodulation and the functional dynamics of piriform cortex. *Chem. Senses* 26: 585–594.
- Linster, C., Wyble, B.P., and Hasselmo, M.E. 1999. Electrical stimulation of the horizontal limb of the diagonal band of Broca modulates population EPSPs in piriform cortex. *J. Neurophysiol.* 81: 2737–2742.
- Lipscomb, B.W., Treloar, H.B., and Greer, C.A. 2002. Novel microglomerular structures in the olfactory bulb of mice. *J. Neurosci.* 22: 766–774.
- Lipscomb, B.W., Treloar, H.B., and Greer, C.A. 2002. Cell surface carbohydrates reveal heterogeneity in olfactory receptor cell axons in the mouse. *Cell Tiss. Res.* 308: 7–17.
- Lisman, J. E. 1999. Relating hippocampal circuitry to function: recall of memory sequences by reciprocal dentate–CA3 interactions. *Neuron* 22: 233–242.
- Liu, R.-J., van den Pol, A.N., and Aghajanian, G.K. 2002. Hypocretins (Orexins) regulate serotonin neurons in the dorsal raphe nucleus by excitatory direct and inhibitory indirect actions. *J. Neurosci.* 22: 9453–9464.
- Liu, X.-B., Honda, C.N., and Jones, E.G. 1995. Distribution of four types of synapse on physiologically identified relay neurons in the ventral posterior thalamic nucleus of the cat. *J. Comp. Neurol.* 352: 69–91.
- Livingstone, M., and Hubel, D.H. 1981. Effects of sleep and arousal on the processing of visual information in the cat. *Nature* 291: 554–561.
- Ljungdahl, A., Hökfelt, T., and Nilsson, G. 1978. Distribution of substance P-like immunoreactivity in the central nervous system of the rat—I. Cell bodies and nerve terminals. *Neuroscience* 3: 861–943.
- Llinás, R. 1974. Eighteenth Bowditch Lecture. Motor aspects of cerebellar control. *Physiologist.* 17: 19–46.
- Llinás, R. 1981. Electrophysiology of the cerebellar networks. In: *Handbook of Physiology. The Nervous System. Vol. II.* Washington, DC: American Physiological Society, pp. 831–876.
- Llinás, R. 1985. Electrotonic transmission in the mammalian central nervous system. In: *Gap Junctions* (Bennett, M.V.L., and Spray, D.C., eds.) Cold Spring Harbor, NY: Cold Spring Harbor Laboratory, pp. 337–353.
- Llinás, R. 1988. The intrinsic electrophysiological properties of mammalian neurons: Insights into central nervous system function. *Science* 242: 1654–1664.
- Llinás, R. 1990. Intrinsic electrical properties of nerve cells and their role in network oscillation. *Cold Spring Harb. Symp. Quant.* 55: 933–938.
- Llinás, R., Baker, R., and Sotelo, C., 1974. Electrotonic coupling between neurons in cat inferior olive. *J. Neurophysiol.* 37: 560–571.
- Llinás, R., and Hess, R. 1976. Tetrodotoxin-resistant dendritic spikes in avian Purkinje cells. *Soc. Neurosci. Abstr.* 2: 112.
- Llinás, R., and Mühlethaler, M. 1988a. An electrophysiological study of the *in vitro*, perfused brainstem-cerebellum of adult guinea pig. *J. Physiol. (Lond.)* 404: 215–240.
- Llinás, R., and Mühlethaler, M. 1988b. Electrophysiology of guinea-pig cerebellar nuclear cells in the *in vitro* brain stem-cerebellar preparation. *J. Physiol. (Lond.)* 404: 241–258.

- Llinás, R., and Nicholson C. 1971. Electrophysiological properties of dendrites and somata in alligator Purkinje cells. *J. Neurophysiol.* 34: 532–551.
- Llinás, R., and Nicholson, C. 1976. Reversal properties of climbing fiber potential in cat Purkinje cells: an example of a distributed synapse. *J. Neurophysiol.* 39: 311–323.
- Llinás, R., and Sasaki, K. 1989. The functional organization of the olivo-cerebellar system as examined by multiple Purkinje cell recordings. *Eur. J. Neurosci.* 1: 587–602.
- Llinás, R., and Sugimori, M. 1978. Dendritic calcium spiking in mammalian Purkinje cells: In vitro study of its function and development. *Soc. Neurosci. Abstr.* 4: 66.
- Llinás, R., and Sugimori M. 1980a. Electrophysiological properties of in vitro Purkinje cell somata in mammalian cerebellar slices. *J. Physiol. (Lond.)* 305: 171–195.
- Llinás, R., and Sugimori, M. 1980b. Electrophysiological properties of in vitro Purkinje cell dendrites in mammalian cerebellar slices. *J. Physiol. (Lond.)* 305: 197–213.
- Llinás, R., and Volkind, R.A. 1973. The olivo-cerebellar system: functional properties as revealed by harmaline-induced tremor. *Exp. Brain Res.* 18: 69–87.
- Llinás, R., and Welsh, J. 1993. On the cerebellum and motor learning. *Curr. Opin. Neurobiol.* 3: 958–965.
- Llinás, R., and Yarom, Y. 1981a. Electrophysiological properties of mammalian inferior olivary cells in vitro: different types of voltage-dependent conductances. *J. Physiol. (Lond.)* 315: 549–567.
- Llinás, R., and Yarom, Y. 1981b. Properties and distribution of ionic conductances generating electroresponsiveness of mammalian inferior olivary neurones in vitro. *J. Physiol. (Lond.)* 315: 569–584.
- Llinás, R., and Yarom, Y. 1986. Oscillatory properties of guinea pig inferior olivary neurons and their pharmacological modulation: an in vitro study. *J. Physiol. (Lond.)* 376: 163–182.
- Llinás, R., Sugimori, M., Hillman, D.E., and Cherksey, B. 1992. Distribution and functional significance of the P-type, voltage-dependent Ca^{2+} channels in the mammalian nervous system. *Trends Neurosci.* 15: 351–355.
- Lloyd, D.P.C. 1960. Spinal mechanisms involved in somatic activities In: *Handbook of Physiology. Sect. 1: Neurophysiology, Vol. II* (Magoun, H.W., ed.) Washington, DC: American Physiol. Soc., pp. 929–949.
- Lo, F.-S., Lu, S.-M., and Sherman, S.M. 1991. Intracellular and extracellular in vivo recording of different response modes for relay cells of the cat's lateral geniculate nucleus. *Exp. Brain Res.* 83: 317–328.
- Lohmann, C., Myhr, K.L., and Wong, R.O.L. 2002. Transmitter-evoked local calcium release stabilizes developing dendrites. *Nature* 418: 177–181.
- Lois, C., Garcia-Verdugo, J.M., and Alvarez-Buylla, A. 1996. Chain migration of neuronal precursors. *Science* 271: 978–981.
- Loren, I., Emson, P.C., Fahrenkrug, J., Bjorklund, A., Alumets, J., Hakanson, R., and Sundler, F. 1979. Distribution of vasoactive intestinal polypeptide in the rat and mouse brain. *Neuroscience* 4: 1953–1976.
- Lorente de Nó, R. 1934. Studies on the structure of the cerebral cortex II. Continuation of the study of the ammonic system. *J. Psychol. Neurol.* 46: 113–177.
- Lorente de Nó, R. 1949. Cerebral cortex: architecture, intracortical connections, motor projections. In: *Physiology of the Nervous System* (Fulton, J.F., ed.) New York: Oxford University Press, pp. 288–313.
- Lorente de Nó, R. 1981. *The Primary Acoustic Nuclei*. New York: Raven Press.
- Lorincz, A., Notomi, T., Tamas, G., Shigemoto, R., and Nusser, Z. 2002. Polarized and compartment-dependent distribution of HCN⁺ in pyramidal cell dendrites. *Nat. Neurosci.* 5: 1185–1193.

- Lowe, G. 2002. Inhibition of backpropagating action potentials in mitral cell secondary dendrites. *J. Neurophysiol.* 88: 64–85.
- Loy, R., Koziell, D.A., Lindsey, J.D., and Moore, R.Y. 1980. Noradrenergic innervation of the adult rat hippocampal formation. *J. Comp. Neurol.* 189: 699–710.
- Lu, G.W., and Willis, W.D. 1999. Branching and/or collateral projections of spinal dorsal horn neurons. *Brain Res. Rev.* 29: 50–82.
- Lu, S.-M., Guido, W., and Sherman, S.M. 1993. The brainstem parabrachial region controls mode of response to visual stimulation of neurons in the cat's lateral geniculate nucleus. *Vis. Neurosci.* 10: 631–642.
- Lu, S.-M., Guido, W., Vaughan, J.W., and Sherman, S.M. 1995. Latency variability of responses to visual stimuli in cells of the cat's lateral geniculate nucleus. *Exp. Brain Res.* 105: 7–17.
- Luchins, D.J. 1990. A possible role of hippocampal dysfunction in schizophrenic symptomatology. *Biol. Psychiatry* 28: 87–91.
- Lund, J.S., Lund, R.D., Hendrickson, A.E., Bunt, A.H., and Fuchs, A.F. 1975. The origin of efferent pathways from the primary visual cortex, area 17, of the macaque monkey as shown by retrograde transport of horseradish peroxidase. *J. Comp. Neurol.* 164: 287–303.
- Lundberg, A. 1969. Convergence of excitatory and inhibitory action on interneurons in the spinal cord. In: *The Interneuron, UCLA Forum in Medical Sciences* (Brazier, M.A.B., ed.) Berkeley: University of California Press, pp. 231–265.
- Lundberg, A. 1971. Function of the ventral spinocerebellar tract, a new hypothesis. *Exp. Brain Res.* 12: 317–330.
- Lundberg, A. 1975. Control of spinal mechanisms from the brain. In: *The Nervous System. Vol 1: The Basic Neurosciences* (Brady, R., ed.) New York: Raven Press, pp. 253–265.
- Lundberg, A., Malmgren, K., and Schomburg, E.D. 1987. Reflex pathways from group II muscle afferents. 3. Secondary spindle afferents and the FRA: a new hypothesis. *Exp. Brain Res.* 65: 294–306.
- Lundberg, A., and Weight, F.F. 1971. Functional organization of connexions to the ventral spinocerebellar tracts. *Exp. Brain Res.* 12: 295–316.
- Luo, M., and Katz, L.C. 2001. Response correlation maps of neurons in the mammalian olfactory bulb. *Neuron* 32: 1165–1179.
- Luo, M., Pu, M., and Sterling, P. 1996. Volumes of beta and alpha cell dendritic arbors peak in different strata. *Soc. Neurosci. Abstr.* 26: 1603.
- Lüscher, H.R., and Clamann, H.P. 1992. Relation between structure and function in information transfer in spinal monosynaptic reflex. *Physiol. Rev.* 72: 71–99.
- Luskin, M.B. 1993. Restricted proliferation and migration of postnatally generated neurons derived from the forebrain subventricular zone. *Neuron* 11: 173–189.
- Luskin, M.B. 1998. Neuroblasts of the postnatal mammalian forebrain: their phenotype and fate. *J. Neurobiol.* 36: 221–233
- Luskin, M.B., and Price, J.L. 1982. The distribution of axon collaterals from the olfactory bulb and the nucleus of the horizontal limb of the diagonal band to the olfactory cortex, demonstrated by double retrograde labeling techniques. *J. Comp. Neurol.* 209: 249–263.
- Luskin, M.B., and Price, J.L. 1983a. The laminar distribution of intracortical fibers originating in the olfactory cortex of the rat. *J. Comp. Neurol.* 216: 292–302.
- Luskin, M.B., and Price, J.L. 1983b. The topographic organization of associational fibers of the olfactory system in the rat, including centrifugal fibers to the olfactory bulb. *J. Comp. Neurol.* 216: 264–291.
- Lynch, G., and Granger, R. 1991. Serial steps in mercury processing: possible clues from studies of plasticity in the olfactory-hippocampal circuit. In: *Olfaction: A Model System for Computational Neurosciences* (Davis, J.L., and Eichenbaum, H., eds.) Cambridge: MIT Press, pp. 145–165.

- Lyubarsky, A.L., Falsini, B., Pennesi, M.E., Valentini, P., and Pugh Jr., E.N. 1999. UV- and mid-wave-sensitive cone-driven retinal responses of the mouse: a possible phenotype for co-expression of cone photopigments. *J. Neurosci.* 19: 442–455.
- MacDermott, A.B., and Dale, N. 1987. Receptors, ion channels and synaptic potentials underlying the integrative actions of excitatory amino acids. *Trends Neurosci.* 10: 280–284.
- MacDermott, A.B., Mayer, M.L., Westbrook, G.L., Smith, S.J., and Barker, J.L. 1986. NMDA-receptor activation increases cytoplasmic calcium concentrations in cultured spinal cord neurones. *Nature* 321: 519–522.
- MacDermott, A.B., Role, L.W., and Siegelbaum, S.A. 1999. Presynaptic ionotropic receptors and the control of transmitter release. *Annu. Rev. Neurosci.* 22: 443–85.
- Mackay-Sim, A., and Kesteven, S. 1994. Topographic patterns of responsiveness to odorants in the rat olfactory epithelium. *J. Neurophysiol.* 71: 150–160.
- Macmillan, N.A., and Creelman, C.D. 1991. *Detection Theory: A User's Guide*. Cambridge: Cambridge University Press.
- MacNeil, M.A., and Masland, R.H. 1998. Extreme diversity among amacrine cells: implications for function. *Neuron* 20: 971–982.
- Macrides, F., and Chorover, S.L. 1972. Olfactory bulb units: activity correlated with inhalation cycles and odor quality. *Science* 175: 84–87.
- Macrides, F., and Davis, B.J. 1983. The olfactory bulb. In: *Chemical Neuroanatomy* (Emson, P.C., ed.) New York: Raven Press, pp. 391–426.
- Macrides, F., Eichenbaum, H.B., and Forbes, W.B. 1982. Temporal relationship between sniffing and the limbic theta rhythm during odor discrimination reversal learning. *J. Neurosci.* 2: 1705–1717.
- Macrides, F., and Schneider, S.P. 1982. Laminar organization of mitral and tufted cells in the main olfactory bulb of the adult hamster. *J. Comp. Neurol.* 208: 419–430.
- Macrides, F., Schoenfeld, T.A., Marchand, J.E., and Clancy, A.N. 1985. Evidence for morphologically, neurochemically and functionally heterogeneous classes of mitral and tufted cells in the olfactory bulb. *Chem. Senses* 10: 175–202.
- MacVicar, B.A., and Dudek, F.E. 1980. Local synaptic circuits in rat hippocampus interactions between pyramidal cells. *Brain Res.* 184: 220–223.
- Madden, D.R. 2002. The structure and function of glutamate receptor ion channels. *Nat. Rev.* 3: 91–101.
- Madison, D.V., and Nicoll, R.A. 1984. Control of the repetitive discharge of rat CA1 pyramidal neurones *in vitro*. *J. Physiol. (Lond.)* 354: 319–331.
- Madison, D.V., and Nicoll, R.A. 1986a. Actions of noradrenaline recorded intracellularly in rat hippocampal CA1 pyramidal neurones, *in vitro*. *J. Physiol. (Lond.)* 372: 221–244.
- Madison, D.V., and Nicoll, R.A. 1986b. Cyclic adenosine 3',5'-monophosphate mediates beta-receptor actions of noradrenaline in rat hippocampal pyramidal cells. *J. Physiol. (Lond.)* 372: 245–259.
- Madison, D.V., Lancaster, B., and Nicoll, R.A. 1987. Voltage clamp analysis of cholinergic action in the hippocampus. *J. Neurosci.* 7: 733–741.
- Madison, D.V., Malenka, R.C., and Nicoll, R.A. 1991. Mechanisms underlying long-term potentiation of synaptic transmission. *Annu. Rev. Neurosci.* 14: 379–397.
- Magee, J.C. 1998. Dendritic hyperpolarization-activated currents modify the integrative properties of hippocampal CA1 pyramidal neurons. *J. Neurosci.* 18: 7613–7624.
- Magee, J.C. 1999. Voltage-gated ion channels in dendrites In: *Dendrites* (Stuart, G.J., Spruston, N., and Häusser, M., eds.) New York: Oxford University Press, pp. 139–160.
- Magee, J.C., Avery, R.B., Christie, B.R., and Johnston, D. 1996. Dihydropyridine-sensitive, voltage-gated Ca^{2+} channels contribute to the resting intracellular Ca^{2+} concentration of hippocampal CA1 pyramidal neurons. *J. Neurophysiol.* 76: 3460–3470.

- Magee, J.C., Christofi, G., Miyakawa, H., Christie, B., Lasser-Ross, N., and Johnston, D. 1995. Subthreshold synaptic activation of voltage-gated Ca^{2+} channels mediates a localized Ca^{2+} influx into the dendrites of hippocampal pyramidal neurons. *J. Neurophysiol.* 74: 1335–1342.
- Magee, J.C., and Cook, E.P. 2000. Somatic EPSP amplitude is independent of synapse location in hippocampal pyramidal neurons. *Nat. Neurosci.* 3: 895–903.
- Magee, J.C., Hoffman, D., Colbert, C., and Johnston, D. 1998. Electrical and calcium signaling in dendrites of hippocampal pyramidal neurons. *Annu. Rev. Physiol.* 60: 327–346.
- Magee, J.C., and Johnston, D. 1995a. Characterization of single voltage-gated Na^+ and Ca^{2+} channels in apical dendrites of rat CA1 pyramidal neurons. *J. Physiol. (Lond.)* 487: 67–90.
- Magee, J.C., and Johnston, D. 1995b. Synaptic activation of voltage-gated channels in the dendrites of hippocampal pyramidal neurons. *Science* 268: 301–304.
- Magee, J.C., and Johnston, D. 1997. A synaptically controlled, associative signal for Hebbian plasticity in hippocampal neurons. *Science* 275: 209–213.
- Magistretti, J., Brevi, S., and de Curtis, M. 1999. Biophysical and pharmacological diversity of high-voltage-activated calcium currents in layer II neurones of guinea-pig piriform cortex. *J. Physiol. (Lond.)* 518: 705–720.
- Magistretti, J., Brevi, S., and de Curtis, M. 2000. A blocker-resistant, fast-decaying, intermediate-threshold calcium current in palaeocortical pyramidal neurons. *Eur. J. Neurosci.* 12: 2376–2386.
- Magistretti, J., and de Curtis, M. 1998. Low-voltage activated T-type calcium currents are differentially expressed in superficial and deep layers of guinea pig piriform cortex. *J. Neurophysiol.* 79: 808–816.
- Magistretti, P.J., Dietl, M.M., Hof, P.R., Martin, J.-L., Palacios, J.M., Schaad, N., and Schorderet, M. 1988. Vasoactive intestinal peptide as a mediator of intercellular communication in the cerebral cortex: release, receptors, actions, and interactions with norepinephrine. *Ann. N.Y. Acad. Sci.* 527: 110–129.
- Mahowald, M. 1994. *An Analog VLSI System for Stereoscopic Vision*. Boston: Kluwer.
- Mainen, Z.F., Carnevale, N.T., Zador, A.M., Claiborne, B.J., and Brown, T.H. 1996. Electrotonic architecture of hippocampal CA1 pyramidal neurons based on three-dimensional reconstructions. *J. Neurophysiol.* 76: 1904–1923.
- Mainen, Z.F., and Sejnowski, T. 1996. Influence of dendritic structure on firing pattern in model neocortical neurons. *Nature* 382: 362–366.
- Mainland, J.D., Bremner, E.A., Young, N., Johnson, B.N., Khan, R.M., Bensafi, M., and Sobel, N. 2002. Olfactory plasticity—one nostril knows what the other learns. *Nature* 419: 802
- Majewska, A., Brown, E., Ross, J., and Yuste, R. 2000. Mechanisms of calcium decay kinetics in hippocampal spines: role of spine calcium pumps and calcium diffusion through the spine neck in biochemical compartmentalization. *J. Neurosci.* 20: 1722–1734.
- Majewska, A., Tashiro, A., and Yuste, R. 2000. Regulation of spine calcium dynamics by rapid spine motility. *J. Neurosci.* 20: 8262–8268.
- Major, G., Larkman, A.U., Jonas, P., Sakmann, B., and Jack, J.J.B. 1994. Detailed passive cable models of whole-cell recorded CA3 pyramidal neurons in rat hippocampal slices. *J. Neurosci.* 14: 4513–4638.
- Majorossy, K., and Kiss, A. 1976a. Types of interneurons and their participation in the neuronal network of the medial geniculate body. *Exp. Brain Res.* 26: 19–37.
- Majorossy, K., and Kiss, A. 1976b. Specific patterns of neuron arrangement and of synaptic articulation in the medial geniculate body. *Exp. Brain Res.* 26: 1–17.
- Makowski, L., Casper, D.L.D., Phillips, W.C., and Goodenough, D.A. 1977. Gap junction structure. II. Analysis of X-ray diffraction data. *J. Cell Biol.* 74: 629–645.

- Malach, R. 1992. Dendritic sampling across processing streams in monkey striate cortex. *J. Comp. Neurol.* 315: 303–312.
- Malenka, R.C., and Nicoll, R.A. 1999. Long-term potentiation—a decade of progress? *Science* 285, 1870–4.
- Malenka, R.C., and Nicoll, R.A. 1993. NMDA-receptor-dependent synaptic plasticity: multiple forms and mechanisms. *Trends Neurosci.* 16: 521–527.
- Malinow, R., and Miller, J.P. 1986. Postsynaptic hyperpolarization during conditioning reversibly blocks induction of long-term potentiation. *Nature* 320: 529–530.
- Malinow, R., and Malenka, R.C. 2002. AMPA receptor trafficking and synaptic plasticity. *Annu. Rev. Neurosci.* 25: 103–126.
- Malioso, M.-L., Marqueze-Pouey, B., Kuhse, J., and Betz, H. 1991. Widespread expression of glycine receptor subunit mRNAs in the adult and developing rat brain. *EMBO J.* 10: 2401–2409.
- Malnic, B., Hirono, J., Sato, T., and Buck, L.B. 1999. Combinatorial receptor codes for odors. *Cell* 96: 713–723.
- Maltenfort, M., Heckman, C., and Rymer, W. 1998. Decorrelating actions of Renshaw interneurons on the firing of spinal motoneurons within a motor nucleus: a simulation study. *J. Neurophysiol.* 80: 309–323.
- Mancillas, J., Siggins, G., and Bloom, F. 1986. Somatostatin selectively enhances acetylcholine-induced excitations in rat hippocampus and cortex. *Proc. Natl. Acad. Sci. U.S.A.* 83: 7518–7521.
- Mangel, S.C. 1991. Analysis of the horizontal cell contribution to the receptive field surround of ganglion cells in the rabbit retina. *J. Physiol. (Lond.)* 442: 211–234.
- Mangel, S.C., and Dowling, J.E. 1985. Responsiveness and receptive field size of carp horizontal cells are reduced by prolonged darkness and dopamine. *Science* 229: 1107–1109.
- Manis, P.B. 1989. Responses to parallel fiber stimulation in the guinea pig dorsal cochlear nucleus in vitro. *J. Neurophysiol.* 61: 149–161.
- Manis, P.B. 1990. Membrane properties and discharge characteristics of guinea pig dorsal cochlear nucleus neurons studied in vitro. *J. Neurosci.* 10: 2338–2351.
- Manis, P.B., and Marx, S.O. 1991. Outward currents in isolated ventral cochlear nucleus neurons. *J. Neurosci.* 11: 2865–2880.
- Manis, P.B., and Molitor, S.C. 1996. N-Methyl-d-aspartate receptors at parallel fiber synapses in the dorsal cochlear nucleus. *J. Neurophysiol.* 76: 1639–1656.
- Manis, P.B., Spirou, G.A., Wright, D.D., Paydar, S., and Ryugo, D.K. 1994. Physiology and morphology of complex spiking neurons in the guinea pig dorsal cochlear nucleus. *J. Comp. Neurol.* 348: 261–276.
- Manning, K.A., Wilson, J.R., and Uhlrich, D.J. 1996. Histamine-immunoreactive neurons and their innervation of visual regions in the cortex, tectum, and thalamus in the primate *Macaca mulatta*. *J. Comp. Neurol.* 373: 271–282.
- Marek, G.J., and Aghajanian, G.K. 1994. Excitation of interneurons in piriform cortex by 5-hydroxytryptamine: blockade by MDL 100,907, a highly selective 5-HT_{2A} receptor antagonist. *Eur. J. Pharmacol.* 259: 137–141.
- Marek, G.J., and Aghajanian, G.K. 1995. Protein kinase C inhibitors enhance the 5-HT_{2A} receptor-mediated excitatory effects of serotonin on interneurons in rat piriform cortex. *Synapse* 21: 123–130.
- Marek, G.J., and Aghajanian, G.K. 1996. Alpha 1B-adrenoceptor-mediated excitation of piriform cortical interneurons. *Eur. J. Pharmacol.* 305: 95–100.
- Margolis, F.L. 1985. Olfactory marker protein: from PAGE band to cDNA clone. *Trends Neurosci.* 8: 542–546.
- Margolis, F.L., Kawano, T., and Grillo, M. 1986. Ontogeny of carnosine, olfactory marker pro-

- tein and neurotransmitter enzymes in olfactory bulb and olfactory mucosa of the rat. In: *Ontogeny of Olfaction* (Breipohl, W., ed.) Berlin: Springer-Verlag, pp. 107–116.
- Margrie, T.W., Sakmann, B., and Urban, N.N. 2001. Action potential propagation in mitral cell lateral dendrites is decremental and controls recurrent and lateral inhibition in the mammalian olfactory bulb. *Proc. Natl. Acad. Sci. U.S.A.* 98: 319–324.
- Mariani, A.P. 1984. Bipolar cells in monkey retina selective for the cones likely to be blue-sensitive. *Nature* 308: 184–186.
- Mariani, J., Crepel, F., Mikoshiba, K., Changeux, J.P., and Sotelo, C. 1977. Anatomical, physiological and biochemical studies of the cerebellum from Reeler mutant mouse. *Trans. R. Soc. Lond B* 281: 1–28.
- Markham, J., and Fífkova, E. 1986. Actin filament organization within dendrites and dendritic spines during development. *Brain Res.* 392: 263–269.
- Markram, H., and Sakmann, B. 1994. Calcium transients in apical dendrites evoked by single subthreshold excitatory post-synaptic potentials via low voltage-activated calcium channels. *Proc. Natl. Acad. Sci. U.S.A.* 91: 5207–5211.
- Markram, H., and Tsodyks, M. 1996. Redistribution of synaptic efficacy between neocortical pyramidal neurons. *Nature* 382: 807–810.
- Markram, H., Gupta, A., Uziel, A., Wang, Y., and Tsodyks, M. 1998. Information processing with frequency-dependent synaptic connections. *Neurobiol. Learn. Mem.* 70: 101–112.
- Markram, H., Helm, P.J., and Sakmann, B. 1995. Dendritic calcium transients evoked by single back-propagating action potentials in rat neocortical pyramidal neurons. *J. Physiol. (Lond.)* 485: 1–20.
- Markram, H., Lubke, J., Frotscher, M., and Sakmann, B. 1997a. Regulation of synaptic efficacy by coincidence of postsynaptic APs and EPSPs. *Science* 275: 213–215.
- Markram, H., Lubke, J., Frotscher, M., Roth, A., and Sakmann, B. 1997b. Physiology and anatomy of synaptic connections between thick tufted paramidial neurons in the developing rat neocortex. *J. Physiol. (Lond.)* 500: 409–440.
- Marr, D., and Poggio, T. 1979. A computational theory of human stereo vision. *Proc. R. Soc. Lond. B. Biol. Sci.* 204: 301–328.
- Marrion, N.V. 1997. Control of M-current. *Annu. Rev. Physiol.* 59: 483–504.
- Martin, A.R. 1977. Junctional transmission. II. Presynaptic mechanisms. In: *Handbook of Physiology, Section I, The Nervous System, Vol. I: The Cellular Biology of Neurons* (Kandel, E.R., ed.) Bethesda: American Physiological Society, pp. 329–355.
- Martin, K.A.C. 1988. The Wellcome Prize Lecture: from single cells to simple circuits in the cerebral cortex. *Q. J. Exp. Physiol.* 73: 637–702.
- Martin, P.R. 1986. The projection of different retinal ganglion cell classes to the dorsal lateral geniculate nucleus in the hooded rat. *Exp. Brain Res.* 62: 77–88.
- Martin, P.R., Lee, B.B., White, A.J.R., Solomon, S.G., and Rüttiger, L. 2001. Chromatic sensitivity of ganglion cells in the peripheral primate retina. *Nature* 410: 933–936.
- Martin, S.J., Grimwood, P. D., and Morris, R. G. 2000. Synaptic plasticity and memory: an evaluation of the hypothesis. *Annu. Rev. Neurosci.* 23: 649–711.
- Martina, M., Royer, S., and Pare, D. 2001. Propagation of neocortical inputs in the perirhinal cortex. *J. Neurosci.* 21: 2878–2888.
- Marty, A., and Llano, I. 1995. Modulation of inhibitory synapses in the mammalian brain. *Curr. Opin. Neurobiol.* 5: 335–341.
- Masland, R.H. 1986. The functional architecture of the retina. *Sci. Am.* 254: 102–111.
- Masland, R.H. 2001. The fundamental plan of the retina. *Nat. Neurosci.* 4: 877–886.
- Masland, R.H., Mills, J.W., and Cassidy, C. 1984. The functions of acetylcholine in the rabbit retina. *Proc. R. Soc. Lond. B* 223: 121–139.
- Maslim, J., and Stone, J. 1986. Synaptogenesis in the retina of the cat. *Brain Res.* 373: 35–48.

- Mason, A., and Larkman, A. 1990. Correlations between morphology and electrophysiology of pyramidal neurons in slices of rat visual cortex. II. Electrophysiology. *J. Neurosci.* 10: 1415–1428.
- Mason, A., Nicoll, A., and Stratford, K. 1991. Synaptic transmission between individual pyramidal neurons of the rat visual cortex in vitro. *J. Neurosci.* 11: 72–84.
- Massey, S.C., and Maguire, G. 1995. Excitatory amino acids and synaptic transmission. In: *The Role of Glutamate in Retina Circuitry* (Wheal, H.V., and Thomsin, A.M., eds.) London: Academic Press, pp. 201–227.
- Massey, S.C., and Redburn, D.A. 1985. Light evoked release of acetylcholine in response to a single flash: cholinergic amacrine cells receive ON and OFF input. *Brain Res.* 328: 374–377.
- Masterton, R.B., and Granger, E.M. 1988. Role of the acoustic striae in hearing: contribution of dorsal and intermediate striae to detection of noises and tones. *J. Neurophysiol.* 60: 1841–1860.
- Masterton, R.B., Granger, E.M., and Glendenning, K.K. 1994. Role of acoustic striae in hearing—mechanism for enhancement of sound detection in cats. *Hear. Res.* 73: 209–222.
- Mastronarde, D.N. 1983. Correlated firing of cat retinal ganglion cells. II. Responses of X- and Y-cells to single quantal events. *J. Neurophysiol.* 49: 325–349.
- Mastronarde, D.N. 1987. Two classes of single-input X-cells in cat lateral geniculate nucleus. I. Receptive field properties and classification of cells. *J. Neurophysiol.* 57: 357–380.
- Masu, M., Iwakabe, H., Tagawa, Y., Miyoshi, T., Yamashita, M., Fukuda, Y., Sasaki, H., Hiroi, K., Nakamura, Y., and Shigemoto, R. 1995. Specific deficit on the ON response in visual transmission by targeted disruption of the mGluR6 gene. *Cell* 80: 757–765.
- Mata, N.L., Radu, R.A., Clemmons, R.C., and Travis, G.H. 2002. Isomerization and oxidation of vitamin A in cone-dominant retina: a novel pathway for visual-pigment regeneration in daylight. *Neuron* 36: 69–80.
- Mates, S., and Lund, J. 1983. Neuronal composition and development of lamina 4c of monkey striate cortex. *J. Comp. Neurol.* 221: 60–90.
- Mathers, L.H. 1972. The synaptic organization of the cortical projection to the pulvinar of the squirrel monkey. *J. Comp. Neurol.* 146: 43–60.
- Matsumoto, R. 1989. GABA receptors: are cellular differences reflected in function? *Brain Res. Revs.* 14: 203–225.
- Matthews, G. 1996. Neurotransmitter release. *Annu. Rev. Neurosci.* 19: 219–233.
- Matthews, M.A., Willis, W.D., and Williams, V. 1971. Dendrite bundles in lamina IX of cat spinal cord: a possible source for electrical interaction between motoneurons. *Anat. Rec.* 171: 313–327.
- Matthews, P.B.C. 1972. *Mammalian Muscle Receptors and Their Central Actions*. London: Arnold.
- Matthews, P.B.C. 1981. Muscle spindles: their messages and their fusimotor supply In: *Handbook of Physiology, Section 1: The Nervous System. Vol. II. Motor Control, Part 1*, Bethesda: American Physiological Society, pp. 189–228.
- Maturana, H.R., Lettvin, J.Y., McCulloch, W.S., and Pitts, W.H. 1960. Anatomy and physiology of vision in the frog (*Rana pipiens*). *J. Gen. Physiol.* 43: 129–175.
- Maxwell, D.J., Christie, W.M., Ottersen, O.P., and Storm-Mathisen, J. 1990a. Terminals of group Ia primary afferent fibres in Clarke's column are enriched with L-glutamate-like immunoreactivity. *Brain Res.* 510: 346–350.
- Maxwell, D.J., Christie, W.M., Short, A.D., and Brown, A.G. 1990b. Direct observations of synapses between GABA-immunoreactive boutons and muscle afferent terminals in lamina VI of the cat's spinal cord. *Brain Res.* 530: 215–222.
- May, B.J. 2000. Role of the dorsal cochlear nucleus in the sound localization behavior of cats. *Hear. Res.* 148: 74–87.

- May, B.J., LePrell, G.S., and Sachs, M.B. 1998. Vowel representations in the ventral cochlear nucleus of the cat: effects of level, background noise, and behavioral state. *J. Neurophysiol.* 79: 1755–1767.
- Mayer, M.L., and Westbrook, G.L. 1987. The physiology of excitatory amino acids in the vertebrate central nervous system. *Prog. Neurobiol.* 28: 197–276.
- Mayer, M.L., Westbrook, G.L., and Guthrie, P.B. 1984. Voltage-dependent block by Mg^{2+} of NMDA responses in spinal cord neurones. *Nature* 309: 261–263.
- McArdle, C.B., Dowling, J.E., and Masland, R.H. 1977. Development of outer segments and synapses in the rabbit retina. *J. Comp. Neurol.* 175: 253–274.
- McBain, C.J., and Fisahn, A. 2001. Interneurons unbound. *Nat. Rev. Neurosci.* 2: 11–23.
- McBride, W.J., Aprison, M.H., and Kusano, K. 1976. Contents of several amino acids in the cerebellum, brain stem and cerebrum of the ‘staggerer’, ‘weaver’ and ‘nervous’ neurologically mutant mice. *J. Neurochem.* 26: 867–870.
- McCarley, R.W., Benoit, O., and Barrionuevo, G. 1983. Lateral geniculate nucleus unitary discharge in sleep and waking state- and rate-specific aspects. *J. Neurophysiol.* 50: 798–818.
- McClurkin, J.W., and Marrocco, R.T. 1984. Visual cortical input alters spatial tuning in monkey lateral geniculate nucleus cells. *J. Physiol (Lond.)* 348: 135–152.
- McClurkin, J.W., Optican, L.M., and Richmond, B.J. 1994. Cortical feedback increases visual information transmitted by monkey parvocellular lateral geniculate nucleus neurons. *Vis. Neurosci.* 11: 601–617.
- McCollum, J., Larson, J., Otto, T., Schottler, F., Granger, R., and Lynch, G. 1991. Short-latency single unit processing in olfactory cortex. *J. Cogn. Neurosci.* 3: 293–299.
- McCormick, D.A. 1989. Cholinergic and noradrenergic modulation of thalamocortical processing. *Trends Neurosci.* 12: 215–221.
- McCormick, D.A. 1989b. GABA as an inhibitory neurotransmitter in the human cerebral cortex. *J. Neurophysiol.* 62: 1018–1027.
- McCormick, D.A. 1990. Membrane properties and neurotransmitter actions. In: *The Synaptic Organization of the Brain*, 3rd ed. (Shepherd, G.M. ed.) New York: Oxford University Press, pp. 32–66.
- McCormick, D.A. 1992. Neurotransmitter actions in the thalamus and cerebral cortex and their role in neuromodulation of thalamocortical activity. *Prog. Neurobiol.* 39: 337–388.
- McCormick, D.A., and Bal, T. 1994. Sensory gating mechanisms of the thalamus. *Curr. Opin. Neurobiol.* 4: 550–556.
- McCormick, D.A., and Bal, T. 1997. Sleep and arousal: thalamocortical mechanisms. *Annu. Rev. Neurosci.* 20: 185–215.
- McCormick, D.A., Connors, B., Lighthall, J., and Prince, D. 1985. Comparative electrophysiology of pyramidal and sparsely spiny stellate neurons of the neocortex. *J. Neurophysiol.* 59: 782–806.
- McCormick, D.A., and Feuser, H.R. 1990. Functional implications of burst firing and single spike activity in lateral geniculate relay neurons. *Neuroscience* 39: 103–113.
- McCormick, D.A., and Gray, C. 1996. Chattering cells: superficial pyramidal neurons contributing to the generation of synchronous oscillations in the visual cortex. *Science* 274: 109–113.
- McCormick, D.A., and Huguenard, J.R. 1992. A model of the electrophysiological properties of thalamocortical relay neurons. *J. Neurophysiol.* 68: 1384–1400.
- McCormick, D.A., and Pape, H.-C. 1988. Acetylcholine inhibits identified interneurons in the cat lateral geniculate nucleus. *Nature* 334: 246–248.
- McCormick, D.A., and Pape, H.-C. 1990a. Noradrenergic and serotonergic modulation of a hyperpolarization-activated cation current in thalamic relay neurones. *J. Physiol. (Lond.)* 431: 319–342.

- McCormick, D.A., and Pape, H.-C. 1990b. Properties of a hyperpolarization-activated cation current and its role in rhythmic oscillation in thalamic relay neurones. *J. Physiol. (Lond.)* 431: 291–318.
- McCormick, D.A., and Prince, D.A. 1985. Two types of muscarinic response to acetylcholine in mammalian cortical neurons. *Proc. Natl. Acad. Sci. U.S.A.* 82: 6344–6348.
- McCormick, D.A., and Prince, D.A. 1986a. Acetylcholine induces burst firing in thalamic reticular neurones by activating a potassium conductance. *Nature* 319: 402–405.
- McCormick, D.A., and Prince, D.A. 1986b. Mechanisms of action of acetylcholine in the guinea-pig cerebral cortex. *J. Physiol. (Lond.)* 375: 169–194.
- McCormick, D.A., and Prince, D.A. 1987a. Actions of acetylcholine in the guinea-pig and cat medial and lateral geniculate nuclei, *in vitro*. *J. Physiol. (Lond.)* 392: 147–165.
- McCormick, D.A., and Prince, D.A. 1987b. Acetylcholine causes rapid nicotinic excitation in the medial habenular nucleus of guinea pig, *in vitro*. *J. Neurosci.* 7: 742–752.
- McCormick, D.A., and Von Krosigk, M. 1992. Corticothalamic activation modulates thalamic firing through glutamate “metabotropic” receptors. *Proc. Natl. Acad. Sci. U.S.A.* 89: 2774–2778.
- McCormick, D.A., and Wang, Z. 1991. Serotonin and noradrenaline excite GABAergic neurones in the guinea-pig and cat nucleus reticularis thalami. *J. Physiol. (Lond.)* 442: 235–255.
- McCormick, D.A., Wang, Z., and Huguenard, J. 1993. Neurotransmitter control of neocortical neuronal activity and excitability. *Cereb. Cortex* 3: 387–398.
- McCormick, D.A., and Williamson, A. 1989. Convergence and divergence of neurotransmitter action in the human cerebral cortex. *Proc. Natl. Acad. Sci. U.S.A.* 86: 8098–8102.
- McCormick, D.A., and Williamson, A. 1991. Modulation of neuronal firing mode in cat and guinea pig LGNd by histamine: possible cellular mechanisms of histaminergic control of arousal. *J. Neurosci.* 11: 3188–3199.
- McCurdy, M.L., and Hamm, T.M. 1992. Recurrent collaterals of motoneurons projecting to distal muscles in the cat hindlimb. *J. Neurophysiol.* 67: 1359–66.
- McGeer, P.L., McGeer, E.G., Sherer, U., and Sinh, K. 1977. A glutamatergic corticostriatal path? *Brain Res.* 128: 369–373.
- McGehee, D.S., and Role, L.W. 1996. Presynaptic ionotropic receptors. *Curr. Opin. Neurobiol.* 6: 342–349.
- McGinty, J.F., Henriksen, S.J., Goldstein, A., Terenius, L., and Bloom, F.E. 1983. Dynorphin is contained within hippocampal mossy fibers immunochemical alterations after kainic acid administration and colchicine. *Proc. Natl. Acad. Sci. U.S.A.* 80: 589–593.
- McGuire, B.A., Stevens, J.K., and Sterling, P. 1984. Microcircuitry of bipolar cells in cat retina. *J. Neurosci.* 4: 2920–2938.
- McHugh, T.J., Blum, K.I., Tsien, J.Z., Tonegawa, S., and Wilson, M.A. 1996. Impaired hippocampal representation of space in CA1-specific NMDAR1 knockout mice. *Cell* 87: 1339–1349.
- McIlwain, J.T. 1964. Receptive fields of optic tract axons and lateral geniculate cells: peripheral extent and barbiturate sensitivity. *J. Neurophysiol.* 27: 1154–1173.
- McIlwain, J.T. 1966. Some evidence concerning the physiological basis of the periphery effect in the cat’s brain. *Exp. Brain Res.* 1: 265–271.
- McLaughlin, B.J., Woods, J.G., Saito, K., Barber, R., Vaughn, J.E., Roberts, E., and Wu, J. 1974. The fine structural localization of glutamate decarboxylase in synaptic terminals of rodent cerebellum. *Brain Res.* 76: 377–391.
- McLennan, H. 1971. The pharmacology of inhibition of mitral cells in the olfactory bulb. *Brain Res.* 29: 177–187.
- McLennan, H. 1983. Receptors for the excitatory amino acids in the mammalian central nervous system. *Progr. Neurobiol.* 20: 251–271.

- McMahon, L.L., and Kauer, J.A. 1997. Hippocampal interneurons express a novel form of synaptic plasticity. *Neuron* 18: 295–305.
- McNaughton, B.L. 1982. Long-term synaptic enhancement and short-term potentiation in rat fascia dentata act through different mechanisms. *J. Physiol. (Lond.)* 324: 249–262.
- McQuiston, A.R., and Katz, L.C. 2001. Electrophysiology of interneurons in the glomerular layer of the rat olfactory bulb. *J. Neurophysiol.* 86: 1899–1907.
- Mead, C. 1990. Neuromorphic electronic systems. *Proc. IEEE* 78: 1629–1636.
- Medina, J.F., Nores, W.L., Ohyama, T., and Mauk, M.D. 2000. Mechanisms of cerebellar learning suggested by eyelid conditioning. *Curr. Opin. Neurobiol.* 10: 717–724.
- Megias, M., Emri, Z., Freund, T.F., and Gulyas, A.I. 2001. Total number and distribution of inhibitory and excitatory synapses on hippocampal CA1 pyramidal cells. *Neuroscience* 102: 527–540.
- Mehraein, P., Yamada, M., and Tarnowska-Dziduszko, E. 1975. Quantitative study on dendrites and dendritic spines in Alzheimer's disease and senile dementia. In: *Advances in Neurology* (Kreutzberg, G.W., ed.) New York: Raven Press, pp. 453–458.
- Mehta, M.R., Quirk, M.C., and Wilson, M.A. 2000. Experience-dependent asymmetric shape of hippocampal receptive fields. *Neuron* 25: 707–15.
- Meister, M. 1996. Multineuronal codes in retinal signaling. *Proc. Natl. Acad. Sci. U.S.A.* 93: 609–614.
- Meister, M., and Berry II, M.J. 1999. The neural code of the retina. *Neuron* 22: 435–450.
- Meister, M., and Bonhoeffer, T. 2001. Tuning and topography in an odor map on the rat olfactory bulb. *J. Neurosci.* 21: 1351–1360.
- Meister, M., Pine, J., and Baylor, D.A. 1994. Multi-neuronal signals from the retina: acquisition and analysis. *J. Neurosci. Methods* 51: 95–106.
- Meister, M., Wong, R.O.L., Baylor, D.A., and Shatz, C.J. 1991. Synchronous bursts of action potentials in ganglion cells of the developing mammalian retina. *Science* 252: 939–943.
- Mel, B. 1993. Synaptic integration in excitable dendritic trees. *J. Neurophysiol.* 70: 1086–1101.
- Mendell, L., Collins, W., and Koerber, H. 1990. How are Ia synapses distributed on spinal motoneurons to permit orderly recruitment? In: *The Segmental Motor System* (Binder, M., and Mendell, L., ed.) New York: Oxford University Press, pp. 308–327.
- Mendell, L.M., and Henneman, E. 1971. Terminals of single Ia fibers: Location, density, and distribution within a pool of 300 homonymous motoneurons. *J. Neurophysiol.* 34: 171–187.
- Meng, X.W., Ohara, P.T., and Ralston, H.J. 1996. Nitric oxide synthase immunoreactivity distinguishes a sub-population of GABA-immunoreactive neurons in the ventrobasal complex of the cat. *Brain Res.* 728: 111–115.
- Merabet, L., Desautels, A., Minville, K., and Casanova, C. 1998. Motion integration in a thalamic visual nucleus. *Nature* 396: 265–268.
- Meulders, M., and Godfraind, J.M. 1969. [Influence of arousal on the size of the visual receptive fields of supragenulate and geniculate neurons in the intact alert cat and in the "cerveau isole" cat] [in French]. *Exp. Brain Res.* 9: 201–220.
- Mickus, T., Jung, H.Y., and Spruston, N. 1999. Properties of slow, cumulative sodium channel inactivation in rat hippocampal CA1 pyramidal neurons. *Biophys. J.* 76: 846–860.
- Middlebrooks, J.C. 1992. Narrow-band sound localization related to external ear acoustics. *J. Acoust. Soc. Am.* 92: 2607–2624.
- Midtgaard J. 1992. Stellate cell inhibition of Purkinje cells in the turtle cerebellum *in vitro*. *J. Physiol. (Lond.)* 457: 355–367.
- Midtgaard, J. 1994. Processing of information from different sources: spatial synaptic integration in the dendrites of vertebrate CNS neurons. *Trends Neurosci.* 17: 166–173.
- Migliore, M., and Shepherd, G.M. 2002. Emerging rules for the distributions of active dendritic conductances. *Nat. Neurosci. Revs.* 3: 362–370.

- Milam, A.H., Dacey, D.M., and Dizhoor, A.M. 1993. Recoverin immunoreactivity in mammalian cone bipolar cells. *Vis. Neurosci.* 10: 1–12.
- Miles, R. 1990. Variation in strength of inhibitory synapses in the CA3 region of guinea-pig hippocampus in vitro. *J. Physiol. (Lond.)* 431: 659–676.
- Miles, R., Toth, K., Gulyas, A.I., Hajos, H., and Freund, T.F. 1996. Differences between somatic and dendritic inhibition in the hippocampus. *Neuron* 16: 815–823.
- Miles, R., and Wong, R.K.S. 1984. Unitary inhibitory synaptic potentials in the guinea-pig hippocampus in vitro. *J. Physiol. (Lond.)* 356: 97–113.
- Miles, R., and Wong, R.K.S. 1986. Excitatory synaptic interactions between CA3 neurones in the guinea-pig hippocampus. *J. Physiol. (Lond.)* 373: 397–418.
- Miller, C. 1989. Genetic manipulation of ion channels: a new approach to structure and mechanism. *Neuron* 2: 1195–1205.
- Miller, J.P., Rall, W., and Rinzel, J. 1985. Synaptic amplification by active membrane in dendritic spines. *Brain Res.* 325: 325–330.
- Miller, R.F., and Bloomfield, S.A. 1983. Electroanatomy of a unique amacrine cell in the rabbit retina. *Proc. Natl. Acad. Sci. U.S.A.* 80: 3069–3073.
- Milner, B., Squire, L.R., and Kandel, E.R. 1998. Cognitive neuroscience and the study of memory. *Neuron* 20: 445–468.
- Mills, S.L., and Massey, S.C. 1991. Labeling and distribution of AII amacrine cells in the rabbit retina. *J. Comp. Neurol.* 304: 491–501.
- Mills, S.L., and Massey, S.C. 1994. Distribution and coverage of A- and B-type horizontal cells stained with neurobiotin in the rabbit retina. *Vis. Neurosci.* 11: 549–560.
- Mills, S.L., and Massey, S.C. 1995. Differential properties of two gap junctional pathways made by AII amacrine cells. *Nature* 377: 734–737.
- Mills, S.L., and Massey, S.C. 1999. AII amacrine cells limit scotopic acuity in central macaque retina: a confocal analysis of calretinin labeling. *J. Comp. Neurol.* 411: 19–34.
- Mintz, I.M., and Bean, B.P. 1993. GABA-B receptor inhibition of P-type Ca^{2+} channels in central neurons. *Neuron* 10: 889–898.
- Misgeld, U., and Frotscher, M. 1986. Postsynaptic-GABAergic inhibition of non-pyramidal neurons in the guinea-pig hippocampus. *Neuroscience* 19: 193–206.
- Mitchison, G. 1992. Axonal trees and cortical architecture. *Trends Neurosci.* 15: 122–126.
- Mitzdorf, U. 1985. Current source-density method and application in cat cerebral cortex: investigation of evoked potentials and EEG phenomena. *Physiol. Rev.* 65: 37–100.
- Miyakawa, H., Ross, W.N., Jaffe, D., Callaway, J.C., Lasser-Ross, N., Lisman, J.E., and Johnston, D. 1992. Synaptically activated increases in Ca^{2+} concentration in hippocampal CA1 pyramidal cells are primarily due to voltage-gated Ca^{2+} channels. *Neuron* 9: 1163–1173.
- Miyashita, C., and Chang, Y. 1988. Neuronal correlate of pictorial short-term memory in the primate temporal cortex. *Nature* 331: 68–70.
- Miyashita, Y. 1988. Neuronal correlate of visual associative long-term memory in the primate temporal cortex. *Nature* 335: 817–820.
- Mody, I., Koninck, Y.D., Otis, T.S., and Soltesz, I. 1994. Bridging the cleft at GABA synapses in the brain. *Trends Neurosci.* 17: 517–525.
- Molitor, S.C., and Manis, P.B. 1999. Voltage-gated Ca^{2+} conductances in acutely isolated guinea pig dorsal cochlear nucleus neurons. *J. Neurophysiol.* 81: 985–998.
- Mollon, J.D., and Bowmaker, J.K. 1992. The spatial arrangement of cones in the primate fovea. *Nature* 360: 677–679.
- Mombaerts, P. 1999. Molecular biology of odorant receptors in vertebrates. *Annu. Rev. Neurosci.* 22: 487–509.
- Mombaerts, P. 1999. Seven-transmembrane proteins as odorant and chemosensory receptors. *Science* 286: 707–711.

- Mombaerts, P., Wang, F., Dulac, C., Chao, S.K., Nemes, A., Mendelsohn, M., Edmondson, J., and Axel, R. 1996. Visualizing an olfactory sensory map. *Cell* 87: 675–686.
- Momiyama, T., and Koga, E. 2000. Dopamine D2-like receptors selectively block N-type Ca^{2+} channels to reduce GABA release onto rat striatal cholinergic interneurons. *J. Physiol. (Lond.)* 533: 479–492.
- Monaghan, D.T., Holets, V.R., Toy, D.W., and Cotman, C.W. 1983. Anatomical distributions of four pharmacologically distinct [3H]-1-glutamate binding sites. *Nature* 306: 176–179.
- Montague, A.A., and Greer, C.A. 1999. Differential distribution of ionotropic glutamate receptor subunits in the rat olfactory bulb. *J. Comp. Neurol.* 405: 233–246.
- Montero, V.M. 1987. Ultrastructural identification of synaptic terminals from the axon of type 3 interneurons in the cat lateral geniculate nucleus. *J. Comp. Neurol.* 264: 268–283.
- Montero, V.M. 1994. Quantitative immunogold evidence for enrichment of glutamate but not aspartate in synaptic terminals of retino-geniculate, geniculo-cortical, and cortico-geniculate axons in the cat. *Vis. Neurosci.* 11: 675–681.
- Montgomery, J.C., Coombs, S., Conley, R.A., and Bodznick, D. 1995. Hindbrain sensory processing in lateral line, electrosensory, and auditory systems: a comparative overview of anatomical and functional similarities. *Auditory Neurosci.* 1: 207–231.
- Monti-Graziadei, G., Stanley, R., and Graziadei, P. 1980. The olfactory marker protein in the olfactory system of the mouse during development. *Neuroscience* 5: 1239–1252.
- Moody, C.I., and Sillito, A.M. 1988. The role of the N-methyl-d-aspartate (NMDA) receptor in the transmission of visual information in the feline dorsal lateral geniculate nucleus (dLGN). *J. Physiol. (Lond.)* 396: 62P.
- Moore, B.C.J. 1989. *An Introduction to the Psychology of Hearing*. London: Academic Press.
- Moore, G.P., Segundo, J.P., Perkel, D.H., and Levitan, H. 1970. Statistical signs of synaptic interaction in neurons. *Biophys. J.* 10: 876–900.
- Moore, R.Y., and Card, J.P. 1984. Noradrenaline-containing neuron systems. In: *Handbook of Chemical Neuroanatomy, Vol. 2: Classical Transmitters in the CNS, Part I* (Bjorklund, A., and Hökfelt, T., eds.) Amsterdam: Elsevier, pp. 123–156.
- Moran, D., Rowles, J., and Jafek, B. 1982. Electronmicroscopy of human olfactory epithelium reveals a new cell type: the microvillar cell. *Brain Res.* 253: 39–46.
- Morest, D.K. 1964. The neuronal architecture of the medial geniculate body of the cat. *J. Anat. (Lond.)* 98: 611–630.
- Morest, D.K. 1971. Dendrodendritic synapses of cells that have axons: the fine structure of the Golgi type II cell in the medial geniculate body of the cat. *Zeitsch. Anat. Entwicklungsgeschichte* 133: 216–246.
- Morest, D.K. 1975. Synaptic relationships of Golgi type II cells in the medial geniculate body of the cat. *J. Comp. Neurol.* 162: 157–193.
- Morgan, S. L., and Teyler, T. J. 1999. VDCCs and NMDARs underlie two forms of LTP in CA1 hippocampus in vivo. *J. Neurophysiol.* 82, 736–740.
- Morgans, C.W. 2001. Localization of the α_{1F} calcium channel subunit in the rat retina. *Invest. Ophthalmol. Vis. Sci.* 42: 2414–2418.
- Mori, J., Kishi, K., and Ojima, H. 1983. Distribution of dendrites of mitral, displaced mitral, tufted, and granule cells in the rabbit olfactory bulb. *J. Comp. Neurol.* 219: 339–355.
- Mori, K. 1987. Membrane and synaptic properties of identified neurons in the olfactory bulb. *Prog. Neurobiol.* 29: 274–320.
- Mori, K., Mataga, N., and Imamura, K. 1992. Differential specificities of single mitral cells in rabbit olfactory bulb for a homologous series of fatty acid odor molecules. *J. Neurophysiol.* 67: 786–789.
- Mori, K., Nagao, H., and Yoshihara, Y. 1999. The olfactory bulb: coding and processing of odor molecule information. *Science* 286: 711–715.

- Mori, K., Nowycky, M.C., and Shepherd, G.M. 1981a. Electrophysiological analysis of mitral cells in the isolated turtle olfactory bulb. *J. Physiol. (Lond.)* 314: 281–294.
- Mori, K., Nowycky, M.C., and Shepherd, G.M. 1981b. Analysis of synaptic potentials in mitral cells in the isolated turtle olfactory bulb. *J. Physiol. (Lond.)* 314: 295–309.
- Mori, K., Nowycky, M.C., and Shepherd, G.M. 1981c. Analysis of a long-duration inhibitory potential in mitral cells in the isolated turtle olfactory bulb. *J. Physiol. (Lond.)* 314: 311–320.
- Mori, K., Nowycky, M.C., and Shepherd, G.M. 1982. Impulse activity in presynaptic dendrites: analysis of mitral cells in the isolated turtle olfactory bulb. *J. Neurosci.* 2: 497–502.
- Mori, K., and Shepherd, G.M. 1994. Emerging principles of molecular signal processing by mitral/tufted cells in the olfactory bulb. *Semin. Cell Biol.* 5: 65–74.
- Mori, K., and Yoshihara, Y. 1995. Molecular recognition and olfactory processing in the mammalian olfactory system. *Prog. Neurobiol.* 45: 585–619.
- Morrison, J.H., Benoit, R., Magistretti, P.J., Ling, N., and Bloom, F.E. 1982. Immunohistochemical distribution of pro-somatostatin-related peptides in hippocampus. *Neurosci. Lett.* 34: 137–142.
- Moruzzi, G., and Magoun, H.W. 1949. Brain stem reticular formation and activation of the EEG. *Electroencephalogr. Clin. Neurophysiol.* 1: 455–473.
- Mosbacher, J., Schoepfer, R., Monyer, H., Burnashev, N., Seeburg, P.H., and Ruppertsberg, J.P. 1994. A molecular determinant for submillisecond desensitization in glutamate receptors. *Science* 266: 1059–1062.
- Moschovakis, A.K., Burke, R.E., and Fyffe, R.E.W. 1991a. The size and dendritic structure of HRP-labeled gamma motoneurons in the cat spinal cord. *J. Comp. Neurol.* 311: 531–545.
- Moschovakis, A.K., Sholomenko, G.N., and Burke, R.E. 1991b. Differential control of short latency cutaneous excitation in cat FDL motoneurons during fictive locomotion. *Exp. Brain Res.* 83: 489–501.
- Mosko, S., Lynch, G., and Cotman, C.W. 1973. The distribution of septal projections to the hippocampus of the rat. *J. Comp. Neurol.* 152: 163–174.
- Mott, D.D., and Lewis, D.V. 1991. Facilitation of the induction of long-term potentiation by GABAB receptors. *Science* 252: 1718–1720.
- Moyano, H.F., Cinelli, A.R., and Molina, J.C. 1985. Current generators and properties of early components evoked in rat olfactory cortex. *Brain Res. Bull.* 15: 237–248.
- Mugnaini, E. 1985. GABA neurons in the superficial layers of rat dorsal cochlear nucleus: light and electron microscopic immunocytochemistry. *J. Comp. Neurol.* 235: 537–570.
- Mugnaini, E., and Morgan, J.I. 1987. The neuropeptide cerebellin is a marker for two similar neuronal circuits in rat brain. *Proc. Natl. Acad. Sci. U.S.A.* 84: 8692–8696.
- Mugnaini, E., Oertel, W.H., and Wouterlood, F.F. 1984. Immunocytochemical localization of GABA neurons and dopamine neurons in the rat main and accessory olfactory bulbs. *Neurosci. Lett.* 47: 221–226.
- Mugnaini, E., Osen, K.K., Dahl, A.L., Friedrich Jr., V.L., and Korte, G. 1980. Fine structure of granule cells and related interneurons (termed Golgi cells) in the cochlear nuclear complex of cat, rat, and mouse. *J. Neurocytol.* 9: 537–570.
- Mugnaini, E., Warr, W.B., and Osen, K.K. 1980. Distribution and light microscopic features of granule cells in the cochlear nuclei of cat, rat, and mouse. *J. Comp. Neurol.* 191: 581–606.
- Muhlethaler, M., Walton, K., and Llinás, R. 1993. The isolated and perfused brain of the guinea-pig *in vitro*. *Eur. J. Neurosci.* 5: 915–926.
- Muir, R.B., and Porter, R. 1973. The effect of a preceding stimulus on temporal facilitation at corticomotoneuronal synapses. *J. Physiol. (Lond.)* 228: 749–763.
- Mukherjee, P., and Kaplan, E. 1995. Dynamics of neurons in the cat lateral geniculate nucleus *in vivo* electrophysiology and computational modeling. *J. Neurophysiol.* 74: 1222–1243.
- Mulders, W.H., Winter, I.M., and Robertson, D. 2002. Dual action of olivocochlear collaterals in the guinea pig cochlear nucleus. *Hear. Res.* 174: 264–280.

- Mulkey, R.M., and Malenka, R.C. 1992. Mechanisms underlying induction of homosynaptic long-term depression in area CA1 of the hippocampus. *Neuron* 9: 967–975.
- Müller, B., and Peichl, L. 1993. Horizontal cells in the cone-dominated tree shrew retina: morphology, photoreceptor contacts, and topographical distribution. *J. Neurosci.* 13: 3628–3646.
- Muller, W., and Connor, J. 1991. Dendritic spines as individual neuronal compartments for synaptic Ca^{2+} responses. *Neuron* 354: 73–76.
- Mulligan, K., and Tork, I. 1988. Serotonergic innervation of the cat cerebral cortex. *J. Comp. Neurol.* 270: 86–110.
- Mumford, D. 1994. Neuronal architectures for pattern theoretic problems. In: *Large-Scale Neuronal Theories of the Brain* (Koch, C., and Davis, J. eds.). Cambridge: MIT Press, pp. 125–152.
- Munson, J., and Sypert, G. 1979a. Properties of single central Ia afferent fibres projecting to motoneurons. *J. Physiol. (Lond.)* 296: 315–327.
- Munson, J., and Sypert, G. 1979b. Properties of single fiber excitatory post-synaptic potentials in triceps surae motoneurons. *J. Physiol. (Lond.)* 296: 329–342.
- Murakami, M., Miyachi, E.-I., and Takahashi, K.-I. 1995. Modulation of gap junctions between horizontal cells by second messengers. In: *Progress in Retinal and Eye Research*. London: Elsevier Science, pp. 197–221.
- Muresan, V., Lyass, A., and Schnapp, B.J. 1999. The kinesin motor KIF3A is a component of the presynaptic ribbon in vertebrate photoreceptors. *J. Neurosci.* 19: 1027–1037.
- Murphy, P.C., and Sillito, A.M. 1996. Functional morphology of the feedback pathway from area 17 of the cat visual cortex to the lateral geniculate nucleus. *J. Neurosci.* 16: 1180–1192.
- Murphy, P.C., Duckett, S.G., and Sillito, A.M. 1999. Feedback connections to the lateral geniculate nucleus and cortical response properties. *Science* 286: 1552–1554.
- Murthy, K.S.K., Ledbetter, W.D., Eidelberg, E., Cameron, W.E., and Petit, J. 1982. Histochemical evidence for the existence of skeletofusimotor (β) innervation in the primate. *Exp. Brain Res.* 46: 186–190.
- Musicant, A.D., Chan, J.C.K., and Hind, J.E. 1990. Direction-dependent spectral properties of cat external ear: new data and cross-species comparisons. *J. Acoust. Soc. Am.* 87: 757–781.
- Naber, P.A., Lopes da Silva, F.H., and Witter, M.P. 2001. Reciprocal connections between the entorhinal cortex and hippocampal fields CA1 and the subiculum are in register with the projections from CA1 to the subiculum. *Hippocampus* 11: 99–104.
- Naegele, J., and Barnstable, C. 1989. Molecular determinants of GABAergic local circuit neurons in the cerebral cortex. *Trends Neurosci.* 12: 28–34.
- Nafstad, P.H.J. 1967. An electron microscope study on the termination of the perforant path fibres in the hippocampus and the fascia dentata. *Z. Zellforsch.* 76: 532–542.
- Nagao, H., Yamaguchi, M., Takahashi, Y., and Mori, K. 2002. Grouping and representation of odorant receptors in domains of the olfactory bulb sensory map. *Microsc. Res. Tech.* 58: 168–175.
- Nakamura, H., Gattass, R., Desimone, R., and Ungerleider, L.G. 1993. The modular organization of projections from areas V1 and V2 to areas V4 and TEO in macaques. *J. Neurosci.* 13: 3681–3691.
- Nakamura, Y., McGuire, B.A., and Sterling, P. 1980. Interplexiform cell in cat retina: Identification by uptake of gamma-[3H]aminobutyric acid and serial reconstruction. *Proc. Natl. Acad. Sci. U.S.A.* 77: 658–661.
- Nakanishi, H., Kita, H., and Kitai, S.T. 1991. Intracellular study of rat entopeduncular nucleus neurons in an in vitro slice preparation response to subthalamic stimulation. *Brain Res.* 549: 285–291.
- Nakazawa, K., Quirk, M.C., Chitwood, R.A., Watanabe, M., Yeckel, M.F., Sun, L.D., Kato, A., Carr, C.A., Johnston, D., Wilson, M.A., and Tonegawa, S. 2002. Requirement for hippocampal CA3 NMDA receptors in associative memory recall. *Science* 297: 211–8.

- Nambu, A., and Linás, R. 1994. Electrophysiology of globus pallidus neurons in vitro. *J. Neurophysiol.* 72: 1127–1139.
- Narasimhan, K., and Linden, D.J. 1996. Defining a minimal computational unit for cerebellar long-term depression. *Neuron* 17: 333–41.
- Nardone, A., Romano, C., and Schieppati, M. 1989. Selective recruitment of high-threshold human motor units during voluntary isotonic lengthening of active muscles. *J. Physiol. (Lond.)* 409: 451–471.
- Nawy, S. 1999. The metabotropic receptor mGluR6 may signal through G_o, but not phosphodiesterase, in retinal bipolar cells. *J. Neurosci.* 19: 2938–2944.
- Nawy, S., and Jahr, C.E. 1990. Suppression by glutamate of cGMP-activated conductance in retinal bipolar cells. *Nature* 346: 269–271.
- Nayeem, N., Green, T., I.M., and Barnard, E. 1994. Quaternary structure of the native GABA_A receptor determined by electron microscopic image analysis. *J. Neurochem.* 62: 815–818.
- Nayeem, N., Green, T., Martin, I., and Barnard, E. 1994. Quaternary structure of the native GABA_A receptor determined by electron microscopic image analysis. *J. Neurochem.* 62: 815–8.
- Neer, E.J. 1995. Heterotrimeric G proteins: organizers of transmembrane signals. *Cell* 80: 249–257.
- Neher, E. 1971. Two fast transient current components during voltage clamp on snail neurons. *J. Gen. Physiol.* 58: 36–53.
- Neher, E., and Sakmann, B. 1976. Single-channel currents recorded from membrane of denervated frog muscle fibers. *Nature* 260: 799–802.
- Neher, E., and Sakmann, B. 1992. The patch clamp technique. *Sci. Am.* 266: 28–35.
- Neitz, J., Carroll, J., Yamauchi, Y., Neitz, M., and Williams, D.R. 2002. Color perception is mediated by a plastic neural mechanism that is adjustable in adults. *Neuron* 35: 783–792.
- Neitz, M., Neitz, J., and Jacobs, G.H. 1991. Spectral tuning of pigments underlying red-green color vision. *Science* 252: 971–974.
- Nelken, I., and Young, E.D. 1994. Two separate inhibitory mechanisms shape the responses of dorsal cochlear nucleus type IV units to narrowband and wideband stimuli. *J. Neurophysiol.* 71: 2446–2462.
- Nelken, I., and Young, E.D. 1996. Why do cats need a dorsal cochlear nucleus? *Rev. Clin. Basic Pharmacol.* 7: 199–220.
- Nelson, P., Famiglietti, E.V., and Kolb, H. 1978. Intracellular staining reveals different levels of stratification for ON- and OFF-center ganglion cells of the cat retina. *J. Neurophysiol.* 41: 472–483.
- Nelson, P.G. 1966. Interaction between spinal motoneurons of the cat. *J. Neurophysiol.* 29: 275–287.
- Nelson, R. 1977. Cat cones have rod input: a comparison of the response properties of cones and horizontal cell bodies in the retina of the cat. *J. Comp. Neurol.* 172: 109–136.
- Nelson, R. 1982. AII amacrine cells quicken time course of rod signals in the cat retina. *J. Neurophysiol.* 47: 928–947.
- Nelson, S. 2002. Cortical microcircuits: diverse or canonical? *Neuron* 36: 19–27.
- Nelson, R., and Kolb, H. 1983. Synaptic patterns and response properties of bipolar and ganglion cells in the cat retina. *Vis. Res.* 23: 1183–1195.
- Nelson, R., and Kolb, H. 1985. A17: a broad-field amacrine cell in the rod system of the cat retina. *J. Neurophysiol.* 54: 592–614.
- Nemeth, P.M. 1990. Metabolic fiber types and influences on their transformation. In: *The Segmental Motor System* (Binder, M.D., and Mendell, L.M., eds.) New York: Oxford University Press, pp. 258–277.
- Nemitz, J.W., and Goldberg, S.J. 1983. Neuronal responses of rat pyriform cortex to odor stimulation: an extracellular and intracellular study. *J. Neurophysiol.* 49: 188–203.

- Nernst, W. 1888. On the kinetics of substances in solution. [Translated from *Z. Physik. Chemie* 2.] In: *Cell Membrane Permeability and Transport* (Kepner, G.R., ed.). 1979 Stroudsburg, PA: Dowden, Hutchinson and Ross pp. 613–622, 634–637.
- Neves, S.R., Ram, P.T., and Iyengar, R. 2002. G protein pathways. *Science* 296: 1636–1639.
- Neveu, D., and Zucker, R. 1996. Postsynaptic levels of $[Ca^{2+}]_i$ needed to trigger LTD and LTP. *Neuron* 16: 619–629.
- Neville, K.R., and Lytton, W.W. 1999. Potentiation of Ca^{2+} influx through NMDA channels by action potentials: a computer model. *NeuroReport* 10: 3711–3716.
- Newberry, N.R., and Nicoll, R.A. 1985. Comparison of the action of baclofen with gamma-aminobutyric acid on rat hippocampal pyramidal cells in vitro. *J. Physiol. (Lond.)* 360: 161–185.
- Newman, E., and Reichenbach, A. 1996. The Müller cell: a functional element of the retina. *Trends Neurosci.* 19: 307–312.
- Newman, E.A. 1986. High potassium conductance in astrocyte endfeet. *Science* 233: 453–454.
- Newman, E.A. 1987. Distribution of potassium conductance in mammalian muller(glial) cells: a comparative study. *J. Neurosci.* 7: 2423–2432.
- Newman, E.A. 2003. Glial cell inhibition of neurons by release of ATP. (in press)
- Nguyen, P.V., Marin, L., and Atwood, H.L. 1997. Synaptic physiology and mitochondrial function in crayfish tonic and phasic motor neurons. *J. Neurophysiol.* 78: 281–294.
- Nicholls, J.G., Martin, A.R., and Wallace, B.G. 1992. *From Neuron to Brain*, 3rd edition. Sunderland, MA: Sinauer Associates.
- Nickell, W.T., and Shipley, M.T. 1993. Evidence for presynaptic inhibition of the olfactory commissural pathway by cholinergic agonists and stimulation of the nucleus of the diagonal band. *J. Neurosci.* 13: 650–659.
- Nickell, W.T., Behbehani, M.M., and Shipley, M.T. 1994. Evidence for GABAB-mediated inhibition of transmission from the olfactory nerve to mitral cells in the rat olfactory bulb. *Brain Res. Bull.* 35: 119–123.
- Nicol, M.J., and Walmsley, B. 2002. Ultrastructural basis of synaptic transmission between endbulbs of Held and bushy cells in the rat cochlear nucleus. *J. Physiol. (Lond.)* 539: 713–723.
- Nicola, S.M., Surmeier, D.J., and Malenka, R.C. 2000. Dopaminergic modulation of neuronal excitability in the striatum and nucleus accumbens. *Annu. Rev. Neurosci.* 23: 185–215.
- Nicolelis, M.A., and Fanselow, E.E. 2002. Thalamocortical optimization of tactile processing according to behavioral state. [erratum appears in *Nat. Neurosci.* (2002) 5:704.]. *Nat. Neurosci.* 5: 517–523.
- Nicoll, R.A. 1970. Recurrent excitation of secondary olfactory neurons: a possible mechanism for signal amplification. *Science* 171: 824–825.
- Nicoll, R.A. 1971. Pharmacological evidence for GABA as the transmitter in granule cell inhibition in the olfactory bulb. *Brain Res.* 35: 137–149.
- Nicoll, R.A. 1988. The coupling of neurotransmitter receptors to ion channels in the brain. *Science* 241: 545–551.
- Nicoll, R.A., and Malenka, R.C. 1995. Contrasting properties of two forms of long-term potentiation in the hippocampus. *Nature* 377: 115–118.
- Nicoll, R.A., Alger, B.E., and Jahr, C.E. 1980a. Enkephalin blocks inhibitory pathways in the vertebrate CNS. *Nature* 287: 22–25.
- Nicoll, R.A., Alger, B.E., and Jahr, C.E. 1980b. Peptides as putative excitatory neurotransmitters: carnosine, enkephalin, substance P and TRH. *Proc. R. Soc. Lond. B.* 210: 133–149.
- Nicoll, R.A., Kauer, J.A., and Malenka, R.C. 1988. The current excitement in long-term potentiation. *Neuron* 1: 97–103.
- Nicoll, R.A., Malenka, R.C., and Kauer, J.A. 1990. Functional comparison of neurotransmitter receptor subtypes in mammalian central nervous system. *Physiol. Rev.* 70: 513–565.

- Nielsen, J., and Kagamihara, Y. 1993. Differential projection of the sural nerve to early and late recruited human tibialis anterior motor units: change of recruitment gain. *Acta Physiol. Scand.* 147: 385–401.
- Nielsen, J., Petersen, N., Deuschl, G., and Ballegaard, M. 1993. Task-related changes in the effect of magnetic brain-stimulation on spinal neurons in man. *J. Physiol. (Lond.)* 471: 223–243.
- Nimchinsky, E.A., Sabatini, B.L., and Svoboda, K. 2002. Structure and function of dendritic spines. *Annu. Rev. Physiol.* 64: 313–353.
- Nini, A., Fiengold, A., Slovlin, H., and Bergman, H. 1995. Neurons in the globus pallidus do not show correlated activity in the normal monkey, but phase-locked oscillations appear in the MPTP model of parkinsonism. *J. Neurophysiol.* 74: 1800–1805.
- Nisenbaum, E.S., and Wilson, C.J. 1995. Potassium currents responsible for inward and outward rectification in rat neostriatal spiny projection neurons. *J. Neurosci.* 15: 4449–4463.
- Nisenbaum, E.S., Wilson, C.J., Foehring, R.C., and Surmeier, D.J. 1996. Isolation and characterization of a persistent potassium current in neostriatal neurons. *J. Neurophysiol.* 76: 1180–1194.
- Nishimura, Y., and Rakic, P. 1987a. Development of the rhesus monkey retina. II. A three-dimensional analysis of the sequences of synaptic combinations in the inner plexiform layer. *J. Comp. Neurol.* 262: 290–313.
- Nishimura, Y., and Rakic, P. 1987b. Synaptogenesis in primate retina proceeds from the ganglion cells towards the photoreceptors. *Neurosci. Res. Suppl.* 6: 253–268.
- Nistri, A. 1983. Spinal cord pharmacology of GABA and chemically related amino acids. In: *Handbook of the Spinal Cord, Vol. 1: Pharmacology* (Davidoff, R.E., ed.) New York: Marcel Dekker, pp. 45–104.
- Noda, H. 1975. Depression in the excitability of relay cells of lateral geniculate nucleus following saccadic eye movements in the cat. *J. Physiol. (Lond.)* 249: 87–102.
- Nomura, A., Shigemoto, R., Nakamura, Y., Okamoto, N., Mizuno, N., and Nakanishi, S. 1994. Developmentally regulated postsynaptic localization of a metabotropic glutamate-receptor in rat rod bipolar cells. *Cell* 77: 361–369.
- North, R.A. 1987. Receptors of individual neurones. *Neuroscience* 17: 899–907.
- Nowycky, M.C., Fox, A.P., and Tsien, R.W. 1985. Three types of neuronal calcium channel with different calcium agonist sensitivity. *Nature* 316: 440–443.
- Nowycky, M.C., Mori, K., and Shepherd, G.M. 1981a. GABAergic mechanisms of dendrodendritic synapses in isolated turtle olfactory bulb. *J. Neurophysiol.* 46: 693–648.
- Nowycky, M.C., Mori, K., and Shepherd, G.M. 1981b. Blockade of synaptic inhibition reveals long-lasting synaptic excitation in isolated turtle olfactory bulb. *J. Neurophysiol.* 46: 649–658.
- Nyakas, C., Luiten, P.G.M., Spencer, D.G., and Traber, J. 1987. Detailed projection patterns of septal and diagonal band efferents to the hippocampus in the rat with emphasis on innervation of CA1 and dentate gyrus. *Brain Res. Bull.* 18: 533–545.
- O'Keefe, J. 1979. A review of the hippocampal place cells. *Prog. Neurobiol.* 13: 419–439.
- O'Leary, J.L. 1937. Structure of the primary olfactory cortex of the mouse. *J. Comp. Neurol.* 67: 1–31.
- O'Malley, D.M., Sandell, J.H., and Masland, R.H. 1994. Co-release of acetylcholine and GABA by the starburst amacrine cells. *J. Neurosci.* 12: 1394–1408.
- Obata, K., Ito, M., Ochi, R., and Sato, N. 1967. Pharmacological properties of the postsynaptic inhibition by Purkinje cell axons and the action of gamma-aminobutyric acid on Deiters neurons. *Exp. Brain Res.* 4: 43–57.
- Obata, K., Takeda, K., and Shinozaki, H. 1970. Further study on pharmacological properties of the cerebellar-induced inhibition of Deiters neurones. *Exp. Brain Res.* 11: 327–342.

- O'Brien, B.J., Isayama, T., Richardson, R., and Berson, D.M. 2002. Intrinsic physiological properties of cat retinal ganglion cells. *J. Physiol. (Lond.)* 538: 787–802.
- O'Donovan, M.J., Pinter, M.J., Dum, R.P., and Burke, R.E. 1982. The actions of FDL and FHL muscles in intact cats: Functional dissociation between anatomical synergists. *J. Neurophysiol.* 47: 1126–1143.
- Oertel, D. 1983. Synaptic responses and electrical properties of cells in brain slices of the mouse anteroventral cochlear nucleus. *J. Neurosci.* 3: 2043–2053.
- Oertel, D. 1997. Encoding of timing in the brain stem auditory nuclei of vertebrates. *Neuron* 19: 959–962.
- Oertel, D., and Wu, S.H. 1989. Morphology and physiology of cells in slice preparations of the dorsal cochlear nucleus of mice. *J. Comp. Neurol.* 283: 228–247.
- Oertel, D., Wu, S.H., Garb, M.W., and Dizack, C. 1990. Morphology and physiology of cells in slice preparations of the posteroventral cochlear nucleus of mice. *J. Comp. Neurol.* 295: 136–154.
- Oertel, D., Wu, S.H., and Hirsch, J.A. 1988. Electrical characteristics of cells and neuronal circuitry in the cochlear nuclei studied with intracellular recordings from brain slices. In: *Auditory Function: Neurobiological Bases of Hearing* (Edelman, G.M., Gall, W.E., and Cowan, W.M., eds.) New York: Wiley, pp. 313–336.
- Oertel, W.H., Schmechel, D.E., Mugnaini, E., Tappaz, M.L., and Kopin, I.J. 1981. Immunocytochemical localization of glutamate decarboxylase in rat cerebellum with a new antiserum. *Neuroscience* 6: 2715–2735.
- Ogata, N., and Ohishi, Y. 2002. Molecular diversity of structure and function of the voltage-gated Na⁺ channels. *Jpn. J. Pharmacol.* 88: 365–377.
- Oertel, W.H., Tappaz, M.L., Berod, A., and Mugnaini, E. 1982. Two-color immunohistochemistry for dopamine and GABA neurons in rat substantia nigra and zona incerta. *Brain Res. Bull.* 9: 463–474.
- Ogata, N., and Ohishi, Y. 2002. Molecular diversity of structure and function of the voltage-gated Na⁺ channels. *Jpn. J. Pharmacol.* 88: 365–377.
- Ogawa, M., Miyata, T., Nakajima, K., Yagu, K., Seike, M., Ikenaka, K., Yamamoto, H., and Mikoshiba, K. 1995. The Reeler gene-associated antigen in Cajal-Retzius neurons is a crucial molecule for laminar organization of cortical neurons. *Neuron* 14: 899–912.
- Ogawa, T., Ito, S., and Kato, H. 1981. Membrane characteristics of visual cortical neurons in *in vitro* slices. *Brain Res.* 226: 315–319.
- Ogawa, T., Kato, H., and Ito, S. 1986. Studies on inhibitory neurotransmission in visual cortex *in vitro*. In: *Visual Neuroscience* (Pettigrew, J., Sanderson, K., and Levick, W., eds.) Cambridge: Cambridge University Press, pp. 280–289.
- Ogren, M.P., and Hendrickson, A.E. 1979. The morphology and distribution of striate cortex terminals in the inferior and lateral subdivisions of the Macaca monkey pulvinar. *J. Comp. Neurol.* 188: 179–199.
- Ohara, P.T., and Lieberman, A.R. 1985. The thalamic reticular nucleus of the adult rat experimental anatomical studies. *J. Neurocytol.* 14: 365–411.
- Ohara, P.T., Lieberman, A.R., Hunt, S.P., and Wu, J.Y. 1983. Neural elements containing glutamic acid decarboxylase (GAD) in the dorsal lateral geniculate nucleus of the rat: immunohistochemical studies by light and electron microscopy. *Neuroscience* 8: 189–211.
- Ohlroge, M., Doucet, J.R., and Ryugo, D.K. 2001. Projections of the pontine nuclei to the cochlear nucleus in rats. *J. Comp. Neurol.* 436: 290–303.
- Ohtsuka, T. 1985. Relation of spectral types to oil droplets in cones of turtle retina. *Science* 229: 874–877.
- Ojima, H. 1994. Terminal morphology and distribution of corticothalamic fibers originating from layers 5 and 6 of cat primary auditory cortex. *Cereb. Cortex* 4: 646–663.

- Ojima, H., Mori, K., and Kishi, K. 1984. The trajectory of mitral cell axons in the rabbit olfactory cortex revealed by intracellular HRP injection. *J. Comp. Neurol.* 230: 77–87.
- Okamoto, K., Quastel, D.M.J., and Quastel, J.H. 1976. Action of amino acids and convulsants on cerebellar spontaneous action potentials in vitro: Effects of deprivation of Ca^{2+} , K^+ or Na^+ . *Brain Res.* 206: 371–386.
- Okamoto, K., and Sakai, Y. 1981. Inhibitory actions of taurocyamine, hypotaurine, homotaurine, taurine and GABA on spike discharges of Purkinje cells, and localization of sensitive sites, in guinea pig cerebellar slices. *Brain Res.* 206: 371–386.
- O'Leary, J.L. 1937. Structure of the primary olfactory cortex of the mouse. *J. Comp. Neurol.* 67: 1–31.
- Oleskevich, S., Alvarez, F., and Walmsley, B. 1999. Glycinergic miniature synaptic currents and receptor cluster sizes differ between spinal cord interneurons. *J. Neurophysiol.* 82: 312–319.
- Oleskevich, S., and Descarries, L. 1990. Quantified distribution of the serotonin innervation in adult rat hippocampus. *Neuroscience* 34: 19–33.
- Oliver, D.L., and Huerta, M.F. 1992. Inferior and superior colliculi. In: *The Mammalian Auditory Pathway: Neuroanatomy* (Webster, D.B., Popper, A.N., and Fay, R.R., eds.) New York: Springer-Verlag, pp. 168–221.
- Olson, D., and Breckenridge, B. 1976. Calcium ion effects on guanylate cyclase of brain. *Life Sci.* 18: 935–940.
- O'Malley, D.M., Sandell, J.H., and Masland, R.H. 1994. Co-release of acetylcholine and GABA by the starburst amacrine cells. *J. Neurosci.* 12: 1394–1408.
- Ono, K., Tomasiewicz, H., Magnuson, T., and Rutishauser, U. 1994. N-CAM mutation inhibits tangential neuronal migration and is phenocopied by enzymatic removal of polysialic acid. *Neuron* 13: 595–609.
- Oorschot, D.E. 1996. Total number of neurons in the neostriatal, pallidal, subthalamic, and substantia nigral nuclei of the rat basal ganglia—a stereological study using the Cavalieri and optical disector methods. *J. Comp. Neurol.* 366: 580–599.
- Örnung, G., Shupliakov, O., Ottersen, O.P., Storm-Mathisen, J., and Cullheim, S. 1994. Immunohistochemical evidence for coexistence of glycine and GABA in nerve terminals on cat spinal motoneurons: an ultrastructural study. *NeuroReport* 5: 889–892.
- Orona, E., Rainer, E., and Scott, J. 1984. Dendritic and axonal organization of mitral and tufted cells in the rat olfactory bulb. *J. Comp. Neurol.* 226: 346–356.
- Orona, E., Scott, J., and Rainer, E. 1983. Different granule cell populations innervate superficial and deep regions of the external plexiform layer in rat olfactory bulb. *J. Comp. Neurol.* 217: 227–237.
- Osborn, C.E., and Poppele, R.E. 1993. Sensory integration by the dorsal spinocerebellar tract circuitry. *Neuroscience* 54: 945–956.
- Osen, K.K. 1969. Cytoarchitecture of the cochlear nuclei in the cat. *J. Comp. Neurol.* 136: 453–482.
- Osen, K.K. 1970a. Course and termination of the primary afferents in the cochlear nuclei of the cat. *Arch. Ital. Biol.* 108: 21–51.
- Osen, K.K. 1970b. Afferent and efferent connections of three well-defined cell types of the cat cochlear nucleus. In: *Excitatory Synaptic Mechanisms* (Anderson, P., and Jansen, J.K.S., eds.) Oslo: Universitetsforlaget, pp. 295–300.
- Osen, K.K. 1983. Orientation of dendritic arbors studied in Golgi sections of the cat dorsal cochlear nucleus. In: *Mechanisms of Hearing* (Webster, W.R., and Aitkin, L.M., eds.) Clayton: Monash University Press, pp. 83–89.
- Osen, K.K., Ottersen, O.P., and Storm-Mathisen, J. 1990. Colocalization of glycine-like and GABA-like immunoreactivities. A semiquantitative study of individual neurons in the dorsal cochlear nucleus of cat. In: *Glycine Neurotransmission* (Ottersen, O.P., and Storm-Mathisen, J., eds.) New York: John Wiley & Sons, pp. 417–451.

- Osen, K.K., Storm-Mathisen, J., Ottersen, O.P., and Dihle, B. 1995. Glutamate is concentrated in and released from parallel fiber terminals in the dorsal cochlear nucleus: a quantitative immunocytochemical analysis in guinea pigs. *J. Comp. Neurol.* 357: 482–500.
- Ostapoff, E.M., Benson, C.G., and Saint Marie, R.L. 1997. GABA- and glycine-immunoreactive projections from the superior olivary complex to the cochlear nucleus in guinea pig. *J. Comp. Neurol.* 381: 500–511.
- Ostapoff, E.M., Feng, J.J., and Morest, D.K. 1994. A physiological and structural study of neuron types in the cochlear nucleus. II. Neuron types and their structural correlation with response properties. *J. Comp. Neurol.* 346: 19–42.
- Ostapoff, E.M., and Morest, D.K. 1991. Synaptic organization of globular bushy cells in the ventral cochlear nucleus of the cat: a quantitative study. *J. Comp. Neurol.* 314: 598–613.
- Ottersen, O.P., and Laake, J.H. 1992. Light and electron microscopic immunocytochemistry of putative neurotransmitter amino acids in the cerebellum with some observations on the distribution of glutamine. In: *The Cerebellum Revisited* (Linás, R., and Sotelo, C., eds.) New York: Springer-Verlag, pp. 116–134.
- Ottersen, O.P. 1993. Neurotransmitters in the cerebellum. *Rev. Neurol. (Paris)*. 149: 629–636.
- Ottersen, O.P., Laake, J.H., and Storm-Mathisen, J. 1990a. Demonstration of a releasable pool of glutamate in cerebellar mossy and parallel fibre terminals by means of light and electron microscopic immunocytochemistry. *Arch. Ital. Biol.* 128: 111–125.
- Ottersen, O.P., Storm-Mathisen, J., and Laake, J.H. 1990b. Cellular and subcellular localization of glycine studied by quantitative electron microscopic immunocytochemistry. In: *Glycine Neurotransmission* (Ottersen, O.P., and Storm-Mathisen, J., eds.) Chichester: Wiley, pp. 303–328.
- Otto, T., and Eichenbaum, H. 1992. Olfactory learning and memory in the rat: a “model system” for studies of the neurobiology of memory. In: *The Science of Olfaction* (Chobor, K.L., and Serby, M., eds.) New York: Springer-Verlag, pp. 213–244.
- Ouardouz, M., and Lacaille, J.C. 1997. Properties of unitary IPSCs in hippocampal pyramidal cells originating from different types of interneurons in young rats. *J. Neurophysiol.* 77: 1939–1949.
- Oyster, C.W., Takahashi, E.S., Cilluffo, M., and Brecha, N.C. 1985. Morphology and distribution of tyrosine hydroxylase-like immunoreactive neurons in the cat retina. *Proc. Natl. Acad. Sci. U.S.A.* 82: 6335–6339.
- Packer, O., Hendrickson, A., and Curcio, C. 1989. Photoreceptor topography of the retina in the adult pigtail Macaque (*Macaca nemestrina*). *J. Comp. Neurol.* 288: 165–183.
- Packer, O.S., Williams, D.R., and Bensinger, D.G. 1996. Photopigment transmittance imaging of the primate photoreceptor mosaic. *J. Neurosci.* 16: 2251–2260.
- Palay, S.L., and Chan-Palay, V. 1974. *Cerebellar Cortex: Cytology and Organization*. New York: Springer-Verlag.
- Palkovits, M., and Brownstein, M.J. 1985. Distribution of neuropeptides in the central nervous system using biochemical micromethods. In: *Handbook of Chemical Neuroanatomy*, Vol. 4: GABA and Neuropeptides in the CNS, Part I (Björklund, A., and Hökfelt, T., eds.) Amsterdam: Elsevier, pp. 1–71.
- Palmer, A.R., Jiang, D., and Marshall, D.H. 1996. Responses of ventral cochlear nucleus onset and chopper units as a function of signal bandwidth. *J. Neurophysiol.* 75: 780–794.
- Palmer, L.A., and Davis, T.L. 1981. Receptive field structure in cat striate cortex. *J. Neurophysiol.* 46: 260–276.
- Panico, J., and Sterling, P. 1995. Retinal neurons and vessels are not fractal but space filling. *J. Comp. Neurol.* 361: 479–490.
- Paolini, A.G., and Clark, G.M. 1999. Intracellular responses of onset chopper neurons in the ventral cochlear nucleus to tones: evidence for dual-component processing. *J. Neurophysiol.* 81: 2347–2359.

- Paolini, A.G., Clark, G.M., and Burkitt, A.N. 1997. Intracellular responses of the rat cochlear nucleus to sound and its role in temporal coding. *NeuroReport* 8: 3415–3421.
- Papadopoulos, G., Parnevelas, J., and Buijs, R. 1987. Light and electron microscopic analysis of the noradrenaline innervation of the rat visual cortex. *J. Neurocytol.* 18: 1–10.
- Pape, H.-C., and Mager, R. 1992. Nitric oxide controls oscillatory activity in thalamocortical neurons. *Neuron* 9: 441–448.
- Pape, H.-C., and McCormick, D.A. 1989. Noradrenaline and serotonin selectively modulate thalamic burst firing by enhancing a hyperpolarization-activated cation current. *Nature* 340: 715–718.
- Pape, H.-C., and McCormick, D.A. 1995. Electrophysiological and pharmacological properties of interneurons in the cat dorsal lateral geniculate nucleus. *Neuroscience* 68: 1105–1125.
- Pape, H.-C., Budde, T., Mager, R., and Kisvárdy, Z.F. 1994. Prevention of Ca^{2+} -mediated action potentials in GABAergic local circuit neurones of rat thalamus by a transient K^{+} current. *J. Physiol. (Lond.)* 478: 403–422.
- Pape, H.-C. 1996. Queer current and pacemaker: the hyperpolarization-activated cation current in neurons. *Annu. Rev. Physiol.* 58: 299–327.
- Papp, E., Leinekugel, X., Henze, D.A., Lee, J., and Buzsáki, G. 2001. The apical shaft of CA1 pyramidal cells is under GABAergic interneuronal control. *Neuroscience* 102: 715–721.
- Parent, A., Bouchard, C., and Smith, Y. 1984. The striatopallidal and striatonigral projections—two distinct fiber systems in primate. *Brain Res.* 303: 385–390.
- Parent, A., Charara, A., and Pinault, D. 1995. Single striatofugal axons arborizing in both pallidal segments and in the substantia nigra in primates. *Brain Res.* 689: 280–284.
- Parham, K., and Kim, D.O. 1995. Spontaneous and sound-evoked discharge characteristics of complex-spiking neurons in the dorsal cochlear nucleus of the unanesthetized decerebrate cat. *J. Neurophysiol.* 73: 550–561.
- Parham, K., Bonaiuto, G., Carlson, S., Turner, J.G., D'Angelo, W.R., Bross, L.S., Fox, A., Willott, J.F., and D.O., K. 2000. Purkinje cell degeneration and control mice: responses of single units in the dorsal cochlear nucleus and the acoustic startle response. *Hear. Res.* 148: 137–152.
- Parnavelas, J. 2000. The origin and migration of cortical neurones: new vistas. *Trends Neurosci.* 23: 126–131.
- Parnevelas, J., and Papadopoulos, G. 1989. The monoaminergic innervation of the cerebral cortex is not diffuse and nonspecific. *Trends Neurosci.* 12: 315–319.
- Parra, P., Gulyas, A.I., and Miles, R. 1998. How many subtypes of inhibitory cells in the hippocampus? *Neuron* 20: 983–993.
- Parsons, J.E., Lim, E., and Voigt, H.F. 2001. Type III units in the gerbil dorsal cochlear nucleus may be spectral notch detectors. *Ann. Biomed. Eng.* 29: 887–896.
- Parsons, T., and Sterling, P. 2003. Synaptic ribbon: conveyor belt or safety belt? *Neuron* 37: 379–382.
- Parsons, T.D., Lenzi, D., Almers, W., and Roberts, W.M. 1994. Calcium-triggered exocytosis and endocytosis in an isolated presynaptic cell: Capacitance measurements in saccular hair cells. *Neuron* 13: 875–883.
- Passingham, R. 1982. *The Human Primate*. Oxford: W.H. Freeman.
- Patel, N.C., Carden, W.B., and Bickford, M.E. 1999. Synaptic targets of cholinergic terminals in the cat lateral posterior nucleus. *J. Comp. Neurol.* 410: 31–41.
- Paternostro, M.A., Reyher, C.K.H., and Brunjes, P.C. 1995. Intracellular injections of Lucifer Yellow into lightly fixed mitral cells reveal neuronal dye-coupling in the developing rat olfactory bulb. *Dev. Brain Res.* 84: 1–10.
- Patil, M.M., and Hasselmo, M.E. 1999. Modulation of inhibitory synaptic potentials in the piriform cortex. *J. Neurophysiol.* 81: 2103–2118.
- Patil, M.M., Linster, C., Lubenov, E., and Hasselmo, M.E. 1998. Cholinergic agonist carbachol

- enables associative long-term potentiation in piriform cortex slices. *J. Neurophysiol.* 80: 2467–2474.
- Pattnaik, B., Jellali, A., Sahel, J., Dreyfus, H., and Picaud, S. 2000. GABA_C receptors are localized with microtubule-associated protein 1B in mammalian cone photoreceptors. *J. Neurosci.* 20: 6789–6796.
- Patuzzi, R. 1996. Cochlear micromechanics and macromechanics. In: *The Cochlea* (Dallos, P., Popper, A.N., and Fay, R.R., eds.) New York: Springer-Verlag, pp. 186–257.
- Paxinos, G., and Watson, C. 1986. *The Rat Brain in Stereotaxic Coordinates*. San Diego: Academic Press.
- Peacock, R.A. 1993. Physiological evidence for two distinct GABA-A responses in rat hippocampus. *Neuron* 10: 189–200.
- Pearson, J.C., and Haines, D.E. 1980. Somatosensory thalamus of a prosimian primate (*Galago senegalensis*). II. An HRP and Golgi study of the ventral posterolateral nucleus (VPL). *J. Comp. Neurol.* 190: 559–580.
- Pedarzani, P., and Storm, J.F. 1993. PKA mediates the effects of monoamine transmitters on the K⁺ current underlying the slow spike frequency adaptation in hippocampal neurons. *Neuron* 11: 1023–1035.
- Pedersen, P.E., Jastreboff, P.J., Stewart, W.B., and Shepherd, G.M. 1986. Mapping of an olfactory receptor population that projects to a specific region in the rat olfactory bulb. *J. Comp. Neurol.* 250: 93–108.
- Pederson, P.L., and Carafoli, E. 1987. Ion motive ATPases. I. Ubiquity, properties, and significance to cell function. *Trends Biochem. Sci.* 12: 146–150.
- Peichl, L. 1991. Alpha ganglion cells in mammalian retinae: common properties, species differences, and some comments on other ganglion cells. *Vis. Neurosci.* 7: 155–169.
- Peichl, L., and González-Soriano, J. 1994. Morphological types of horizontal cell in rodent retinae: a comparison of rat, mouse, gerbil, and guinea pig. *Vis. Neurosci.* 11: 501–517.
- Peng, Y., and Frank, E. 1989a. Activation of GABA-B receptors causes presynaptic inhibition at synapses between muscle spindle afferents and motoneurons in the spinal cord of bullfrogs. *J. Neurosci.* 9: 1502–1515.
- Peng, Y., and Frank, E. 1989b. Activation of GABA-A receptors causes presynaptic and postsynaptic inhibition at synapses between muscle spindle afferents and motoneurons in the spinal cord of bullfrogs. *J. Neurosci.* 9: 1516–1522.
- Peng, Y.-W., Blackstone, C.D., Haganir, R.L., and Yau, K.-W. 1995. Distribution of glutamate receptor subtypes in the vertebrate retina. *Neuroscience* 66: 483–497.
- Penn, A.A., Wong, R.O.L., and Shatz, C.J. 1994. Neuronal coupling in the developing mammalian retina. *J. Neurosci.* 14: 3805–3815.
- Penney, J.B. Jr., and Young, A.B. 1983. Speculations on the functional anatomy of basal ganglia disorders. *Annu. Rev. Neurosci.* 6: 73–94
- Penny, G.R., Afsharpour, S., and Kitai, S.T. 1986. The glutamate decarboxylase immunoreactive, met-enkephalin-immunoreactive and substance P-immunoreactive neurons in the neostriatum of the rat and cat. Evidence for partial population overlap. *Neuroscience* 17: 1011–1045.
- Perkel, D.H., and Perkel, D.J. 1985. Dendritic spines: role of active membrane in modulating synaptic efficacy. *Brain Res.* 325: 331–335.
- Perry, V.H., Oehler, R., and Cowey, A. 1984. Retinal ganglion cells that project to the dorsal lateral geniculate nucleus in the macaque monkey. *Neuroscience* 12: 1101–1123.
- Peters, A. 1984. Chandelier cells. In: *Cerebral Cortex: Cellular Components of the Cerebral Cortex* (Peters, A., and Jones, E., eds.) New York: Plenum Press, pp. 361–380.
- Peters, A. 1987. Number of neurons and synapses in the primary visual cortex. In: *Cerebral Cortex, Vol. 6: Further Aspects of Cortical Functions Including Hippocampus* (Jones, E., and Peters, A., eds.) New York: Plenum Press, pp. 267–294.

- Peters, A., and Kaiserman-Abramof, I.R. 1970. The small pyramidal neuron of the rat cerebral cortex. The perikaryon, dendrites and spines. *Am. J. Anat.* 127: 321–356.
- Peters, A., and Regidor, J. 1981. A reassessment of the forms of nonpyramidal neurons in area 17 of cat visual cortex. *J. Comp. Neurol.* 203: 685–716.
- Peters, B.N., and Masland, R.H. 1996. Responses to light of starburst amacrine cells. *J. Neurophysiol.* 75: 469–480.
- Peterson, B.B., and Dacey, D.M. 1999. Morphology of wide-field, monostratified ganglion cells of the human retina. *Vis. Neurosci.* 16: 107–120.
- Peterson, G.E., and Barney, H.L. 1952. Control methods used in a study of the vowels. *J. Acoust. Soc. Am.* 24: 175–184.
- Petralia, R.S., Rubio, M.E., Wang, Y.X., and Wenthold, R.J. 2000. Differential distribution of glutamate receptors in the cochlear nuclei. *Hear. Res.* 147: 59–69.
- Petralia, R.S., Wang, Y.X., Zhao, H.M., and Wenthold, R.J. 1996. Ionotropic and metabotropic glutamate receptors show unique postsynaptic, presynaptic, and glial localizations in the dorsal cochlear nucleus. *J. Comp. Neurol.* 372: 356–383.
- Petralia, R.S., and Wenthold, R.J. 1992. Light and electron immunocytochemical localization of AMPA-selective glutamate receptors in the rat brain. *J. Comp. Neurol.* 318: 329–354.
- Pettigrew, J. 1982. Pharmacological control of cortical plasticity. *Retina* 2: 360–372.
- Pfeiffer, R.R. 1966. Classification of response patterns of spike discharges for units in the cochlear nucleus: tone burst stimulation. *Exp. Brain Res.* 1: 220–235.
- Pfeiffer, R.R., and Kim, D.O. 1975. Cochlear nerve fiber responses: distribution along the cochlear partition. *J. Acoust. Soc. Am.* 58: 867–869.
- Phelps, P.E., Houser, C.R., and Vaughn, J.E. 1985. Immunocytochemical localization of choline acetyltransferase within the rat neostriatum: a correlated light and electron microscopic study of cholinergic neurons and synapses. *J. Comp. Neurol.* 238: 286–307.
- Phillips, C.G. 1959. Actions of antidromic pyramidal volleys on single Betz cells in the cat. *Q. J. Exp. Physiol.* 44: 1–25.
- Phillips, C.G. 1969. Motor apparatus of the baboon's hand. *Proc. R. Soc. Biol.* 173: 141–174.
- Phillips, C.G., Powell, T.P.S., and Shepherd, G.M. 1963. Responses of mitral cells to stimulation of the lateral olfactory tract in the rabbit. *J. Physiol. (Lond.)* 168: 65–88.
- Phillis, J.W. 1968. Acetylcholinesterase in the feline cerebellum. *J. Neurochem.* 15: 691–698.
- Phillis, J.W., and Wu, P.H. 1981. Catecholamines and the sodium pump in excitable cells. *Prog. Neurobiol.* 17: 141–184.
- Piccolino, M. 1986. Cajal and the retina: a 100-year retrospective. *Trends Neurosci.* 9: 521–525.
- Piccolino, M. 1995. Cross-talk between cones and horizontal cells through the feedback circuit. In: *Neurobiology and Clinical Aspects of the Outer Retina* (Djamgoz, M.B.A., Archer, S., and Vallerga, S., eds.) London: Chapman & Hall, pp. 221–248.
- Piccolino, M., Neyton, J., and Gerschenfeld, H.M. 1984. Decrease of gap-junction permeability induced by dopamine and cyclic adenosine 3',5'-monophosphate in horizontal cells of turtle retina. *J. Neurosci.* 4: 2477–2488.
- Pickel V.M., Segal M., and Bloom F.E., 1974. A radioautographic study of the efferent pathways of the nucleus locus coeruleus. *J. Comp. Neurol.* 155: 15–42.
- Pickles, J.O. 1988. *An Introduction to the Physiology of Hearing*. New York: Academic Press.
- Pierce, J.P., and Mendell, L.M. 1993. Quantitative ultrastructure of Ia boutons in the ventral horn: scaling and positional relationships. *J. Neurosci.* 13: 4748–4763.
- Pierrot-Deseilligny, E. 1996. Transmission of the cortical command for human voluntary movement through cervical propriospinal premotoneurons. *Prog. Neurobiol.* 48: 489–517.
- Pilpel, Y., and Lancet, D. 1999. The variable and conserved interfaces of modeled olfactory receptor proteins. *Prot. Sci.* 8: 969–977.

- Pinault, D., Smith, Y., and Deschenes, M. 1997. Dendrodendritic and axoaxonic synapses in the thalamic reticular nucleus of the adult rat. *J. Neuroscience*. 17: 3215–3233.
- Pinching, A.J. 1971. Myelinated dendritic segments in the monkey olfactory bulb. *Brain Res.* 29: 133–138.
- Pinching, A.J., and Powell, T.P.S. 1971a. The neuron types of the glomerular layer of the olfactory bulb. *J. Cell Sci.* 9: 305–345.
- Pinching, A.J., and Powell, T.P.S. 1971b. The neuropil of the glomeruli of the olfactory bulb. *J. Cell Sci.* 9: 347–377.
- Pinco, M., and Lev-Tov, A. 1993. Synaptic excitation of alpha-motoneurons by dorsal root afferents in the neonatal rat spinal cord. *J. Neurophysiol.* 70: 406–417.
- Pinco, M., and Lev-Tov, A. 1993. Modulation of monosynaptic excitation in the neonatal rat spinal cord. *J. Neurophysiol* 70: 1151–1158.
- Pineda, J.C., Galarraga, E., Bargas, J., Cristancho, M., and Aceves, J. 1992. Charybdotoxin and apamin sensitivity of the calcium-dependent repolarization and the afterhyperpolarization in neostriatal neurons. *J. Neurophysiol.* 68: 287–294.
- Pinsky, P., and Rinzel, J. 1994. Intrinsic and network rhythmogenesis in a reduced Traub model for Ca3 neurons. *J. Comput. Neuroscience* 1: 39–60.
- Pinter, M.J., Burke, R.E., O'Donovan, M.J., and Dum, R.P. 1982. Supraspinal facilitation of cutaneous polysynaptic EPSPs in cat medial gastrocnemius motoneurons. *Exp. Brain Res.* 45: 133–143.
- Piredda, S., and Gale, K. 1985. A crucial epileptogenic site in the deep prepiriform cortex. *Nature* 317: 623–625.
- Pisani, A., Bonsi, P., Centonze, D., Calabresi, P., and Bernardi, G. 2000. Activation of D2-like dopamine receptors reduces synaptic inputs to striatal cholinergic interneurons. *J. Neurosci.* 20:RC69(1–6).
- Pitkanen, A., Pikkarainen, M., Nurminen, N., and Ylinen, A. 2000. Reciprocal connections between the amygdala and the hippocampal formation, perirhinal cortex, and postrhinal cortex in rat. A review. *Ann. NY Acad. Sci.* 911: 369–391.
- Plummer, K.L., Manning, K.A., Levey, A.I., Rees, H.D., and Uhrich, D.J. 1999. Muscarinic receptor subtypes in the lateral geniculate nucleus: a light and electron microscopic analysis. *J. Comp. Neurol.* 404: 408–425.
- Pollen, D., and Lux, H. 1966. Conductance changes during inhibitory postsynaptic potentials in normal and strychninized cortical neurons. *J. Neurophysiol.* 29: 367–381.
- Polyak, S.L. 1941. *The Retina*. Chicago: University of Chicago Press.
- Porter, J., Cauli, B., Staiger, J., Lambolez, B., Rossler, J., and Aunat, E. 1998. Properties of bipolar VIPergic interneurons and their excitation by pyramidal neurons in the rat neocortex. *Eur. J. Neurosci.* 10: 3617–3628.
- Porter, R. 1987. Corticomotoneuronal projections: Synaptic events related to skilled movement. *Proc. R. Soc. Lond. B* 231: 147–168.
- Potashner, S.J., Benson, C.G., Ostapoff, E.M., Lindberg, N., and Morest, D.K. 1993. Glycine and GABA: transmitter candidates of projections descending to the cochlear nucleus. In: *The Mammalian Cochlear Nuclei: Organization and Function* (Merchán, M.A., Juiz, J.M., Godfrey, D.A., and Mugnaini, E., eds.) New York: Plenum, pp.
- Potter, S.M., Zheng, C., Koos, D.S., Feinstein, P., Fraser, S.E., and Mombaerts, P. 2001. Structure and emergence of specific olfactory glomeruli in the mouse. *J. Neurosci.* 21: 9713–9723.
- Potts, A.M., Hodges, D., Shelman, C.B., Fritz, K.J., Levy, N.S., and Mangnall, Y. 1972. Morphology of the primate optic nerve. I. Method and total fiber count. *Invest. Ophthalmol. Vis. Sci.* 11: 980–988.
- Pourcho, R.G. 1982. Dopaminergic amacrine cells in the cat retina. *Brain Res.* 252: 101–109.

- Pourcho, R.G., and Goebel, D.J. 1987. Visualization of endogenous glycine in cat retina: an immunocytochemical study with Fab fragments. *J. Neurosci.* 7: 1189–1197.
- Pourcho, R.G., and Owczarzak, M.T. 1989. Distribution of GABA immunoreactivity in the cat retina: a light- and electron-microscopic study. *Vis. Neurosci.* 2: 425–435.
- Pourcho, R.G., and Owczarzak, M.T. 1991. Glycine receptor immunoreactivity is localized at amacrine synapses in cat retina. *Vis. Neurosci.* 7: 611–618.
- Pourcho, R.G., Qin, P., and Goebel, D.J. 2001. Cellular and subcellular distribution of NMDA receptor subunit NR2B in the retina. *J. Comp. Neurol.* 433: 75–85.
- Powell, T., and Mountcastle, V.B. 1959. Some aspects of the functional organization of the cortex of the postcentral gyrus of the monkey: a correlation of findings obtained on a single unit analysis with cytoarchitecture. *Bull. Johns Hopkins Hosp.* 105: 133–162.
- Powell, T.P.S. 1981. Certain aspects of the intrinsic organisation of the cerebral cortex. In *Brain Mechanisms and Perceptual Awareness* (Pompeiano, O., and Ajmone-Marsan, C., eds.) New York: Raven Press, pp. 1–19.
- Powers, R., and Binder, M. 2001. Input-output functions of mammalian motoneurons. *Rev. Physiol. Biochem. Pharmacol.* 143: 137–263.
- Pratt, C.A., and Jordan, L. 1987. Ia inhibitory interneurons and Renshaw cells as contributors to the spinal mechanisms of fictive locomotion. *J. Neurophysiol.* 57: 56–71.
- Precht, W., and Yoshida, M. 1971. Blockage of caudate-evoked inhibition of neurons in the substantia nigra by picrotoxin. *Brain Res.* 32: 229–233.
- Prensa, L., and Parent, A. 2001. The nigrostriatal pathway in the rat: A single-axon study of the relationship between dorsal and ventral tier nigral neurons and the striosome/matrix striatal compartments. *J. Neurosci.* 21: 7247–7260.
- Preuss, T.M., Beck, P.D., and Kaas, J.H. 1993. Areal, modular, and connectional organization of visual cortex in a prosimian primate, the slow loris (*Nycticebus coucang*). *Brain Behav. Evol.* 42: 321–335.
- Price, J.L. 1973. An autoradiographic study of complementary laminar patterns of termination of afferent fibers to the olfactory cortex. *J. Comp. Neurol.* 150: 87–108.
- Price, J.L. 1985. Beyond the primary olfactory cortex. Olfactory-related areas in the neocortex, thalamus and hypothalamus. *Chem. Senses* 10: 239–258.
- Price, J.L. 1987. The central olfactory and accessory olfactory systems. In: *Neurobiology of Taste and Smell* (Finger, T.E., and Silver, W.L., eds.) New York: John Wiley & Sons, pp. 179–203.
- Price, J.L., and Powell, T.P.S. 1970a. The morphology of granule cells of the olfactory bulb. *J. Cell. Sci.* 7: 91–123.
- Price, J.L., and Powell, T.P.S. 1970b. The synaptology of the granule cells of the olfactory bulb. *J. Cell. Sci.* 7: 125–155.
- Price, J.L., and Sprich, W.W. 1975. Observations on the lateral olfactory tract of the rat. *J. Comp. Neurol.* 162: 321–336.
- Price, J.L., Carmichael, S.T., Carnes, K.M., Clugnut, M.C., Kuroda, M., and Ray, J.P. 1991. Olfactory input to the prefrontal cortex. In: *Olfaction. Model System for Computational Neuroscience* (Davis, J.L., and Eichenbaum, H., eds.) Cambridge, MA: MIT Press, pp. 101–120.
- Price, J.L., Slotnick, B.M., and Revial, M.F. 1991b. Olfactory projections to the hypothalamus. *J. Comp. Neurol.* 306: 447–461.
- Prince, D.A., and Huguenard, J.R. 1988. Functional properties of neocortical neurons. In: *Neurobiology of the Neocortex* (Rakic, P., and Singer, W., eds.) Chichester: John Wiley & Sons, pp. 153–176.
- Prochazka, A. 1996. Proprioceptive feedback and movement regulation. In: *Handbook of Physiology. Section 12, Exercise: Regulation and Integration of Multiple Systems* (Rowell, L., and Shepherd, J., ed.) New York: American Physiological Society, pp. 89–127.

- Protopapas, A.D., and Bower, J.M. 2000. Physiological characterization of layer III non-pyramidal neurons in piriform (olfactory) cortex of rat. *Brain Res.* 865: 1–11.
- Pu, M., and Amthor, F.R. 1990. Dendritic morphologies of retinal ganglion cells projecting to the nucleus of the optic tract in the rabbit. *J. Comp. Neurol.* 302: 657–674.
- Pugh, E.N., Jr., 2000. Rhodopsin flash photolysis in man. *J. Physiol.* 248: 393–412.
- Pugh E.N., Jr., and Lamb, T.D. 1993. Amplification and kinetics of the activation steps in phototransduction. *Biochim. Biophys. Acta* 1141: 111–149.
- Puul, E. 1983. Actions and interactions of S-glutamate in the spinal cord. In: *Handbook of the Spinal Cord, Vol. 1: Pharmacology* (Davidoff, R.A., ed.) New York: Marcel Dekker, pp. 105–169.
- Puopolo, M., and Belluzzi, O. 1998. Functional heterogeneity of periglomerular cells in the rat olfactory bulb. *Eur. J. Neurosci.* 10: 1073–1083.
- Puopolo, M., and Belluzzi, O. 2001. NMDA-dependent, network-driven oscillatory activity induced by bicuculline or removal of Mg^{2+} in rat olfactory bulb neurons. *Eur. J. Neurosci.* 13: 92–102.
- Puopolo, M., Kratskin, I., and Belluzzi, O. 1998. Direct inhibitory effect of taurine on relay neurones of the rat olfactory bulb in vitro. *NeuroReport* 9: 2319–2323.
- Purkinje J.E., 1837. Über die gangliösen Körperchen in verschiedenen Theilen des Gehirns. *Berüberd. Versamm. deutscher Naturf. u. Aerzte in Prag* S. 179.
- Purpura, D.P. 1974. Dendritic spine “dysgenesis” and mental retardation. *Science* 186: 1126–1128.
- Purves, D., Augustine, G.J., Fitzpatrick, D., Katz, L.C., Lamantia, A.-S., and McNamara, J.O. 1997. *Neuroscience*. Sunderland, MA: Sinauer.
- Qin, P., and Pourcho, R.G. 1999a. AMPA-selective glutamate receptor subunits GluR2 and GluR4 in the cat retina: an immunocytochemical study. *Vis. Neurosci.* 16: 1105–1114.
- Qin, P., and Pourcho, R.G. 1999b. Localization of AMPA-selective glutamate receptor subunits in the cat retina: a light- and electron-microscopic study. *Vis. Neurosci.* 16: 169–177.
- Racine, R.J., Moore, K.-A., and Evans, C. 1991. Kindling-induced potentiation in the piriform cortex. *Brain Res.* 556: 218–225.
- Rack, P.M.H. 1981. Limitations of somatosensory feedback in control of posture and movement. In: *Handbook of Physiology, Section 1: The Nervous System, Vol. II: Motor Control, Part 1* (Brooks, V.B., ed.) Bethesda, American Physiological Society, pp. 229–256.
- Rackowski, D., and Fitzpatrick, D. 1989. Organization of cholinergic synapses in the cat’s dorsal lateral geniculate and perigeniculate nuclei. *J. Comp. Neurol.* 288: 676–690.
- Radpour, S., and Thomson, A.M. 1991. Coactivation of local circuit NMDA receptor mediated EPSPs induces lasting enhancement of minimal Schaffer collateral EPSPs in slices of rat hippocampus. *Eur. J. Neurosci.* 3: 602–613.
- Ragsdale, C.W.J., and Graybiel, A.M. 1991. Compartmental organization of the thalamostriatal connection in the cat. *J. Comp. Neurol.* 311: 134–167.
- Raisman, G. 2001. Olfactory ensheathing cells—another miracle cure for spinal cord injury? *Nat. Rev. Neurosci.* 2: 369–375.
- Rakic, P. 1971. Guidance of neurons migrating to the fetal monkey neocortex. *Brain Res.* 33: 471–476.
- Rakic, P. 1995. A small step for the cell, a giant leap for mankind: a hypothesis of neocortical expansion during evolution. *Trends Neurosci.* 18: 383–388.
- Rakic, P. (ed.) 1976a. *Local Circuit Neurons*. Cambridge, MA: MIT Press.
- Rakic, P. 1976b. Prenatal genesis of connections subserving ocular dominance in the rhesus monkey. *Nature* 261: 467–471.
- Rakic, P., Bourgeois, J.P., Eckenhoff, M.F., Zecevic, N., and Goldman-Rakic, P.S. 1986. Con-

- current overproduction of synapses in diverse regions of the primate cerebral cortex. *Science* 232: 232–235.
- Rakic, P., and Riley, K.P. 1983. Overproduction and elimination of retinal axons in the fetal rhesus monkey. *Science* 219: 1441–1444.
- Rall, W. 1957. Membrane time constant of motoneurons. *Science* 126: 454–455.
- Rall, W. 1959a. Dendritic current distribution and whole neuron properties. *Naval Med. Res. Inst. Res. Report NM 01-05-00.01.01.*
- Rall, W. 1959b. Branching dendritic trees and motoneuron membrane resistivity. *Exp. Neurol.* 1: 491–527.
- Rall, W. 1960. Membrane potential transients and membrane time constant of motoneurons. *Exp. Neurol.* 2: 503–532.
- Rall, W. 1962. Electrophysiology of a dendritic neuron model. *Biophys. J.* 2: 145–167.
- Rall, W. 1964. Theoretical significance of dendritic trees for neuronal input-output relations. In: *Neural Theory and Modeling* (Reiss, R.F., ed.) Stanford, CA: Stanford University Press, pp. 73–97.
- Rall, W. 1967. Distinguishing theoretical synaptic potentials computed for different somadendritic distributions of synaptic input. *J. Neurophysiol.* 30: 1138–1168.
- Rall, W. 1970. Cable properties of dendrites and effects of synaptic location. In: *Excitatory Synaptic Mechanisms* (Andersen, P., and Jansen, J.K.S., eds.) Oslo: Universitetsforlag, pp. 175–187.
- Rall, W. 1974a. Dendritic spines and synaptic potency. In: *Studies in Neurophysiology* (Porter, R., ed.) Cambridge: Cambridge University Press, pp. 203–209.
- Rall, W. 1974b. Dendritic spines, synaptic potency in neuronal plasticity. In: *Cellular Mechanisms Subservicing Changes in Neuronal Activity* (Woody, C.D., Brown, K.A., Crow, T.J., and Knispel, J.D., eds.) Los Angeles: Brain Information Service, pp. 13–21.
- Rall, W. 1977. Core conductor theory and cable properties of neurons. In: *The Nervous System, Vol. I: Cellular Biology of Neurons, Part 1* (Kandel, E.R., ed.) Bethesda: American Physiological Society, pp. 39–97.
- Rall, W. 1989. Cable theory for dendritic neurons. In: *Methods in Neuronal Modeling* (Koch, C., and Segev, I., eds.) Cambridge, MA: MIT Press, pp. 9–62.
- Rall, W., Burke, R.E., Holmes, W.R., Jack, J.J.B., Redman, S.J., and Segev, I. 1992. Matching dendritic neuron models to experimental data. *Physiol. Revs.* 72: S159–S186.
- Rall, W., Burke, R.E., Nelson, P.G., Smith, T.G., and Frank, K. 1967. The dendritic location of synapses and possible mechanisms for the monosynaptic EPSP in motoneurons. *J. Neurophysiol.* 30: 1169–1193.
- Rall, W., and Hunt, C.C. 1956. Analysis of reflex variability in terms of partially correlated excitability fluctuations in a population of motoneurons. *J. Gen. Physiol.* 39: 397–422.
- Rall, W., and Rinzel, J. 1973. Branch input resistance and steady attenuation for input to one branch of a dendritic neuron model. *Biophys. J.* 13: 648–688.
- Rall, W., and Segev, I. 1987. Functional possibilities for synapses on dendrites and on dendritic spines. In: *Synaptic Function* (Edelman, G.M., Gall, W.F., and Cowan, W.M., eds.) New York: John Wiley & Sons, pp. 605–636.
- Rall, W., and Shepherd, G.M. 1968. Theoretical reconstruction of field potentials and dendrodendritic synaptic interactions in olfactory bulb. *J. Neurophysiol.* 31: 884–915.
- Rall, W., Shepherd, G.M., Reese, T.S., and Brightman, M.W. 1966. Dendrodendritic synaptic pathway for inhibition in the olfactory bulb. *Exp. Neurol.* 14: 44–56.
- Ralston, H.J. 1969. The synaptic organization of lemniscal projections to the ventrobasal thalamus of the cat. *Brain Res.* 14: 99–116.
- Ralston, H.J. 1971. Evidence for presynaptic dendrites and a proposal for their mechanism of action. *Nature* 230: 585–587.

- Ralston, H.J. 1983. The synaptic organization of the ventrobasal thalamus in the rat, cat, and monkey. In *Somatosensory Integration in the Thalamus* (Macchi, G., Rustioni, A., and Spreafico, R., eds.) Amsterdam: Elsevier, pp. 241–250.
- Ralston, H.J., Ohara, P.T., Ralston, D.D., and Chazal, G. 1988. The neuronal and synaptic organization of the cat and primate somatosensory thalamus. In: *Cellular Thalamic Mechanisms* (Bentivoglio, M., and Spreafico, R., eds.) Amsterdam: Elsevier, pp 127–141.
- Raman, I., and Trussell, L.O. 1992. The kinetics of the responses to glutamate and kainate in neurons of the avian cochlear nucleus. *Neuron* 9: 173–186.
- Raman, I.M., and Bean, B.P. 1999. Ionic currents underlying spontaneous action potentials in isolated cerebellar Purkinje neurons. *J. Neurosci.* 19: 1663–1674.
- Raman, I.M., Zhang, S., and Trussell, L.O. 1994. Pathway-specific variants of AMPA receptors and their contribution to neuronal signaling. *J. Neurosci.* 14: 4998–5010.
- Ramcharan, E.J., Gnadt, J.W., and Sherman, S.M. 2000. Burst and tonic firing in thalamic cells of unanesthetized, behaving monkeys. *Vis. Neurosci.* 17: 55–62.
- Ramcharan, E., Gnadt, J.W., and Sherman, S.M. 2001. The effects of saccadic eye movements on the activity of geniculate relay neurons in the monkey. *Vis. Neurosci.* 18: 253–258.
- Ramoa, A., Campbell, G., and Shatz, C.J. 1988. Dendritic growth and remodeling of cat retinal ganglion cells during fetal and postnatal development. *J. Neurosci.* 8: 4239–4261.
- Ramon y Cajal, S. 1911. *Histologie du Système Nerveux de l'Homme et des Vertébrés*, Volume II. Paris: Maloine.
- Ramon-Cueto, A., and Valverde, F. 1995. Olfactory bulb ensheathing glia: a unique cell type with axonal growth-promoting properties. *Glia* 14: 163–173.
- Ramón-Moliner, E. 1977. The reciprocal synapses of the olfactory bulb: questioning the evidence. *Brain Res.* 128: 1–20.
- Randall, A., and Tsien, R.W. 1995. Pharmacological dissection of multiple types of Ca^{2+} channel currents in rat cerebellar granule neurons. *J. Neurosci.* 15: 2995–3012.
- Rao, R., Buchsbaum, G., and Sterling, P. 1994a. Rate of quantal transmitter release at the mammalian rod synapse. *Biophys. J.* 67: 57–63.
- Rao, R., Buchsbaum, G., and Sterling, P. 1994b. Minimum rate of transmitter release at a cone active zone. *Invest. Ophthalmol. Vis. Sci. Abstr.* 35: 2125.
- Rao-Mirotnik, R., Buchsbaum, G., and Sterling, P. 1998. Transmitter concentration at a three-dimensional synapse. *J. Neurophysiol.* 80: 3163–3172.
- Rao-Mirotnik, R., Harkins, A., Buchsbaum, G., and Sterling, P. 1995. Mammalian rod terminal: architecture of a binary synapse. *Neuron* 14: 561–569.
- Rash J.E., Staines W.A., Yasumura T., Patel D., Furman C.S., Stelmack G.L., and Nagy J.I. 2000. Immunogold evidence that neuronal gap junctions in adult rat brain and spinal cord contain connexin-36 but not connexin-32 or connexin-43. *Proc. Natl. Acad. Sci. U.S.A.* 97: 7573–7578.
- Ratliff, F. 1965. *Mach Bands: Quantitative Studies on Neural Networks in the Retina*. San Francisco: Holden-Day.
- Raviola, E., and Gilula, N.B. 1973. Gap junctions between photoreceptor cells in the vertebrate retina. *Proc. Natl. Acad. Sci. U.S.A.* 70: 1677–1681.
- Ray, J.P., and Price, J.L. 1992. The organization of the thalamocortical connections of the mediodorsal thalamic nucleus in the rat, related to the ventral forebrain-prefrontal cortex topography. *J. Comp. Neurol.* 323: 167–197.
- Reader, T., Ferron, A., Descarries, L., and Jasper, H. 1979. Modulatory role for biogenic amines in the cerebral cortex: microiontophoretic studies. *Brain Res.* 160: 217–229.
- Redman, S.J. 1973. The attenuation of passively propagating dendritic potentials in a motoneurone cable model. *J. Physiol. (Lond.)* 234: 637–664.
- Redman, S.J. 1990. Quantal analysis of synaptic potentials in neurons of the central nervous system. *Physiol. Rev.* 70: 165–198.

- Redman, S.J., and Walmsley, B. 1983a. Amplitude fluctuations in synaptic potentials evoked in cat spinal motoneurons at identified group Ia synapses. *J. Physiol. (Lond.)* 343: 135–145.
- Redman, S.J., and Walmsley, B. 1983b. The time course of synaptic potentials evoked in cat spinal motoneurons at identified group Ia synapses. *J. Physiol. (Lond.)* 343: 117–133.
- Reece, L.J., and Schwartzkroin, P.A. 1991. Effects of cholinergic agonists on two non-pyramidal cell types in rat hippocampal slices. *Brain Res.* 566: 115–126.
- Reed, M.C., and Blum, J.J. 1995. A computational model for signal processing by the dorsal cochlear nucleus, I: Responses to pure tones. *J. Acoust. Soc. Am.* 97: 425–438.
- Reep, R.L., and Winans, S.S. 1982. Efferent connections of dorsal and ventral agranular insular cortex in the hamster, *Mesocricetus auratus*. *Neuroscience* 7: 2609–2635.
- Reese, B.E. 1988. 'Hidden lamination' in the dorsal lateral geniculate nucleus. The functional organization of this thalamic region in the rat. *Brain Res.* 472: 119–137.
- Reese, T.S., and Brightman, M.W. 1970. Olfactory surface and central olfactory connections in some vertebrates. In: *Taste and Smell in Vertebrates* (Wolstenholme, G.E.W., and Knight, J., eds.) London: J & A Churchill, pp. 115–149.
- Reese, T.S., and Shepherd, G.M. 1972. Dendro-dendritic synapses in the central nervous system. In: *Structure and Function of Synapses* (Pappas, G.D., and Purpura, D.P., eds.) New York: Raven Press, pp. 121–136.
- Regehr, W.G., Delaney, K.R., and Tank, D.W. 1994. The role of presynaptic calcium in short-term enhancement at the hippocampal mossy fiber synapse. *J. Neurosci.* 14: 523–537.
- Regehr, W.G., and Tank, D.W. 1992. Calcium concentration dynamics produced by synaptic activation of CA1 hippocampal pyramidal cells. *J. Neurosci.* 12: 4202–4223.
- Regehr, W.G., and Tank, D.W. 1994. Dendritic calcium dynamics. *Curr. Opin. Neurobiol.* 4: 373–382.
- Reh, T., and Constantine-Paton, M. 1984. Retinal ganglion cell terminals change their projection sites during larval development of *Rana pipiens*. *J. Neurosci.* 4: 442–457.
- Reid, R.C., and Alonso, J.M. 1995. Specificity of monosynaptic connections from thalamus to visual cortex. *Nature* 378: 281–284.
- Reid, R.C., and Alonso, J.M. 1996. The processing and encoding of information in the visual cortex. *Curr. Opin. Neurobiol.* 6: 475–480.
- Reid, R.C., and Shapley, R.M. 2002. Space and time maps of cone photoreceptor signals in macaque lateral geniculate nucleus. *J. Neurosci.* 22: 6158–6175.
- Reisine, T., and Bell, G.I. 1995. Molecular properties of somatostatin receptors. *Neuroscience* 67: 777–790.
- Reithmeier, R.A.F. 1994. Mammalian exchangers and co-transporters. *Curr. Opin. Cell Biol.* 6: 583–594.
- Rekling, J., Funk, G., Bayliss, D., Dong, X.-W., and Feldman, J. 2000. Synaptic control of motoneuronal excitability. *Physiol. Rev.* 80: 767–852.
- Remez, R.E., Rubin, P.E., Pisoni, D.B., and Carrell, T.D. 1981. Speech perception without traditional speech cues. *Science* 212: 947–950.
- Ressler, K.J., Sullivan, S.L., and Buck, L.B. 1993. A zonal organization of odorant receptor gene expression in the olfactory epithelium. *Cell* 73: 597–609.
- Ressler, K.J., Sullivan, S.L., and Buck, L.B. 1994. Information coding in the olfactory system: evidence for a stereotyped and highly organized epitope map in the olfactory bulb. *Cell* 79: 1245–1255.
- Rexed, B. 1952. The cytoarchitectonic organization of the spinal cord in the cat. *J. Comp. Neurol.* 96: 415–496.
- Reyes, A.D., Rubel, E.W., and Spain, W.J. 1994. Membrane properties underlying the firing of neurons in the avian cochlear nucleus. *J. Neurosci.* 14: 5352–5364.
- Reyher, C.K., Lubke, J., Larsen, W.J., Hendrix, G.M., Shipley, M.T., and Baumgarten, H.G. 1991.

- Olfactory bulb granule cell aggregates: morphological evidence for interperikaryal electrotonic coupling via gap junctions. *J. Neurosci.* 11: 1485–1495.
- Reymond, L. 1985. Spatial visual acuity of the eagle *Aquila audax*: a behavioural, optical and anatomical investigation. *Vision Res.* 25: 1477–1491.
- Reynolds, J.N., and Wickens, J.R. 2001. A cellular mechanism of reward-related learning. *Nature* 413: 67–70.
- Rhoades, B.K., and Freeman, W.J. 1990. Excitatory actions of GABA in the rat olfactory bulb. *Soc. Neurosci. Abstr.* 16: 403.
- Rhode, W.S. 1999. Vertical cell responses to sound in cat dorsal cochlear nucleus. *J. Neurophysiol.* 82: 1019–1032.
- Rhode, W.S., and Smith, P.H. 1986. Encoding timing and intensity in the ventral cochlear nucleus of the cat. *J. Neurophysiol.* 56: 261–286.
- Rhode, W.S., Smith, P.H., and Oertel, D. 1983b. Physiological response properties of cells labeled intracellularly with horseradish peroxidase in cat dorsal cochlear nucleus. *J. Comp. Neurol.* 213: 426–447.
- Rhode, W.S., and Greenberg, S. 1994a. Encoding of amplitude modulation in the cochlear nucleus of the cat. *J. Neurophysiol.* 71: 1797–1825.
- Rhode, W.S., and Greenberg, S. 1994b. Lateral suppression and inhibition in the cochlear nucleus of the cat. *J. Neurophysiol.* 71: 493–514.
- Rhode, W.S., Oertel, D., and Smith, P.H. 1983a. Physiological response properties of cells labeled intracellularly with horseradish peroxidase in cat ventral cochlear nucleus. *J. Comp. Neurol.* 213: 448–463.
- Ribak, C. 1978. Aspinous and sparsely-spinous stellate neurons in the visual cortex of rats contain glutamic acid decarboxylase. *J. Neurocytol.* 7: 461–478.
- Ribak, C.E., and Seress, L. 1983. Five types of basket cell in the hippocampal dentate gyrus: a combined Golgi and electron microscopic study. *J. Neurocytol.* 12: 577–597.
- Ribak, C.E., Seress, L., and Amaral, D.G. 1985. The development, ultrastructure and synaptic connections of the mossy cells of the dentate gyrus. *J. Neurocytol.* 14: 835–857.
- Ribak, C.E., Vaughn, J.E., and Saito, K. 1978. Immunocytochemical localization of glutamic acid decarboxylase in neuronal somata following colchicine inhibition of axonal transport. *Brain Res.* 140: 315–332.
- Ribak, C.E., Vaughn, J.E., Saito, K., Barber, R., and Roberts, E. 1977. Glutamate decarboxylase localization in neurons in the olfactory bulb. *Brain Res.* 126: 1–18.
- Richardson, T.L., Turner, R.W., and Miller, J.J. 1987. Action-potential discharge in hippocampal CA1 pyramidal neurons: current source-density analysis. *J. Neurophysiol.* 58: 981–996.
- Richmond, B., Wurtz, R., and Sato, T. 1983. Visual responses of inferior temporal neurons in the awake rhesus monkey. *J. Neurophysiol.* 50: 1415–1432.
- Rieke, F. 2001. Temporal contrast adaptation in salamander bipolar cells. *J. Neurosci.* 21: 9445–9454.
- Rieke, F., and Schwartz, E.A. 1996. Asynchronous transmitter release: control of exocytosis and endocytosis at the salamander rod synapse. *J. Physiol. (Lond.)* 493: 1–8.
- Rihn, L.L., and Claiborne, B.J. 1990. Dendritic growth and regression in rat dentate granule cells during late postnatal development. *Dev. Brain Res.* 54: 115–124.
- Ringham, G.L. 1971. Origin of nerve impulse in slowly adapting stretch receptor of crayfish. *J. Neurophysiol.* 34: 773–784.
- Rinik, E. 1972. Organization of thalamic connections from motor and somatosensory cortical areas in the cat. In: *Corticothalamic Projections and Sensorimotor Activities* (Frigyesi, T., Rinik, E., and Yahr, M.D., eds.) New York: Raven Press, pp. 57–90.
- Rinzel, J., and Rall, W. 1974. Transient response in a dendritic neuronal model for current injected at one branch. *Biophys. J.* 14: 759–790.

- Rivadulla, C., Rodriguez, R., Martinez-Conde, S., Acuña, C., and Cudeiro, J. 1996. The influence of nitric oxide on perigeniculate GABAergic cell activity in the anaesthetized cat. *Eur. J. Neurosci.* 8: 2459–2466.
- Roberts, E., Chase, T.N., and Tower, D.B. 1976. *GABA in Nervous System Function*. New York: Raven Press.
- Roberts, G.W., Woodhams, P.L., Polak, J.M., and Crow, T.J. 1982. Distribution of neuropeptides in the limbic system of the rat: the amygdaloid complex. *Neuroscience* 7: 99–131.
- Roberts, P.J., Storm-Mathisen, J., and Johnston, G.A.R. 1981. *Glutamate Transmission in the Central Nervous System*. Chichester: John Wiley & Sons.
- Roberts, R.C., Force, M., and Kung, L. 2002. Dopaminergic synapses in the matrix of the ventrolateral striatum. *Synapse* 45: 78–85.
- Robson, J.A., and Hall, W.C. 1977. The organization of the pulvinar in the grey squirrel (*Sciurus carolinensis*). II. Synaptic organization and comparisons with the dorsal lateral geniculate nucleus. *J. Comp. Neurol.* 173: 389–416.
- Rochefort, C., Gheusi, G., Vincent, J.D., and Lledo, P.M. 2002. Enriched odor exposure increases the number of newborn neurons in the adult olfactory bulb and improves odor memory. *J. Neurosci.* 22: 2679–2689.
- Rockland, K.S. 1996. Two types of corticopulvinar terminations: round (type 2) and elongate (type 1). *J. Comp. Neurol.* 368: 57–87.
- Rockland, K.S., and Pandya, D.N. 1981. Cortical connections of the occipital lobe in the rhesus monkey. Interconnections between areas 17, 18, 19 and the superior temporal sulcus. *Brain Res.* 212: 249–270.
- Rodieck, R.W. 1965. Quantitative analysis of cat retinal ganglion cell response to visual stimuli. *Vis. Res.* 5: 583–601.
- Rodieck, R.W. 1989. Starburst amacrine cells of the primate retina. *J. Comp. Neurol.* 285: 18–37.
- Rodieck, R.W., and Brening, R.K. 1983. Retinal ganglion cells: properties, types, genera, pathways and trans-species comparisons. *Brain Behav. Evol.* 23: 121–164.
- Rodieck, R.W., and Watanabe, M. 1993. Survey of the morphology of macaque retinal ganglion cells that project to the pretectum, superior colliculus, and parvocellular laminae of the lateral geniculate nucleus. *J. Comp. Neurol.* 338: 289–303.
- Rodieck, R.W., Brening, R.K., and Watanabe, M. 1993. The origin of parallel visual pathways. In: *Contrast Sensitivity* (Shapley, R., and Lam, D.M.-K, eds.) Cambridge, MA: MIT Press, pp. 117–144.
- Rodrigo, J., Suburo, A.M., Bentura, M.L., Fernandez, T., Nakade, S., Mikoshiba, K., Martinez-Murillo, R., and Polak, J.M. 1993. Distribution of the inositol 1,4,5-trisphosphate receptor, P400, in adult rat brain. *J. Comp. Neurol.* 337: 493–517.
- Rodriguez, R., and Haberly, L.B. 1989. Analysis of synaptic events in the opossum piriform cortex with improved current source density techniques. *J. Neurophysiol.* 61: 702–718.
- Roffler-Tarlov, S., and Turey, M. 1982. The content of amino acids in the developing cerebellar cortex and deep cerebellar nuclei of granule cell deficient mutant mice. *Brain Res.* 247: 65–73.
- Rohde, B.H., Rea, M.A., Simon, J.R., and McBride, W.J. 1979. Effects of X-irradiation induced loss of cerebellar granule cells on the synaptosomal levels and the high affinity uptake of amino acids. *J. Neurochem.* 32: 1431–1435.
- Röhlich, P., Van Veen, T., and Szél, A. 1994. Two different visual pigments in one retinal cone cell. *Neuron* 13: 1159–1166.
- Röhrenbeck, J., Wässle, H., and Boycott, B.B. 1989. Horizontal cells in the monkey retina: immunocytochemical staining with antibodies against calcium binding proteins. *Eur. J. Neurosci.* 1: 407–420.

- Rolls, E.T. 2000. Functions of the primate temporal lobe cortical visual areas in invariant visual object and face recognition. *Neuron* 27: 205–218.
- Roman, F.S., Chaillan, F.A., and Soumireu-Mourat, B. 1993. Long-term potentiation in rat piriform cortex following discrimination learning. *Brain Res.* 601: 265–272.
- Roman, F.S., Staubli, U., and Lynch, G. 1987. Evidence for synaptic potentiation in a cortical network during learning. *Brain Res.* 418: 221–226.
- Romanes, G.J. 1951. The motor cell columns of the lumbo-sacral spinal cord of the cat. *J. Comp. Neurol.* 94: 313–363.
- Romer, A.S. 1969. Vertebrate history with special reference to factors related to cerebellar evolution. In: *Neurobiology of Cerebellar Evolution and Development* (Llinás, R., ed.) Chicago: American Medical Association, pp. 1–18.
- Roorda, A., and Williams, D.R. 1999. The arrangement of the three cone classes in the living human eye. *Nature* 397: 520–522.
- Ropert, N., Miles, R., and Korn, H. 1990. Characteristics of miniature inhibitory postsynaptic currents in CA1 pyramidal neurones of rat hippocampus. *J. Physiol. (Lond.)* 428: 707–722.
- Rose, A. 1973. *Vision: Human and Electronic*. New York: Plenum Press.
- Rose, D., and Dobson, V.G. 1985. *Models of the Visual Cortex*. New York: John Wiley & Sons.
- Rose, M. 1928. Die Inselrinde des Menschen und der Tiere. *J. Psychol. Neurol. (Leipzig)* 37: 467–624.
- Rose, P.K., and Richmond, F.J.R. 1981. White-matter dendrites in the upper cervical spinal cord of the adult cat: a light and electron microscopic study. *J. Comp. Neurol.* 199: 191–203.
- Roska, B., Nemeth, E., and Werblin, F.S. 1998. Response to change is facilitated by a three-neuron disinhibitory pathway in the tiger salamander retina. *J. Neurosci.* 18: 3451–3459.
- Roska, B., and Werblin, F. 2001. Vertical interactions across ten parallel, stacked representations in the mammalian retina. *Nature* 410: 583–587.
- Ross, W.N., and Werman, J.R. 1986. Mapping calcium transients in the dendrites of Purkinje cells from the guinea-pig cerebellum in vitro. *J. Physiol. (Lond.)* 389: 319–336.
- Rossi, D.J., Alford, S., Mugnaini, E., and Slater, N.T. 1995. Properties of transmission at a giant glutamatergic synapse in cerebellum: the mossy fiber-unipolar brush cell synapse. *J. Neurophysiol.* 74: 24–42.
- Rossignol, S. 1996. Neural control of stereotypic limb movements. In: *Handbook of Physiology, Section 12. Exercise: Regulation and Integration of Multiple Systems* (Rowell, L.B., and Shepherd, J.T., ed.) Bethesda: American Physiological Society, pp. 173–216.
- Rossignol, S., and Dubuc, R. 1994. Spinal pattern generation. *Curr. Opin. Neurobiol.* 4: 894–902.
- Rothman, J.S. 1999. *Physiological and Theoretical Analysis of Potassium Conductances in Ventral Cochlear Nucleus Neurons*. Ph.D. thesis, Baltimore: Johns Hopkins University.
- Rothman, J.S., and Young, E.D. 1996. Enhancement of neural synchronization in computational models of ventral cochlear nucleus bushy cells. *Auditory Neurosci.* 2: 47–62.
- Rothman, J.S., Young, E.D., and Manis, P.B. 1993. Convergence of auditory nerve fibers onto bushy cells in the ventral cochlear nucleus: implications of a computational model. *J. Neurophysiol.* 70: 2562–2583.
- Rotter, A., Birdsall, N.J.M., Burgen, A.S.V., Field, P.M., Hulme, E.C., and Raisman, G. 1977. Muscarinic receptors in the central nervous system of the rat. I. Technique for autoradiographic localization of the binding of [3H] propylbenzilylcholine mustard and its distribution in the forebrain. *Brain Res. Rev.* 1: 141–165.
- Rouiller, E.M., Cronin-Schreiber, R., Fekete, D.M., and Ryugo, D.K. 1986. The central projections of intracellularly labeled auditory nerve fibers in cats: An analysis of terminal morphology. *J. Comp. Neurol.* 249: 261–278.

- Rouiller, E.M., and Ryugo, D.K. 1984. Intracellular marking of physiologically characterized cells in the ventral cochlear nucleus of the cat. *J. Comp. Neurol.* 225: 167–186.
- Rousselot, P., Lois, C., and Alvarez-Buylla, A. 1995. Embryonic (PSA) N-CAM reveals chains of migrating neuroblasts between the lateral ventricle and the olfactory bulb of adult mice. *J. Comp. Neurol.* 351: 51–61.
- Royal, S.J., and Key, B. 1999. Development of P2 olfactory glomeruli in P2–internal ribosome entry site-tau-LacZ transgenic mice. *J. Neurosci.* 19: 9856–9864.
- Royet, J.-P., Souchier, C., Jourdan, R., and Ploye, H. 1988. Morphometric study of the glomerular population in the mouse olfactory bulb: numerical density and size distribution along the rostrocaudal axis. *J. Comp. Neurol.* 270: 559–568.
- Royet, J.-P., Distel, H., Hudson, R., and Gervais, R. 1998. A re-estimation of the number of glomeruli and mitral cells in the olfactory bulb of the rabbit. *Brain Res.* 788: 35–42.
- Rubenstein, J.L.R., Martinez, S., Shimura, K., and Puelles, L. 1994. The embryonic vertebrate forebrain. *Science* 266: 578–580.
- Rubenstein, J.L.R., Shimura, K., Martinez, S., and Puelles, L. 1998. Regionalization of the prosencephalic neural plate. *Annu. Rev. Neurosci.* 21: 445–477.
- Rubin, R.D., and Katz, L.C. 1999. Optical imaging of odorant representations in the mammalian olfactory bulb. *Neuron* 23: 499–511.
- Rubio, M.E., and Wenthold, R.J. 1997. Glutamate receptors are selectively targeted to postsynaptic sites in neurons. *Neuron* 18: 939–950.
- Rudomin, P. 1990. Presynaptic inhibition of muscle spindle and tendon organ afferents in the mammalian spinal cord. *Trends Neurosci.* 13: 499–505.
- Rudomin, P., and Schmidt, R. 1999. Presynaptic inhibition in the vertebrate spinal cord revisited. *Exp. Brain Res.* 129: 1–37.
- Rudomin, P., Burke, R.E., Nunez, R., Madrid, J., and Dutton, H. 1975. Control by presynaptic correlation: a mechanism affecting information transmission from Ia fibers to motoneurons. *J. Neurophysiol.* 38: 267–284.
- Rudy, B. 1988. Diversity and ubiquity of K⁺ channels. *Neuroscience* 25: 729–749.
- Rumberger, A., Schmidt, M., Lohmann, H., and K.-Hoffmann, P. 1998. Correlation of electrophysiology, morphology, and functions in corticotectal and cortico pretectal projection neurons in rat visual cortex. *Exp. Brain Res.* 119: 375–390.
- Rumelhart, D., and McClelland, J. 1986. *Parallel Distributed Processing*. Cambridge, MA: MIT Press.
- Ruth, R.E., Collier, T.J., and Routtenberg, A. 1982. Topography between the entorhinal cortex and the dentate septotemporal axis in rats: I. Medial and intermediate entorhinal projecting cells. *J. Comp. Neurol.* 209: 69–78.
- Ruth, R.E., Collier, T.J., and Routtenberg, A. 1988. Topographical relationship between the entorhinal cortex and the septotemporal axis of the dentate gyrus in rats: II. Cells projecting from lateral entorhinal subdivisions. *J. Comp. Neurol.* 270: 506–516.
- Ryall, R. 1981. Patterns of recurrent excitation and mutual inhibition of cat Renshaw cells. *J. Physiol. (Lond.)* 316: 439–452.
- Ryall, R.W., Piercey, M.F., and Polosa, C. 1971. Intersegmental and intrasegmental distribution of mutual inhibition of Renshaw cells. *J. Neurophysiol.* 34: 700–707.
- Ryugo, D.K. 1992. The auditory nerve: Peripheral innervation, cell body morphology, and central projections. In: *The Mammalian Auditory Pathway: Neuroanatomy* (Webster, D.B., Popper, A.N., and Fay, R.R., eds.) New York: Springer-Verlag, pp. 23–65.
- Ryugo, D.K., and Fekete, D.M. 1982. Morphology of primary axosomatic endings in the anteroventral cochlear nucleus of the cat: a study of the endbulbs of Held. *J. Comp. Neurol.* 210: 239–257.

- Ryugo, D.K., and Sento, S. 1991. Synaptic connections of the auditory nerve in cats: relationship between endbulbs of Held and spherical bushy cells. *J. Comp. Neurol.* 305: 35–48.
- Ryugo, D.K., and Willard, F.H. 1985. The dorsal cochlear nucleus of the mouse: a light microscopic analysis of neurons that project to the inferior colliculus. *J. Comp. Neurol.* 242: 381–396.
- Ryugo, D.K., Pongstaporn, T., Wright, D.D., and Sharp, A.H. 1995. Inositol 1,4,5-triphosphate receptors: immunocytochemical localization in the dorsal cochlear nucleus. *J. Comp. Neurol.* 358: 102–118.
- Saar, D., Grossman, Y., and Barkai, E. 1998. Reduced after-hyperpolarization in rat piriform cortex pyramidal neurons is associated with increased learning capability during operant conditioning. *Eur. J. Neurosci.* 10: 1518–1523.
- Saar, D., Grossman, Y., and Barkai, E. 2001. Long-lasting cholinergic modulation underlies rule learning in rats. *J. Neurosci.* 21: 1385–1392.
- Sachs, M.B., and Abbas, P.J. 1974. Rate versus level functions for auditory-nerve fibers in cats: tone-burst stimuli. *J. Acoust. Soc. Am.* 56: 1835–1847.
- Sachs, M.B., and Young, E.D. 1979. Encoding of steady-state vowels in the auditory nerve: representation in terms of discharge rate. *J. Acoust. Soc. Am.* 66: 470–479.
- Sachs, M.B., Wang, X., and Molitor, S.C. 1993. Cross-correlation analysis and phase-locking in a model of the ventral cochlear nucleus stellate cell. In: *The Mammalian Cochlear Nuclei: Organization and Function* (Merchán, M.A., Juiz, M., and Godfrey, D.A., eds.) New York: Plenum Press, pp. 411–420.
- Sagar, S.M. 1987. Somatostatin-like immunoreactive material in the rabbit retina: immunohistochemical staining using monoclonal antibodies. *J. Comp. Neurol.* 266: 291–299.
- Sah, P., and Faber, E.S.L. 2002. Channels underlying neuronal calcium-activated potassium currents. *Prog. Neurobiol.* 66: 345–353.
- Saint Marie, R.L., Benson, C.G., Ostapoff, E.M., and Morest, D.K. 1991. Glycine immunoreactive projections from the dorsal to the anteroventral cochlear nucleus. *Hear. Res.* 51: 11–28.
- Saito, H.-A. 1983. Morphology of physiologically identified X-, Y-, and W-type retinal ganglion cells of the cat. *J. Comp. Neurol.* 221: 279–288.
- Saito, T. 1999. Development and regeneration of the retina. In: *The Retinal Basis of Vision* (Toyoda, J., Murakami, M., Kaneko, A., and Saito, T., eds.) Tokyo: Elsevier.
- Saito, T., Kujiraoka, T., Yonaha, T., and Chino, Y. 1985. Reexamination of photoreceptor-bipolar connectivity patterns in carp retina: HRP-EM and Golgi-EM studies. *J. Comp. Neurol.* 236: 141–160.
- Sakai, H.M., and Naka, K.-I. 1985. Novel pathway connecting the outer and inner vertebrate retina. *Nature* 315: 570–571.
- Sakmann, B. 1992. Elementary steps in synaptic transmission revealed by currents through single ion channels. *Science* 256: 503–512.
- Sakmann, B., and Creutzfeldt, O.D. 1969. Scotopic and mesopic light adaptation in the cat's retina. *Pflügers Arch.* 313: 168–185.
- Salin, P.-A., and Bullier, J. 1995. Corticocortical connections in the visual system: Structure and function. *Physiol. Rev.* 75: 107–154.
- Salin, P.-A., Lledo, P.M., Vincent, J.D., and Charpak, S. 2001. Dendritic glutamate autoreceptors modulate signal processing in rat mitral cells. *J. Neurophysiol.* 85: 1275–1282.
- Salkoff, L., Baker, K., Butler, A., Covarrubias, M., Pak, M.D., and Wei, A. 1992. An essential 'set' of K⁺ channels conserved in flies, mice, and humans. *Trends Neurosci.* 15: 161–166.
- Sallaz, M., and Jourdan, F. 1992. Apomorphine disrupts odour-induced patterns of glomerular activation in the olfactory bulb. *NeuroReport* 3: 833–836.

- Sallaz, M., and Jourdan, F. 1993. C-fos expression and 2-deoxyglucose uptake in the olfactory bulb of odour-stimulated awake rats. *NeuroReport* 4: 55–58.
- Salt, T.E. 1988. Electrophysiological studies of excitatory amino acid neurotransmitters in the ventrobasal thalamus. In: *Cellular Thalamic Mechanisms* (Macchi, G., Bentivoglio, M., and Spreafico, R., eds.) Amsterdam: Elsevier, pp. 297–310.
- Salt, T.E., and Eaton, S.A. 1991. Sensory excitatory postsynaptic potentials mediated by NMDA and non-NMDA receptors in the thalamus *in vivo*. *Eur. J. Neurosci.* 3: 296–300.
- Salt, T.E., and Eaton, S.A. 1996. Functions of ionotropic and metabotropic glutamate receptors in sensory transmission in the mammalian thalamus. *Prog. Neurobiol.* 48: 55–72.
- Salt, T.E., and Sillito, A. 1984. The action of somatostatin (SST) on the response properties of cells in the cat's visual cortex. *J. Physiol. (Lond.)* 350: 28P.
- Salzman, C., and Newsome, W. 1994. Neural mechanisms for forming a perceptual decision. *Science* 264: 231–237.
- Sanchez-Vives, M.V., Bal, T., Kim, U., Von Krosigk, M., and McCormick, D.A. 1996. Are the interlaminar zones of the ferret dorsal lateral geniculate nucleus actually part of the perigeniculate nucleus? *J. Neurosci.* 16: 5923–5941.
- Sandell, J.H. 1985. NADPH diaphorase cells in the mammalian inner retina. *J. Comp. Neurol.* 238: 466–472.
- Sandell, J.H., and Masland, R.H. 1986. A system of indoleamine-accumulating neurons in the rabbit retina. *J. Neurosci.* 6: 3331–3347.
- Sanderson, K.J. 1971. Visual field projection columns and magnification factors in the lateral geniculate nucleus of the cat. *Exp. Brain Res.* 13: 159–177.
- Sandmann, D., Boycott, B.B., and Peichl, L. 1996. The horizontal cells of artiodactyl retinae: a comparison with Cajal's descriptions. *Vis. Neurosci.* 13: 735–746.
- Sandoval, M.E., and Cotman, C.W. 1978. Evaluation of glutamate as a neurotransmitter of cerebellar parallel fibers. *Neuroscience* 3: 199–206.
- Sanes, D.H., Reh, T.A., and Harris, W.A. 2000. *Development of the Nervous System*. New York: Academic.
- Sanides, F., and Sanides, D. 1972. The "extraverted neurons" of the mammalian cerebral cortex. *Z. Anat. Entwickl.-Gesch.* 136: 272–293.
- Sanides-Kohlrausch, C., and Wahle, P. 1990. VIP- and PHI-immunoreactivity in olfactory centers of the adult cat. *J. Comp. Neurol.* 294: 325–339.
- Sasaki, T., and Kaneko, A. 1996. L-glutamate-induced responses in OFF-type bipolar cells of the cat retina. *Vision Res.* 36: 787–795.
- Sashihara, S., Greer, C.A., Oh, Y., and Waxman, S.G. 1996. Cell-specific differential expression of Na⁺-channel B1-subunit mRNA in the olfactory system during postnatal development and after denervation. *J. Neurosci.* 16: 702–713.
- Sassoè-Pognetto, M., Cantino, D., Panzanelli, P., Verdun Di Cantogno, L., Giustetto, M., Margolis, F.L., De Biasi, S., and Fasolo, A. 1993. Presynaptic co-localization of carnosine and glutamate in olfactory neurons. *NeuroReport* 5: 7–10.
- Sassoè-Pognetto, M., and Ottersen, O.P. 2000. Organization of ionotropic glutamate receptors at dendrodendritic synapses in the rat olfactory bulb. *J. Neurosci.* 20: 2192–2201.
- Sassoè-Pognetto, M., Wässle, H., and Grünert, U. 1994. Glycinergic synapses in the rod pathway of the rat retina: cone bipolar cells express the alpha-1 subunit of the glycine receptor. *J. Neurosci.* 14: 5131–5146.
- Sato, T., Hirono, J., Tonoike, M., and Takebayashi, M. 1994. Tuning specificities to aliphatic odorants in mouse olfactory receptor neurons and their local distribution. *J. Neurophysiol.* 72: 2980–2989.
- Satoh, H., Kaneda, M., and Kaneko, A. 2001. Intracellular chloride concentration is higher in rod bipolar cells than in cone bipolar cells of the mouse retina. *Neurosci. Lett.* 310: 161–164.

- Satou, M., Mori, K., Tazawa, Y., and Takagi, S.F. 1982. Long-lasting disinhibition in pyriform cortex of the rabbit. *J. Neurophysiol.* 48: 1157–1163.
- Satou, M., Mori, K., Tazawa, Y., and Takagi, S.F. 1983a. Neuronal pathways for activation of inhibitory interneurons in pyriform cortex of the rabbit. *J. Neurophysiol.* 50: 74–88.
- Satou, M., Mori, K., Tazawa, Y., and Takagi, S.F. 1983b. Interneurons mediating fast postsynaptic inhibition in pyriform cortex of the rabbit. *J. Neurophysiol.* 50: 89–101.
- Saul, A.B., and Humphrey, A.L. 1990. Spinal and temporal response properties of lagged and nonlagged cells in cat lateral geniculate nucleus. *J. Neurophysiol.* 64: 206–224.
- Saul, A.B., and Humphrey, A.L. 1992. Evidence of input from lagged cells in the lateral geniculate nucleus to simple cells in cortical area 17 of the cat. *J. Neurophysiol.* 68: 1190–1208.
- Savage, G.L., and Banks, M.S. 1992. Scotopic visual efficiency: constraints by optics, receptor properties, and rod pooling. *Vis. Res.* 32: 645–656.
- Sayer, R., Schwandt, P., and Crill, W. 1992. Metabotropic glutamate receptor-mediated suppression of L-type calcium current in acutely isolated neocortical neurons. *J. Neurophysiol.* 68: 833–842.
- Scatton, B., Simon, H., Moal, M.L., and Bischoff, S. 1980. Origins of dopaminergic innervation of the rat hippocampal formation. *Neurosci. Lett.* 18: 125–131.
- Scharfman, H., and Sarvey, J. 1987. Responses to GABA recorded from identified rat visual cortical neurons. *Neuroscience* 23: 407–422.
- Scharfman, H.E. 1994. EPSPs of dentate gyrus granule cells during epileptiform bursts of dentate hilar “mossy” cells and area CA3 pyramidal cells in disinhibited rat hippocampal slices. *J. Neurosci.* 14: 6041–6057.
- Scharfman, H.E. 1995. Electrophysiological evidence that dentate hilar mossy cells are excitatory and innervate both granule cells and interneurons. *J. Neurophysiol.* 74: 179–194.
- Scharfman, H.E., and Schwartzkroin, P.A. 1988. Electrophysiology of morphologically identified mossy cells of the dentate hilus recorded in guinea pig hippocampal slices. *J. Neurosci.* 8: 3812–3821.
- Scharfman, H.E., Kunkel, D.D., and Schwartzkroin, P.A. 1990a. Synaptic connections of dentate granule cells and hilar neurons: results of paired intracellular recordings and intracellular horseradish peroxidase injections. *Neuroscience* 37: 693–707.
- Scharfman, H.E., Lu, S.-M., Guido, W., Adams, P.R., and Sherman, S.M. 1990b. N-Methyl-D-aspartate (NMDA) receptors contribute to excitatory postsynaptic potentials of cat lateral geniculate neurons recorded in thalamic slices. *Proc. Natl. Acad. Sci. U.S.A.* 87: 4548–4552.
- Scheibel, A.B., and Conrad, A.S. 1993. Hippocampal dysgenesis in mutant mouse and schizophrenic man—is there a relationship? *Schizophr. Bull.* 19: 21–33.
- Scheibel, M.E., and Scheibel, A.B. 1973. Hippocampal pathology in temporal lobe epilepsy. A Golgi survey. In: *Epilepsy, Its Phenomena in Man* (Brazier, M.A.B., ed.) New York: Academic Press, pp. 315–337.
- Schein, S. 1988. Anatomy of macaque fovea and spatial densities of neurones in foveal representation. *J. Comp. Neurol.* 269: 479–505.
- Schein, S.J., and de Monasterio, F.M. 1987. Mapping of retinal and geniculate neurons onto striate cortex of macaque. *J. Neurosci.* 7: 996–1009.
- Schiller, J., Helmchen, F., and Sakmann, B. 1995. Spatial profile of dendritic calcium transients evoked by action potentials in rat neocortical pyramidal neurones. *J. Physiol. (Lond.)* 487: 583–600.
- Schiller, J., Schiller, Y., Stuart, G., and Sakmann, B. 1997. Calcium action potentials restricted to distal apical dendrites of rat neocortical pyramidal neurones. *J. Physiol. (Lond.)* 505: 605–616.
- Schiller, P.H., Sandell, J.H., and Maunsell, J.H.R. 1986. Functions of the ON and OFF channels of the visual system. *Nature* 322: 824–825.

- Schlaggar, B., Fox, K., and O'Leary, D. 1993. Postsynaptic control of plasticity in developing somatosensory cortex. *Nature* 364: 623–626.
- Schmechel, D., Vickery, B., Fitzpatrick, D., and Elde, R. 1984. GABAergic neurons of mammalian cerebral cortex: widespread subclass defined by somatostatin content. *Neurosci. Lett.* 47: 227–232.
- Schmid, S., Guthmann, A., Ruppertsberg, J.P., and Herbert, H. 2001. Expression of AMPA receptor subunit flip/flop splice variants in the rat auditory brainstem and inferior colliculus. *J. Comp. Neurol.* 430: 160–171.
- Schmidt, B., and Jordan, L. 2000. The role of serotonin in reflex modulation and locomotor rhythm production in the mammalian spinal cord. *Brain Res. Bull.* 53: 689–710.
- Schmidt, M., Humphrey, M.F., and Wässle, H. 1987. Action and localization of acetylcholine in the cat retina. *J. Neurophysiol.* 58: 997–1015.
- Schmielau, F., and Singer, W. 1977. The role of visual cortex for binocular interactions in the cat lateral geniculate nucleus. *Brain Res.* 120: 354–361.
- Schnapf, J.L., Nunn, B.J., Meister, M., and Baylor, D.A. 1990. Visual transduction in cones of the monkey *Macaca fascicularis*. *J. Physiol. (Lond.)* 427: 681–713.
- Schneeweis, D.M., and Schnapf, J.L. 1995. Photovoltage of rods and cones in the macaque retina. *Science* 268: 1053–1056.
- Schneeweis, D.M., and Schnapf, J.L. 1999. The photovoltage of Macaque cone photoreceptors: adaptation, noise, and kinetics. *J. Neurosci.* 19: 1203–1216.
- Schneider, G.E. 1969. Two visual systems. *Science* 163: 895–902.
- Schneider, S.P., and Fyffe, R.E.W. 1992. Involvement of GABA and glycine in recurrent inhibition of spinal motoneurons. *J. Neurophysiol.* 68: 397–406.
- Schneider, S.P., and Macrides, F. 1978. Laminar distribution of interneurons in the main olfactory bulb of adult hamster. *Brain Res. Bull.* 3: 73–82.
- Schneider, S.P., and Scott, J.W. 1983. Orthodromic response properties of rat olfactory bulb mitral and tufted cells correlate with their projection patterns. *J. Neurophysiol.* 50: 358–378.
- Schoenbaum, G., Chiba, A.A., and Gallagher, M. 1999. Neural encoding in orbitofrontal cortex and basolateral amygdala during olfactory discrimination learning. *J. Neurosci.* 19: 1876–1884.
- Schoenbaum, G., and Eichenbaum, H. 1995. Information coding in the rodent prefrontal cortex. I. Single-neuron activity in orbitofrontal cortex compared with that in pyriform cortex. *J. Neurophysiol.* 74: 733–750.
- Schoenfeld, T.A., Marchand, J.E., and Macrides, F. 1985. Topographic organization of tufted cell axonal projections in the hamster main olfactory bulb: an intrabulbar associational system. *J. Comp. Neurol.* 235: 503–518.
- Schoepfer, R., Monyer, H., Sommer, B., Wisden, W., Sprengel, R., Kuner, T., Lomeli, H., Herb, A., Kohler, M., Burnashev, N., Gunther, W., Ruppertsberg, P., and Seeburg, P. 1994. Molecular biology of glutamate receptors. *Prog. Neurobiol.* 42: 353–357.
- Schoepp, D.D., and Conn, P.J. 1993. Metabotropic glutamate receptors in brain function and pathology. *Trends Pharmacol. Sci.* 14: 13–20.
- Schofield, B.R. 1995. Projections from the cochlear nucleus to the superior paraolivary nucleus in guinea pigs. *J. Comp. Neurol.* 360: 135–149.
- Schofield, B.R., and Cant, N.B. 1996. Origins and targets of commissural connections between the cochlear nuclei in guinea pigs. *J. Comp. Neurol.* 375: 128–146.
- Scholfield, C.N. 1978a. Electrical properties of neurones in the olfactory cortex slice in vitro. *J. Physiol. (Lond.)* 275: 535–546.
- Scholfield, C.N. 1978b. A depolarizing inhibitory potential in neurones of the olfactory cortex in vitro. *J. Physiol. (Lond.)* 275: 547–557.
- Schomburg, E.D., and Behrends, H.B. The possibility of phase-dependent monosynaptic and

- polysynaptic Ia excitation to homonymous motoneurons during fictive locomotion. *Brain Res.* 143: 533–7, 1978.
- Schoppa, N.E., Kinzie, J.M., Sahara, Y., Segerson, T.P., and Westbrook, G.L. 1998. Dendrodendritic inhibition in the olfactory bulb is driven by NMDA receptors. *J. Neurosci.* 18: 6790–6802.
- Schoppa, N.E., and Westbrook, G.L. 1999. Regulation of synaptic timing in the olfactory bulb by an A-type potassium current. *Nat. Neurosci.* 2: 1106–1113.
- Schoppa, N.E., and Westbrook, G.L. 2001. Glomerulus-specific synchronization of mitral cells in the olfactory bulb. *Neuron* 31: 639–651.
- Schoppa, N.E., and Westbrook, G.L. 2002. AMPA autoreceptors drive correlated spiking in olfactory bulb glomeruli. *Nature Neurosci.* 5: 1194–1202.
- Schultz, W. 1998. Predictive reward signal of dopaminergic neurons. *J. Neurophysiol.* 80: 1–27.
- Schultz, W., Dayan, P., and Montague, R.R. 1997. A neural substrate of prediction and reward. *Science* 275: 1593–1599.
- Schultz, W., Romo, R., Ljungberg, T., Mirenowicz, J., Hollerman, J.R., and Dickenson, A. 1995. Reward-related signals carried by dopamine neurons. In: *Models of Information Processing in the Basal Ganglia* (J.C. Houk, J.L. Davis, and D.G. Beiser, eds.). Cambridge, MA: MIT Press, pp. 233–248.
- Schulz, P.E., Cook, E.P., and Johnston, D. 1994. Changes in paired-pulse facilitation suggest presynaptic involvement in long-term potentiation. *J. Neurosci.* 14: 5325–5337.
- Schulz, P.E., and Fitzgibbons, J.C. 1997. Differing mechanisms of expression for short-term and long-term potentiation. *J. Neurophysiol.* 78: 321–334.
- Schuman, E.M., and Madison, D.V. 1991. A requirement for the intercellular messenger nitric oxide in long-term potentiation. *Science* 254: 1503–1506.
- Schuman, E.M., and Madison, D.V. 1994. Nitric oxide and synaptic function. *Annu. Rev. Neurosci.* 17: 153–183.
- Schwartz, G.A., Kostek, C., Ahmad, N., Dibble, C., Pays, L., and Puschel, A.W. 2000. Semaphorin 3A is required for guidance of olfactory axons in mice. *J. Neurosci.* 20: 7691–7697.
- Schwartz, E. 1987. Depolarization without calcium can release gamma-aminobutyric acid from a retinal neuron. *Science* 238: 350–355.
- Schwartz, M.L., Dekker, J.J., and Goldman-Rakic, P.S. 1991. Dual mode of corticothalamic synaptic termination in the mediodorsal nucleus of the rhesus monkey. *J. Comp. Neurol.* 309: 289–304.
- Schwartz, S.P., and Coleman, P.D. 1981. Neurons of origin of the perforant path. *Exp. Neurol.* 74: 305–312.
- Schwartzkroin, P.A. 1975. Characteristics of CA1 neurons recorded intracellularly in the hippocampal in vitro slice preparation. *Brain Res.* 85: 423–436.
- Schwartzkroin, P.A. 1977. Further characteristics of hippocampal CA1 cells in vitro. *Brain Res.* 128: 53–68.
- Schwartzkroin, P.A. 1986. Regulation of excitability in hippocampal neurons. In: *The Hippocampus* (Isaacson, R.L., and Pribram, K.H., eds.) New York: Plenum Press, pp. 113–136.
- Schwartzkroin, P.A., and Kunkel, D.D. 1985. Morphology of identified interneurons in the CA1 regions of guinea pig hippocampus. *J. Comp. Neurol.* 232: 205–218.
- Schwartzkroin, P.A., and Mathers, L.H. 1978. Physiological and morphological identification of a nonpyramidal hippocampal cell type. *Brain Res.* 157: 1–10.
- Schwartzkroin, P.A., and Slawsky, M. 1977. Probable calcium spikes in hippocampal neurons. *Brain Res.* 135: 157–161.
- Schwindt, P. 1992. Ionic currents governing input-output relations of Betz cells. In: *Single Neuron Computation* (McKenna, J.D.T., and Zornetzer, S., eds.) Orlando, FL: Academic Press, pp. 235–258.

- Schwandt, P., and Crill, W.E. 1977. A persistent negative resistance in cat lumbar motoneurons. *Brain Res.* 120: 173–178.
- Schwandt, P., and Crill, W. 1980. Properties of a persistent inward current in normal and TEA-injected motoneurons. *J. Neurophysiol.* 43: 1700–1724.
- Schwandt, P., Spain, W., Foehring, R., Chubb, M., and Crill, W. 1988a. Slow conductances in neurons from cat sensorimotor cortex in vitro and their role in slow excitability changes. *J. Neurophysiol.* 59: 450–467.
- Schwandt, P., Spain, W., Foehring, R., Stafstrom, C., Chubb, M., and Crill, W.E. 1988b. Multiple potassium conductances and their functions in neurons from cat sensorimotor cortex in vitro. *J. Neurophysiol.* 59: 424–449.
- Schwob, J.E. 1992. The biochemistry of olfactory neurons: Stages of differentiation and neuronal subsets. In: *Science of Olfaction* (Serby, M.J., and Chobor, K.L., eds.) New York: Springer-Verlag, pp. 80–125.
- Schwob, J.E. 2002. Neural regeneration and the peripheral olfactory system. *Anat. Rec.* 269: 33–49.
- Schwob, J.E., and Price, J.L. 1978. The cortical projection of the olfactory bulb: development in fetal and neonatal rats correlated with quantitative variations in adult rats. *Brain Res.* 151: 369–374.
- Scott, J.W. 1981. Electrophysiological identification of mitral and tufted cells and distributions of their axons in olfactory system of the rat. *J. Neurophysiol.* 46: 918–931.
- Scott, J.W., and Harrison, T.A. 1987. The olfactory bulb: anatomy and physiology. In: *Neurobiology of Taste and Smell* (Finger, T.E., and Silver, W.K., eds.) New York: John Wiley & Sons, pp. 151–178.
- Scott, J.W., McBride, R.L., and Schneider, S.P. 1980. The organization of projections from the olfactory bulb to the piriform cortex and olfactory tubercle in the rat. *J. Comp. Neurol.* 194: 519–534.
- Scoville, W.B., and Milner, B. 1957. Loss of recent memory after bilateral hippocampal lesions. *J. Neurol. Psychiatry* 20: 11–21.
- Segal, M. 2002. Changing views of Cajal's neuron: the case of the dendritic spine. *Prog. Brain Res.* 136: 101–107.
- Segev, I. 1995. Cable and compartmental models of dendritic trees. In: *The Book of Genesis, Exploring Realistic Neural Models with the GEneral NEural Simulation System* (Bower, J.M., and Beeman, D., eds.) New York: Springer-Verlag, pp. 53–82.
- Segev, I., Fleshman, J.W., and Burke, R.E. 1989. Compartmental models of complex neurons. In: *Methods in Neuronal Modeling: From Synapse to Network* (Koch, C., and Segev, I., eds.) Cambridge, MA: MIT Press, pp. 63–93.
- Segev, I., Fleshman, J.W., and Burke, R.E. 1990a. Computer simulation of group Ia EPSPs using morphologically realistic models of cat α -motoneurons. *J. Neurophysiol.* 64: 648–660.
- Segev, I., and London, M. 1999. A theoretical view of passive and active dendrites. In: *Dendrites* (Stuart, G.J., Spruston, N., and Häusser, M., ed.) New York: Oxford University Press, pp. 205–230.
- Segev, I., and Rall, W. 1988. Computational study of an excitable dendritic spine. *J. Neurophysiol.* 60: 499–523.
- Segev, I., Rinzal, J., and Shepherd, G.M. (eds.). 1995. *The Theoretical Foundation of Dendritic Function*. Cambridge, MA: MIT Press.
- Sejnowski, T., Koch, C., and Churchland, P. 1988. Computational neuroscience. *Science* 241: 1299–1306.
- Selemon, L.D., and Goldman-Rakic, P.S. 1985. Longitudinal topography and interdigitation of corticostriatal projections in the rhesus monkey. *J. Neurosci.* 5: 776–794.
- Selverston, A., Elson, R., Rabinovich, M., Huerta, R., and Abarbanel, H. 1998. Basic principles

- for generating motor output in the stomatogastric ganglion. In: *Neuronal Mechanisms for Generating Locomotor Activity* (Kiehn, O., Harris-Warrick, R.M., Jordan, L.M., Hultborn, H., and Kudo, N., eds.) New York, NY: N.Y. Acad. Sci., pp. 35–50.
- Senaris, R.M., Humphrey, P.P., and Emson, P.C. 1994. Distribution of somatostatin receptors 1, 2 and 3 mRNA in rat brain and pituitary. *Eur. J. Neurosci.* 6: 1883–1896.
- Sengpiel, F., and Bonhoeffer, T. 2002. Orientation specificity of contrast adaptation in visual cortical pinwheel centres and iso-orientation domains. *Eur. J. Neurosci.* 15: 876–86.
- Sento, S., and Ryugo, D.K. 1989. Endbulbs of Held and spherical bushy cells in cats: morphological correlates with physiological properties. *J. Comp. Neurol.* 280: 553–562.
- Seress, L., Abraham, H., Paleszter, M., and Gallyas, F. 2001. Granule cells are the main source of excitatory input to a subpopulation of GABAergic hippocampal neurons as revealed by electron microscopic double staining for zinc histochemistry and parvalbumin immunocytochemistry. *Exp. Brain Res.* 136: 456–462.
- Seress, L., and Ribak, C.E. 1984. Direct commissural connections to the basket cells of the hippocampal dentate gyrus: anatomical evidence for feed-forward inhibition. *J. Neurocytol.* 13: 215–225.
- Shadlen, M., and Newsome, W. 1996. Motion perception: seeing and deciding. *Proc. Natl. Acad. Sci. U.S.A.* 93: 628–633.
- Shamma, S. 1998. Spatial and temporal processing in central auditory networks. In: *Methods in Neuronal Modeling: From Ions to Networks* (Koch, C., and Segev, I., eds.) Cambridge, MA: MIT Press, pp. 411–460.
- Shannon, C.E., and Weaver, W. 1949. *The Mathematical Theory of Communication*. Urbana, IL: University of Illinois Press.
- Shannon, R.V., Zeng, F.-G., Kamath, V., Wygonski, J., and Ekelid, M. 1995. Speech recognition with primarily temporal cues. *Science* 270: 303–304.
- Shapley, R., and Lennie, P. 1985. Spatial frequency analysis in the visual system. *Annu. Rev. Neurosci.* 8: 547–583.
- Shapley, R., and Perry, V.H. 1986. Cat and monkey retinal ganglion cells and their visual functional roles. *Trends Neurosci.* 9: 229–235.
- Shapley, R.M., and Victor, J.D. 1978. The effect of contrast on the transfer properties of cat retinal ganglion cells. *J. Physiol. (Lond.)* 285: 275–298.
- Shapovalov, A.I., and Shiraev, B.I. 1980. Dual mode of junctional transmission at synapses between single primary afferent fibers and motoneurons in amphibian. *J. Physiol. (Lond.)* 306: 1–15.
- Shapovalov, A.I., and Shiraev, B.L. 1982. Selective modulation of chemical transmission at a dual-action synapse (with special reference to baclofen). *Gen. Physiol. Biophys.* 1: 423–433.
- Sharp, F.R., Kauer, J.S., and Shepherd, G.M. 1975. Local sites of activity-related glucose metabolism in rat olfactory bulb during olfactory stimulation. *Brain Res.* 98: 596–600.
- Sharp, F.R., Kauer, J.S., and Shepherd, G.M. 1977. Laminar analysis of 2-deoxyglucose uptake in olfactory bulb and olfactory cortex of rabbit and rat. *J. Neurophysiol.* 40: 800–813.
- Sharpe, L.T., and Stockman, A. 1999. Rod pathway: the importance of seeing nothing. *Trends Neurosci.* 22: 497–504.
- Sharrard, W.J.W. 1955. The distribution of the permanent paralysis in the lower limb in poliomyelitis. *J. Bone Joint Surg.* 37: 540–558.
- Sheldon, P.W., and Aghajanian, G.K. 1990. Serotonin (5-HT) induces IPSPs in pyramidal layer cells of rat piriform cortex: evidence for the involvement of a 5-HT₂-activated interneuron. *Brain Res.* 506: 62–69.
- Sheldon, P.W., and Aghajanian, G.K. 1991. Excitatory responses to serotonin (5-HT) in neurons of the rat piriform cortex: evidence for mediation by 5-HT_{1C} receptors in pyramidal cells and 5-HT₂ receptors in interneurons. *Synapse* 9: 208–218.

- Shen, G., Chen, W.R., Midtgaard, J., Shepherd, G.M., and Hines, M.L. 1999. Computational analysis of action potential initiation in mitral cell soma and dendrites based on dual patch recordings. *J. Neurophysiol.* 82: 3006–3020.
- Shepherd, G., Brayton, R., Miller, J., Segev, I., Rinzel, J., and Rall, W. 1985. Signal enhancement in distal cortical dendrites by means of interactions between active dendritic spines. *Proc. Natl. Acad. Sci. U.S.A.* 82: 2192–2195.
- Shepherd, G.M. 1963. Neuronal systems controlling mitral cell excitability. *J. Physiol. (Lond.)* 168: 101–117.
- Shepherd, G.M. 1972a. The neuron doctrine: a revision of functional concepts. *Yale J. Biol. Med.* 45: 584–599.
- Shepherd, G.M. 1972b. Synaptic organization of the mammalian olfactory bulb. *Physiol. Rev.* 52: 864–917.
- Shepherd, G.M. 1974. *The Synaptic Organization of the Brain*. New York: Oxford University Press.
- Shepherd, G.M. 1978. Microcircuits in the nervous system. *Sci. Am.* 238: 93–103.
- Shepherd, G.M. 1979. *The Synaptic Organization of the Brain*, 2nd edition. New York: Oxford University Press.
- Shepherd, G.M. 1988a. A basic circuit for cortical organization. In: *Perspectives on Memory Research* (Gazzaniga, M., ed.) Cambridge, MA: MIT Press, pp. 93–134.
- Shepherd, G.M. 1988b. Studies of development and plasticity in the olfactory sensory neuron. *J. Physiol. (Paris)* 83: 240–245.
- Shepherd, G.M. 1990. The significance of real neuron architectures for neural network simulations. In: *Computational Neuroscience* (Schwartz, E., ed.) Cambridge, MA: MIT Press.
- Shepherd, G.M. 1991a. Computational structure of the olfactory system. In: *Olfaction: A Model System for Computational Neuroscience* (Davis, J.L., and Eichenbaum, H., eds.) Cambridge, MA: MIT Press, pp. 3–41.
- Shepherd, G.M. 1991b. *Foundations of the Neuron Doctrine*. New York: Oxford University Press.
- Shepherd, G.M. 1992. Modules for molecules. *Nature* 358: 457–458.
- Shepherd, G.M. 1994a. Discrimination of molecular signals by the olfactory receptor neuron. *Neuron* 13: 771–790.
- Shepherd, G.M. 1994b. *Neurobiology*, 3rd edition. New York: Oxford University Press.
- Shepherd, G.M. 1996. The dendritic spine: a multifunctional integrative unit. *J. Neurophysiol.* 75: 2197–2210.
- Shepherd, G.M. 2003a. Electrotonic properties of axons and dendrites. In *Fundamental Neuroscience* (Squire, L.R., Bloom, F.E., McConnell, S.K., Roberts, J.L., Spitzer, N.C., and Zigmond, M.J., eds.) New York: Academic Press, pp. 115–139.
- Shepherd, G.M. 2003b. Information processing in complex dendrites. In *Fundamental Neuroscience* (Squire, L.R., Bloom, F.E., McConnell, S.K., Roberts, J.L., Spitzer, N.C., and Zigmond, M.J., eds.) New York: Academic Press, pp. 319–338.
- Shepherd, G.M., and Brayton, R.K. 1979. Computer simulation of a dendrodendritic synaptic circuit for self- and lateral-inhibition in the olfactory bulb. *Brain Res.* 175: 377–382.
- Shepherd, G.M., and Brayton, R.K. 1987. Logic operations are properties of computer-simulated interactions between excitable dendritic spines. *Neuroscience* 21: 151–166.
- Shepherd, G.M., and Firestein, S. 1991a. Making scents of olfactory transduction. *Curr. Biol.* 1: 204–206.
- Shepherd, G.M., Carnevale, N.T., and Woolf, T.B. 1989a. Comparisons between active properties of distal dendritic branches and spines: implications for neuronal computations. *J. Cogn. Neurosci.* 1: 273–286.
- Shepherd, G.M., and Firestein, S. 1991b. Toward a pharmacology of odor receptors and the processing of odor images. *J. Steroid Biochem. Mol. Biol.* 39: 538–592.

- Shepherd, G.M., and Greer, C.A. 1988. The dendritic spine: Adaptations of structure and function for different types of synaptic integration. In: *Intrinsic Determinants of Neuronal Form and Function* (Lassek, R., ed.) New York: Alan R. Liss, pp. 245–262.
- Shepherd, G.M.G., and Corey, D.P. 1992. Sensational science. Sensory transduction: 45th annual symposium of the Society of General Physiologists, Marine Biological Laboratory, Woods Hole, MA, September 5–8, 1991. *New Biologist* 4: 48–52.
- Shepherd, G.M.G., and Corey, D.P. 1994. The extent of adaptation in bullfrog saccular hair cells. *J. Neurosci.* 14: 6217–6229.
- Shepherd, G.M.G., Barres, B.A., and Corey, D.P. 1989b. “Bundle blot” purification and initial protein characterization of hair cell stereocilia. *Proc. Natl. Acad. Sci. U.S.A.* 86: 4973–4977.
- Shepherd, G.M.G., and Harris, K.M. 1998. Three-dimensional structure and composition of CA3->CA1 axons in rat hippocampal slices: implications for presynaptic connectivity and compartmentalization. *J. Neurosci.* 18: 8300–8310.
- Sherman, S.M. 1985. Functional organization of the W-, X-, and Y-cell pathways in the cat: a review and hypothesis. In: *Progress in Psychobiology and Physiological Psychology* (Sprague, J.M., and Epstein, A.N., eds.) Orlando: Academic Press, pp. 233–314.
- Sherman, S.M. 1988. Functional organization of the cat’s lateral geniculate nucleus. In: *Cellular Thalamic Mechanisms* (Macchi, G., Bentivoglio, M., and Spreafico, R., eds.) Amsterdam: Elsevier, pp. 163–183.
- Sherman, S.M. 1993. Dynamic gating of retinal transmission to the visual cortex by the lateral geniculate nucleus. In: *Thalamic Networks for Relay and Modulation* (Minciacchi, D., Molinari, M., Macchi, G., and Jones, E.G., eds.) Oxford: Pergamon Press, pp. 61–79.
- Sherman, S.M. 1995. Dual response modes in lateral geniculate neurons: mechanisms and functions. *Vis. Neurosci.* 13: 205–213.
- Sherman, S.M. 2001. Tonic and burst firing: dual modes of thalamocortical relay. *Trends Neurosci.* 24: 122–126.
- Sherman, S.M., and Friedlander, M.J. 1988. Identification of X versus Y properties for interneurons in the A-laminae of the cat’s lateral geniculate nucleus. *Exp. Brain. Res.* 73: 384–392.
- Sherman, S.M., and Guillery, R.W. 1998. On the actions that one nerve cell can have on another: distinguishing “drivers” from “modulators.” *Proc. Natl. Acad. Sci. U.S.A.* 95: 7121–7126.
- Sherman, S.M., and Guillery, R.W. 1996. The functional organization of thalamocortical relays. *J. Neurophysiol.* 76: 1367–1395.
- Sherman, S.M., and Guillery, R.W. 2001. Exploring the Thalamus. San Diego: Academic Press.
- Sherman, S.M., and Guillery, R.W. 2002. The role of thalamus in the flow of information to cortex. *Phil. Trans. R. Soc. Lond. B* 357: 1695–1708.
- Sherman, S.M., and Koch, C. 1986. The control of retinogeniculate transmission in the mammalian lateral geniculate nucleus. *Exp. Brain. Res.* 63: 1–20.
- Sherman, S.M., and Spear P.D. 1982. Organization of visual pathways in normal and visually deprived cats. *Physiol. Rev.* 62: 738–855.
- Sherrington, C. 1941. *Man on His Nature*. Cambridge: Cambridge University Press.
- Shibuki, K., and Okada, D. 1991. Endogenous nitric oxide release required for long-term depression in the cerebellum. *Nature* 349: 326–328.
- Shields, C.R., Tran, M.N., Wong, R.O.L., and Lukasiewicz, P.D. 2000. Distinct ionotropic GABA receptors mediate presynaptic and postsynaptic inhibition in retinal bipolar cells. *J. Neurosci.* 20: 2673–2682.
- Shiells, R.A., and Falk, G. 1990. Glutamate receptors of rod bipolar cells are linked to a cyclic GMP cascade via a G-protein. *Proc. R. Soc. Lond. B* 242: 91–94.
- Shiells, R.A., and Falk, G. 1999. A rise in intracellular Ca²⁺ underlies light adaptation in dogfish retinal ‘on’ bipolar cells. *J. Physiol.* 514: 343–350.

- Shigemoto, R., Kinoshita A., Wada, E., Nomura, S., Ohishi, H., Takada, M., Flor, P.J., Neki, A., Abe, T., Nakanishi, S., et al. 1997. Differential presynaptic localization of metabotropic glutamate receptor subtypes in the rat hippocampus. *J. Neurosci.* 17: 7503–7522.
- Shik, M., Severin, F., and Orlovsky, G. 1966. Control of walking and running by means of electrical stimulation of the midbrain. *Biophysics* 11: 756–765.
- Shinoda, Y., Futami, T., Mitoma, H., and Yokota, J. 1988. Morphology of single neurones in the cerebello-rubrospinal system. *Behav. Brain Res.* 28: 59–64.
- Shinoda, Y., Ohgaki, T., and Futami, T. 1986. The morphology of single lateral vestibulospinal tract axons in the lower cervical spinal cord of the cat. *J. Comp. Neurol.* 249: 226–241.
- Shinoda Y., Sugiuchi Y., Futami T., and Izawa R. 1992. Axon collaterals of mossy fibers from the pontine nucleus in the cerebellar dentate nucleus. *J. Neurophysiol.* 67: 547–560.
- Shinoda, Y., Yamaguchi, T., and Futami, T. 1986b. Multiple axon collaterals of single corticospinal axons in the cat spinal cord. *J. Neurophysiol.* 55: 425–448.
- Shinozaki, H., and Konishi, S. 1970. Actions of several antihelmintics and insecticides on rat cortical neurones. *Brain Res.* 24: 368–371.
- Shiple, M.T. 1974. Presubiculum afferents to the entorhinal area and the papez circuit. *Brain Res.* 67: 162–168.
- Shiple, M.T., and Ennis, M. 1996. Functional organization of olfactory system. *J. Neurobiol.* 30: 123–176.
- Shiple, M.T., McLean, J.H., and Ennis, M. 1995. Olfactory system. In: *The Rat Nervous System*, 2nd edition (Paxinos, G., ed.) San Diego: Academic Press, pp. 899–926.
- Shupliakov, O., Örnung, G., Brodin, L., Ulfhake, B., Ottersen, O.P., Storm-Mathisen, J., and Cullheim, S. 1993. Immunocytochemical localization of amino acid neurotransmitter candidates in the ventral horn of the cat spinal cord: a light microscopic study. *Exp. Brain Res.* 96: 404–418.
- Siggins G.R., Hoffer B.J., and Bloom F.E. 1971a. Studies on norepinephrine-containing afferents to Purkinje cells of rat cerebellum. 3. Evidence for mediation of norepinephrine effects by cyclic 3',5'-adenosine monophosphate. *Brain Res.* 25: 535–553.
- Siggins, G.R., Hoffer, B.J., Oliver, A.P., and Bloom, F.E. 1971b. Activation of a central noradrenergic projection to the cerebellum. *Nature* 233: 481–483.
- Siggins, G.R., Oliver, A.P., Hoffer, B.J., and Bloom, F.E. 1971c. Cyclic adenosine monophosphate and norepinephrine: effects on transmembrane properties of cerebellar Purkinje cells. *Science* 171: 192–194.
- Sik, A., Tamamaki, N., and Freund, T.F. 1993. Complete axon arborization of a single CA3 pyramidal cell in the rat hippocampus, and its relationship with postsynaptic parvalbumin-containing interneurons. *Eur. J. Neurosci.* 5: 1719–1728.
- Siklos, L., Rickmann, M., Joo, F., Freeman, W.J., and Wolff, J.R. 1995. Chloride is preferentially accumulated in a subpopulation of dendrites and periglomerular cells of the main olfactory bulb in adult rats. *Neuroscience* 64: 165–172.
- Sillito, A. 1975. The effectiveness of bicuculline as an antagonist of GABA and visually evoked inhibition in the cat's striate cortex. *J. Physiol. (Lond.)* 250: 287–304.
- Sillito, A., and Kemp, J. 1983. Cholinergic modulation of the functional organization of the cat visual cortex. *Brain Res.* 289: 143–155.
- Sillito, A.M., Kemp, J.A., Wilson, J.A., and Berardi, N. 1980. A re-evaluation of the mechanisms underlying simple cell orientation selectivity. *Brain Res.* 194: 517–520.
- Sillito, A.M., Cudeiro, J., and Murphy, P.C. 1993. Orientation sensitive elements in the corticofugal influence on centre-surround interactions in the dorsal lateral geniculate nucleus. *Exp. Brain Res.* 93: 6–16.
- Sillito, A.M., and Jones, H.E. 2002. Cortico-thalamic interactions in the transfer of visual information. *Phil. Trans. R. Soc. Lond. B.* 357:1739–1752.

- Sillito, A.M., Jones, H.E., Gerstein, G.L., and West, D.C. 1994. Feature-linked synchronization of thalamic relay cell firing induced by feedback from the visual cortex. *Nature* 369: 479–482.
- Simon, S.M., Moal, M.L., and Calas, A. 1979. Efferents and afferents of the ventral tegmental-A-10-region studied after local injection of (3H) leucine and horseradish peroxidase. *Brain Res.* 175: 1–23.
- Singer, J.H., Mirotznik, R.R., and Feller, M.B. 2001. Potentiation of L-type calcium channels reveals nonsynaptic mechanisms that correlate spontaneous activity in the developing mammalian retina. *J. Neurosci.* 21: 8514–8522.
- Singer, M.S. 2000. Analysis of the molecular basis for octanal interactions in the expressed rat 17 olfactory receptor. *Chem. Senses* 25: 155–165.
- Singer, M.S., Oliveira, L., Vriend, G., and Shepherd, G.M. 1995a. Potential ligand-binding residues in rat olfactory receptors identified by correlated mutation analysis. *Receptors and Channels* 3: 89–95.
- Singer, M.S., and Shepherd, G.M. 1994. Molecular modeling of ligand-receptor interactions in the OR5 olfactory receptor. *NeuroReport* 5: 1297–1300.
- Singer, M.S., Shepherd, G.M., and Greer, C.A. 1995b. Olfactory receptors guide axons. *Nature* 377: 19–20.
- Singer, W. 1977. Control of thalamic transmission by corticofugal and ascending reticular pathways in the visual system. *Physiol. Rev.* 57: 386–420.
- Singer, W. 1994. Putative functions of temporal correlations in neocortical processing. In: *Large-Scale Neuronal Theories of the Brain* (Koch, C., and Davis, J. eds.) Cambridge: MA: Bradford Books, pp. 201–237.
- Singer, W. 1999. Neuronal synchrony: a versatile code for the definition of relations? *Neuron* 24: 49–65.
- Singer, W., and Gray, C.M. 1995. Visual feature integration and the temporal correlation hypothesis. *Annu. Rev. Neurosci.* 18: 555–586.
- Sjostrom, P.J., and Nelson, S.B. 2002. Spike timing, calcium signals and synaptic plasticity. *Curr. Opin. Neurobiol.* 12: 305–314.
- Skeen, L.C., and Hall, W.C. 1977. Efferent projections of the main and accessory olfactory bulb in the tree shrew (*Tupaia glis*). *J. Comp. Neurol.* 172: 1–36.
- Skou, J.C. 1988. Overview: the Na-K pump. *Methods Enzymol.* 156: 1–25.
- Sloper, J. 1972. Gap junctions between dendrites in the primate neocortex. *Brain Res.* 44: 641–646.
- Sloper, J., Hiorns, R., and Powell, T. 1979. A qualitative and quantitative electron microscope study of the neurons in the primate motor and somatic sensory cortices. *Phil. Trans. R. Soc. Lond. B* 285: 141–171.
- Sloper, J.J., and Powell, T.P.S. 1979a. An experimental electronmicroscopic study of afferent connections to the primate motor and somatic sensory cortices. *Phil. Trans. R. Soc. Lond. B* 285: 199–266.
- Sloper, J.J., and Powell, T.P.S. 1979b. Ultrastructural features of the sensorimotor cortex of the primate. *Phil. Trans. R. Soc. Lond. B* 285: 123–139.
- Sloviter, R.S., Dichter, M.A., Rachinsky, T.L., Dean, E., Goodman, J.H., Sollas, A.L., and Martin, D.L. 1996. Basal expression and induction of glutamate decarboxylase and GABA in excitatory granule cells of the rat and monkey hippocampal dentate gyrus. *J. Comp. Neurol.* 373: 593–618.
- Smallman, H.S., MacLeod, D.I.A., He, S., and Kentridge, R.W. 1996. Fine grain of the neural representation of human spatial vision. *J. Neurosci.* 16: 1852–1859.
- Smiley, J., and Goldman-Rakic, P. 1993. Heterogenous targets of dopamine synapses in monkey prefrontal cortex demonstrated by serial electron microscopy: a laminar analysis using the

- silver-enhanced diaminobenzidine sulfide (SEDS) immunolabelling technique. *Cerebral Cortex* 3: 223–228.
- Smirnakis, S.M., Berry, M.J., II, Warland, D.K., Bialek, W., and Meister, M. 1997. Adaptation of retinal processing to image contrast and spatial scale. *Nature* 386: 69–73.
- Smith, G.D., and Sherman, S.M. 2002. Detectability of excitatory versus inhibitory drive in an integrate-and-fire-or-burst thalamocortical relay neuron model. *J. Neurosci.* 22:10242–10250.
- Smith, J.L., Betts, B., Edgerton, V.R., and Zernicke, R.F. 1980. Rapid ankle extension during paw shakes: selective recruitment of fast ankle extensors. *J. Neurophysiol.* 43: 612–620.
- Smith, P.H. 1995. Structural and functional differences distinguish principal from nonprincipal cells in the guinea pig MSO slice. *J. Neurophysiol.* 73: 1653–1667.
- Smith, P.H., and Rhode, W.S. 1985. Electron microscopic features of physiologically characterized, HRP-labeled fusiform cells in the cat dorsal cochlear nucleus. *J. Comp. Neurol.* 237: 127–143.
- Smith, P.H., and Rhode, W.S. 1987. Characterization of HRP-labeled globular bushy cells in the cat anteroventral cochlear nucleus. *J. Comp. Neurol.* 266: 360–375.
- Smith, P.H., and Rhode, W.S. 1989. Structural and functional properties distinguish two types of multipolar cells in the ventral cochlear nucleus. *J. Comp. Neurol.* 282: 595–616.
- Smith, P.H., Joris, P.X., Banks, M.I., and Yin, T.C.T. 1993. Responses of cochlear nucleus cells and projections of their axons. In: *The Mammalian Cochlear Nuclei: Organization and Function* (Merchán, M.A., Juiz, J.M., Godfrey, D.A., and Mugnaini, E., eds.) New York: Plenum, pp. 349–360.
- Smith, R.G. 1995. Simulation of an anatomically-defined local circuit: the cone-horizontal cell network in cat retina. *Vis. Neurosci.* 12: 545–561.
- Smith, R.G., Freed, M.A., and Sterling, P. 1986. Microcircuitry of the dark-adapted cat retina: functional architecture of the rod-cone network. *J. Neurosci.* 6: 3505–3517.
- Smith, R.G., and Sterling, P. 1990. Cone receptive field in cat retina computed from microcircuitry. *Vis. Neurosci.* 5: 453–461.
- Smith, R.G., and Vardi, N. 1995. Simulation of the AII amacrine cell of mammalian retina: Functional consequences of electrical coupling and regenerative membrane properties. *Vis. Neurosci.* 12: 851–860.
- Smith, T., Wuerker, R., and Frank, K. 1967. Membrane impedance changes during synaptic transmission in cat spinal motoneurons. *J. Neurophysiol.* 30: 1072–1096.
- Smith, Y., Paré, D., Deschênes, M., Parent, A., and Steriade, M. 1988. Cholinergic and non-cholinergic projections from the upper brainstem core to the visual thalamus in the cat. *Exp. Brain Res.* 70: 166–180.
- Smithson, K.G., Weiss, M.L., and Hatton, G.I. 1989. Supraoptic nucleus afferents from the main olfactory bulb. I. Anatomical evidence from anterograde and retrograde tracers in rat. *Neuroscience* 31: 277–287.
- Snyder, S.H. 1992. Nitric oxide and neurons. *Curr. Opin. Neurobiol.* 2: 323–327.
- Sobel, N., Prabhakaran, V., Desmond, J.E., Glover, G.H., Goode, R.L., Sullivan, E.V., and Gabrieli, J.D. 1998. Sniffing and smelling: separate subsystems in the human olfactory cortex. *Nature* 392: 282–286.
- Sobel, N., Prabhakaran, V., Zhao, Z., Desmond, J.E., Glover, G.H., Sullivan, E.V., and Gabrieli, J.D. 2000. Time course of odorant-induced activation in the human primary olfactory cortex. *J. Neurophysiol.* 83: 537–551.
- Sofroniew, M.V., Campbell, P.E., Cuello, A.C., and Eckenstein, F. 1985. Central cholinergic neurons visualized by immunohistochemical detection of choline acetyltransferase. In: *The Rat Nervous System, Vol. 1: Forebrain and Midbrain* (Paxinos, G., ed.) Orlando: FL: Academic Press, pp. 471–485.

- Sokolov, M., Lyubarsky, A., Strissel, K.J., Savchenko, A.B., Govardovskii, V.I., and Pugh, E.N., Jr. 2002. Massive light-driven translocation of transducin between the two major compartments of rod cells: a novel mechanism of light adaptation. *Neuron* 34: 95–106.
- Somers, D., Nelson, S., and Sur, M. 1995. An emergent model of orientation selectivity in cat visual cortical simple cells. *J. Neurosci.* 15: 5448–5465.
- Somogyi, G., Hajdu, F., and Tombol, T. 1978. Ultrastructure of the anterior ventral and anterior medial nuclei of the cat thalamus. *Exp. Brain Res.* 31: 417–431.
- Somogyi, P. 1977. A specific 'axo-axonal' interneuron in the visual cortex of the rat. *Brain Res.* 136: 345–350.
- Somogyi, P., and Cowey, A. 1981. Combined Golgi and electron microscope study on the synapses formed by double bouquet cells in the visual cortex of the cat and monkey. *J. Comp. Neurol* 195: 547–566.
- Somogyi, P., Hodgson, A., Smith, A., Nunzi, M., Gorio, A., and Wu, J.-Y. 1984. Differential populations of GABAergic neurons in the visual cortex and hippocampus of the cat contain somatostatin- or cholecystokinin-immunoreactive material. *J. Neurosci.* 4: 2590–2603.
- Somogyi, P., Bolam, J.P., and Smith, A.D. 1981. Monosynaptic cortical input and local axon collaterals of identified striato nigral neurons. A light and electron microscopic study using the Golgi-peroxidase transport-degeneration procedure. *J. Comp. Neurol.* 195: 567–584.
- Somogyi, P., Freund, T.F., and Cowey, A.D. 1982. The axo-axonic interneuron in the cerebral cortex of the rat, cat and monkey. *Neuroscience* 7: 2577–2607.
- Somogyi, P., Freund, T.F., Hodgson, A.J., Somogyi, J., Berboukas, D., and Chubb, I.W. 1985. Identified axo-axonic cells are immunoreactive for GABA in the hippocampus and visual cortex of the cat. *Brain Res.* 332: 143–149.
- Somogyi, P., Halasy, K., Somogyi, J., Storm-Mathisen, J., and Ottersen, O.P. 1986. Quantification of immunogold reveals enrichment of glutamate in mossy and parallel fiber terminals in cat cerebellum. *Neuroscience* 19: 1045–1050.
- Somogyi, P., Kisvárdy, Z., Martin, K., and Whitteridge, D. 1983. Synaptic connections of morphologically identified and physiologically characterized large basket cells in the striate cortex of the cat. *Neuroscience* 10: 261–294.
- Somogyi, P., Takagi, H., Richards, J.G., and Mohler, H. 1989. Subcellular localization of benzodiazepine/GABA_A receptors in the cerebellum of rat, cat, and monkey using monoclonal antibodies. *J. Neurosci.* 9: 2197–2209.
- Sonnhof, U., Richter, D.W., and Taugner, R. 1977. Electrotonic coupling between frog spinal motoneurons. An electrophysiological and morphological study. *Brain Res.* 138: 197–215.
- Soriano, E., and Frotscher, M. 1989. A GABAergic axo-axonic cell in the fascia dentata controls the main excitatory hippocampal pathway. *Brain Res.* 503: 170–174.
- Soriano, E., and Frotscher, M. 1993. Spiny nonpyramidal neurons in the CA3 region of the rat hippocampus are glutamate-like immunoreactive and receive convergent mossy fiber input. *J. Comp. Neurol.* 333: 435–448.
- Soriano, E., and Frotscher, M. 1994. Mossy cells of the rat fascia dentata are glutamate-immunoresistive. *Hippocampus.* 4: 65–69.
- Sorra, K.E., and Harris, K.M. 1993. Occurrence and three-dimensional structure of multiple synapses between individual radiatum axons and their target pyramidal cells in hippocampal area CA1. *J. Neurosci.* 13: 3736–3748.
- Sotelo, C., Gotow, T., and Wassef, M. 1986. Localization of glutamate acid-decarboxylase immunoreactive axon terminals in the inferior olive of the rat with special emphasis on anatomical relations between GABAergic synapses and dendrodendritic gap junctions. *J. Comp. Neurol.* 252: 32–50.
- Sotelo, C., Hillman, D.E., Zamora, A.J., and Llinás, R. 1975. Climbing fiber deafferentiation: its action on Purkinje cell dendritic spines. *Brain Res.* 98: 574–581.

- Sotelo C., Llinás R., and Baker, R. 1974. Structural study of inferior olivary nucleus of the cat: morphological correlates of electrotonic coupling. *J. Neurophysiol.* 37: 541–559.
- Sotelo, C., Privat, A., and Drian, M. 1972. Localization of [3H]GABA in tissue culture of rat cerebellum using electron microscopy radioautography. *Brain Res.* 45: 302–308.
- Soucy, E., Nirenberg, S., Nathans, J., and Meister, M. 1998. A novel signaling pathway from rod photoreceptors to ganglion cells in mammalian retina. *Neuron* 21: 481–493.
- Spencer, W.A., and Kandel, E.R. 1961. Electrophysiology of hippocampal neurons. IV. Fast prepotentials. *J. Neurophysiol.* 24: 272–285.
- Spirou, G.A., Brownell, W.E., and Zidanic, M. 1990. Recordings from cat trapezoid body and HRP labeling of globular bushy cell axons. *J. Neurophysiol.* 63: 1169–1190.
- Spirou, G.A., Davis, K.A., Nelken, I., and Young, E.D. 1999. Spectral integration by type II interneurons in dorsal cochlear nucleus. *J. Neurophysiol.* 82: 648–663.
- Spirou, G.A., May, B.J., Wright, D.D., and Ryugo, D.K. 1993. Frequency organization of the dorsal cochlear nucleus in cats. *J. Comp. Neurol.* 329: 36–52.
- Spirou, G.A., and Young, E.D. 1991. Organization of dorsal cochlear nucleus type IV unit response maps and their relationship to activation by bandlimited noise. *J. Neurophysiol.* 65: 1750–1768.
- Spoendlin, H. 1973. The innervation of the cochlear receptor. In: *Basic Mechanisms in Hearing* (Møller, A.R., ed.) New York: Academic Press, pp. 185–230.
- Spors, H., and Grinvald, A. 2002. Spatio-temporal dynamics of odor representations in the mammalian olfactory bulb. *Neuron* 34: 301–15.
- Spragu, J.M., Berlucchi, G., Di Berardino, A. 1970. The superior colliculus and pretectum in visually guided behavior and visual discrimination in the cat. *Brain Behav. Evol.* 3: 285–294.
- Sprague, J.M. 1966. Interaction of cortex and superior colliculus in mediation of visually guided behavior in the cat. *Science* 153: 1544–1547.
- Sprague, J.M. 1972. The superior colliculus and pretectum in visual behavior. *Invest. Ophthalmol.* 11: 473–482.
- Spreafico, R., Schmechel, D.E., Ellis, L.C., Jr., and Rustioni, A. 1983. Cortical relay neurons and interneurons in the n. ventralis posterolateralis of cats: a horseradish peroxidase, electron-microscopic Golgi and immunocytochemical study. *Neuroscience* 9: 491–509.
- Spruston, N., Jaffe, D., and Johnston, D. 1994. Dendritic attenuation of synaptic potentials and currents: the role of passive membrane properties. *Trends Neurosci.* 17: 161–166.
- Spruston, N., and Johnston, D. 1992. Perforated patch-clamp analysis of the passive membrane properties of three classes of hippocampal neurons. *J. Neurophysiol.* 67: 508–529.
- Spruston, N., Lubke, J., and Frotscher, M. 1997. Interneurons in the stratum lucidum of the rat hippocampus: an anatomical and electrophysiological characterization. *J. Comp. Neurol.* 385: 427–440.
- Spruston, N., Schiller, Y., Stuart, G., and Sakmann, B. 1995. Activity-dependent action potential invasion and calcium influx into hippocampal CA1 dendrites. *Science* 268: 297–300.
- Spruston, N., Stuart, G.J., and Häusser, M. 1999. Dendritic integration. In: *Dendrites* (Stuart, G.J., Spruston, N., and Häusser, M., ed.) New York: Oxford University Press, pp. 231–270.
- Srinivasan, M.V., Laughlin, S.B., and Dubs, A. 1982. Predictive coding: a fresh view of inhibition in the retina. *Proc. R. Soc. Lond. B* 216: 427–459.
- St. John, J.A., Tisay, K.T., Caras, I.W., and Key, B. 2000. Expression of EphA5 during development of the olfactory nerve pathway in rat. *J. Comp. Neurol.* 416: 540–550.
- Stafford, D.K., and Dacey, D. 1997. Physiology of the A1 amacrine: a spiking axon-bearing interneuron of the macaque monkey retina. *Vis. Neurosci.* 14: 507–522.
- Stafstrom, C., Schwindt, P., and Crill, W. 1984. Repetitive firing in layer V neurons from cat neocortex in vitro. *J. Neurophysiol.* 52: 264–277.

- Stafstrom, C.E., Schwindt, P., and Crill, W. 1982. Negative slope conductance due to a persistent subthreshold sodium current in cat neocortical neurons in vitro. *Brain Res.* 236: 221–226.
- Stafstrom, C.E., Schwindt, P.C., Chubb, M.C., and Crill, W.E. 1985. Properties of persistent sodium conductance and calcium conductance of layer V neurons from cat sensorimotor cortex in vitro. *J. Neurophysiol.* 53: 153–170.
- Staley, K.J., Otis, T.S., and Mody, I. 1992. Membrane properties of dentate gyrus granule cells: comparison of sharp microelectrode and whole-cell recordings. *J. Neurophysiol.* 67: 1346–1358.
- Staley, K.J., Soldo, B.L., and Proctor, W.R. 1995. Ionic mechanisms of neuronal excitation by inhibitory gabaa receptors. *Science* 269: 977–981.
- Staubli, U., Fraser, D., Faraday, R., and Lynch, G. 1987. Olfaction and the “data” memory system in rats. *Behav. Neurosci.* 101: 757–765.
- Staubli, U., Fraser, D., Kessler, M., and Lynch, G. 1986. Studies on retrograde and anterograde amnesia of olfactory memory after denervation of the hippocampus by entorhinal cortex lesions. *Behav. Neural Biol.* 46: 432–444.
- Staubli, U., Thibault, O., DiLorenzo, M., and Lynch, G. 1989. Antagonism of NMDA receptors impairs acquisition but not retention of olfactory memory. *Behav. Neurosci.* 103: 54–60.
- Stea, A., Soong, T.W., and Snutch, T.P. 1995. Voltage-gated calcium channels. In: *Handbook of Receptors and Channels. Ligand- and Voltage-Gated Ion Channels* (North, R.A., ed.) London: CRC Press, pp. 113–152.
- Stein, J.J., Johnson, S.A., and Berson, D.M. 1996. Distribution and coverage of beta cells in the cat retina. *J. Comp. Neurol.* 372: 597–617.
- Stein, P., and Smith, J. 1997. Neural and biomechanical control strategies for different forms of vertebrate hindlimb motor tasks. In: *Neurons, Networks and Behavior* (Stein, P., Grillner, S., Selverston, A., and Stuart, D., eds.) Cambridge, MA: MIT Press, pp. 61–73.
- Steinberg, R.H. 1969. Rod and cone contributions to S-potentials from the cat retina. *Vis. Res.* 9: 1319–1329.
- Steinberg, R.H., Reid, M., and Lacy, P.L. 1973. The distribution of rods and cones in the retina of the cat (*Felis domesticus*). *J. Comp. Neurol.* 148: 229–248.
- Stengaard-Pedersen, K., Fredens, K., and Larsson, L.I. 1981. Enkephalin and zinc in the hippocampal mossy fiber system. *Brain Res.* 212: 230–233.
- Stent, G.S. 1973. A physiological mechanism for Hebb’s postulate of learning. *Proc. Natl. Acad. Sci. U.S.A.* 70: 997–1001.
- Steriade, M., and Contreras, D. 1995. Relations between cortical and thalamic cellular events during transition from sleep patterns to paroxysmal activity. *J. Neurosci.* 15: 623–642.
- Steriade, M., Datta, S., Paré, D., Oakson, G., and Curró Dossi, R. 1990a. Neuronal activities in brain-stem cholinergic nuclei related to tonic activation processes in thalamocortical systems. *J. Neurosci.* 10: 2541–2559.
- Steriade, M., Domich, L., Oakson, G., and Deschênes, M. 1987. The deafferented reticular thalamic nucleus generates spindle rhythmicity. *J. Neurophysiol.* 57: 260–273.
- Steriade, M., Jones, E.G., and Llinás, R. 1990b. *Thalamic Oscillations and Signalling*. New York: John Wiley & Sons.
- Steriade, M., and Llinás, R. 1988. The functional states of the thalamus and the associated neuronal interplay. *Physiol. Rev.* 68: 649–742.
- Steriade, M., and McCarley, R.W. 1990. *Brainstem Control of Wakefulness and Sleep*. New York: Plenum Press.
- Steriade, M., McCormick, D.A., and Sejnowski, T.J. 1993. Thalamocortical oscillations in the sleeping and aroused brain. *Science* 262: 679–685.
- Sterling, P. 1983. Microcircuitry of the cat retina. *Annu. Rev. Neurosci.* 6: 149–185.
- Sterling, P. 1995. Tuning retinal circuits. *Nature* 377: 676–677.

- Sterling, P., Calkins, D.J., Klug, K.J., Schein, S.J., and Tsukamoto, Y. 1994. Parallel pathways from primate fovea. *Invest. Ophthalmol. Vis. Sci. Abstr.* 35: 2001.
- Sterling, P., Cohen, E., Freed, M.A., and Smith, R.G. 1987. Microcircuitry of the ON-beta ganglion cell in daylight, twilight and starlight. *Neurosci. Res. (Suppl.)* 6: 5269–5285.
- Sterling, P., Cohen, E., Smith, R.G., and Tsukamoto, Y. 1992. Retinal circuits for daylight: why ballplayers don't wear shades. In: *Analysis and Modeling of Neural Systems* (Eeckman, F.H., ed.) Boston: Kluwer Academic Publishers, pp. 143–162.
- Sterling, P., Freed, M.A., and Smith, R.G. 1988. Architecture of the rod and cone circuits to the ON-beta ganglion cell. *J. Neurosci.* 8: 623–642.
- Sterling, P., Smith, R.G., Rao, R., and Vardi, N. 1995. Functional architecture of mammalian outer retina and bipolar cells. In: *Neurobiology and Clinical Aspects of the Outer Retina* (Archer, S., Djamgoz, M.B.A., and Vallerga, S., eds.) London: Chapman & Hall, pp. 325–348.
- Stevens, C.F., and Tsujimoto, T. 1995. Estimates for the pool size of releasable quanta at a single central synapse and for the time required to refill the pool. *Proc. Natl. Acad. Sci. U.S.A.* 92: 846–849.
- Stevens, C.F., and Wang, Y. 1994. Changes in reliability of synaptic function as a mechanism for plasticity. *Nature* 371: 704–707.
- Stevens, C.F., and Wang, Y. 1995. Facilitation and depression at single central synapses. *Neuron* 14: 795–802.
- Stevens, J.R., Phillips, I., and Beaurepaire, R. 1988. gamma-vinyl GABA in endopiriform area suppresses kindled amygdala seizures. *Epilepsia* 29: 404–411.
- Steward, O. 1976. Topographic organization of the projections from the entorhinal area to the hippocampal formation of the rat. *J. Comp. Neurol.* 167: 285–314.
- Steward, O., and Scoville, S.A. 1976. Cells of origin of entorhinal cortical afferents to the hippocampus and fascia dentata of the rat. *J. Comp. Neurol.* 169: 347–370.
- Stewart, W.B., Kauer, J.S., and Shepherd, G.M. 1979. Functional organization of rat olfactory bulb analysed by the 2–deoxyglucose method. *J. Comp. Neurol.* 185: 715–734.
- Stockman, A., Sharpe, L.T., R  ther, K., and Nordby, K. 1995. Two signals in the human rod visual system: a model based on electrophysiological data. *Vis. Neurosci.* 12: 951–970.
- Stone, J. 1983. *Parallel Processing in the Visual System*. New York: Plenum Press.
- Stone, J., and Fukuda, Y. 1974. Properties of cat retinal ganglion cells: a comparison of W-cells with X- and Y-cells. *J. Neurophysiol.* 37: 722–748.
- Stone, L.S. 1950. The role of retinal pigment cells in regenerating neural retinae of adult salamander eyes. *J. Exp. Zool.* 113: 9–32.
- Stone, T., and Taylor, D. 1977. Microiontophoretic studies of the effects of cyclic nucleotides on excitability of neurones in the rat cerebral cortex. *J. Physiol. (Lond.)* 266: 523–543.
- Storm, J.F. 1990. Potassium currents in hippocampal pyramidal cells. *Prog. Brain Res.* 83: 161–187.
- Storm-Mathisen, J. 1977. Localization of transmitter candidates in the brain: the hippocampal formation as a model. *Prog. Neurobiol.* 8: 119–181.
- Storm-Mathisen, J., and Fonnum, F. 1972. Localization of transmitter candidates in the hippocampal region. *Prog. Brain Res.* 36: 41–58.
- Stratford, K.J., Tarczy-Hornoch, K., Martin, K.A.C., Bannister, N.J., and Jack, J.J.B. 1996. Excitatory synaptic inputs to spiny stellate cells in cat visual cortex. *Nature* 382: 258–261.
- Strettoi, E., Dacheux, R.F., and Raviola, E. 1990. Synaptic connections of rod bipolar cells in the inner plexiform layer of the rabbit retina. *J. Comp. Neurol.* 295: 449–466.
- Stricker, C., Field, A.C., and Redman, S.J. 1996. Statistical analysis of amplitude fluctuations in EPSCs evoked in rat CA1 pyramidal neurones *in vitro*. *J. Physiol. (Lond.)* 490: 419–441.
- Stripling, J.S., and Patneau, D.K. 1999. Potentiation of late components in olfactory bulb and piriform cortex requires activation of cortical association fibers. *Brain Res.* 841: 27–42.

- Stripling, J.S., Patneau, D.K., and Gramlich, C.A. 1988. Selective long-term potentiation in the pyriform cortex. *Brain Res.* 441: 281–291.
- Stripling, J.S., Patneau, D.K., and Gramlich, C.A. 1991. Characterization and anatomical distribution of selective long-term potentiation in the olfactory forebrain. *Brain Res.* 542: 107–122.
- Strotmann, J., Wanner, I., Krieger, J., Raming, K., and Breer, H. 1992. Expression of odorant receptors in spatially restricted subsets of chemosensory neurones. *Neuroreport* 3: 1053–1056.
- Struble, R.G., Desmond, N.L., and Levy, W.B. 1978. Anatomical evidence for interlamellar inhibition in the fascia dentata. *Brain Res.* 152: 580–585.
- Struble, R.G., and Walters, C.P. 1982. Light microscopic differentiation of two populations of rat olfactory bulb granule cells. *Brain Res.* 236: 237–251.
- Stryker, M.P., and Zahs, K.R. 1983. On and off sublaminae in the lateral geniculate nucleus of the ferret. *J. Neurosci.* 3: 1943–1951.
- Stuart, G.J., and Redman, S.J. 1992. The role of GABA-A and GABA-B receptors in presynaptic inhibition of Ia EPSPs in cat spinal motoneurons. *J. Physiol. (Lond.)* 447: 675–692.
- Stuart, G.J., and Sakmann, B. 1994. Active propagation of somatic action potentials into neocortical pyramidal cell dendrites. *Nature* 367: 69–72.
- Stuart, G.J., and Spruston, N. 1995. Probing dendritic function with patch pipettes. *Curr. Opin. Neurobiol.* 5: 389–394.
- Stuart, G.J., Dodt, H.U., and Sakmann, B. 1993. Patch-clamp recordings from the soma and dendrites of neurones in brain slices using infrared video microscopy. *Pflügers Arch.* 423: 511–518.
- Stuart, G.J., and Redman, S.J. 1992. The role of GABA-A and GABA-B receptors in presynaptic inhibition of Ia EPSPs in cat spinal motoneurons. *J. Physiol. (Lond.)* 447: 675–92.
- Stuart, G.J., Spruston, N., and Häusser, M. (eds.) 1999. *Dendrites*. Oxford, UK: Oxford University Press.
- Stuart, G.J., Spruston, N., Sakmann, B., and Häusser, M. 1997. Action potential initiation and backpropagation in neurons of the mammalian CNS. *Trends Neurosci.* 20: 125–131.
- Study, R., and Barker, J. 1981. Diazepam and (-) pentobarbital: fluctuation analysis reveals different mechanisms for potentiation of gamma-amino-butyric acid responses in cultured neurons. *Proc. Natl. Acad. Sci. U.S.A.* 78: 7180–7184.
- Suarez, H., Koch, C., and Douglas, R. 1995. Modeling direction selectivity of simple cells in striate visual cortex using the canonical microcircuit. *J. Neurosci.* 15: 6700–6719.
- Sugihara I., Lang E.J., and Llinás R., 1993. Uniform olivocerebellar conduction time underlies Purkinje cell complex spike synchronicity in the rat cerebellum. *J. Physiol. Lond.* 470, 243–271.
- Sugihara, I., Wu, H.-S., and Shinoda, Y. 2001. The entire trajectories of single olivocerebellar axons in the cerebellar cortex and their contribution to cerebellar compartmentalization. *J. Neurosci.* 21, 7715–7723.
- Sugimori, M., and Llinás, R. 1981. Localization of ionic conductances in soma-dendritic regions of Purkinje cells: an in vitro study of guinea pig cerebellar slices. *Soc. Neurosci. Abstr.* 7, 76.
- Sugimori, M., Llinás, R., and Angelides, A. 1986. Fluorescence localization of tetrodotoxin receptors in mammalian cerebellar cortex in vitro. *Soc. Neurosci. Abstr.* 12: 463.
- Sugimori, M., Preston, R.J., and Kitai, S.T. 1978. Response properties and electrical constants of caudate nucleus neurons in the cat. *J. Neurophysiol.* 41: 1662–1675.
- Sung, K-W., Choi, S., and Lovinger, D.M. 2001. Activation of Group I mGluRs is necessary for induction of long-term depression at striatal synapses. *J. Neurophysiol.* 86: 2405–2412.
- Super, H., and Uylings, H. 2001. The early differentiation of the neocortex: a hypothesis on neocortical evolution. *Cereb. Cortex* 11: 1101–1109.

- Sur, M., Esguerra, M., Garraghty, P.E., Kritzer, M.F., and Sherman, S.M. 1987. Morphology of physiologically identified retinogeniculate X- and Y-axons in the cat. *J. Neurophysiol.* 58: 1–32.
- Surmeier, D.J., Cantrell, A.R., and Carter-Russell, H. 1995. Dopaminergic and cholinergic modulation of calcium conductances in neostriatal neurons. In: *Molecular and Cellular Mechanisms of Neostriatal Function* (Ariano, M.A., and Surmeier, D.J., eds.) Austin: R.G. Landes, pp. 193–216.
- Surmeier, D.J., Eberwine, J., Wilson, C.J., Cao, Y., Stefani, A., and Kitai, S.T. 1992. Dopamine receptor subtypes colocalize in rat striatonigral neurons. *Proc. Natl. Acad. Sci. U.S.A.* 89: 10178–10182.
- Surmeier, D.J., and Kitai, S.T. 1993. D1 and D2 Dopamine Receptor Modulation of Sodium and Potassium Currents in Rat Neostriatal Neurons. Oxford: Elsevier.
- Surmeier, D.J., Song, W.-J., and Yan, Z. 1996. Coordinated expression of dopamine receptors in neostriatal medium spiny neurons. *J. Neurosci.* 16: 6579–6591.
- Sutherland, G.R., and McNaughton, B. 2000. Memory trace reactivation in hippocampal and neocortical neuronal ensembles. *Curr. Opin. Neurobiol.* 10: 180–6.
- Svirskis, G., and Hounsgaard, J. 1997. Depolarization-induced facilitation of a plateau-generating current in ventral horn neurons in the turtle spinal cord. *J. Neurophysiol.* 78: 1740–1742.
- Svoboda, K., Denk, W., and Kleinfeld, D. 1997. In vivo dendritic calcium dynamics in neocortical pyramidal cells. *Nature* 385: 161–165.
- Swadlow, H.A., and Gusev, A.G. 2001. The impact of ‘bursting’ thalamic impulses at a neocortical synapse. *Nat. Neurosci.* 4: 402–408.
- Swadlow, H.A., Gusev, A.G., and Bezdudnaya, T. 2002. Activation of a cortical column by a thalamocortical impulse. *J. Neurosci.* 22: 7766–7773.
- Swanson, G.T., Kamboj, S.K., and Cull-Candy, S.G. 1997. Single-channel properties of recombinant AMPA receptors depend on RNA editing, splice variation, and subunit composition. *J. Neurosci.* 17: 58–69.
- Swanson, L.W. 1978. The anatomical organization of septo-hippocampal projections. In: *Functions of the Septo-Hippocampal System* (CIBA Foundation Vol. 58). Amsterdam: Elsevier North Holland, pp. 25–48.
- Swanson, L.W. 1981. A direct projection from Ammon’s horn to prefrontal cortex in the rat. *Brain Res.* 217: 150–154.
- Swanson, L.W. 1982. The projections of the ventral tegmental area and adjacent regions: a combined fluorescent retrograde tracer and immunofluorescence study in the rat. *Brain Res. Bull.* 9: 321–353.
- Swanson, L.W., and Cowan, W.M. 1975. Hippocampus-hypothalamic connections: origin in subicular cortex, not ammon’s horn. *Science* 25: 303–304.
- Swanson, L.W., and Cowan, W.M. 1977. An autoradiographic study of the organization of the efferent connections of the hippocampal formation in the rat. *J. Comp. Neurol.* 172: 49–84.
- Swanson, L.W., and Hartman, B.K. 1975. The central adrenergic system. An immunofluorescence study of the location of cell bodies and their efferent connections in the rat utilizing dopamine-B-hydroxylase as a marker. *J. Comp. Neurol.* 163: 467–506.
- Swanson, L.W., Köhler, C., and Björklund, A. 1987. The limbic region. I: the septohippocampal system. In: *Handbook of Chemical Neuroanatomy, Vol. 5: Integrated Systems of the CNS, Part I* (Björklund, A., Hökfelt, T., and Swanson, L.W., eds.) New York: Elsevier Science Publishing, pp. 125–227.
- Swanson, L.W., Sawchenko, P.E., and Cowan, W.M. 1980. Evidence that the commissural, associational and septal projections of the regio inferior of the hippocampus arise from the same neurons. *Brain Res.* 197: 207–212.

- Swanson, L.W., Wyss, J.M., and Cowan, W.M. 1978. An autoradiographic study of the organization of intrahippocampal association pathways in the rat. *J. Comp. Neurol.* 181: 681–716.
- Sweatt, J.D. 2003. *Mechanisms of Memory*. New York: Academic Press.
- Swindale, N. 1981. Dendritic spines only connect. *Trends Neurosci.* 4: 240–241.
- Switzer, R.C., de Olmos, J., and Heimer, L. 1985. Olfactory system. In: *The Rat Nervous System: Forebrain and Midbrain* (Paxinos, G., ed.) San Diego: Academic Press, pp. 1–36.
- Switzer, R.C.I., Hill, J., and Heimer, L. 1982. The globus pallidus and its rostroventral extension into the olfactory tubercle of the rat: a cyto- and chemoarchitectural study. *Neuroscience* 7: 1891–1904.
- Sypert, G.W., and Munson, J.B. 1984. Excitatory synapses. In: *Handbook of the Spinal Cord, Vol. 1: Physiology* (Davidoff, R.E., ed.) New York: Marcel Dekker, pp. 315–384.
- Szél, A., Diamanstein, T., and Röhlich, P. 1988. Identification of the blue sensitive cones in the mammalian retina by anti-visual pigment antibody. *J. Comp. Neurol.* 273: 593–602.
- Szél, A., Röhlich, P., Caffé, A.R., Juliussn, B., Aguirre, G., and Van Veen, T. 1992. Unique topographic separation of two spectral classes of cones in the mouse retina. *J. Comp. Neurol.* 325: 327–342.
- Szentágothai, J. 1973. Synaptology of the visual cortex. In: *Handbook of Sensory Physiology, Vol. VII/3: Central Processing of Visual Information, Part B: Visual Centers in the Brain* (Jung, R., ed.) Berlin: Springer-Verlag, pp. 269–324.
- Szentágothai, J. 1978. The neuron network of the cerebral cortex: a functional interpretation. *Proc. R. Soc. Lond. B* 201: 219–248.
- Szot, P., Bale, T.L., and Dorsa, D.M. 1994. Distribution of messenger RNA for the vasopressin V1a receptor in the CNS of male and female rats. *Mol. Brain Res.* 24: 1–10.
- Tachibana, M., and Kaneko, A. 1984. Gamma-aminobutyric acid acts at axon terminals of turtle photoreceptors: difference in sensitivity among cell types. *Proc. Natl. Acad. Sci. U.S.A.* 81: 7961–7964.
- Tachibanaki, S., Tsushima, S., and Kawamura, S. 2001. Low amplification and fast visual pigment phosphorylation as mechanisms characterizing cone photoresponses. *Proc. Natl. Acad. Sci. U.S.A.* 98: 14044–14049.
- Takagi, H., Somogyi, P., Somogyi, J., and Smith, A.D. 1983. Fine structural studies of a type of somatostatin-immunoreactive neuron and its synaptic connections in the rat neostriatum—a correlated light and electron microscopic study. *J. Comp. Neurol.* 214: 1–16.
- Takagi, S.F. 1986. Studies on the olfactory nervous system in the Old World monkey. *Prog. Neurobiol.* 27: 195–250.
- Takeuchi Y., Kimura H., and Sano Y., 1982. Immunohistochemical demonstration of serotonin-containing nerve fibers in the cerebellum. *Cell Tiss. Res.* 226, 1–12.
- Takikawa, Y., Kawagoe, R., and Hikosaka, O. 2002. Reward-dependent spatial selectivity of anticipatory activity in monkey caudate neurons. *J. Neurophysiol.* 87: 508–515.
- Talley, E., Solorzano, G., Lei, Q., Kim, D., and Bayliss, D. 2001. CNS distribution of members of the two-pore domain (KCNK) potassium channel family. *J. Neurosci.* 21: 7491–7505.
- Tamamaki, N., Abe, K., and Nijyo, Y. 1987. Columnar organization in the subiculum formed by axon branches originating from single CA1 pyramidal neurons in the rat hippocampus. *Brain Res.* 412: 156–160.
- Tamamaki, N., Abe, K., and Nijyo, Y. 1988. Three-dimensional analysis of the whole axonal arbors originating from single CA2 pyramidal neurons in the rat hippocampus with the aid of a computer graphic technique. *Brain Res.* 452: 255–272.
- Tamamaki, N., Uhlrich, D.J., and Sherman, S.M. 1994. Morphology of physiologically identified retinal X and Y axons in the cat's thalamus and midbrain as revealed by intra-axonal injection of biocytin. *J. Comp. Neurol.* 354: 583–607.

- Tamamaki, N., Watanabe, K., and Nojyo, Y. 1984. A whole image of the hippocampal pyramidal neuron revealed by intracellular pressure-injection of horseradish peroxidase. *Brain Res.* 307: 336–340.
- Tamas, G., Somogyi, P., and Buhl, E. 1998. Differentially interconnected networks of GABAergic interneurons in the visual cortex of the cat. *J. Neurosci.* 18: 4255–4270.
- Tamura, T., Nakatani, K., and Yau, K.-W. 1989. Light adaptation in cat retinal rods. *Science* 245: 755–758.
- Tamura, T., Nakatani, K., and Yau, K.-W. 1991. Calcium feedback and sensitivity regulation in primate rods. *J. Gen. Physiol.* 98: 91–130.
- Tanabe, T., Iino, M., and Takagi, S.F. 1975a. Discrimination of odors in olfactory bulb, pyriform-amygdaloid areas, and orbitofrontal cortex of the monkey. *J. Neurophysiol.* 38: 1284–1296.
- Tanabe, T., Yarita, H., Iino, M., Ooshima, Y., and Takagi, S.F. 1975b. An olfactory projection area in orbitofrontal cortex of the monkey. *J. Neurophysiol.* 38: 1269–1283.
- Tanaka, K., Saito, H.-A., Fukada, Y., and Moriya, M. 1991. Coding visual images of objects in the inferotemporal cortex of the macaque monkey. *J. Physiol. (Lond.)* 66: 170–189.
- Tang, A.C., and Hasselmo, M.E. 1994. Selective suppression of intrinsic but not afferent fiber synaptic transmission by baclofen in the piriform (olfactory) cortex. *Brain Res.* 659: 75–81.
- Tank, D.S., Sugimori, M., Connor, J.A., and Llinás, R. 1988. Spatially resolved calcium dynamics of mammalian Purkinje cells in cerebellar slices. *Science* 242: 773–777.
- Tank, D.W., and Hopfield, J.J. 1987. Neural computation by concentrating information in time. *Proc. Natl. Acad. Sci. U.S.A.* 84: 1896–1900.
- Tarczy-Hornoch, K., Martin, K.A.C., Jack, J.J.B., and Stratford, K. 1998. Synaptic interactions between smooth and spiny neurones in layer 4 of cat visual cortex *in vitro*. *J. Physiol. (Lond.)* 508: 351–363.
- Taube, J.S. 1995. Head direction cells recorded in the anterior thalamic nuclei of freely moving rats. *J. Neurosci.* 15: 70–86.
- Tauchi, M., and Masland, R.H. 1984. The shape and arrangement of the cholinergic neurons in the rabbit retina. *Proc. R. Soc. Lond. B* 223: 101–119.
- Taylor, C.P., and Dudek, F.E. 1984. Excitation of hippocampal pyramidal cells by electrical field effect. *J. Neurophysiol.* 52: 126–142.
- Taylor, W.R. 1996. Response properties of long-range axon-bearing amacrine cells in the dark-adapted rabbit retina. *Vis. Neurosci.* 13: 599–604.
- Taylor, W.R. 1999. TTX attenuates surround inhibition in rabbit retinal ganglion cells. *Vis. Neurosci.* 16: 285–290.
- Taylor, W.R., and Morgans, C. 1998. Localization and properties of voltage-gated calcium channels in cone photoreceptors of *Tupaia belangeri*. *Vis. Neurosci.* 15: 541–552.
- Taylor, W.R., and Wässle, H. 1995. Receptive field properties of starburst cholinergic amacrine cells in the rabbit retina. *Eur. J. Neurosci.* 7: 2308–2321.
- Teicher, M.H., Stewart, W.B., Kauer, J.S., and Shepherd, G.M. 1980. Suckling pheromone stimulation of a modified glomerular region in the developing rat olfactory bulb revealed by the 2-deoxyglucose method. *Brain Res.* 194: 530–535.
- ten Bruggencate, G., and Engberg, I. 1971. Iontophoretic studies in Deiters' nucleus of the inhibitory actions of GABA and related amino acids and the interactions of strychnine and picrotoxin. *Brain Res.* 25: 431–448.
- Teranishi, T., Negishi, K., and Kato, S. 1984. Regulatory effect of dopamine on spatial properties of horizontal cells in carp retina. *J. Neurosci.* 4: 1271–1280.
- Terman, D., Rubin, J.E., Yew, A.C., and Wilson, C.J. 2002. Activity patterns in a model for the subthalamopallidal network of the basal ganglia. *J. Neurosci.* 22: 2963–2976.
- Teyler, T.J., Cavus, I., Coussens, C., DiScenna, P., Grover, L., Lee, Y.P., and Little, Z. 1994.

- Multideterminant role of calcium in hippocampal synaptic plasticity. *Hippocampus* 4: 623–634.
- Thalmann, R.H. 1988. Evidence that guanosine triphosphate (GTP)-binding proteins control a synaptic response in brain effect of pertussis toxin and GTPf1S on the late inhibitory postsynaptic potential of hippocampal CA3 neurons. *J. Neurosci.* 8: 4589–4602.
- Thanos, P.K., and Slotnick, B.M. 1997. Short-term odor memory: effects of posterior transection of the lateral olfactory tract in the rat. *Physiol. Behav.* 61: 903–906.
- Thomas, M.J., Watabe, A.M., Moody, T.D., Makhinson, M., and O'Dell, T.J. 1998. Postsynaptic complex spike bursting enables the induction of LTP by theta frequency synaptic stimulation. *J. Neurosci.* 18: 7118–26.
- Thomas, R.C. 1972. Electrogenic sodium pump in nerve and muscle cells. *Physiol. Rev.* 52: 563–594.
- Thomas, T.M., Smith, Y., Levey, A.I., and Hersch, S.M. 2000. Cortical inputs to m2-immunoreactive striatal interneurons in rat and monkey. *Synapse* 37: 252–261.
- Thompson, A.M., and Thompson, G.C. 1991. Posteroventral cochlear nucleus projections to olivocochlear neurons. *J. Comp. Neurol.* 303: 267–285.
- Thompson, S.M., Deisz, R.A., and Prince, D.A. 1988. Relative contributions of passive equilibrium and active transport to the distribution of chloride in mammalian cortical neurons. *J. Neurophysiol.* 60: 105–124.
- Thomson, A. 2000. Facilitation, augmentation and potentiation at central synapses. *Trends Neurosci.* 23: 305–312.
- Thomson, A., and Bannister, A. 1999. Release-independent depression at pyramidal inputs onto specific cell targets: dual recordings in slices of rat cortex. *J. Physiol. (Lond.)* 519: 57–70.
- Thomson, A., Deuchars, J., and West, D. 1993. Large, deep layer pyramid-pyramid single axon epp's in slices of rat motor cortex display paired pulse and frequency-dependent depression, mediated presynaptically and self-facilitation mediated postsynaptically. *J. Neurosci.* 70: 2354–2369.
- Thomson, A., Deuchars, J., and West, D. 1995. Properties of single axon excitatory postsynaptic potentials elicited in spiny interneurons by action potentials in pyramidal neurons in slices of rat neocortex. *Neuroscience* 69: 727–738.
- Thomson, A.M., Girdlestone, D., and West, D.C. 1988. Voltage-dependent currents prolong single axon postsynaptic potentials in layer III pyramidal neurons in rat neocortical slices. *J. Neurophysiol.* 6: 1896–1907.
- Thomson, A.M., West, D.C., and Deuchars, J. 1994. Temporal and spatial properties of local circuits in neocortex. *Trends Neurosci.* 17: 119–126.
- Thurbon, D., Field, A., and Redman, S. 1994. Electrotonic profiles of interneurons in stratum pyramidale of the CA1 region of rat hippocampus. *J. Neurophysiol.* 71: 1948–1958.
- Thurbon, D., Lüscher, H.-R., Hofstetter, T., and Redman, S. 1998. Passive electrical properties of ventral horn neurons in rat spinal cord slices. *J. Neurophysiol.* 79: 2485–2502.
- Tigges, J., and Tigges, M. 1985. Subcortical sources of direct projections to visual cortex. In: *Cerebral Cortex*, Vol. 3 (Peters, A., and Jones, E., eds.) New York: Plenum Press, pp. 351–378.
- Toida, K., Kosaka, K., Aika, Y., and Kosaka, T. 2000. Chemically defined neuron groups and their subpopulations in the glomerular layer of the rat main olfactory bulb—IV. Intra-glomerular synapses of tyrosine hydroxylase-immunoreactive neurons. *Neuroscience* 101: 11–17.
- Tolbert, L.P., and Morest, D.K. 1982a. The neuronal architecture of the anteroventral cochlear nucleus of the cat in the region of the cochlear nerve root: Golgi and Nissl methods. *Neuroscience* 7: 3013–3030.
- Tolbert, L.P., and Morest, D.K. 1982b. The neuronal architecture of the anteroventral cochlear

- nucleus of the cat in the region of the cochlear nerve root: electron microscopy. *Neuroscience* 7: 3030–3053.
- Torigoe, Y., Blanks, R.H., and Precht, W. 1986. Anatomical studies on the nucleus reticularis tegmenti pontis in the pigmented rat. II. Subcortical afferents demonstrated by the retrograde transport of horseradish peroxidase. *J. Comp. Neurol.* 243: 88–105.
- Toth, K., and Freund, T.F. 1992. Calbindin D28k-containing nonpyramidal cells in the rat hippocampus: their immunoreactivity for GABA and projection to the medial septum. *Neuroscience* 49: 793–805.
- Townes-Anderson, E., Dacheux, R.F., and Raviola, E. 1988. Rod photoreceptors dissociated from the adult rabbit retina. *J. Neurosci.* 8: 320–331.
- Townes-Anderson, E., MacLeish, P.R., and Raviola, E. 1985. Rod cells dissociated from mature salamander retina: ultrastructure and uptake of horseradish peroxidase. *J. Cell Biol.* 100: 175–188.
- Toyama, K., Matsunami, K., Ohno, T., and Tokashiki, S. 1974. An intracellular study of neuronal organization in the visual cortex. *Exp. Brain Res.* 21: 45–66.
- Traub, R.D., and Llinás, R. 1977. The spatial distribution of ionic conductances in normal and axotomized motoneurons. *Neuroscience* 2: 829–849.
- Traub, R.D., and Llinás, R. 1979. Hippocampal pyramidal cells' significance of dendritic ionic conductances for neuronal function and epileptogenesis. *J. Neurophysiol.* 42: 476–496.
- Traub, R.D., and Miles, R. 1991. *Neuronal Networks of the Hippocampus*. Cambridge: Cambridge University Press.
- Traub, R.D., Miles, R., and Wong, R.K.S. 1989. Model of the origin of rhythmic population oscillations in the hippocampal slice. *Science* 243: 1319–1325.
- Traub, R.D., and Wong, R.K.S. 1981. Penicillin-induced epileptiform activity in the hippocampal slice: a model of synchronization of CA3 pyramidal cell bursting. *Neuroscience* 6: 223–230.
- Treloar, H.B., Feinstein, P., Mombaerts, P., and Greer, C.A. 2002. Specificity of glomerular targeting by olfactory sensory axons. *J. Neurosci.* 22: 2469–2477.
- Treloar, H.B., Purcell, A.L., and Greer, C.A. 1999. Glomerular formation in the developing rat olfactory bulb. *J. Comp. Neurol.* 413: 289–304.
- Treloar, H.B., Walters, E., Margolis, F., and Key, B. 1996. Olfactory glomeruli are innervated by more than one distinct subset of primary sensory olfactory neurons in mice. *J. Comp. Neurol.* 367: 550–562.
- Triller A., Cluzeaud F., and Korn H., 1987. Gamma-aminobutyric acid-containing terminals can be apposed to glycine receptors at central synapses. *J. Cell Biol.* 104: 947–956.
- Trombley, P.Q. 1992. Norepinephrine inhibits calcium currents and EPSPs via a G-protein-coupled mechanism in olfactory bulb neurons. *J. Neurosci.* 12: 3992–3998.
- Trombley, P.Q., and Shepherd, G.M. 1993. Synaptic transmission and modulation in the olfactory bulb. *Curr. Opin. Neurobiol.* 3: 540–547.
- Trombley, P.Q., and Shepherd, G.M. 1994. Glycine exerts potent inhibitory actions on mammalian olfactory bulb neurons. *J. Neurophysiol.* 71: 761–767.
- Trombley, P.Q., and Shepherd, G.M. 1997. The olfactory bulb. In: *Encyclopedia of Neuroscience* (Edelman, G., and Smith, B., eds.) Amsterdam: Elsevier.
- Tsai, K.Y., Carnevale, N.T., Caliborne, B.J., and Brown, T.H. 1994. Efficient mapping from neuroanatomical to electrotonic space. *Network* 5: 21–46.
- Tseng, G.-F., and Haberly, L.B. 1988. Characterization of synaptically mediated fast and slow inhibitory processes in piriform cortex in an in vitro slice preparation. *J. Neurophysiol.* 59: 1352–1376.
- Tseng, G.-F., and Haberly, L.B. 1989a. Deep neurons in piriform cortex. I. Morphology and synaptically evoked responses including a unique high amplitude paired shock facilitation. *J. Neurophysiol.* 62: 369–385.

- Tseng, G.-F., and Haberly, L.B. 1989b. Deep neurons in piriform cortex. II. Membrane properties that underlie unusual synaptic responses. *J. Neurophysiol.* 62: 386–400.
- Tsien, R.W., Ellinor, P.T., and Horne, W.A. 1991. Molecular diversity of voltage-dependent Ca^{2+} channels. *Trends Pharmacol. Sci.* 12: 349–354.
- Tsien, R.W., Lipscombe, D., Madison, D.V., Bley, K.R., and Fox, A.P. 1988. Multiple types of neuronal calcium channels and their selective modulation. *Trends Neurosci.* 11: 431–438.
- Tsodyks, M., Pawelzik, K., and Markram, H. 1998. Neural networks with dynamic synapses. *Trends Neurosci.* 10: 821–835.
- Tsubokawa, H., and Ross, W.N. 1996. IPSPs modulate spike backpropagation and associated $[\text{Ca}^{2+}]_i$ changes in the dendrites of hippocampal CA1 pyramidal neurons. *J. Neurophysiol.* 76: 2896–2906.
- Tsukahara, N., Toyama, K., and Kosaka, K. 1967. Electrical activity of red nucleus neurons investigated with intracellular microelectrodes. *Exp. Brain Res.* 4: 18–33.
- Tsukamoto, Y., and Sterling, P. 1991. Spatial summation by ganglion cells: some consequences for the efficient encoding of natural scenes. *Neurosci. Res. Suppl.* 15: S185–S198.
- Tsukamoto, Y., Masarachia, P., Schein, S.J., and Sterling, P. 1992. Gap junctions between the pedicles of macaque foveal cones. *Vis. Res.* 32: 1809–1815.
- Tsukamoto, Y., Morigiwa, K., Ueda, M., and Sterling, P. 2001. Microcircuits for night vision in mouse retina. *J. Neurosci.* 21: 8616–8623.
- Tsukamoto, Y., Smith, R.G., and Sterling, P. 1990. “Collective coding” of correlated cone signals in the retinal ganglion cell. *Proc. Natl. Acad. Sci. U.S.A.* 87: 1860–1864.
- Tsumoto, T., Eckart, W., and Creutzfeld, O. 1979. Modification of orientation sensitivity of cat visual cortex neurons by removal of GABA-mediated inhibition. *Exp. Brain Res.* 46: 157–169.
- Tsumoto, T., and Suda, K. 1979. Cross-depression: an electrophysiological manifestation of binocular competition in developing visual cortex. *Brain Res.* 168: 190–194.
- Tsumoto, T., and Suda, K. 1980. Three groups of cortico-geniculate neurons and their distribution in binocular and monocular segments of cat striate cortex. *J. Comp. Neurol.* 193: 223–236.
- Tunstall, M.J., Oorschot, D.E., Kean, A., and Wickens, J.R. 2002. Inhibitory interactions between spiny projection neurons in the rat striatum. *J. Neurophysiol.* 88: 1263–1269.
- Turkin, V., Monroe, K., and Hamm, T. 1998. Organization of recurrent inhibition and facilitation in motor nuclei innervating ankle muscles of the cat. *J. Neurophysiol.* 79: 778–790.
- Turner, C.P., and Perez-Polo, J.R. 1993. Expression of p75NGFR in the olfactory system following peripheral deafferentation. *NeuroReport* 4: 1023–1026.
- Turner, R.W., Meyers, D.E.R., Richardson, T.L., and Barker, J.L. 1991. The site for initiation of action potential discharge over the somatodendritic axis of rat hippocampal CA1 pyramidal neurons. *J. Neurosci.* 11: 2270–2280.
- Turrigiano, G. 1999. Homeostatic plasticity in neuronal networks: the more things change, the more they stay the same. *Trends Neurosci.* 22: 221–227.
- Turrigiano, G.G., Leslie, K., Desai, N., Rutherford, L., and Nelson, S. 1998. Activity-dependent scaling of quantal amplitude in neocortical neurons. *Nature* 391: 892–896.
- Uchida, N., Takahashi, Y.K., Tanifuji, M., and Mori, K. 2000. Odor maps in the mammalian olfactory bulb: domain organization and odorant structural features. *Nature Neurosci.* 3: 1035–1043.
- Uchiyama, H., and Barlow, R.B. 1994. Centrifugal inputs enhance responses of retinal ganglion cells in the Japanese quail without changing their spatial coding properties. *Vision Res.* 34: 2189–2194.
- Uchiyama, Y., and Ito, H. 1993. Target cells for the isthmo-optic fibers in the retina of the Japanese quail. *Neurosci. Lett.* 154: 35–38.
- Uhlrich, D.J., Cucchiari, J.B., Humphrey, A.L., and Sherman, S.M. 1991. Morphology and ax-

- onal projection patterns of individual neurons in the cat perigeniculate nucleus. *J. Neurophysiol.* 65: 1528–1541.
- Uhlrich, D.J., Manning, K.A., and Xue, J.T. 2002. Effects of activation of the histaminergic tuberomammillary nucleus on visual responses of neurons in the dorsal lateral geniculate nucleus. *J. Neuroscience* 22: 1098–1107.
- Uhlrich, D.J., Manning, K.A., and Pienkowski, T.P. 1993. The histaminergic innervation of the lateral geniculate complex in the cat. *Vis. Neurosci.* 10: 225–235.
- Ulfhake, B., and Cullheim, S. 1981. A quantitative light microscopic study of the dendrites of cat spinal γ -motoneurons after intracellular staining with horseradish peroxidase. *J. Comp. Neurol.* 202: 585–596.
- Ulfhake, B., and Kellerth, J.-O. 1981. A quantitative light microscopic study of the dendrites of cat spinal α -motoneurons after intracellular staining with horseradish peroxidase. *J. Comp. Neurol.* 202: 571–584.
- Ulfhake, B., Arvidsson, U., Cullheim, S., Hökfelt, T., Brodin, E., Verhofstad, A., and Visser, T. 1987. An ultrastructural study of 5-hydroxytryptamine-, thyrotropin-releasing hormone- and substance P-immunoreactive axonal boutons in the motor nucleus of spinal cord segments L7-S1 in the adult cat. *Neuroscience* 23: 917–929.
- Updyke, B.V. 1977. Topographic organization of the projections from cortical areas 17, 18, and 19 onto the thalamus, pretectum and superior colliculus in the cat. *J. Comp. Neurol.* 173: 81–122.
- Urban, N.N., and Sakmann, B. 2002. Reciprocal intraglomerular excitation and intra- and interglomerular lateral inhibition between mouse olfactory bulb mitral cells. *J. Physiol.* 542: 355–367.
- Usrey, W.M., and Fitzpatrick, D. 1996. Specificity in the axonal connections of layer VI neurons in tree shrew striate cortex: evidence for distinct granular and supragranular systems. *J. Neurosci.* 16: 1203–1218.
- Valcana, T., Hudson, D., and Timiras, P.S. 1972. Effects of X-irradiation on the content of amino acids in the developing rat cerebellum. *J. Neurochem.* 19: 2229–2232.
- Valverde, F. 1965. *Studies on the Piriform Lobe*. Cambridge, MA: Harvard University Press.
- Valverde, F., and Lopez-Mascaraque, L. 1991. Neuroglial arrangements in the olfactory glomeruli of the hedgehog. *J. Comp. Neurol.* 307: 658–674.
- van Daal, J.H.H.M., Zanderink, H.E.A., Jenks, B.G., and van Abellen, J.H.F. 1989. Distribution of dynorphin B and methionine-enkephalin in the mouse hippocampus: Influence of genotype. *Neurosci. Lett.* 97: 241–244.
- van den Pol, A.N., and Gorcs, T. 1988. Glycine and glycine receptor immunoreactivity in brain and spinal cord. *J. Neurosci.* 8: 472–492.
- van Eden, C., Hoorneman, E., Buijs, R., Matthijssen, M., Geffard, M., and Uylings, H. 1987. Immunocytochemical localization of dopamine in the prefrontal cortex of the rat at light and electron microscopic level. *Neuroscience* 22: 849–862.
- Van Essen, D.C. 1985. Functional organization of primate visual cortex. In: *Cerebral Cortex* (Peters, A., and Jones, E.G., eds.) New York: Plenum Press, pp. 259–329.
- Van Essen, D.C., and Maunsell, J.H.R. 1983. Hierarchical organization and functional streams in the visual cortex. *Trends Neurosci.* 6: 370–375.
- Van Essen, D.C., Anderson, C.H., and Felleman, D.J. 1992. Information processing in the primate visual system: an integrated systems perspective. *Science* 255: 419–423.
- Van Essen, D.C., Felleman, D.J., DeYoe, E.A., Olvarria, J., and Knierim, J.J. 1990. Modular and hierarchical organization of extrastriate visual cortex in the macaque monkey. *Cold Spring Harb. Symp. Quant. Biol.* 55: 679–696.
- van Groen, T., and Wyss, J.M. 1990. Extrinsic projections from area CA1 of the rat hippocampus. Olfactory, cortical, subcortical and bilateral hippocampal formation projections. *J. Comp. Neurol.* 302: 515–528.

- van Groen, T., and Wyss, J.M. 1992. Connections of the retrosplenial dysgranular cortex in the rat. *J. Comp. Neurol.* 315: 200–216.
- van Groen, T., Kadish, I., and Wyss, J.M. 2002. Role of the anterodorsal and anteroventral nuclei of the thalamus in spatial memory in the rat. *Behav. Brain Res.* 132: 19–28.
- van Hateren, J.H. 1992. A theory of maximizing sensory information. *Biol. Cybern.* 68: 23–29.
- van Hateren, J.H. 1993. Spatiotemporal contrast sensitivity of early vision. *Vis. Res.* 33: 257–267.
- Van Horn, S.C., Erişir, A., and Sherman, S.M. 2000. The relative distribution of synapses in the A laminae of the lateral geniculate nucleus of the cat. *J. Comp. Neurol.* 416: 509–520.
- Van Horn, S.C., Erişir, A., and Sherman, S.M. 1997. Re-evaluation of relative distribution of synaptic terminals in the LGN of cats. *Soc. Neurosci. Abstr.*
- Van Keulen, L. 1981. Autogenetic recurrent inhibition of individual spinal motoneurons of the cat. *Neurosci. Lett.* 21: 297–300.
- van Rossum, M.C.W., and Smith, R.G. 1998. Noise removal at the rod synapse of mammalian retina. *Vis. Neurosci.* 15: 809–821.
- Van Tasell, D.J., Soli, S.D., Kirby, V.M., and Widin, G.P. 1987. Speech waveform envelope cues for consonant recognition. *J. Acoust. Soc. Am.* 82: 1152–1161.
- Vandermaelen, C.P., and Aghajanian, G.K. 1983. Electrophysiological and pharmacological characterization of serotonergic dorsal raphe neurons recorded extracellularly and intracellularly in rat brain slices. *Brain Res.* 289: 109–119.
- Vanderwolf, C.H. 1992. Hippocampal activity, olfaction, and sniffing: an olfactory input to the dentate gyrus. *Brain Res.* 593: 197–208.
- Vaney, D.I. 1985. The morphology and topographic distribution of AII amacrine cells in the cat retina. *Proc. R. Soc. Lond. B* 224: 475–488.
- Vaney, D.I. 1986. Morphological identification of serotonin-accumulating neurons in the living retina. *Science* 233: 444–446.
- Vaney, D.I. 1990. The mosaic of amacrine cells in mammalian retina. In: *Progress in Retinal Research* (Osborne, N., and Chader, J., eds.). Oxford: Pergamon Press, pp. 49–100.
- Vaney, D.I. 1993. The coupling pattern of axon-bearing horizontal cells in the mammalian retina. *Proc. R. Soc. Lond. B* 252: 93–101.
- Vaney, D.I. 1994a. Patterns of neuronal coupling in the retina. *Prog. Retina Eye Res.* 13: 301–355.
- Vaney, D.I. 1994b. Territorial organization of direction-selective ganglion cells in rabbit retina. *J. Neurosci.* 14: 6301–6316.
- Vaney, D.I. 2002a. Retinal amacrine cells. In: *The Visual Neurosciences* (Chap. 25). (Chalupa, L., and Werner, J.S., eds.) Cambridge, Mass: MIT Press.
- Vaney, D.I. 2002b. Retinal neurons: cell types and coupled networks. In *Changing Views of Cajal's Neuron* (Chapter 18). (Azmitia, E.C., De Felipe, J., Jones, E.G., Rakic, P., and Ribak, C.E., eds.) Elsevier: Amsterdam.
- Vaney, D.I., and Collin, S.P. 1989a. Dendritic relationships between cholinergic amacrine cells and direction-selective retinal ganglion cells. In: *Neurobiology of the Inner Retina* (Weiler, R., and Osborne, N.N., eds.) Berlin: Springer-Verlag, pp. 157–168.
- Vaney, D.I., and Young, H.M. 1988a. GABA-like immunoreactivity in cholinergic amacrine cells of the rabbit retina. *Brain Res.* 438: 369–373.
- Vaney, D.I., and Young, H.M. 1988b. GABA-like immunoreactivity in NADPH-diaphorase amacrine cells of the rabbit retina. *Brain Res.* 474: 380–385.
- Vaney, D.I., Collin, S.P., and Young, H.M. 1989a. Dendritic relationships between cholinergic amacrine cells and direction-selective retinal ganglion cells. In: *Neurobiology of the Inner Retina* (Weiler, R., and Osborne, N.N., eds.) Berlin: Springer-Verlag, pp.
- Vaney, D.I., Gynther, I.C., and Young, H.M. 1991. Rod-signal interneurons in the rabbit retina: 2. AII amacrine cells. *J. Comp. Neurol.* 310: 154–169.
- Vaney, D.I., Nelson, J.C., and Pow, D.V. 1998. Neurotransmitter coupling through gap junctions in the retina. *J. Neurosci.* 18: 10594–10602.

- Vaney, D.I., Peichl, L., Wässle, H., and Illing, R.-B. 1981. Almost all ganglion cells in the rabbit retina project to the superior colliculus. *Brain Res* 212: 447–453.
- Vaney, D.I., Whittington, G.E., and Young, H.M. 1989b. The morphology and topographic distribution of substance-P-like immunoreactive amacrine cells in the cat retina. *Proc. R. Soc. Lond. B* 237: 471–488.
- Vardi, N. 1998. The alpha subunit of Go localizes in the dendritic tips of ON bipolar cells. *J. Comp. Neurol.* 395: 43–52.
- Vardi, N., and Auerbach, P. 1995. Specific cell types in cat retina express different forms of glutamic acid decarboxylase. *J. Comp. Neurol.* 351: 374–384.
- Vardi, N., and Morigiwa, K. 1997. ON cone bipolar cells in rat express the metabotropic receptor mGluR6. *Vis. Neurosci.* 14: 789–794.
- Vardi, N., and Shi, Y.-J. 1996. Identification of GABA containing bipolar cells in cat retina. *Invest. Ophthalmol. Vis. Sci. Abstr.* S418.
- Vardi, N., and Smith, R.G. 1996. The AII amacrine network: Coupling can increase correlated activity. *Vis. Res.* 36: 3743–3757.
- Vardi, N., and Sterling, P. 1994. Subcellular localization of GABAA receptor on bipolar cells in macaque and human retina. *Vis. Res.* 34: 1235–1246.
- Vardi, N., Duvoisin, R.M., Wu, G., and Sterling, P. 2000a. Localization of mGluR6 to dendrites of ON bipolar cells in primate retina. *J. Comp. Neurol.* 423: 402–412.
- Vardi, N., Kaufman, D.L., Sterling, P. 1994. Horizontal cells in cat and monkey retina express different isoforms of glutamic acid decarboxylase. *Vis. Neurosci.* 11: 135–142.
- Vardi, N., Masarachia, P., and Sterling, P. 1989. Structure of the starburst amacrine network and its association with alpha ganglion cells. *J. Comp. Neurol.* 288: 601–611.
- Vardi, N., Masarachia, P., and Sterling, P. 1992. Immunoreactivity to GABAA receptor in the outer plexiform layer of the cat retina. *J. Comp. Neurol.* 320: 394–397.
- Vardi, N., Matesic, D.F., Manning, D.R., Liebman, P.A., and Sterling, P. 1993. Identification of a G-protein in depolarizing rod bipolar cells. *Vis. Neurosci.* 10: 473–478.
- Vardi, N., Morigiwa, K., Wang, T.-L., Shi, Y.-J., and Sterling, P. 1998. Neurochemistry of the mammalian cone 'synaptic complex'. *Vis. Res.* 38: 1359–1369.
- Vardi, N., Zhang, L.-L., Payne, J.A., and Sterling, P. 2000b. Evidence that different cation chloride cotransporters in retinal neurons allow opposite responses to GABA. *J. Neurosci.* 20: 7657–7663.
- Vasilaki, A., Hatzilaris, E., Liapakis, G., Georgoussi, Z., and Thermos, K. 1996. Somatostatin receptor subtypes (SSTR2) in the rabbit retina. *Soc. Neurosci. Abstr.* 22: 180.
- Vassar, R., Chao, S.K., Sitcheran, R., Nunez, J.M., Vossahl, L.B., and Axel, R. 1994. Topographic organization of sensory projections to the olfactory bulb. *Cell* 79: 981–991.
- Vassar, R., Ngai, J., and Axel, R. 1993. Spatial segregation of odorant receptor expression in the mammalian olfactory epithelium. *Cell* 74: 309–318.
- Velte, T.J., and Masland, R.H. 1999. Action potentials in the dendrites of retinal ganglion cells. *J. Neurophysiol.* 81: 1412–1417.
- Verney, C., Alvarez, C., Geffard, M., and Berger, B. 1990. Ultra-structural double-labelling study of dopamine terminals and GABA-containing neurons in rat anteromedial cerebral cortex. *Eur. J. Neurosci.* 2: 960.
- Veruki, M.L., and Hartveit, E. 2002. AII (rod) amacrine cells form a network of electrically coupled interneurons in the mammalian retina. *Neuron* 33: 935–946.
- Veruki, M.L., and Wässle, H. 1996. Immunohistochemical localization of dopamine D1 receptors in rat retina. *Eur. J. Neurosci.* 8: 2286–2297.
- Victor, J.D. 1987. The dynamics of the cat retinal X cell centre. *J. Physiol. (Lond.)* 386: 219–246.
- Victor, J.D., Shapley, R.M., and Knight, B.W. 1977. Nonlinear analysis of cat retinal ganglion cells in the frequency domain. *Proc. Natl. Acad. Sci. U.S.A.* 74: 3068–3072.

- Viitala, J., Korpimäki, E., Palokangas, P., and Koivula, M. 1995. Attraction of kestrels to vole scent marks visible in ultraviolet light. *Nature* 373: 425–427.
- Vincent, S., Satoh, K., Armstrong, D., and Fibiger, H. 1983. Substance P in the ascending cholinergic reticular system. *Nature* 306: 688–691.
- Vincent, S.R., and Kimura, H. 1992. Histochemical mapping of nitric oxide synthase in the rat brain. *Neuroscience* 46: 755–784.
- Vincent, S.R., Johansson, O., Hökfelt, T., Skirboll, L., Elde, R.P., Terenius, L., Kimmel, J., and Goldstein, M. 1983b. NADPH-diaphorase—a selective histochemical marker for striatal neurons containing both somatostatin- and avian pancreatic polypeptide (APP)-like immunoreactivities. *J. Comp. Neurol.* 217: 252–263.
- Vincent, S.R., Satoh, K., Armstrong, D., and Fibiger, H. 1983a. Substance P in the ascending cholinergic reticular system. *Nature* 306: 688–691.
- Vogel, M. 1978. Postnatal development of the cat's retina. *Adv. Anat. Embryol. Cell Biol.* 54: 7–64.
- Voight, T., and Wässle, H. 1987. Dopaminergic innervation of AII amacrine cells in mammalian retina. *J. Neurosci.* 7: 4115–4128.
- Voigt, H.F., and Young, E.D. 1990. Cross-correlation analysis of inhibitory interactions in dorsal cochlear nucleus. *J. Neurophysiol.* 64: 1590–1610.
- Vollenweider, F.X., Cuenod, M., and Do, K.Q. 1990. Effect of climbing fiber deprivation on release of endogenous aspartate, glutamate, and homocysteate in slices of rat cerebellar hemispheres and vermis. *J. Neurochem.* 54: 1533–1540.
- von der Malsburg, C. 1981. The correlation theory of brain function. Internal Report of the Dept. of Neurobiology of the Max Plank Institute for Biophysical Chemistry, Göttingen. 81: 2.
- von Gersdorff, H., and Matthews, G. 1994. Dynamics of synaptic vesicle fusion and membrane retrieval in synaptic terminals. *Nature* 367: 735–739.
- von Gersdorff, H., Vardi, E., Matthews, G., and Sterling, P. 1996. Evidence that vesicles on the synaptic ribbon of retinal bipolar neurons can be rapidly released. *Neuron* 16: 1221–1227.
- von Krosigk, M., Bal, T., and McCormick, D.A. 1993. Cellular mechanisms of a synchronized oscillation in the thalamus. *Science* 261: 361–364.
- Voogd, J., and Bigaré, F. 1980. Topographical distribution of olivary and corticonuclear fibers in the cerebellum: a review. In: *The Inferior Olivary Nucleus* (Courville, J., de Montigny, C., and Lamarre, Y., eds.). New York: Raven Press, pp. 207–234.
- Vu, T.Q., Payne, J.A., and Copenhagen, D. 2000. Localization and developmental expression patterns of the neuronal K-Cl cotransporter (KCC2) in the rat retina. *J. Neurosci.* 20: 1414–1423.
- Wachowiak, M., and Cohen, L.B. 2001. Representation of odorants by receptor neuron input to the mouse olfactory bulb. *Neuron* 32: 723–735.
- Wada, E., Wada, K., Boulter, J., Deneris, E., Heinemann, S., Patrick, J., and Swanson, L.W. 1989. Distribution of alpha2, alpha3, alpha4, and beta2 neuronal nicotinic receptor subunit mRNAs in the central nervous system—a hybridization histochemical study in the rat. *J. Comp. Neurol.* 284: 314–335.
- Wagner, J.J., and Alger, B.E. 1996. Homosynaptic LTD and depotentiation: do they differ in name only? *Hippocampus* 6: 24–29.
- Wahle, P. 1993. Differential regulation of substance P and somatostatin in Martinotti cells of the developing cat visual cortex. *J. Comp. Neurol.* 329: 519–538.
- Wainer, B.H., Levey, A.I., Rye, D.B., Mesulam, M.M., and Mufson, E.J. 1985. Cholinergic and non-cholinergic septohippocampal pathways. *Neurosci. Lett.* 54: 45–52.
- Walker, A.E. 1938. *The Primate Thalamus*. Chicago, IL.: University of Chicago Press.
- Walker, M. C., Ruiz, A., and Kullmann, D. M. 2001. Monosynaptic GABAergic signaling from

- dentate to CA3 with a pharmacological and physiological profile typical of mossy fiber synapses. *Neuron* 29: 703–15.
- Walmsley, B. 1991. Central synaptic transmission: Studies at the connection between primary afferent fibres and dorsal spinocerebellar tract (DSCT) neurones in Clarke's column of the spinal cord. *Prog. Neurobiol.* 36: 391–423.
- Walmsley, B. 1995. Interpretation of 'quantal' peaks in distributions of evoked synaptic transmission at central synapses. *Proc. R. Soc. Lond. B* 261: 245–250.
- Walmsley, B., and Bolton, P.S. 1994. An *in vivo* pharmacological study of single group Ia fibre contacts with motoneurons in the cat spinal cord. *J. Physiol. (Lond.)* 481: 731–741.
- Walmsley, B., and Edwards, F.R. 1988. Nonuniform release probabilities underlie quantal synaptic transmission at a mammalian excitatory central synapse. *J. Neurophysiol.* 60: 889–908.
- Walmsley, B., Hodgson, J.A., and Burke, R.E. 1978. Forces produced by medial gastrocnemius and soleus muscles during locomotion in freely moving cats. *J. Neurophysiol.* 41: 1203–1216.
- Walmsley, B., and Tracey, D.J. 1981. An intracellular study of Renshaw cells. *Brain Res.* 223: 170–175.
- Walmsley, B., Wieniawa-Narkiewicz, E., and Nicol, M.J. 1985. The ultrastructural basis for synaptic transmission between primary muscle afferents and neurons in Clarke's column of the cat. *J. Neurosci.* 5: 2095–2106.
- Wan, H., and Cahusac, P. 1995. The effects of 1-ap4 and 1-serine-o-phosphate on inhibition in primary somatosensory cortex of the adult rat *in vivo*. *Neuropharm.* 34: 1053–1062.
- Wang, F., Nemes, A., Mendelsohn, M., and Axel, R. 1998. Odorant receptors govern the formation of a precise topographic map. *Cell* 93: 47–60.
- Wang, J.H., and Kelly, P.T. 1996. Regulation of synaptic facilitation by postsynaptic Ca²¹/CaM pathways in hippocampal CA1 neurons. *J. Neurophysiol.* 76: 276–286.
- Wang, S., Bickford, M.E., Van Horn, S.C., Erisir, A., Godwin, D.W., and Sherman, S.M. 2001. Synaptic targets of thalamic reticular nucleus terminals in the visual thalamus of the cat. *J. Comp. Neurol.* 440: 321–341.
- Wang, S.T., Eisenback, M.A., and Bickford, M.E. 2002a. Relative distribution of synapses in the pulvinar nucleus of the cat: implications regarding the "driver/modulator" theory of thalamic function. *J. Comp. Neurol.* 454: 482–494.
- Wang, S.T., Eisenback, M.A., Datskovskaia, A., Boyce, M., and Bickford, M.E. 2002b. GABAergic pretectal terminals contact GABAergic interneurons in the cat dorsal lateral geniculate nucleus. *NeuroscienceLett* 323: 141–145.
- Wang, X., and Sachs, M.B. 1994. Neural encoding of single-formant stimuli in the cat. II. Responses of anteroventral cochlear nucleus neurons. *J. Neurophysiol.* 71: 59–78.
- Wang, X.Y., McKenzie, J.S., and Kemm, R.E. 1996. Whole-cell K1 currents in identified olfactory bulb output neurones of rat. *J. Physiol. (Lond.)* 490: 63–77.
- Wang, Y., Gupta, A., Toledo, M.,-Rodriguez, Wu, C., and Markram, H. 2002. Anatomical, physiological, molecular and circuit properties of nest basket cells in the developing somatosensory cortex. *Cereb. Cortex* 12: 395–410.
- Wang, Y.X., Wenthold, R.J., Ottersen, O.P., and Petralia, R.S. 1998. Endbulb synapses in the anteroventral cochlear nucleus express a specific subset of AMPA-type glutamate receptor subunits. *J. Neurosci.* 18: 1148–1160.
- Wang, Z., and McCormick, D.A. 1993. Control of firing mode of corticotectal and corticopontine layer V burst-generating neurons by norepinephrine, acetylcholine and 1s, 3r-ACPD. *J. Neurosci.* 13: 2199–2216.
- Wässle, H. 2003. *The Cone Pedicle, the First Synapse in the Retina. The Neural Basis of Early Vision.* Tokyo: Springer-Verlag.
- Wässle, H., and Boycott, B.B. 1991. Functional architecture of the mammalian retina. *Physiol. Rev.* 71: 447–480.

- Wässle, H., and Chun, M.-H. 1988. Dopaminergic and indoleamine-accumulating amacrine cells express GABA-like immunoreactivity in the cat retina. *J. Neurosci.* 8: 3383–3394.
- Wässle, H., and Chun, M.H. 1989. GABA-like immunoreactivity in the cat retina: light microscopy. *J. Comp. Neurol.* 279: 43–54.
- Wässle, H., and Illing, R.-B. 1980. The retinal projection to the superior colliculus in the cat: a quantitative study with HRP. *J. Comp. Neurol.* 190: 333–356.
- Wässle, H., and Riemann, H.J. 1978. The mosaic of nerve cells in the mammalian retina. *Proc. R. Soc. Lond. B* 200: 441–461.
- Wässle, H., Boycott, B.B., and Illing, R.B. 1981a. Morphology and mosaic of ON- and OFF-beta cells in the cat retina and some functional considerations. *Proc. R. Soc. B* 212: 177–195.
- Wässle, H., Boycott, B.B., and Peichl, L. 1978a. Receptor contacts of horizontal cells in the retina of the domestic cat. *Proc. R. Soc. Lond. B* 203: 247–267.
- Wässle, H., Grünert, U., Chun, M.-H., and Boycott, B.B. 1995. The rod pathway of the macaque monkey retina: identification of AII-amacrine cells with antibodies against calretinin. *J. Comp. Neurol.* 361: 537–551.
- Wässle, H., Grünert, U., Martin, P.R., and Boycott, B.B. 1994. Immunocytochemical characterization and spatial distribution of midget bipolar cells in the macaque monkey retina. *Vision Res.* 34: 561–579.
- Wässle, H., Grünert, U., Röhrenbeck, J., and Boycott, B.B. 1989. Cortical magnification factor and the ganglion cell density of the primate retina. *Nature* 341: 643–646.
- Wässle, H., Peichl, L., and Boycott, B. 1981b. Dendritic territories of cat retinal ganglion cells. *Nature* 292: 344–345.
- Wässle, H., Peichl, L., and Boycott, B.B. 1978b. Topography of horizontal cells in the retina of the domestic cat. *Proc. R. Soc. Lond. B* 203: 269–291.
- Wässle, H., Peichl, L., and Boycott, B.B. 1981c. Morphology and topography of ON- and OFF-alpha cells in the cat retina. *Proc. R. Soc. B Lond.* 212: 157–175.
- Wässle, H., Yamashita, M., Greferath, U., Grünert, U., and Müller, F. 1991. The rod bipolar cell of the mammalian retina. *Vis. Neurosci.* 7: 99–112.
- Watanabe, M., and Rodieck, R.W. 1989. Parasol and midget ganglion cells of the primate retina. *J. Comp. Neurol.* 289: 434–454.
- Waterhouse, B., Azizi, B.R., and Woodward, S.A.D. 1990. Modulation of rat cortical area 17. Neuronal responses to moving visual stimuli during norepinephrine and serotonin microiontophoresis. *Brain Res.* 514: 276–292.
- Waterhouse, B., C.-Lin, S., Burne, R., and Woodward, D. 1983. The distribution of neocortical projection neurons in the locus coeruleus. *J. Comp. Neurol.* 217: 418–431.
- Waterhouse, B., R, B., Azizi, S.A., and Woodward, D. 1990. Modulation of rat cortical area 17. Neuronal responses to moving visual stimuli during norepinephrine and serotonin microiontophoresis. *Brain Res.* 514: 276–292.
- Watkins, J.C., and Olverman, H.J. 1987. Agonists and antagonists for excitatory amino acid receptors. *Trends Neurosci.* 10: 265–272.
- Weedman, D.L., and Ryugo, D.K. 1996. Projections from auditory cortex to the cochlear nucleus in rats: Synapses on granule cell dendrites. *J. Comp. Neurol.* 371: 311–324.
- Weedman, D.L., Pongstaporn, T., and Ryugo, D.K. 1996. Ultrastructural study of the granule cell domain of the cochlear nucleus in rats: mossy fiber endings and their targets. *J. Comp. Neurol.* 369: 345–360.
- Wehr, M., and Laurent, G. 1996. Odour encoding by temporal sequences of firing in oscillating neural assemblies. *Nature* 384: 161–164.
- Weiler, R., Pottek, M., He, S., and Vaney, D.I. 2000. Modulation of coupling between retinal horizontal cells by retinoic acid and endogenous dopamine. *Brain Res.* 32: 121–129.
- Weinberg, R.J., and Rustioni, A. 1987. A cuneocochlear pathway in the rat. *Neuroscience* 20: 209–219.

- Wellis, D.P., and Kauer, J.S. 1993. GABAA and glutamate receptor involvement in dendrodendritic synaptic interactions from salamander olfactory bulb. *J. Physiol. (Lond.)* 469: 315–339.
- Wellis, D.P., and Scott, J.W. 1987. Intracellular recordings of odor-induced responses in the rat olfactory bulb. *Chem. Senses* 12: 707.
- Wellis, D.P., and Scott, J.W. 1990. Intracellular responses of identified rat olfactory bulb interneurons to electrical and odor stimulation. *J. Neurophysiol.* 64: 932–947.
- Welsh J.P., Lang E.J., Sugihara I., and Llinás R., 1995. Dynamic organization of motor control within the olivocerebellar system. *Nature* 374: 453–457.
- Wenthold, R.J. 1979. Release of endogenous glutamic acid, aspartic acid and GABA from cochlear nucleus slices. *Brain Res.* 162: 338–343.
- Wenthold, R.J. 1987. Evidence for a glycinergic pathway connecting the two cochlear nuclei: an immunocytochemical and retrograde transport study. *Brain Res.* 415: 183–187.
- Wenthold, R.J. 1991. Neurotransmitters of brainstem auditory nuclei. In: *Neurobiology of Hearing: The Central Auditory System* (Altschuler, R.A., Bobbin, R.P., Clopton, B.M., and Hoffman, D.W., eds.) New York: Raven Press, pp. 121–139.
- Wenthold, R.J., Huie, D., Altschuler, R.A., and Reeks, K.A. 1987. Glycine immunoreactivity localized in the cochlear nucleus and superior olivary complex. *Neuroscience* 22: 897–912.
- Wenthold, R.J., Parakkal, M.H., Oberdorfer, M.D., and Altschuler, R.A. 1988. Glycine receptor immunoreactivity in the ventral cochlear nucleus. *J. Comp. Neurol.* 276: 423–435.
- Werblin, F.S., and Dowling, J.E. 1969. Organization of the retina of the mudpuppy, *Necturus maculosus*. II. Intracellular recording. *J. Neurophysiol.* 32: 339–355.
- Westbrook, G.L. 1994. Glutamate receptor update. *Curr. Opin. Neurobiol.* 4: 337–346.
- Westenbroek, R.E., Ahljianian, M.K., and Catterall, W.A. 1990. Clustering of L-type Ca^{2+} channels at the base of major dendrites in hippocampal pyramidal neurons. *Nature* 347: 281–284.
- Westenbroek, R.E., Westrum, L.E., Hendrickson, A.E., and Wu, J.-Y. 1987. Immunocytochemical localization of cholecystokinin and glutamic acid decarboxylase during normal development in the prepyriform cortex of rats. *Dev. Brain Res.* 34: 191–206.
- Westrum, L.E. 1970. Observations on initial segments of axons in the prepyriform cortex of the rat. *J. Comp. Neurol.* 139: 337–356.
- Wheeler, D.B., Randall, A., and Tsien, R.W. 1994. Roles of N-type and Q-type Ca^{2+} channels in supporting hippocampal synaptic transmission. *Science* 264: 107–111.
- White, C.A., Chalupa, L.M., Johnson, D., and Brecha, N.C. 1990. Somatostatin-immunoreactive cells in the adult cat retina. *J. Comp. Neurol.* 293: 134–150.
- White, E.L. 1972. Synaptic organization in the olfactory glomerulus of the mouse. *Brain Res.* 37: 69–80.
- White, E.L. 1989. *Cortical Circuits*. Boston, MA: Birkhauser.
- White, E.L., and Rock, M. 1980. Three-dimensional aspects and synaptic relationships of a Golgi-impregnated spiny stellate cell reconstructed from serial thin sections. *J. Neurocytol.* 9: 615–636.
- White, G., Levy, W.B., and Steward, O. 1990. Spatial overlap between populations of synapses determines the extent of their associative interaction during the induction of long-term potentiation and depression. *J. Neurophysiol.* 64: 1186–1198.
- White, J.A., Young, E.D., and Manis, P.B. 1994. The electrotonic structure of regular-spiking neurons in the ventral cochlear nucleus may determine their response properties. *J. Neurophysiol.* 71: 1774–1786.
- Wickens, J.R., Begg, A.J., and Arbuthnott, G.W. 1996. Dopamine reverses the depression of rat cortico-striatal synapses which normally follows high frequency stimulation of cortex in vitro. *Neuroscience* 70: 1–5.
- Wickens, J.R., and Kötter, R. 1995. Cellular models of reinforcement. In: *Models of Informa-*

- tion Processing in the Basal Ganglia (J.C. Houk, J.L. Davis and D.G. Beiser, eds.). Cambridge, MA:MIT Press, pp. 187–214.
- Wickesberg, R.E., and Oertel, D. 1988. Tonotopic projection from the dorsal to the anteroventral cochlear nucleus of mice. *J. Comp. Neurol.* 268: 389–399.
- Wickesberg, R.E., and Oertel, D. 1990. Delayed, frequency-specific inhibition in the cochlear nuclei of mice: A mechanism for monaural echo suppression. *J. Neurosci.* 10: 1762–1768.
- Wickesberg, R.E., and Oertel, D. 1991. Tuberculoventral neurons project to the multipolar cell area but not to the octopus cell area of the posteroventral cochlear nucleus. *J. Comp. Neurol.* 15: 457–468.
- Wickesberg, R.E., and Oertel, D. 1989. Auditory nerve neurotransmitter acts on a kainate receptor: evidence from intracellular recordings in brain slices from mice. *Brain Res.* 486: 39–48.
- Wickesberg, R.E., Whitlon, D., and Oertel, D. 1994. In vitro modulation of somatic glycine-like immunoreactivity in presumed glycinergic neurons. *J. Comp. Neurol.* 339: 311–327.
- Wightman, F.L., and Kistler, D.J. 1992. The dominant role of low-frequency interaural time differences in sound localization. *J. Acoust. Soc. Am.* 91: 1648–1661.
- Wigstrom, H., and Gustafsson, B. 1983. Facilitated induction of hippocampal long-lasting potentiation during blockade of inhibition. *Nature* 301: 603–604.
- Wigstrom, H., Gustafsson, B., Huang, Y.Y., and Abraham, W.C. 1986. Hippocampal long-term potentiation is induced by pairing single afferent volleys with intracellularly injected depolarizing current pulses. *Acta. Physiol. Scand.* 126: 317–319.
- Wiklund L., Toggenburger G., and Cuenod, M. 1982. Aspartate: possible neurotransmitter in cerebellar climbing fibers. *Science.* 216: 78–80.
- Williams, D.R. 1992. Photoreceptor sampling and aliasing in human vision. In: *Tutorials in Optics* (Moore, D.T., ed.) Optical Society of America, Rochester, NY: pp. 15–27.
- Williams, D.R., MacLeod, D.I.A., and Hayhoe, M.M. 1981. Punctate sensitivity of the blue-sensitive mechanism. *Vision Res.* 21: 1357–1375.
- Williams, D.R., Sekiguchi, N., and Brainard, D. 1993b. Color, contrast sensitivity, and the cone mosaic. *Proc. Natl. Acad. Sci. U.S.A.* 90: 9770–9777.
- Williams, J.T., North, R.A., Shefner, S.A., Nishi, S., and Egan, T.M. 1984. Membrane properties of rat locus coeruleus neurones. *Neuroscience* 13: 137–156.
- Williams, R.W., and Herrup, K. 1988. The control of neuron number. *Annu. Rev. Neurosci.* 11: 423–453.
- Williams, R.W., Bastiani, M.J., and Chalupa, L. 1983. Loss of axons in the cat optic nerve following fetal unilateral enucleation: An electron microscopic analysis. *J. Neurosci.* 3: 133–144.
- Williams, R.W., Bastiani, M.J., Lia, B., and Chalupa, L.M. 1996. Growth cones, dying axons, and developmental fluctuations in the fiber population of the cat's optic nerve. *J. Comp. Neurol.* 246: 32–69.
- Williams, R.W., Cavada, C., and Reinoso-Suárez, F. 1993a. Rapid evolution of the visual system: A cellular assay of the retina and dorsal lateral geniculate nucleus of the Spanish wildcat and the domestic cat. *J. Neurosci.* 13: 208–228.
- Williams, S.H., and Constanti, A. 1988. Quantitative effects of some muscarinic agonists on evoked surface-negative field potentials recorded from the guinea-pig olfactory cortex slice. *British J. Pharmacol.* 93: 846–854.
- Williams, S.H., and Johnston, D. 1993. Muscarinic cholinergic inhibition of glutamatergic transmission. In: *Presynaptic Receptors in the Mammalian Brain* (Dunwiddie, T.V., and Lovinger, D.M., eds.) Boston: Burkhauser, pp. 27–41.
- Williams, S.H., and Johnston, D. 1996. Actions of endogenous opioids on NMDA receptor-independent long-term potentiation in area CA3 of the hippocampus. *J. Neurosci.* 16: 3652–3660.

- Willis, W.D., and Coggeshall, R.E. 1991. *Sensory Mechanisms of the Spinal Cord*. New York: Plenum Press.
- Willott, J.F., and Bross, L.S. 1990. Morphology of the octopus cell area of the cochlear nucleus in young and aging C57BL/6J and CBA/J mice. *J. Comp. Neurol.* 300: 61–81.
- Wilson, C.J. 1986a. Postsynaptic potentials evoked in spiny neostriatal projection neurons by stimulation of ipsilateral or contralateral neocortex. *Brain Res.* 367: 201–213.
- Wilson, C.J. 1986b. Three-dimensional analysis of dendritic spines by means of HVEM. *J. Electron Microsc.* 35(Suppl.): 1151–1155.
- Wilson, C.J. 1992. Dendritic morphology, inward rectification and the functional properties of neostriatal neurons. In: *Single Neuron Computation* (McKenna, T., Davis, J., and Zornetzer, S.F., eds.) San Diego: Academic Press, pp. 141–171.
- Wilson, C.J., Chang, H.T., and Kitai, S.T. 1982. Origins of post-synaptic potentials evoked in identified neostriatal neurons by stimulation in substantia nigra. *Exp. Brain Res.* 45: 157–167.
- Wilson, C.J., Chang, H.T., and Kitai, S.T. 1983a. Origins of postsynaptic potentials evoked in spiny neostriatal projection neurons by thalamic stimulation in the rat. *Exp. Brain Res.* 51: 217–226.
- Wilson, C.J., Chang, H.T., and Kitai, S.T. 1990. Firing patterns and synaptic potentials of identified giant aspiny interneurons in the rat neostriatum. *J. Neurosci.* 10: 508–519.
- Wilson, C.J., and Groves, P.M. 1980. Fine structure and synaptic connections of the common spiny neuron of the rat neostriatum. *J. Comp. Neurol.* 194: 599–615.
- Wilson, C.J., and Groves, P.M. 1981. Spontaneous firing patterns of identified spiny neurons in the rat neostriatum. *Brain Res.* 22: 67–80.
- Wilson, C.J., Groves, P.M., Kitai, S.T., and Linder, J.C. 1983b. Three-dimensional structure of dendritic spines in the rat neostriatum. *J. Neurosci.* 3: 383–398.
- Wilson, C.J., and Kawaguchi, Y. 1996. The origins of two-state spontaneous membrane potential fluctuations of neostriatal spiny neurons. *J. Neurosci.* 16: 2397–2410.
- Wilson, D.A. 1997. Binocular interactions in the rat piriform cortex. *J. Neurophysiol.* 78: 160–169.
- Wilson, D.A. 1998a. Habituation of odor responses in the rat anterior piriform cortex. *J. Neurophysiol.* 79: 1425–1440.
- Wilson, D.A. 1998b. Synaptic correlates of odor habituation in the rat anterior piriform cortex. *J. Neurophysiol.* 80: 998–1001.
- Wilson, D.A. 2000a. Comparison of odor receptive field plasticity in the rat olfactory bulb and anterior piriform cortex. *J. Neurophysiol.* 84: 3036–3042.
- Wilson, D.A. 2000b. Odor specificity of habituation in the rat anterior piriform cortex. *J. Neurophysiol.* 83: 139–145.
- Wilson, D.A. 2001a. Receptive fields in the rat piriform cortex. *Chem. Senses* 26: 577–584.
- Wilson, D.A. 2001b. Scopolamine enhances generalization between odor representations in rat olfactory cortex. *Learning & Memory* 8: 279–285.
- Wilson, D.A., and Leon, M. 1987a. Abrupt decrease in synaptic inhibition in the postnatal rat olfactory bulb. *Brain Res.* 430: 134–138.
- Wilson, D.A., and Leon, M. 1987b. Evidence of lateral synaptic interactions in olfactory bulb output cell responses to odors. *Brain Res.* 417: 175–180.
- Wilson, H.R. 1999. *Spikes, Decisions, and Actions: The Dynamical Foundations of Neuroscience*. Oxford: Oxford Press.
- Wilson, J.R., Friedlander, M.J., and Sherman, S.M. 1984. Fine structural morphology of identified X- and Y-cells in the cat's lateral geniculate nucleus. *Proc. R. Soc. Lond. B* 221: 411–436.
- Wilson, J.R., Friedlander, M.J., and Sherman, S.M. 1984. Fine structural morphology of identified X- and Y-cells in the cat's lateral geniculate nucleus. *Proc. R. Soc. Lond. B Biol. Sci.* 221: 441–436.

- Wilson, M. 2002. Retinal processing: smaller babies thrown out with bathwater. *Curr. Biol.* 12: R625–R627.
- Wilson, M. 2003. Retinal synapses. In: *The Visual Neurosciences* (Chalupa, L., and Werner, J.S., eds.). Cambridge, Mass.: MIT Press, pp.
- Wilson, M.A., and Bower, J.M. 1988. A computer simulation of olfactory cortex with functional implications for storage and retrieval of olfactory information. In: *Neural Information Processing Systems* (Anderson, D.Z., ed.). New York: American Institute of Physics, pp. 114–126.
- Wilson, M.A., and McNaughton, B.L. 1993. Dynamics of the hippocampal ensemble code for space. *Science* 261: 1055–1058.
- Wilson, M.A., and McNaughton, B.L. 1994. Reactivation of hippocampal ensemble memories during sleep. *Science* 265: 676–679.
- Wilson, R.I., and Nicoll, R.A. 2002. Endocannabinoid signaling in the brain. *Science* 296: 678–682.
- Winter, I.M., and Palmer, A.R. 1995. Level dependence of cochlear nucleus onset unit responses and facilitation by second tones or broadband noise. *J. Neurophysiol.* 73: 141–159.
- Witkovsky, P., Nicholson, C., Rice, M.E., and Bohmaker, K. 1993. Extracellular dopamine concentration in the retina of the clawed frog, *Xenopus laevis*. *Proc. Natl. Acad. Sci. U.S.A.* 90: 5667–5671.
- Witter, M.P., and Groenewegen, H. 1992. Organizational principles of hippocampal connections. In: *The Temporal Lobes and the Limbic System* (Trimble, M., and Bolwig, T., eds.) Wrightson Biomedical Publishing, pp. 37–60.
- Witter, M.P., Ostendorf, R.H., and Groenewegen, H.J. 1990. Heterogeneity in the dorsal subiculum of the rat. Distinct neuronal zones project to different cortical and subcortical targets. *Eur. J. Neurosci.* 2: 718–725.
- Wong, R., and Watkins, D. 1982. Cellular factors influencing GABA responses in hippocampal pyramidal cells. *J. Neurophysiol.* 48: 938–951.
- Wong, R.K.S., and Prince, D.A. 1978. Participation of calcium spikes during intrinsic burst firing in hippocampal neurons. *Brain Res.* 159: 385–390.
- Wong, R.K.S., Prince, D.A., and Basbaum, A.I. 1979. Intradendritic recordings from hippocampal neurons. *Proc. Natl. Acad. Sci. U.S.A.* 76: 986–990.
- Wong, R.O.L., and Oakley, D.M. 1996. Changing patterns of spontaneous bursting activity of On and Off retinal ganglion cells during development. *Neuron* 16: 1087–1095.
- Wong, R.O.L., Chernjavsky, A., Smith, S.J., and Shatz, C.J. 1995. Early functional neural networks in the developing retina. *Nature* 374: 716–718.
- Wong, R.O.L., Herrmann, K., and Shatz, C.J. 1991. Remodeling of retinal ganglion cell dendrites in the absence of action potential activity. *J. Neurobiol.* 22: 685–697.
- Wong-Riley, M., and Carroll, E. 1984. Quantitative light and electron microscopic analysis of cytochrome oxidase-rich zones in v11 prestriate cortex of the squirrel monkey. *J. Comp. Neurol.* 222: 18–37.
- Woo, C.C., Coopersmith, R., and Leon, M. 1987. Localized changes in olfactory bulb morphology associated with early olfactory learning. *J. Comp. Neurol.* 263: 113–125.
- Wolf, T.B., and Greer, C.A. 1994. Local communication within dendritic spines: Models of second messenger diffusion in granule cell spines of the mammalian olfactory bulb. *Synapse* 17: 247–267.
- Wolf, T.B., Shepherd, G.M., and Greer, C.A. 1988. Models of local electrical interactions within spiny dendrites of granule cells in mouse olfactory bulb. *Soc. Neurosci. Abstr.* 14: 620.
- Wolf, T.B., Shepherd, G.M., and Greer, C.A. 1991a. Local information processing in dendritic trees: subsets of spines in granule cells of the mammalian olfactory bulb. *J. Neurosci.* 11: 1837–1854.

- Woolf, T.B., Shepherd, G.M., and Greer, C.A. 1991b. Serial reconstructions of granule cell spines in the mammalian olfactory bulb. *Synapse* 7: 181–192.
- Woolley, D.E., and Timiras, P.S. 1965. Prepyriform electrical activity in the rat during high altitude exposure. *Electroencephalogr. Clin. Neurophysiol.* 18: 680–690.
- Woolsey, T., and Van der Loos, H. 1970. The structural organization of layer IV in the somatosensory region (S1) of mouse cortex. The description of a cortical field composed of discrete cytoarchitectonic units. *Brain Res.* 17: 205–242.
- Woolsey, T., and Van, H., der Loos 1970. The structural organization of layer IV in the somatosensory region (S1) of mouse cortex. The description of a cortical field composed of discrete cytoarchitectonic units. *Brain Res.* 17: 205–242.
- Wouterlood, F.G., and Härtig, W. 1995. Calretinin-immunoreactivity in mitral cells of the rat olfactory bulb. *Brain Res.* 682: 93–100.
- Wouterlood, F.G., and Mugnaini, E. 1984. Cartwheel neurons of the dorsal cochlear nucleus. A Golgi-electron microscopic study in the rat. *J. Comp. Neurol.* 227: 136–157.
- Wouterlood, F.G., Mugnaini, E., Osen, K.K., and Dahl, A.-L. 1984. Stellate neurons in rat dorsal cochlear nucleus studied with combined Golgi impregnation and electron microscopy: synaptic connections and mutual coupling by gap junctions. *J. Neurocytol.* 13: 639–664.
- Wouterlood, F.G., Saldana, E., and Witter, M.P. 1990. Projection from the nucleus reuniens thalami to the hippocampal region: Light and electron microscopic tracing study in the rat with the anterograde tracer Phaseolus vulgaris-leucoagglutinin. *J. Comp. Neurol.* 296: 179–203.
- Wright, D.D., Blackstone, C.D., Haganir, R.L., and Ryugo, D.K. 1996. Immunocytochemical localization of the mGluR1a receptor in the dorsal cochlear nucleus. *J. Comp. Neurol.* 364: 729–745.
- Wróbel, A. 1981. Light level induced reorganization of cat's lateral geniculate nucleus receptive fields: a spatiotemporal study. *Acta Neurobiol. Exp.* 41: 447–466.
- Wu, S.H., and Oertel, D. 1984. Intracellular injection with horseradish peroxidase of physiologically characterized stellate and bushy cells in slices of mouse anteroventral cochlear nucleus. *J. Neurosci.* 4: 1577–1588.
- Wu, S.H., and Oertel, D. 1986. Inhibitory circuitry in the ventral cochlear nucleus is probably mediated by glycine. *J. Neurosci.* 6: 2691–2706.
- Wu, S.H., and Oertel, D. 1987. Maturation of synapses and electrical properties of cells in the cochlear nuclei. *Hearing Res.* 30: 99–110.
- Wu, S.M. 1992. Feedback connections and operation of the outer plexiform layer of the retina. *Curr. Opin. Neurobiol.* 2: 462–468.
- Wyss, J.M., Swanson, L.W., and Cowan, W.M. 1979a. Evidence for an input to the molecular layer and the stratum granulosum of the dentate gyrus from the supramammillary region of the hypothalamus. *Anat. Embryol.* 156: 165–176.
- Wyss, J.M., Swanson, L.W., and Cowan, W.M. 1979b. A study of subcortical afferents to the hippocampal formation in the rat. *Neuroscience* 4: 463–476.
- Wyss, J.M., and van Groen, T. 1992. Connections between the retrosplenial cortex and the hippocampal formation in the rat: a review. *Hippocampus* 2: 1–11.
- Xiang, M., Zhou, L., and Nathans, J. 1996. Similarities and differences among inner retinal neurons revealed by the expression of reporter transgenes controlled by Brn-3a, Brn-3b, and Brn-3c promoter sequences. *Vis. Neurosci.* 13: 955–962.
- Xiang, Z., Greenwood, A.C., Kairiss, E.W., and Brown, T.H. 1994. Quantal mechanism of long-term potentiation in hippocampal mossy-fiber synapses. *J. Neurophysiol.* 71: 2552–2556.
- Xie, C.W., and Lewis, D.V. 1995. Endogenous opioids regulate long-term potentiation of synaptic inhibition in the dentate gyrus of rat hippocampus. *J. Neurosci.* 15: 3788–3795.
- Xin, D., and Bloomfield, S.A. 1997. Tracer coupling pattern of amacrine and ganglion cells in the rabbit retina. *J. Comp. Neurol.* 383: 512–528.

- Xin, D., and Bloomfield, S.A. 1999. Comparison of the responses of AII amacrine cells in the dark- and light-adapted rabbit retina. *Vis. Neurosci.* 16: 653–665.
- Xiong, W., and Chen, W.R. 2002. Dynamic gating of spike propagation in the mitral cell lateral dendrites. *Neuron* 34: 115–126.
- Xu, F., Liu, N., Kida, I., Rothman, D.L., Hyder, F., and Shepherd, G.M. 2003. Odor maps of aldehydes and esters revealed by fMRI in the mouse olfactory bulb. *Proc. Natl. Acad. Sci. USA* (in press).
- Xu, Z.C., Wilson, C.J., and Emson, P.C. 1991. Restoration of thalamostriatal projections in rat neostriatal grafts: An electron microscopic analysis. *J. Comp. Neurol.* 303: 22–34.
- Yamamoto T., Fukuda M., and Llinás R., 2001. Bilaterally synchronous complex spike Purkinje cell activity in the mammalian cerebellum. *Eur. J. Neurosci.* 13: 327–339.
- Yan, Z., and Surmeier, D.J. 1996. Muscarinic (m2/m4) receptors reduce N- and P-type Ca^{2+} currents in rat neostriatal cholinergic interneurons through a fast, membrane-delimited, G-protein pathway. *J. Neurosci.* 16: 2592–2604.
- Yan, Z., Flores-Hernandez, J.I., and Surmeier, D.J. 2001. Coordinated expression of muscarinic receptor messenger RNAs in striatal medium spiny neurons. *Neuroscience* 103: 1017–1024.
- Yang, G., and Masland, R.H. 1992. Direct visualization of the dendritic and receptive fields of directionally selective retinal ganglion cells. *Science* 258: 1949–1952.
- Yau, K.-W. 1994. Phototransduction mechanism in retinal rods and cones. *Invest. Ophthalmol. Vis. Sci.* 35: 9–32.
- Ye, Y., Machado, D.G., and Kim, D.O. 2000. Projection of the marginal shell of the anteroventral cochlear nucleus to olivocochlear neurons in the cat. *J. Comp. Neurol.* 420: 127–138.
- Yeckel, M. F., Kapur, A., and Johnston, D. 1999. Multiple forms of LTP in hippocampal CA3 neurons use a common postsynaptic mechanism. *Nat. Neurosci.* 2: 625–33.
- Yeckel, M.F., and Berger, T.W. 1990. Feedforward excitation of the hippocampus by afferents from the entorhinal cortex: redefinition of the role of the trisynaptic pathway. *Proc. Natl. Acad. Sci. U.S.A.* 87: 5832–5836.
- Yeckel, M.F., and Berger, T.W. 1995. Monosynaptic excitation of hippocampal CA1 pyramidal cells by afferents from the entorhinal cortex. *Hippocampus* 5: 108–114.
- Yellen, G. 2002. The voltage-gated potassium channels and their relatives. *Nature* 419: 35–42.
- Yeterian, E.H., and Hoesen, G. 1978. Cortico-striate projections in the rhesus monkey. The organization of certain cortico-caudate connections. *Brain Res.* 139: 43–63.
- Yin, T.C.T. 2002. Neural mechanisms of encoding binaural localization cues in the auditory brainstem. In: *Integrative Functions in the Mammalian Auditory Pathway* (Oertel, D., Popper, A.N., and Fay, R.R., eds.). New York: Springer, pp. 99–159.
- Yokoi, M., Mori, K., and Nakanishi, S. 1995. Refinement of odor molecule tuning by dendrodendritic synaptic inhibition in the olfactory bulb. *Proc. Natl. Acad. Sci. U.S.A.* 92: 3371–3375.
- Yoshimura, R., Kiyama, H., Kimura, T., Araki, T., Maeno, H., Tanizawa, O., and Tohyama, M. 1993. Localization of oxytocin receptor messenger ribonucleic acid in the rat brain. *Endocrinology* 133: 1239–1246.
- Young, A.B., and Macdonald, R.L. 1983. Glycine as a spine cord neurotransmitter. In: *Handbook of the Spinal Cord*, Vol. 1: Pharmacology (Davidoff, R.E., ed.) New York: Marcel Dekker, pp. 1–43.
- Young, A.B., Oster-Granite, M.L., Herndon, R.M., and Snyder, S.H. 1974. Glutamic acid: Selective depletion by viral induced granule cell loss in hamster cerebellum. *Brain Res.* 73: 1–13.
- Young, E.D. 1980. Identification of response properties of ascending axons from dorsal cochlear nucleus. *Brain Res.* 200: 23–38.
- Young, E.D., and Brownell, W.E. 1976. Responses to tones and noise of single cells in dorsal cochlear nucleus of unanesthetized cats. *J. Neurophysiol.* 39: 282–300.

- Young, E.D., and Davis, K.A. 2001. Circuitry and function of the dorsal cochlear nucleus. In: *Integrative Functions in the Mammalian Auditory Pathway* (Oertel, D., Popper, A.N., and Fay, R.R., eds.) New York: Springer Verlag, pp. 160–206.
- Young, E.D., and Voigt, H.F. 1981. The internal organization of the dorsal cochlear nucleus. In: *Neuronal Mechanisms of Hearing* (Syka, J., and Aitkin, L. eds.) New York: Plenum Press, pp. 127–133.
- Young, E.D. Robert, J.M., and Shofner, W.P. 1988. Regularity and latency of units in ventral cochlear nucleus: implications for unit classification and generation of response properties. *J. Neurophysiol.* 60: 1–29.
- Young, H.M., and Vaney, D.I. 1991. Rod-signal interneurons in the rabbit retina: 1. Rod bipolar cells. *J. Comp. Neurol.* 310: 139–153.
- Young, M., and Yamane, S. 1992. Sparse population coding of faces in the inferotemporal cortex. *Science* 256: 1327–1331.
- Young, M.P. 1992. Objective analysis of the topological organization of the primate cortical visual system. *Nature* 358: 152–155.
- Young, M.P., and Yamane, S. 1992. Sparse population coding of faces in the inferotemporal cortex. *Science* 256: 1327–1331.
- Young, W.S., III, Alheid, G.F., and Heimer, L. 1984. The ventral pallidal projection to the mediodorsal thalamus. A study with fluorescent retrograde tracers and immunohistofluorescence. *J. Neurosci.* 4: 1626–1638.
- Youngentob, S.L., Kent, P.F., Schwob, J.E., and Tzoumaka, E. 1995. Mucosal inherent activity patterns in the rat: Evidence from voltage-sensitive dyes. *J. Neurophysiol.* 73: 387–398.
- Youngentob, S.L., Mozell, M.M., Sheehe, P.R., and Hornung, D.E. 1987. A quantitative analysis of sniffing strategies in rats performing odor detection tasks. *Physiol. Behav.* 41: 59–69.
- Yu, J.J., and Young, E.D. 2000. Linear and nonlinear pathways of spectral information transmission in the cochlear nucleus. *Proc. Natl. Acad. Sci. U.S.A.* 97: 11780–11786.
- Yuan, B., Morrow, T.J., and Casey, K.L. 1986. Corticofugal influences of S1 cortex on ventrobasal thalamic neurons in the awake rat. *J. Neurosci.* 6: 3611–3617.
- Yuan, L.L., Adams, J.P., Swank, M., Sweatt, J.D., and Johnston, D. 2002. Protein kinase modulation of dendritic K⁺ channels in hippocampus involves a mitogen-activated protein kinase pathway. *J. Neurosci.* 22: 4860–8.
- Yung, K., Smith, A.D., Levey, A.I., and Bolam, J.P. 1996. Synaptic connections between spiny neurons of the direct and indirect pathways in the neostriatum of the rat—Evidence from dopamine receptor and neuropeptide staining. *Eur. J. Neurosci.* 8: 861–869.
- Yuste, R., and Bonhoeffer, T. 2001. Morphological changes in dendritic spines associated with long-term synaptic plasticity. *Nature* 24: 1071–1089.
- Yuste, R., and Denk, W. 1995. Dendritic spines as basic functional units of neuronal integration. *Nature* 375: 682–684.
- Yuste, R., and Majewska, A. 2001. On the function of dendritic spines. *Neuroscientist.* 7: 387–395.
- Yuste, R., and Tank, D.W. 1996. Dendritic integration in mammalian neurons, a century after Cajal. *Neuron* 16: 701–716.
- Yuste, R., Gutnick, M., Saar, D., Delaney, K., and Tank, D. 1994. Calcium accumulations in dendrites from neocortical neurons: An apical band and evidence for functional compartments. *Neuron* 13: 23–43.
- Yuste, R., Majewska, A., and Holthoff, K. 2000. From form to function: Calcium compartmentalization in dendritic spines. *Nat. Neurosci.* 3: 653–659.
- Zaborszky, L., Heimer, L., Eckenstein, F., and Leranth, C. 1986. GABAergic input to cholinergic forebrain neurons: An ultrastructural study using retrograde tracing of HRP and double immunolabeling. *J. Comp. Neurol.* 250: 282–295.
- Zador, A., and Koch, C. 1994. Linearized models of calcium dynamics: Formal equivalence to the cable equation. *J. Neurosci.* 14: 4705–4715.

- Zador, A., Koch, C., and Brown, T. 1990. Biophysical model of a hebbian synapse. *Proc. Natl. Acad. Sci. U.S.A.* 87: 6718–6722.
- Zarbin, M.A., Innis, R.B., Wamsley, J.K., Snyder, S.H., and Kuhar, M.J. 1983. Autoradiographic localization of cholecystokinin receptors in rodent brain. *J. Neurosci.* 3: 877–906.
- Zeki, S., and Shipp, S. 1988. The functional logic of cortical connections. *Nature* 335: 311–317.
- Zengel, J.E., Reid, S.A., Sypert, G.W., and Munson, J.B. 1985. Membrane electrical properties and prediction of motor-unit type of cat medial gastrocnemius motoneurons in the cat. *J. Neurophysiol.* 53: 1323–1344.
- Zhan, X.J., Cox, C.L., and Sherman, S.M. 2000. Dendritic depolarization efficiently attenuates low threshold calcium spikes in thalamic relay cells. *J. Neurosci.* 20: 3909–3914.
- Zhan, X.J., Cox, C.L., Rinzel, J., and Sherman, S.M. 1999. Current clamp and modeling studies of low threshold calcium spikes in cells of the cat's lateral geniculate nucleus. *J. Neurophysiol.* 81: 2360–2373.
- Zhang, C., and Restrepo, D. 2002. Expression of connexin 45 in the olfactory system. *Brain Res.* 929: 37–47.
- Zhang, L., Freed, M., Sterling, P., and Vardi, N. 2003. Developmental switch in the retina of chloride-cation cotransporters from NKCC to KCCC2 mediates the switch of GABA from excitatory to inhibitory.
- Zhang, N., and Ottersen, O.P. 1993. In search of the identity of the cerebellar climbing fiber transmitter: immunocytochemical studies in rats. *Can. J. Neurol. Sci.* 20 (Suppl. 3), S36–S42.
- Zhang, N., Walberg, F., Laake, J.H., Meldrum, B.S., and Ottersen, O.P. 1990. Aspartate-like and glutamate-like immunoreactivities in the inferior olive and climbing fibre system: a light microscopic and semiquantitative electron microscopic study in rat and baboon (*Papio anubis*). *Neuroscience.* 38: 61–80.
- Zhang, S., and Oertel, D. 1993a. Cartwheel and superficial stellate cells of the dorsal cochlear nucleus of mice: Intracellular recordings in slices. *J. Neurophysiol.* 69: 1384–1397.
- Zhang, S., and Oertel, D. 1993b. Giant cells of the dorsal cochlear nucleus of mice: Intracellular recordings in slices. *J. Neurophysiol.* 69: 1398–1408.
- Zhang, S., and Oertel, D. 1993c. Tuberculoventral cells of the dorsal cochlear nucleus of mice: Intracellular recordings in slices. *J. Neurophysiol.* 69: 1409–1421.
- Zhang, S., and Oertel, D. 1994. Neuronal circuits associated with the output of the dorsal cochlear nucleus through fusiform cells. *J. Neurophysiol.* 71: 914–930.
- Zhang, S., and Trussell, L.O. 1994. Voltage clamp analysis of excitatory synaptic transmission in the avian nucleus magnocellularis. *J. Physiol. (Lond.)* 480: 123–136.
- Zhang, X., and Firestein S. 2002. The olfactory receptor gene superfamily of the mouse. *Nat. Neurosci.* 5: 124–133.
- Zhang, Z.W., and Deschênes, M. 1997. Intracortical axonal projections of lamina VI cells of the primary somatosensory cortex in the rat: A single-cell labeling study. *J. Neurosci.* 17: 6365–6379.
- Zhao, H.Q., Firestein, S., and Greer, C.A. 1994. NADPH-diaphorase localization in the olfactory system. *NeuroReport* 6: 149–152.
- Zhao, H., Ivic, L., Otaki, J.M., Hashimoto, M., Mikoshiba, K., and Firestein, S. 1998. Functional expression of a mammalian odorant receptor. *Science* 279: 237–242.
- Zheng, T., and Wilson, C.J. 2002. Corticostriatal combinatorics: The implications of corticostriatal axonal arborizations. *J. Neurophysiol.* 87: 1007–1017.
- Zheng, C., Feinstein, P., Bozza, T., Rodriguez, I., and Mombaerts, P. 2000. Peripheral olfactory projections are differentially affected in mice deficient in a cyclic nucleotide-gated channel subunit. *Neuron* 26: 81–91.
- Zheng, L.M., and Jourdan, F. 1988. Atypical olfactory glomeruli contain original olfactory axon terminals: An ultrastructural horseradish peroxidase study in the rat. *Neuroscience* 26: 367–378.

- Zhou, F.M., Liang, Y., and Dani, J.A. 2001. Endogenous nicotinic cholinergic activity regulates dopamine release in the striatum. *Nat. Neurosci.* 4: 1224–1249.
- Zhou, L., Yoshioka, T., and Nathans, J. 1996. Retina-derived POU-domain factor-1: A complex POU-domain gene implicated in the development of retinal ganglion and amacrine cells. *J. Neurosci.* 16: 2261–2274.
- Zhou, Q., Godwin, D.W., Bickford, M.E., Sherman, S.M., and Adams, P.R. 1994. Relay cells and local GABAergic cells contribute to responses mediated by metabotropic glutamate receptors in cat LGN. *Soc. Neurosci. Abstr.* 20: 133.
- Zhou, Q., Godwin, D.W., O'Malley, D.M., and Adams, P.R. 1997. Visualization of calcium influx through channels that shape size burst and tonic firing modes of thalamic relay cells. *J. Neurophysiol.* 77: 2816–2825.
- Zhou, Z.J. 2001a. A critical role of the strychnine-sensitive glycinergic system in spontaneous retinal waves of the developing rabbit. *J. Neurosci.* 21: 5158–5168.
- Zhou, Z.J. 2001b. The function of the cholinergic system in the developing mammalian retina. *Prog. Brain Res.* 131: 599–613.
- Zhou, Z.J., and Fain, G.L. 1995. Neurotransmitter receptors of starburst amacrine cells in rabbit retinal slices. *J. Neurosci.* 15: 5334–5345.
- Zhu, J.J., Uhrlich, D.J., and Lytton, W.W. 1999. Burst firing in identified rat geniculate interneurons. *Neurosci.* 91: 1445–1460.
- Zhuo, M., Zhang, W., Son, H., Mansuy, I., Sobel, R.A., Seidman, J., and Kandel, E.R. 1999. A selective role of calcineurin α in synaptic depotentiation in hippocampus. *Proc. Natl. Acad. Sci. U.S.A.* 96: 4650–5.
- Zibrowski, E.M., and Vanderwolf, C.H. 1997. Oscillatory fast wave activity in the rat pyriform cortex: relations to olfaction and behavior. *Brain Res.* 766: 39–49.
- Zibrowski, E.M., Hoh, T.E., and Vanderwolf, C.H. 1998. Fast wave activity in the rat rhinencephalon: elicitation by the odors of phytochemicals, organic solvents, and a rodent predator. *Brain Res.* 80: 207–215.
- Zinyuk, L.E., Datiche, F., and Cattarelli, M. 2001. Cell activity in the anterior pyriform cortex during an olfactory learning in the rat. *Behav. Brain Res.* 124: 29–32.
- Zipp, F., Nitsch, R., Soriano, E., and Frotscher, M. 1989. Entorhinal fibers form synaptic contacts on parvalbumin-immunoreactive neurons in the rat fascia dentata. *Brain Res.* 495: 161–166.
- Zipser, D., and Andersen, R. 1988. A back-propagation programmed network that simulates response properties of a subset of posterior parietal neurons. *Nature* 331: 679–684.
- Ziskind-Conhaim, L. 1990. NMDA receptors mediate poly- and monosynaptic potentials in motoneurons of rat embryos. *J. Neurosci.* 10: 125–135.
- Zola-Morgan, S., Squire, L.R., and Amaral, D.G. 1986. Human amnesia and the medial temporal region: Enduring memory impairment following a bilateral lesion limited to field CA1 of the hippocampus. *J. Neurosci.* 6: 2950–2967.
- Zou, D.J., Greer, C.A., and Firestein, S. 2002. Expression pattern of alpha CaMKII in the mouse main olfactory bulb. *J. Comp. Neurol.* 443: 226–236.
- Zou, Z., Horowitz, L.F., Montmayeur, J.P., Snapper, S., and Buck, L.B. 2001. Genetic tracing reveals a stereotyped sensory map in the olfactory cortex. *Nature* 414: 173–179.
- Zucker, C.L., and Dowling, J.E. 1987. Centrifugal fibres synapse on dopaminergic interplexiform cells in the teleost retina. *Nature* 330: 166–168.
- Zucker, R., and Regehr, W. 2002. Short-term synaptic plasticity. *Annu. Rev. Physiol.* 64: 355–405.

INDEX

- Accessory olfactory bulb (AOB), 184–185, 215, 216
Accommodation, 110
Acetylcholine (ACh), 21, 62, 64, 69, 202, 299, 343, 402. *See also* Cholinergic neurons
 in hippocampus, 480–481
 in neocortex, 515, 528, 541–542
 in olfactory cortex, 442–443
Action potential initiation, 45–47
 sites within neuron for, 24, 203–204, 299–301, 489–493, 544
Action potential threshold, 46
Action potentials (APs), 45–47, 487, 489, 532
 back-propagating, 25, 491–495
 carried by auditory-nerve fibers, 128
 spine, 23, 546–547
Activation and inactivation gates, 336–338
Active zone, 3
Actor units, 412
Adenosine monophosphate. *See* AMP
Afferent depolarization, primary, 97, 98
Afferent drivers, 357–359
Afferent fibers, 166, 167, 364, 365, 372–373, 425, 432
Afferent input, 419, 433–435
Afferent system
 horizontal organization, 425
 synaptic hierarchy in primary, 90, 91
Afferents, 168. *See also* Group Ia afferents
 brainstem, 323–324
 cortical, 321–323, 366–367
 corticothalamic driver, 355–356
 driving, 321
 flexor reflex, 81
 monoaminergic, 298–299
 in neocortex, 512–516
 nigrostriatal, 367
 primary, 81
 thalamic, 314–315, 366–367, 512–514
Afterdepolarization (ADP), 527, 542
Afterhyperpolarization (AHP), 338, 476, 527–532
Afterhyperpolarizing current (I_{AHP}), 23, 49, 51, 56, 58, 71, 75–76, 111, 338
Agranular cortex, 499
AII cells, 223–225, 249, 267–269
Allelic exclusion, 168
Alpha-motoneurons, 82–83, 88, 112
Alzheimer's disease, 497
Amacrine cells, 20–21, 33, 35, 217, 228–229, 231, 237, 252–253
 starburst, 21, 249
AMP (adenosine monophosphate), 57
AMPA receptors, 139–141, 190–193, 197, 199–200, 296
 GluR, 94, 139, 208
 kainate and, 65, 66, 479, 535
 NMDA and, 190, 208, 341, 441, 479, 480, 535
Amplification, 10
Anterior division of the VCN (AVCN), 127–129, 137
Anterior olfactory cortex (AOC), 416
Anterior olfactory nucleus (AON), 169
Anterior piriform cortex (APC), 418, 419, 425, 426, 433, 439–440, 449
Anterior thalamic nuclei, 312
Ascending branch (a.b.), 127
Aspiny neurons, 170
Associational connections, 420, 469
ATP (adenosine triphosphate), 48
Auditory-nerve fibers (ANFs), 125–126, 128, 132, 134, 140, 144, 149
 action potentials carried by, 128
 ANF type, 125–126, 136
 in AVCN, 137
 best frequency threshold, 162
 bushy cells and, 130, 143, 148
 cell types, convergence, and, 143
 chopper neurons and, 153, 157, 158, 160
 collaterals of, 129
 defined, 126
 glutamate and glutamine in terminals of, 139
 innervation of cochlear nucleus cell by, 129
 low spontaneous rate, 159
 multipolar cells and, 130, 137, 151
 octopus cells and, 130, 137, 139, 149
 phase-locking in, 156, 157
 primarylike neurons and, 155
 primarylike responses and, 146, 148
 spontaneous firing rates, 158
Augmentation, 484
Autoinhibition, 72
Axo-axonic cells, 460, 465. *See also* Chandelier cells
Axon, initial segment of, 90

Back propagation
 of action potentials, 25, 491–495
 in network, 552
Baclofen, 538

- Barbiturates, 538
- Barlow, H. B., 548–549
- Basal forebrain, 324
- Basal ganglia, 361–363
 anatomy, 361–363
 basic circuit, 377–379
 direct and indirect pathways, 363, 368,
 381–382
 mosaic organization of neostriatum,
 379–381
- dendritic membrane properties, 382–387
 cholinergic interneurons, 387–390
 GABA/parvalbumin fast spiking
 interneurons, 390
 GABA/SOM/NO interneurons, 391
- functional operations
 complex integrative tasks, 406–413
 natural firing patterns, 403–406
- neuronal elements, 364, 365
 cell populations, 372–374
 efferent axons, 371
 inputs, 366–367
 interneurons, 368, 370–371
 principal neuron, 368, 369
- synaptic actions
 of cortical and thalamic inputs, 391–394
 input fibers, 391
 intrinsic connections, 400–403
 of substantia nigra inputs, 397–400
 synaptic plasticity, 394–397
- synaptic connections, 374
 axon collateral, 376
 cortical and thalamic, 375
 interneuron, 376
 output, 376–377
 substantia nigra, 375
- Basket cells, 277–280, 298, 428, 460, 508, 509,
 520–521
- Benzodiazepines, 538
- Best frequency (BF), 125, 127, 145, 157–159,
 162
- Beta oscillation, 437
- Beta-motoneurons, 83
- Bicuculline, 189–190, 298, 538, 539
- Binary signal, 221
- Bipolar neurons, 217, 222, 429
 ON vs. OFF, 223–225, 240–241, 247, 251,
 254, 257, 262, 263
- Bistable membrane responses, 111
- Bistratified cells, 460, 462
- Bitufted cells, 429
- Blobs, 523
- Boutons, synaptic, 86–88, 90, 96
 single, 113
- Brain nitric oxide synthase (BNOS), 327
- Brain-derived neurotrophic factor (BDNF), 535
- Brainstem afferents, 323–324
- Brainstem inputs, 343–344, 350
- Branch point failure, 95
- Bruce effect, 215
- Brush cells, unipolar, 134
- Buildup responses to sound, 151
- Burst and tonic relay response modes
 anatomical relationship of modulator inputs to
 T channels, 348
 control of response mode, 347–348
 detectability, 347
 linearity, 345–347
 signal transmission during burst and tonic
 firing, 344–345
- Burst mode of firing, 338, 339
- Bursting, as “wake-up call,” 347
- Bushy cells, 128, 130, 138, 147, 154
 auditory-nerve fibers and, 130, 143
 EPSP in, 149
 globular, 129, 131, 136, 137, 143, 144, 148,
 155
 phase-locking in, 155–157
 primarylike responses from, 146–149
 spherical, 129–131, 136, 137, 140, 143, 144,
 146
- CA3 neurons, 464, 467, 482, 483. *See also under*
 Hippocampus, synaptic connections
- Cable equation, 543
- Cable model of dendrites, 90–93, 202–208,
 384–386, 488–489, 542–543
- Calbindin, 326
- Calcium binding proteins, 326
- Calcium (Ca²⁺), 483, 491
 intracellular concentration of, 302
- Calcium (Ca²⁺) conductances, 336–339,
 528–530
 in hippocampus, 489–495
 low threshold, 336
 in mitral cells, 189, 205
 in neocortex, 528–530
 in olfactory cortex, 444–445
 in photoreceptors, 248
 in Purkinje cells, 288
 in thalamic cells, 336
- Calcium (Ca²⁺) currents, 49, 53. *See also*
 Calcium (Ca²⁺) conductances
 decrease in, 72
 high-threshold, 53–54
 low-threshold, 54–55
- Calcium (Ca²⁺)-activated K⁺ currents, 56
- Canonical circuits, regional, 34–38, 556–558
- Canonical cortex circuit, 37–38, 556–558

- Canonical neuron, concept of, 25–27
- Cardinal neurons, 549
- Cartwheel (Ca) cells, 131–133, 138, 145, 151–152
- Cation conductance, hyperpolarization-activated, 340
- Central pattern generator (CPG), 118–122
- Centrifugal fibers, 201–202, 231
- Centrifugal inputs, 169–170
- Cerebellar cortex
 - basic circuit organization, 284, 285
 - cerebellar cortex-deep nuclei circuit, 286–287
 - climbing fiber circuit, 286
 - mossy fiber circuit, 284–285
 - dendritic properties
 - functional circuits, 304–309
 - microelectrode recordings, 299–301
 - optical recording, 302–304
 - granular layer. *See* Granule cell layer
 - intrinsic membrane properties, 287
 - cerebellar nuclear cells, 288–290
 - Purkinje cells, 287–288
 - molecular layer, 281–283, 294
 - neuronal elements, 273–274
 - cerebellar nuclei, 271, 278–279
 - geometric organization of, 273
 - input elements, 274–275
 - intrinsic elements, 277–278
 - output elements, 276–277
 - neurotransmitters, 297–299
 - synaptic actions, 290–292, 294–295
 - inhibitory synapses, 292–295
 - modulation of excitatory synapses, 295–296
 - synaptic connections, 279–284
 - cerebellar nuclei, 283–284
- Cerebellar nuclear neurons
 - intrinsic properties, 289–290
 - Purkinje cell action on, 294–295
 - response to white matter stimulation, 307
- Cerebellar nuclei, 271
- Cerebellum, 28, 271–272
- Chandelier cells, 70, 429, 465, 511, 521. *See also* Axo-axonic cells
- Chattering cells, 530
- Chestnut cells, 134
- Choline acetyltransferase (ChAT), 299
- Cholinergic fibers, 202
- Cholinergic interneurons, 370, 376, 387–390, 401, 402, 404, 411
- Cholinergic neurons. *See also* Acetylcholine
 - pacemaking by, 387–389
- Cholinergic responses, nicotinic, 64–65
- Chopper neurons, 153, 154, 156
 - stimulus spectrum representation in, 157–160
- Chopping, 146
- Clastrum, 516
- Climbing fiber circuit, 286
- Climbing fibers (CF), 274, 275, 290–291, 304
- Climbing fibers-Purkinje cell connection, 281
- Cl⁻-mediated IPSP, 430, 437
- Cochlear nucleus, 125–126
 - basic circuit, 143–145
 - circuit functions, 155–163
 - membrane properties and integration of inputs, 146–152
 - models of somatic and dendritic properties, 153–155
 - neuronal elements and synaptic connections, 126–130
 - numbers of cell types and convergence, 143
 - synaptic connections, 134–136
- Commissural connections, 420
- Complex spikes, 290
- Cone bipolar circuit, 264
- Connectionist models of cortical function, 549
- Connectivity, patterns of, 8
- Connexins, 519
- Contextual modulation, 183
- Contrast gain control, 351
- Cortical canonical circuit, 37–38, 536–558
- Corticogeniculate inputs, 342
- Corticothalamic driver afferents, 355–356
- Cruciform axodendritic, 366
- Current source-density (CSD) analysis, 431, 436, 445, 447
- Cyclic nucleotide-gated (CNG) channel, 201
- Cytoarchitectonics, defined, 499
- Deep pyramidal cells (DP), 417, 421
- Delay non-match to sample (DNMS), 496
- Delayed rectifier, 338
- Dendrites, 2. *See also specific topics*
 - “filtering” by, 489
 - primary, 170, 203
 - secondary, 170, 203, 205
 - and synaptic action in spinal cord, 90–94
- Dendritic branch units, 15, 19, 21
- Dendritic branches, secondary, 202
- Dendritic cells, granule cell, 178
- Dendritic computation, 15–17
- Dendritic integration and dendritic subunits, 15–19
- Dendritic location, and somatic EPSPs, 90, 92
- Dendritic processes, visualization of
 - by current source-density (CSD) analysis, 431–432
- Dendritic shaft, primary, 202
- Dendritic spine units, 17–19

- Dendritic spines, 206–207, 421. *See also under*
 Neocortex
 fine structure, 17, 18
 functions that have been ascribed to, 20
 inhibition, 547
 nonsaturating, 547
 saturating, 546
- Dendritic subunits, 7
- Dendritic tips, bipolar, 240
- Dendritic trees, 7, 15
- Dendrodendritic reciprocal excitatory-inhibitory synapses, 215
- Dendrodendritic synaptic actions in olfactory bulb, 186–187
 field potentials, 188–189
 oscillatory activity, 187–188
 presynaptic mechanisms, 192
 recurrent excitation, 190, 192
 tests of dendrodendritic interactions, 189–191
- Dentate granule cells (DGC), 28, 464–466
- Dentate gyrus (DG), 458, 463
 interneurons in, 460, 461
 synaptic connections
 extrinsic inputs, 466–467
 outputs, 467–468
- Dentate-CA3, 28
- Depolarization, 45–46, 50, 69, 111, 112, 151.
See also Ionic currents, types of
 gradient of, 203
 primary afferent, 97–98
- Depotentiation, 487
- Derecruitment, 109–110
- Descending branch (d.b.), 127
- Direction(al) selectivity, 31–33
- Distributed synapse, 290
- D-multipolar cells, 129–131, 136, 143–145, 151, 159, 162
- Dopamine, 515
- Dopaminergic neurons, 253, 397–400, 411–413
 reward-prediction-related responses of, 408–412
- Dopaminergic synapses, 375, 399
- Dorsal acoustic striae (DAS), 128, 133, 144
- Dorsal cochlear nucleus (DCN), 127–129, 144, 145, 152
 cell types, 131–134
 feature detection, 160–163
 response maps of type II and IV neurons in, 160–162
 synapses, 140–143
- Dorsal cortex, 28
- Dorsal raphe nucleus, 324, 363
- Dorsal spinocerebellar tract neurons (DSCT), 107, 108
- Dorsal thalamus. *See* Thalamus
- Dorsal turtle cortex, 36, 37
- Double bouquet neurons, 510, 521–522
- Dreaming, 55
- Duty-cycle units, 116
- Dyad, 242
- Electrical coupling, 8
- Electrotonic interactions, 113–114
- Embryonic development of neocortex, 501–503
- Endbulbs (EB), 136, 137
- Endopiriform nucleus, 417
- Entorhinal cortex, 466
- Entorhinal-hippocampal system, compared with olfactory system, 454
- Ephaptic interactions, 60–61, 87
- Epileptiform activity, 483, 494
- EPSP-IPSP sequence. *See* Excitatory-inhibition (EPSP-IPSP) sequence
- Eulaminate cortex, 501
- Exchange of small molecules, 8
- Excitatory amino acid (EAA) responses, 65–67, 94
- Excitatory postsynaptic potentials (EPSPs), 3–4, 11, 12, 22, 25, 75–76
 in basal ganglia, 391–394, 396, 397
 in bushy cells, 149
 in cerebellum, 290–295, 297, 307
 in cochlear nucleus, 137, 139, 149, 153
 composite, 90, 91
 in glomerular synaptic actions, 192–193, 208
 group Ia, 96–97, 113
 in hippocampus, 475–477, 480, 482, 484, 489, 493–495
 in mitral cells, 192–193
 in neocortex, 536, 543
 in octopus cells, 149
 in olfactory cortex, 430, 433, 435–437, 445–447
 integration of, 447
 passive return current and electrotonic spread of, 445–447
 polysynaptic, 114
 single-bouton, 90, 91, 113
 single-fiber, 90, 91
 somatic, 97
 effect of dendritic location on, 90, 92
 local vs., 94
 in spinal cord, 90–92, 94–98, 106, 107, 113, 114, 119–120, 206
 in thalamus, 341, 344, 353
- Excitatory synaptic currents (EPSCs), 142
- Excitatory-inhibition (EPSP-IPSP) sequence, 213, 307, 308, 475–477
- Excitatory-inhibitory interactions, types of, 11

- Extensor digitorum longus (EDL), 118, 120–122
- External plexiform layer (EPL), 170, 173, 177–179, 205–206
 development and plasticity, 179
- Exteroceptors, 81
- Eye movements, “pursuit”
 foveal architecture implies, 237–238
- Fan-in, 11
- Fan-out, 9
- Fast spiking cells, 530–531
- Fast spiking interneurons, 390
- Fastigial nucleus, 278
- Feedback (FB) excitation, 29–30
- Feedback (FB) inhibition, 14, 427
- Feedback neural networks, 553, 555
- Feedback pathways, 516
- Feedforward (FF) excitation, 28–29
- Feedforward (FF) inhibition, 12–14, 427
- Feedforward networks, 451, 453, 552, 553, 555
- Feedforward pathways, 516, 522
- Fiber systems, association
 horizontal organization, 425–426
- Fiber volley, 475
- Flexion reflex, 100
- Flexor, 106
- Flexor digitorum longus (FDL), 117, 118, 120–122
- Flexor hallucis longus (FHL), 117, 120
- Flexor reflex afferents (FRAs), 81
- Foveola, 233, 237–238
- Fusiform cells. *See* Pyramidal (Py) cells
- GABA (gamma-aminobutyric acid), 21
 in amacrine cells, 252–253
 in basal ganglia, 371, 400
 in cerebellum, 297–298
 in cochlear nucleus, 134, 143
 in granule cells, 200
 in hippocampus, 472, 481
 inhibitory actions, 245
 K^+ conductance and, 69
 molecular mechanisms of ionotropic amino acids and, 61
 in neocortex, 515, 537–541
 in olfactory bulb, 200, 208, 215
 in olfactory cortex, 442
 in outer plexiform layer of retina, 241
 primary afferent depolarization and, 97–98
 in retina, 241, 245, 251–253
 in spinal cord, 97–98, 103
 in thalamus, 331, 343
- GABA_A and GABA_B receptors, 97–98, 197, 199–200, 341, 342, 430–431, 481, 538–539
- GABAergic activity, 304–306
 inhibitory responses, 74
- GABAergic cells, 199, 278–279, 330, 401, 428, 429, 465, 472, 503, 524, 556–557
- GABAergic inhibition, axo-axonic, 429, 521
- GABAergic input, 324, 330, 331
- GABA-mediated IPSPs, 67, 68, 440
- GABA/parvalbumin-containing interneurons, 370–371, 396, 400, 401, 411
- GABA/SOM/NO interneurons, 391, 401, 402, 411
- Gamma oscillation, 435–437
- Gamma-motoneurons, 82–83
 static vs. dynamic, 83
- Ganglion cell receptive field, 254–257
- Ganglion cells, retinal, 217, 225–227, 236, 243–245, 252
 alpha and beta, 226
 forms and function, 225–226
- Gap junctions, 59, 241–242, 286, 518–519
- Gating
 by different mechanisms, 8
 in thalamus, 344
- Gating actions of neurotransmitters, 72, 73
- Gemmules, 173
- Genes, level of, 7
- Giant (Gi) cells, 128, 129, 132, 133, 144
- gK. *See* Potassium (K^+) conductance
- Glia, 180–181, 238. *See also* Müller cells
- Glial cells, 231
- Global integration, 27
- Global modulation, 27
- Globular bushy cells (GBCs), 129, 131, 136, 137, 143, 144, 148, 155
- Globus pallidus (GP), 363, 371, 372, 376
 external segment (GPe), 363, 372, 376–377, 381
 internal segment (GPi), 363, 372, 377
- Glomerular complex, modified, 184
- Glomerular dendritic tuft, 202
- Glomerular layer (GL) cells, 172, 194–196
 dopaminergic cells, 196, 198
 excitatory properties, 194, 195
 GABAergic, 199
 synaptic relations between, 198
- Glomerular layer (GL) of olfactory bulb
 development and plasticity, 176–177
 interglomerular connections, 176
 interglomerular microcircuits, 182
 intraglomerular connections, 175–176
 intraglomerular microcircuits, 182
- Glomerular modules form odor image, 210–211

- Glomerular synapses, 142
- Glomerular synaptic actions, EPSPs in, 192–193, 208
- Glomerular tuft, 202–203
synchronization by, 208–209
- Glomeruli, 168, 169, 214, 279
defined, 183
necklace, 184
olfactory, 168–169, 183
synaptic triadic arrangements, 319
- Glutamate (GLU), 61, 66, 190, 192–193, 208–209, 215
in cerebellum, 297
in cochlear nucleus, 139–141
in hippocampus, 478, 479
mGluR6 receptor, 251
in neocortex, 541
in olfactory bulb, 190–194, 196–199
in olfactory cortex, 441–442
in thalamus, 341–342
in ventral horn, 94–95
- Glutamate receptors (GluRs), 94, 95, 139–141, 208, 251, 535–536
metabotropic, 251, 342
- Glutamic acid decarboxylase (GAD), 252, 298, 402
- Glycine, as neurotransmitter, 67, 69
in cochlear nucleus, 143
in olfactory bulb, 200
in ventral horn, 100
- Goldman-Hodgkin-Katz (GHK), 44
- Golgi cell dendrite (Gcd), 281, 283
- Golgi cells (GCs), 134, 277, 281–284
- G-proteins, 481
- Graded actions, 11
- Graded signal, 221
- Grandmother cell scheme, 549
- Granule (Gr) cells (GCs), 28
in cerebellum, 277
in cochlear nucleus, 131–134, 142, 144, 145, 163
deep (G_{II}), 173
dendrodendritic microcircuit between mitral and, 189
in hippocampus, 467
intermediate (G_I), 173
in olfactory bulb, 177, 186–188, 200, 205–207
superficial (G_{III}), 173
synchronization by, 208
- Granule cell dendritic spines (Grs), 178
- Granule cell layer
in cerebellar cortex, 274, 279, 280, 293–294
in olfactory bulb, 170, 173–174
- Group Ia afferents, 88, 90–94
anatomy, 88–90
disynaptic Ia reciprocal system, 99–100
modulation of transmitter release at Ia synapses, 96
neurotransmitter receptors, 94–95
physiology, 90
quantization of synaptic action, 95
- Group Ia excitatory transmission. *See also* Excitatory postsynaptic potentials
mechanisms of, 94
- Group Ia inhibition, synaptic organization of, 106, 107
- Group Ia reciprocal inhibition, disynaptic, 105–106
- Hebb's postulate for learning, 493–494
- High-threshold currents, 50
- High-voltage activated currents (HVA), 53–54
- Hilar pathways, 482
- Hippocampal cortex, 28
- Hippocampal formation, 415, 455, 456
basic circuits, 462–463
cytoarchitectonic divisions, 457–458
- Hippocampus, 60, 455–457
dendritic properties, 488
active, 489–493
dendritic integration of synaptic and action potentials, 493–495
passive, 489
diseases, 497–498
learning and memory, 494, 496–497
neuronal elements
interneurons, 460–462
principal neurons, 458–460
three-dimensional position and layers of rat, 457–458
neurotransmitter receptors
excitatory neurotransmitters, 478–481
inhibitory neurotransmitters, 481–482
specific pathways, 482–484
physiological and pharmacological properties
basic response, 474
extracellular responses, 475–476
inhibitory synapses, 478
intracellular responses, 476–477
physiology and biophysics of synaptic actions, 477–478
synaptic connections
of CA1, 473–474
of CA2, 472–473
of CA3, 469–472
of dentate gyrus, 464–468
of subiculum, 474
synaptic plasticity, 484
depression, 485, 487–488

- facilitation, 484
 - long-term plasticities, 485
 - long-term potentiation, 485–487
 - post-tetanic potentiation, 484–485
 - short-term plasticities, 484
- Homocysteate, 297
- Homotypical cortex, 501
- Hopfield network, 451, 553–554
- Horizontal cell spines, 240
- Horizontal cells, 217, 227–228, 241, 429
- Horizontal limb of the diagonal band (HDB), 169
- Horizontal plane, sound localization in, 155–157
- Hubel-Wiesel models of visual cortex circuits, 522
- Hyperpolarization, 43, 70, 151. *See also* Ionic currents, types of
 - currents activated by, 57
- Hyperpolarization-activated conductance, 340
- Hyperpolarizing inhibition, 11

- I_A (neurotransmitter), decrease in, 72
- I_{AHP} (neurotransmitter), decrease in, 70–71
- I_H (hyperpolarization-activated), 149, 388
- I_M (neurotransmitter), decrease in, 71–72
- Inactivation (kinetics), 45–46, 50
 - removal of, 50
- Induction phase, 485
- Inferior colliculus (IC), 128, 129, 133
- Information processing, specific, 17–19
- Inhibitory operations, 12–14, 30–34. *See also specific operations*
- Inhibitory postsynaptic potentials (IPSPs), 69. *See also* Excitatory-inhibition (EPSP-IPSP) sequence
 - in basal ganglia, 400–401
 - in cerebellum, 290, 292, 307, 308
 - defined, 4
 - disynaptic, 99
 - in neocortex, 537
 - in olfactory bulb, 213
 - in olfactory cortex, 430
 - reciprocal Ia, 99
 - recurrent, 102–103
 - slow vs. fast, 69, 342
 - in spinal cord, 99
 - in thalamus, 342
- Initial segment-soma dendritic (IS-SD) break, 287
- Inner hair cells (IHCs), 125–126, 128
- Input convergence, 103
- Input fibers, 2
- Input processing, 35
- Intermediate acoustic striae (IAS), 128, 144
- Internal plexiform layer (IPL), 170–171

- Interneurons, 422. *See also* Local/intrinsic neurons
 - in basal ganglia, 368, 370–371, 376, 387–391, 401–403
 - excitatory, 460
 - in olfactory bulb, 166, 167
 - recurrent inhibition through Renshaw, 102–104
 - segmental/local, 84
 - spontaneous firing patterns of hippocampal, 478
- Interplexiform cells, 229
- Intralaminar nuclei, 314
- Intrinsic associational connections, 426
- Intrinsic operations, 35
- Invagination, 240
- Ionic channels, 47
- Ionic currents, types of, 48–58
- Ionic pumps, 47–48
- Ionotropic amino acid synapses, molecular mechanisms of, 61–62
- Ionotropic receptors, 62, 340–342, 481
- Ions
 - distribution across neuronal membranes, 39, 40
 - equilibrium potentials, 39–42
 - permeability, 43, 45
- IPIC, 111, 114
- Ipsilateral associational-commissural projection, 465
- Irregularity, 146
- Islets, 173
- Isofrequency sheets, 132–133

- Juxtaglomerular (JG) cells, 172

- Kainate receptors, 65, 66, 479, 535
- Kinesin, 240
- Koniocortex, 499

- Large multipolar (M_L) cells, 417. *See also* Multipolar (M) cells
- Last-order interneurons, 120
- Lateral geniculate nucleus (LGN), 312, 326, 327, 351
 - interneurons, 325, 333, 335
 - main connections, 320
 - relay cells, 325, 333. *See also* Thalamic relay neurons
 - burst and tonic firing for, 338, 339, 346
 - synaptic inputs onto X and Y cells, 328
- Lateral habenular nucleus, 363
- Lateral inhibition, 13, 14, 429
 - mediates odor contrast enhancement, 214–215

- Lateral nucleus of trapezoid body (LnTB), 128, 129
- Lateral olfactory tract (LOT), 170, 171, 416, 418, 419, 433, 436, 439, 447
- Lateral superior olivary (LSO), 128, 129, 155
- Laterodorsal nucleus, 312
- Light intensity range, 220–221
- Limulus eye, 33
- Lobe output cells, 213
- Local activity-dependent changes, 26
- Local circuit interactions, 31–33
- Local decision point, 26
- Local/intrinsic circuits, 7, 27
excitatory operations, 27–30
inhibitory operations, 30–34
- Local/intrinsic neurons, 3. *See also* Interneurons
- Locomotion
fictive, 105, 116–118
spatial facilitation of cutaneous reflexes during, 118–122
motor neuron activity patterns in, 116–118
- Locomotor drive potentials (LDPs), 119–121
- Locomotor inhibition, 118
- Locus coeruleus (LC), 169, 323
- Longitudinal axodendritic pattern, 371
- Long-lasting (L) current, 50
- Long-term depression (LTD)
in basal ganglia, 394–396, 411
in cerebellum, 295, 296
in cochlear nucleus, 141, 142
in hippocampus, 485–488
in neocortex, 533–535
in olfactory cortex, 440
synaptic plasticity and, 394–396, 411
- Long-term potentiation (LTP), 67, 410–411
associative, 439–440
associative learning and, 19
in basal ganglia, 394–396, 411
in cochlear nucleus, 141, 142
in hippocampus, 485–487, 494
in neocortex, 533–535, 546
NMDA-dependent homosynaptic, 437–439
regulation of, 440–441
synaptic plasticity and, 394–396, 486
- Lorentz de N6, 522
- Low-threshold currents, 50, 148
- Low-threshold spikes (LTSs), 290, 336, 396, 530
- Magnesium ions (Mg^{2+}), 65, 66
- Magnification factor of projection, 512
- Martinotti cell, 510–511
- Matrix, 379, 380
- Medial gastrocnemius (MG) motor units, 84
- Medial geniculate nucleus, 312
- Medial lemniscus, 321
- Medial nucleus of trapezoid body (MnTB), 128, 129
- Medial plantar (MPL) nerve, 118–122
- Medial superior olivary (MSO), 128, 129, 155–157
- Mediodorsal nucleus, 312
- Membrane conductance, increasing, 41, 43
- Membrane depolarization. *See* Depolarization
- Membrane potential, resting, 43–45, 50
- Membrane properties. *See also* Resistance
intrinsic, 31, 58
- Membranes and ionic currents, 39–43
- Memory storage in accessory olfactory bulb, 216
- Metabotropic glutamate receptors, 342
- Metabotropic receptors, 62, 251, 340–342, 344, 481
- Microcircuits, synaptic, 7–14
cortical, 557
simplest types of, 9
- Middle temporal visual area (MT), 501
- Midget bipolar terminal (MB), 243
- Midget ganglion cell (MG), 243
- Midget (M) cells, 226, 234, 254
- Mitral cell dendritic tree, 202–205
- Mitral cell membrane properties, synchronization by, 209
- Mitral cells, 21, 24, 25, 189
in olfactory bulb, 170–171, 184, 185–187, 192–194, 199, 213, 214
synaptic activation by olfactory nerve volleys, 192, 193
- Modified glomerular complex (MGC), 184
- Modulation, 70
- Modulatory gating, 27
- Molecular layer, 274
- Molecular receptive range (MRR), concept of, 211–212, 215
- Monoaminergic afferents, 298–299
- Monoaminergic inhibition, 294
- Monoamines, 514
in olfactory cortex, 443
- Mossy fiber activation of Purkinje cells, 292, 293
- Mossy fiber axonal plexus, 464
- Mossy fiber circuit, 284–285
- Mossy fiber rosettes, 274
- Mossy fiber-parallel fiber pathway, 274–275, 304, 309
- Mossy fibers (MF)
in cerebellum, 275, 299
in hippocampus, 458–459, 467–468, 482–483
- Motoneurons (MNs), 81–84
- Motor coordination, 272
- Movement control, 359
- Müller cells, 231
spatial density, 238

- Multipolar (M) cells, 129–131, 154, 417, 428, 429. *See also* T-multipolar cells
 auditory-nerve fibers and, 130, 151
- Muscarine-sensitive K^+ currents, 57
- Muscarinic receptors, 480–481
- Muscle unit, 83
- Myeloarchitectonics, 499
- Myotatic unit, 89
- NADPH-diaphorase, 371
- Neocortex, 28, 36, 37, 499–501
 amino acid neurotransmitters, 540–542
 basic circuit, 522–523
 cortical output, 523–525
 corticocortical connections, 516
 dendrites, 542–544
 active properties, 544–545
 dendritic spines, 545
 biochemical compartments, 547–548
 electrical models, 545–547
 embryonic development, 501–503
 functional operations
 neural networks compared with cortical circuits, 552–554
 new designs for visual circuits, 550–551
 parallel processing in neural networks, 551–552
 single neurons vs. neural networks, 549–550
 static and dynamic connectivity, 555–558
 neuronal elements, 503–512
 afferents, 512–516
 considerations of cortical wiring, 516–517
 smooth neurons, 507–512, 520–522
 spiny neurons, 503–507, 519–520
 synaptic actions, 525
 electrical properties of IPSP, 539–540
 excitatory synapses, 535–536
 inhibitory synapses, 537–539
 neuronal excitability, 525–532
 synaptic dynamics, 532–535
 synaptic connections, 518–522
 types, 517–519
- Neostriatum, 362. *See also* Basal ganglia
 afferent fibers and neuron types, 364, 365, 372–373
 mosaic organization, 379–381
- Nernst equation, 41–42
- Nerve impulse. *See* Action potential
- Nervous system, organization of, 2–3
- Neural images, multiple, 217
- Neural network models, 451–453, 549, 555–556.
See also under Neocortex, functional operations
- Neuromodulation vs. neurotransmission, 62–63
- Neuromuscular junction (NMJ), 10, 83
- Neuron, 7
 concept of canonical, 25–27
 as integrative unit, 22–27
- Neuron doctrine, 548
- Neuronal communication, types of, 58–63
- Neuronal computation, biophysics of, 22
- Neuronal elements, triad of, 2–3
- Neuronal operations and underlying biophysical mechanisms, 22, 23
- Neurone doctrine, 237
- Neuronism, 237
- Neuropeptides, 200–201, 443, 542
- Neurotransmitter responses in CNS, common, 62–63
- Neurotransmitters. *See also specific neurotransmitters*
 ionic actions, 63–74
- Nicotinic cholinergic responses, 64–65
- Nicotinic receptors, 402
- Nigrostriatal afferents, 367
- Nitric oxide (NO), 5, 201, 402
- Nitric oxide synthase (NOS), 5, 201
- NMDA (*N*-methyl-D-aspartate)
 dendrodendritic interactions and, 190
 excitatory amino acid responses and, 65–67
- NMDA component of EPSP, 341, 394, 441, 480
- NMDA (ion) channels, 394, 440
- NMDA receptors. *See also* Glutamate
 in basal ganglia, 394
 GluR, 95
 in hippocampus, 479, 487–488
 in neocortex, 533
 in olfactory bulb, 190, 208, 209
 in olfactory cortex, 441
 in retina, 250
 in spinal cord, 95
 in thalamus, 341
- NMDA-dependent homosynaptic LTP, 437–439
- Noradrenaline (NA), 344, 514–515
- Noradrenaline (NA)-containing fibers, 201
- Norepinephrine, 514–515, 542
 and excitability of pyramidal neurons, 70–71
- Nucleus of lateral lemniscus (nLL), 128, 129
- Octopus cells (O), 129–131, 136–139, 144, 145
 auditory-nerve fibers and, 130, 137, 139, 149
 onset units from, 149–151
- Odor. *See also* Olfactory bulb; Olfactory cortex
 fast and slow oscillatory rhythms evoked by, 433–435
- Odor contrast enhancement, lateral inhibition mediates, 214–215

- Odor discrimination, functional mechanisms in, 212–214
- Odor image, glomerular modules form, 210–211
- Odor maps on olfactory bulb, methods for demonstrating, 210
- Odor memory, modulation of recurrent inhibition mediates, 215–216
- “Odor opponent” interactions, 215
- Odor stimulation, responses to, 447–451
- Odor-induced slow-temporal patterning of afferent input, 433–435
- Olfactory bulb, 14, 34–35, 165
- activity patterns elicited by, 210, 211
 - basic circuit, 181
 - centrifugal modulation, 185–186
 - input processing, 181, 182
 - output control, 181, 183
 - parallel pathways, 183–185
 - dendritic properties, 202–209
 - synchronization depends on, 208–209
 - functional circuits, 210–216
 - neuronal elements, 166–167
 - cell populations, 174
 - inputs, 168–170
 - intrinsic neurons, 172–174
 - oscillatory activity in neurons, 208–209
 - principal neurons, 170–172
 - neurotransmitters and neuromodulators, 196–202
 - gaseous messengers, 201
 - return projections from olfactory cortex to, 420
 - synaptic actions, 186
 - dendrodendritic, 186–192
 - glomerular, 192–196
 - synaptic connections, 174
 - external plexiform layer, 177–179
 - glia, 180–181
 - glomerular layer, 175–177
 - granule cell layer, 179–180
- Olfactory cortex, 28, 169, 415–416. *See also* Piriform cortex
- defined, 415
 - excitatory circuitry
 - horizontal organization of afferent system, 425
 - horizontal organization of association fiber systems, 425–426
 - laminar organization, 423–424
 - functional operations, 447–453
 - comparisons with other cortical systems, 453–454
 - inhibitory circuitry, 426–429
 - membrane and dendritic properties
 - electrotonic structure, 443–444
 - integrative processes, 445–447
 - voltage-dependent processes, 444–445
 - neuronal elements, 417–420
 - afferent input, 419
 - cytoarchitecture, 416–417
 - neuromodulatory inputs, 419–420
 - nonpyramidal neurons, 422
 - numbers of pyramidal cells, 422
 - outputs, 420–421
 - principal neuron, 421
 - neurotransmitters, 441–443
 - primary, 454
 - synaptic actions, 433–437
 - afferent stimulation evokes series of postsynaptic currents, 433
 - dendritic processes, 431–432
 - synaptic potentials and currents, 430–431
 - synaptic connections, 422–423
- Olfactory cortical areas, connections between, 415–416, 420
- Olfactory discrimination and memory, role of olfactory cortex in, 451–453
- Olfactory pathway, 166
- main, 183
- Olfactory receptor neurons (ORNs), 450
- Olfactory sensory neurons, 196
- Olfactory system, patterns of connectivity in, 450
- Olivocerebellar circuit, 307–309
- Onset units, 149
- Optic nerve, 321
- Optic stalk, 217
- Optic tract, nucleus of, 324
- Organelles, 7
- Output control, 35
- Output convergence, 103
- P cells. *See* Midget (M) cells
- Pacemaker activity, 53
- Paired-pulse facilitation (PPF), 483
- Parabigeminal nucleus, 324
- Parabrachial inputs, 343
- Parabrachial region, 323
- Parabrachial triad, 319–320
- Parallel fibers (p.f.), 144, 275, 280–283
- Parolivary nucleus (PON), 128, 129
- Paravermis, 278
- Parvalbumin, 326
- Patches, striatal, 379
- Pathways, interregional, 7
- Pauser responses to sound, 151
- Paw shake reflex, 115
- Pedunculopontine tegmental nucleus, 323
- Peptides. *See* Neuropeptides
- Perceptrons. *See* Feedforward networks
- Perforant pathway, 482

- Periglomerular (PG) cells, 172, 199, 207–208
- Periolivary nuclei (PON), 129
- Permeability, ionic, 43, 45
- Persistent current. *See* Long-lasting (L) current
- Phaclofen, 539
- Phase-locking
 - in bushy cells, 155–157
 - defined, 156
- Photon noise, 258, 266
- Photoreceptors, 217–220
 - intensity range, 220–221
 - isolated rod, 220
 - spectral sensitivity, 221–222
- Pinso terminale, 281
- Piriform cortex, 415
 - anterior, 418, 419, 425, 426, 433, 439–440, 449
 - current-voltage relationship for deep pyramidal cell in, 444
 - inhibitory circuitry, 427–428
 - patterns of afferent fiber distribution to, 425
 - subdivisions of, 417–419
 - synaptic events evoked by afferent-fiber stimulation in, 432
 - synaptic plasticity and its regulation in, 437–441
 - temporal patterns of activity in, 433–437
- Place cells, 496
- Plasticity, homeostatic, 535
- Plateau potentials, 51–52, 111, 112
- Population excitatory postsynaptic potential (pEPSP), 475–476
- Posterior division of the VCN (PVCN), 127–130
- Posterior piriform cortex (PPC), 418, 419, 424–426, 432, 433, 439–440
 - “dispersive propagation” of afferent-evoked response in, 433, 434
- Postsynaptic inhibition, microcircuits that mediate different types of, 13
- Postsynaptic potentials (PSPs), 11, 122. *See also* Excitatory postsynaptic potentials; Inhibitory postsynaptic potentials
 - fast, 64–69
 - latencies of mono- and disynaptic, 99
 - separation of, 12
 - slow, 69–74
- Postsynaptic process, 3, 5
- Post-tetanic depression (PTD), 96
- Post-tetanic potentiation (PTP), 96, 484–485
- Potassium (K^+) channels, 336–338
- Potassium (K^+) conductance (gK), 338, 340
 - in cochlear nucleus cells, 148
 - in hippocampus, 489–495
 - increase in, 69–70
 - low-threshold, 148
 - in motor neurons, 93
 - in neocortex, 526–528
 - in neostriatal neurons, 382–387
 - in olfactory bulb cells, 195, 203–205
 - in olfactory cortex, 444–445
 - in thalamic cells, 336
- Potassium (K^+) currents, 49, 55, 526–528. *See also* Ionic currents
 - decrease in, 70–72
 - delayed rectifier, 56
 - transient, 56–57
- Potassium (K^+) ions, 40
- Potassium (K^+)-mediated IPSP, 430
- Potentialiation, 67
- Prediction units, 412
- Predictive coding, 261
- Prepiriform cortex. *See* Piriform cortex
- Prepotential, 147
- Presynaptic control, 9, 14
- Presynaptic inhibition, 9, 12
- Presynaptic process, 3, 5
- Primary afferent depolarization (PAD), 97, 98
- Primary afferents, 81
- Primarylike neurons, 153–156
- Primarylike responses, 146
 - from bushy cells, 146–149
- Primarylike-with-notch (pri-N) responses, 148
- Principal neurons. *See* Relay neurons
- Projection neurons, 3, 369. *See also* Thalamic relay neurons
- Proprioceptors, 81
- Propriospinal neurons, 84–85
- Protein molecular components of cells, 7
- Pspike, 475
- Pulvinar region, 314, 355
- Purkinje cell connectivity, plasticity of, 283
- Purkinje cell dendrite (Pcd), 280, 281
- Purkinje cell layer of cerebellum, 279–281
- Purkinje cells (PC), 28, 244
 - in cerebellar cortex, 287–288
 - in cerebellum, 276–277. *See also* Cerebellum climbing fiber activation, 290–291
- Pyramidal cell layer of hippocampus, 458–460
- Pyramidal (Py) cells (PC)
 - in cochlear nucleus, 129, 131–133, 138, 144, 151–152
 - cortical, 24–30, 421
 - activation of excitatory inputs to, 74, 75
 - norepinephrine and excitability of, 70–71
 - synaptic potentials generated in, 68
 - deep, 417, 421
 - in hippocampus, 458
 - in neocortex, 504–506
 - in olfactory cortex, 421
- Pyramidal cortex. *See* Piriform cortex

- Quantal actions, 11
Quantum, 477
- Raphe nucleus (Ra), 169
Rapidly inactivating current, 50
Rate coding, 110
Rebound response, 290, 307
Receptor molecules, 62
Reciprocal synapses, 14, 242
Recruitment, 109
Recurrent collaterals, 170
Recurrent excitation, 29, 104, 190, 192, 556–558
Recurrent inhibition, 13, 14
 disynaptic, 102–104
Recurrent networks, 451–453, 554
Recurrent pathways, 483–484, 522
Re-excitation, 29. *See also* Recurrent excitation
Reflex, stretch
 synaptic organization in, 101
Reflex interneurons. *See* Spinal interneurons,
 dynamic control of
Reflex pathways, 100–101
Reflex responses, automatic
 vs. voluntary motor acts, 100–101
Reflex systems, disynaptic, 106–108
Reflexes, multisynaptic, 101–108
Regio inferior, 459
Regio superior, 459
Regional circuits, basic. *See* Canonical circuits
Reinforcement learning, 409–412
Relay neurons, 3. *See also* Thalamic relay
 neurons
Release failure, 95
Release probabilities, 10
Remote inhibition, 97
Renshaw cells, 102–104
Renshaw inhibition, 14
Renshaw interneurons, recurrent inhibition
 through, 102–104
Repetitive discharge of neocortical cells,
 530–532
Repolarization, 45
Resistance/resistivity, 91–93, 110
Respiratory modulation, 433–435
Retention of sign, 10
Reticularism, 237
Retina, 34–35, 217–219, 269
 dendritic and axonal properties
 amacrine cells, 252–253
 bipolar to ganglion and amacrine cells, 252
 horizontal to photoreceptor and bipolar
 cells, 251–252
 individual retinal neurons are electronically
 compact, 250
 neurotransmitters and postsynaptic
 receptors, 250
 patterns of functional polarization, 248–250
 photoreceptors to horizontal and bipolar
 cells, 250–251
 development, 244–246
 efficiency, 253–254
 functional circuits, 253–254
 for daylight, twilight, and starlight, 264–269
 for ganglion cell receptive field, 254–257
 how retinal circuits serve vision
 efficient coding strategies, 260–265
 natural scenes contain fine detail at low
 contrast, 257–260
 transmitting low-contrast neural image, 260
 neuronal elements
 cell populations, 231–238
 input elements, 218–222
 intrinsic elements for forward transmission,
 222–225
 intrinsic elements for lateral transmission,
 227–231
 output elements, 225–227
 synaptic connections
 inner plexiform layer, 242–244
 outer plexiform layer (OPL), 238–242
Retinal triad, 320
Retinogeniculate inputs, 341–342
Retrograde messengers, 5
Retrograde signaling, 73–74
Retzius-Cajal neuron, 510
Rhodopsin (Rh), 248, 253, 268
Rhythmic bursting, 344–345
Rhythmic generation, 31, 32
Ribbon synapse, 238–241
Rod bipolar circuit, 264
- Saclophen, 539
Safety factors for synaptic transmission, 10
Scaling principle, 203
Schaffer collateral projection, 463
Schaffer collaterals, 469, 484
Scratch reflex, 100, 101
Semilunar cells (S), 417, 421, 424
Septotemporal axis (S-T), 456, 457
Serotonin (5-HT), 111, 515
Serotonin-containing fibers, 201–202
“Sharp wave” activity, 483
Short-axon (SA) cells, 172
 deep, 174
Shunting inhibition, 70, 430
Signal-to-noise enhancement, 8
Signal-to-noise (S/N) ratio, 260–263
Silent synapses, 10

- Silent/shunting inhibition, 11
- Simple spikes, 292
- Single-fiber group Ia ESPSs (sfEPSPs), 95
- Size principle, 110, 113, 184
- Sleep, transition to, 55
- Sodium (Na^+) conductances, 336
- Sodium (Na^+) currents, 49–53, 525–526. *See also* Sodium (Na^+) conductances
- in hippocampus, 489–495
 - in mitral cells, 203–205
 - in neocortex, 525–526
 - in neostriatal neurons, 382–384
 - in olfactory cortex, 444–445
 - in photoreceptors, 248
 - in Purkinje cells, 287
 - in thalamic cells, 336
- Solitary cells of Meynert, 505
- Soluble guanylate cyclase (sGC), 201
- Somas, 2. *See also* different cells
- Somatostatin (SOM)/nitric oxide synthetase (NOS)-containing interneurons, 370, 371, 402
- Sound, buildup and pauser responses to, 151
- Sound localization in horizontal plane, 155–157
- Spatial contrast, 32–34
- Spatial facilitation, 105, 106
- Spatial summation, 11
- nonlinear, 264
- Specific local information processing, 26
- Spherical bushy cells (SBC), 129–131, 136, 137, 140, 143, 144, 146
- Spike. *See* Action potential
- Spike frequency adaptation, 56, 70, 527
- Spike-timing dependent (synaptic) plasticity (STDP), 440, 486, 487, 533
- Spillover effect, 190
- Spinal circuits, synaptic organization of, 100–108
- Spinal cord, 79, 122–123
- in action, 109–116
 - anatomy, 80
 - excitatory systems, 98–99. *See also* Group Ia afferents
 - motor unit recruitment
 - alternative recruitment patterns, 114–116
 - functional consequences, 116
 - intrinsic motoneuron properties related to, 110–111
 - synaptic organization underlying, 112–113, 115
 - motor units, 83–84
 - properties, 84, 85
 - recruitment, 109–110
 - types of, 83–84
- neuronal elements, 79–86
 - postsynaptic excitation, 88–96
 - postsynaptic inhibition, 99–100
 - presynaptic inhibition, 86, 96–98
 - synaptic action in, 86–88
 - synaptic organization of ascending tracts, 108–109
 - “relay” vs. integrative” functions, 108
 - synthesis, 109
- Spinal interneurons, 84–86, 101–102. *See also* Renshaw interneurons
- dynamic control of, 116–122
- Spindles, 348, 349
- Spine action potentials, 546–547
- Spines. *See also* Dendritic spines
- horizontal cell, 240
- Spiny branchlets, 281
- Spiny neurons, 170. *See also* Pyramidal (Py) cells
- in basal ganglia, 369. *See also* Basal ganglia conditions for induction of LTD and LTP into, 394–395
 - dendritic membrane properties and, 382–387
 - intrinsic connections and, 400–401
 - synaptic types of neostriatal, 374–377
 - “sparsely,” 504
- Spiny stellate (St) cells, 506–507
- Spontaneous rate fibers, high vs. low, 158–159
- Starburst amacrine cell, 21, 249
- State dependence, 106–108, 118
- Stellate (St) cells (SC), 28, 132, 134, 277–278, 298
- spiny, 506–507
- Stretch reflex inhibition, 118
- Striatal interneurons, cortical and thalamic inputs to, 396–397
- Striate cortex, 225
- Striatum. *See* Neostriatum
- Striosomes, 379, 380
- Stumbling corrective reaction, 122
- Subiculum, 474
- Substantia nigra, 371, 375, 397–400
- pars reticulata (SNr), 363
- Substantia nigra pars compacta (SNc), 363
- Subthalamic nucleus, 363
- Superficial peroneal (SP) nerve, 118–122
- Superficial pyramidal cells (SP), 417, 421
- Superior colliculus, 324, 363
- “Surround” mechanism reduces redundancy, 261–262
- Sustained current. *See* Long-lasting (L) current
- Synapse(s), 61–63
- as basic unit of neural circuit organization, 3–6

- Synapse(s) (*continued*)
 defined, 3
 as integrative micro-unit, 7
 mechanisms involved in signaling at, 3–5
 as multifunctional multitemporal unit, 3–5
 types of, 5–6
 types 1 and 2, 5–6
- Synaptic and intrinsic currents, 74–77
- Synaptic circuits. *See also* Canonical circuits;
 Local/intrinsic circuits
 development of, 8
 levels of organization of, 6–8
- Synaptic cleft, 61
- Synaptic convergence, 9, 11–12, 14
- Synaptic density, 113
- Synaptic divergence, 9, 14
- Synaptic efficacy, factors that control, 113–115
- Synaptic integration, 488
- Synaptic organization, 1–3. *See also specific topics*
 as multidisciplinary and multilevel subject, 1
- Synaptic scaling/normalization, 489
- Synaptic strength. *See* Synaptic efficacy
- Synaptic summation, as fundamentally nonlinear, 11
- Synaptic system, 113
- Synaptic terminal, types of, 316–318
- Synaptic transmission in reverse. *See* Retrograde signaling
- Synchronization, 8, 10
- T channels, 336–338
 anatomical relationship of modulator inputs to, 348
- Temporal contrast, 32, 34
- Temporal differentiation, 13
- Temporal summation, 11
- Terminal tuft (T), 19
- Tetanic depression, 96
- Tetrodotoxin (TTX), 287–288, 290, 301, 383, 495
- Thalamic afferents, 366–367, 512–514
- Thalamic neurons, 74–75
- Thalamic nuclear groups, major, 312–314
- Thalamic nucleus, major types of afferent to, 314–315
- Thalamic relay neurons, 314, 324–326, 329–334
 classes of, 325–326
 firing mode, 58, 72–73
 inputs to, 328–329
 noradrenaline's effects on, 344
- Thalamic relay(s)
 first and higher order, 312, 353–356
 gating and other transformations in, 344, 348–350
 brainstem inputs, 350
 burst and tonic relay response modes, 344–348
 cortical inputs from layer 6, 350–351
- Thalamic reticular nucleus, 331, 332
 cells of, 328
 inputs from, 323, 348–350
- Thalamocortical cells (TC), 28
- Thalamocortical relationships, 355–356
- Thalamus, 311–312, 359, 363
 basic neuronal circuit, 329
 component populations, 329–330
 intrinsic circuitry, 330–332
 dendritic cable properties, 332–334
 drivers and modulators, 314, 351–353
 general organization, 312–315
 maps, 315–316
 parallel processing, 315
 how it relates to motor outputs, 357
 motor links of first order afferent drivers, 357–358
 motor links of higher order afferent drivers, 358–359
 relationships of sensory perception to mechanisms of motor control, 359
- interneurons, 326–327, 334, 342
 inputs to, 329
- membrane properties, 334–340
 of monkey, 312–313
- neuronal elements, 316, 324–327
 electron microscopic appearance of, 316–320
 inputs, 320–324
 synaptic connections, 328–329
 synaptic transmission
 brainstem inputs, 343–344
 GABAergic inputs, 342–343
 glutamatergic inputs, 341–342
 ionotropic and metabotropic receptors, 340–341
- Theta, 485
- Theta burst pairing, 485–486
- Theta burst stimulation, 485
- Thorny excrescence, 467–468
- Tibialis anterior (TA), 117
- T-multipolar cells, 129, 130, 136, 138, 143–147, 159
 chopper responses from, 146
- Tonic mode of firing, 338, 339. *See also* Burst and tonic relay response modes
- Tonotopic map, 125
- Tract cells, 85
- Transient current, 50
- Transmitter substance, 3
- Transverse axis (TRANS), 456, 457

- Trapezoid body (TB), 128–130, 144
Trigger features, 550
Trisynaptic circuit, 463
Tuberculoventral cells. *See* Vertical (tuberculoventral) cells
Tuberomammillary nucleus of hypothalamus, 324
Tufted cell membrane properties, synchronization by, 209
Tufted cells, 171–172, 184, 194, 199
 external (T_e), 171
 internal (T_i), 171
 middle (T_m), 171
“Twitching spine” hypothesis, 546
Two-port, nonreciprocal, 3
Tyrosine hydroxylase (TH), 375
- Varicosity/bouton, 7
Ventral anterior thalamic nuclei, 312
Ventral cochlear nucleus (VCN), 144, 145
 anterior division, 127–129, 137
 cell types in, 129–131
 posterior division, 127–130
 synapses in, 136–140
Ventral horn, synaptic types in, 86, 87
Ventral horn interneurons, 86
Ventral lateral thalamic nuclei, 312
Ventral nucleus of lateral lemniscus (VnLL), 129
Ventral posterior thalamic nuclei, 312
Ventral spinocerebellar tract neurons (VSCT), 107–109
Ventral thalamus, 311
Ventricular cells, symmetrical and asymmetrical modes of division, 501–503
Ventricular zone (VZ), 501–503
Vermis, 278
Vertical (tuberculoventral) cells (V), 132, 133, 138
Vesicles, synaptic, 3–6, 61, 240, 268
Visual cortex, basic circuit for, 524–525
Visual system, compared with olfactory system, 454
Visual transduction, 246–248
Voltage clamp, 45
Voltage-dependent channels, 336–338
Voltage-dependent processes, 444–445
Voltage-gated Ca^{2+} channels (VGCCs), 192, 493
Voltage-gated currents, 45, 47, 51
 high-voltage activated currents, 53–54
Voltage-gated Na^+ channels, 489–491
Voltage-sensitive ion channels, 47
Voltage-sensitive membrane currents, 45, 149
Vomeronasal organ (VNO), 185
- Waking, transition to, 55
Waveform of stimulus, 157